BIOMARKERS AND PATHOGENESIS OF ALPHA-SYNUCLEIN IN PARKINSON'S DISEASE

EDITED BY: Pingyi Xu, Shaomin Li, Liu Jun, Yun-Cheng Wu, Shaogang Qu and Hao Deng

PUBLISHED IN: Frontiers in Aging Neuroscience and Frontiers in Genetics



frontiers Research Topics



frontiers

Frontiers eBook Copyright Statement

The copyright in the text of individual articles in this eBook is the property of their respective authors or their respective institutions or funders. The copyright in graphics and images within each article may be subject to copyright of other parties. In both cases this is subject to a license granted to Frontiers.

The compilation of articles constituting this eBook is the property of Frontiers.

Each article within this eBook, and the eBook itself, are published under the most recent version of the Creative Commons CC-BY licence. The version current at the date of publication of this eBook is CC-BY 4.0. If the CC-BY licence is updated, the licence granted by Frontiers is automatically updated to the new version.

When exercising any right under the CC-BY licence, Frontiers must be attributed as the original publisher of the article or eBook, as applicable.

Authors have the responsibility of ensuring that any graphics or other materials which are the property of others may be included in the CC-BY licence, but this should be checked before relying on the CC-BY licence to reproduce those materials. Any copyright notices relating to those materials must be complied with.

Copyright and source acknowledgement notices may not be removed and must be displayed in any copy, derivative work or partial copy which includes the elements in question.

All copyright, and all rights therein, are protected by national and international copyright laws. The above represents a summary only. For further information please read Frontiers' Conditions for Website Use and Copyright Statement, and the applicable CC-BY licence.

ISSN 1664-8714
ISBN 978-2-88974-143-4
DOI 10.3389/978-2-88974-143-4

About Frontiers

Frontiers is more than just an open-access publisher of scholarly articles: it is a pioneering approach to the world of academia, radically improving the way scholarly research is managed. The grand vision of Frontiers is a world where all people have an equal opportunity to seek, share and generate knowledge. Frontiers provides immediate and permanent online open access to all its publications, but this alone is not enough to realize our grand goals.

Frontiers Journal Series

The Frontiers Journal Series is a multi-tier and interdisciplinary set of open-access, online journals, promising a paradigm shift from the current review, selection and dissemination processes in academic publishing. All Frontiers journals are driven by researchers for researchers; therefore, they constitute a service to the scholarly community. At the same time, the Frontiers Journal Series operates on a revolutionary invention, the tiered publishing system, initially addressing specific communities of scholars, and gradually climbing up to broader public understanding, thus serving the interests of the lay society, too.

Dedication to Quality

Each Frontiers article is a landmark of the highest quality, thanks to genuinely collaborative interactions between authors and review editors, who include some of the world's best academicians. Research must be certified by peers before entering a stream of knowledge that may eventually reach the public - and shape society; therefore, Frontiers only applies the most rigorous and unbiased reviews.
Frontiers revolutionizes research publishing by freely delivering the most outstanding research, evaluated with no bias from both the academic and social point of view. By applying the most advanced information technologies, Frontiers is catapulting scholarly publishing into a new generation.

What are Frontiers Research Topics?

Frontiers Research Topics are very popular trademarks of the Frontiers Journals Series: they are collections of at least ten articles, all centered on a particular subject. With their unique mix of varied contributions from Original Research to Review Articles, Frontiers Research Topics unify the most influential researchers, the latest key findings and historical advances in a hot research area! Find out more on how to host your own Frontiers Research Topic or contribute to one as an author by contacting the Frontiers Editorial Office: frontiersin.org/about/contact

BIOMARKERS AND PATHOGENESIS OF ALPHA-SYNUCLEIN IN PARKINSON'S DISEASE

Topic Editors:
Pingyi Xu, First Affiliated Hospital of Guangzhou Medical University, China
Shaomin Li, Harvard Medical School, Boston, United States
Liu Jun, Shanghai Jiao Tong University, China
Yun-Cheng Wu, Shanghai Jiao Tong University School of Medicine, China
Shaogang Qu, Southern Medical University, China
Hao Deng, Central South University, China

Citation: Xu, P., Li, S., Jun, L., Wu, Y.-C., Qu, S., Deng, H., eds. (2022). Biomarkers and Pathogenesis of Alpha-Synuclein in Parkinson's Disease.
Lausanne: Frontiers Media SA. doi: 10.3389/978-2-88974-143-4

Table of Contents

06 ***Editorial: Biomarkers and Pathogenesis of Alpha-Synuclein in Parkinson's Disease***
Puyu Li, Pingyi Xu and Jun Liu

10 ***Changes of Amide Proton Transfer Imaging in Multiple System Atrophy Parkinsonism Type***
Shuhua Li, Piu Chan, Chunmei Li, Haibo Chen, Min Chen, Wen Su, Kai Li, Na Lu, Lu Yu, Defa Chu and Pu-Yeh Wu

20 ***The cis-Regulatory Element of SNCA Intron 4 Modulates Susceptibility to Parkinson's Disease in Han Chinese***
Shi-Guo Zhu, Hui Lu, Miao Mao, Zhao-Feng Li, Lei Cui, Begench Ovlyakulov, Xiong Zhang and Jian-Hong Zhu

27 ***Parkinson's Disease With Depression: The Correlations Between Neuroinflammatory Factors and Neurotransmitters in Cerebrospinal Fluid***
Teng-hong Lian, Peng Guo, Ya-nan Zhang, Jing-hui Li, Li-xia Li, Du-yu Ding, Da-ning Li, Wei-jiao Zhang, Hui-ying Guan, Xiao-min Wang and Wei Zhang

35 ***Corticospinal Tract Impairment of Patients With Parkinson's Disease: Triple Stimulation Technique Findings***
Dan Xu, Qingyun Ding and Han Wang

41 ***Different Perivascular Space Burdens in Idiopathic Rapid Eye Movement Sleep Behavior Disorder and Parkinson's Disease***
Xiao-li Si, Lu-yan Gu, Zhe Song, Cheng Zhou, Yi Fang, Chong-yao Jin, Jing-jing Wu, Ting Gao, Tao Guo, Xiao-jun Guan, Xiao-jun Xu, Xin-zhen Yin, Ya-ping Yan, Min-min Zhang and Jia-li Pu

52 ***Characterization of EEG Data Revealing Relationships With Cognitive and Motor Symptoms in Parkinson's Disease: A Systematic Review***
Qing Wang, Lin Meng, Jun Pang, Xiaodong Zhu and Dong Ming

66 ***Alpha-Synuclein Accumulation and Its Phosphorylation in the Enteric Nervous System of Patients Without Neurodegeneration: An Explorative Study***
Lu-Lu Bu, Kai-Xun Huang, De-Zhi Zheng, Dan-Yu Lin, Ying Chen, Xiu-Na Jing, Yan-Ran Liang and En-Xiang Tao

76 ***LncRNA-T199678 Mitigates α-Synuclein-Induced Dopaminergic Neuron Injury via miR-101-3p***
Lu-Lu Bu, Ying-Yu Xie, Dan-Yu Lin, Ying Chen, Xiu-Na Jing, Yan-Ran Liang, Su-Dan Peng, Kai-Xun Huang and En-Xiang Tao

88 ***Aberrant Amplitude of Low-Frequency Fluctuations in Different Frequency Bands in Patients With Parkinson's Disease***
Zhaoxiu Wang, Yanjun Liu, Xiuhang Ruan, Yuting Li, E. Li, Guoqin Zhang, Mengyan Li and Xinhua Wei

102 ***Regulatory Roles of Bone in Neurodegenerative Diseases***
Zhengran Yu, Zemin Ling, Lin Lu, Jin Zhao, Xiang Chen, Pingyi Xu and Xuenong Zou

118 ***Sporadic Parkinson's Disease Potential Risk Loci Identified in Han Ancestry of Chinese Mainland***

Bo Wang, Xin Liu, Shengyuan Xu, Zheng Liu, Yu Zhu, Xiong Zhang and Renshi Xu

132 ***A Comprehensive Phenotype of Non-motor Impairments and Distribution of Alpha-Synuclein Deposition in Parkinsonism-Induced Mice by a Combination Injection of MPTP and Probenecid***

Na-Ra Han, Yu-Kang Kim, Sora Ahn, Tae-Yeon Hwang, Hyejung Lee and Hi-Joon Park

147 ***Mini Review: Correlations of Cognitive Domains With Cerebrospinal Fluid α-Synuclein Levels in Patients With Parkinson's Disease***

Hidetomo Murakami, Kenjiro Ono, Tomotaka Shiraishi, Tadashi Umehara, Shusaku Omoto and Yasuyuki Iguchi

155 ***Mild Cognitive Impairment Patients Have Higher Regulatory T-Cell Proportions Compared With Alzheimer's Disease-Related Dementia Patients***

Jiping Fu, Jinhai Duan, Jianwei Mo, Hao Xiao, Yuedong Huang, Weiping Chen, Shaotong Xiang, Fan Yang, Yongjun Chen and Shuwen Xu

162 ***Increased Plasma Heme Oxygenase-1 Levels in Patients With Early-Stage Parkinson's Disease***

Wenhua Sun, Jinhua Zheng, Jianjun Ma, Zhidong Wang, Xiaoxue Shi, Mingjian Li, Shen Huang, Shiyu Hu, Zhenxiang Zhao and Dongsheng Li

171 ***Bone-Derived Factors as Potential Biomarkers for Parkinson's Disease***

Yuwan Lin, Miaomiao Zhou, Wei Dai, Wenyuan Guo, Jiewen Qiu, Zhiling Zhang, Mingshu Mo, Liuyan Ding, Panghai Ye, Yijuan Wu, Xiaoqin Zhu, Zhuohua Wu, Pingyi Xu and Xiang Chen

178 ***Preanalytical Stability of CSF Total and Oligomeric Alpha-Synuclein***

Ilham Y. Abdi, Nour K. Majbour, Eline A. J. Willemse, Wilma D. J. van de Berg, Brit Mollenhauer, Charlotte E. Teunissen and Omar M. El-Agnaf

186 ***α-Synuclein Up-regulates Monoamine Oxidase A Expression and Activity* via *Trans-Acting Transcription Factor 1***

Congcong Jia, Cheng Cheng, Tianbai Li, Xi Chen, Yuting Yang, Xinyao Liu, Song Li and Weidong Le

195 ***Biomarkers and the Role of α-Synuclein in Parkinson's Disease***

Tingting Du, Le Wang, Weijin Liu, Guanyu Zhu, Yingchuan Chen and Jianguo Zhang

210 ***Fatty Acid-Binding Protein 3 Expression in the Brain and Skin in Human Synucleinopathies***

Hideki Oizumi, Kenshi Yamasaki, Hiroyoshi Suzuki, Takafumi Hasegawa, Yoko Sugimura, Toru Baba, Kohji Fukunaga and Atsushi Takeda

220 ***Co-registration Analysis of Fluorodopa and Fluorodeoxyglucose Positron Emission Tomography for Differentiating Multiple System Atrophy Parkinsonism Type From Parkinson's Disease***

Wen-biao Xian, Xin-chong Shi, Gan-hua Luo, Chang Yi, Xiang-song Zhang and Zhong Pei

229 ***Decreased Exosomal Acetylcholinesterase Activity in the Plasma of Patients With Parkinson's Disease***
Kyu Hwan Shim, Han Gyeol Go, Heewon Bae, Da-Eun Jeong, Danyeong Kim, Young Chul Youn, SangYun Kim, Seong Soo A. An and Min Ju Kang

236 ***Cortical Structural Connectivity Alterations and Potential Pathogenesis in Mid-Stage Sporadic Parkinson's Disease***
Xia Deng, Zheng Liu, Qin Kang, Lin Lu, Yu Zhu and Renshi Xu

249 ***The Cross-Links of Endoplasmic Reticulum Stress, Autophagy, and Neurodegeneration in Parkinson's Disease***
Haigang Ren, Wanqing Zhai, Xiaojun Lu and Guanghui Wang

267 ***Identifying Mild Cognitive Impairment in Parkinson's Disease With Electroencephalogram Functional Connectivity***
Min Cai, Ge Dang, Xiaolin Su, Lin Zhu, Xue Shi, Sixuan Che, Xiaoyong Lan, Xiaoguang Luo and Yi Guo

277 ***PKC Delta Activation Promotes Endoplasmic Reticulum Stress (ERS) and NLR Family Pyrin Domain-Containing 3 (NLRP3) Inflammasome Activation Subsequent to Asynuclein-Induced Microglial Activation: Involvement of Thioredoxin-Interacting Protein (TXNIP)/Thioredoxin (Trx) Redoxisome Pathway***
Manikandan Samidurai, Bharathi N. Palanisamy, Alejandra Bargues-Carot, Monica Hepker, Naveen Kondru, Sireesha Manne, Gary Zenitsky, Huajun Jin, Vellareddy Anantharam, Anumantha G. Kanthasamy and Arthi Kanthasamy

299 ***Alpha-Synuclein as a Biomarker of Parkinson's Disease: Good, but Not Good Enough***
Upasana Ganguly, Sukhpal Singh, Soumya Pal, Suvarna Prasad, Bimal K. Agrawal, Reena V. Saini and Sasanka Chakrabarti

318 ***Development and Validation of a Prognostic Model for Cognitive Impairment in Parkinson's Disease With REM Sleep Behavior Disorder***
Fangzheng Chen, Yuanyuan Li, Guanyu Ye, Liche Zhou, Xiaolan Bian and Jun Liu

329 ***Genetic Analysis and Literature Review of* SNCA *Variants in Parkinson's Disease***
Yi Guo, Yan Sun, Zhi Song, Wen Zheng, Wei Xiong, Yan Yang, Lamei Yuan and Hao Deng

336 ***Significant Difference of Immune Cell Fractions and Their Correlations With Differential Expression Genes in Parkinson's Disease***
Yilin Huang, Huisheng Liu, Jiaqi Hu, Chongyin Han, Zhenggang Zhong, Wei Luo, Yuhu Zhang and Fei Ling

346 ***Detection of Cerebrospinal Fluid Neurofilament Light Chain as a Marker for Alpha-Synucleinopathies***
Sezgi Canaslan, Matthias Schmitz, Anna Villar-Piqué, Fabian Maass, Karin Gmitterová, Daniela Varges, Paul Lingor, Franc Llorens, Peter Hermann and Inga Zerr

354 ***Alterations of Erythrocytic Phosphorylated Alpha-Synuclein in Different Subtypes and Stages of Parkinson's Disease***
Xu-Ying Li, Wei Li, Xin Li, Xu-Ran Li, Linjuan Sun, Weiwei Yang, Yanning Cai, Zhigang Chen, Jun Wu, Chaodong Wang and Shun Yu

frontiers in Aging Neuroscience

EDITORIAL
published: 05 October 2021
doi: 10.3389/fnagi.2021.776873

Editorial: Biomarkers and Pathogenesis of Alpha-Synuclein in Parkinson's Disease

*Puyu Li, Pingyi Xu and Jun Liu**

Department of Neurology, Ruijin Hospital Afflicted to Shanghai Jiaotong University School of Medicine, Shanghai, China

Keywords: alpha-synuclein (α-synuclein), Parkinson's disease, biomarker (BM), pathogenesis (nervous system), predictor

Editorial on the Research Topic

Biomarkers and Pathogenesis of Alpha-Synuclein in Parkinson's Disease

The recognition of Alpha-Synuclein (α-Syn) as an essential player in the pathobiology of human neurodegenerative diseases has spurred substantial efforts to understand its biochemical and pathological function. This *Frontiers in Aging Neuroscience* Topic contains a series of high-quality original articles and updated reviews covering recent 2-year progression in various aspects of α-Syn expressions in blood, saliva, and cerebrospinal fluid (CSF), and pathological processes in regulating human neurodegenerative disorders as well as its feasibility as an early predictive biomarker. Parkinson's disease (PD) is a typical disease in α-synucleinopathies, presenting dominantly with clinical symptoms of motor impairment. PD is characterized by progressive chronic neurodegeneration and loss of dopaminergic (DA) neurons in brain, mainly substantia nigra. Meanwhile, dementia with Lewy bodies (DLB), and multiple system atrophy (MSA) belong to this devastating neurodegenerative category. Currently, PD cannot be completely cured or reversed, and existing treatment strategies have limited efficacy in the early stages. Therefore, there is an imperative need to clarify the pathogenesis of PD and find early identifications of it. However, the detailed etiology and pathogenesis remain no consensus. This Research Topic aims to generate a multidimensional discussion linking clinical analysis with basic experiment unveiling the fundamental mechanisms of PD. Then filtrate the current effective biomarkers for preclinical detection and clinical evaluation on this basis. As a result, building a predictive model contributes to a deeper understanding of the mechanism of PD, so as to better guide clinical applications.

Various attempts made by the researchers to develop preclinical and clinical investigations encompassing genetics, immunology, microbiology, neuroimaging, and neurophysiology to clarify the molecular mechanisms and identify useful biomarkers for the disease diagnosis. There are two valuable systematic reviews on this topic, which comprehensively describe the current research status. In the first place, Du et al. summarizes useful biomarkers for the diagnosis of PD, as well as how the biomarkers α-Syn could potentially be used as a biomarker for PD step by step from genetics, immunology, fluid and tissue, imaging, as well as neurophysiology. As a general overview, Ganguly et al. also evaluate the overall effectiveness of α-Syn in forecasting PD progression. In view of the overwhelming importance of α-Syn in the pathogenesis, a detailed analysis is then made of various studies to establish the biomarker potential of this protein in PD. Knowledge of the α-Syn-related novel biomarkers for preclinical detection and clinical evaluation serve to identify the disease-predictive biomarkers more effectively, which are critical for precise diagnosis and therapeutic approaches.

Early warning biomarkers have become a hot topic recently due to the need for diagnosis and treatment in forepart. Inchoate detection and differential diagnosis of parkinsonism-type MSA

OPEN ACCESS

Edited and reviewed by:
Thomas Wisniewski,
NYU Grossman School of Medicine, United States

****Correspondence:***
Jun Liu
jly0520@hotmail.com

Received: *14 September 2021*
Accepted: *20 September 2021*
Published: *05 October 2021*

Citation:
Li P, Xu P and Liu J (2021) Editorial: Biomarkers and Pathogenesis of Alpha-Synuclein in Parkinson's Disease. Front. Aging Neurosci. 13:776873. doi: 10.3389/fnagi.2021.776873

(MSA-P) and PD are in great clinical need, as aging can lead to many diseases that are difficult to detect at early stage. This urgent issue is also addressed by Li et al. in this case by studying the role of neuroimaging in the diagnosis of MSA-P. Using a novel magnetic resonance technology, amide proton transfer (APT) imaging, which is a well-studied chemical exchange saturation transfer imaging for its sensitivity to mobile protons and peptides in tissues. Next, Xian et al. demonstrate the diagnostic value of co-registration analysis of ^{18}F-flurodeoxyglucose (^{18}F-FDG) and ^{18}F-Dopa positron emission tomography (PET) for differentiating MSA-P from PD. Segmentation analysis of the rabbit-shaped appearance of the striatum segment of PET images not only could distinguish PD and MSA-P patients from healthy controls (HCs).

Rapid eye movement sleep behavior disorder (RBD) is marked by repeated nocturnal sleep-related normal skeletal muscle atonia with remarkable motor disturbances and dream enactment behaviors, and the existence of RBD can be considered as an omnipotent precursor to PD. Therefore, scholars have started with exploring the interconnected mechanisms between RBD and PD and the course progression to identify early predictive indicators of PD. The article by Si et al. assess the clinical significance of magnetic resonance imaging (MRI)-visible enlarged perivascular space (EPVS) in patients with idiopathic RBD (iRBD) and PD. Their study indicates that iRBD patients had significantly greater EPVS burdens than PD patients. Specifically, higher EPVS burdens in centrum semiovale (CSO) and basal ganglia might be independent risk factors for iRBD, and the higher the value the more severe the clinical symptoms. Then, Chen et al. combine clinical assessments, dopamine transporter (DAT) imaging data, CSF and genetic data of PD patients to minister to develop a prognostic model for predicting mild cognitive impairment (MCI) in PD-RBD patients. As CI is one of the most common non-motor symptoms in PD, incidence of CI in PD patients increases as the disease progresses, thus investigating risk factors and predictive model for CI may contribute to a better understanding of the PD-RBD phenotype and help decelerate the MCI process in PD-RBD patients in clinical practice.

The central nervous system (CNS) is so sophisticated and fragile that is vulnerable to injury, pathogen, or neurodegeneration. In the process of aging and degradation, the activation of the innate immune system occurs. The inflammasome is a signal complex that regulates immune cells, chiefly microglial, leading to the release of pro-inflammatory factors. Consequently, pro-inflammatory factors aggravate the neuro-inflammatory response, neurological degeneration, and eventually upset the brain metabolic balance. It can be deduced that analyzing the inflammatory factors in CSF is more meaningful to investigate brain neuroinflammation. For instance, studies have shown that immune dysfunction may lead to aberrant α-Syn aggregation and transmission in the brain. The article by Lian et al. tackles this issue and suggests that neuroinflammatory factors in CSF, especially tumor necrosis factor (TNF)-α, may cause damage to dopamine (DA) neurons and induce the depletion of DA, which is related to the occurrence and development in PD patients who accompanied with depression. Also, adaptive immune system, including lymphocyte subpopulations and cytokines, is involved in the PD pathogenesis. The article by Huang et al. analyzes integrated substantia nigra (SN) and gene expression by CIBERSPOT and identifies the function of key immune cell types in PD. They propose the immune response modifying the genetic background as a factor influencing the synaptic pathway in PD pathology. Another popular inflammation topic normally discussed in pathogenesis of neurodegenerative disease is gut-brain axis. The gut-brain axis is a two-way regulating axis for the interaction between gastrointestinal function and the CNS, and the nerve-endocrine-immune network is an important connection method. Following this clue, Bu, Huang, et al. assess α-Syn immune-neuron reactivity and expression patterns. Contrary to our expectations, they propose that gastrointestinal pathology couldn't be facilitated for diagnosing α-synucleinopathies, including PD. The deposit of α-Syn is age-dependent rather than neurodegenerative-unique in the enteric nervous system (ENS) of patients.

Apart from aging, genetic dysfunction is widely considered to be a key risk factor of PD, and is repeatedly discussed when exploring the etiology and pathology of α-Syn. So far, at least 23 genes and independent risk signals related to PD have been discovered. Among them, it is indisputable that the α-synuclein gene (*SNCA*) is the first identified pathogenic gene that causes autosomal dominant PD, and its abnormal protein aggregation is regarded as the main pathological symbol of patients. Based on this understanding, Guo et al. evaluates the associations between the *SNCA* gene variants and PD through conventional whole-exome sequencing (WES) and sanger sequencing. Beyond expectations, the result shows that variants located in the coding regions of the *SNCA* gene may have less or no role in the development of PD in the Han Chinese population, which implies the inescapable role of ethnic differences in PD development. Therefore, in order to verify the function of *SNCA*, it is necessary to carry out cohort comparisons with large samples of multiple races in the future. Neuro regulation is the result of multi-gene collaboration. Both α-Syn and Monoamine oxidase A (MAOA) are long deemed as the pivotal pathogenesis of PD, Jia et al. further explores the close crosstalk between these two co-regulation molecules. At the same time, Bu, Xie et al. reveal that overexpression of long non-coding RNA (lncRNA)-T199678 mitigates the α-Syn-induced dopaminergic neuron injury, including oxidative stress, abnormal cell cycle, and apoptosis, which contributed to promote PD. This study praises a new molecular target for further genetic pathway investigation in PD.

Multiple system diseases often occur in the elderly. It is often found that patients with neurodegenerative diseases are complicated by osteoporosis, and fractures are more likely to be found in the prodromal phase of PD in clinical practice. As the main supporting and protecting organs of our body, bone is also an active immune and endocrine organ. It can secrete a variety of bone-derived factors, interact with the brain through various bone-derived cells, and participate in the pathophysiology of various diseases. First, the article by Yu et al. reviews the latest research studying the impact of

bone-derived cells and bone-controlled immune system on the brain, summarizes the roles of the bone-brain axis in the progression of neurodegenerative diseases and evaluates how these factors are implicated in the progress of α-synucleinopathies diseases and their potential use in the diagnosis and treatment of these diseases. On the other hand, Lin et al. guaranteed the combined assessment of plasma and CSF of osteocalcin (OCN) or osteopontin (OPN) could be candidate biomarkers in differentiating PD patients from HCs. Besides, inflammation may be involved in the interaction between these two bone-derived factors and PD, which partly explains the various modulating effects of bone physiological processes on the CNS.

New methods and molecules are gradually being tried for scientific research. Recently, exosomal biomarkers have been involved in embedding the acknowledgment and diagnosis of neurodegenerative disorders. Exosomes are small extracellular vesicles coming from different cell types and can contain different molecular components such as proteins, lipids, and RNA. Previous reports have demonstrated increased exosomal α-Syn in patients with PD in comparison to HCs. In this context, the exosomal acetylcholinesterase (AChE) and α-Syn are quantified and the inner relationships with clinical symptom are simultaneously scouted by Shim et al. supporting the occurrence of cholinergic dysfunction on motor deficits in PD. The mechanisms of progressive loss of DA neurons in PD include a variety of cellular processes such as α-Syn aggregation, mitochondrial damage, oxidative stress, calcium homeostasis dysfunction, interruption of axonal transport, and neuroinflammatory damage. These abnormal phenomena can disturb the balance of protein homeostasis in PD. In a review by Ren et al., the cross-linking mechanisms of endoplasmic reticulum (ER) stress-induced unfolded protein response (UPR) and the dysregulated autophagy in DA neurodegeneration are systematically addressed.

Neuroimaging is also a traditional technique for detecting the connectivity of brain functions, which is often used in interpreting the static state and dynamic changes of patients in clinical research. Focusing on the brain imaging network in aging, it is wildly acknowledged that PD patients depict abnormal spontaneous neural activity in resting-state functional magnetic resonance imaging (r-fMRI). Wang Z. et al. target at the amplitude of low-frequency fluctuations (ALFF) and discover that PD patients exhibited different tendencies in several brain regions, emphasizing the diversity of widespread abnormal brain activities related to PD, and suggesting that the abnormalities of ALFF in specific frequency bands would be helpful in detecting the neural changes in PD. Expect for traditional neuroimaging, nowadays researchers use more controllable electrophysiological tools, such as TMS, to reveal the conduction blocks caused by structural abnormalities or neurodegenerative diseases. The article by Xu et al. applies a more sensitive and accurate method, triple stimulation technique (TST), to quantitatively assess the integrity and impairment of corticospinal pathway in PD patients.

Present research regards the electroencephalogram (EEG) as a promising method to study real-time brain dynamic changes in patients with PD. Compared with other functional imaging methods, EEG has high temporal resolution, in which specific frequency analysis enables accurately investigating connectivity fluctuations. Firstly, the review by Wang Q. et al. summarizes recent research on EEG characterization related to the cognitive and motor functions in PD patients and discussed its potential to be used as diagnostic biomarkers. Abnormalities in β and δ frequency bands are, respectively the main manifestation of dyskinesia and cognitive decline in PD. In conclude, the unique time-frequency characteristics of EEG could provide further insight into disrupted sensorimotor networks in PD with motor deficits, such as FOG, dyskinesia, and dystonia in a real-world environment. Several of the contributors to this topic recognized the need to promote cognition of older people. The exploration of specific brain regions for PD cognitive impairment is ongoing. The dorsolateral prefrontal cortex (DLPFC) transmits afferent projections to the caudate nucleus and putamen and participates in advanced cognitive functions, which is recognized as an important area related to CI. Furthermore, Cai et al. compare the posterior middle frontal gyrus-based functional connectivity differences between PD patients with MCI and normal cognitive PD patients. As discussed previously in this editorial, this topic accumulates growing evidence that cognitive dysfunction of PD patients is different from the cognitive function of normal aging people.

In summary, PD is a neurodegenerative disease caused by the combined action of genes, age, and environment. The underlying pathological mechanism involves multiple circuits such as gene regulation, neuroimmune, biochemical factors, and neurophysiology, which requires further exploration by establishing multi-factor model. On the other hand, biomarkers can help clinicians reduce the chance of misdiagnosis and help them monitor the improvement of disease pathology during anti-Parkinson's disease drug trials. However, the inconsistent research conclusions in the same direction remind us that many methodological issues related to the detection and quantification of α-syn need to be further verified for their feasibility. At the same time, large sample of long-term follow-up studies comparing the motor dysfunction of different neurodegenerative diseases are needed.

AUTHOR CONTRIBUTIONS

JL and PL decided on the basic framework of the editorial, and PL wrote the initial version of the manuscript. Also, JL and PX revised the work. All the authors approved of the final edition for publication.

ACKNOWLEDGMENTS

We are grateful to each author for the remarkable contributions to this topic.

Conflict of Interest: The authors declare that the research was conducted in the absence of any commercial or financial relationships that could be construed as a potential conflict of interest.

Publisher's Note: All claims expressed in this article are solely those of the authors and do not necessarily represent those of their affiliated organizations, or those of the publisher, the editors and the reviewers. Any product that may be evaluated in this article, or claim that may be made by its manufacturer, is not guaranteed or endorsed by the publisher.

Copyright © 2021 Li, Xu and Liu. This is an open-access article distributed under the terms of the Creative Commons Attribution License (CC BY). The use, distribution or reproduction in other forums is permitted, provided the original author(s) and the copyright owner(s) are credited and that the original publication in this journal is cited, in accordance with accepted academic practice. No use, distribution or reproduction is permitted which does not comply with these terms.

frontiers in Aging Neuroscience

ORIGINAL RESEARCH
published: 30 September 2020
doi: 10.3389/fnagi.2020.572421

Changes of Amide Proton Transfer Imaging in Multiple System Atrophy Parkinsonism Type

Shuhua Li[1,2], Piu Chan[1], Chunmei Li[3], Haibo Chen[2], Min Chen[3], Wen Su[2], Kai Li[2], Na Lu[3,4], Lu Yu[3], Defa Chu[5] and Pu-Yeh Wu[6]*

[1]Department of Neurobiology and Neurology, Xuanwu Hospital, Capital Medical University, Beijing, China, [2]Department of Neurology, Beijing Hospital, National Center of Gerontology, Institute of Geriatric Medicine, Chinese Academy of Medical Sciences, Beijing, China, [3]Department of Radiology, Beijing Hospital, National Center of Gerontology, Institute of Geriatric Medicine, Chinese Academy of Medical Sciences, Beijing, China, [4]Graduate School of Peking Union Medical College, Beijing, China, [5]Department of Statistics, Beijing Hospital, National Center of Gerontology, Institute of Geriatric Medicine, Chinese Academy of Medical Sciences, Beijing, China, [6]GE Healthcare, MR Research China, Beijing, China

OPEN ACCESS

Edited by:
Shaomin Li,
Brigham and Women's Hospital and Harvard Medical School, United States

Reviewed by:
Jifeng Guo,
Central South University, China
Junli Zhen,
Second Hospital of Hebei Medical University, China

***Correspondence:**
Piu Chan
pbchan@hotmail.com

Received: *14 June 2020*
Accepted: *02 September 2020*
Published: *30 September 2020*

Citation:
Li S, Chan P, Li C, Chen H, Chen M, Su W, Li K, Lu N, Yu L, Chu D and Wu P-Y (2020) Changes of Amide Proton Transfer Imaging in Multiple System Atrophy Parkinsonism Type. Front. Aging Neurosci. 12:572421. doi: 10.3389/fnagi.2020.572421

Multiple system atrophy (MSA), an atypical parkinsonism of alpha-synucleinopathies, has no specific biomarker of diagnosis. According to different combinations of symptoms, MSA can be classified as parkinsonism-type MSA (MSA-P) and cerebellar-type MSA (MSA-C; Watanabe et al., 2018). Amide proton transfer (APT) imaging is by far the most studied chemical exchange saturation transfer imaging for its sensitivity to mobile protons and peptides in tissues. We hypothesize that APT imaging may be a feasible biomarker of MSA-P. Twenty MSA-P patients and 20 age-matched normal controls were enrolled in this study and underwent MR exams on a 3.0-T MR scanner. Magnetization transfer spectra at 3.5 ppm were acquired at two transverse slices of the head, including the midbrain and the basal ganglia. Mann–Whitney *U* test was used to compare the asymmetrical magnetization transfer ratio (MTR_{asym}) difference between MSA-P patients and normal controls. The APT MTR_{asym} values of MSA patients in the red nucleus (RN) (SN; $P = 0.000$), substantia nigra ($P = 0.000$), thalamus ($P = 0.000$), and putamen ($P = 0.013$) were significantly higher than those in normal controls. There was a negative correlation between APT MTR_{asym} and the score of part III of the Unified Parkinson Disease Rating Scale ($R = -0.338$, $P = 0.044$) in the putamen, while there was a positive correlation between the APT MTR_{asym} and the rate of motor symptom progression ($R = 0.406$, $P = 0.017$) in the RN. These findings suggest that APT MTR_{asym} changes are found and may be of value in the diagnosis of MSA-P.

Keywords: APT imaging, magnetic resonance imaging, biomarker, multiple system atrophy, parkinsonism

INTRODUCTION

Multiple system atrophy (MSA) is an adult-onset, health-threatening, sporadic, and progressive neurodegenerative disorder (Watanabe et al., 2002, 2018; Fanciulli and Wenning, 2015). Clinical manifestations caused by neuronal degenerations in striatonigral, olivopontocerebellar, and autonomic nervous systems include progressive dopamine-resistant parkinsonism, cerebellar ataxia, autonomic failure, and pyramidal signs (Fanciulli and Wenning, 2015; Watanabe et al., 2018). According to different combinations of symptoms, MSA can be classified as parkinsonism-type MSA (MSA-P) and cerebellar-type MSA (MSA-C; Watanabe et al., 2018) and diagnosed as probable and possible MSA. The time from onset of symptoms to diagnosis of probable MSA ranges from 1 to 10 years, with a median time of 2 years (Watanabe et al., 2002). Only 57.4% of MSA patients have both motor and autonomic manifestations within 2 years of disease onset, indicating that more than 40% of patients had symptoms involving only one system and could hardly be diagnosed in the first 2 years of the disease (Watanabe et al., 2002). Therefore, there is a great clinical need for biomarkers that can help early diagnosis of MSA. Although magnetic resonance imaging (MRI) is widely used for helping the diagnosis and differential diagnosis of MSA, conventional MRI has a limited role, particularly at the early stage (Watanabe et al., 2018). Previous studies have reported normal findings in conventional MRI for approximately 60% of MSA-P patients within 2 years of disease onset (Watanabe et al., 2002), and hence, other MRI methods that enable better early diagnosis of MSA are desirable.

Chemical exchange saturation transfer (CEST) imaging is a new method that has emerged in recent years (Henkelman et al., 2001; Vinogradov et al., 2013; Zhou et al., 2019), which enables the detection of endogenous or exogenous metabolites by observing the transferred saturation effects between the metabolite and water (Kogan et al., 2013). Amide proton transfer (APT) imaging, also known as amide CEST, is by far the most studied branch of CEST imaging because of its feasibility and robustness at 3.0 T and its sensitivity to mobile protons and peptides in tissues (Zhou et al., 2003). Other branches of CEST, such as amine CEST or hydroxyl CEST, are more feasible under higher magnetic field strengths. Previous studies have shown that APT imaging at 3.0 T has potential clinical value in diagnosis of brain tumors (Zhou et al., 2011), breast tumors (Dula et al., 2013), cerebral ischemia disease (Tietze et al., 2014; Harston et al., 2015; Jones et al., 2018), and Parkinson's disease (PD; Li et al., 2014, 2015, 2017).

Previous studies have found neuronal losses and accumulation of abnormal cytoplasmic proteins (such as α-synuclein), gliosis, and microgliosis in the striatonigral pathway, including the red nucleus (RN), substantia nigra (SN), globus pallidus, thalamus, caudate, and putamen, in MSA-P patients (Ahmed et al., 2012). These pathological changes may be the basis for the possibility of APT imaging in MSA-P patients. We hypothesize that these pathological changes may lead to the modified APT imaging effects, and hence, APT imaging may be a feasible biomarker of MSA-P. The purpose of this study is to evaluate the feasibility of APT imaging in the diagnosis of MSA-P. We selected MSA-P and not MSA-C at the same time in this study for the following reasons. First, as a common type of MSA, it is difficult to differentiate PD, dementia with Lewy bodies, and progressive supranuclear palsy from MSA-P in the early stage of the disease. Thus, there is a great clinical demand for early detection and differential diagnosis of MSA-P. Second, if MSA-C and MSA-P are selected at the same time, more slices (slices covered RN and SN, basal ganglia, pons, cerebellum, and inferior olive) of the APT image will be performed with longer scan time, which will make the patients intolerant.

We conducted subgroup studies to evaluate the feasibility of APT imaging in diagnosis of MSA-P in different subgroups. There were two parts in subgroup studies. Patients were classified into probable and possible MSA-P subgroups according to the second consensus statement on the diagnosis of MSA (Gilman et al., 2008) in part 1, and patients were classified into conventional MRI positive MSA-P subgroup and conventional MRI negative MSA-P subgroup according to the visual assessment to conventional MRI in part 2. We compared the difference in APT imaging between each subgroup of MSA-P and normal controls (NCs) and evaluated the feasibility of APT imaging in subgroups of MSA-P. Furthermore, the correlations were evaluated between APT imaging signal intensity and the course of disease, age, the score of part III of the Unified Parkinson Disease Rating Scale (UPDRS III), rate of motor symptom progression, and Hoehn–Yahr scale (H&Y) score.

MATERIALS AND METHODS

Subjects and Clinical Assessments

Twenty consecutive MSA-P patients (10 males and 10 females, mean age 66.5 ± 6.8 years) and 20 NCs (eight males and 12 females; mean age 67.9 ± 9.3 years) were recruited for this study. MSA-P patients were diagnosed according to the second consensus statement on the diagnosis of MSA (Gilman et al., 2008) by two experienced movement disorder specialists (19 and 24 years of experience).

The inclusion criteria for MSA-P patients were as follows: (Watanabe et al., 2018) probable MSA-P patients should have a sporadic, progressive adult-onset disorder including rigorously defined autonomic failure and poorly levodopa-responsive parkinsonism; and (Fanciulli and Wenning, 2015) possible MSA-P patients should have a sporadic, progressive adult-onset disease parkinsonism and at least one feature suggesting autonomic dysfunction plus another feature such as a clinical or neuroimaging abnormality (Gilman et al., 2008). Age-matched controls without neurological disorders were also enrolled. The exclusion criteria for all participants were as follows: (Watanabe et al., 2018) a history of exposure to antidopaminergic drugs; (Fanciulli and Wenning, 2015) head trauma; (Watanabe et al., 2002) stroke; (Vinogradov et al., 2013) central nervous system infection; (Henkelman et al., 2001) other neurologic or psychiatric diseases; and (Zhou et al., 2019) a structural lesion or hydrocephalus on brain MR images.

General information, medical history, and treatment information were collected and recorded *via* face-to-face consultation at the time of enrollment. The UPDRS III and H&Y scale were used to evaluate the motor impairment of MSA-P patients. The rate of motor symptom progression is defined as the UPDRS III score divided by the disease duration.

The protocol was approved by the ethics committee of Beijing Hospital (registration number: 2018BJYYEC-050–01). Each subject in this study signed informed consent forms prior to participation.

MRI Acquisition

All participants underwent MRI examinations on a 3.0-T whole-body MRI system (SIGNA Pioneer, GE Healthcare, Milwaukee, WI, USA) equipped with a 16-channel head and neck coil. Conventional MRI, including axial T1-weighted imaging (T1WI), axial T2-weighted imaging (T2WI) with fat suppression, and diffusion-weighted imaging (DWI), was acquired to evaluate changes within and/or around the putamen and the brain stem and to exclude subjects with structural abnormality.

For each participant, the APT image was prescribed and performed on two slices with reference to T2WI images; one slice covered the RN and SN, and the other slice covered the basal ganglia region. For saturation pulse in APT, a train of four Fermi-filtered pulses with a duration of 400 ms and amplitude of 2 μT was used. For acquisition of APT, 2D echo-planar imaging (EPI) with the following parameters was used: TR/TE = 2, 500/26.2 ms, flip angle = 20°, field of view = 240 × 240 mm, matrix = 128 × 128, and slice thickness = 5 mm, and NEX = 2. The frequency offsets acquired were 5,000, 1,996, 768, 640, 576, 512, 480, 448, 416, 384, 320, 256, 192, 128, 96, 64, 32, 0, −32, −64, −96, −128, −192, −256, −320, −384, −416, −448, −480, −512, −576, −640, and −768 Hz.

Data Processing

Hyperintense putaminal rim (HPR), putaminal atrophy, and hot cross bun were visually assessed by two radiologists (NL and LY, 2 and 6 years of experience, respectively) and two neurologists (SL and KL, 20 and 12 years of experience, respectively). The T2-hyperintense rim, located predominantly at the dorsolateral margin of the putamen, was evaluated as HPR in our study.

Magnetization transfer ratio asymmetry (MTR_{asym}) was further performed on an AW4.6 GE workstation. The APT MTR_{asym} was calculated as MTR_{asym} (3.5 ppm) = Ssat (−3.5 ppm)/S0 − Ssat (+3.5 ppm)/S0, in which Ssat is the signal intensity with selective saturation, while S0 is not (Zhou et al., 2013). B0 inhomogeneity was corrected on a pixel-by-pixel basis. The data of APT MTR_{asym} were presented in percentage (%).

T2WI was used to evaluate the function of APT images in our study mainly because T2WI could show SN and RN better than T1WI. Two radiologists (NL and LY) analyzed the quantitative MTR_{asym} images and compared the difference between MSA-P patients and NCs. Six regions of interest (ROIs), including RN, SN, globus pallidus, thalamus, caudate, and putamen of both hemispheres, were manually drawn based on T2WI images. ROIs from one representative subject overlaid on top of his own T2WI images and APT MTR_{asym} maps are as shown in **Figures 1**, **2**.

Statistical Analysis

All statistical analyses were performed using SPSS 25.0 (IBM, Armonk, NY, USA). The average APT MTR_{asym} at 3.5 ppm and the standard deviation were measured and calculated for each

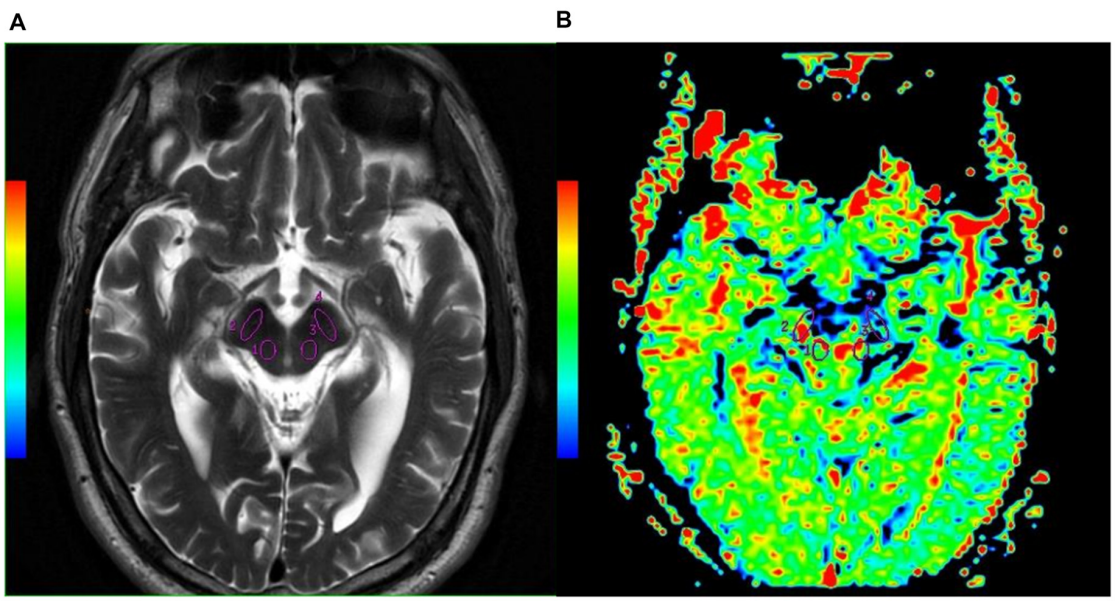


FIGURE 1 | Examples of the definition of the regions of interest (ROIs) in the midbrain for quantitative analysis. **(A)** Axial T2WI and **(B)** axial image of amide proton transfer (APT). Refer to the T2WI to delineate the red nucleus (RN; Watanabe et al., 2002, 2018) and substantia nigra (SN; Vinogradov et al., 2013; Fanciulli and Wenning, 2015).

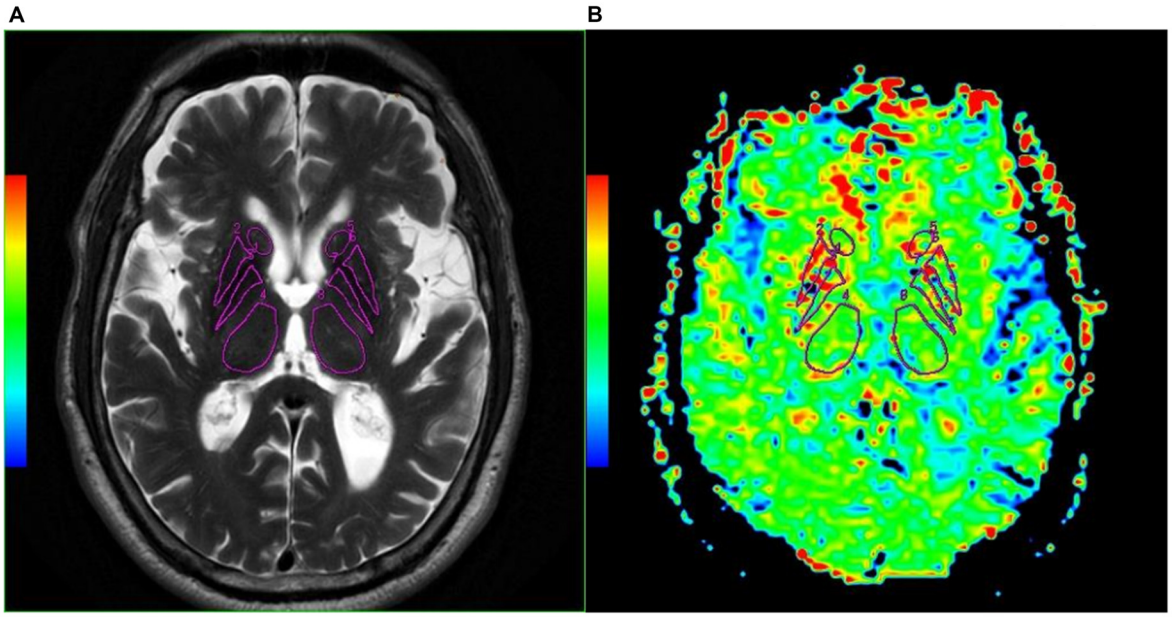


FIGURE 2 | Examples of the definition of the ROIs in the basal ganglia for quantitative analysis. **(A)** Axial T2WI and **(B)** axial image of APT. Refer to the T2WI to delineate the caudate (Henkelman et al., 2001; Watanabe et al., 2018), putamen (Fanciulli and Wenning, 2015; Zhou et al., 2019), globus pallidus (Watanabe et al., 2002; Kogan et al., 2013), and thalamus (Zhou et al., 2003; Vinogradov et al., 2013).

ROI. To compare the difference of APT MTR_{asym} (3.5 ppm) between MSA-P patients and NCs, a *t*-test was used if the data were normally distributed, and Mann–Whitney *U* test was used if the data were not normally distributed. A chi-square test was conducted to examine the clinical differences of categorical variables. Spearman rank correlation test was used to compare the correlation between APT MTR_{asym} and its related factors. The level of significance was set at $P < 0.05$.

RESULTS

Demographic and Clinical Features

All MSA-P subjects had autonomic nervous system impairment and parkinsonism. Twelve MSA-P patients (seven females and five males) were diagnosed as clinically probable MSA-P patients, and eight MSA-P patients (two females and six males) as clinically possible MSA-P. Three probable MSA-P subjects had minor cerebellar symptoms, autonomic nervous system impairment, and parkinsonism. Two patients in possible MSA-P group had cerebellar symptoms. There was no statistically significant difference in age ($P = 0.605$) and gender ($P = 0.525$) between MSA-P and NCs. No statistically significant difference in age and gender was observed between each diagnostic category subgroup of MSA-P and NCs. The detailed information is shown in **Table 1**.

Compared to possible MSA-P patients, the probable MSA-P patients showed higher average UPDRS III scores ($P = 0.001$). There was no statistically significant difference in disease duration ($P = 0.516$), H&Y scale ($P = 0.208$), and rate of motor symptom progression ($P = 0.735$) between probable and possible MSA-P patients. The detailed information is shown in **Table 2**.

Conventional MRI Features for MSA-P Patients and NCs

No morphological abnormity was found within and around the putamen and the pons in NCs using conventional MRI. Hot cross bun was not found in our MSA-P patients, and putaminal changes were found in seven MSA-P patients (HPR in one patient, putaminal atrophy in three patients, and possible putaminal atrophy in three patients). So common abnormalities within and around the putamen (HPR and putaminal atrophy) can be observed in 35% of the MSA-P patients (7/20) at 3.0-T conventional MRI. The incidence of putaminal atrophy is 30%.

There were seven conventional MRI positive MSA-P patients (three males and four females) and 13 conventional MRI negative MSA-P patients (seven males and six females) in this study. No statistically significant difference in age and gender was observed between each subgroup (conventional MRI positive MSA-P subgroup and conventional MRI negative MSA-P subgroup) of MSA-P and NCs. Detailed information is shown in **Table 1**.

Compared with conventional MRI negative MSA-P patients, conventional MRI positive MSA-P patients showed higher rate of motor symptom progression scores ($P = 0.047$). No statistically significant difference in disease duration ($P = 0.154$), UPDRS scores ($P = 0.397$), and H&Y scale ($P = 0.653$) was observed between conventional MRI negative MSA-P patients and conventional MRI positive MSA-P patients. Detailed information is shown in **Table 2**.

TABLE 1 | Demographic information of the subjects.

	NCs	MSA-P	MSA-P probable	MSA-P possible	MSA-P MRI+	MSA-P MRI−	z/χ^2 NCs vs.	*P*-value
Sample size	20	20	12	8	7	13		-
Age (years)[a] mean ± SD	67.9 ± 9.3	66.5 ± 6.8	67.4 ± 7.4	68.5 ± 3.62	66.1 ± 4.1	68.7 ± 7.3	MSA-P, 0.522	0.605
							MSA-P probable, −0.234	0.815
							MSA-P possible, −0.055	0.956
							MSA-P MRI+, −0.166	0.868
							MSA-P MRI−, −0.390	0.679
Gender[b] (female/male)	12/8	10/10	7/5	2/6	4/3	6/7	MSA-P, 0.404	0.525
							MSA-P probable, 0.009	0.926
							MSA-P possible, 2.800	0.094
							MSA-P MRI+, −0.018	0.895
							MSA-P MRI−, −0.179	0.493

NCs, normal controls; MSA-P, multiple system atrophy—parkinsonism type; MSA-P MRI+, multiple system atrophy—parkinsonism type conventional MRI positive; MSA-P MRI−, multiple system atrophy—parkinsonism type conventional MRI negative; [a]Independent t-test; [b]Chi-square tests.

TABLE 2 | Basic clinical information of the MSA-P patients.

	MSA-P	MSA-P probable	MSA-P possible	*z*	*P*-value	MSA-P MRI+	MSA-P MRI−	*z*	*P*-value
Sample size	20	12	8	-	-	7	13	-	-
Disease duration (years), mean ± SD	2.5 ± 1.7	2.4 ± 1.8	2.5 ± 0.8	0.649	0.516	1.9 ± 1.2	2.9 ± 1.5	−1.427	0.154
Hoehn and Yahr staging, mean ± SD	2.9 ± 0.8	3.1 ± 2.6	2.6 ± 0.5	1.258	0.208	3.0 ± 0.8	2.8 ± 0.8	−0.449	0.653
UPDRS III, mean ± SD	31.5 ± 16.2	36.8 ± 17.1	23.9 ± 9.3	−3.390	0.001	36.1 ± 14.1	30.3 ± 17.3	−0.847	0.397
RMSP, mean ± SD	18.4 ± 16.0	18.9 ± 16.1	18.1 ± 12.0	0.338	0.735	26.9 ± 16.9	13.8 ± 10.7	−1.987	0.047

MSA-P, multiple system atrophy—parkinsonism type; UPDRS III, the third part of the Unified Parkinson Disease Rating Scale; RMSP, rate of motor symptom progression. Mann–Whitney U test was used for the data listed in this table.

Changes of APT Imaging in MSA-P Patients

MSA-P vs. NCs

Compared with NCs, the MSA-P patients showed higher APT MTR_{asym} values in the regions of the RN (P = 0.000), SN (P = 0.000), thalamus (P = 0.000), and putamen (P = 0.001). In the regions of the caudate, the APT MTR_{asym} was higher in MSA-P patients than in NCs but did not reach statistical significance (P = 0.061). There was no significant difference in the APT MTR_{asym} values of the globus pallidus (P = 0.692) between MSA-P patients and NCs.

Figure 3 shows the representative APT MTR_{asym} images of a probable MSA-P patient (female, 73 years old, H&Y scale of 3, disease duration of 3 years) and a NC (male, 60 years old). **Table 3** and **Figure 4** show the comparison of APT MTR_{asym} in the six ROIs between the MSA-P group and NCs.

Probable MSA-P and Possible MSA-P vs. NCs

Compared with NCs, probable MSA-P patients showed higher APT MTR_{asym} values in the RN (P = 0.000), SN (P = 0.000), thalamus (P = 0.001), caudate (P = 0.023), and putamen (P = 0.001). No statistically significant difference was found between probable MSA-P patients and NCs for the APT MTR_{asym} values in the globus pallidus (P = 0.836). Compared with NCs, possible MSA-P patients showed higher APT MTR_{asym} values in the RN (P = 0.006), SN (P = 0.000), and thalamus (P = 0.005). No statistically significant difference was found between possible MSA-P patients and NCs in the putamen (P = 0.050), globus pallidus (P = 0.650), and caudate (P = 0.164).

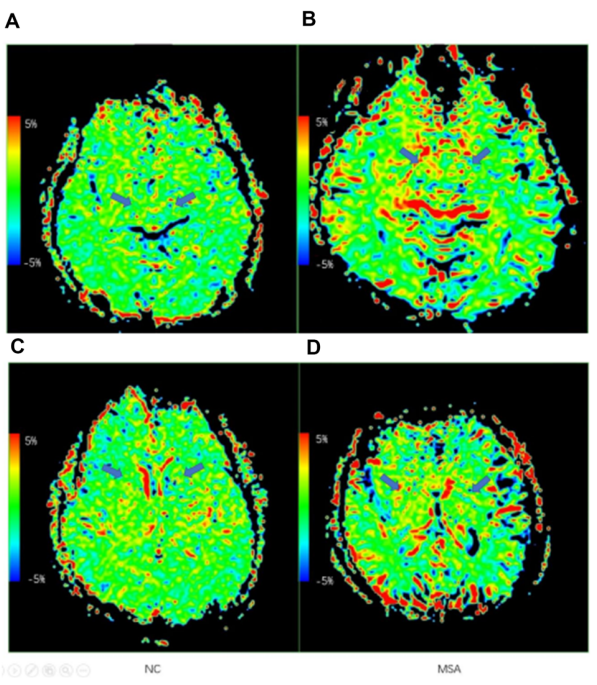


FIGURE 3 | Examples of the APT maps of a normal control and an multiple system atrophy (MSA) patient. **(A,C)** Axial images of APT imaging in a normal control. **(B,D)** Axial images of APT imaging in an MSA patient. The arrows show the difference of the RN, SN, and basal ganglia region.

TABLE 3 | Changes in APT MTR_{asym} among MSA-P and controls.

APT MTR_{asym} (mean ± SE)	NCs (n = 20)	MSA-P (n = 20)	z	P-value
RN	0.42 ± 0.08	1.4 ± 0.15	−4.838	0.000
SN	0.34 ± 0.14	1.40 ± 0.15	−5.682	0.000
Caud	0.67 ± 0.11	1.12 ± 0.16	−1.874	0.061
Thal	0.59 ± 0.11	1.00 ± 0.10	−4.291	0.000
GP	1.02 ± 0.09	0.85 ± 0.08	−0.396	0.692
Put	0.70 ± 0.08	1.08 ± 0.10	−3.278	0.001

MSA-P, multiple system atrophy—parkinsonism type; RN, red nucleus; SN, substantia nigra; Caud, caudate; Thal, thalamus; GP, globus pallidus; Put, putamen. Mann–Whitney U test was used for the data listed in this table.

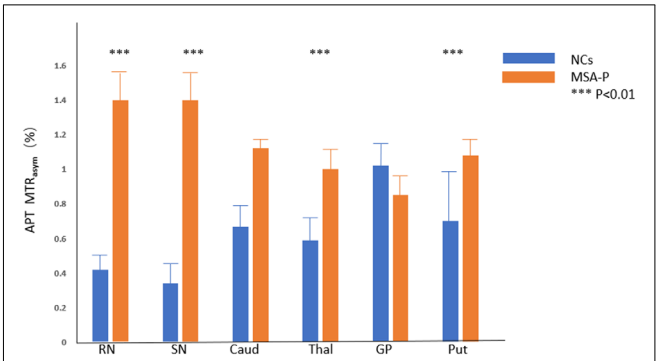


FIGURE 4 | Comparison of average MTR_{asym} (3.5 ppm, %) between MSA patients and NCs. RN = red nucleus, SN = substantia nigra, Caud = caudate, Thal = thalamus, GP = globus pallidus, Put = putamen. ***$p < 0.01$.

Compared with possible MSA-P patients, probable MSA-P patients showed higher APT MTR_{asym} values in the RN (P = 0.001), caudate (P = 0.013), and putamen (P = 0.010). No statistically significant difference was found between probable MSA-P and possible MSA-P patients in the SN (P = 0.516), thalamus (P = 0.868), and globus pallidus (P = 0.340). Detailed information is shown in **Table 4**.

Conventional MRI Positive MSA-P Patients and Conventional MRI Negative MSA-P Patients vs. NCs

Compared with NCs, conventional MRI positive MSA-P patients showed higher APT MTR_{asym} values in the RN (P = 0.001), SN (P = 0.000), thalamus (P = 0.012), and caudate (P = 0.045). No statistically significant difference was found between conventional MRI positive MSA-P patients and NCs in the putamen (P = 0.228) and globus pallidus (P = 0.515). Compared with NCs, conventional MRI negative MSA-P patients showed higher APT MTR_{asym} values in the RN (P = 0.000), SN (P = 0.000), thalamus (P = 0.000), and putamen (P = 0.000). No statistically significant difference was found between conventional MRI negative MSA-P patients and NCs in the caudate (P = 0.065) and globus pallidus (P = 0.325). No statistically significant difference was found between conventional MRI positive MSA-P patients and conventional MRI negative MSA-P patients in the above-mentioned regions. Detailed information is shown in **Table 5**.

Summary for Changes of APT Imaging in MSA-P Patients

To summarize the main results (Watanabe et al., 2018), the APT MTR_{asym} values in the RN, SN, and thalamus were capable of differentiating MSA-P from NCs regardless of diagnostic categories and conventional MRI results; (Fanciulli and Wenning, 2015) the APT MTR_{asym} values in the putamen were also capable of differentiating MSA-P from NCs, especially for probable MSA-P patients; (Watanabe et al., 2002) the APT MTR_{asym} values were increased in the RN, SN, thalamus, and putamen in conventional MRI negative MSA-P patients, which indicates that APT imaging may be more sensitive than conventional MRI.

Correlation Analysis

The APT MTR_{asym} at the putamen was negatively correlated with the UPDRS III score (P = 0.044), and the APT MTR_{asym} at the RN was positively correlated with rate of motor symptom progression (P = 0.017). There was no correlation between the course of disease, age, H&Y, and APT MTR_{asym}. Detailed information is shown in **Table 6**.

DISCUSSION

This preliminary study demonstrated that the APT MTR_{asym} values in the RN, SN, thalamus, and putamen were higher in MSA-P patients as compared to those in healthy controls. A potential link with the pathophysiological mechanism of MSA-P was supported by the negative correlation between the APT MTR_{asym} at the putamen with the UPDRS III score.

MSA is an orphan disease (orphan number, ORPHAN102[1]; Fanciulli and Wenning, 2015), and the diagnosis of MSA at an early stage is challenging. A recent study reported that the clinicopathological consistency of MSA was only 62% (Koga et al., 2015). Multimodal MRI technology is often applied in the diagnosis of MSA patients (Pradhan and Tandon, 2017; Krismer et al., 2019). Several MRI findings have been reported in MSA-P patients, including the presence of a bilateral T2-hyperintense rim bordering the dorsolateral margins of the putamen (the "HPR sign"), T2-putaminal hypointensity (T2H), and atrophy of the putamen, middle cerebellar peduncles (MCP), cerebellum, or pons (Massey et al., 2012). In our study, the incidence of these morphological abnormalities within and around the putamen was only 35% in MSA-P patients at 3.0-T conventional MRI, and the incidence of putaminal atrophy was 30%. The incidence of these abnormalities was relatively low in MSA-P patients at conventional MRI, probably because our patients had a shorter duration of illness and relatively mild symptoms. Previous studies found that putaminal atrophy often occurs in advanced MSA-P patients, with a high specificity (92.3%) in distinguishing MSA-P from PD but a low sensitivity (44.4%; Feng et al., 2015), and our results were consistent with theirs. HPR incidence of our study was only 5%. The low incidence of HPR indicated that HPR was not a sensitive biomarker for early diagnosis of MSA-P. T2 "putaminal rim sign" and putaminal hypointensity were

[1]www.orpha.net

TABLE 4 | Changes in APT MTR_{asym} among probable MSA-P, possible MSA-P, and controls.

APT MTR_{asym} (mean ± SD)	NCs (n = 20)	MSA-P probable (n = 12)	MSA-P possible (n = 8)	z	P-value
RN	0.42 ± 1.03	1.56 ± 0.47	1.13 ± 1.55	NCs vs. MSA-P probable, −4.693	0.000
				NCs vs. MSA-P possible, −2.759	0.006
				MSA-P probable vs. possible, −3.390	0.001
SN	0.34 ± 1.02	1.31 ± 0.96	1.55 ± 0.50	NCs vs. MSA-P probable, −4.650	0.000
				NCs vs. MSA-P possible, −4.527	0.000
				MSA-P probable vs. possible, −0.649	0.516
Caud	0.67 ± 1.04	1.19 ± 0.82	1.08 ± 0.39	NCs vs. MSA-P probable, −2.274	0.023
				NCs vs. MSA-P possible, −1.392	0.164
				MSA-P probable vs. possible, −2.482	0.013
Thal	0.59 ± 0.63	0.85 ± 0.85	1.04 ± 0.33	NCs vs. MSA-P probable, −3.426	0.001
				NCs vs. MSA-P possible, −2.794	0.005
				MSA-P probable vs. possible, −0.167	0.868
GP	1.02 ± 0.38	0.85 ± 0.66	0.85 ± 0.33	NCs vs. MSA-P probable, −0.208	0.836
				NCs vs. MSA-P possible, −0.454	0.650
				MSA-P probable vs. possible, −0.953	0.340
Put	0.70 ± 0.64	1.10 ± 0.56	1.04 ± 0.32	NCs vs. MSA-P probable, −3.187	0.001
				NCs vs. MSA-P possible, −1.960	0.050
				MSA-P probable vs. possible, −2.573	0.010

MSA-P, multiple system atrophy—parkinsonism type; RN, red nucleus; SN, substantia nigra; Caud, caudate; Thal, thalamus; GP, globus pallidus; Put, putamen. Mann–Whitney U test was used for the data listed in this table.

compared in one study using a 3.0-T MRI scanner; the result also indicated that HPR could not provide adequate diagnostic assistance in MSA-P patients (Lee et al., 2005). So far, the overall sensitivity of conventional MRI in diagnosing MSA-P especially at an early stage remains low.

In this study, the feasibility of using APT imaging in the diagnosis of MSA-P was evaluated. APT imaging has been reported to detect variations of proteins in diseases including brain tumors and PD. The accumulation of abnormal proteins in the central nervous system in a number of the neurodegenerative diseases has been reported in several pathological studies (Ito et al., 2009; Peden and Ironside, 2012; Fanciulli and Wenning, 2015). In MSA, oligodendroglia cytoplasmic inclusions (also known as Papp–Lantos bodies) are pathological hallmarks. Accumulated misfolded α-synuclein is a major component of the Papp–Lantos bodies (Spillantini et al., 1998; Ito et al., 2009; Peden and Ironside, 2012). These pathological characteristics form the basis of novel potential biomarker for MSA-P.

Our results showed that the APT MTR_{asym} values in the RN, SN, thalamus, and putamen were higher in MSA-P

TABLE 5 | Changes in APT MTR_{asym} among MSA-P MRI+, MSA-P MRI−, and controls.

APT MTR_{asym} (mean ± SD)	NCs (n = 20)	MSA-P MRI+ (n = 7)	MSA-P MRI− (n = 13)	Z	P-value
RN	0.42 ± 1.03	1.46 ± 0.63	1.40 ± 0.29	NCs vs. MSA MRI+, −3.247	0.001
				NCs vs. MSA MRI−, −4.363	0.000
				MSA MRI+ vs. MSA MRI−, −1.064	0.287
SN	0.34 ± 1.02	1.59 ± 0.53	1.30 ± 0.93	NCs vs. MSA MRI+, −4.398	0.000
				NCs vs. MSA MRI−, −4.747	0.000
				MSA MRI+ vs. MSA MRI−, −0.330	0.741
Caud	0.67 ± 1.04	1.25 ± 0.23	1.08 ± 0.85	NCs vs. MSA MRI+, −2.004	0.045
				NCs vs. MSA MRI−, −1.844	0.065
				MSA MRI+ vs. MSA MRI−, −0.348	0.728
Thal	0.59 ± 0.63	0.84 ± 0.83	0.98 ± 0.58	NCs vs. MSA MRI+, −2.508	0.012
				NCs vs. MSA MRI−, −3.627	0.000
				MSA MRI+ vs. MSA MRI−, −0.121	0.904
GP	1.02 ± 0.38	1.02 ± 0.27	0.75 ± 0.65	NCs vs. MSA MRI+, −0.651	0.515
				NCs vs. MSA MRI−, −0.985	0.325
				MSA MRI+ vs. MSA MRI−, −1.211	0.226
Put	0.70 ± 0.64	0.99 ± 0.31	1.13 ± 0.56	NCs vs. MSA MRI+, −1.204	0.228
				NCs vs. MSA MRI−, −3.548	0.000
				MSA MRI+ vs. MSA MRI−, −0.938	0.348

MSA-P MRI+, multiple system atrophy—parkinsonism type conventional MRI positive; MSA-P MRI−, multiple system atrophy—parkinsonism type conventional MRI negative; RN, red nucleus; SN, substantia nigra; Caud, caudate; Thal, thalamus; GP, globus pallidus; Put, putamen. Mann–Whitney U test was used for the data listed in this table.

TABLE 6 | Correlation analysis of APT-MTR_{asym} in MSA-P patients.

	Age		Disease duration		H&Y		UPDRS III		Rate of progress	
	R	*P*	*R*	*P*	*R*	*P*	*R*	*P*	*R*	*P*
RN	−0.025	0.890	−0.135	0.446	0.388	0.124	0.154	0.386	0.406	0.017*
SN	−0.015	0.933	−0.281	0.101	0.201	0.440	0.058	0.746	0.163	0.356
Caud	−0.290	0.096	−0.012	0.942	0.332	0.164	0.044	0.797	0.009	0.960
Thal	−0.033	0.846	−0.071	0.670	0.020	0.934	−0.106	0.537	−0.014	0.934
GP	−0.248	0.133	−0.151	0.537	−0.298	0.215	−0.012	0.962	0.061	0.723
Put	0.320	0.065	−0.214	0.196	−0.345	0.148	−0.338	0.044*	−0.007	0.967

*RN, red nucleus; SN, substantia nigra; Caud, caudate; Thal, thalamus; GP, globus pallidus; Put, putamen. Spearman rank correlation test was used for the data listed in this table. *$P < 0.05$.*

patients than in NCs. These observations may be attributed to the pathophysiological mechanism of MSA-P. In MSA-P, the primary pathological impairment regions are the nigrostriatal pathway, which may lead to abnormalities in the SN, RN, thalamus, and putamen (Wenning et al., 1997; Ahmed et al., 2012). The pathological characteristics were consistent with the results of this study that the APT MTR_{asym} difference was mainly observed in the RN, SN, thalamus, and putamen as the primary foci in MSA-P patients.

The main pathological abnormalities of MSA-P are neuronal loss and/or gliosis in the putamen and SN. One study found that MSA patients had more microglia in the brain than healthy controls (Salvesen et al., 2015). There were extensive microgliosis in the RN, putamen, globus pallidus, and subthalamic nucleus. The pathological hallmark of MSA is glial cytoplasmic inclusions (GCIs), and the key neuropathological manifestation of MSA is a broad spectrum of neuronal loss, gliosis, and myelin pallor. Neuronal loss may lead to a decrease of the APT MTR_{asym} due to a reduction of the water-exchanging chemicals, while gliosis, microgliosis, and GCIs may have an opposite effect. For MSA patients at the early stage of the disease, neuronal loss is relatively mild and the pathological change is often overlooked without special staining for gliosis (Wenning et al., 1997). Our findings of higher APT MTR_{asym} in MSA-P patients than in NCs suggested that the accumulation of abnormal cytoplasmic protein, gliosis, and microgliosis is more severe than neuronal loss on account of most of the MSA-P patients in our group. These findings support that APT imaging may be a potential biomarker in the diagnosis of MSA-P.

The results showed that the APT MTR_{asym} values in the globus pallidus had no statistically significant difference between MSA-P patients and NCs. This also may be attributed to the pathophysiological mechanism of MSA-P. Compared with the SN and putamen, the pathological changes of the globus pallidus were relatively mild (Wenning et al., 1997). According to the neuropathological grading of striatonigral degeneration (SND/MSA-P), the neuropathological changes (atrophy, neuronal loss, gliosis, and GCIs) in the globus pallidus were relatively mild, especially in grades I and II (Jellinger et al., 2005). For MSA-P patients at the early stage of the disease in our study, the accumulation of abnormal cytoplasmic protein, gliosis, and microgliosis may be equivalent to neuronal loss in the globus pallidus, the APT MTR_{asym} values were relatively normal in the globus pallidus.

Our results of subgroup analysis showed that the APT MTR_{asym} values in the RN, SN, and thalamus were capable of differentiating MSA-P from NCs regardless of diagnostic categories and conventional MRI results. The results indicate that the RN, SN, and thalamus may be the main foci of APT imaging in MSA diagnosis. The APT MTR_{asym} values in the putamen were also capable of differentiating probable MSA-P and possible MSA-P from NCs.

The APT MTR_{asym} values in the putamen were sensitive enough to distinguish conventional MRI negative MSA-P from NCs but not sensitive enough to distinguish conventional MRI positive MSA-P from NCs. HPR and putaminal atrophy were the main MRI features in our conventional MRI positive MSA-P patients. Posterior putaminal atrophy is related with neuronal loss and gliosis in the posterior putamen, and HPR is related to degeneration in the external capsule and/or lateral margin of the putamen (Matsusue et al., 2008). Compared with conventional MRI negative MSA-P patients, the conventional MRI positive patients had more severe neuronal loss, and loss of neurons led to a decrease in APT MTR_{asym} values. So compared with conventional MRI negative MSA-P patients, the conventional MRI positive MSA-P patients had lower APT MTR_{asym}. As a result, APT MTR_{asym} values in the putamen were not sensitive enough to distinguish conventional MRI positive MSA-P from NCs. This may dynamically reflect the course of the disease. The APT MTR_{asym} values were increased in the RN, SN, thalamus, and putamen in conventional MRI negative MSA-P patients, which indicates that APT imaging may be more sensitive than conventional MRI to some extent.

We also did correlation analysis. The correlation coefficient was not very high, but it was still statistically significant. Correlation analysis found that there was a negative correlation between the APT MTR_{asym} of the putamen and the score of UPDRS III. As mentioned above, the decrease of APT MTR_{asym} was related to the loss of neurons. The result indicated that neuronal loss in the putamen may be closely related to the motor impairment in MSA-P patients. Wenning et al. also found that akinesia and rigidity were significantly correlated with the cell loss in the putamen, which was in line with our findings (Wenning et al., 1997). Our findings support that APT imaging may be a potential biomarker to evaluate motor function and the pathophysiological mechanism of MSA-P.

Correlation analysis also found that the APT MTR_{asym} at the RN was positively correlated with the rate of motor

symptom progression. Previous work had reported that there were extensive microgliosis in the RN, putamen, and globus pallidus with neuronal loss in the putamen and globus pallidus (Salvesen et al., 2015). So compared with the putamen and globus pallidum, the RN may be a region that reveals microgliosis. The increase of APT MTR_{asym} in the RN may reflect the degree of microgliosis in the brain, and this microglia-dependent inflammatory processes may be related to the rate of motor symptom progression in MSA-P pathogenesis. Our findings support that APT imaging might also be applied to predict motor symptom progress of MSA-P. The above speculations, which were based on the results of this study and previous clinicopathological studies, need to be further investigated by prospective studies.

Several studies have found that APT MTR_{asym} in the SN of PD patients is lower than that in NCs (Tambasco et al., 2003; Anik et al., 2007; Morgen et al., 2011; Li et al., 2014). These results were related to the pathological abnormalities in the SN, which could lead to the decrease of water-exchanging chemicals. Based on these results, a number of studies have used CEST imaging as an imaging biomarker in diagnosis of PD (Li et al., 2014, 2015). A study found significantly increased APT MTR_{asym} in the globus pallidus, putamen, and caudate in PD patients compared with health controls (Fanciulli and Wenning, 2015). There was no significant difference in APT MTR_{asym} of the RN between PD and healthy controls (Anik et al., 2007; Morgen et al., 2011). Our results differ from previous studies on PD, suggesting that APT imaging may be helpful in differentiating MSA-P from PD. Further studies are required to evaluate the feasibility of APT imaging in differential diagnosis between MSA-P patients and PD in the future.

There were several limitations in this study. First, the sample size of the MSA-P group or the subgroup was limited. Longitudinal and large sample size studies are needed in the future. Second, only two slices of APT imaging were obtained in this study, which may lead to an inconsistency in ROI definition. Simultaneous comparison of the pons and cerebellum was insufficient; 3D volumetric acquisitions may allow better capturing of the brain regions of interest in the future. Third, ROI-based measurements were performed and compared in this study on a pathological basis. A pixel-by-pixel analysis based on the standard brain template may allow for the investigation of other brain regions. Finally, other auxiliary methods which can be applied as the diagnosis criteria of the MSA-P, for example, FDG-PET, were not compared.

In conclusion, our study identified that APT imaging may have potential value in diagnosis of MSA-P patients as well as in predicting the motor symptom progression of MSA-P. More investigations are needed for further evaluation of APT imaging in differential diagnosis of atypical parkinsonism.

DATA AVAILABILITY STATEMENT

The raw data supporting the conclusions of this article will be made available by the authors, without undue reservation.

ETHICS STATEMENT

The studies involving human participants were reviewed and approved by The ethics committee of Beijing Hospital. The patients/participants provided their written informed consent to participate in this study.

AUTHOR CONTRIBUTIONS

SL was involved in all study phases. CL and MC assisted with the study design, helped execute the MRI examination, and contributed to manuscript preparation. HC assisted with the study design, referred subjects, and contributed to manuscript preparation. WS and KL referred subjects. NL and LY helped execute MRI examination and analyzed the quantitative MTR_{asym}. DC assisted with statistical analysis and interpretation and provided manuscript critique. P-YW helped review the manuscript and provided manuscript critique. PC assisted with the study design, provided clinical oversight during study, and provided manuscript critique. All authors contributed to the article and approved the submitted version.

FUNDING

This study was supported by the Ministry of Science and Technology of the People's Republic of China (No. 2017ZX09304026) and the National Key R&D Program of China (No. 2018YFC1312001).

REFERENCES

Ahmed, Z., Asi, Y. T., Sailer, A., Lees, A. J., Houlden, H., Revesz, T., et al. (2012). The neuropathology, pathophysiology and genetics of multiple system atrophy. *Neuropathol. Appl. Neurobiol.* 38, 4–24. doi: 10.1111/j.1365-2990.2012.01268.x

Anik, Y., Iseri, P., Demirci, A., Komsuoglu, S., and Inan, N. (2007). Magnetization transfer ratio in early period of Parkinson disease. *Acad. Radiol.* 14, 189–192. doi: 10.1016/j.acra.2006.11.005

Dula, A. N., Arlinghaus, L. R., Dortch, R. D., Dewey, B. E., Whisenant, J. G., Ayers, G. D., et al. (2013). Amide proton transfer imaging of the breast at 3 T: establishing reproducibility and possible feasibility assessing chemotherapy response. *Magn. Reson. Med.* 70, 216–224. doi: 10.1002/mrm.24450

Fanciulli, A., and Wenning, G. K. (2015). Multiple-system atrophy. *N. Engl. J. Med.* 372, 249–263. doi: 10.1056/NEJMra1311488

Feng, J.-Y., Huang, B., Yang, W.-Q., Zhang, Y.-H., Wang, L.-M., Wang, L.-J., et al. (2015). The putaminal abnormalities on 3.0T magnetic resonance imaging: can they separate parkinsonism-predominant multiple system atrophy from Parkinson's disease? *Acta Radiol.* 56, 322–328. doi: 10.1177/0284185114524090

Gilman, S., Wenning, G. K., Low, P. A., Brooks, D. J., Mathias, C. J., Trojanowski, J. Q., et al. (2008). Second consensus statement on the diagnosis of multiple system atrophy. *Neurology* 71, 670–676. doi: 10.1212/01.wnl.0000324625.00404.15

Harston, G. W., Tee, Y. K., Blockley, N., Okell, T. W., Thandeswaran, S., Shaya, G., et al. (2015). Identifying the ischaemic penumbra using pH-weighted magnetic resonance imaging. *Brain* 138, 36–42. doi: 10.1093/brain/awu374

Henkelman, R. M., Stanisz, G. J., and Graham, S. J. (2001). Magnetization transfer in MRI: a review. *NMR Biomed.* 14, 57–64. doi: 10.1002/nbm.683

Ito, S., Shirai, W., and Hattori, T. (2009). Putaminal hyperintensity on T1-weighted MR imaging in patients with the Parkinson variant of multiple system atrophy. *Am. J. Neuroradiol.* 30, 689–692. doi: 10.3174/ajnr.a1443

Jellinger, K. A., Seppi, K., and Wenning, G. K. (2005). Grading of neuropathology in multiple system atrophy: proposal for a novel scale. *Mov. Disord.* 20, S29–S36. doi: 10.1002/mds.20537

Jones, K. M., Pollard, A. C., and Pagel, M. D. (2018). Clinical applications of chemical exchange saturation transfer (CEST) MRI. *J. Magn. Reson. Imaging.* 47, 11–27. doi: 10.1002/jmri.25838

Koga, S., Aoki, N., Uitti, R. J., van Gerpen, J. A., Cheshire, W. P., Josephs, K. A., et al. (2015). When, DLB, PD and PSP masquerade as MSA: an autopsy study of 134 patients. *Neurology* 85, 404–412. doi: 10.1212/WNL.0000000000001807

Kogan, F., Hariharan, H., and Reddy, R. (2013). Chemical exchange saturation transfer (CEST) imaging: description of technique and potential clinical applications. *Curr. Radiol. Rep.* 1, 102–114. doi: 10.1007/s40134-013-0010-3

Krismer, F., Seppi, K., Göbel, G., Steiger, R., Zucal, I., Boesch, S., et al. (2019). Morphometric MRI profiles of multiple system atrophy variants and implications for differential diagnosis. *Mov. Disord.* 34, 1041–1048. doi: 10.1002/mds.27669

Lee, W. H., Lee, C. C., Shyu, W. C., Chong, P. N., and Lin, S. Z. (2005). Hyperintense putaminal rim sign is not a hallmark of multiple system atrophy at 3T. *AJNR Am. J. Neuroradiol.* 26, 2238–2242.

Li, C., Chen, M., Zhao, X., Wang, R., Chen, H., Su, W., et al. (2017). Chemical exchange saturation transfer MRI signal loss of the substantia nigra as an imaging biomarker to evaluate the diagnosis and severity of Parkinson's disease. *Front. Neurosci.* 11:489. doi: 10.3389/fnins.2017.00489

Li, C., Peng, S., Wang, R., Chen, H., Su, W., Zhao, X., et al. (2014). Chemical exchange saturation transfer MR imaging of Parkinson's disease at 3 tesla. *Eur. Radiol.* 24, 2631–2639. doi: 10.1007/s00330-014-3241-7

Li, C., Wang, R., Chen, H., Su, W., Li, S., Zhao, X., et al. (2015). Chemical exchange saturation transfer MR imaging is superior to diffusion-tensor imaging in the diagnosis and severity evaluation of Parkinson's disease: a study on substantia nigra and striatum. *Front. Aging Neurosci.* 7:198. doi: 10.3389/fnagi.2015.00198

Massey, L. A., Micallef, C., Paviour, D. C., O'Sullivan, S. S., Ling, H., Williams, D. R., et al. (2012). Conventional magnetic resonance imaging in confirmed progressive supranuclear palsy and multiple system atrophy. *Mov. Disord.* 27, 1754–1762. doi: 10.1002/mds.24968

Matsusue, E., Fujii, S., Kanasaki, Y., Sugihara, S., Miyata, H., Ohama, E., et al. (2008). Putaminal lesion in multiple system atrophy: postmortem MR-pathological correlations. *Neuroradiology* 50, 559–567. doi: 10.1007/s00234-008-0381-y

Morgen, K., Sammer, G., Weber, L., Aslan, B., Müller, C., Bachmann, G. F., et al. (2011). Structural brain abnormalities in patients with Parkinson disease: a comparative voxel-based analysis using T1-weighted MR imaging and magnetization transfer imaging. *Am. J. Neuroradiol.* 32, 2080–2086. doi: 10.3174/ajnr.a2837

Peden, A. H., and Ironside, J. W. (2012). Molecular pathology in neurodegenerative diseases. *Curr. Drug Targets.* 13, 1548–1559. doi: 10.2174/138945012803530134

Pradhan, S., and Tandon, R. (2017). Relevance of non-specific MRI features in multiple system atrophy. *Clin. Neurol. Neurosurg.* 159, 29–33. doi: 10.1016/j.clineuro.2017.05.008

Salvesen, L., Ullerup, B. H., Sunay, F. B., Brudek, T., Løkkegaard, A., Agander, T. K., et al. (2015). Changes in total cell numbers of the basal ganglia in patients with multiple system atrophy—a stereological study. *Neurobiol. Dis.* 74, 104–113. doi: 10.1016/j.nbd.2014.11.008

Spillantini, M. G., Crowther, R. A., Jakes, R., Cairns, N. J., Lantos, P. L., and Goedert, M. (1998). Filamentous α-synuclein inclusions link multiple system atrophy with Parkinson's disease and dementia with Lewy bodies. *Neurosci. Lett.* 251, 205–208. doi: 10.1016/s0304-3940(98)00504-7

Tambasco, N., Pelliccioli, G. P., Chiarini, P., Montanari, G. E., Leone, F., Mancini, M. L., et al. (2003). Magnetization transfer changes of grey and white matter in Parkinson's disease. *Neuroradiology* 45, 224–230. doi: 10.1007/s00234-002-0925-5

Tietze, A., Blicher, J., Mikkelsen, I. K., Ostergaard, L., Strother, M. K., Smith, S. A., et al. (2014). Assessment of ischemic penumbra in patients with hyperacute stroke using amide proton transfer (APT) chemical exchange saturation transfer (CEST) MRI. *NMR Biomed.* 27, 163–174. doi: 10.1002/nbm.3048

Vinogradov, E., Sherry, A. D., and Lenkinski, R. E. (2013). CEST: from basic principles to applications, challenges and opportunities. *J. Magn. Reson.* 229, 155–172. doi: 10.1016/j.jmr.2012.11.024

Watanabe, H., Riku, Y., Hara, K., Kawabata, K., Nakamura, T., Ito, M., et al. (2018). Clinical and imaging features of multiple system atrophy: challenges for an early and clinically definitive diagnosis. *J. Mov. Disord.* 11, 107–120. doi: 10.14802/jmd.18020

Watanabe, H., Saito, Y., Terao, S., Ando, T., Kachi, T., Mukai, E., et al. (2002). Progression and prognosis in multiple system atrophy: an analysis of 230 Japanese patients. *Brain* 125, 1070–1083. doi: 10.1093/brain/awf117

Wenning, G. K., Tison, F., Ben Shlomo, Y., Daniel, S. E., and Quinn, N. P. (1997). Multiple system atrophy: a review of 203 pathologically proven cases. *Mov. Disord.* 12, 133–147. doi: 10.1002/mds.870120203

Zhou, J., Heo, H.-Y., Knutsson, L., van Zijl, P. C. M., and Jiang, S. (2019). APT-weighted MRI: techniques, current neuro applications and challenging issues. *J. Magn. Reson. Imaging* 50, 347–364. doi: 10.1002/jmri.26645

Zhou, J., Hong, X., Zhao, X., Gao, J.-H., and Yuan, J. (2013). APT-weighted and NOE-weighted image contrasts in glioma with different RF saturation powers based on magnetization transfer ratio asymmetry analyses. *Magn. Reson. Med.* 70, 320–327. doi: 10.1002/mrm.24784

Zhou, J., Payen, J.-F., Wilson, D. A., Traystman, R. J., and van Zijl, P. C. (2003). Using the amide proton signals of intracellular proteins and peptides to detect pH effects in MRI. *Nat. Med.* 9, 1085–1090. doi: 10.1038/nm907

Zhou, J., Tryggestad, E., Wen, Z., Lal, B., Zhou, T., Grossman, R., et al. (2011). Differentiation between glioma and radiation necrosis using molecular magnetic resonance imaging of endogenous proteins and peptides. *Nat. Med.* 17, 130–134. doi: 10.1038/nm.2268

Conflict of Interest: P-YW was employed by company GE Healthcare.

The remaining authors declare that the research was conducted in the absence of any commercial or financial relationships that could be construed as a potential conflict of interest.

Copyright © 2020 Li, Chan, Li, Chen, Chen, Su, Li, Lu, Yu, Chu and Wu. This is an open-access article distributed under the terms of the Creative Commons Attribution License (CC BY). The use, distribution or reproduction in other forums is permitted, provided the original author(s) and the copyright owner(s) are credited and that the original publication in this journal is cited, in accordance with accepted academic practice. No use, distribution or reproduction is permitted which does not comply with these terms.

frontiers in Genetics

ORIGINAL RESEARCH
published: 23 October 2020
doi: 10.3389/fgene.2020.590365

The cis-Regulatory Element of SNCA Intron 4 Modulates Susceptibility to Parkinson's Disease in Han Chinese

Shi-Guo Zhu[1,2†], Hui Lu[2†], Miao Mao[2], Zhao-Feng Li[2], Lei Cui[2], Begench Ovlyakulov[1], Xiong Zhang[1] and Jian-Hong Zhu[1,2*]*

[1]Department of Geriatrics and Neurology, The Second Affiliated Hospital and Yuying Children's Hospital, Wenzhou Medical University, Wenzhou, China, [2]Department of Preventive Medicine, Wenzhou Medical University, Wenzhou, China

OPEN ACCESS

Edited by:
Hao Deng,
Central South University, China

Reviewed by:
Qiying Sun,
Central South University, China
Atif Adnan,
China Medical University, China

***Correspondence:**
Jian-Hong Zhu
jhzhu@wmu.edu.cn
Xiong Zhang
zhangxiong98@gmail.com

†These authors have contributed equally to this work

Specialty section:
This article was submitted to Genetics of Common and Rare Diseases, a section of the journal Frontiers in Genetics

Received: 03 August 2020
Accepted: 16 September 2020
Published: 23 October 2020

Citation:
Zhu S-G, Lu H, Mao M, Li Z-F, Cui L, Ovlyakulov B, Zhang X and Zhu J-H (2020) The cis-Regulatory Element of SNCA Intron 4 Modulates Susceptibility to Parkinson's Disease in Han Chinese. Front. Genet. 11:590365. doi: 10.3389/fgene.2020.590365

Objective: A novel functional cis-regulatory element (CRE) located at *SNCA* intron 4 has recently been identified in association with Parkinson's disease (PD) risk in European descendants. We aimed to investigate whether this CRE is associated with PD in Han Chinese ethnicity.

Methods: A Chinese cohort comprising 513 sporadic PD patients and 517 controls was recruited. CRE variants were identified by sequencing and then analyzed.

Results: A total of nine variants were detected, namely eight single nucleotide variants and one new insertion variant. Two variants, rs17016188 and rs7684892, had minor allele frequency greater than 5%. A difference of rs17016188 was observed in males with the C allele serving as a recessive risk factor ($p = 0.001$, OR = 2.349, 95% CI = 1.414–3.901) following Bonferroni correction. Haplotypes of rs17016188 and rs7684892 showed distribution differences in the total and the male populations ($p = 0.002$ and 4.08×10^{-5}, respectively). Among the haplotypes, rs17016188/T-rs7684892/G was associated with a reduced risk for PD ($p = 4.8 \times 10^{-4}$, OR = 0.731, 95% CI = 0.614–0.872).

Conclusions: Our results provide insight into how the *SNCA* intron 4 CRE harbors variants and its contribution to PD risk in Chinese ethnicity.

Keywords: Parkinson's disease, SNCA, cis-regulatory element, association, variant

INTRODUCTION

Parkinson's disease (PD) is a common neurodegenerative disease characterized by the progressive loss of dopaminergic neurons in the substantia nigra and the formation of Lewy bodies. Considerable progress has been made to understand the genetic underpinning of PD. Monogenic mutations such as in genes of *SNCA*, *LRRK2*, and *Parkin* have been well defined to cause hereditary PD (Obeso et al., 2017). A number of independent risk variants including *SNCA*/rs356182, *RIT2*/rs12456492, and *SIPA1L2*/rs10797576 have been consistently identified to associate with sporadic PD (Nalls et al., 2014; Wang et al., 2015; Zou et al., 2018).

SNCA and its product α-synuclein are at the convergence of PD genetically and pathologically. It has been intensively investigated in regard with its causative genetic mutations and risk variants. Patients with *SNCA* duplication or triplication exhibit a dosage effect in disease onset, severity, and progression (Obeso et al., 2017). The encoded α-synuclein is the main component of Lewy body inclusion, and dopaminergic neurons are particularly vulnerable to the toxic α-synuclein aggregates (Alegre-Abarrategui et al., 2019). In recent years, misfolded α-synuclein is considered possessing prion-like properties, propagating between neurons, neurons and glia cells, and even between animals (Makin, 2016).

By analyzing open chromatins of midbrain dopaminergic neurons and their correlations with putative enhancers, McClymont et al. (2018) recently revealed a novel functional cis-regulatory element (CRE; chr4: 90,721,063–90,722,122; hg19) located at *SNCA* intron 4. Variants of this CRE were shown to be associated with elevated PD risk in non-Hispanic Caucasians of European descent and be able to impact DNA-binding capacity of a set of proteins. Also, DNase hypersensitivity site analysis showed an interaction between the CRE and the *SNCA* promoter (Thurman et al., 2012; Wang et al., 2018). However, whether this *SNCA* CRE is associated with PD risk in other ethnicities remains unknown. In this study, we recruited a total of 1,020 individuals of Han Chinese descent and aimed to investigate those bearing CRE variants and their associations with PD risk.

MATERIALS AND METHODS

Subjects

Enrolled in this study were 513 sporadic PD patients (264 males and 249 females) and 507 controls (287 males and 220 females) of Han Chinese ethnicity from southeast China. The median ages of the patients and controls were 64 (interquartile range, 55–71) and 65 (interquartile range, 60–73) years, respectively, following a normality test. PD patients were diagnosed by two movement disorder specialists according to the UK Parkinson's disease Society Brain Bank Criteria. Patients with a family history of PD or with secondary and atypical Parkinsonism were excluded. Control subjects were free of neurological disorders according to medical history and physical and laboratory examinations. All subjects participating in the study signed written informed consent. The study was approved by the Ethics Committee of the Second Affiliated Hospital and Yuying Children's Hospital, Wenzhou Medical University (No. KYKT2018-15, 03/02/2018).

Genotyping

Genomic DNA was extracted from human peripheral blood using an extraction kit from Tiangen (Beijing, China). The CRE fragment was amplified by polymerase chain reaction (PCR) in 20 μl of reaction mixture that contained 2 μl DNA template, 10 μl 2 × PCR Master Mix (Vazyme, Nanjing, China), and 1 μl of each primer. The primer pair was 5'-GGG AGG GAA CTA TGG AGG CAT C-3' and 5'-GGC CTA GCA GGG CGA GAA TAG-3'. The PCR condition was initial denaturation at 95°C for 3 min, followed by 30 cycles of 95°C for 30 s, 60°C for 30 s, and 72°C for 60 s, and a final extension at 72°C for 5 min. Variants were identified by bidirectional Sanger sequencing (BGI, Shanghai, China).

Data Analysis

Sequence data were analyzed using Lasergene (DNASTAR). Statistical analyses were performed using the statistical package of Predictive Analytics Software 18.0 (PASW, version 18.0) for Windows. Hardy-Weinberg equilibrium in genotype distribution, as well as differences in gender, genotype, allele, and haplotype frequencies, was assessed using the χ^2 test. Mann-Whitney *U* test was used to evaluate age difference. Variants with significant difference were further analyzed using binary logistic regression model with gender and age as covariates. Haplotype association analysis was evaluated using SHEsis (Shi and He, 2005; Li et al., 2009). Linkage disequilibrium structure and r^2 values of the *SNCA* loci were extracted from LDlink with the LDmatrix tool in the 1,000 Genomes Chinese population (Machiela and Chanock, 2015) and were plotted with R.[1] Statistical significance was considered when $p < 0.05$.

RESULTS

Identification of Variants in the CRE Region of SNCA Intron 4

A total of nine variants were detected in the CRE region out of the 1,020 subjects (**Table 1**). Among these variants, eight were single nucleotide variation and one was insertion variation. Two single nucleotide variants, rs17016188 and rs7684892, had minor allele frequencies greater than 5%. The other six single nucleotide variants were found in heterozygous carriers. Based on the TOPMed project,[2] the chr4: 90,721,599 (G > A) discovered in a PD patient was a new variant, and the rs1245859102 discovered in a control was a new G > T transversion instead of the usual G > A transition. The homozygous insertion variant, chr4: 90,722,259, was discovered in a control subject (**Table 1**).

Association Analysis of the Variants rs1701688 and rs7684892 With PD Risk

Genotype distribution of both rs17016188 and rs7684892 met with Hardy-Weinberg equilibrium ($p > 0.05$). The gender frequencies in the PD cases and controls were comparable ($p > 0.05$). There was a difference in age between the two groups ($p < 0.05$). Allele frequencies of

[1]https://www.r-project.org/
[2]https://www.nhlbiwgs.org

TABLE 1 | Identified variants and their allele and genotype frequencies in PD cases and controls.

Variant	Minor allele	Subject	Allele, *n* (%)		Genotype, *n* (%)		
			Minor	Major	Hm minor	Heterozygous	Hm major
chr4: 90,722,259 (insertion)	GAGGAA	Control	2 (0.2)	1,013 (99.8)	1 (0.2)	0 (0.0)	506 (99.8)
		PD	0 (0.0)	1,026 (100.0)	0 (0.0)	0 (0.0)	513 (100.0)
rs1245859102 (G/T)	T	Control	1 (0.1)	1,013 (99.9)	0 (0.0)	1 (0.2)	506 (99.8)
		PD	0 (0.0)	1,026 (100.0)	0 (0.0)	0 (0.0)	513 (100.0)
rs2737024 (A/G)	G	Control	0 (0.0)	1,014 (100.0)	0 (0.0)	0 (0.0)	507 (100.0)
		PD	2 (0.2)	1,024 (99.8)	0 (0.0)	2 (0.4)	511 (99.6)
chr4: 90,721,599 (G/A)	A	Control	0 (0.0)	1,014 (100.0)	0 (0.0)	0 (0.0)	507 (100.0)
		PD	1 (0.1)	1,025 (99.9)	0 (0.0)	1 (0.2)	512 (99.8)
rs2583959 (C/G)	G	Control	0 (0.0)	1,014 (100.0)	0 (0.0)	0 (0.0)	507 (100.0)
		PD	2 (0.2)	1,024 (99.8)	0 (0.0)	2 (0.4)	511 (99.6)
rs17016188 (T/C)	C	Control	345 (34.0)	669 (66.0)	61 (12.0)	223 (44.0)	223 (44.0)
		PD	392 (38.2)	634 (61.8)	86 (16.8)	220 (42.9)	207 (40.4)
rs7684892 (G/A)	A	Control	190 (18.7)	824 (81.3)	18 (3.6)	154 (30.4)	335 (66.1)
		PD	228 (22.2)	798 (77.8)	27 (5.3)	174 (33.9)	312 (60.8)
rs1389820774 (C/T)	T	Control	1 (0.1)	1,013 (99.9)	0 (0.0)	1 (0.2)	506 (99.8)
		PD	5 (0.5)	1,021 (99.5)	0 (0.0)	5 (1.0)	508 (99.0)
rs1560531460 (T/A)	A	Control	1 (0.1)	1,013 (99.9)	0 (0.0)	1 (0.2)	506 (99.8)
		PD	1 (0.1)	1,025 (99.9)	0 (0.0)	1 (0.2)	512 (99.8)

Hm, homozygous; PD, Parkinson's disease.

TABLE 2 | Association analysis of rs17016188 and rs7684892 with PD risk.

Variant	Allele, *n* (%)		OR (95% CI)	*p*	Genotype, *n* (%)			*p*
rs17016188	T	C			TT	CT	CC	
Control	669 (66.0)	345 (34.0)			223 (44.0)	223 (44.0)	61 (12.0)	
PD	634 (61.8)	392 (38.2)	1.199 (1.001–1.437)	0.049	207 (40.4)	220 (42.9)	86 (16.8)	0.089
Male control	388 (67.6)	186 (32.4)			127 (44.3)	134 (46.7)	26 (9.1)	
Male PD	313 (59.3)	215 (40.7)	1.433 (1.120–1.833)	0.004*	99 (37.5)	115 (43.6)	50 (18.9)	0.003*
Female control	281 (63.9)	159 (36.1)			96 (43.6)	89 (40.5)	35 (15.9)	
Female PD	321 (64.5)	177 (35.5)	0.974 (0.746–1.273)	0.850	108 (43.4)	105 (42.2)	36 (14.5)	0.884
rs7684892	G	A			GG	AG	AA	
Control	824 (81.3)	190 (18.7)			335 (66.1)	154 (30.4)	18 (3.6)	
PD	798 (77.8)	228 (22.2)	1.239 (0.999–1.537)	0.051	312 (60.8)	174 (33.9)	27 (5.3)	0.149
Male control	474 (82.6)	100 (17.4)			196 (68.3)	82 (28.6)	9 (3.1)	
Male PD	409 (77.5)	119 (22.5)	1.379 (1.025–1.856)	0.033	163 (61.7)	83 (31.4)	18 (6.8)	0.079
Female control	350 (79.6)	90 (20.5)			139 (63.2)	72 (32.7)	9 (4.1)	
Female PD	389 (78.1)	109 (21.9)	1.090 (0.796–1.492)	0.592	149 (59.8)	91 (36.8)	9 (3.6)	0.680

*CI, confidence interval; OR, odds ratio; PD, Parkinson's disease. *Indicates $p < 0.025$ after Bonferroni correction.*

both rs17016188 and rs7684892 showed marginal associations with PD risk in the total population (p = 0.049 and 0.051, respectively; **Table 2**). After Bonferroni correction, the difference, that is $p < 0.025$, was found in the male group in rs17016188 (allele: p = 0.004, OR = 1.433, 95% CI = 1.120–1.833; genotype: p = 0.003). Further multivariate analysis of rs17016188 with age adjusted confirmed the difference in the males with the C allele serving as a recessive risk factor (p = 0.001, OR = 2.349, 95% CI = 1.414–3.901; **Table 3**).

Haplotype Analysis of rs1701688 and rs7684892 in Association With PD

Haplotypes were constructed to understand the combined effect of rs17016188 and rs7684892 on PD risk (**Table 4**). The two variants displayed a linkage disequilibrium with r^2 = 0.146 and D' = 0.9993 in the cohort. Out of four potential combinations, three haplotypes were detected except for the rs17016188/C-rs7684892/A. An overall significance in haplotype distribution was found in the total and male populations (p = 0.002 and 4.08×10^{-5}, respectively), but not in the females. The haplotype, rs17016188/T-rs7684892/G, exhibited a protective effect against PD in the total population ($p = 4.8 \times 10^{-4}$, OR = 0.731, 95% CI = 0.614–0.872) and in the males ($p = 7.14 \times 10^{-6}$, OR = 0.577, 95% CI = 0.453–0.734).

Linkage disequilibrium structure was subsequently constructed in the 1,000 Genomes data to understand how the two CRE variants might be interacting with other *SNCA* variants (**Figure 1**). Of the variants, rs356168 is a previous functionally

TABLE 3 | Multivariate analysis of rs17016188 in the male PD cases and controls adjusted with age.

rs17016188	Genotype, *n* (%)			OR (95% CI)	*p*
	TT	CT	CC		
Control	127 (44.3)	134 (46.7)	26 (9.1)		
PD	99 (37.5)	115 (43.6)	50 (18.9)		
Additive				1.425 (1.114–1.823)	0.005*
Dominant				1.323 (0.941–1.861)	0.108
Recessive				2.349 (1.414–3.901)	0.001*

*CI, confidence interval; OR, odds ratio; PD, Parkinson's disease. *Indicates $p < 0.05$.*

TABLE 4 | Haplotype frequencies of rs17016188 and rs7684892 in PD cases and controls.

rs17016188	rs7684892	Control, *n* (%)	PD, *n* (%)	OR (95% CI)	*p*
Total					
T	G	479 (47.2)	406 (39.6)	0.731 (0.614–0.872)	4.8×10^{-4}*
C	G	345 (34.0)	392 (38.2)	1.199 (1.001–1.437)	0.049
T	A	190 (18.7)	228 (22.2)	1.239 (0.999–1.538)	0.051
Total		1,014 (100)	1,026 (100)		0.002*
Men					
T	G	288 (50.2)	194 (36.7)	0.577 (0.453–0.734)	7.14×10^{-6}*
C	G	186 (32.4)	215 (40.7)	1.433 (1.120–1.833)	0.004*
T	A	100 (17.4)	119 (22.5)	1.380 (1.025–1.857)	0.033
Total		574 (100)	528 (100)		4.08×10^{-5}*
Women					
T	G	191 (43.4)	212 (42.6)	0.966 (0.746–1.252)	0.796
C	G	159 (36.1)	177 (35.5)	0.974 (0.746–1.273)	0.850
T	A	90 (20.5)	109 (21.9)	1.090 (0.796–1.492)	0.592
Total		440 (100)	498 (100)		0.866

*CI, confidence interval; OR, odds ratio; PD, Parkinson's disease. *Indicates $p < 0.017$ after Bonferroni correction.*

validated variant (Soldner et al., 2016) and rs356182 is the lead variant of genome-wide associated studies (GWAS; Nalls et al., 2014; Chang et al., 2017). The rest are a panel of PD-associated variants identified across *SNCA* in Chinese ethnicity (Li et al., 2019). The linkage disequilibrium analysis showed a low linkage disequilibrium structure between the CRE variants (rs1701688 and rs7684892) and the previously reported *SNCA* sites.

DISCUSSION

SNCA is a central piece of the genetic puzzle leading to PD pathogenesis. The recent advance of the *SNCA* intron 4 CRE in association with PD risk warrants further identification in additional ethnicities. The current study involving a Chinese population reveals nine variants, including one new rare variant (chr4: 90,721,599; G > A) and one variant with different nucleotide replacement (rs124589102; G > T). Four variants, namely rs17016188, rs7684892, rs2737024, and rs2583959, are common between ours and the 14 variants discovered in the European descendants (McClymont et al., 2018; **Figure 2**).

Current knowledge of biologically related noncoding variation is limited. It is considered that CRE candidates may serve functional roles in regulating gene expression (Snyder et al., 2020). Recent studies have highlighted the importance of CREs harboring functional variation as well as their regulated genes (Maurano et al., 2012; Thurman et al., 2012; Soldner et al., 2016; McClymont et al., 2018). For instance, the CRE in *SNCA* intron 4 may affect the midbrain-specific expression of *SNCA*, and the variants within the CRE can disturb binding affinity of a set of proteins, including NOVA1, APOBEC3C, PEG10, SNRPA, and CHMP5. Three of them, PEG10, SNRPA, and CHMP5, show increased affinities of binding to the minor risk allele, that is, G of rs2583959 or G of rs2737024. To understand whether the CRE variants are independently connected to PD, eight known PD-associated *SNCA* risk variants, including those functionally validated and leading in GWAS studies (Nalls et al., 2014; Soldner et al., 2016; Chang et al., 2017), and those identified in a Chinese population (Li et al., 2019), are used for linkage disequilibrium analysis. Results suggest that the CRE variants rs1701688 and rs7684892 and the resulting haplotypes are independent in association with PD. Though detailed mechanisms and consequences remain to be further explored, it is possible that the variants within the CRE, independently or in concert with additional variation, may influence *SNCA* expression and/or susceptibility of catecholaminergic neurons.

In line with the previous results (McClymont et al., 2018), both rs17016188 and rs7684892 show minor allele frequency over 5% and are not associated with PD risk in the overall population. While the gender-stratified analysis was not presented in the earlier study, our results suggest an impact of rs17016188 on PD risk in males. Similar results were also found in the PD-associated protective haplotype, rs17016188/T-rs7684892/G. It is not clear how gender bias occurs in the *SNCA* CRE variant and haplotype, which may need further verification in other populations. Nonetheless, the gender bias per se is not surprising for genetic association with PD risk (Palacios et al., 2010; Klebe et al., 2013; Wang et al., 2015). The male-to-female ratio of PD prevalence is approximately at 3:2 (de Lau and Breteler, 2006), probably due to genes in the sex chromosomes and sex hormone-related mechanisms (Jurado-Coronel et al., 2018).

The other two variants, rs2737024 and rs2583959, whose minor allele frequencies are above 5% in the Caucasian population, are significantly associated with PD risk (Heckman et al., 2012; McClymont et al., 2018). In contrast, it is reported that rs2583959 is not associated with multiple system atrophy

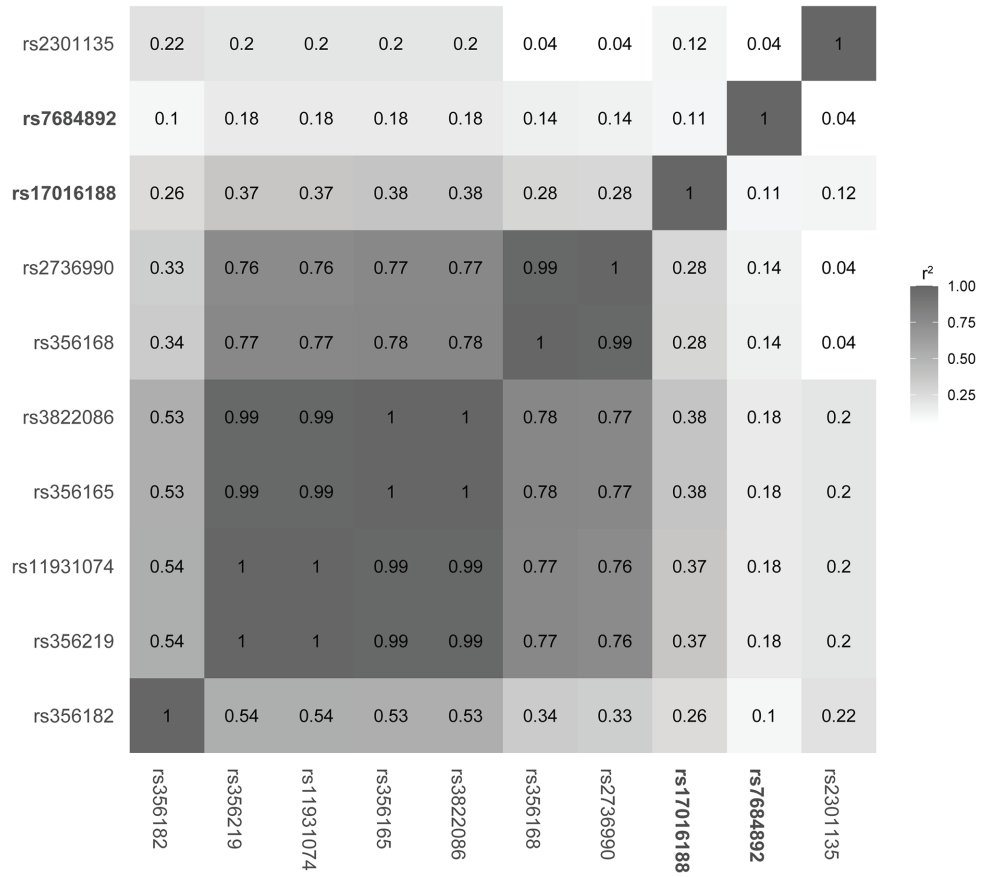


FIGURE 1 | Linkage disequilibrium structure of the *SNCA* loci.

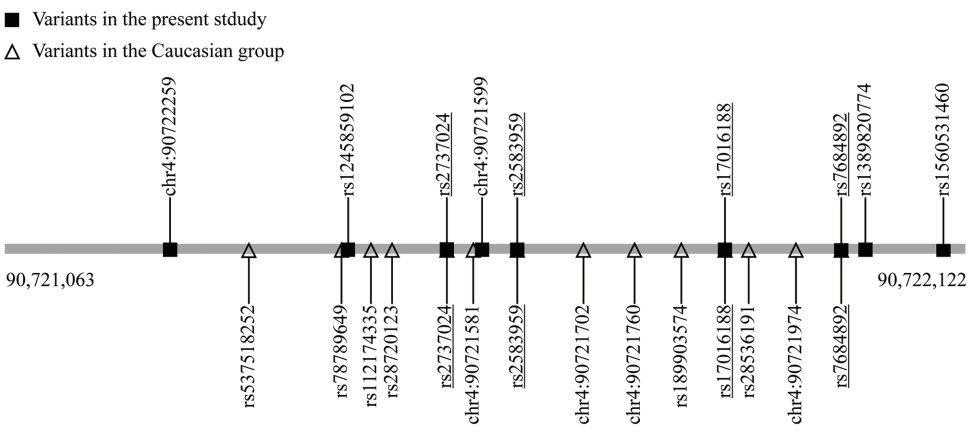


FIGURE 2 | The variants in the *SNCA* intron 4 CRE. The underlined are the shared variants.

and essential tremor (Al-Chalabi et al., 2009; Ross et al., 2011). Interestingly, both variants are rare single nucleotide polymorphisms in the Chinese population. Each variant is only found in two PD patients in heterozygous form, and coincidentally, their carriers are identical individuals. Although their frequencies are distinct between the Chinese and Caucasian populations, our results support the previous findings that the minor alleles of rs2737024 and rs2583959 aggravated PD

risk and the two variants were in strong linkage disequilibrium (McClymont et al., 2018).

In conclusion, the current study reveals nine variants in the *SNCA* intron 4 CRE and demonstrates their associations with PD risk in a Chinese population. Our results provide further insight into how this specific gene regulatory region of *SNCA* harbors variants contributing to PD risk in different ethnicities.

DATA AVAILABILITY STATEMENT

The original contributions presented in the study are included in the article/supplementary material, further inquiries can be directed to the corresponding authors.

ETHICS STATEMENT

The studies involving human participants were reviewed and approved by the Ethics Committee of the Second Affiliated Hospital and Yuying Children's Hospital, Wenzhou Medical University. The patients/participants provided their written informed consent to participate in this study.

AUTHOR CONTRIBUTIONS

J-HZ and XZ designed the research. XZ, S-GZ, and BO collected and managed the samples. S-GZ, HL, and MM conducted the experiments. S-GZ, Z-FL, and LC analyzed the data. J-HZ and S-GZ wrote the manuscript. All authors contributed to the article and approved the submitted version.

FUNDING

This work was supported by funding from Zhejiang Provincial Natural Science Foundation (LD19H090001 and LZ19H090002), National Natural Science Foundation of China (81771380 and 81771510), Zhejiang Provincial Medical Technology Program (2019KY445), Wenzhou Municipal Science and Technology Bureau (Y20190074 and C20170003), and Wenzhou Medical University (QTJ10024 and 89218014).

ACKNOWLEDGMENTS

The authors thank all of the subjects participating in this study and the colleagues for the management of the patients.

REFERENCES

Al-Chalabi, A., Dürr, A., Wood, N. W., Parkinson, M. H., Camuzat, A., Hulot, J. S., et al. (2009). Genetic variants of the alpha-synuclein gene SNCA are associated with multiple system atrophy. *PLoS One* 4:e7114. doi: 10.1371/journal.pone.0007114

Alegre-Abarrategui, J., Brimblecombe, K. R., Roberts, R. F., Velentza-Almpani, E., Tilley, B. S., Bengoa-Vergniory, N., et al. (2019). Selective vulnerability in alpha-synucleinopathies. *Acta Neuropathol.* 138, 681–704. doi: 10.1007/s00401-019-02010-2

Chang, D., Nalls, M. A., Hallgrímsdóttir, I. B., Hunkapiller, J., van der Brug, M., Cai, F., et al. (2017). A meta-analysis of genome-wide association studies identifies 17 new Parkinson's disease risk loci. *Nat. Genet.* 49, 1511–1516. doi: 10.1038/ng.3955

de Lau, L. M., and Breteler, M. M. (2006). Epidemiology of Parkinson's disease. *Lancet Neurol.* 5, 525–535. doi: 10.1016/s1474-4422(06)70471-9

Heckman, M. G., Soto-Ortolaza, A. I., Diehl, N. N., Carrasquillo, M. M., Uitti, R. J., Wszolek, Z. K., et al. (2012). Evaluation of the role of SNCA variants in survival without neurological disease. *PLoS One* 7:e42877. doi: 10.1371/journal.pone.0042877

Jurado-Coronel, J. C., Cabezas, R., Avila Rodriguez, M. F., Echeverria, V., Garcia-Segura, L. M., and Barreto, G. E. (2018). Sex differences in Parkinson's disease: features on clinical symptoms, treatment outcome, sexual hormones and genetics. *Front. Neuroendocrinol.* 50, 18–30. doi: 10.1016/j.yfrne.2017.09.002

Klebe, S., Golmard, J. L., Nalls, M. A., Saad, M., Singleton, A. B., Bras, J. M., et al. (2013). The Val158Met COMT polymorphism is a modifier of the age at onset in Parkinson's disease with a sexual dimorphism. *J. Neurol. Neurosurg. Psychiatry* 84, 666–673. doi: 10.1136/jnnp-2012-304475

Li, G., Ma, J., Cui, S., He, Y., Xiao, Q., Liu, J., et al. (2019). Parkinson's disease in China: a forty-year growing track of bedside work. *Transl. Neurodegener.* 8:22. doi: 10.1186/s40035-019-0162-z

Li, Z., Zhang, Z., He, Z., Tang, W., Li, T., Zeng, Z., et al. (2009). A partition-ligation-combination-subdivision EM algorithm for haplotype inference with multiallelic markers: update of the SHEsis (http://analysis.bio-x.cn). *Cell Res.* 19, 519–523. doi: 10.1038/cr.2009.33

Machiela, M. J., and Chanock, S. J. (2015). LDlink: a web-based application for exploring population-specific haplotype structure and linking correlated alleles of possible functional variants. *Bioinformatics* 31, 3555–3557. doi: 10.1093/bioinformatics/btv402

Makin, S. (2016). Pathology: the prion principle. *Nature* 538, S13–S16. doi: 10.1038/538S13a

Maurano, M. T., Humbert, R., Rynes, E., Thurman, R. E., Haugen, E., Wang, H., et al. (2012). Systematic localization of common disease-associated variation in regulatory DNA. *Science* 337, 1190–1195. doi: 10.1126/science.1222794

McClymont, S. A., Hook, P. W., Soto, A. I., Reed, X., Law, W. D., Kerans, S. J., et al. (2018). Parkinson-associated SNCA enhancer variants revealed by open chromatin in mouse dopamine neurons. *Am. J. Hum. Genet.* 103, 874–892. doi: 10.1016/j.ajhg.2018.10.018

Nalls, M. A., Pankratz, N., Lill, C. M., Do, C. B., Hernandez, D. G., Saad, M., et al. (2014). Large-scale meta-analysis of genome-wide association data identifies six new risk loci for Parkinson's disease. *Nat. Genet.* 46, 989–993. doi: 10.1038/ng.3043

Obeso, J. A., Stamelou, M., Goetz, C. G., Poewe, W., Lang, A. E., Weintraub, D., et al. (2017). Past, present, and future of Parkinson's disease: a special essay on the 200th Anniversary of the Shaking Palsy. *Mov. Disord.* 32, 1264–1310. doi: 10.1002/mds.27115

Palacios, N., Weisskopf, M., Simon, K., Gao, X., Schwarzschild, M., and Ascherio, A. (2010). Polymorphisms of caffeine metabolism and estrogen receptor genes and risk of Parkinson's disease in men and women. *Parkinsonism Relat. Disord.* 16, 370–375. doi: 10.1016/j.parkreldis.2010.02.012

Ross, O. A., Conneely, K. N., Wang, T., Vilarino-Guell, C., Soto-Ortolaza, A. I., Rajput, A., et al. (2011). Genetic variants of α-synuclein are not associated with essential tremor. *Mov. Disord.* 26, 2552–2556. doi: 10.1002/mds.23909

Shi, Y. Y., and He, L. (2005). SHEsis, a powerful software platform for analyses of linkage disequilibrium, haplotype construction, and genetic association at polymorphism loci. *Cell Res.* 15, 97–98. doi: 10.1038/sj.cr.7290272

Snyder, M. P., Gingeras, T. R., Moore, J. E., Weng, Z., Gerstein, M. B., Ren, B., et al. (2020). Perspectives on ENCODE. *Nature* 583, 693–698. doi: 10.1038/s41586-020-2449-8

Soldner, F., Stelzer, Y., Shivalila, C. S., Abraham, B. J., Latourelle, J. C., Barrasa, M. I., et al. (2016). Parkinson-associated risk variant in distal enhancer of α-synuclein modulates target gene expression. *Nature* 533, 95–99. doi: 10.1038/nature17939

Thurman, R. E., Rynes, E., Humbert, R., Vierstra, J., Maurano, M. T., Haugen, E., et al. (2012). The accessible chromatin landscape of the human genome. *Nature* 489, 75–82. doi: 10.1038/nature11232

Wang, J. Y., Gong, M. Y., Ye, Y. L., Ye, J. M., Lin, G. L., Zhuang, Q. Q., et al. (2015). The RIT2 and STX1B polymorphisms are associated with Parkinson's disease. *Parkinsonism Relat. Disord.* 21, 300–302. doi: 10.1016/j.parkreldis.2014.12.006

Wang, Y., Song, F., Zhang, B., Zhang, L., Xu, J., Kuang, D., et al. (2018). The 3D Genome Browser: a web-based browser for visualizing 3D genome organization and long-range chromatin interactions. *Genome Biol.* 19:151. doi: 10.1186/s13059-018-1519-9

Zou, M., Li, R., Wang, J. Y., Wang, K., Wang, Y. N., Li, Y., et al. (2018). Association analyses of variants of SIPA1L2, MIR4697, GCH1, VPS13C, and DDRGK1 with Parkinson's disease in East Asians. *Neurobiol. Aging* 68, 159.e157–159.e114. doi: 10.1016/j.neurobiolaging.2018.03.005

Conflict of Interest: The authors declare that the research was conducted in the absence of any commercial or financial relationships that could be construed as a potential conflict of interest.

Copyright © 2020 Zhu, Lu, Mao, Li, Cui, Ovlyakulov, Zhang and Zhu. This is an open-access article distributed under the terms of the Creative Commons Attribution License (CC BY). The use, distribution or reproduction in other forums is permitted, provided the original author(s) and the copyright owner(s) are credited and that the original publication in this journal is cited, in accordance with accepted academic practice. No use, distribution or reproduction is permitted which does not comply with these terms.

frontiers in Aging Neuroscience

ORIGINAL RESEARCH
published: 23 October 2020
doi: 10.3389/fnagi.2020.574776

Parkinson's Disease With Depression: The Correlations Between Neuroinflammatory Factors and Neurotransmitters in Cerebrospinal Fluid

*Teng-hong Lian[1], Peng Guo[1], Ya-nan Zhang[2], Jing-hui Li[1], Li-xia Li[3], Du-yu Ding[1], Da-ning Li[1], Wei-jiao Zhang[1], Hui-ying Guan[1], Xiao-min Wang[4] and Wei Zhang[5,6,7,8]**

[1]*Department of Neurology, Beijing Tiantan Hospital, Capital Medical University, Beijing, China,* [2]*Department of Blood Transfusion, Beijing Tiantan Hospital, Capital Medical University, Beijing, China,* [3]*Department of General Internal Medicine, Beijing Tiantan Hospital, Capital Medical University, Beijing, China,* [4]*Department of Physiology, Capital Medical University, Beijing, China,* [5]*Center for Cognitive Neurology, Department of Neurology, Beijing Tiantan Hospital, Capital Medical University, Beijing, China,* [6]*China National Clinical Research Center for Neurological Disease, Beijing Tiantan Hospital, Capital Medical University, Beijing, China,* [7]*Center of Parkinson's Disease, Beijing Institute for Brain Disorders, Beijing, China,* [8]*Beijing Key Laboratory on Parkinson Disease, Beijing, China*

OPEN ACCESS

Edited by:
Pingyi Xu,
First Affiliated Hospital of Guangzhou Medical University, China

Reviewed by:
Zhong Pei,
Sun Yat-Sen University, China
Nicola B. Mercuri,
University of Rome Tor Vergata, Italy

***Correspondence:**
Wei Zhang
ttyyzw@163.com

Received: *21 June 2020*
Accepted: *24 August 2020*
Published: *23 October 2020*

Citation:
Lian T-h, Guo P, Zhang Y-n, Li J-h, Li L-x, Ding D-y, Li D-n, Zhang W-j, Guan H-y, Wang X-m and Zhang W (2020) Parkinson's Disease With Depression: The Correlations Between Neuroinflammatory Factors and Neurotransmitters in Cerebrospinal Fluid. Front. Aging Neurosci. 12:574776. doi: 10.3389/fnagi.2020.574776

Background: To explore the changes of neuroinflammatory factors in cerebrospinal fluid (CSF) and their correlation with monoamine neurotransmitters in Parkinson's disease (PD) with depression (PD-D) patients.

Methods: Neuroinflammatory factors and neurotransmitters in CSF were measured and compared between PD with no depression (PD-ND) and PD-D groups. The relationship between PD-D and neuroinflammatory factors was studied by binary logistic regression equation, and the related factors of PD-D were adjusted. The correlations of the levels of neuroinflammatory factors and neurotransmitters in PD-D group were analyzed.

Results: The levels of tumor necrosis factor (TNF)-α in CSF from PD-D group were significantly higher and there were no significant differences in the levels of interleukin-1β, prostaglandin (PG) E_2, hydrogen peroxide (H_2O_2), and nitric oxide (NO). The 24-item Hamilton Depression Scale (HAMD-24) score was positively correlated with the level of TNF-α in CSF. Binary logistic regression showed that the OR of CSF TNF-α level was 1.035 (95% CI 1.002–1.069). The level of dopamine (DA) in CSF of PD-D group was significantly lower than that in PD-ND group. TNF-α level was negatively correlated with DA level in CSF from PD patients ($r = -0.320$, $P = 0.003$).

Conclusions: Neuroinflammatory factors, especially TNF-α, may play an important role in PD-D. It may cause damage to DA neurons and lead to the depletion of DA, which is related to the occurrence and development of PD-D.

Keywords: Parkinson's disease, depression, neuroinflammatory factors, neurotransmitters, cerebrospinal fluid

INTRODUCTION

Parkinson's disease (PD) is the second most common neurodegenerative disorder with a number of characteristic motor symptoms, including rest tremor, rigidity, bradykinesia, and gait and postural instabilities (Jankovic, 2008). Additionally, PD patients also have a variety of non-motor symptoms, such as mood abnormality, sleep disturbance, autonomic dysfunction, cognitive impairment, etc. Depression is one of the most common non-motor symptoms of PD (Cosentino et al., 2013). Compared with healthy controls, PD with depression (PD-D) patients displayed a higher morbidity, which was 40% at the early stage and reached up to 70% at advanced stage of disease (Reijnders et al., 2008; Cosentino et al., 2013). However, both diagnosis and treatment of PD-D have not been given enough attention for patients. The failures to diagnose PD-D and offer timely treatment significantly compromise the life quality of both PD patients and their caregivers (Goodarzi et al., 2016). Importantly, the underlying mechanisms of PD-D are not clearly elucidated, and thus effective therapy for PD-D patients still needs to be developed.

Increasing studies showed that primary depression was closely related to inflammation (Kohler et al., 2016). In the clusters of inflammatory markers measured, C-reactive protein (CRP) level in plasma was found to be significantly correlated with the severity of depressive symptoms (Felger et al., 2020). Furthermore, repetitive transcranial magnetic stimulation exerted an anti-depressant effect *via* an anti-inflammation mechanism in a mouse model of primary depression (Tian et al., 2020), indicating the pivotal role of inflammation on primary depression.

It can be suspected that inflammation probably also plays a role on the depression caused by neurodegenerative disease, like PD. We know that it is more meaningful to investigate brain neuroinflammation by detecting the inflammatory factors in cerebrospinal fluid (CSF) than peripheral inflammation by measuring the inflammatory factors in plasma from PD-D patients. Although non-motor symptoms of PD, including cognitive impairment (Sanjari Moghaddam et al., 2018), pure apathy (Wang et al., 2016) and sleep disorders (Wang et al., 2016), particularly rapid eye movement sleep behavior disorder (RBD) (Hu et al., 2015), were significantly correlated with multiple neuroinflammatory factors in CSF demonstrated by our and other investigations, there were very few studies about the relationship between PD-D and brain neuroinflammation. For example, Lindqvist et al. (2013) found that the more severe depression was significantly associated with the higher CRP level in CSF from 71 non-demented PD patients. However, there are no studies in large samples with more neuroinflammatory factors in CSF from PD-D patients measured and analyzed.

It is known that the alterations of neurotransmitters may serve as the biochemical basis of PD-D. The dysfunctions of dopamine (DA; Lian et al., 2018), 5-hydroxytryptamine (5-HT; Zhuo et al., 2017; Lian et al., 2018), and norepinephrine (NE; Zhuo et al., 2017) systems as well as their interaction in the brain were related to PD-D. Through analysis of neurotransmitters in CSF from PD patients, our previous study showed that, compared with 5-HT and NE, only DA level in PD-D group was significantly reduced compared with that in PD with no depression (PD-ND) group. Moreover, the score of the 24-item Hamilton Depression Scale (HAMD-24) had a negative correlation only with DA level in CSF (Lian et al., 2018). Therefore, DA may play a more important role in PD-D. Additionally, it was found that alleviating inflammation prevented dopaminergic neurodegeneration (Chen et al., 2019) and increased DA level (Wang et al., 2015) in a mouse PD model. However, there was no investigation exploring the correlations of neuroinflammatory factors with neurotransmitters in CSF from PD-D patients.

In this study, HAMD-24 was used to assess the depressive symptoms of PD patients; the levels of neuroinflammatory factors, including hydrogen peroxide (H_2O_2), nitric oxide (NO), tumor necrosis factor (TNF)-α, IL (interleukin)-1β, IL-6, prostaglandin (PG)E_2, and neurotransmitters, including DA, 5-HT, and NE in CSF, were measured and compared between PD-D and PD-ND groups; the correlations among the score of HAMD-24, the levels of neuroinflammatory factors, and neurotransmitters in PD-D group were analyzed.

MATERIALS AND METHODS

Participants

PD Patients

PD patients were consecutively recruited according to the 2015 International Parkinson and Movement Disorders Society (MDS) diagnostic criteria for PD (Postuma et al., 2015).

This study was approved by Beijing Tiantan Hospital ethics committee. Written informed consents were obtained from all participants in this study.

PD-D and PD-ND Patients

Inclusion criteria: PD-D was established by the diagnostic criteria for PD with depression (Starkstein et al., 2011). HAMD-24 recommended by PD-D diagnostic criterion for assessing depressive symptoms of PD includes seven factors: anxiety/somatization, weight loss, cognitive impairment, circadian fluctuations, retardation, sleep disturbances, and hopelessness, by which the clinical characteristics of depressive patients are clearly and explicitly reflected. PD patients with a total score of HAMD-24 $\geq$8 points were assigned to PD-D group, in which 8–19 points, 20–34 points, and $\geq$35 points were categorized as mild, moderate, and severe depression, respectively. PD patients with a total score of HAMD-24 $<$ 8 points were assigned to PD-ND group.

Exclusion criteria: PD patients who met the following criteria were excluded: (1) other central nervous systemic diseases; (2) severe systemic diseases; (3) depression caused by organic mental disorders, psychoactive substances, addictive substances, etc.; (4) infections and immune diseases; and (5) usage of anti-depressants.

Clinical Assessments for PD Patients

A total of 86 PD patients were consecutively recruited from the Beijing Tiantan Hospital, Capital Medical University, at the baseline, among which 58 cases met the PD-D inclusion and exclusion criteria and the remaining 28 cases were with PD-ND.

Collection of Demographic Information

Medical information, including gender, age, age of onset, duration of disease, side of onset, education level, and anti-PD therapy, including levodopa equivalent daily dose (LEDD), the types of drugs, the duration of taking drugs, etc., were collected.

Assessment of Motor Function

Disease severity: the severity of PD was assessed by using the Hoehn-Yahr (H-Y) stage.

Motor symptoms: the motor symptoms of PD patients, including tremor, bradykinesia, rigidity, and postural and gait abnormalities, were assessed during the "off" period. The higher the total score of UPDRS III, the worse the motor symptoms.

Motor phenotypes: according to Jankovic's clinical phenotype classification, PD patients were divided into three motor phenotypes, including tremor-dominant (TD), postural instability and gait difficulty (PIGD), and mixed types (Jankovic et al., 1990). Tremor was assessed by item 16, 20, and 21, and PIGD was assessed by item 13, 14, 15, 29, and 30 in UPDRS III. Motor phenotype was determined by the ratio of average tremor score and PIGD score, and the ratio of $\geq$1.5, $\leq$1.0, and 1.0–1.5 were identified as TD, PIGD, and mixed types, respectively.

Assessments of Non-motor Symptoms

Non-motor symptoms: cognitive impairment was assessed by the Montreal Cognitive Assessment Scale (MoCA; Hoops et al., 2009); anxiety was assessed by the 14-item Hamilton Anxiety Scale (HAMA-14; Hamilton, 1959); fatigue was assessed by the 14-item Chalder Fatigue Scale (FS-14; Chalder et al., 1993); RBD was assessed by the RBD Screening Questionnaire (RBDSQ; Zea-Sevilla and Martínez-Martin, 2014); autonomic dysfunction was assessed by the Scale for Outcomes in PD for Autonomic Symptoms (SCOPA-AUT; Visser et al., 2004); restless legs syndrome (RLS) was assessed by RLS Severity Rating Scale (RLSRS; Walters et al., 2003).

Assessment of the Activities of Daily Living (ADL)

ADL, including basic ADL (BADL) and instrumental ADL (IADL), was assessed by the ADL Scale (Holroyd et al., 2005).

Measurements of Neuroinflammatory Factors and Neurotransmitters in CSF

Collection and Processing of CSF

Anti-PD drugs were withdrawn for 12–14 h if the patients' condition allowed and longer time was considered unethical by our ethical committee. Because the medical washout period should be three times the $t_{1/2}$ of the anti-PD drugs, the subjects taking drugs with long $t_{1/2}$, including controlled release Sinemet (Sinement CR), Pramipexole, and controlled-release Piribedil (Piribedil CR), were excluded in the analyses of neurotransmitters.

Under fasting conditions, 5 ml of CSF was taken in a polypropylene tube through lumbar puncture between 7 and 9 a.m. CSF samples were centrifuged immediately at 3,000 rpm at 4°C. Then, approximately 0.5-ml volume of CSF was aliquoted into separate Nunc cryotubes and kept frozen at −80°C until usage in the assays (Lian et al., 2018).

Measurements of Neuroinflammatory Factors in CSF

The levels of H_2O_2 and NO in CSF from PD patients were measured by the A064 assay kit and A012 assay kit (Jiancheng Bioengineering Institute, Nanjing, China), respectively, by the chemical colorimetric method (Wang et al., 2016).

The levels of TNF-α, IL-1β, IL-6 and PGE_2 in CSF from PD patients were measured by the enzyme linked immunosorbent assay. Kit 1R040, 1R350, and D6050 (R&D Systems parent company, USA) were used for TNF-α, IL-1β, and IL-6, respectively. Kit CSB-E07965h (CUSABIO Technology Limited Liability Company, USA) was used for PGE_2.

Measurements of Neurotransmitters in CSF

The levels of DA, 5-HT, and NE in CSF from PD patients were measured by high-performance liquid chromatography (Lian et al., 2018). LC-MS-MS 6410 chromatograph and Phenomenex 150 × 2 mm and 150 × 3 mm chromatographic columns were from the Agilent Company (California, USA), and the standard sample was from Sigma Company (California, USA).

Statistical Analyses

Statistical analyses were performed by using SPSS Statistics 20.0. A *P*-value of less than an alpha level of 0.05 was defined as statistically significant.

The levels of neuroinflammatory factors in CFS between PD-D and PD-ND groups were compared. Normal distributed measurement data were presented as means ± standard deviations, and non-normal distributed measurement data were presented as median (first quartile, third quartile). In the analyses between PD-D and PD-ND groups, those that meet the normal distribution and the homogeneity of variance were compared by *t* test; the rest of the data were compared by Mann–Whitney *U* test.

Bivariate correlation analysis was performed between HAMD-24 score and the level of neuroinflammatory factors in CSF from PD patients.

Binary logistic regression analysis was used to investigate the relationship between PD-D and the level of neuroinflammatory factors in CSF. In the binary logistic regression equation, neuroinflammatory factors in CSF with statistical differences in single-factor analysis and in the bivariate correlation analysis were respectively set as covariates and put into multi-logistic regression models, whereas with or without depression in PD was set as a dependent variable (PD-D = 1, PD-ND = 0).

RESULTS

Demographic Variables, Motor Function, Non-motor Symptoms, and ADL of PD-D and PD-ND Groups

Demographic variables, the scores of motor symptoms, non-motor symptoms, and ADL were compared between PD-D and PD-ND groups (**Table 1**). The data displayed that PD-D group had significantly lower education level, higher UPDRS III score, greater proportion of PIGD type, higher scores of HAMA, FS, RBDSQ, and SCOPA-AUT scales, and lower score of ADL scale than PD-ND group ($P < 0.05$).

Comparisons of Neuroinflammatory Factors in CSF Between PD-D and PD-ND Groups

The levels of neuroinflammatory factors, including H_2O_2, NO, TNF-α, IL-1β, IL-6, and PGE_2 in CSF from PD-D and PD-ND groups, were compared (**Table 2**). The results showed that TNF-α level in CSF from PD-D group was significantly increased compared with that from PD-ND group (31.321 pg/ml vs. 21.530 pg/ml, $P < 0.05$). However, there was no significant difference in the levels of H_2O_2, NO, IL-1β, IL-6, and PGE_2 in CSF between the two groups.

The Relationship Between PD-D and Neuroinflammatory Factors in CSF

The correlation between the score of HAMD-24 and the levels of H_2O_2, NO, TNF-α, IL-1β, IL-6, and PGE_2 in CSF from PD patients was analyzed (**Table 3**). It was found that HAMD-24 score had a positive correlation with TNF-α level in CSF ($r = 0.247$, $P = 0.022$). However, no significant relationship between HAMD-24 score and the levels of H_2O_2, NO, IL-1β, IL-6, and PGE_2 in CSF was observed between the two groups.

Binary logistic regression analysis was further performed to investigate the correlation between PD-D and TNF-α level in CSF (**Table 4**). The results suggested that the OR of TNF-α level was 1.035, and the 95% CI was 1.003–1.069 ($P < 0.05$) after the adjusting the risk factors of PD-D, including PIGD type, and the scores of HAMA-24 and UPDRS III scales observed in our previous study.

Comparisons of Neurotransmitters in CSF Between PD-D and PD-ND Groups

The levels of DA, 5-HT, and NE in CSF from PD-D and PD-ND groups were then compared (**Table 5**). It was observed that DA level in PD-D group was significantly reduced compared with that in PD-ND group. However, the levels of 5-HT and NE were not significantly different between the two groups.

TABLE 1 | Demographic variables, scores of motor function, non-motor symptoms, and ADL in PD with depression (PD-D) and PD with no depression (PD-ND) groups; $^{**}P < 0.01$, $^{*}P < 0.05$.

	PD-ND group (28 cases)	PD-D group (58 cases)	*P*
Demographic variables			
Female (*n*, %)	13 (46.43%)	27 (46.55%)	0.991
Age [year, median (Q1–Q3)]	60.50 (51.75–70.00)	60.00 (56.00–68.00)	0.938
Age of onset (year, $\overline{X} \pm s$)	57.39 ± 10.76	56.44 ± 9.30	0.676
Disease duration [year, median (Q1–Q3)]	3.00 (2.00–5.00)	3.00 (1.50–5.00)	0.683
Low education level (<9 years; *n*, %)	7 (25.00%)	28 (48.28%)	0.040*
Side of onset (*n*, %)	14 (50.00%)	26 (44.83%)	0.652
LEDD [mg, median (Q1–Q3)]	0.00 (0.00–1.87)	1.06 (0.00–2.25)	0.329
Motor function			
H–Y stage (*n*, %)			
Early stage (stage 1–2.5)	23 (82.14%)	51 (87.93%)	0.515
Advanced stage (stage 3–5)	5 (17.86%)	7 (12.07%)	
Total UPDRS III score [point, median (Q1–Q3)]	16.00 (12.00–29.25)	29.50 (20.75–42.00)	0.001**
Tremor	3.00 (2.00–7.50)	5.00 (3.00–7.00)	
Rigidity	2.00 (0.25–4.75)	5.00 (2.00–8.25)	
Bradykinesia	6.50 (4.25–12.00)	12.00 (8.00–17.00)	
Postural instability/gait difficulty	2.50 (2.00–4.00)	4.00 (2.00–6.00)	
Motor phenotypes (*n*, %)			
PIGD type	11 (39.29)	55 (94.83%)	<0.001**
TD type	6 (21.43%)	3 (5.17%)	
Mixed type	11 (39.29%)	0 (0.00%)	
Non-motor symptoms			
MoCA [point, median (Q1–Q3)]	21.50 (17.00–24.00)	18.50 (14.50–25.00)	0.631
HAMA-14 [point, median (Q1–Q3)]	2.00 (1.00–3.75)	10.00 (7.00–17.5)	<0.001**
FS-14 [point, median (Q1–Q3)]	7.00 (3.25–9.50)	10 (7.00–12.00)	0.003**
RBDSQ [point, median (Q1–Q3)]	1.00 (0.00–4.00)	4.00 (1.00–5.50)	0.018*
SCOPA-AUT [point, median (Q1–Q3)]	31.50 (28.25–36.25)	35.50 (31.00–40.75)	0.004**
RLSRS [point, median (Q1–Q3)]	0.00 (0.00–8.00)	0.00 (0.00–15.25)	0.108
ADL			
ADL [point, median (Q1–Q3)]	23.00 (20.00–30.75)	32.00 (23.75–43.00)	0.003**

TABLE 2 | Levels of neuroinflammatory factors in cerebrospinal fluid (CSF) from PD-D and PD-ND groups; *$P < 0.05$.

	PD-ND group (28 cases)	PD-D group (58 cases)	*P*
H_2O_2 [mmol/L, median (Q1–Q3)]	3.342 (1.931–12.532)	2.580 (1.973–9.772)	0.311
NO [mmol/L, median (Q1–Q3)]	53.892 (42.784–75.000)	52.821 (35.682–74.603)	0.839
TNF-α [pg/ml, median (Q1–Q3)]	21.530 (17.054–33.689)	31.321 (19.682–73.178)	0.027*
IL-1β [pg/ml, median (Q1–Q3)]	12.401 (10.297–22.112)	17.078 (11.079–23.522)	0.394
IL-6 [pg/ml, median (Q1–Q3)]	3.436 (1.885–5.552)	3.498 (1.885–5.802)	0.749
PGE_2 [pg/ml, median (Q1–Q3)]	13.096 (3.692–16.004)	10.043 (5.540–15.621)	0.847

H_2O_2, hydrogen peroxide; NO, nitric oxide; TNF-α, tumor necrosis factor-α; IL-1β, interleukin-1β; IL-6, interleukin-6; PGE_2, prostaglandin E_2.

The Relationship Between Neuroinflammatory Factors and Neurotransmitters in CSF From PD-D Group

The correlational analysis between DA and TNF-α level in CSF from PD-D group was further conducted. The results showed that DA level in CSF had a significant and negative correlation with TNF-α level in CSF from PD-D group ($r = -0.320$, $P = 0.003$).

TABLE 3 | Correlation between the score of 24-item Hamilton Depression Scale (HAMD-24) and the levels of neuroinflammatory factors in CSF from PD patients; *$P < 0.05$.

	R	*P*
H_2O_2	−0.176	1.704
NO	−0.016	0.882
TNF-α	0.247	0.022*
IL-1β	0.004	0.970
IL-6	0.145	0.260
PGE_2	0.068	0.534

H_2O_2, hydrogen peroxide; NO, nitric oxide; TNF-α, tumor necrosis factor-α; IL-1β, interleukin-1β; IL-6, interleukin-6; PGE_2, prostaglandin E_2.

DISCUSSION

In this study, 63.15% of all patients was diagnosed with PD-D. Compared with PD-ND group, PD-D group had significantly severer motor symptoms, more non-motor symptoms, and poor ADL (**Table 1**). This is the same with our previous research, which indicated that motor symptoms, PIGD type, anxiety, and fatigue were the significant influencing factors of PD-D (Lian et al., 2018).

Increasing evidences indicated that neuroinflammation featured by the microglial overactivation plays a vital role on the pathogenesis and progression of neurodegenerative disorders, like PD (Streit et al., 1999; Olson and Miller, 2004; Li and Zhang, 2016). Autopsy results from PD brains showed the overactivated microglia in the substantia nigra (McGeer et al., 1988). Microglia, accounting for about 10% of glial cells, are the immune cells in the brain and protect human body against damage through eliminating harmful irritants, pathogens, and dead cells (Cláudio et al., 2013) under normal conditions. However, when brain homeostasis is disturbed by various stimuli, microglia are overactivated and initiate neuroinflammatory process, robustly producing series of neuroinflammatory factors, including TNF-α, IL-1β, IL-6, etc. (Hanisch, 2002; Wilms et al., 2007), as well as a variety of harmful free radicals, such as H_2O_2 and NO (Block et al., 2007; Gao et al., 2012). In the PD animal model, it was found that microglial activation resulted in pathogenic changes of α-synuclein, which consequently led to Lewy body formation (Theodore et al., 2008). Neuroinflammation causes DA neuronal death, and the dead neurons release the content, for example, α-synuclein, etc., into extracellular spaces, further evoking microglial activation and progressive DA neurodegeneration. Therefore, neuroinflammation is an important mechanism underlying the development and deterioration of PD (Alcalay, 2016).

Depression was considered to be a microglial disease (Yirmiya et al., 2015). In a mouse model of depression induced by a strong pathogen lipopolysaccharide (LPS), the expression of Toll-like receptor 2 in microglia was evidently increased, while RNA levels of neuroinflammatory factors, such as IL-1β and IL-6, in the cortex and hippocampus were significantly enhanced. Minocycline, a tetracycline antibiotic, significantly reduced the levels of the above neuroinflammatory factors and thus improved depressive symptoms, indicating that depression was closely related to microglial activation. Thus, anti-neuroinflammatory drugs improved depressive symptoms by reducing microglial activation (Henry et al., 2008).

In this investigation, an array of neuroinflammatory factors, including H_2O_2, NO, TNF-α, IL-1β, IL-6, and PGE_2 in CSF from PD patients, were measured and compared. The results demonstrated that TNF-α level in CSF from PD-D group was prominently elevated compared with that from PD-ND group (**Table 2**). Further analysis indicated that the severer the depressive symptoms, the higher the TNF-α level in CSF (**Table 3**), and this close correlation was still strong after adjusting the risk factors of PD-D (**Table 4**). It was confirmed that in PD patients, a variety of pathological processes led to microglial activation, which might contribute to DA neuronal death by releasing cytotoxic inflammatory factors, such as TNF-α, IL-1β, IL-6, and so on. Among all these factors, TNF-α was a strong neuroinflammatory factor involved. It might have a direct damaging effect on DA neurons by activating an intracellular death pathway coupled with its receptor expressed on the cell surface. The neuroinflammatory factor might also stimulate the expression of iNOS within microglial (and possibly astroglial) cells and lead to the production of toxic amounts of NO, H_2O_2, etc. In turn, these free radicals could potentiate the expression

TABLE 4 | Binary logistic regression analysis of TNF-α in CSF from PD-D group; *$P < 0.05$.

	B	OR	95% CI	*P*
HAMA-24 score	0.032	1.033	0.968–1.102	0.333
PIGD type	0.478	1.613	1.176–2.213	0.003
UPDRS III score	−2.573	0.076	0.008–0.75	0.027
FS-14 score	0.007	1.007	0.748–1.356	0.962
TNF-α level in CSF	0.034	1.035	1.002–1.069	0.039*
Constant number	−3.429	0.032		0.023

The model corrects HAMA score, PIGD type, UPDRS III score, and FS score. HAMA-14, 14-item Hamilton Anxiety Scale; PIGD, postural instability and gait difficulty; UPDRS III, Unified Parkinson's Disease Rating Scale III; FS-14, 14-item Chalder Fatigue Scale; TNF-α, tumor necrosis factor-α.

TABLE 5 | Levels of neurotransmitters in CSF from PD-D and PD-ND groups; *$P < 0.05$.

	PD-ND group (28 cases)	PD-D group (58 cases)	*P*
DA (fg/ml, $\overline{X} \pm s$)	7.6111 ± 2.510	6.232 ± 2.151	0.011*
5-HT (fg/ml, $\overline{X} \pm s$)	18.459 ± 7.373	14.892 ± 8.367	0.061
NE (fg/ml, $\overline{X} \pm s$)	502.111 ± 124.634	497.076 ± 125.207	0.865

DA, dopamine; 5-HT, 5-hydroxytryptamine; NE, norepinephrine.

and release of TNF-α by adjacent microglial cells, thereby amplifying further the inflammatory reaction (Chertoff et al., 2011). Therefore, TNF-α plays an important role in the loss of DA neurons.

TNF-α could be detrimental or protective under different context. TNF-α mediated biological reactions through TNF receptor I and II (TNF-RI and TNF-RII; Montgomery and Bowers, 2012), both of which were homologous single-channel transmembrane glycoproteins with different structures. TNF-α was believed to elicit cytotoxicity and apoptosis when it was combined with TNF-RI, and promote cell survival, proliferation, and protective cellular responses when it was combined with TNF-RII (Hanisch, 2002). These differential effects of TNF-RI and TNF-RII are dependent on cell type, environment, age, and the activation status of those cells (Montgomery and Bowers, 2012). It was also found that there were specific regional differences and dual effects of TNF-α signaling in the brain; for example, TNF-α was a promoter of neurodegeneration in the striatum and a protector of neurodegeneration in the hippocampus (Sriram et al., 2006). Moreover, the effect of TNF-α on brain may be determined by the level and time of expression. Chronic expression of low TNF-α level reduced the nigrostriatal neurodegeneration, while high TNF-α level induced progressive neuronal loss (Chertoff et al., 2011). In PD patients, neuroinflammation plays key roles in the dysfunction and death of DA neurons. It was reported that the levels of both TNF-α and TNF-RI in the striatum and substantia nigra were significantly increased (Mogi et al., 2000; McCoy et al., 2006). TNF-α immunoreactive glial cells were found in the substantia nigra of PD patients but not in those of healthy controls (Boka et al., 1994). Dopaminergic neurons might be sensitive to TNF-α, and the elevated TNF-α may lead to DA neuronal death in PD. In this study, it was found that the higher the level of TNF-α in CSF, the severer the symptoms of depression in PD patients. Hence, we speculated that the elevated TNF-α might be predominantly combined with TNF-RI and produce oxidation–reduction reaction, accordingly playing a significantly negative role on PD-D.

The pathophysiology of PD-D might be related to the changes in neurotransmitter systems (Remy et al., 2005). However, there are very limited studies on the levels of neurotransmitters in CSF from PD-D group. In this investigation, a line of neurotransmitters, including DA, 5-HT, and NE in CSF from PD-D and PD-ND groups, were measured and compared. The results indicated that, compared with 5-HT and NE, DA level in PD-D group was significantly reduced compared with that in PD-ND group, indicating a more important role of DA on PD-D than 5-HT and NE (Lian et al., 2018).

Since neuroinflammatory factor TNF-α and neurotransmitter DA were both highly associated with PD-D, we then asked the question of whether there was a relationship between TNF-α and DA in CSF from the PD-D group. Thus, we finally performed correlational analysis between them, and the results revealed that the higher the TNF-α level, the lower the DA level in CSF from PD-D group, indicating that DA neurons in PD-D brains might be highly susceptible to the damage induced by neuroinflammatory factor TNF-α (McGeer and McGeer, 2008). In the LPS-induced PD animal model, neuroinflammation indicated by microglial overactivation specifically caused permanent damage to DA neurons in the substantia nigra but not to γ-aminobutyric acid neurons in the cortex (Herrera et al., 2000). Here, we inferred that neuroinflammation indicated by the significantly enhanced TNF-α in CSF might cause serious damage to DA neurons and consequent dramatic depletion of DA, which was correlated to the occurrence and progression of PD-D.

This study has the following limitations. It was difficult to obtain CSF from all PD patients due to old age, hyperostosis, etc. Currently, we are collecting CSF from PD patients with the aim of confirming the results from the current study. Because an observational study is limited for drawing final conclusions, a longitudinal study is being performed to figure out the correlations among depression, the levels of neuroinflammatory factors, and neurotransmitters in CSF from PD patients for a prolonged period.

DATA AVAILABILITY STATEMENT

The raw data supporting the conclusions of this article will be made available by the authors, without undue reservation.

ETHICS STATEMENT

The studies involving human participants were reviewed and approved by Beijing Tiantan Hospital ethics committee. The patients/participants provided their written informed consent to participate in this study.

AUTHOR CONTRIBUTIONS

T-hL: drafted the manuscript, study design, analysis of data, accepts responsibility for conduct of research, gave final approval, acquisition of data, and statistical analysis. PG: analysis of data, acquisition of data, accepts responsibility for the conduct of research, and gave final approval. Y-nZ, W-jZ, H-yG, and X-mW: accepts responsibility for the conduct of research, and gave final approval. J-hL: assisted in drafting the manuscript, accepts responsibility for the conduct of research, and gave final approval. L-xL, D-yD, and D-nL: acquisition of data, accepts responsibility for the conduct of research, and gave final approval. W-jZ: study design, analysis of data, accepts responsibility for the conduct of research, gave final approval, acquisition of data, statistical analysis, and study supervision.

FUNDING

This work was supported by the National Key Research and Development Program of China (2016YFC1306000 and 2016YFC1306300); the National Key R&D Program of China–European Commission Horizon 2020 (2017YFE0118800-779238); the National Natural Science Foundation of China (81970992, 81571229, 81071015, and 30770745); the Key Technology R&D Program of the Beijing Municipal Education Commission (kz201610025030); the Key Project of the Natural Science Foundation of Beijing, China (4161004); the Natural Science Foundation of Beijing, China (7082032); the Project of Scientific and Technological Development of Traditional Chinese Medicine in Beijing (JJ2018-48); the Capital Clinical Characteristic Application Research (Z121107001012161); the High Level Technical Personnel Training Project of Beijing Health System, China (2009-3-26); the Project of Beijing Institute for Brain Disorders (BIBD-PXM2013_014226_07_000084); the Excellent Personnel Training Project of Beijing, China (20071D0300400076); Important National Science and Technology Specific Projects (2011ZX09102-003-01); the National Key Technology Research and Development Program of the Ministry of Science and Technology of China (2013BAI09B03); the Project of Construction of Innovative Teams and Teacher Career Development for Universities and Colleges Under Beijing Municipality (IDHT20140514); Beijing Healthcare Research Project, China (JING-15-2); the Basic-Clinical Research Cooperation Funding of Capital Medical University, China (2015-JL-PT-X04, 10JL49, and 14JL15); the Natural Science Foundation of Capital Medical University, Beijing, China (PYZ2018077); and Youth Research Funding, Beijing Tiantan Hospital, Capital Medical University, China (2015-YQN-14, 2015-YQN-15, and 2015-YQN-17).

REFERENCES

Alcalay, R. N. (2016). Cytokines as potential biomarkers of Parkinson disease. *JAMA Neurol.* 73, 1282–1284. doi: 10.1001/jamaneurol.2016.3335

Block, M. L., Zecca, L., and Hong, J. S. (2007). Microglia-mediated neurotoxicity: uncovering the molecular mechanisms. *Nat. Rev. Neurosci.* 8, 57–69. doi: 10.1038/nrn2038

Boka, G., Anglade, P., Wallach, D., Javoy-Agid, F., Agid, Y., and Hirsch, E. C. (1994). Immunocytochemical analysis of tumor necrosis factor and its receptors in Parkinson's disease. *Neurosci. Lett.* 172, 151–154. doi: 10.1016/0304-3940(94)90684-x

Chalder, T., Berelowitz, G., Pawlikowska, T., Watts, L., Wessely, S., Wright, D., et al. (1993). Development of a fatigue scale. *J. Psychosom. Res.* 37, 147–153. doi: 10.1016/0022-3999(93)90081-p

Chen, L., Xue, L., Zheng, J., Tian, X., Zhang, Y., and Tong, Q. (2019). PPARss/delta agonist alleviates NLRP3 inflammasome-mediated neuroinflammation in the MPTP mouse model of Parkinson's disease. *Behav. Brain Res.* 356, 483–489. doi: 10.1016/j.bbr.2018.06.005

Chertoff, M., Di Paolo, N., Schoeneberg, A., Depino, A., Ferrari, C., Wurst, W., et al. (2011). Neuroprotective and neurodegenerative effects of the chronic expression of tumor necrosis factor α in the nigrostriatal dopaminergic circuit of adult mice. *Exp. Neurol.* 227, 237–251. doi: 10.1016/j.expneurol.2010.11.010

Cláudio, N., Dalet, A., Gatti, E., and Pierre, P. (2013). Mapping the crossroads of immune activation and cellular stress response pathways. *EMBO J.* 32, 1214–1224. doi: 10.1038/emboj.2013.80

Cosentino, C., Nuñez, Y., and Torres, L. (2013). Frequency of non-motor symptoms in Peruvian patients with Parkinson's disease. *Arq. Neuropsiquiatr.* 71, 216–219. doi: 10.1590/0004-282x20130005

Felger, J. C., Haroon, E., Patel, T. A., Goldsmith, D. R., Wommack, E. C., Woolwine, B. J., et al. (2020). What does plasma CRP tell us about peripheral and central inflammation in depression? *Mol. Psychiatry* 25, 1301–1311. doi: 10.1038/s41380-018-0096-3

Gao, H. M., Zhou, H., and Hong, J. S. (2012). NADPH oxidases: novel therapeutic targets for neurodegenerative diseases. *Trends Pharmacol. Sci.* 33, 295–303. doi: 10.1016/j.tips.2012.03.008

Goodarzi, Z., Mrklas, K. J., Roberts, D. J., Jette, N., Pringsheim, T., and Holroyd-Leduc, J. (2016). Detecting depression in Parkinson disease: a systematic review and meta-analysis. *Neurology* 87, 426–437. doi: 10.1212/wnl.0000000000002898

Hamilton, M. (1959). The assessment of anxiety states by rating. *Br. J. Med. Psychol.* 32, 50–55. doi: 10.1111/j.2044-8341.1959.tb00467.x

Hanisch, U. K. (2002). Microglia as a source and target of cytokines. *Glia* 40, 140–155. doi: 10.1002/glia.10161

Henry, C. J., Huang, Y., Wynne, A., Hanke, M., Himler, J., Bailey, M. T., et al. (2008). Minocycline attenuates lipopolysaccharide (LPS)-induced neuroinflammation, sickness behavior, and anhedonia. *J. Neuroinflammation* 5:15. doi: 10.1186/1742-2094-5-15

Herrera, A. J., Castaño, A., Venero, J. L., Cano, J., and Machado, A. (2000). The single intranigral injection of LPS as a new model for studying the selective effects of inflammatory reactions on dopaminergic system. *Neurobiol. Dis.* 7, 429–447. doi: 10.1006/nbdi.2000.0289

Holroyd, S., Currie, L. J., and Wooten, G. F. (2005). Depression is associated with impairment of ADL, not motor function in Parkinson disease. *Neurology* 64, 2134–2135. doi: 10.1212/01.WNL.0000165958.12724.0D

Hoops, S., Nazem, S., Siderowf, A. D., Duda, J. E., Xie, S. X., Stern, M. B., et al. (2009). Validity of the MoCA and MMSE in the detection of MCI and dementia in Parkinson disease. *Neurology* 73, 1738–1745. doi: 10.1212/WNL.0b013e3181c34b47

Hu, Y., Yu, S. Y., Zuo, L. J., Cao, C. J., Wang, F., Chen, Z. J., et al. (2015). Parkinson disease with REM sleep behavior disorder: features, α-synuclein, and inflammation. *Neurology* 84, 888–894. doi: 10.1212/WNL.0000000000001308

Jankovic, J. (2008). Parkinson's disease: clinical features and diagnosis. *J. Neurol. Neurosurg. Psychiatry* 79, 368–376. doi: 10.1136/jnnp.2007.131045

Jankovic, J., McDermott, M., Carter, J., Gauthier, S., Goetz, C., Golbe, L., et al. (1990). Variable expression of Parkinson's disease: a base-line analysis of the DATATOP cohort. The Parkinson Study Group. *Neurology* 40, 1529–1534. doi: 10.1212/wnl.40.10.1529

Kohler, O., Krogh, J., Mors, O., and Benros, M. E. (2016). Inflammation in depression and the potential for anti-inflammatory treatment. *Curr. Neuropharmacol.* 14, 732–742. doi: 10.2174/1570159x14666151208113700

Li, T., and Zhang, S. (2016). Microgliosis in the injured brain: infiltrating cells and reactive microglia both play a role. *Neuroscientist* 22, 165–170. doi: 10.1177/1073858415572079

Lian, T. H., Guo, P., Zuo, L. J., Hu, Y., Yu, S. Y., Liu, L., et al. (2018). An investigation on the clinical features and neurochemical changes in Parkinson's disease with depression. *Front. Psychiatry* 9:723. doi: 10.3389/fpsyt.2018.00723

Lindqvist, D., Hall, S., Surova, Y., Nielsen, H. M., Janelidze, S., Brundin, L., et al. (2013). Cerebrospinal fluid inflammatory markers in Parkinson's disease—associations with depression, fatigue and cognitive impairment. *Brain Behav. Immun.* 33, 183–189. doi: 10.1016/j.bbi.2013.07.007

McCoy, M. K., Martinez, T. N., Ruhn, K. A., Szymkowski, D. E., Smith, C. G., Botterman, B. R., et al. (2006). Blocking soluble tumor necrosis factor signaling with dominant-negative tumor necrosis factor inhibitor attenuates loss of dopaminergic neurons in models of Parkinson's disease. *J. Neurosci.* 26, 9365–9375. doi: 10.1523/JNEUROSCI.1504-06.2006

McGeer, P. L., Itagaki, S., Boyes, B. E., and McGeer, E. G. (1988). Reactive microglia are positive for HLA-DR in the substantia nigra of Parkinson's and Alzheimer's disease brains. *Neurology* 38, 1285–1291. doi: 10.1212/wnl.38.8.1285

McGeer, P. L., and McGeer, E. G. (2008). Glial reactions in Parkinson's disease. *Mov. Disord.* 23, 474–483. doi: 10.1002/mds.21751

Mogi, M., Togari, A., Kondo, T., Mizuno, Y., Komure, O., Kuno, S., et al. (2000). Caspase activities and tumor necrosis factor receptor R1 (p55) level are elevated in the substantia nigra from parkinsonian brain. *J. Neural Transm.* 107, 335–341. doi: 10.1007/s007020050028

Montgomery, S. L., and Bowers, W. J. (2012). Tumor necrosis factor-α and the roles it plays in homeostatic and degenerative processes within the central nervous system. *J. Neuroimmune Pharmacol.* 7, 42–59. doi: 10.1007/s11481-011-9287-2

Olson, J. K., and Miller, S. D. (2004). Microglia initiate central nervous system innate and adaptive immune responses through multiple TLRs. *J. Immunol.* 173, 3916–3924. doi: 10.4049/jimmunol.173.6.3916

Postuma, R. B., Berg, D., Stern, M., Poewe, W., Olanow, C. W., Oertel, W., et al. (2015). MDS clinical diagnostic criteria for Parkinson's disease. *Mov. Disord.* 30, 1591–1601. doi: 10.1002/mds.26424

Reijnders, J. S., Ehrt, U., Weber, W. E., Aarsland, D., and Leentjens, A. F. (2008). A systematic review of prevalence studies of depression in Parkinson's disease. *Mov. Disord.* 23, 183–189; quiz 313. doi: 10.1002/mds.21803

Remy, P., Doder, M., Lees, A., Turjanski, N., and Brooks, D. (2005). Depression in Parkinson's disease: loss of dopamine and noradrenaline innervation in the limbic system. *Brain* 128, 1314–1322. doi: 10.1093/brain/awh445

Sanjari Moghaddam, H., Valitabar, Z., Ashraf-Ganjouei, A., Mojtahed Zadeh, M., Ghazi Sherbaf, F., and Aarabi, M. H. (2018). Cerebrospinal fluid C-reactive protein in Parkinson's disease: associations with motor and non-motor symptoms. *Neuromolecular Med.* 20, 376–385. doi: 10.1007/s12017-018-8499-5

Sriram, K., Matheson, J. M., Benkovic, S. A., Miller, D. B., Luster, M. I., and O'Callaghan, J. P. (2006). Deficiency of TNF receptors suppresses microglial activation and alters the susceptibility of brain regions to MPTP-induced neurotoxicity: role of TNF-α. *FASEB J.* 20, 670–682. doi: 10.1096/fj.05-5106com

Starkstein, S., Dragovic, M., Jorge, R., Brockman, S., Merello, M., Robinson, R. G., et al. (2011). Diagnostic criteria for depression in Parkinson's disease: a study of symptom patterns using latent class analysis. *Mov. Disord.* 26, 2239–2245. doi: 10.1002/mds.23836

Streit, W. J., Walter, S. A., and Pennell, N. A. (1999). Reactive microgliosis. *Prog. Neurobiol.* 57, 563–581. doi: 10.1016/s0301-0082(98)00069-0

Theodore, S., Cao, S., Mclean, P. J., and Standaert, D. G. (2008). Targeted overexpression of human α-synuclein triggers microglial activation and an adaptive immune response in a mouse model of Parkinson disease. *J. Neuropathol. Exp. Neurol.* 67, 1149–1158. doi: 10.1097/nen.0b013e31818e5e99

Tian, L., Sun, S. S., Cui, L. B., Wang, S. Q., Peng, Z. W., Tan, Q. R., et al. (2020). Repetitive transcranial magnetic stimulation elicits antidepressant- and anxiolytic-like effect *via* nuclear factor-E2-related factor 2-mediated anti-inflammation mechanism in rats. *Neuroscience* 429, 119–133. doi: 10.1016/j.neuroscience.2019.12.025

Visser, M., Marinus, J., Stiggelbout, A. M., and Van Hilten, J. J. (2004). Assessment of autonomic dysfunction in Parkinson's disease: the SCOPA-AUT. *Mov. Disord.* 19, 1306–1312. doi: 10.1002/mds.20153

Walters, A. S., Lebrocq, C., Dhar, A., Hening, W., Rosen, R., Allen, R. P., et al. (2003). Validation of the international restless legs syndrome study group rating scale for restless legs syndrome. *Sleep Med.* 4, 121–132. doi: 10.1016/s1389-9457(02)00258-7

Wang, S., Jing, H., Yang, H., Liu, Z., Guo, H., Chai, L., et al. (2015). Tanshinone I selectively suppresses pro-inflammatory genes expression in activated microglia and prevents nigrostriatal dopaminergic neurodegeneration in a mouse model of Parkinson's disease. *J. Ethnopharmacol.* 164, 247–255. doi: 10.1016/j.jep.2015.01.042

Wang, F., Yu, S. Y., Zuo, L. J., Cao, C. J., Hu, Y., Chen, Z. J., et al. (2016). Excessive iron and α-synuclein oligomer in brain are relevant to pure apathy in Parkinson disease. *J. Geriatr. Psychiatry Neurol.* 29, 187–194. doi: 10.1177/0891988716632918

Wilms, H., Zecca, L., Rosenstiel, P., Sievers, J., Deuschl, G., and Lucius, R. (2007). Inflammation in Parkinson's diseases and other neurodegenerative diseases: cause and therapeutic implications. *Curr. Pharm. Des.* 13, 1925–1928. doi: 10.2174/138161207780858429

Yirmiya, R., Rimmerman, N., and Reshef, R. (2015). Depression as a microglial disease. *Trends Neurosci.* 38, 637–658. doi: 10.1016/j.tins.2015.08.001

Zea-Sevilla, M. A., and Martínez-Martin, P. (2014). Rating scales and questionnaires for assessment of sleep disorders in Parkinson's disease: what they inform about? *J. Neural Transm.* 121, S33–S40. doi: 10.1007/s00702-014-1217-z

Zhuo, C., Xue, R., Luo, L., Ji, F., Tian, H., Qu, H., et al. (2017). Efficacy of antidepressive medication for depression in Parkinson disease: a network meta-analysis. *Medicine* 96:e6698. doi: 10.1097/md.0000000000006698

Conflict of Interest: The authors declare that the research was conducted in the absence of any commercial or financial relationships that could be construed as a potential conflict of interest.

Copyright © 2020 Lian, Guo, Zhang, Li, Li, Ding, Li, Zhang, Guan, Wang and Zhang. This is an open-access article distributed under the terms of the Creative Commons Attribution License (CC BY). The use, distribution or reproduction in other forums is permitted, provided the original author(s) and the copyright owner(s) are credited and that the original publication in this journal is cited, in accordance with accepted academic practice. No use, distribution or reproduction is permitted which does not comply with these terms.

frontiers in Aging Neuroscience

ORIGINAL RESEARCH
published: 04 November 2020
doi: 10.3389/fnagi.2020.588085

Corticospinal Tract Impairment of Patients With Parkinson's Disease: Triple Stimulation Technique Findings

*Dan Xu, Qingyun Ding and Han Wang**

Department of Neurology, Peking Union Medical College Hospital, Chinese Academy of Medical Sciences, Beijing, China

Background: Corticospinal tract impairment is no longer an absolute exclusion in the updated Movement Disorder Society Parkinson's disease criteria. Triple stimulation technique (TST) is an accurate method to quantitatively assess the integrity and impairment of corticospinal pathway in a variety of neurological diseases. This study aims to evaluate the corticospinal tract impairment in Parkinson's disease (PD) patients using TST.

Methods: Ten PD patients, 19 multiple-system atrophy parkinsonian variant (MSA-P) patients, and 12 healthy controls (HC) were sequentially recruited in this study. Information of age, disease duration, pyramidal signs, and Hoehn and Yahr (H&Y) stage was obtained from all patients. The TST was assessed at right abductor digiti minimi for HCs and both sides for patients. The Chi-square test was used for categorical variables, and variance analysis was performed for continuous variables in comparing the difference among PD, MSA-P, and HC, plus the *post hoc* tests for pairwise comparisons.

Results: All subjects were age and gender matched. There was no significant difference in disease duration ($p = 0.855$), H-Y stage ($p = 0.067$), and the percentage of pyramidal signs present ($p = 0.581$) between MSA-P and PD patients. The mean TST ratio was 55.5 ± 32.2%, 81.7 ± 19.8%, and 96.8 ± 3.0% for PD, MSA-P, and HCs, correspondingly. PD patients had a significant lower TST amplitude ratio than MSA-P and HCs. The TST ratio of MSA-P was lower than HCs, but there was no significant difference ($p = 0.160$). Additionally, it was significantly higher in percentage of abnormal TST ratio between PD patients and MSA-P ($p = 0.010$).

Conclusion: Corticospinal tract impairment is not a rare manifestation in PD and can be quantitatively evaluated with TST. The result needs to be verified in amplified sample.

Keywords: Parkinson's disease, multiple system atrophy, triple stimulation technique, corticospinal tract, pyramidal sign

OPEN ACCESS

Edited by:
Pingyi Xu,
First Affiliated Hospital of Guangzhou Medical University, China

Reviewed by:
Hao Deng,
Central South University, China
Liu Jun,
Shanghai Jiao Tong University, China

***Correspondence:**
Han Wang
18600044179@163.com

Received: *28 July 2020*
Accepted: *09 October 2020*
Published: *04 November 2020*

Citation:
Xu D, Ding Q and Wang H (2020) Corticospinal Tract Impairment of Patients With Parkinson's Disease: Triple Stimulation Technique Findings. Front. Aging Neurosci. 12:588085. doi: 10.3389/fnagi.2020.588085

INTRODUCTION

Parkinson's disease (PD) is the second most common neurodegenerative disease worldwide with rising incidence and prevalence alongside a changing population demographic (Pringsheim et al., 2014). The complicated motor and non-motor symptoms suggest extensive involvement of the central, peripheral, and enteric nervous systems (Braak and Del Tredici, 2017). PD is more like

a syndrome than an entity. With the continuous development in our understanding of PD, the diagnostic criteria have been updated (Braak and Del Tredici, 2017). In 2015, the Movement Disorder Society (MDS) task force introduced the clinical diagnostic criteria for PD (Postuma et al., 2015). Several of the items differed from the United Kingdom (UK) Brain Bank criteria, which previously had been used widely. For instance, pyramidal tract impairment is recognized as one of the "red flags" for MDS-PD diagnosis, which is in contrast to the United Kingdom Brain Bank criteria that consider it an absolute exclusion (Hughes et al., 1992). This can cause confusion since multiple-system atrophy parkinsonian variant (MSA-P), a rare neurodegenerative disorder that often needs to be differentiated from PD, usually presents with pyramidal tract impairment (Gilman et al., 2008). Thus, it is worthwhile to investigate corticospinal tract impairment in both diseases.

There is some neuroimaging evidence that supports corticospinal tract impairment in PD. Over the past several years, important neuroimaging findings have revealed that PD is not confined to the nigrostriatal dopaminergic pathway and also involves the cortico-basal ganglia-thalamo-cortical neural network (Burciu and Vaillancourt, 2018). Taylor et al. (2018) observed significant increases in white matter fractional anisotropy (FA) in a widespread anatomical network that included the corticospinal tract and subcortical white matter in a 1-year longitudinal study that used diffusion tensor imaging (DTI). A meta-analysis of DTI studies in PD demonstrated that DTI was sensitive for identifying differences in the corticospinal tract between patients with PD and healthy controls (HCs) (Atkinson-Clement et al., 2017). The increased FA in the motor tract of PD suggested compensatory neuroplasticity or selective neurodegeneration (Mole et al., 2016). Evidence to support this has been reported in a transcranial magnetic stimulation (TMS) study. As a conventional electrophysiological tool, TMS was developed by Barker et al. in 1985 (Barker et al., 1985) and was used to non-invasively detect corticospinal or corticobulbar pathways (Groppa et al., 2012). Central motor conduction time (CMCT) of TMS represents the maximum conduction velocity of corticospinal axons (Cantello et al., 2002). A significant reduction in CMCT in patients with PD compared with healthy controls was first reported by Kandler et al. (1990). Other alterations of motor cortical function, such as decreased relaxed threshold and central silence period duration, have also been detected using TMS in patients with PD (Cantello et al., 2002). These neuroimaging and electrophysiological findings indicate structural and functional changes of the corticospinal tract in PD patients.

Compared with TMS, triple-stimulation technique (TST) is a more accurate method to quantitatively assess the integrity and impairment of the corticospinal pathway in a variety of diseases, such as multiple sclerosis (Magistris et al., 1999), amyotrophic lateral sclerosis (Rösler et al., 2000; Grapperon et al., 2014), and stroke (Tan et al., 2013). It has been demonstrated to be 2.75 times more sensitive than conventional TMS techniques for revealing corticospinal conduction blocks caused by severe demyelination or neurodegenerative processes (Magistris et al., 1999). The TST amplitude ratio reflects the proportion of the activated spinal motor neurons; $\geq$90% is considered normal, according to a previous study (Eusebio et al., 2007). In movement disorders, decreased TST ratios have been found in spinocerebellar ataxia type 6, while conventional TMS parameters were shown to be similar in controls (Sakuma et al., 2005). There have been a few studies using TST in PD patients, but none have reported abnormal TST results (Eusebio et al., 2007; Jang et al., 2014). However, given the evidence from the neuroimaging and neurophysiology studies, normal TST results in PD are surprising (Eusebio et al., 2007). A possible reason for these results is that both of the studies were performed before the MDS-PD criteria were being published (Postuma et al., 2015). Parkinsonian patients who had pyramidal signs had to be absolutely excluded from the diagnosis of PD, in accordance with the United Kingdom Brain Bank criteria (Hughes et al., 1992). To the best of our knowledge, no study since 2015 has assessed corticospinal tract involvement in PD using TST.

In this pilot study, we performed TST to quantitatively assess the involvement of the cortico-spinal tract in patients with clinically diagnosed PD, according to MDS-PD and MSA-P criteria.

MATERIALS AND METHODS

Subjects

We prospectively recruited 19 parkinsonian variant patients of probable MSA-P who satisfied the consensus criteria (Gilman et al., 2008), 10 clinically diagnosed late-onset PD patients who fulfilled the 2015 MDS-PD criteria (Postuma et al., 2015), and 12 age-matched HCs from the neurology department of Peking Union Medical College Hospital. We obtained demographic and clinical information, including age, symptom duration, pyramidal signs, and Hoehn and Yahr (H&Y) stage. Signs of pyramidal signs were defined as a positive Babinski or Chaddock sign that was documented in the patients' medical records. Otherwise, none of the patients had remarkable medical history that could explain the pyramidal signs. We acquired brain and spinal magnetic resonance images (MRIs). Participants who had MRI abnormalities that could affect the corticospinal pathway, such as lacunar infarctions, white matter lesions, or other lesions, were excluded from the study. All HCs had no remarkable medical history or signs on physical examination. All participants gave written informed consent.

Triple-Stimulation Technique

Electromyography of the bilateral abductor digiti-minimi (ADM) was recorded in MSA-P and PD patients from surface electrodes using a Viking IV electromyography machine (Nicolet Biomedical, Madison, WI, United States). In HCs, electromyography of the left ADM was recorded. Bandpass filters were set at 20–2000 Hz. We performed TST using the MagPro Compact stimulator (Dantec Company, Copenhagen, Denmark) and a standard figure-of-eight TMS coil. The coil was held tangentially to the scalp, at a 45° angle from the posterior–anterior axis, with the handle pointing posterior–laterally. The motor hotspot for ADM was identified by applying single-pulse

stimuli over the corresponding scalp area to evoke the largest motor-evoked potential (MEP).

Triple stimulation technique has been well described in previous studies (Magistris et al., 1999; Groppa et al., 2012). Examples of the TST recordings are shown in **Figure 1** (Magistris et al., 1998). Briefly, three stimuli with appropriate delays were given in a sequence as follows: TMS at the motor cortex, supramaximal electrical stimuli to the ulnar nerve at the wrist, and supramaximal electrical stimuli at Erb's point. Two collisions occurred, and we obtained the TST test. The first delay was calculated as the MEP latency minus the compound muscle action potential (CMAP) latency (at the wrist). The second delay was Erb's latency minus the CMAP latency (at the wrist). We then replaced the TMS at the motor cortex with the stimuli at Erb's point with an adjusted delay and acquired the TST control curve. Finally, we calculated the baseline-to-negative peak amplitude ratio using the following formula: TST amplitude ratio = TST test amplitude/TST control amplitude.

Statistical Analysis

The distribution of the categorical variables (gender, pyramidal signs, and H&Y stage) is presented as frequencies, and the continuous variables (age and disease duration) are presented as means ± standard deviations. A chi-square test was used for the categorical variables. For data with normal distributions, we used a one-way ANOVA and *post hoc* analyses to compare the TST ratios. All analyses were performed using the SPSS 22.0 software package.

RESULTS

Subjects

The demographic and clinical characteristics of the subjects are summarized in **Table 1**. Age and gender were comparable between patients and HCs. The mean disease duration of MSA-P and PD was 2.71 and 2.90 years, respectively. There was no significant difference in disease duration or H&Y stage between MSA-P and PD patients. Patients were divided into three subgroups on the basis of the presence or absence of pyramidal signs: unilaterally present, bilaterally present, and bilaterally absent. There was no significant difference between MSA-P and PD patients in the presence of pyramidal signs ($p = 0.393$) or the percentage of pyramidal signs present ($p = 0.581$).

TST

Data obtained from TST are summarized in **Table 2**. All HCs presented with TST ratios within the normal range (≥90%). The

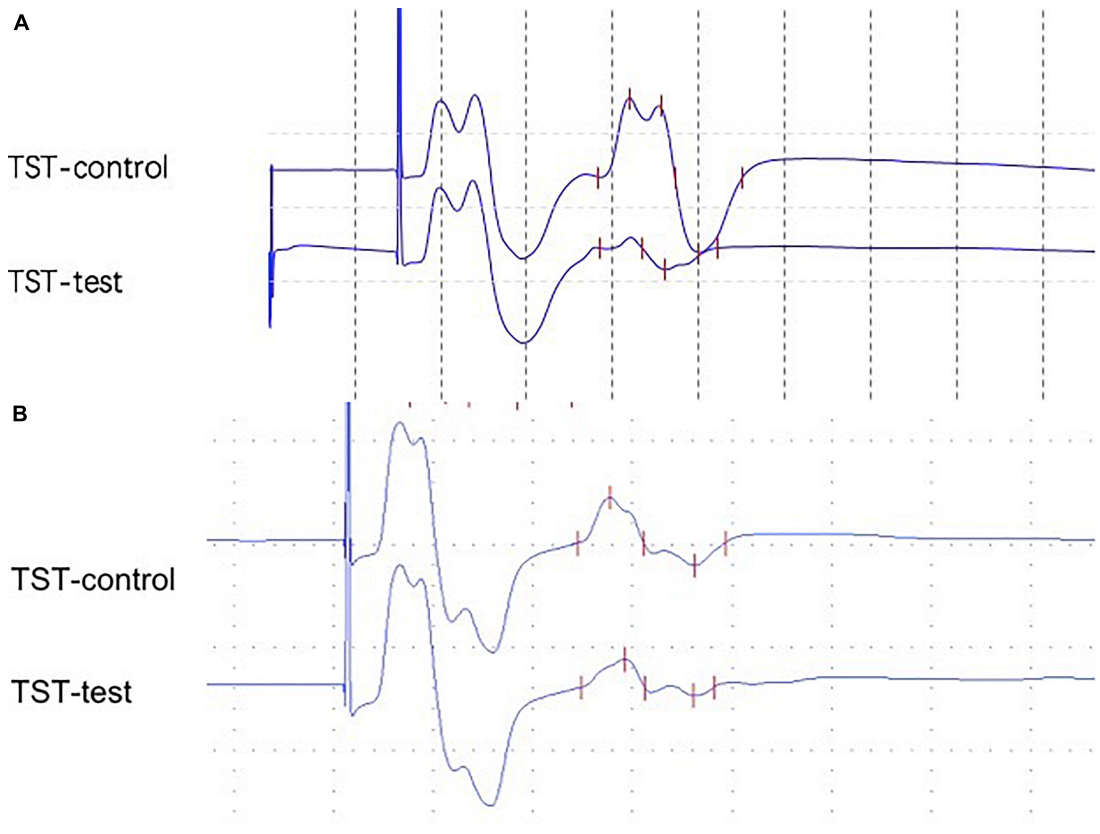


FIGURE 1 | (A) Abnormal TST ratio (21.0%) from a 59-year-old female with a 2-year PD (patient 21). **(B)** Abnormal TST ratio (53.0%) from a 48-year-old male with a 1-year MSA-P (patient 2).

TABLE 1 | Demographic and clinical characters of patients and healthy controls.

	PD (n = 10)	MSA-P (n = 19)	HC (n = 12)	p-value
Age (years)	59.3 ± 4.4	57.6 ± 7.7	54.6 ± 9.6	0.347
Gender (male/female)	5/5	10/9	10/2	0.167*
Disease duration (years)	2.90 ± 2.69	2.71 ± 2.59	NA	0.855
Age of symptom onset	56.4 ± 3.7	55.1 ± 6.3	NA	0.549
Pyramidal sign (number)			NA	0.393*
Unilaterally present	1	6		
Bilaterally present	4	7		
Absent	5	6		
Percentage of pyramidal sign present#	45.0%	52.6%	NA	0.581*
H&Y stage			NA	0.067*
Stage 1	6	4		
Stage 2	4	11		
Stage 3	0	4		
Stage 4	0	0		
Average	1.4 ± 0.5	2.0 ± 0.7	NA	

These values represent the mean ± standard deviation or the number of patients.
**Chi-squared test.*
#Percentage of pyramidal sign present = (number of unilaterally present + 2 × number of bilaterally present)/(the number of patient × 2) × 100%.
PD, Parkinson's disease; MSA-P, multiple-system atrophy parkinsonian variant; HCs, healthy controls; H&Y stage, Hoehn and Yahr stage; NA, not applicable.

TABLE 2 | Comparison of TST ratio in different groups.

	PD (n = 10)	MSA-P (n = 19)	HC (n = 12)	
TST ratio (%)	55.5 ± 32.2	81.7 ± 19.8	96.8 ± 3.0	
P-value*	0.000			
P-value (MSA-P and HC)	0.160			
P-value (PD and HC)	0.000			
P-value (MSA-P and PD)	0.010			
Percentage of abnormal TST ratio#	80.0%	36.8%	NA	p = 0.002

The TST ratio was presented as mean ± SD.
**One-way ANOVA, post hoc analysis was performed using the Scheffe test.*
#TST ratio<90% was considered abnormal. Percentage of abnormal TST ratio = (number of unilaterally abnormal + 2 × number of bilaterally abnormal)/(the number of patient × 2) × 100%.
MSA-P, multiple-system atrophy parkinsonian variant; PD, Parkinson's disease; HCs, healthy controls; TST, triple-stimulation technique; NA, not applicable.

TST ratio was significantly different among the three groups ($p < 0.001$). According to the *post hoc* analysis, PD patients had a significantly lower TST amplitude ratio (55.5 ± 32.2) compared with patients with MSA-P ($p = 0.010$) and HCs ($p < 0.001$). The TST ratio of patients with MSA-P (81.7 ± 19.8) was lower than that of HCs (96.8 ± 3.0), but this did not reach statistical significance ($p = 0.160$). Abnormal TST ratios (TST ratio <90%) were significantly more common in PD patients than in the other groups ($p = 0.002$). Representative TST curves of patients are shown in **Figure 1**. Detailed clinical and electrophysiological findings of patients and HCs are shown in **Supplementary Table 1**.

DISCUSSION

According to MDS-PD criteria, a parkinsonian patient with pyramidal signs might fulfill the diagnosis of clinically probable PD, provided that the patient has no absolute exclusion criteria or totals more than two red flags and has sufficient supportive criteria to counterbalance any red flags. All PD patients in this study were consistent with clinically probable PD. The presence of pyramidal signs in patients with PD and MSA-P in our study was 45 and 52.6%, respectively, which was not significantly different. Corticospinal tract impairment is common in patients with MSA-P. Pyramidal signs, which represent upper motor neuron (UMN) impairment, are considered one of the key clinical features of MSA-P (Eusebio et al., 2007). In a postmortem clinicopathological study of seven MSA-P cases, five patients had a positive Babinski sign. Furthermore, loss of Betz cells and presence of glial cytoplasmic inclusions in the primary motor cortex were confirmed by pathology examination in all cases, which was in accordance with UMN impairment (Tsuchiya et al., 2000). To the best of our knowledge, our study is the first to report pyramidal signs in PD.

The decreased TST ratios in our study also revealed profound corticospinal tract impairment in PD. Compared with MSA-P, TST ratio decreases in PD patients were much more prominent. A previous study reported cortico-spinal impairment in 50% of MSA-P patients, with a mean TST ratio of 86.6%

(Eusebio et al., 2007). TST ratios were lower in MSA-P patients than HCs; however, this was not statistically significant. In our study, the average TST ratios of MSA-P patients and HCs were 81.7 and 96.8%, respectively, which is consistent with previous studies (Eusebio et al., 2007; Jang et al., 2014). Neuroimaging studies have demonstrated corticospinal tract impairment in patients with PD using DTI (Atkinson-Clement et al., 2017; Taylor et al., 2018). Increased FA in the motor tracts of PD patients suggests either compensatory neuroplasticity or selective neurodegeneration (Mole et al., 2016). To the best of our knowledge, this is the first study showing corticospinal tract impairment using TST.

Although TST ratio decreases in PD might be consistent with previous neuroimaging and electrophysiologic evidence, it was surprising that the TST ratio was much lower in PD patients than in MSA-P patients. Given that there was no significant difference in disease duration or H&Y stage between MSA-P and PD patients, this can only be explained by the updated diagnostic criteria for PD. Our TST ratio results were also lower than previous reports using PD patients as a control group. Jang et al. (2014) compared TST ratios of patients with PD, patients with vascular Parkinsonism (VP), and HCs. They found that the TST ratio of PD patients was similar to that of HCs (96.42 $\pm$ 5.11 vs. 97.70 $\pm$ 3.82%) and significantly higher than that of VP patients (71.59 $\pm$ 11.86%). Eusebio et al. (2007) reported that the TST ratio of PD patients was 99.1%, which was not different from HCs. Both of these studies were performed before the MDS-PD criteria were published; therefore, the pyramidal signs were absent. In contrast, pyramidal signs were present in almost half of the PD patients in our study, which might be directly associated with our TST findings.

There are shortcomings in our study. First, the sample size was limited. Further studies of TST with a larger sample are encouraged to explicitly investigate corticospinal pathway impairment in PD patients. Second, during the examination of pyramidal signs, no quantitative evaluation or interrater reliability analyses were performed, which may have introduced bias in the pyramidal sign results. Third, the neuroimaging methods used to determine abnormalities were performed in different hospitals. Therefore, the differences in scanning conditions may also have introduced bias. Repeated standardized neuroimaging data are necessary to fully exclude alternative causes of pyramidal signs in future studies. Finally, no neuroimaging sequence specific to corticospinal tract evaluation, such as DTI, was acquired.

In summary, our study showed profound decreases in TST ratios in patients with clinically probable PD. The results suggest that corticospinal tract impairment is not rare in PD and therefore warrants further observation and investigation. TST could be used to quantitatively evaluate corticospinal tract impairment and further our understanding of the pathophysiology of PD.

DATA AVAILABILITY STATEMENT

The raw data supporting the conclusions of this article will be made available by the authors, without undue reservation.

ETHICS STATEMENT

The studies involving human participants were reviewed and approved by the Ethics Committee of Peking Union Medical College Hospital. The patients/participants provided their written informed consent to participate in this study. Written informed consent was obtained from the individual(s) for the publication of any potentially identifiable images or data included in this article.

AUTHOR CONTRIBUTIONS

DX: analyse the data and writing the article. QYD: perform all the TST and data collection. HW: design the study, recruit patients, and revise the article. All authors contributed to the article and approved the submitted version.

FUNDING

This research was supported by the Non-profit Central Research Institute Fund of Chinese Academy of Medical Science. Fund number: NWB20204179.

SUPPLEMENTARY MATERIAL

The Supplementary Material for this article can be found online at: https://www.frontiersin.org/articles/10.3389/fnagi.2020.588085/full#supplementary-material

REFERENCES

Atkinson-Clement, C., Pinto, S., Eusebio, A., and Coulon, O. (2017). Diffusion tensor imaging in Parkinson's disease: review and meta-analysis. *Neuroimage Clin.* 16, 98–110. doi: 10.1016/j.nicl.2017.07.011

Barker, A. T., Jalinous, R., and Freeston, I. L. (1985). Non-invasive magnetic stimulation of human motor cortex. *Lancet* 1, 1106–1107. doi: 10.1016/s0140-6736(85)92413-4

Braak, H., and Del Tredici, K. (2017). Neuropathological staging of brain pathology in sporadic Parkinson's disease: separating the wheat from the chaff. *J. Parkinsons Dis.* 7, S71–S85. doi: 10.3233/jpd-179001

Burciu, R. G., and Vaillancourt, D. E. (2018). Imaging of motor cortex physiology in Parkinson's Disease. *Mov. Disord.* 33, 1688–1699. doi: 10.1002/mds.102

Cantello, R., Tarletti, R., and Civardi, C. (2002). Transcranial magnetic stimulation and Parkinson's disease. *Brain Res. Brain Res. Rev.* 38, 309–327. doi: 10.1016/s0165-0173(01)00158-8

Eusebio, A., Azulay, J. P., Witjas, T., Rico, A., and Attarian, S. (2007). Assessment of cortico-spinal tract impairment in multiple system atrophy using transcranial magnetic stimulation. *Clin. Neurophysiol.* 118, 815–823. doi: 10.1016/j.clinph.2007.01.004

Gilman, S., Wenning, G. K., Low, P. A., Brooks, D. J., Mathias, C. J., Trojanowski, J. Q., et al. (2008). Second consensus statement on the diagnosis of multiple

system atrophy. *Neurology* 71, 670–676. doi: 10.1212/01.wnl.0000324625.00404.15

Grapperon, A. M., Verschueren, A., Duclos, Y., Confort-Gouny, S., Soulier, E., Loundou, A. D., et al. (2014). Association between structural and functional corticospinal involvement in amyotrophic lateral sclerosis assessed by diffusion tensor MRI and triple stimulation technique. *Muscle Nerve* 49, 551–557. doi: 10.1002/mus.23957

Groppa, S., Oliviero, A., Eisen, A., Quartarone, A., Cohen, L. G., Mall, V., et al. (2012). A practical guide to diagnostic transcranial magnetic stimulation: report of an IFCN committee. *Clin. Neurophysiol.* 123, 858–882. doi: 10.1016/j.clinph.2012.01.010

Hughes, A. J., Daniel, S. E., Kilford, L., and Lees, A. J. (1992). Accuracy of clinical diagnosis of idiopathic Parkinson's disease: a clinico-pathological study of 100 cases. *J. Neurol. Neurosurg. Psychiatry* 55, 181–184. doi: 10.1136/jnnp.55.3.181

Jang, W., Park, J., Kim, J. S., Youn, J., Oh, E., Jo, K. D., et al. (2014). Triple stimulation technique findings in vascular Parkinsonism and Parkinson's disease. *Clin. Neurophysiol.* 125, 1834–1839. doi: 10.1016/j.clinph.2014.01.008

Kandler, R. H., Jarratt, J. A., Sagar, H. J., Gumpert, E. J., Venables, G. S., Davies-Jones, G. A., et al. (1990). Abnormalities of central motor conduction in Parkinson's disease. *J. Neurol. Sci.* 100, 94–97. doi: 10.1016/0022-510x(90)90018-i

Magistris, M. R., Rösler, K. M., Truffert, A., Landis, T., and Hess, C. W. (1999). A clinical study of motor evoked potentials using a triple stimulation technique. *Brain* 122(Pt 2), 265–279. doi: 10.1093/brain/122.2.265

Magistris, M. R., Rosler, K. M., Truffert, A., and Myers, J. P. (1998). Transcranial stimulation excites virtually all motor neurons supplying the target muscle. A demonstration and a method improving the study of motor evoked potentials. *Brain* 121(Pt 3), 437–450. doi: 10.1093/brain/121.3.437

Mole, J. P., Subramanian, L., Bracht, T., Morris, H., Metzler-Baddeley, C., and Linden, D. E. (2016). Increased fractional anisotropy in the motor tracts of Parkinson's disease suggests compensatory neuroplasticity or selective neurodegeneration. *Eur. Radiol.* 26, 3327–3335. doi: 10.1007/s00330-015-4178-1

Postuma, R. B., Berg, D., Stern, M., Poewe, W., Olanow, C. W., Oertel, W., et al. (2015). MDS clinical diagnostic criteria for Parkinson's disease. *Mov. Disord.* 30, 1591–1601. doi: 10.1002/mds.26424

Pringsheim, T., Jette, N., Frolkis, A., and Steeves, T. D. (2014). The prevalence of Parkinson's disease: a systematic review and meta-analysis. *Mov. Disord.* 29, 1583–1590. doi: 10.1002/mds.25945

Rösler, K. M., Truffert, A., Hess, C. W., and Magistris, M. R. (2000). Quantification of upper motor neuron loss in amyotrophic lateral sclerosis. *Clin. Neurophysiol.* 111, 2208–2218. doi: 10.1016/s1388-2457(00)00481-8

Sakuma, K., Adachi, Y., Fukuda, H., Kai, T., and Nakashima, K. (2005). Triple stimulation technique in patients with spinocerebellar ataxia type 6. *Clin. Neurophysiol.* 116, 2586–2591. doi: 10.1016/j.clinph.2005.04.015

Tan, F., Wang, X., Li, H. Q., Lu, L., Li, M., Li, J. H., et al. (2013). A randomized controlled pilot study of the triple stimulation technique in the assessment of electroacupuncture for motor function recovery in patients with acute ischemic stroke. *Evid. Based Complement Alternat. Med.* 2013:431986. doi: 10.1155/2013/431986

Taylor, K. I., Sambataro, F., Boess, F., Bertolino, A., and Dukart, J. (2018). Progressive decline in gray and white matter integrity in de novo Parkinson's Disease: an analysis of longitudinal parkinson progression markers initiative diffusion tensor imaging data. *Front.Aging Neurosci.* 10:318. doi: 10.3389/fnagi.2018.00318

Tsuchiya, K., Ozawa, E., Haga, C., Watabiki, S., Ikeda, M., Sano, M., et al. (2000). Constant involvement of the Betz cells and pyramidal tract in multiple system atrophy: a clinicopathological study of seven autopsy cases. *Acta Neuropathol.* 99, 628–636. doi: 10.1007/s004010051173

Conflict of Interest: The authors declare that the research was conducted in the absence of any commercial or financial relationships that could be construed as a potential conflict of interest.

Copyright © 2020 Xu, Ding and Wang. This is an open-access article distributed under the terms of the Creative Commons Attribution License (CC BY). The use, distribution or reproduction in other forums is permitted, provided the original author(s) and the copyright owner(s) are credited and that the original publication in this journal is cited, in accordance with accepted academic practice. No use, distribution or reproduction is permitted which does not comply with these terms.

frontiers in Aging Neuroscience

ORIGINAL RESEARCH
published: 05 November 2020
doi: 10.3389/fnagi.2020.580853

Different Perivascular Space Burdens in Idiopathic Rapid Eye Movement Sleep Behavior Disorder and Parkinson's Disease

*Xiao-li Si[1†], Lu-yan Gu[1†], Zhe Song[1], Cheng Zhou[2], Yi Fang[1], Chong-yao Jin[1], Jing-jing Wu[2], Ting Gao[1], Tao Guo[2], Xiao-jun Guan[2], Xiao-jun Xu[2], Xin-zhen Yin[1], Ya-ping Yan[1], Min-min Zhang[2] and Jia-li Pu[1]**

[1] Department of Neurology, The Second Affiliated Hospital, College of Medicine, Zhejiang University, Hangzhou, China,
[2] Department of Radiology, The Second Affiliated Hospital, College of Medicine, Zhejiang University, Hangzhou, China

Background: Excessive aggregation of α-synuclein is the key pathophysiological feature of Parkinson's disease (PD). Rapid eye movement sleep behavior disorder (RBD) is also associated with synucleinopathies and considered as a powerful predictor of PD. Growing evidence suggests the diminished clearance of α-synuclein may be partly attributable to poor interstitial fluid drainage, which can be reflected by magnetic resonance imaging (MRI)-visible enlarged perivascular space (EPVS). However, the effect of MRI-visible EPVS on iRBD and PD, and their correlation with clinical characteristics remain unclear.

Objective: To evaluate the clinical and neuroimaging significance of MRI-visible EPVS in iRBD and PD patients.

Methods: We enrolled 33 iRBD patients, 82 PD (with and without RBD) patients, and 35 healthy controls (HCs), who underwent clinical evaluation and 3.0 Tesla MRI. Two neurologists assessed MRI-visible EPVS in centrum semiovale (CSO), basal ganglia (BG), substantia nigra (SN), and brainstem (BS). Independent risk factors for iRBD and PD were investigated using multivariable logistic regression analysis. Spearman analysis was used to test the correlation of MRI-visible EPVS with clinical characteristics of patients.

Results: iRBD patients had significantly higher EPVS burdens (CSO, BG, SN, and BS) than PD patients. Higher CSO-EPVS and BS-EPVS burdens were independent risk factors for iRBD. Furthermore, higher CSO-EPVS and SN-EPVS burdens were positively correlated with the severity of clinical symptom in iRBD patients, and higher BG-EPVS burden was positively correlated with the severity of cognitive impairment in PD patients.

Conclusion: iRBD and PD patients have different MRI-visible EPVS burdens, which may be related with a compensatory mechanism in glymphatic system. Lower MRI-visible EPVS burden in PD patients may be a manifestation of severe brain waste drainage dysfunction. These findings shed light on the pathophysiologic relationship between iRBD and PD with respect to neuroimaging marker of PD.

Keywords: Parkinson's disease, REM sleep behavior disorder, perivascular space, glymphatic system, white matter hyperintensity

OPEN ACCESS

Edited by:
Liu Jun,
Shanghai Jiao Tong University, China

Reviewed by:
Weili Yang,
Jinan University, China
Dennis Qing Wang,
Southern Medical University, China

****Correspondence:***
Jia-li Pu
jialipu@zju.edu.cn

† These authors have contributed equally to this work

Received: *07 July 2020*
Accepted: *20 October 2020*
Published: *05 November 2020*

Citation:
Si X-l, Gu L-y, Song Z, Zhou C, Fang Y, Jin C-y, Wu J-j, Gao T, Guo T, Guan X-j, Xu X-j, Yin X-z, Yan Y-p, Zhang M-m and Pu J-l (2020) Different Perivascular Space Burdens in Idiopathic Rapid Eye Movement Sleep Behavior Disorder and Parkinson's Disease. Front. Aging Neurosci. 12:580853. doi: 10.3389/fnagi.2020.580853

INTRODUCTION

Parkinson's disease (PD) is an age-related neurodegenerative disorder that is caused by the loss of dopaminergic (DA) neurons in the substantia nigra (SN) and is characterized by misfolded α-synuclein in Lewy bodies (Sulzer and Surmeier, 2013). Apart from classical motor symptoms, PD is also associated with a broad spectrum of non-motor symptoms, including autonomic dysfunction, sensory symptoms, neuropsychiatric dysfunction and sleep disturbances (Poewe, 2008; Xie et al., 2019; LeWitt et al., 2020).

Before the appearance of PD classical motor symptoms, at least 60% DA neurons have degenerated (Si et al., 2017). Therefore, detecting a premotor marker which aids in primary prevention of PD is in urgent need. Rapid eye movement (REM) sleep behavior disorder (RBD), which is characterized by recurrent nocturnal dream enactment behavior during REM sleep without normal muscle atonia, commonly accompanies PD and even precede the onset of PD (Arnulf, 2012). A growing number of studies have focused on idiopathic RBD (iRBD) to be an prodromal marker of PD (Schenck et al., 2013; Xie et al., 2019; Zhang et al., 2020). iRBD is strongly associated with synucleinopathy and there is a long time interval (∼10 years) between the onset of iRBD and PD, which provides the time window for disease-modifying therapies (Xie et al., 2019). However, it is challenging to make assumptions about the phenoconversion and disease subtypes that may subsequently follow iRBD (Qian and Huang, 2019). As imaging is less susceptible to subjectivity and drug influence, the establishment of neuroimaging markers to detect brain changes in patients with iRBD and PD is promising, and may be a valuable method for predicting PD disease progression.

Glymphatic system, the lymphatic drainage system of central nervous system (CNS), may contribute to the clearance of α-synuclein (Jessen et al., 2015; Li et al., 2020). Perivascular spaces (PVSs), also known as Virchow-Robin spaces, form a network of spaces around microvessels that are dedicated to cerebrospinal fluid (CSF) transportation and metabolic waste drainage, are major component of the glymphatic system (Iliff et al., 2012; Jessen et al., 2015; Mestre et al., 2017). However, normal PVSs are invisible on conventional structural magnetic resonance image (MRI) and can only be visualized when enlarged (Potter et al., 2015). Enlarged PVSs (EPVSs) are spaces with diameters less than 3 mm, which are visible on MRI. MRI-visible EPVSs are commonly found in centrum semiovale (CSO), basal ganglia (BG), and brainstem (BS), with high signals on T2-weighted images and low signals on T1-weighted and fluid attenuated inversion recovery (FLAIR) images (Wardlaw et al., 2013b). MRI-visible EPVS burden is a cerebral small vessel disease (SVD) and is predictive of cognitive impairment in cerebrovascular disease (Halliday et al., 2014; Gutierrez et al., 2017). Yet it likely resembles obstruction by protein and stagnation of fluid (Brown et al., 2018), which may contribute to the development of neurodegenerative diseases (Banerjee et al., 2017), including PD and iRBD (Laitinen et al., 2000; Xie et al., 2013; Park Y. W. et al., 2019). However, the effect of MRI-visible EPVSs in iRBD and PD patients, and their correlation with clinical characteristics remains unclear.

Therefore, by evaluating MRI-visible EPVS burdens in CSO, BG, SN and BS, we investigated the clinical significance of MRI-visible EPVS in iRBD and PD patients. To the best of our knowledge, this is the first study to investigate the relationship between these two closely linked diseases in terms of neuroimaging-based markers, which may shed light on the pathophysiology of iRBD and PD.

MATERIALS AND METHODS

Study Design and Participants

This study was approved by the ethics committee of the Second Affiliated Hospital of the Zhejiang University School of Medicine, and written consent was obtained from each participant. The participants were selected from the outpatient clinic of the Department of Neurology of the Second Affiliated Hospital of the Zhejiang University School of Medicine for adjacent communities, between January 2017 and August 2019. Patients who met the American Academy of Sleep Medicine criteria for iRBD were assigned to the iRBD group (American Academy of Sleep Medicine, 2014), while patients who met the Movement Disorder Society's Clinical Diagnostic Criteria for PD were assigned to the PD group (Postuma et al., 2015). The criteria of classification of PD with symptomatic RBD (PD-sRBD) group and PD without RBD (PD-nRBD) group was according to REM Sleep Behavior Disorder Questionnaire-Hong Kong (RBDQ-HK) scale (Shen et al., 2014). Age- and sex-matched community volunteers served as healthy controls (HCs). Potential participants who met the following exclusion criteria were excluded: (1) sleep-related epilepsy, obstructive sleep apnea hypopnea syndrome, night terror/sleepwalking, nocturnal paroxysmal dystonia, or secondary RBD caused by drugs; (2) other neurodegenerative diseases, such as dementia with Lewy bodies (DLB), multiple system atrophy (MSA), progressive supranuclear palsy, or secondary PD caused by drugs; (3) experience of a cerebrovascular accident, such as cerebral hemorrhage, cerebral infarction, subarachnoid hemorrhage, etc.; (4) cerebral structural abnormality, such as brain trauma and brain tumor; (5) have severe cognitive dysfunction [Montreal Cognitive Assessment (MoCA) score $<$ 10 and/or Mini-Mental State Examination (MMSE) score $<$9] (Dalrymple-Alford et al., 2010; Arevalo-Rodriguez et al., 2015); (6) inability to undergo MRI due to contraindications, such as metal implants and mental disorders; and (7) refusal to sign the informed consent form. In total, 35 age- and sex- matched HCs, 33 patients with iRBD, and 82 patients with PD (43 PD-nRBD and 39 PD-sRBD patients) were enrolled. All the participants underwent clinical evaluation and 3.0 Tesla (3.0T) MRI scan.

Clinical Assessment

We performed clinical evaluation of all the participants, including detailed personal information, medical history, and neurological and neuropsychological examination. The severity and stage of PD were evaluated with the Unified Parkinson's

Disease Rating Scale (UPDRS) and the Hoehn-Yahr scale (H-Y stage), respectively. The RBDQ-HK scale was used to evaluate the severity of iRBD patients and classify the PD-sRBD and PD-nRBD groups (using a cut-off score of 17/18 points for the overall scale and 7/8 points for the factor II subscale of the RBDQ-HK) (Shen et al., 2014). In addition, we performed the MMSE and MoCA scales to evaluate cognitive function. The participants' demographic and clinical characteristics are summarized in **Table 1**.

MRI Acquisition

Standardized T2 and FLAIR images were acquired from all the participants at the Department of Radiology of the Second Affiliated Hospital of the Zhejiang University School of Medicine, using the same 3.0 Tesla MRI scanner (GE Discovery 750). The images for each participant were obtained in one session, and all the MRIs were obtained in the same orientation and slice positions. We acquired the T2 gradient recalled echo (GRE) images with the following imaging parameters: repetition time (TR) = 3,000 ms, echo time (TE) = 102 ms, flip angle = 90°, field of view = 240 mm× 240 mm, matrix size = 256 × 256 pixels, and slice number/thickness = 38/4.0 mm. FLAIR GRE-images were obtained using the following parameters: TR = 11,000 ms, TE = 147 ms, flip angle = 90°, field of view = 220 mm× 220 mm, matrix size = 256 × 256 pixels, and slice number/thickness = 42/4.0 mm.

Quantification of MRI-Visible EPVS

MRI-visible EPVS was defined as a fluid-filled space (1–3 mm in diameter) that followed the typical course of a vessel, whose space had a signal intensity similar to CSF on all sequences. Evaluation was done by two trained neurologists (S.XL and G.LY), according to the STandards for ReportIng Vascular changes on nEuroimaging (STRIVE) criteria (Wardlaw et al., 2013a; Hilal et al., 2018b; **Figure 1**). These two neurologists were blinded to the clinical data. Discrepancies were resolved by negotiation. The numbers of MRI-visible EPVS in both hemispheres were assessed and added together. We selected the slices of CSO, BG, and BS with the highest numbers of EPVS after scanning all the relevant slices. We also selected the specific region of SN that we have marked in **Figure 1A**. The inter-rater reliability was good for BG-EPVS (Spearman's rank correlation

TABLE 1 | Baseline characteristics and Imaging findings according to disease classification.

	HC	iRBD	PD		*P*-value	
			PD-nRBD	PD-sRBD	HC vs. RBD vs. PD	HC vs. RBD vs. PD-nRBD vs. PD-sRBD
n (%)	35 (23.2)	33 (21.9)	43 (28.5)	39 (27.9)	–	–
Clinical variables						
Age, years, mean (SD)	61.3 (7.0)	65.6 (8.9)	59.2 (12.1)	61.8 (8.3)	0.056	0.109
Sex, male, n (%)	12 (34.3)	17 (51.5)	21 (48.8)	26 (66.7)	0.075	0.051
Smoking, n (%)	5 (14.3)	10 (30.3)	7 (16.3)	12 (30.8)	0.283	0.118
Hypertension, n (%)	11 (31.4)	8 (24.2)	13 (30.2)	9 (23.1)	0.617	0.686
Hyperlipidaemia, n (%)	4 (11.4)	4 (12.1)	2 (4.7)	1 (2.6)	0.167	0.294
Diabetes mellitus, n (%)	1 (2.9)	2 (6.1)	1 (2.3)	4 (10.3)	0.759	0.379
MMSE, mean (SD)	27.5 (2.5)	27.2 (3.0)	26.5 (4.6)	26.3 (3.9)	0.589	0.675
MoCA, mean (SD)	24.3 (3.4)	22.6 (4.5)	21.5 (6.2)	20.9 (5.4)	**0.022**	**0.034**
RBDQ-HK, mean (SD)	7.4 (4.7)	39.4 (12.9)	7.5 (4.8)	27.1 (13.4)	**0.000**	**0.000**
RBDQ-HK II, mean (SD)	0.9 (1.7)	24.5 (10.9)	2.1 (2.4)	16.5 (10.5)	**0.000**	**0.000**
Disease duration, years, mean (SD)	–	–	3.8 (3.7)	4.6 (5.3)	–	0.346*
UPDRS total, mean (SD)	–	–	30.6 (19.2)	31.2 (18.3)	–	0.446*
UPDRS I	–	–	1.5 (1.6)	1.5 (2.0)	–	0.965*
UPDRS II	–	–	8.3 (5.7)	8.8 (5.4)	–	0.530*
UPDRS III	–	–	19.9 (13.6)	20.3 (12.5)	–	0.492*
UPDRS IV	–	–	0.9 (1.7)	0.8 (1.1)	–	0.675*
H-Y stage, mean (SD)	–	–	2.2 (0.9)	2.0 (0.6)	–	0.435*
Imaging findings						
CSO-EPVS, mean (SD)	17.0 (7.9)	21.3 (8.5)	16.3 (10.4)	17.1 (8.6)	**0.019**	**0.034**
BG-EPVS, mean (SD)	12.4 (3.7)	15.0 (5.4)	11.0 (6.2)	12.1 (7.3)	**0.001**	**0.002**
SN-EPVS, mean (SD)	1.9 (1.1)	2.7 (1.7)	1.8 (1.3)	1.5 (1.1)	**0.024**	**0.038**
BS-EPVS, mean (SD)	2.3 (1.5)	3.3 (1.6)	2.6 (1.6)	2.2 (1.4)	**0.020**	**0.023**
WMH score, mean (SD)	2.3 (1.6)	2.4 (1.4)	1.9 (1.4)	1.8 (1.3)	0.056	0.122

MMSE, Mini-mental State Examination; MoCA, Montreal Cognitive Assessment; RBDQ-HK, REM Sleep Behavior Disorder Questionnaire-Hong Kong; UPDRS, United Parkinson's Disease Rate Scale; H-Y stage, Hoehn-Yahr stage; EPVS, enlarged perivascular space; CSO, centrum semiovale; BG, basal ganglia; SN,substantia nigra; BS, brainstem; WMH, white matter hyperintensity.

**P-values reflect comparisons between PD-nRBD and PD-sRBD groups using Mann-Whitney U-tests. P-value < 0.05.*

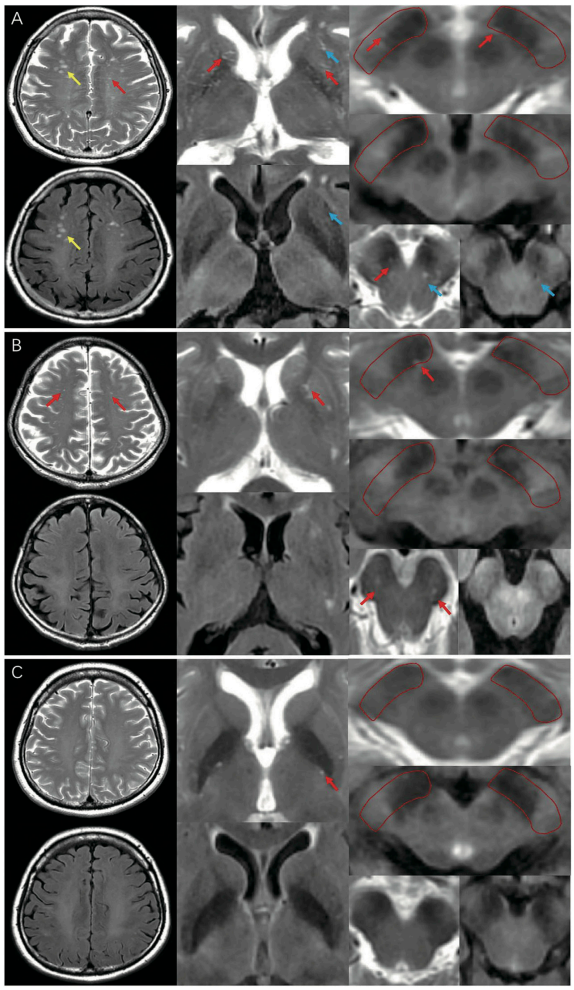


FIGURE 1 | MRI-visible EPVS on T2 and FLAIR imaging. Red arrows indicate EPVS: an EPVS was defined as a fluid-filled space from 1 to 3 mm in diameter with high signal on T2 and low signal on FLAIR imaging, without a perilesional halo. Yellow arrows indicate WMH: a WMH was defined as a lesion with variable size in the white matter, with high signal on both T2 and FLAIR imaging. Blue arrows indicate lacunes: a lacune was defined as a lesion 3–15 mm in diameter with high signal on T2 and a perilesional halo on FLAIR imaging. **(A)** A representative of EPVS in iRBD group (frequent/severe grade CSO, BG-EPVS, with EPVS in SN and BS); **(B)** A representative of EPVS in HC group (moderate grade CSO, BG-EPVS, with EPVS in SN and BS); **(C)** A representative of EPVS in PD group (none/mild grade CSO, BG-EPVS, without EPVS in SN or BS). EPVS, enlarged perivascular spaces; FLAIR: fluid attenuated inversion recovery; WMH, white matter hyperintensity; CSO, centrum semiovale; BG, basal ganglia; SN, substantia nigra; BS, brainstem; MRI, magnetic resonance imaging.

coefficient, intraclass correlation coefficient [ICC] = 0.58) and CSO-EPVS (ICC = 0.46), and excellent for SN-EPVS (ICC = 0.88) and BS-EPVS (ICC = 0.89), respectively.

Measurement of White Matter Hyperintensity

White matter hyperintensities (WMHs) were defined as signal abnormalities of variable sizes in the white matter, which exhibited hyperintensity on T2-weighted images, such as FLAIR, without cavitation (that is, the signal is different from that of CSF) according to STRIVE criteria (Wardlaw et al., 2013a; **Figure 1**). We used the Fazekas scale to grade periventricular (PV) WMHs (PVWMHs) and deep WMHs (DWMHs). PVWMH scores were 0 = absent, 1 = caps or pencil-thin lining, 2 = smooth halo, and 3 = irregular PV lesions extending into the deep white matter. DWMH scores were 0 = absent, 1 = punctate foci, 2 = beginning confluence of foci, and 3 = large confluent areas (Fazekas et al., 1987). The total WMH (Fazekas) score was calculated by summing the scores of these two regions, and a total score >3 was defined as severe WMH (Park et al., 2019). WMHs were rated by two trained neurologists (S.Z and Z.C). Discrepancies were resolved by negotiation.

Statistical Analysis

Data were entered into Microsoft Excel, and statistical analyses were performed with Statistical Package for the Social Sciences 18.0 (IBM, Chicago, IL, United States). Statistical plots were generated using GraphPad Prism 7.0a (GraphPad Inc., San Diego, CA, United States). The results are expressed as mean ± standard deviation (mean ± SD) for continuous variables and as frequencies for categorical variables. The Kolmogorov-Smirnov test was used to determine the normality of the distribution of the variables. Demographic data, clinical variables, and MRI-visible EPVS were compared using independent *t*-tests for normally distributed continuous variables, and Mann-Whitney *U* test and Kruskal-Wallis test for continuous variables that were not normally distributed. Kruskal-Wallis Multiple Compare (Nemenyi test) was used for multiple comparisons, and a corrected $P < 0.05$ was considered statistically significant. We performed both univariate and multivariate logistic regression analyses. Variables of interest in the univariate analysis ($P < 0.05$) and previously known demographic and clinical risk factors, including age, sex, smoking, hypertension, hyperlipidemia, diabetes mellitus, MoCA score, MRI-visible EPVS, and WMH score, were included in the multivariable models by using backward elimination according to the likelihood ratio, with a variable selection criterion of $P < 0.05$. We estimated the area under the receiver operating characteristic curve (AUC) to assess the predictive ability of the multivariable models. Spearman's rank correlation was used to evaluate the bivariate associations between number of EPVS and RBDQ-HK (total and subscale II) scores, UPDRS (total and III) scores, and MoCA scores in HC, iRBD, and PD groups. $P < 0.05$ was regarded as statistically significant.

RESULTS

Sample and Participant Characteristics

In total, 239 participants completed the clinical data collection and underwent 3.0T MRI. Based on the inclusion and exclusion criteria, the data of 33 iRBD patients, 82 PD patients (43 PD-nRBD and 39 PD-sRBD patients), and 35 HCs were analyzed for the study. The demographic and clinical characteristics of the participants are summarized in **Table 1**. There was no significant

difference among the four groups ($P > 0.05$ with Kruskal-Wallis test) with respect to baseline age, sex, smoking, hypertension, hyperlipidemia, diabetes mellitus, or MMSE scores. The PD-sRBD group had lower MoCA scores (20.9 ± 5.4 vs. 24.3 ± 3.4, $P = 0.023$) than HC group. The iRBD and PD-sRBD groups had higher RBDQ-HK (total and II) scores ($P < 0.05$) than the HC and PD-nRBD groups. A subgroup analysis between PD-nRBD group and PD-sRBD group found no significant difference in demographic or clinical characteristics of patients [including disease duration, UPDRS scores (I, II, III, IV, and total), and Hoehn-Yahr stage] in these two groups ($P > 0.05$).

Distribution of EPVSs

The imaging characteristics (numbers of EPVS and WMH scores) of the four groups are summarized in **Table 1** and **Figure 2**. Kruskal-Wallis Multiple Compare was used for multiple comparisons. The subgroup analysis between HC and iRBD groups showed that iRBD group had higher numbers of CSO-, BG-, and SN-EPVS burdens ($P > 0.05$), and higher BS-EPVSs (3.3 ± 1.6 vs. 2.3 ± 1.5, $P = 0.032$) than HC group. The subgroup analysis between iRBD and PD groups showed that iRBD group had significantly higher numbers of CSO-EPVS (21.3 ± 8.5 vs. 16.7 ± 9.5, $P = 0.015$), BG-EPVS (15.0 ± 5.4 vs. 11.5 ± 6.7, $P = 0.001$), SN-EPVS (2.7 ± 1.7 vs. 1.7 ± 1.2, $P = 0.020$), and BS-EPVS (3.3 ± 1.6 vs. 2.4 ± 1.5, $P = 0.044$) than PD group. There was no significant difference in numbers of EPVS between PD and HC groups ($P > 0.05$). There was no significant difference of WMH scores in these four groups ($P > 0.05$) (**Table 1** and **Figure 2A**). Among PD patients, the iRBD group had significant higher numbers of CSO-EPVS (21.3 ± 8.5 vs. 16.3 ± 10.4, $P = 0.022$) and BG-EPVS (15.0 ± 5.4 vs. 11.0 ± 6.2, $P = 0.003$) than PD-nRBD group, while iRBD group had significantly higher numbers of BG-EPVS (15.0 ± 5.4 vs. 12.1 ± 7.3, $P = 0.010$), SN-EPVS (2.7 ± 1.7 vs. 1.5 ± 1.1, $P = 0.025$), and BS-EPVS (3.3 ± 1.6 vs. 2.2 ± 1.4, $P = 0.034$) than PD-sRBD group. There was no significant difference in numbers of EPVS between PD-nRBD and PD-sRBD groups (**Figure 2B**).

Logistic Regression Results

The univariate analysis of the HC and iRBD groups showed that higher numbers of CSO-EPVS (OR = 1.07; 95% CI: 1.00–1.14), BG-EPVS (OR = 1.13; 95% CI: 1.01–1.27), SN-EPVS (OR = 1.47; 95% CI: 1.02–2.12), and BS-EPVS (OR = 1.50; 95% CI: 1.06–2.13) were associated with the diagnosis of iRBD ($P < 0.05$). In multivariable analysis, lower MoCA score (OR = 0.79; 95% CI: 0.66–0.94, P = 0.008), and higher numbers of CSO-EPVS (OR = 1.10; 95% CI: 1.00–1.21, P = 0.048) and BS-EPVS (OR = 1.95; 95% CI = 1.18–3.23, $P = 0.010$) were independent risk factors for iRBD (**Table 2**). The model achieved an AUC of 0.68 (95% CI: 0.55–0.81).

The univariate analysis of the entire sample showed that lower MoCA score (OR = 0.91; 95% CI: 0.85–0.98), fewer BG-EPVS (OR = 0.94; 95% CI: 0.89–0.99) and SN-EPVS (OR = 0.71; 95% CI: 0.55–0.92), and lower WMH score (OR = 0.76; 95% CI: 0.60–0.95) were associated with the diagnosis of PD. The multivariate analysis found that female sex (OR = 0.33; 95% CI = 0.13–0.83, $P = 0.019$), lower MoCA score (OR = 0.89; 95% CI: 0.82–0.97, $P = 0.008$), and fewer SN-EPVS (OR = 0.73; 95% CI = 0.53–1.00, $P = 0.048$) were independent risk factors for PD (**Table 3**). This model achieved an AUC of 0.57 (95% CI: 0.47–0.66).

Correlation Analysis of EPVS With Clinical Characteristics

The results of the correlation analysis of numbers of MRI-visible EPVS with clinical features in iRBD and PD patients are shown in **Figure 3**. Spearman's rank correlation showed that numbers of SN-EPVS and CSO-EPVS were positively correlated with RBDQ-HK total scores ($r = 0.333$, $P = 0.058$; and $r = 0.334$, $P = 0.057$, respectively) and RBDQ-HK II scores ($r = 0.411$, $P = 0.018$; and $r = 0.356$, $P = 0.042$, respectively) in iRBD group, but not in HC and PD groups ($P > 0.05$) (**Figures 3A,B**). Spearman's rank correlation also showed that the number of BG-EPVS was negatively correlated with MoCA score ($r = -0.333$, $P = 0.002$) in PD group, but not in HC and iRBD groups ($P > 0.05$) (**Figures 3C,D**). There was no correlation between MRI-visible EPVS numbers with UPDRS (total and III) score or H-Y stage in PD group ($P > 0.05$).

DISCUSSION

In this study, we assessed the clinical significance of MRI-visible EPVS in patients with iRBD and PD. Our study indicated that iRBD patients had significantly greater EPVS burdens (CSO, BG, SN, and BS) than PD patients. Moreover, iRBD patients had significantly greater EPVS burdens (CSO, BG) than PD without RBD, and significantly greater EPVS burdens (BG, SN, and BS) than PD with RBD. Higher CSO-EPVS and BS-EPVS burdens might be independent risk factors for iRBD, and higher CSO-EPVS and SN-EPVS burdens were positively correlated with the severity of clinical symptom in iRBD patients. Furthermore, higher BG-EPVS burden was positively correlated with the severity of cognitive impairment in PD patients.

Parkinson's disease is characterized by the excessive aggregation of α-synuclein (Dehay et al., 2015). A range of mechanisms are involved in the pathogenesis of synucleinopathies, including oxidative stress, neuroinflammation and mitochondrial dysfunction (Blandini, 2013; Xu et al., 2019; Yang et al., 2020). Among them, inflammation has been recognized as the key factor (Wang et al., 2020; Zheng et al., 2020). Kishimoto et al. (2019) revealed that gut microbiota changes were associated with intestinal inflammation, which may contribute to α-synuclein misfolding (Zheng et al., 2020). By measuring serum superoxide dismutase (SOD) with lipoprotein cholesterol and CRP, respectively, in PD patients, (Yang et al., 2020) found the lower level of SOD along with cholesterol, HDL-C and LDL-C, and higher C-reactive protein (CRP) levels were correlated with the severity of PD. iRBD is considered to be associated with synucleinopathies, such as PD, dementia with Lewy bodies (DLB), and multiple system atrophy (MSA), and usually precedes the onset of first motor symptom of these diseases (Reichmann, 2017; Zhang et al., 2020). In iRBD patients, increased microglial

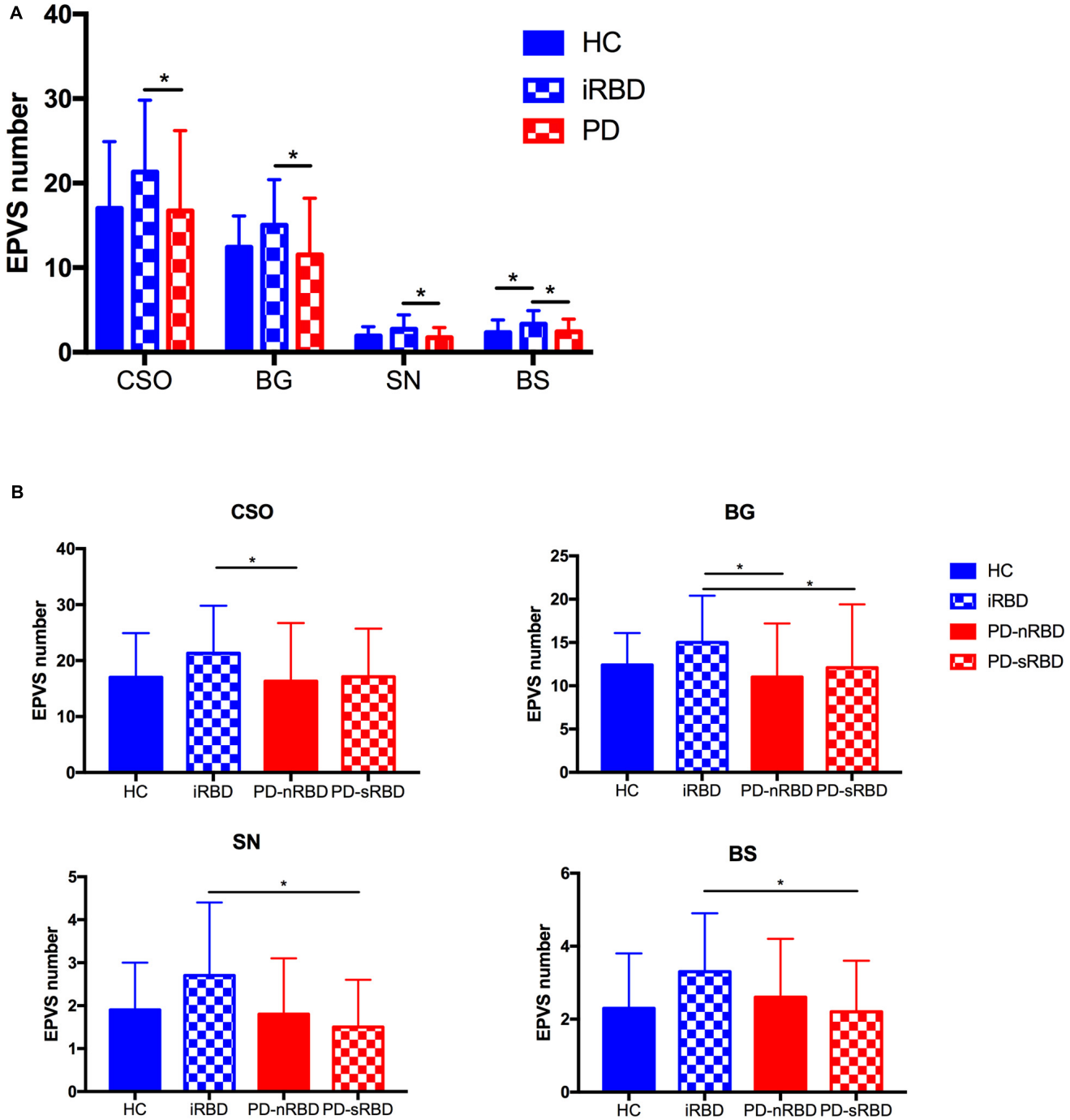


FIGURE 2 | (A) Comparison of numbers of EPVS among HC, iRBD, and PD (with or without RBD) groups; **(B)** Comparison of numbers of CSO-EPVS, BG-EPVS, SN-EPVS, and BS-EPVS (mean ± SD) among HC, iRBD, PD-nRBD, and PD-sRBD groups. *$P < 0.05$. HC, healthy control; iRBD, idiopathic rapid eye movement sleep behavior disorder; PD, Parkinson's disease; PD-nRBD, Parkinson's disease without symptomatic RBD; PD-sRBD, Parkinson's disease with symptomatic RBD; EPVS, enlarged perivascular space; CSO, centrum semiovale; BG, basal ganglia; SN, substantia nigra; BS, brainstem; SD, standard deviation.

activation was detected by positron emission tomography in the SN, implying that neuroinflammation may have occur in the early pathophysiological stage of α-synucleinopathies, including the prodromal phase of PD (Stokholm et al., 2017; Zhang et al., 2020).

Recently, the term "glymphatic" has been applied to the PVS system, based on its similarities to the lymphatic system in other tissue (Weller et al., 2009; Jessen et al., 2015). This waste drainage system can transport soluble proteins – such as amyloid beta (Aβ), whose deposition is thought to be the main pathogenic

TABLE 2 | Logistic regression analysis for clinical and imaging predictors of iRBD.

Variables	Univariate		Multivariable	
	OR (95% CI)	*P*-value	OR (95% CI)	*P*-value
Clinical variables				
Age, years	1.05 (0.99–1.12)	0.082	–	–
Sex, male	0.49 (0.19-1.30)	0.153	–	–
Smoking	2.25 (0.67–7.61)	0.192	–	–
Hypertension	1.63 (0.57–4.70)	0.365	–	–
Hyperlipidaemia	1.29 (0.27–6.26)	0.752	–	–
Diabetes mellitus	0.29 (0.03–2.98)	0.300	–	–
MoCA	0.89 (0.78–1.01)	0.080	0.79 (0.66–0.94)	**0.008**
Imaging findings				
CSO-EPVS	1.07 (1.00–1.14)	**0.041**	1.10 (1.00–1.21)	**0.048**
BG-EPVS	1.13 (1.01–1.27)	**0.030**	–	–
SN-EPVS	1.47 (1.02–2.12)	**0.037**	–	–
BS-EPVS	1.50 (1.06–2.13)	**0.022**	1.95 (1.18–3.23)	**0.010**
WMH score	1.05 (0.77–1.44)	0.760	–	**–**

OR, odds ratio; MoCA, Montreal Cognitive Assessment; EPVS, enlarged perivascular spaces; CSO, centrum semiovale; BG, basal ganglia; SN, substantia nigra; BS, brainstem; WMH, white matter hyperintensity. P-value < 0.05.

TABLE 3 | Logistic regression analysis for clinical and imaging predictors of PD.

Variables	Univariate		Multivariable	
	OR (95% CI)	*P*-value	OR (95% CI)	*P*-value
Clinical variables				
Age, years	0.97 (0.94–1.00)	0.068	–	–
Sex, male	0.55 (0.29–1.06)	0.075	0.33 (0.13–0.83)	**0.019**
Smoking	1.01 (0.46–2.19)	0.987	–	–
Hypertension	1.14 (0.56–2.32)	0.726	–	–
Hyperlipidaemia	3.51 (0.89–13.80)	0.072	–	–
Diabetes mellitus	0.71 (0.16–3.09)	0.649	–	–
MoCA	0.91 (0.85–0.98)	**0.008**	0.89 (0.82–0.97)	**0.008**
Imaging findings				
CSO-EPVS	0.97 (0.94–1.01)	0.102	–	–
BG-EPVS	0.94 (0.89–0.99)	**0.031**	–	–
SN-EPVS	0.71 (0.55–0.92)	**0.009**	0.73 (0.53–1.00)	**0.048**
BS-EPVS	0.86 (0.70–1.07)	0.172	–	–
WMH score	0.76 (0.60–0.95)	**0.017**	–	–

OR, odds ratio; MoCA, Montreal Cognitive Assessment; EPVS, enlarged perivascular spaces; CSO, centrum semiovale; BG, basal ganglia; SN, substantia nigra; BS, brainstem; WMH, White matter hyperintensity. P-value < 0.05.

factor in AD – from the brain interstitial fluid (ISF) into the PVS system (Banerjee et al., 2017). However, the PVS system of fluid drainage and waste clearance is not fully understood. PVS burden has been associated with brain atrophy with aging, inflammation leading to increased oxygen consumption, cerebrovascular reactivity and hypoperfusion, and disruption of the blood-brain barrier (Joutel et al., 2010; Aribisala et al., 2014; Adams et al., 2015; Rost et al., 2018; Ghali et al., 2020). Recent findings suggest that the PVS system may be an immunological hotspot, which is the site of antigen presentation and tissue-resident memory T-cell reactivation (Smolders et al., 2020). Moreover, higher level of inflammation markers (CRP, interleukin-6, et al.) are associated with MRI-visible EPVS burdens, but not with WMH (Aribisala et al., 2014; Hilal et al., 2018a; Yang et al., 2020). These evidence link inflammation to the PVS system, as its malfunction may impair the clearance of α-synuclein aggregation, and causes subsequent progression of iRBD and PD. Therefore, we propose that MRI-visible EPVS burden may indicate obstruction by protein and stagnation of fluid (Brown et al., 2018), which serves as an imaging marker of neurodegenerative diseases, including PD and iRBD.

Studies on the relationship between EPVS and clinical characteristics of PD are limited. There was no significant difference in numbers of EPVS between PD (with and without RBD) and HC groups in the present study. We consider the following explanations for this observation. First, EPVS, which is a type of cerebral SVD, may play the same role as cerebrovascular factors that influence some aspects of the symptoms of PD. Second, dopamine has been shown to increase excitotoxic ischemic damage in experimental models, whereas dopamine antagonists ameliorate such effects, suggesting that decreased dopamine may be a protective factor for cerebrovascular disease (Lotharius et al., 1999). In addition, smoking is a confirmed protective factor for PD, yet it is associated with increased risk of stroke.

Parkinson's disease patients frequently suffer from mild cognitive impairment (MCI) (MoCA score more than 21 and less than 26) (Litvan et al., 2012), who are at higher risk of developing dementia compared to PD patients with normal cognition (PD-NC) (Kehagia et al., 2010). Several lines of evidence suggested the inflammatory risk factors (Trefoil Factor 3, neutrophils, lymphocytes, et al.) in PD may modulate underlying neurodegeneration particularly in relation to dementia (Stojkovic et al., 2018; Zou et al., 2018; Nicoletti et al., 2020; Wang et al., 2020). It is promising to detect MRI-visible EPVS burden as a marker of cognitive decline in PD. Park Y. W. et al. (2019) suggested that PD-MCI subgroup had a higher BG-PVS burden than PD-NC subgroup. In our cohort, MoCA scores were low in all four groups. However, several Chinese validation studies of the application of MoCA to identify patients with dementia showed lower thresholds than those found in international populations, due to the differences in regional culture and level of education, especially in older patients (Zheng et al., 2012; Huang et al., 2018). The MoCA scores in our study were similar to the data in the above Chinese studies. We found the BG-EPVS burden was positively correlated with the severity of cognitive impairment in PD, which is consistent with previous studies. Recently, (Jia et al., 2019) found PD-MCI patients exclusively exhibited atrophy in the right entorhinal cortex compared to PD-NC by examining structural MRI. Further studies may investigate in the correlation between MRI-visible EPVSs and other neuroanatomical states in the cognitive aspect of PD.

There was no significant difference of EPVS burdens between PD patients with RBD and those without RBD in our cohort. We consider the following explanations for this observation. First, MRI-visible EPVSs, which may indicate diminished glymphatic clearance of α-synuclein (Jessen et al., 2015; Zou et al., 2019), were potentially related to the clinical events in PD (Laitinen et al., 2000). However, there was no significant

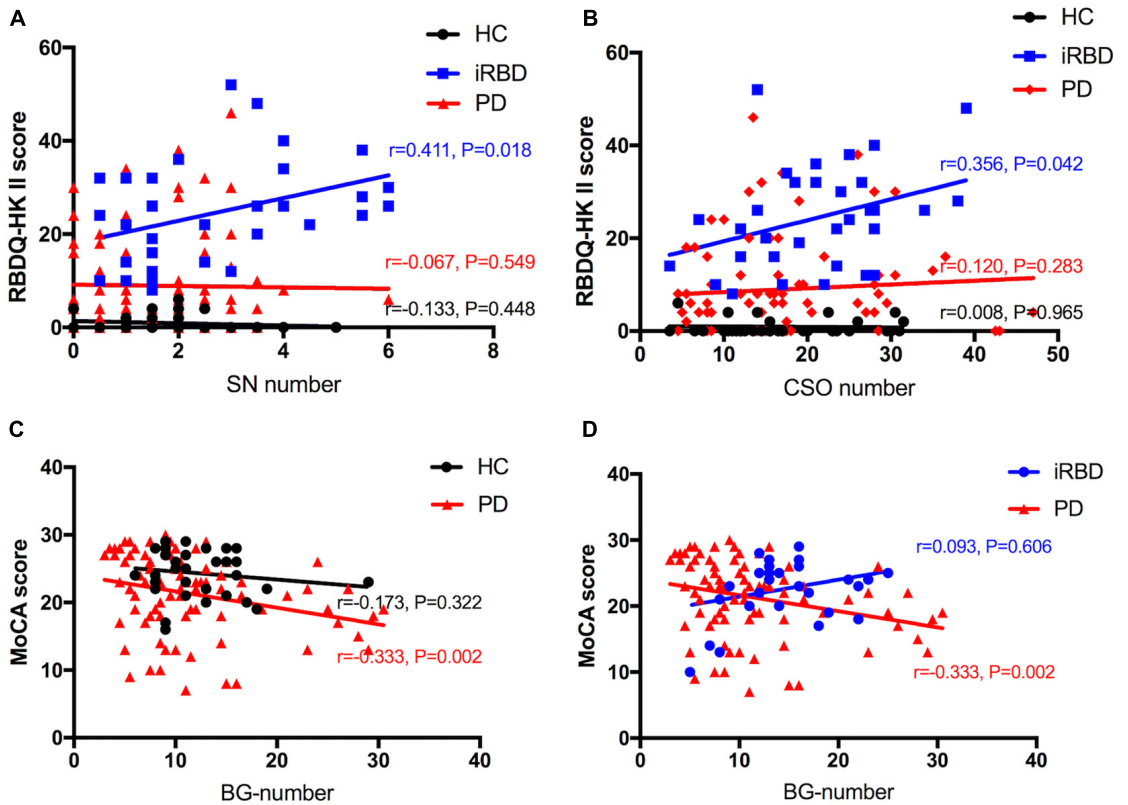


FIGURE 3 | A–D: Correlation between number of EPVS and clinical features among HC, iRBD, and PD groups. HC, healthy control; iRBD, idiopathic rapid eye movement sleep behavior disorder; PD, Parkinson's disease; EPVS, enlarged perivascular space; CSO, centrum semiovale; SN, substantia nigra; RBDQ-HK: Rapid Eye Movement Sleep Behavior Disorder Questionnaire-Hong Kong; MoCA: Montreal Cognitive Assessment.

difference in demographic or clinical characteristics in these two groups. Second, although iRBD shows a high rate of conversion to PD, only a minority of newly diagnosed PD cases show RBD (Sixel-Doring et al., 2014), and the sequence of the occurrence of RBD and the typical clinical symptoms of PD are diverse, which may be the result of individual differences, the exposure environment, and other factors. Therefore, neuropathological changes in the brain in PD with RBD phenotype are not yet conclusive, and further animal and human studies are required to elucidate this process (Schenck et al., 2013; Tekriwal et al., 2017).

Intriguingly, it is documented that the glymphatic system drains ISF and metabolic waste via PVSs more effectively during sleep (Xie et al., 2013). Therefore, it is plausible that sleep-related disorders disrupt waste clearance mechanisms via PVS system and potentially contribute to the accumulation of toxic proteins such as beta amyloid (Aβ), τ-protein, and α-synuclein. Quite recently, (Del Brutto et al., 2019) suggested that poor sleep efficiency was independently associated with BG-EPVSs. Sleep involves transitions between three different states: wakefulness, REM sleep, and non-REM sleep. RBD is characterized by loss of paralysis during REM sleep, allowing patients to act out vivid, often unpleasant dreams (Schenck et al., 2013). Therefore, it is conceivable that sleep-related disorders in iRBD may alter these clearance mechanisms, thus favoring a higher EPVS burden. Most insights into RBD have been drawn from animal lesion studies and functional models, which show that REM sleep regulation predominantly involved the key pontine centers, with additional modulation by the SN, BG, and frontal cortex (St Louis and Boeve, 2017). According to the Braak's hypothesis, RBD emerges when α-synuclein pathology affects brainstem areas that are involved in sleep regulation (Braak et al., 2003). Our study revealed a relationship between iRBD and higher EPVS burdens in CSO, BG, SN, and BS. Moreover, CSO-EPVS and SN-EPVS may be positively correlated with the severity of clinical symptoms in iRBD. This is the first clinical study to specifically report such clinical associations.

Contrary to previous theories that MRI-visible EPVS indicates poor waste clearance and predicts worse clinical outcomes (Abbott et al., 2018), we found iRBD patients had significantly higher EPVS burdens (CSO, BG, SN, and BS) than PD patients. Recently, a study found a significantly lower MRI-visible EPVS volume in the anterosuperior medial temporal lobe in some patients with early cognitive decline (Sepehrband et al., 2020). This suggested impaired signaling due to MRI-visible EPVS might be a manifestation of severe brain waste drainage dysfunction, which is consistent with our result.

In iRBD patients, sleep disruption during REM and neuroinflammation may lead to the increased metability deposition and α-synuclein aggregation, thus favoring a high EPVS burden. As the disease progresses, poor PVS drainage may cause increased deposition of metabolites and α-synuclein aggregation, and in a vicious cycle, increased α-synuclein aggregation may obstruct the PVS drainage system further, leading to lower MRI-visible EPVS burdens in PD. However, the underlying mechanism requires further verification. Finally, it is not clear whether lower EPVS burdens result from PD progression and impaired clearance of fluid, or conversely, that impaired fluid clearance occurs as a result of EPVS. However, our results demonstrated that, as a prodromal marker of PD, patients with iRBD obviously had higher EPVS burdens than patients with PD, either with or without RBD symptoms. We therefore speculate that EPVS burden may play a compensatory role in the process of iRBD developing into PD, and as the disease progresses, adaptation may become decompensatory. Further research based on this mechanism is needed to elucidate this process.

Limitations

This study has several limitations. First, there is limited sample size, and future research with a larger sample size is required to examine the reproducibility of the current findings in other cohorts. Second, according to the second edition of the International Classification of Sleep Disorders, polysomnography is essential to establish the criterion for the diagnosis of RBD, however, it is costly, labor-intensive, and impractical to perform in large study populations. Some of the iRBD patients underwent polysomnography, and others were tested with RBDQ-HK scale in this study. RBDQ-HK is a self-administered questionnaire, and its scores (total and factor 2) are useful and validated RBD screening instruments. It has also been demonstrated to have satisfactory reliability and validity as a tool for screening for the severity of iRBD, especially in east China (Shen et al., 2014). Third, we calculated EPVS numbers manually, and this is time-consuming and prone to subjectivity. Automated, computational quantification methods may be necessary for assessing EPVS in the future. However, as our analysis methods are simple with good inter-rater reliability, they can be applied easily in clinical practice. Finally, this is a neuroimaging study that only reflects the different EPVS patterns in iRBD and PD patients in a cross-sectional study. To investigate how iRBD patients transit to PD over time and demonstrate an underlying mechanism for this transition, we will follow-up these patients for a longitudinal cohort study to make the conclusions more solid in the future.

CONCLUSION

Our study provides evidence that iRBD and PD patients have different MRI-visible EPVS burdens. iRBD patients have significantly higher EPVS burdens than PD patients, an interesting observation that requires further evaluation, as it may be relevant to the mechanism of glymphatic system clearance caused by α-synuclein aggregation. Further research based on a comprehensive consideration of EPVS burden and the association between MRI-visible EPVS and α-synuclein aggregation is necessary to clarify the mechanisms underlying these findings.

DATA AVAILABILITY STATEMENT

The raw data supporting the conclusions of this article will be made available by the authors, without undue reservation.

ETHICS STATEMENT

The study involving human participants was reviewed and approved by the ethics committee of the Second Affiliated Hospital of the Zhejiang University School of Medicine, and written consent was obtained from each participant. The patients/participants provided their written i nformed consent to participate in this study. Written informed consent was obtained from the individual(s) for the publication of any potentially identifiable images or data included in this article.

AUTHOR CONTRIBUTIONS

XS: conceptualization, data curation, formal analysis, validation, and writing original draft. LG: conceptualization, data curation, validation, and writing original draft. ZS and CZ: data curation, validation, and writing original draft. CJ, JW, and TG: investigation and data curation. TG and YF: investigation and formal analysis. XG and XX: methodology and Formal analysis. XY and YY: investigation, methodology, review and editing. MZ: funding acquisition and resources. JP: project administration, resources, supervision, review and editing. All the authors read and approved the final manuscript.

FUNDING

This work was supported by the National Natural Science Foundation of China (No. 81771216), the 13th Five-year Plan for National Key Research and Development Program of China (No. 2016YFC1306600), the National Natural Science Foundation of China (No. 81971577), the Key Research and Development Program of Zhejiang Province (No. 2020C03020), and the project funded by China Postdoctoral Science Foundation (No. 2019M662082).

ACKNOWLEDGMENTS

We thank the patients and their relatives for their contribution. We would like to thank Editage (www.editage.cn) for English language editing.

REFERENCES

Abbott, N. J., Pizzo, M. E., Preston, J. E., Janigro, D., and Thorne, R. G. (2018). The role of brain barriers in fluid movement in the CNS: is there a 'glymphatic' system? *Acta Neuropathol.* 135, 387–407. doi: 10.1007/s00401-018-1812-4

Adams, H. H., Hilal, S., Schwingenschuh, P., Wittfeld, K., van der Lee, S. J., DeCarli, C., et al. (2015). A priori collaboration in population imaging: the Uniform Neuro-Imaging of Virchow-Robin spaces enlargement consortium. *Alzheimers Dement.* 1, 513–520. doi: 10.1016/j.dadm.2015.10.004

American Academy of Sleep Medicine (2014). *International Classification of Sleep Disorders*, 3rd Edn. Darien, IL: American Academy of Sleep Medicine.

Arevalo-Rodriguez, I., Smailagic, N., Roque, I. F. M., Ciapponi, A., Sanchez-Perez, E., Giannakou, A., et al. (2015). Mini-Mental State Examination (MMSE) for the detection of Alzheimer's disease and other dementias in people with mild cognitive impairment (MCI). *Cochrane Database Syst. Rev.* 2015:CD010783. doi: 10.1002/14651858.CD010783.pub2

Aribisala, B. S., Wiseman, S., Morris, Z., Valdes-Hernandez, M. C., Royle, N. A., Maniega, S. M., et al. (2014). Circulating inflammatory markers are associated with magnetic resonance imaging-visible perivascular spaces but not directly with white matter hyperintensities. *Stroke* 45, 605–607. doi: 10.1161/STROKEAHA.113.004059

Arnulf, I. (2012). REM sleep behavior disorder: motor manifestations and pathophysiology. *Mov. Disord.* 27, 677–689. doi: 10.1002/mds.24957

Banerjee, G., Kim, H. J., Fox, Z., Jager, H. R., Wilson, D., Charidimou, A., et al. (2017). MRI-visible perivascular space location is associated with Alzheimer's disease independently of amyloid burden. *Brain* 140, 1107–1116. doi: 10.1093/brain/awx003

Blandini, F. (2013). Neural and immune mechanisms in the pathogenesis of Parkinson's disease. *J. Neuroimmune Pharmacol.* 8, 189–201. doi: 10.1007/s11481-013-9435-y

Brown, R., Benveniste, H., Black, S. E., Charpak, S., Dichgans, M., Joutel, A., et al. (2018). Understanding the role of the perivascular space in cerebral small vessel disease. *Cardiovasc. Res.* 114, 1462–1473. doi: 10.1093/cvr/cvy113

Dalrymple-Alford, J. C., MacAskill, M. R., Nakas, C. T., Livingston, L., Graham, C., Crucian, G. P., et al. (2010). The MoCA: well-suited screen for cognitive impairment in Parkinson disease. *Neurology* 75, 1717–1725. doi: 10.1212/WNL.0b013e3181fc29c9

Dehay, B., Bourdenx, M., Gorry, P., Przedborski, S., Vila, M., Hunot, S., et al. (2015). Targeting alpha-synuclein for treatment of Parkinson's disease: mechanistic and therapeutic considerations. *Lancet Neurol.* 14, 855–866. doi: 10.1016/S1474-4422(15)00006-X

Del Brutto, O. H., Mera, R. M., Costa, A. F., and Castillo, P. R. (2019). Effect of heart rate variability on the association between the apnea-hypopnea index and cerebral small vessel disease. *Stroke* 50, 2486–2491. doi: 10.1161/STROKEAHA.119.026095

Fazekas, F., Chawluk, J. B., Alavi, A., Hurtig, H. I., and Zimmerman, R. A. (1987). MR signal abnormalities at 1.5 T in Alzheimer's dementia and normal aging. *Am. J. Neuroradiol.* 8, 421–426.

Ghali, M. G. Z., Marchenko, V., Yasargil, M. G., and Ghali, G. Z. (2020). Structure and function of the perivascular fluid compartment and vertebral venous plexus: illumining a novel theory on mechanisms underlying the pathogenesis of Alzheimer's, cerebral small vessel, and neurodegenerative diseases. *Neurobiol. Dis.* 144:105022. doi: 10.1016/j.nbd.2020.105022

Goedert, M., Spillantini, M. G., Del Tredici, K., and Braak, H. (2013). 100 years of lewy pathology. *Nat. Rev. Neurol.* 9, 13–24. doi: 10.1038/nrneurol.2012.242

Gutierrez, J., Elkind, M. S. V., Dong, C., Di Tullio, M., Rundek, T., Sacco, R. L., et al. (2017). Brain perivascular spaces as biomarkers of vascular risk: results from the Northern Manhattan study. *AJNR Am. J. Neuroradiol.* 38, 862–867. doi: 10.3174/ajnr.A5129

Halliday, G. M., Leverenz, J. B., Schneider, J. S., and Adler, C. H. (2014). The neurobiological basis of cognitive impairment in Parkinson's disease. *Mov. Disord.* 29, 634–650. doi: 10.1002/mds.25857

Hilal, S., Ikram, M. A., Verbeek, M. M., Franco, O. H., Stoops, E., Vanderstichele, H., et al. (2018a). C-Reactive protein, plasma amyloid-beta levels, and their interaction with magnetic resonance imaging markers. *Stroke* 49, 2692–2698. doi: 10.1161/STROKEAHA.118.022317

Hilal, S., Tan, C. S., Adams, H. H. H., Habes, M., Mok, V., Venketasubramanian, N., et al. (2018b). Enlarged perivascular spaces and cognition: a meta-analysis of 5 population-based studies. *Neurology* 91, e832–e842. doi: 10.1212/WNL.0000000000006079

Huang, L., Chen, K. L., Lin, B. Y., Tang, L., Zhao, Q. H., Lv, Y. R., et al. (2018). Chinese version of Montreal cognitive assessment basic for discrimination among different severities of Alzheimer's disease. *Neuropsychiatr. Dis. Treat.* 14, 2133–2140. doi: 10.2147/NDT.S174293

Iliff, J. J., Wang, M., Liao, Y., Plogg, B. A., Peng, W., Gundersen, G. A., et al. (2012). A paravascular pathway facilitates CSF flow through the brain parenchyma and the clearance of interstitial solutes, including amyloid beta. *Sci. Transl. Med.* 4:147ra111. doi: 10.1126/scitranslmed.3003748

Jessen, N. A., Munk, A. S., Lundgaard, I., and Nedergaard, M. (2015). The glymphatic system: a beginner's guide. *Neurochem. Res.* 40, 2583–2599. doi: 10.1007/s11064-015-1581-6

Jia, X., Wang, Z., Yang, T., Li, Y., Gao, S., Wu, G., et al. (2019). Entorhinal cortex atrophy in early, drug-naive parkinson's disease with mild cognitive impairment. *Aging Dis.* 10, 1221–1232. doi: 10.14336/AD.2018.1116

Joutel, A., Monet-Lepretre, M., Gosele, C., Baron-Menguy, C., Hammes, A., Schmidt, S., et al. (2010). Cerebrovascular dysfunction and microcirculation rarefaction precede white matter lesions in a mouse genetic model of cerebral ischemic small vessel disease. *J. Clin. Invest.* 120, 433–445. doi: 10.1172/JCI39733

Kehagia, A. A., Barker, R. A., and Robbins, T. W. (2010). Neuropsychological and clinical heterogeneity of cognitive impairment and dementia in patients with Parkinson's disease. *Lancet Neurol.* 9, 1200–1213. doi: 10.1016/S1474-4422(10)70212-X

Kishimoto, Y., Zhu, W., Hosoda, W., Sen, J. M., and Mattson, M. P. (2019). Chronic mild gut inflammation accelerates brain neuropathology and motor dysfunction in alpha-synuclein mutant mice. *Neuromolecular Med.* 21, 239–249. doi: 10.1007/s12017-019-08539-5

Laitinen, L. V., Chudy, D., Tengvar, M., Hariz, M. I., and Bergenheim, A. T. (2000). Dilated perivascular spaces in the putamen and pallidum in patients with Parkinson's disease scheduled for pallidotomy: a comparison between MRI findings and clinical symptoms and signs. *Mov. Disord.* 15, 1139–1144. doi: 10.1002/1531-8257(200011)15:6<1139::aid-mds1012>3.0.co;2-e

LeWitt, P. A., Kymes, S., and Hauser, R. A. (2020). Parkinson disease and orthostatic hypotension in the elderly: recognition and management of risk factors for falls. *Aging Dis.* 11, 679–691. doi: 10.14336/AD.2019.0805

Li, Y., Zhu, Z., Chen, J., Zhang, M., Yang, Y., and Huang, P. (2020). Dilated perivascular space in the midbrain may reflect dopamine neuronal degeneration in Parkinson's Disease. *Front. Aging Neurosci.* 12:161. doi: 10.3389/fnagi.2020.00161

Litvan, I., Goldman, J. G., Troster, A. I., Schmand, B. A., Weintraub, D., Petersen, R. C., et al. (2012). Diagnostic criteria for mild cognitive impairment in Parkinson's disease: movement disorder society task force guidelines. *Mov. Disord.* 27, 349–356. doi: 10.1002/mds.24893

Lotharius, J., Dugan, L. L., and O'Malley, K. L. (1999). Distinct mechanisms underlie neurotoxin-mediated cell death in cultured dopaminergic neurons. *J. Neurosci.* 19, 1284–1293. doi: 10.1523/jneurosci.19-04-01284.1999

Mestre, H., Kostrikov, S., Mehta, R. I., and Nedergaard, M. (2017). Perivascular spaces, glymphatic dysfunction, and small vessel disease. *Clin. Sci.* 131, 2257–2274. doi: 10.1042/CS20160381

Nicoletti, A., Luca, A., Baschi, R., Cicero, C. E., Mostile, G., Davi, M., et al. (2020). Vascular risk factors, white matter lesions and cognitive impairment in Parkinson's disease: the PACOS longitudinal study. *J. Neurol.* doi: 10.1007/s00415-020-10189-8 [Epub ahead of print].

Park, M., Moon, Y., Han, S. H., Kim, H. K., and Moon, W. J. (2019). Myelin loss in white matter hyperintensities and normal-appearing white matter of cognitively impaired patients: a quantitative synthetic magnetic resonance imaging study. *Eur. Radiol.* 29, 4914–4921. doi: 10.1007/s00330-018-5836-x

Park, Y. W., Shin, N. Y., Chung, S. J., Kim, J., Lim, S. M., Lee, P. H., et al. (2019). Magnetic resonance imaging-visible perivascular spaces in basal ganglia predict cognitive decline in Parkinson's disease. *Mov. Disord.* 34, 1672–1679. doi: 10.1002/mds.27798

Poewe, W. (2008). Non-motor symptoms in Parkinson's disease. *Eur. J. Neurol.* 15(Suppl. 1), 14–20. doi: 10.1111/j.1468-1331.2008.02056.x

Postuma, R. B., Berg, D., Stern, M., Poewe, W., Olanow, C. W., Oertel, W., et al. (2015). MDS clinical diagnostic criteria for Parkinson's disease. *Mov. Disord.* 30, 1591–1601. doi: 10.1002/mds.26424

Potter, G. M., Chappell, F. M., Morris, Z., and Wardlaw, J. M. (2015). Cerebral perivascular spaces visible on magnetic resonance imaging: development of a qualitative rating scale and its observer reliability. *Cerebrovasc. Dis.* 39, 224–231. doi: 10.1159/000375153

Qian, E., and Huang, Y. (2019). Subtyping of Parkinson's disease - where are we up to? *Aging Dis.* 10, 1130–1139. doi: 10.14336/AD.2019.0112

Reichmann, H. (2017). Premotor diagnosis of Parkinson's disease. *Neurosci. Bull.* 33, 526–534. doi: 10.1007/s12264-017-0159-5

Rost, N. S., Cougo, P., Lorenzano, S., Li, H., Cloonan, L., Bouts, M. J., et al. (2018). Diffuse microvascular dysfunction and loss of white matter integrity predict poor outcomes in patients with acute ischemic stroke. *J. Cereb. Blood Flow Metab.* 38, 75–86. doi: 10.1177/0271678X17706449

Schenck, C. H., Boeve, B. F., and Mahowald, M. W. (2013). Delayed emergence of a parkinsonian disorder or dementia in 81% of older men initially diagnosed with idiopathic rapid eye movement sleep behavior disorder: a 16-year update on a previously reported series. *Sleep Med.* 14, 744–748. doi: 10.1016/j.sleep.2012.10.009

Sepehrband, F., Barisano, G., Sheikh-Bahaei, N., Choupan, J., Cabeen, R. P., Crawford, M. S., et al. (2020). Alteration of perivascular spaces in early cognitive decline. *bioRxiv* doi: 10.1101/2020.01.30.927350

Shen, S. S., Shen, Y., Xiong, K. P., Chen, J., Mao, C. J., Huang, J. Y., et al. (2014). Validation study of REM sleep behavior disorder questionnaire-Hong Kong (RBDQ-HK) in east China. *Sleep Med.* 15, 952–958. doi: 10.1016/j.sleep.2014.03.020

Si, X., Pu, J., and Zhang, B. (2017). Structure, distribution, and genetic profile of alpha-synuclein and their potential clinical application in Parkinson's disease. *J. Mov. Disord.* 10, 69–79. doi: 10.14802/jmd.16061

Sixel-Doring, F., Trautmann, E., Mollenhauer, B., and Trenkwalder, C. (2014). Rapid eye movement sleep behavioral events: a new marker for neurodegeneration in early Parkinson disease? *Sleep* 37, 431–438. doi: 10.5665/sleep.3468

Smolders, J., Fransen, N. L., Hsiao, C. C., Hamann, J., and Huitinga, I. (2020). Perivascular tissue resident memory T cells as therapeutic target in multiple sclerosis. *Expert Rev. Neurother.* 20, 835–848. doi: 10.1080/14737175.2020.1776609

St Louis, E. K., and Boeve, B. F. (2017). REM sleep behavior disorder: diagnosis, clinical implications, and future directions. *Mayo Clin. Proc.* 92, 1723–1736. doi: 10.1016/j.mayocp.2017.09.007

Stojkovic, T., Stefanova, E., Soldatovic, I., Markovic, V., Stankovic, I., Petrovic, I., et al. (2018). Exploring the relationship between motor impairment, vascular burden and cognition in Parkinson's disease. *J. Neurol.* 265, 1320–1327. doi: 10.1007/s00415-018-8838-3

Stokholm, M. G., Iranzo, A., Ostergaard, K., Serradell, M., Otto, M., Svendsen, K. B., et al. (2017). Assessment of neuroinflammation in patients with idiopathic rapid-eye-movement sleep behaviour disorder: a case-control study. *Lancet Neurol.* 16, 789–796. doi: 10.1016/S1474-4422(17)30173-4

Sulzer, D., and Surmeier, D. J. (2013). Neuronal vulnerability, pathogenesis, and Parkinson's disease. *Mov. Disord.* 28, 715–724. doi: 10.1002/mds.25187

Tekriwal, A., Kern, D. S., Tsai, J., Ince, N. F., Wu, J., Thompson, J. A., et al. (2017). REM sleep behaviour disorder: prodromal and mechanistic insights for Parkinson's disease. *J. Neurol. Neurosurg. Psychiatry* 88, 445–451. doi: 10.1136/jnnp-2016-314471

Wang, T., Yuan, F., Chen, Z., Zhu, S., Chang, Z., Yang, W., et al. (2020). Vascular, inflammatory and metabolic risk factors in relation to dementia in Parkinson's disease patients with type 2 diabetes mellitus. *Aging* 12, 15682–15704. doi: 10.18632/aging.103776

Wardlaw, J. M., Smith, E. E., Biessels, G. J., Cordonnier, C., Fazekas, F., Frayne, R., et al. (2013a). Neuroimaging standards for research into small vessel disease and its contribution to ageing and neurodegeneration. *Lancet Neurol.* 12, 822–838. doi: 10.1016/S1474-4422(13)70124-8

Wardlaw, J. M., Smith, C., and Dichgans, M. (2013b). Mechanisms of sporadic cerebral small vessel disease: insights from neuroimaging. *Lancet Neurol.* 12, 483–497. doi: 10.1016/S1474-4422(13)70060-7

Weller, R. O., Djuanda, E., Yow, H. Y., and Carare, R. O. (2009). Lymphatic drainage of the brain and the pathophysiology of neurological disease. *Acta Neuropathol.* 117, 1–14. doi: 10.1007/s00401-008-0457-0

Xie, F., Gao, X., Yang, W., Chang, Z., Yang, X., Wei, X., et al. (2019). Advances in the research of risk factors and prodromal biomarkers of Parkinson's disease. *ACS Chem. Neurosci.* 10, 973–990. doi: 10.1021/acschemneuro.8b00520

Xie, L., Kang, H., Xu, Q., Chen, M. J., Liao, Y., Thiyagarajan, M., et al. (2013). Sleep drives metabolite clearance from the adult brain. *Science* 342, 373–377. doi: 10.1126/science.1241224

Xu, J., Fu, X., Pan, M., Zhou, X., Chen, Z., Wang, D., et al. (2019). Mitochondrial creatine kinase is decreased in the serum of idiopathic Parkinson's disease patients. *Aging Dis.* 10, 601–610. doi: 10.14336/AD.2018.0615

Yang, W., Chang, Z., Que, R., Weng, G., Deng, B., Wang, T., et al. (2020). Contra-directional expression of plasma superoxide dismutase with lipoprotein cholesterol and high-sensitivity C-reactive protein as important markers of Parkinson's disease severity. *Front. Aging Neurosci.* 12:53. doi: 10.3389/fnagi.2020.00053

Zhang, F., Niu, L., Liu, X., Liu, Y., Li, S., Yu, H., et al. (2020). Rapid eye movement sleep behavior disorder and neurodegenerative diseases: an update. *Aging Dis.* 11, 315–326. doi: 10.14336/AD.2019.0324

Zhang, H., Wang, T., Li, Y., Mao, W., Hao, S., Huang, Z., et al. (2020). Plasma immune markers in an idiopathic REM sleep behavior disorder cohort. *Parkinson. Relat. Disord.* 78, 145–150. doi: 10.1016/j.parkreldis.2020.07.017

Zheng, L., Teng, E. L., Varma, R., Mack, W. J., Mungas, D., Lu, P. H., et al. (2012). Chinese-language montreal cognitive assessment for cantonese or mandarin speakers: age, education, and gender effects. *Int. J. Alzheimers Dis.* 2012:204623. doi: 10.1155/2012/204623

Zheng, W., He, R., Yan, Z., Huang, Y., Huang, W., Cai, Z., et al. (2020). Regulation of immune-driven pathogenesis in Parkinson's disease by gut microbiota. *Brain Behav. Immun.* 87, 890–897. doi: 10.1016/j.bbi.2020.01.009

Zou, J., Chen, Z., Liang, C., Fu, Y., Wei, X., Lu, J., et al. (2018). Trefoil Factor 3, cholinesterase and homocysteine: potential predictors for Parkinson's disease dementia and vascular parkinsonism dementia in advanced stage. *Aging Dis.* 9, 51–65. doi: 10.14336/AD.2017.0416

Zou, W., Pu, T., Feng, W., Lu, M., Zheng, Y., Du, R., et al. (2019). Blocking meningeal lymphatic drainage aggravates Parkinson's disease-like pathology in mice overexpressing mutated alpha-synuclein. *Transl. Neurodegener.* 8:7. doi: 10.1186/s40035-019-0147-y

Conflict of Interest: The authors declare that the research was conducted in the absence of any commercial or financial relationships that could be construed as a potential conflict of interest.

Copyright © 2020 Si, Gu, Song, Zhou, Fang, Jin, Wu, Gao, Guo, Guan, Xu, Yin, Yan, Zhang and Pu. This is an open-access article distributed under the terms of the Creative Commons Attribution License (CC BY). The use, distribution or reproduction in other forums is permitted, provided the original author(s) and the copyright owner(s) are credited and that the original publication in this journal is cited, in accordance with accepted academic practice. No use, distribution or reproduction is permitted which does not comply with these terms.

frontiers in Aging Neuroscience

SYSTEMATIC REVIEW
published: 10 November 2020
doi: 10.3389/fnagi.2020.587396

Characterization of EEG Data Revealing Relationships With Cognitive and Motor Symptoms in Parkinson's Disease: A Systematic Review

Qing Wang[1†], *Lin Meng*[1†], *Jun Pang*[1], *Xiaodong Zhu*[2*] *and Dong Ming*[1*]

[1] *Academy of Medical Engineering and Translational Medicine, Tianjin University, Tianjin, China,* [2] *Department of Neurology, Tianjin Medical University General Hospital, Tianjin, China*

Recent research regards the electroencephalogram (EEG) as a promising method to study real-time brain dynamic changes in patients with Parkinson's disease (PD), but a deeper understanding is needed to discern coincident pathophysiology, patterns of changes, and diagnosis. This review summarized recent research on EEG characterization related to the cognitive and motor functions in PD patients and discussed its potential to be used as diagnostic biomarkers. Thirty papers out of 220 published from 2010 to 2020 were reviewed. Movement abnormalities and cognitive decline are related to changes in EEG spectrum and event-related potentials (ERPs) during typical oddball paradigms and/or combined motor tasks. Abnormalities in β and δ frequency bands are, respectively the main manifestation of dyskinesia and cognitive decline in PD. The review showed that PD patients have noteworthy changes in specific EEG characterizations, however, the underlying mechanism of the interrelation between gait and cognitive is still unclear. Understanding the specific nature of the relationship is essential for development of novel invasive clinical diagnostic and therapeutic methods.

Keywords: Parkinson's disease (PD), electroencephalogram (EEG), motor disorders, cognitive decline, freezing of gait (FOG), dementia

OPEN ACCESS

Edited by:
Liu Jun,
Shanghai Jiao Tong University, China

Reviewed by:
Qinyong Ye,
Fujian Medical University, China
Xavier Xifró,
University of Girona, Spain

***Correspondence:**
Xiaodong Zhu
zxd3516@tmu.edu.cn
Dong Ming
richardming@tju.edu.cn

[†] These authors have contributed equally to this work and share first authorship

Received: *05 August 2020*
Accepted: *06 October 2020*
Published: *10 November 2020*

Citation:
Wang Q, Meng L, Pang J, Zhu X and Ming D (2020) Characterization of EEG Data Revealing Relationships With Cognitive and Motor Symptoms in Parkinson's Disease: A Systematic Review. Front. Aging Neurosci. 12:587396. doi: 10.3389/fnagi.2020.587396

INTRODUCTION

Parkinson's disease (PD) is the second most common neurodegenerative disease after Alzheimer's disease (AD) (Galvez et al., 2018). The degeneration of the basal nucleus nigrostriatal pathway leads to the loss of the dopaminergic neurons, which will result in multiple motor and non-motor symptoms (Martinez-Martin et al., 2011; Galvez et al., 2018). The motor symptoms mainly appear as resting tremor, postural instability, or gait impairment whilst patients would also demonstrate non-motor symptoms, such as depression, anxiety, sleep disorders, and cognitive dysfunctions (Latreille et al., 2015; Galvez et al., 2018). These consequential features of PD contribute to reduced quality of life and increased the risk of disability and mortality in patients with PD.

Gait is no longer regarded as an automated activity, and instead, the role of central nervous system (CNS) and the interaction between motion control and movement execution is drawn more and more attention. Studies in recent decades has revealed a relationship between cognitive

dysfunction and motor symptoms of postural instability/gait disability (PIGD) (Martinez-Martin, 2011). Evidence have shown that cognitive functions, especially execution function and attention function, play significant roles in gait regulation (Maruyama and Yanagisawa, 2006; Amboni et al., 2008). Although the precise mechanism underlying PIGD, especially for severe symptoms, such as freezing of gait (FOG), are not completely understood. It has been shown that impaired cognitive functions can reduce motor autonomy of PD patients (Lewis and Barker, 2009), which comprises postural and gait stability (Robinovitch et al., 2013). Such cognitive dysfunctions (i.e., executive function impairment) are significantly related to motor symptoms (Maruyama and Yanagisawa, 2006; Amboni et al., 2008), suggesting that it can be considered as a predictor of PD.

Neuroimaging technologies have been widely used to study the regulation effect of cognition on motor control. Previous research has demonstrated that FOG might be related with dysfunction of the cortical frontal and parietal regions, and increased activation of the frontal region related to attention network has been observed in PD patients (Rushworth et al., 2002; Wager et al., 2004; Peterson et al., 2014; Maidan et al., 2016b). However, current studies have certain limitations as they were mostly performed in a constrained environment due to the immobility of scanner equipment.

Recent mobile brain/body imaging techniques based on electroencephalogram (EEG) allow the acquisition and real-time analysis of brain dynamics during active unrestrained movements (Nathan and Contreras-Vidal, 2016). The approach has been applied to distinguish brain dysfunctions of PD patients (Handojoseno et al., 2018; Wagner et al., 2019). In general, PD patients show a slowing tendency of global EEG activity where a decrease of beta and gamma power whilst an increase of power in the theta and alpha bands have been observed to be significantly related to cognitive processes, such as motivation, emotion, and decision-making (Handojoseno et al., 2013). Event-related potentials (ERPs) do not only reflect cognitive decline but also could indicate motor disorders in PD (Georgiev et al., 2015; Butler et al., 2017; Delval et al., 2018; Maidan et al., 2019).

Despite a certain amount of studies about characterizing EEG patterns in PD have been published, changes of EEG features related to cognition and motor dysfunctions have not been discussed in detail. Therefore, the aim of this article is to provide a literature review of characterizations of EEG signals related to PD's cognitive and motor functions and discuss its potential to be used as a novel method in clinic diagnosis.

METHODS

This review follows a PICO search strategy based on the research question about the brain mechanism related to cognition and motor dysfunctions in PD. The EEG features of PD patients were summarized and compared to healthy controls, as well as other neurodegenerative diseases, such as DLB and AD.

In this review, PubMed, Web of Science databases and EMBASE were systematically searched for relevant literature from 2010 to 2020. Three sets of keywords were used for the literature search: (i) "Parkinson's disease"; (ii) "EEG" or "Electroencephalography"; (iii) "Dual task" or "cognition and motor" or "cognitive and motor." Papers that have the term of keywords (i & ii & iii) located within the title and/or abstract were included in this review. In addition to the systematic electronic database search, a targeted search of bibliographies of relevant articles was also performed to identify any additional papers for inclusion.

Only original, full-text articles published in English between January 2010 and June 2020 that investigate the cognitive and motor impairments with scalp EEG analysis in patients with PD were considered in this review. Articles were excluded if they: (i) did not use scalp EEG signals to study features associated with cognitive and/or motor symptoms; (ii) studied on other neurological diseases, such as Alzheimer's disease, multiple system atrophy, Huntington's disease, and Binswanger disease; (iii) were review articles.

RESULTS

Search Results

Using the search method mentioned above, a total of 152 articles were retrieved in the Web of Science database and 66 articles were retrieved in the PubMed database. After duplicate and unrelated papers were removed after initial screening, a total of 51 articles were excluded according to the criteria, of which, 38 were excluded according to the exclusion criteria (i), 8 according to the criteria (ii), 2 according to the criteria (iii) and 3 due to only healthy people participated in the studies. Two relevant articles were identified based on the targeted search in the review article. Therefore, a total of 30 articles were selected for inclusion in this review. A modified PRISMA diagram as shown in **Figure 1** illustrates the screening and inclusion process.

Participants

Fourteen papers enrolled only PD patients with and/or without motor or cognitive impairment in the experiments while the rest of studies aimed to identify difference in EEG features during cognitive and/or motion tasks for PD group compared with healthy control (HC) group ($n = 14$) or patient group with other neurodegenerative disease ($n = 2$), such as AD or Lewy body dementia (LBD). The PD patient demographic characteristics and clinical scores are summarized in **Table 1**.

Assessment of Cognitive and Motor Functions

More than half of the studies utilized motor and/or cognitive tasks, some of which combined oddball paradigm (Kotz and Gunter, 2015; Muente et al., 2015; Waechter et al., 2015; Tard et al., 2016; Possti et al., 2020) in order to analyze dual task execution difficulty and investigate the interrelation of the cognitive decline and motor impairment in PD patients. Motor tasks include the standardized Timed up and Go Test (Quynh Tran et al., 2016; Handojoseno et al., 2018), bilateral cyclical ankle movements (Yoshida et al., 2018), lower-limb pedaling motor task (Singh et al., 2020), and repetitive movements of

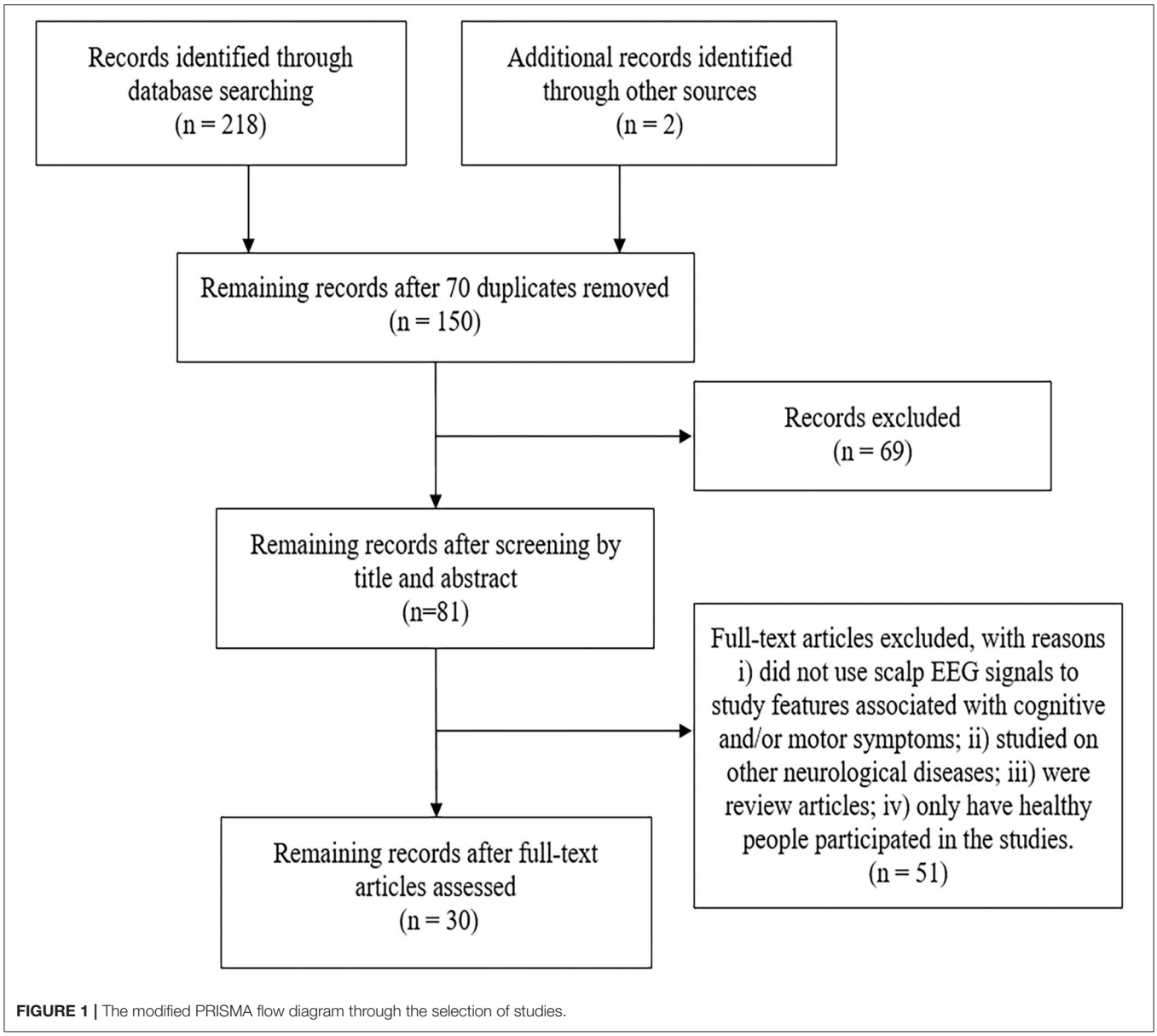


FIGURE 1 | The modified PRISMA flow diagram through the selection of studies.

a specific finger (Herz et al., 2014), while the common Simon task (van Wouwe et al., 2014; Singh et al., 2018), and other customized tasks that require more cognitive processing (Palmer et al., 2010; Yuvaraj et al., 2014; Melloni et al., 2015; Solis-Vivanco et al., 2015) were used to accomplish the cognitive tasks. Three other studies established simple auditory and/or visual oddball paradigms to assess PD cognitive and motor symptoms (Georgiev et al., 2015; Butler et al., 2017; Maidan et al., 2019). The characterizations of EEG signals include: EEG frequency spectrum characteristics, evoked potentials and cortical-muscle coherence (CMC). The remaining 11 papers (37%) used resting state EEG to investigate possible biomarkers for cognitive decline in PD patients (Schlede et al., 2011; Caviness et al., 2015, 2016; Latreille et al., 2015; Cozac et al., 2016; Utianski et al., 2016; Arnaldi et al., 2017), evaluate therapeutic effects (Galvez et al., 2018; Babiloni et al., 2019), and distinguish PDD patients from other dementia patients, such as AD and DLB (Babiloni et al., 2011; Bliwise et al., 2014). The EEG frequency spectrum characteristics (the spectral power and/or power density), the event-related desynchronization/synchronization (ERD/ERS), and the EEG connectivity were studied in rest state EEG while sleep EEG, microstate analysis and the grand total EEG (GTE) score were also investigated in PD patients.

DISCUSSION

This study has evaluated the temporal and spectral characteristics of EEG as well as cortico-muscular coherence (CMC) in PD patients. The definable slowing EEG activity can reflect decreased

TABLE 1 | PD patient demographic characteristics and clinical scores (Mean ± SD) are summarized.

References	Number	Age (year)	Gender (male)	Disease duration (year)	H&Y stage	UPDRS-III	Cognition score
Palmer et al. (2010)	7	63.7 ± 7.1	5	7.1 ± 2.8	–	–	–
Babiloni et al. (2011)	13	72 ± 0	4	–	–	–	17.2 ± 0[b]
Schlede et al. (2011)	19	70.7 ± 0	15	–	–	30.0 ± 0	28.0 ± 0[b]
Bliwise et al. (2014)	64	63.0 ± 9.7	42	5.6 ± 4.0	–	17.6 ± 8.9	28.6 ± 1.7[b]
Herz et al. (2014)	11	60.5 ± 9.4	8	8 ± 5.2	–	17.9 ± 10.9	–
van Wouwe et al. (2014)	10	63.1 ± 0	6	3.52 ± 0	–	13.2 ± 0	29.2 ± 0[b]
Yuvaraj et al. (2014)	20	59.0 ± 5.6	10	5.8 ± 3.5	2.3 ± 0.6	17.1 ± 3.2	26.9 ± 1.5[b]
Caviness et al. (2015)	71	73.7 ± 8.0	43	8.5 ± 4.9	2.27 ± 0.71	22 ± 12	27.8 ± 2.0[b]
Georgiev et al. (2015)	14	60.4 ± 12.3	–	3.5 ± 3.0	1.8 ± 0.4	28.6 ± 7.7	27.6 ± 1.6[a]
Kotz and Gunter (2015)	1	58	1	14	3–4	47	–
Latreille et al. (2015)	68	64.9 ± 0	46	4.5 ± 0	2.3 ± 0	22.5 ± 0	–
Muente et al. (2015)	12	66.5 ± 8.9	5	10.4 ± 6.8	–	22.3 ± 12.9	–
Melloni et al. (2015)	14	56.0 ± 11.2	7	22.0 ± 12.4	6.5 ± 3.5	2.4 ± 0.7	–
Solis-Vivanco et al. (2011)	55	58.5 ± 8.6	33	5.2 ± 3.4	–	–	26.7 ± 2.1[b]
Waechter et al. (2015)	16	64.7 ± 6.2	11	8.9 ± 7.0	2 ± 0.4	30.1 ± 14.8	25.4 ± 2.7[a]
Caviness et al. (2016)	134	75.9 ± 8.2	–	11.4 ± 6.7	2.6 ± 0.9	27.8 ± 14.8	–
Cozac et al. (2016)	37	67 ± 0	25	8 ± 0	–	14 ± 0	–
Quynh Tran et al. (2016)	4	–	3	–	–	–	–
Tard et al. (2016)	25	61.3 ± 8.2	–	7.1 ± 3.1	2.3 ± 0.7	18.0 ± 8.9	27.7 ± 2.2[b]
Utianski et al. (2016)	88	76.4 ± 7.5	–	11.8 ± 6.8	2.6 ± 1.0	27.3 ± 14.4	–
Arnaldi et al. (2017)	54	68.6 ± 7.2	30	13.6 ± 9.9	1.6 ± 0.5	13.4 ± 5.8	28.9 ± 1.1[b]
Butler et al. (2017)	20	63.9 ± 7.8	12	10.25 ± 9.9	2.5 ± 0.4	28.7 ± 12.0	25.2 ± 2.9[a]
Galvez et al. (2018)	14	62.0 ± 6.1	6	7.2 ± 4.9	2.1 ± 0.7	–	–
Handojoseno et al. (2018)	16	70.9 ± 6.9	16	8.6 ± 6.6	2.8 ± 0.6	42.5 ± 14.3	–
Singh et al. (2018)	28	69.8 ± 8.6	17	12.5 ± 3.8	–	22.1 ± 10.1	28.6 ± 1.1[b]
Yoshida et al. (2018)	9	62 ± 6.2	9	10.1 ± 5.2	–	17.6 ± 6.2	26.9 ± 1.7[a]
Babiloni et al. (2019)	120	72.1 ± 0	52	–	–	–	24.4 ± 0[b]
Maidan et al. (2019)	10	60.5 ± 0	6	2.9 ± 0	–	20.2 ± 0	25.2 ± 0[a]
Possti et al. (2020)	6	57.7 ± 0	5	2.9 ± 0	–	21.8 ± 0	25.8 ± 0[a]
Singh et al. (2020)	26	67.4 ± 0	17	6.2 ± 0	2 ± 0	14.9 ± 0	23.3 ± 0[a]

SD = 0 means that SD value was not provided in the article. SD, standard deviation.
[a] *The Montreal Cognitive Assessment (MoCA) scale was used for cognitive level evaluation.*
[b] *The Mini-Mental State Examination (MMSE) scale was used for cognitive level evaluation.*

cognitive level of patients with PD while negative correlation between the GTE score and cognitive state was observed. Reduced ERPs represent the cognitive decline and attention deficits that can be associated with severity of motor symptoms. Abnormalities in β and δ frequency bands are the main manifestation of dyskinesia and cognitive decline in Parkinson's disease, respectively.

EEG Spectral Characteristics

EEG spectral pattern is usually characterized in the range of 0–30 Hz with five internationally agreed frequency bands: δ (0–4 Hz), θ (5–7 Hz), α (8–13 Hz), β (14–30 Hz), and γ (>30 Hz) bands. It is one of the most studied EEG features in PD patients. Studies showed that cognitive deficits are correlated with a slowing of EEG frequencies. Compared to non-demented PD patients, PD patients with dementia (PDD) have increased amplitude in lower frequency bands (i.e., θ and δ bands) and decreased amplitude in higher frequency bands (i.e., α and β bands; Soikkeli et al., 1991; Stoffers et al., 2007; Caviness et al., 2015; Arnaldi et al., 2017; Geraedts et al., 2018). More studies revealed the increased activities in θ and δ bands of EEG in PD patients (Babiloni et al., 2011; Caviness et al., 2016). Cozac et al. (2016) analyzed low frequency bands and demonstrated that global relative median power (GRMP) spectra of θ band can be used to predict cognitive decline. Despite the attenuated mid-frontal θ activity associated with disease duration, PD patients exhibited increased central θ power and decreased occipital θ power (Palmer et al., 2010; Singh et al., 2018). The abnormality of posterior cortical θ rhythm based on cortical source mapping of resting state EEG was observed in Babiloni et al. (2011). The θ relative band power of PD patients with mild cognitive impairment (PD-MCI) was higher than that of cognitively normal PD patients (PD-CogNl). An increasing trend was observed in the δ band power from PD-CogNl to PD-MCI to PDD (Caviness et al., 2016). Longitudinal changes of neuropsychological test were mostly related to the change of δ

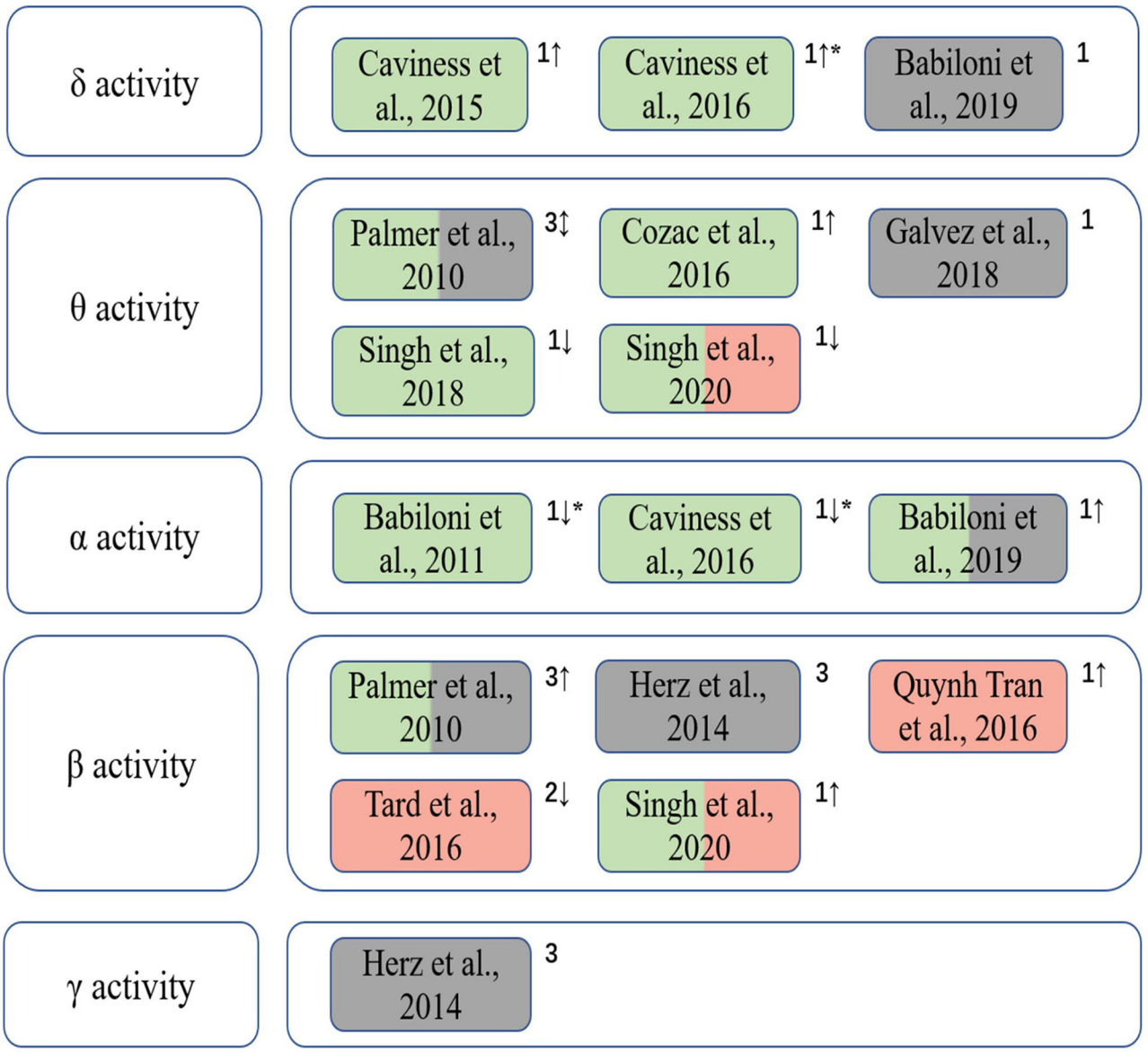


FIGURE 2 | The correlation between EEG spectral characteristics in different frequency bands and cognition and motor functions of PD patients. Green indicates that the EEG spectral characteristics is correlated with cognitive function; red indicates that it is correlated with motor performance; gray indicates that EEG spectral patterns are used to assess clinical treatment outcomes. 1, spectral power/power density; 2, event-related desynchronization/synchronization (ERD/ERS); 3, EEG connectivity; "↑," the increase trend; "↓," the decrease trend; "↕," different trends of EEG spectral characteristics in various brain regions when cognitive and/or motor symptoms appear; "*" indicates that the gradual changes of EEG features of patients from PD-CogNl to PD-MCI to PDD manifest decrements in cognitive level.

power for PD patients with mild to moderate motor impairment (Caviness et al., 2015). PD patients had higher diffuse δ source compared to HC group which may lead to abnormal sources of central δ rhythms in PDD patients (Babiloni et al., 2011, 2019). The increased power in δ band could be the main feature of the deterioration of cognitive impairment, which is closely related to the incidence of PDD (Caviness et al., 2015, 2016).

Event-related desynchronization (ERD) and event-related synchronization (ERS) are considered to indicate the activation of the motor cortex during planning, executing and completing a movement (Heinrichs-Graham et al., 2014; Tard et al., 2016; Delval et al., 2018). Previous studies have shown the α band rhythm display an essential role in motor processing and enhanced β band oscillation may reflect motor control deficits during movement preparation (Cahn et al., 2013; Tard et al., 2016; Delval et al., 2018). The diminished β power ERD and prolonged β ERS in an attentional experiment suggest that the coupling between attention and motor preparation was impaired in PD-FOG (Tard et al., 2016). The relative bandpower in α band showed a decreasing trend in the longitudinal changes from

PD-CogNl to PD-MCI to PDD as well as cortical changes were observed in PD patients (Babiloni et al., 2011, 2019; Caviness et al., 2016). PD patients had lower occipital α source compared to HC whilst PDD patients showed increased frontal-temporal α source and abnormal sources of posterior cortical β1 rhythm (Soikkeli et al., 1991; Babiloni et al., 2011, 2019). As the changes of β band power are related to gait initiation failure (GIF) events, abnormal β oscillation may be a biomarker of motor impairment in PD patients (Palmer et al., 2010; Quynh Tran et al., 2016).

The efficient neural communication between premotor and motor cortical areas was critical for motor control (Herz et al., 2014). The decrease in γ band power was observed in resting state EEG of PD patients (Stoffers et al., 2007). PD patients exhibited a loss of γ-γ coupling from the lateral premotor cortex (lPM) to the supplementary motor area (SMA) when performing repetitive movements of the right index finger at maximal rate. Cross-frequency coupling of the slow and fast band activities might facilitate information transmission across brain networks (Canolty and Knight, 2010). $Kappa_w$ was used to evaluate the weighted brain network and found the parameters increased in the θ and β bands while decreased in the δ and α bands in PD patients compared to healthy participants (Utianski et al., 2016). The results showed a hub shifting in the bands and peak background frequency exists in both higher and lower frequency bands. The shift from α/δ to θ/β coupling suggests a change in cortical network in PD (Utianski et al., 2016), and the enhancement of θ/β coupling from primary motor cortex (M1) to the lateral premotor cortex (LPM) is related to the improvement of levodopa-induced motor function (Herz et al., 2014). The brain graph theory network analysis based on EEG signals indicated that the network breakdown is associated with cognitive decline, manifested as less connectivity and decreased global network efficiency with a loss of highly connected cortical hubs (Utianski et al., 2016).

Changes of EEG spectrum can be associated with clinical assessment scales and motion performance. The power of θ and β bands are, respectively related to the scores of Montreal Cognitive Assessment (MoCA) and the motor part of the Unified Parkinson's Disease Rating Scale (UPDRS-III) (Singh et al., 2020). PD-FOG patients showed increased β power and decreased θ power in mid-frontal region when performing a lower-limb pedaling motor task needing intentional initiation and stopping of movement (Singh et al., 2020). The θ, α, and β activities in left posterior parietal cortex (PPC) were positively correlated to the motion parameters during single or dual task walking (conversation/email sending), indicating that the left PPC may be involved in sensory motor integration and gait control (Pizzamiglio et al., 2018). Studies also found that the power of δ, θ, and γ bands was significantly increased during the planning and execution stages of motor (particularly in the execution stage), followed by decreases in α, β, and low-γ bands after an execution cue (Combrisson et al., 2017; Delval et al., 2018).

Figure 2 summarizes the included studies on EEG spectrum characteristics related to Parkinson's disease in this review. A significant interrelation was observed between β band power changes and dyskinesias, whilst abnormalities in θ and δ bands were associated to cognitive decline in PD patients. The changes of the spectrum characteristics can be used to assess the cognitive and motor abilities of PD patients during treatments as a dynamic and quantitative method.

Event-Related Potentials (ERPs)

Event-related potentials (ERPs) refer to event-related voltage changes in brain regions in response to specific stimuli (e.g., visual, auditory, and somatosensory stimuli). The ERPs provide a powerful method for exploring the ongoing EEG activity that are time-locked to sensory, motor, and cognitive events, and can be used as an electrophysiological indicator of cognitive function (Butler et al., 2017; Maidan et al., 2019). **Table 2** summarizes ERP-related studies included in this review. The results demonstrate that changes of ERPs have been utilized to identify cognitive decline and abnormal attention distribution of PD patients, and can be applied to investigate the correlation between cognitive and motor functions. All studies investigated ERPs induced by visual or auditory stimuli ($n = 10$), and five studies also discussed event-related potentials while performing motor tasks ($n = 5$).

Auditory and/or Visual ERPs

The P300 ERP is the most investigated neural markers of attention and cognition. Studies have shown that changes in the amplitude and latency of the P300 ERP are related to attention and cognitive decline (Georgiev et al., 2015; Maidan et al., 2019). An increase of P3b latency was observed in PD patients in visual and/or auditory oddball paradigms and associated with disease severity, cognitive dysfunction and impaired activities (Matsui et al., 2007; Da Silva Lopes et al., 2014). It is shown in **Figure 3A** that PD patients had a significantly smaller amplitude of P3b in random number generation (RNG) task compared to that in ordered number generation (ONG) task. The execution of RNG task may require greater attention resources, therefore less random behavior in PD patients was observed due to depleted attention resources (Muente et al., 2015). As there is a relationship between the decrease of P3a amplitude and the duration and severity of PD, the P3a is regarded as a potential cognitive marker for the development of mild to moderate PD patients (Solis-Vivanco et al., 2015). The changes of EEG in PD patients can be used to identify the drug effect during treatment in which P3a amplitude is mainly related to motor symptoms and dopaminergic medication (Georgiev et al., 2015). However, it should be noted that the P300 ERP is highly sensitive to cognitive decline and attention disorders, which may also occur in other neurodegenerative diseases, such as AD (Maidan et al., 2019). Further study on P300 in a large representative sample will be needed to support the potential use of P300 as a biomarker for PD patients.

Another measure commonly used to study ERPs is Event-Related Spectral Perturbation (ERSP), which evaluated the spectral power within various frequency bands (Possti et al., 2020). Changes in brain dynamics in the power of different frequency bands, i.e., delta, theta, alpha, and beta bands, were observed when PD patients, healthy elder, and young subjects participated in an auditory oddball cognitive task performed during standing and walking on a treadmill (Possti et al., 2020). PD patients showed higher alpha

TABLE 2 | Summary of experimental paradigms and main results of induced ERPs.

Induced method	ERPs induced	References	Subjects	Experimental paradigm	Main results
Visual/auditory stimulations only	P300	Georgiev et al., 2015	14 PD patients, 13 HC	Auditory three stimuli Oddball paradigm: 500 and 1,000 Hz, white noise. Visual Oddball paradigm: a small light blue circle at 4.36°, circle at 5.72°, checkerboard pattern. Subjects were asked to count the times the target stimulus appeared.	Dopaminergic drugs significantly increase the P3a amplitude in PD patients, but only in response to error select stimuli in hearing rather than vision.
		Muente et al., 2015	12 PD patients, 12 HC	Auditory Oddball paradigm: 635 and 435 Hz. Subjects should press the key of 1–9 to form RNG/ONG when hearing the standard stimulus, and press the 0 key when hearing the target.	Compared with ONG, P3b amplitude in PD patients is significantly smaller when generating RNG. But in HC group, it is similar in two conditions.
	P300, MMN, RON	Solis-Vivanco et al., 2015	55 PD patients, 24 HC	Auditory experiment: 1,000 Hz (90%), 1,100 Hz (10%). Subjects are asked to distinguish the sound and press the corresponding button at full speed.	Both the duration and severity of PD have important effects on P3a amplitude. The amplitude of P3a in PD is significantly lower than that in HC, especially in patients with H&Y stage 2 and 3.
	P600	Kotz and Gunter, 2015	1 advanced PD patient	Auditory Oddball paradigm: 600 and 660 Hz. Subjects should count the number of target stimuli. They then receive a language part in which passively listening to grammatically correct and incorrect sentences. Sections 2 and 3 give subjects auditory stimulus of progress/waltz before the language part while section 1 and 4 not.	External auditory cues seem to completely restore the P600 potential of PD patients in response to a syntactic expectancy violation, such as March (4/4).
	LRP, P300	Butler et al., 2017	10 PD-FOG, 10 PD-nFOG	Visual Oddball paradigm: a vertical green cross blinking in the screen, cross rotating 45°. Subjects were asked to press the button immediately after the target.	The LRP in PD-FOG appears earlier and has a larger amplitude. The LRP amplitude is significantly correlated with the FAB score, but not with the disease severity indicators such as H & Y and UPDRS-III scores.
Merging motor tasks	P300	Waechter et al., 2015	9 PD-FOG, 7 PD-nFOG	VR technology provides a virtual corridor which subjects walk through. They complete the visual Oddball task at the same time: "+," "×." Subjects are required to press the button when seeing target. Finally, repeating the above experiment in a sitting position.	The P3b component in walking/sitting experiments could not be detected in PD-FOG if the data is stimulus-locked, while P3b is clearly visible when respond-locked (lock to the button press).
		Maidan et al., 2019	11 healthy young adults, 10 healthy older adults, 10 PD patients	Auditory Oddball paradigm while standing or walking on the treadmill: 600 Hz pure tone bursts, 1,200 Hz. Subjects need to count how many times the target stimulus appeared.	The P300 latency of the elderly and PD patients is prolonged during walking, but the P300 amplitude only reduces in PD patients; better motor and cognitive abilities are associated with shorter P300 latency.
	N1, P2, P3	Tard et al., 2016	12 PD-FOG, 13 PD-nFOG, 13 HC	Auditory Oddball paradigm: 1,000 and 2,000 Hz. Subjects need to press the button after the target stimulus. Simultaneously performing a motor preparation task: taking right foot to start walking as soon as the screen shows "go."	The ERP characteristics of three groups are not significantly different. As a post-perceptual marker of FOG, EEG oscillations are more sensitive than ERP.

LRP, lateralized readiness potential; SDN, step-cue delay negative; RNG, random number generation; ONG, ordered number generation; MRP, movement-related brain potential; CPP, centroparietal positivity; APA, anticipatory postural adjustments; VR, virtual reality; H&Y, Hoehn and Yahr scale; UPDRS III, the motor part of the Unified Parkinson's Disease Rating Scale.

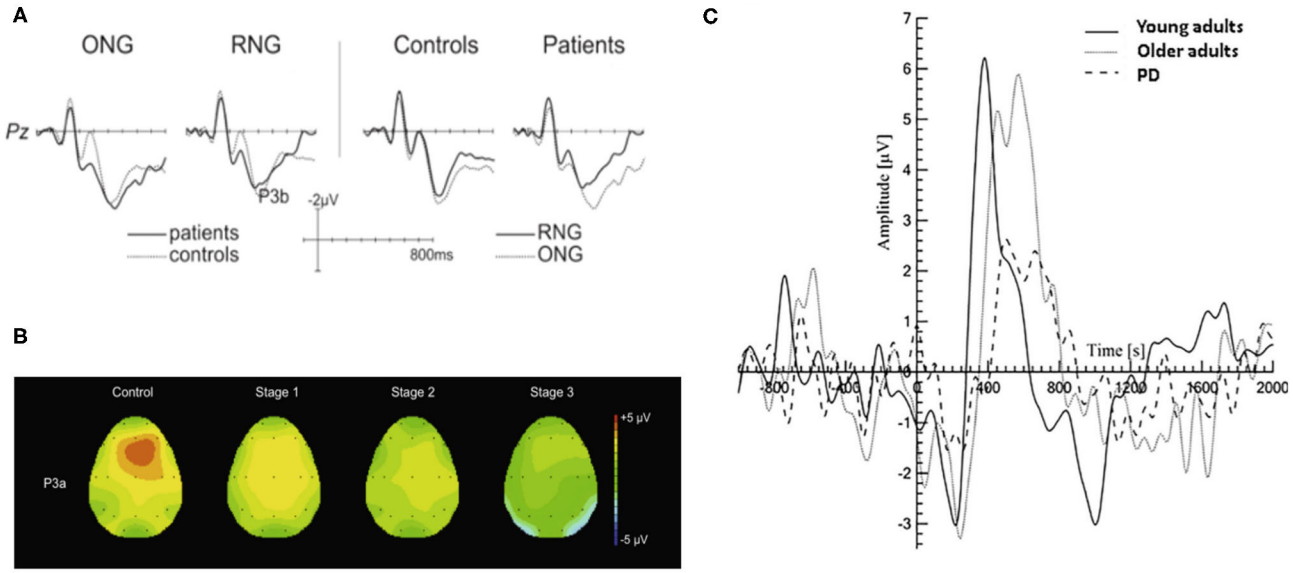


FIGURE 3 | Typical P300 changes in PD patients. **(A)** A more pronounced reduction in P3b amplitude during the RNG task was observed than that with ONG task (Muente et al., 2015). **(B)** Topographic maps of P3a in HC group and PD patients in three H&Y stages (stage 1, 2, 3) during an auditory oddball paradigm. The P3a showed a frontocentral distribution and its amplitude was negatively associated with the severity of PD (Solis-Vivanco et al., 2015). **(C)** The P300 amplitude is significantly smaller in PD patients (dash line) compared to those in young and older adults (solid black line and gray line, respectively) during walking (Maidan et al., 2019). HC, healthy control; H&Y, Hoehn and Yahr scale; RNG, random number generation; ONG, ordered number generation. (Image sources were adapted with granted copyright permission.) **Figure 3A** is available at IOS Press through Muente et al. (2015).

and beta power during single and dual task compared to older adults, while an early lower delta power was also found during dual task. The phenomenon suggests that further modulation of readiness and attention is required in elders and PD patients and leads to larger recruitment of brain resources.

Unexpected changes in task-irrelevant auditory stimuli are usually accompanied by the elicited ERP components associated with attention orientation, such as novelty-P3a, mismatch negativity (MMN), reorientation negativity (RON). They are collectively referred as "distraction potential" and have been used to study the brain mechanism of involuntary attention (IA) in PD patients (Solis-Vivanco et al., 2011). As shown in **Figure 3B**, Solis-Vivanco et al. (2015) found that PD patients, especially those receiving anti-PD drug treatments, had reduced P3a amplitudes in the frontal, central, and temporal regions during distracting oddball tasks. The changes in novelty detection and/or the direction of attention were only observed in severe PD patients (Karayanidis et al., 1995; Georgiev et al., 2015; Solis-Vivanco et al., 2015). It suggests that the MMN might be potential in identifying patients with PD dementia (PDD) (Bronnick et al., 2010). Solis-Vivanco et al. (2011) also studied the role of RON in assessing cognitive function of PD patients. Comparing with drug-naïve patients, RON amplitude of patients receiving drug treatment was significantly higher and closer to HC group, indicating that dopamine therapy can also regulate the reorientation of attention. It is proven that there is a correlation between RON latency and the behavioral outcome of advanced PD patients (Georgiev et al., 2015; Solis-Vivanco et al., 2015). Despite the above-mentioned potentials, Kotz and Gunter (2015) firstly studied the P600 potential in one patient with advanced PD for reflecting language-related deficits.

Movement-Related Potentials

Understanding the neural mechanism underlying the cognitive-motor interference may have implications for predicting the decrement in dual task performance. The P300 ERP is regarded as an index of the amount of resources allocated to stimulus processing. The reduced amplitude of P300 is associated with worse attentional concentration and the longer latency is related to motor and cognitive abnormalities (Polich, 2007; Maidan et al., 2019). PD patients showed a decrease amplitude and an increased peak latency of P300 during sitting and walking tasks as shown in **Figure 3C**, but its amplitude when performing oddball task during standing is similar to those in healthy elderly and young groups (Yilmaz et al., 2017; Maidan et al., 2019). There is no significant association between FOG symptom and ERPs. The ERPs elicited in auditory oddball paradigm may not be suitable as a biomarker of FOG symptoms (Tard et al., 2016).

The lateralized readiness potential (LRP) reflects the preparation of motor activity and it is modulated by participants' observed response. Due to the lack of motor preparation in PD caused by dysfunctions in supplementary motor area (SMA) (D'Ostilio et al., 2013), the LRP might occur earlier and have larger amplitude in PD-FOG when comparing to PD-nFOG (Butler et al., 2017). The increased activation in the prefrontal cortex area in the occurrence of FOG suggests that PD patients

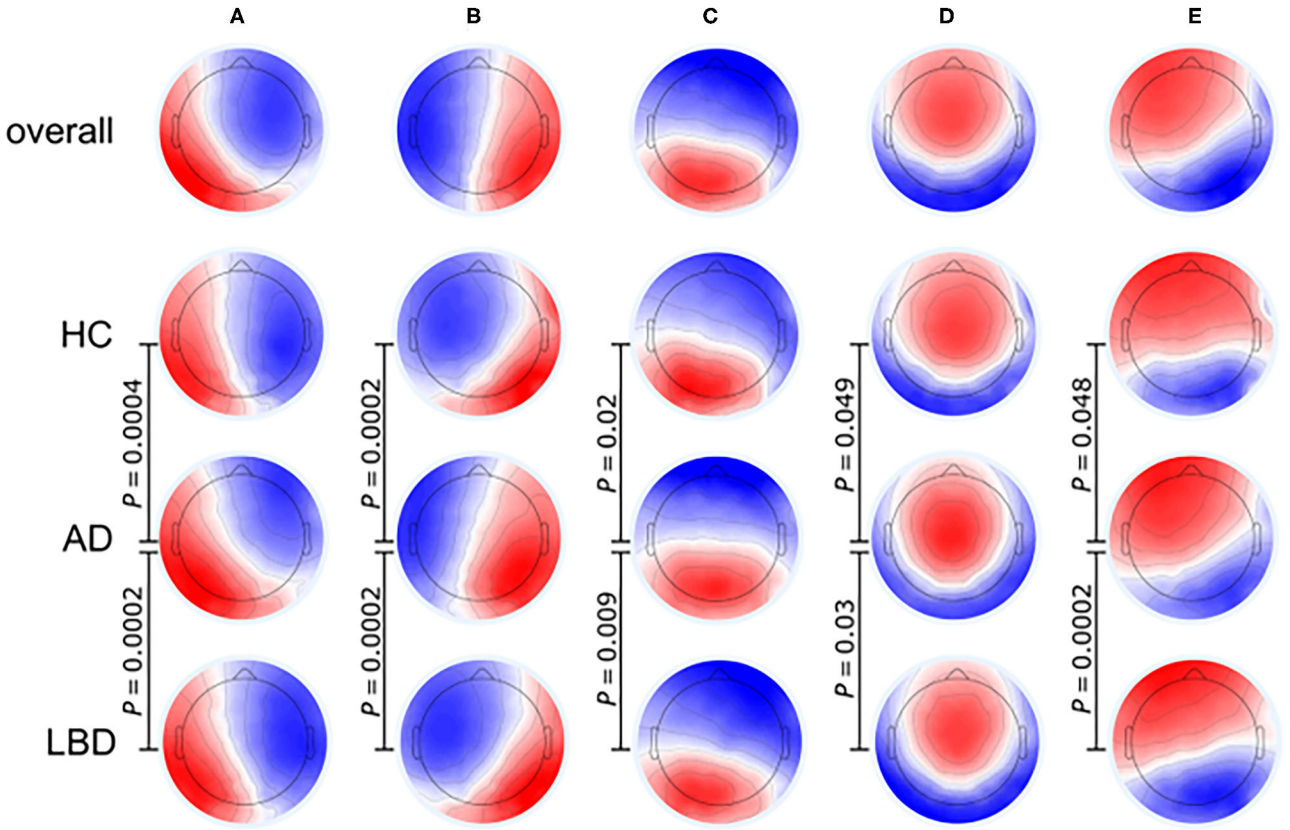


FIGURE 4 | Microstate class topographies for dynamic brain activities in Alzheimer's disease (AD) and Lewy body dementia (LBD) patients compared to healthy control (HC) group. The EEG signal was divided into a group of short, non-overlapping and quasi-stable microstates where the microstates **(A–E)** were related to over 70% of changes in brain activities. *P*-values result from comparing the group topographies between groups using TANOVA. (Image source: Schumacher et al., 2019b: use permitted under the Creative Commons CC BY license).

with FOG would need more attentional source (probably from the lateral premotor area) compared with PD-nFOG. The change in LRP reflects over-recruitment of the lateral premotor area in order to compensate for SMA deficits, and it also indicates that the main defect of FOG might occur in the motor preparation stage (Shine et al., 2013). As the LRP can be regarded as a movement-related brain potential, the results from van Wouwe et al. (2014) demonstrated that inhibition of motor cortex is important to alleviate PD symptoms. Another study also found that PD patients had reduced motor potential (MP) and impaired action-sentence compatibility effect (Melloni et al., 2015).

Other EEG studies in PD

EEG Microstates

EEG signals can be segmented into many different short topographies (microstates) which can be clustered into a limited number of landscape (Koenig et al., 1999). EEG microstates reflect a transient and stable brain topology on a millisecond temporal level and provide a powerful perspective on the dynamic changes of the brain. It has been proved that EEG microstate features, especially its duration, were associated with the cognition and perception, and different cognitive functions were related to specific microstates (Britz et al., 2010; Van de Ville et al., 2010; Milz et al., 2016). **Figure 4** illustrates that the EEG microstate analysis can be used for investigating brain activity changes in neurodegenerative diseases. Compared to AD and HC groups, patients with Lewy body dementia (LBD) have longer durations of all microstate classes and the number of distinct microstates per second is also reduced (Schumacher et al., 2019b). As the fluctuation of cognitive and attentional disorders is an important feature of Lewy body dementia, the severity of cognitive fluctuation is positively associated with the slowing of microstate dynamics (McKeith et al., 2005, 2017).

The slowing of microstate dynamics indicates a relative loss of brain variability at resting state in patients with LBD (Schumacher et al., 2019b), which is consistent with the loss of brain network flexibility observed in previous fMRI studies (McIntosh et al., 2008; Jia et al., 2014; Schumacher et al., 2019a). The average duration of microstates in LBD patients is inversely related to dynamic functional connections between the basal ganglia and thalamus or large cortical networks, indicating that the dynamic interactions in the cortical-basal ganglia-thalamic loop participate in the regulation of global microstate dynamics

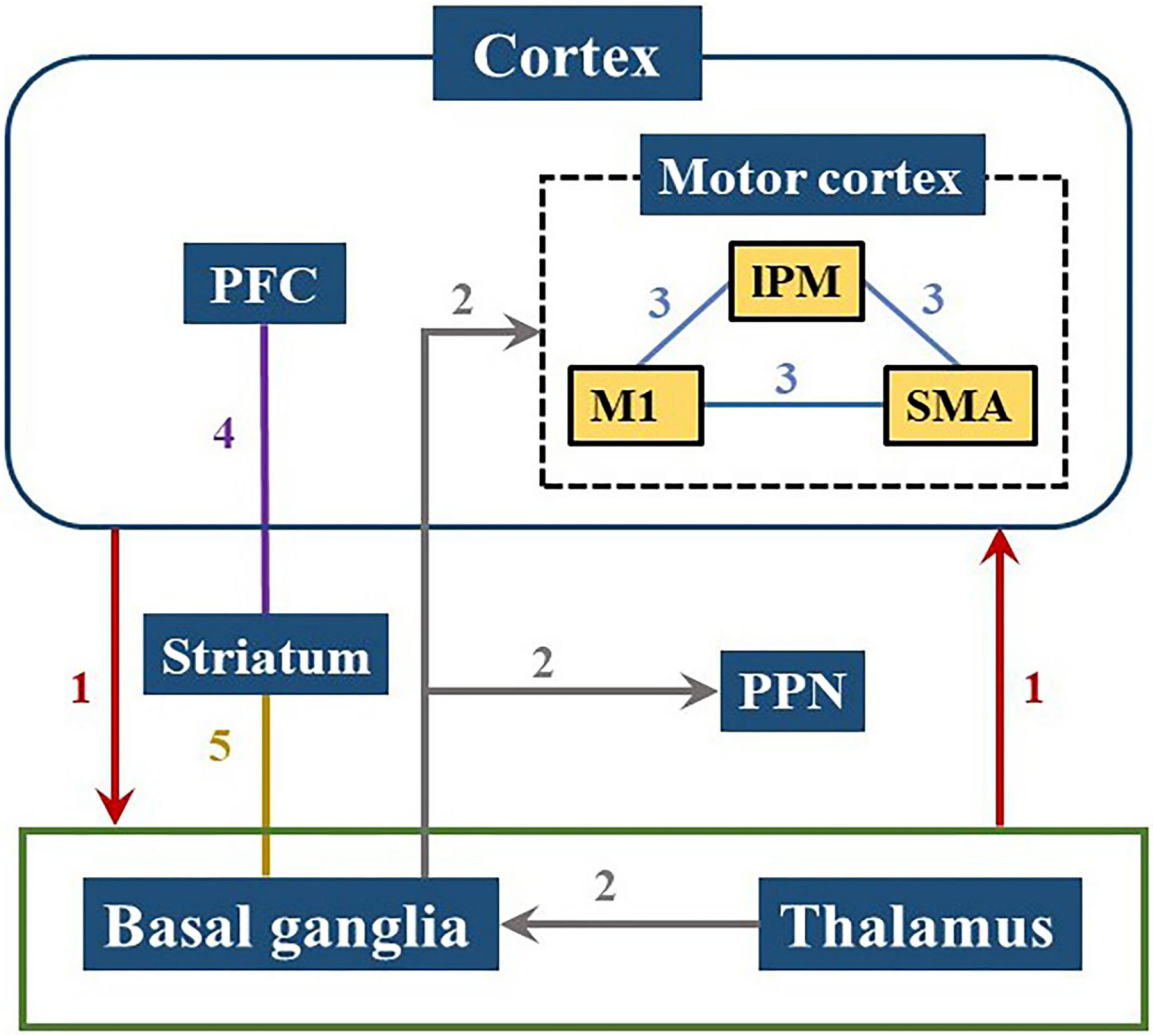


FIGURE 5 | Brain pathways involved in PD cognitive and motor dysfunctions. Neural information is transmitted from the cerebral cortex to the basal ganglia or thalamus and back to the cortex as shown in path 1. Path 2 demonstrates that the input from the thalamus in the basal ganglia is projected to the motor cortex or PPN, reflecting the pathological activities within the ganglia which can affect motor control process. The internal connection of the motor cortex in path 3 has a great influence on motor functions of PD patients. Path 4 and 5 are related to the striatum showing that the frontostriatal circuit and the basal ganglia-striatal circuit are both damaged in PD patients. PFC, prefrontal cortex; IPM, lateral premotor cortex; M1, primary motor cortex; SMA, supplementary motor area; PPN, pedunculopontine nucleus.

and the subcortical abnormalities have a significant impact on the overall function of the whole brain network (Bell and Shine, 2016; Schumacher et al., 2018).

Sleep EEG

Recent studies show that sleep spindle and slow waves might facilitate understanding the mechanism of brain plasticity and the results have been related to human cognitive ability. However, the potential use of sleep EEG as a biomarker of cognitive decline in PD is still unclear (Latreille et al., 2015). In a longitudinal study, PD patients who develop dementia after 4.5 years of follow-up study showed decreased density and amplitude of sleep spindle in baseline polysomnography at the posterior cortical area: The PDD patients had most decrease in sleep spindles density, followed by PD patients without dementia, and the HC group has the least (Latreille et al., 2015). The result indicates that the sleep spindle density might be used a potential marker of cognitive decline in PD.

Cognitive fluctuation is a noteworthy feature of DLB rather than PD (Bliwise et al., 2014). In comparison of the coefficients of variation (COVs) based on the polysomnography, DLB patients have significantly greater cognitive fluctuation that PD patients even when they have similar level of cognitive impairment. Although PD patients have smaller amplitude of slow waves compared to healthy people, there is no significant difference observed between patients with different cognitive levels. Slow waves might not be suitable for predicting the cognitive function (Latreille et al., 2015).

Grand Total EEG (GTE) Score

The grand total EEG (GTE) score is a rating scale for clinical EEG analysis which can be used for the diagnosis of AD and LBD. It can distinguish between AD and other types of dementia (Pijnenburg et al., 2008). The original GTE score consists of six subscales: (i) frequency of rhythmic background activity, (ii) diffuse slow activity, (iii) reactivity of rhythmic background activity, (iv) paroxysmal activity, (v) focal abnormalities, and (vi) sharp wave activity. A negative relationship between scores (i)–(iii) and cognitive decline was observed in Schlede et al. (2011) by analyzing the correlation between GTE scores and cognitive levels in PD patients. The scores could be potential to identify MCI, which is a common non-motor symptom in PD and regarded as a transitional state between normal cognition and PDD.

Cortico-Muscular Coherence (CMC)

The cortico-muscular coherence (CMC) reflects functional coupling between the cortical activity and muscle activity (Wagner et al., 2019). It has been widely used in studies to assess the recovery of motor function after stroke by quantifying interaction between the motor cortex and controlled muscles, however the CMC is rarely used in PD patients (Ushiyama et al., 2011; Zheng et al., 2018).

The findings in CMC features of PD patients are not yet consistent. Several studies have shown that PD patients exhibit motor abnormalities during ankle movement (Yoshida et al., 2018; Zheng et al., 2018). Although there was no difference in CMC even when movement performance significantly varied between PD patients and age-matched HC group (Andrykiewicz et al., 2007). The increased CMC of the midline cortical areas and tibialis anterior muscle in β band during maximum dorsiflexion and plantarflexion is opposite to results from previous study in which decreased β band CMC in PD patients during continuous isometric wrist extension was found (Omlor et al., 2007). Levels of cortico-muscular β band coherence during forearm contraction were found to be similar in patients with PD and HC group (Pollok et al., 2012). Different sensorimotor loops are responsible for upper and lower limb movements, which may explain the inconsistent results among the existing studies. The task-related and movement-related effect of CMC should be concerned when researchers investigate changes of functional interactions between brain activity and movement kinematics using CMC analysis.

Changes of Brain Networks in PD

PD patients have less global efficiency and functional connectivity of the brain network during the cognitive level declines (Utianski et al., 2016), which might be caused by pathological oscillations and abnormal regulation in the cortico-basal ganglia-thalamic-cortical pathways (Palmer et al., 2010; Herz et al., 2014). Studies have shown that the motor and cognitive dysfunction of PD patients can be related to abnormal changes in multiple pathways involving several brain regions, mainly including the basal ganglia (BG), thalamus, and frontal region. The changes of brain networks in PD were summarized in **Figure 5**.

The BG circuits play a key role in high-level cognitive function and motor control (Melloni et al., 2015). The loss of dopamine impacts the network between the prefrontal cortex and BG which leads to inability to coordinate the selection and inhibition of conflict responses (Aron et al., 2007). The damage of the BG-cortical motor network consisting the loop from the frontal lobe to BG/thalamus and back to the cortex, may cause downstream influence on the cortical-subcortical connectivity and interfere with the cortical-subcortical motor network (Garcia and Ibanez, 2014; Melloni et al., 2015). Moreover, the cortical-BG-thalamic circuit is an important contributor to large-scale network communication in the brain, in which the dynamic interaction of the various components plays a role in the regulation of brain dynamics (Bell and Shine, 2016). Several different locations in the frontal area are connected to specific areas of the striatum and thalamus through parallel circuits (Cummings, 1995). Pathologic activities in the ganglia are input from the thalamus to the BG, and then projected to the motor cortex or pedunculopontine nucleus (PPN) (Lanciego et al., 2012; Hunnicutt et al., 2014; Yoshida et al., 2018). Dysfunction within these circuits lead to symptomatic progression in PD, such as cognitive issues.

Insufficient motor preparation in PD patients is mainly caused by supplementary motor area (SMA) dysfunction and can be compensated by overrecruiting larger cortical areas, such as lateral premotor cortex (lPM) (D'Ostilio et al., 2013; Butler et al., 2017). Both lPM and SMA are located in Brodmann Area 6 (BA 6), while the primary motor cortex (M1) is in Brodmann Area 4 (BA 4). These three regions are all located near the precentral gyrus and the connections between them (shown as Path 3 in **Figure 5**) affect movement function in PD (Herz et al., 2014). Increased activities in the prefrontal cortex (PFC) has been observed in PD patients during dual-task walking, which indicates a potential compensation mechanism involving the recruitment of attention networks (Holtzer et al., 2015; Maidan et al., 2016a, 2019). The activation of the PFC has been proven to have an essential role in cognitive control (Singh et al., 2018) and also involve in initiation and execution of movement (Singh et al., 2020).

Limitations and Perspectives

The EEG analysis provides parameters to quantitatively evaluate cognitive deficits related to the severity of PD, making it a promising approach to assess the therapeutic efficacy. Galvez et al. (2018) investigated the possibility of binaural-rhythmic sound simulation to be applied as an effective therapy using EEG data. The results showed that the decrease of θ power in PD patients after receiving auditory stimuli, demonstrating that the changes of EEG in PD patients could detect the drug effect before and after the treatment (Georgiev et al., 2015). The P3a amplitude is mainly related to motor symptoms and dopaminergic medication. Moreover, the onset of FOG could be identified by tracking the dynamic changes of EEG (Shine et al., 2014; Handojoseno et al., 2015, 2018). Handojoseno et al. (2018) established a classifier with a sensitivity of 85.86% and a specificity of 80.5% for

the prediction of the transition period of FOG (5 s before FOG onset).

Studies have shown that EEG energy power, entropy, and signal correlation are significantly related to FOG symptom in PD. However, the relationship between cognitive and motor symptoms in PD is not well-understood. Current studies have a variety of sample size and experimental setting (Herz et al., 2014; Georgiev et al., 2015; Singh et al., 2018), thus leading to inconsistent conclusions. Further studies are needed to elucidate the relative contributions of EEG patterns on reflecting the cognitive and motor symptoms and their relationship. A better understanding of neural mechanism based on EEG analysis related to PD is crucial to develop novel invasive clinical diagnostic and therapeutic methods.

CONCLUSION

This paper reviewed recent 10 years studies related to cognitive and motor deficits in PD patients using EEG analysis. The studies show that PD patients have significant changes in specific EEG patterns compared to healthy people. Movement abnormalities and cognitive decline can be related to changes in EEG spectrum and ERPs during typical oddball paradigms and/or combined motor tasks. The unique time-frequency characteristics of EEG could provide further insight into disrupted sensorimotor networks in PD with motor deficits, such as FOG, dyskinesia, and dystonia in a real-world environment. However, the mechanism underlying interaction between gait and cognition still needs to be further studied.

DATA AVAILABILITY STATEMENT

The original contributions presented in the study are included in the article/supplementary material, further inquiries can be directed to the corresponding author/s.

AUTHOR CONTRIBUTIONS

LM, QW, XZ, and DM: conception and design of the study. QW and JP: acquisition, analysis, and interpretation of literatures. QW and LM: drafting the manuscript. All authors critically revised the draft and approved the final version.

FUNDING

This work was supported by National Key R&D Program of China (2016YFC1306501), Ministry of Science and Technology of China (2016YFC1306500 and 2016YFC1306504), the Science & Technology Development Fund of Tianjin Education Commission for Higher Education (2017ZD10), and Tianjin University Talent Support Grant (2020XRY-0014). National Natural Science Foundation of China (No. 82001921).

REFERENCES

Amboni, M., Cozzolino, A., Longo, K., Picillo, M., and Barone, P. (2008). Freezing of gait and executive functions in patients with Parkinson's disease. *Mov. Disord.* 23, 395–400. doi: 10.1002/mds.21850

Andrykiewicz, A., Patino, L., Naranjo, J. R., Witte, M., Hepp-Reymond, M.-C., and Kristeva, R. (2007). Corticomuscular synchronization with small and large dynamic force output. *BMC Neurosci.* 8:101. doi: 10.1186/1471-2202-8-101

Arnaldi, D., De Carli, F., Fama, F., Brugnolo, A., Girtler, N., Picco, A., et al. (2017). Prediction of cognitive worsening in *de novo* parkinson's disease: clinical use of biomarkers. *Mov. Disord.* 32, 1738–1747. doi: 10.1002/mds.27190

Aron, A. R., Behrens, T. E., Smith, S., Frank, M. J., and Poldrack, R. A. (2007). Triangulating a cognitive control network using diffusion-weighted magnetic resonance imaging (MRI) and functional MRI. *J. Neurosci.* 27, 3743–3752. doi: 10.1523/JNEUROSCI.0519-07.2007

Babiloni, C., De Pandis, M. F., Vecchio, F., Buffo, P., Sorpresi, F., Frisoni, G. B., et al. (2011). Cortical sources of resting state electroencephalographic rhythms in parkinson's disease related dementia and alzheimer's disease. *Clin. Neurophysiol.* 122, 2355–2364. doi: 10.1016/j.clinph.2011.03.029

Babiloni, C., Del Percio, C., Lizio, R., Noce, G., Lopez, S., Soricelli, A., et al. (2019). Levodopa may affect cortical excitability in parkinson's disease patients with cognitive deficits as revealed by reduced activity of cortical sources of resting state electroencephalographic rhythms. *Neurobiol. Aging* 73, 9–20. doi: 10.1016/j.neurobiolaging.2018.08.010

Bell, P. T., and Shine, J. M. (2016). Subcortical contributions to large-scale network communication. *Neurosci. Biobehav. Rev.* 71, 313–322. doi: 10.1016/j.neubiorev.2016.08.036

Bliwise, D. L., Scullin, M. K., and Trotti, L. M. (2014). Fluctuations in cognition and alertness vary independently in dementia with lewy bodies. *Mov. Disord.* 29, 83–89. doi: 10.1002/mds.25707

Britz, J., Van De Ville, D., and Michel, C. M. (2010). BOLD correlates of EEG topography reveal rapid resting-state network dynamics. *Neuroimage* 52, 1162–1170. doi: 10.1016/j.neuroimage.2010.02.052

Bronnick, K. S., Nordby, H., Larsen, J. P., and Aarsland, D. (2010). Disturbance of automatic auditory change detection in dementia associated with parkinson's disease: a mismatch negativity study. *Neurobiol. Aging* 31, 104–113. doi: 10.1016/j.neurobiolaging.2008.02.021

Butler, J. S., Fearon, C., Killane, I., Waechter, S. M., Reilly, R. B., and Lynch, T. (2017). Motor preparation rather than decision-making differentiates parkinson's disease patients with and without freezing of gait. *Clin. Neurophysiol.* 128, 463–471. doi: 10.1016/j.clinph.2016.12.019

Cahn, B. R., Delorme, A., and Polich, J. (2013). Event-related delta, theta, alpha and gamma correlates to auditory oddball processing during vipassana meditation. *Soc. Cogn. Affect. Neurosci.* 8, 100–111. doi: 10.1093/scan/nss060

Canolty, R. T., and Knight, R. T. (2010). The functional role of cross-frequency coupling. *Trends Cogn. Sci.* 14, 506–515. doi: 10.1016/j.tics.2010.09.001

Caviness, J. N., Hentz, J. G., Belden, C. M., Shill, H. A., Driver-Dunckley, E. D., Sabbagh, M. N., et al. (2015). Longitudinal EEG changes correlate with cognitive measure deterioration in parkinson's disease. *J. Parkinsons Dis.* 5, 117–124. doi: 10.3233/JPD-140480

Caviness, J. N., Utianski, R. L., Hentz, J. G., Beach, T. G., Dugger, B. N., Shill, H. A., et al. (2016). Differential spectral quantitative electroencephalography patterns between control and Parkinson's disease cohorts. *Eur. J. Neurol.* 23, 387–392. doi: 10.1111/ene.12878

Combrisson, E., Perrone-Bertolotti, M., Soto, J. L. P., Alamian, G., Kahane, P., Lachaux, J. P., et al. (2017). From intentions to actions: neural oscillations encode motor processes through phase, amplitude and phase-amplitude coupling. *Neuroimage* 147, 473–487. doi: 10.1016/j.neuroimage.2016.11.042

Cozac, V. V., Chaturvedi, M., Hatz, F., Meyer, A., Fuhr, P., and Gschwandtner, U. (2016). Increase of EEG Spectral theta power indicates higher risk of the development of severe cognitive decline in parkinson's disease after 3 years. *Front. Aging Neurosci.* 8:284. doi: 10.3389/fnagi.2016.00284

Cummings, J. L. (1995). Anatomic and behavioral aspects of frontal-subcortical circuits. *Ann. N. Y. Acad. Sci.* 769, 1–13. doi: 10.1111/j.1749-6632.1995.tb38127.x

Da Silva Lopes, M., de Souza Melo, A., and Nobrega, A. C. (2014). Delayed latencies of auditory evoked potential P300 are associated with the severity of Parkinson's disease in older patients. *Arq. Neuropsiquiatr.* 72, 296–300. doi: 10.1590/0004-282X20140005

Delval, A., Braquet, A., Dirhoussi, N., Bayot, M., Derambure, P., Defebvre, L., et al. (2018). Motor preparation of step initiation: error-related cortical oscillations. *Neuroscience* 393, 12–23. doi: 10.1016/j.neuroscience.2018.09.046

D'Ostilio, K., Deville, B., Cremers, J., Grandjean, J., Skawiniak, E., Delvaux, V., et al. (2013). Role of the supplementary motor area in the automatic activation of motor plans in *de novo* Parkinson's disease patients. *Neurosci. Res.* 76, 173–177. doi: 10.1016/j.neures.2013.04.002

Galvez, G., Recuero, M., Canuet, L., and Del-Pozo, F. (2018). Short-term effects of binaural beats on eeg power, functional connectivity, cognition, gait and anxiety in Parkinson's disease. *Int. J. Neural Syst* 28:17500551. doi: 10.1142/S0129065717500551

Garcia, A. M., and Ibanez, A. (2014). Words in motion: motor-language coupling in Parkinson's disease. *Transl. Neurosci.* 5, 152–159. doi: 10.2478/s13380-014-0218-6

Georgiev, D., Jahanshahi, M., Dreo, J., Cus, A., Pirtosek, Z., and Repovs, G. (2015). Dopaminergic medication alters auditory distractor processing in Parkinson's disease. *Acta Psychol.* 156, 45–56. doi: 10.1016/j.actpsy.2015.02.001

Geraedts, V. J., Boon, L. I., Marinus, J., Gouw, A. A., van Hilten, J. J., Stam, C. J., et al. (2018). Clinical correlates of quantitative EEG in Parkinson disease a systematic review. *Neurology* 91, 871–883. doi: 10.1212/WNL.0000000000006473

Handojoseno, A. M. A., Naik, G. R., Gilat, M., Shine, J. M., Nguyen, T. N., Ly, Q. T., et al. (2018). Prediction of freezing of gait in patients with parkinson's disease using EEG signals. *Stud. Health Technol. Inform* 246, 124–131. doi: 10.3233/978-1-61499-845-7-124

Handojoseno, A. M. A., Shine, J. M., Nguyen, T. N., Tran, Y., Lewis, S. J. G. and Nguyen, H. T. (2013). "Using EEG spatial correlation, cross frequency energy, and wavelet coefficients for the prediction of freezing of gait in Parkinson's disease patients," in *2013 35th Annual International Conference Of the IEEE Engineering In Medicine And Biology Society* (Osaka: IEEE), 4263–4266.

Handojoseno, A. M. A., Shine, J. M., Nguyen, T. N., Tran, Y., Lewis, S. J. G., and Nguyen, H. T. (2015). Analysis and prediction of the freezing of gait using EEG brain dynamics. *IEEE Trans. Neural Syst. Rehabil. Eng.* 23, 887–896. doi: 10.1109/TNSRE.2014.2381254

Heinrichs-Graham, E., Wilson, T. W., Santamaria, P. M., Heithoff, S. K., Torres-Russotto, D., Hutter-Saunders, J. A. L., et al. (2014). Neuromagnetic evidence of abnormal movement-related beta desynchronization in parkinson's disease. *Cereb. Cortex* 24, 2669–2678. doi: 10.1093/cercor/bht121

Herz, D. M., Florin, E., Christensen, M. S., Reck, C., Barbe, M. T., Tscheuschler, M. K., et al. (2014). Dopamine replacement modulates oscillatory coupling between premotor and motor cortical areas in parkinson's disease. *Cereb. Cortex* 24, 2873–2883. doi: 10.1093/cercor/bht140

Holtzer, R., Mahoney, J. R., Izzetoglu, M., Wang, C. L., England, S., and Verghese, J. (2015). Online fronto-cortical control of simple and attention-demanding locomotion in humans. *Neuroimage* 112, 152–159. doi: 10.1016/j.neuroimage.2015.03.002

Hunnicutt, B. J., Long, B. R., Kusefoglu, D., Gertz, K. J., Zhong, H. N., and Mao, T. Y. (2014). A comprehensive thalamocortical projection map at the mesoscopic level. *Nat. Neurosci.* 17, 1276–1285. doi: 10.1038/nn.3780

Jia, H., Hu, X., and Deshpande, G. (2014). Behavioral relevance of the dynamics of the functional brain connectome. *Brain Connect.* 4, 741–759. doi: 10.1089/brain.2014.0300

Karayanidis, F., Andrews, S., Ward, P. B., and Michie, P. T. (1995). ERP indices of auditory selective attention in aging and Parkinson's disease. *Psychophysiology* 32, 335–350. doi: 10.1111/j.1469-8986.1995.tb01216.x

Koenig, T., Lehmann, D., Merlo, M. C. G., Kochi, K., Hell, D., and Koukkou, M. (1999). A deviant EEG brain microstate in acute, neuroleptic-naive schizophrenics at rest. *Eur. Arch. Psychiatry Clin. Neurosci.* 249, 205–211. doi: 10.1007/s004060050088

Kotz, S. A., and Gunter, T. C. (2015). Can rhythmic auditory cuing remediate language-related deficits in Parkinson's disease? *Ann N Y Acad Sci.* 1337, 62–68. doi: 10.1111/nyas.12657

Lanciego, J. L., Luquin, N., and Obeso, J. A. (2012). Functional neuroanatomy of the basal ganglia. *Cold Spring Harb. Perspect. Med.* 2:a009621. doi: 10.1101/cshperspect.a009621

Latreille, V., Carrier, J., Lafortune, M., Postuma, R. B., Bertrand, J.-A., Panisset, M., et al. (2015). Sleep spindles in Parkinson's disease may predict the development of dementia. *Neurobiol. Aging* 36, 1083–1090. doi: 10.1016/j.neurobiolaging.2014.09.009

Lewis, S. J. G., and Barker, R. A. (2009). A pathophysiological model of freezing of gait in Parkinson's disease. *Parkinsonism Relat. Disord.* 15, 333–338. doi: 10.1016/j.parkreldis.2008.08.006

Maidan, I., Fahoum, F., Shustak, S., Gazit, E., Patashov, D., Tchertov, D., et al. (2019). Changes in event-related potentials during dual task walking in aging and Parkinson's disease. *Clin. Neurophysiol.* 130, 224–230. doi: 10.1016/j.clinph.2018.11.019

Maidan, I., Nieuwhof, F., Bernad-Elazari, H., Reelick, M. F., Bloem, B. R., Giladi, N., et al. (2016a). The role of the frontal lobe in complex walking among patients with parkinson's disease and healthy older adults: an fNIRS study. *Neurorehabil. Neural Repair.* 30, 963–971. doi: 10.1177/1545968316650426

Maidan, I., Rosenberg-Katz, K., Jacob, Y., Giladi, N., Deutsch, J. E., Hausdorff, J. M., et al. (2016b). Altered brain activation in complex walking conditions in patients with Parkinson's disease. *Parkinsonism Relat. Disord.* 25, 91–96. doi: 10.1016/j.parkreldis.2016.01.025

Martinez-Martin, P. (2011). The importance of non-motor disturbances to quality of life in Parkinson's disease. *J. Neurol. Sci.* 310, 12–16. doi: 10.1016/j.jns.2011.05.006

Martinez-Martin, P., Rodriguez-Blazquez, C., Kurtis, M. M., Chaudhuri, K. R., and Grp, N. V. (2011). The impact of non-motor symptoms on health-related quality of life of patients with parkinson's disease. *Mov. Disord.* 26, 399–406. doi: 10.1002/mds.23462

Maruyama, T., and Yanagisawa, N. (2006). Cognitive impact on freezing of gait in Parkinson's disease. *Parkinsonism Relat. Disord.* 12, S77–S82. doi: 10.1016/j.parkreldis.2006.05.024

Matsui, H., Nishinaka, K., Oda, M., Kubori, T., and Udaka, F. (2007). Auditory event-related potentials in Parkinson's disease: prominent correlation with attention. *Parkinsonism Relat. Disord.* 13, 394–398. doi: 10.1016/j.parkreldis.2006.12.012

McIntosh, A. R., Kovacevic, N., and Itier, R. J. (2008). Increased brain signal variability accompanies lower behavioral variability in development. *PLoS Comput. Biol.* 4:e1000106. doi: 10.1371/journal.pcbi.1000106

McKeith, I. G., Boeve, B. F., Dickson, D. W., Halliday, G., Taylor, J.-P., Weintraub, D., et al. (2017). Diagnosis and management of dementia with lewy bodies fourth consensus report of the DLB consortium. *Neurology* 89, 88–100. doi: 10.1212/WNL.0000000000004058

McKeith, I. G., Dickson, D. W., Lowe, J., Emre, M., O'Brien, J. T., Feldman, H., et al. (2005). Diagnosis and management of dementia with lewy bodies - third report of the DLB consortium. *Neurology* 65, 1863–1872. doi: 10.1212/01.wnl.0000187889.17253.b1

Melloni, M., Sedeno, L., Hesse, E., Garcia-Cordero, I., Mikulan, E., Plastino, A., et al. (2015). Cortical dynamics and subcortical signatures of motor-language coupling in Parkinson's disease. *Sci. Rep.* 5:11899. doi: 10.1038/srep11899

Milz, P., Faber, P. L., Lehmann, D., Koenig, T., Kochi, K., and Pascual-Marqui, R. D. (2016). The functional significance of EEG microstates-associations with modalities of thinking. *Neuroimage* 125, 643–656. doi: 10.1016/j.neuroimage.2015.08.023

Muente, T. F., Joppich, G., Daeuper, J., Schrader, C., Dengler, R., and Heldmann, M. (2015). Random number generation and executive functions in parkinson's disease: an event-related brain potential study. *J. Parkinsons Dis.* 5, 613–620. doi: 10.3233/JPD-150575

Nathan, K., and Contreras-Vidal, J. L. (2016). Negligible motion artifacts in scalp electroencephalography (EEG) during treadmill walking. *Front. Hum. Neurosci.* 9:708. doi: 10.3389/fnhum.2015.00708

Omlor, W., Patino, L., Hepp-Reymond, M.-C., and Kristeva, R. (2007). Gamma-range corticomuscular coherence during dynamic force output. *Neuroimage* 34, 1191–1198. doi: 10.1016/j.neuroimage.2006.10.018

Palmer, S. J., Lee, P. W.-H., Wang, Z. J., Au, W.-L., and McKeown, M. J. (2010). theta, beta but not alpha-band EEG connectivity has implications for dual task performance in Parkinson's disease. *Parkinsonism Relat. Disord.* 16, 393–397. doi: 10.1016/j.parkreldis.2010.03.001

Peterson, D. S., Pickett, K. A., Duncan, R. P., Perlmutter, J. S., and Earhart, G. M. (2014). Brain activity during complex imagined gait tasks in Parkinson disease. *Clin. Neurophysiol.* 125, 995–1005. doi: 10.1016/j.clinph.2013.10.008

Pijnenburg, Y. A. L., Strijers, R. L. M., Made, Y. V., van der Flier, W. M., Scheltens, P., and Stam, C. J. (2008). Investigation of resting-state EEG functional connectivity in frontotemporal lobar degeneration. *Clin. Neurophysiol.* 119, 1732–1738. doi: 10.1016/j.clinph.2008.02.024

Pizzamiglio, S., Abdalla, H., Naeem, U., and Turner, D. L. (2018). Neural predictors of gait stability when walking freely in the real-world. *J. Neuroeng. Rehabil.* 15:11. doi: 10.1186/s12984-018-0357-z

Polich, J. (2007). Updating p300: an integrative theory of P3a and P3b. *Clin. Neurophysiol.* 118, 2128–2148. doi: 10.1016/j.clinph.2007.04.019

Pollok, B., Krause, V., Martsch, W., Wach, C., Schnitzler, A., and Sudmeyer, M. (2012). Motor-cortical oscillations in early stages of Parkinson's disease. *J. Physiol. Lond.* 590, 3203–3212. doi: 10.1113/jphysiol.2012.231316

Possti, D., Fahoum, F., Sosnik, R., Giladi, N., Hausdorff, J. M., Mirelman, A., et al. (2020). Changes in the EEG spectral power during dual-task walking with aging and Parkinson's disease: initial findings using event-related spectral perturbation analysis. *J. Neurol.* doi: 10.1007/s00415-020-10104-1

Quynh Tran, L., Handojoseno, A. M. A., Gilat, M., Nghia, N., Chai, R., Yvonne, T., et al. (2016). "Detection of gait initiation failure in parkinson's disease patients using EEG signals," in *2016 38th Annual International Conference of the IEEE Engineering in Medicine and Biology Society,* eds J. Patton, R. Barbieri, J. Ji, E. Jabbari, S. Dokos, R. Mukkamala, et al., (Orlando: IEEE), 1599–1602.

Robinovitch, S. N., Feldman, F., Yang, Y. J., Schonnop, R., Leung, P. M., Sarraf, T., et al. (2013). Video capture of the circumstances of falls in elderly people residing in long-term care: an observational study. *Lancet* 381, 47–54. doi: 10.1016/S0140-6736(12)61263-X

Rushworth, M. F. S., Hadland, K. A., Paus, T., and Sipila, P. K. (2002). Role of the human medial frontal cortex in task switching: a combined fMRI and TMS study. *J. Neurophysiol.* 87, 2577–2592. doi: 10.1152/jn.2002.87.5.2577

Schlede, N., Zimmermann, R., Ehrensperger, M. M., Gschwandtner, U., Hardmeier, M., Hatz, F., et al. (2011). Clinical EEG in cognitively impaired patients with Parkinson's disease. *J. Neurol. Sci.* 310, 75–78. doi: 10.1016/j.jns.2011.05.034

Schumacher, J., Peraza, L. R., Firbank, M., Thomas, A. J., Kaiser, M., Gallaghe, P., et al. (2019a). Dynamic functional connectivity changes in dementia with lewy bodies and Alzheimer's disease. *Neuroimage Clin.* 22:101812. doi: 10.1016/j.nicl.2019.101812

Schumacher, J., Peraza, L. R., Firbank, M., Thomas, A. J., Kaiser, M., Gallagher, P., et al. (2018). Functional connectivity in dementia with lewy bodies: a within- and between-network analysis. *Hum. Brain Mapp.* 39, 1118–1129. doi: 10.1002/hbm.23901

Schumacher, J., Peraza, L. R., Firbank, M., Thomas, A. J., Kaiser, M., Gallagher, P., et al. (2019b). Dysfunctional brain dynamics and their origin in lewy body dementia. *Brain* 142, 1767–1782. doi: 10.1093/brain/awz069

Shine, J. M., Handojoseno, A. M. A., Nguyen, T. N., Tran, Y., Naismith, S. L., Nguyen, H., et al. (2014). Abnormal patterns of theta frequency oscillations during the temporal evolution of freezing of gait in Parkinson's disease. *Clin. Neurophysiol.* 125, 569–576. doi: 10.1016/j.clinph.2013.09.006

Shine, J. M., Matar, E., Ward, P. B., Bolitho, S. J., Gilat, M., Pearson, M., et al. (2013). Exploring the cortical and subcortical functional magnetic resonance imaging changes associated with freezing in Parkinson's disease. *Brain* 136, 1204–1215. doi: 10.1093/brain/awt049

Singh, A., Cole, R. C., Espinoza, A. I., Brown, D., Cavanagh, J. F., and Narayanan, N. S. (2020). Frontal theta and beta oscillations during lower-limb movement in Parkinson's disease. *Clin. Neurophysiol.* 131, 694–702. doi: 10.1016/j.clinph.2019.12.399

Singh, A., Richardson, S. P., Narayanan, N., and Cavanagh, J. F. (2018). Mid-frontal theta activity is diminished during cognitive control in Parkinson's disease. *Neuropsychologia* 117, 113–122. doi: 10.1016/j.neuropsychologia.2018.05.020

Soikkeli, R., Partanen, J., Soininen, H., Paakkonen, A., and Riekkinen, P. Sr. (1991). Slowing of EEG in Parkinson's disease. *Electroencephalogr. Clin. Neurophysiol.* 79, 159–165. doi: 10.1016/0013-4694(91)90134-P

Solis-Vivanco, R., Ricardo-Garcell, J., Rodriguez-Camacho, M., Prado-Alcala, R. A., Rodriguez, U., Rodriguez-Violante, M., et al. (2011). Involuntary attention impairment in early Parkinson's disease: an event-related potential study. *Neurosci. Lett.* 495, 144–149. doi: 10.1016/j.neulet.2011.03.058

Solis-Vivanco, R., Rodriguez-Violante, M., Rodriguez-Agudelo, Y., Schilmann, A., Rodriguez-Ortiz, U., and Ricardo-Garcell, J. (2015). The P3a wave: a reliable neurophysiological measure of Parkinson's disease duration and severity. *Clin. Neurophysiol.* 126, 2142–2149. doi: 10.1016/j.clinph.2014.12.024

Stoffers, D., Bosboom, J. L. W., Deijen, J. B., Wolters, E. C., Berendse, H. W., and Stam, C. J. (2007). Slowing of oscillatory brain activity is a stable characteristic of Parkinson's disease without dementia. *Brain* 130, 1847–1860. doi: 10.1093/brain/awm034

Tard, C., Dujardin, K., Bourriez, J.-L., Molaee-Ardekani, B., Derambure, P., Defebvre, L., et al. (2016). Attention modulation during motor preparation in Parkinsonian freezers: a time-frequency EEG study. *Clin. Neurophysiol.* 127, 3506–3515. doi: 10.1016/j.clinph.2016.09.014

Ushiyama, J., Suzuki, T., Masakado, Y., Hase, K., Kimura, A., Liu, M., et al. (2011). Between-subject variance in the magnitude of corticomuscular coherence during tonic isometric contraction of the tibialis anterior muscle in healthy young adults. *J. Neurophysiol.* 106, 1379–1388. doi: 10.1152/jn.00193.2011

Utianski, R. L., Caviness, J. N., van Straaten, E. C. W., Beach, T. G., Dugger, B. N., Shill, H. A., et al. (2016). Graph theory network function in Parkinson's disease assessed with electroencephalography. *Clin. Neurophysiol.* 127, 2228–2236. doi: 10.1016/j.clinph.2016.02.017

Van de Ville, D., Britz, J., and Michel, C. M. (2010). EEG microstate sequences in healthy humans at rest reveal scale-free dynamics. *Proc. Natl. Acad. Sci. U.S.A.* 107, 18179–18184. doi: 10.1073/pnas.1007841107

van Wouwe, N. C., van den Wildenberg, W. P. M., Claassen, D. O., Kanoff, K., Bashore, T. R., and Wylie, S. A. (2014). Speed pressure in conflict situations impedes inhibitory action control in Parkinson's disease. *Biol. Psychol.* 101, 44–60. doi: 10.1016/j.biopsycho.2014.07.002

Waechter, S. M., Fearon, C., McDonnell, C., Gallego, J., Quinlivan, B., Killane, I., et al. (2015). "The impact of dual tasking on cognitive performance in a Parkinson's disease cohort with and without freezing of gait: an EEG and behavioral based approach," in *2015 7th International Ieee/Embs Conference on Neural Engineering* (Montpellier), 1072–1075. doi: 10.1109/NER.2015.7146813

Wager, T. D., Jonides, J., and Reading, S. (2004). Neuroimaging studies of shifting attention: a meta-analysis. *Neuroimage* 22, 1679–1693. doi: 10.1016/j.neuroimage.2004.03.052

Wagner, J., Martinez-Canino, R., and Makeig, S. (2019). Trial-by-trial source-resolved EEG responses to gait task challenges predict subsequent step adaptation. *Neuroimage* 199, 691–703. doi: 10.1016/j.neuroimage.2019.06.018

Yilmaz, F. T., Ozkaynak, S. S., and Barcin, E. (2017). Contribution of auditory P300 test to the diagnosis of mild cognitive impairment in Parkinson's disease. *Neurol. Sci.* 38, 2103–2109. doi: 10.1007/s10072-017-3106-3

Yoshida, T., Masani, K., Zabjek, K., Popovic, M. R., and Chen, R. (2018). Dynamic cortical participation during bilateral, cyclical ankle movements: effects of Parkinson's disease. *PLoS ONE* 13:e0196177. doi: 10.1371/journal.pone.0196177

Yuvaraj, R., Murugappan, M., Ibrahim, N. M., Sundaraj, K., Omar, M. I., Mohamad, K., et al. (2014). Detection of emotions in Parkinson's disease using higher order spectral features from brain's electrical activity. *Biomed. Signal Process. Control* 14, 108–116. doi: 10.1016/j.bspc.2014.07.005

Zheng, Y., Peng, Y., Xu, G., Li, L., and Wang, J. (2018). Using corticomuscular coherence to reflect function recovery of paretic upper limb after stroke: a case study. *Front. Neurol.* 8:728. doi: 10.3389/fneur.2017.00728

Conflict of Interest: The authors declare that the research was conducted in the absence of any commercial or financial relationships that could be construed as a potential conflict of interest.

Copyright © 2020 Wang, Meng, Pang, Zhu and Ming. This is an open-access article distributed under the terms of the Creative Commons Attribution License (CC BY). The use, distribution or reproduction in other forums is permitted, provided the original author(s) and the copyright owner(s) are credited and that the original publication in this journal is cited, in accordance with accepted academic practice. No use, distribution or reproduction is permitted which does not comply with these terms.

frontiers in Aging Neuroscience

ORIGINAL RESEARCH
published: 23 November 2020
doi: 10.3389/fnagi.2020.575481

Alpha-Synuclein Accumulation and Its Phosphorylation in the Enteric Nervous System of Patients Without Neurodegeneration: An Explorative Study

Lu-Lu Bu[1,2†], Kai-Xun Huang[1,3†], De-Zhi Zheng[1,2†], Dan-Yu Lin[1,3], Ying Chen[1,2], Xiu-Na Jing[1,2], Yan-Ran Liang[1,2] and En-Xiang Tao[1,2*]*

[1] Department of Neurology, Sun Yat-sen Memorial Hospital, Sun Yat-sen University, Guangzhou, China, [2] Guangdong Provincial Key Laboratory of Malignant Tumor Epigenetics and Gene Regulation, Sun Yat-sen Memorial Hospital, Sun Yat-sen University, Guangzhou, China, [3] Department of Neurology, The Eighth Affiliated Hospital, Sun Yat-sen University, Shenzhen, China

Alpha-synuclein (α-Syn) is widely distributed and involved in the regulation of the nervous system. The phosphorylation of α-Syn at serine 129 (p^{Ser129}α-Syn) is known to be closely associated with α-Synucleinopathies, especially Parkinson's disease (PD). The present study aimed to explore the α-Syn accumulation and its phosphorylation in the enteric nervous system (ENS) in patients without neurodegeneration. Patients who underwent colorectal surgery for either malignant or benign tumors that were not suitable for endoscopic resection ($n = 19$) were recruited to obtain normal intestinal specimens, which were used to assess α-Syn immunoreactivity patterns using α-Syn and p^{Ser129}α-Syn antibodies. Furthermore, the sub-location of α-Syn in neurons was identified by α-Syn/neurofilament double staining. Semi-quantitative counting was used to evaluate the expression of α-Syn and p^{Ser129}α-Syn in the ENS. Positive staining of α-Syn was detected in all intestinal layers in patients with non-neurodegenerative diseases. There was no significant correlation between the distribution of α-Syn and age ($p = 0.554$) or tumor stage ($p = 0.751$). Positive staining for p^{Ser129}α-Syn was only observed in the submucosa and myenteric plexus layers. The accumulation of p^{Ser129}α-Syn increased with age. In addition, we found that the degenerative changes of the ENS were related to the degree of tumor malignancy ($p = 0.022$). The deposits of α-Syn were present in the ENS of patients with non-neurodegenerative disorders; particularly the age-dependent expression of p^{Ser129}α-Syn in the submucosa and myenteric plexus. The current findings of α-Syn immunostaining in the ENS under near non-pathological conditions weaken the basis of using α-Syn pathology as a suitable hallmark to diagnose α-Synucleinopathies including PD. However, our data provided unique perspectives to study gastrointestinal dysfunction in non-neurodegenerative disorders. These findings provide new evidence to elucidate the neuropathological characteristics and α-Syn pathology pattern of the ENS in non-neurodegenerative conditions.

Keywords: α-Synuclein, α-synucleinopathies, enteric nervous system, non-neurodegenerative disorder, pathology

OPEN ACCESS

Edited by:
Shaogang Qu,
Southern Medical University, China

Reviewed by:
David J. Koss,
Newcastle University, United Kingdom
Tetsuya Asakawa,
Fujian University of Traditional Chinese Medicine, China

***Correspondence:**
En-Xiang Tao
taoex@mail.sysu.edu.cn
Xiu-Na Jing
jingxn3@mail.sysu.edu.cn

†These authors have contributed equally to this work

Received: *23 June 2020*
Accepted: *09 October 2020*
Published: *23 November 2020*

Citation:
Bu L-L, Huang K-X, Zheng D-Z, Lin D-Y, Chen Y, Jing X-N, Liang Y-R and Tao E-X (2020) Alpha-Synuclein Accumulation and Its Phosphorylation in the Enteric Nervous System of Patients Without Neurodegeneration: An Explorative Study. Front. Aging Neurosci. 12:575481. doi: 10.3389/fnagi.2020.575481

INTRODUCTION

Alpha-synuclein (α-Syn) is widely distributed in the nervous system and is involved in the regulation of synaptic plasticity, as well as the packaging and trafficking of vesicles (Fortin et al., 2004; Wislet-Gendebien et al., 2006). The physiological role of α-Syn is often associated with the exocytotic and synaptic machinery controlling neurotransmitter release (Alegre-Abarrategui et al., 2019).

The complexity of α-Syn pathology mainly reflects its ability to form a broad range of structures, its diverse post-translational modification status, and its ability to associate with both lipid and protein chaperones (Alegre-Abarrategui et al., 2019). The monomeric form of α-Syn is generally considered to be non-pathogenic and has profound implications for neuronal physiology. Under certain circumstances, α-Syn would fold from its natural state into pathogenic forms comprising oligomers and polymers, and could converge into a fibrous filament, called the fiber precursor (preformed fibrils, PFFs). Insoluble fibrils of phosphorylated α-Syn (p-α-Syn) have also been implicated in inducing the pathological progress of neurodegenerative disorders (Peng et al., 2018; Bieri et al., 2019), of which phosphorylation at serine 129 (p^{Ser129}α-Syn) has been shown to be the most abundant form in intracellular inclusion bodies in the brain of patients with PD (Oueslati, 2016). The term α-Synucleinopathies refers to neurodegenerative disorders that share the key pathological feature of neuronal loss accompanied by the presence of α-Syn inclusions, including Parkinson's disease (PD), dementia with Lewy bodies (DLB), and multiple system atrophy (MSA). Besides these typical α-Synucleinopathies, patients with Alzheimer's disease (AD) also show an overlap of α-Syn, Aβ plaques, and tau tangle pathologies (Lippa et al., 1998).

Pathologically, α-Syn spreads between neurons like prions, which induces more monomeric α-Syn misfolding or over-modification, and is then deposited in neurons to form Lewy bodies (LBs), leading to neurotoxicity (Mao et al., 2016; Lim and Lee, 2017; Urrea et al., 2018). LB pathology in α-Synucleinopathies is not confined to the central nervous system (CNS). The involvement of the peripheral autonomic nervous system was first observed more than 50 years ago (den and Bethlem, 1960). The enteric nervous system (ENS) is composed of neurons embedded in the gastrointestinal tract and is known as the "second brain" (Rao and Gershon, 2016; Chalazonitis and Rao, 2018). Neurons and enteric glial cells in the ENS form the gastrointestinal ganglia, also known as the nerve plexus, mainly comprising the submucosal and myenteric plexus (Sprenger et al., 2015). Mounting evidence indicates that α-Syn is present in the ENS of patients with PD and related disorders (Lee et al., 2018). As reported by Del Tredici and Braak (2016), α-Syn pathology could commence in the ENS and then spread to the brain to participate in the pathogenesis and progression of PD (Braak et al., 2003; Breen et al., 2019). In a post-mortem study, α-Syn was identified in both patients with PD and in pathologically defined cases of sporadic DLB, but it was not detected in the controls (Annerino et al., 2012). However, more recent evidence has indicated that α-Syn is a normal constituent of the ENS and thus exists in healthy controls as well as patients with PD (Bottner et al., 2012; Gold et al., 2013; Antunes et al., 2016; Shin et al., 2017). Although considerable progress has been made in determining the distribution pattern of α-Syn pathology, variation in the status of α-Syn in healthy people still remains.

Few data are available on the normal spatial expression profile and distribution pattern of α-Syn in the ENS. Therefore, this study aimed to explore the status of α-Syn accumulation and its phosphorylation in the human ENS of patients with non-neurodegenerative diseases, i.e., approximating to non-pathological conditions. We employed the normal intestine tissues of 19 patients that underwent colorectal surgery for malignant or benign tumors who were not suitable for endoscopic resection to investigate α-Syn pathology in the normal ENS. The results showed that deposits of α-Syn and p^{Ser129}α-Syn in the ENS could be detected in people with non-neurodegenerative disorders. The results revealed the neuropathological characteristics and α-Syn pathology pattern of ENS in non-neurodegenerative conditions and might indicate that the α-Syn pathology of the ENS represents physiological deposition.

MATERIALS AND METHODS

Participants

This study was approved by the Ethics Committee of Sun Yat-sen Memorial Hospital, Sun Yat-sen University, Guangzhou, China (Approval number: 2015 Lun Bei NO. 50). All the involved patients [11 male and 8 female, aged 39–84 years (mean age, 65)] attended Sun Yat-sen Memorial Hospital. Written informed consent for this research was obtained from all individuals prior to surgery. Intestinal specimens were obtained from patients who underwent colorectal surgery for malignant or benign tumors that were not suitable for endoscopic resection. A 2 cm-wide sample of the intestinal tract was taken as the initial specimen within a safe distance (10 cm) from the tumor (Bottner et al., 2012). Specimens were subdivided into Ileum (Il), right colon (Rc), left colon (Lc), and rectum (Re) groups.

All patients underwent a complete pre-operative neurological examination to rule out neurodegenerative disease-related symptoms, particularly cognitive impairment and PD-related symptoms. Patients with a history of neurological or psychiatric disorders were excluded. All patients were assessed for the presence of PD using the diagnostic criteria for PD issued by the International Parkinson and movement disorder society in 2015 (Postuma et al., 2015). The TNM (Tumor-Node-Metastasis) stage of each subject was assessed according to the Classification of Malignant Tumor, 8th Edition, published by the Union for International Cancer Control in 2016. Then, the patients were staged according to their prognosis (0–IV), together with the pathological results. There were eight tumor sub-stages, comprising stages 0, I, IIa–IIb, IIIa–IIIc, and IVa, respectively. A score of 0 was indicative of a tumor free status, although evidence of inflammation was present.

TABLE 1 | Demographic and clinical data of patients underwent colorectal surgery.

Age	31–40 ($n = 1$)	41–50 ($n = 2$)	51–60 ($n = 6$)	61–70 ($n = 4$)	71–80 ($n = 4$)	81–90 ($n = 2$)
Specimens	Ileum ($n = 3$)	Right colon ($n = 4$)		Left colon ($n = 4$)		Rectum ($n = 8$)
Tumor stage	0 ($n = 1$)	I ($n = 3$)	II ($n = 6$)	III ($n = 7$)		IV ($n = 2$)

Immunohistochemistry and Quantitative Analysis

Immunostaining of neurofilaments (NFs), α-Syn and pathologic α-Syn were employed to assess their distribution patterns. For immunohistochemical staining, the initial tissue was immersed in 4% neutral formalin solution for fixation within 1 h after tissue extraction. All specimens were fixed for more than 48 h. Then, a 1.5 cm × 1.5 cm full-thickness intestinal sample was selected for paraffin embedding and preparation. Continuous sectioning was performed, and the thickness of each section was 4 μm.

After baking (60°C, 1.5–2 h), xylene dewaxing, and gradient alcohol (100–90–75%) dehydration, antigen retrieval of the samples on the slides was performed in a microwave oven with high fire for 10 min and medium-high fire for 10 min, using sodium citrate solution (0.01 mol/L, pH 6.0). Then, the sections were blocked using an endogenous peroxidase blocker (10 min) and 5% goat serum (15 min). They were then incubated with primary antibodies (anti-α-Syn-monoclonal antibody, 1:500, ab138501, Abcam, Cambridge, MA, USA; anti-neurofilament-polyclonal antibody, 1:500, ab235991, Abcam; and an anti-phospho-α-Syn (Ser129) antibody, 1:500, MABN826, Millipore, Billerica, MA, USA) at 4°C overnight, followed by incubation with a biotin-conjugated secondary antibody (1:3,000; BA-1000, Vector Laboratories, Burlingame, CA, USA) for 15 min at room temperature (RT) and horseradish peroxidase (HRP)-labeled streptavidin (1:1,000, PK-6100; Vector Laboratories) for 10 min at RT. After reaction with 3,3′-Diaminobenzidine (DAB) peroxidase substrate (SK-4100, Vector Laboratories), the slides were stained with hematoxylin, dried, and sealed with neutral resin. Detailed steps of immunohistochemistry are provided in the **Supplementary Material**. All other reagents were acquired from Sigma-Aldrich (Shanghai, China).

The immunohistochemically-stained sections were imaged using a Nikon eclipse 80 microscope and counted as follows: 1. The NF positive neuron count. The number of positive neurons in the myenteric plexus were counted at high magnification (20×) and the NF statistic was determined by the number of neurons observed and divided by the number of visual fields observed; 2. α-Syn expression. A semi-quantitative counting method was used to record the frequency of α-Syn expression, as 0- absence, 1- sparse (≤ 1/4 positive staining area), and 2- small amount (≤ 2/4 positive staining area), 3- common (≤ 3/4 positive staining area), 4- rich (> 3/4 positive staining area) according to criteria from a previous study (Lebouvier et al., 2010). For this study, the positive staining area referred to the proportion of the positively stained nerve plexus in the entire enteric nerve plexus of a complete specimen, rather than taking an average of the positive rates of several random fields; 3. p^{Ser129}α-Syn. In a high power field of view, starting from one end of the myenteric plexus of the specimen, we obtained the visual fields of the specimen covering the entire myenteric plexus without overlap. Five visual fields across the plexus were assigned at random for counting, and the ratio of p^{Ser129}α-Syn positive neurons was generated from the mean of the number of p^{Ser129}α-Syn positive neurons divided by the total number of neurons across the five inspected fields was calculated.

Statistical Analysis

The rostro caudal gradient of LBs in the gastrointestinal nervous system prompted us to divide the samples into four groups according to the sampling site, namely, the ileum group (Il); right colon group (Rc); left colon group (Lc), including the descending colon and sigmoid colon; and the rectum group (Re). This was done to exclude the influence of different sampling sites and to verify the rostro caudal gradient.

All experiments were performed in triplicate. Data are expressed as the mean ± SD. Data normality was tested using the Kolmogorov-Smirnov test. Differences between means were evaluated using a one-way analysis of variance (ANOVA) test followed by a homogeneity test using IBM SPSS Statistics 20 software (IBM Corp., Armonk, NY, USA). A least significant difference (LSD)-*t*-test was used for multiple comparisons, including the inter-group comparison of NF and p^{Ser129}α-Syn. For semi-quantitative analysis, the Kruskal–Wallis test was used to compare multiple samples between groups. The correlations were analyzed using Pearson correlation, except for the correlation analysis involving α-Syn and tumor staging, which was analyzed using the Spearman correlation test. The statistical significance was set at $^{*}P < 0.05$, $^{**}P < 0.01$, and $^{***}P < 0.001$).

RESULTS

Characteristics of the Population

A total of 11 male and 8 female patients, aged between 39 and 84 years old, consented to participate and were enrolled in this study. They underwent colorectal surgery for either malignant tumors of the intestinal tract or benign tumors and were not suitable for endoscopic resection. The basic demographic data of patients in this study are shown in **Table 1**. Clinical information, including sex, age, admission and discharge diagnosis, pathological diagnosis, tumor stage, levels of tumor markers were obtained and are presented in the **Supplementary Materials**.

Distribution of Neurons in the ENS of Patients With Non-neurodegenerative Diseases

NF staining was identified throughout the intestinal tract (100%). However, neurons in the mucosa and submucosa were too scattered to count and rate. The myenteric plexus was selected for comparison among the groups. Representative immunostaining of NFs in the myenteric plexus is shown in **Figure 1**. Fine staining of NFs (brown color) could be seen in the perikaryon of neurons in the myenteric plexus (black arrows in **Figures 1B,D**). No statistically significant difference was found in age distribution between the groups ($p = 0.822$). There were inter-group differences in the NF counts among the Rc, Lc, and Re groups (one-way ANOVA, $F = 3.564$, $df = 18$, $p = 0.040$, followed by a LSD-t *post-hoc* test: The Rc group 1.07 ± 0.82 *vs*. the Lc group 3.66 ± 0.62, $p = 0.010$; the Rc group 1.07 ± 0.82 *vs*. the Re group 3.11 ± 1.35, $p = 0.017$) (**Figure 1E**). The neuronal distribution in the myenteric plexus was not correlated with age (Pearson correlation, $p = 0.281$) (**Figure 1F**).

Distribution and Expression of α-Syn and Pathological α-Syn in the ENS

Immunohistochemical staining showed that the deposition of α-Syn could be detected in all specimens of the submucosa, muscularis propria, myenteric plexus, and part of the mucosa (12/19, 63%) (**Figure 2**). **Figure 2** shows representative images of α-Syn in the myenteric plexus (**Figure 2A**), and the mucosa (**Figure 2C**) obtained via immunostaining. Non-specific staining interference was excluded. The Kruskal–Wallis test showed that there was no significant difference in the expression of α-Syn among groups in the myenteric plexus (Kruskal–Wallis test, $p = 0.812$) (**Figure 2E**). The deposition of α-Syn showed no significant correlation with age in the myenteric plexus (Pearson correlation, $p = 0.554$) (**Figure 2F**), whereas it positively correlated with the count of neurons (Pearson correlation, $R = 0.592$, $p = 0.008$) (**Figure 2G**). Semi-quantitative counting for α-Syn expression in the intestinal tract was defined according to a previous study, as shown in **Figure 3**.

The deposition of p^{S129}α-Syn was observed only in the submucosa and the myenteric plexus and was detected in the cytoplasm of neurons. We used serial section staining to analyze co-localization. The representative distribution and expression of pathological α-Syn were observed, as shown in **Figures 4A–D**. Not all neurons in the myenteric plexus had p^{S129}α-Syn deposits. No significant difference was observed in the deposition of p^{S129}α-Syn between groups (one-way ANOVA, $F = 0.452$, $df = 17$, $p = 0.720$) (**Figure 4E**). Correlation analysis indicated that there was an age-dependent deposition of p^{S129}α-Syn in the myenteric plexus ($R = 0.643$, $p = 0.004$) (**Figure 4F**), suggesting that the deposition of p^{S129}α-Syn in the ENS myenteric plexus increased with age. However, the deposition of p^{S129}α-Syn and the count of neurons in the myenteric plexus showed no correlation ($p = 0.958$) (**Figure 4G**).

α-Syn Pathology of the ENS and Its Correlation With Tumor Malignancy

All subjects included in this study were patients with primary intestinal tumors; therefore, excluding the neoplastic effect was necessary to analyze the influence of tumor malignancy on the α-Syn pathology. The Kruskal–Wallis test showed no statistically significant differences in the tumor stage among the four groups ($p = 0.751$). Spearman correlation analysis suggested a negative correlation between the tumor stage and the NF counts in the myenteric plexus of the ENS (Pearson correlation, $R = -0.522$, $p = 0.022$) (**Figure 5A**). There was no significant correlation between the deposition of α-Syn and tumor stage in the myenteric plexus (Spearman correlation, $p = 0.095$) (**Figure 5B**). Furthermore, the deposition of p^{Ser129}α-Syn did not correlate with the tumor stage (Pearson correlation, $p = 0.566$) (**Figure 5C**). Taken together, these findings suggested that α-Syn pathology in ENS might not be affected by tumor malignancy.

DISCUSSION

In the present study, we explored the distribution of α-Syn and its phosphorylation modification in the non-neurodegenerative intestinal tracts. We employed full-thickness normal intestinal tissues from 19 patients with non-neurodegenerative diseases to explore the levels of α-Syn and phosphorylated α-Syn via immunohistochemistry staining. We found that in the intestinal tissues of patients without neurodegeneration, accumulation of α-Syn and p^{Ser129}α-Syn were detected within the submucosal and myenteric plexus, as well as in enteric nerve fibers. This evidence argues against the role of ENS immunostaining of α-Syn as a diagnostic hallmark for α-Synucleinopathies and related neurodegenerative disorders. Our findings indicated that the level of p^{Ser129}α-Syn was age-dependent in the myenteric plexus, suggesting that the accumulation of α-Syn in the ENS might be a physiological change.

The presence of α-Syn inclusions is a common hallmark of α-Synucleinopathies. However, why it would accumulate in the ENS remains unknown. Without a clear understanding of the function of α-Syn and why it would accumulate in a nerve cell, we cannot unravel the pathophysiology of diseases such as PD. Previous studies using antibodies against α-Syn and p-α-Syn in the ENS of patients with neurodegenerative diseases have yielded conflicting results. Reports have suggested the accumulation of α-Syn in the ENS in animals and humans under both physiological and pathological states. A previous report investigating α-Syn immunoreactivity in biopsies of the distal sigmoid colon in 10 patients suggested that immunostaining of nerve fibers of the colonic submucosa was observed in all PD biopsies, but not the controls (Shannon et al., 2012). In addition, α-Syn was identified both in patients with PD and in pathologically-defined cases of sporadic DLB, but not in the controls (Annerino et al., 2012). α-Syn deposits could be observed in the ENS in MSA (Pouclet et al., 2012). In contrast, however, other studies found that α-Syn was a normal constituent of the ENS and was thus present both in healthy controls and participants with PD (Bottner et al., 2012; Gold et al., 2013;

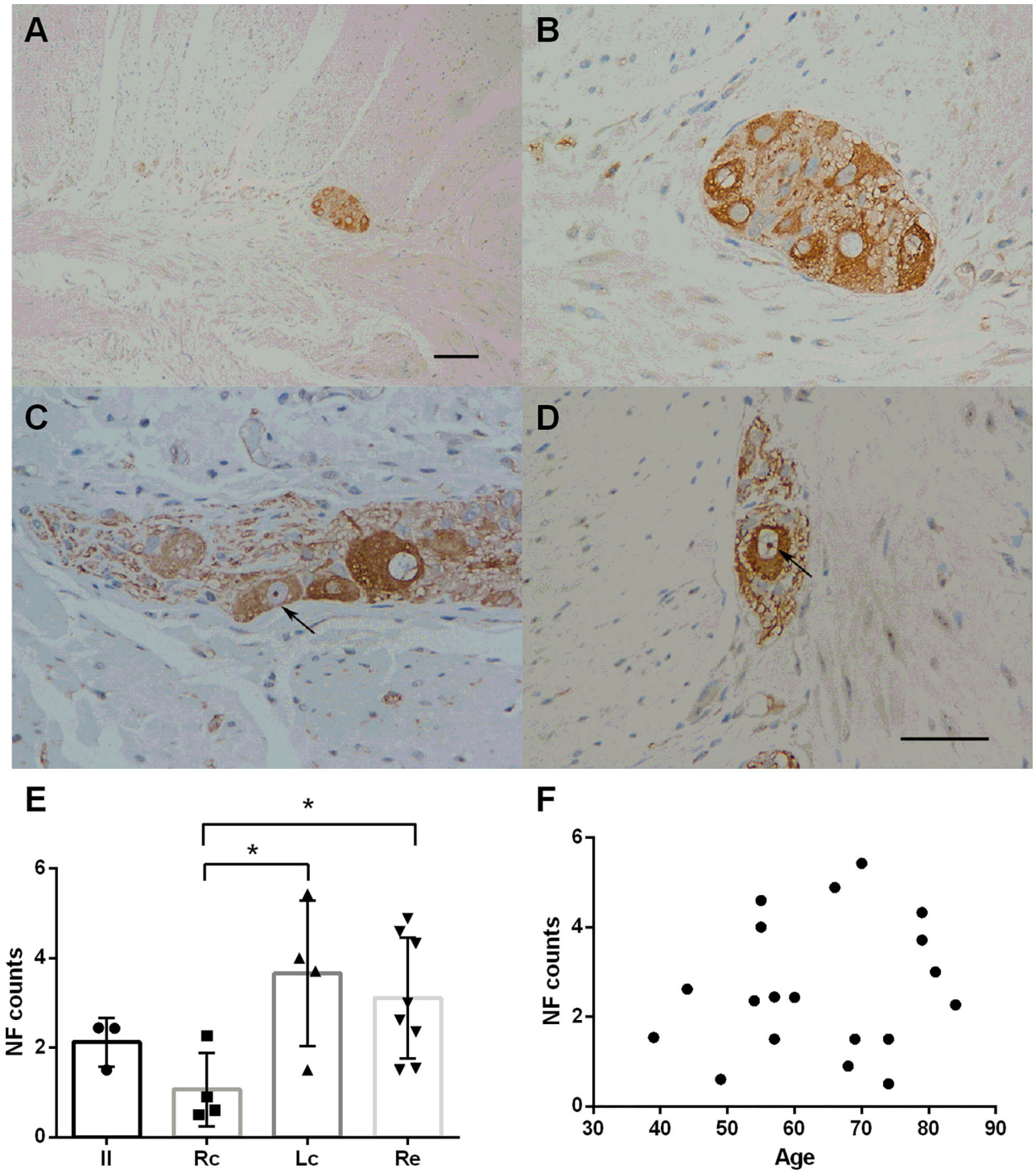


FIGURE 1 | Immunostaining of neurofilaments (NFs) in the myenteric plexus. **(A–D)** Immunostaining of NFs in the myenteric plexus. Representative image of the myenteric nerve plexus located between the two muscle layers (longitudinal and circular muscles), comprised of many nerve plexus sections on the cut surface **(A)**. Fine staining of NF-positive profiles (brown color) could be seen in the perikaryon of neurons in the myenteric plexus. The nuclei of the neurons were lightly stained and some nucleoli could be seen (black arrows in **C,D**). Hematoxylin counterstain, scale bars = 100 μm **(A)**, 50 μm **(B–D)**. **(E)** Quantitative analysis of the NF-positive neuron count in the myenteric plexus. The count is subdivided into the ileum (Il), right colon (RC), left colon (LC), and rectum (RE). Inter-group differences are reported as per one-way ANOVA ($F = 3.564$, $df = 18$, $p = 0.040$) followed by an LSD-t *post-hoc* test (RC group 1.07 ± 0.82 *vs*. the LC group 3.66 ± 0.62, $p = 0.010$; RC group 1.07 ± 0.82 *vs.* the RE group 3.11 ± 1.35, $p = 0.017$). Data are shown as NF positive neurons per visual field for individual cases and the group mean ± SD is also shown. **(F)** Scatter plot of the NF-positive neuron count within the myenteric plexus with age. No significant correlation was observed (Pearson correlation, $p = 0.499$). * = $p < 0.05$.

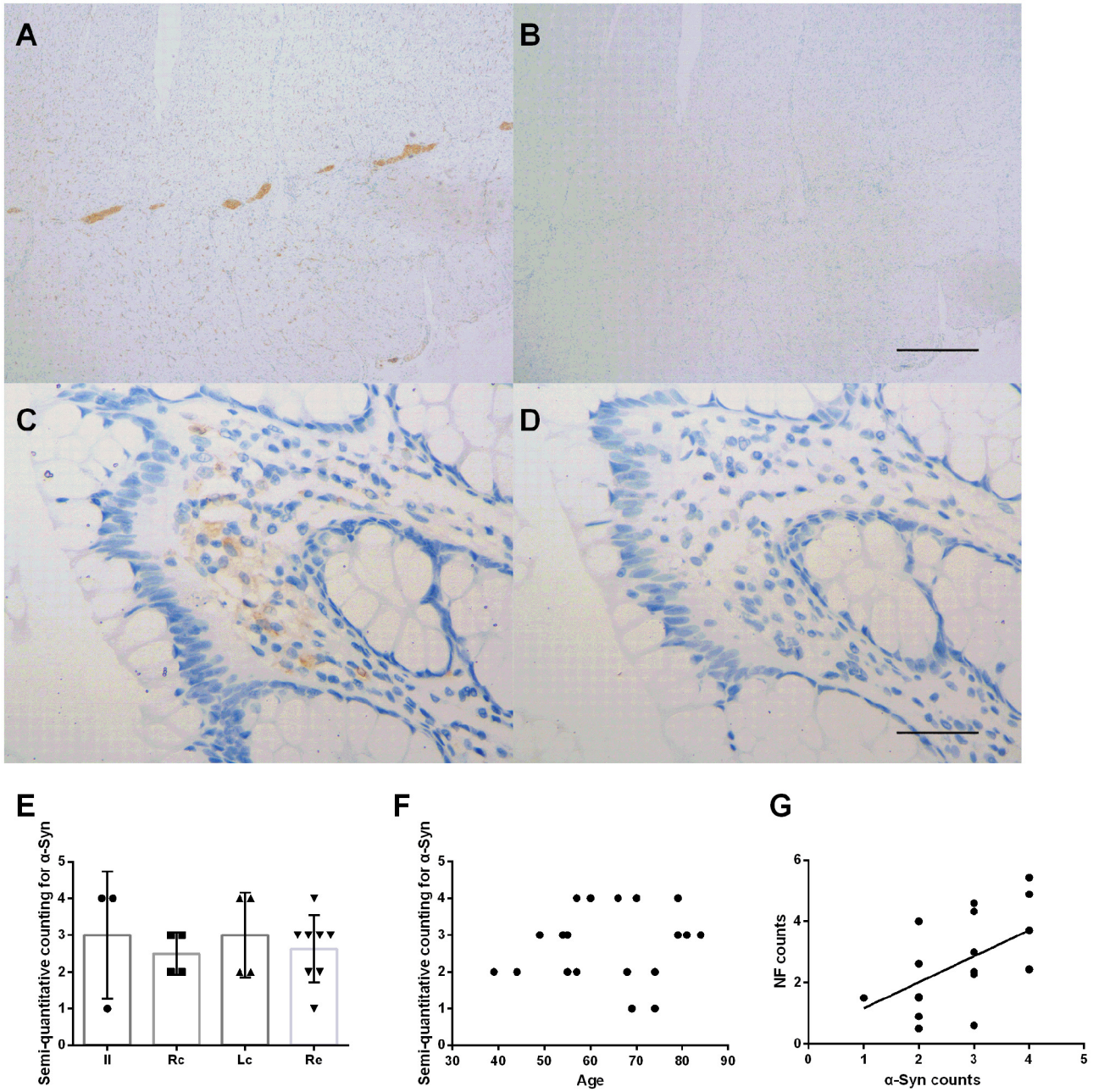


FIGURE 2 | Characteristic of α-Syn immunoreactive signals in the myenteric plexus. **(A–D)**. Representative image of immunostaining for α-Syn in the myenteric plexus. α-Syn immunoreactive signals (brown color) in the myenteric plexus **(A)**, and the mucosa **(C)**. **(B,D)** Are negative controls. Hematoxylin counterstain, scale bars = 500 μm **(A,B)**, 50 μm **(C,D)**. **(E)** Specimens were subdivided into the ileum (Il), right colon (Rc), left colon (Lc), and rectum (Re). Semi-quantitative analysis of α-Syn immunoreactive signals among the groups in the myenteric plexus (Kruskal–Wallis test, $p = 0.812$). Data shown as mean± SD. **(F)** Scatter plot of the semi-quantitative analysis of α-Syn immunoreactive signals within the myenteric plexus with age. No significant correlation was observed (Pearson correlation, $p = 0.554$). **(G)** Scatter plot of the NF-positive neuron count within the myenteric plexus with α-Syn showed a positive correlation (Pearson correlation, $R = 0.592$, $p = 0.008$).

Antunes et al., 2016; Shin et al., 2017). Aggregated α-Syn and p^{Ser129}α-Syn were present in individuals with and without PD (Visanji et al., 2015). In a human post-mortem study on elderly subjects without neurological diseases, α-Syn immunoreactivity was observed in the brainstem, olfactory nerves, spinal cord, and the peripheral nervous system (Bloch et al., 2006). There are several possible reasons for the inconsistencies between the results of past studies on α-Syn in the ENS. These include differences in the sites and depths of biopsies, and the antibodies and histological techniques used. Previous studies proved a

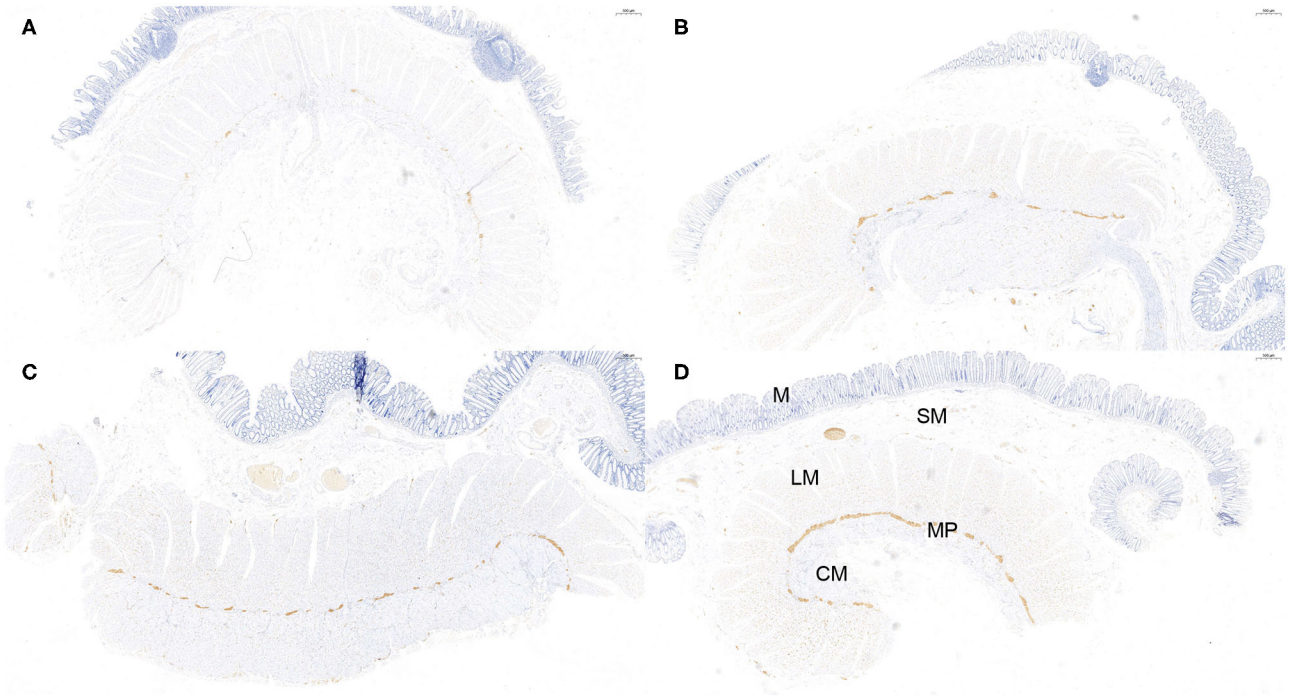


FIGURE 3 | Semi-quantitative counting for α-Syn expression in the myenteric plexus. All layers of the intestine were shown. From top to bottom: The mucosa (M), submucosa (SM), longitudinal muscularis (LM), myenteric plexus (MP), and circular muscularis (CM), respectively. The expression of α-Syn was defined as 1- sparse (≤ 1/4 positive staining area) **(A)**, 2- small amount (≤ 2/4 positive staining area) **(B)**, 3-common (≤ 3/4 positive staining area) **(C)**, and 4-rich (> 3/4 positive staining area) **(D)**, according to a previous study. The "positive" stained area here refers to the length of the positively stained myenteric plexus as a proportion of the total length of the specimen. Hematoxylin counterstain, scale bars = 500 μm.

rostro-caudal gradient of α-Syn expression, with greater density of expression in rostral portions as compared to the more caudal portions of the gastrointestinal tract (Beach et al., 2010; Gelpi et al., 2014). It suggested that localization of biopsies along the gastrointestinal tract and the difference in intestinal staining intensity might be critical factors that could be standardized in studies of enteric α-Syn immunohistochemistry, and may be responsible for previous discrepancies in results. These findings raise the question of whether α-Syn immunostaining in the ENS holds promise as a diagnostic hallmark and represents the pathological state.

Our study is consistent with previous immunohistochemical studies on intestinal biopsies, in which α-Syn pathology in the ENS is not a proper indicator of α-Synucleinopathies. The presence of α-Syn in the human ENS appears to be a normal finding. In contrast to native α-Syn immunoreactivity, which remained uniform regardless of the patients' age, we found that the level of p^{Ser129}α-Syn was age-dependent in the myenteric plexus of the ENS. Normal development and aging could be major contributing factors to α-Syn pathology. Correlation analysis showed that the counts of neurons in the myenteric plexus correlated positively with the accumulation of α-Syn ($p = 0.008$). It is also supported the hypothesis that the accumulation of α-Syn is a physiological phenomenon.

Data from previous human studies have shown that p^{Ser129}α-Syn occurs in the adult brain physiologically (Muntane et al., 2012). Another study found that the presence of LBs was not associated with the severity of neurodegeneration in the CNS (Schulz-Schaeffer, 2010). We found that p^{Ser129}α-Syn levels increased with age, and previous studies indicated that the pathology of p^{Ser129}α-Syn was not limited to PD, and was implicated in several neurodegenerative diseases (Paleologou et al., 2010; Vaikath et al., 2019). Therefore, we speculated that p^{Ser129}α-Syn might reflect the aging process to a certain extent, rather than just neurodegeneration. These changes can also be found in patients without neurodegenerative disorders; therefore, these changes might not be regarded as a hallmark in patients with neurodegenerative disorders, particularly PD.

Correlation analysis showed that there was no significant correlation between the distribution of p^{Ser129}α-Syn and age or tumor stage. While the presence of p^{Ser129}α-Syn was observed only in the submucosa and myenteric plexus, the age-dependent pattern indicated that this pathological change represented constant accumulation with age. Additionally, we found that the degenerative changes of the ENS were related to the degree of tumor malignancy.

The significance of this research was to determine the importance of α-Syn pathology as an intestinal hallmark for neurodegenerative disorders. We showed that positive staining of α-Syn was also detected in normal intestinal specimens of the human ENS. The pathological change of p^{Ser129}α-Syn was

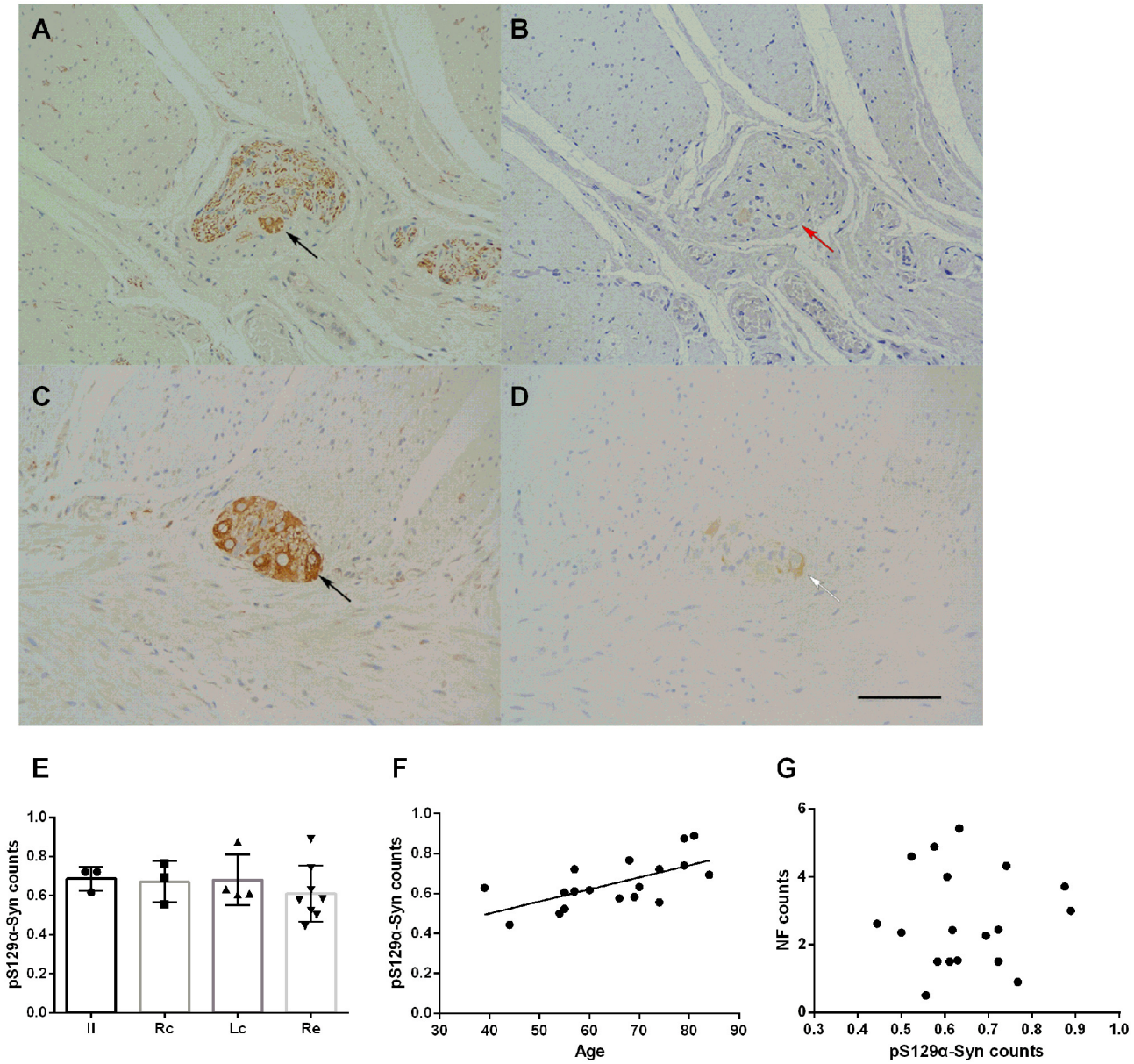


FIGURE 4 | Characteristic of p^{S129}α-Syn immunoreactive signals in the myenteric plexus **(A–D)**. Representative image of NF immunoreactivity in the myenteric plexus (black arrows in **A,C**). p^{S129}α-Syn immunoreactivity in the human myenteric plexus **(B,D)** (brown color). Co-localization of NFs and p^{S129}α-Syn (white arrow in **D**). Not all neurons with positive NF staining have p^{S129}α-Syn deposition (red arrow in **B**). Hematoxylin counterstain, bars =50 μm. **(E)** Quantitative analysis of the p^{S129}α-Syn-positive count in the myenteric plexus. Specimens were subdivided into the Ileum(Il), right colon (RC), left colon (LC), and rectum (RE). Inter-group differences are reported as per one-way ANOVA ($F = 0.452$, $df = 17$, $p = 0.720$) followed by LSD-t *post-hoc* test. Data are shown as p^{S129}α-Syn positive neurons per visual field for individual cases and the group mean ± SD is also shown. **(F)** Scatter plot of the p^{S129}α-Syn-positive neuron count within the myenteric plexus with age showed a positive correlation (Pearson correlation, $R = 0.643$, $p = 0.004$). **(G)** Scatter plot of p^{S129}α-Syn immunoreactive signals within the myenteric plexus with the NF-positive neuron count. No significant correlation was observed (Pearson correlation, $p = 0.958$).

observed to constantly accumulate with age in the ENS and might not be strictly regarded as a pathological correlation. In addition, there was no significant correlation between the α-Syn pathology of the ENS and tumor malignancy. These results suggested that α-Syn pathology in the ENS is not suitable as a hallmark of α-Synucleinopathies such as PD.

There are several limitations to this study. The recruitment challenges arising from the need to obtain full-thickness intestinal specimens meant that patients with neurodegenerative disorders and healthy individuals are lacking in the current study. Further studies are needed to compare these groups and to investigate the role of α-Syn pathology in the ENS.

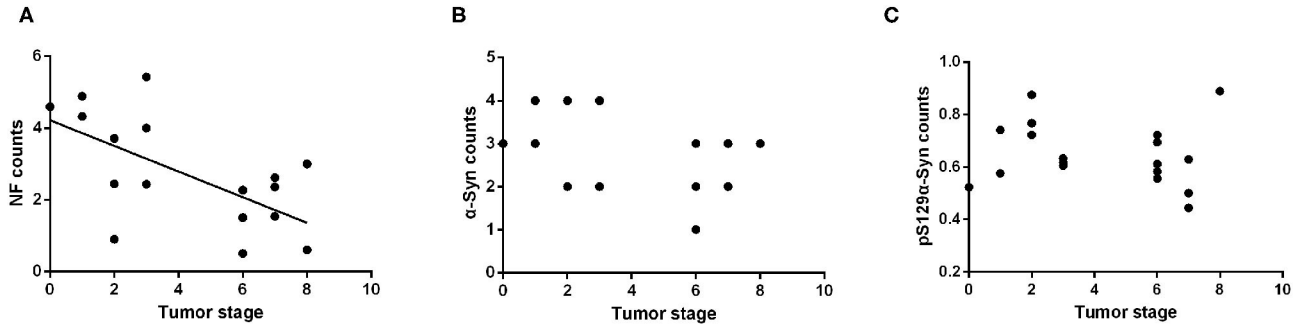


FIGURE 5 | Correlation analysis between the α-Syn pathology of the ENS and tumor malignancy. **(A)** Scatter plot of p^{S129}α-Syn immunoreactive signals within the myenteric plexus with tumor malignancy; a negative correlation was observed (Pearson correlation, $R = -0.522$, $p = 0.022$). **(B)** Scatter plot of α-Syn immunoreactive signals within the myenteric plexus with tumor malignancy; no significant correlation was observed (Spearman correlation, $p = 0.095$). **(C)** Scatter plot of p^{S129}α-Syn immunoreactive signals within the myenteric plexus with tumor malignancy; no significant correlation was observed (Pearson correlation, $p = 0.566$).

We should also determine whether this deposit is pathogenic, related to the digestive tract, or caused by extrapyramidal symptoms. The present study was insufficient to show the different forms of α-Syn, such as the prefibrillar forms and oligomers. Furthermore, only a small group of tumor patients were enrolled in this study. Our results may be limited by the sample size and the lack of intestinal tissue from patients with α-Synucleinopathies, including PD. In addition, the differences in intestinal staining intensity (under different conditions) between non-neurodegenerative cases and neurodegenerative cases might also cause different results. However, in the current study, we only focused on exploring the α-Syn status in the nearly normal ENS. Further studies involving larger samples and patients with neurodegeneration patients are required to provide stronger evidence for our conclusions.

CONCLUSION

Overall, we found that deposits of α-Syn in the ENS were presented in people with non-neurodegenerative disorders in a physiological state. In particular, the age-dependent appearance of p^{Ser129}α-Syn was observed in the submucosa and myenteric plexus. This finding weakens the basis and reliability of gastrointestinal pathology as an auxiliary diagnosis for α-Synucleinopathies, including PD.

DATA AVAILABILITY STATEMENT

The original contributions presented in the study are included in the article/**Supplementary Materials**, further inquiries can be directed to the corresponding author/s.

ETHICS STATEMENT

The studies involving human participants were reviewed and approved by Ethics Committee of Sun Yat-sen Memorial Hospital, Sun Yat-sen University, Guangzhou, China. The patients/participants provided their written informed consent to participate in this study.

AUTHOR CONTRIBUTIONS

E-XT, Y-RL, and X-NJ designed the experiments and critically revised the manuscript. K-XH and D-ZZ performed the experiments. L-LB and D-YL collected patient information and specimens. L-LB, YC, and X-NJ analyzed and interpreted the data. L-LB and X-NJ wrote the manuscript. All authors read and approved the final manuscript. All authors contributed to the article and approved the submitted version.

FUNDING

This work was supported by the National Natural Science Foundation of China (Grant Numbers 81503052, 81571244, 81771378, and 81971195), the Natural Science Foundation of Guangdong Province (Grant Numbers 2017A030313840 and 2018A0303130205), the Key Field Research and Development Program of Guangdong Province (Grant Number 2018B030337001), the Yat-sen Scholarship for Young Scientists, Key Laboratory of Malignant Tumor Molecular Mechanism and Translational Medicine of Guangzhou Bureau of Science and Information Technology (Grant Number [2013]163), and the Key Laboratory of Malignant Tumor Gene Regulation and Target Therapy of Guangdong Higher Education Institutes (Grant Number KLB09001).

SUPPLEMENTARY MATERIAL

The Supplementary Material for this article can be found online at: https://www.frontiersin.org/articles/10.3389/fnagi.2020.575481/full#supplementary-material

REFERENCES

Alegre-Abarrategui, J., Brimblecombe, K. R., Roberts, R. F., Velentza-Almpani, E., Tilley, B. S., Bengoa-Vergniory, N., et al. (2019). Selective vulnerability in α-synucleinopathies. *Acta Neuropathol.* 138, 681–704. doi: 10.1007/s00401-019-02010-2

Annerino, D. M., Arshad, S., Taylor, G. M., Adler, C. H., Beach, T. G., and Greene, J. G. (2012). Parkinson's disease is not associated with gastrointestinal myenteric ganglion neuron loss. *Acta Neuropathol.* 124, 665–680. doi: 10.1007/s00401-012-1040-2

Antunes, L., Frasquilho, S., Ostaszewski, M., Weber, J., Longhino, L., Antony, P., et al. (2016). Similar α-Synuclein staining in the colon mucosa in patients with Parkinson's disease and controls. *Mov. Disord.* 31, 1567–1570. doi: 10.1002/mds.26702

Beach, T. G., Adler, C. H., Sue, L. I., Vedders, L., Lue, L., White Iii, C. L., et al. (2010). Multi-organ distribution of phosphorylated α-synuclein histopathology in subjects with Lewy body disorders. *Acta Neuropathol.* 119, 689–702. doi: 10.1007/s00401-010-0664-3

Bieri, G., Brahic, M., Bousset, L., Couthouis, J., Kramer, N. J., Ma, R., et al. (2019). LRRK2 modifies α-syn pathology and spread in mouse models and human neurons. *Acta Neuropathol.* 137, 961–980. doi: 10.1007/s00401-019-01995-0

Bloch, A., Probst, A., Bissig, H., Adams, H., and Tolnay, M. (2006). Alpha-synuclein pathology of the spinal and peripheral autonomic nervous system in neurologically unimpaired elderly subjects. *Neuropathol. Appl. Neurobiol.* 32, 284–295. doi: 10.1111/j.1365-2990.2006.00727.x

Bottner, M., Zorenkov, D., Hellwig, I., Barrenschee, M., Harde, J., Fricke, T., et al. (2012). Expression pattern and localization of α-synuclein in the human enteric nervous system. *Neurobiol. Dis.* 48, 474–480. doi: 10.1016/j.nbd.2012.07.018

Braak, H., Rub, U., Gai, W. P., and Del Tredici, K. (2003). Idiopathic Parkinson's disease: possible routes by which vulnerable neuronal types may be subject to neuroinvasion by an unknown pathogen. *J. Neural Transm.* 110, 517–536. doi: 10.1007/s00702-002-0808-2

Breen, D. P., Halliday, G. M., and Lang, A. E. (2019). Gut-brain axis and the spread of α-synuclein pathology: vagal highway or dead end? *Mov. Disord.* 34, 307–316. doi: 10.1002/mds.27556

Chalazonitis, A., and Rao, M. (2018). Enteric nervous system manifestations of neurodegenerative disease. *Brain. Res.* 1693(Pt B), 207–213. doi: 10.1016/j.brainres.2018.01.011

Del Tredici, K., and Braak, H. (2016). Review: sporadic Parkinson's disease: development and distribution of α-synuclein pathology. *Neuropathol. Appl. Neurobiol.* 42, 33–50. doi: 10.1111/nan.12298

den, H. J. W., and Bethlem, J. (1960). The distribution of Lewy bodies in the central and autonomic nervous systems in idiopathic paralysis agitans. *J Neurol. Neurosurg. Psychiatry* 23, 283–290. doi: 10.1136/jnnp.23.4.283

Fortin, D. L., Troyer, M. D., Nakamura, K., Kubo, S., Anthony, M. D., and Edwards, R. H. (2004). Lipid rafts mediate the synaptic localization of α-synuclein. *J. Neurosci.* 24, 6715–6723. doi: 10.1523/JNEUROSCI.1594-04.2004

Gelpi, E., Navarro-Otano, J., Tolosa, E., Gaig, C., Compta, Y., Rey, M. J., et al. (2014). Multiple organ involvement by α-synuclein pathology in Lewy body disorders. *Mov. Disord.* 29, 1010–1018. doi: 10.1002/mds.25776

Gold, A., Turkalp, Z. T., and Munoz, D. G. (2013). Enteric α-synuclein expression is increased in Parkinson's disease but not Alzheimer's disease. *Mov. Disord.* 28, 237–240. doi: 10.1002/mds.25298

Lebouvier, T., Neunlist, M., Bruley des Varannes, S., Coron, E., Drouard, A., N'Guyen, J. M., et al. (2010). Colonic biopsies to assess the neuropathology of Parkinson's disease and its relationship with symptoms. *PLoS ONE* 5:e12728. doi: 10.1371/journal.pone.0012728

Lee, H. J., Jung, K. W., Chung, S. J., Hong, S. M., Kim, J., Lee, J. H., et al. (2018). Relation of enteric α-synuclein to gastrointestinal dysfunction in patients with Parkinson's disease and in neurologically intact subjects. *J. Neurogastroenterol. Motil.* 24, 469–478. doi: 10.5056/jnm17141

Lim, Y. J., and Lee, S. J. (2017). Are exosomes the vehicle for protein aggregate propagation in neurodegenerative diseases? *Acta. Neuropathol. Commun.* 5:64. doi: 10.1186/s40478-017-0467-z

Lippa, C. F., Fujiwara, H., Mann, D. M., Giasson, B., Baba, M., Schmidt, M. L., et al. (1998). Lewy bodies contain altered α-synuclein in brains of many familial Alzheimer's disease patients with mutations in presenilin and amyloid precursor protein genes. *Am. J. Pathol.* 153, 1365–1370. doi: 10.1016/S0002-9440(10)65722-7

Mao, X., Ou, M. T., Karuppagounder, S. S., Kam, T. I., Yin, X., Xiong, Y., et al. (2016). Pathological α-synuclein transmission initiated by binding lymphocyte-activation gene 3. *Science* 353:aah3374. doi: 10.1126/science.aah3374

Muntane, G., Ferrer, I., and Martinez-Vicente, M. (2012). α-synuclein phosphorylation and truncation are normal events in the adult human brain. *Neuroscience* 200, 106–119. doi: 10.1016/j.neuroscience.2011.10.042

Oueslati, A. (2016). Implication of Alpha-Synuclein Phosphorylation at S129 in Synucleinopathies: what have we learned in the last decade? *J. Parkinsons Dis.* 6, 39–51. doi: 10.3233/JPD-160779

Paleologou, K. E., Oueslati, A., Shakked, G., Rospigliosi, C. C., Kim, H. Y., Lamberto, G. R., et al. (2010). Phosphorylation at S87 is enhanced in synucleinopathies, inhibits α-synuclein oligomerization, and influences synuclein-membrane interactions. *J. Neurosci.* 30, 3184–3198. doi: 10.1523/JNEUROSCI.5922-09.2010

Peng, C., Gathagan, R. J., Covell, D. J., Medellin, C., Stieber, A., Robinson, J. L., et al. (2018). Cellular milieu imparts distinct pathological α-synuclein strains in α-synucleinopathies. *Nature* 557, 558–563. doi: 10.1038/s41586-018-0104-4

Postuma, R. B., Berg, D., Stern, M., Poewe, W., Olanow, C. W., Oertel, W., et al. (2015). MDS clinical diagnostic criteria for Parkinson's disease. *Mov. Disord.* 30, 1591–1601. doi: 10.1002/mds.26424

Pouclet, H., Lebouvier, T., Coron, E., Rouaud, T., Flamant, M., Toulgoat, F., et al. (2012). Analysis of colonic α-synuclein pathology in multiple system atrophy. *Parkinsonism Relat. Disord.* 18, 893–895. doi: 10.1016/j.parkreldis.2012.04.020

Rao, M., and Gershon, M. D. (2016). The bowel and beyond: the enteric nervous system in neurological disorders. *Nat. Rev. Gastroenterol. Hepatol.* 13, 517–528. doi: 10.1038/nrgastro.2016.107

Schulz-Schaeffer, W. J. (2010). The synaptic pathology of α-synuclein aggregation in dementia with Lewy bodies, Parkinson's disease and Parkinson's disease dementia. *Acta Neuropathol.* 120, 131–143. doi: 10.1007/s00401-010-0711-0

Shannon, K. M., Keshavarzian, A., Mutlu, E., Dodiya, H. B., Daian, D., Jaglin, J. A., et al. (2012). Alpha-synuclein in colonic submucosa in early untreated Parkinson's disease. *Mov. Disord.* 27, 709–715. doi: 10.1002/mds.23838

Shin, C., Park, S. H., Yun, J. Y., Shin, J. H., Yang, H. K., Lee, H. J., et al. (2017). Fundamental limit of α-synuclein pathology in gastrointestinal biopsy as a pathologic biomarker of Parkinson's disease: comparison with surgical specimens. *Parkinsonism Relat. Disord.* 44, 73–78. doi: 10.1016/j.parkreldis.2017.09.001

Sprenger, F. S., Stefanova, N., Gelpi, E., Seppi, K., Navarro-Otano, J., Offner, F., et al. (2015). Enteric nervous system α-synuclein immunoreactivity in idiopathic REM sleep behavior disorder. *Neurology* 85, 1761–1768. doi: 10.1212/WNL.0000000000002126

Urrea, L., Segura-Feliu, M., Masuda-Suzukake, M., Hervera, A., Pedraz, L., Garcia-Aznar, J. M., et al. (2018). Involvement of Cellular Prion Protein in α-Synuclein Transport in Neurons. *Mol. Neurobiol.* 55, 1847–1860. doi: 10.1007/s12035-017-0451-4

Vaikath, N. N., Erskine, D., Morris, C. M., Majbour, N. K., Vekrellis, K., Li, J. Y., et al. (2019). Heterogeneity in α-synuclein subtypes and their expression in cortical brain tissue lysates from Lewy body diseases and Alzheimer's disease. *Neuropathol. Appl. Neurobiol.* 45, 597–608. doi: 10.1111/nan.12531

Visanji, N. P., Marras, C., Kern, D. S., Al Dakheel, A., Gao, A., Liu, L. W., et al. (2015). Colonic mucosal a-synuclein lacks specificity as a biomarker for Parkinson disease. *Neurology* 84, 609–616. doi: 10.1212/WNL.0000000000001240

Wislet-Gendebien, S., D'Souza, C., Kawarai, T., St George-Hyslop, P., Westaway, D., Fraser, P., et al. (2006). Cytosolic proteins regulate α-synuclein dissociation from presynaptic membranes. *J. Biol. Chem.* 281, 32148–32155. doi: 10.1074/jbc.M605965200

Conflict of Interest: The authors declare that the research was conducted in the absence of any commercial or financial relationships that could be construed as a potential conflict of interest.

Copyright © 2020 Bu, Huang, Zheng, Lin, Chen, Jing, Liang and Tao. This is an open-access article distributed under the terms of the Creative Commons Attribution License (CC BY). The use, distribution or reproduction in other forums is permitted, provided the original author(s) and the copyright owner(s) are credited and that the original publication in this journal is cited, in accordance with accepted academic practice. No use, distribution or reproduction is permitted which does not comply with these terms.

frontiers in Aging Neuroscience

ORIGINAL RESEARCH
published: 24 November 2020
doi: 10.3389/fnagi.2020.599246

LncRNA-T199678 Mitigates α-Synuclein-Induced Dopaminergic Neuron Injury via miR-101-3p

Lu-Lu Bu[1,2†], Ying-Yu Xie[1,2†], Dan-Yu Lin[3], Ying Chen[1,2], Xiu-Na Jing[1,2], Yan-Ran Liang[1,2], Su-Dan Peng[1,2], Kai-Xun Huang[3] and En-Xiang Tao[1,2*]*

[1] Department of Neurology, Sun Yat-sen Memorial Hospital, Sun Yat-sen University, Guangzhou, China, [2] Guangdong Provincial Key Laboratory of Malignant Tumor Epigenetics and Gene Regulation, Sun Yat-sen Memorial Hospital, Sun Yat-sen University, Guangzhou, China, [3] Department of Neurology, The Eighth Affiliated Hospital, Sun Yat-sen University, Shenzhen, China

Parkinson's disease (PD) is the second most common neurodegenerative disorder characterized by dopaminergic neuron death and the abnormal accumulation and aggregation of α-synuclein (α-Syn) in the substantia nigra (SN). Although the abnormal accumulation of α-Syn can solely promote and accelerate the progress of PD, the underlying molecular mechanisms remain unknown. Mounting evidence confirms that the abnormal expression of long non-coding RNA (lncRNA) plays an important role in PD. Our previous study found that exogenous α-Syn induced the downregulation of lncRNA-T199678 in SH-SY5Y cells via a gene microarray analysis. This finding suggested that lncRNA-T199678 might have a potential pathological role in the pathogenesis of PD. This study aimed to explore the influence of lncRNA-T199678 on α-Syn-induced dopaminergic neuron injury. Overexpression of lncRNA-T199678 ameliorated the neuron injury induced by α-Syn via regulating oxidative stress, cell cycle, and apoptosis. Studies indicate lncRNAs could regulate posttranscriptional gene expression via regulating the downstream microRNA (miRNA). To discover the downstream molecular target of lncRNA-T199678, the following experiment found out that miR-101-3p was a potential target for lncRNA-T199678. Further study showed that the upregulation of lncRNA-T199678 reduced α-Syn-induced neuronal damage through miR-101-3p in SH-SY5Y cells and lncRNA-T199678 was responsible for the α-Syn-induced intracellular oxidative stress, dysfunction of the cell cycle, and apoptosis. All in all, lncRNA-T199678 mitigated the α-Syn-induced dopaminergic neuron injury via targeting miR-101-3p, which contributed to promote PD. Our results highlighted the role of lncRNA-T199678 in mitigating dopaminergic neuron injury in PD and revealed a new molecular target for PD.

Keywords: Parkinson's disease, lncRNA-T199678, miRNA-101-3p, dopaminergic neuron injury, α-synuclein

OPEN ACCESS

Edited by:
Shaogang Qu,
Southern Medical University, China

Reviewed by:
Tao Wang,
Huazhong University of Science and Technology, China
Jifeng Guo,
Central South University, China

***Correspondence:**
En-Xiang Tao
taoex@mail.sysu.edu.cn
Dan-Yu Lin
daisylamdy@163.com

† These authors have contributed equally to this work

Received: *26 August 2020*
Accepted: *21 October 2020*
Published: *24 November 2020*

Citation:
Bu L-L, Xie Y-Y, Lin D-Y, Chen Y, Jing X-N, Liang Y-R, Peng S-D, Huang K-X and Tao E-X (2020) LncRNA-T199678 Mitigates α-Synuclein-Induced Dopaminergic Neuron Injury via miR-101-3p. Front. Aging Neurosci. 12:599246. doi: 10.3389/fnagi.2020.599246

INTRODUCTION

Parkinson disease (PD) is a progressive neurodegenerative disease classified clinically as a movement disorder and pathologically by nigrostriatal dopamine depletion, and the residual dopaminergic neurons contained Lewy bodies with α-synuclein (α-Syn) misfolding and abnormal aggregation (Dorsey et al., 2007; Kalia and Lang, 2015; Poewe et al., 2017). At present, PD cannot be

completely cured and existing therapeutic strategies have limited efficacy at the early stages of PD (Charvin et al., 2018). Therefore, it is in urgent need to clarify the pathogenesis of PD and find new therapeutic targets for PD.

Misfolding and abnormal aggregation of α-Syn are the core features of Parkinson's disease (Fayyad et al., 2019). However, the specific mechanism of α-Syn-induced cell damage is still not clear. Exogenous α-Syn induces abnormal aggregation and misfolding of α-Syn in normal cells. Long non-coding RNAs (lncRNAs) play an important role in a variety of physiology and pathology conditions in neurodegenerative diseases. Mounting evidence shows that lncRNAs are demonstrated to be equipped with multiple functions in PD (Chen et al., 2018; Lu et al., 2018; Wang et al., 2018b). To be specific, lncRNAs have been found to regulate α-Syn expression and aggregation (Liu and Lu, 2018; Xu et al., 2018), mitochondrial dysfunction (Yan et al., 2018; Xie et al., 2019), apoptosis (Ding et al., 2019; Lin et al., 2019), neuroinflammation (Fragkouli and Doxakis, 2014), and autophagy (Yan et al., 2018) in PD. In the specimen of the brain, the expression of 87 lncRNAs in the substantia nigra of PD patients was significantly changed (Ni et al., 2017). Among which, lncRNA AL049437 and lncRNA AK021630 were verified, via experimental test, to promote or inhibit the occurrence of PD, respectively. Also, besides brain tissue, abnormal expression of lncRNAs was also found in peripheral blood and cerebrospinal fluid of PD patients. Studies indicated that more than 6,000 lncRNAs were detected in peripheral blood leukocytes of PD patients, of which 13 lncRNAs decreased and among which 4 abnormally expressed lncRNAs were reversed after deep brain stimulation (DBS) (Soreq et al., 2015). Despite many exciting advances in lncRNA biology, the relationship between lncRNAs and PD pathogenesis remains elusive.

In our preliminary study, clear downregulation of lncRNA-T199678 (G046036) was noted in the exogenous α-Syn-induced SH-SY5Y cell model of PD by gene microarray (Lin et al., 2018). Subsequently, we confirmed that the expression level of lncRNA-T199678 was reduced in the α-Syn-induced SH-SY5Y cell model. Yet the function of lncRNA-T199678 in PD pathogenesis has not been rigorously studied. To address this point, in the present study we investigated the profile of lncRNA-T199678 in the α-Syn-induced SH-SY5Y cell model. We found that α-Syn downregulated lncRNA-T199678, which targeted miR-101-3p, thus aggravating neuron injury in PD. Therefore, this study explores the function of lncRNA-T199678 in the etiology and pathogenesis of PD and providing scientific clues for lncRNA-based treatments of this neurodegenerative disorder.

MATERIALS AND METHODS

Cell Culture

SH-SY5Y cells were obtained from the Cell Bank of the Chinese Academy of Medical Science (Shanghai, China). Cells were cultured in Dulbecco's modified Eagle's medium (DMEM; Gibco, Carlsbad, CA, USA) containing 10% fetal bovine serum (FBS; Invitrogen, Carlsbad, CA, USA), 100 U/mL penicillin, and 100 μg/mL streptomycin in a humidified atmosphere with 5% CO_2 at 37°C.

Preparation for α-Syn Oligomer

The powder of α-Syn monomer was kindly donated by Professor Yu Shun, Department of Neurology, Xuanwu Hospital, Capital Medical University. The powder was dissolved in 0.01 M PBS to a final concentration of 25 μM (pH = 7.4), filtered and sterilized, and then incubated at 37°C for 72 h with oscillations for 100–150 R/min.

RNA Extraction and qPCR

The medium was aspirated, and cells were washed once with PBS. RNA was extracted using the Trizol (Takara, Japan) according to kit instructions. The concentration and quality of RNA were detected by NanoDrop ND-1000. cDNA was prepared using the Prime Script™ RT Reagent Kit (Takara, Japan) according to the manufacturer's instructions and diluted 1:10 in double-distilled water before qPCR plate preparation.

qPCR was performed in 96-well plates, using SYBR(R) Premix Ex Taq™. β-Actin was used as a housekeeping gene for SH-SY5Y cells. All data were calculated by the $2^{-\Delta\Delta Ct}$ method. (Primer sequences were detailed as follows).

Primer	Sequences
lncRNA-T199678-R	5′-TCTATTTTGTTGGTTTTCGG-3′
lncRNA-T199678-F	5′-ATGCTTTCGCTCTGGTCT-3′
β-Actin-F	5′-TGTCCACCTTCCAGCAGATGT-3′
β-Actin-R	5′-AGCTCAGTAACAGTCCGCCTAG-3′
hsa-miR-101-3p-F	5′-ACACTCCAGCTGGGTACAGTACTGTGATAAC-3′
hsa-miR-101-3p-R	5′-CTCAACTGGTGTCGTGGA-3′
hsa-miR-101-3p-RT	5′-CTCAACTGGTGTCGTGGAGTCGGCAATTCAGTTGAGTTCA GTTA-3′

In situ Hybridization

An appropriate amount of cells was inoculated into confocal dishes and treated in groups. Fixed with 4% paraformaldehyde at room temperature for 10 min, the cells were washed with PBS for 5 min, three times. One microliter precooled permeable solution (Triton-X100, Sigma, USA) was added to each well and stood at 4°C for 5 min. The permeable solution was discarded, and the cells were washed with PBS for 5 min, three times. The following *in situ* hybridization experiments were carried out according to the instructions of fluorescent *in situ* hybridization kit of Guangzhou Ruibo Biotechnology Co., Ltd. 200 μL of the pre-hybrid solution was added to each well and sealed at 37°C for 30 min. At the same time, the hybrid solution was preheated at 37°C. In the dark conditions, a mixed storage solution of 2.5 μl 20 μM lncRNA FISH Probe or control FISH Probe was added to the 100-μl hybrid solution. Then, the pre-hybrid solution was discarded in each well, and a 100-μL probe hybrid solution-containing probe was added overnight at 37°C in the absence of light. Hybrid lotions I, II, and III were preheated to 42°C; the cells were washed with hybrid lotion I for three times, 5 min each time in dark conditions and then washed with hybrid lotion II and hybrid lotion III once, 5 min each time. Next, the cells were washed with PBS, 5 min at room temperature, and 4′,6-Diamidino-2-Phenylindole, Dihydrochloride-stained for 10 min in dark conditions. Cells were washed with PBS for three times,

5 min each time. A fluorescence quenching agent was added under dark conditions (Wuhan Baodu Bio-Engineering Co., Ltd., China), and fluorescence detection was carried out by a confocal microscope (Zeiss LSM, Germany) (maximum excitation light length was 555 nm, maximum emission wavelength was 570 nm).

RNA Transfection and Interference

LncRNA-T199678-overexpressed plasmid PCDNA3.1-T199678 (PC-T199678) and its negative control (pcDNA3.1), lncRNA-T199678 Smart Silence (siT199678) and its negative control (siNC), and the miR-101-3p mimic and NC mimic were synthesized by Ruibo Biotechnology Co., Ltd. (Guangzhou, China). A Lipofectamine 3000 transfection agent (Invitrogen) was used for transfection according to the specification. The expressions of lncRNA-T199678 and miR-101-3p were detected by qPCR.

RNA Immunoprecipitation

The RNA immunoprecipitation was performed by using a Magna RIP Kit (Product NO. 17-701, Millipore, USA). In brief, SH-SY5Ycells were cells were lysed by RIP lysis (Shanghai Beyotime Biotechnology Co., Ltd., China), and cell lysates (100 μL) were incubated with RIP buffer containing magnetic beads conjugated with the human anti-Ago2 antibody (1:1000, Abcam 32381) or negative control normal mouse IgG (Millipore) at 4°C overnight. Then immunoprecipitated RNA was extracted. Purified RNA was subjected to further study.

Detection of Intracellular ROS

Intracellular ROS was detected using an oxidation-sensitive fluorescent probe (DCFH-DA) (Shanghai Beyotime Biotechnology Co., Ltd., China). Cells were incubated with 10 μmol/L DCFH-DA at 37°C for 20 min according to the manufacturer's instructions. The cells were washed three times with serum-free cell culture medium to fully remove DCFH-DA. Fluorescence of DCFH was detected by flow cytometry, and the excitation wavelength of 488 nm and emission wavelength of 525 nm were used to detect the fluorescence intensity before and after stimulation in real time.

Cell Cycle Analysis

Cell cycles were measured using the cell cycle kit (Product NO. BMS500FI-300) from Thermo Fisher, USA. The cells were digested by pancreatic enzymes. The supernatant was removed by centrifugation at 1,000 rpm for 5 min and then resuspended in PBS and fixed with 2 mL precooled 70% ethanol for 24 h at 4°C. After fixation, the supernatant was removed after centrifugation at 1,000 rpm for 5 min and washed with PBS. The precipitated cells were added with 50 μl RNA enzyme and 450 μl propidium iodide (PI) staining solution for flow cytometry within 4 h.

Cell Apoptosis Analysis

The apoptosis of the neurons was measured using an Annexin/V-FITC apoptosis detection kit (Product NO. BMS500FI-300, Thermo Fisher, USA) according to the manufacturer's instructions. The neurons were harvested in the EP and spun down for 5 min at 1000 rpm. Cells were washed in ice-cold PBS and resuspended in a 1 × binding buffer. Then 5 μl of Annexin V-FITC was added to the cell suspension and incubated for 15 min at room temperature. Lastly, 10 μl PI buffer was added and analyzed immediately by flow cytometry.

Statistical Analysis

All *in vitro* experiments were performed in triplicate, and each assay was repeated three times. The mean values from the triplicate measurements were used for statistical analysis. Data were presented as mean ± standard deviation (SD). Comparisons between two groups were performed with Student's *t*-test, and multiple comparisons of more than two groups were performed with one-way ANOVA followed by Tukey's multiple-comparison tests using GraphPad Prism 5. $P < 0.05$ was considered statistically significant.

RESULTS

Exogenous α-Syn Induces Stable Downregulation of lncRNA-T199678 Expression in SH-SY5Y Cells

Our previous research screened a significant downregulated lncRNA-T199678 in the differential expression gene in the pathologically α-Syn-induced group via a gene chip (Lin et al., 2018). To determine whether lncRNA-T199678 was involved in α-Syn-induced dopaminergic neuron damage, the relative expression of lncRNA-T199678 was detected via qPCR. In the α-Syn-challenged SH-SY5Y cell line, the expression of lncRNA-T199678 was markedly decreased when comparing to the control group (**Figure 1A**, $P < 0.05$). Therefore, to explore the function of lncRNA-T199678, we constructed lncRNA-T199678 overexpression and silencing cell lines as shown in **Figure 1B**. The lncRNA-T199678 expression was lower in the α-Syn-challenged SH-SY5Y cell line, as examined by RT-qPCR (**Figure 1A**, $P < 0.05$). These results indicated that lncRNA-T199678 may be a key player in α-Syn-mediated dopaminergic neuron loss.

Sub-Localization of lncRNA-T199678 in SH-SY5Y Cells

The localization of lncRNA in the cell is closely related to its function. Therefore, we studied the sub-localization of lncRNA-T199678 in the cell. We found that most lncRNA-T199678 in SH-SY5Y cells were located in the cytoplasm via taking U6 located in the nucleus and 18S located in the cytoplasm as the control, and with only a small amount in the nucleus. The results are shown in **Figure 1C**.

Overexpressed lncRNA-T199678 Reverses α-Syn-Induced Cell Injury

To further examine the effect of lncRNA-T199678 on the α-Syn-mediated dopaminergic neuron loss, we constructed lncRNA-T199678 overexpression and silencing cell lines in α-Syn-induced SH-SY5Y cells, followed by detection of the ROS to clear the oxidative stress injury via DCFH-DA probe and flow cytometry. Our results indicated that the level of ROS was significantly increased in the α-Syn-treated group

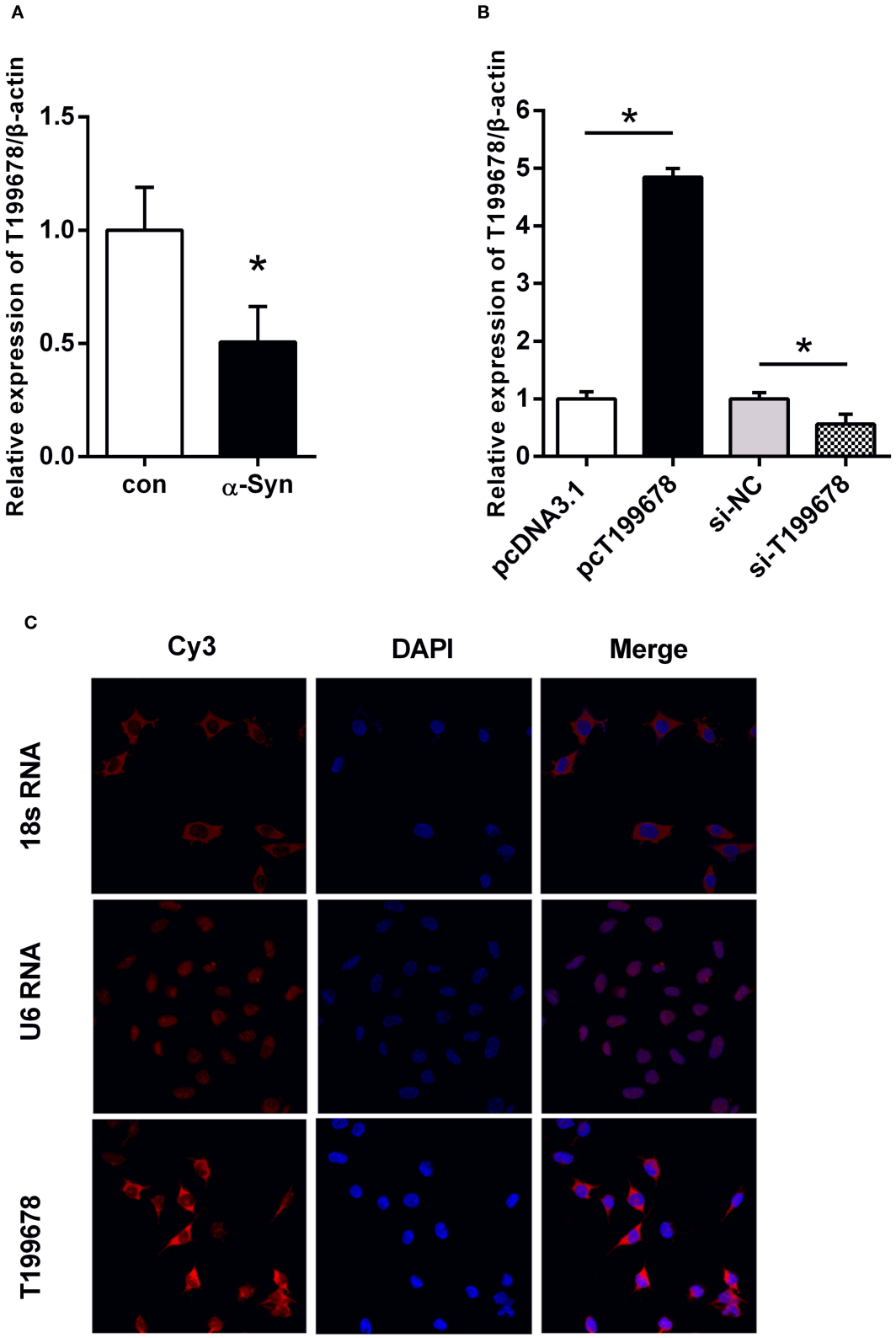


FIGURE 1 | The level and sub-localization of lncRNA-T199678 in α-Syn-challenged SH-SY5Y cells**. (A)** Relative expression of lncRNA-T199678 was markedly decreased in α-Syn-challenged SH-SY5Y cells by qPCR ($p < 0.05$, compared with the control group). **(B)** Relative expression of lncRNA-T199678 in lncRNA-T199678 overexpression and silencing cell lines by qPCR. **(C)** Sub-localization of lncRNA-T199678 in SH-SY5Y cells. Taking U6 located in the nucleus and 18S located in the cytoplasm as the control, most lncRNA-T199678 in the SH-SY5Y cell line were located in the cytoplasm. *$P < 0.05$.

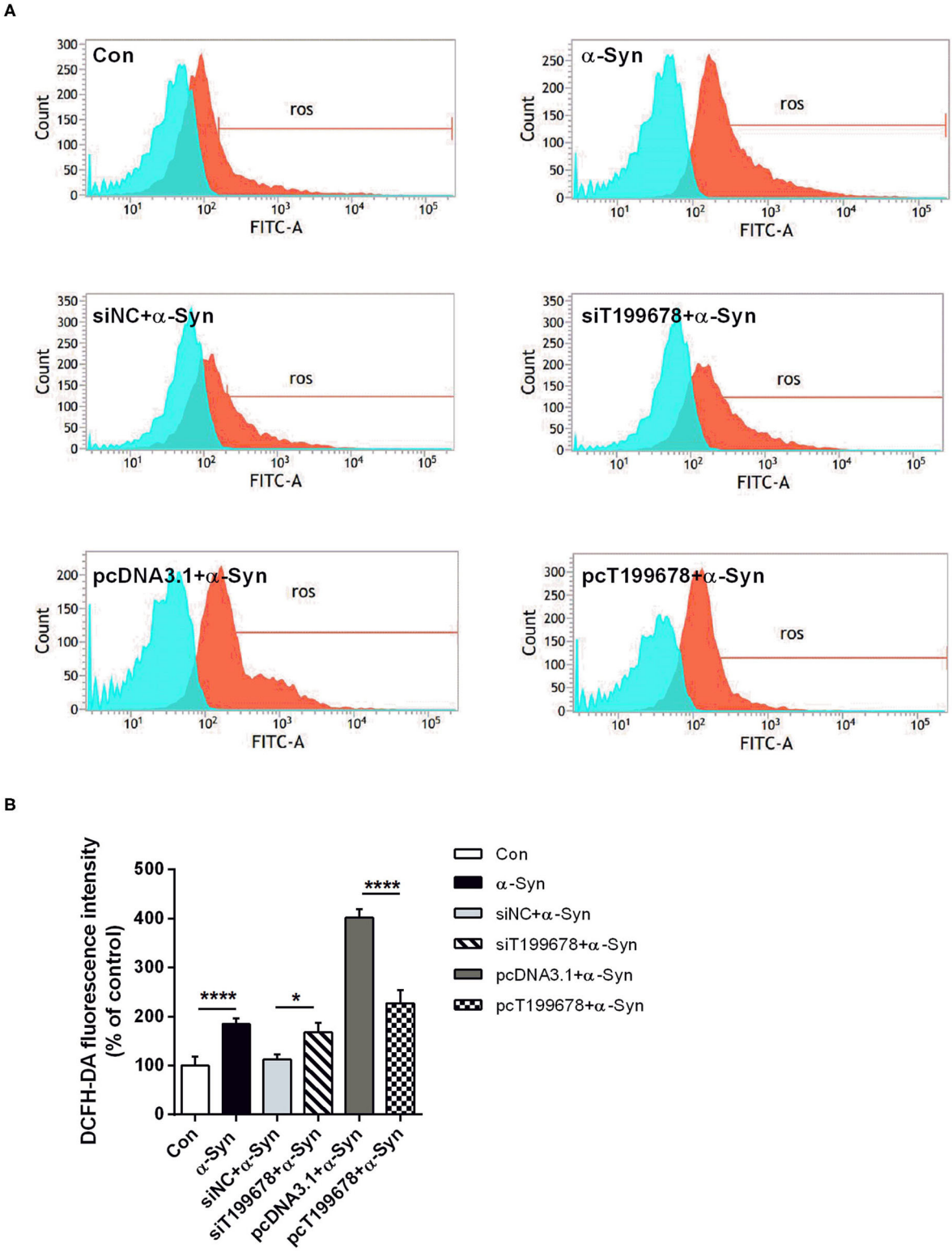


FIGURE 2 | Interference of lncRNA-T199678 ameliorated intracellular oxidative stress induced by α-Syn. SH-SY5Y cells were divided into six groups: control (wild type), α-Syn, siNC+α-Syn, siT199678+α-Syn, pcDNA3.1+α-Syn, and pc T199678+α-Syn. **(A)** Oxidative stress injury (ROS) was detected via DCFH-DA probe and flow cytometry. **(B)** Fluorescence of DCFH-DA was detected by flow cytometry (one-way ANOVA, $F = 143.1$, df $= 23$, $P < 0.0001$, followed by Tukey's multiple-comparison tests: Control vs. α-Syn, $^{****}P < 0.0001$; siNC+α-Syn vs. siT199678+α-Syn, $^{*}P < 0.05$; pcDNA3.1+α-Syn vs. pc T199678+α-Syn, $^{****}P < 0.0001$).

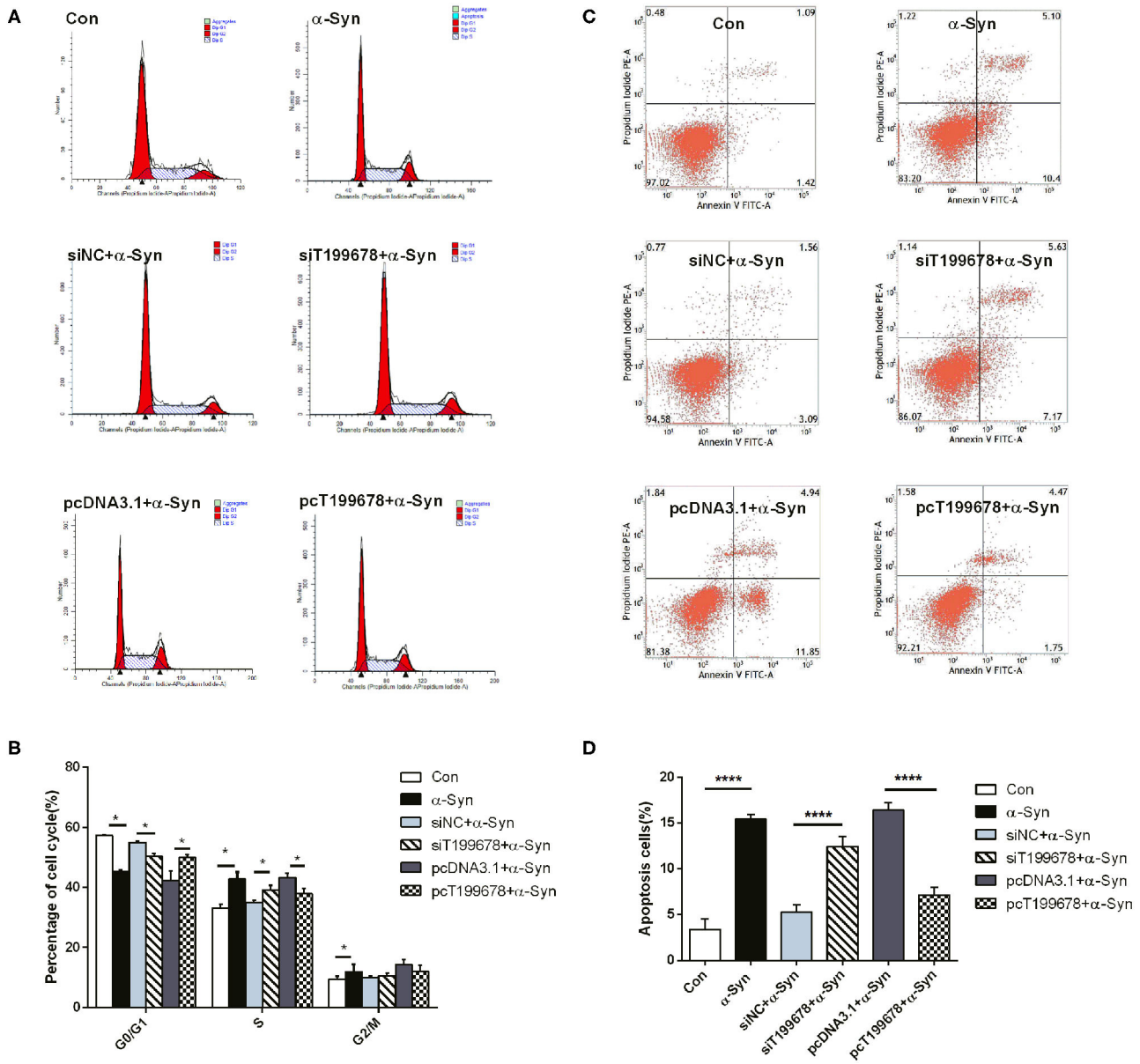


FIGURE 3 | lncRNA-T199678 mitigated α-Syn-induced cell cycle abnormality and apoptosis. SH-SY5Y cells were divided into six groups: control (wild type), α-Syn, siNC+α-Syn, siT199678+α-Syn, pcDNA3.1+α-Syn, and pc T199678+α-Syn. **(A,B)** The proportion of cells in the G0/G1, S, and G2/M phases in cell cycle via flow cytometry (both in the G0/G1 phase and S phase, one-way ANOVA, $P < 0.01$, followed by Tukey's multiple-comparison tests: Control vs. α-Syn, $^{*}P < 0.05$; siNC+α-Syn vs. si T199678+α-Syn, $^{*}P < 0.05$; pcDNA3.1+α-Syn vs. pc T199678+α-Syn, $^{*}P < 0.05$). **(C,D)** Percentage of apoptotic cells was quantified using flow cytometry (one-way ANOVA, $F = 115.3$, df = 17, $P < 0.0001$, followed by Tukey's multiple-comparison tests: control vs. α-Syn, $^{****}P < 0.0001$; siNC+α-Syn vs. siT199678+α-Syn, $^{****}P < 0.0001$; pcDNA3.1+α-Syn vs. pc T199678+α-Syn, $^{****}P < 0.0001$).

and lncRNA-T199678 silencing group (one-way ANOVA, $F = 143.1$, df = 23, $P < 0.0001$, followed by Tukey's multiple-comparison tests: control vs. α-Syn, $^{****}P < 0.0001$; siNC+α-Syn vs. siT199678+α-Syn, $^{*}P < 0.05$; **Figures 2A,B**), while overexpression of lncRNA-T199678 could reverse intracellular oxidative stress induced by exogenous α-Syn (pcDNA3.1+α-Syn vs. pc T199678+α-Syn, $^{****}P < 0.0001$; **Figures 2A,B**). Next, we determined the influence of lncRNA-T199678 on cell cycles, results of which suggested a reverse of cell cycles in an α-Syn-induced cell model with overexpressed lncRNA-T199678 (**Figures 3A,B**). The data from the cell cycle assay exhibited that the proportion of cells in the G0/G1 phase decreased and that in the S phase increased both in the α-Syn-treated group and in the lncRNA-T199678 silencing group (**Figures 3A,B**). Then, Annexin V-FITC/PI apoptosis detection kit and flow cytometry were used to measure differences in cell apoptosis.

The percentage of apoptotic cells was significantly increased in the α-Syn-treated group and lncRNA-T199678 silencing group (one-way ANOVA, $F = 115.3$, df $= 17$, $P < 0.0001$, followed by Tukey's multiple-comparison tests: control vs. α-Syn, $^{****}P < 0.0001$; siNC+α-Syn vs. siT199678+α-Syn, $^{****}P < 0.0001$; **Figures 3C,D**), while the apoptosis was proved to be inhibited after overexpression of lncRNA-T199678 along with α-Syn treatment (one-way ANOVA, $F = 115.3$, df $= 17$, $P < 0.0001$, followed by Tukey's multiple-comparison tests: pcDNA3.1+α-Syn vs. pc T199678+α-Syn, $^{****}P < 0.0001$; **Figures 3C,D**). Taken together, we found that lncRNA-T199678 reversed the oxidative stress, cell cycle abnormality, and apoptosis induced by α-Syn. These results indicated that lncRNA-T199678 attenuated the α-Syn-induced dopaminergic neuron damage.

Interaction Between lncRNA-T199678 and miR-101-3p in SH-SY5Y Cells

To investigate the downstream regulatory mechanism of lncRNA-T199678, the interactional binding sites between lncRNA-T199678 and miR-101-3p were predicted via the bioinformatics method (https://bibiserv.cebitec.uni-bielefeld.de/rnahybrid/, RNAhybrid prediction tools, **Figure 4A**), and the direct binding between them in SH-SY5Y cells was evaluated with RIP (RNA-binding protein immunoprecipitation) assay. Previous studies show that when lncRNA competitively binds miRNA in the form of ceRNA, lncRNA binds to miRNA and RNA-induced silencing complex (RISC), since Ago2 (Argonaute 2) is the core component of RISC, and ceRNA combined with miRNA can also bind to Ago2. We detected the expression of Ago2 in SH-SY5Y cells by Western blot (**Figure 4B**). Compared with IgG, lncRNA-T199678 and miR-101-3p were abundantly detected in the Ago2 antibody precipitation complex (**Figure 4C**), which suggested that lncRNA-T199678 had a similar function of ceRNA and could competitively bind to microRNA in the Ago2 complex. Thus, we confirmed the binding of miR-101-3p to lncRNA-T199678, suggesting miR-101-3p as a target of lncRNA-T199678.

Furthermore, we explored the effects of lncRNA-T199678 on the expression of miR-101-3p by qPCR. Overexpressed lncRNA-T199678 significantly downregulated the expression of miR-101-3p (**Figure 5A**), and we constructed a miR-101-3p overexpression cell line (miR-101-3p mimic) to study its role in lncRNA-T199678-mediated α-Syn-induced cell damage (**Figure 5B**).

Overexpression of lncRNA-T199678 Improved Dopaminergic Neuron Activity That Is Affected by α-Syn Through miR-101-3p

Next, we investigated the effect of overexpression of lncRNA-T199678 and miR-101-3p on α-Syn-induced dopaminergic neuron injury. The results showed that the rescue effect of overexpression of lncRNA-T199678 on the damage of dopaminergic neurons induced by α-Syn was halted after co-expression of lncRNA-T199678 and miR-101-3p (**Figures 6**, **7**). Our results indicated that oxidative stress (level of ROS) was significantly enhanced by α-Syn but inhibited after pcT199678 transfection, which was terminally reversed by miR-101-3p mimic (**Figures 6A,B**). Cell cycle redistribution (mitotic catastrophe) (**Figures 7A,B**) and neuron apoptosis (**Figures 7C,D**) were induced by α-Syn but suppressed by overexpression of lncRNA-T199678, but they were both reemerged by a miR-101-3p mimic. It could be concluded that overexpression of lncRNA-T199678 improved α-Syn-damaged neuron activity through miR-101-3p.

DISCUSSION

Researches on PD have attracted a lot of attention, and abnormal accumulation and aggregation of α-Syn are generally considered as the core hallmark of PD pathogenesis (Spillantini et al., 1997); however, the underlying mechanism is still unclear. Accumulating evidences have illuminated that lncRNAs are abnormally expressed in PD and correlated with its pathology (Wu and Kuo, 2020). In the present study, we identified the downregulation of a novel lncRNA-T199678 in the α-Syn-challenged SH-SY5Y cell lines (Lin et al., 2018). This study is conducted to investigate how lncRNA-T199678 affects the α-Syn-induced neuronal damage by regulating miR-101-3p. Collectively, our study revealed that α-Syn mediated neuron injury by downregulation of lncRNA-T199678. Overexpression of lncRNA-T199678 ameliorated the DA neuron injury induced by α-Syn via regulating oxidative stress, cell cycle, and apoptosis. In the mechanism of action of lncRNA, the regulation network of lncRNA–miRNA–mRNA is the most typical regulation mode of lncRNA. Thus, we further explore the lncRNA–miRNA network and found an interaction between lncRNA-T199678 and miR-101-3p. The following study showed that lncRNA-T199678 mediated α-Syn-induced neuron injury via targeting miR-101-3p, which contributes to improving PD. With this study performed, the pathogenesis of PD was further understood; meanwhile, the potential neuroprotective effect and significance of lncRNA-T199678 in PD were explained, providing novel perspectives into PD progression and treatment.

Accumulating evidences have illuminated that lncRNAs have been participated in disrupting mitochondrial function, regulating α-Syn expression and Lewy body formation, mediating apoptosis, and other mechanisms of PD pathogenesis (Lyu et al., 2019). The lncRNA, NEAT1, regulates the transcription of α-Syn, participates in α-Syn-associated apoptosis (Liu and Lu, 2018), and regulates MPP (+)-induced neuronal injury by targeting miR-124 (Xie et al., 2019). The lncRNA, SNHG14, induces dopaminergic neuron injury by regulating α-Syn via targeting miR-133b (Zhang et al., 2019). LncRNA-p21 prevents the targeting of SCNA mRNA, promotes caspase 3 activation, mediates Bcl family-initiated apoptosis, and regulates neuroinflammation via the upregulation of multiple inflammatory cytokines (Xu et al., 2018; Ding et al., 2019). In the MPTP-treated model, lncRNA MALAT1 associated with α-Syn, leading to the increased stability and expression of α-Syn, exhibiting its crucial role in promoting PD progression (Zhang et al., 2016). In our study, the downregulation of

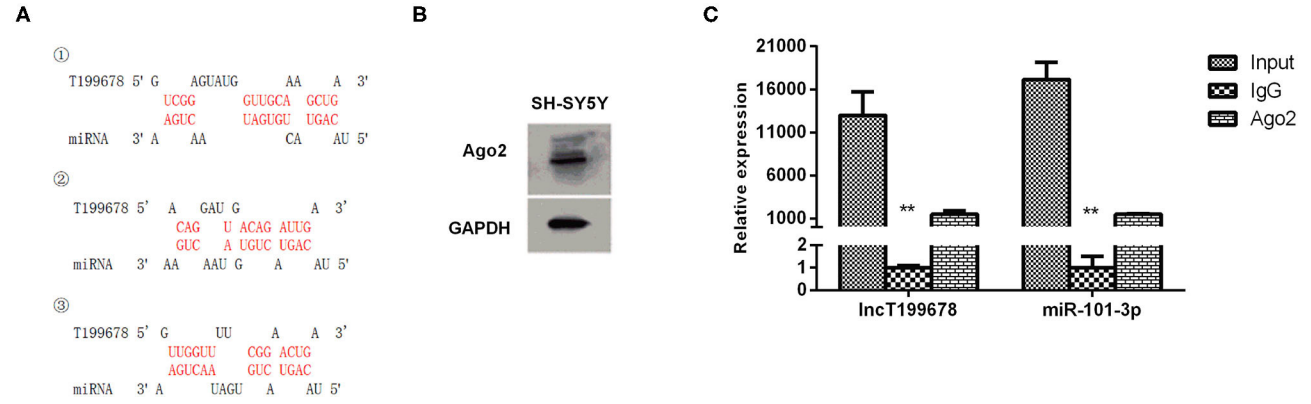


FIGURE 4 | lncRNA-T199678 and miR-101-3p in SH-SY5Y cells. **(A)** The potential-binding sites between lncRNA-T199678 and miR-101-3p were shown. **(B)** The expression of Ago2 in SH-SY5Y cells by Western blot. **(C)** Ago2-RNA immunoprecipitation (RIP) followed by qPCR was conducted to determine lncRNA-T199678 endogenously associated with miR-101-3p (**$P < 0.01$).

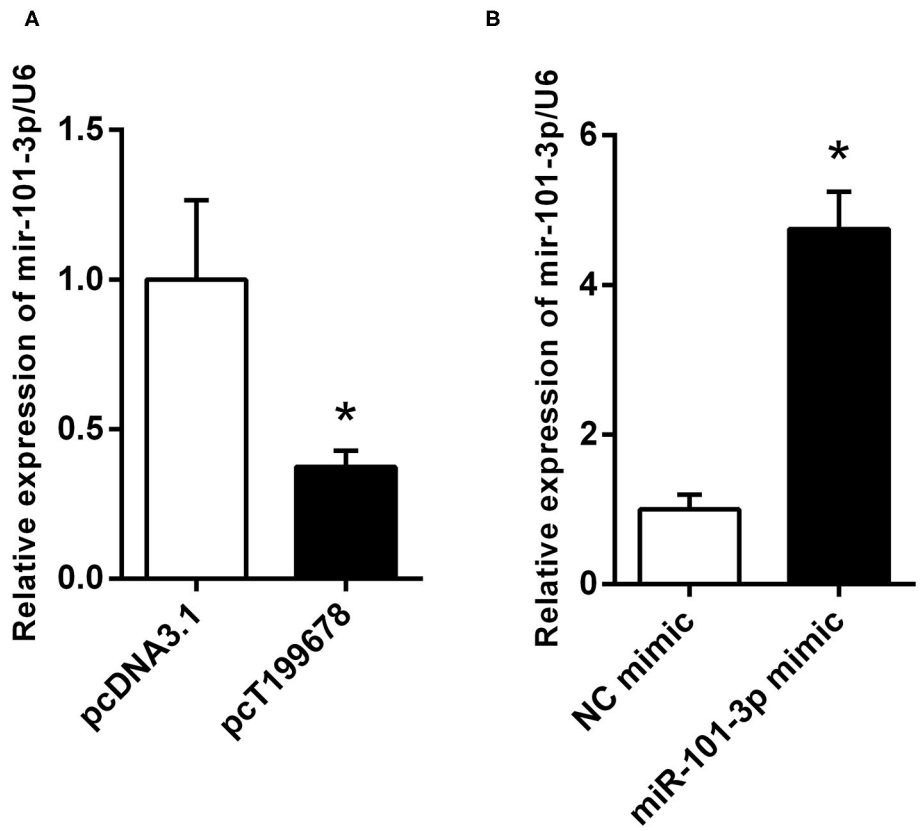


FIGURE 5 | lncRNA-T199678 regulated the expression of miR-101-3p. **(A)** Overexpressed lncRNA-T199678 significantly downregulated the expression of miR-101-3p via qPCR (*$P < 0.05$). **(B)** Construction of overexpressed miR-101-3p in the SH-SY5Y cell line (*$P < 0.05$).

lncRNA-T199678 was identified in the α-Syn-mediated neuron injury, and upregulation of miR-101-3p via binding with lncRNA-T199678 was further involved in the α-Syn-induced dopaminergic neuron injury. It was the first time that the action mechanism of α-Syn was uncovered in PD development by regulating lncRNA-T199678 and the involvement of miR-101-3p in the neuronal injury was also highlighted.

The functions of lncRNAs are closely related to their location. lncRNAs located in the cytoplasm mainly regulate the posttranscription of genes. LncRNAs can directly interact with

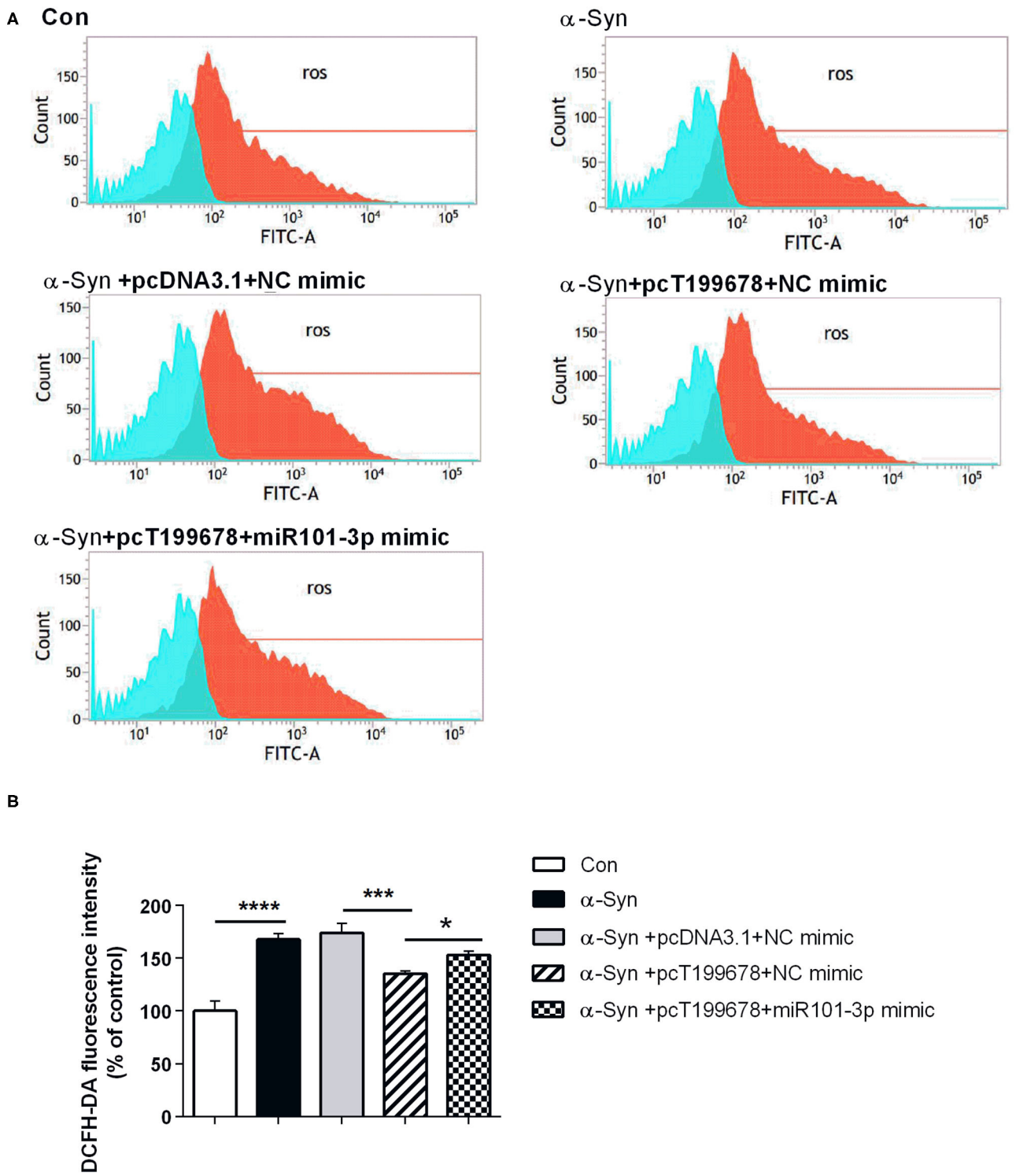


FIGURE 6 | Overexpression of lncRNA-T199678 decreased the ROS production that was affected by α-Syn through miR-101-3p. SH-SY5Y cells were divided into five groups: control (wild type), α-Syn, α-Syn+pcDNA3.1+NC mimic, α-Syn+pcT199678+NC mimic, and α-Syn+pc T199678+ miR-101-3p mimic. **(A)** The oxidative stress (level of ROS) was detected by flow cytometry. **(B)** Fluorescence of DCFH-DA was detected by flow cytometry (one-way ANOVA, $F = 60.30$, df = 14, $P < 0.0001$, followed by Tukey's multiple-comparison tests: control vs. α-Syn, $^{****}P < 0.0001$; α-Syn+pcDNA3.1+NC mimic vs. α-Syn+pcT199678+NC mimic, $^{***}P < 0.001$; α-Syn+pcT199678+NC mimic, α-Syn+pc T199678+ miR-101-3p mimic, $^{*}P < 0.05$).

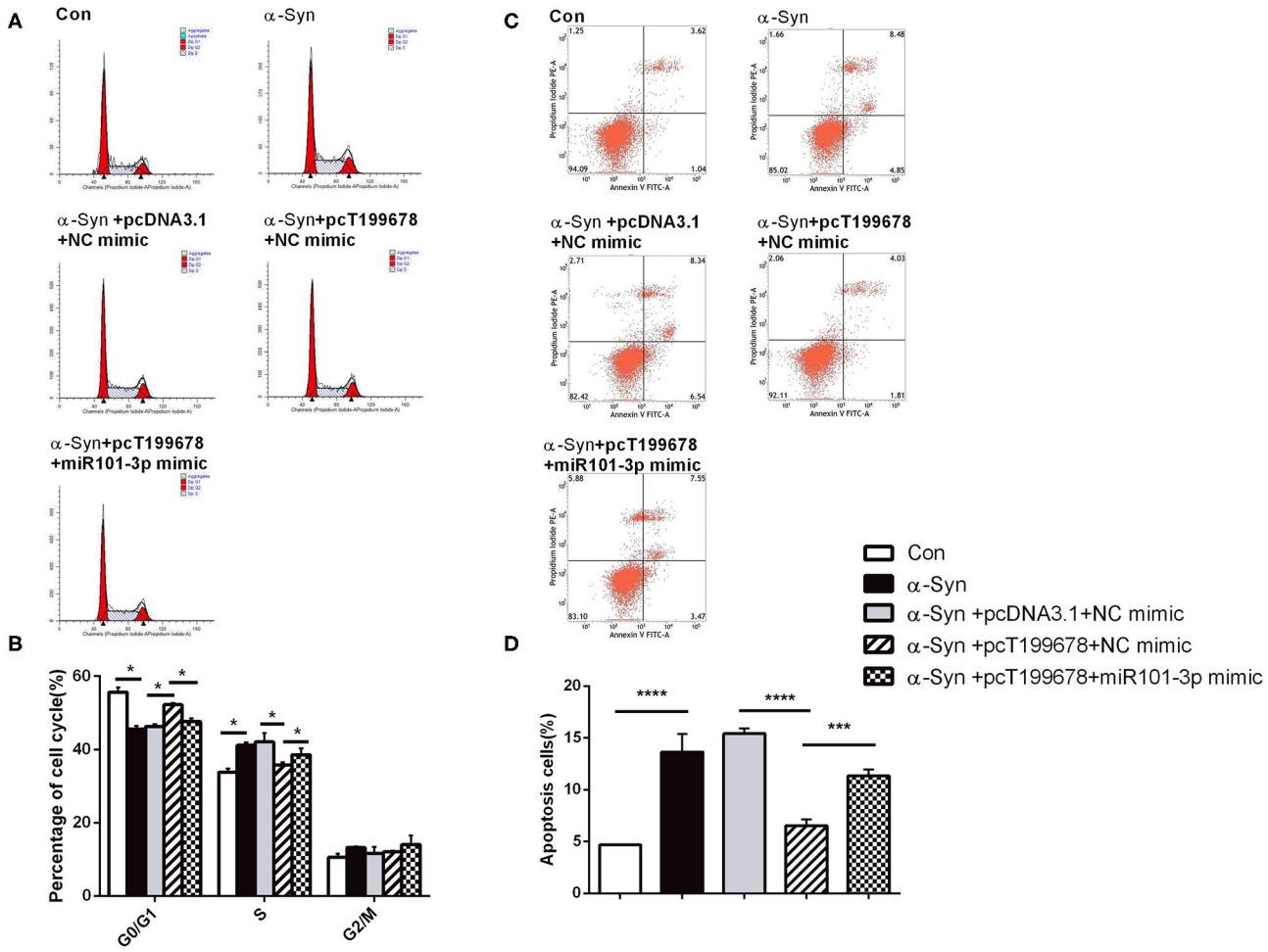


FIGURE 7 | lncRNA-T199678 mitigated α-Syn induced cell cycle abnormality and apoptosis via miR-101-3p**.** SH-SY5Y cells were divided into five groups: control (wild type), α-Syn, α-Syn+pcDNA3.1+NC mimic, α-Syn+pcT199678+NC mimic, and α-Syn+pc T199678+ miR-101-3p mimic. **(A,B)** The proportion of cells in the G0/G1, S, and G2/M phases in cell cycle via flow cytometry (both in the G0/G1 phase and S phase, one-way ANOVA, $P < 0.01$, followed by Tukey's multiple-comparison tests: control vs. α-Syn, $^{*}P < 0.05$; α-Syn+pcDNA3.1+NC mimic vs. α-Syn+pcT199678+NC mimic, $^{*}P < 0.05$; α-Syn+pcT199678+NC mimic, α-Syn+pc T199678+ miR-101-3p mimic, $^{*}P < 0.05$). **(C,D)** Percentage of apoptotic cells was quantified using flow cytometry (one-way ANOVA, $F = 76.52$, df = 14, $P < 0.0001$, followed by Tukey's multiple-comparison tests: control vs. α-Syn, $^{****}P < 0.0001$; α-Syn+pcDNA3.1+NC mimic vs. α-Syn+pcT199678+NC mimic, $^{****}P < 0.0001$; α-Syn+pcT199678+NC mimic, α-Syn+pc T199678+ miR-101-3p mimic,$^{***}P < 0.001$).

mRNA to promote or inhibit mRNA translation by stabilizing or promoting the degradation of mRNA. On the other hand, lncRNAs can also act as precursors of miRNAs or bind with miRNAs to prevent transcriptional inhibition of target genes, resulting in increased expression of target genes. LncRNAs located in the nucleus play their roles mainly through epigenetic regulation of chromatin silencing, transcriptional regulation, and selective splicing of pre-miRNAs (Zhang et al., 2014). Our results showed that most lncRNA-T199678 in the SH-SY5Y cell line were located in the cytoplasm (**Figure 1C**). This demonstrated the direction to explore its function, and the following experiment found miR-101-3p was a potential target for lncRNA-T199678. The etiology of PD has been explained by several hypotheses; loss of dopaminergic neuron is considered one of the most prevalent mechanisms. α-Syn could induce the loss of dopaminergic neurons by different biological processes including oxidative stress, cell cycle regulation, and cell apoptosis. Also, oxidative stress, cell cycle abnormality, and apoptosis are closely related and represent classic, stable, and objective index to reflect the damage of dopaminergic neurons. Pathological α-Syn induces mitochondrial dysfunction, leading to oxidative stress. Meanwhile, ROS can activate ATM, induce DNA damage, and activate the downstream p53 and finally trigger mitochondria-mediated apoptosis. The activation of ATM and DNA damage could drive the cell cycle reinitiation by regulating pRb phosphorylation, and the cell cycle reactivation induces E2F-1 expression and finally mediates cell apoptosis through p53-dependent or non-dependent pathways (Lee et al., 2003; Hoglinger et al., 2007).

Therefore, the alterations of these factors were employed to evaluate the potential function of lncRNA T199678 in the α-Syn-induced cell model. Overexpression of lncRNA-T199678 reversed

the α-Syn-induced oxidative stress, cell cycle abnormality, and apoptosis, suggesting that lncRNA-T199678 may play a protective role in the α-Syn-induced dopaminergic neuron damage. Our results suggested that miR-101-3p was identified as a novel target of lncRNA-T199678, hinting that the function of lncRNA-T199678 may be uncovered in more human diseases related to miR-101-3p. LncRNA-T199678 may act as a ceRNA to regulate the expression of miR-101-3p. Our study illustrated the upregulation of miR-101-3p in neuron injury induced by α-Syn, and lncRNA-T199678 promoted α-Syn-induced oxidative stress, cell cycle abnormality, and apoptosis via miR-101-3p. Previous studies showed that miR-101 significantly increased in the striatum of patients with multiple system atrophy. Overexpression of miR-101 led to the accumulation of α-Syn and autophagy defects in oligodendrocytes (Valera et al., 2017). In the PD model, it was found that lncRNA MiRt2 could inhibit TNF-α-induced inflammatory damage by downregulating miR-101 (Han et al., 2019). Apart from its role in PD, miR-101 has been elucidated as a promoter of apoptosis in a variety of cancer cells (Wang et al., 2018a). Besides, miR-101 could enhance the sensitivity of breast cancer cells to oxidative stress by inhibiting the expression of Nrf2, suggesting its role in the process of oxidative stress (Yi et al., 2019). All of the above have shown that miR-101-3p played a key role in the occurrence and development of a variety of diseases including PD.

From the results, it is clear that the downregulation of lncRNA-T199678 promotes dopaminergic dependent oxidative stress injury in PD by upregulating miR-101-3p. Our study offers new clues for the role of the α-Syn/lncRNA-T199678/miR-101-3p axis in PD and emphasizes a new direction for the clinical treatment of PD. Nevertheless, further studies are still required for better elucidation of the specific mechanism of lncRNA-T199678 on PD. Hopefully, lncRNA-based treatments will someday be realized as new medicines to prevent the onset and extend survival in patients with devastating neurodegenerative diseases like PD.

There are several limitations in this study. The specific target genes and signal pathways of miR-101-3p mediated the cell damage need to be further studied. This kind of uncertainty undoubtedly increases the difficulty of miR-101-3p in identifying specific downstream targets in clinical applications. Further studies are needed to identify the downstream genes and pathways mediated by miR-101-3p. Only bioinformatics methods were used to predict the binding sites of lncRNA-T199678 and miR-101-3p, while the specific binding sites still need to be further verified by experimental studies. Moreover, in this study, only cell models were studied; whether α-Syn mediates dopaminergic neuron injury by downregulating the expression of lncRNA-T199678 remains to be further studied in animal models.

CONCLUSIONS

In conclusion, we clarified that a stable low expression of lncRNA-T199678 in α-Syn induced neuron injury, therefore resulting in increased ROS production, abnormal cell cycle, and apoptosis. Furthermore, we found that lncRNA-T199678 mediated α-Syn-induced neuron damage via upregulating miR-101-3p, which contributes to improving PD pathology. Overexpression of lncRNA-T199678 reversed the damage of α-Syn to the neurons via downregulating miR-101-3p. The downregulation of lncRNA-T199678 may be an important mechanism of exogenous α-Syn-mediated dopaminergic neuron injury. Taken together, our study highlighted the initial target of exogenous α-Syn, and the role of lncRNA-T199678 in PD pathogenesis, and emphasized its regulatory relationship with miR-101-3p, providing a new theoretical hypothesis and foundation for the clinical treatment of PD.

DATA AVAILABILITY STATEMENT

The raw data supporting the conclusions of this article will be made available by the authors, without undue reservation.

AUTHOR CONTRIBUTIONS

E-XT and Y-RL designed the experiments and critically revised the manuscript. Y-YX, D-YL, S-DP, and K-XH performed the experiments. L-LB, YC, and X-NJ analyzed and interpreted the data. L-LB and D-YL wrote the manuscript. All authors have read and approved the final manuscript, contributed to the article, and approved the submitted version.

FUNDING

This work was supported by the National Natural Science Foundation of China (Grant Numbers 81503052, 81571244, 81771378, and 81971195), Natural Science Foundation of Guangdong Province (Grant Numbers 2017A030313840 and 2018A0303130205), Key Field Research and Development Program of Guangdong Province (Grant Number 2018B030337001), Yat-Sen Scholarship for Young Scientists (Grant Number YXQH202020), Key Laboratory of Malignant Tumor Molecular Mechanism and Translational Medicine of Guangzhou Bureau of Science and Information Technology (Grant Number [2013]163), and Key Laboratory of Malignant Tumor Gene Regulation and Target Therapy of Guangdong Higher Education Institutes (Grant Number KLB09001).

REFERENCES

Charvin, D., Medori, R., Hauser, R. A., and Rascol, O. (2018). Therapeutic strategies for Parkinson disease: beyond dopaminergic drugs. *Nat. Rev. Drug Discov.* 17, 804–822. doi: 10.1038/nrd.2018.136

Chen, Q., Huang, X., and Li, R. (2018). lncRNA MALAT1/miR-205-5p axis regulates MPP(+)-induced cell apoptosis in MN9D cells by directly targeting LRRK2. *Am. J. Transl. Res.* 10, 563–572.

Ding, X. M., Zhao, L. J., Qiao, H. Y., Wu, S. L., and Wang, X. H. (2019). Long non-coding RNA-p21 regulates MPP(+)-induced neuronal injury by targeting

miR-625 and derepressing TRPM2 in SH-SY5Y cells. *Chem. Biol. Interact.* 307, 73–81. doi: 10.1016/j.cbi.2019.04.017

Dorsey, E. R., Constantinescu, R., Thompson, J. P., Biglan, K. M., Holloway, R. G., Kieburtz, K., et al. (2007). Projected number of people with Parkinson disease in the most populous nations, 2005 through 2030. *Neurology* 68, 384–386. doi: 10.1212/01.wnl.0000247740.47667.03

Fayyad, M., Salim, S., Majbour, N., Erskine, D., Stoops, E., Mollenhauer, B., et al. (2019). Parkinson's disease biomarkers based on alpha-synuclein. *J. Neurochem.* 150, 626–636. doi: 10.1111/jnc.14809

Fragkouli, A., and Doxakis, E. (2014). miR-7 and miR-153 protect neurons against MPP(+)-induced cell death via upregulation of mTOR pathway. *Front. Cell Neurosci.* 8:182. doi: 10.3389/fncel.2014.00182

Han, Y., Kang, C., Kang, M., Quan, W., Gao, H., and Zhong, Z. (2019). Long non-coding RNA Mirt2 prevents TNF-alpha-triggered inflammation via the repression of microRNA-101. *Int. Immunopharmacol.* 76:105878. doi: 10.1016/j.intimp.2019.105878

Hoglinger, G. U., Breunig, J. J., Depboylu, C., Rouaux, C., Michel, P. P., Alvarez-Fischer, D., et al. (2007). The pRb/E2F cell-cycle pathway mediates cell death in Parkinson's disease. *Proc. Natl. Acad. Sci. U.S.A.* 104, 3585–3590. doi: 10.1073/pnas.0611671104

Kalia, L. V., and Lang, A. E. (2015). Parkinson's disease. *Lancet* 386, 896–912. doi: 10.1016/S0140-6736(14)61393-3

Lee, S. S., Kim, Y. M., Junn, E., Lee, G., Park, K. H., Tanaka, M., et al. (2003). Cell cycle aberrations by alpha-synuclein over-expression and cyclin B immunoreactivity in Lewy bodies. *Neurobiol. Aging* 24, 687–696. doi: 10.1016/S0197-4580(02)00196-3

Lin, D., Liang, Y., Jing, X., Chen, Y., Lei, M., Zeng, Z., et al. (2018). Microarray analysis of an synthetic alpha-synuclein induced cellular model reveals the expression profile of long non-coding RNA in Parkinson's disease. *Brain Res.* 1678, 384–396. doi: 10.1016/j.brainres.2017.11.007

Lin, Q., Hou, S., Dai, Y., Jiang, N., and Lin, Y. (2019). LncRNA HOTAIR targets miR-126-5p to promote the progression of Parkinson's disease through RAB3IP. *Biol. Chem.* 400, 1217–1228. doi: 10.1515/hsz-2018-0431

Liu, Y., and Lu, Z. (2018). Long non-coding RNA NEAT1 mediates the toxic of Parkinson's disease induced by MPTP/MPP+ via regulation of gene expression. *Clin. Exp. Pharmacol. Physiol.* 45, 841–848. doi: 10.1111/1440-1681.12932

Lu, M., Sun, W. L., Shen, J., Wei, M., Chen, B., Qi, Y. J., et al. (2018). LncRNA-UCA1 promotes PD development by upregulating SNCA. *Eur. Rev. Med. Pharmacol. Sci.* 22, 7908–7915. doi: 10.26355/eurrev_201811_16417

Lyu, Y., Bai, L., and Qin, C. (2019). Long noncoding RNAs in neurodevelopment and Parkinson's disease. *Animal Model. Exp. Med.* 2, 239–251. doi: 10.1002/ame2.12093

Ni, Y., Huang, H., Chen, Y., Cao, M., Zhou, H., and Zhang, Y. (2017). Investigation of long non-coding RNA expression profiles in the Substantia Nigra of Parkinson's disease. *Cell Mol. Neurobiol.* 37, 329–338. doi: 10.1007/s10571-016-0373-0

Poewe, W., Seppi, K., Tanner, C. M., Halliday, G. M., Brundin, P., Volkmann, J., et al. (2017). Parkinson disease. *Nat. Rev. Dis. Primers* 3:17013. doi: 10.1038/nrdp.2017.13

Soreq, L., Salomonis, N., Guffanti, A., Bergman, H., Israel, Z., and Soreq, H. (2015). Whole transcriptome RNA sequencing data from blood leukocytes derived from Parkinson's disease patients prior to and following deep brain stimulation treatment. *Genom. Data* 3, 57–60. doi: 10.1016/j.gdata.2014.11.009

Spillantini, M. G., Schmidt, M. L., Lee, V. M., Trojanowski, J. Q., Jakes, R., and Goedert, M. (1997). Alpha-synuclein in Lewy bodies. *Nature* 388, 839–840. doi: 10.1038/42166

Valera, E., Spencer, B., Mott, J., Trejo, M., Adame, A., Mante, M., et al. (2017). MicroRNA-101 modulates autophagy and oligodendroglial alpha-synuclein accumulation in multiple system atrophy. *Front. Mol. Neurosci.* 10:329. doi: 10.3389/fnmol.2017.00329

Wang, C. Z., Deng, F., Li, H., Wang, D. D., Zhang, W., Ding, L., et al. (2018a). MiR-101: a potential therapeutic target of cancers. *Am. J. Transl. Res.* 10, 3310–3321.

Wang, L., Yang, H., Wang, Q., Zhang, Q., Wang, Z., Zhang, Q., et al. (2018b). Paraquat and MPTP induce alteration in the expression profile of long noncoding RNAs in the substantia nigra of mice: role of the transcription factor Nrf2. *Toxicol. Lett.* 291, 11–28. doi: 10.1016/j.toxlet.2018.04.002

Wu, Y. Y., and Kuo, H. C. (2020). Functional roles and networks of non-coding RNAs in the pathogenesis of neurodegenerative diseases. *J. Biomed. Sci.* 27:49. doi: 10.1186/s12929-020-00636-z

Xie, S. P., Zhou, F., Li, J., and Duan, S. J. (2019). NEAT1 regulates MPP(+)-induced neuronal injury by targeting miR-124 in neuroblastoma cells. *Neurosci. Lett.* 708:134340. doi: 10.1016/j.neulet.2019.134340

Xu, X., Zhuang, C., Wu, Z., Qiu, H., Feng, H., and Wu, J. (2018). LincRNA-p21 inhibits cell viability and promotes cell apoptosis in Parkinson's disease through activating alpha-synuclein expression. *Biomed. Res. Int.* 2018:8181374. doi: 10.1155/2018/8181374

Yan, W., Chen, Z. Y., Chen, J. Q., and Chen, H. M. (2018). LncRNA NEAT1 promotes autophagy in MPTP-induced Parkinson's disease through stabilizing PINK1 protein. *Biochem. Biophys. Res. Commun.* 496, 1019–1024. doi: 10.1016/j.bbrc.2017.12.149

Yi, J., Huang, W. Z., Wen, Y. Q., and Yi, Y. C. (2019). Effect of miR-101 on proliferation and oxidative stress-induced apoptosis of breast cancer cells via Nrf2 signaling pathway. *Eur. Rev. Med. Pharmacol. Sci.* 23, 8931–8939. doi: 10.26355/eurrev_201910_19291

Zhang, K., Shi, Z. M., Chang, Y. N., Hu, Z. M., Qi, H. X., and Hong, W. (2014). The ways of action of long non-coding RNAs in cytoplasm and nucleus. *Gene* 547, 1–9. doi: 10.1016/j.gene.2014.06.043

Zhang, L. M., Wang, M. H., Yang, H. C., Tian, T., Sun, G. F., Ji, Y. F., et al. (2019). Dopaminergic neuron injury in Parkinson's disease is mitigated by interfering lncRNA SNHG14 expression to regulate the miR-133b/ alpha-synuclein pathway. *Aging (Albany NY)* 11, 9264–9279. doi: 10.18632/aging.102330

Zhang, Q. S., Wang, Z. H., Zhang, J. L., Duan, Y. L., Li, G. F., and Zheng, D. L. (2016). Beta-asarone protects against MPTP-induced Parkinson's disease via regulating long non-coding RNA MALAT1 and inhibiting alpha-synuclein protein expression. *Biomed. Pharmacother.* 83, 153–159. doi: 10.1016/j.biopha.2016.06.017

Conflict of Interest: The authors declare that the research was conducted in the absence of any commercial or financial relationships that could be construed as a potential conflict of interest.

Copyright © 2020 Bu, Xie, Lin, Chen, Jing, Liang, Peng, Huang and Tao. This is an open-access article distributed under the terms of the Creative Commons Attribution License (CC BY). The use, distribution or reproduction in other forums is permitted, provided the original author(s) and the copyright owner(s) are credited and that the original publication in this journal is cited, in accordance with accepted academic practice. No use, distribution or reproduction is permitted which does not comply with these terms.

frontiers in Aging Neuroscience

ORIGINAL RESEARCH
published: 03 December 2020
doi: 10.3389/fnagi.2020.576682

Aberrant Amplitude of Low-Frequency Fluctuations in Different Frequency Bands in Patients With Parkinson's Disease

Zhaoxiu Wang[1†], Yanjun Liu[2,5†], Xiuhang Ruan[1], Yuting Li[1], E. Li[3], Guoqin Zhang[3], Mengyan Li[4] and Xinhua Wei[1]*

[1] Department of Radiology, Guangzhou First People's Hospital, School of Medicine, South China University of Technology, Guangzhou, China, [2] Institute of Biomedical and Health Engineering, Shenzhen Institutes of Advanced Technology, Chinese Academy of Sciences, Shenzhen, China, [3] Department of Radiology, Guangzhou First People's Hospital, Guangzhou Medical University, Guangzhou, China, [4] Department of Neurology, Guangzhou First People's Hospital, School of Medicine, South China University of Technology, Guangzhou, China, [5] Padova Neuroscience Center (PNC), University of Padova, Padua, Italy

OPEN ACCESS

Edited by:
Zhigang Liu,
Northwest A&F University, China

Reviewed by:
Feng Liu,
Tianjin Medical University General Hospital, China
Gong-Jun Ji,
Anhui Medical University, China
Yu-Feng Zang,
Hangzhou Normal University, China

***Correspondence:**
Xinhua Wei
eyxinhuawei@163.com

[†] These authors have contributed equally to this work and share first authorship

Received: 26 June 2020
Accepted: 26 October 2020
Published: 03 December 2020

Citation:
Wang Z, Liu Y, Ruan X, Li Y, Li E, Zhang G, Li M and Wei X (2020) Aberrant Amplitude of Low-Frequency Fluctuations in Different Frequency Bands in Patients With Parkinson's Disease. Front. Aging Neurosci. 12:576682. doi: 10.3389/fnagi.2020.576682

Previous studies reported abnormal spontaneous neural activity in Parkinson's disease (PD) patients using resting-state functional magnetic resonance imaging (R-fMRI). However, the frequency-dependent neural activity in PD is largely unknown. Here, 35 PD patients and 35 age- and education-matched healthy controls (HCs) underwent R-fMRI scanning to investigate abnormal spontaneous neural activity of PD using the amplitude of low-frequency fluctuation (ALFF) approach within the conventional band (typical band: 0.01–0.08 Hz) and specific frequency bands (slow-5: 0.010–0.027 Hz and slow-4: 0.027–0.073 Hz). Compared with HCs, PD patients exhibited increased ALFF in the parieto-temporo-occipital regions, such as the bilateral inferior temporal gyrus/fusiform gyrus (ITG/FG) and left angular gyrus/posterior middle temporal gyrus (AG/pMTG), and displayed decreased ALFF in the left cerebellum, right precuneus, and left postcentral gyrus/supramarginal gyrus (PostC/SMG) in the typical band. PD patients showed greater increased ALFF in the left caudate/putamen, left anterior cingulate cortex/medial superior frontal gyrus (ACC/mSFG), left middle cingulate cortex (MCC), right ITG, and left hippocampus, along with greater decreased ALFF in the left pallidum in the slow-5 band, whereas greater increased ALFF in the left ITG/FG/hippocampus accompanied by greater decreased ALFF in the precentral gyrus/PostC was found in the slow-4 band (uncorrected). Additionally, the left caudate/putamen was positively correlated with levodopa equivalent daily dose (LEDD), Hoehn and Yahr (HY) stage, and disease duration. Our results suggest that PD is related to widespread abnormal brain activities and that the abnormalities of ALFF in PD are associated with specific frequency bands. Future studies should take frequency band effects into account when examining spontaneous neural activity in PD.

Keywords: resting-state functional MRI, Parkinson's disease, amplitude of low-frequency fluctuation, frequency band, spontaneous brain activity

INTRODUCTION

As one of the most common neurodegenerative disorders, Parkinson's disease (PD) is characterized by motor symptoms, such as resting tremor, bradykinesia, rigidity, postural instability, and non-motor symptoms, including autonomic dysfunction, mood disorders, and cognitive impairments (Herrington et al., 2017). The main neuropathological characteristics of PD are the loss of dopamine neurons in the substantia nigra and the formation of intracellular Lewy inclusion bodies; however, these characteristics do not sufficiently explain the heterogeneity of symptoms and the progression of the disease (Tuovinen et al., 2018). To date, the underlying disease-related neural mechanism has not been completely understood.

Advanced neuroimaging techniques have been extensively employed to explore the neural substrates of neurologic and psychiatric diseases. Positron emission tomography (PET) or single photon emission computed tomography (SPECT) studies have shown that PD patients present abnormal cerebral metabolism in the basal ganglia and some cortical regions (Thobois et al., 2001; Albrecht et al., 2019). Resting-state functional magnetic resonance imaging (R-fMRI) reveals the phenomenon of spontaneous neuronal activity at rest by examining spontaneous fluctuations of the blood oxygen level-dependent (BOLD) signal, providing a reliable measure of baseline brain activity (Gusnard et al., 2001; Fox and Raichle, 2007; Liu et al., 2013). Using R-fMRI, Wu et al. (2011) and Tuovinen et al. (2018) reported PD patients existed abnormal connectivity in the cortico-striato-thalamic loop and cortico-basal-cerebellar connectome in PD patients. As a reliable measure of the magnitude of spontaneous BOLD signals, the amplitude of low-frequency fluctuations (ALFF) has been widely applied to assess spontaneous neural activity related to cerebral physiological and pathological states (Skidmore et al., 2013; Zhang et al., 2015; Wang et al., 2016). Tang et al. (2017) reported decreased ALFF in the bilateral lingual gyrus and left putamen in PD patients compared with healthy controls. Furthermore, a meta-analysis (Pan et al., 2017) reported that the most consistent and replicable findings in PD patients were decreased ALFF in the bilateral supplementary motor areas, left putamen, left premotor cortex, and left inferior parietal gyrus and increased ALFF in the right inferior parietal gyrus.

To date, most ALFF studies in PD have focused on the conventional low-frequency band of 0.01–0.08 Hz (Skidmore et al., 2013; Xiang et al., 2016) because the BOLD signal of this band is thought to reflect spontaneous brain activity (Fox and Raichle, 2007). However, studies have proposed that different frequencies of neural oscillations in the human brain may be sensitive to activity in different regions and can be applied to reflect distinct physiological functions of brain activity (Buzsaki and Draguhn, 2004; Zuo et al., 2010). The frequency spectrum was decomposed into five different frequency bands, including slow-6 (0–0.01 Hz), slow-5 (0.01–0.027 Hz), slow-4 (0.027–0.073 Hz), slow-3 (0.073–0.198 Hz), and slow-2 (0.198–0.25 Hz). Slow-6, slow-3, and slow-2 oscillations were discarded because they mainly reflect very low-frequency drift, white matter signals, and high-frequency physiological noise, whereas slow-4 and slow-5 oscillations primarily correlated with gray matter are beneficial to identify correlations of functional processing and diseases (Salvador et al., 2008; Zuo et al., 2010). Low-frequency oscillations at different frequency bands exhibit different properties and physiological functions (Zuo et al., 2010). Indeed, by examining the ALFF in the slow-4 and slow-5 bands, frequency-dependent brain changes were detected in schizophrenia (Yu et al., 2014), major depressive disorder (Wang et al., 2016), social anxiety disorder (Zhang et al., 2015), and Alzheimer's disease (Liu et al., 2014). By performing an independent validation study, a meta-analysis (Wang et al., 2018) suggested that decreased ALFF in the putamen was the most consistent finding in PD patients and was mainly found in the subfrequency band of slow-4, but the only two original studies (Zhang et al., 2013; Hou et al., 2014) on these subfrequency analyses may have been performed on different medication statuses. These results require further research. The condition of dopaminergic medication was actually unclear in the study of Zhang et al. (2013), whereas another ALFF study of PD in the subfrequency band was definitely performed in the off-medication state (Hou et al., 2014). Dopaminergic drugs have been proven to profoundly modulate the power and coherence of low-frequency oscillations in cortico-striato-thalamic systems (Honey et al., 2003). To our knowledge, no research has investigated the frequency-dependent ALFF in an on-medication state in PD patients to date. It would be necessary to differentiate the frequency bands to examine the ALFF in PD patients in the on-medication state.

We hypothesized that the changes in ALFF in PD are associated with the frequency band. In the current study, we investigated the altered ALFF of PD patients in the on-medication state in the typical band (0.01–0.08 Hz) and further in specific frequency bands (slow-5: 0.01–0.027 Hz; slow-4: 0.027–0.073 Hz). Moreover, correlations between the abnormal ALFF values and clinical measures were also explored. We expected that the characteristics of spontaneous neural activity in PD will be discovered in a specific frequency band.

MATERIALS AND METHODS

Subjects

In this study, we recruited 37 patients diagnosed with PD who were partly overlapped with our previous study focusing on global synchronization (Li et al., 2019) and 36 matched healthy controls (HCs), which was accordant with the normal control in this paper. PD patients were diagnosed according to the clinical criteria of the Movement Disorder Society (MDS) (Postuma et al., 2015). The exclusion criteria for PD patients were as follows: (i) diagnosis uncertain for PD or suspicious of parkinsonism syndrome (vascular, drug-induced, toxin-induced, and postinfectious parkinsonism); (ii) a history of brain surgery (thalamotomy and posteroventral pallidotomy, deep brain stimulation, and organ transplantation); (iii) severe cardiovascular disease, respiratory disease, or severe symptoms of dementia that fail to cooperate; (iv) a pacemaker embedded in the body, which is forbidden in MRI scan. All of the

PD patients received a stable dose of levodopa medication treatment and were in the on-medication state during clinical assessments and MRI data collection. No drug-naïve patients were included in this study. The HC subjects were healthy with no history of neurological disease, no psychiatric illness, and no neuroanatomical abnormalities and were included as Mini-Mental State Exam (MMSE) (Folstein et al., 1975) ≥24. Both PD and HC subjects were enrolled from Guangzhou First People's Hospital. This research was approved by the Institutional Review Board (IRB) of Guangzhou First People's Hospital, and all participants provided written informed consent before the scan.

Clinical Assessments

Clinical assessments (including motor and non-motor symptoms) were measured across all PD patients. The severity of motor symptoms was recorded using the motor part (part III) of the Unified Parkinson's Disease Rating Scale (UPDRS-III) (Goetz et al., 2008), and the severity of PD was evaluated by the Hoehn and Yahr (HY) scale (Hoehn and Yahr, 1998). Higher UPDRS-III scores indicated decreased movement ability. All participants underwent MMSE evaluations to measure general cognitive abilities. The levodopa equivalent daily dose (LEDD) was also collected from all PD patients.

Data Acquisition

All imaging data were obtained using a 3-T MRI scanner (Magnetom Verio, Siemens Healthcare, Erlangen, Germany). Head movement was minimized by using foam padding, and scanner noise was diminished by earplugs. All of the subjects were required to lie quietly and remain awake with their eyes

TABLE 1 | Demographic and clinical characteristics.

	PD (n = 35)	HC (n = 35)	Statistical p-value
Age (years old) (range)	63.31 ± 10.45 (35–90)	59.57 ± 5.94 (47–81)	0.0679
Gender (female/male)	21/14	24/11	NA
Education years	9.94 ± 3.50	11.08 ± 2.84	0.1388
Mean FD (mm)	0.08 ± 0.04	0.09 ± 0.06	0.3556
Disease duration (years)	4.54 ± 4.30	NA	NA
MMSE	25.31 ± 4.46	27.88 ± 2.10	0.0026
HY	2.34 ± 0.74	NA	NA
UPDRS-III	32.00 ± 15.84	NA	NA
LEDD (mg)	459.81 ± 389.56	NA	NA

PD, patients with Parkinson's disease; HC, healthy controls; FD, framewise displacement of Jenkinson; MMSE, Mini-Mental State Examination; HY, Hoehn and Yahr scale; UPDRS-III, part three (motor part) of Unified Parkinson's Disease Rating Scale; LEDD, levodopa equivalent daily dose. Data are presented as mean ± standard deviation. The statistical p-value was obtained by two-sample t-tests with a significance level of $p < 0.05$.

TABLE 2 | Brain regions showing ALFF differences between groups in typical band and the main effect of group.

Brain regions	BA	Cluster size (voxels/mm^3)	MNI coordinates (x y z)	Peak t-value
Typical band (0.01–0.08 Hz)				
R-ITG/FG/ParaHip	20/21/36	74/1,998	63 −9 −27	4.33
L-FG/ITG	20	80/2,160	−33 −12 −30	4.79
L-AG/Pmtg	39/21	60/1,620	−63 −57 21	5.24
L-Cuneus/calcarine	23/17	50/1,350	−18 −60 24	5.20
L-PostC/SMG	48/3	50/1,350	−42 −24 33	−5.11
R-Precuneus	5/7	51/1,377	6 −54 63	−4.89
L-Cerebellum_6	NA	88/2,376	−18 −63 −27	−4.68
Main effect of group (slow-5 and slow-4)				
R-FG/ParaHip	20/36	62/1,674	39 −21 −27	4.09
R-ITG	21/20	55/1,485	63 −9 −27	4.55
L-FG/ITG	20	66/1,782	−36 −9 −39	4.62
L-AG/pMTG	39/21	61/1,647	−63 −57 21	4.99
L-Cuneus/Calcarine	23/17	47/1,269	−18 −60 24	4.94
L-PostC/SMG	48/3	49/1,323	−42 −24 33	−5.46
R-Precuneus	5/7	50/1,350	6 −54 63	−5.03
L-Cerebellum_6	NA	81/2,187	−18 −63 −27	−4.72

BA, Brodmann's area; MNI, Montreal Neurological Institute; L/R, left/right; ITG, inferior temporal gyrus; FG, fusiform gyrus; ParaHip, parahippocampus gyrus; AG, angular gyrus; pMTG, posterior middle temporal gyrus; PostC, postcentral gyrus; SMG, supramarginal gyrus. The results in the typical band were obtained by two-sample t-tests, and the results of main group effects were obtained by two-way repeated-measures ANOVA [GRF corrected, voxel $p < 0.005$, cluster $p < 0.05$, threshold of $t > 2.91$, cluster size >46 voxels (1,242 mm^3)]. Positive (negative) t-value indicates that PD patients had higher (lower) ALFF.

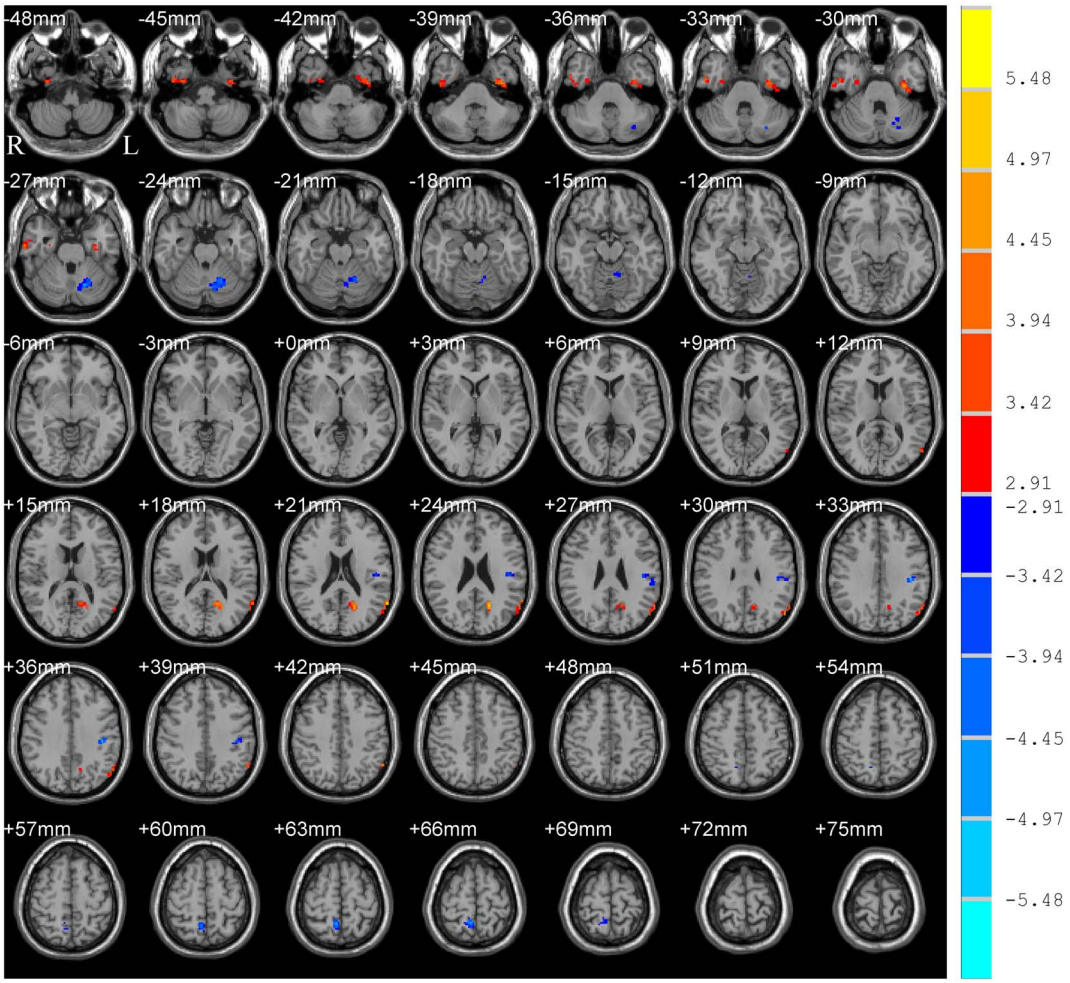


FIGURE 1 | T-map of ALFF differences in the typical band (0.01–0.08 Hz). The results were obtained by two-sample *t*-test [GRF corrected, voxel $p < 0.005$, cluster $p < 0.05$, threshold of $t > 2.91$, and cluster size >46 voxels (1,242 mm^3)]. The color bar on the right indicates statistical *t*-value. Warm (cold) overlays indicate higher (lower) ALFF in PD patients. L/R, left/right.

closed during the whole scanning process. The functional images were obtained using an echo-planar imaging sequence with the following parameters: repetition time (TR) = 2,000 ms, echo time (TE) = 21 ms, flip angle (FA) = 78, matrix size = 64 × 64, slice thickness = 4 mm, pixel spacing = 3.5 mm × 3.5 mm, and field of view (FOV) = 224 mm × 224 mm. After the functional scan, T1-weighted images were acquired with the following parameters: TR = 1,900 ms, TE = 2.22 ms, matrix = 256 × 215, FA = 9, pixel spacing = 0.488 × 0.488, and slice thickness = 1 mm.

Data Preprocessing

All imaging data were preprocessed and analyzed using the toolkits of DPABI[1] and Statistical Parametric Mapping (SPM12)[2] on a MATLAB platform. Preprocessing procedures included the following: (i) removal of the first 10 volumes from 220 volumes to allow the subjects to adapt to the circumstances; (ii) slice timing correction for acquisition delay between slices; (iii) head-motion correction (excessive motion was defined as translation or rotation of >2.5 or 2.5°mm); (iv) regression of nuisance covariates including linear trend, white matter signals, cerebral spinal fluid signal, and Friston-24 parameters of head motions; (v) spatial normalization into the Montreal Neurological Institute (MNI) space by DARTEL (Ashburner, 2007) with a resampled voxel size of 3 × 3 × 3 mm^3; (vi) before smoothing with a 6-mm full width at half maximum Gaussian kernel, data were separately filtered using the typical band (0.01–0.08 Hz), slow-5 band (0.01–0.027 Hz), and slow-4 band (0.027–0.073 Hz).

ALFF Analysis

All voxels were converted from the time domain to the frequency domain using a fast Fourier transform to obtain the power spectrum. Then, the average square root of the power spectrum for each voxel was computed and regarded as ALFF (Zang et al., 2007). For standardization, all ALFF maps were converted into

[1]http://www.rfmri.org/dpabi

[2]http://www.fil.ion.ucl.ac.uk/spm

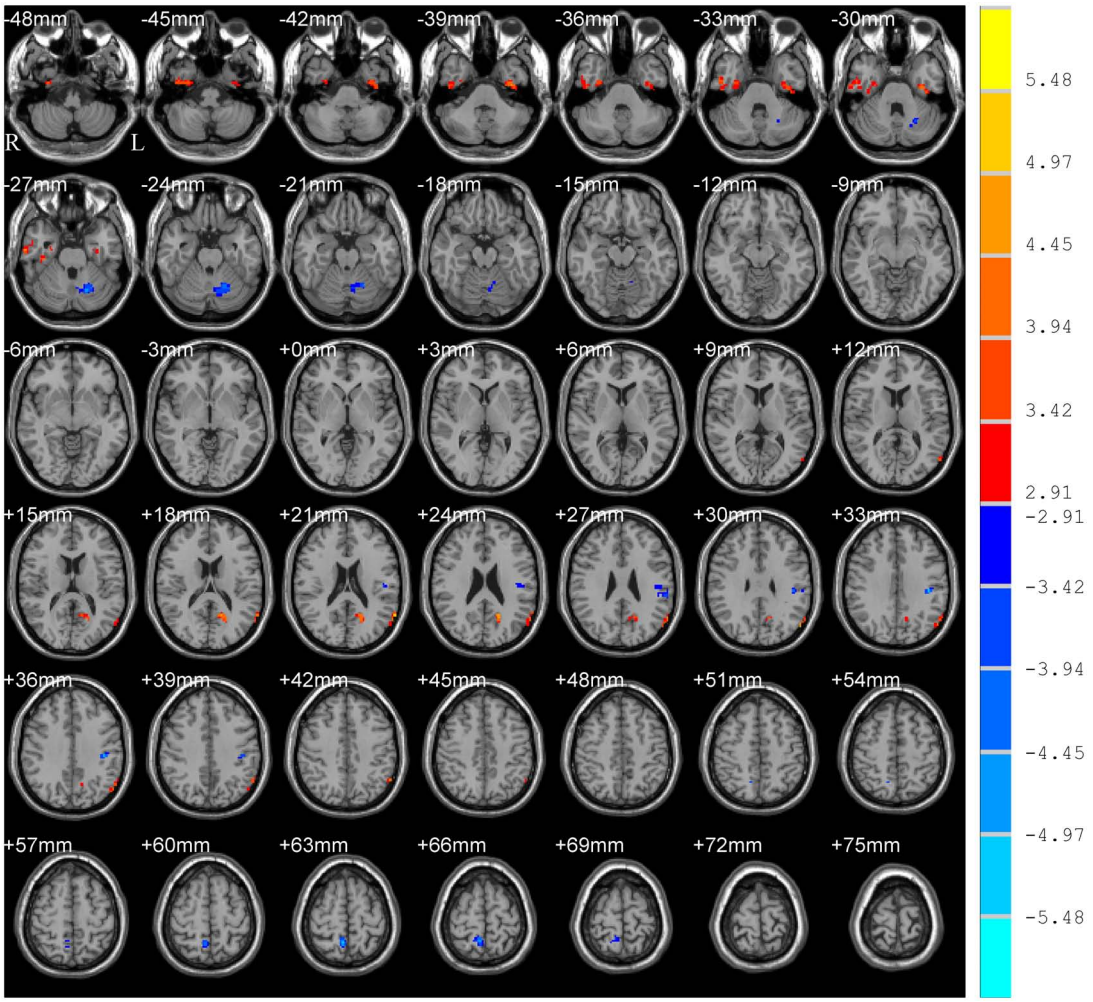


FIGURE 2 | Main effect of group on ALFF. The results were obtained by two-way repeated-measures ANOVA [GRF corrected, voxel $p < 0.005$, cluster $p < 0.05$, threshold of $t > 2.91$, and cluster size >46 voxels (1,242 mm^3)]. The color bar on the right indicates statistical t-value. Warm (cold) overlays indicate higher (lower) ALFF in PD patients. L/R, left/right.

z-maps by subtracting the global mean value and then dividing by the standard deviation. The subsequent statistical and correlative analyses were based on the standardized ALFF maps.

Statistical Analysis

To obtain demographic and clinical characteristics, group differences between the PD and HC groups in age, mean framewise displacement (FD) (Jenkinson et al., 2002), education year, and MMSE scores were analyzed using a two-sample t-test, and $p < 0.05$ was considered statistically significant.

To explore the ALFF differences between two groups, firstly, a two-sample t-test was performed on ALFF maps of a typical band (0.01–0.08 Hz) within gray matter mask (threshold at 20%), with age, gender, and head motions (mean FD) as covariates. Then, mixed effect analysis was performed on two groups and their ALFF of slow-5 and slow-4, by applying two-way repeated-measure analysis of variance (ANOVA) to examine the effects of group and frequency band, with group (PD and HC) serving as a between-subject factor and frequency band (slow-4 and slow-5) as a repeated-measures factor. Furthermore, within the brain regions showing interactions of group and frequency band, *post hoc* two-sample t-tests were performed between PD and HC for slow-5 and slow-4, respectively. Additionally, on account of abnormal ALFF in the caudate/putamen widely reported in previous studies, ANOVA was also examined within the bilateral caudate and putamen, which were extracted from the automated anatomical label (AAL) template. All statistical maps were corrected by Gaussian random field (GRF) with voxel $p < 0.005$ (or $p < 0.05$) and cluster $p < 0.05$.

Brain regions exhibiting significant ALFF differences between the PD and HC were extracted as regions of interest (ROIs). To identify the relationships between the mean ALFF value of these regions and clinical measurements, the Pearson correlation analysis was applied separately, and all correlative results were corrected by the false discovery rate (FDR) with $p < 0.05$.

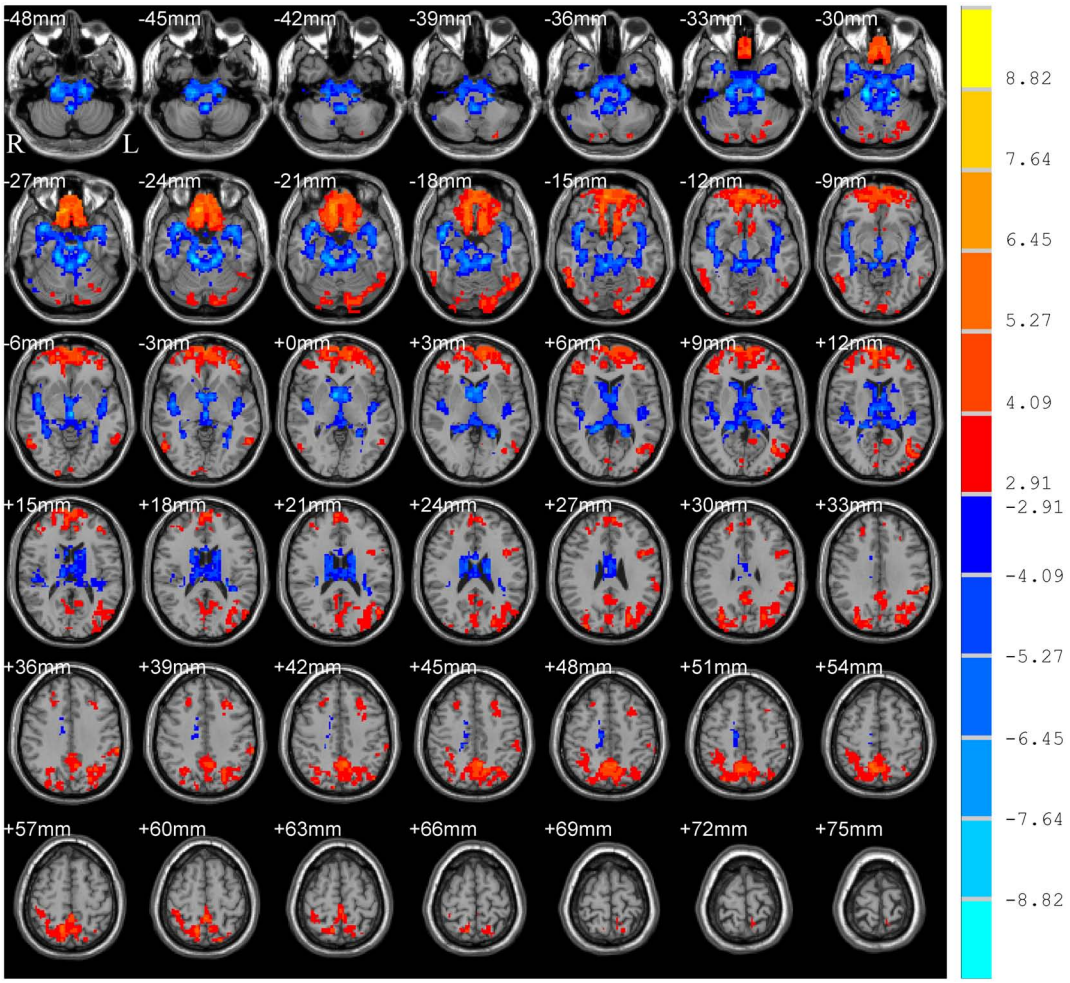


FIGURE 3 | Main effect of frequency band on ALFF. The results were obtained by two-way repeated-measures ANOVA [GRF corrected, voxel $p < 0.005$, cluster $p < 0.05$, threshold of $t > 2.91$, and cluster size >39 voxels (1,053 mm^3)]. The color bar on the right indicates statistical *t*-value. Warm (cold) overlays indicate higher (lower) ALFF in slow-5 band than in slow-4. L/R, left/right.

TABLE 3 | *Post hoc* analysis based on the interaction between group and frequency band.

Brain regions	BA	Cluster size (voxels/mm^3)	MNI coordinates (x y z)	Peak *t*-value
Slow-5 (0.01–0.027 Hz)				
L-Caudate/Putamen	NA	28/756	−18 15 18	4.95
L-ACC/mSFG	32	37/999	−12 51 12	4.11
L-MCC	32	27/729	−12 18 36	3.95
R-ITG	20	27/729	51 −15 −33	4.16
R-ACC	32	23/621	15 42 21	3.28
L-Hippocampus	37	15/405	−30 −36 3	3.72
L-Pallidum	NA	17/459	−24 −6 −3	−5.03
Slow-4 (0.027–0.073 Hz)				
L-ITG/FG/Hippocampus	20	54/1,458	−36 −3 −42	3.72
L-PreC/PostC	6	16/432	−36 0 30	−3.08

The results were obtained by two-way repeated-measures ANOVA ($p < 0.05$, $F > 3.98$, uncorrected) and post hoc two-sample t-test (voxel $p < 0.05$, threshold of $t > 2.00$, uncorrected). BA, Brodmann's area; MNI, Montreal Neurological Institute; L/R, left/right; ACC/MCC, anterior/middle cingulate cortex; mSFG, medial superior frontal gyrus; ITG, inferior temporal gyrus; FG, fusiform gyrus; PreC/PostC, precentral/postcentral gyrus.

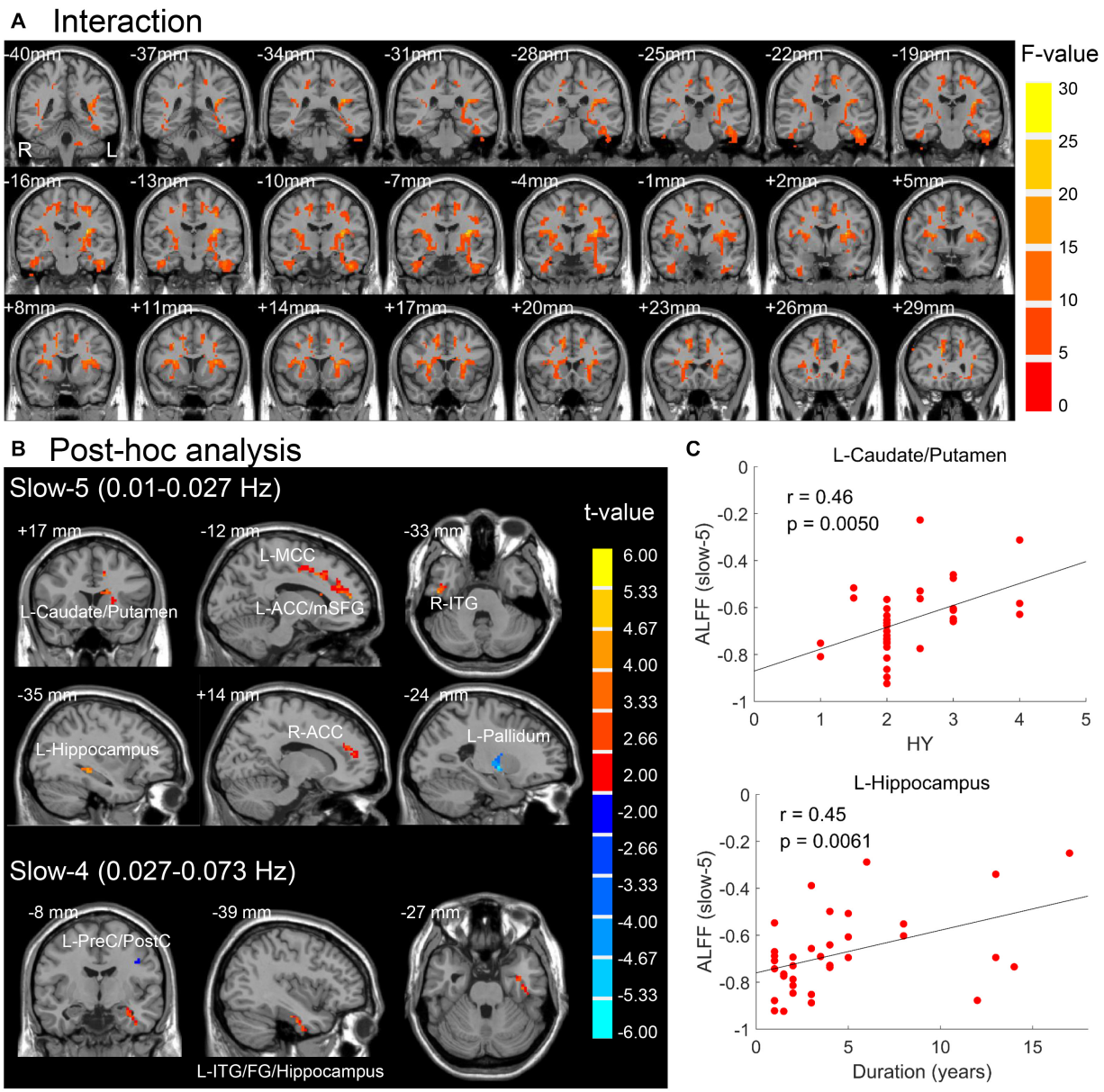


FIGURE 4 | (A) Interaction effect between group and frequency band ($p < 0.05$, $F > 3.98$, uncorrected). **(B)** *Post hoc* two-sample *t*-test for slow-5 and slow-4 (voxel $p < 0.05$, threshold of $t > 2.00$, uncorrected). Warm (cold) overlays indicate higher (lower) ALFF in PD than in HC. **(C)** Significant correlations between mean ALFF of brain regions in panel (**B**) and clinical assessments (FDR corrected, $p < 0.05$). L/R, left/right; ACC/MCC, anterior/middle cingulate cortex; mSFG, medial superior frontal gyrus; ITG, inferior temporal gyrus; FG, fusiform gyrus; PreC/PostC, precentral/postcentral gyrus; HY, Hoehn and Yahr scale.

RESULTS

Demographic and Clinical Data

According to the criteria of excessive head motion mentioned previously, the R-fMRI data from two patients and one control were excluded due to excessive head motion. Demographic and clinical details of the remaining 35 patients and 35 controls are presented in **Table 1**. No significant differences ($p > 0.05$) were observed between the PD and HC groups in age, years of education, and mean head motions (mean FD). As expected, significant group differences in MMSE scores ($p = 0.0026$) were noted. PD patients exhibited lower MMSE scores than did HC subjects.

ALFF Analysis

Significant group differences in typical bands are presented in **Table 2** and **Figure 1**. Compared to HC subjects, the PD patients exhibited significantly increased ALFF in the right inferior temporal gyrus/fusiform gyrus/parahippocampus (ITG/FG/ParaHip), left FG/ITG, left angular gyrus/posterior middle temporal

gyrus (AG/pMTG), and left cuneus/calcarine, accompanied by decreased ALFF in the left postcentral/supramarginal gyrus (PostC/SMG), right precuneus, and left cerebellum.

The main effect of group (PD and HC) is shown in **Table 2** and **Figure 2**, which displayed accordant brain regions reported in typical bands that confirmed the group differences. The main effect of the frequency band (slow-5 and slow-4) is shown in **Figure 3**. Brain regions showing significant increased ALFF in the slow-5 band were identified in the bilateral middle prefrontal cortex, bilateral precuneus/posterior cingulate cortex, bilateral occipital/ITG/MTG, left SMG, and left posterior cerebellum, whereas increased ALFF in the slow-4 band was found in the bilateral superior temporal gyrus/Heschl gyrus, bilateral insula, bilateral caudate, bilateral hippocampus, and bilateral anterior cerebellum. It is obvious that greater ALFF in the slow-5 band was identified in

TABLE 4 | Correlative analysis of clinical assessments.

Brain regions	Frequency band	LEDD		HY		Duration		UPDRS-III		MMSE	
		R	*P*	*r*	*P*	*R*	*P*	*r*	*p*	*R*	*p*
Brain regions of group analysis of typical band											
R-ITG/FG/ParaHip	typical	0.02	0.9275	0.25	0.1521	0.20	0.2523	0.14	0.4299	−0.14	
L-FG/ITG	typical	−0.02	0.9212	0.17	0.3281	0.33	0.0561	0.16	0.3714	−0.12	0.4748
L-AG/pMTG	typical	−0.13	0.4487	−0.23	0.1747	−0.24	0.1628	−0.13	0.4642	0.10	0.5722
L-Cuneus/Calcarine	typical	−0.06	0.7213	−0.05	0.7916	−0.17	0.3219	0.04	0.8115	−0.01	0.9646
L-PostC/SMG	typical	−0.17	0.3360	−0.18	0.2977	−0.22	0.2106	−0.38	0.0250	0.20	0.2577
R-Precuneus	typical	−0.14	0.4162	−0.40	0.0178	−0.26	0.1252	−0.42	0.0128	0.22	0.2014
L-Cerebellum_6	typical	−0.28	0.1076	−0.10	0.5557	−0.05	0.7888	−0.18	0.2985	0.24	0.1629
Brain regions of group effect											
R-FG/ParaHip	slow-5	0.00	0.9906	0.21	0.2293	0.23	0.1794	0.10	0.5670	−0.29	0.0929
	slow-4	−0.09	0.6055	0.13	0.4529	0.18	0.3111	0.04	0.8077	−0.13	0.4537
R-ITG	slow-5	0.16	0.3474	0.26	0.1271	0.18	0.2904	0.29	0.0909	0.11	0.5186
	slow-4	0.10	0.5668	0.26	0.1268	0.00	0.9888	0.22	0.2057	−0.09	0.5901
L-FG/ITG	slow-5	0.10	0.5664	0.29	0.0867	0.43	0.0095	0.30	0.0804	−0.12	0.4814
	slow-4	−0.09	0.6190	0.10	0.5625	0.23	0.1865	0.08	0.6289	−0.10	0.5763
L-AG/pMTG	slow-5	−0.01	0.9554	−0.15	0.3931	−0.10	0.5735	−0.02	0.9111	0.05	0.7619
	slow-4	−0.17	0.3167	−0.25	0.1474	−0.29	0.0886	−0.13	0.4606	0.07	0.6801
L-Cuneus/Calcarine	slow-5	−0.13	0.4695	0.07	0.6835	−0.07	0.6788	0.04	0.7989	−0.03	0.8598
	slow-4	−0.01	0.9463	−0.10	0.5835	−0.20	0.2602	0.07	0.6738	−0.10	0.5570
L-PostC/SMG	slow-5	−0.20	0.2436	−0.30	0.0756	−0.34	0.0444	**−0.50**	**0.0021***	0.21	0.2176
	slow-4	−0.13	0.4435	−0.06	0.7320	−0.13	0.4549	−0.24	0.1587	0.15	0.3746
R-Precuneus	slow-5	−0.11	0.5456	−0.34	0.0482	−0.21	0.2243	−0.37	0.0291	0.35	0.0393
	slow-4	−0.17	0.3333	−0.42	0.0120	−0.28	0.1037	−0.43	0.0109	0.17	0.3312
L-Cerebellum_6	slow-5	−0.28	0.0982	−0.21	0.2263	−0.14	0.4083	−0.24	0.1628	−0.05	0.7851
	slow-4	−0.19	0.2711	−0.01	0.9726	0.12	0.5076	−0.08	0.6558	0.31	0.0716
Brain regions of *post hoc* analysis											
L-Caudate/Putamen	slow-5	0.29	0.0920	**0.46**	**0.0050***	0.40	0.0187	0.22	0.2084	−0.30	0.0793
L-ACC/mSFG	slow-5	−0.09	0.6086	0.13	0.4627	0.31	0.0689	0.19	0.2733	−0.08	0.6303
L-MCC	slow-5	−0.06	0.7503	0.11	0.5235	0.01	0.9364	0.10	0.5696	−0.09	0.6209
R-ITG	slow-5	0.06	0.7396	0.21	0.2312	0.24	0.1736	0.17	0.3382	−0.09	0.6008
R-ACC	slow-5	−0.26	0.1342	0.10	0.5677	0.10	0.5597	0.25	0.1410	0.05	0.7848
L-Hippocampus	slow-5	0.18	0.3070	0.31	0.0746	**0.45**	**0.0061***	0.19	0.2630	−0.01	0.9354
L-Pallidum	slow-5	0.16	0.3707	0.08	0.6543	0.04	0.8197	0.03	0.8511	−0.03	0.8596
L-ITG/FG/Hippocampus	slow-4	0.05	0.7646	0.30	0.0807	0.35	0.0365	0.28	0.1021	−0.07	0.6883
L-PreC/PostC	slow-4	−0.11	0.5126	−0.29	0.0902	−0.33	0.0606	−0.15	0.3963	0.20	0.2493
Bran regions of analysis within bilateral caudate/putamen											
L-Caudate/Putamen	slow-5	**0.37**	**0.0282***	**0.51**	**0.0020***	**0.44**	**0.0081***	0.21	0.2179	−0.23	0.1933
	slow-4	**0.40**	**0.0177***	**0.54**	**0.0008***	**0.44**	**0.0080***	0.24	0.1685	−0.06	0.7201

The meaning of the bold values is equal to "" meaning signiffcant results after correction by false discovery rate (FDR) with $p < 0.05$.*

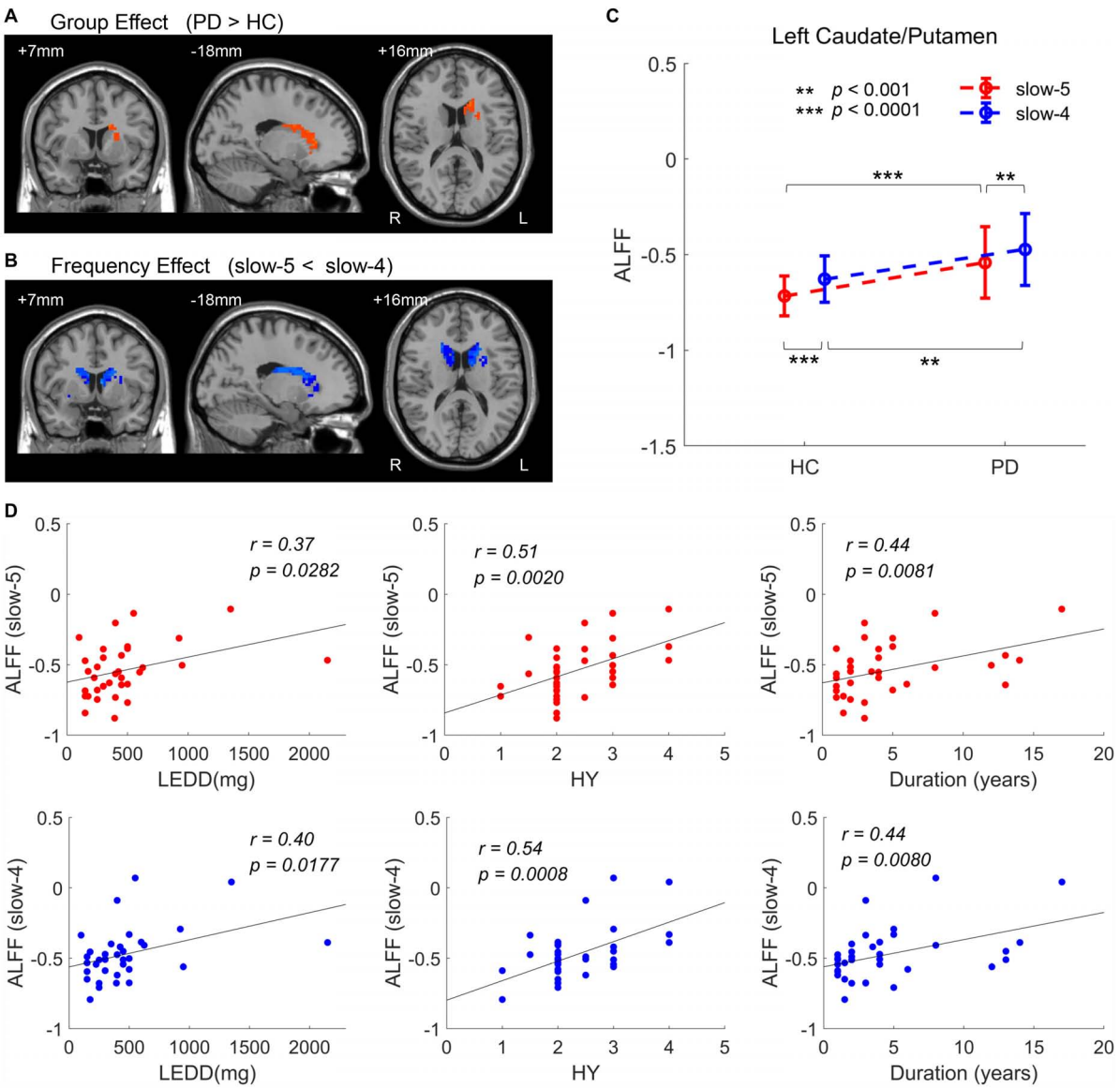


FIGURE 5 | ANOVA within the bilateral caudate/putamen. **(A)** Group effect [GRF corrected, voxel $p < 0.05$, cluster $p < 0.05$, threshold of $t > 2.00$, and cluster size >69 voxels (1,863 mm^3)]. **(B)** Frequency effect [GRF corrected, voxel $p < 0.05$, cluster $p < 0.05$, threshold of $t > 2.00$, and cluster size >50 voxels (1,350 mm^3)]. **(C)** ALFF of two groups within the significant region of group effect, the left caudate/putamen. **(D)** Clinical correlations within the significant region of group effect (the left caudate/putamen) (FDR corrected, $p < 0.05$). L/R, left/right; LEDD, levodopa equivalent daily dose; HY, Hoehn and Yahr scale. $^{**}p < 0.001$, $^{***}p < 0.0001$.

widespread cortical regions, whereas greater ALFF in the slow-4 band was identified mainly in the temporal cortex and subcortical regions.

The brain regions resulted from interactions between frequency band and group on ALFF ($p < 0.05$, $F > 3.98$, uncorrected) are located in the basal ganglia, insula, ITG, FG, hippocampus gyrus, supplementary motor area, anterior and middle cingulate cortex, medial superior frontal gyrus, and cerebellum (**Figure 4A**). After *post hoc* analysis (voxel $p < 0.05$, threshold of $t > 2.00$, uncorrected), the brain regions demonstrating greater increased ALFF in PD patients in the slow-5 band were identified in the left caudate/putamen, left anterior cingulate cortex/medial superior frontal gyrus (ACC/mSFG), left middle cingulate cortex (MCC), right ITG, right ACC, and left hippocampus, along with greater decreased ALFF in left pallidum, whereas accompanied by greater decreased ALFF in the precentral gyrus/PostC, greater increased ALFF of PD was identified in left ITG/FG/hippocampus in the slow-4 band (**Table 3** and **Figure 4B**). The abnormal left caudate/putamen in the slow-5 band was positively correlated with the HY stage, and the left hippocampus was positively correlated with disease duration as shown in **Figure 4C** and **Table 4** ($p < 0.05$, FDR corrected).

Results of analysis within the bilateral caudate/putamen were shown in **Figure 5**. Statistical maps were corrected by GRF with voxel $p < 0.05$ ($t > 2.00$) and cluster $p < 0.05$. Analysis of group effect showed that PD had higher ALFF in the left caudate/putamen (113 voxels, 3,051 mm^3) (**Figure 5A**). Analysis of frequency band effect demonstrated that ALFF of slow-4 was observed to be higher than slow-5 in the bilateral caudate/putamen (516 voxels, 13,932 mm^3) (**Figure 5B**). No significant results were found in the interaction analysis under GRF correction with voxel $p < 0.05$. Additionally, for both the two groups and two frequency bands, ALFF signals were extracted from the left caudate/putamen within which showed a significant group effect, respectively. In addition to the group effect, significantly higher ALFF of slow-4 than that of slow-5 was observed in the two groups in the left caudate/putamen (**Figure 5C**). The ALFF of PD showing a group effect in **Figure 5A** was positively correlated with LEDD, HY stage, and disease duration in both slow-5 and slow-4 bands (**Figure 5D** and **Table 4**). All results of correlation between the abnormal brain regions with the clinical assessments are shown in **Table 4**. Besides the significant correlations mentioned previously, the decreased ALFF in the left PostC/SMG showing a group effect (**Table 2** and **Figure 2**) was negatively correlated with UPDRS-III score ($p < 0.05$, FDR corrected).

DISCUSSION

Using the ALFF method, our study found that compared with the HC group, PD patients exhibited significantly abnormal ALFF in widespread brain regions. Moreover, the abnormal ALFF in some brain areas was different in specific frequency bands. Our results suggest that PD is associated with widespread abnormal brain activities and that the abnormalities are associated with specific frequency bands.

ALFF Differences Between the PD and HC Groups

In this study, we observed increased ALFF in PD patients predominantly in several parieto-temporo-occipital regions, such as ITG/FG and AG/pMTG, which is thought to be crucial to visual and semantic functions (Kravitz et al., 2013; Davey et al., 2015). A study of PD with hallucination (Yao et al., 2015) in the "on" state found that PD patients with or without hallucination exhibited similar increased ALFF in the medial temporal lobe and temporo-parietal gyrus compared with HC, which was consistent with our results. Abnormal regional cerebral blood flow has been observed in the right FG, MTG, and superior temple gyrus in PD patients with visual hallucinations in the on-medication condition (Oishi et al., 2005). However, increased ALFF in some temporal regions (e.g., the left superior temporal gyrus, left ITG, and right FG) was also observed in PD patients in another study, but the medication condition was unclear (Zhang et al., 2015). Although the exact mechanisms underlying these findings are not clear, it is tempting to hypothesize that increased ALFF in these cortices may imply greater neuronal activities at rest and possibly intend to maintain the function or may be related to the therapy of dopamine drugs.

Lower ALFF in the left cerebellum was discovered in our study compared with controls, which was consistent with several R-fMRI studies (Skidmore et al., 2013; Zhang et al., 2013). However, much evidence has demonstrated that hyperactivation in the cerebellum exists in PD patients who withdrew from medication for at least 12 h (Yu et al., 2007; Wu et al., 2010). Generally, pathological impairments should be more severe as disease progresses because dopaminergic degeneration develops gradually (Jankovic, 2005). The major roles of the cerebellum in PD include pathological and compensatory effects. The compensatory effect exists and strengthens at a relatively early stage to maintain relatively motor and non-motor functions. However, as the pathological effects progress gradually, the compensatory effect may diminish or eventually fail at the advanced stage. The decreased ALFF in the cerebellum might be related to dopaminergic medication that weakens the compensatory effect or to serious pathological progression that does not respond to dopaminergic medication.

Similarly, a previously reported decrease in ALFF in the right precuneus and left PostC/SMG (Cavanna and Trimble, 2006; Juenger et al., 2011) that is closely related to cognitive and somatosensory functions was also observed in this study. A study of non-demented PD in the "ON" state showed that cerebral blood flow (CBF) in the precuneus was significantly reduced (Syrimi et al., 2017). Furthermore, precuneus hypoperfusion was identified in a perfusion study of PD with mild cognitive impairment, and reduced precuneus function connectivity in the striatum was further detected in participants' off-medication state (Jia et al., 2018). Diminished activation within the somatosensory cortex has been demonstrated in PD patients; furthermore, dopaminergic medications did not alter the deficient activation of the primary somatosensory cortex (Nelson et al., 2018). It seems that decreased ALFF in the precuneus and somatosensory cortex might be induced by pathological changes in dopaminergic degeneration and was uneasily corrected by dopaminergic medication.

Numerous studies have reported abnormal spontaneous brain activities in some regions important for motor control. A meta-analysis (Pan et al., 2017) showed that decreased ALFFs in the bilateral supplementary motor areas and left premotor cortex were the most consistent and replicable findings related to motor function in PD patients, which were not found in our study. Moreover, it has been proven that spontaneous brain activity deficits in the left premotor cortex, inferior frontal gyrus, and supplementary motor area can been restored after treatment and were no longer different from those in controls (Possin et al., 2013). The normalization of ALFF in the motor areas in this study is likely related to dopaminergic medication.

ALFF Differences Between the Frequency Bands

In this study, the main effect of the frequency band obviously showed that greater ALFF in the slow-5 band was identified in widespread cortical regions, whereas greater ALFF in the slow-4

band was identified mainly in the temporal cortex and subcortical regions. These results are consistent with the frequency effect analysis in other studies (Han et al., 2011; Hou et al., 2014; Liu et al., 2014). The slow-5 band (0.010–0.027 Hz), which has more power, is associated with the integration of large-scale neural networks and long-distance connectivity and localized mainly to the prefrontal, parietal, and occipital cortex, whereas the slow-4 band (0.027–0.073 Hz), which has less power, is linked with more local neural activity and short connections and localized more within the temporal cortex and subcortical structures, such as the thalamus and basal ganglia (Zuo et al., 2010; Baria et al., 2011). The human brain is a complex biological system generating a multitude of oscillatory waves that cover a wide range of frequencies, and the signals within different frequency bands may be derived from distinct oscillators with specific properties and physiological functions (Buzsaki and Draguhn, 2004). However, the origins, relationships, and specific physiological functions of different frequency bands have not be completely clarified to date. Because BOLD oscillations have been proven to directly associate with electroencephalographic signals (He et al., 2008), future work can identify the neurophysiological basis of specific frequency bands by combining R-fMRI with electroencephalographic recordings.

Frequency-Dependent Changes in ALFF in PD Patients

The abnormal ALFF in some brain areas of PD patients (**Table 3** and **Figure 4B**) was detected different in specific frequency bands (uncorrected). Especially, the increased ALFF in the left caudate/putamen was more prominent in the slow-5 band compared with the slow-4 band in our on-medication research. Decreased ALFF in the caudate was observed in the slow-4 band in a study performed in the off-medication state (Hou et al., 2014). Studies related to the specific frequency band of PD are rare, and no exactly consistent and generally accepted results have been detected to date. One brain region may present multiple oscillations belonging to different frequency bands. The inconsistent changes of the brain region within the same frequency band may result from various reasons, such as the heterogeneity in samples and the confounding effect (e.g., ON medication or OFF medication) on results between group comparisons. Research on dopaminergic drug effects has proven that the functional connectivity of the caudate nucleus can be modulated specifically by dopaminergic drugs (Honey et al., 2003). Several previous studies showed that levodopa administration can normalize the activity pattern in PD, including increasing neural activity in the striatum (including the caudate and putamen) (Kraft et al., 2009; Wu et al., 2009). It is likely that in PD, hypoactivation in the striatum as the consequence of disorder progression-related pathological neural changes may be more sensitively explored in the slow-4 band, whereas hyperactivation in the striatum as the neural alterations related to dopaminergic drugs may be more sensitively detected in the slow-5 band. The differences of PD-related activity between frequency bands suggested that the abnormalities in intrinsic brain activity in PD patients were associated with specific frequency bands. The properly chosen frequency band can be helpful to more sensitively explore PD-related neural changes.

Although ANOVA was performed within the gray matter mask, the cluster of the left caudate/putamen seemingly has a low percentage, extending to the white matter of the underlying mask, which was difficult to calculate. Besides pathological changes of neural bodies mainly located in the gray matter or gray matter nuclei, studies have demonstrated that damage to the projecting axons of substantia nigral neurons also happened in PD (Tagliaferro et al., 2015). Most previous studies of low-frequency fluctuation were focused on the gray matter for its postsynaptic potential, whereas Ji et al. (2017) considered that low-frequency BOLD fluctuations in the white matter were also significant and can be used to estimate the dynamic functioning of fiber tracts. Ji et al. (2019) have found decreased structural–functional coupling in the left corticospinal tract, and this tract displayed abnormally increased functional connectivity within the left PostC and left putamen in PD patients. More functional investigation of the white matter may be helpful to understand the pathophysiology of PD.

Correlation Analysis

The left caudate/putamen detected in the slow-5 band as a result from ANOVA and *post hoc* analysis was positively correlated with the HY stage. Moreover, the left caudate/putamen resulting from the group effect of ANOVA in the template of the bilateral caudate/putamen was positively correlated with LEDD, HY stage, and disease duration. These accordant positive correlations indicate that as the disease continues, the course progresses, and the LEDD increases, the neural activity in the left caudate/putamen becomes more intensive. PD is a progressive neurodegenerative disorder caused by the gradual degeneration of dopaminergic nigrostriatal neurons. As the disease continues and the course progresses, the LEDD gradually increases. The striatum and thalamus were thought to be the regions with the most prominent response to levodopa within the cortico-subcortical motor circuit (Kraft et al., 2009). ALFF in the caudate nucleus has also been detected to be positively correlated with the dose of levodopa in an R-fMRI study (Hou et al., 2014). In the on-medication state, it can be easily understood that the positive correlation was mainly attributed to dopaminergic medication in our study.

The negative correlation of the left PostC/SMG with the UPDRS-III score found in our study means that the brain activity of the left PostC/SMG gradually decreased as motor dysfunction worsened. The PostC is a cortical center for somatosensory processing, and abnormalities in this region may be responsible for the disrupted perception of tactile, painful, thermal, and proprioceptive inputs in PD. More importantly, it may superimpose the so-called abnormal background noise on motor function, hampering sensorimotor integration and ultimately resulting in clinical motor symptoms (Conte et al., 2013). Indeed, different from the past understanding, motor symptoms in PD are not purely motor problems now; it has been proven to be associated with types of cognitive impairments (Wojtala et al., 2019). PD subjects have demonstrated diminished activation within the somatosensory cortex, and it was insensitive

to dopaminergic medications (Nelson et al., 2018). A meta-analysis (Ji et al., 2018) found that abnormalities of the PostC were unaffected by medication as well. Overall, the abnormal neural activity in the PostC of PD patients decreases as symptoms progress and has the potential to be used as a biomarker for predicting the severity of PD.

Although the findings of our study are encouraging, several limitations must be addressed. First, the present study was limited by a relatively small sample size. Therefore, the results of the current study should be replicated with a larger sample. Second, although the age was included as a covariate to reduce its effect, age was not well matched between the PD and HC groups because the *p*-value of age is actually not large enough. Third, we were unable to distinguish all the effects of medication on neural activity from progression-related pathological neural change. With further available comparison studies, investigation of PD related to "on" or "off" medication states will be more important.

CONCLUSION

In the present study, we found that PD patients exhibited increased ALFF in many parieto-temporo-occipital regions along with decreased ALFF in the cerebellum and some parietal cortex in a typical band. In particular, we found that the abnormalities of activity in some brain regions, such as the left caudate/putamen, in PD patients are different in specific frequency bands (uncorrected). Our findings suggest that the use of specific frequency bands will be helpful in detecting the neural changes in PD, which should be considered in future works.

DATA AVAILABILITY STATEMENT

The raw data supporting the conclusions of this article will be made available by the authors, without undue reservation.

ETHICS STATEMENT

The studies involving human participants were reviewed and approved by Institutional Review Board (IRB) of Guangzhou First People's Hospital. The patients/participants provided their written informed consent to participate in this study.

AUTHOR CONTRIBUTIONS

ZW wrote the manuscript. ZW, YaL, and XW conceived of the idea and performed the literature review. YuL, ML, and XR performed the data analysis. YuL, EL, and GZ contributed to the data collection. All authors interpreted the results, reviewed the manuscript, and joined the discussion of the manuscript.

FUNDING

This research was partly supported by the National Key Research and Development Plan of China (2019YFC0118805), the National Science Foundation of China (81871846), the Science and Technology Planning Project of Guangzhou (201804010032), the Guangzhou Science and Technology Project of Health (20201A011004), the Featured Clinical Technique of Guangzhou (2019TS46), and the China Scholarship Council.

ACKNOWLEDGMENTS

We are grateful to all participants for their participation in our study.

REFERENCES

Albrecht, F., Ballarini, T., Neumann, J., and Schroeter, M. L. (2019). FDG-PET hypometabolism is more sensitive than MRI atrophy in Parkinson's disease: a whole-brain multimodal imaging meta-analysis. *Neuroimage Clin.* 21:101594. doi: 10.1016/j.nicl.2018.11.004

Ashburner, J. (2007). A fast diffeomorphic image registration algorithm. *Neuroimage* 38, 95–113. doi: 10.1016/j.neuroimage.2007.07.007

Baria, A. T., Baliki, M. N., Parrish, T., and Apkarian, A. V. (2011). Anatomical and functional assemblies of brain BOLD oscillations. *J. Neurosci.* 31, 7910–7919. doi: 10.1523/JNEUROSCI.1296-11.2011

Buzsaki, G., and Draguhn, A. (2004). Neuronal oscillations in cortical networks. *Science* 304, 1926–1929. doi: 10.1126/science.1099745

Cavanna, A. E., and Trimble, M. R. (2006). The precuneus: a review of its functional anatomy and behavioural correlates. *Brain* 129, 564–583. doi: 10.1093/brain/awl004

Conte, A., Khan, N., Defazio, G., Rothwell, J. C., and Berardelli, A. (2013). Pathophysiology of somatosensory abnormalities in Parkinson disease. *Nat. Rev. Neurol.* 9, 687–697. doi: 10.1038/nrneurol.2013.224

Davey, J., Cornelissen, P. L., Thompson, H. E., Sonkusare, S., Hallam, G., Smallwood, J., et al. (2015). Automatic and controlled semantic retrieval: TMS reveals distinct contributions of posterior middle temporal gyrus and angular gyrus. *Neurosci.* 35, 15230–15239. doi: 10.1523/JNEUROSCI.4705-14.2015

Folstein, M. F., Folstein, S. E., and McHugh, P. R. (1975). "Mini-mental state". A practical method for grading the cognitive state of patients for the clinician. *J. Psychiatric Res.* 12, 189–198. doi: 10.1016/0022-3956(75)90026-6

Fox, M. D., and Raichle, M. E. (2007). Spontaneous fluctuations in brain activity observed with functional magnetic resonance imaging. *Nat. Rev. Neurosci.* 8, 700–711. doi: 10.1038/nrn2201

Goetz, C. G., Tilley, B. C., Shaftman, S. R., Stebbins, G. T., Fahn, S., and Martinez-Martin, P. (2008). Movement disorder society-sponsored revision of the Unified Parkinson's Disease Rating Scale (MDS-UPDRS): scale presentation and clinimetric testing results. *Mov. Disord.* 23, 2129–2170. doi: 10.1002/mds.22340

Gusnard, D. A., Raichle, M. E., and Raichle, M. E. (2001). Searching for a baseline: functional imaging and the resting human brain. *Nat. Rev. Neurosci.* 2, 685–694. doi: 10.1038/35094500

Han, Y., Wang, J., Zhao, Z., Min, B., Lu, J., and Li, K. (2011). Frequency-dependent changes in the amplitude of low-frequency fluctuations in amnestic mild cognitive impairment: a resting-state fMRI study. *Neuroimage* 55, 287–295. doi: 10.1016/j.neuroimage.2010.11.059

He, B. J., Snyder, A. Z., Zempel, J. M., Smyth, M. D., and Raichle, M. E. (2008). Electrophysiological correlates of the brain's intrinsic large-scale functional architecture. *Proc. Natl. Acad. Sci. U.S.A.* 105, 16039–16044. doi: 10.1073/pnas.0807010105

Herrington, T. M., Briscoe, J., and Eskandar, E. (2017). Structural and functional network dysfunction in Parkinson Disease. *Radiology* 285, 725–727. doi: 10.1148/radiol.247172401

Hoehn, M. M., and Yahr, M. D. (1998). Parkinsonism: onset, progression, and mortality. 1967. *Neurology* 50, 316–318. doi: 10.1212/wnl.50.2.318

Honey, G. D., Suckling, J., Zelaya, F., Long, C., Routledge, C., and Jackson, S. (2003). Dopaminergic drug effects on physiological connectivity in a human cortico-striato-thalamic system. *Brain* 126, 1767–1781. doi: 10.1093/brain/awg184

Hou, Y., Wu, X., Hallett, M., Chan, P., and Wu, T. (2014). Frequency-dependent neural activity in Parkinson's disease. *Hum. Brain Mapp.* 35, 5815–5833. doi: 10.1002/hbm.22587

Jankovic, J. (2005). Progression of Parkinson disease: are we making progress in charting the course? *Arch. Neurol.* 62, 351–352. doi: 10.1001/archneur.62.3.351

Jenkinson, M., Bannister, P., Brady, M., and Smith, S. (2002). Improved optimization for the robust and accurate linear registration and motion correction of brain images. *Neuroimage* 17, 825–841. doi: 10.1016/s1053-8119(02)91132-8

Ji, G. J., Hu, P., Liu, T. T., Li, Y., Chen, X., and Zhu, C. (2018). Functional connectivity of the corticobasal ganglia-thalamocortical network in parkinson disease: a systematic review and meta-analysis with cross-validation. *Radiology* 287, 973–982. doi: 10.1148/radiol.2018172183

Ji, G. J., Liao, W., Chen, F. F., Zhang, L., and Wang, K. (2017). Low-frequency blood oxygen level-dependent fluctuations in the brain white matter: more than just noise(Article). *Sci. Bull.* 62, 656–657.

Ji, G. J., Ren, C., Li, Y., Sun, J., Liu, T., and Gao, Y. (2019). Regional and network properties of white matter function in Parkinson's disease. *Hum. Brain Mapp.* 40, 1253–1263. doi: 10.1002/hbm.24444

Jia, X., Li, Y., Li, K., Liang, P., and Fu, X. (2018). Precuneus dysfunction in Parkinson's Disease with mild cognitive impairment. *Front. Aging Neurosci.* 10:427. doi: 10.3389/fnagi.2018.00427

Juenger, H., de Haan, B., Krageloh-Mann, I., Staudt, M., and Karnath, H. O. (2011). Early determination of somatosensory cortex in the human brain. *Cereb. Cortex* 21, 1827–1831. doi: 10.1093/cercor/bhq258

Kraft, E., Loichinger, W., Diepers, M., Lule, D., Schwarz, J., and Ludolph, A. C. (2009). Levodopa-induced striatal activation in Parkinson's disease: a functional MRI study. *Parkinsonism Relat. Disord.* 15, 558–563. doi: 10.1016/j.parkreldis.2009.02.005

Kravitz, D. J., Saleem, K. S., Baker, C. I., Ungerleider, L. G., and Mishkin, M. (2013). The ventral visual pathway: an expanded neural framework for the processing of object quality. *Trends Cogn. Sci.* 17, 26–49. doi: 10.1016/j.tics.2012.10.011

Li, M., Liu, Y., Chen, H., Hu, G., Yu, S., and Ruan, X. (2019). altered global synchronizations in patients with Parkinson's disease: a resting-state fMRI study. *Front. Aging Neurosci.* 11:139. doi: 10.3389/fnagi.2019.00139

Liu, F., Guo, W., Liu, L., Long, Z., Ma, C., and Xue, Z. (2013). Abnormal amplitude low-frequency oscillations in medication-naive, first-episode patients with major depressive disorder: a resting-state fMRI study. *J. Affect. Disord.* 146, 401–406. doi: 10.1016/j.jad.2012.10.001

Liu, X., Wang, S., Zhang, X., Wang, Z., Tian, X., and He, Y. (2014). Abnormal amplitude of low-frequency fluctuations of intrinsic brain activity in Alzheimer's disease. *J. Alzheimers Dis.* 40, 387–397. doi: 10.3233/JAD-131322

Nelson, A. J., Hoque, T., Gunraj, C., and Chen, R. (2018). Altered somatosensory processing in Parkinson's disease and modulation by dopaminergic medications. *Parkinsonism Relat. Disord.* 53, 76–81. doi: 10.1016/j.parkreldis.2018.05.002

Oishi, N., Udaka, F., Kameyama, M., Sawamoto, N., Hashikawa, K., and Fukuyama, H. (2005). Regional cerebral blood flow in Parkinson disease with nonpsychotic visual hallucinations. *Neurology* 65, 1708–1715. doi: 10.1212/01.wnl.0000187116.13370.e0

Pan, P., Zhang, Y., Liu, Y., Zhang, H., Guan, D., and Xu, Y. (2017). Abnormalities of regional brain function in Parkinson's disease: a meta-analysis of resting state functional magnetic resonance imaging studies. *Sci. Rep.* 7:40469. doi: 10.1038/srep40469

Possin, K. L., Kang, G. A., Guo, C., Fine, E. M., Trujillo, A. J., and Racine, C. A. (2013). Rivastigmine is associated with restoration of left frontal brain activity in Parkinson's disease. *Mov. Disord.* 28, 1384–1390. doi: 10.1002/mds.25575

Postuma, R. B., Berg, D., Stern, M., Poewe, W., Olanow, C. W., and Oertel, W. (2015). MDS clinical diagnostic criteria for Parkinson's disease. *Mov. Disord.* 30, 1591–1601. doi: 10.1002/mds.26424

Salvador, R., Martinez, A., Pomarol-Clotet, E., Gomar, J., Vila, F., and Sarro, S. (2008). A simple view of the brain through a frequency-specific functional connectivity measure. *Neuroimage* 39, 279–289. doi: 10.1016/j.neuroimage.2007.08.018

Skidmore, F. M., Yang, M., Baxter, L., von Deneen, K. M., Collingwood, J., and He, G. (2013). Reliability analysis of the resting state can sensitively and specifically identify the presence of Parkinson disease. *Neuroimage* 75, 249–261. doi: 10.1016/j.neuroimage.2011.06.056

Syrimi, Z. J., Vojtisek, L., Eliasova, I., Viskova, J., Svatkova, A., and Vanicek, J. (2017). Arterial spin labelling detects posterior cortical hypoperfusion in non-demented patients with Parkinson's disease. *J. Neural Transm.* 124, 551–557. doi: 10.1007/s00702-017-1703-1

Tagliaferro, P., Kareva, T., Oo, T. F., Yarygina, O., Kholodilov, N., and Burke, R. E. (2015). An early axonopathy in a hLRRK2(R1441G) transgenic model of Parkinson disease. *Neurobiol. Di.* 82, 359–371. doi: 10.1016/j.nbd.2015.07.009

Tang, Y., Meng, L., Wan, C. M., Liu, Z. H., Liao, W. H., and Yan, X. X. (2017). Identifying the presence of Parkinson's disease using low-frequency fluctuations in BOLD signals. *Neurosci. Lett.* 645, 1–6. doi: 10.1016/j.neulet.2017.02.056

Thobois, S., Guillouet, S., and Broussolle, E. (2001). Contributions of PET and SPECT to the understanding of the pathophysiology of Parkinson's disease. *Neurophysiol. Clin. -Clin. Neurophysiol.* 31, 321–340. doi: 10.1016/s0987-7053(01)00273-8

Tuovinen, N., Seppi, K., de Pasquale, F., Muller, C., Nocker, M., and Schocke, M. (2018). The reorganization of functional architecture in the early-stages of Parkinson's disease. *Parkinsonism Relat. Disord.* 50, 61–68. doi: 10.1016/j.parkreldis.2018.02.013

Wang, J., Zhang, J. R., Zang, Y. F., and Wu, T. (2018). Consistent decreased activity in the putamen in Parkinson's disease: a meta-analysis and an independent validation of resting-state fMRI. *GigaScience* 7:giy071. doi: 10.1093/gigascience/giy071

Wang, L., Kong, Q., Li, K., Su, Y., Zeng, Y., and Zhang, Q. (2016). Frequency-dependent changes in amplitude of low-frequency oscillations in depression: a resting-state fMRI study. *Neurosci. Lett.* 614, 105–111. doi: 10.1016/j.neulet.2016.01.012

Wojtala, J., Heber, I. A., Neuser, P., Heller, J., Kalbe, E., and Rehberg, S. P. (2019). Cognitive decline in Parkinson's disease: the impact of the motor phenotype on cognition. *J. Neurol. Neurosurg. Psychiatry* 90, 171–179. doi: 10.1136/jnnp-2018-319008

Wu, T., Long, X., Zang, Y., Wang, L., Hallett, M., and Li, K. (2009). Regional homogeneity changes in patients with Parkinson's disease. *Hum. Brain Mapp.* 30, 1502–1510. doi: 10.1002/hbm.20622

Wu, T., Wang, L., Hallett, M., Chen, Y., Li, K., and Chan, P. (2011). Effective connectivity of brain networks during self-initiated movement in Parkinson's disease. *Neuroimage* 55, 204–215. doi: 10.1016/j.neuroimage.2010.11.074

Wu, T., Wang, L., Hallett, M., Li, K., and Chan, P. (2010). Neural correlates of bimanual anti-phase and in-phase movements in Parkinson's disease. *Brain* 133, 2394–2409. doi: 10.1093/brain/awq151

Xiang, J., Jia, X., Li, H., Qin, J., Liang, P., and Li, K. (2016). Altered spontaneous brain activity in cortical and subcortical regions in Parkinson's Disease. *Parkinsons Dis.* 2016:5246021. doi: 10.1155/2016/5246021

Yao, N., Pang, S., Cheung, C., Chang, R. S., Lau, K. K., and Suckling, J. (2015). Resting activity in visual and corticostriatal pathways in Parkinson's disease with hallucinations. *Parkinsonism Relat. Disord.* 21, 131–137. doi: 10.1016/j.parkreldis.2014.11.020

Yu, H., Sternad, D., Corcos, D. M., and Vaillancourt, D. E. (2007). Role of hyperactive cerebellum and motor cortex in Parkinson's disease. *Neuroimage* 35, 222–233. doi: 10.1016/j.neuroimage.2006.11.047

Yu, R., Chien, Y. L., Wang, H. L., Liu, C. M., Liu, C. C., and Hwang, T. J. (2014). Frequency-specific alternations in the amplitude of low-frequency fluctuations in schizophrenia. *Hum. Brain Mapp.* 35, 627–637. doi: 10.1002/hbm.22203

Zang, Y. F., He, Y., Zhu, C. Z., Cao, Q. J., Sui, M. Q., and Liang, M. (2007). Altered baseline brain activity in children with ADHD revealed by resting-state functional MRI. *Brain Dev.* 29, 83–91. doi: 10.1016/j.braindev.2006.07.002

Zhang, J., Wei, L., Hu, X., Zhang, Y., Zhou, D., and Li, C. (2013). Specific frequency band of amplitude low-frequency fluctuation predicts Parkinson's disease. *Behav. Brain Res.* 252, 18–23. doi: 10.1016/j.bbr.2013.05.039

Zhang, Y., Zhu, C., Chen, H., Duan, X., Lu, F., and Li, M. (2015). Frequency-dependent alterations in the amplitude of low-frequency fluctuations in social anxiety disorder. *J. Affect. Disord.* 174, 329–335. doi: 10.1016/j.jad.2014.12.001

Zuo, X. N., Di Martino, A., Kelly, C., Shehzad, Z. E., Gee, D. G., and Klein, D. F. (2010). The oscillating brain: complex and reliable. *Neuroimage* 49, 1432–1445. doi: 10.1016/j.neuroimage.2009.09.037

Conflict of Interest: The authors declare that the research was conducted in the absence of any commercial or financial relationships that could be construed as a potential conflict of interest.

Copyright © 2020 Wang, Liu, Ruan, Li, Li, Zhang, Li and Wei. This is an open-access article distributed under the terms of the Creative Commons Attribution License (CC BY). The use, distribution or reproduction in other forums is permitted, provided the original author(s) and the copyright owner(s) are credited and that the original publication in this journal is cited, in accordance with accepted academic practice. No use, distribution or reproduction is permitted which does not comply with these terms.

frontiers in Aging Neuroscience

REVIEW
published: 21 December 2020
doi: 10.3389/fnagi.2020.610581

Regulatory Roles of Bone in Neurodegenerative Diseases

Zhengran Yu[1†], Zemin Ling[1†], Lin Lu[2†], Jin Zhao[2], Xiang Chen[2], Pingyi Xu[2] and Xuenong Zou[1*]*

[1]Guangdong Provincial Key Laboratory of Orthopaedics and Traumatology, Orthopaedic Research Institute/Department of Spine Surgery, The First Affiliated Hospital of Sun Yat-sen University, Guangzhou, China, [2]Department of Neurology, The First Affiliated Hospital of Guangzhou Medical University, Guangzhou, China

Osteoporosis and neurodegenerative diseases are two kinds of common disorders of the elderly, which often co-occur. Previous studies have shown the skeletal and central nervous systems are closely related to pathophysiology. As the main structural scaffold of the body, the bone is also a reservoir for stem cells, a primary lymphoid organ, and an important endocrine organ. It can interact with the brain through various bone-derived cells, mostly the mesenchymal and hematopoietic stem cells (HSCs). The bone marrow is also a place for generating immune cells, which could greatly influence brain functions. Finally, the proteins secreted by bones (osteokines) also play important roles in the growth and function of the brain. This article reviews the latest research studying the impact of bone-derived cells, bone-controlled immune system, and bone-secreted proteins on the brain, and evaluates how these factors are implicated in the progress of neurodegenerative diseases and their potential use in the diagnosis and treatment of these diseases.

Keywords: bone, bone marrow, neurodegenerative diseases, mesenchymal stem cells, immune, osteokines

OPEN ACCESS

Edited by:
Daniel Ortuño-Sahagún, University of Guadalajara, Mexico

Reviewed by:
Michele D'Angelo, University of L'Aquila, Italy
Vanessa Castelli, University of L'Aquila, Italy

***Correspondence:**
Xuenong Zou
zxnong@hotmail.com; zouxuen@mail.sysu.edu.cn
Pingyi Xu
pingyixu@sina.com

†These authors have contributed equally to this work

Received: *26 September 2020*
Accepted: *24 November 2020*
Published: *21 December 2020*

Citation:
Yu Z, Ling Z, Lu L, Zhao J, Chen X, Xu P and Zou X (2020) Regulatory Roles of Bone in Neurodegenerative Diseases. Front. Aging Neurosci. 12:610581. doi: 10.3389/fnagi.2020.610581

INTRODUCTION

Neurodegenerative diseases are characterized by the gradual loss of structure and function of selectively vulnerable neurons in different regions of the brain, affecting millions of people worldwide. Neurodegenerative disorders can be clinically identified by their representative features, mostly exhibiting extrapyramidal and/or pyramidal movement disorders, cognitive or behavioral disorders. Most patients suffer multiple clinical symptoms rather than pure phenotype (Dugger and Dickson, 2017). The related mechanism of neurodegenerative diseases has been studied. For example, the most common kind of dementia worldwide, Alzheimer's disease (AD), is pathologically characterized by the extracellular amyloid-β (Aβ) peptides accumulation in senile plaques and the formation of intracytoplasmic neurofibrillary tangles in the brain (Querfurth and LaFerla, 2010; Livingston et al., 2017). And Parkinson's disease (PD) is characterized by loss of dopaminergic neurons and insufficient synthesis of dopamine in the substantia nigra (SN) area (Dauer and Przedborski, 2003; Maiti et al., 2017), and the accumulation of intracytoplasmic α-synuclein polymers (Lewy bodies) in the brain (Goldman et al., 1983). Multiple sclerosis (MS) which shows both neuroinflammatory and neurodegenerative characteristics had been found it results from chronic demyelinating of the central nervous system (CNS; Compston and Coles, 2008). For the majority of MS patients (85–90%), tissue damage is more caused by inflammation rather than neuronal degeneration in the first 5–12 years of onset, whereas the balance between

inflammatory response and neuronal degeneration shifts to the latter at the secondary stage of progression. However, for a minor proportion of MS patients (10–15%), neuronal degeneration plays a major role throughout the disease (Steinman, 2009).

With the increasing trend of social aging, neurodegenerative diseases and osteoporosis have become severe social issues. The bone-related effect in neurodegenerative diseases has so far gained an increased awareness of several epidemiological findings. A meta-analytic study showed that compared with healthy controls, AD patients have a lower hip bone mineral density and are more likely to suffer from hip fractures (Zhao Y. et al., 2012). Also, osteoporosis is regarded as a risk factor for AD, since osteoporosis correlates with the cognitive deficit and its severity in adults older than 50 (Zhou et al., 2011; Kang et al., 2018). Many PD patients have compulsory trunk scoliosis, known as Pisa syndrome, which causes severe late complications of disability (Poewe et al., 2017). In a more common scenario, AD or PD patients suffer from bone fracture, osteoarthritis, restricted movement, bed ulcer, and even death caused by severe osteoporosis. Osteoporosis and an abnormal amount of bone-derived factors in turn promote the progression of AD and PD, especially in women over 60 years old (Yuan et al., 2019).

Bone is a multifaceted, dynamic tissue, which participated in movement facilitation, mineral metabolism, immune cell generation, and mesenchymal stem cells (MSCs) or hematopoietic stem cells (HSCs) breading. Since the bone marrow (BM) contains enormous amounts of MSCs and serves as the primary lymphoid organ, both of which have already been proved to have effects on the brain by many studies, the significance of bone in the regulation of CNS homeostasis is un-doubtable. Moreover, some hormones or "osteokines" from bone cells such as osteocalcin (OCN), osteopontin (OPN), and fibroblast growth factor (FGF) 23 have endocrine functions (Vervloet et al., 2014; Han Y. et al., 2018). These proteins can act on the brain directly or indirectly by regulating phosphate homeostasis or systemic energy metabolism (Han Y. et al., 2018; Yuan et al., 2019). This review aims to clarify the inter-relationship between the bone and brain and to discuss its potential therapeutic implications for neurodegenerative diseases.

BM-DERIVED CELLS

The bone organ consists of bone and Bone marrow(BM), both of which function as a single unit (Compston, 2002). BM is a soft and viscous tissue enclosed within the bone cortex, containing HSCs and MSCs. HSCs are responsible for producing blood cells, including leukocytes, monocytes, erythrocytes, and platelets, while MSCs are contributed to osteoclasts and osteoblasts' origination. These stem cells are tightly involved in the neurodegenerative progressions. Transplantation of young BM can rejuvenate the hematopoietic system and preserve cognitive function in old recipient mice, suggesting the beneficial effects of BM to the brain (Castellano et al., 2015; Das et al., 2019). Several pathways are contributed to the beneficial effects such as these BM-derived cells migrating directly into the brain to exert their toxicant clearance, immuno-modulative and neuro-generative functions, or *via* secreting exosomes to enter the brain and execute their biological functions (Soulet and Rivest, 2008; Dennie et al., 2016; Nakano et al., 2016; Han K. H. et al., 2018; **Figure 1**).

BM-Derived Microglia-Like Cells

Microglia are the primary immune effector cells in the CNS. These cells are monocytes that originated from mesodermal that invade the developing CNS in the embryonic period when the blood-brain barrier (BBB) is not fully formed. In addition to the primary resident microglia, another type of microglia that originates from precursors cells in the BM has been identified in the brain (Soulet and Rivest, 2008). To distinguish them from the originally brain-resident microglia cells, microglial cells originating from the outside of the brain are referred to as "microglia-like cells" (Han K. H. et al., 2018). Although BM-derived microglia-like cells can enter the CNS under normal physiological conditions, they are preferentially presented in regions suffering from neurodegeneration or exogenous insults (Soulet and Rivest, 2008). In the case of ischemic stroke, peripheral monocytes can migrate into the brain at the injury site and differentiate into ramified microglial-like cells (Priller et al., 2001a,b; Soulet and Rivest, 2008). This is even true for facial nerve axotomy and hypoglossal nerve axotomy models, in both cases the mouse models' BBBs are not damaged (Priller et al., 2001a,b; Soulet and Rivest, 2008). *In vitro* studies showed Aβ-eliminating microglia-like cells could be differentiated from the BM-derived HSCs (Kuroda et al., 2020b) monocyte (Simard et al., 2006) and CD11b- or CD115-positive cells (Lebson et al., 2010; Koronyo et al., 2015). Further mechanism study showed that cells from the human and mouse BM can become microglia-like cells under the stimulation of colony-stimulating factor-1 (Kuroda et al., 2020a). An *in vivo* study showed that BM-derived microglia-like cells can move through the BBB and accumulate inside the brain in a CCR2 chemokine-dependent manner (El Khoury and Luster, 2008). The decreased CCR2 expression can reduce microglia accumulation and increase the level of Aβ in the brain, suggesting that early microglial accumulation can promote Aβ clearance in AD mouse models (El Khoury and Luster, 2008).

We reviewed the BM-derived microglia-like cells' contribution to microgliosis in neurodegenerative diseases. Researchers transferred GFP-labeled myeloid cells into the BM of irradiated AD mice, and these GFP-labeled cells were later detected in the senile plaques in the brains (Simard et al., 2006). Similarly, early and rapid recruitment of BM-derived microglia to the brain also occurs in prion disease, bacterial meningitis, and PD mouse models (Kokovay and Cunningham, 2005; Djukic et al., 2006). Intracerebral injection of externally differentiated BM-derived microglia-like cells can also decrease Aβ deposits and improved cognitive function in AD mouse models (Kawanishi et al., 2018). These injected microglia-like cells can automatically migrate toward Aβ plaques, and reduce the number and area of these plaques (Lampron et al., 2011). Another study used a novel transgenic AD mouse to demonstrate that it is the peripheral blood-originated microglia, rather than their resident counterparts, that are capable of phagocytosing Aβ deposits (Simard et al., 2006). Besides, BM-derived microglia-like

cells could also stimulate the phagocytic functions of brain-resident microglia *in vitro* and *in vivo*, *via* secreting large sums of transforming growth factor-β (TGF-β; Kuroda et al., 2020a). All these results suggest that BM-derived microglia-like cells have potential cell-based disease-modifying therapy against neurodegenerative diseases, especially AD.

BM-MSCs

Bone marrow MSCs (BM-MSCs) are pluripotent stem cells inside the BM. It has been proved that BM-MSCs can move into the brain and develop neuronal markers such as nestin, doublecortin, and NeuN under physiological conditions (Dennie et al., 2016). The CCR5 plays a critical role in regulating the BM-MSCs' migration into the brain, both in physiological conditions and in response to injury (Dennie et al., 2016). Thus, BM-derived progenitors can migrate to the brain and become neurons at least in part, by firstly differentiating into neuronal precursor cells (Dennie et al., 2016). Apart from that, BM-MSCs can migrate to the brain and exert strong neuroprotective effects *via* regulating neurogenesis, apoptosis, angiogenesis, immunomodulation, and eliminating Aβ plaques in the brain (Naaldijk et al., 2017; Qin et al., 2020).

Transplanted BM-MSCs could significantly diminish the hippocampal Aβ plaques by activating several Aβ-degrading enzymes (Jha et al., 2015). Since vascular damage is also a pathogenic factor of AD, BM-MSCs can promote angiogenesis in the AD brain by secreting vascular endothelial growth factor (VEGF), epidermal growth factor (EGF), FGF-2, and Ang-1 (Gallina et al., 2015), and thus favor the cognitive and behavioral recovery (Garcia et al., 2014). The MSCs can also exert neuroprotective effects by secreting neurotrophic factors such as neurotrophin-3 (NT-3), hepatocyte growth factor (HGF), and brain-derived neurotrophic factor (BDNF; Wang et al., 2010). These factors stimulate endogenous regeneration and contribute to neurobehavioral function recovery. Animal studies demonstrate that the immunomodulatory effect of BM-MSCs plays a vital role in AD treatment as well (Salem et al., 2014; Zhang et al., 2020). Transplanted BM-MSCs can attract microglia-like cells by secreting CCL5 both *in vitro* and in the AD brain (Lee J. K. et al., 2012). Despite this, the activation levels of microglia and astrocyte were decreased in AD mice brains after BM-MSCs transplantation, manifested as the cerebral Iba-1 levels were down-regulated (Yokokawa et al., 2019). Our previous study showed that the transplanted BM-MSCs could inactivate microglia in the peri-infarct area *via* the CD200-CD200R1 signaling (Li et al., 2019). Also, BM-MSCs could lower expressional levels of pro-inflammatory genes, cytokines, and enzymes in astrocytes (Schäfer et al., 2012; Naaldijk et al., 2017). However, other studies report that the BM-MSCs could accelerate the microglia activation and thus the Aβ clearance in the AD brain (Lee et al., 2009). The BM-MSCs could also significantly increase the number of ChAT-positive cells and the intensity of ChAT spots in AD brains, which is an indicator for neurogenesis, neuronal differentiation, and integration (Mezey and Chandross, 2000; Mezey et al., 2000; Sanchez-Ramos et al., 2000). Nestin in neural cells, a neural precursor biomarker, is also up-regulated in the brain following the BM-MSC transplantation (Sanchez-Ramos et al., 2000). In fact, cells in different neurogenic stages, including proliferation, differentiation, migration, targeting, and integration, could be found in the hippocampus after the BM-MSC treatment (Perry et al., 2012).

Furthermore, BM-MSCs can alleviate cognitive defects related to various neurological disorders including traumatic brain injury (TBI), PD, and stroke by secreting microvesicles (MV) or exosomes (Xiong et al., 2017; Yang et al., 2017). It has been hypothesized that vesicles from BM-MSCs facilitate the transference of various functional factors, including regulatory non-coding RNAs, lipids, and proteins (Reza-Zaldivar et al., 2018). These regulatory factors within the MSC-derived exosomes are reported to act on critical cellular pathophysiological processes, such as energy metabolism, inflammation, and migration (Nakano et al., 2016; Borger et al., 2017). Li et al. (2017) reported that MSC-oriented exosomes shift the M1 microglia polarization toward an M2 phenotype, which ameliorates neuroinflammation and promotes functional recovery in a TBI model. Nakano et al. (2016) reported that BM-MSC-derived exosomes can alleviate the learning and cognitive damage in Streptozotocin (STZ)-induced diabetic mice by alleviating oxidative stress and promoting synaptogenesis. Functional miRNAs in exosomes might be an important mediator to inhibit neuronal apoptosis, promote synaptic plasticity and remodeling, and accelerate functional recovery (Xin et al., 2013, 2017; Cheng et al., 2018). For example, Xin et al. (2012, 2013) reported that MSC-released exosomes can transfer miR-133b into astrocytes and neurons in stroke rat models, and thereby promote the neurite outgrowth in the ischemic area. The authors further demonstrated the miR-133b exerts their neuroprotective function *via* decreasing the Ras homolog gene family member A (RhoA) and connective tissue growth factor (CTGF) expression. Besides, a study based on miRNA profiling and qPCR demonstrated the upregulation of miR-146a-5p in senescent MSCs and MSC-MVs (Lei et al., 2017). MiR-146a were also significantly upregulated in peripheral blood and cerebral spinal fluid (CSF) during the progression of AD, amyotrophic lateral sclerosis (ALS), and MS (Viswambharan et al., 2017). The miR-146a transferred by BM-MSCs-secreted exosomes is a key regulator in suppressing the astrocytic inflammation and protecting diabetic rats from cognitive decline (Kubota et al., 2018). Other neuroprotective mechanisms of MiR-146a-5p include inhibiting the NF-κB signaling (Iyer et al., 2012) and promoting remyelination (Zhang et al., 2017).

However, the neuroprotective functions of MSCs may be restricted with age, since both the number and function of MSCs are decreased (Lee et al., 2010; Bang et al., 2016). The senescent MSCs commonly present enlarged and more granular morphology, limited proliferation and differentiation capacity, and a distinct secretory phenotype referred to as "senescence-associated secretory phenotype" (SASP; Watanabe et al., 2017). The senescence of MSCs is believed to be the underlying cause of osteoporosis (Román et al., 2017), and neurodegenerative diseases including AD and PD (Lei et al., 2017). Furthermore, MSCs in the senescent late period release higher levels but smaller-sized MSC-MVs than the early passage of MSCs

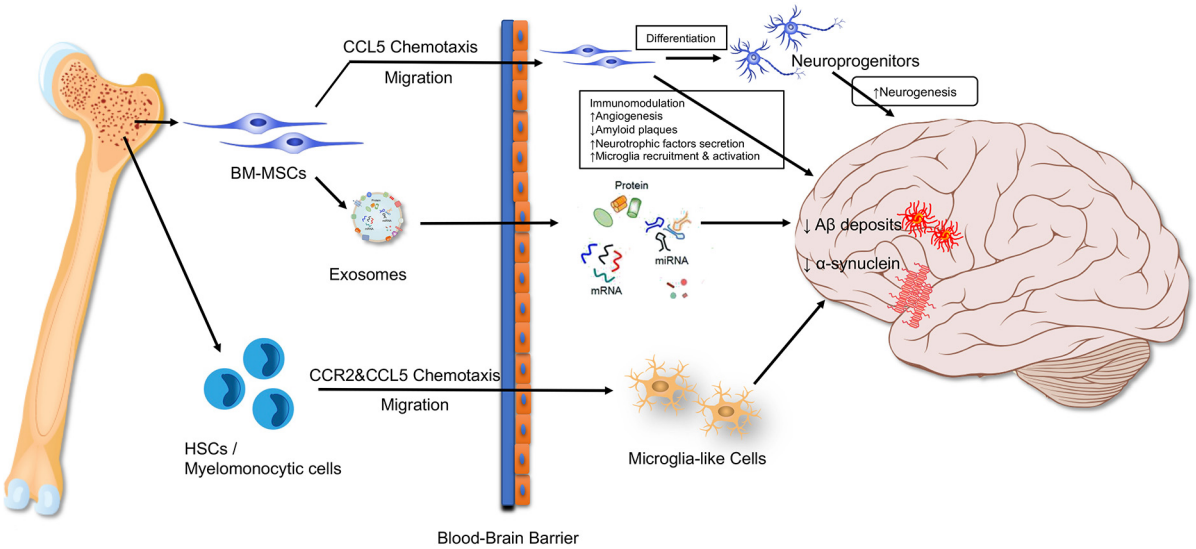


FIGURE 1 | Bone marrow-derived cells influence the brain. BM-MSC, bone marrow mesenchymal stem cell; HSC, hematopoietic stem cell.

(Lei et al., 2017), which correlated with the phenomenon that the levels of myeloid MVs in plasma and cerebrospinal fluid were positively associated with neurodegenerative disease (Joshi et al., 2014).

In conclusion, BM-MSCs can migrate into the brain to differentiate toward neurons themselves, or recruit microglia cells for toxicant clearance. BM-MSCs can also promote neuronal repair and functional recovery by secreting exosomes. However, BM-MSC's curative effects decreased greatly in the aging process.

BM-CONTROLLED IMMUNE SYSTEM

The BM is the primary organ for producing common lymphoid progenitors (CLPs), which are responsible for generating innate and adaptive immune cells (Zhao E. et al., 2012). This is why the BM is called the primary lymphoid organ. The function of the BM and CNS is closely interconnected. There are norepinephrine (NE)-releasing sympathetic nerve fibers in BM, which are essential for preserving the HSC niche, promoting the HSC mobility, and regulating their differentiation into immune cells (Maryanovich et al., 2018). At the same time, the changes in the immune system originated from the BM will also affect the functions of the CNS by various mechanisms, including promoting inflammatory cytokines secretion, microglial activation, neuronal apoptosis, demyelination, and tissue damage (Liang et al., 2017). With age, the hematopoietic tissue is gradually replaced by fat tissue, and the proliferative and developmental capacity of HSCs, as well as the lymphogenic capacity decrease (Geiger et al., 2013). Studies have shown that the pathogenesis of AD and PD may be related to systemic immune dysfunction, especially to the T cell subtypes (Pellicano et al., 2012). Compared with the age-matched controls, the difference of immunity in AD patients was greater than that caused by age. The immune alterations mainly include less naïve T cells, more terminated-differentiated cells, and more dysfunctional Treg cells in AD patients. In PD patients, CD4+ and CD8+ T lymphocytes are found aggregated around the SN compacta (Brochard et al., 2009). These CD4+ cells are highly pro-inflammatory, which can promote the microglia activation and the degeneration of dopaminergic neurons. These studies suggest that immune alterations can contribute to the progression of neurodegenerative diseases (**Figure 2**).

CD8⁺ T Cells

CD8+ T cells also referred to as cytotoxic T lymphocytes (CTL), play vital roles in the immune system to defend against intracellular pathogens by secreting pro-inflammatory cytokines, primarily the TNF-α and IFN-γ, or directly killing target cells *via* Fas/FasL interactions or cytotoxic granules containing perforin and granzymes (Harty et al., 2000). CD8+ T cells are also related to the pathogenesis of neurodegenerative diseases. Studies indicated that the CD8+ T cells outnumber the CD4+ T cells in MS lesions (Goverman et al., 2005). Moreover, the injection of CD8+ myelin-specific T cells rather than myelin-specific CD4+ T cells into wild-type mice can induce a demyelinating disease similar to MS, suggesting CD8+ T cells' unique roles in the pathogenesis of MS (Huseby et al., 2001; Goverman, 2009). Furthermore, in the brains of both postmortem human PD specimens and PD mouse models, CD8+ T cells are often located next to the activated microglia and degenerating neurons in the SN area, which indicates that these cells might be implicated in PD neuronal loss (Brochard et al., 2009). Additionally, CD8+ T cells mediated inflammation and IFN-γ levels are associated with microstructural tissue damage and neurological deficits in AD patients (Baglio et al., 2013; Lueg et al., 2015).

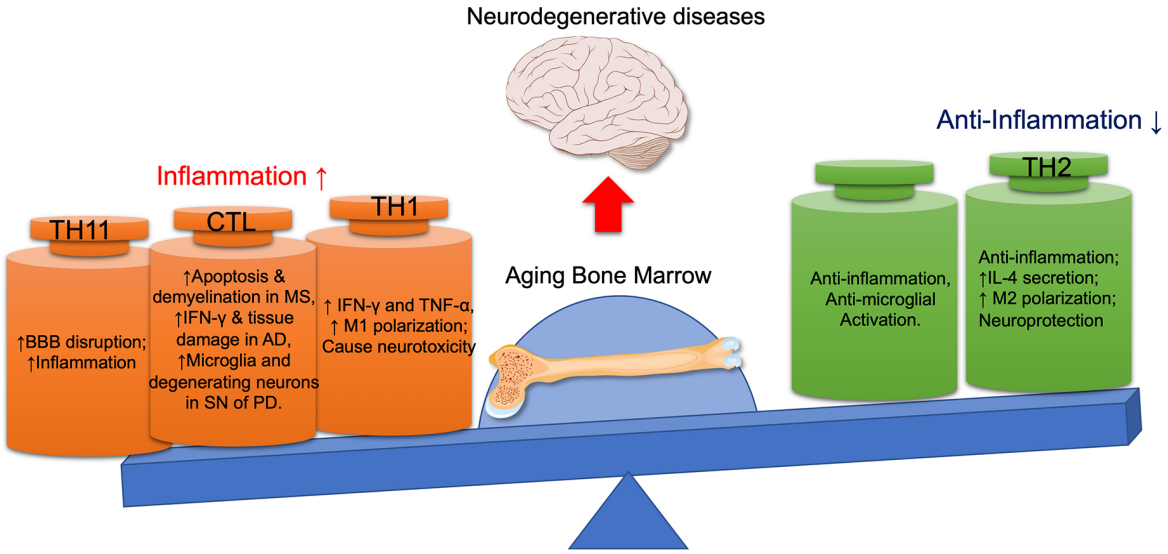


FIGURE 2 | The detrimental and beneficial roles of different immune cells in neurodegenerative diseases. With the aging bone marrow, pro-inflammatory lymphocytes (CTL, Th1, Th17) are activated, while immunomodulatory lymphocytes (Th2, Tregs) are suppressed, thus promoting the progression of neurodegenerative diseases. AD, Alzheimer's disease; BBB, blood-brain barrier; CTL, cytotoxic T lymphocyte; IFN-γ, interferon-γ; MS, multiple sclerosis; PD, Parkinson disease; SN, substantia nigra; TNF-α, tumor necrosis factor-α.

Th1 Cells

CD4+ Th1 cells referred to as type 1 T helper cells are characterized by T-bet expression and Type 1 cytokines (mainly IFN-γ, TNF-α, and IL-2) secretion (Romagnani, 2014). CD4+ Th1 infiltration in the brain is seen in various neurodegenerative diseases (Liang et al., 2017). Browne et al. (2013) showed that Th cells infiltrated in the brains of APP/PS1 mouse models secrete abundant IFN-γ and IL-17, suggesting these Th cells are mainly the Th1 and Th17 subsets. They further demonstrated that it is the Th1 cells, but not Th2 nor Th17 cells, that cause microglial activation, Aβ plaque burden increase, and impaired cognitive function in APP/PS1 mouse models (Browne et al., 2013). Much of the Th1 cell-mediated inflammatory damage in the context of neurodegenerative diseases can be attributed to the release of pro-inflammatory cytokines and the M1 polarization of macrophages and microglia. These cellular processes could significantly aggravate neurodegenerative diseases by promoting neurotoxicity and tissue damage in the brain (Sanchez-Guajardo et al., 2013). Administrating anti-IFN-γ antibody and immunomodulative TGF-β in AD mouse models could effectively alleviate the Th1 cell-mediated neuroinflammation and cognitive decline (Browne et al., 2013; Chen et al., 2015). However, some studies show the beneficial roles of Th1 cells in AD pathology. Intracerebroventricular (ICV) injection of Aβ-specific Th1 cells lowers the Aβ levels and enhances neurogenesis, while exerts no impact on apoptosis in AD mouse models (Fisher et al., 2014). Thus, it seems that different routes of Th cells migration into the brain might play different roles in neurodegeneration.

Th2 Cells

CD4+ Th2 cells are T helper cells expressing the GATA3 and producing Type-2 cytokines (mainly IL-4, IL-5, IL-9, and IL-13; Walker and McKenzie, 2018). Th2 cells mainly exhibit an anti-inflammatory function, such as suppressing the Th1-related IFN-γ-driven immune response and inducing macrophage to polarize into an M2-like phenotype (Walker and McKenzie, 2018). In the Th1/Th2 balance paradigm, the Th1-secreted IFN-γ and Th2-derived IL-10 inhibit the proliferation of each other's cells. CD4+ Th2 cells mainly exhibit neuroprotective properties in the context of neurodegenerative diseases. For example, myelin basic protein (MBP)-primed Th2 cells can enter the brain and restrict the AD and PD neurotoxicant induced microglial inflammation (Roy and Pahan, 2013). In MS models, Th2 cells can inhibit the activation of lipopolysaccharide (LPS)-stimulated microglia *via* direct cell contact, and ultimately inhibit its IL-1b and nitric oxide production (Roy and Pahan, 2013). Additionally, MBP-primed Th2 cells can even induce the neurotrophic molecules (including BDNF and NT-3) expression in microglia and astroglia *via* direct cell contact (Roy et al., 2007).

Th17 Cells

Th17 cells are CD4+ Th cells expressing the RORγτ transcriptional factors and secreting characteristic cytokines including IL-17 and IL-22 (Annunziato et al., 2013). They are involved in the progression of neurodegenerative diseases, mainly by secreting IL-17 to recruit inflammatory neutrophils and IL-22 to stimulate epithelial cells generating antimicrobial peptides (Saresella et al., 2011). Saresella et al. (2011) analyzed the function of various T lymphocytes in AD patients and compared the data with those of mild cognitive impairment participants or aged-matched healthy people. They found that the Th17 lymphocytes are significantly increased in AD. In MS or experimental autoimmune encephalomyelitis (EAE), Th17 cells secrete cytokines to

act on IL-17 and IL-22 receptors on the BBB endothelium, causing BBB damage and subsequent neural inflammation (Kebir et al., 2007).

Interestingly, Th17 is tightly associated with bone destruction. In postmenopausal osteoporosis patients, serum IL-17A is significantly higher, while the IFN-γ and IL-4 are significantly lower, suggesting osteoporosis may be more associated with the Th17 cells rather than the Th1 or Th2 cells (Zhang et al., 2015). The further study demonstrates IL-17A is pro-osteoclastogenic at the cellular level (Le Goff et al., 2019). *In vivo* study shows that although IL-17A is not required for normal bone homeostasis, it plays a vital role in bone loss of ovariectomized osteoporosis mouse models. Furthermore, preliminary data from clinical trials show that anti-IL-17A antibodies stabilize bone density in inflammatory arthritis (Le Goff et al., 2019). These results suggest an inter-relationship between osteoporosis and neurodegenerative diseases.

Treg Cells

Regulatory T cells (Tregs) are T cells expressing the CD4+CD25+Foxp3+ surface markers. They inhibit immune response and thus to maintain homeostasis and self-tolerance. Treg cells play a substantial role in slowing down the progression of ALS by lowering pro-inflammatory cytokine expressions and reducing microglial activation in mouse models (Beers et al., 2011). The mechanisms behind are associated with Tregs' secretion of immuno-modulative cytokines (TGF-β, IL-10, and IL-4) which inhibits the microglia and pro-inflammatory T cells activation (Beers et al., 2011; Xie et al., 2015). However, functional Tregs are usually deficient in patients with neurodegenerative diseases for several reasons. Under normal physiological conditions, 30% of $CD4^+$ T cells are functional Treg cells in BM (Zou et al., 2004), and over 15% of CD4+ T cells in rat cerebrum are Treg cells (Xie et al., 2015). However, the absolute lymphocyte numbers and the percentage of Treg subsets were both decreased in the BM and peripheral blood of the aged participants, indicating the Treg production in BM is reduced (Freitas et al., 2019). Moreover, a decrease of functional Treg seems to be closely related to MS, since the relapsed MS patients have fewer Tregs and significantly reduced Treg/Th17 ratio in the peripheral blood compared with healthy individuals (Jamshidian et al., 2013). Furthermore, Tregs are extremely rare or even undetectable in MS brain lesions, which might be due to Treg's impaired migration across the BBB (Fritzsching et al., 2011). *In vitro* studies show healthy Tregs can cross the human brain endothelium easily, whereas the migration ability of Tregs in MS patients is severely impaired (Schneider-Hohendorf et al., 2010). Moreover, their neural protective functionality might also be hindered in neurodegenerative disease because of the Th17 subset's inhibitory effect on Tregs. Treg cells rely on TGF-β, which is competitively bound by the abundant Th17 cells in a neurodegenerative context, for differentiation and maintenance (Afzali et al., 2010). However, Tregs can be transformed into pro-inflammatory Th17 cells themselves in some circumstances (Afzali et al., 2010). These multiple factors result in low Treg levels in neurodegenerative patients.

BONE SECRETORY PROTEINS

Previous evidence showed that several bone cell-secreted hormones or "osteokines" have endocrine functions, such as OCN, OPN, FGF23, Lipocalin 2(LCN2), osteoprotegerin (OPG), sclerostin (SOST), and Dickkopf-1 (DKK1; Vervloet et al., 2014; Han Y. et al., 2018). Most of these proteins are produced by osteoblasts and osteocytes and have roles in regulating phosphate and systemic energy metabolism (Han Y. et al., 2018). Osteoblasts-secreted OCN regulates energy metabolism, reproduction, and cognition (Zoch et al., 2016; Mizokami et al., 2017; Obri et al., 2018). OPN in the osseous tissue is released from osteoblasts and osteoclasts and is associated with bone destruction and suppression of ectopic calcification (Lund et al., 2009; Uede, 2011). It mainly regulates phosphate homeostasis (Huang et al., 2013). LCN2 secreted by osteoblasts can act on the brain to suppress appetite (Mosialou et al., 2017). OPG is synthesized by osteoblasts and its main function is to antagonize the effects of receptor activator of nuclear factor-kappa-B ligand (RANKL; Bonnet, 2017; Rochette et al., 2019). Both SOST and DKK1 (Ke et al., 2012) are mainly secreted by osteocytes and function through antagonizing the canonical Wnt pathway. These bone secretory proteins are reported to play diverse roles in neurodegenerative diseases (**Table 1**).

OCN

OCN is uniquely secreted by osteoblasts (Hauschka et al., 1975; Price et al., 1976) and is thus a specific biomarker for bone formation (Ducy et al., 1996; Ducy, 2011). OCN is also an important regulator of energy metabolism, as it can enhance insulin secretion, decrease insulin resistance, improve glucose tolerance and blood lipid profile, and regulate brown adipose tissue differentiation (Karsenty and Ferron, 2012; Wei et al., 2014).

OCN, uncarboxylated in most circumstances, can pass through the BBB and bind specifically with neurons in the brainstem, thalamus, and hypothalamus (Oury et al., 2013; Shan et al., 2019). Upon binding, OCN can influence the signals that regulate neurotransmitter syntheses, such as decreasing the synthesis of glutamate decarboxylase 1 (Gad1), an enzyme involved in GABA biosynthesis, and increasing the tyrosine hydroxylase (Th) and tryptophan hydroxylase 2 (Tph2) synthesis, which are the key enzymes involved in the serotonin, dopamine, and norepinephrine generation in the brainstem and midbrain explants (Oury et al., 2013). In the hippocampus, OCN mainly combines with neurons' Gpr158/Gaq receptors, and functions in part by activating IP3 and promoting the secretion of BDNF (Khrimian et al., 2017), a molecule well known to promote hippocampal-dependent memory (Hall et al., 2000; Dean et al., 2009). Adult mice lacking OCN displayed a substantial increase in anxiety-like behavior and had a major deficit in memory and learning (Nakazawa et al., 2002; Oury et al., 2013). Anatomically, the brains of OCN–/– mice are consistently smaller, mainly in the hippocampal region, and often lost the corpus callosum compared with wild-type littermates (Nakazawa et al., 2002; Oury et al., 2013). OCN–/– mice injected with OCN showed

TABLE 1 | Bone secretory proteins and their different effects in the brain.

	Origin	Neuroprotective effects on the brain	Neurotoxic effects on the brain
OCN	Osteoblast	↑MN (5-HT, DA, NE) and ↓ GABA production; ↑BDNF; ↓Inflammation; Beneficial for AD and PD.	
OPN	Osteoblasts, osteoclasts, myelomonocytic cells	↑Monocyte-macrophage' recruitment and M2 polarization in AD; ↑Aβ clearance in AD; ↓Apoptosis in AD; Either neuroprotective or neurotoxic in PD; Protects dopaminergic cells in PD *via* RGD-binding domain.	↑Pro-inflammatory mediators in MS; ↑Autoreactive immune cells in MS; Associate with nigral cell death and glial response in PD.
FGF23	Osteoblasts, osteocytes		↓Vitamin D, exacerbate AD and PD; ↓Serum phosphate, cause ion dysregulation; FGF23 deficiency causes ectopic calcification, neuronal loss, and cognition damages.
LCN2	Osteoblast		Inhibit remyelination in MS; Synergistic neurotoxic effects with Aβ, TNF-α or LPS; ↑Apoptosis and neuronal death in MS, PD, AD; ↓TNFR2's neuroprotective effects.
OPG	Osteoblast	Inhibit RNAKL and TRAIL; ↓Aβ toxicity and prevent AD; ↓Vascular calcification and prevent vascular dementia.	
DKK1	Osteocytes, osteoblasts, BM-MSCs		↓Wnt's neuroprotective effects; ↑Aβ toxicity; ↓Neural synapses; Risk factor for AD.

Abbreviations: OCN, osteocalcin; OPN, osteopontin; OPG, osteoprotegerin; FGF23, fibroblast growth factor 23; LCN2, Lipocalin 2; DKK1, Dickkopf-1; MN, Monoamides; 5-HT, serotonin; DA, dopamine; NE, norepinephrine; GABA, γ-aminobutyric acid; RGD, arginine-glycine-aspartic acid; RANKL, receptor activator of the nuclear factor-kappa-B ligand; TRAIL, TNF-related apoptosis-inducing ligand; BDNF, brain-derived neurotrophic factor; AD, Alzheimer's disease; MS, multiple sclerosis PD, Parkinson's disease; TNFR2, tumor necrosis factor receptor 2; LPS, lipopolysaccharide; TNF-α, tumor necrosis factor-α.

ameliorated anxiety and depression, and improved memory and learning abilities (Mera et al., 2016). OCN also has neuroprotective effects in the context of PD. As mentioned above, OCN could enhance dopamine synthesis in neurons, thereby reducing the Th loss and relieving the PD symptoms in PD rat models (Guo et al., 2018; Obri et al., 2018). Also, OCN could modulate neuroinflammation in the SN of PD rats by inhibiting astrocyte and microglia proliferation, together with partially decreased levels of TNF-α and IL-1β (Guo et al., 2018).

OPN

OPN was first discovered as a protein to anchor osteoclast to the mineral surface of bones, thereby to facilitate the osteolytic process (Reinholt et al., 1990). Serum OPN levels have negative correlations with bone mineral density in postmenopausal women (Cho et al., 2013). OPN is mainly secreted by osteoblasts, osteoclasts, and BM-derived myelomonocytic cells (Lund et al., 2009; Uede, 2011). In the brain, OPN is a constituent of the normal extracellular matrix and is expressed mainly in the basal ganglia, especially in the substantia nigra (SN; Iczkiewicz et al., 2004). In neurodegenerative diseases, OPN is considered to play dual roles in neuroinflammation and neuroprotection (Carecchio and Comi, 2011; Yu et al., 2017).

Previous studies showed OPN's detrimental role in MS. Abundant OPN transcript was found in plaques dissected from MS patients' brains, while it was absent in the control group (Chabas et al., 2001). Further study demonstrated that OPN-deficient mice had a milder disease course than wild type animals, and displayed only a single relapse without subsequent exacerbations or progression (Chabas et al., 2001; Jansson et al., 2002). Administrating OPN-deficient EAE mice with recombinant OPN exacerbates the disease (Hur et al., 2007). Two mechanisms may be involved in OPN's detrimental effects: by stimulating the pro-inflammatory mediators in MS lesions, and by inhibiting the apoptosis of autoreactive immune cells (Carecchio and Comi, 2011). In contrast, the OPN is mainly studied for its anti-inflammatory and anti-apoptotic properties in PD (Khan et al., 2002; Lund et al., 2009; Rittling and Singh, 2015). Iczkiewicz et al. (2010) showed that the arginine-glycine-aspartic acid (RGD)-binding domain of OPN protects dopaminergic cells against toxic insult induced by MPP+ and LPS. Also, the OPN's effect decline with age, a major predisposing factor for PD, further reinforced the hypothesis (Hwang et al., 1994). However, Maetzler et al. (2007) showed that OPN knock-out PD mice displayed less nigral cell death and a lower glial response compared to wild-type PD mice. He also reported that PD patients' serum and CSF OPN levels were higher, with CSF levels positively correlated with concomitant dementia and serum levels with more severe motor symptoms, suggesting OPN may promote the PD progression (Maetzler et al., 2007). In the context of AD, studies show OPN can promote the monocyte-macrophage' recruitment into AD mouse brains, and their polarization towards an anti-inflammatory, highly phagocytic phenotype

to facilitate Aβ clearance (Rentsendorj et al., 2018). The FDA-approved anti-AD drug glatiramer acetate increases the plasma levels of OPN, and therefore promotes a macrophage phenotype that is highly phagocytic of Aβ and anti-inflammatory (Rentsendorj et al., 2018). Also, OPN can bind to the CD44 receptor and exert its anti-apoptotic function (Lin and Yang-Yen, 2001). This may be another potential mechanism for OPN to protect neurons from injury in AD.

Therefore, we can conclude that the levels of OPN increase with age. OPN accelerates the progression of bone demineralization, while exerts different influence on various kinds of neurodegenerative disorders.

FGF-23

FGF-23 is mainly secreted by osteoblasts and osteocytes. It suppresses the phosphate resorption and 1, 25(OH)2D3 production in the kidney by binding to FGFR1 and its co-receptor Klotho (Urakawa et al., 2006). FGF-23 changes significantly in the aging process (Cardoso et al., 2018). Still, FGF-23 is an independent predictor for dementia and AD, after adjusting for age, sex, cardiovascular disease, diabetes mellitus, etc. (McGrath et al., 2019). In another study, researchers used high-resolution MRI to find out that increased FGF-23 was associated with axonal loss and white matter disruption in the frontal lobe only in patients with cardiovascular risk factors (Marebwa et al., 2018). FGF-23-deficient mice show ectopic calcifications in the brain, fewer immature neurons in the sub-granular zone (SGZ), and significant cognitive impairment compared with wild type controls (Kunert et al., 2017; Laszczyk et al., 2019). Mice overexpressing FGF-23 also showed impaired spatial learning and memory (Liu et al., 2011). However, these peripheral symptoms could be largely alleviated by dietary correction of phosphate levels (Morishita et al., 2001; Liu et al., 2011), suggesting that FGF-23 may indirectly affect brain health and cognition, but probably by affecting phosphate homeostasis which acts synergistically with renal or cardiovascular risk factors.

Another explanation is that too much FGF-23 may exacerbate neurodegenerative diseases by decreasing the level of vitamin D3. FGF-23 suppresses the vitamin D3 production by blocking the 1α-hydroxylase in the renal proximal and distal tubules (Karsenty and Olson, 2016). The detrimental effects of vitamin D deficiency on the brain and its roles in neurodegenerative diseases have already been elaborated on in other studies (Koduah et al., 2017; Lv et al., 2020).

In conclusion, an abnormal amount (too much or too little) of FGF-23 is sufficient to affect brain function and cognition, most likely through an indirect way by affecting ion (phosphate) and/or vitamin D homeostasis.

LCN2

LCN2 is an endocrine hormone secreted by osteoblasts and can suppress appetite by crossing the BBB to bind to the melanocortin-4 receptor (MC4R) in the brainstem (Mosialou et al., 2017). Besides, LCN2 can promote insulin resistance and cause hyperglycemia, diabetes, cardiovascular disease, and metabolic syndrome (Yan et al., 2007). LCN2 can also be secreted by neutrophils and glial cells, and play essential roles in inflammation, infection, and injury to cells (Pinyopornpanish et al., 2019).

LCN2 acts through its two receptors, 24p3R and megalin (Chakraborty et al., 2012), both of which can be found in the brain in basal and pathological conditions (Ip et al., 2011). LCN2 production is increased in progressive MS patients, and this effect could be relieved by the MS-treating drug natalizumab (Al Nimer et al., 2016). Further *in vitro* study shows that LCN2 plays detrimental roles by inhibiting remyelination in a dose-dependent manner (Al Nimer et al., 2016). LCN2 is also upregulated in the SN of PD patients and neurotoxin-induced PD animal models (Kim et al., 2016). The higher LCN2 levels could disrupt the SN dopaminergic projection and contribute to abnormal locomotor behaviors through neurotoxic iron accumulation and neuroinflammation, which were alleviated in LCN2-deficient mice (Kim et al., 2016). LCN2 is significantly decreased in CSF of AD patients and increased in brain regions related to AD pathology (Naudé et al., 2012). *in vitro* study demonstrates that LCN2 makes nerve cells susceptible to Aβ toxicity, and suppresses the neural protective tumor necrosis factor receptor 2 (TNFR2) signaling pathway in neurons (Naudé et al., 2012).

In animal experiments, ICV injection of recombinant mouse LCN2 protein can cause neuronal death in the hippocampal CA1 area and cognitive dysfunction (Kim et al., 2017). Moreover, LCN2 usually acts synergistically and exacerbates the neurotoxic effects of Aβ, TNF-α, or LPS (Mesquita et al., 2014; Yang et al., 2017). The expression of 24p3R increases after the administration of Aβ (Mesquita et al., 2014). An increase in cell death is reported when astrocytes or neurons are co-cultured with LCN2 and Aβ (Marebwa et al., 2018), and the depletion of LCN2 helps to protect astrocytes from Aβ toxicity (Mesquita et al., 2014). Also, LCN2 could undermine the neuroprotective effect of the TNFR2 signaling pathway induced by TNF-α (Hemmings and Restuccia, 2012; Naudé et al., 2012). Further *in vitro* studies demonstrate that LCN2 can directly induce neuronal apoptosis through the BCL2 mediated cell death signaling pathway in a time and dose-dependent manner (Lee S. et al., 2012; Bi et al., 2013).

In short, LCN2 could exert pro-apoptotic effects on brain cells and increase the susceptibility of neurons to toxic stimuli. LCN2 could also increase glial activity, increase inflammation, and inhibit remyelination.

OPG

OPG is a soluble glycoprotein that belongs to the TNF receptor superfamily. It is a decoy receptor for RANKL and TNF-related apoptosis-inducing ligand (TRAIL), and thus inhibits the association of RANKL and TRAIL with their receptors. It is secreted by osteoblast and prevents the RANKL from binding to its receptor on osteoclasts, thereby inhibiting the osteolysis (Bonnet, 2017; Rochette et al., 2019). Increased blood levels of OPG are associated with osteoporosis in postmenopausal women (Yano et al., 1999).

High OPG levels are also detected in the CSF, and as the OPG level in the CSF increases with age, it may play a role in inflammatory and degenerative disorders of the CNS (Hofbauer et al., 2004). A study demonstrates that after adjusting for age, sex, and APOE ε4 allele, OPG is an independent predictor of AD and vascular dementia (Emanuele et al., 2004). OPG might influence cognition by affecting the immune environment and the perfusion of the brain. For the former, studies have demonstrated that the RANKL/RANK signaling suppresses inflammation through a Toll-like receptor pathway in microglia. Increased OPG could inhibit the RANKL/RANK signaling and aggravate the post-ischemic inflammation (Shimamura et al., 2014). Whereas for the latter, the RANK/RANKL/OPG triad might play a critical role in vascular calcification (Rochette et al., 2019). Therefore, OPG can prevent vascular calcification as a RANKL inhibitor (Wu et al., 2013). Emanuele et al. (2004) measured plasma OPG levels in vascular dementia patients and compared them with OPG in AD and age-matched healthy individuals. They found that compared with the non-demented control group, OPG concentrations were significantly higher in both vascular dementia and AD patients, wherein the OPG level in vascular dementia was the highest. These results were interpreted to be that OPG could mirror atherosclerotic disease, most so in vascular dementia and that vascular factors may also play a role in the pathogenesis of AD (Emanuele et al., 2004). Increases of OPG in vascular dementia can be regarded as a compensatory defense mechanism to relieve the atherosclerotic burden (Schoppet et al., 2002).

DKK1

Both DKK1 and SOST are soluble Wnt inhibitors (Ke et al., 2012). Although these two molecules share some homologies in action, they have distinct biological effects and different expression patterns (Gifre et al., 2013). The DKK1 and SOST use a different receptor to inhibit the low-density lipoprotein receptor-related protein (LRP)5-LRP6 receptor complex formation (Monroe et al., 2012). The SOST protein seems to be a specific Wnt inhibitor because it is almost exclusively bone-derived, and is predominantly secreted by osteocytes and osteoclast precursors (Poole et al., 2005; Vervloet et al., 2014). Although DKK1 is also mainly expressed by osteocytes, osteoblasts, and BM-MSCs, it is not as highly selective as SOST (Han Y. et al., 2018). We mainly focus on the DKK1 in this review, since it is more deeply involved in brain pathologies, while the SOST is found unrelated to cognition change (Ross et al., 2018).

Wnt signaling has been proven to have strong neuroprotective effects, and can even regulate neo-neuronal generation in the adult brain (Inestrosa and Varela-Nallar, 2014). Wnt signaling activation facilitates synaptic remodeling and memory consolidation (Inestrosa and Varela-Nallar, 2014). Therefore, it is easy to understand that Dkk1, a Wnt signaling inhibitor, is associated with the severity of neurodegenerative diseases (Ross et al., 2018). The expression of DKK1 in the brain tissue, CSF, and plasma of AD patients and animal models increases significantly compared to healthy controls (Caricasole et al., 2004; Rosi et al., 2010). It has also been reported that at high concentrations, DKK1 can pass through the BBB, and thus accelerate the AD progression (Ren et al., 2019). Some studies show that the occurrence of familial/early-onset AD, sporadic/late-onset AD, and patient's cognitive decline are related to DKK1 and Wnt/β-catenin signaling disruptions (Scott and Brann, 2013). The increased expression of DKK1 inhibits the Wnt signaling pathway, which further increases the tau phosphorylation, while the DKK1 knock-out inhibits the formation of neurofibrillary tangles, and reduces the neurotoxicity of Aβ (Caricasole et al., 2004). Further study shows that injecting different concentrations of DKK1 into the dorsal hippocampus can lead to object recognition memory loss, which is regulated by the canonical Wnt-dependent signaling pathway (Fortress and Frick, 2016). DKK1 could also aggravate the Aβ-induced neuronal apoptosis and synaptic loss by blocking the Wnt signaling pathway (Purro et al., 2012). Other related studies show that short-term exposure to Aβ in mouse brain slices increases the DKK1 expression and reduces the synaptic formation (Matrisciano et al., 2011), while injecting DKK1-specific antibodies could alleviate the Aβ-induced damage to neuronal synapses (Huang et al., 2018). Some scholars suggest that the endogenous Wnt ligands, which are inhibited by DKK1, are vital to maintaining the neuronal synapses (Purro et al., 2014). Also, the potential therapeutic effects of the DKK1 inhibitor may be associated with synaptic preservation and hippocampal circuit reconstruction (Marzo et al., 2016; Ortiz-Matamoros and Arias, 2018). Animal tests show that inhibiting DKK1 improves subjects' spatial memory tasks (Marzo et al., 2016; Ortiz-Matamoros and Arias, 2018) and their electrophysiological findings (Marzo et al., 2016).

POTENTIAL THERAPEUTIC IMPLICATIONS

BM-Derived Cells

After the transplantation of BM-MSCs, learning ability and spatial memory performance were significantly improved in AD animal models (Ohsawa et al., 2008; Kanamaru et al., 2015; Safar et al., 2016). It was revealed that the gene expression patterns are altered in AD brains, and the alterations are correlated with the severity of neuropathology (Qin et al., 2020). Transplantation of BM-MSCs could also alter some gene levels in the AD brains, such as genes related to pro-inflammatory cytokines, enzymes, receptors, and intermediate filaments. These differentially expressed representative genes are mostly responsible for neuropathological phenotypes in AD (Qin et al., 2020).

In terms of feasibility, the intravenous delivery of stem cells is convenient and sufficient to lower the levels of cerebral amyloidosis (Salem et al., 2014; Harach et al., 2017). The intravenous transplanted stem cells could be easily detected in the brain parenchyma, i.e., could be found in the hippocampus 1 h after administration (Harach et al., 2017), and expressed neuronal phenotypes in the brain for 1-6 months (Brazelton et al., 2000). The expression of male BM-MSCs' *sry* gene in female AD model's brain tissue proves that exogenous stem cells with intravenous delivery could successfully migrate to the brain injury site (Salem et al., 2014). As for the cell dose for intravenous administration, our previous data showed

5×10^5 BM-MSCs is an appropriate dose for treating ischemic stroke in rats (He et al., 2016). The optimal cell dose for AD and other neurodegenerative disease therapies are remained to be explored.

Bone-Derived Exosomes

Previous studies report positive correlations between MVs in CSF and neurodegenerative diseases and show that many exosomes are enriched with undigested lysosomal substrates, such as Aβ and APP (Malm et al., 2016). However, these MVs are mainly derived from inflammatory cells, microglia, or tumor (Rajendran et al., 2006; Saman et al., 2012, 2014; Joshi et al., 2014; Levy, 2017), and there is no evidence suggested that BM-derived exosomes can cause or exacerbate neurodegenerative diseases. Some studies indicate that using stem cell-secreted exosomes as an alternative therapeutic would be much safer compared with stem cell transplantation (Smith et al., 2020). Administrating exosomes rather than viable replicating cells can mitigate many complications and therefore be much safer (Smith et al., 2020). The transplanted stem cells may persist or be amplified even after treatment is terminated. The transplanted stem cells' potential of differentiating into other cell types has also raised long-term safety concerns (Breitbach et al., 2007).

Apart from its innate therapeutic effect discussed above, exosomes from the BM can be modified into appropriate nanocarriers to transport siRNA. To strengthen exosomes' targeting ability, researchers reshaped them by attaching neuron-specific Rabies Viral Glycoprotein (RVG) peptides onto their surface (Alvarez-Erviti et al., 2011). The remodeled RVG exosomes successfully transported the GAPDH siRNA into targeted neurons, oligodendrocytes, and microglia, and subsequently downregulated the BACE1 gene expression, which is crucial in the AD progression.

Bone Secretory Proteins

Several bone-secreted proteins were summarized above as regulators of CNS homeostasis and neurodegenerative diseases. Although the direct use of these bone-secreted proteins as drugs to treat neurodegenerative diseases are rare, a few studies indicated that these proteins might be indirectly involved in other therapeutics. For example, metformin could ameliorate spatial memory loss (Ahmed et al., 2017), reduce stress-induced behaviors (Mourya et al., 2018), and relieve the related symptoms in the PD mouse model (Katila et al., 2017). Metformin can affect OCN and related bone diseases. In an osteoporosis mouse model, metformin could ameliorate the bone loss with the increased OCN expression level (Liu et al., 2019). The drug could also improve the osteogenic functions of adipose-derived stromal cells by increasing the OCN expression and AMPK signaling (Smieszek et al., 2018). It should be noted that AMPK is also a regulator for brain energy metabolism (Garza-Lombó et al., 2018), which are related to cognition and motor coordination (Kobilo et al., 2014), and can inhibit NF-κB signaling and inflammation (Salminen et al., 2011). Moreover, metformin can behavior by increasing the BDNF secretion (Katila et al., 2017; Fatemi et al., 2019), which coordinates with OCN's effect in age-related memory loss (Khrimian et al., 2017). These findings suggested that metformin therapy could influence brain functions, wherein the OCN may act as a mediator in promoting neurotrophic signal, energy metabolism, and immune modulation. A role for OCN may also be implicated in exercise-induced cognitive improvement through the IL-6/gp130/OCN axis (Shan et al., 2019). Moreover, the MS-treating drug natalizumab and the anti-AD drug glatiramer acetate mentioned above are another two examples to treat neurodegenerative diseases *via* the mechanisms related to bone secretory proteins. The two drugs reduce the LCN2 or increase the OPN expression, respectively.

Before clinical application, further studies on specific bone regulative processes and their effects on the brain are required. For example, even though BM-derived cells can enter the CNS and become neural progenitors or microglia-like cells, more details about how this process is controlled *in vivo* should be elucidated (Ajami et al., 2007; Mildner et al., 2007). Moreover, most studies examining the bone-derived cells or molecules' roles in neurodegenerative diseases were performed in mouse models rather than in patients. These results should further be confirmed in human samples. Furthermore, except for OCN and DKK1, there is still a lack of direct evidence to show that these bone-secreted osteokines can cross the BBB and influence the neurodegenerative diseases' course. Although these cytokines are mainly secreted from the bone, and show altered expression in the context of neurodegenerative diseases, most osteokines above are not bone-specific and some of them can be secreted within the brain. It remains to be determined how these osteokines are evolved in the process of bone-brain crosstalk and contribute to the progression of neurodegenerative diseases by using bone-defect models. Last but not least, although bone is a primary lymphoid organ, it does not sufficiently control the entire immune system, other factors are also needed for triggering the onset of neurodegenerative diseases. Although there are still many difficulties, the potential application of bone-based therapy in neurodegenerative diseases is worthy of further experimental and clinical studies.

CONCLUSIONS

Elderly people are prone to osteoporosis and neurodegenerative diseases including cognitive decline, PD, and MS. All these disorders have common soil, mainly the metabolic-related disorders and immune dysregulation, suggesting the bone and brain may be closely interacted. When anyone of the two sides breaks, the whole interconnected balanced system collapses. Finding out the interactive mechanisms and looking for early detection and intervention may be a promising way to prevent the disease progress. This review summarizes the roles of the bone-brain axis in the progression of neurodegenerative diseases. We focus on the effects of BM-derived cells, mainly the microglia-like cells and MSCs, the BM-controlled immune system, and the bone secreted proteins on the brain. Evidence from experimental studies is encouraging, wherein bone-derived cells and factors can influence brain

development, neurotransmitter synthesis, ion homeostasis, neuroinflammation, and neurotoxicant clearance. Therefore, targeting and modulating bone physiological processes can be promising for developing novel therapeutic approaches for neurodegenerative diseases.

AUTHOR CONTRIBUTIONS

ZY drafted the article. ZL and LL revised it critically for important intellectual content. JZ and XC contributed to the revision of the manuscript and figure illustrations. XZ and PX made substantial contributions to the conception and design of the review and gave final approval of the version to be published. All authors contributed to the article and approved the submitted version.

FUNDING

This work was supported in part by grants from National Key R&D Program of China (2016YFC1306601 and 2017YFC1310300), National Natural Science Foundation of China (32071341, 82071416, 31430030, 81901282, 81870992, and 81870856), Natural Science Foundation of Guangdong, China (2017A030308004), Science and Technology Program of Guangzhou, China (201804020011), and Technology project of Guangzhou (2018-1202-SF-0019 and 2019ZD09).

REFERENCES

Afzali, B., Mitchell, P., Lechler, R. I., John, S., and Lombardi, G. (2010). Translational mini-review series on Th17 cells: induction of interleukin-17 production by regulatory T cells. *Clin. Exp. Immunol.* 159, 120–130. doi: 10.1111/j.1365-2249.2009.04038.x

Ahmed, S., Mahmood, Z., Javed, A., Hashmi, S. N., Zerr, I., Zafar, S., et al. (2017). Effect of metformin on adult hippocampal neurogenesis: comparison with donepezil and links to cognition. *J. Mol. Neurosci.* 62, 88–98. doi: 10.1007/s12031-017-0915-z

Ajami, B., Bennett, J. L., Krieger, C., Tetzlaff, W., and Rossi, F. M. (2007). Local self-renewal can sustain CNS microglia maintenance and function throughout adult life. *Nat. Neurosci.* 10, 1538–1543. doi: 10.1038/nn2014

Al Nimer, F., Elliott, C., Bergman, J., Khademi, M., Dring, A. M., Aeinehband, S., et al. (2016). Lipocalin-2 is increased in progressive multiple sclerosis and inhibits remyelination. *Neurol. Neuroimmunol. Neuroinflamm.* 3:e191. doi: 10.1212/NXI.0000000000000191

Alvarez-Erviti, L., Seow, Y., Yin, H., Betts, C., Lakhal, S., and Wood, M. J. (2011). Delivery of siRNA to the mouse brain by systemic injection of targeted exosomes. *Nat. Biotechnol.* 29, 341–345. doi: 10.1038/nbt.1807

Annunziato, F., Cosmi, L., Liotta, F., Maggi, E., and Romagnani, S. (2013). Main features of human T helper 17 cells. *Ann. N Y Acad. Sci.* 1284, 66–70. doi: 10.1111/nyas.12075

Baglio, F., Saresella, M., Preti, M. G., Cabinio, M., Griffanti, L., Marventano, I., et al. (2013). Neuroinflammation and brain functional disconnection in Alzheimer's disease. *Front. Aging Neurosci.* 5:81. doi: 10.3389/fnagi.2013.00081

Bang, O. Y., Kim, E. H., Cha, J. M., and Moon, G. J. (2016). Adult stem cell therapy for stroke: challenges and progress. *J. Stroke* 18, 256–266. doi: 10.5853/jos.2016.01263

Beers, D. R., Henkel, J. S., Zhao, W., Wang, J., Huang, A., Wen, S., et al. (2011). Endogenous regulatory T lymphocytes ameliorate amyotrophic lateral sclerosis in mice and correlate with disease progression in patients with amyotrophic lateral sclerosis. *Brain* 134, 1293–1314. doi: 10.1093/brain/awr074

Bi, F., Huang, C., Tong, J., Qiu, G., Huang, B., Wu, Q., et al. (2013). Reactive astrocytes secrete lcn2 to promote neuron death. *Proc. Natl. Acad. Sci. U S A* 110, 4069–4074. doi: 10.1073/pnas.1218497110

Bonnet, N. (2017). Bone-derived factors: a new gateway to regulate glycemia. *Calcif. Tissue Int.* 100, 174–183. doi: 10.1007/s00223-016-0210-y

Borger, V., Bremer, M., Ferrer-Tur, R., Gockeln, L., Stambouli, O., Becic, A., et al. (2017). Mesenchymal stem/stromal cell-derived extracellular vesicles and their potential as novel immunomodulatory therapeutic agents. *Int. J. Mol. Sci.* 18:1450. doi: 10.3390/ijms18071450

Brazelton, T. R., Rossi, F. M., Keshet, G. I., and Blau, H. M. (2000). From marrow to brain: expression of neuronal phenotypes in adult mice. *Science* 290, 1775–1779. doi: 10.1126/science.290.5497.1775

Breitbach, M., Bostani, T., Roell, W., Xia, Y., Dewald, O., Nygren, J. M., et al. (2007). Potential risks of bone marrow cell transplantation into infarcted hearts. *Blood* 110, 1362–1369. doi: 10.1182/blood-2006-12-063412

Brochard, V., Combadiere, B., Prigent, A., Laouar, Y., Perrin, A., Beray-Berthat, V., et al. (2009). Infiltration of CD4+ lymphocytes into the brain contributes to neurodegeneration in a mouse model of Parkinson disease. *J. Clin. Invest.* 119, 182–192. doi: 10.1172/JCI36470

Browne, T. C., McQuillan, K., McManus, R. M., O'Reilly, J. A., Mills, K. H., and Lynch, M. A. (2013). IFN-γ Production by amyloid β-specific Th1 cells promotes microglial activation and increases plaque burden in a mouse model of Alzheimer's disease. *J. Immunol.* 190, 2241–2251. doi: 10.4049/jimmunol.1200947

Cardoso, A. L., Fernandes, A., Aguilar-Pimentel, J. A., de Angelis, M. H., Guedes, J. R., Brito, M. A., et al. (2018). Towards frailty biomarkers: candidates from genes and pathways regulated in aging and age-related diseases. *Ageing Res. Rev.* 47, 214–277. doi: 10.1016/j.arr.2018.07.004

Carecchio, M., and Comi, C. (2011). The role of osteopontin in neurodegenerative diseases. *J. Alzheimers Dis.* 25, 179–185. doi: 10.3233/JAD-2011-102151

Caricasole, A., Copani, A., Caraci, F., Aronica, E., Rozemuller, A. J., Caruso, A., et al. (2004). Induction of Dickkopf-1, a negative modulator of the Wnt pathway, is associated with neuronal degeneration in Alzheimer's brain. *J. Neurosci.* 24, 6021–6027. doi: 10.1523/JNEUROSCI.1381-04.2004

Castellano, J. M., Kirby, E. D., and Wyss-Coray, T. (2015). Blood-borne revitalization of the aged brain. *JAMA Neurol.* 72, 1191–1194. doi: 10.1001/jamaneurol.2015.1616

Chabas, D., Baranzini, S. E., Mitchell, D., Bernard, C. C., Rittling, S. R., Denhardt, D. T., et al. (2001). The influence of the proinflammatory cytokine, osteopontin, on autoimmune demyelinating disease. *Science* 294, 1731–1735. doi: 10.1126/science.1062960

Chakraborty, S., Kaur, S., Guha, S., and Batra, S. K. (2012). The multifaceted roles of neutrophil gelatinase associated lipocalin (NGAL) in inflammation and cancer. *Biochim. Biophys. Acta* 1826, 129–169. doi: 10.1016/j.bbcan.2012.03.008

Chen, J.-H., Ke, K.-F., Lu, J.-H., Qiu, Y.-H., and Peng, Y.-P. (2015). Protection of TGF-β1 against neuroinflammation and neurodegeneration in Aβ1–42-induced Alzheimer's disease model rats. *PLoS One* 10:e0116549. doi: 10.1371/journal.pone.0116549

Cheng, X., Zhang, G., Zhang, L., Hu, Y., Zhang, K., Sun, X., et al. (2018). Mesenchymal stem cells deliver exogenous miR-21 *via* exosomes to inhibit nucleus pulposus cell apoptosis and reduce intervertebral disc degeneration. *J. Cell. Mol. Med.* 22, 261–276. doi: 10.1111/jcmm.13316

Cho, E.-H., Cho, K.-H., Lee, H. A., and Kim, S.-W. (2013). High serum osteopontin levels are associated with low bone mineral density in postmenopausal women. *J. Korean Med. Sci.* 28, 1496–1499. doi: 10.3346/jkms.2013.28.10.1496

Compston, J. E. (2002). Bone marrow and bone: a functional unit. *J. Endocrinol.* 173, 387–394. doi: 10.1677/joe.0.1730387

Compston, A., and Coles, A. (2008). Multiple sclerosis. *Lancet* 372, 1502–1517. doi: 10.1016/S0140-6736(08)61620-7

Das, M. M., Godoy, M., Chen, S., Moser, V. A., Avalos, P., Roxas, K. M., et al. (2019). Young bone marrow transplantation preserves learning and memory in old mice. *Commun. Biol.* 2:73. doi: 10.1038/s42003-019-0298-5

Dauer, W., and Przedborski, S. (2003). Parkinson's disease: mechanisms and models. *Neuron* 39, 889–909. doi: 10.1016/s0896-6273(03)00568-3

Dean, C., Liu, H., Dunning, F. M., Chang, P. Y., Jackson, M. B., and Chapman, E. R. (2009). Synaptotagmin-IV modulates synaptic function and

long-term potentiation by regulating BDNF release. *Nat. Neurosci.* 12, 767–776. doi: 10.1038/nn.2315

Dennie, D., Louboutin, J. P., and Strayer, D. S. (2016). Migration of bone marrow progenitor cells in the adult brain of rats and rabbits. *World J. Stem Cells* 8, 136–157. doi: 10.4252/wjsc.v8.i4.136

Djukic, M., Mildner, A., Schmidt, H., Czesnik, D., Bruck, W., Priller, J., et al. (2006). Circulating monocytes engraft in the brain, differentiate into microglia and contribute to the pathology following meningitis in mice. *Brain* 129, 2394–2403. doi: 10.1093/brain/awl206

Ducy, P. (2011). The role of osteocalcin in the endocrine cross-talk between bone remodelling and energy metabolism. *Diabetologia* 54, 1291–1297. doi: 10.1007/s00125-011-2155-z

Ducy, P., Desbois, C., Boyce, B., Pinero, G., Story, B., Dunstan, C., et al. (1996). Increased bone formation in osteocalcin-deficient mice. *Nature* 382, 448–452. doi: 10.1038/382448a0

Dugger, B. N., and Dickson, D. W. (2017). Pathology of neurodegenerative diseases. *Cold Spring Harb. Perspect. Biol.* 9:a028035. doi: 10.1101/cshperspect.a028035

El Khoury, J., and Luster, A. D. (2008). Mechanisms of microglia accumulation in Alzheimer's disease: therapeutic implications. *Trends Pharmacol. Sci.* 29, 626–632. doi: 10.1016/j.tips.2008.08.004

Emanuele, E., Peros, E., Scioli, G. A., D'Angelo, A., Olivieri, C., Montagna, L., et al. (2004). Plasma osteoprotegerin as a biochemical marker for vascular dementia and Alzheimer's disease. *Int. J. Mol. Med.* 13, 849–853. doi: 10.3892/ijmm.13.6.849

Fatemi, I., Delrobaee, F., Bahmani, M., Shamsizadeh, A., and Allahtavakoli, M. (2019). The effect of the anti-diabetic drug metformin on behavioral manifestations associated with ovariectomy in mice. *Neurosci. Lett.* 690, 95–98. doi: 10.1016/j.neulet.2018.10.024

Fisher, Y., Strominger, I., Biton, S., Nemirovsky, A., Baron, R., and Monsonego, A. (2014). Th1 polarization of T cells injected into the cerebrospinal fluid induces brain immunosurveillance. *J. Immunol.* 192, 92–102. doi: 10.4049/jimmunol.1301707

Fortress, A. M., and Frick, K. M. (2016). Hippocampal Wnt signaling: memory regulation and hormone interactions. *Neuroscientist* 22, 278–294. doi: 10.1177/1073858415574728

Freitas, G. R. R., da Luz Fernandes, M., Agena, F., Jaluul, O., Silva, S. C., Lemos, F. B. C., et al. (2019). Aging and end stage renal disease cause a decrease in absolute circulating lymphocyte counts with a shift to a memory profile and diverge in treg population. *Aging Dis.* 10, 49–61. doi: 10.14336/AD.2018.0318

Fritzsching, B., Haas, J., Konig, F., Kunz, P., Fritzsching, E., Poschl, J., et al. (2011). Intracerebral human regulatory T cells: analysis of CD4+ CD25+ FOXP3+ T cells in brain lesions and cerebrospinal fluid of multiple sclerosis patients. *PLoS One* 6:e17988. doi: 10.1371/journal.pone.0017988

Gallina, C., Turinetto, V., and Giachino, C. (2015). A new paradigm in cardiac regeneration: the mesenchymal stem cell secretome. *Stem Cells Int.* 2015:765846. doi: 10.1155/2015/765846

Garcia, K. O., Ornellas, F. L., Martin, P. K., Patti, C. L., Mello, L. E., Frussa-Filho, R., et al. (2014). Therapeutic effects of the transplantation of VEGF overexpressing bone marrow mesenchymal stem cells in the hippocampus of murine model of Alzheimer's disease. *Front. Aging Neurosci.* 6:30. doi: 10.3389/fnagi.2014.00030

Garza-Lombó, C., Schroder, A., Reyes-Reyes, E. M., and Franco, R. (2018). mTOR/AMPK signaling in the brain: cell metabolism, proteostasis and survival. *Curr. Opin. Toxicol.* 8, 102–110. doi: 10.1016/j.cotox.2018.05.002

Geiger, H., de Haan, G., and Florian, M. C. (2013). The ageing haematopoietic stem cell compartment. *Nat. Rev. Immunol.* 13, 376–389. doi: 10.1038/nri3433

Gifre, L., Ruiz-Gaspà, S., Monegal, A., Nomdedeu, B., Filella, X., Guañabens, N., et al. (2013). Effect of glucocorticoid treatment on Wnt signalling antagonists (sclerostin and Dkk-1) and their relationship with bone turnover. *Bone* 57, 272–276. doi: 10.1016/j.bone.2013.08.016

Goldman, J. E., Yen, S. H., Chiu, F. C., and Peress, N. S. (1983). Lewy bodies of Parkinson's disease contain neurofilament antigens. *Science* 221, 1082–1084. doi: 10.1126/science.6308771

Goverman, J. (2009). Autoimmune T cell responses in the central nervous system. *Nat. Rev. Immunol.* 9, 393–407. doi: 10.1038/nri2550

Goverman, J., Perchellet, A., and Huseby, E. S. (2005). The role of CD8(+) T cells in multiple sclerosis and its animal models. *Curr. Drug Targets Inflamm. Allergy* 4, 239–245. doi: 10.2174/1568010053586264

Guo, X.-Z., Shan, C., Hou, Y.-F., Zhu, G., Tao, B., Sun, L. H., et al. (2018). Osteocalcin ameliorates motor dysfunction in a 6-hydroxydopamine-induced Parkinson's disease rat model through AKT/GSK3β signaling. *Front. Mol. Neurosci.* 11:343. doi: 10.3389/fnmol.2018.00343

Hall, J., Thomas, K. L., and Everitt, B. J. (2000). Rapid and selective induction of BDNF expression in the hippocampus during contextual learning. *Nat. Neurosci.* 3, 533–535. doi: 10.1038/75698

Han, K. H., Arlian, B. M., Macauley, M. S., Paulson, J. C., and Lerner, R. A. (2018). Migration-based selections of antibodies that convert bone marrow into trafficking microglia-like cells that reduce brain amyloid β. *Proc. Natl. Acad. Sci. U S A* 115, E372–E381. doi: 10.1073/pnas.1719259115

Han, Y., You, X., Xing, W., Zhang, Z., and Zou, W. (2018). Paracrine and endocrine actions of bone-the functions of secretory proteins from osteoblasts, osteocytes, and osteoclasts. *Bone Res.* 6:16. doi: 10.1038/s41413-018-0019-6

Harach, T., Jammes, F., Muller, C., Duthilleul, N., Cheatham, V., Zufferey, V., et al. (2017). Administrations of human adult ischemia-tolerant mesenchymal stem cells and factors reduce amyloid β pathology in a mouse model of Alzheimer's disease. *Neurobiol. Aging* 51, 83–96. doi: 10.1016/j.neurobiolaging.2016.11.009

Harty, J. T., Tvinnereim, A. R., and White, D. W. (2000). CD8+ T cell effector mechanisms in resistance to infection. *Annu. Rev. Immunol.* 18, 275–308. doi: 10.1146/annurev.immunol.18.1.275

Hauschka, P. V., Lian, J. B., and Gallop, P. M. (1975). Direct identification of the calcium-binding amino acid, γ-carboxyglutamate, in mineralized tissue. *Proc. Natl. Acad. Sci. U S A* 72, 3925–3929. doi: 10.1073/pnas.72.10.3925

He, B., Yao, Q., Liang, Z., Lin, J., Xie, Y., Li, S., et al. (2016). The dose of intravenously transplanted bone marrow stromal cells determines the therapeutic effect on vascular remodeling in a rat model of ischemic stroke. *Cell Transplant.* 25, 2173–2185. doi: 10.3727/096368916X692627

Hemmings, B. A., and Restuccia, D. F. (2012). PI3K-PKB/Akt pathway. *Cold Spring Harb. Perspect. Biol.* 4:a011189. doi: 10.1101/cshperspect.a011189

Hofbauer, L. C., Cepok, S., and Hemmer, B. (2004). Osteoprotegerin is highly expressed in the spinal cord and cerebrospinal fluid. *Acta Neuropathol.* 107, 575–577, author reply 578. doi: 10.1007/s00401-004-0854-y

Huang, X., Jiang, Y., and Xia, W. (2013). FGF23 and phosphate wasting disorders. *Bone Res.* 1, 120–132. doi: 10.4248/BR201302002

Huang, Y., Liu, L., and Liu, A. (2018). Dickkopf-1: current knowledge and related diseases. *Life Sci.* 209, 249–254. doi: 10.1016/j.lfs.2018.08.019

Hur, E. M., Youssef, S., Haws, M. E., Zhang, S. Y., Sobel, R. A., and Steinman, L. (2007). Osteopontin-induced relapse and progression of autoimmune brain disease through enhanced survival of activated T cells. *Nat. Immunol.* 8, 74–83. doi: 10.1038/ni1415

Huseby, E. S., Liggitt, D., Brabb, T., Schnabel, B., Ohlen, C., and Goverman, J. (2001). A pathogenic role for myelin-specific CD8(+) T cells in a model for multiple sclerosis. *J. Exp. Med.* 194, 669–676. doi: 10.1084/jem.194.5.669

Hwang, S. M., Wilson, P. D., Laskin, J. D., and Denhardt, D. T. (1994). Age and development-related changes in osteopontin and nitric oxide synthase mRNA levels in human kidney proximal tubule epithelial cells: contrasting responses to hypoxia and reoxygenation. *J. Cell. Physiol.* 160, 61–68. doi: 10.1002/jcp.1041600108

Iczkiewicz, J., Broom, L., Cooper, J. D., Wong, A. M., Rose, S., and Jenner, P. (2010). The RGD-containing peptide fragment of osteopontin protects tyrosine hydroxylase positive cells against toxic insult in primary ventral mesencephalic cultures and in the rat substantia nigra. *J. Neurochem.* 114, 1792–1804. doi: 10.1111/j.1471-4159.2010.06896.x

Iczkiewicz, J., Rose, S., and Jenner, P. (2004). Osteopontin (Eta-1) is present in the rat basal ganglia. *Mol. Brain Res.* 132, 64–72. doi: 10.1016/j.molbrainres.2004.09.013

Inestrosa, N. C., and Varela-Nallar, L. (2014). Wnt signaling in the nervous system and in Alzheimer's disease. *J. Mol. Cell Biol.* 6, 64–74. doi: 10.1093/jmcb/mjt051

Ip, J. P. K., Nocon, A. L., Hofer, M. J., Lim, S. L., Muller, M., and Campbell, I. L. (2011). Lipocalin 2 in the central nervous system host response to systemic lipopolysaccharide administration. *J. Neuroinflammation* 8:124. doi: 10.1186/1742-2094-8-124

Iyer, A., Zurolo, E., Prabowo, A., Fluiter, K., Spliet, W. G., van Rijen, P. C., et al. (2012). MicroRNA-146a: a key regulator of astrocyte-mediated inflammatory response. *PLoS One* 7:e44789. doi: 10.1371/journal.pone.0044789

Jamshidian, A., Shaygannejad, V., Pourazar, A., Zarkesh-Esfahani, S. H., and Gharagozloo, M. (2013). Biased Treg/Th17 balance away from regulatory toward inflammatory phenotype in relapsed multiple sclerosis and its correlation with severity of symptoms. *J. Neuroimmunol.* 262, 106–112. doi: 10.1016/j.jneuroim.2013.06.007

Jansson, M., Panoutsakopoulou, V., Baker, J., Klein, L., and Cantor, H. (2002). Cutting edge: attenuated experimental autoimmune encephalomyelitis in eta-1/osteopontin-deficient mice. *J. Immunol.* 168, 2096–2099. doi: 10.4049/jimmunol.168.5.2096

Jha, N. K., Jha, S. K., Kumar, D., Kejriwal, N., Sharma, R., Ambasta, R. K., et al. (2015). Impact of insulin degrading enzyme and neprilysin in Alzheimer's disease biology: characterization of putative cognates for therapeutic applications. *J. Alzheimers Dis.* 48, 891–917. doi: 10.3233/JAD-150379

Joshi, P., Turola, E., Ruiz, A., Bergami, A., Libera, D. D., Benussi, L., et al. (2014). Microglia convert aggregated amyloid-β into neurotoxic forms through the shedding of microvesicles. *Cell Death Differ.* 21, 582–593. doi: 10.1038/cdd.2013.180

Kanamaru, T., Kamimura, N., Yokota, T., Nishimaki, K., Iuchi, K., Lee, H., et al. (2015). Intravenous transplantation of bone marrow-derived mononuclear cells prevents memory impairment in transgenic mouse models of Alzheimer's disease. *Brain Res.* 1605, 49–58. doi: 10.1016/j.brainres.2015.02.011

Kang, H. G., Park, H. Y., Ryu, H. U., and Suk, S. H. (2018). Bone mineral loss and cognitive impairment: the PRESENT project. *Medicine* 97:e12755. doi: 10.1097/MD.0000000000012755

Karsenty, G., and Ferron, M. (2012). The contribution of bone to whole-organism physiology. *Nature* 481, 314–320. doi: 10.1038/nature10763

Karsenty, G., and Olson, E. N. (2016). Bone and muscle endocrine functions: unexpected paradigms of inter-organ communication. *Cell* 164, 1248–1256. doi: 10.1016/j.cell.2016.02.043

Katila, N., Bhurtel, S., Shadfar, S., Srivastav, S., Neupane, S., Ojha, U., et al. (2017). Metformin lowers α-synuclein phosphorylation and upregulates neurotrophic factor in the MPTP mouse model of Parkinson's disease. *Neuropharmacology* 125, 396–407. doi: 10.1016/j.neuropharm.2017.08.015

Kawanishi, S., Takata, K., Itezono, S., Nagayama, H., Konoya, S., Chisaki, Y., et al. (2018). Bone-marrow-derived microglia-like cells ameliorate brain amyloid pathology and cognitive impairment in a mouse model of Alzheimer's disease. *J. Alzheimers Dis.* 64, 563–585. doi: 10.3233/JAD-170994

Ke, H. Z., Richards, W. G., Li, X., and Ominsky, M. S. (2012). Sclerostin and Dickkopf-1 as therapeutic targets in bone diseases. *Endocr. Rev.* 33, 747–783. doi: 10.1210/er.2011-1060

Kebir, H., Kreymborg, K., Ifergan, I., Dodelet-Devillers, A., Cayrol, R., Bernard, M., et al. (2007). Human TH17 lymphocytes promote blood-brain barrier disruption and central nervous system inflammation. *Nat. Med.* 13, 1173–1175. doi: 10.1038/nm1651

Khan, S. A., Lopez-Chua, C. A., Zhang, J., Fisher, L. W., Sorensen, E. S., and Denhardt, D. T. (2002). Soluble osteopontin inhibits apoptosis of adherent endothelial cells deprived of growth factors. *J. Cell Biochem.* 85, 728–736. doi: 10.1002/jcb.10170

Khrimian, L., Obri, A., Ramos-Brossier, M., Rousseaud, A., Moriceau, S., Nicot, A. S., et al. (2017). Gpr158 mediates osteocalcin's regulation of cognition. *J. Exp. Med.* 214, 2859–2873. doi: 10.1084/jem.20171320

Kim, B.-W., Jeong, K. H., Kim, J.-H., Jin, M., Kim, J.-H., Lee, M.-G., et al. (2016). Pathogenic upregulation of glial lipocalin-2 in the Parkinsonian dopaminergic System. *J. Neurosci.* 36, 5608–5622. doi: 10.1523/JNEUROSCI.4261-15.2016

Kim, J.-H., Ko, P.-W., Lee, H.-W., Jeong, J.-Y., Lee, M.-G., Kim, J.-H., et al. (2017). Astrocyte-derived lipocalin-2 mediates hippocampal damage and cognitive deficits in experimental models of vascular dementia. *Glia* 65, 1471–1490. doi: 10.1002/glia.23174

Kobilo, T., Guerrieri, D., Zhang, Y., Collica, S. C., Becker, K. G., and van Praag, H. (2014). AMPK agonist AICAR improves cognition and motor coordination in young and aged mice. *Learn. Mem.* 21, 119–126. doi: 10.1101/lm.033332.113

Koduah, P., Paul, F., and Dorr, J.-M. (2017). Vitamin D in the prevention, prediction and treatment of neurodegenerative and neuroinflammatory diseases. *EPMA J.* 8, 313–325. doi: 10.1007/s13167-017-0120-8

Kokovay, E., and Cunningham, L. A. (2005). Bone marrow-derived microglia contribute to the neuroinflammatory response and express iNOS in the MPTP mouse model of Parkinson's disease. *Neurobiol. Dis.* 19, 471–478. doi: 10.1016/j.nbd.2005.01.023

Koronyo, Y., Salumbides, B. C., Sheyn, J., Pelissier, L., Li, S., Ljubimov, V., et al. (2015). Therapeutic effects of glatiramer acetate and grafted CD115(+) monocytes in a mouse model of Alzheimer's disease. *Brain* 138, 2399–2422. doi: 10.1093/brain/awv150

Kubota, K., Nakano, M., Kobayashi, E., Mizue, Y., Chikenji, T., Otani, M., et al. (2018). An enriched environment prevents diabetes-induced cognitive impairment in rats by enhancing exosomal miR-146a secretion from endogenous bone marrow-derived mesenchymal stem cells. *PLoS One* 13:e0204252. doi: 10.1371/journal.pone.0204252

Kunert, S. K., Hartmann, H., Haffner, D., and Leifheit-Nestler, M. (2017). Klotho and fibroblast growth factor 23 in cerebrospinal fluid in children. *J. Bone Miner. Metab.* 35, 215–226. doi: 10.1007/s00774-016-0746-y

Kuroda, E., Nishimura, K., Kawanishi, S., Sueyoshi, M., Ueno, F., Toji, Y., et al. (2020a). Mouse bone marrow-derived microglia-like cells secrete transforming growth factor-β1 and promote microglial aβ phagocytosis and reduction of brain aβ. *Neuroscience* 438, 217–228. doi: 10.1016/j.neuroscience.2020.05.004

Kuroda, E., Takata, K., Nishimura, K., Oka, H., Sueyoshi, M., Aitani, M., et al. (2020b). Peripheral blood-derived microglia-like cells decrease amyloid-β burden and ameliorate cognitive impairment in a mouse model of Alzheimer's disease. *J. Alzheimers Dis.* 73, 413–429. doi: 10.3233/JAD-190974

Lampron, A., Gosselin, D., and Rivest, S. (2011). Targeting the hematopoietic system for the treatment of Alzheimer's disease. *Brain Behav. Immun.* 25, S71–79. doi: 10.1016/j.bbi.2010.12.018

Laszczyk, A. M., Nettles, D., Pollock, T. A., Fox, S., Garcia, M. L., Wang, J., et al. (2019). FGF-23 deficiency impairs hippocampal-dependent cognitive function. *eNeuro* 6:ENEURO.0469-18.2019. doi: 10.1523/ENEURO.0469-18.2019

Lebson, L., Nash, K., Kamath, S., Herber, D., Carty, N., Lee, D. C., et al. (2010). Trafficking CD11b-positive blood cells deliver therapeutic genes to the brain of amyloid-depositing transgenic mice. *J. Neurosci.* 30, 9651–9658. doi: 10.1523/JNEUROSCI.0329-10.2010

Lee, J. S., Hong, J. M., Moon, G. J., Lee, P. H., Ahn, Y. H., Bang, O. Y., et al. (2010). A long-term follow-up study of intravenous autologous mesenchymal stem cell transplantation in patients with ischemic stroke. *Stem Cells* 28, 1099–1106. doi: 10.1002/stem.430

Lee, J. K., Jin, H. K., and Bae, J.-S. (2009). Bone marrow-derived mesenchymal stem cells reduce brain amyloid-β deposition and accelerate the activation of microglia in an acutely induced Alzheimer's disease mouse model. *Neurosci. Lett.* 450, 136–141. doi: 10.1016/j.neulet.2008.11.059

Lee, S., Lee, W.-H., Lee, M.-S., Mori, K., and Suk, K. (2012). Regulation by lipocalin-2 of neuronal cell death, migration, and morphology. *J. Neurosci. Res.* 90, 540–550. doi: 10.1002/jnr.22779

Lee, J. K., Schuchman, E. H., Jin, H. K., and Bae, J. S. (2012). Soluble CCL5 derived from bone marrow-derived mesenchymal stem cells and activated by amyloid β ameliorates Alzheimer's disease in mice by recruiting bone marrow-induced microglia immune responses. *Stem Cells* 30, 1544–1555. doi: 10.1002/stem.1125

Le Goff, B., Bouvard, B., Lequerre, T., Lespessailles, E., Marotte, H., Pers, Y. M., et al. (2019). Implication of IL-17 in bone loss and structural damage in inflammatory rheumatic diseases. *Mediators Inflamm.* 2019:8659302. doi: 10.1155/2019/8659302

Lei, Q., Liu, T., Gao, F., Xie, H., Sun, L., Zhao, A., et al. (2017). Microvesicles as potential biomarkers for the identification of senescence in human mesenchymal stem cells. *Theranostics* 7, 2673–2689. doi: 10.7150/thno.18915

Levy, E. (2017). Exosomes in the diseased brain: first insights from *in vivo* studies. *Front. Neurosci.* 11:142. doi: 10.3389/fnins.2017.00142

Li, Y., Yang, Y.-Y., Ren, J.-L., Xu, F., Chen, F.-M., and Li, A. (2017). Exosomes secreted by stem cells from human exfoliated deciduous teeth contribute to functional recovery after traumatic brain injury by shifting microglia M1/M2 polarization in rats. *Stem Cell Res. Ther.* 8:198. doi: 10.1186/s13287-017-0648-5

Li, Z., Ye, H., Cai, X., Sun, W., He, B., Yang, Z., et al. (2019). Bone marrow-mesenchymal stem cells modulate microglial activation in the peri-infarct area in rats during the acute phase of stroke. *Brain Res. Bull.* 153, 324–333. doi: 10.1016/j.brainresbull.2019.10.001

Liang, Z., Zhao, Y., Ruan, L., Zhu, L., Jin, K., Zhuge, Q., et al. (2017). Impact of aging immune system on neurodegeneration and potential immunotherapies. *Prog. Neurobiol.* 157, 2–28. doi: 10.1016/j.pneurobio.2017.07.006

Lin, Y. H., and Yang-Yen, H. F. (2001). The osteopontin-CD44 survival signal involves activation of the phosphatidylinositol 3-kinase/Akt signaling pathway. *J. Biol. Chem.* 276, 46024–46030. doi: 10.1074/jbc.M105132200

Liu, P., Chen, L., Bai, X., Karaplis, A., Miao, D., and Gu, N. (2011). Impairment of spatial learning and memory in transgenic mice overexpressing human fibroblast growth factor-23. *Brain Res.* 1412, 9–17. doi: 10.1016/j.brainres.2011.07.028

Liu, Q., Xu, X., Yang, Z., Liu, Y., Wu, X., Huang, Z., et al. (2019). Metformin alleviates the bone loss induced by ketogenic diet: an *in vivo* study in mice. *Calcif. Tissue Int.* 104, 59–69. doi: 10.1007/s00223-018-0468-3

Livingston, G., Sommerlad, A., Orgeta, V., Costafreda, S. G., Huntley, J., Ames, D., et al. (2017). Dementia prevention, intervention, and care. *Lancet* 390, 2673–2734. doi: 10.1016/S0140-6736(17)31363-6

Lueg, G., Gross, C. C., Lohmann, H., Johnen, A., Kemmling, A., Deppe, M., et al. (2015). Clinical relevance of specific T-cell activation in the blood and cerebrospinal fluid of patients with mild Alzheimer's disease. *Neurobiol. Aging* 36, 81–89. doi: 10.1016/j.neurobiolaging.2014.08.008

Lund, S. A., Giachelli, C. M., and Scatena, M. (2009). The role of osteopontin in inflammatory processes. *J. Cell Commun. Signal.* 3, 311–322. doi: 10.1007/s12079-009-0068-0

Lv, L., Tan, X., Peng, X., Bai, R., Xiao, Q., Zou, T., et al. (2020). The relationships of vitamin D, vitamin D receptor gene polymorphisms and vitamin D supplementation with Parkinson's disease. *Transl. Neurodegener.* 9:34. doi: 10.1186/s40035-020-00213-2

Maetzler, W., Berg, D., Schalamberidze, N., Melms, A., Schott, K., Mueller, J. C., et al. (2007). Osteopontin is elevated in Parkinson's disease and its absence leads to reduced neurodegeneration in the MPTP model. *Neurobiol. Dis.* 25, 473–482. doi: 10.1016/j.nbd.2006.10.020

Maiti, P., Manna, J., and Dunbar, G. L. (2017). Current understanding of the molecular mechanisms in Parkinson's disease: targets for potential treatments. *Transl. Neurodegener.* 6:28. doi: 10.1186/s40035-017-0099-z

Malm, T., Loppi, S., and Kanninen, K. M. (2016). Exosomes in Alzheimer's disease. *Neurochem. Int.* 97, 193–199. doi: 10.1016/j.neuint.2016.04.011

Marebwa, B. K., Adams, R. J., Magwood, G. S., Kindy, M., Wilmskoetter, J., Wolf, M., et al. (2018). Fibroblast growth factor23 is associated with axonal integrity and neural network architecture in the human frontal lobes. *PLoS One* 13:e0203460. doi: 10.1371/journal.pone.0203460

Maryanovich, M., Takeishi, S., and Frenette, P. S. (2018). Neural regulation of bone and bone marrow. *Cold Spring Harb. Perspect. Med.* 8:a031344. doi: 10.1101/cshperspect.a031344

Marzo, A., Galli, S., Lopes, D., McLeod, F., Podpolny, M., Segovia-Roldan, M., et al. (2016). Reversal of synapse degeneration by restoring wnt signaling in the adult hippocampus. *Curr. Biol.* 26, 2551–2561. doi: 10.1016/j.cub.2016.07.024

Matrisciano, F., Busceti, C. L., Bucci, D., Orlando, R., Caruso, A., Molinaro, G., et al. (2011). Induction of the Wnt antagonist Dickkopf-1 is involved in stress-induced hippocampal damage. *PLoS One* 6:e16447. doi: 10.1371/journal.pone.0016447

McGrath, E. R., Himali, J. J., Levy, D., Conner, S. C., Pase, M. P., Abraham, C. R., et al. (2019). Circulating fibroblast growth factor 23 levels and incident dementia: the Framingham heart study. *PLoS One* 14:e0213321. doi: 10.1371/journal.pone.0213321

Mera, P., Laue, K., Ferron, M., Confavreux, C., Wei, J., Galan-Diez, M., et al. (2016). Osteocalcin signaling in myofibers is necessary and sufficient for optimum adaptation to exercise. *Cell Metab.* 23, 1078–1092. doi: 10.1016/j.cmet.2016.05.004

Mesquita, S. D., Ferreira, A. C., Falcao, A. M., Sousa, J. C., Oliveira, T. G., Correia-Neves, M., et al. (2014). Lipocalin 2 modulates the cellular response to amyloid β. *Cell Death Differ.* 21, 1588–1599. doi: 10.1038/cdd.2014.68

Mezey, E., and Chandross, K. J. (2000). Bone marrow: a possible alternative source of cells in the adult nervous system. *Eur. J. Pharmacol.* 405, 297–302. doi: 10.1016/s0014-2999(00)00561-6

Mezey, E., Chandross, K. J., Harta, G., Maki, R. A., and McKercher, S. R. (2000). Turning blood into brain: cells bearing neuronal antigens generated *in vivo* from bone marrow. *Science* 290, 1779–1782. doi: 10.1126/science.290.5497.1779

Mildner, A., Schmidt, H., Nitsche, M., Merkler, D., Hanisch, U. K., Mack, M., et al. (2007). Microglia in the adult brain arise from Ly-6ChiCCR2+ monocytes only under defined host conditions. *Nat. Neurosci.* 10, 1544–1553. doi: 10.1038/nn2015

Mizokami, A., Kawakubo-Yasukochi, T., and Hirata, M. (2017). Osteocalcin and its endocrine functions. *Biochem. Pharmacol.* 132, 1–8. doi: 10.1016/j.bcp.2017.02.001

Monroe, D. G., McGee-Lawrence, M. E., Oursler, M. J., and Westendorf, J. J. (2012). Update on Wnt signaling in bone cell biology and bone disease. *Gene* 492, 1–18. doi: 10.1016/j.gene.2011.10.044

Morishita, K., Shirai, A., Kubota, M., Katakura, Y., Nabeshima, Y., Takeshige, K., et al. (2001). The progression of aging in klotho mutant mice can be modified by dietary phosphorus and zinc. *J. Nutr.* 131, 3182–3188. doi: 10.1093/jn/131.12.3182

Mosialou, I., Shikhel, S., Liu, J.-M., Maurizi, A., Luo, N., He, Z., et al. (2017). MC4R-dependent suppression of appetite by bone-derived lipocalin 2. *Nature* 543, 385–390. doi: 10.1038/nature21697

Mourya, A., Akhtar, A., Ahuja, S., Sah, S. P., and Kumar, A. (2018). Synergistic action of ursolic acid and metformin in experimental model of insulin resistance and related behavioral alterations. *Eur. J. Pharmacol.* 835, 31–40. doi: 10.1016/j.ejphar.2018.07.056

Naaldijk, Y., Jäger, C., Fabian, C., Leovsky, C., Bluher, A., Rudolph, L., et al. (2017). Effect of systemic transplantation of bone marrow-derived mesenchymal stem cells on neuropathology markers in APP/PS1 Alzheimer mice. *Neuropathol. Appl. Neurobiol.* 43, 299–314. doi: 10.1111/nan.12319

Nakano, M., Nagaishi, K., Konari, N., Saito, Y., Chikenji, T., Mizue, Y., et al. (2016). Bone marrow-derived mesenchymal stem cells improve diabetes-induced cognitive impairment by exosome transfer into damaged neurons and astrocytes. *Sci. Rep.* 6:24805. doi: 10.1038/srep24805

Nakazawa, K., Quirk, M. C., Chitwood, R. A., Watanabe, M., Yeckel, M. F., Sun, L. D., et al. (2002). Requirement for hippocampal CA3 NMDA receptors in associative memory recall. *Science* 297, 211–218. doi: 10.1126/science.1071795

Naudé, P. J., Nyakas, C., Eiden, L. E., Ait-Ali, D., van der Heide, R., Engelborghs, S., et al. (2012). Lipocalin 2: novel component of proinflammatory signaling in Alzheimer's disease. *FASEB J.* 26, 2811–2823. doi: 10.1096/fj.11-202457

Obri, A., Khrimian, L., Karsenty, G., and Oury, F. (2018). Osteocalcin in the brain: from embryonic development to age-related decline in cognition. *Nat. Rev. Endocrinol.* 14, 174–182. doi: 10.1038/nrendo.2017.181

Ohsawa, I., Nishimaki, K., Murakami, Y., Suzuki, Y., Ishikawa, M., and Ohta, S. (2008). Age-dependent neurodegeneration accompanying memory loss in transgenic mice defective in mitochondrial aldehyde dehydrogenase 2 activity. *J. Neurosci.* 28, 6239–6249. doi: 10.1523/JNEUROSCI.4956-07.2008

Ortiz-Matamoros, A., and Arias, C. (2018). Chronic infusion of Wnt7a, Wnt5a and Dkk-1 in the adult hippocampus induces structural synaptic changes and modifies anxiety and memory performance. *Brain Res. Bull.* 139, 243–255. doi: 10.1016/j.brainresbull.2018.03.008

Oury, F., Khrimian, L., Denny, C. A., Gardin, A., Chamouni, A., Goeden, N., et al. (2013). Maternal and offspring pools of osteocalcin influence brain development and functions. *Cell* 155, 228–241. doi: 10.1016/j.cell.2013.08.042

Pellicano, M., Larbi, A., Goldeck, D., Colonna-Romano, G., Buffa, S., Bulati, M., et al. (2012). Immune profiling of Alzheimer patients. *J. Neuroimmunol.* 242, 52–59. doi: 10.1016/j.jneuroim.2011.11.005

Perry, E. K., Johnson, M., Ekonomou, A., Perry, R. H., Ballard, C., and Attems, J. (2012). Neurogenic abnormalities in Alzheimer's disease differ between stages of neurogenesis and are partly related to cholinergic pathology. *Neurobiol. Dis.* 47, 155–162. doi: 10.1016/j.nbd.2012.03.033

Pinyopornpanish, K., Chattipakorn, N., and Chattipakorn, S. C. (2019). Lipocalin-2: its perspectives in brain pathology and possible roles in cognition. *J. Neuroendocrinol.* 31:e12779. doi: 10.1111/jne.12779

Poewe, W., Seppi, K., Tanner, C. M., Halliday, G. M., Brundin, P., Volkmann, J., et al. (2017). Parkinson disease. *Nat. Rev. Dis. Primers* 3:17013. doi: 10.1038/nrdp.2017.13

Poole, K. E., van Bezooijen, R. L., Loveridge, N., Hamersma, H., Papapoulos, S. E., Lowik, C. W., et al. (2005). Sclerostin is a delayed secreted product of osteocytes that inhibits bone formation. *FASEB J.* 19, 1842–1844. doi: 10.1096/fj.05-4221fje

Price, P. A., Otsuka, A. A., Poser, J. W., Kristaponis, J., and Raman, N. (1976). Characterization of a γ-carboxyglutamic acid-containing protein from bone. *Proc. Natl. Acad. Sci. U S A* 73, 1447–1451. doi: 10.1073/pnas.73.5.1447

Priller, J., Flügel, A., Wehner, T., Boentert, M., Haas, C. A., Prinz, M., et al. (2001a). Targeting gene-modified hematopoietic cells to the central nervous system: use of green fluorescent protein uncovers microglial engraftment. *Nat. Med.* 7, 1356–1361. doi: 10.1038/nm1201-1356

Priller, J., Persons, D. A., Klett, F. F., Kempermann, G., Kreutzberg, G. W., and Dirnagl, U. (2001b). Neogenesis of cerebellar Purkinje neurons from gene-marked bone marrow cells *in vivo*. *J. Cell Biol.* 155, 733–738. doi: 10.1083/jcb.200105103

Purro, S. A., Dickins, E. M., and Salinas, P. C. (2012). The secreted Wnt antagonist Dickkopf-1 is required for amyloid β-mediated synaptic loss. *J. Neurosci.* 32, 3492–3498. doi: 10.1523/JNEUROSCI.4562-11.2012

Purro, S. A., Galli, S., and Salinas, P. C. (2014). Dysfunction of Wnt signaling and synaptic disassembly in neurodegenerative diseases. *J. Mol. Cell Biol.* 6, 75–80. doi: 10.1093/jmcb/mjt049

Qin, C., Lu, Y., Wang, K., Bai, L., Shi, G., Huang, Y., et al. (2020). Transplantation of bone marrow mesenchymal stem cells improves cognitive deficits and alleviates neuropathology in animal models of Alzheimer's disease: a meta-analytic review on potential mechanisms. *Transl. Neurodegener.* 9:20. doi: 10.1186/s40035-020-00199-x

Querfurth, H. W., and LaFerla, F. M. (2010). Alzheimer's disease. *N. Engl. J. Med.* 362, 329–344. doi: 10.1056/NEJMra0909142

Rajendran, L., Honsho, M., Zahn, T. R., Keller, P., Geiger, K. D., Verkade, P., et al. (2006). Alzheimer's disease β-amyloid peptides are released in association with exosomes. *Proc. Natl. Acad. Sci. U S A* 103, 11172–11177. doi: 10.1073/pnas.0603838103

Reinholt, F. P., Hultenby, K., Oldberg, A., and Heinegard, D. (1990). Osteopontin—a possible anchor of osteoclasts to bone. *Proc. Natl. Acad. Sci. U S A* 87, 4473–4475. doi: 10.1073/pnas.87.12.4473

Ren, C., Gu, X., Li, H., Lei, S., Wang, Z., Wang, J., et al. (2019). The role of DKK1 in Alzheimer's disease: a potential intervention point of brain damage prevention? *Pharmacol. Res.* 144, 331–335. doi: 10.1016/j.phrs.2019.04.033

Rentsendorj, A., Sheyn, J., Fuchs, D. T., Daley, D., Salumbides, B. C., Schubloom, H. E., et al. (2018). A novel role for osteopontin in macrophage-mediated amyloid-β clearance in Alzheimer's models. *Brain Behav. Immun.* 67, 163–180. doi: 10.1016/j.bbi.2017.08.019

Reza-Zaldivar, E. E., Hernandez-Sapiens, M. A., Minjarez, B., Gutierrez-Mercado, Y. K., Marquez-Aguirre, A. L., and Canales-Aguirre, A. A. (2018). Potential effects of MSC-derived exosomes in neuroplasticity in Alzheimer's disease. *Front. Cell. Neurosci.* 12:317. doi: 10.3389/fncel.2018.00317

Rittling, S. R., and Singh, R. (2015). Osteopontin in Immune-mediated Diseases. *J. Dent. Res.* 94, 1638–1645. doi: 10.1177/0022034515605270

Rochette, L., Meloux, A., Rigal, E., Zeller, M., Malka, G., Cottin, Y., et al. (2019). The role of osteoprotegerin in vascular calcification and bone metabolism: the basis for developing new therapeutics. *Calcif. Tissue Int.* 105, 239–251. doi: 10.1007/s00223-019-00573-6

Romagnani, S. (2014). T cell subpopulations. *Chem. Immunol. Allergy* 100, 155–164. doi: 10.1159/000358622

Román, F., Urra, C., Porras, O., Pino, A. M., Rosen, C. J., and Rodriguez, J. P. (2017). Real-time H_2 O_2 measurements in bone marrow mesenchymal stem cells (MSCs) show increased antioxidant capacity in cells from osteoporotic women. *J. Cell Biochem.* 118, 585–593. doi: 10.1002/jcb.25739

Rosi, M. C., Luccarini, I., Grossi, C., Fiorentini, A., Spillantini, M. G., Prisco, A., et al. (2010). Increased Dickkopf-1 expression in transgenic mouse models of neurodegenerative disease. *J. Neurochem.* 112, 1539–1551. doi: 10.1111/j.1471-4159.2009.06566.x

Ross, R. D., Shah, R. C., Leurgans, S., Bottiglieri, T., Wilson, R. S., and Sumner, D. R. (2018). Circulating Dkk1 and TRAIL are associated with cognitive decline in community-dwelling, older adults with cognitive concerns. *J. Gerontol. A Biol. Sci. Med. Sci.* 73, 1688–1694. doi: 10.1093/gerona/glx252

Roy, A., Liu, X., and Pahan, K. (2007). Myelin basic protein-primed T cells induce neurotrophins in glial cells *via* αvβ3 [corrected] integrin. *J. Biol. Chem.* 282, 32222–32232. doi: 10.1074/jbc.M702899200

Roy, A., and Pahan, K. (2013). Myelin basic protein-primed T helper 2 cells suppress microglial activation *via* αVβ3 integrin: implications for multiple sclerosis. *J. Clin. Cell. Immunol.* 7:158. doi: 10.4172/2155-9899.1000158

Safar, M. M., Arab, H. H., Rizk, S. M., and El-Maraghy, S. A. (2016). Bone marrow-derived endothelial progenitor cells protect against scopolamine-induced alzheimer-like pathological aberrations. *Mol. Neurobiol.* 53, 1403–1418. doi: 10.1007/s12035-014-9051-8

Salem, A. M., Ahmed, H. H., Atta, H. M., Ghazy, M. A., and Aglan, H. A. (2014). Potential of bone marrow mesenchymal stem cells in management of Alzheimer's disease in female rats. *Cell Biol. Int.* 38, 1367–1383. doi: 10.1002/cbin.10331

Salminen, A., Hyttinen, J. M., and Kaarniranta, K. (2011). AMP-activated protein kinase inhibits NF-kappaB signaling and inflammation: impact on healthspan and lifespan. *J. Mol. Med.* 89, 667–676. doi: 10.1007/s00109-011-0748-0

Saman, S., Kim, W., Raya, M., Visnick, Y., Miro, S., Saman, S., et al. (2012). Exosome-associated tau is secreted in tauopathy models and is selectively phosphorylated in cerebrospinal fluid in early Alzheimer disease. *J. Biol. Chem.* 287, 3842–3849. doi: 10.1074/jbc.M111.277061

Saman, S., Lee, N. C., Inoyo, I., Jin, J., Li, Z., Doyle, T., et al. (2014). Proteins recruited to exosomes by tau overexpression implicate novel cellular mechanisms linking tau secretion with Alzheimer's disease. *J. Alzheimers Dis.* 40, S47–70. doi: 10.3233/JAD-132135

Sanchez-Guajardo, V., Barnum, C. J., Tansey, M. G., and Romero-Ramos, M. (2013). Neuroimmunological processes in Parkinson's disease and their relation to α-synuclein: microglia as the referee between neuronal processes and peripheral immunity. *ASN Neuro* 5, 113–139. doi: 10.1042/AN20120066

Sanchez-Ramos, J., Song, S., Cardozo-Pelaez, F., Hazzi, C., Stedeford, T., Willing, A., et al. (2000). Adult bone marrow stromal cells differentiate into neural cells *in vitro*. *Exp. Neurol.* 164, 247–256. doi: 10.1006/exnr.2000.7389

Saresella, M., Calabrese, E., Marventano, I., Piancone, F., Gatti, A., Alberoni, M., et al. (2011). Increased activity of Th-17 and Th-9 lymphocytes and a skewing of the post-thymic differentiation pathway are seen in Alzheimer's disease. *Brain Behav. Immun.* 25, 539–547. doi: 10.1016/j.bbi.2010.12.004

Schäfer, S., Calas, A. G., Vergouts, M., and Hermans, E. (2012). Immunomodulatory influence of bone marrow-derived mesenchymal stem cells on neuroinflammation in astrocyte cultures. *J. Neuroimmunol.* 249, 40–48. doi: 10.1016/j.jneuroim.2012.04.018

Schneider-Hohendorf, T., Stenner, M. P., Weidenfeller, C., Zozulya, A. L., Simon, O. J., Schwab, N., et al. (2010). Regulatory T cells exhibit enhanced migratory characteristics, a feature impaired in patients with multiple sclerosis. *Eur. J. Immunol.* 40, 3581–3590. doi: 10.1002/eji.201040558

Schoppet, M., Preissner, K. T., and Hofbauer, L. C. (2002). RANK ligand osteoprotegerin: paracrine regulators of bone metabolism and vascular function. *Arterioscler. Thromb. Vasc. Biol.* 22, 549–553. doi: 10.1161/01.atv.0000012303.37971.da

Scott, E. L., and Brann, D. W. (2013). Estrogen regulation of Dkk1 and Wnt/β-Catenin signaling in neurodegenerative disease. *Brain Res.* 1514, 63–74. doi: 10.1016/j.brainres.2012.12.015

Shan, C., Ghosh, A., Guo, X.-Z., Wang, S.-M., Hou, Y.-F., Li, S.-T., et al. (2019). Roles for osteocalcin in brain signalling: implications in cognition- and motor-related disorders. *Mol. Brain* 12:23. doi: 10.1186/s13041-019-0444-5

Shimamura, M., Nakagami, H., Osako, M. K., Kurinami, H., Koriyama, H., Zhengda, P., et al. (2014). OPG/RANKL/RANK axis is a critical inflammatory signaling system in ischemic brain in mice. *Proc. Natl. Acad. Sci. U S A* 111, 8191–8196. doi: 10.1073/pnas.1400544111

Simard, A. R., Soulet, D., Gowing, G., Julien, J. P., and Rivest, S. (2006). Bone marrow-derived microglia play a critical role in restricting senile plaque formation in Alzheimer's disease. *Neuron* 49, 489–502. doi: 10.1016/j.neuron.2006.01.022

Smieszek, A., Tomaszewski, K. A., Kornicka, K., and Marycz, K. (2018). Metformin promotes osteogenic differentiation of adipose-derived stromal cells and exerts pro-osteogenic effect stimulating bone regeneration. *J. Clin. Med.* 7:482. doi: 10.3390/jcm7120482

Smith, S. M., Giedzinski, E., Angulo, M. C., Lui, T., Lu, C., Park, A. L., et al. (2020). Functional equivalence of stem cell and stem cell-derived extracellular vesicle transplantation to repair the irradiated brain. *Stem Cells Transl. Med.* 9, 93–105. doi: 10.1002/sctm.18-0227

Soulet, D., and Rivest, S. (2008). Bone-marrow-derived microglia: myth or reality? *Curr. Opin. Pharmacol.* 8, 508–518. doi: 10.1016/j.coph.2008.04.002

Steinman, L. (2009). A molecular trio in relapse and remission in multiple sclerosis. *Nat. Rev. Immunol.* 9, 440–447. doi: 10.1038/nri2548

Uede, T. (2011). Osteopontin, intrinsic tissue regulator of intractable inflammatory diseases. *Pathol. Int.* 61, 265–280. doi: 10.1111/j.1440-1827.2011.02649.x

Urakawa, I., Yamazaki, Y., Shimada, T., Iijima, K., Hasegawa, H., Okawa, K., et al. (2006). Klotho converts canonical FGF receptor into a specific receptor for FGF23. *Nature* 444, 770–774. doi: 10.1038/nature05315

Vervloet, M. G., Massy, Z. A., Brandenburg, V. M., Mazzaferro, S., Cozzolino, M., Ureña-Torres, P., et al. (2014). Bone: a new endocrine organ at the heart of chronic kidney disease and mineral and bone disorders. *Lancet Diabetes Endocrinol.* 2, 427–436. doi: 10.1016/S2213-8587(14)70059-2

Viswambharan, V., Thanseem, I., Vasu, M. M., Poovathinal, S. A., and Anitha, A. (2017). miRNAs as biomarkers of neurodegenerative disorders. *Biomark. Med.* 11, 151–167. doi: 10.2217/bmm-2016-0242

Walker, J. A., and McKenzie, A. N. J. (2018). TH2 cell development and function. *Nat. Rev. Immunol.* 18, 121–133. doi: 10.1038/nri.2017.118

Wang, F., Yasuhara, T., Shingo, T., Kameda, M., Tajiri, N., Yuan, W. J., et al. (2010). Intravenous administration of mesenchymal stem cells exerts therapeutic effects on parkinsonian model of rats: focusing on neuroprotective effects of stromal cell-derived factor-1α. *BMC Neurosci.* 11:52. doi: 10.1186/1471-2202-11-52

Watanabe, S., Kawamoto, S., Ohtani, N., and Hara, E. (2017). Impact of senescence-associated secretory phenotype and its potential as a therapeutic target for senescence-associated diseases. *Cancer Sci.* 108, 563–569. doi: 10.1111/cas.13184

Wei, J., Hanna, T., Suda, N., Karsenty, G., and Ducy, P. (2014). Osteocalcin promotes β-cell proliferation during development and adulthood through Gprc6a. *Diabetes* 63, 1021–1031. doi: 10.2337/db13-0887

Wu, M., Rementer, C., and Giachelli, C. M. (2013). Vascular calcification: an update on mechanisms and challenges in treatment. *Calcif. Tissue Int.* 93, 365–373. doi: 10.1007/s00223-013-9712-z

Xie, L., Choudhury, G. R., Winters, A., Yang, S. H., and Jin, K. (2015). Cerebral regulatory T cells restrain microglia/macrophage-mediated inflammatory responses *via* IL-10. *Eur. J. Immunol.* 45, 180–191. doi: 10.1002/eji.201444823

Xin, H., Li, Y., Buller, B., Katakowski, M., Zhang, Y., Wang, X., et al. (2012). Exosome-mediated transfer of miR-133b from multipotent mesenchymal stromal cells to neural cells contributes to neurite outgrowth. *Stem Cells* 30, 1556–1564. doi: 10.1002/stem.1129

Xin, H., Li, Y., Liu, Z., Wang, X., Shang, X., Cui, Y., et al. (2013). MiR-133b promotes neural plasticity and functional recovery after treatment of stroke with multipotent mesenchymal stromal cells in rats *via* transfer of exosome-enriched extracellular particles. *Stem Cells* 31, 2737–2746. doi: 10.1002/stem.1409

Xin, H., Wang, F., Li, Y., Lu, Q. E., Cheung, W. L., Zhang, Y., et al. (2017). Secondary release of exosomes from astrocytes contributes to the increase in neural plasticity and improvement of functional recovery after stroke in rats treated with exosomes harvested from microrna 133b-overexpressing multipotent mesenchymal stromal cells. *Cell Transplant.* 26, 243–257. doi: 10.3727/096368916X693031

Xiong, Y., Mahmood, A., and Chopp, M. (2017). Emerging potential of exosomes for treatment of traumatic brain injury. *Neural Regen. Res.* 12, 19–22. doi: 10.4103/1673-5374.198966

Yan, Q. W., Yang, Q., Mody, N., Graham, T. E., Hsu, C. H., Xu, Z., et al. (2007). The adipokine lipocalin 2 is regulated by obesity and promotes insulin resistance. *Diabetes* 56, 2533–2540. doi: 10.2337/db07-0007

Yang, Y., Ye, Y., Su, X., He, J., Bai, W., and He, X. (2017). MSCs-derived exosomes and neuroinflammation, neurogenesis and therapy of traumatic brain injury. *Front. Cell. Neurosci.* 11:55. doi: 10.3389/fncel.2017.00055

Yano, K., Tsuda, E., Washida, N., Kobayashi, F., Goto, M., Harada, A., et al. (1999). Immunological characterization of circulating osteoprotegerin/osteoclastogenesis inhibitory factor: increased serum concentrations in postmenopausal women with osteoporosis. *J. Bone Miner. Res.* 14, 518–527. doi: 10.1359/jbmr.1999.14.4.518

Yokokawa, K., Iwahara, N., Hisahara, S., Emoto, M. C., Saito, T., Suzuki, H., et al. (2019). Transplantation of mesenchymal stem cells improves amyloid-β pathology by modifying microglial function and suppressing oxidative stress. *J. Alzheimers Dis.* 72, 867–884. doi: 10.3233/JAD-190817

Yu, H., Liu, X., and Zhong, Y. (2017). The effect of osteopontin on microglia. *Biomed. Res. Int.* 2017:1879437. doi: 10.1155/2017/1879437

Yuan, J., Meloni, B. P., Shi, T., Bonser, A., Papadimitriou, J. M., Mastaglia, F. L., et al. (2019). The potential influence of bone-derived modulators on the progression of Alzheimer's disease. *J. Alzheimers Dis.* 69, 59–70. doi: 10.3233/JAD-181249

Zhang, L., Dong, Z. F., and Zhang, J. Y. (2020). Immunomodulatory role of mesenchymal stem cells in Alzheimer's disease. *Life Sci.* 246:117405. doi: 10.1016/j.lfs.2020.117405

Zhang, J., Fu, Q., Ren, Z., Wang, Y., Wang, C., Shen, T., et al. (2015). Changes of serum cytokines-related Th1/Th2/Th17 concentration in patients with postmenopausal osteoporosis. *Gynecol. Endocrinol.* 31, 183–190. doi: 10.3109/09513590.2014.975683

Zhang, J., Zhang, Z. G., Lu, M., Wang, X., Shang, X., Elias, S. B., et al. (2017). MiR-146a promotes remyelination in a cuprizone model of demyelinating injury. *Neuroscience* 348, 252–263. doi: 10.1016/j.neuroscience.2017.02.029

Zhao, Y., Shen, L., and Ji, H. F. (2012). Alzheimer's disease and risk of hip fracture: a meta-analysis study. *Sci. World J.* 2012:872173. doi: 10.1100/2012/872173

Zhao, E., Xu, H., Wang, L., Kryczek, I., Wu, K., Hu, Y., et al. (2012). Bone marrow and the control of immunity. *Cell. Mol. Immunol.* 9, 11–19. doi: 10.1038/cmi.2011.47

Zhou, R., Deng, J., Zhang, M., Zhou, H. D., and Wang, Y. J. (2011). Association between bone mineral density and the risk of Alzheimer's disease. *J. Alzheimers Dis.* 24, 101–108. doi: 10.3233/JAD-2010-101467

Zoch, M. L., Clemens, T. L., and Riddle, R. C. (2016). New insights into the biology of osteocalcin. *Bone* 82, 42–49. doi: 10.1016/j.bone.2015.05.046

Zou, L., Barnett, B., Safah, H., Larussa, V. F., Evdemon-Hogan, M., Mottram, P., et al. (2004). Bone marrow is a reservoir for CD4+CD25+ regulatory T cells that traffic through CXCL12/CXCR4 signals. *Cancer Res.* 64, 8451–8455. doi: 10.1158/0008-5472.CAN-04-1987

Conflict of Interest: The authors declare that the research was conducted in the absence of any commercial or financial relationships that could be construed as a potential conflict of interest.

Copyright © 2020 Yu, Ling, Lu, Zhao, Chen, Xu and Zou. This is an open-access article distributed under the terms of the Creative Commons Attribution License (CC BY). The use, distribution or reproduction in other forums is permitted, provided the original author(s) and the copyright owner(s) are credited and that the original publication in this journal is cited, in accordance with accepted academic practice. No use, distribution or reproduction is permitted which does not comply with these terms.

frontiers in Aging Neuroscience

ORIGINAL RESEARCH
published: 12 January 2021
doi: 10.3389/fnagi.2020.603793

Sporadic Parkinson's Disease Potential Risk Loci Identified in Han Ancestry of Chinese Mainland

Bo Wang[1†], Xin Liu[2†], Shengyuan Xu[2†], Zheng Liu[3†], Yu Zhu[2], Xiong Zhang[4] and Renshi Xu[1,2*]*

[1] Department of Neurology, The First Affiliated Hospital of Nanchang University, Nanchang, China, [2] Department of Neurology, Jiangxi Provincial People's Hospital, The Affiliated People's Hospital of Nanchang University, Nanchang, China, [3] Department of Neurology, First Affiliated Hospital of Gannan Medical University, Ganzhou, China, [4] Department of Neurology, Maoming People's Hospital, Maoming, China

Recent investigations demonstrated that genetic factors might play an important role in sporadic Parkinson's disease (sPD). To clarify the specific loci susceptibility to sPD, we analyze the relationship between 30 candidate single nucleotide polymorphisms (SNPs) and sPD in the population of Han ancestry from Chinese mainland (HACM) by using genome-wide association study, sequenom massARRAY, DNA sequence, and biological information analysis. Results showed that the subjects carrying the T allele of rs863108 and rs28499371 exhibited a decreased risk for sPD. The subjects carrying the T allele of rs80315856 exhibited an increased risk for sPD. The A/T genotype of rs863108 and the C/T genotype of rs28499371 were a potential increased risk for sPD, and the G/T genotype of rs80315856 and T/T genotype of rs2270568 were a potential decreased risk for sPD. The minor allele frequency (MAF) of rs80315856 and rs2270568 was higher in sPD. The T allele of rs80315856 and rs2270568 might be a risk locus for sPD. Our data suggested that the alteration of these SNPs might play some roles through changing/affecting LINC01524/LOC105372666, DMRT2/SMARCA2, PLEKHN1, and FLJ23172/FNDC3B genes in the pathogenesis of sPD.

Keywords: genetic polymorphism, single nucleotide polymorphisms, pathogenesis, sporadic Parkinson's disease, Chinese Han ancestry

OPEN ACCESS

Edited by:
Pingyi Xu,
First Affiliated Hospital of Guangzhou Medical University, China

Reviewed by:
Eirini Kanata,
Aristotle University of Thessaloniki, Greece
Jia-Da Li,
Central South University, China

****Correspondence:***
Xiong Zhang
xiong715@126.com
Renshi Xu
13767015770@163.com;
xurenshi@ncu.edu.cn

† These authors have contributed equally to this work and share first authorship

Received: *07 September 2020*
Accepted: *30 November 2020*
Published: *12 January 2021*

Citation:
Wang B, Liu X, Xu S, Liu Z, Zhu Y, Zhang X and Xu R (2021) Sporadic Parkinson's Disease Potential Risk Loci Identified in Han Ancestry of Chinese Mainland. Front. Aging Neurosci. 12:603793. doi: 10.3389/fnagi.2020.603793

INTRODUCTION

Sporadic Parkinson's disease (sPD) is a progressive neurodegenerative disease, which is characterized by signs and symptoms of progressive motor and non-motor dysfunctions. Due to the presence of Lewy bodies in dopamine (DA) neuron in the substantia nigra of the midbrain, the typical pathological features of sPD mainly display the progressive loss of DA neurons in the substantia nigra of the midbrain. The degenerated DA neurons in sPD primarily occur in the substantia nigra pars compacta (SNc) projected to striatum. sPD is one of commonest neurodegenerative diseases and occupies approximately 1% in the populations of more than 65 years (Marsden, 1994).

The characterized clinical manifestations of sPD include motor and non-motor symptoms. The typical clinical motor symptoms of sPD mainly consist of rest tremors, rigidity, bradykinesia, and posture disorder (Fahn, 2003; Cummings et al., 2011). The motor symptoms of sPD begin to

manifest only after more than 50% dopaminergic neurons loss in SNc and a significant deficit of 70–80% striatal DA concentration in striatum. Besides motor manifestations, sPD reveals lots of non-motor symptoms. The commonest non-motor symptoms include anxiety, depression, olfactory hyposmia, the dysfunction of autonomic nerves (e.g., orthostatic symptoms, urine incontinence, and constipation), dyssomnia, behavioral disorders, and cognitive dysfunction (Göttlich et al., 2013; Khoo et al., 2013). sPD is a complex, multifactorial disease that can have diverse genetic, biological, and environmental influences (Polito et al., 2016). Although sPD patients lack evidential family history and definitive genetic basis, the familial forms of Parkinson's disease (PD) have inferred that sPD might be closely associated with some genetic factors (Singleton et al., 2013). Up to now the etiology of sPD is still unclear, but it is convincing that the interaction of genetic factor, environmental factor, and aging together contributes to this disease (Kalia and Lang, 2015).

Over last two decades, we have witnessed a revolution in the field of sPD genetics. Great advances have been made in identifying many single nucleotide polymorphisms (SNPs) that confer a risk for sPD, which has subsequently led to an improved understanding of molecular pathways involved in the sPD pathogenesis. Despite this success, it is predicted that only relatively small proportion of phenotypic variability has been explained by genetics. Therefore, the heritable components of sPD are still waiting to be identified, and exploring the genetic architecture of sPD constitutes a critical effort in identifying the therapeutic targets of sPD. Although substantial progress has helped us to better understand the mechanism of sPD, the route to sPD-disease-modifying drugs is a lengthy one (Billingsley et al., 2018).

Although genetic and environmental factors currently have been shown to lead to sPD, the etiology of sPD remains elusive (Fahn, 2003). On the past unremitting effort, researchers have shed light on the relationship between some candidate genetic factors and sPD in different populations (von Otter et al., 2014; Rozenkrantz et al., 2016; Soldner et al., 2016; Wang et al., 2016; Yang et al., 2016). These genetic factors included SNPs, rearrangements, and insertion/deletion polymorphisms; however, very few studies have been evaluated in Chinese populations, especially in the Han ancestry of Chinese mainland (HACM).

To this end, in this study, we chose 30 most possible associated candidate SNPs from the results of our and other related previous study (Hu et al., 2016) to further analyze their susceptibility in 398 sPD patients and 430 controls from HACM. We discovered that the polymorphisms of rs863108, rs80315856, rs28499371, and rs2270568 were possibly associated with the pathogenesis of sPD from HACM. Furthermore, we also explored their potential biological functions and relationships in the pathogenesis of sPD. Our results suggested that the subject carrying the T allele (A/T + T/T) of rs863108 and the T allele (C/T + T/T) of rs28499371 exhibited a decreased risk for sPD. The subject carrying the T allele (T/T + G/T) of rs80315856 exhibited an increased risk for sPD. The A/T genotype of rs863108 and the C/T genotype of rs28499371 were a potential increased risk for sPD, and the G/T genotype of rs80315856 and the T/T genotype of rs2270568 were a potential decreased risk for sPD. The minor allele frequency (MAF) of rs80315856 was higher in sPD patients (8%) than in controls (6%). The MAF of rs2270568 was higher in sPD patients (47%) than in the controls (43%). The T allele of rs80315856 and rs2270568 may be the risk loci for sPD. These polymorphisms alteration might change or affect the structures and functions of LINC01524/LOC105372666, DMRT2/SMARCA2, PLEKHN1, and FLJ23172/FNDC3B genes to exert some effects in the pathogenesis of sPD.

MATERIALS AND METHODS

Human Subjects

sPD and control dataset was created from two affiliated hospitals of the university, The First Affiliated Hospital of Nanchang University and The Affiliated Guangdong General Hospital of Nan Fang Medical University. All recruited sPD and control subjects were from HACM in Chinese southern regions (Jiangxi and Guangdong Province). Informed consent was signed by all participants in this study. All sPD patients were diagnosed according to clinical diagnostic criteria for sPD in China (Li et al., 2017). All subjects underwent the same evaluation process including records of medical history, Mini-Mental State Exam, PD family history, related diseases in their first-degree relatives, the toxicant exposure associated with sPD, related indispensable biochemical test, and brain and spinal magnetic resonance imaging to eliminate other neurological diseases that might mimic the clinical image of PD (e.g., tumors, demyelinated disorders, cerebral vascular disease, and Parkinsonism).

Studied populations were composed of 648 sPD and 680 controls. Among them, 250 sPD and 250 controls were used for genome-wide association study (GWAS) analysis (Hu et al., 2016); 398 sPD and 430 controls were used for the polymorphism analysis of 30 most possible associated candidate SNPs (**Tables 1**, **2**). The male and female ratio of sPD was 215 (54.02%) and 183 (45.98%), and that of controls were 261 (60.69%) and 169 (39.31%). The mean (range) age of sPD was 60.99 ± 0.56 years, and that of controls were 62.06 ± 0.60 years (**Table 1**). Male subjects were more than female subjects because sPD affected more men than women, and our data exhibited a slight gender disparity. The age of the control subjects was older than that of sPD patients, which aimed to minimize the age bias that the control subjects were too young to develop sPD. Moreover, we also intend to avoid the age-related factors associated with sPD. For example, the sPD patients of early and late onset would be

TABLE 1 | Basic characteristics of study subjects.

	Cases (*n* = 398)	Controls (*n* = 430)	*P*-value
Male [n (%)]	215 (54.02)	261 (60.69)	
Female [n (%)]	183 (45.98)	169 (39.31)	0.052
Age (years)	60.99 ± 0.56	62.06 ± 0.60	0.199

n, number.

TABLE 2 | All SNPs were chosen in the association study.

Our previous pooling GWAS scanning SNPs						Function region SNPs and validated hot SNPs			
Gene	**Chro**	**SNP ID**	**Position**	**OR (95%CI)**	***P*-value**	**SNP ID**	**Position**	**Function region**	**MAF in CHP**
TSG1/MANEA	6	rs9445283	95,187,922	8.2 (5.70–11.78)	1.37461E-27				
PDE10A	6	rs880121	166,068,329	3.72 (2.75–5.04)	4.47044E-17				
MDGA2	14	rs9323124	47,466,177	3.97 (2.91–5.42)	3.44125E-19	rsl2590500[a,b]	46,957,434	Missense	0.073
ATPBD4/LOC100288892	15	rsl7534343	36,296,150	4.30 (3.16–5.85)	7.4025E-16				
ZFP64/TSHZ2	20	rs863108	51,255,111	6.59 (4.2–10.20)	4.98978E-13				
PAQR3/ARD1B	4	rs201453169	80,119,145	0.18 (0.12–0.25)	2.15365E-14				
FLJ23172/FNDC3B	3	rs73180248	171,699,046	3.97 (2.82–5.60)	1.35108E-05	rs2270568[a]	172,329,071	Synonymous	0.476
CYPIBl/C2orf58	2	rs163090	38,313,632	0.36 (0.26–0.50)	5.42354E-09				
ANXA1/LOC100132423	9	rs10746953	76,917,840	2.62 (1.91–3.60)	5.35053E-09				
FLJ35379	13	rs61959631	76,477,028	2.37 (1.78–3.14)	7.34753E-09	rs7652177[a,d]	172,251,287	Missense	0.39
PLEKHN1	1	rs3829740	909,238	2.63 (1.91–3.63)	1.47259E-08	rs28499371[a]	966,748	Missense	0.131
						rs3829738[a]	973,929	Missense	0.248
DMRT2/SMARCA2	9	rs80315856	1,261,774	0.29 (0.19–0.44)	1.1753E-08	rs2279984[a]	1,048,496	Promoter	0.417
						rsl2002058[a]	1048,945	Promoter	0.136
ZNF396/IN080C	18	rsl362858	32,986,600	2.68 (1.92–3.73)	3.62598E-05				
C3orf67/LOC339902	3	rs6783485	59,427,797	0.20 (0.12–0.35)	2.05182E-08				
LOC285194/IGSF11	3	rsl879553	118,615,463	2.83 (1.98–4.04)	3.28729E-08				
FGF10/MRPS30	5	rsl3153459	44,515,935	2.45 (1.79–3.34)	3.17573E-08				
BARX1/PTPDC1	9	rsl0993010	96,749,048	2.29 (1.72–3.06)	6.5853E-08	rsll793856[a]	93,952,209	Synonymous	0.073
						sl91789925[a]	93,955,005	Missense	0.092
COL5A2	2	rslll86	189,897,394	2.79 (1.94–4.03)	1.37461E-27	rsl0197596[a,c]	189,039,507	Synonymous	0.117
						rs6434312[a,c]	189,043,211	Synonymous	0.107
						rsll691604[a]	189,180,039	Promoter	0.286

Chro, Chromosome; SNP, Single nucleotide polymorphism; GWAS, Genome wide association study; OR, Odds ratio; CI, Confidence interval; MD, Missing Data; CHP, Chinese Han populations. [a]*Hu et al. (2016).* [b]*Hellquist et al. (2009).* [c]*Li et al. (2014).* [d]*Allen et al. (2010). The underlined values indicates position in chromosome.*

eliminated. The disease course of sPD patients was controlled within 3–5 years after onset, which would preclude the sPD patients of rapid and slow progression. The sPD patients with atypical clinical manifestations were eliminated yet. Based on the above enrolled factors of subjects, therefore, in our study, the sPD patients with typical age, clinical course, and phenotype were enrolled. This study was approved by the Institutional Review Board of the Hospital Human Ethics Committee of The First Affiliated Hospital of Nanchang University and The Affiliated Guangdong General Hospital of Nan Fang Medical University.

Selection of SNPs

Based on the information of candidate genes and the purpose of this study, the screen scheme of candidate SNPs initially was formulated. In our previous pooling GWAS of 250 sPD patients and 250 control subjects from HACM, we revealed that 18 SNPs, including rs9445283 (kgp154172) in TSG1/MANEA, rs880121 (kgp8130520) in PDE10A, rs9323124 in MDGA2, rs17534343 (kgp11333367) in ATPBD4/LOC100288892, rs863108 (kgp4156164) in ZFP64/TSHZ2, rs201453169 (kgp9482779) in PAQR3/ARD1B, rs73180248 (kgp760898) in FLJ23172/FNDC3B, rs163090 (kgp11353523) in CYP1B1/C2orf58, rs10746953 in ANXA1/LOC100130911, rs61959631 (kgp9550589) in FLJ35379/LOC100132423, rs3829740 (kgp7172368) in PLEKHN1, rs80315856 (kgp10769919) in DMRT2/SMARCA2, rs1362858 in ZNF396/INO80C, rs6783485 in C3orf67/LOC339902, rs1879553 in LOC285194/IGSF11, rs13153459 in FGF10/MRPS30, rs10993010 (kgp6542803) in BARX1/PTPDC1, and rs11186 in COL5 A2, were strongly associated with sPD from HACM because their significance threshold was $p < 3.7 \times 10^{-5}$ (Hu et al., 2016). The above SNPs were not reported to be associated with sPD before our study (Hu et al., 2016). Moreover, we screened the previously reported candidate SNPs related with the pathogenesis of sPD by the screen methods of function region SNPs and validated hot SNPs (**Supplementary Table 1**). We found that 12 SNPs, which consisted of rs12590500 in MDGA2 (Hellquist et al., 2009; Hu et al., 2016); rs28499371 and rs3829738 in PLEKHN1 (Hu et al., 2016); rs10197596, rs6434312 (Li et al., 2014; Hu et al., 2016), and rs11691604 in COL5A2 (Hu et al., 2016); rs11793856 and rs191789925 in BARX1 (Hu et al., 2016); rs2279984 and rs12002058 in DMRT2 (Hu et al., 2016); and rs7652177 (Allen et al., 2010; Hu et al., 2016) and rs2270568 in FLJ23172/FNDC3B (Hu et al., 2016) were the possible susceptible SNPs of sPD based on the result of function region SNPs and validated hot SNPs screen (**Supplementary Table 1**). In addition, 12 additional SNPs were selected so as to (a) be within the wider loci indicated by the previous GWAS in Han Chinese and (b) reside within functional regions. Therefore, in this study, 30

SNPs were chosen to further ascertain their association with the pathogenesis of sPD (**Table 2**).

Screen Methods of Function Region SNPs and Validated Hot SNPs Screen of Function Region SNPs

The functional SNPs screening of MAF > 0.025 in the Chinese Han population was conducted in two databases of HapMap[1] and 1000 Genomes[2] in exons, 5′ untranslated region (UTR), promoter, and 3′ UTR regions of candidate gene SNPs in the Geneview of National Center for Biotechnology Information (NCBI) website, which further verified the researched state in the relevant literature. The function of selected SNPs was predicted through http://snpinfo.niehs.nih.gov/, and their functions stated in some documents were also tagged.

Screen of Validated Hot SNPs

Through searching the literature in the PubMed of NCBI and Google, we carried out the literature research of related SNPs of candidate genes and screened the susceptible SNPs. Screened SNPs were verified by MAF in the Chinese Han populations in the HapMap and 1000 Genomes database (see text footnotes 1, 2). SNPs of MAF < 0.025 is abandoned.

SNPs Genotype of Sequenom Mass Array

SNPs genotype was performed by sequenom massARRAY platform (Sequenom, San Diego, CA, United States) according to manufacturer's instructions. Thirty SNPs were genotyped. For quality control, 5% of the samples underwent repeated genotype; 100% of the results was consistent. This experiment was conducted by Wuhan Icongene Biological Technology Co., Ltd (Contract number: BMSW20170807LHY0063).

Major Reagents and Apparatuses

Major reagents used in the experiments were the following: DNA extraction kit (BioTeKe Corpration), HotStar Taq (5 U/μl), shrimp alkaline phosphatase (SAP) buffer, SAP enzyme, iPLEX buffer plus, iPLEX termination mix, iPLEX enzyme, and massARRAY TYPER4.0 (Agena, Inc.). The main apparatuses applied for this research were as follows: nucleic acid automatic extractor (BioTeKe Corpration), nanoDrop2000 (Thermo Fisher Scientific, United States), Veriti-384 PCR reactor (ABI, United States), 384-well spectroCHIP bioarray chip®, massARRAY nanodispenser spotting machine, and massARRAY analyzer 4.0 mass spectrometer (Agena, Inc.).

Performance of 384-Well PCR Reactions

DNA assays were conducted by 384-well PCR reactions in this study. The experimental processes were as follows: (1) a PCR mixture was prepared with the following descriptions—1.85 μl ddH_2O, 0.625 μl 10 × PCR buffer with 15 mM $MgCl_2$, 0.325 μl 25 mM $MgCl_2$, 0.1 μl deoxyribonucleotide triphosphate (dNTP) mix (25 mM), 0.1 μl HotStar Taq PCR enzyme (5 U/μl), 1 μl primer mixture (0.5 μM), 1 μl DNA template (20 ng/μl), a total of 5 μl volume; (2) 5 μl PCR mixture was added to each well of 384-well microtiter plate; (3) the microtiter plate was centrifuged at 1,000 rpm for 1 min; and (4) the 384-well microtiter plate was thermocycled in the following amplified conditions—94°C degeneration for 20 s, 56°C annealing for 30 s, and 72°C extension for 1 min, a total of 45 cycles. The primers in **Supplementary Table 2** were used in the above 384-well PCR reactions.

Preparation of SAP Enzyme Solution

The SAP enzyme solution was prepared with the following descriptions: mixed 1.53 μl RNase-free ddH_2O, 0.3 μl 1 U/μl SAP enzyme, and 0.17 μl 10 × SAP buffer in a 2-μl tube; held the 1.5-mL tube containing the SAP enzyme solution onto a vortex to mix the solution for 5 s; and centrifuged the SAP enzyme solution at 5,000 rpm for 10 s.

Treatment of PCR Production by SAP Enzyme

Two microliters SAP enzyme solution was added into each well of 384-well sample microtiter plate. The 384-well sample microtiter plate was sealed using a plate sealing film, centrifuged at 1,000 rpm for 1 min, and incubated as follows: 37°C for 20 min and 85°C for 5 min.

Preparation of High Plex iPLEX Gold Reaction Mixture

The high plex iPLEX gold reaction mixture was prepared as follows: 0.619 μl RNase-free ddH_2O, 0.2 μl iPLEX buffer plus, 0.2 μl iPLEX termination mixture, 0.94 μl iPLEX extend primer mixture (7 μM/14 μM), 0.041 μl 1 × iPLEX enzyme, and 7 μl PCR/SAP reaction solution were added to a total of 9 μl volume; the mixture was centrifuged in a microtiter plate at 1,000 rpm for 1 min.

High Plex iPLEX® Gold Assay

The 2 μl high plex iPLEX gold reaction mixture was added into the 384-well sample microtiter plate. The 384-well sample microtiter plate was sealed with a plate sealing film, centrifuged at 1,000 rpm for 1 min, and thermocycled as follows: 94°C degeneration for 30 s (94°C degeneration for 5 s, 52°C annealing for 5 s, 80°C extension for 5 s, 5 cycles), 52°C annealing for 5 s, and 72°C extension for 3 min, a total of 40 cycles. The primers in **Supplementary Table 2** were used.

Cleanup of High Plex iPLEX Gold Reaction Products

The cleanup of high plex iPLEX gold reaction products involved adding water and cleaning. The processes performed were as follows: the sample microtiter plate was resined; the clean resin was spread onto a 384-well dimple plate; nanopure water was added into each well of the 384-well sample microtiter plate and then the clean resin was added; and the 384-well sample microtiter plate was rotated and centrifuged.

[1] http://hapmap.ncbi.nlm.nih.gov/

[2] http://browser.1000genomes.org/

Acquirement of Spectra

The ACQUIRE module controlled massARRAY analyzer compact was used to acquire spectra from SpectroCHIPs. Each SpectroCHIP spectra was processed and analyze by massARRAY TYPER 4.0 software.

Sanger Sequence of DNA

For each SNPs, the Sanger sequence of samples subset was performed on an ABI3500 (ABI3730xl; Applied Biosystems, Inc., CA) to confirm the genotyping of sequenom massARRAY. Their nucleotide variants were analyzed with DNASTARLaser gene software (Version v7.1) and compared with DNA sequence from NCBI GeneBank. This experiment was performed by Wuhan Icongene Biological Technology Co., Ltd (Contract number: XM171114-471).

Function Prediction of rs863108, rs80315856, rs28499371, and rs2270568

The functional prediction of polymorphisms in rs863108 of the LINC01524/LOC105372666 gene, rs80315856 of the DMRT2/SMARCA2 gene, rs28499371 of the PLEKHN1 gene, and rs2270568 of the FLJ23172/FNDC3B gene was further conducted, which included transcription factor binding sites (Alkema et al., 2004), pathogenicity, protein structure domain, protein family evolution, protein Q494U1 homology modeling, and secondary structure of protein Q53EP0. The transcription factor binding sites in the sequence 1,500 bp upstream in the mutation position was analyzed using Mscan[3]. Human messenger RNA (mRNA) sequences were downloaded from the Ensemble website of version GRCh38 and formatted as database. The sequence of mutation position was applied to Blast against the database. Blast with an e-value cutoff e-15 was performed to obtain hits with the database. The pathogenicity prediction of the mutation site was analyzed using polyphen database[4] and sift database[5]. Pathogenicity screening was performed with a polyphen pathogenicity score cutoff of 0.8 and sift pathogenicity score cutoff of 0.05. Coding protein sequence was retrieved from uniprot database[6]. Protein structure domain was analyzed using NCBI CDD database with input sequence and default parameter. For protein family evolution analysis, an evolution tree was drawn by gene tree tool in the Ensemble database. Multiple alignment sequence was extracted from gene tree results and was applied to draw seqLogo figure using weblogo software[7]. Protein Q494U1 homology modeling was analyzed using I-Tasser software[8] with *ab initio* algorithm. The modeling structures of the mutation and origin proteins were aligned using SuperPose software[9]. The secondary structure of protein Q53EP0 was retrieved by SWISS-MODEL database[10]; the protein secondary structure of mutation sites was exhibited in the structure.

[3]http://cisreg.cmmt.ubc.ca/cgi-bin/mscan/MSCAN

[4]http://genetics.bwh.harvard.edu/pph2/

[5]http://sift.jcvi.org/

[6]http://www.uniprot.org

[7]http://weblogo.berkeley.edu/

[8]https://zhanglab.ccmb.med.umich.edu/I-TASSER/

[9]http://wishart.biology.ualberta.cn/SuperPose/

[10]https://swissmodel.expasy.org

Statistical Analysis

Statistical analysis was performed using SPSS (Version 18.0) statistical software (SPSS, Chicago, IL, United States). Hardy–Weinberg equilibrium (HWE) was first evaluated in healthy controls. Pearson chi-square test was used to compare the frequency of allele and genotypes in both cases and controls. MAF and odds ratios (ORs) with 95% confidence intervals (CI) were estimated to determine the role of each SNPs in sPD patients and controls. Two-tailed $p < 0.05$ were considered as statistical significance.

RESULTS

Identification of Genetic Association Between 30 SNPs and sPD

We analyzed the association of 30 SNPs (**Table 2**) and sPD in an independent Chinese population using sequenom massARRAY technology. Four novel SNPs of rs863108 in the LINC01524/LOC105372666 gene (Chr 20:52638572), rs80315856 in the DMRT2/SMARCA2 gene (Chr 9:1261774), rs28499371 in the PLEKHN1 gene (Chr 1:966748), and rs2270568 in the FLJ23172/FNDC3B gene (Chr 3:172329071) were identified in our study.

The allelic and genotypic frequencies are summarized in **Tables 3**, **4**. Four novel SNPs were identified as follows: rs863108, rs80315856, rs28499371, and rs2270568. The subjects carrying the T allele (A/T + T/T) of rs863108 (*OR* = 0.73, 95% *CI* = 0.55–0.97, $p = 0.029$) and the subjects carrying T allele (C/T + T/T) of rs28499371 (*OR* = 0.75, 95% *CI* = 0.56–1.00, $p = 0.05$) exhibited a decreased risk for sPD in comparison with other subjects. The subjects carrying the T allele (T/T + G/T) of rs80315856 (*OR* = 1.51, 95% *CI* = 1.05–2.19, $p = 0.027$) exhibited an increased risk for sPD in comparison with other subjects. The subjects carrying the T allele (T/T + C/T) of rs2270568 (*OR* = 1.23, 95% *CI* = 0.94–1.61, $p = 0.133$) exhibited no significance in comparison with other subjects (**Table 3**). The A/T genotype of rs863108 and C/T genotype of rs28499371 were a potential increased risk for sPD, and the G/T genotype of rs80315856 and the T/T genotype of rs2270568 were a potential decreased risk for sPD compared with other genotypes (**Table 3**). The MAF of rs80315856 (*OR* = 1.460, 95% *CI* = 1.027–2.077, $p = 0.034$) was significantly different between sPD patients and controls. The MAF of rs80315856 was higher in sPD patients (8%) than in controls (6%). The MAF of rs2270568 (*OR* = 1.217, 95% *CI* = 1.020–1.452, $p = 0.029$) was significantly different between sPD patients and controls. The MAF of rs2270568 was higher in sPD patients (47%) than in controls (43%). The T allele of rs80315856 and rs2270568 may be the risk loci of sPD. The MAF of rs863108 and rs28499371 did not find any significant difference between sPD patients and controls (**Table 4**).

Confirmation of Variation Position in rs863108, rs80315856, rs28499371, and rs2270568

After performing a sequenom massARRAY array, we randomly drew 10 samples of each SNPs to reconfirm

TABLE 3 | Association between four SNPs and the risk of sPD in the Chinese Han population.

SNP	Genotype	Cases	Controls	OR (95% CI)	*P*-value
rs863108	A/A	145 (0.29)	112 (0.23)	1	Ref
(Chr 20:52638572 T > A)	A/T	243 (0.48)	267 (0.54)	0.7 (0.52–0.95)	0.022
	T/T	114 (0.23)	112 (0.23)	0.79 (0.55–1.13)	0.188
	T/T + A/T	357	379	0.73 (0.55–0.97)	0.029
rs80315856	G/G	428 (0.842)	445 (0.89)	1	Ref
(Chr 9:1261774 G > T)	G/T	79 (0.156)	54 (0.108)	1.52 (1.05–2.20)	0.026
	T/T	1 (0.002)	1 (0.002)	1.04 (0.06–16.68)	1.00
	T/T + G/T	80	55	1.51 (1.05–2.19)	0.027
rs28499371	C/C	402 (0.79)	359 (0.74)	1	Ref
(Chr 1:966748 C > T)	C/T	96 (0.19)	119 (0.24)	0.72 (0.53–0.98)	0.034
	T/T	10 (0.02)	8 (0.02)	1.12 (0.44–2.86)	0.823
	T/T + C/T	106	127	0.75 (0.56–1.00)	0.050
rs2270568	C/C	141 (0.28)	158 (0.32)	1	Ref
(Chr 3:172329071 T > C)	C/T	252 (0.50)	249 (0.51)	1.13 (0.85–1.51)	0.390
	T/T	115 (0.22)	85 (0.17)	1.52 (1.06–2.17)	0.024
	T/T + C/T	367	334	1.23 (0.94–1.61)	0.133

SNP, single nucleotide polymorphism; CI, confidence interval; OR, odds ratio; sPD, sporadic Parkinson's disease; p significance at < 0.05. All p-values were calculated by means of chi-squared test.

TABLE 4 | Allele frequencies of four SNPs in sPD cases and controls groups.

SNPs	Allele	Cases	Controls	χ^2	*P*	OR (95% CI)
rs80315856	G (Major)	935 (0.92)	944 (0.94)			0.685 (0.481–0.974)
	T (Minor)	81 (0.08)	56 (0.06)	4.478	0.034	1.460 (1.027–2.077)
rs2270568	C (Major)	534 (0.53)	565 (0.57)			0.822 (0.689–0.980)
	T (Minor)	482 (0.47)	419 (0.43)	4.769	0.029	1.217 (1.020–1.452)

SNPs, single nucleotide polymorphism; CI, confidence interval; OR, odds ratio; sPD, sporadic Parkinson's disease; χ^2, chi-squared test. p significance at < 0.05. The data weren't shown in this table, because the MAF of rs863108 and rs28499371 didn't find any significant difference between sPD patients and controls (The p-value of χ^2-test > 0.05).

the genotypes of rs863108, rs80315856, rs28499371, and rs2270568 by conducting DNA Sanger sequence on an ABI3500. Sequencing results coincided with that from our sequenom massARRAY array. The polymorphism of rs863108 in the LINC01524/LOC105372666 gene was a T > A variation (**Figure 1A**). The polymorphism of rs80315856 in the DMRT2/SMARCA2 gene was a G > A variation (**Figure 1B**). The polymorphism of rs28499371 in the PLEKHN1 gene was a C > T variation (**Figure 1C**). The polymorphism of rs2270568 in the FLJ23172/FNDC3B gene was a T > C variation (**Figure 1D** and **Table 3**).

General Mutation Information and Prediction of Transcription Factor Binding Site of rs863108

The mutation information of rs863108 (*Homo sapiens*) was retrieved from NCBI dbSNP database[11] as shown in **Figure 2A**. The LINC01524/LOC105372666 mutation site of rs863108 located in the Chr20:52638572 changed from T to A as shown in **Figure 2B**. The transcription factor binding site was predicted at distances from 166 to 154 bp upstream of LINC01524/LOC105372666 as shown in **Figure 2C**.

General Mutation Information, Pathogenicity Prediction, Analysis of Structure Domain, Protein Family Evolution, and Structure Modeling of rs28499371

rs28499371 (*H. sapiens*) information was retrieved from NCBI dbSNP database (see text footnote 11) as shown in **Figure 3A**. The mutation site located in Chr1:966748 changed from C to T (**Figure 3A**). This mutation is missense variant, which leads to codon change from GCT to GTT and amino acid change from A to V in the 43rd position of PLEKHN1 coding protein (**Figure 3A**). The pathogenicity prediction of mutation site was conducted as shown in **Figure 3B**. This mutation was predicted to be benign with a score of 0.208 (sensitivity, 0.92; specificity, 0.88) (**Figure 3B**). The result showed that PLEKHN1 was PH-like super family in **Figure 3C**. The mutation site was in the 43rd amino acid position and did not appear in the protein structure domain (**Figure 3C**). The PLEKHN1 evolution tree was drawn by the gene tree tool in Ensemble database, and 80 orthologous genes were

[11]https://www.ncbi.nlm.nih.gov/snp/

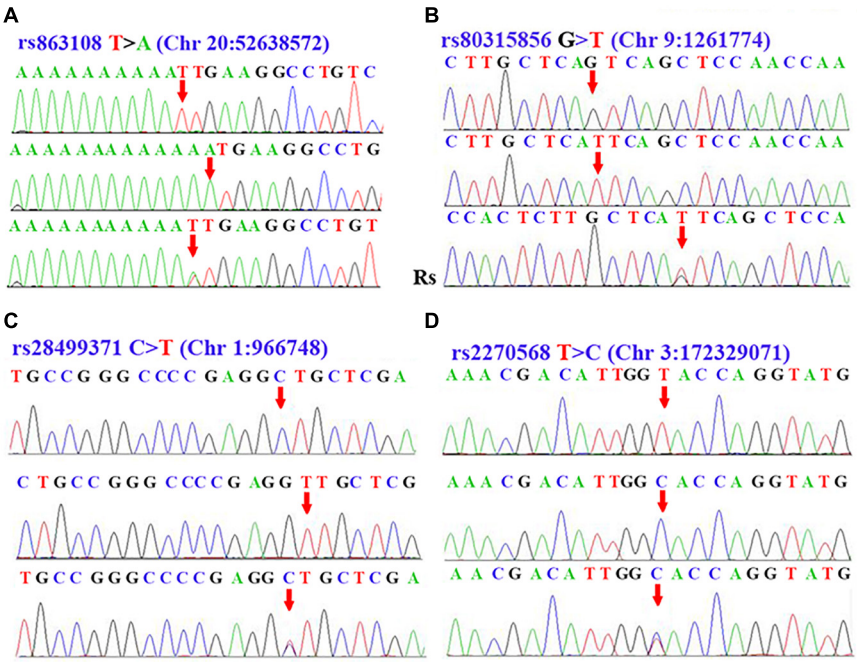


FIGURE 1 | Sequence data of rs863108, rs80315856, rs28499371, and rs2270568. **(A)** Peak graph showing T > A variation of rs863108 in LINC01524/LOC105372666 gene. **(B)** Peak graph showing G > T variation of rs80315856 in DMRT2/SMARCA2. **(C)** Peak graph showing C > T variation of rs28499371 in PLEKHN1. **(D)** Peak graph showing T > C variation of rs2270568 in FLJ23172/FNDC3B. The variant loci were indicated by the red arrow. The Rs in the Panel **(B)** was the abbreviation of reverse sequence, which indicate that the Rs sequence in the Panel **(B)** was the result of reverse DNA sequence.

found in the database as shown in **Figure 3D**. Multiple alignment sequences were extracted from the gene tree result and were applied to draw seqlogo figure using weblogo software[12] as shown in **Figure 3E**. The mutation sites located in the 143rd amino acid position and main mutations were A, E, G, and S. In those mutations, A is the most important, and V is rare. V mutation may lead to pathogenicity (**Figures 3D,E**). Structure modeling analysis was conducted. The modeling structures of mutation and origin proteins are showed in **Figures 4A,B**. In **Figure 4**, red represents origin protein structure, blue represents mutation protein structure. The neighborhood partial structure is retained in **Figure 4A**. The mutation amino acid is located at the center of protein pocket, which may influence neighborhood structure.

General Mutation Information, Pathogenicity Prediction, and Structure Modeling of rs2270568 Mutation

rs2270568 (*H. sapiens*) information was retrieved from NCBI dbSNP database (see text footnote 11) as shown in **Figure 5A**. The mutation site of rs2270568 located in Chr3:172046861 changed from T to C (**Figure 5A**). A total of 2,869 pathogenicity sites were screened by databases, and multiple pathogenicity sites were found near the rs2270568 mutation site as shown in **Figure 5B**. These pathogenicity sites led to the change in amino acid (**Figure 5B**). Mutation sites appeared between the coil and beta sheet, which were pathogenicity mutation regions with high frequency occurrence. The pathogenicity site near the mutation site may influence protein function and the regulation mechanism of disease (**Figure 5C**).

[12]http://weblogo.berkeley.edu/

DISCUSSION

In this study, we found that four SNPs were possibly associated with sPD in HACM, rs863108 in the LINC01524/LOC105372666 gene, rs80315856 in the DMRT2/SMARCA2 gene (Hu et al., 2016), rs28499371 in the PLEKHN1 gene (Hu et al., 2016), and rs2270568 in the FLJ23172/FNDC3B gene (Hu et al., 2016). Among them, two SNPs of rs863108 and rs80315856 were our previously reported SNPs (Hu et al., 2016). This study further certified our past studied result (Hu et al., 2016).

LINC01524, long intergenic non-protein coding RNA 1524, locates in 20q13.2 and consists of 3 exons, which belongs to the non-coding RNA (ncRNA) gene type. LOC105372666 locates in 20q13.2 and consists of 18 exons, belonging to the ncRNA gene type. LINC01524 and LOC105372666 are mainly expressed in the human testis tissue (Strausberg et al., 2002; Fagerberg et al., 2014). In this study, we found that the T > A variation of rs863108 polymorphism in the LINC01524/LOC105372666 gene was possibly associated with the risk of sPD from HACM. At present, the relationship and pathogenesis about the LINC01524/LOC105372666 gene with sPD have not been reported. Based on the LINC01524/LOC105372666 gene mainly expressed in the human testis tissue that generate androgen, we

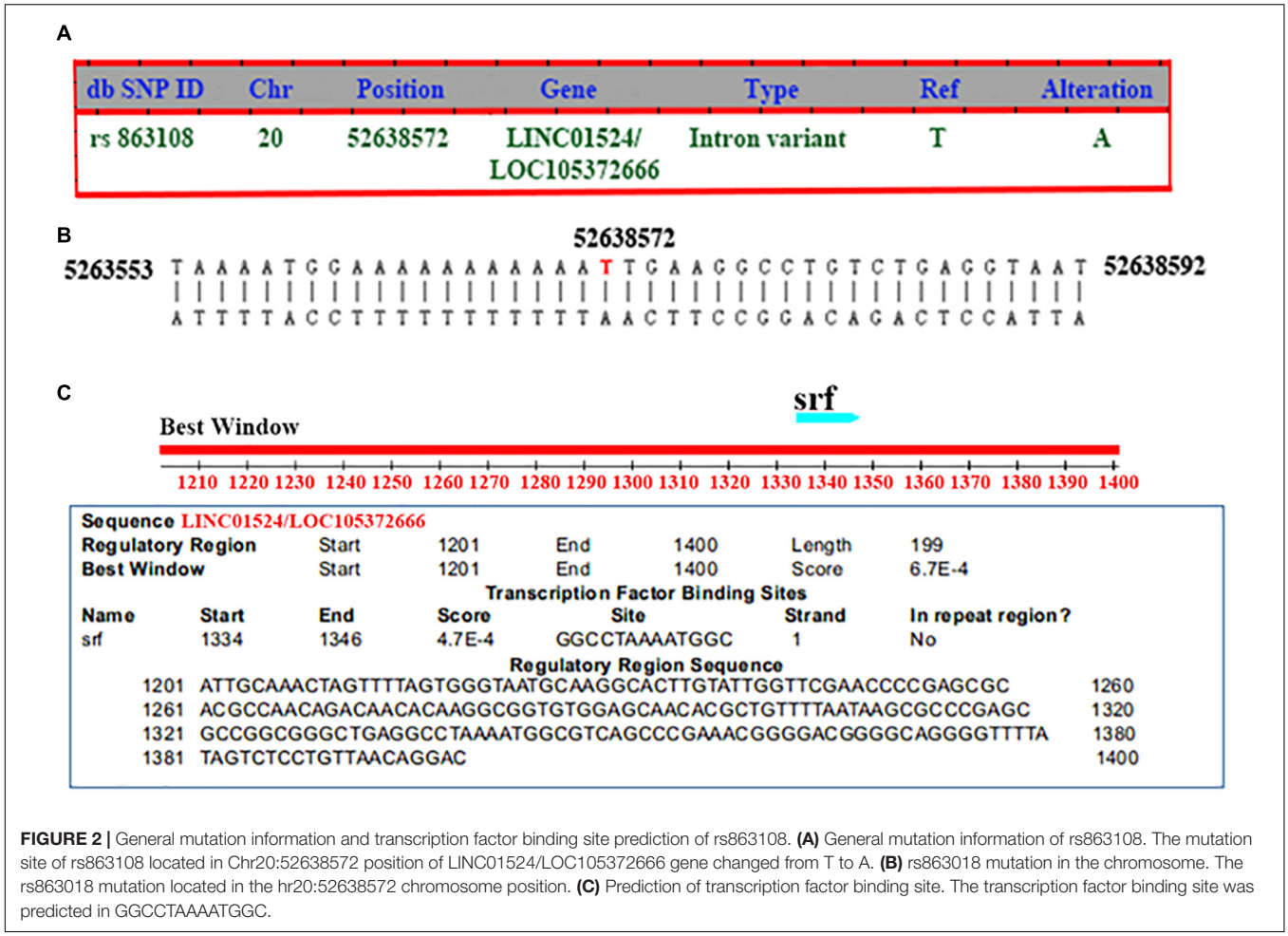


FIGURE 2 | General mutation information and transcription factor binding site prediction of rs863108. **(A)** General mutation information of rs863108. The mutation site of rs863108 located in Chr20:52638572 position of LINC01524/LOC105372666 gene changed from T to A. **(B)** rs863018 mutation in the chromosome. The rs863018 mutation located in the hr20:52638572 chromosome position. **(C)** Prediction of transcription factor binding site. The transcription factor binding site was predicted in GGCCTAAAATGGC.

hypothesized whether the pathogenesis of sPD was associated with the reduced secretion of androgen, as morbidity of sPD is higher in male than in female, and the partial sPD patients are accompanied with sexual dysfunction, which might be related with the abnormal expression of the LINC01524/LOC105372666 gene that contributes to the decrease in androgen level. The rs863108 polymorphism is a non-protein coding RNA in the LINC01524/LOC105372666 gene, which might play some roles in the pathogenesis of sPD through indirectly affecting the metabolism of androgen. The androgen hormone is closely associated with the pathogenesis of sPD, which is suggested to exert a protective effect in the brain (Snyder et al., 2018). Therefore, steroids and drugs altering endocrine conditions could have a potential curing effect for sPD. Sex hormones, particularly estrogen, progesterone, androgen, and dehydroepirosterone, play a protective effect in animal models and human studies of sPD. Drugs affecting the estrogen neurotransmission such as selective estrogen receptor modulators or affecting the steroid metabolism such as 5α-reductase inhibitors could be repositioned for the treatment of sPD. Sex steroids are also the modulator of neurotransmission; thus, they could repurpose to treat sPD motor symptoms and modulate the response to sPD medication (Bourque et al., 2019).

DMRT2, doublesex- and mab-3-related transcription factor 2, locates in 9p24.3, consists of nine exons, and is mainly expressed in the kidney, fat, lung, brain, colon, testis, lymph node, placenta, prostate, salivary gland, and esophagus (Fagerberg et al., 2014). DMRT2 shares a doublesex- and mab DNA-binding domain involved in sex determination. This gene also is associated with gonadal dysgenesis and XY sex reversal (Ottolenghi et al., 2000). Hence, this gene is one of candidates for sex-determining genes on chromosome 9.

SMARCA2 locates in 9p24.3 and consists of 38 exons. This gene comprehensively expresses in almost all tissues of the body and ubiquitously expresses in the ovary, testis, brain, thyroid, urinary bladder, and fat (Fagerberg et al., 2014). Possible functions consist of ATP binding, DNA-dependent ATPase activity (Xu et al., 2007), chromatin binding, helicase activity, histone binding, protein binding (Batsché et al., 2006; Tréand et al., 2006; Abramovitz et al., 2008; Kowenz-Leutz et al., 2010; Sahni et al., 2015; Garrido-Urbani et al., 2016), transcription coactivator activity (Abramovitz et al., 2008), and the DNA binding of transcription regulatory region (Abramovitz et al., 2008).

Our study showed that subjects carrying the T allele (T/T + G/T) of rs80315856 in the DMRT2/SMARCA2 gene

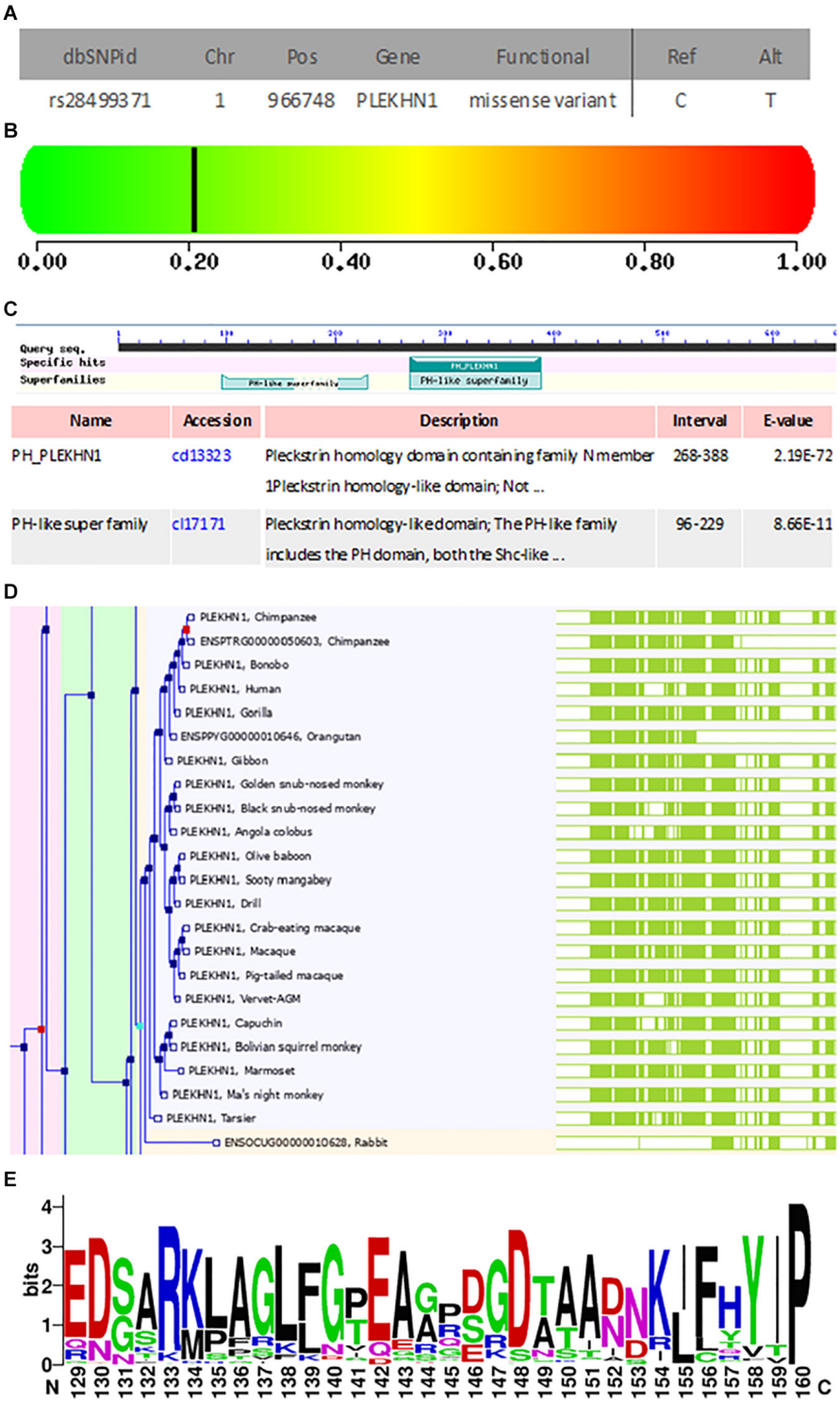


FIGURE 3 | General mutation information, pathogenicity prediction, structure domain analysis, and protein family evolution analysis of rs28499371. **(A)** General mutation information. The mutation site located in the Chr1:966748 changed from C to T. This mutation is a missense variant, which leads to the codon change from GCT to GTT and the amino acid change from A to V in the 43rd position of the coding protein. **(B)** Pathogenicity prediction of A43V mutation site. This mutation is predicted to be benign with a score of 0.208 (sensitivity, 0.92; specificity, 0.88). **(C)** PLEKHN1 structure domain analysis. PLEKHN1 is the PH-like super family. **(D,E)** The mutation site was in the 43rd amino acid position and did not appear in the protein structure domain. Analysis of protein family evolution. **(D)** PLEKHN1 gene evolution tree. **(E)** PLEKHN1 weblogo. The mutation sites located in the 143rd amino acid position and the main mutations are A, E, G, and S. In those mutations, A is the most important, and V is rare. The V mutation may lead to the pathogenicity.

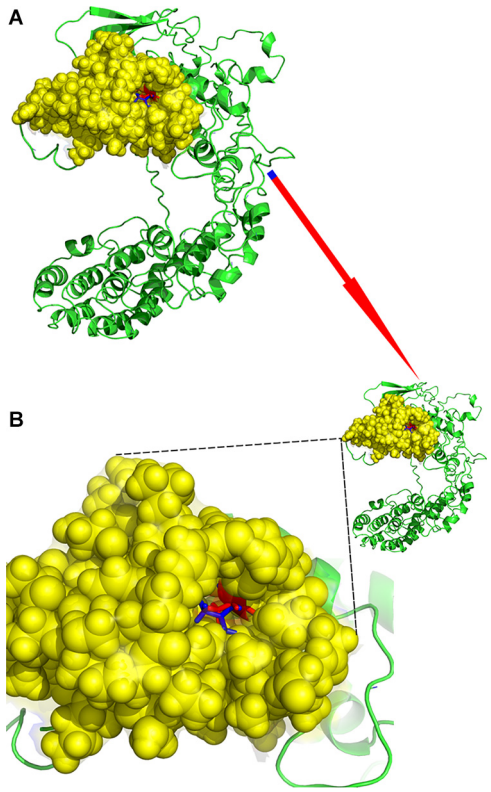


FIGURE 4 | Structure modeling analysis of rs28499371. **(A)** Protein alignment. **(B)** Mutation structure. The neighborhood partial structure was retained. The mutation amino acid was located at the center of protein pocket, and this may influence the neighborhood structure. Red represents the origin protein structure; blue represents the mutation protein structure.

increased the risk of sPD compared with other subjects. The relationship between DMRT2/SMARCA2 gene and sPD and their pathogeneses has not been studied yet. According to the above reviewed literatures, we suggested that the polymorphism of rs80315856 might be associated to the following elements. (1) The DMRT2 gene is a doublesex- and mab-3-related transcription factor, which decides the sexual gonadal genesis. Therefore, the alteration of rs80315856 polymorphism might affect the expression of male and female hormone, and the secretion of sexual hormone, especially the ratio of male and female hormone in a life time, might result in the imbalance of male and female hormone ratio following age increase, which results in sPD. The polymorphism alteration of DMRT2 gene might be one of the reasons of middle and elder population onset and the male domination of sPD. The polymorphism alteration of rs80315856 in the DMRT2/SMARCA2 gene was consistent with the rs863108 polymorphism in the LINC01524/LOC105372666 gene, which might further indicate that the disorder of sexual hormone secretion or metabolism was associated with the pathogenesis of sPD (Bourque et al., 2019). (2) The alteration of rs80315856 in the DMRT2/SMARCA2 gene might have an effect on DNA-binding transcription factor activity (Abramovitz et al., 2008), RNA polymerase II-specific, RNA polymerase II regulatory region sequence-specific DNA binding (Muchardt and Yaniv, 1993; Huuskonen et al., 2005; Xu et al., 2007), embryonic skeletal system development, the positive regulation of myotome development, the positive regulation of transcription by RNA polymerase II (Huuskonen et al., 2005; Xu et al., 2007), and the regulation of somitogenesis in the pathogensis of sPD. (3) The rs80315856 may also change the metal ion balance because of the change in metal ion binding and protein homodimerization activity, which might be associated with abnormal iron ion deposition in the pathogenesis of sPD (Jomova et al., 2010). (4) SMARCA2 gene codes ATP-dependent helicase that is associated with the actin-dependent regulator of chromatin a2, brahma homolog, global transcription activator homologous sequence, protein brahma homolog, and sucrose non-fermenting 2-like protein 2. Possible functions mainly take part in the metabolizing of energy in tissues and cells including the brain. The abnormal polymorphism of rs80315856 in the SMARCA2 gene might change the energy metabolization including the production of ATP and the balance of oxygen free radical generation and elimination. Our results further implied that the disorder of reactive oxygen species (ROS) is one of the possible pathogenesis of sPD, through regulating the transcription of certain genes by altering the chromatin structure around those genes, encoding the protein of partially large ATP-dependent chromatin, remodeling complex SNF/SWI, and generating the alternatively spliced transcript variants encoding different isoforms containing CAG length polymorphism.

PLEKHN1, also known as CLPABP, is pleckstrin homology domain containing N1. It locates in 1p36.33 and consists of 15 exons and is mainly expressed in the skin, esophagus, stomach, urinary bladder, and prostate (Fagerberg et al., 2014). PLEKHN1 majorly distributes in the cytoskeleton (Sano et al., 2008), mitochondrial membrane (Nishino et al., 2016; Kuriyama et al., 2018), mitochondrion (Sano et al., 2008; Maeda et al., 2018), and plasma membrane.

Our results showed that subjects carrying T allele (C/T + T/T) of rs28499371 in the PLEKHN1 gene decreased the risk of sPD compared with other subjects. The functional prediction of the mutation site and the structure domain analysis of rs28499371 revealed that missense mutation led to codon change from GCT to GTT and the amino acid change from A to V in the 43rd position of PLEKHN1 coding protein (**Figure 3A**). The pathogenicity prediction of the mutation site was benign, which might not result in pathogenicity. However, the structure domain analysis showed that the mutation sites located in the 143rd amino acid position and the main mutations are A, E, G, and S. In those mutations, A is the most important, and V is rare. The V mutation may lead to the pathogenicity (**Figures 3D,E**). The structure modeling analysis of rs28499371 found that the mutation amino acid is located at the center of the protein pocket, which may influence the neighborhood structure.

Besides our previous published study (Hu et al., 2016), the relationship and potential mechanism between PLEKHN1 and sPD have not been reported up to now. Because PLEKHN1 majorly distributes in the mitochondrion, we hypothesized that the alteration of rs28499371 polymorphism might be associated with the mitochondrion damage in the pathogenesis of sPD.

A

dbSNPid	Chr	Pos	Gene	Functional	Ref	Alt
rs2270568	3	172046861	FNDC3B	synonymous variant	T	C

B

Chro	Start	End	Ref	Mut	PolyPhen Score	Sift Score	Code	Base	Amino	Mut Base	Mut Amino
3	172046854	172046854	A	G	0.966	0.01	172046853,172046854,172046855	GAC	D	GGC	G
3	172046854	172046854	A	C	0.993	0.01	172046853,172046854,172046855	GAC	D	GCC	A
3	172046854	172046854	A	T	0.988	0.05	172046853,172046854,172046855	GAC	D	GTC	V
3	172046859	172046859	G	A	1	0	172046859,172046860,172046861	GGT	G	AGT	S
3	172046859	172046859	G	C	1	0	172046859,172046860,172046861	GGT	G	CGT	R
3	172046859	172046859	G	T	1	0	172046859,172046860,172046861	GGT	G	TGT	C
3	172046860	172046860	G	A	0.999	0	172046859,172046860,172046861	GGT	G	GAT	D
3	172046860	172046860	G	T	1	0	172046859,172046860,172046861	GGT	G	GTT	V
3	172046860	172046860	G	C	1	0	172046859,172046860,172046861	GGT	G	GCT	A
3	172046865	172046865	A	T	0.999	0	172046865,172046866,172048331	AGT	S	TGT	C
3	172046865	172046865	A	C	0.999	0.02	172046865,172046866,172048331	AGT	S	CGT	R
3	172046866	172046866	G	A	0.967	0	172046865,172046866,172048331	AGT	S	AAT	N
3	172046866	172046866	G	T	1	0	172046865,172046866,172048331	AGT	S	ATT	I
3	172048331	172048331	T	G	0.999	0.02	172046865,172046866,172048331	AGT	S	AGG	R
3	172048331	172048331	T	A	0.999	0.02	172046865,172046866,172048331	AGT	S	AGA	R

C

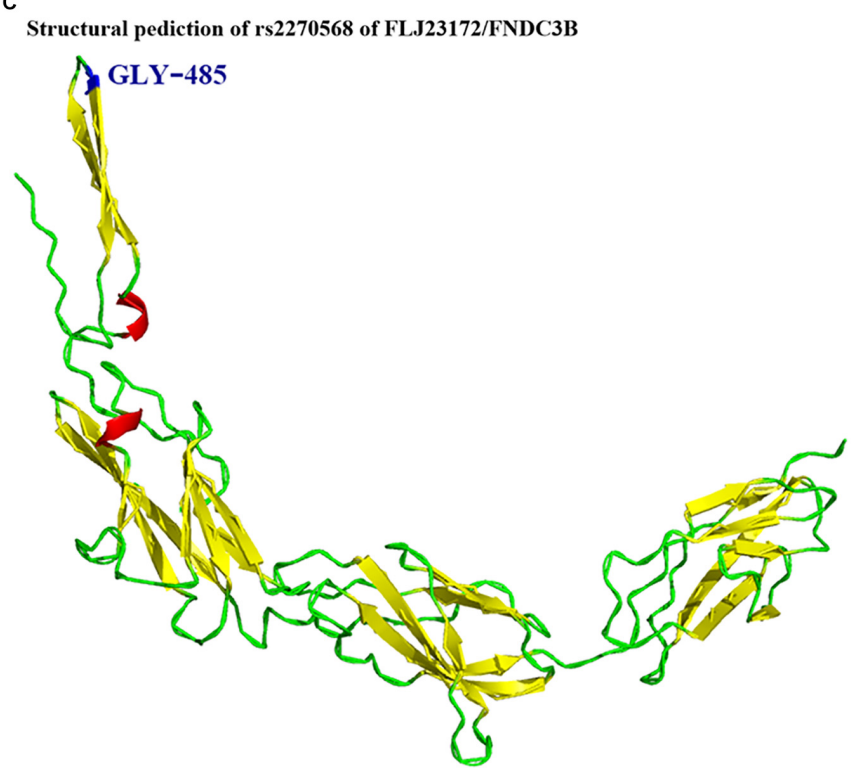


FIGURE 5 | General mutation information, pathogenicity prediction, and structure modeling of rs2270568. **(A)** The mutation site of rs2270568 located in Chr3:172046861 position changed from T to C. **(B)** Multiple pathogenicity site near rs2270568. The 2,869 pathogenicity sites were screened by the databases, and the multiple pathogenicity sites were found near the rs2270568 mutation site as shown in the figure. These pathogenicity sites lead to the change in amino acid. **(C)** Structure modeling of mutation. The mutation site appeared between the coil and beta sheet, which were the pathogenicity mutation region with high frequency occurrence. The pathogenicity sites near the mutation site may influence the protein function and the disease regulation mechanism. However, this protein function may not be much influenced by the mutation site. Blue represents the mutation site, red represents the alpha helix, yellow represents the beta sheet, and green represents the random coil.

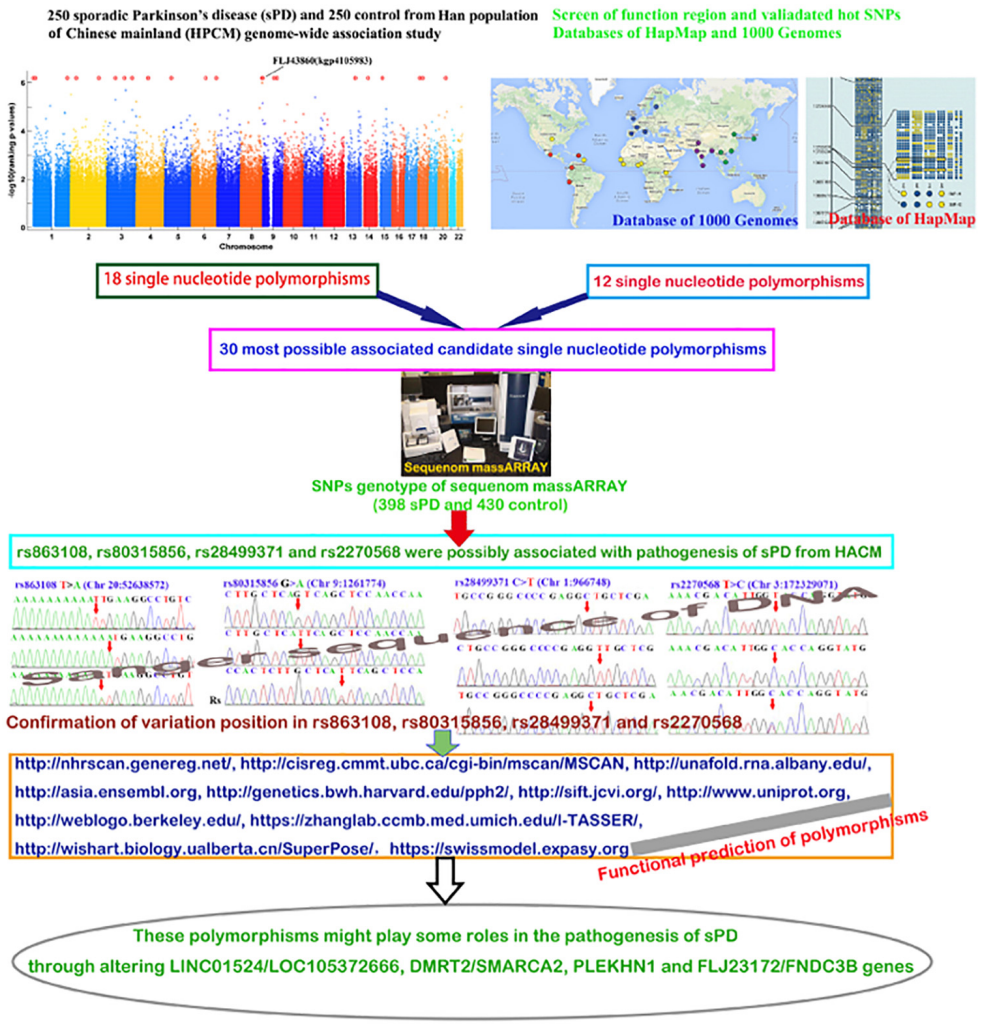


FIGURE 6 | The studied diagrammatic sketch. This figure generally described the design, procedures, methods, results, and conclusion.

Furthermore, respiratory chain impairment is a key feature in sPD patients, and there is a growing evidence that links proteins encoded by PD-associated genes to disturbances in the mitochondrial function (Grünewald et al., 2019). PLEKHN1 mainly takes part in the phospholipid-related functions including the phosphatidic acid, phosphatidylinositol phosphate, and phosphatidylserine binding (Sano et al., 2008); these functions play important biological effects in the production of nerve myelin sheath; moreover, PLEKHN1 also participates in the processes of 3′-UTR-mediated mRNA destabilization (Maeda et al., 2018), positive apoptotic regulation, and hypoxia response (Kuriyama et al., 2018). Therefore, we suggest that the alteration of rs28499371 polymorphism in the PLEKHN1 gene might play some pathophysiological roles in the pathogenesis of sPD through affecting the production of nerve myelin sheath, the destabilization of 3′-UTR-mediated mRNA, the regulation of neural cell apoptosis, and the response of hypoxia, subsequently contributing to nerve myelin sheath deletion, excessive neural cell apoptosis, and increased ROS production, which ultimately result in the death of the DA neuron in sPD.

FLJ23172, also known as TMEM212 gene, locates in 3q26.31, consists of five exons, and majorly expresses in the lung, endometrium, testis, and prostate (Fagerberg et al., 2014). FNDC3B, also known as FAD104, PRO4979, and YVTM2421, locates in 3q26.31, consists of 30 exons, and ubiquitously expresses in the ovary, testis, brain, thyroid, urinary bladder, fat, adrenal tissue, and endometrium (Fagerberg et al., 2014). This gene codes the protein of fibronectin type III domain-containing protein 3B and also includes HCV NS5A-binding protein 37 and factor for adipocyte differentiation 104. The possible function is RNA binding (Castello et al., 2012).

Our results revealed that subjects carrying the T allele (T/T + C/T) of rs2270568 exhibited no significance when compared with other subjects, and the G/T genotype of rs2270568 decreased the risk of sPD when compared with other genotypes (**Table 3**). The MAF of rs2270568 was significantly higher in

sPD patients than that in controls, which implied that the T allele of rs2270568 was a risk locus for sPD. The pathogenicity prediction and the structure modeling of rs2270568 indicated that the mutation site of rs2270568 resulted in a nucleotide alteration from T to C (**Figure 5A**). The variant is synonymous and resides within a pathogenicity region, which may suggest its potential involvement in the disease (**Figure 5B**). Although the mutation site appeared between the coil and beta sheet, which were the pathogenicity mutation region with high frequency occurrence, this protein function might not be influenced by the mutation site. However, the pathogenicity sites near the mutation site might influence the protein function and the disease regulation mechanism (**Figure 5C**). FLJ23172 majorly expresses in the testis and prostate; therefore, we speculated that alteration of rs2270568 polymorphism might affect the secretion of androgen and progesterone and participate in the pathogenesis of sPD (Bourque et al., 2019). FNDC3B ubiquitously expresses in the testis, brain, and adrenal tissues, which implied that the rs2270568 polymorphism alteration might regulate the secretion of prostaglandin, androgen, and adrenocortical hormones, and play some effects in sPD (Bourque et al., 2019). The accurate mechanisms about the relationship between FLJ23172/FNDC3B and the pathogenesis of sPD need to be further studied.

CONCLUSION

In general, our data supported that four polymorphisms of rs863108, rs80315856, rs28499371, and rs2270568 possibly were associated with the pathogenesis of sPD in HACM and further identified two previous reported SNPs of rs863108 and rs80315856. The alteration of rs863108, rs80315856, rs28499371, and rs2270568 polymorphism might affect the metabolism of sexual hormones including estrogen, progesterone, androgen, dehydroepirosterone, prostaglandin, and adrenocortical hormones; the increase in ROS production induced by abnormal iron ion deposition and hypoxia response; the increase in neural cell apoptosis; and the deletion of nerve myelin sheath in the pathogenesis of sPD in HACM (**Figure 6**).

DATA AVAILABILITY STATEMENT

The original contributions presented in the study are included in the article/**Supplementary Material**, further inquiries can be directed to the corresponding authors.

ETHICS STATEMENT

This study was approved by the Institutional Review Board of the Hospital Human Ethics Committee of The First Affiliated Hospital of Nanchang University and The Affiliated Guangdong General Hospital of Nan Fang Medical University. The patients/participants provided their written informed consent to participate in this study.

AUTHOR CONTRIBUTIONS

RX, BW, and XZ conceived and designed the experiments and wrote the manuscript. BW, XL, SX, ZL, and YZ performed the experiments and analyzed the data. RX contributed to the reagents, materials, and analysis tools. RX and BW processed the figures. All authors have been involved in the drafting, critical revision, and final approval of the manuscript for publication, and agreed to be accountable for all aspects of the work in ensuring that questions related to the accuracy or integrity of any part of the work are appropriately investigated and resolved.

FUNDING

This work was supported by grants from the National Natural Science Foundation of China (30560042, 81160161, and 81360198), the Education Department of Jiangxi Province (GJJ13198 and GJJ170021), the Jiangxi Provincial Department of Science and Technology [(2014)-47, 20142BBG70062, and 20171BAB215022], the Health and Family Planning Commission of Jiangxi Province (20181019), and the Natural Science Foundation of Guangdong Province (2019A1515011341). The funders had no role in study design, data collection and analysis, decision to publish, or preparation of the manuscript.

SUPPLEMENTARY MATERIAL

The Supplementary Material for this article can be found online at: https://www.frontiersin.org/articles/10.3389/fnagi.2020.603793/full#supplementary-material

REFERENCES

Abramovitz, L., Shapira, T., Ben-Dror, I., Dror, V., Granot, L., Rousso, T., et al. (2008). Dual role of NRSF/REST in activation and repression of the glucocorticoid response. *J. Biol. Chem.* 283, 110–119. doi: 10.1074/jbc.M707366200

Alkema, W. B., Johansson, O., Lagergren, J., and Wasserman, W. W. (2004). MSCAN: identification of functional clusters of transcription factor binding sites. *Nucleic. Acids. Res.* 32, W195–W198. doi: 10.1093/nar/gkh387

Allen, H. L., Estrada, K., Lettre, G., Berndt, S. I., Weedon, M. N., Rivadeneira, F., et al. (2010). Hundreds of variants clustered in genomic loci and biological pathways affect human height. *Nature* 467, 832–838. doi: 10.1038/nature09410

Batsché, E., Yaniv, M., and Muchardt, C. (2006). The human SWI/SNF subunit Brm is a regulator of alternative splicing. *Nat. Struct. Mol Biol.* 13, 22–29. doi: 10.1038/nsmb1030

Billingsley, K. J., Bandres-Ciga, S., Saez-Atienzar, S., and Singleton, A. B. (2018). Genetic risk factors in Parkinson's disease. *Cell Tissue Res.* 373, 9–20.

Bourque, M., Morissette, M., and Di Paolo, T. (2019). Repurposing sex steroids and related drugs as potential treatment for Parkinson's disease. *Neuropharmacology* 147, 37–54. doi: 10.1016/j.neuropharm.2018.04.005

Castello, A., Fischer, B., Eichelbaum, K., Horos, R., Beckmann, B. M., Strein, C., et al. (2012). Insights into RNA biology from an atlas of mammalian mRNA-binding proteins. *Cell* 149, 1393–1406. doi: 10.1016/j.cell.2012.04.031

Cummings, J. L., Henchcliffe, C., Schaier, S., Simuni, T., Waxman, A., and Kemp, P. (2011). The role of dopaminergic imaging in patients with symptoms of dopaminergic system neurodegeneration. *Brain* 134, 3146–3166. doi: 10.1093/brain/awr177

Fagerberg, L., Hallström, B. M., Oksvold, P., Kampf, C., Djureinovic, D., Odeberg, J., et al. (2014). Analysis of the human tissue-specific expression by genome-wide integration of transcriptomics and antibody-based proteomics. *Mol. Cell Proteomics.* 13, 397–406. doi: 10.1074/mcp.M113.035600

Fahn, S. (2003). Description of Parkinson's disease as a clinical syndrome. *Ann. N. Y. Acad. Sci.* 991, 1–14. doi: 10.1111/j.1749-6632.2003.tb07458.x

Garrido-Urbani, S., Garg, P., Ghossoub, R., Arnold, R., Lembo, F., Sundell, G. N., et al. (2016). Proteomic peptide phage display uncovers novel interactions of the PDZ1-2 supramodule of syntenin. *FEBS. Lett.* 590, 3–12. doi: 10.1002/1873-3468.12037

Göttlich, M., Münte, T. F., Heldmann, M., Kasten, M., Hagenah, J., and Krämer, U. M. (2013). Altered resting state brain networks in Parkinson's disease. *PLoS. One* 8:e77336. doi: 10.1371/journal.pone.0077336

Grünewald, A., Kumar, K. R., and Sue, C. M. (2019). New insights into the complex role of mitochondria in Parkinson's disease. *Prog. Neurobiol.* 177, 73–93. doi: 10.1016/j.pneurobio.2018.09.003

Hellquist, A., Zucchelli, M., Lindgren, C. M., Saarialho-Kere, U., Järvinen, T. M., Koskenmies, S., et al. (2009). Identification of MAMDC1 as a candidate susceptibility gene for systemic lupus erythematosus (SLE). *PLoS One* 4:e8037. doi: 10.1371/journal.pone.0008037

Huuskonen, J., Vishnu, M., Fielding, P. E., and Fielding, C. J. (2005). Activation of ATP-binding cassette transporter A1 transcription by chromatin remodeling complex. *Arterioscler. Thromb. Vasc. Biol.* 25, 1180–1185. doi: 10.1161/01.ATV.0000163186.58462.c5

Hu, Y., Deng, L., Zhang, J., Fang, X., Mei, P., Cao, X., et al. (2016). A pooling genome-wide association study combining a pathway analysis for typical sporadic Parkinson's disease in the han population of Chinese Mainland. *Mol. Neurobiol.* 53, 4302–4318. doi: 10.1007/s12035-015-9331-y

Jomova, K., Vondrakova, D., Lawson, M., and Valko, M. (2010). Metals, oxidative stress and neurodegenerative disorders. *Mol. Cell Biochem.* 345, 91–104. doi: 10.1007/s11010-010-0563-x

Kalia, L. V., and Lang, A. E. (2015). Parkinson's disease. *Lancet* 386, 896–912. doi: 10.1016/S0140-6736(14)61393-3

Khoo, T. K., Yarnall, A. J., Duncan, G. W., Coleman, S., O'Brien, J. T., Brooks, D. J., et al. (2013). The spectrum of nonmotor symptoms in early Parkinson disease. *Neurology* 80, 276–281. doi: 10.1212/WNL.0b013e31827deb74

Kowenz-Leutz, E., Pless, O., Dittmar, G., Knoblich, M., and Leutz, A. (2010). Crosstalk between C/EBPbeta phosphorylation, arginine methylation, and SWI/SNF/Mediator implies an indexing transcription factor code. *EMBO. J.* 29, 1105–1115. doi: 10.1038/emboj.2010.3

Kuriyama, S., Tsuji, T., and Sakuma, T. (2018). PLEKHN1 promotes apoptosis by enhancing Bax-Bak hetro-oligomerization through interaction with Bid in human colon cancer. *Cell Death Discov.* 4:11. doi: 10.1038/s41420-017-0006-5

Li, J., Jin, M., Wang, L., Qin, B., and Wang, K. (2017). MDS clinical diagnostic criteria for Parkinson's disease in China. *J. Neurol.* 264, 476–481. doi: 10.1007/s00415-016-8370-2

Li, S., Cui, Y., and Romero, R. (2014). Entropy-based selection for maternal-fetal genotype incompatibility with application to preterm prelabor rupture of membranes. *BMC Genet.* 15:66. doi: 10.1186/1471-2156-15-66

Maeda, A., Uchida, M., Nishikawa, S., Nishino, T., and Konishi, H. (2018). Role of N-myristoylation in stability and subcellular localization of the CLPABP protein. *Biochem. Biophys. Res. Commun.* 495, 1249–1256. doi: 10.1016/j.bbrc.2017.11.112

Marsden, C. D. (1994). Parkinson's disease. *J. Neurol. Neurosurg. Psychiatry* 57, 672–681. doi: 10.1136/jnnp.57.6.672

Muchardt, C., and Yaniv, M. (1993). A human homologue of Saccharomyces cerevisiae SNF2/SWI2 and Drosophila brm genes potentiates transcriptional activation by the glucocorticoid receptor. *EMBO. J.* 12, 4279–4290. doi: 10.1002/j.1460-2075.1993.tb06112.x

Nishino, T., Matsunaga, R., Jikihara, H., Uchida, M., Maeda, A., Qi, G., et al. (2016). Antagonizing effect of CLPABP on the function of HuR as a regulator of ARE-containing leptin mRNA stability and the effect of its depletion on obesity in old male mouse. *Biochim. Biophys. Acta* 1861, 1816–1827. doi: 10.1016/j.bbalip.2016.09.006

Ottolenghi, C., Veitia, R., Barbieri, M., Fellous, M., and McElreavey, K. (2000). The human doublesex-related gene, DMRT2, is homologous to a gene involved in somitogenesis and encodes a potential bicistronic transcript. *Genomics* 64, 179–186. doi: 10.1006/geno.2000.6120

Polito, L., Greco, A., and Seripa, D. (2016). Genetic profile, environmental exposure, and their interaction in Parkinson's Disease. *Parkinsons Dis.* 2016:6465793. doi: 10.1155/2016/6465793

Rozenkrantz, L., Gan-Or, Z., Gana-Weisz, M., Mirelman, A., Giladi, N., Bar-Shira, A., et al. (2016). SEPT14 Is associated with a reduced risk for Parkinson's disease and expressed in human brain. *J. Mol. Neurosci.* 59, 343–350. doi: 10.1007/s12031-016-0738-3

Sahni, N., Yi, S., Taipale, M., Bass, J. I. J., Coulombe-Huntington, J., Yang, F., et al. (2015). Widespread macromolecular interaction perturbations in human genetic disorders. *Cell* 161, 647–660. doi: 10.1016/j.cell.2015.04.013

Sano, E., Shono, S., Tashiro, K., Konishi, H., Yamauchi, E., and Taniguchi, H. (2008). Novel tyrosine phosphorylated and cardiolipin- binding protein CLPABP functions as mitochondrial RNA granule. *Biochim. Biophys. Acta* 1783, 1036–1047. doi: 10.1016/j.bbamcr.2007

Singleton, A. B., Farrer, M. J., and Bonifati, V. (2013). The genetics of Parkinson's disease: progress and therapeutic implications. *Mov. Disord.* 28, 14–23. doi: 10.1002/mds.25249

Snyder, B., Duong, P., Trieu, J., and Cunningham, R. L. (2018). Androgens modulate chronic intermittent hypoxia effects on brain and behavior. *Horm. Behav.* 106, 62–73. doi: 10.1016/j.yhbeh.2018.09.005

Soldner, F., Stelzer, Y., Shivalila, C. S., Abraham, B. J., Latourelle, J. C., Barrasa, M. I., et al. (2016). Parkinson-associated risk variant in distal enhancer of alpha-synuclein modulates target gene expression. *Nature* 533, 95–99. doi: 10.1038/nature17939

Strausberg, R. L., Feingold, E. A., Grouse, L. H., Derge, J. G., Klausner, R. D., Collins, F. S., et al. (2002). Generation and initial analysis of more than 15,000 full-length human and mouse cDNA sequences. *Proc. Natl. Acad. Sci. USA.* 99, 16899–16903. doi: 10.1073/pnas.242603899

Tréand, C., du, Chéné, I., Brès, V., Kiernan, R., Benarous, R., et al. (2006). Requirement for SWI/SNF chromatin-remodeling complex in Tat-mediated activation of the HIV-1 promoter. *EMBO J.* 25, 1690–1699. doi: 10.1038/sj.emboj.7601074

von Otter, M., Bergström, P., Quattrone, A., De Marco, E. V., Annesi, G., Söderkvist, P., et al. (2014). Genetic associations of Nrf2-encoding NFE2L2 variants with Parkinson's disease-a multicenter study. *BMC Med. Genet.* 15:131. doi: 10.1186/s12881-014-0131-4

Wang, L., Maldonado, L., Beecham, G. W., Martin, E. R., Evatt, M. L., Ritchie, J. C., et al. (2016). DNA variants in CACNA1C modify Parkinson disease risk only when vitamin D level is deficient. *Neurol. Genet.* 2:e72. doi: 10.1212/NXG.0000000000000072

Xu, Y., Zhang, J., and Chen, X. (2007). The activity of p53 is differentially regulated by Brm- and Brg1-containing SWI/SNF chromatin remodeling complexes. *J. Biol. Chem.* 282, 37429–37435. doi: 10.1074/jbc.M706039200

Yang, X., Zhao, Q., An, R., Zhou, H., Lin, Z., and Xu, Y. (2016). SNP rs1805874 of the calbindin1 gene is associated with Parkinson's disease in Han Chinese. *Genet. Test. Mol. Biomarkers* 20, 753–757. doi: 10.1089/gtmb.2016.0149

Conflict of Interest: The authors declare that the research was conducted in the absence of any commercial or financial relationships that could be construed as a potential conflict of interest.

Copyright © 2021 Wang, Liu, Xu, Liu, Zhu, Zhang and Xu. This is an open-access article distributed under the terms of the Creative Commons Attribution License (CC BY). The use, distribution or reproduction in other forums is permitted, provided the original author(s) and the copyright owner(s) are credited and that the original publication in this journal is cited, in accordance with accepted academic practice. No use, distribution or reproduction is permitted which does not comply with these terms.

frontiers in Aging Neuroscience

ORIGINAL RESEARCH
published: 13 January 2021
doi: 10.3389/fnagi.2020.599045

A Comprehensive Phenotype of Non-motor Impairments and Distribution of Alpha-Synuclein Deposition in Parkinsonism-Induced Mice by a Combination Injection of MPTP and Probenecid

Na-Ra Han[1,2], Yu-Kang Kim[1,2], Sora Ahn[1], Tae-Yeon Hwang[1,3], Hyejung Lee[3] and Hi-Joon Park[1,2]**

[1] Integrative Parkinson's Disease Research Group, Acupuncture and Meridian Science Research Center, Kyung Hee University, Seoul, South Korea, [2] Department of Anatomy & Information Sciences, College of Korean Medicine, Kyung Hee University, Seoul, South Korea, [3] Department of Meridian & Acupoints, College of Korean Medicine, Kyung Hee University, Seoul, South Korea

OPEN ACCESS

Edited by:
Shaomin Li,
Brigham and Women's Hospital and Harvard Medical School, United States

Reviewed by:
Gabriela Mercado,
Van Andel Institute, United States
Jifeng Guo,
Central South University, China

***Correspondence:**
Hyejung Lee
hjlee@khu.ac.kr
Hi-Joon Park
acufind@khu.ac.kr

Received: 26 August 2020
Accepted: 21 December 2020
Published: 13 January 2021

Citation:
Han N-R, Kim Y-K, Ahn S, Hwang T-Y, Lee H and Park H-J (2021) A Comprehensive Phenotype of Non-motor Impairments and Distribution of Alpha-Synuclein Deposition in Parkinsonism-Induced Mice by a Combination Injection of MPTP and Probenecid. Front. Aging Neurosci. 12:599045. doi: 10.3389/fnagi.2020.599045

Parkinson's disease (PD) is characterized by non-motor symptoms as well as motor deficits. The non-motor symptoms rarely appear individually and occur simultaneously with motor deficits or independently. However, a comprehensive research on the non-motor symptoms using an experimental model of PD remains poorly understood. The aim of the current study is to establish a chronic mouse model of PD mimicking the comprehensive non-motor symptoms of human PD by injection of 1-methyl-4-phenyl-1,2,3,6-tetrahydropyridine (MPTP) and probenecid (MPTP/p). The non-motor and motor symptoms were evaluated by performing buried food, short-term olfactory memory, hot plate, open field, tail suspension, Y maze, novel object recognition, bead expulsion, one-h stool collection, rotarod, rearing, catalepsy, and akinesia tests after 10 injections of MPTP/p into mice. The expression levels of α-synuclein, glial fibrillary acidic protein (GFAP), tyrosine hydroxylase (TH) or DJ-1 were analyzed by Western blotting or immunostaining. MPTP/p-treated mice achieved to reproduce the key features of non-motor symptoms including olfactory deficit, thermal hyperalgesia, anxiety, depression, cognitive decline, and gastrointestinal dysfunction in addition to motor deficits. The MPTP/p-treated mice also showed the high levels of α-synuclein and low levels of TH and DJ-1 in striatum, substantia nigra, olfactory bulb, hippocampus, amygdala, prefrontal cortex, locus coeruleus, or colon. In addition, the expression levels of phosphorylated-α-synuclein and GFAP were elevated in the striatum and substantia nigra in the MPTP/p-treated mice. Taken together, our study clarifies that the chronic MPTP/p-treated mice have a variety of non-motor dysfunctions as well as motor

abnormalities by α-synuclein overexpression and dopaminergic depletion. Therefore, the study of comprehensive phenotypes of non-motor symptoms in one PD model would advance in-depth understandings of neuropathological alternations and contribute to future strategies for PD treatment.

Keywords: Parkinson's disease, non-motor symptoms, α-synuclein, 1-methyl-4-phenyl-1,2,3,6-tetrahydropyridine and probenecid, behavior tests

INTRODUCTION

Parkinson's disease (PD) is currently regarded as the most common neurodegenerative disorder following Alzheimer's disease, that affects over 5 million people worldwide and 1–3% of people over 50 years of age (Meissner et al., 2011; Lashuel et al., 2013). PD is mainly characterized by motor deficits including tremor or rigidity (Dauer and Przedborski, 2003). These motor deficits result from severe loss of dopaminergic nigrostriatal neurons (Maiti et al., 2017). Recently, however, a wide range of non-motor symptoms such as olfactory deficit or cognitive decline is known to be strongly associated with PD pathological processes and significantly affect the quality of life of PD patients (Schapira et al., 2017; Monastero et al., 2018; Liu et al., 2020).

α-synuclein is a major pathological protein that underlies PD pathogenesis (Butkovich et al., 2018). The widespread aggregation of α-synuclein is a neuropathological hallmark of PD (Dehay et al., 2015). The progressive and abnormal accumulation of α-synuclein in various brains regions leads to neurodegeneration and impairment of neurotransmitter release (Lashuel et al., 2013). In addition, the overexpression of α-synuclein in striatum, substantia nigra, olfactory bulb, hippocampus, amygdala, prefrontal cortex, locus coeruleus, and colon are involved in non-motor features such as anxiety, depression or cognitive decline (Jellinger, 2011; Shannon et al., 2012; Flores-Cuadrado et al., 2016; Schapira et al., 2017; Butkovich et al., 2018; Henrich et al., 2018; Stoyka et al., 2020). The high level of phosphorylated (p)-α-synuclein is a pathological deposition of α-synuclein in correlation with the behavioral phenotypes of PD (Canerina-Amaro et al., 2019). One of phosphorylated forms of α-synuclein, pS129, is significantly correlated with PD severity (Wang et al., 2012; Stewart et al., 2015).

Animal models have been developed to identify pathological mechanisms of PD using several neurotoxins such as 1-methyl-4-phenyl-1,2,3,6-tetrahydropyridine (MPTP) as reviewed by Zeng et al. (2018). Among the neurotoxins, MPTP crossed blood–brain barrier after systemic administration and exhibited the notable degeneration of nigrostriatal dopaminergic neurons in a PD model (Zeng et al., 2018). Thus, an MPTP-intoxicated mouse model has been commonly used as an animal PD model (Chan et al., 2007; Jackson-Lewis and Przedborski, 2007). However, the dopamine loss was rapid and not progressive, so it was often difficult to determine the motor disability of PD in most MPTP models (Meredith et al., 2008). Motor deficits appeared in several acute or subacute MPTP mouse models (Li et al., 2016; Sim et al., 2017), but other MPTP models hardly mimicked the motor deficits of human PD (Rousselet et al., 2003; Luchtman et al., 2009; Zhang et al., 2017). Chan et al. (2007) suggested that the chronic injection of both MPTP and probenecid (MPTP/p) induces pathological hallmarks of PD with motor deficits, making it an appropriate excellent choice for pathogenic researches on PD.

The most of PD patients have one or more non-motor symptoms (Shalash et al., 2018). There was a clinically significant correlation among non-motor signs (Bugalho et al., 2016). However, studies using a PD mouse model have been limited to a specific non-motor symptom or the lack of a comprehensive approach to non-motor symptoms (Laloux et al., 2008; Fox et al., 2010; Park et al., 2015; Ellett et al., 2016). The mutual neuropathological study of non-motor symptoms and establishment of an experimental model representing the comprehensive non-motor symptoms of human PD are needed to clarify the complexity of PD. Thus, the aim of the current study is to establish an experimental model of PD with the spectrum of non-motor symptoms in addition to motor impairments caused by the chronic injection of MPTP/p, which mimics characteristics of human PD.

MATERIALS AND METHODS

Animals

Eight-week-old male C57BL/6 mice (24–26 g, Central Laboratories Animal Inc., Seoul, South Korea) were maintained under a standard laboratory condition (12 h light–dark cycle, 55 ± 10% relative humidity and 22 ± 1°C). We used male mice for establishing a PD mouse model with reference to the previous reports (Lei et al., 2012; Brichta et al., 2015; Maatouk et al., 2018). Mice were given *ad libitum* access to water and feed. Experimental procedures were performed with reference to the National Institutes of Health Guide for the Care and Use of Laboratory Animals. The procedures were also approved by the Dongguk University Animal Care Committee (IACUC-2017-023-1).

Experimental Procedures

MPTP (Cat# 16377, Cayman Chemical, Ann Arbor, MI, United States) was dissolved in saline and prepared at a concentration of 25 mg/kg according to a report of Shao et al. (2019). Probenecid (Cat# 14981, Cayman Chemical) was dissolved in dimethyl sulfoxide and prepared at a concentration of 250 mg/kg according to a report of Shao et al. (2019). Experimental procedures (**Figure 1A**) were as follows. Mice were randomly grouped into two groups (MPTP/p group and control group) after a week of acclimatization. MPTP/p was

intraperitoneally administered twice per week for 5 weeks (Chan et al., 2007; Luchtman et al., 2009; Shao et al., 2019). Because probenecid as an adjuvant maintains the effectiveness of neurotoxins of chronic MPTP by reducing the renal excretion of MPTP and its metabolites, probenecid was administered 30 min before the MPTP injection (Meredith et al., 2008; Choi et al., 2018). Control mice were injected with saline and dimethyl sulfoxide twice a week for 5 weeks. Three days after the last injection, on day 35, the non-motor symptoms and motor dysfunctions were evaluated using various behavior tests. All animals were then sacrificed for further study.

Behavior Tests

The behavior tests are listed in **Table 1**. All behavior tests were conducted by blind observers between 9: 00 and 18: 00. On day 35, the mice were first subjected to the rotarod test and buried food test (**Figure 1A**, black; $n = 14$/group). In order to minimize the stress of the experimental animals, mice were randomly divided into two kinds of tests (**Figure 1A**, red; $n = 7$/group and blue; $n = 7$/group) the next day. On day 40, all mice were combined to perform the tail suspension test and akinesia test (black; $n = 14$/group).

Buried Food Test

To assess the olfactory deficit, we performed the buried food test as previously described with a few modifications (Yang and Crawley, 2009). The buried food test measures how quickly food-restricted mice find hidden food. The mice that are unable to find the food within a 15 min period are assumed to have olfactory dysfunctions. Mice usually find the hidden piece of food in a few min (Yang and Crawley, 2009). For the buried food test, a clean mouse cage was filled with clean litter 3–4 cm deep. Mice were subjected to fasting without water and feed 24 h before the test. The mouse was placed in any corner of the cage. The pieces of cheese were buried in a different location. The litter was changed between mice. The time until the mouse found the hidden piece of cheese (when the mouse touched the pellet) was measured.

Short-Term Olfactory Memory Test

We performed the short-term olfactory memory test as another test to evaluate the olfactory deficit as previously described (Petit et al., 2013). It is expected that mice would spend less time sniffing in the second trial (T2) if they remember the odor in the first trial (T1) (Petit et al., 2013). We exposed a mouse to the lemon juice odor at two 5 min-trials separated by 120 s inter-trial intervals. The sniffing time was defined as head up sniffing within 1 cm of the odor source. It was analyzed by video recording and expressed as a percentage of time to sniff the odor at T2 compared to the total time to sniff at both T1 and T2.

Hot Plate Test

The hot plate test was performed to evaluate the thermal hyperalgesia as previously described (Challis et al., 2020). The latency time is measured after the first occurrence of the following endpoint nocifensive behaviors: flinching, hind paw licking or jumping. Since the forefoot is used for grooming and exploration, and not consistently in contact with the metal surface, licking, or withdrawal of the hind paw is considered a more reliable indicator of nociception (Deuis et al., 2017). A mouse was habituated to an unheated hot plate (Bioseb – *In Vivo* Research Instruments, Pinellas Park, FL, United States; Model: BIO-CHP) for 5 min. The latency time taken to elicit the nocifensive behaviors was measured after the mouse was placed on the metal surface maintained at a constant temperature 52.5°C. The cutoff time was set to 40 s to prevent a paw thermal injury.

Open Field Test

To assess the anxiety-related behaviors, we performed the open field test as previously described (Park et al., 2015). Thigmotaxis or wall-hugging behavior is associated with anxiety-related behaviors to avoid wide open areas and regarded as the starting point for anxiety-related tests (Seibenhener and Wooten, 2015). The center zone size was designated as 20 cm × 20 cm (Bailey and Crawley, 2009). A mouse was placed in an open top and square box (40 cm × 40 cm × 24 cm) in a quiet room and able to freely move for 5 min under bright illumination. The box was thoroughly wiped with 10% ethanol between each test to remove any residue. The number of entries into center zone, total movement distance, and central movement distance were analyzed with Smart 3.0 software (Panlab Harvard Apparatus, Barcelona, Spain). Finally, the anxiety-like behavior was examined as a ratio of central/total distance.

Tail Suspension Test

To assess the depression-like behaviors, we performed the tail suspension test as previously described (Badr et al., 2020). The immobility is a behavioral characteristic associated with depression (Cryan et al., 2005). A mouse was suspended 50 cm above the ground using plastic boxes (50 cm × 50 cm × 50 cm) and adhesive tape about 1 cm from the tip of tail. The immobility time was considered when the mouse hung completely motionless. We recorded the immobility time during 6 min.

Y Maze Test

To evaluate the cognitive decline, we performed the Y maze test to analyze immediate spatial working memory as a form of short-term memory as previously described (Yan et al., 2017). Mice generally prefer a new arm rather than returning to the previously visited location in the maze. Spontaneous alternations of mice are considered to enter the other arms in succession, i.e., ABC, BAC or CBA, but not CAC (CAC means repetitive), which means that mice have immediate spatial working memory (Yan et al., 2017). The Y-maze consisted of three white acrylic arms (30 cm × 5 cm × 15 cm) with a common neutral area (triangular neutral zone) in the center (5 cm × 5 cm × 15 cm). A mouse was placed in an arbitrary arm and able to freely explore through the maze for 5 min. The Y maze arms were wiped with 10% ethanol between tests. The alternation was expressed as a ratio of actual alternations to possible alternations (total arm entries – 2). The equation is as follows: alternation (%) = [number of alternations/(total arm entries – 2)] × 100.

Novel Object Recognition Test

We performed the novel object recognition test as another test to evaluate the cognitive decline as previously described

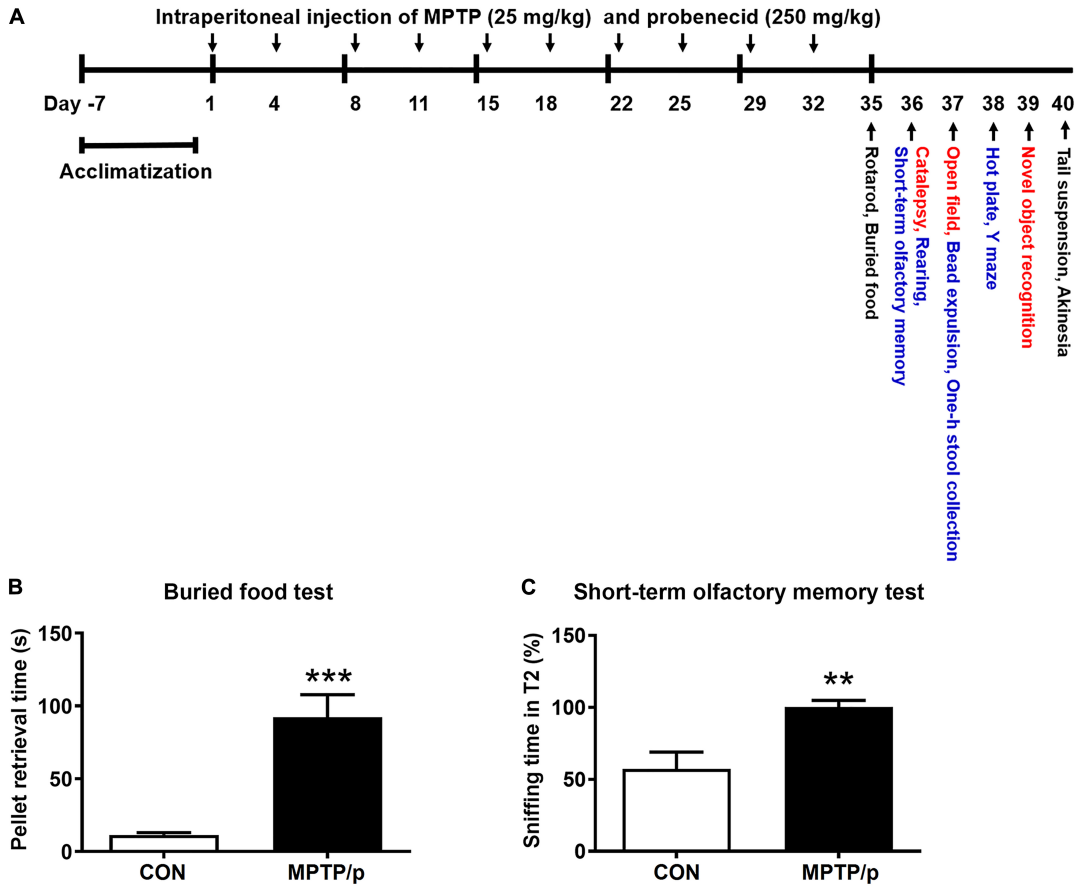


FIGURE 1 | The chronic injection of MPTP/p causes olfactory deficit in mice. **(A)** Scheme of the experimental procedure. MPTP/p was intraperitoneally administered twice a week for 5 weeks, a total of 10 times. On day 35, the mice were first subjected to the rotarod test and buried food test (black; $n = 14$/group). The next day, mice were randomly divided into two kinds of tests (red; $n = 7$/group and blue; $n = 7$/group). On day 40, all mice were combined to perform the tail suspension test and akinesia test (black; $n = 14$/group). **(B)** The time (s) required to find the buried food pellet in the buried food test ($n = 14$/group) on day 35 of exposure to MPTP/p described in Materials and Methods section. **(C)** Time (%) to sniff the odor at T2 compared to the total time to sniff at both T1and T2 in the short-term olfactory memory test ($n = 7$/group) on day 36 of exposure to MPTP/p described in Materials and Methods section. Graphed data are mean ± SEM. Significant differences from values of control mice by unpaired Student's *t*-test are indicated as $^{**}P < 0.01$; $^{***}P < 0.001$. CON, control; MPTP/p, MPTP and probenecid; T1, trial 1; T2, trial 2.

TABLE 1 | Behavior tests.

Impairments of Parkinson's disease	Behavior tests				References
Olfactory deficit	Buried food	Short-term olfactory memory			Yang and Crawley, 2009; Petit et al., 2013
Thermal hyperalgesia	Hot plate				Challis et al., 2020
Anxiety and depression	Open field	Tail suspension			Seibenhener and Wooten, 2015; Badr et al., 2020
Cognitive decline	Y maze	Novel object recognition			Fernandez et al., 2017; Yan et al., 2017
Gastrointestinal dysfunction	Bead expulsion	One-h stool collection			Li et al., 2006; Natale et al., 2010
Motor dysfunction	Rotarod	Rearing	Catalepsy	Akinesia	Lu et al., 2014

with a few modifications (Fernandez et al., 2017). The novel object recognition test is based on the spontaneous characteristic of mice that spend more time exploring novel objects than familiar objects. The choice of exploring novel objects implies the use of cognitive memory and learning (Antunes and Biala, 2012). The novel object recognition test was composed of three sessions (habituation, training and testing). Each session was conducted once a day for three consecutive days. The first day consisted of a 30-min habituation session in a white arena (40 cm × 40 cm × 24 cm). On the second day of training session, the mouse was able to freely move for 10 min after two identical objects were centered. On the third day of testing session, one object (familiar object) was replaced with a novel object. The novel object was made of the same material with different shapes

and colors. The mouse was allowed to explore for 5 min. Through video recording, the exploration time for each object, the number of entries into the novel object zone (within a 3 cm radius of the object) and discrimination index were automatically analyzed by Smart 3.0 software (Panlab Harvard Apparatus). The exploration time for the familiar or novel object during the testing session was measured only when the nose pointed toward the objects at a distance of no more than 2 cm and/or touched or sniffed the object. Memory was determined by the discrimination index as shown by the following equation: [Discrimination index = (novel object exploration time/total exploration time) – (familiar object exploration time/total exploration time) × 100].

Bead Expulsion Test

We performed the bead expulsion test to evaluate the gastrointestinal dysfunction as previously described (Natale et al., 2010). Mice were subjected to fasting without water and feed 24 h before the test. Mice were temporarily anesthetized with isoflurane (Ifran liquid for inhalation, HANA Pharm Co., Seoul, South Korea). The glass 3-mm bead (Cat# 4901003, Paul Marienfeld GmbH & Co. KG, Lauda-Königshofen, Germany) was inserted 2 cm into distal colon. After bead insertion, the mouse was individually placed in a clean plastic cage. Bead expulsion time was measured within 100 min as a time limit. We measured the bead expulsion latency (the time required for the bead expulsion) and expressed the time as a percentage compared to that of control mice.

One-h Stool Collection Test

We performed the one-h stool collection test as another test to evaluate the gastrointestinal dysfunction as previously described (Li et al., 2006). Each mouse was placed in a separate clean plastic cage and observed during the one-h collection period. Stools were collected immediately after being expelled and placed in sealed laboratory tubes. The wet weights of the stools in tube were measured. The stools were then dried in an oven at 65°C. The stool water contents were calculated from differences between the wet and dry stool weights.

Rotarod Test

The rotarod (MED associates Inc., Albans, VT, United States) test was performed to assess the motor dysfunction as previously described (Park et al., 2017; Parker et al., 2018). Briefly, we trained mice for 3–4 days on an accelerated rotarod so that the mice remained on the rotarod. The test was performed three times with the rod accelerating linearly from 3.5 to 35 rpm within 2 min. The test session consisted of 480 s intervals. The time on rod of the mice was measured.

Rearing Test

The rearing test was performed to evaluate the motor impairments as previously described (Park et al., 2017). A mouse was placed in a plastic cylinder (12 cm diameter × 20 cm height) under dim light conditions and adapted for 1 min before the experiment. The number of times the mouse forepaws touched the cylinder wall was counted for 3 min.

Catalepsy Test

The catalepsy test was conducted to assess the ability to correct an abnormally imposed body position (Lu et al., 2014) as previously described with a few modifications (Bardin et al., 2006). The two forelimbs of mouse were placed on a horizontal raised metal bar (1 cm diameter, 5 cm above the table) and their hindlimbs were placed on the floor of the apparatus. The time (latency time) during which both forelimbs remained on the bar was recorded before removing both forelimbs from the bar. The test was repeated three times (inter-trial interval: 1 min) and cutoff time was set to 180 s.

Akinesia Test

We conducted the akinesia test to assess the latency time to move all four limbs as previously described with a few modifications (Paul et al., 2017). A mouse was placed on a high and flat surface. A mouse was initially acclimatized for 5 min on the surface (40 cm × 40 cm × 24 cm) before the experiment. The time taken to move all the four limbs was measured. It was repeated 3 times and terminated if the latency exceeded 180 s.

Immunohistochemistry and Quantitative Analysis

Mice were perfused with ice-cold paraformaldehyde (4%) in phosphate buffer (0.2 M). Brains were randomly removed from each group and post-fixed overnight in the fixative. After cryoprotection in sucrose/phosphate buffer (30%), the serial coronal sections of frozen brains were cut to 40 μm by a freezing microtome (Cat# CM1850, Leica, Nussloch, Germany). Free-floating sections were blocked with bovine serum albumin (1%)/phosphate buffer plus Triton X-100 (0.2%) and incubated with an anti-TH antibody (Santa Cruz Biotechnology, Santa Cruz, CA, United States) overnight at room temperature, followed by incubation with biotinylated secondary antibodies (Vector Laboratories, Inc., Burlingame, CA, United States) and ABC reagents (Vectastain Elite ABC kit, Vector Laboratories, Inc.). The sections developed with diaminobenzidine (Sigma-Aldrich Co., St. Louis, MO, United States) were dehydrated and coverslipped. A bright-field microscope (Cat# BX51, Olympus Japan Co., Tokyo, Japan) was used for observing images. The optical density of TH in striatum was analyzed using ImageJ software (National Institute of Health, Bethesda, MD, United States). The number of TH + neurons in substantia nigra was stereologically analyzed with an unbiased optical fractionator method that is not affected by either the volume of substantia nigra or size of the counted neurons. We used a computer-assisted image analysis system consisting of an Axiophot photomicroscope (Carl Zeiss Vision International GmbH, Aalen, Germany) equipped with a computer controlled motorized stage (Ludl Electronics, Hawthorne, NY, United States), a Hitachi HV C20 camera and Stereo Investigator software (MicroBright-Field, Williston, VT, United States). The total number of TH + neurons was calculated as previously described (Mandir et al., 1999).

Western Blot Analysis

Brains were randomly removed from each group. Tissues from striatum, substantia nigra, olfactory bulb, hippocampus,

amygdala, prefrontal cortex, locus coeruleus, and mid part of colon were homogenized in CyQUANT® cell lysis buffer (Invitrogen, Carlsbad, CA, United States). After the homogenates were centrifuged, the protein concentration was measured with a BCA protein assay (Sigma-Aldrich Co.). The equal protein amounts of each sample were combined with SDS-polyacrylamide gel electrophoresis (SDS-PAGE) loading buffer (Biomedic Co., Bucheon, South Korea), heated at 95°C for 10 min, separated by SDS-PAGE gels (10%) and transferred onto nitrocellulose membranes. The membranes blocked with skimmed milk (5%) were incubated with the following primary antibodies: α-synuclein (1:500 dilution, Cell Signaling Technology, Danvers, MA, United States), p-α-synuclein (pS129, 1:200 dilution, Abcam, Cambridge, United Kingdom), glial fibrillary acidic protein (GFAP, astroglial marker, 1:500 dilution, Invitrogen), ionized calcium-binding adapter molecule-1 (Iba-1, microglial marker, 1:500 dilution, Sigma-Aldrich Co.), TH (1:1,000 dilution, Santa Cruz Biotechnology), DJ-1 (1:1,000 dilution, Cell Signaling Technology) and β-actin (1:4,000 dilution, Sigma-Aldrich Co.), followed by horseradish peroxidase-conjugated secondary antibodies (1:10,000 dilution, Pierce Biotechnology, Rockford, IL, United States). Bands were visualized by an enhanced chemiluminescence system (West Pico, Pierce Biotechnology). Densitometry analysis was performed using ImageJ software (National Institute of Health).

Statistical Analysis

All data were analyzed by the unpaired Student's *t*-test depending on the homogeneity of variance (IBM SPSS statistics 23, IBM Corp., Armonk, NY, United States). *P* values lower than 0.05 were considered to be significant. Asterisks signs indicate statistical significance between control mice versus MPTP/p-treated mice: $^{*}P < 0.05$; $^{**}P < 0.01$; $^{***}P < 0.001$. Graphed data are mean ± standard error of the mean (SEM).

RESULTS

The Chronic Injection of MPTP/p Causes Olfactory Deficit in Mice

The most widely studied non-motor feature is olfaction, which has been found to be abnormal in more than 90% of PD patients (Doty et al., 1988). Thus, it was first investigated whether olfactory deficit would be caused in the MPTP/p-induced PD mouse model by performing the buried food test and short-term olfactory memory test. The major parameter of the buried food test is the time required to find the buried food pellet (Yang and Crawley, 2009). The MPTP/p-treated mice significantly increased the retrieval time, showing difficulties in detecting the buried food (**Figure 1B**, $P < 0.0001$). Next, we conducted the short-term olfactory memory test as another olfactory deficit test. As shown in **Figure 1C**, control mice spent less time sniffing the novel odor on the second exposure, behaving as if they remembered having been exposed to the odor before (Petit et al., 2013). However, the MPTP/p-treated mice spent more time sniffing the odor, behaving as if they were unable to remember the odor (**Figure 1C**, $P = 0.0052$).

The Chronic Injection of MPTP/p Causes Thermal Hyperalgesia in Mice

PD patients had hyperalgesia compared to normal controls (Sung et al., 2018a,b). Clinically, hyperalgesia plays an important role in the development of chronic pain (Sung et al., 2018a,b). Thus, we performed the hot plate test for evaluation of nociception in the MPTP/p-treated mice. As shown in **Figure 2**, the MPTP/p-treated mice significantly decreased the latency time, showing the onset of heat sensitivity was significantly advanced compared to control mice when the paws were exposed to heat (**Figure 2**, $P = 0.0037$).

The Chronic Injection of MPTP/p Causes Neuropsychiatric Features in Mice

Anxiety affected approximately 60% of PD patients and was commonly accompanied by depression (Schapira et al., 2017). Thus, we performed the open field test and tail suspension test for evaluation of neuropsychiatric features in the MPTP/p-treated mice. The open field test is most commonly used to measure anxiety-related behaviors as well as ambulatory behaviors after MPTP intoxication (Park et al., 2015; Seibenhener and Wooten, 2015). The MPTP/p-treated mice significantly reduced the number of entries into center zone compared to control mice, suggesting a change in basal anxiety levels of the MPTP/p-treated mice (**Figure 3A**, $P < 0.0001$). The total movement distance ($P = 0.0003$), distance traveled in the center (central movement distance, $P < 0.0001$) and the ratio of central/total distance ($P < 0.0001$) were significantly reduced in the MPTP/p-treated mice (**Figures 3B,C**). In addition, the tail suspension test presented the depressive-like behaviors in the MPTP/p-treated

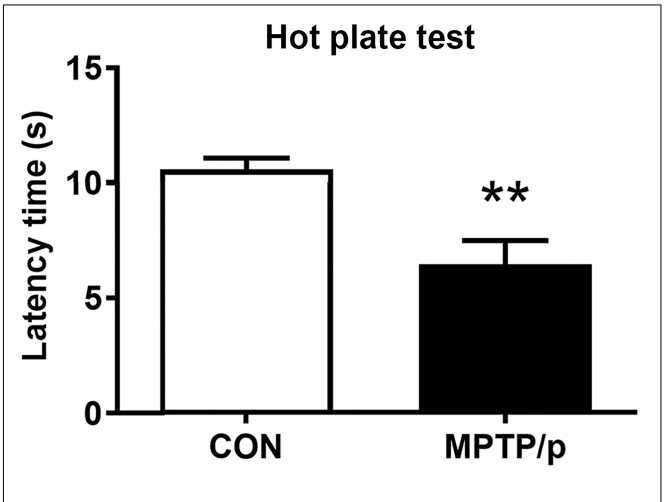


FIGURE 2 | The chronic injection of MPTP/p causes thermal hyperalgesia in mice. MPTP/p was intraperitoneally administered twice a week for 5 weeks, a total of 10 times. The latency time (s) taken to elicit nocifensive behaviors (flinching, hind paw licking, or jumping) in the hot plate test ($n = 7$/group) on day 38 of exposure to MPTP/p described in Materials and Methods section. Values are mean ± SEM. Graphed data are mean ± SEM. Significant differences from values of control mice by unpaired Student's *t*-test are indicated as $^{**}P < 0.01$. CON, control; MPTP/p, MPTP and probenecid.

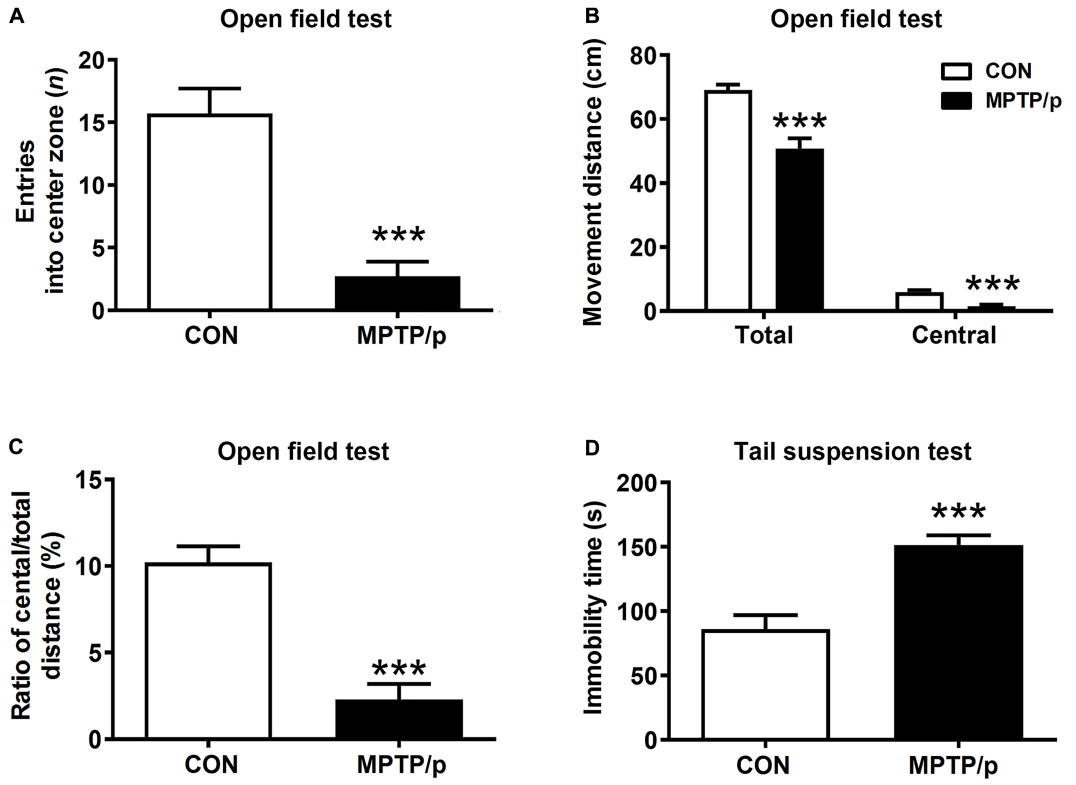


FIGURE 3 | The chronic injection of MPTP/p causes neuropsychiatric features in mice. MPTP/p was intraperitoneally administered twice a week for 5 weeks, a total of 10 times. **(A)** Entries (*n*) into center zone, **(B)** total movement distance (cm) and central movement distance (cm) of their respective tracks and **(C)** ratio (%) of central/total distance in the open field test ($n = 7$/group) on day 37 of exposure to MPTP/p described in Materials and Methods section. **(D)** Immobility time (s) of the tail suspension test ($n = 14$/group) on day 40 of exposure to MPTP/p described in Materials and methods section. Graphed data are mean ± SEM. Significant differences from values of control mice by unpaired Student's *t*-test are indicated as $^{***}P < 0.001$. CON, control; MPTP/p, MPTP and probenecid.

mice with a significant increase in immobility time (**Figure 3D**, $P < 0.0001$).

The Chronic Injection of MPTP/p Causes Cognitive Decline in Mice

People at risk of developing PD had cognitive decline and problems with working memory (Schapira et al., 2017). Thus, we explored whether the MPTP/p-treated mice would be defective in memory and learning by conducting the Y maze test and novel object recognition test. There was a significant difference in the spontaneous alternation between two groups of the Y maze test. The MPTP/p-treated mice significantly decreased the alternation behaviors (**Figure 4A**, $P < 0.0001$). In the novel object recognition test, the MPTP/p-treated mice also showed a significant deficit in the novel object recognition memory. The MPTP/p-treated mice spent significantly less time exploring the novel object (**Figure 4B**, $P = 0.0082$) and significantly more exploring the familiar object compared to control mice (**Figure 4B**, $P = 0.0373$). The number of entries into the novel object zone revealed that control mice preferentially approached to the novel object zone, but the MPTP/p-treated mice showed a striking decrease in the number of entries into the novel object zone (**Figure 4C**, $P = 0.0006$). The discrimination index also indicated that control mice exhibited a significant preference for exploring the novel object, but the MPTP/p-treated mice failed to show this preference (**Figure 4D**, $P = 0.0003$).

The Chronic Injection of MPTP/p Causes Gastrointestinal Dysfunction in Mice

The gastrointestinal dysfunction is one of the most common non-motor impairments observed in PD, which often precedes the development of motor symptoms (O'Sullivan et al., 2008). Thus, we investigated whether the MPTP/p-treated mice would have gastrointestinal disturbances by performing the bead expulsion test and one-h stool collection test. The bead expulsion test, the MPTP/p-treated mice significantly increased the latency time to expel the bead compared to control mice, indicating a delay of enteric motility (**Figure 5A**, $P = 0.0071$). The one-h stool collection test also showed that water contents were significantly decreased by MPTP/p injection, indicating the MPTP/p-treated mice have constipation (**Figure 5B**, $P = 0.0014$).

The Chronic Injection of MPTP/p Disrupts Motor Function in Mice

Additionally, we identified motor dysfunction as a major symptom of PD in the MPTP/p-treated mice by performing

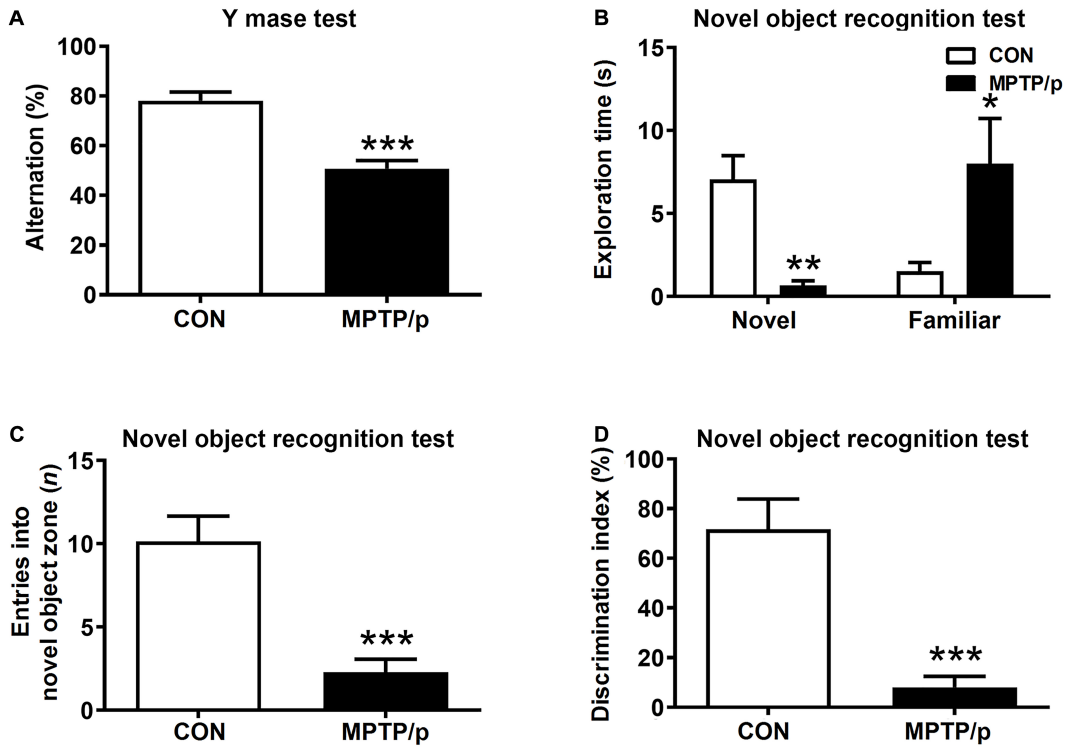


FIGURE 4 | The chronic injection of MPTP/p causes cognitive decline in mice. MPTP/p was intraperitoneally administered twice a week for 5 weeks, a total of 10 times. **(A)** The percentage of alternation behaviors [number of alternations/(total arm entries – 2) × 100] in the Y maze test ($n = 7$/group) on day 38 of exposure to MPTP/p described in Materials and methods section. **(B)** Time (s) exploring the novel object and familiar object, **(C)** entries (*n*) into the novel object zone and **(D)** discrimination index (%) defined by equation [(novel object exploration time/total exploration time) – (familiar object exploration time/total exploration time) × 100] in the novel object recognition test on day 39 of exposure to MPTP/p described in Materials and Methods section ($n = 7$/group). Graphed data are mean ± SEM. Significant differences from values of control mice by unpaired Student's *t*-test are indicated as $^{*}P < 0.05$; $^{**}P < 0.01$; $^{***}P < 0.001$. CON, control; MPTP/p, MPTP and probenecid.

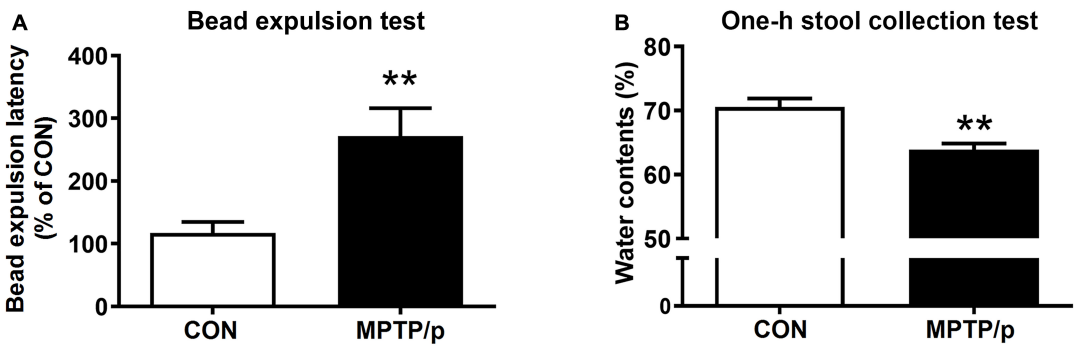


FIGURE 5 | The chronic injection of MPTP/p causes gastrointestinal dysfunction in mice. MPTP/p was intraperitoneally administered twice a week for 5 weeks, a total of 10 times. **(A)** The bead expulsion latency (%) in the bead expulsion test ($n = 7$/group) on day 37 of exposure to MPTP/p described in Materials and Methods section. **(B)** Stool water contents (%) in the one-h stool collection test ($n = 7$/group) on day 37 of exposure to MPTP/p described in Materials and Methods section. Graphed data are mean ± SEM. Significant differences from values of control mice by unpaired Student's *t*-test are indicated as $^{**}P < 0.01$. CON, control; MPTP/p, MPTP and probenecid.

the rotarod test, rearing test, catalepsy test, and akinesia test. As expected, the MPTP/p-treated mice exhibited a significant decrease in the time on rod in the rotarod test, indicating the impaired movement function of the MPTP/p-treated mice (**Supplementary Figure 1A**, $P < 0.0001$). The MPTP/p-treated mice significantly reduced the number of touches on cylinder wall in the rearing test (**Supplementary Figure 1B**, $P < 0.0001$). The catalepsy test (**Supplementary Figure 1C**, $P = 0.0010$) and akinesia test (**Supplementary Figure 1D**, $P < 0.0001$) also showed that the latency times to start

movement were significantly increased in the MPTP/p-treated mice, indicating PD-like abnormal behavior phenotypes of the MPTP/p-treated mice.

The Chronic Injection of MPTP/p Leads to Abnormal Accumulation of α-Synuclein in Mice

α-Synuclein is a major pathological protein underlying PD pathogenesis (Xu and Pu, 2016). Most non-motor dysfunctions in PD are associated with α-synuclein pathology as well as the dopaminergic striatonigral system (Jellinger, 2011). Thus, we examined α-synuclein levels in the striatum and substantia nigra of the MPTP/p-treated mice. As shown in **Figures 6A–D** and **Supplementary Figure 2**, the MPTP/p injection showed significant increases in expression levels of α-synuclein in the striatum ($P = 0.0005$) and substantia nigra ($P = 0.0053$). We further identified the abnormal accumulation of α-synuclein in regions associated with non-motor symptoms, i.e., olfactory bulb (Henrich et al., 2018), hippocampus (Flores-Cuadrado et al., 2016), amygdala (Henrich et al., 2018), prefrontal cortex (Stoyka et al., 2020), locus coeruleus (Butkovich et al., 2018) and colon (Shannon et al., 2012). The results of Western blot at these areas showed a similar trend to the expression levels of α-synuclein of the striatum and substantia nigra. The expression levels of α-synuclein were significantly enhanced in the olfactory bulb ($P = 0.0375$), hippocampus ($P = 0.0012$), amygdala ($P = 0.0308$), prefrontal cortex ($P < 0.0001$), locus coeruleus ($P = 0.0174$) and colon ($P = 0.0027$) of the MPTP/p-treated mice (**Figures 6E–P** and **Supplementary Figure 2**). In addition, the expression levels of p-α-synuclein were significantly increased in the striatum ($P = 0.0127$), substantia nigra ($P = 0.0260$), olfactory bulb ($P = 0.0294$), hippocampus ($P = 0.0273$), amygdala ($P = 0.0043$) and locus coeruleus ($P = 0.0133$) (**Figures 7A–D** and **Supplementary Figures 3A,B, 4A–F,I,J**). Interestingly, the expression levels of GFAP were also significantly increased in the striatum ($P = 0.0320$) and substantia nigra ($P = 0.0322$) (**Figures 7E–H** and **Supplementary Figures 3C,D**). However, the expression levels of p-α-synuclein in the prefrontal cortex and colon (**Supplementary Figures 4G,H,K,L**) and the those of Iba-1 in the striatum and substantia nigra (**Supplementary Figure 5**) showed the trends of increase in the MPTP/p group, but they did not reach statistically significant.

The Chronic Injection of MPTP/p Leads to Dopaminergic Neurons Loss in Mice

Finally, we confirmed the dopaminergic depletion in the MPTP/p-treated mice. TH which is a critical enzyme for dopamine biosynthesis, is commonly used to detect

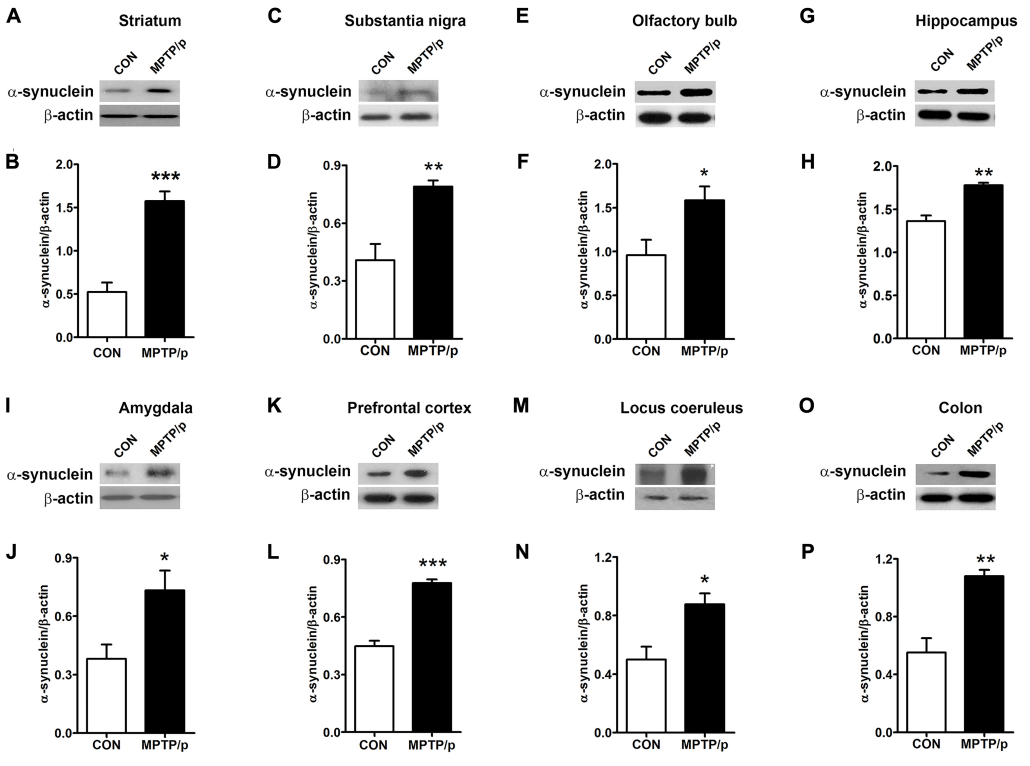


FIGURE 6 | The chronic injection of MPTP/p leads to abnormal accumulation of α-synuclein in mice. Representative images of Western blotting analysis of α-synuclein in panels **(A)** striatum, **(C)** substantia nigra, **(E)** olfactory bulb, **(G)** hippocampus, **(I)** amygdala, **(K)** prefrontal cortex, **(M)** locus coeruleus, and **(O)** colon ($n = 4$/group). The other three Western blot images are shown in **Supplementary Figure 2**. **(B,D,F,H,J,L,N,P)** Quantification of normalized α-synuclein levels in each region. α-synuclein levels were normalized to β-actin levels, a housekeeping gene. Graphed data are mean ± SEM. Significant differences from values of control mice by unpaired Student's *t*-test are indicated as $^*P < 0.05$; $^{**}P < 0.01$; $^{***}P < 0.001$. CON, control; MPTP/p, MPTP and probenecid.

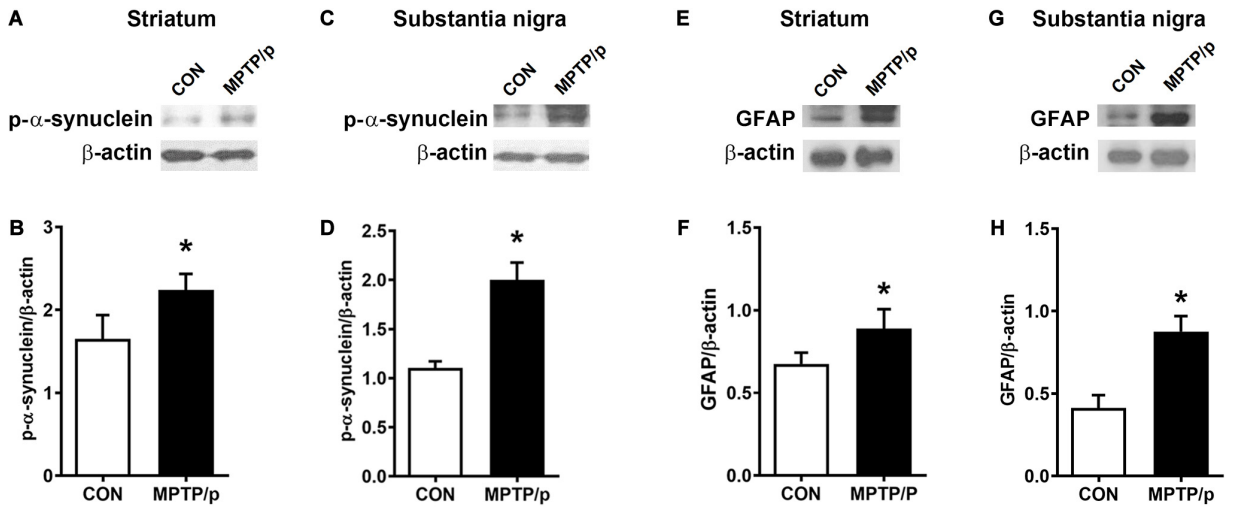


FIGURE 7 | The chronic injection of MPTP/p leads to high expression levels of p-α-synuclein and GFAP in mice. Representative images of Western blotting analysis of p-α-synuclein in panels **(A)** striatum and **(C)** substantia nigra ($n = 4$/group). Representative images of Western blotting analysis of GFAP in panels **(E)** striatum and **(G)** substantia nigra ($n = 4$/group). The other three Western blot images are shown in **Supplementary Figure 3**. **(B,D,F,H)** Quantification of normalized p-α-synuclein levels and GFAP levels in each region. The p-α-synuclein levels and GFAP levels were normalized to β-actin levels, a housekeeping gene. Graphed data are mean ± SEM. Significant differences from values of control mice by unpaired Student's *t*-test are indicated as $^*P < 0.05$. CON, control; MPTP/p, MPTP and probenecid; p-α-synuclein, phosphorylated-α-synuclein; GFAP, glial fibrillary acidic protein.

dopaminergic neurons (Ishikawa et al., 2010). TH is a transcriptional target gene for DJ-1 which is a neuroprotective transcriptional activator (Zhong et al., 2006; Ishikawa et al., 2010). Thus, we clarified whether the non-motor and motor impairments in the MPTP/p-treated mice would result from dopaminergic neurons loss by analyzing TH and DJ-1 levels. The MPTP/p-induced dopaminergic depletion was examined by staining TH in the striatum and substantia nigra. TH + neurons counts were monitored by unbiased stereologic methods. As shown in **Figures 8A,B** the significant losses of both TH + dopaminergic fibers ($P < 0.001$) in the striatum and TH + neurons ($P < 0.0001$) in the substantia nigra were observed in the MPTP/p-treated mice, consistently with the non-motor and motor defective behaviors. The quantified TH expression levels by Western blot analysis were reduced in the striatum ($P < 0.001$) and substantia nigra ($P < 0.001$) of the MPTP/p-treated mice (**Figures 8C–F** and **Supplementary Figure 6**). Also, DJ-1 expression levels were significantly decreased in the striatum ($P = 0.0050$) and substantia nigra ($P = 0.0366$) of the MPTP/p-treated mice (**Figures 8C–F** and **Supplementary Figure 6**), indicating a similar vulnerability of the dopamine neurons observed in PD. Interestingly, DJ-1 expression level was reduced in the olfactory bulb of the MPTP/p-treated mice (**Supplementary Figure 7**, $P < 0.0001$).

DISCUSSION

In the current study, we determined that the chronic injection of MPTP/p caused olfactory deficit by performing the buried food test and short-term olfactory memory test; thermal hyperalgesia by the hot plate test; neuropsychiatric features by the open field test and tail suspension test; cognitive decline by the Y maze test and novel object recognition test; gastrointestinal dysfunction by the bead expulsion test and one-h stool collection test. Moreover, we confirmed that the MPTP/p-treated mice exhibited motor dysfunctions in the rotarod test, rearing test, catalepsy test, and akinesia test. The chronic injection of MPTP/p resulted in high expression levels of α-synuclein in striatum, substantia nigra, olfactory bulb, hippocampus, amygdala, prefrontal cortex, locus coeruleus, and colon, and low expression levels of TH in striatum and substantia nigra. Therefore, the current study established the experimental model of PD representing the comprehensive non-motor symptoms through the abnormal accumulation of α-synuclein and loss of dopaminergic neurons by the chronic injection of MPTP/p.

In PD, the causes of non-motor symptoms are multifactorial and are not described by a single lesion (Jellinger, 2011). The majority of PD patients had more than one non-motor dysfunction and the increased comorbidity of non-motor dysfunctions, which was associated with the severity of PD (Shulman et al., 2001). Autonomic symptoms, anxiety, cognitive decline, dementia, and psychotic episodes were all related to a high risk of depression in PD patients (Santangelo et al., 2014). Gastrointestinal dysfunctions in PD patients were associated with the deterioration of mobility, cognition and communication (Tibar et al., 2018). Although the MPTP-induced mouse models of PD faithfully have reproduced the naturally occurring neurodegeneration, following similar topographical patterns of human PD (Meredith and Rademacher, 2011), the comprehensive alterations in the non-motor functions using the MPTP-treated mice have not been noticed in any one study (Schapira et al., 2017). Dopaminergic neurons died quickly in acute and subchronic MPTP models, whereas the chronic MPTP

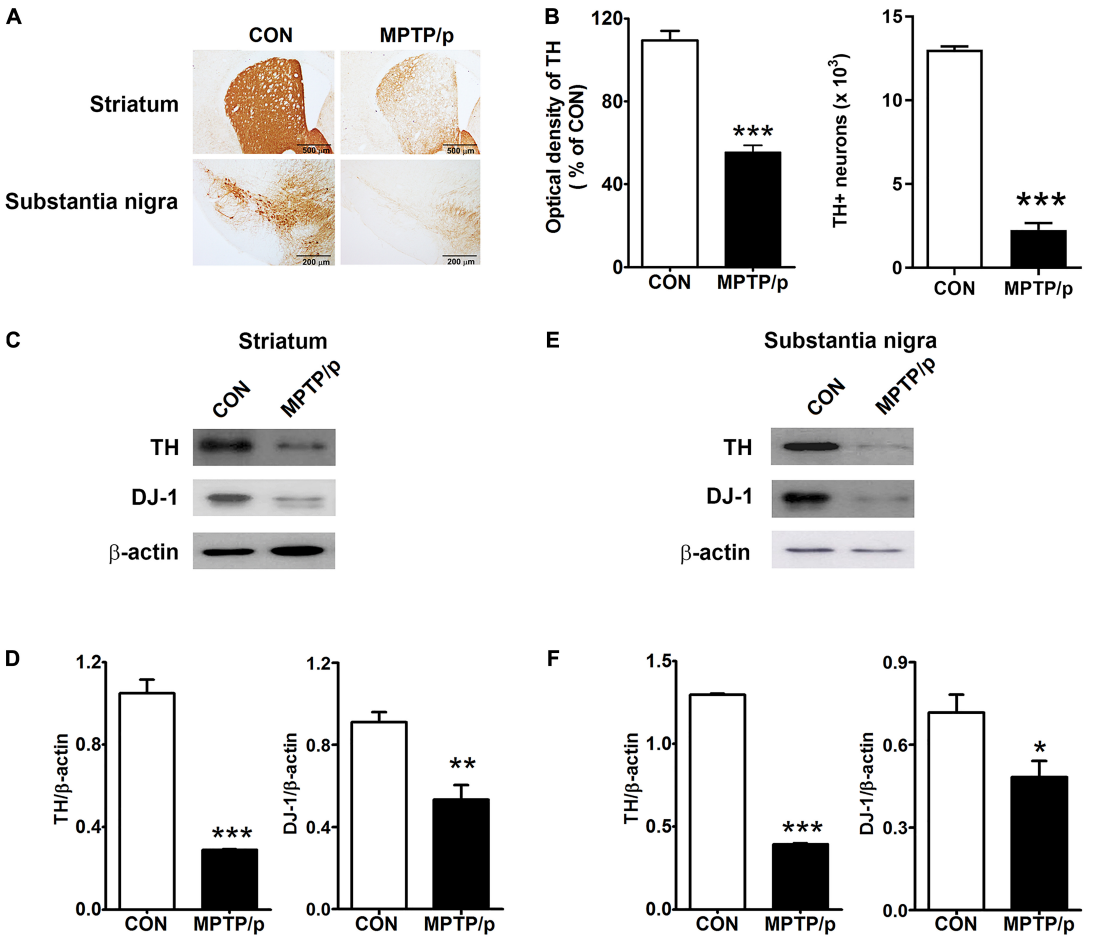


FIGURE 8 | The chronic injection of MPTP/p leads to dopaminergic neurons loss in mice. Microphotographs of **(A, upper)** TH + dopaminergic fibers in striatum and **(A, lower)** TH + dopaminergic neurons in substantia nigra by TH immunostaining ($n = 4$/group). **(B, left panel)** The optical density of TH + dopaminergic fibers in striatum and **(B, right panel)** stereology counts of TH + dopaminergic neurons in substantia nigra. Unbiased stereological counting was conducted in substantia nigra. Representative images of Western blotting analysis using anti-TH and anti-DJ-1 antibodies in panels **(C)** striatum and **(E)** substantia nigra ($n = 4$/group). The other three Western blot images are shown in **Supplementary Figure 6**. Quantification of normalized TH and DJ-1 levels in panels **(D)** striatum and **(F)** substantia nigra. TH and DJ-1 levels were normalized to β-actin levels, a housekeeping gene. Graphed data are mean ± SEM. Significant differences from values of control mice by unpaired Student's *t*-test are indicated as $^{*}P < 0.05$; $^{**}P < 0.01$; $^{***}P < 0.001$. CON, control; MPTP/p, MPTP and probenecid; TH, tyrosine hydroxylase.

model including MPTP/p showed to be more progressive loss of dopaminergic neurons (Meredith and Rademacher, 2011). Thus, in the current study, we injected MPTP/p for 5 weeks and established the experimental chronic mouse model of PD mimicking the comprehensive non-motor dysfunctions of human PD, showing olfactory deficit, thermal hyperalgesia, anxiety, depression, cognitive decline, and gastrointestinal dysfunction by conducting various behavior tests. We clearly characterized the mouse model of PD, fulfilling many of the main criteria of human conditions including non-motor and motor impairments. Although previous studies have reported non-motor symptoms by conducting the buried food test (Choi et al., 2018), open field test (Choi et al., 2018) and bead expulsion test (Choi et al., 2018) in the chronic MPTP/p-treated mice, we conducted the short-term olfactory memory test, hot plate test, tail suspension test, Y maze test, novel object recognition test and one-h stool collection test in the chronic MPTP/p-treated mice for the first time and established the chronic mouse model of PD mimicking the comprehensive non-motor symptoms of human PD. Thus, the current study is noteworthy in that conducting the various behavior tests in one model is a more advanced approach to the symptomatic study in PD patients. However, as animal models using toxins such as 6-OHDA or rotenone have previously been demonstrated to be useful for studying non-motor dysfunctions of human PD (Blesa and Przedborski, 2014), further investigation is needed to characterize the comprehensive non-motor symptoms in various chronic models of PD. The current PD model has been established using male mice with reference to previous reports that the incidence rate of PD in men was higher than that in women (Van Den Eeden et al., 2003; Miller and Cronin-Golomb, 2010). However, further studies are needed in female mice to clarify the current model. Further researches are also required to develop this model system into a validated model as a clinical research platform.

A characteristic neuropathological hallmark of PD is Lewy bodies which consists predominantly of α-synuclein (Spillantini et al., 1997). The appearance of α-synuclein in a series of brain regions coincides with non-motor and motor dysfunctions in PD patients (Gajula Balija et al., 2011; Schirinzi et al., 2019). Hyposmia is implicated in olfactory bulb and amygdala; pain in locus coeruleus containing Lewy bodies and amygdala; anxiety or depression in locus coeruleus; cognitive dysfunction in frontal cortex and hippocampus (Jellinger, 2011; Schapira et al., 2017). In particular, the accumulation of α-synuclein in substantia nigra, olfactory bulb, hippocampus, amygdala, prefrontal cortex, and locus coeruleus replicated non-motor features of human PD pathology such as anxiety or cognitive dysfunction (Flores-Cuadrado et al., 2016; Schapira et al., 2017; Butkovich et al., 2018; Henrich et al., 2018; Stoyka et al., 2020). The accumulation of α-synuclein was also found in colon of PD patients, which innervated the intestine, promoted the progression of α-synuclein pathology to the brain, caused behavioral dysfunction and allowed early detection of PD before the slow onset of motor symptoms (Schapira et al., 2017; Challis et al., 2020). The current study showed the high expression levels of α-synuclein in olfactory bulb, hippocampus, amygdala, prefrontal cortex, locus coeruleus, and colon with the nigrostriatal areas of the MPTP/p-treated mice, which was consistent with previous studies describing that the mice overexpressing α-synuclein in midbrain exhibited the non-motor impairments with progressive motor decline (Nuber et al., 2008; Schapira et al., 2017). The p-α-synuclein, pS129, level was higher in PD patients than healthy controls (Stewart et al., 2015). Our results showed that the expression levels of pS129 were increased in the striatum and substantia nigra of the MPTP/p-treated mice. Thus, the current study suggests that the chronic injection of MPTP/p would reproduce behavioral phenotypes of human PD through the abnormal distribution of α-synuclein in various brain regions and colon. Recently, Kim et al. (2019) established a gastrointestinal α-synuclein-injected PD mouse model characterized by PD with both motor and non-motor symptoms, suggesting it as a new model with α-synucleinopathies, one of the main features of PD. Kim et al. (2019) conducted a variety of behavioral tests and demonstrated that the PD mouse model had several non-motor symptoms, but a significant loss of dopaminergic neurons in substantia nigra and dysfunction of motor and non-motor symptoms were observed at 7 months after α-synuclein injection. Our chronic MPTP/p-injected model has shown that the loss of dopaminergic neurons, the distribution of α-synuclein and comprehensive non-motor symptoms are implicated within a short period of time compared to the previous study of Kim et al. (2019). Thus, we suggest that the current PD mouse model by MPTP/p would be suitable for short-term pharmacological and pathological studies, while the study of Kim et al. (2019) would be suitable for long-term studies by α-synuclein on gut-brain axis in PD.

PD is characterized by motor deficits via a slow and progressive loss of nigral dopaminergic neurons (Maiti et al., 2017). The dopaminergic neurodegeneration of PD is also involved in the genesis of non-motor symptoms (Lee and Koh, 2015). Dopamine is synthesized by l-DOPA converted by TH and l-DOPA decarboxylase (Daubner et al., 2011). DJ-1 has a neuroprotective activity against neurodegeneration in PD and loss of DJ-1 function triggers the onset of PD (Ariga et al., 2013). Our results have revealed the chronic injection of MPTP/p dramatically leads to low expression levels of TH and DJ-1 in striatum and substantia nigra, and the losses of both TH + dopaminergic fibers in striatum and TH + neurons in substantia nigra, which was consistent with previous studies determining chronic effects of MPTP/p injection (Biju et al., 2018; Shao et al., 2019). Astrocytes are associated with the progression of PD by the production of pro-inflammatory cytokines which damage dopaminergic neurons (Rappold and Tieu, 2010). The overexpression of GFAP often occur in PD patients and these alterations of GFAP in astrocytes are involved in the pathogenesis of PD (Clairembault et al., 2014). Emamzadeh and Surguchov (2018) suggested that PD can be identified with high levels of GFAP. The current study showed the elevated levels of GFAP in the striatum and substantia nigra. Thus, we suggest that this model would be excellently suited to study the non-motor dysfunctions of PD by loss of dopaminergic nigrostriatal neurons with high levels of GFAP. However, various proteins, as well as TH and α-synuclein, are involved in the mechanisms underlying pathological and behavioral phenotypes of PD (Blesa and Przedborski, 2014). Whether the presence of various pathologic proteins contributes to these non-motor symptoms of PD will require further study.

Nutrition plays a critical role in both neuroprotection and neurodegeneration of PD (Seidl et al., 2014). The MPTP injection can cause dystrophy in mice, which can lead to weight loss (Sedelis et al., 2001). On the last day of MPTP/p injection, there was a significant difference in body weight between control group and MPTP/p group (**Supplementary Figure 8**, $P < 0.0001$). Although not fully pathologically understood in the current study, body weight loss and nutrition status may have an effect on behavioral tests. Thus, future research is needed to identify the association between body weight and behavioral tests in the current model. Regardless of the limitations, the current study suggests the chronic injection of MPTP/p would reproduce behavioral phenotypes of human PD through the abnormal accumulation of α-synuclein and loss of dopaminergic neurons.

In summary, the current study shows that the chronic intraperitoneal injection of MPTP/p leads to the abnormal accumulation of α-synuclein in a series of brain regions and colon and the degeneration of dopaminergic neurons in the striatum and substantia nigra, which is involved in various non-motor symptoms. Because attention is now focused on non-motor dysfunctions to improve the quality of life of PD patients and the comprehensive focus of non-motor aspects in the experimental model of PD is an evolution from previous studies on the non-motor aspects, the current study will provide significant insights into the various pathological properties of PD. However, further studies are required to clarify the non-motor symptoms of PD pathogenesis through multiple signaling pathways in the current chronic MPTP/p-induced PD model.

DATA AVAILABILITY STATEMENT

The raw data supporting the conclusions of this article will be made available by the authors, without undue reservation.

ETHICS STATEMENT

Experimental procedures were performed with reference to the National Institutes of Health Guide for the Care and Use of Laboratory Animals. The procedures were also approved by the Dongguk University Animal Care Committee (IACUC-2017-023-1).

AUTHOR CONTRIBUTIONS

HL and H-JP supervised the study and reviewed the manuscript. N-RH, Y-KK, SA, T-YH, HL, and H-JP conducted the experiments and data analysis. N-RH wrote the manuscript. All authors contributed to the article and approved the submitted version.

FUNDING

The present research was supported by grants from the National Research Foundation of Korea funded by the Korean government (NRF-2017R1A2B4009963) and from the Korea Institute of Oriental Medicine (grant K18182). This work was supported by a grant from Kyung Hee University in 2018 (KHU- 20181061).

SUPPLEMENTARY MATERIAL

The Supplementary Material for this article can be found online at: https://www.frontiersin.org/articles/10.3389/fnagi.2020.599045/full#supplementary-material

REFERENCES

Antunes, M., and Biala, G. (2012). The novel object recognition memory: neurobiology, test procedure, and its modifications. *Cogn. Process* 13, 93–110. doi: 10.1007/s10339-011-0430-z

Ariga, H., Takahashi-Niki, K., Kato, I., Maita, H., Niki, T., and Iguchi-Ariga, S. M. (2013). Neuroprotective function of DJ-1 in Parkinson's disease. *Oxid. Med. Cell. Longev.* 2013:683920. doi: 10.1155/2013/683920

Badr, A. M., Attia, H. A., and Al-Rasheed, N. (2020). Oleuropein Reverses Repeated Corticosterone-Induced Depressive-Like Behavior in mice: Evidence of Modulating Effect on Biogenic Amines. *Sci. Rep.* 10:3336. doi: 10.1038/s41598-020-60026-1

Bailey, K. R., and Crawley, J. N. (2009). "Anxiety-Related Behaviors in Mice" In *Methods of Behavior Analysis in Neuroscience*. ed. Buccafusco, J. J, 2nd Edn. Boca Raton, FL: CRC Press/Taylor & Francis.

Bardin, L., Kleven, M. S., Barret-Grévoz, C., Depoortère, R., and Newman-Tancredi, A. (2006). Antipsychotic-like vs cataleptogenic actions in mice of novel antipsychotics having D2 antagonist and 5-HT1A agonist properties. *Neuropsychopharmacology* 31, 1869–1879. doi: 10.1038/sj.npp.1300940

Biju, K. C., Evans, R. C., Shrestha, K., Carlisle, D. C. B., Gelfond, J., and Clark, R. A. (2018). Methylene Blue Ameliorates Olfactory Dysfunction and Motor Deficits in a Chronic MPTP/Probenecid Mouse Model of Parkinson's Disease. *Neuroscience* 380, 111–122. doi: 10.1016/j.neuroscience.2018.04.008

Blesa, J., and Przedborski, S. (2014). Parkinson's disease: animal models and dopaminergic cell vulnerability. *Front. Neuroanat.* 8:155. doi: 10.3389/fnana.2014.00155

Brichta, L., Shin, W., Jackson-Lewis, V., Blesa, J., Yap, E. L., Walker, Z., et al. (2015). Identification of neurodegenerative factors using translatome-regulatory network analysis. *Nat. Neurosci.* 18, 1325–1333. doi: 10.1038/nn.4070

Bugalho, P., Lampreia, T., Miguel, R., Mendonça, M. D., Caetano, A., and Barbosa, R. (2016). Non-Motor symptoms in Portuguese Parkinson's Disease patients: correlation and impact on Quality of Life and Activities of Daily Living. *Sci. Rep.* 6:32267. doi: 10.1038/srep32267

Butkovich, L. M., Houser, M. C., and Tansey, M. G. (2018). α-Synuclein and Noradrenergic Modulation of Immune Cells in Parkinson's Disease Pathogenesis. *Front. Neurosci.* 12:626. doi: 10.3389/fnins.2018.00626

Canerina-Amaro, A., Pereda, D., Diaz, M., Rodriguez-Barreto, D., Casañas-Sánchez, V., Heffer, M., et al. (2019). Differential Aggregation and Phosphorylation of Alpha Synuclein in Membrane Compartments Associated With Parkinson Disease. *Front. Neurosci.* 13:382. doi: 10.3389/fnins.2019.00382

Challis, C., Hori, A., Sampson, T. R., Yoo, B. B., Challis, R. C., Hamilton, A. M., et al. (2020). Gut-seeded α-synuclein fibrils promote gut dysfunction and brain pathology specifically in aged mice. *Nat. Neurosci.* 23, 327–336. doi: 10.1038/s41593-020-0589-7

Chan, C. S., Guzman, J. N., Ilijic, E., Mercer, J. N., Rick, C., Tkatch, T., et al. (2007). 'Rejuvenation' protects neurons in mouse models of Parkinson's disease. *Nature* 447, 1081–1086. doi: 10.1038/nature05865

Choi, J. G., Huh, E., Ju, I. G., Kim, N., Yun, J., and Oh, M. S. (2018). 1-Methyl-4-phenyl-1,2,3,6 tetrahydropyridine/probenecid impairs intestinal motility and olfaction in the early stages of Parkinson's disease in mice. *J. Neurol. Sci.* 392, 77–82. doi: 10.1016/j.jns.2018.07.011

Clairembault, T., Kamphuis, W., Leclair-Visonneau, L., Rolli-Derkinderen, M., Coron, E., Neunlist, M., et al. (2014). Enteric GFAP expression and phosphorylation in Parkinson's disease. *J. Neurochem.* 130, 805–815. doi: 10.1111/jnc.12742

Cryan, J. F., Mombereau, C., and Vassout, A. (2005). The tail suspension test as a model for assessing antidepressant activity: review of pharmacological and genetic studies in mice. *Neurosci. Biobehav. Rev.* 29, 571–625. doi: 10.1016/j.neubiorev.2005.03.009

Daubner, S. C., Le, T., and Wang, S. (2011). Tyrosine hydroxylase and regulation of dopamine synthesis. *Arch. Biochem. Biophys.* 508, 1–12. doi: 10.1016/j.abb.2010.12.017

Dauer, W., and Przedborski, S. (2003). Parkinson's disease: mechanisms and models. *Neuron* 39, 889–909. doi: 10.1016/s0896-6273(03)00568-3

Dehay, B., Bourdenx, M., Gorry, P., Przedborski, S., Vila, M., Hunot, S., et al. (2015). Targeting α-synuclein for treatment of Parkinson's disease: mechanistic and therapeutic considerations. *Lancet Neurol.* 14, 855–866. doi: 10.1016/S1474-4422(15)00006-X

Deuis, J. R., Dvorakova, L. S., and Vetter, I. (2017). Methods Used to Evaluate Pain Behaviors in Rodents. *Front. Mol. Neurosci.* 10:284. doi: 10.3389/fnmol.2017.00284

Doty, R. L., Deems, D. A., and Stellar, S. (1988). Olfactory dysfunction in parkinsonism: a general deficit unrelated to neurologic signs, disease stage, or disease duration. *Neurology* 38, 1237–1244. doi: 10.1212/wnl.38.8.1237

Ellett, L. J., Hung, L. W., Munckton, R., Sherratt, N. A., Culvenor, J., Grubman, A., et al. (2016). Restoration of intestinal function in an MPTP model of Parkinson's Disease. *Sci. Rep.* 6:30269. doi: 10.1038/srep30269

Emamzadeh, F. N., and Surguchov, A. (2018). Parkinson's Disease: Biomarkers, Treatment, and Risk Factors. *Front. Neurosci.* 12:612. doi: 10.3389/fnins.2018.00612

Fernandez, S. P., Muzerelle, A., Scotto-Lomassese, S., Barik, J., Gruart, A., Delgado-García, J. M., et al. (2017). Constitutive and Acquired Serotonin Deficiency Alters Memory and Hippocampal Synaptic Plasticity. *Neuropsychopharmacology* 42, 512–523. doi: 10.1038/npp.2016.134

Flores-Cuadrado, A., Ubeda-Bañon, I., Saiz-Sanchez, D., de la Rosa-Prieto, C., and Martinez-Marcos, A. (2016). Hippocampal α-synuclein and interneurons in Parkinson's disease: Data from human and mouse models. *Mov. Disord.* 31, 979–988. doi: 10.1002/mds.26586

Fox, S. H., Visanji, N., Reyes, G., Huot, P., Gomez-Ramirez, J., Johnston, T., et al. (2010). Neuropsychiatric behaviors in the MPTP marmoset model of Parkinson's disease. *Can. J. Neurol. Sci.* 37, 86–95. doi: 10.1017/s0317167100009707

Gajula Balija, M. B., Griesinger, C., Herzig, A., Zweckstetter, M., and Jäckle, H. (2011). Pre-fibrillar α-synuclein mutants cause Parkinson's disease-like non-motor symptoms in Drosophila. *PLoS One* 6:e24701. doi: 10.1371/journal.pone.0024701

Henrich, M. T., Geibl, F. F., Lee, B., Chiu, W. H., Koprich, J. B., Brotchie, J. M., et al. (2018). A53T-α-synuclein overexpression in murine locus coeruleus induces Parkinson's disease-like pathology in neurons and glia. *Acta Neuropathol. Commun.* 6:39. doi: 10.1186/s40478-018-0541-1

Ishikawa, S., Taira, T., Takahashi-Niki, K., Niki, T., Ariga, H., and Iguchi-Ariga, S. M. (2010). Human DJ-1-specific transcriptional activation of tyrosine hydroxylase gene. *J. Biol. Chem.* 285, 39718–39731. doi: 10.1074/jbc.M110.137034

Jackson-Lewis, V., and Przedborski, S. (2007). Protocol for the MPTP mouse model of Parkinson's disease. *Nat. Protoc.* 2, 141–151. doi: 10.1038/nprot.2006.342

Jellinger, K. A. (2011). Synuclein deposition and non-motor symptoms in Parkinson disease. *J. Neurol. Sci.* 310, 107–111. doi: 10.1016/j.jns.2011.04.012

Kim, S., Kwon, S. H., Kam, T. I., Panicker, N., Karuppagounder, S. S., Lee, S., et al. (2019). Transneuronal Propagation of Pathologic α-Synuclein from the Gut to the Brain Models Parkinson's Disease. *Neuron* 103, 627.e–641.e. doi: 10.1016/j.neuron.2019.05.035

Laloux, C., Derambure, P., Houdayer, E., Jacquesson, J. M., Bordet, R., Destée, A., et al. (2008). Effect of dopaminergic substances on sleep/wakefulness in saline- and MPTP-treated mice. *J. Sleep Res.* 17, 101–110. doi: 10.1111/j.1365-2869.2008.00625.x

Lashuel, H. A., Overk, C. R., Oueslati, A., and Masliah, E. (2013). The many faces of α-synuclein: from structure and toxicity to therapeutic target. *Nat. Rev. Neurosci.* 14, 38–48. doi: 10.1038/nrn3406

Lee, H. M., and Koh, S. B. (2015). Many Faces of Parkinson's Disease: Non-Motor Symptoms of Parkinson's Disease. *J. Mov. Disord.* 8, 92–97. doi: 10.14802/jmd.15003

Lei, P., Ayton, S., Finkelstein, D. I., Spoerri, L., Ciccotosto, G. D., Wright, D. K., et al. (2012). Tau deficiency induces parkinsonism with dementia by impairing APP-mediated iron export. *Nat. Med.* 18, 291–295. doi: 10.1038/nm.2613

Li, X. H., Dai, C. F., Chen, L., Zhou, W. T., Han, H. L., and Dong, Z. F. (2016). 7,8-dihydroxyflavone Ameliorates Motor Deficits Via Suppressing α-synuclein Expression and Oxidative Stress in the MPTP-induced Mouse Model of Parkinson's Disease. *CNS Neurosci. Ther.* 22, 617–624. doi: 10.1111/cns.12555

Li, Z. S., Schmauss, C., Cuenca, A., Ratcliffe, E., and Gershon, M. D. (2006). Physiological modulation of intestinal motility by enteric dopaminergic neurons and the D2 receptor: analysis of dopamine receptor expression, location, development, and function in wild-type and knock-out mice. *J. Neurosci.* 26, 2798–2807. doi: 10.1523/JNEUROSCI.4720-05.2006

Liu, R., Umbach, D. M., Tröster, A. I., Huang, X., and Chen, H. (2020). Non-motor symptoms and striatal dopamine transporter binding in early Parkinson's disease. *Parkinsonism Relat. Disord.* 72, 23–30. doi: 10.1016/j.parkreldis.2020.02.001

Lu, W., Karuppagounder, S. S., Springer, D. A., Allen, M. D., Zheng, L., Chao, B., et al. (2014). Genetic deficiency of the mitochondrial protein PGAM5 causes a Parkinson's-like movement disorder. *Nat. Commun.* 5:4930. doi: 10.1038/ncomms5930

Luchtman, D. W., Shao, D., and Song, C. (2009). Behavior, neurotransmitters and inflammation in three regimens of the MPTP mouse model of Parkinson's disease. *Physiol. Behav.* 98, 130–138. doi: 10.1016/j.physbeh.2009.04.021

Maatouk, L., Compagnion, A. C., Sauvage, M. C., Bemelmans, A. P., Leclere-Turbant, S., Cirotteau, V., et al. (2018). TLR9 activation via microglial glucocorticoid receptors contributes to degeneration of midbrain dopamine neurons. *Nat. Commun.* 9:2450. doi: 10.1038/s41467-018-04569-y

Maiti, P., Manna, J., and Dunbar, G. L. (2017). Current understanding of the molecular mechanisms in Parkinson's disease: Targets for potential treatments. *Transl. Neurodegener.* 6:28. doi: 10.1186/s40035-017-0099-z

Mandir, A. S., Przedborski, S., Jackson-Lewis, V., Wang, Z. Q., Simbulan-Rosenthal, C. M., Smulson, M. E., et al. (1999). Poly(ADP-ribose) polymerase activation mediates 1-methyl-4-phenyl-1, 2,3,6-tetrahydropyridine (MPTP)-induced parkinsonism. *Proc. Natl. Acad. Sci. U. S. A.* 96, 5774–5779. doi: 10.1073/pnas.96.10.5774

Meissner, W. G., Frasier, M., Gasser, T., Goetz, C. G., Lozano, A., Piccini, P., et al. (2011). Priorities in Parkinson's disease research. *Nat. Rev. Drug Discov.* 10, 377–393. doi: 10.1038/nrd3430

Meredith, G. E., and Rademacher, D. J. (2011). MPTP mouse models of Parkinson's disease: an update. *J. Parkinsons Dis.* 1, 19–33. doi: 10.3233/JPD-2011-11023

Meredith, G. E., Totterdell, S., Potashkin, J. A., and Surmeier, D. J. (2008). Modeling PD pathogenesis in mice: advantages of a chronic MPTP protocol. *Parkinsonism Relat. Disord.* 14, S112–S115. doi: 10.1016/j.parkreldis.2008.04.012

Miller, I. N., and Cronin-Golomb, A. (2010). Gender differences in Parkinson's disease: clinical characteristics and cognition. *Mov. Disord.* 25, 2695–2703. doi: 10.1002/mds.23388

Monastero, R., Cicero, C. E., Baschi, R., Davì, M., Luca, A., Restivo, V., et al. (2018). Mild cognitive impairment in Parkinson's disease: the Parkinson's disease cognitive study (PACOS). *J. Neurol.* 265, 1050–1058. doi: 10.1007/s00415-018-8800-4

Natale, G., Kastsiushenka, O., Fulceri, F., Ruggieri, S., Paparelli, A., and Fornai, F. (2010). MPTP-induced parkinsonism extends to a subclass of TH-positive neurons in the gut. *Brain Res.* 1355, 195–206. doi: 10.1016/j.brainres.2010.07.076

Nuber, S., Petrasch-Parwez, E., Winner, B., Winkler, J., von Hörsten, S., Schmidt, T., et al. (2008). Neurodegeneration and motor dysfunction in a conditional model of Parkinson's disease. *J. Neurosci.* 28, 2471–2484. doi: 10.1523/JNEUROSCI.3040-07.2008

O'Sullivan, S. S., Williams, D. R., Gallagher, D. A., Massey, L. A., Silveira-Moriyama, L., and Lees, A. J. (2008). Nonmotor symptoms as presenting complaints in Parkinson's disease: a clinicopathological study. *Mov. Disord.* 23, 101–106. doi: 10.1002/mds.21813

Park, J. Y., Kim, S. N., Yoo, J., Jang, J., Lee, A., Oh, J. Y., et al. (2017). Novel Neuroprotective Effects of Melanin-Concentrating Hormone in Parkinson's Disease. *Mol. Neurobiol.* 54, 7706–7721. doi: 10.1007/s12035-016-0258-8

Park, J., Lim, C. S., Seo, H., Park, C. A., Zhuo, M., Kaang, B. K., et al. (2015). Pain perception in acute model mice of Parkinson's disease induced by 1-methyl-4-phenyl-1,2,3,6-tetrahydropyridine (MPTP). *Mol. Pain* 11:28. doi: 10.1186/s12990-015-0026-1

Parker, J. G., Marshall, J. D., Ahanonu, B., Wu, Y. W., Kim, T. H., Grewe, B. F., et al. (2018). Diametric neural ensemble dynamics in parkinsonian and dyskinetic states. *Nature* 557, 177–182. doi: 10.1038/s41586-018-0090-6

Paul, R., Choudhury, A., Kumar, S., Giri, A., Sandhir, R., and Borah, A. (2017). Cholesterol contributes to dopamine-neuronal loss in MPTP mouse model of Parkinson's disease: Involvement of mitochondrial dysfunctions and oxidative stress. *PLoS One* 12:e0171285. doi: 10.1371/journal.pone.0171285

Petit, G. H., Berkovich, E., Hickery, M., Kallunki, P., Fog, K., Fitzer-Attas, C., et al. (2013). Rasagiline ameliorates olfactory deficits in an alpha-synuclein mouse model of Parkinson's disease. *PLoS One* 8:e60691. doi: 10.1371/journal.pone.0060691

Rappold, P. M., and Tieu, K. (2010). Astrocytes and therapeutics for Parkinson's disease. *Neurotherapeutics* 7, 413–423. doi: 10.1016/j.nurt.2010.07.001

Rousselet, E., Joubert, C., Callebert, J., Parain, K., Tremblay, L., Orieux, G., et al. (2003). Behavioral changes are not directly related to striatal monoamine levels, number of nigral neurons, or dose of parkinsonian toxin MPTP in mice. *Neurobiol. Dis.* 14, 218–228. doi: 10.1016/s0969-9961(03)00108-6

Santangelo, G., Vitale, C., Trojano, L., Angrisano, M. G., Picillo, M., Errico, D., et al. (2014). Subthreshold depression and subjective cognitive complaints in Parkinson's disease. *Eur. J. Neurol.* 21, 541–544. doi: 10.1111/ene.12219

Schapira, A. H. V., Chaudhuri, K. R., and Jenner, P. (2017). Non-motor features of Parkinson disease. *Nat. Rev. Neurosci.* 18, 435–450. doi: 10.1038/nrn.2017.62

Schirinzi, T., Sancesario, G. M., Di Lazzaro, G., Biticchi, B., Colona, V. L., Mercuri, N. B., et al. (2019). CSF α-synuclein inversely correlates with non-motor symptoms in a cohort of PD patients. *Parkinsonism Relat. Disord.* 61, 203–206. doi: 10.1016/j.parkreldis.2018.10.018

Sedelis, M., Schwarting, R. K., and Huston, J. P. (2001). Behavioral phenotyping of the MPTP mouse model of Parkinson's disease. *Behav. Brain Res.* 125, 109–125. doi: 10.1016/s0166-4328(01)00309-6

Seibenhener, M. L., and Wooten, M. C. (2015). Use of the Open Field Maze to measure locomotor and anxiety-like behavior in mice. *J. Vis. Exp.* 96:e52434. doi: 10.3791/52434

Seidl, S. E., Santiago, J. A., Bilyk, H., and Potashkin, J. A. (2014). The emerging role of nutrition in Parkinson's disease. *Front. Aging Neurosci.* 6:36. doi: 10.3389/fnagi.2014.00036

Shalash, A. S., Hamid, E., Elrassas, H. H., Bedair, A. S., Abushouk, A. I., Khamis, M., et al. (2018). Non-Motor Symptoms as Predictors of Quality of Life in Egyptian Patients With Parkinson's Disease: A Cross-Sectional Study Using a Culturally Adapted 39-Item Parkinson's Disease Questionnaire. *Front. Neurol.* 9:357. doi: 10.3389/fneur.2018.00357

Shannon, K. M., Keshavarzian, A., Dodiya, H. B., Jakate, S., and Kordower, J. H. (2012). Is alpha-synuclein in the colon a biomarker for premotor Parkinson's disease? *Evidence from 3 cases. Mov. Disord.* 27, 716–719. doi: 10.1002/mds.25020

Shao, Q. H., Chen, Y., Li, F. F., Wang, S., Zhang, X. L., Yuan, Y. H., et al. (2019). TLR4 deficiency has a protective effect in the MPTP/probenecid mouse model of Parkinson's disease. *Acta Pharmacol. Sin.* 40, 1503–1512. doi: 10.1038/s41401-019-0280-2

Shulman, L. M., Taback, R. L., Bean, J., and Weiner, W. J. (2001). Comorbidity of the nonmotor symptoms of Parkinson's disease. *Mov. Disord.* 16, 507–510. doi: 10.1002/mds.1099

Sim, Y., Park, G., Eo, H., Huh, E., Gu, P. S., Hong, S. P., et al. (2017). Protective effects of a herbal extract combination of Bupleurum falcatum, Paeonia suffruticosa, and Angelica dahurica against MPTP-induced neurotoxicity via regulation of nuclear receptor-related 1 protein. *Neuroscience* 340, 166–175. doi: 10.1016/j.neuroscience.2016.10.029

Spillantini, M. G., Schmidt, M. L., Lee, V. M., Trojanowski, J. Q., Jakes, R., and Goedert, M. (1997). Alpha-synuclein in Lewy bodies. *Nature* 388, 839–840. doi: 10.1038/42166

Stewart, T., Sossi, V., Aasly, J. O., Wszolek, Z. K., Uitti, R. J., Hasegawa, K., et al. (2015). Phosphorylated α-synuclein in Parkinson's disease: correlation depends on disease severity. *Acta Neuropathol. Commun.* 3:7. doi: 10.1186/s40478-015-0185-3

Stoyka, L. E., Arrant, A. E., Thrasher, D. R., Russell, D. L., Freire, J., Mahoney, C. L., et al. (2020). Behavioral defects associated with amygdala and cortical dysfunction in mice with seeded α-synuclein inclusions. *Neurobiol. Dis.* 134:104708. doi: 10.1016/j.nbd.2019.104708

Sung, S., Vijiaratnam, N., Chan, D. W. C., Farrell, M., and Evans, A. H. (2018a). Parkinson disease: A systemic review of pain sensitivities and its association with clinical pain and response to dopaminergic stimulation. *J. Neurol. Sci.* 395, 172–206. doi: 10.1016/j.jns.2018.10.013

Sung, S., Vijiaratnam, N., Chan, D. W. C., Farrell, M., and Evans, A. H. (2018b). Pain sensitivity in Parkinson's disease: Systematic review and meta-analysis. *Parkinsonism Relat. Disord.* 48, 17–27. doi: 10.1016/j.parkreldis.2017.12.031

Tibar, H., El Bayad, K., Bouhouche, A., Ait Ben, Haddou, E. H., Benomar, A., et al. (2018). Non-Motor Symptoms of Parkinson's Disease and Their Impact on Quality of Life in a Cohort of Moroccan Patients. *Front. Neurol.* 9:170. doi: 10.3389/fneur.2018.00170

Van Den Eeden, S. K., Tanner, C. M., Bernstein, A. L., Fross, R. D., Leimpeter, A., Bloch, D. A., et al. (2003). Incidence of Parkinson's disease: variation by age, gender, and race/ethnicity. *Am. J. Epidemiol.* 157, 1015–1022. doi: 10.1093/aje/kwg068

Wang, Y., Shi, M., Chung, K. A., Zabetian, C. P., Leverenz, J. B., Berg, D., et al. (2012). Phosphorylated α-synuclein in Parkinson's disease. *Sci. Transl. Med.* 4:121ra20. doi: 10.1126/scitranslmed.3002566

Xu, L., and Pu, J. (2016). Alpha-Synuclein in Parkinson's Disease: From Pathogenetic Dysfunction to Potential Clinical Application. *Parkinsons Dis.* 2016:1720621. doi: 10.1155/2016/1720621

Yan, T., He, B., Wan, S., Xu, M., Yang, H., Xiao, F., et al. (2017). Antidepressant-like effects and cognitive enhancement of Schisandra chinensis in chronic unpredictable mild stress mice and its related mechanism. *Sci. Rep.* 7:6903. doi: 10.1038/s41598-017-07407-1

Yang, M., and Crawley, J. N. (2009). Simple behavioral assessment of mouse olfaction. *Curr. Protoc. Neurosci.* 8:ns0824s48. doi: 10.1002/0471142301.ns0824s48

Zeng, X. S., Geng, W. S., and Jia, J. J. (2018). Neurotoxin-Induced Animal Models of Parkinson Disease: Pathogenic Mechanism and Assessment. *ASN Neuro.* 10:1759091418777438. doi: 10.1177/1759091418777438

Zhang, Q. S., Heng, Y., Mou, Z., Huang, J. Y., Yuan, Y. H., and Chen, N. H. (2017). Reassessment of subacute MPTP-treated mice as animal model of Parkinson's disease. *Acta Pharmacol. Sin.* 38, 1317–1328. doi: 10.1038/aps.2017.49

Zhong, N., Kim, C. Y., Rizzu, P., Geula, C., Porter, D. R., Pothos, E. N., et al. (2006). DJ-1 transcriptionally up-regulates the human tyrosine hydroxylase by inhibiting the sumoylation of pyrimidine tract-binding protein-associated splicing factor. *J. Biol. Chem.* 281, 20940–20948. doi: 10.1074/jbc.M601935200

Conflict of Interest: The authors declare that the research was conducted in the absence of any commercial or financial relationships that could be construed as a potential conflict of interest.

Copyright © 2021 Han, Kim, Ahn, Hwang, Lee and Park. This is an open-access article distributed under the terms of the Creative Commons Attribution License (CC BY). The use, distribution or reproduction in other forums is permitted, provided the original author(s) and the copyright owner(s) are credited and that the original publication in this journal is cited, in accordance with accepted academic practice. No use, distribution or reproduction is permitted which does not comply with these terms.

frontiers in Aging Neuroscience

MINI REVIEW
published: 21 January 2021
doi: 10.3389/fnagi.2020.616357

Mini Review: Correlations of Cognitive Domains With Cerebrospinal Fluid α-Synuclein Levels in Patients With Parkinson's Disease

Hidetomo Murakami[1], *Kenjiro Ono*[2]*, *Tomotaka Shiraishi*[1], *Tadashi Umehara*[1], *Shusaku Omoto*[1] *and Yasuyuki Iguchi*[1]

[1] Department of Neurology, School of Medicine, The Jikei University, Tokyo, Japan, [2] Department of Neurology, School of Medicine, Showa University, Tokyo, Japan

The level of α-synuclein, a component of Lewy bodies, in cerebrospinal fluid (CSF) in Parkinson's disease (PD) has attracted recent attention. Most meta-analyses conclude that CSF levels of α-synuclein are decreased in PD. Patients with PD present with cognitive impairment, including frontal/executive dysfunction in the early phase and later emergence of visuospatial and mnemonic deficits. To examine whether CSF α-synuclein levels reflect the activities of various cognitive domains, we reviewed reports examining the association of these levels with cognitive performance in each domain in PD. Among 13 cross-sectional studies, five showed that a lower CSF α-synuclein level was associated with worse cognitive function. In four of these five reports, frontal/executive function showed this association, suggesting a link of the pathophysiology with Lewy bodies. In three other reports, a higher CSF α-synuclein level was associated with temporal-parieto-occipital cognitive deterioration such as memory. In the other five reports, the CSF α-synuclein level did not correlate with cognitive performance for any domain. In four longitudinal studies, a higher baseline CSF α-synuclein level was associated with a worse cognitive outcome, including cognitive processing speed, visuospatial function and memory in two, but not with any cognitive outcome in the other two. The different associations may reflect the heterogeneous pathophysiology in PD, including different pathogenic proteins, neurotransmitters. Thus, more studies of the association between cognitive domains and CSF levels of pathogenic proteins are warranted.

Keywords: Parkinson's disease, cerebrospinal fluid, α-synuclein, Lewy body, cognitive domain, frontal/executive function

OPEN ACCESS

Edited by:
Pingyi Xu,
First Affiliated Hospital of Guangzhou Medical University, China

Reviewed by:
Dag Aarsland,
King's College London, United Kingdom
Davide Chiasserini,
University of Perugia, Italy

***Correspondence:**
Kenjiro Ono
onoken@med.showa-u.ac.jp

Received: *12 October 2020*
Accepted: *29 December 2020*
Published: *21 January 2021*

Citation:
Murakami H, Ono K, Shiraishi T, Umehara T, Omoto S and Iguchi Y (2021) Mini Review: Correlations of Cognitive Domains With Cerebrospinal Fluid α-Synuclein Levels in Patients With Parkinson's Disease. Front. Aging Neurosci. 12:616357. doi: 10.3389/fnagi.2020.616357

INTRODUCTION

Parkinson's disease (PD) is a common neurodegenerative disease that presents with motor and various non-motor symptoms, including cognitive impairment. Such impairment of frontal/executive function, such as flexibility, planning, and working memory, is common as early cognitive impairment in PD (Williams-Gray et al., 2007; Kehagia et al., 2010). As the disease

progresses, posterior cortically based cognitive deficits, such as visuospatial and mnemonic deficits, become apparent as the major symptoms of PD with dementia (PDD) (Kehagia et al., 2010; Collins and Williams-Gray, 2016). A dementia syndrome affects two or more cognitive domains and causes social and occupational impairment.

The presence of Lewy bodies consisting of α-synuclein is the pathological hallmark of the disease. According to Braak's theory, Lewy bodies are deposited in the brainstem in the early stage, then progress through the limbic and subcortical regions, and eventually are distributed over the neocortex in a later stage (Braak et al., 2003). Cerebrospinal fluid (CSF) is in close contact with the brain, and CSF levels of α-synuclein may reflect the pathology and progression of clinical symptoms. The CSF α-synuclein level has previously been compared with global/composite cognitive assessments using the mini-mental state examination (MMSE) and other scales, but no association was observed in cross-sectional (Park et al., 2011; Parnetti et al., 2011; Wennström et al., 2013) and longitudinal (Parnetti et al., 2014; Mollenhauer et al., 2019) studies. Several previous reports have compared the association of the CSF α-synuclein level with cognitive performance in each domain, but a review of the findings in these reports has not been published. Here, we review the studies that examined this association and we discuss factors that may mediate differences in correlations.

SEARCH STRATEGY AND SELECTION CRITERIA

We searched for reports on correlations of CSF total α-synuclein, but not other specific types such as oligomeric and phosphorylated α-synuclein, levels and cognitive assessments in each domain in the PubMed database, using a combination of keywords of "cerebrospinal fluid, synuclein and Parkinson" with "cognitive function" or "executive" or "visuospatial" or "memory" or "attention" or "language." Quoted papers in eligible studies were traced to ensure all relevant studies were included. Papers from any year that evaluated the relationship of the CSF α-synuclein level with assessment of a precise cognitive domain were included. The search was performed from 29th June to 1st August 2020, and 98 papers were found. However, 86 of these papers that did not mention the association between the CSF α-synuclein level and cognitive performance or that used a composite assessment such as the total MMSE or Montreal Cognitive Assessment (MoCA) score were excluded.

ASSOCIATION BETWEEN THE CSF α-SYNUCLEIN LEVEL AND COGNITIVE PERFORMANCE

Eligible Studies

Twelve papers examining associations of CSF α-synuclein levels and cognitive function in single domains were included in the study (**Table 1**). Three of these reports included two or three associations (Stewart et al., 2014; Compta et al., 2015; Førland et al., 2018), and 13 cross-sectional results were used from the 12 papers (**Tables 1A–C**). Five showed that a lower CSF α-synuclein level was associated with worse cognitive function in certain domains (**Table 1A**) and three showed that a higher CSF α-synuclein level was associated with worse cognitive performance in some domains (**Table 1B**). The other 5 results indicated that the CSF α-synuclein level did not correlate with cognitive performance in any domain (**Table 1C**). There were 4 longitudinal studies, of which two showed that a higher CSF α-synuclein level predicted worse cognitive outcome (**Table 1D**) and the other two showed no association (**Tables 1E,F**).

Cross-Sectional Assessments

Results Showing That a Lower CSF α-Synuclein Level Indicates Worse Frontal/Executive Cognitive Function

Four of the five reports in **Table 1A** showed an association of frontal/executive function with the CSF α-synuclein level. Compta et al. (2015) showed dysfunction in phonetic fluency was associated with low CSF α-synuclein in 41 PD patients with a wide range of cognitive status from normal cognition to dementia (21 patients without dementia). The CSF α-synuclein level also showed significant correlations with thickness in the frontal cortex in patients with idiopathic rapid-eye-movement sleep behavior disorder (iRBD) as a prodoromal stage of PD and PD without dementia (Compta et al., 2015). Skogseth et al. (2015) showed that low CSF α-synuclein was significantly associated with phonemic fluency and attention, but not with posterior cortical domains, such as memory and visuospatial domains, in PD and PD with mild cognitive impairment (PD-MCI). We have shown that lower CSF α-synuclein is associated with worse performance in a judgement subtest that assesses planning and executive function, but not with subtests assessing other cognitive domains in patients with PD, PD-MCI and PDD (Murakami et al., 2019). In these four studies, CSF α-synuclein levels were also correlated with CSF levels of amyloid-β 1-42 and total tau.

Results Showing That a Lower CSF α-Synuclein Level Indicates Worse Posterior Cognitive Function

Stewart et al. (2014) found that lower CSF α-synuclein was correlated with worse performance of memory at the beginning of phase I of the deprenyl and tocopherol antioxidative therapy of Parkinsonism (DATATOP) study, which included drug-naïve early PD patients (**Table 1A**).

Results Showing That a Higher CSF α-Synuclein Level Indicates Worse Posterior Cognitive Function

All three results in **Table 1B** showed an association of higher CSF α-synuclein with worse performance in posterior, but not frontal, cortical cognitive function, such as memory, naming and semantic fluency. At the beginning of phase 2 of the DATATOP study, when motor symptoms in patients on selegiline, tocopherol, both drugs or placebo had progressed to a state requiring L-dopa therapy, higher CSF α-synuclein was associated with worse verbal learning and memory score in PD without dementia (Stewart et al., 2014). Compta et al. (2015) showed that CSF α-synuclein was significantly higher in patients with a worse score for naming and memory compared to those

TABLE 1 | Results of cross-sectional or longitudinal studies of the association between the CSF alpha-synuclein level and cognitive performance in each domain.

Study	Number of participants	Age (range)	Disease duration (range)	H and Y (range)	MMSE (range)	Duration of follow up	Associated cognitive domain	Analysis of α-synuclein level (manufacturer of the assay)
A. Lower CSF α-synuclein indicates worse cognitive function in a crosssectional study								
Compta et al. (2015)	PD: 41 (without/with dementia 21/20)	68/73.5[a]	10/9 years[a]	3/4[a]	28/18[a]	–	Phonetic fluency	ELISA
		(63.50–73.50)/(66.00–78.00)[b]	(7.00–15.75)/(7.25–11.50)[b]	(2–3)/(3–5)[b]	(27–29)/(16–22)[b]			(Invitrogen: KHB0061)
Compta et al. (2015)	PD without dementia: 21	68[a]	10 years[a]	3[a]	28[a]	–	Phonemic fluency,	ELISA
		(63.50–73.50)[b]	(7.00–15.75)[b]	(2–3)[b]	(27–29)[b]		visuospatial function	(Invitrogen: KHB0061)
Skogseth et al. (2015)	PD-NC and PD-MCI: 414	61.3 ± 9.7	4.0 months[a]	N.A.	N.A.	–	Phonemic fluency, attention	ELISA
		(N.A)	(2.0–8.0 months)[b]	(N.A.)	(N.A.)			(Covance)
Murakami et al. (2019)	PD, PD-MCI and PDD: 27	72.3 ± 9.2	1.3 ± 1.2 years	N.A.	21.7 ± 5.5[c]	–	Planning, executive	ELISA
		(47–84)	(0–5)	(N.A.)	(9–28)			(Covance)
Stewart et al. (2014) -phase 1	PD without dementia: 350	60.90 ± 9.21	2.08 ± 1.39 years	1.5[a]	28.86 ± 1.44	–	Memory	Luminex assay
		(34–79)	(0–7)	(1.0–2.5)	(23–30)			(Luminex)
B. Higher CSF α-synuclein indicates worse cognitive function in a crosssectional study								
Stewart et al. (2014) -phase 2	PD: 266	62.64 ± 9.03	3.80 ± 1.45 years	2.0[a]	28.74 ± 2.30	–	Verbal learning, memory	Luminex assay
		(37–80)	(1–8)	(1.0–4.0)	(8–30)			(Luminex)
Compta et al. (2015)	PD: 41(without/with dementia 21/20)	68/73.5[a]	10/9 years[a]	3/4[a]	28/18[a]	–	Naming, memory	ELISA
		(63.50–73.50)/(66.00–78.00)[b]	(7.00–15.75)/(7.25–11.50)[b]	(2–3)/(3–5)[b]	(27–29)/(16–22)[b]			(Invitrogen: KHB0061)
Wijeyekoon et al. (2020)	PD: 35	65.4 ± 7.6	5.4 ± 5.6 years	N.A.	90.3 ± 9.4[d]	–	Semantic fluency	ECL
		(N.A.)	(N.A.)	(N.A.)	(N.A.)			(Meso Scale Diagnostics)
C. Results showing no association between CSF α-synuclein level and cognitive function in any domain in a crosssectional study								
Buddhala et al. (2015)	PD without dementia: 77	66.9 ± 8.5[e]	4.9 ± 4.0 years[e]	N.A.	N.A.	–	None	ELISA
		(N.A.)	(N.A.)	(N.A.)	(N.A.)			(Covance)
Yarnall et al. (2014)	PD-NC and PD-MCI: 67	64.5 ± 9.4	5.3 ± 5.6 months	N.A.	25.2 ± 3.3[c]	–	None	ELISA
		(N.A.)	(N.A.)	(N.A.)	(N.A.)			(N.A.)
Førland et al. (2018)	PD: 56	69.1[a]	4.8 years[a]	2[a]	28.5[a]	–	None	ELISA
		(56.1–78.5)	(N.A.)	(1.0–3.0)	(23.0–30.0)			(BioLegend: #844101)

(Continued)

TABLE 1 | Continued

Study	Number of participants	Age (range)	Disease duration (range)	H and Y (range)	MMSE (range)	Duration of follow up	Associated cognitive domain	Analysis of α-synuclein level (manufacturer of the assay)
Kang et al. (2013)	PD: 63	62 ± 10	0.4 years[a]	1.65 ± 0.51	27.2 ± 2.0[c]	–	None	ELISA
		(59–64)[f]	(0.0–2.6)	(1–2)	(26.7–27.7)[f]			(Covance)
Stav et al. (2015)	PD without dementia: 31	64.65 ± 6.53	2.5 ± 1.2 years	1.5[a]	28.58 ± 1.59	–	None	ECL
		(47–74)	(1–6)	(1.0–2.5)	(22–30)			(Meso Scale Discovery)
D. Higher CSF α-synuclein predicts worse outcome in cognition in a longitudinal study								
Hall et al. (2015)	PD without dementia: 42	67.5[a]	7 years[a]	2.25[a]	29[a]	2 years	Cognitive processing speed	Luminex assay
		(60.5–73.25)[b]	(4.0–10.25)[b]	(1–2.5)[b]	(27–29)[b]			(Luminex)
Stewart et al. (2014)	PD: 266	62.64 ± 9.03	3.80 ± 1.45 years	2.0[a]	28.74 ± 2.30	Up to 6.9 years	Verbal learning, memory, visuospatial working memory	Luminex assay
		(37–80)	(1–8)	(1.0–4.0)	(8–30)	(average 1.8 years)		(Luminex)
E. Baseline CSF α-synuclein level does not predict cognitive decline in a longitudinal study								
Førland et al. (2018)	PD: 56	69.1[a]	4.8 years[a]	2[a]	28.5[a]	2 to 4 years	None	ELISA
		(56.1–78.5)	(N.A.)	(1.0–3.0)	(23.0–30.0)			(BioLegend: #844101)
F. Change in CSF α-synuclein is not associated with worsening of cognitive function in a longitudinal study								
Hall et al. (2016)	PD without dementia: 63	64.7 ± 9.4	5.5 ± 4.0 years	2.0 ± 0.7	28.5 ± 1.4	2 years	None	ELISA
		(N.A.)	(N.A.)	(N.A.)	(N.A.)			(Covance)

Data are presented as mean (±standard deviation) unless otherwise indicated.

[a]Median, [b]Interquartile range, [c]Montreal cognitive assessment (MoCA), [d]Addenbrooke's Cognitive Examination- Revised (ACE-R), [e]median ± standard deviation, [f]95% confidence interval.

N.A.: not available.

ECL, Electrochemiluminescence; ELISA, Enzyme-Linked ImmunoSorbent Assay; H and Y, Hoehn and Yahr scale; MCI, mild cognitive impairment; MMSE, Mini-mental state examination; NC, normal cognition; SD, standard deviation.

with better scores in 41 PD patients with a wide range of cognitive function. In this cohort, CSF levels of α-synuclein correlated with those of amyloid-β 1-42 and total tau. Wijeyekoon et al. (2020) showed that the CSF α-synuclein level was negatively correlated negatively with semantic fluency score and positively with the CSF level of amyloid-β 1-42 in PD.

Results Showing no Association of CSF α-Synuclein Levels With Cognitive Function in any Domain

In the five results in **Table 1C**, the CSF α-synuclein level showed no association with any domains of cognitive assessment, including frontal/executive, attention, memory, visuospatial functions and others in PD without dementia (Buddhala et al., 2015; Stav et al., 2015), PD with normal cognition and MCI (Yarnall et al., 2014) and PD with a wide range of cognitive status (Kang et al., 2013; Førland et al., 2018). CSF α-synuclein levels were correlated with those of amyloid-β 1-42 (Buddhala et al., 2015) and total tau (Kang et al., 2013; Buddhala et al., 2015).

Longitudinal Assessments

Two of four longitudinal studies showed that higher baseline CSF α-synuclein was associated with future worsening of cognitive function (**Table 1D**). Hall et al. (2015) found an association of higher baseline CSF α-synuclein with worsening in cognitive processing speed, but not with memory and word fluency at 2 years follow-up in 42 PD patients without dementia. Stewart et al. (2014) showed that lower baseline CSF α-synuclein was associated with preservation of assessment scores for verbal learning, memory and visuospatial working memory after follow-up for up to 6.9 years in PD without dementia. In contrast, Førland et al. (2018) found that CSF α-synuclein levels did not predict longitudinal cognitive decline in executive function memory and visuospatial function after 2–4 years follow-up in PD patients (**Table 1E**). Hall et al. (2016) followed 63 PD patients without dementia for 2 years and found that an increase in CSF α-synuclein did not correlate with a change in the letter fluency task (**Table 1F**).

POSSIBLE FACTORS AFFECTING THE ASSOCIATION BETWEEN CSF α-SYNUCLEIN LEVEL AND COGNITIVE FUNCTION

Role of Change in the Dynamics of CSF α-Synuclein Over Time

Among the five cross-sectional results showing that lower CSF α-synuclein was associated with worse cognitive function, four showed an association with frontal/executive function (**Table 1A**). Among the cognitive domains, frontal-executive impairment is common as an early cognitive impairment in PD due to dysfunction in the frontostriatal circuit (Lewis et al., 2003; Williams-Gray et al., 2007). α-Synuclein aggregates to form oligomers that have neurotoxic effects and play an important role in the pathogenesis of PD (Ono, 2017). Meta-analyses showing that the CSF α-synuclein level in PD patients is lower than that in normal controls (Zhou et al., 2015; Eusebi et al., 2017) are consistent with aggregation and intracellular sequestering in Lewy bodies (Stewart et al., 2014; Mollenhauer et al., 2019). CSF α-synuclein in relatively early PD has been shown to decrease during 24–36 months of observation in drug-naïve PD patients (Mollenhauer et al., 2019) and during the phase I DATATOP study cohort (Stewart et al., 2014). Therefore, the association of lower CSF α-synuclein with worse frontal/executive function supports the idea that this dysfunction emerges during concurrent aggregation of α-synuclein and formation of Lewy body in relatively early PD. The finding that lower CSF α-synuclein was associated with frontal cortical thinning in patients with iRBD as a prodromal stage of PD and PD without dementia (Compta et al., 2015) supports the emergence of frontal/executive dysfunction with concurrent development of Lewy body pathology in the frontal cortex. Therefore, a lower α-synuclein level may reflect frontal/executive impairment as an early cognitive dysfunction in PD.

In contrast with the above results for frontal/executive function, there are reports showing associations of a higher CSF α-synuclein level with worse cognitive assessment in cross-sectional studies (**Table 1B**) and worse cognitive outcome in longitudinal studies (**Table 1D**). CSF α-synuclein has been found to increase over time in PD with a disease duration of >5 years (Hall et al., 2016) and in patients receiving levodopa treatment (Majbour et al., 2016). Thus, there may be a point at which CSF α-synuclein turns from decreasing to increasing in the progressive course of PD. The increase in CSF is suggested to be due to release of the pathogenic protein as a result of neural damage (Lleó et al., 2015), and these results support the idea that as neuronal damage progress, cognitive function also deteriorates. The association of high CSF α-synuclein with posterior cortical thinning in PDD also support this idea (Compta et al., 2015).

Among cognitive domains, worse posterior cortical cognitive domains, a hallmark of dementia in PD, have been associated with both higher (**Table 1B**) and lower (**Table 1A**) CSF α-synuclein levels. This opposite association may also be due to the bimodal change in CSF α-synuclein level, which decreases in the relatively early phase and increases in the later phase of PD. We found no report showing that worse frontal/executive function was associated with a higher CSF level in the search for this review. Therefore, the association of lower α-synuclein with worse frontal/executive function observed before the turning point of the CSF α-synuclein level supports frontal/executive impairment as an earlier symptom in PD.

Although we conceptually view patients in a cohort as being earlier or later stage cases with regard to the association between CSF α-synuclein and cognitive function, we cannot distinguish "earlier" or "later" patients using clinically obtainable information. For example, there are overlaps in patient background factors, such as age, disease duration and clinical symptoms, among cohort groups presenting with each type of association. However, we believe that the existence of positive and negative associations signifies differences in disease duration and pathophysiology linked to α-synuclein among the cognitive domains.

Involvement of Pathogenic Proteins Other Than α-Synuclein

There were five results showing no association between CSF α-synuclein and cognitive assessments (**Tables 1C,E,F**). This indicates that the pathophysiological background of cognitive dysfunction cannot be explained by the CSF α-synuclein level as a single biomarker. There are some reports showing an association between a reduced CSF amyloid-β 1-42 level and cognitive deterioration in PD (Lim et al., 2019). Decreased CSF amyloid-β 1-42 is a confirmed biomarker for Alzheimer's disease (AD), and this decrease is suggested to be due to formation of aggregates such as senile plaque. In PD progression, posterior cortically based dysfunction is known to become dominant due to pathological findings in AD (Collins and Williams-Gray, 2016). PD often presents with an AD pathology such as senile plaques and neurofibrillary tangles (Apaydin et al., 2002), and several experimental studies have explained the co-pathology of AD and PD. α-synuclein has been shown to co-aggregate with amyloid-β 1-42 (Ono et al., 2012) and tau (Guo et al., 2013), and some of the studies in this review showed that CSF α-synuclein levels were correlated with those of amyloid-β 1-42 (Buddhala et al., 2015; Compta et al., 2015; Skogseth et al., 2015; Hall et al., 2016; Murakami et al., 2019; Wijeyekoon et al., 2020) and tau (Kang et al., 2013; Buddhala et al., 2015; Compta et al., 2015; Hall et al., 2015, 2016; Skogseth et al., 2015; Murakami et al., 2019). These reports support an interaction of α-synuclein with amyloid beta and tau in the progressive course of PD and cognitive deterioration. Amyloid-β 1-42 and tau also contribute to progression of PD, but this contribution may not be reflected by the CSF α-synuclein level.

Involvement of Other Factors

Changes in the titers of neurotransmitters in the central nervous system during the progressive course of PD partially contribute to variation in the association between CSF α-synuclein levels and cognitive performance in each domain. Frontal/executive function in early PD is dopaminergic (Kehagia et al., 2010) and dopaminergic medication can be effective (Murakami et al., 2017). Frontal/executive function, but not memory or visuospatial function, was shown to correlate with striatal dopaminergic deficits on ^{123}I-Ioflupane SPECT (Siepel et al., 2014), whereas a dopaminergic titer that is too high can impair frontal/executive function (Kehagia et al., 2010). Lewy body pathology has also been suggested to contribute to frontostriatal dopaminergic depletion and frontal atrophy (Stav et al., 2015). Therefore, the association between CSF α-synuclein level and frontal/executive function can be affected by dopamine.

Cholinergic dysfunction with an AD-like pathophysiology also contributes to cognitive deterioration in PD and has a key role in progression to PDD (Kehagia et al., 2010). Cholinergic drugs are effective for cognitive impairment in PD (Aarsland et al., 2002; Ravina et al., 2005), and cholinergic activity can affect the association between CSF α-synuclein levels and cognitive assessments. Other neurotransmitters, such as noradrenaline, also contribute to some domains of cognitive function in PD (Kehagia et al., 2010). Therefore, associations among pathological findings linked to pathogenic proteins, affected neurotransmitters, cognitive performance and lesions linked to the cognitive domain are of great interest, and it is important to determine the mechanism by which pathogenic proteins produce specificity for lesions and neurotransmitters.

PD is associated with neuronal inflammation and α-synuclein can activate microglia and astrocytes (Surendranathan et al., 2015). CSF levels of inflammatory cytokines, such as IL-1β, IL-6 and others, are increased in PD (Mogi et al., 1996; Chen et al., 2018), and the CSF α-synuclein level is associated with that of inflammation markers such as IL-1β (Hu et al., 2015), serum amyloid A (SAA), IL-8 and chitinase-3-like protein 1 (YKL-40) (Hall et al., 2018) in PD. Higher levels of CSF inflammatory markers such as CRP, SAA, IL-6 and IL-8 have been associated with worse cognition, such as cognitive speed, attention and letter fluency (Hall et al., 2018). Cortical microglial activity assessed by ^{11}C-RPK11195 PET was negatively correlated with glucose metabolism in the temporo-parietal-occipital cortex, and the level of microglial activity in the temporoparietal, occipital and frontal cortex showed an inverse correlation with MMSE scores in PDD patients (Fan et al., 2015). Therefore, the status of neuronal inflammation can affect the association between the CSF α-synuclein level and cognitive function.

Various genetic factors also affect the pathology and cognitive function in PD. Correlations between cortical thinning and CSF α-synuclein levels are opposite based on two types of the SNCA rs356191 single nucleotide polymorphism, and the correlated cortical lesion also differs in PD (Sampedro et al., 2018). Some heterogeneities such as the microtubule-associated protein tau (MAPT) genotype (Williams-Gray et al., 2009) and apolipoprotein E subtype (Tsuang et al., 2013) influence development of dementia in PD. The catechol-O-methyltransferase (COMT) genotype is known to affect frontal/executive function (Williams-Gray et al., 2009). Therefore, genetic factors may also affect the association between CSF α-synuclein levels and cognitive function, and contribute to the heterogeneity in cognitive function.

In each study, CSF α-synuclein levels were assessed using different methods, such as Enzyme-Linked Immunosorbent Assay (ELISA), Electrochemiluminescence (ECL) and Luminex assay (**Table 1**). All 4 reports showing lower CSF α-synuclein

TABLE 2 | Suggested factors that affect cognitive performance during the conceptual disease stage.

Relatively early stage (Impairment in frontal/executive function is associated with lower CSF α-synuclein level)
Lewy body pathology
Dopaminergic deficit
Relatively later stage (Impairment in posterior cortically based cognitive domains are associated with higher CSF α-synuclein level)
Alzheimer's pathology
Deficit of acetylcholine or another neurotransmitter
Unspecified (unknown) stage
Neuronal inflammation
Genetic factors

level indicates worse frontal/executive function used ELISA (**Table 1A**). Whereas, studies showing the other type of association between CSF α-synuclein level and cognition used various assays (**Tables 1B–F**). Therefore, the method to assess CSF α-synuclein level should be paid attention in the future study.

Suggested factors that affect cognitive performance during the conceptual disease stage are summarized in **Table 2**.

CONCLUSION AND FUTURE PERSPECTIVE

Reports on relationships of CSF α-synuclein levels with cognitive performance in each domain have shown various associations. The type of association with the CSF α-synuclein level has tended to differ between frontal/executive and posterior cortical cognitive domains. Pathophysiology and phase of the disease in which α-synuclein pathology contributes may differ based on the cognitive domain. Therefore, it is important to focus on impairment in each cognitive domain when evaluating the pathophysiology of PD. At present, the mechanism for each type of association is uncertain, and the type of association in each cohort cannot be predicted using available information in clinical practice. Investigation of cohorts presenting with different types of association between CSF α-synuclein levels and cognitive performance in each domain will contribute to unveiling the pathophysiology of cognitive function in PD. However, as shown in this review, there are still only a few reports on associations of CSF pathogenic proteins and cognitive function. This is a limitation of the review, and further clinical studies in other cohorts and more studies on α-synuclein metabolism and PD pathogenesis are required.

AUTHOR CONTRIBUTIONS

HM and KO planned and wrote the manuscript. TS, TU, SO, and YI read and approved the final manuscript. All authors contributed to the article and approved the submitted version.

FUNDING

This work was supported by Strategic Research Program for Brain Sciences from Japan Agency for Medical Research and Development (jp20dm0107158) (KO).

REFERENCES

Aarsland, D., Laake,. K., Larsen, J. P., and Janvin, C. (2002). Donepezil for cognitive impairment in Parkinson's disease: a randomised controlled study. *J. Neurol. Neurosurg. Psychiatry* 72, 708–712. doi: 10.1136/jnnp.72.6.708

Apaydin, H., Ahlskog, J. E., Parisi, J. E., Boeve, B. F., and Dickson, D. W. (2002). Parkinson disease neuropathology: later-developing dementia and loss of the levodopa response. *Arch. Neurol.* 59, 102–112. doi: 10.1001/archneur.59.1.102

Braak, H., Tredici, K. D., Rüb, U., de Vos, R. A. I., Jansen Steur, E. N. H., and Braak, E. (2003). Staging of brain pathology related to sporadic Parkinson's disease. *Neurobiol. Aging* 24, 197–211. doi: 10.1016/S0197-4580(02)00065-9

Buddhala, C., Campbell, M. C., Perlmutter, J. S., and Kotzbauer, P. T. (2015). Correlation between decreased CSF α-synuclein and Aβ1–42 in Parkinson disease. *Neurobiol. Aging* 36, 476–484. doi: 10.1016/j.neurobiolaging.2014.07.043

Chen, X., Hu, Y., Cao, Z., Liu, Q., and Cheng, Y. (2018). Cerebrospinal fluid inflammatory cytokine aberrations in Alzheimer's disease, Parkinson's disease and amyotrophic lateral sclerosis: A systematic review and meta-analysis. *Front. Immunol.* 9:2122. doi: 10.3389/fimmu.2018.02122

Collins, L. M., and Williams-Gray, C. H. (2016). The genetic basis of cognitive impairment and dementia in Parkinson's disease. *Front. Psychiatry* 7:89. doi: 10.3389/fpsyt.2016.00089

Compta, Y., Valente, T., Saura, J., Segura, B., Iranzo, Á., Serradell, M., et al. (2015). Correlates of cerebrospinal fluid levels of oligomeric- and total-α-synuclein in premotor, motor and dementia stages of Parkinson's disease. *J. Neurol.* 262, 294–306. doi: 10.1007/s00415-014-7560-z

Eusebi, P., Giannandrea, D., Biscetti, L., Abraha, I., Chiasserini, D., Orso, M., et al. (2017). Diagnostic utility of cerebrospinal fluid α-synuclein in Parkinson's disease: a systematic review and meta-analysis. *Mov. Disord.* 32, 1389–1400. doi: 10.1002/mds.27110

Fan, Z., Aman, Y., Ahmed, I., Chetelat, G., Landeau, B., Chaudhuri, K. R., et al. (2015). Influence of microglial activation on neuronal function in Alzheimer's and Parkinson's disease dementia. *Alzheimers Dement.* 11, 608–621. doi: 10.1016/j.jalz.2014.06.016

Førland, M. G., Öhrfelt, A., Dalen, I., Tysnes, O.-B., and Blennow, K., Zetterberg, H., et al. (2018). Evolution of cerebrospinal fluid total α-synuclein in Parkinson's disease. *Parkinson. Relat. Disord.* 49, 4–8. doi: 10.1016/j.parkreldis.2018.01.018

Guo, J. L., Covell, D. J., Daniels, J. P., Iba, M., Stieber, A., Zhang, B., et al. (2013). Distinct α-synuclein strains differentially promote tau inclusions in neurons. *Cell* 154, 103–117. doi: 10.1016/j.cell.2013.05.057

Hall, S., Janelidze, S., Surova, Y., Widner, H., Zetterberg, H., and Hansson, O. (2018). Cerebrospinal fluid concentrations of inflammatory markers in Parkinson's disease and atypical parkinsonian disorders. *Sci. Rep.* 8:13276. doi: 10.1038/s41598-018-31517-z

Hall, S., Surova, Y., Öhrfelt, A., Blennow, K., Zetterberg, H., and Hansson, O. (2016). Longitudinal measurements of cerebrospinal fluid biomarkers in Parkinson's disease. *Mov. Disord.* 31, 898–905. doi: 10.1002/mds.26578

Hall, S., Surova, Y., Öhrfelt, A., Zetterberg, H., Lindqvist, D., and Hansson, O. (2015). CSF biomarkers and clinical progression of Parkinson disease. *Neurology* 84, 57–63. doi: 10.1212/WNL.0000000000001098

Hu, Y., Yu, S.-Y., Zuo, L.-J., Cao, C.-J., Wang, F., Chen, Z.-J., et al. (2015). Parkinson disease with REM sleep behavior disorder: features, α-synuclein, and inflammation. *Neurology* 84, 888–894. doi: 10.1212/WNL.0000000000001308

Kang, J. H., Irwin, D. J., Chen-Plotkin, A. S., Siderowf, A., Caspell, C., Coffey, C. S., et al. (2013). Association of cerebrospinal fluid β-amyloid 1-42, T-tau, P-tau181, and α-synuclein levels with clinical features of drug-naive patients with early Parkinson disease. *JAMA. Neurol.* 70, 1277–1287. doi: 10.1001/jamaneurol.2013.3861

Kehagia, A. A., Barker, R. A., and Robbins, T. W. (2010). Neuropsychological and clinical heterogeneity of cognitive impairment and dementia in patients with Parkinson's disease. *Lancet Neurol.* 9, 1200–1213. doi: 10.1016/S1474-4422(10)70212-X

Lewis, S. J. G., Dove, A., Robbins, T. W., Barker, R. A., and Owen, A. M. (2003). Cognitive impairments in early Parkinson's disease are accompanied by reductions in activity in frontostriatal neural circuitry. *J. Neurosci.* 23, 6351–6356. doi: 10.1523/JNEUROSCI.23-15-06351.2003

Lim, E. W., Aarsland, D., Ffytche, D., Taddei, R. N., van Wamelen, D. J., and Wan, W. M. (2019). Amyloid-β and Parkinson's disease. *J. Neurol.* 266, 2605–2619. doi: 10.1007/s00415-018-9100-8

Lleó, A., Cavedo, E., Parnetti, L., Vanderstichele, H., Herukka, S. K., Andreasen, N., et al. (2015). Cerebrospinal fluid biomarkers in trials for Alzheimer and Parkinson diseases. *Nat. Rev. Neurol.* 11, 41–55. doi: 10.1038/nrneurol.2014.232

Majbour, N. K., Vaikath, N. N., Eusebi, P., Chiasserini, D., Ardah, M., Varghese, S., et al. (2016). Longitudinal changes in CSF α-synuclein

species reflect Parkinson's disease progression. *Mov. Disord.* 31, 1535–1542. doi: 10.1002/mds.26754

Mogi, M., Harada, M., Narabayashi, H., Inagaki, H., Minami, M., and Nagatsu, T. (1996). Interleukin (IL)-1 beta, IL-2, IL-4, IL-6 and transforming growth factor-α levels are elevated in ventricular cerebrospinal fluid in juvenile parkinsonism and Parkinson's disease. *Neurosci. Lett.* 211, 13–16. doi: 10.1016/0304-3940(96)12706-3

Mollenhauer, B., Caspell-Garcia, C. J., Coffey, C. S., Taylor, P., Singleton, A., Shaw, L. M., et al. (2019). Longitudinal analyses of cerebrospinal fluid α-Synuclein in prodromal and early Parkinson's disease. *Mov. Disord.* 34, 1354–1364. doi: 10.1002/mds.27806

Murakami, H., Nohara, T., Shozawa, H., Owan, Y., Kuroda, T., Yano, S., et al. (2017). Effects of dopaminergic drug adjustment on executive function in different clinical stages of Parkinson's disease. *Neuropsychiatr. Dis. Treat.* 13, 2719–2726. doi: 10.2147/NDT.S145916

Murakami, H., Tokuda, T., El-Agnaf, O. M. A., Ohmichi, T., Miki, A., Ohashi, H., et al. (2019). Correlated levels of cerebrospinal fluid pathogenic proteins in drug-naïve Parkinson's disease. *BMC Neurol.* 19:113. doi: 10.1186/s12883-019-1346-y

Ono, K. (2017). The oligomer hypothesis in α-synucleinopathy. *Neurochem. Res.* 42, 3362–3371. doi: 10.1007/s11064-017-2382-x

Ono, K., Takahashi, R., Ikeda, T., and Yamada, M. (2012). Cross-seeding effects of amyloid β-protein and α-synuclein. *J. Neurochem.* 122, 883–890. doi: 10.1111/j.1471-4159.2012.07847.x

Park, M. J., Cheon, S.-M., Bae, H.-R., Kim, S.-H., and Kim, J. W. (2011). Elevated levels of α-synuclein oligomer in the cerebrospinal fluid of drug-naïve patients with Parkinson's disease. *J. Clin. Neurol.* 7, 215–222. doi: 10.3988/jcn.2011.7.4.215

Parnetti, L., Chiasserini, D., Bellomo, G., Giannandrea, D., Carlo, C. D., Qureshi, M. M., et al. (2011). Cerebrospinal fluid Tau/α-synuclein ratio in Parkinson's disease and degenerative dementias. *Mov. Disord.* 26, 1428–1435. doi: 10.1002/mds.23670

Parnetti, L., Farotti, L., Eusebi, P., Chiasserini, D., Carlo, C. D., Giannandrea, D., et al. (2014). Differential role of CSF α-synuclein species, tau, and Aβ42 in Parkinson's disease. *Front. Aging Neurosci.* 6:53. doi: 10.3389/fnagi.2014.00053

Ravina, B., Putt, M., Siderowf, A., Farrar, J. T., Gillespie, M., Crawley, A., et al. (2005). Donepezil for dementia in Parkinson's disease: a randomised, double blind, placebo controlled, crossover study. *J. Neurol. Neurosurg. Psychiatry* 76, 934–939. doi: 10.1136/jnnp.2004.050682

Sampedro, F., Marín-Lahoz, J., Martínez-Horta, S., Pagonabarraga, J., and Kulisevsky, J. (2018). Cortical thinning associated with age and CSF biomarkers in early Parkinson's disease is modified by the SNCA rs356181 polymorphism. *Neurodegener. Dis.* 18, 233–238. doi: 10.1159/000493103

Siepel, F. J., Brønnick, K. S., Booij, J., Ravina, B. M., Lebedev, A. V., Pereira, J. B., et al. (2014). Cognitive executive impairment and dopaminergic deficits in de novo Parkinson's disease. *Mov. Disord.* 29, 1802–1808. doi: 10.1002/mds.26051

Skogseth, R. E., Bronnick, K., Pereira, J. B., Mollenhauer, B., Weintraub, D., Fladby, T., et al. (2015). Associations between cerebrospinal fluid biomarkers and cognition in early untreated Parkinson's disease. *J. Parkinson. Dis.* 5, 783–792. doi: 10.3233/JPD-150682

Stav, A. L., Aarsland, D., Johansen, K. K., Hessen, E., Auning, E., and Fladby, T. (2015). Amyloid-β and α-synuclein cerebrospinal fluid biomarkers and cognition in early Parkinson's disease. *Parkinson. Relat. Disord.* 21, 758–764. doi: 10.1016/j.parkreldis.2015.04.027

Stewart, T., Liu, C., Ginghina, C., Cain, K. C., Auinger, P., Cholerton, B., et al. (2014). Cerebrospinal fluid α-synuclein predicts cognitive decline in Parkinson disease progression in the DATATOP cohort. *Am. J. Pathol.* 184, 966–975. doi: 10.1016/j.ajpath.2013.12.007

Surendranathan, A., Rowe, J. B., and O'Brien, J. T. (2015). Neuroinflammation in Lewy body dementia. *Parkinson. Relat. Disord.* 21, 1398–1406. doi: 10.1016/j.parkreldis.2015.10.009

Tsuang, D., Leverenz, J. B., Lopez, O. L., Hamilton, R. L., Bennett, D. A., Schneider, J. A., et al. (2013). APOE ε4 increases risk for dementia in pure synucleinopathies. *JAMA. Neurol.* 70, 223–228. doi: 10.1001/jamaneurol.2013.600

Wennström, M., Surova, Y., Hall, S., Nilsson, C., Minthon, L., Boström, F., et al. (2013). Low CSF levels of both α-synuclein and the α-synuclein cleaving enzyme neurosin in patients with synucleinopathy. *PLoS ONE* 8:e53250. doi: 10.1371/journal.pone.0053250

Wijeyekoon, R. S., Moore, S. F., Farrell, K., Breen, D. P., Barker, R. A., and Williams-Gray, C. H. (2020). Cerebrospinal fluid cytokines and neurodegeneration-associated proteins in Parkinson's disease. *Mov. Disord.* 35, 1062–1066. doi: 10.1002/mds.28015

Williams-Gray, C. H., Evans, J. R., Goris, A., Foltynie, T., Ban, M., Robbins, T. W., et al. (2009). The distinct cognitive syndromes of Parkinson's disease: 5 year follow-up of the CamPaIGN cohort. *Brain* 132, 2958–2969. doi: 10.1093/brain/awp245

Williams-Gray,. C. H., Foltynie, T., Brayne, C. E. G., Robbins, T. W., and Barker, R. A. (2007). Evolution of cognitive dysfunction in an incident Parkinson's disease cohort. *Brain* 130, 1787–1798. doi: 10.1093/brain/awm111

Yarnall, A. J., Breen, D. P., Duncan, G. W., Khoo, T. K., Coleman, S. Y., Firbank, M. J., et al. (2014). Characterizing mild cognitive impairment in incident Parkinson disease: the ICICLE-PD study. *Neurology* 82, 308–316. doi: 10.1212/WNL.0000000000000066

Zhou, B., Wen, M., Yu, W.-F., Zhang, C.-L., and Jiao, L. (2015). The diagnostic and differential diagnosis utility of cerebrospinal fluid α -Synuclein levels in Parkinson's disease: a meta-analysis. *Parkinson. Dis.* 2015:567386. doi: 10.1155/2015/567386

Conflict of Interest: The authors declare that the research was conducted in the absence of any commercial or financial relationships that could be construed as a potential conflict of interest.

Copyright © 2021 Murakami, Ono, Shiraishi, Umehara, Omoto and Iguchi. This is an open-access article distributed under the terms of the Creative Commons Attribution License (CC BY). The use, distribution or reproduction in other forums is permitted, provided the original author(s) and the copyright owner(s) are credited and that the original publication in this journal is cited, in accordance with accepted academic practice. No use, distribution or reproduction is permitted which does not comply with these terms.

frontiers in Aging Neuroscience

ORIGINAL RESEARCH
published: 22 January 2021
doi: 10.3389/fnagi.2020.624304

Mild Cognitive Impairment Patients Have Higher Regulatory T-Cell Proportions Compared With Alzheimer's Disease-Related Dementia Patients

Jiping Fu[1,2†], Jinhai Duan[1†], Jianwei Mo[1], Hao Xiao[1], Yuedong Huang[1], Weiping Chen[1], Shaotong Xiang[1], Fan Yang[1], Yongjun Chen[1] and Shuwen Xu[1]*

[1] Eastern Department of Neurology, Guangdong Geriatrics Institute, Guangdong Provincial People's Hospital, Guangdong Academy of Medical Sciences, Guangzhou, China, [2] Department of Neurology, First Affiliated Hospital of Shantou University Medical College, Shantou, China

Objectives: The role of neuroinflammation in the pathogenesis of Alzheimer's disease (AD) has attracted much attention recently. Regulatory T-cells (Tregs) play an important role in modulating inflammation. We aimed to explore the Treg-related immunosuppression status at different stages of AD.

Methods: Thirty healthy control (HC) subjects, 26 patients with mild cognitive impairment (MCI), 30 patients with mild probable AD-related dementia, and 28 patients with moderate-to-severe probable AD-related dementia underwent detailed clinical history taking, structural MRI scanning, and neuropsychological assessment. Peripheral blood samples were taken to measure the percentage of $CD4^+CD25^+CD127^{low/-}$ Tregs by flow cytometry and the levels of interleukin (IL-10), interleukin (IL-35), and transforming growth factor β (TGF-β) by ELISA.

Results: The percentage of Tregs in the blood of MCI patients was the highest (9.24%); there was a significant difference between patients with MCI and patients with probable AD-related dementia. The level of TGF-β in patients with MCI (47.02 ng/ml) was significantly increased compared with patients with AD-related dementia. There were positive correlations between Treg percentage, IL-35, and Mini-mental state evaluation scores in patients with MCI and probable AD-related dementia.

Conclusions: Patients with MCI have stronger Treg-related immunosuppression status compared with patients with probable AD-related dementia.

Keywords: Alzheimer's disease, neuroinflammation, regulatory T-cells, immunosuppression, cytokines

OPEN ACCESS

Edited by:
Pingyi Xu,
First Affiliated Hospital of Guangzhou Medical University, China

Reviewed by:
Carlo Riccardi,
University of Perugia, Italy
Caterina Motta,
Santa Lucia Foundation (IRCCS), Italy

***Correspondence:**
Shuwen Xu
xsw9133new@sina.com

[†] These authors have contributed equally to this work

Received: *31 October 2020*
Accepted: *21 December 2020*
Published: *22 January 2021*

Citation:
Fu J, Duan J, Mo J, Xiao H, Huang Y, Chen W, Xiang S, Yang F, Chen Y and Xu S (2021) Mild Cognitive Impairment Patients Have Higher Regulatory T-Cell Proportions Compared With Alzheimer's Disease-Related Dementia Patients. Front. Aging Neurosci. 12:624304. doi: 10.3389/fnagi.2020.624304

INTRODUCTION

Alzheimer's disease (AD), the most common cause of dementia in the elderly, is a global health concern with a huge burden for individuals and society. However, the pathogenesis of AD remains unknown. The failure of several drug clinical trials targeting beta amyloid (Aβ) in recent years has led to the question of the most widely known amyloid hypothesis (Panza et al., 2019). In addition to senile plaques and neurofibrillary tangles, chronic neuroinflammation is the third

major pathological feature of AD (Kinney et al., 2018), and inflammatory responses have been observed in AD autopsy studies (Gomez-Nicola and Boche, 2015; Knezevic and Mizrahi, 2018). One study showed that the number of naive T-cells in patients with AD were reduced, while the effector memory T-cells were increased (Larbi et al., 2009). The innate immune cells, such as natural killer cells and neutrophils, in patients with mild cognitive impairment (MCI) were upregulated compared with those of patients with mild AD-related dementia (Le Page et al., 2015). Recent studies have shown that the most important component of senile plaque-Aβ has antimicrobial properties (Moir et al., 2018), suggesting that patients with AD may be immune to unidentified substances derived from chronic viral, bacterial, or fungal infections. The immune changes associated with the development and progression of AD have already been the hotspot in the field of AD research.

Immune regulation is the key to maintaining a stable internal environment of the human body. The human body produces rapid and specific responses through the strict regulation of the immune system once a pathogen attacks. In the regressive phase, these responses need to be inhibited to prevent chronic inflammation and tissue damage. Immunoregulatory cells—regulatory T-cells (Tregs) [cell phenotype can be defined as $CD4^+CD25^+Foxp3^+$, Tregs hardly express CD127, so they can also be expressed by $CD4^+CD25^+CD127^{low/-}$ (Seddiki et al., 2006)], participate in this important regulatory mechanism through the secretion of anti-inflammatory cytokines, such as interleukin-10 (IL-10), interleukin-35 (IL-35), transforming growth factor beta (TGF-β), and cell-cell contact, to prevent the occurrence of chronic inflammation and autoimmunity (Campbell, 2015). In amyotrophic lateral sclerosis (ALS), Tregs have protective effects that can delay the disease progression, and early reduction of Foxp3 levels can be used to screen patients with rapid progression (Zhao et al., 2012; Henkel et al., 2013). The accumulation of Tregs in cancer patients, such as breast cancer and liver cancer, was associated with poor prognosis. In addition to immunomodulatory effects, Tregs play a role in maintaining homeostasis and repairing damage in non-lymphoid organs (Spitz et al., 2016; Ito et al., 2019).

There is an immune imbalance in patients with AD, and microglia and astrocytes release cytotoxic substances, such as pro-inflammatory cytokines and oxygen free radicals, to cause neuronal damage and death (Hardy and Selkoe, 2002). Exploring the inhibitory inflammatory response in patients with AD is of great significance for understanding the pathogenesis of AD. There are few reports on the role of Tregs in AD and the findings are inconsistent (Rosenkranz et al., 2007; Saresella et al., 2010; Le Page et al., 2017). One of the studies found that the suppressive activity of Tregs was increased in patients with AD (Rosenkranz et al., 2007), while the other two studies found that the frequencies of Tregs were increased in patients with MCI. In the AD-related dementia stage, Tregs were reduced instead (Saresella et al., 2010; Le Page et al., 2017). Two animal experiments have different conclusions about the role of Tregs in AD due to the different stages of the AD mice models (Baruch et al., 2015; Dansokho et al., 2016). IL-35 is a newly discovered pure immunosuppressive cytokine mainly produced by Tregs, which plays an important role in various autoimmune diseases (Su et al., 2018). However, the expression status of IL-35 in AD has yet to be elucidated clearly. Since inflammation in patients with AD is a chronic progressive process, the effects of Tregs in different stages may be different. The aim of this study was to measure the levels of Tregs and their related cytokines (IL10, IL35, and TGF-β) in the peripheral blood of patients with probable AD and to understand the Treg-related immunosuppression status at different stages of AD.

MATERIALS AND METHODS

Subjects

Patients with MCI and probable AD-related dementia were clinically diagnosed according to the 2011 National Institute on Aging-Alzheimer's Association (NIA-AA) workgroups on diagnostic guidelines for AD. The clinical dementia rating (CDR) scale was used to differentiate the severity of AD-related dementia (mild dementia: CDR = 1 point, moderate-to-severe dementia: CDR ≥ 2 points). Subjects who had a history of trauma, cerebrovascular disease, intracranial infection, mental disorder, and autoimmune disease were excluded. Each subject underwent clinical evaluation, neuropsychological assessment, laboratory examination, and head structural MRI. Mini-mental state evaluation (MMSE), Montreal cognitive assessment (MoCA), Hamilton anxiety scale (HAMA), Hamilton depression scale (HAMD), The Bayer Activities of Daily Living Scale (B-ADL), and Hachinski ischemia scale (HIS) were performed, except for patients with very severe AD-related dementia because they could not complete full scale assessment. The study enrolled 26 subjects with MCI, 30 patients with mild AD-related dementia, and 28 patients with moderate-to-severe AD from October 2017 to September 2018 in outpatient and inpatient departments of Guangdong Provincial People's Hospital. Another 30 healthy control (HC) subjects were selected as the control group. The research protocol was approved by Guangdong Provincial People's Hospital. All subjects or their guardians were informed of the content and the purpose of the study. All of them volunteered to participate in the study and signed written informed consent. Additional details of the clinical data of patients are summarized in **Table 1**.

Tregs Analysis by Flow Cytometry

Fluorochrome-labeled monoclonal antibodies mainly CD4-FITC, CD127-PE, and CD25-APC (eBioscience, San Diego, USA), which identified Tregs, were added to flow measuring tubes. Fifty microliters of whole blood samples treated with EDTA-K3 were added to the tube, mixed well, and incubated for 20 min at room temperature in the dark. Then, the samples were added with 2 ml RBC lysing buffer and mixed well to lyse RBC, incubated for 10 min at room temperature in the dark, and centrifuged, after which the supernatant was discarded. Later, they were washed with 2 ml phosphate buffered saline containing 0.5% bovine serum albumin and centrifuged at 1,000 rpm for 5 min, after which the supernatant was discarded. The cells were resuspended in 300 μl fixative solution and placed at 4°C in the dark. Data were acquired by flow cytometry; fixed cells

TABLE 1 | Patients' clinical data, percentage of Tregs, and related cytokine levels of four groups.

Parameters	HC ($n = 30$)	MCI ($n = 26$)	Mild AD ($n = 30$)	Mod&severe AD ($n = 28$)	X^2/F/H	*P*-value
Sex (M/F)	16/14	16/10	18/12	15/13	0.628	0.890
Age (years)	73.03 ± 9.21	75.19 ± 11.45	79.23 ± 10.54	79.39 ± 17.13	1.864	0.140
Education (years)	13.43 ± 3.79	12.85 ± 3.02	10.50 ± 5.19	11.21 ± 3.92	7.227	0.065
MMSE (score)	28.63 ± 1.35	25.46 ± 2.79	20.07 ± 3.36	11.54 ± 6.68	92.933	0.000
Tregs (%)	8.19 ± 1.97	9.24 ± 2.38	7.78 ± 1.26	7.42 ± 1.61	11.645	0.009
IL10 (pg/ml)	30.51 ± 17.06	32.89 ± 22.66	28.01 ± 12.31	32.38 ± 16.72	0.721	0.868
TGF-β (ng/ml)	37.92 ± 12.03	47.02 ± 16.28	38.31 ± 10.49	34.83 ± 7.87	9.885	0.020
IL35 (pg/ml)	21.17 ± 18.72	24.75 ± 26.33	19.95 ± 13.07	15.75 ± 12.12	1.386	0.709

HC, healthy control; MCI, mild cognitive impairment; AD, Alzheimer's disease; Mod&severe, moderate and severe; MMSE, Mini-mental state evaluation; Tregs, regulatory T-cells; IL-10, interleukin-10; TGF-β, transforming growth factor β; IL-35, interleukin-35.

were analyzed using CellQuest/Diva software within 24 h; and the percentage of $CD4^+CD25^+CD127^{lo/-}$ cells was obtained in $CD4^+$ lymphocytes.

IL-10, IL-35, and TGF-β Quantification

Sera were collected following the centrifugation of non-anticoagulated whole blood (1,000 $\times g$, 20 min). Samples were frozen at −80°C until the day of analysis. The concentrations of IL-10, IL-35, and TGF-β were determined by ELISA technology. All experimental procedures were carried out in accordance with the instructions of the ELIAS kit (IL-35: XpressBio, Frederick, MD, USA; IL-10 and TGF-β: 4A Biotech Co, Beijing, China). A standard curve was drawn based on the concentrations of the standard solution and their OD_{450} value. The concentrations of IL-10, IL-35, and TGF-β in the sample can be calculated from the standard curve according to their OD values.

Statistical Analysis

Data were processed using Statistical Package for the Social Sciences (SPSS) 25 software. For count data, the chi-square test was conducted. For normally distributed data, one-way ANOVA was conducted. A comparison involving non-normally distributed variables was conducted by the Kruskal–Wallis H test. For significant Kruskal–Wallis tests, pairwise comparisons were completed using the Mann–Whitney *U*-test with Bonferroni correction. The relationship between Tregs, IL-10, IL-35, TGF-β, and cognitive function was calculated by Spearman's correlation analysis after controlling for age. Only patients with MCI and AD were included in the correlation analyses.

RESULTS

The Percentage of Tregs and Concentrations of IL-10, IL-35, and TGF-β Comparison Among Four Groups

1) The percentage of Tregs in the blood of patients with MCI was the highest (9.24%), followed by HC subjects (8.19%), and the proportion of Tregs in patients with moderate-to-severe AD-related dementia was the lowest (7.42%). There was a significant difference in the percentage of Tregs between patients with MCI and patients with moderate-to-severe AD-related dementia (the value of p was 0.004; **Table 1** and **Figure 1**).
2) The level of TGF-β in patients with MCI (47.02 ng/ml) was the highest and significantly increased compared with patients with moderate-to-severe AD-related dementia (the value of p was 0.002), the group that had the lowest level of TGF-β (34.83 ng/ml; **Table 1** and **Figure 1**).
3) There were no significant differences in the levels of IL-10 and IL-35 among the four groups (**Table 1**).
4) The percentage of Tregs and the level of TGF-β in patients with MCI were significantly increased compared with patients with AD-related dementia, which were composed of patients with mild and moderate-to-severe AD-related dementia (for Tregs, the value of p was 0.002; for TGF-β, the value of p was 0.003).

Correlation Between Tregs, IL-10, IL-35, TGF-β, and Cognitive Function in Patients With MCI and AD-Related Dementia

There was a positive correlation between the percentage with Tregs and the scores of MMSE (the partial correlation coefficient was 0.445, the value of p was < 0.001). A mild, positive significant correlation was found between MMSE scores and TGF-β (the partial correlation coefficient was 0.292, the value of p was 0.007), MMSE scores, and IL-35 (the partial correlation coefficient was 0.285, the value of p was 0.009). There was no correlation between IL-10 and MMSE scores (**Figure 2**).

DISCUSSION AND CONCLUSION

The immune system plays a key role in the pathogenesis of AD. Autopsy found that activated microglia clustered around amyloid plaques (Calsolaro and Edison, 2016). Many AD-risk genes, including CR1, CD33, and TREM2, are related to the immune system (Jones et al., 2010; Hollingworth et al., 2011). Clinical studies using PET ligands that bind to activated microglia provide further *in vivo* evidence for understanding the role of neuroinflammation in patients with AD (Hamelin et al., 2016). Whether or when neuroinflammation is protective, harmful, or

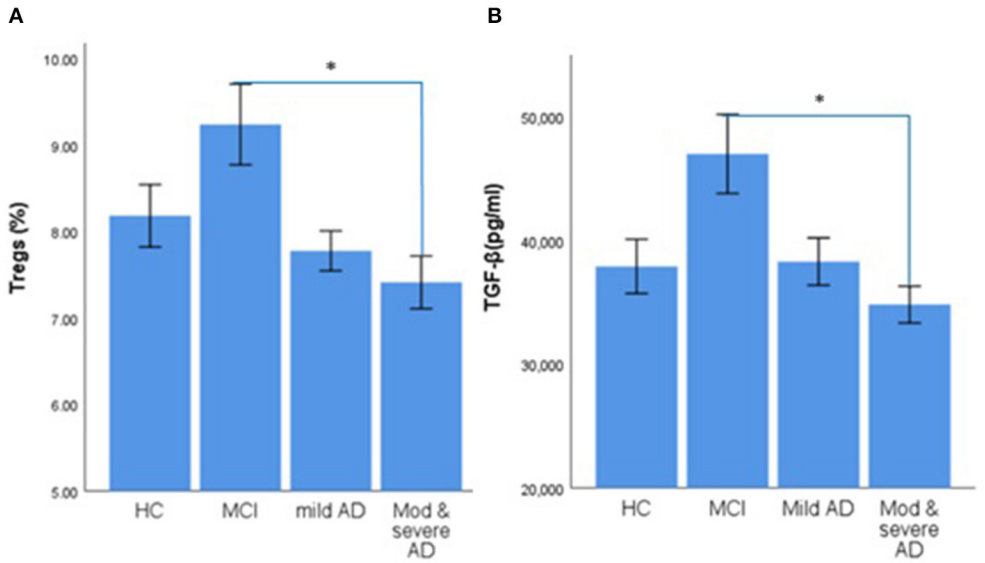


FIGURE 1 | Error bar charts show the difference in mean ± standard error of the mean (SEM) values of regulatory T cells (Tregs) and transforming growth factor β (TGF-β) in peripheral blood of healthy control (HC), mild cognitive impairment (MCI), mild Alzheimer's Disease (AD) dementia, and moderate-to-severe AD dementia subjects. **(A)** Percentage of $CD^{4+}CD^{25+}CDl27^{low/-}$ Tregs. **(B)** The Concentration of TGF-β. The asterisks (*) means $p < 0.0083$.

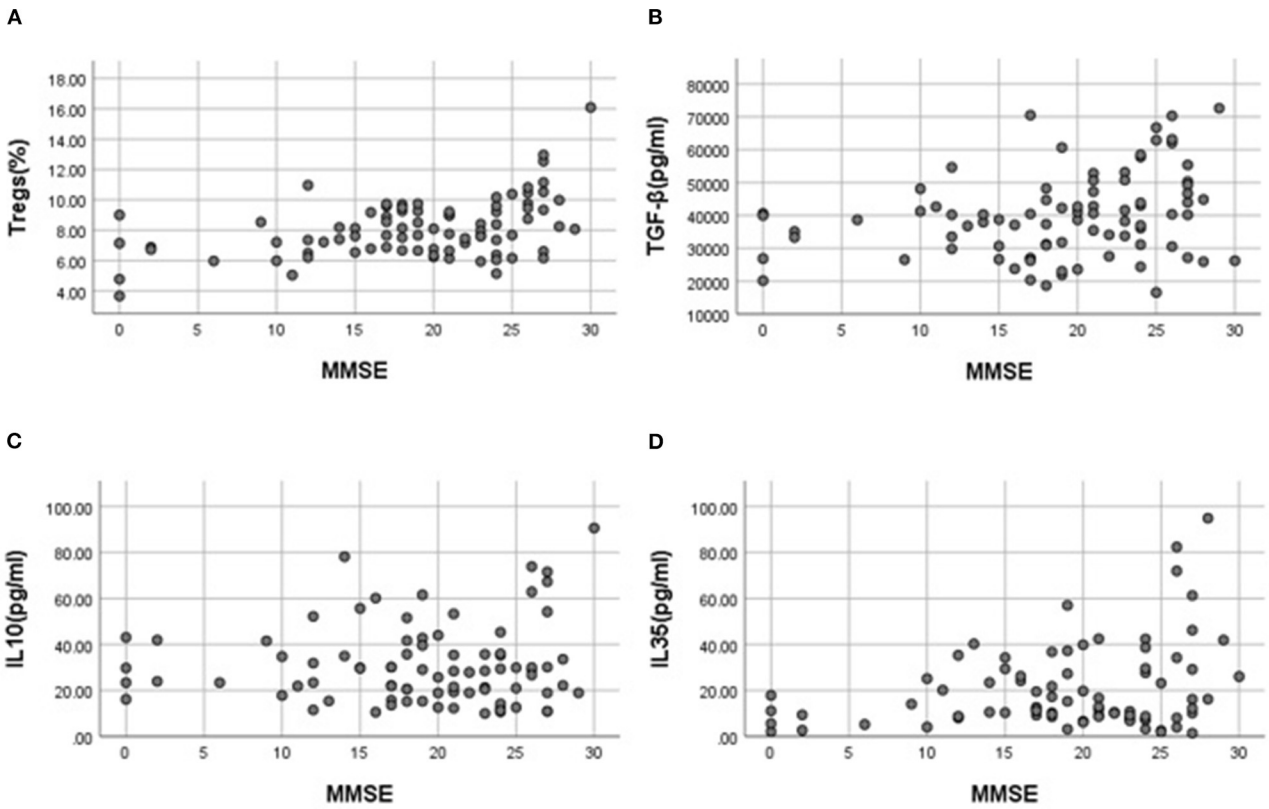


FIGURE 2 | Scatter plots show correlation between regulatory T cells (Tregs), transforming growth factor β (TGF-β), interleukin 10 (IL10), interleukin 35 (IL35), and cognitive function after controlling for age in MCI and AD dementia patients. **(A)** Correlation between percentage of $CD^{4+}CD^{25+}CDl27^{low/-}$ Tregs and Mini-mental state evaluation (MMSE) scores (the partial correlation coefficient was 0.445, *P-value* was 0.001). **(B)** Correlation between concentration of TGF-β and MMSE scores ($P > 0.05$). **(C)** Correlation between concentration of IL10 and MMSE scores ($P > 0.05$). **(D)** Correlation between concentration of IL35 and MMSE scores (the partial correlation coefficient was 0.285, *P-value* was 0.009).

both may depend on the stage of the disease and the genetic subtype. The lymphoid system in the brain can drain the central nervous system (CNS)-derived antigen and produce acquired immunity against CNS. The CNS-derived antigen is mainly drained through adjacent structures such as choroid plexus (CP), pia mater space, and deep cervical lymph nodes. Dendritic cells, T cells infiltrate into the brain through the same pathway (Korn and Kallies, 2017).

Our study found that patients with MCI had the highest proportion of Tregs, followed by HC subjects, and patients with moderate-to-severe probable AD-related dementia had the lowest proportion of Tregs. Among the inhibitory cytokines secreted by Tregs, patients with MCI had the highest level of TGF-β, which was statistically significant compared with patients with AD-related dementia. The data above indicated that patients with MCI had enhanced the immunosuppressive function, which was consistent with two other studies (Saresella et al., 2010; Le Page et al., 2017). Saresella et al. (2010) found that the subpopulation of Tregs with the most powerful suppressive ability, $PD1^{-}CD4^{+}CD25^{+}Foxp3^{+}$ Tregs, was significantly increased in patients with MCI, and Treg-mediated immunosuppression was stronger compared to that of HC and patients with AD-related dementia. Other studies reported that the early stage of patients with AD had an enhanced pro-inflammatory response (Heneka et al., 2015; Yasuno et al., 2017; Oberstein et al., 2018). Patients with MCI had an increased proportion of Th17 (Oberstein et al., 2018). The proportion of peripheral cytotoxic T-cells had increased even in the preclinical stage of AD with no cognitive changes but with only the deposition of Aβ (Yasuno et al., 2017). Combined with the similar study published in 2017 (Le Page et al., 2017), we could speculate that the proportion of Tregs and TGF-β levels in patients with MCI may be a compensatory increase to reduce the excessive immune response. In AD-related dementia stage, especially in moderate-to-severe AD-related dementia stage, the compensatory mechanism disappears, the protective effect of Tregs and TGF-β disappears. Larbi et al. (2009) found that the distribution of $CD4^{+}CD25^{+}$Tregs gradually shifted to memory subpopulation with age, and the proportion of all Treg subgroups in patients with AD-related dementia decreased compared with healthy elderly patients. Recently, a study also found that the percentage of total Tregs and resting Tregs significantly decreased in the middle stage of patients with AD, as compared to HC subjects, suggesting an impairment of the immune reserve in patients with AD-related dementia (Ciccocioppo et al., 2019). The adaptive immune system of patients with AD-related dementia was affected by continuous antigenic stimulation, which may result in premature immunosenescence. In our study, the proportion of Tregs, as well as Treg-related cytokines, IL-35, and TGF-β, positively correlated with the MMSE score. The worse the cognitive function, the lower was the proportion of Tregs and Treg-related cytokines. The premature immunosenescence may explain why the proportion of Tregs in patients with moderate-to-severe AD-related dementia decreased in the study.

The above studies indicated that Tregs might be involved in the pathogenesis of AD, but it is not clear through which mechanism Tregs can affect the pathological process of AD. Baruch et al. (2015) found that the transient depletion of Tregs increased the production of IFN-γ at the CP in 5XFAD mice and upregulated the expression of leukocyte trafficking molecules such as ICAM-1, CXCL10, and CCL2 by the CP, followed by an increased accumulation of mononuclear-macrophages at cerebral site of plaque formation. Cerebral Aβ plaque burden in the brain was reduced and cognitive decline was reversed. On the contrary, an increased number of peripheral Tregs in 5XFAD mice was associated with higher burden of cerebral Aβ plaque and worse cognitive function.

However, some animal studies drew the opposite conclusion. Dansokho et al. (2016) found that transient clearance of Tregs significantly reduced the aggregation of activated microglia to Aβ and accelerated the cognitive impairment of mice but did not change the deposition of Aβ, while the expansion of Tregs increased the number of plaque-associated microglial cells and improved the cognitive function. Further analysis suggested that Tregs may contribute to promote a type I IFN-dependent beneficial activation profile of microglial in response to amyloid deposition (Dansokho et al., 2016).

The role of Tregs in AD animal models is inconsistent across different studies, probably due to the modulation of Tregs in AD mice models at different disease stages. Baruch et al. (2015) interfered peripheral Tregs in 5XFAD mice at 4–5 months old after significant pathological changes, such as the deposition of Aβ and gliosis, have developed, whereas Dansokho et al. (2016) modulated Tregs in APPPS1 mice at 5–6 weeks of age when the deposition of Aβ and gliosis has just emerged. At early disease stages, Tregs may promote type I IFN-dependent beneficial activation profile in microglia. At later disease stages, the accumulation of brain-derived signals associated with disease progression may lead to different responsiveness of CP to Tregs, resulting in Treg-mediated alteration of CP and impaired recruitment of inflammation-resolving leukocytes to CNS. It is still necessary to do more studies to explore the changes of Tregs in different stages of AD and how the changes affect the course of AD.

There were several limitations in this study: (1) The authors did not follow-up the changes of cognition and the frequency of Tregs and its related cytokines in enrolled subjects. The relationship between Tregs and the progression of the disease could not be clarified. (2) The sample sizes were small and the statistical power of the study was low. (3) The subjects did not get a spinal tap, so the number of Tregs in cerebrospinal fluid (CSF) could not be detected, and the immune suppression status of patients with AD could not be accurately reflected. (4) We did not include any CSF biomarkers or PET imaging that some patients with MCI or dementia with other etiologies may be enrolled in; this could lead to confounding result. A study published in 2018 detected the Aβ and tau protein in patients with MCI, and found that there was no difference between HC and MCI due to AD (Oberstein et al., 2018). Therefore, it is necessary to expand the sample sizes to further explore the changes in the number and function of Tregs in the peripheral blood and CSF of patients with AD.

DATA AVAILABILITY STATEMENT

The raw data supporting the conclusions of this article will be made available by the authors, without undue reservation.

ETHICS STATEMENT

The studies involving human participants were reviewed and approved by Guangdong Provincial People's Hospital. The patients/participants provided their written informed consent to participate in this study. Written informed consent was obtained from the individual(s) for the publication of any potentially identifiable images or data included in this article.

AUTHOR CONTRIBUTIONS

SXu and JD: designed and conceptualized the study. JF: analyzed the data and drafted the manuscript for the intellectual content. JM, HX, YH, and WC: a major role in the acquisition of clinical data and implementation of neuropsychological scale assessment. FY, SXi, and YC: detected the level of Tregs, IL-10, IL-35, and TGF-β in the peripheral blood. All authors contributed to the article and approved the submitted version.

FUNDING

This work was supported by Natural Science of Foundation of Guangdong Province, China (Nos. 7300973 and S2012010009108), the Science and Technology Plan Foundation of Guangdong Province (No. 2020A1414040027), and the Science and Technology Plan Foundation of Guangzhou (No. 201904010066).

ACKNOWLEDGMENTS

We gratefully acknowledge Dr. Maohua Zhou and staff of Guangdong Provincial People's Hospital Laboratory for their help in guiding Tregs and its related cytokines testing.

REFERENCES

Baruch, K., Rosenzweig, N., Kertser, A., Deczkowska, A., Sharif, A. M., Spinrad, A., et al. (2015). Breaking immune tolerance by targeting Foxp3(+) regulatory T cells mitigates Alzheimer's disease pathology. *Nat. Commun.* 6:7967. doi: 10.1038/ncomms8967

Calsolaro, V., and Edison, P. (2016). Neuroinflammation in Alzheimer's disease: current evidence and future directions. *Alzheimer's Dement.* 12, 719–732. doi: 10.1016/j.jalz.2016.02.010

Campbell, D. J. (2015). Control of regulatory T cell migration, function, and homeostasis. *J. Immunol.* 195, 2507–2513. doi: 10.4049/jimmunol.1500801

Ciccocioppo, F., Lanuti, P., Pierdomenico, L., Simeone, P., Bologna, G., Ercolino, E., et al. (2019). The characterization of regulatory T-cell profiles in Alzheimer's disease and multiple sclerosis. *Sci. Rep.* 9:8788. doi: 10.1038/s41598-019-45433-3

Dansokho, C., Ait Ahmed, D., Aid, S., Toly-Ndour, C., Chaigneau, T., Calle, V., et al. (2016). Regulatory T cells delay disease progression in Alzheimer-like pathology. *Brain* 139(Pt 4), 1237–1251. doi: 10.1093/brain/awv408

Gomez-Nicola, D., and Boche, D. (2015). Post-mortem analysis of neuroinflammatory changes in human Alzheimer's disease. *Alzheimer's Res. Ther.* 7:42. doi: 10.1186/s13195-015-0126-1

Hamelin, L., Lagarde, J., Dorothee, G., Leroy, C., Labit, M., Comley, R. A., et al. (2016). Early and protective microglial activation in Alzheimer's disease: a prospective study using 18F-DPA-714 PET imaging. *Brain* 139(Pt 4), 1252–1264. doi: 10.1093/brain/aww017

Hardy, J., and Selkoe, D. J. (2002). The amyloid hypothesis of Alzheimer's disease: progress and problems on the road to therapeutics. *Science* 297, 353–356. doi: 10.1126/science.1072994

Heneka, M. T., Golenbock, D. T., and Latz, E. (2015). Innate immunity in Alzheimer's disease. *Nat. Immunol.* 16, 229–236. doi: 10.1038/ni.3102

Henkel, J. S., Beers, D. R., Wen, S., Rivera, A. L., Toennis, K. M., Appel, J. E., et al. (2013). Regulatory T-lymphocytes mediate amyotrophic lateral sclerosis progression and survival. *EMBO Mol. Med.* 5, 64–79. doi: 10.1002/emmm.201201544

Hollingworth, P., Harold, D., Sims, R., Gerrish, A., Lambert, J. C., Carrasquillo, M. M., et al. (2011). Common variants at ABCA7, MS4A6A/MS4A4E, EPHA1, CD33 and CD2AP are associated with Alzheimer's disease. *Nat. Genet.* 43, 429–435. doi: 10.1038/ng.803

Ito, M., Komai, K., Mise-Omata, S., Iizuka-Koga, M., Noguchi, Y., Kondo, T., et al. (2019). Brain regulatory T cells suppress astrogliosis and potentiate neurological recovery. *Nature* 565, 246–250. doi: 10.1038/s41586-018-0824-5

Jones, L., Holmans, P. A., Hamshere, M. L., Harold, D., Moskvina, V., Ivanov, D., et al. (2010). Genetic evidence implicates the immune system and cholesterol metabolism in the aetiology of Alzheimer's disease. *PLoS ONE.* 5:e13950. doi: 10.1371/journal.pone.0013950

Kinney, J. W., Bemiller, S. M., Murtishaw, A. S., Leisgang, A. M., Salazar, A. M., and Lamb, B. T. (2018). Inflammation as a central mechanism in Alzheimer's disease. *Alzheimer's Dement.* 4, 575–590. doi: 10.1016/j.trci.2018.06.014

Knezevic, D., and Mizrahi, R. (2018). Molecular imaging of neuroinflammation in Alzheimer's disease and mild cognitive impairment. *Prog. Neuropsychopharmacol. Biol. Psychiatry.* 80(Pt B), 123–131. doi: 10.1016/j.pnpbp.2017.05.007

Korn, T., and Kallies, A. (2017). T cell responses in the central nervous system. *Nat. Rev. Immunol.* 17, 179–194. doi: 10.1038/nri.2016.144

Larbi, A., Pawelec, G., Witkowski, J. M., Schipper, H. M., Derhovanessian, E., Goldeck, D., et al. (2009). Dramatic shifts in circulating CD4 but not CD8 T cell subsets in mild Alzheimer's disease. *J. Alzheimer's Dis.* 17, 91–103. doi: 10.3233/JAD-2009-1015

Le Page, A., Bourgade, K., Lamoureux, J., Frost, E., Pawelec, G., Larbi, A., et al. (2015). NK cells are activated in amnestic mild cognitive impairment but not in mild Alzheimer's disease patients. *J. Alzheimer's Dis.* 46, 93–107. doi: 10.3233/JAD-143054

Le Page, A., Garneau, H., Dupuis, G., Frost, E. H., Larbi, A., Witkowski, J. M., et al. (2017). Differential phenotypes of myeloid-derived suppressor and t regulatory cells and cytokine levels in amnestic mild cognitive impairment subjects compared to mild alzheimer diseased patients. *Front. Immunol.* 8:783. doi: 10.3389/fimmu.2017.00783

Moir, R. D., Lathe, R., and Tanzi, R. E. (2018). The antimicrobial protection hypothesis of Alzheimer's disease. *Alzheimer's Dement.* 14, 1602–1614. doi: 10.1016/j.jalz.2018.06.3040

Oberstein, T. J., Taha, L., Spitzer, P., Hellstern, J., Herrmann, M., Kornhuber, J., et al. (2018). Imbalance of circulating Th17 and regulatory T cells in Alzheimer's disease: a case control study. *Front. Immunol.* 9:1213. doi: 10.3389/fimmu.2018.01213

Panza, F., Lozupone, M., Seripa, D., and Imbimbo, B. P. (2019). Amyloid-beta immunotherapy for alzheimer disease: is it now a long shot? *Ann. Neurol.* 85, 303–315. doi: 10.1002/ana.25410

Rosenkranz, D., Weyer, S., Tolosa, E., Gaenslen, A., Berg, D., Leyhe, T., et al. (2007). Higher frequency of regulatory T cells in the elderly and increased suppressive activity in neurodegeneration. *J. Neuroimmunol.* 188, 117–127. doi: 10.1016/j.jneuroim.2007.05.011

Saresella, M., Calabrese, E., Marventano, I., Piancone, F., Gatti, A., Calvo, M. G., et al. (2010). PD1 negative and PD1 positive CD4+ T regulatory cells in mild

cognitive impairment and Alzheimer's disease. *J. Alzheimer's Dis.* 21, 927–938. doi: 10.3233/JAD-2010-091696

Seddiki, N., Santner-Nanan, B., Martinson, J., Zaunders, J., Sasson, S., Landay, A., et al. (2006). Expression of interleukin (IL)-2 and IL-7 receptors discriminates between human regulatory and activated T cells. *J. Exp. Med.* 203, 1693–1700. doi: 10.1084/jem.20060468

Spitz, C., Winkels, H., Burger, C., Weber, C., Lutgens, E., Hansson, G. K., et al. (2016). Regulatory T cells in atherosclerosis: critical immune regulatory function and therapeutic potential. *Cell. Mol. Life Sci.* 73, 901–922. doi: 10.1007/s00018-015-2080-2

Su, L. C., Liu, X. Y., Huang, A. F., and Xu, W. D. (2018). Emerging role of IL-35 in inflammatory autoimmune diseases. *Autoimmun. Rev.* 17, 665–673. doi: 10.1016/j.autrev.2018.01.017

Yasuno, F., Kazui, H., Kajimoto, K., Ihara, M., Morita, N., Taguchi, A., et al. (2017). Mutual effect of cerebral amyloid beta and peripheral lymphocytes in cognitively normal older individuals. *Int. J. Geriatr. Psychiatry.* 32, e93–e99. doi: 10.1002/gps.4660

Zhao, W., Beers, D. R., Liao, B., Henkel, J. S., and Appel, S. H. (2012). Regulatory T lymphocytes from ALS mice suppress microglia and effector T lymphocytes through different cytokine-mediated mechanisms. *Neurobiol. Dis.* 48, 418–428. doi: 10.1016/j.nbd.2012.07.008

Conflict of Interest: The authors declare that the research was conducted in the absence of any commercial or financial relationships that could be construed as a potential conflict of interest.

Copyright © 2021 Fu, Duan, Mo, Xiao, Huang, Chen, Xiang, Yang, Chen and Xu. This is an open-access article distributed under the terms of the Creative Commons Attribution License (CC BY). The use, distribution or reproduction in other forums is permitted, provided the original author(s) and the copyright owner(s) are credited and that the original publication in this journal is cited, in accordance with accepted academic practice. No use, distribution or reproduction is permitted which does not comply with these terms.

frontiers in Aging Neuroscience

ORIGINAL RESEARCH
published: 12 February 2021
doi: 10.3389/fnagi.2021.621508

Increased Plasma Heme Oxygenase-1 Levels in Patients With Early-Stage Parkinson's Disease

Wenhua Sun[1,2], Jinhua Zheng[1,2,3], Jianjun Ma[1,2,3]*, Zhidong Wang[1,2], Xiaoxue Shi[1,2], Mingjian Li[2,3], Shen Huang[1,2], Shiyu Hu[2,3], Zhenxiang Zhao[1,2,3] and Dongsheng Li[1,2,3]*

[1]*Department of Neurology, People's Hospital of Zhengzhou University, Zhengzhou, China,* [2]*Department of Neurology, Henan Provincial People's Hospital, Zhengzhou, China,* [3]*Department of Neurology, People's Hospital of Henan University, Zhengzhou, China*

Introduction: Heme oxygenase-1 (HO-1) is a 32 kDa stress-response protein implicated in the pathogenesis of Parkinson's disease (PD). Biliverdin is derived from heme through a reaction mediated by HO-1 and protects cells from oxidative stress. However, iron and carbon monoxide produced by the catabolism of HO-1 exert detrimental effects on patients with PD. The purpose of this study was to determine whether plasma HO-1 levels represent a biomarker of PD and to further explore the underlying mechanism of increased HO-1 levels by applying voxel-based morphometry (VBM).

Methods: We measured plasma HO-1 levels using an enzyme-linked immunosorbent assay (ELISA) in 156 subjects, including 81 patients with early- and advanced-stage PD and 75 subjects without PD. The analyses were adjusted to control for confounders such as age, sex, and medication. We analyzed T1-weighted magnetic resonance imaging (MRI) data from 74 patients with PD using VBM to elucidate the association between altered brain volumes and HO-1 levels. Then, we compared performance on MMSE sub-items between PD patients with low and high levels of HO-1 using Mann–Whitney *U* tests.

Results: Plasma HO-1 levels were significantly elevated in PD patients, predominantly those with early-stage PD, compared with controls ($p < 0.05$). The optimal cutoff value for patients with early PD was 2.245 ng/ml HO-1 [area under the curve (AUC) = 0.654]. Plasma HO-1 levels were unaffected by sex, age, and medications ($p > 0.05$). The right hippocampal volume was decreased in the subset of PD patients with high HO-1 levels ($p < 0.05$). A weak correlation was observed between right hippocampal volume and plasma HO-1 levels ($r = -0.273$, $p = 0.018$). There was no difference in total MMSE scores between the low- and high-HO-1 groups ($p > 0.05$), but the high-HO-1 group had higher language scores than the low-HO-1 group ($p < 0.05$).

Conclusions: Plasma HO-1 levels may be a promising biomarker of early PD. Moreover, a high plasma concentration of the HO-1 protein is associated with a reduction in right hippocampal volume.

Keywords: biomarker, heme oxygenase-1, Parkinson's disease, plasma, voxel-based morphometry

OPEN ACCESS

Edited by:
Shaomin Li,
Brigham and Women's Hospital and Harvard Medical School, United States

Reviewed by:
Marisa Cressatti,
Jewish General Hospital, Canada
Jong-Min Kim,
Seoul National University Bundang Hospital, South Korea

****Correspondence:***
Jianjun Ma
majj1124@163.com
Jinhua Zheng
731763795@qq.com

Received: *26 October 2020*
Accepted: *22 January 2021*
Published: *12 February 2021*

Citation:
Sun W, Zheng J, Ma J, Wang Z, Shi X, Li M, Huang S, Hu S, Zhao Z and Li D (2021) Increased Plasma Heme Oxygenase-1 Levels in Patients With Early-Stage Parkinson's Disease. Front. Aging Neurosci. 13:621508. doi: 10.3389/fnagi.2021.621508

INTRODUCTION

Parkinson's disease (PD) is a movement disorder characterized by the loss of dopaminergic neurons in the substantia nigra and the formation of Lewy bodies induced by the aggregation of α-synuclein. Although pharmacological dopamine substitution (L-DOPA treatment) or deep brain stimulation (DBS) have been used to control the symptoms of PD and improve the quality of life up to decades after the onset of disease, these treatments are not very effective at preventing PD progression. Therefore, PD is a neurodegenerative disease that may ultimately lead to severe disability as it progresses (Poewe et al., 2017).

To date, the diagnosis of PD has been based on clinical criteria (Hughes et al., 1992). However, more than half of dopaminergic neurons are typically lost before a patient is diagnosed with PD. The long preclinical phase of PD offers the potential to administer disease-modifying treatments; therefore, an easily accessible biomarker that reflects the process of neurodegeneration is needed to diagnose the disease and predict disease progression in individual patients. Thus, a reliable biomarker would have great potential to help distinguish patients with PD from healthy persons, particularly in the early stages of the disease.

Heme oxygenase-1 (HO-1) is a 32 kDa cellular stress protein of the superfamily that metabolizes heme into biliverdin, iron, and carbon monoxide in cooperation with NADPH cytochrome P450 reductase in the brain and other tissues exposed to oxidative stress. This enzyme is primarily located and functions in the endoplasmic reticulum. Biliverdin is then further oxidized to bilirubin by biliverdin reductase, which helps restore a more favorable tissue redox microenvironment (Maines, 1988; Keyse and Tyrrell, 1989). The neuroprotective effect of HO-1 has been well studied in PD. For example, failure of proteasome degradation results in the formation of misfolded proteins, which is an important mechanism of α-synuclein accumulation in PD. Meanwhile, overexpression of HO-1 has been shown to facilitate α-synuclein proteasomal degradation in M17 neuroma cells (Song et al., 2009). Heme-derived CO in glial cells plays an important role in the dopaminergic neuroprotective effect of 2′, 3′-dihydroxy-4′,6′-dimethoxychalcone (DDC) through cell-to-cell communication (Masaki et al., 2017). Simvastatin prevents oxidative stress by enhancing the expression of the antioxidant protein HO-1 in a 6-OHDA-induced PD model (Tong et al., 2018). On the other hand, the following results indicate that overactivation of HO-1 in neurons may be deleterious in PD. Overexpression of HO-1 has been demonstrated in astrocytes in postmortem PD samples (Schipper, 2004). Moreover, excessive upregulation of HO-1 promotes the accumulation of non-transferrin-bound iron deposits, mitochondrial dysfunction, macrophages, and oxidative stress (Schipper, 1999; Song et al., 2006; Zukor et al., 2009). Previous studies have reported that selective overexpression of HO-1 in astrocytes in GFAP.HMOX1 transgenic mice from 8.5 to 19 months of age lead to the behavioral, neuropathologic, and molecular biological characteristics of parkinsonism (Song et al., 2017). Based on these findings, HO-1 may be a double-edged sword, and some clinical studies have investigated this hypothesis. Significantly higher serum (Mateo et al., 2010) and salivary HO-1 levels (Song et al., 2018) have been reported in patients with PD than in normal controls, prompting the hypothesis that HO-1 levels in biological fluids represent a promising marker of PD and may be used to assess the extent of neurodegeneration.

Voxel-based morphometry (VBM) is a widely used automated neuroanatomical image analysis technique that compares the local concentrations or volumes of gray and white matter in voxels (Yousaf et al., 2018). In the past decade, VBM has been widely used in neurological research, including studies of PD (van Mierlo et al., 2015; Goto et al., 2018; Xuan et al., 2019; Wolters et al., 2020). Here, we chose to investigate potential differences in the voxels of brain regions between patients with high and low plasma HO-1 levels (using the mean value as the dividing point) by applying this structural imaging technique at an anatomical level to explore the mechanism of the differences in HO-1 levels in PD patients.

In the present study, we sought to determine by ELISA whether plasma-derived HO-1 protein concentrations are elevated in patients with idiopathic PD and to explore structural neuroimaging to elucidate the mechanism underlying the variability of HO-1 levels in the blood of these patients.

MATERIALS AND METHODS

Participants

All participants were recruited from the Henan Provincial People's Hospital. This study included 156 participants: 81 patients with PD and 75 healthy controls. After initial inclusion, seven subjects with PD and incomplete relevant imaging data were excluded. The final sample for structural MRI analyses consisted of 74 patients with PD. The inclusion criteria were as follows: (1) a diagnosis of PD was made by an experienced neurologist; and (2) PD was diagnosed according to the United Kingdom Brain Bank Clinical Diagnostic Criteria (Hughes et al., 1992). Patients with secondary parkinsonism or atypical parkinsonian syndromes (including multiple system atrophy, progressive supranuclear palsy, dementia with Lewy bodies, and cortical–basal ganglionic degeneration) and individuals with the systemic inflammatory disease were excluded from the study.

The patients with idiopathic PD were in the "on" period when they were evaluated using different scales. The severity of motor symptoms was evaluated using the Hoehn & Yahr stages (H & Y stages) and United Parkinson's disease (PD) Rating Scale-III (UPDRSIII; Goetz et al., 2008). Cognition was assessed with the Mini-Mental State Examination (MMSE). The MMSE was divided into eight subitems: (1) orientation to time and place (10 points); (2) immediate registration (three points); (3) divided attention (five points); (4) delayed recall (three points); (5) language (four points); (6) following a three-step command (three points); (7) writing a sentence (one point); and (8) copying a figure (one point; Ringman et al., 2007). The patients were on PD medication, including carbidopa/levodopa and dopamine agonists, to relieve their symptoms; however, exposure to these medications can influence plasma HO-1 concentrations and thereby act as a confounding

factor. Also, there are more than a dozen anti-PD medications, and patients with PD usually take two or more medications. We consulted the drug treatment history of the PD patients and used a previously reported formula to calculate the equivalent daily doses of L-DOPA (LEDD; Tomlinson et al., 2010).

Meanwhile, 75 sex-matched subjects without PD were recruited from the Outpatient Physical Examination Department of Henan Provincial People's Hospital. The inclusion criteria for control subjects were as follows: (1) no history of neurological disease or psychiatric disorders; (2) no brain injury; and (3) no diabetes mellitus, hypertension, cardiovascular disease, or systemic diseases (inflammation, infection, cancer, et cetera). The inclusion and exclusion criteria were strictly enforced to minimize the potential for confounders.

We divided patients with PD into those in the early stages (H&Y stage I and H&Y stage II) and those in the advanced stages (H&Y stage III and H&Y stage IV) to investigate the relationship between plasma HO-1 levels and disease progression. This study was approved by the ethics committee of Henan Provincial People's Hospital. All study participants and their guardians provided written informed consent. The methodology used in this study was implemented according to recognized guidelines.

Blood Sampling and Analysis of Plasma HO-1 Levels

Early in the morning (7:00 am) after an overnight fast, a 5-ml blood sample was collected from each participant into a tube containing the anticoagulant EDTA. The blood samples were centrifuged (2,500 *g* for 15 min) at 25°C within 1 h of collection. The supernatant was collected, divided into 1.5 ml centrifuge tubes, and stored at −80°C until analysis. Plasma HO-1 levels in subjects with and without PD were measured using a human HO-1 sandwich ELISA kit (Catalog Number: ADI-EKS-800; Enzo Life Sciences Inc., Farmingdale, NY, USA) according to the manufacturer's protocol. A standard curve generated with purified HO-1 was used to calculate the HO-1 concentration of each sample from the absorbance at λ = 450 nm (Li Volti et al., 2010). The sensitivity of the HO-1 (human) ELISA kit was determined to be 0.78 ng/ml. The standard curve had a range of 0.78–25 ng/ml. The intra-assay coefficient of variation of the HO-1 (human) ELISA kit was determined to be <10%. All samples were analyzed in duplicate and processed in the first freeze-thaw cycle.

Neuroimaging Data Acquisition and Preprocessing

All MRI scans were acquired using a Siemens MAGNETOM Prisma 3 T MRI scanner with a 64-channel head coil. Structural images were obtained using a 3D MRI magnetization-prepared rapid gradient-echo (MPRAGE) T1-weighted sequence [matrix = 256 × 256; flip angle = 4°; field of view (FOV) = 256 × 256 mm; slice thickness = 1 mm; TR = 5,000 ms; echo time (TE) = 3.43 ms; voxel size = 1 × 1 × 1 mm].

The quality of the acquired MRI scans was visually assessed to exclude scans with severe vascular lesions, space-occupying lesions, or motion artifacts. VBM was performed with SPM8[1] running on MATLAB 2013b. T1 image preprocessing was implemented using VBM8[2] as follows (Chard et al., 2002): (1) format conversion: the DICOM images were converted to a parsable NIFTI format; (2) normalization: after image registration, all anatomical images were registered to the Montreal Neurological Institute (MNI) coordinate space with a voxel size of 1 × 1 × 1 mm^3; (3) segmentation: the brain tissue was segmented into gray matter (GM), white matter, and cerebrospinal fluid; (4) smoothing: the normalized modulated images were smoothed with an 8-mm full-width at half-maximum (FWHM) Gaussian kernel.

Whole-Brain and Region-of-Interest (ROI) Analyses

The modulated and smoothed GM data were subjected to whole-brain analysis using a two-sample *t*-test. Two sets of between-group analyses were performed on the differences in GM volume using a two-sample *t*-test in SPM8. Age and sex were included as covariates. First, the whole-brain significance threshold was set to $p < 0.05$ for multiple comparisons using familywise error correction at the voxel level. Since *in vivo* evidence of a correlation between GM and HO-1 levels in patients with PD has never been reported, the data were also presented using a less stringent, uncorrected threshold ($p < 0.001$, cluster threshold = 10 voxels) to detect subtle morphological changes. Based on the results of an exploratory whole-brain analysis, we also performed ROI analyses focusing on the right hippocampus. The brain areas with identified intergroup differences served as ROIs. The XJVIEWER[3] module was applied to save the ROIs as a mask, and the GM volume of the ROI was extracted using REST1.2[4]. Finally, the results of the SPM8 analysis were visualized using MRICRON[5] and Adobe Photoshop 2019 (Adobe Systems Incorporated, San Jose, CA, USA).

Statistics

The normality of distributions was assessed by the Shapiro–Wilk (SW) normality test (Henderson, 2006). Normally distributed continuous data are expressed as the mean ± standard deviation (SD). Data that did not conform to the normal distribution are presented as the median (first quartile, third quartile). Pearson's chi-square test was used to compare the distributions of categorical variables between groups. Two-group comparisons of normally distributed variables were performed using *t*-tests. One-way ANOVA was performed to compare variables among three or more groups. Variables that did not fit the normal distribution were assessed using the Mann–Whitney *U* test (two groups) or the Kruskal–Wallis (KW) rank-sum test (three or more groups).

Spearman's rank correlation coefficient was calculated to assess whether HO-1 levels were related to medications, and the

[1]http://www.fil.ion.ucl.ac.uk/spm/software/spm8
[2]http://dbm.neuro.uni-jena.de
[3]http://www.alivelearn.net/xjview/ad.php
[4]http://restfmri.net/forum/rest_v12
[5]https://www.nitrc.org/projects/mricron

correlation between plasma HO-1 levels and ROI volumes was analyzed by calculating the Pearson correlation coefficient.

The accuracy of plasma HO-1 levels in diagnosing patients with PD was assessed by constructing a receiver operating characteristic curve. The point with the maximum Youden index on the ROC curve was considered the optimum HO-1 cutoff point to diagnose the disease.

Statistical analyses were performed using SPSS software version 25 (IBM, USA). Graphs were generated with GraphPad Prism version 8.0 (GraphPad Prism Software, Inc., San Diego, CA, USA). A value of $p < 0.05$ was considered to indicate a statistically significant difference.

RESULTS

Of the 156 study subjects, 81 (51.9%) were diagnosed with idiopathic PD, and 75 (48.1%) were non-PD controls. The clinical characteristics of patients with PD are summarized in **Table 1**. No intergroup differences in sex were observed ($p = 0.985$), but patients with PD were older than controls ($p < 0.001$).

There were no statistically significant differences in HO-1 levels among the three groups (early PD patients, advanced PD patients and healthy controls) in either men or women [male: 2.39 (2.11, 2.97) vs. 2.38 (2.02, 2.61) vs. 2.18 (1.70, 2.61) ng/ml, $p = 0.176$; female: 2.34 ± 0.60 vs. 2.10 ± 0.53 vs. 2.01 ± 0.41 ng/ml, $p = 0.053$; **Supplementary Figure 1**]. Furthermore, comparison of HO-1 levels between men and women in the early PD, the advanced PD, and control groups also showed no significant differences [early PD: 2.39 ± 0.75 vs. 2.34 ± 0.60 ng/ml, $p = 0.81$; advanced PD: 2.33 ± 0.58 vs. 2.10 ± 0.53 ng/ml, $p = 0.22$; normal controls: 2.18 (1.70, 2.61) vs. 2.07 (1.74, 2.28) ng/ml, $p = 0.25$; **Supplementary Figures 1B–D**]. We also performed the same stratified analysis with age as a confounding factor. Subjects aged ≥60 years and < 60 years were defined as elderly and young, respectively. When the levels of HO-1 were compared among the early PD, advanced PD and control groups in young and elderly subjects, the results showed no statistically significant differences [young subjects: 2.43 (1.99, 2.97) vs. 2.19 (1.62, 2.61) vs. 2.16 (1.73, 2.39) ng/ml, $p = 0.15$; elder subjects: 2.34 ± 0.70 vs. 2.23 ± 0.56 vs. 2.02 ± 0.49 ng/ml, $p = 0.22$; **Supplementary Figure 1E**]. Comparison of HO-1 levels between young and elderly individuals in the early PD, advanced PD, and normal control groups also showed no significant differences [early PD: 2.42 ± 0.62 vs. 2.34 ± 0.70 ng/ml, $p = 0.75$; advanced PD: 2.19 ± 0.60 vs. 2.23 ± 0.56 ng/ml, $p = 0.84$; normal controls: 2.16 (1.73, 2.39) vs. 2.09 (1.68, 2.33) ng/ml, $p = 0.69$; **Supplementary Figures 1F–H**].

Plasma HO-1 levels were significantly increased in PD patients compared with the control group [2.37 (1.98, 2.67) vs. 2.13 (1.73, 2.37) ng/ml; $p = 0.006$; **Figure 1A**]. Significantly higher HO-1 levels were observed in the participants with early PD than in the controls [2.43 (2.00, 2.79) vs. 2.13 (1.73, 2.37) ng/ml; $p = 0.004$; **Figure 1B**]. Although higher plasma HO-1 levels were detected in the subjects with advanced PD than in the healthy controls, this difference was not statistically significant [2.35 (1.68, 2.54) vs. 2.13 (1.73, 2.37) ng/ml; $p = 0.139$; **Figure 1C**]. In addition, differences in HO-1 concentrations based on H & Y stage were not significant [2.35 ± 0.89 vs. 2.37 ± 0.62 vs. 2.23 ± 0.58 vs. 2.15 ± 0.53 ng/ml; $p = 0.787$; **Supplementary Figure 3**].

There was no significant difference in LEDD levels among H & Y stages I-IV [400 (262.50, 631.25) vs. 400.00 (200.00, 600.00) vs. 450 (287.50, 600.00) vs. 400.00 (375.00, 737.50), $p = 0.917$; **Supplementary Figure 2A**]. The median LEDD in the 81 patients with PD was 400.00 mg. However, no significant correlation was observed between plasma HO-1 levels and LEDD ($r = -0.015$, $p = 0.892$; **Supplementary Figure 2B**).

In order to evaluate the utility of HO-1 as a candidate biomarker of PD, an ROC curve was generated to distinguish PD patients in general from controls; the optimal cutoff value was found to be 2.255 ng/ml (sensitivity = 68%, specifity = 61.7%, AUC = 0.627, $p = 0.006$); the cutoff value for early-stage PD was 2.245 ng/ml (sensitivity = 66%, specifity = 66.7%, AUC = 0.654, $p = 0.004$). Plasma HO-1 levels did not differ between patients with advanced PD and the control group (sensitivity = 55.9%, specifity = 73.3%, AUC = 0.589, $p = 0.139$; **Figure 2**).

Each volumetric image section in the high-HO-1 group showed a reduced area of the right hippocampus compared to the low-HO-1 group (**Figure 3A**). Brain regions with different volumes between the low- and high-HO-1 groups are summarized in **Table 2**. As shown in **Figure 3B**, the volume of the ROI was significantly higher in the low-HO-1 group than in the high-HO-1 group after the extraction of volumes in different brain areas ($p = 0.002$). Additionally, the correlation analysis indicated a weak but significant negative correlation between the ROI volumes and plasma HO-1 levels in the PD group ($r = -0.273$, $p = 0.018$; **Figure 3C**). There was no significant difference in MMSE scores between the low- and

TABLE 1 | Clinical characteristics between PD group and controls.

	PD ($n = 81$)	Control ($n = 75$)	p-value
Gender (male/female)	42/39	39/36	0.985
Age (years)	64.00 (57.50, 67.00)	51 (47, 57)	<0.001*
Age of onset (years)	58.00 (50.00, 61.50)	NA	
Disease duration (years)	5.00 (4.00, 9.00)	NA	
Hoehn & Yahr scale	2.00 (2.00, 3.00)	NA	
UPDRS III	38.99 ± 16.37	NA	
LEDD (mg)	400.00 (212.50, 600.00)	NA	
MMSE	26.00 (24.00, 28.00)	NA	

*Mean ± standard deviation or median (interquartile range). UPDRS, United Parkinson's Disease Rating Scale; MMSE, Mini-Mental State Examination; LEDD, The equivalent daily dose of L-DOPA; HO-1, Heme Oxygenase-1; PD, Parkinson's disease; NA, not available. *$p < 0.05$.*

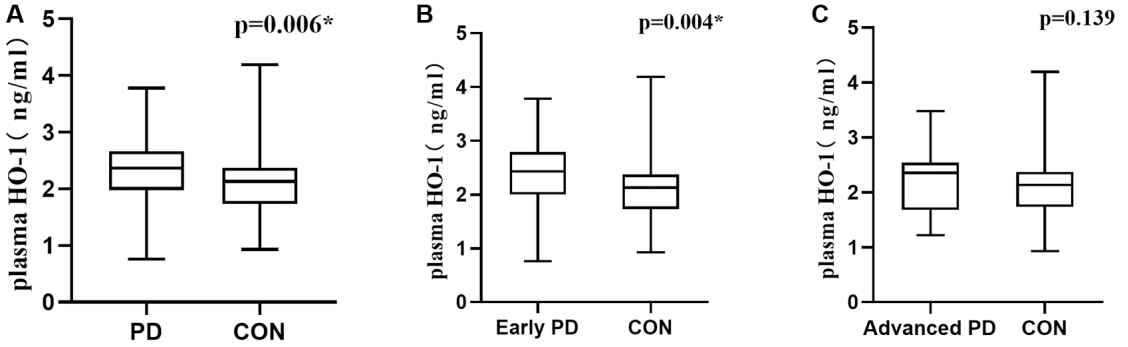
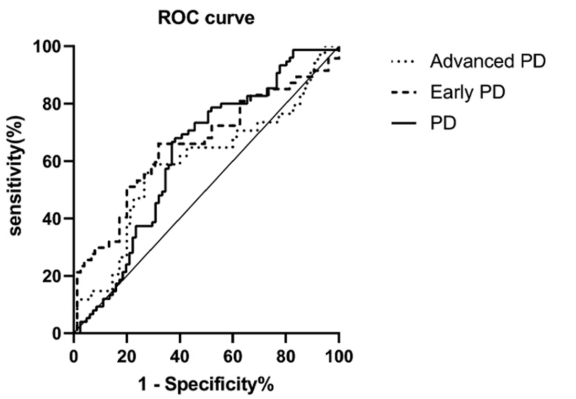


FIGURE 1 | Plasma HO-1 levels in PD patients and control subjects. **(A)** Increased plasma HO-1 levels in the PD group compared with control subjects. **(B)** HO-1 levels in the PD group with early-stage were highly increased in the plasma compared with the controls. **(C)** Plasma HO-1 levels were elevated in the advanced PD group relative to the control group, but no statistically significant. PD, Parkinson's disease; CON, normal controls; HO-1, Heme Oxygenase-1. The central line in each box indicates the median, box edges mark the first and third quartiles, and limits of the vertical lines show ranges. *$p < 0.05$.



	PD	Early PD	Advanced PD
Cutoff value(ng/ml)	2.255	2.245	2.335
Sentivity	0.680	0.660	0.559
Specifity	0.617	0.667	0.733
AUC	0.627	0.654	0.589
p	0.006	0.004	0.139

FIGURE 2 | ROC curve for plasma HO-1 levels comparing PD group, early PD group, advanced PD group, and healthy control group. ROC curve, receiver operating characteristic curve; AUC, area under the curve; PD, Parkinson's disease.

high-HO-1 groups [26.00 (23.00, 28.00) vs. 26.00 (24.75, 28.00), $p = 0.533$; **Table 3**]. However, the low-HO-1 group had lower language scores than the high-HO-1 group [3.00 (3.00, 4.00) vs. 4.00 (3.00, 4.00), $p = 0.018$; **Table 3**].

DISCUSSION

Plasma is more accessible and frequently sampled than cerebrospinal fluid, and the assessment of plasma is inexpensive compared to PET-CT imaging techniques. In this study, we used plasma HO-1 levels to distinguish patients with PD from healthy controls in a large cohort. Concentrations of the HO-1 protein were significantly increased in patients with PD, particularly those in the early stage of the disease, compared to normal controls. VBM features are not suitable as markers, but they may improve our understanding of the potential pathophysiological mechanism underlying the differences in regional brain volume. Increased levels of the HO-1 protein were associated with a reduced right hippocampal volume.

HO-1 is the rate-limiting enzyme in the endoplasmic reticulum that converts the pro-oxidant heme into biliverdin, iron, and carbon monoxide in the presence of oxidative stress (Maines, 1988; Keyse and Tyrrell, 1989). HO-1 expression was observed in the neuromelanin-containing (dopaminergic) neurons of the substantia nigra compacta of postmortem brain tissues from patients with PD (Schipper et al., 1998). Considerable evidence implicates oxidative stress as a primary pathogenic mechanism underlying the death of most dopaminergic neurons in patients with PD (Blesa et al., 2015). The promoter of the HO-1 gene contains a heat shock element, and its expression is substantially upregulated in response to oxidative stress. The induction of HO-1 expression in redox tissues provides cytoprotection from oxidative damage through the production of bile pigments (bilirubin and biliverdin) with free radical-scavenging capabilities (Stocker, 1990). On the other hand, HO-1-mediated heme degradation releases free iron and CO, which exacerbates oxidative damage by producing free radicals within the mitochondrial compartment. However, little is known about the exact mechanism by which HO-1 participates in oxidative stress in patients with PD. Based on accumulating evidence, the HO-1 protein is present in peripheral body fluids, such as plasma (Bao et al., 2010; Signorelli et al., 2016; Kishimoto et al., 2018a,b, 2020). Plasma HO-1 is leaked or secreted from epithelial and endothelial cells of different tissues that are subjected to oxidative stress. Additionally, the induction of HO-1 expression may be necessary and

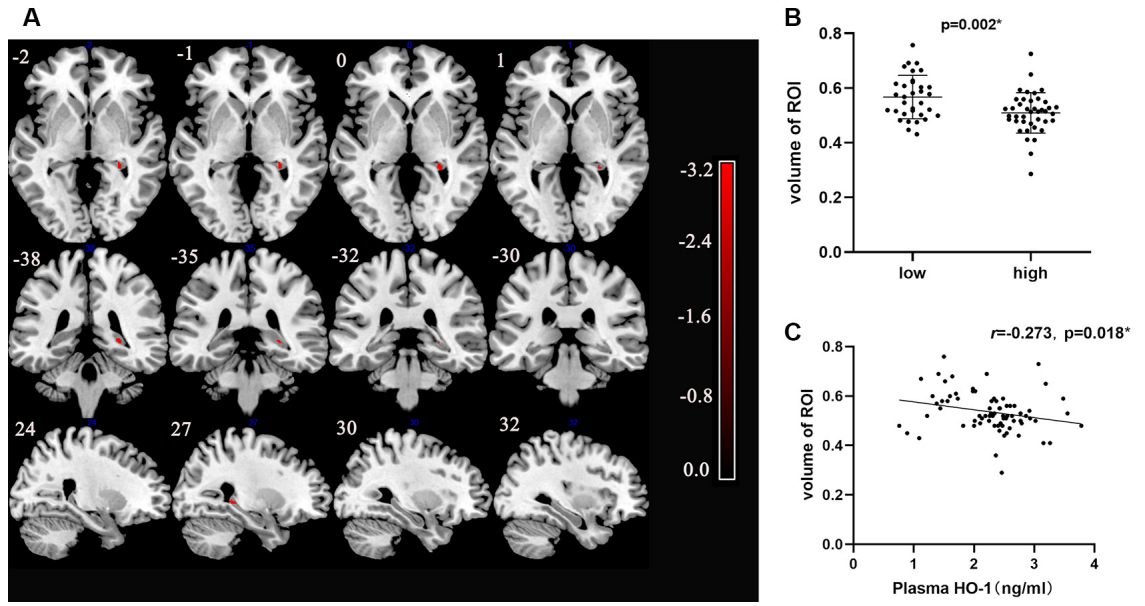


FIGURE 3 | VBM analysis of differences in brain areas between low and high levels HO-1 groups. **(A)** The figure shows T1-weighted imaging-based VBM analysis of the whole-brain about series of sections images. Statistically significant reduction in clusters of right hippocampal concentration in high HO-1 PD group compared with that in low HO-1 PD subjects is shown. Only clusters comprising at least 10 suprathreshold voxels were included in the analysis and are shown in the figure. To help visualization, shaded red sections were added to highlight all clusters. Color-bar indicates the level of concentration by the depth of the color. **(B)** Comparison of the volume of two groups with different HO-1 levels. **(C)** Correlation between HO-1 level and right hippocampal volume. HO-1, Heme Oxygenase-1; VBM, Voxel-Based Morphometry. *$p < 0.05$.

TABLE 2 | Overview of VBM results (ROI analyses).

Region	Side	Cluster size	BA	MNI coordinates			*T*-value
				X	Y	Z	
Low > high							
Hippocampus	Right	20	36	27	−38	−18	−3.42
High > low*							

*Differences of brain region comparing low and high HO-1 groups. *Means no areas were statistically significant different. BA, Brodmann's Area; MNI, Montreal neurological institute; VBM, voxel-based morphometry; T-value is statistical t by two-sample t-test.*

TABLE 3 | MMSE and subscale score differences.

Items	Low	High	*p*-value
Orientation to time and place (10)	10.00 (9.00, 10.00)	10.00 (9.00, 10.00)	0.838
Immediate registration (3)	3.00 (3.00, 3.00)	3.00 (3.00, 3.00)	0.120
Divided attention (5)	4.00 (3.00, 5.00)	4.00 (2.75, 5.00)	0.803
Delayed recall (3)	3.00 (2.00, 3.00)	3.00 (1.75, 3.00)	0.331
Language (4)	3.00 (3.00, 4.00)	4.00 (3.00, 4.00)	0.018*
Following a three-step command (3)	3.00 (3.00, 3.00)	3.00 (3.00, 3.00)	0.118
Writing a sentence (1)	1.00 (0.00, 1.00)	1.00 (0.75, 1.00)	0.853
Copying a figure (1)	0.00 (0.00, 1.00)	0.00 (0.00, 1.00)	0.593
MMSE	26.00 (23.00, 28.00)	26.00 (24.75, 28.00)	0.533

*Detailed cognitive function between low and high HO-1 levels groups. Data not conforming to a normal distribution were represented by median (interquartile range). HO-1, Heme Oxygenase-1; MMSE, Mini-mental State Examination. *$p < 0.05$.*

sufficient to provide protection after damage. Thus, plasma HO-1 levels are abnormal and elevated in patients with PD, a pathological condition, relative to the normal condition in healthy subjects.

As in previous studies (Mateo et al., 2010; Song et al., 2018), peripheral HO-1 levels were higher in patients with PD than in controls in the present study, and the difference was not affected by age, sex, or medication. Paradoxically, Schipper et al. (2000) did not observe a significant difference in plasma HO-1 levels between a small group of patients with PD and normal elderly subjects. A probable explanation for this discrepancy is the use of different methods to measure HO-1 levels in the two groups, along with the recruitment of subjects from different areas. A large cohort of patients with PD was

used to investigate plasma HO-1 levels in the present study. Moreover, plasma HO-1 levels displayed moderate sensitivity and specificity in distinguishing PD patients from controls in the diagnosis of PD. In addition to the results discussed above, HO-1 concentrations were significantly increased in patients with early PD compared to controls without the disease, but there was no such difference between patients with advanced PD and healthy subjects. Our observations were consistent with those of a previous study (Song et al., 2018), where the level of HO-1 in patients with idiopathic PD peaked early and started decreasing as the disease progressed. As exemplified by a temporary elevation of particular chemicals in some patients with acute diseases, HO-1 protects against challenges or noxious stimuli resulting from oxidative damage in patients with early-stage PD. On the other hand, based on evidence from cell culture, animal model, and human neuropathology studies in the literature before this study, predominant HO-1 expression in astrocytes is considered a necessary and sufficient condition for excessive brain iron deposition, oxidative stress, mitochondrial dysfunction, and macroautophagy (Schipper et al., 2019). Hence, we hypothesized that the decreased level of HO-1 in patients with advanced-stage PD may be due to a mechanism by which the body defends against damage caused by HO-1 overexpression after the pathological features of PD have developed. Although HO-1 levels were markedly increased in the early stage of PD, plasma HO-1 levels must be measured in a larger number of patients with idiopathic PD.

The expression levels of HO-1 exhibited significant differences at various stages of PD. Therefore, we explored differences in the anatomical structures of brain regions in patients with different HO-1 levels. Interestingly, our VBM analysis showed a decrease in the volume of the right hippocampus in the group of PD patients presenting high HO-1 levels compared with the group presenting low HO-1 levels. According to Schipper et al. (1995) HO-1 was significantly overexpressed in hippocampal neurons and astrocytes in patients with AD relative to controls, as analyzed using immunoblotting, which confirmed an association between the hippocampus and HO-1 levels. Although this association was identified in patients with AD, both diseases are neurodegenerative diseases. GFAP.HMOX1 mice exhibit dysgenesis of the hippocampal dentate gyrus (Song et al., 2012). This model confirms the presence of hippocampal atrophy in mice overexpressing HO-1. Consistent with these results, we observed a reduction in hippocampal volume in patients with high peripheral plasma HO-1 concentrations. However, it is unclear why the volume reduction is limited to the right side of the hippocampus and whether the volumes of specific hippocampal subregions are decreased.

Also, we performed a simple cognitive function test (the MMSE) in PD patients with low and high HO-1 levels. The results showed that there was no significant intergroup difference in total MMSE scores. Several studies have reported that volumetric measurements of the hippocampus are the most significant predictor of AD among patients and that they may even precede the onset of clinical symptoms (Fox et al., 1996; Kaye et al., 1997; Jack et al., 1999). Additionally, hippocampal volume atrophy is a very sensitive indicator of cognitive impairment not only in people with AD but also in a broader population (Wolf et al., 2001). Taken together, the results imply that the reduction in hippocampal volume does not indicate impaired cognition. Perhaps this volume reduction occurs before the onset of cognitive impairment. The reason why the MMSE results were negative in this study may be that the clinical symptoms had not yet developed, although there were already structural changes. Regarding the specific sub-items of the MMSE, the reason for our results might be the limited specificity of the sub-items. More detailed data on cognitive function will be needed to compare the cognition of the two groups in future work. Our results also suggest that the correlation between hippocampal volume and HO-1 levels is complicated. Ultimately, plasma HO-1 is more promising than brain volumetric features as a marker of early PD, and increased plasma HO-1 is accompanied by a reduction in hippocampal volume, which can serve as a warning in the predementia stages.

The main strength of this study is that it is one of very few to measure peripheral plasma HO-1 levels in PD patients and control subjects in a sample size that allows statistical comparisons. Moreover, the anatomy of the brain was altered by HO-1 levels, advancing the current understanding of the underlying pathophysiological mechanism of HO-1. However, the study has some limitations. First, abnormal HO-1 levels have been observed in diseases of other organs, such as hypertension, diabetes, and cardiovascular disease (Bao et al., 2010; Signorelli et al., 2016; Kishimoto et al., 2018a,b, 2020). Although healthy controls with these complications were excluded from the study, these cofounders were still present in patients with PD. Second, plasma HO-1 concentrations in patients with atypical Parkinsonism, such as multiple system atrophy (MSA) and progressive supranuclear palsy (PSP), need to be measured in the future to determine the specificity of HO-1 as a marker of idiopathic PD. Third, larger sample size is warranted to analyze the role of HO-1 levels in predicting the progression of PD. In contrast to cross-sectional studies, a more accurate and appropriate approach would be to assess HO-1 levels and measure changes in the volumes of different brain structures in follow-up studies.

CONCLUSION

Based on our findings, plasma HO-1 levels are a promising biomarker for diagnosing early PD and may assist clinicians in achieving unexpectedly good treatment outcomes by intervening in the early stage of the disease. Moreover, we observed a correlation between high HO-1 levels and GM volume in the hippocampus. Given the significance of reduced hippocampal volume, high HO-1 levels accompanied by a reduction in hippocampal volume in early PD may be a warning sign of cognitive impairment. Also, inhibiting HO-1 overexpression in response to nociceptive stimuli at a critical time in the development of PD might be an effective method for managing neurodegeneration.

DATA AVAILABILITY STATEMENT

The raw data supporting the conclusions of this article will be made available by the authors, without undue reservation.

ETHICS STATEMENT

The studies involving human participants were reviewed and approved by Medical Ethics Committee of Henan Provincial People's Hospital. The patients/participants provided their written informed consent to participate in this study.

AUTHOR CONTRIBUTIONS

WS, JM, and JZ completed the research design. WS performed the experiments. ZW, XS, and ML conducted the literature search and data collection. SH, SYH, ZZ, and DL performed the statistical analysis and interpretation of data. WS, JM, and JZ were responsible for writing the manuscript. All authors contributed to the article and approved the submitted version.

FUNDING

This study was supported by Henan Province Science and Technology Development Plan (192102310085) and Henan Province Medical Science and Technology Research Program (201701018).

SUPPLEMENTARY MATERIAL

The Supplementary Material for this article can be found online at: https://www.frontiersin.org/articles/10.3389/fnagi.2021.621508/full#supplementary-material.

REFERENCES

Bao, W., Song, F., Li, X., Rong, S., Yang, W., Zhang, M., et al. (2010). Plasma heme oxygenase-1 concentration is elevated in individuals with type 2 diabetes mellitus. *PLoS One* 5:e12371. doi: 10.1371/journal.pone.0012371

Blesa, J., Trigo-Damas, I., Quiroga-Varela, A., and Jackson-Lewis, V. R. (2015). Oxidative stress and Parkinson's disease. *Front. Neuroanat.* 9:91. doi: 10.3389/fnana.2015.00091

Chard, D. T., Parker, G. J. M., Griffin, C. M. B., Thompson, A. J., and Miller, D. H. (2002). The reproducibility and sensitivity of brain tissue volume measurements derived from an SPM-based segmentation methodology. *J. Magn. Reson. Imaging* 15, 259–267. doi: 10.1002/jmri.10064

Fox, N. C., Warrington, E. K., Freeborough, P. A., Hartikainen, P., Kennedy, A. M., Stevens, J. M., et al. (1996). Presymptomatic hippocampal atrophy in Alzheimer's disease. a longitudinal MRI study. *Brain* 119, 2001–2007. doi: 10.1093/brain/119.6.2001

Goetz, C. G., Tilley, B. C., Shaftman, S. R., Stebbins, G. T., Fahn, S., Martinez-Martin, P., et al. (2008). Movement disorder society-sponsored revision of the unified Parkinson's disease rating scale (MDS-UPDRS): scale presentation and clinimetric testing results. *Mov. Disord.* 23, 2129–2170. doi: 10.1002/mds.22340

Goto, M., Kamagata, K., Hatano, T., Hattori, N., Abe, O., Aoki, S., et al. (2018). Depressive symptoms in Parkinson's disease are related to decreased left hippocampal volume: correlation with the 15-item shortened version of the geriatric depression scale. *Acta. Radiol.* 59, 341–345. doi: 10.1177/0284185117719100

Henderson, A. R. (2006). Testing experimental data for univariate normality. *Clin. Chim. Acta* 366, 112–129. doi: 10.1016/j.cca.2005.11.007

Hughes, A. J., Daniel, S. E., Kilford, L., and Lees, A. J. (1992). Accuracy of clinical diagnosis of idiopathic Parkinson's disease: a clinico-pathological study of 100 cases. *J. Neurol. Neurosurg. Psychiatry* 55, 181–184. doi: 10.1136/jnnp.55.3.181

Jack, C. R. Jr., Petersen, R. C., Xu, Y. C., O'Brien, P. C., Smith, G. E., Ivnik, R. J., et al. (1999). Prediction of AD with MRI-based hippocampal volume in mild cognitive impairment. *Neurology* 52, 1397–1403. doi: 10.1212/wnl.52.7.1397

Kaye, J. A., Swihart, T., Howieson, D., Dame, A., Moore, M. M., Karnos, T., et al. (1997). Volume loss of the hippocampus and temporal lobe in healthy elderly persons destined to develop dementia. *Neurology* 48, 1297–1304. doi: 10.1212/wnl.48.5.1297

Keyse, S. M., and Tyrrell, R. M. (1989). Heme oxygenase is the major 32-kDa stress protein induced in human skin fibroblasts by UVA radiation, hydrogen peroxide, and sodium arsenite. *Proc. Natl. Acad. Sci. U S A* 86, 99–103. doi: 10.1073/pnas.86.1.99

Kishimoto, Y., Ibe, S., Saita, E., Sasaki, K., Niki, H., Miura, K., et al. (2018a). Plasma heme oxygenase-1 levels in patients with coronary and peripheral artery diseases. *Dis. Markers* 2018:6138124. doi: 10.1155/2018/6138124

Kishimoto, Y., Sasaki, K., Saita, E., Niki, H., Ohmori, R., Kondo, K., et al. (2018b). Plasma heme oxygenase-1 levels and carotid atherosclerosis. *Stroke* 49, 2230–2232. doi: 10.1161/STROKEAHA.118.022256

Kishimoto, Y., Niki, H., Saita, E., Ibe, S., Umei, T., Miura, K., et al. (2020). Blood levels of heme oxygenase-1 versus bilirubin in patients with coronary artery disease. *Clin. Chim. Acta.* 504, 30–35. doi: 10.1016/j.cca.2020.01.030

Li Volti, G., Galvano, F., Frigiola, A., Guccione, S., Di Giacomo, C., Forte, S., et al. (2010). Potential immunoregulatory role of heme oxygenase-1 in human milk: a combined biochemical and molecular modeling approach. *J. Nutr. Biochem.* 21, 865–871. doi: 10.1016/j.jnutbio.2009.06.011

Maines, M. D. (1988). Heme oxygenase: function, multiplicity, regulatory mechanisms, and clinical applications. *FASEB J.* 2, 2557–2568.

Masaki, Y., Izumi, Y., Matsumura, A., Akaike, A., and Kume, T. (2017). Protective effect of Nrf2-ARE activator isolated from green perilla leaves on dopaminergic neuronal loss in a Parkinson's disease model. *Eur. J. Pharmacol.* 798, 26–34. doi: 10.1016/j.ejphar.2017.02.005

Mateo, I., Infante, J., Sánchez-Juan, P., García-Gorostiaga, I., Rodríguez-Rodríguez, E., Vázquez-Higuera, J. L., et al. (2010). Serum heme oxygenase-1 levels are increased in Parkinson's disease but not in Alzheimer's disease. *Acta. Neurol. Scand.* 121, 136–138. doi: 10.1111/j.1600-0404.2009.01261.x

Poewe, W., Seppi, K., Tanner, C. M., Halliday, G. M., Brundin, P., Volkmann, J., et al. (2017). Parkinson disease. *Nat. Rev. Dis. Primers* 3:17013. doi: 10.1038/nrdp.2017.13

Ringman, J. M., Rodriguez, Y., Diaz-Olavarrieta, C., Chavez, M., Thompson, M., Fairbanks, L., et al. (2007). Performance on MMSE sub-items and education level in presenilin-1 mutation carriers without dementia. *Int. Psychogeriatr.* 19, 323–332. doi: 10.1017/S1041610206003772

Schipper, H. M. (1999). Glial HO-1 expression, iron deposition and oxidative stress in neurodegenerative diseases. *Neurotox. Res.* 1, 57–70. doi: 10.1007/BF03033339

Schipper, H. M. (2004). Heme oxygenase-1: transducer of pathological brain iron sequestration under oxidative stress. *Ann. N. Y. Acad. Sci.* 1012, 84–93. doi: 10.1196/annals.1306.007

Schipper, H. M., Chertkow, H., Mehindate, K., Frankel, D., Melmed, C., and Bergman, H. (2000). Evaluation of heme oxygenase-1 as a systemic biological marker of sporadic AD. *Neurology* 54, 1297–1304. doi: 10.1212/wnl.54.6.1297

Schipper, H. M., Cisse, S., and Stopa, E. G. (1995). Expression of heme oxygenase-1 in the senescent and Alzheimer-diseased brain. *Ann. Neurol.* 37, 758–768. doi: 10.1002/ana.410370609

Schipper, H. M., Liberman, A., and Stopa, E. G. (1998). Neural heme oxygenase-1 expression in idiopathic Parkinson's disease. *Exp. Neurol.* 150, 60–68. doi: 10.1006/exnr.1997.6752

Schipper, H. M., Song, W., Tavitian, A., and Cressatti, M. (2019). The sinister face of heme oxygenase-1 in brain aging and disease. *Prog. Neurobiol.* 172, 40–70. doi: 10.1016/j.pneurobio.2018.06.008

Signorelli, S. S., Volsi, G. L., Fiore, V., Mangiafico, M., Barbagallo, I., Parenti, R., et al. (2016). Plasma heme oxygenase-1 is decreased in peripheral artery disease patients. *Mol. Med. Rep.* 14, 3459–3463. doi: 10.3892/mmr.2016.5644

Song, W., Cressatti, M., Zukor, H., Liberman, A., Galindez, C., and Schipper, H. M. (2017). Parkinsonian features in aging GFAP.HMOX1 transgenic mice overexpressing human HO-1 in the astroglial compartment. *Neurobiol. Aging* 58, 163–179. doi: 10.1016/j.neurobiolaging.2017.06.017

Song, W., Kothari, V., Velly, A. M., Cressatti, M., Liberman, A., Gornitsky, M., et al. (2018). Evaluation of salivary heme oxygenase-1 as a potential biomarker of early Parkinson's disease. *Mov. Disord.* 33, 583–591. doi: 10.1002/mds.27328

Song, W., Patel, A., Qureshi, H. Y., Han, D., Schipper, H. M., and Paudel, H. K. (2009). The parkinson disease-associated a30p mutation stabilizes alpha-synuclein against proteasomal degradation triggered by heme oxygenase-1 over-expression in human neuroblastoma cells. *J. Neurochem.* 110, 719–733. doi: 10.1111/j.1471-4159.2009.06165.x

Song, W., Su, H., Song, S., Paudel, H. K., and Schipper, H. M. (2006). Over-expression of heme oxygenase-1 promotes oxidative mitochondrial damage in rat astroglia. *J. Cell Physiol.* 206, 655–663. doi: 10.1002/jcp.20509

Song, W., Zukor, H., Lin, S. H., Hascalovici, J., Liberman, A., Tavitian, A., et al. (2012). Schizophrenia-like features in transgenic mice overexpressing human HO-1 in the astrocytic compartment. *J. Neurosci.* 32, 10841–10853. doi: 10.1523/JNEUROSCI.6469-11.2012

Stocker, R. (1990). Induction of heme oxygenase as a defence against oxidative stress. *Free Radic. Res. Commun.* 9, 101–112. doi: 10.3109/10715769009148577

Tomlinson, C. L., Stowe, R., Patel, S., Rick, C., Gray, R., and Clarke, C. E. (2010). Systematic review of levodopa dose equivalency reporting in Parkinson's disease. *Mov. Disord.* 25, 2649–2653. doi: 10.1002/mds.23429

Tong, H., Zhang, X., Meng, X., Lu, L., Mai, D., and Qu, S. (2018). Simvastatin inhibits activation of NADPH oxidase/p38 MAPK pathway and enhances expression of antioxidant protein in parkinson disease models. *Front. Mol. Neurosci.* 11:165. doi: 10.3389/fnmol.2018.00165

van Mierlo, T. J., Chung, C., Foncke, E. M., Berendse, H. W., and van den Heuvel, O. A. (2015). Depressive symptoms in Parkinson's disease are related to decreased hippocampus and amygdala volume. *Mov. Disord.* 30, 245–252. doi: 10.1002/mds.26112

Wolf, H., Grunwald, M., Kruggel, F., Riedel-Heller, S. G., Angerhöfer, S., Hojjatoleslami, A., et al. (2001). Hippocampal volume discriminates between normal cognition; questionable and mild dementia in the elderly. *Neurobiol. Aging* 22, 177–186. doi: 10.1016/s0197-4580(00)00238-4

Wolters, A. F., Moonen, A. J. H., Lopes, R., Leentjens, A. F. G., Duits, A. A., Defebvre, L., et al. (2020). Grey matter abnormalities are associated only with severe cognitive decline in early stages of Parkinson's disease. *Cortex* 123, 1–11. doi: 10.1016/j.cortex.2019.09.015

Xuan, M., Guan, X., Huang, P., Shen, Z., Gu, Q., Yu, X., et al. (2019). Different patterns of gray matter density in early- and middle-late-onset Parkinson's disease: a voxel-based morphometry study. *Brain Imag. Behav.* 13, 172–179. doi: 10.1007/s11682-017-9745-4

Yousaf, T., Dervenoulas, G., and Politis, M. (2018). Advances in MRI methodology. *Int. Rev. Neurobiol.* 141, 31–76. doi: 10.1016/bs.irn.2018.08.008

Zukor, H., Song, W., Liberman, A., Mui, J., Vali, H., Fillebeen, C., et al. (2009). HO-1-mediated macroautophagy: a mechanism for unregulated iron deposition in aging and degenerating neural tissues. *J. Neurochem.* 109, 776–791. doi: 10.1111/j.1471-4159.2009.06007.x

Conflict of Interest: The authors declare that the research was conducted in the absence of any commercial or financial relationships that could be construed as a potential conflict of interest.

Copyright © 2021 Sun, Zheng, Ma, Wang, Shi, Li, Huang, Hu, Zhao and Li. This is an open-access article distributed under the terms of the Creative Commons Attribution License (CC BY). The use, distribution or reproduction in other forums is permitted, provided the original author(s) and the copyright owner(s) are credited and that the original publication in this journal is cited, in accordance with accepted academic practice. No use, distribution or reproduction is permitted which does not comply with these terms.

frontiers in Aging Neuroscience

BRIEF RESEARCH REPORT
published: 24 February 2021
doi: 10.3389/fnagi.2021.634213

Bone-Derived Factors as Potential Biomarkers for Parkinson's Disease

Yuwan Lin[1†], Miaomiao Zhou[1†], Wei Dai[1†], Wenyuan Guo[1], Jiewen Qiu[1], Zhiling Zhang[1], Mingshu Mo[1], Liuyan Ding[1], Panghai Ye[1], Yijuan Wu[1], Xiaoqin Zhu[2], Zhuohua Wu[1], Pingyi Xu[1]* and Xiang Chen[1]**

[1]Department of Neurology, The First Affiliated Hospital of Guangzhou Medical University, Guangzhou, China, [2]Department of Physiology, School of Basic Medical Sciences, Guangzhou Medical University, Guangzhou, China

Background: Parkinson's disease (PD) and osteoporosis are both common aging diseases. It is reported that PD has a close relationship with osteoporosis and bone secretory proteins may be involved in disease progression.

Objectives: To detect the bone-derived factors in plasma and cerebrospinal fluid (CSF) of patients with PD and evaluate their correlations with C-reaction protein (CRP) level, motor impairment, and Hoehn-Yahr (HY) stage of the disease.

Methods: We included 250 PD patients and 250 controls. Levels of osteocalcin (OCN), osteopontin (OPN), osteoprotegerin (OPG), Sclerostin (SO), Bone morphogenetic protein 2 (BMP2), and Dickkopf-1 (DKK-1) in plasma and CSF were measured by custom protein antibody arrays. Data were analyzed using Mann–Whitney *U*-test and Spearman's receptor activator of NF-κB (RANK) correlation.

Results: Plasma levels of OCN and OPN were correlated with CRP levels and HY stage and motor impairment of PD. Furthermore, the plasma assessment with CSF detection may enhance their potential prediction on PD.

Conclusions: OCN and OPN may serve as potential biomarkers for PD. The inflammation response may be involved in the cross-talk between the two factors and PD.

Keywords: Parkinson's disease, bone-derived factors, osteocalcin, osteopontin, C-reaction protein

OPEN ACCESS

Edited by:
Ramesh Kandimalla, Texas Tech University Health Sciences Center, United States

Reviewed by:
Maria E. Jimenez-Capdeville, Autonomous University of San Luis Potosí, Mexico
Michele D'Angelo, University of L'Aquila, Italy

***Correspondence:**
Xiang Chen
wuliancx@163.com
Pingyi Xu
pingyi123@hotmail.com
Zhuohua Wu
zhh88w@126.com

†These authors have contributed equally to this work

Received: *27 November 2020*
Accepted: *29 January 2021*
Published: *24 February 2021*

Citation:
Lin Y, Zhou M, Dai W, Guo W, Qiu J, Zhang Z, Mo M, Ding L, Ye P, Wu Y, Zhu X, Wu Z, Xu P and Chen X (2021) Bone-Derived Factors as Potential Biomarkers for Parkinson's Disease. Front. Aging Neurosci. 13:634213. doi: 10.3389/fnagi.2021.634213

INTRODUCTION

Parkinson's disease (PD) is one of the most common neurodegenerative disorders. It is investigated that approximately 7.4–23.4% of the patients with PD suffered from osteoporosis as a result of immobility, vitamin D deficiency, hyperhomocysteinemia, malnutrition, and muscle weakness (Choi et al., 2017). Besides, fractures can also be found more commonly in the prodromal period of PD compared to controls (Camacho-Soto et al., 2020). Both of these indicate that osteoporosis may be a hidden non-motor syndrome of PD and bone metabolism has a close relationship with the development of PD (Metta et al., 2017). Bone has traditionally been considered a structural organ that supports the movement of the body and protects the internal organs. However, an increasing number of studies have shown that the skeleton could also be an active endocrine organ that secretes many kinds of

bone-derived factors and contributes to the pathophysiology of many diseases, such as Alzheimer's disease, diabetes mellitus, cardiovascular, chronic kidney disease (Rentsendorj et al., 2018; Xu et al., 2018). In this study, we aimed to clarify the levels of OCN, OPN, OPG, SO, BMP2, and DKK-1 in the plasma and CSF of PD patients and identify candidate biomarkers for detection of PD. We also investigated the relevance of these bone-derived factors with CRP and motor dysfunction and disease progression.

MATERIALS AND METHODS

Subjects

This study enrolled 500 participants, including 250 PD, and 250 healthy controls (HCs). Among the participants, 400 were collected for plasma (200 PD, 200 HCs), 100 were collected for CSF (50 PD, 50 controls). PD patients were diagnosed following the Movement Disorder Society Clinical Diagnostic Criteria. All patients included in this study were tested negative for secondary forms of parkinsonism, neurological/psychiatric, diabetes mellitus, thyroid disease, history of metabolic bone disorders, renal dysfunction and failure, and severe cardiovascular and systemic diseases affecting the overall health of participants. Controls were matched with PD patients regarding their age and gender. All participants were recruited from the First Affiliated Hospital of Guangzhou Medical University. This study was approved by the Institutional Ethics Board Committee of the First Affiliated Hospital of Guangzhou Medical University and all participants provided written informed consent.

Plasma and CSF Collection

The blood samples of 200 HCs and 200 patients with PD were collected in early morning (7 a.m. – 9 a.m.) and were centrifuged (2,500 *g* for 15 min at 4° C) within 1 h of the collection (Redmond et al., 2016). CSF samples were collected by lumbar puncture from 50 controls and 50 patients with PD. CSF samples had no blood contamination (leukocyte number count fewer than 5 cells/μl and erythrocyte number fewer than 200 cells/μl). Sample aliquots were stored in cryotubes at −80°C before testing.

Measurement of Bone-Derived Factors in Plasma and CSF

The levels of bone-derived factors were measured using custom protein antibody arrays (RayBiotech[1]). First of all, a captured antibody was bound to the glass surface. Then the standard protein cocktail, 50–100 μl plasma or CSF samples were added to the platform and incubated for 1–2 h. Second, a second biotin-labeled detection antibody was added and incubated for 1–2 h, which can recognize a different epitope of bone-derived factors. Next, the streptavidin-conjugated Cy3 equivalent dye which could visualize the cytokine-antibody-biotin complex was added and incubated for 1 h. Last, the data was scanned and performed by using a laser scanner.

[1]http://raybiotech.com

Measurement of CRP in Plasma and CSF

The levels of CRP in plasma and CSF were measured by immunoturbidimetric assays. For the estimation of CRP levels, an automatic biochemical analyzer was used according to the manual instruction.

Statistical Analysis

Data statistics were carried out by SPSS, version 21, and GraphPad Prism version 6. Student's *t*-tests or Mann–Whitney *U* test was used to assess the difference of continuous variables between PD and HC groups. Differences between groups for categorical variables were assessed by using chi-square tests. Spearman coefficient calculation and the Kruskal–Wallis *H* test were used to analyze possible correlations between parameters of interest. Receiver operating characteristics (ROC) curves were used to determine the diagnostic performance of studied bone-derived factors in differentiating PD patients from controls. The accuracy of a biomarker in predicting PD was assessed by calculating the area under the ROC curve (AUC). Values of $P < 0.05$ were considered significant.

RESULTS

For this study, we obtained plasma samples from 200 PD patients and 200 age- and gender-matched controls, and CSF samples from 50 PD patients and 50 age- and gender-matched controls. The detectable rates of six bone-derived factors in plasma and five bone-derived factors in CSF were more than 90%. SO in CSF analysis was excluded due to the low detection rate (52%). In plasma, levels of OCN [PD vs. HC, 11,716.4pg/ml (8,052.7–14,679.4) vs. 4833.1 pg/ml (1,953.1–8,847.8), $P < 0.001$] and OPN [PD vs. HC, 16,733.7 pg/ml (12,446.0–19,981.3)vs 12,333.7 pg/ml (6,341.4–16,882.7), $P < 0.001$] were increased in the PD patients relative to the controls. In contrast, levels of OPG [PD vs HC, 130.7 pg/ml (89.4–207) vs. 169.5 pg/ml (113.1–245), $P < 0.001$] and BMP2 [PD vs. HC, 11.8 pg/ml (8–20.9) vs. 17.9 pg/ml (9.37–31.5), $P < 0.001$] were decreased in the PD patients compared to those in controls (**Table 1**, **Figures 1A–D**). However, no significant difference in plasma SO and DKK1 levels were found between the two groups (**Supplementary Figure 1**). In CSF, patients with PD had significantly lower levels of OCN [14,817.5 pg/ml (8,145.9–18,998.3) vs. 18,264 pg/ml (12,835.5–22,342.3), $P = 0.002$; **Figure 1A**] and OPG [204.3 pg/ml (107.3–307) vs. 282.7 pg/ml (215.3–444.1), $P = 0.008$; **Figure 1C**] relative to HC. There was no significant difference in OPN, BMP2, or DKK1 levels in CSF between the two groups (**Table 1**, **Figures 1B,D**, and **Supplementary Figure 1**).

To evaluate whether these bone-derived factors could be the potential biomarkers for PD risk, the natural-logarithm values of these levels were analyzed using ROC curves. Compared with the HC group, the AUCs for the plasma and CSF levels of OCN in PD patients were 0.863 (95% *CI* = 0.771–0.928) and 0.67 (95% *CI* = 0.559–0.769), respectively. Moreover, the AUC was higher when the combined assessment of plasma and CSF OCN in PD patients at 0.869 (95% *CI* = 0.778–0.993; **Figure 1E**). The AUCs for plasma, CSF, and

TABLE 1 | Demographics and protein levels of six bone-derived factors in plasma and cerebrospinal fluid (CSF) in two groups.

Clinical characteristics	Plasma		*P*-value	CSF		*P*-value
	PD	Con		PD	Con	
Gender (Male/Female)	113/87	108/92	0.688	29/21	27/23	0.84
Age (SD), years	63.2 (11.2)	63.3 (12.3)	0.935	57.6 (11.1)	59 (10.2)	0.518
SBP (SD), mm Hg	122.2 (10.32)	123.6 (11.9)	0.298	121.4 (12.5)	122.4 (10.6)	0.579
DBP (SD), mm Hg	75.2 (7.0)	74.6 (7.5)	0.215	74.5 (7.3)	73.9 (7.5)	0.553
H-Y	2.3 (0.8)	-	-	2.2 (0.6)	-	-
UPDRS-III	33.1 (11.6)	-	-	32.4 (11.7)	-	-
CRP, median (IQR), mg/l	3.3 (1.8–4.5)	2.1 (1.1–2.9)	<0.001	0.15 (0.12–0.17)	0.032 (0.01–0.04)	0.006
OCN, median (IQR), pg/ml	11,716.4 (805 2.7–14,679.4)	4,833.1 (195 3.1–8,847.8)	<0.001	14,817.5 (814 5.9–18,998.3)	18,264 (1283 5.5–22,342.3)	0.002
OPN, median (IQR), pg/ml	16,733.7 (124 46.0–19,981.3)	12,333.7 (634 1.4–16,882.7)	<0.001	93,16.1 (695 5.1–11,378.3)	8,189.4 (662 9.2–10736.8)	0.124
OPG, median (IQR), pg/ml	130.7 (89.4–207)	169.5 (113.1–245)	<0.001	204.3 (107.3–307)	282.7 (215.3–444.1)	0.008
SO, median (IQR), pg/ml	651.4 (321.1–1068.7)	748.6 (372.6–1272.2)	0.147	-	-	-
BMP2, median (IQR), pg/ml	11.8 (8–20.9)	17.9 (9.37–31.5)	<0.001	44.3 (22–84.1)	45 (27.5–60.5)	0.900
DKK1, median (IQR), pg/ml	45.6 (15.8–141.1)	63.6 (24.8–135.4)	0.067	16.2 (5.2–56.3)	33.46 (18.1–54.7)	0.080

Data are represented as Mean (SD), median (IQR), or n. P-value was considered significant when < 0.05, PD, Parkinson's disease; con, Controls; SBP, systolic blood pressure; DBP, diastolic blood pressure; H-Y, Hoehn and Yahr, UPDRS-III, Unified Parkinson's Disease Rating Scale part III (motor score). CRP, C-reaction protein; OCN, Osteocalcin; OPN, Osteopontin; OPG, Osteoprotegerin; SO, Sclerostin; BMP2, Bone morphogenetic protein 2; DKK-1, Dickkopf-1; IQR, Interquartile range.

the combined assessment of OPN when comparing PD patients with control groups were 0.73 (95% *CI* = 0.632–0.814), 0.589 (95% *CI* = 0.486–0.687), and 0.739 (95% *CI* = 0.641–0.822), respectively (**Figure 1F**). The AUCs for plasma, CSF, and the combined assessment of OPG and BMP2 were less than 0.7 (**Supplementary Figure 1**). Further, the plasma level of OCN and OPN were correlated with the Hoehn and Yahr disease stage (**Figures 1H–K**) and the Movement Disorders Society-Unified Parkinson's Disease Rating Scale-III score (MDS-UPDRS III; **Figures 1G–J**). Inflammation was involved both in the pathology of osteoporosis and PD, we next analyzed the relationship between CRP and these bone-derived factors. We found that significant correlations existed between plasma OCN and OPN and CRP levels in PD (**Figures 1I–L**). However, no correlation was identified between these factors and CRP in CSF.

DISCUSSION

Several studies have focused on the questions of comorbidity of PD and osteoporosis. The relationship between bone-derived factors and the risk of PD remains unclear. In the present study, we tested six bone-derived factors and found increased levels of OCN and OPN and decreased levels of OPG and BMP2 in plasma of PD patients. And levels of OCN and OPG were lower in CSF of PD relative to controls. Furthermore, we identified that plasma OCN and OPN were correlated with the disease stage and motor impairment. CRP was correlated with plasma levels of OCN and OPN. Combined assessment of plasma and CSF of OCN or OPN would be a better biomarker for differentiating PD patients from HCs.

OCN is one of the most abundant bone-specific non-collagenous proteins secreted primarily by osteoblasts and is often used as a biomarker for bone formation. In recent years, OCN has been regarded as a bone-derived hormone that plays important roles in physiological and pathological processes (Wei and Karsenty, 2015). In the brain, the uncarboxylated form of OCN can accumulate in the brainstem, thalamus, and hypothalamus, influencing various neurotransmitters synthesis and signalings (Shan et al., 2019). Several types of research indicated that OCN offers its protective function in PD. OCN can bind with the neurons in the midbrain and interacts with the dopamine transporter through heterotrimeric G protein's βγ subunit, and thus facilitating the formation of dopamine neurotransmitters (Garcia-Olivares et al., 2017). Intervention with OCN could relieve the behavioral dysfunction symptoms and reduce the tyrosine hydroxylase loss in the nigrostriatal system in PD rat models (Guo et al., 2018). Also, OCN could modulate neuroinflammation in the substantia nigra (SN) of PD rats by inhibiting astrocyte and microglia proliferation, together with partially decreased levels of TNF-α and IL-1β. Further studies confirmed that OCN corrected motor dysfunction, inhibited the neuroinflammatory responses, and reduced dopaminergic neuronal injury *via* the AKT/GSK3β signaling pathway in an animal model of PD (Guo et al., 2018). Additionally, OCN has an important role in brain development. OCN is required during embryonic development for proper neuronal development (Moser and van der Eerden, 2018). In OCN-deficient mice, the brains were smaller and less developed than control mice. OCN was also indicated to have a significant impact on cognition. Serum OCN levels

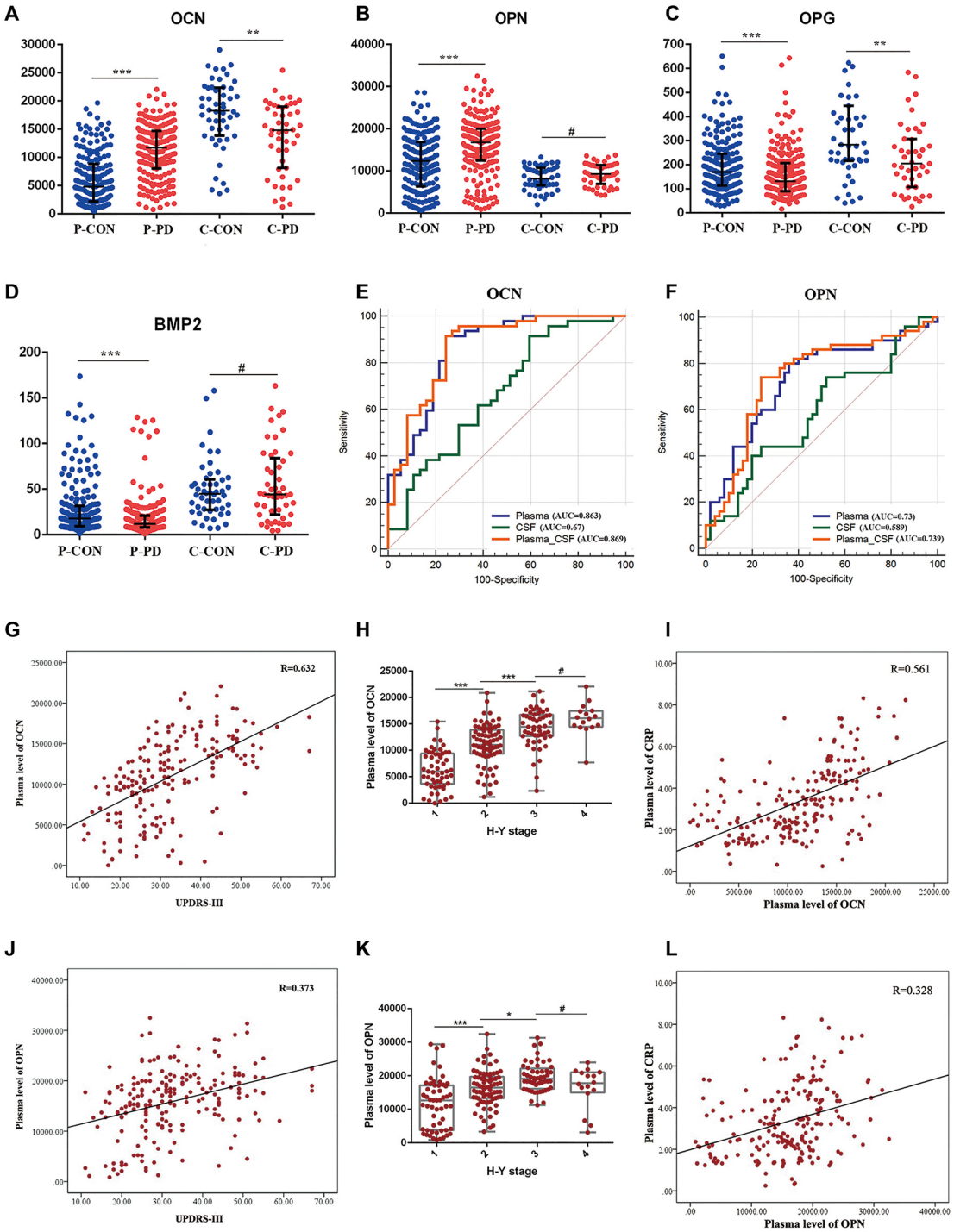


FIGURE 1 | Expression levels, receiver operating characteristics (ROC) analysis, and correlation analysis of selected bone-derived factors of Parkinson's disease (PD) relative to healthy control (HC). **(A–D)** Presents the concentrations of osteocalcin (OCN), osteopontin (OPN), osteoprotegerin (OPG), and bone morphogenetic protein 2 (BMP2) 1 in plasma (P) and cerebrospinal fluid (CSF; **C**) of PD and HC (CON). Data are presented as median and interquartile range (IQR; $^{**}P < 0.01$, $^{***}P < 0.001$, $^{\#}P = 0.05$ from Mann–Whitney test). **(E,F)** ROC curves of plasma, CSF, and combined plasma and CSF (Plasma-CSF) of OCN and OPN were analyzed. AUC, area under the curve. **(G)** Scatter diagram of the correlation between the plasma level of OCN and Unified Parkinson's Disease Rating Scale part III (UPDRS-III) of PD patients ($r = 0.632$, $P < 0.001$). **(H)** The relationship of plasma level of OCN and Hoehn and Yahr (H-Y) stage of PD patients, ($^{***}P < 0.001$, $^{*}P < 0.05$, $^{\#}P = 0.05$). **(I)** Correlation between the plasma level of OCN and C-reaction protein (CRP) of PD patients ($r = 0.561$, $P < 0.001$). **(J)** Scatter diagram of the correlation between the plasma level of OPN and UPDRS-III of PD patients ($r = 0.373$, $P < 0.001$). **(K)** The relationship of plasma level of OPN and H-Y stage of PD patients ($^{***}P < 0.001$ $^{*}P < 0.05$, $^{\#}P = 0.05$). **(L)** Correlation between the plasma level of OPN and CRP of PD patients ($r = 0.328$, $P < 0.001$).

were correlated with cognitive performance in aged women and obese patients (Bradburn et al., 2016; Puig et al., 2016). OCN-deficient mice were more susceptible to suffer from cognitive defects and exogenous OCN could protect against cognitive function in mice (Khrimian et al., 2017). In the peripheral, OCN acts as a regulator of the activity of osteoclasts and also maintains the energy homeostasis by improving glucose metabolism, insulin sensitivity (Mizokami et al., 2017). OCN also plays an important role in inflammation. The OCN treatment in obese mice could reduce substantially the expression of proinflammatory cytokines, chemokine, and inflammasome-related genes. Furthermore, OCN treatment prevents infiltration of lymphocytes and fibrosis and reduces the density of macrophages in crown-like structures (Guedes et al., 2018). Also, both carboxylated and uncarboxylated OCN increase secretion of adiponectin and the anti-inflammatory cytokine interleukin 10 (Hill et al., 2014). In this study, we found that the plasma level of OCN was increased, however, the CSF level of OCN was decreased in PD patients. This may be accounted for by the different roles of OCN in peripheral circulation and the central nervous system. Given the role of OCN in protecting dopaminergic neurons, improving cognition, and preventing anxiety and depression the low expression level of OCN in CSF indicates its involvement in motor and non-motor symptoms of PD. Plasma level of OCN correlated with CRP and H-Y stage of PD patients indicates inflammation may be a potential bridge between OCN and progression of PD. However, no correlation was identified between OCN and CRP in CSF, indicating that other mechanisms are involved in PD in the central nervous system. Furthermore, compared to analyzing plasma or CSF OCN alone, the combined assessment is more effective in differentiating PD patients from HCs, and the plasma level of OCN was correlated with the disease stage and motor impairment. All these results highlight the essential roles of OCN in the pathology of PD.

OPN is a glycosylated phosphoprotein belonging to the small integrin-binding ligand, N-linked glycoprotein (SIBLING) family of proteins (Pang et al., 2019). It is highly expressed by bone marrow-derived myelomonocytic cells and can act both as a matrix protein and as a cytokine. As a multifunctional protein, OPN plays significant roles in regulating reactive oxygen species production, levels of inflammatory cytokines, and apoptotic signals (Rentsendorj et al., 2018). OPN was reported to be involved in the pathology of various brain diseases, such as Alzheimer's disease (AD), multiple sclerosis, and traumatic brain injury *via* neuroprotective and repair-promoting effects (Carecchio and Comi, 2011; Rentsendorj et al., 2018). In PD, the function of OPN mainly derives from its anti-inflammatory and anti-apoptotic properties, as well as its role in regulating reactive oxygen species (ROS) production, and cytokine levels (Khan et al., 2002; Lund et al., 2009; Rittling and Singh, 2015). Also, OPN is expressed in SN and in nigral dopaminergic neurons (DAs) and its expression is decreased in surviving dopaminergic neurons in PD, suggesting a potential role of OPN in neuroprotection of PD. Further study showed that the arginine-glycine-aspartic acid (RGD)-containing domain of OPN, could protect tyrosine hydroxylase (TH)-positive cells against toxic insult induced by MPP^+ and LPS, indicating that this peptide fragment of OPN may be necessary for the survival of TH cells and have neuroprotective properties relevant to Parkinson's disease (Iczkiewicz et al., 2010). However, OPN knockout mice displayed less nigral cell death and a decreased glial response in a 1-methyl-4-phenyl-1,2,3,6-tetrahydropyridine (MPTP) induced animal model of PD (Maetzler et al., 2007; Carecchio and Comi, 2011). This suggests that OPN may act as a double-edged sword triggering neuronal toxicity or functioning as a neuroprotectant in PD. The inflammatory response may be one of the mechanisms of OPN in PD as there is a significant correlation between OPN and CRP. Maetzler et al. (2007) have reported that OPN was upregulated both in the plasma and CSF of PD patients, however, we only identified a higher level of OCN in the plasma of PD patients. The incongruence might be owing to the difference in disease stage, ethnic or environmental factors and more studies are needed to reveal the function of OPN in PD.

OPG is a tumor necrosis factor (TNF) receptor superfamily protein and expressed mainly by bone marrow stromal cells, but can also be induced in B lymphocytes and dendritic cells (Schoppet et al., 2007; Li et al., 2014). OPG plays essential roles in receptor activator of nuclear factor kappa-B (NF-kB) ligand (RANKL)–receptor activator of NF-κB (RANK)–OPG axis to regulate bone metabolisms, organogenesis, immune tolerance, and cancer (Walsh and Choi, 2014). In this study, although OPG may not be a biomarker for PD, the decreased levels of OPG in the plasma and CSF of PD patients indicated its involvement in the pathophysiology of the disease. In a small sample size study (N = 26), the serum levels of OPG were higher in PD patients than in controls (P = 0.04); (Alrafiah et al., 2019). However, in an animal model of AD, the plasma levels of OPG were down-regulated (Ali et al., 2019). The different results may be due to the sample size, disease severity, or detection sensitivity, and further investigations with a larger sample size are required to verify the findings of the present study.

BMP2 is a transforming growth factor-β (TGF-β) superfamily protein that plays significant roles in skeletal development, anti-inflammatory, and embryonic development (Grgurevic et al., 2016). In PD, BMP2 can facilitate the transformation of neural stem cells to DAs and promote neurite growth (Jordan et al., 1997). BMP2 overexpression can protect against neurotoxin-induced or A53T-α-synuclein-induced DAs degeneration by canonical sma and mothers against decapentaplegic (Smad) signaling pathway (Goulding et al., 2019). In this study, we found that BMP2 was downregulated in the plasma of PD patients than in HCs. All these results indicate that BMP2 may act as a neurotrophic factor for PD.

In conclusion, we analyzed six bone-derived factors and revealed abnormal expression levels of OCN, OPN, OPG, and BMP2 in plasma or CSF of PD. We identified that plasma levels of OCN and OPN were correlated with CRP, H-Y stage, and motor impairment. Our study also suggests that combined assessment of plasma and CSF of OCN may enhance their potential for predicting PD. Inflammation response may be

involved in the cross-talk between these two factors and PD. These findings may contribute to the functional understanding of PD pathophysiology. However, further studies are needed to confirm our findings and to illustrate the roles of inflammation or immune mechanisms involved in the factors on PD.

DATA AVAILABILITY STATEMENT

The originale contributions presented in the study are included in the article, further inquiries can be directed to the corresponding authors.

ETHICS STATEMENT

The studies involving human participants were reviewed and approved by Medical Ethics Committee of The First Affiliated Hospital of Guangzhou Medical University. The patients/participants provided their written informed consent to participate in this study.

AUTHOR CONTRIBUTIONS

PX and ZW: research project conception. XC and MM: research project organization. YL, MZ, WD, JQ, LD, and PY: research project execution. WG, YW, ZZ, and MM: statistical analysis execution. ZW and XZ: statistical analysis—review and critique. XC: manuscript—writing of the first draft. ZW and PX: manuscript—review and critique. All authors read and approved the final manuscript.

FUNDING

This article was supported by National Key R&D Program of China (2016YFC1306601 and 2017YFC1306002), National Natural Science Foundation of China (81901282, 81870992, 81870856, U1603281, 81771891, 81401462, 82071444, and 82071416), Guangdong Basic and Applied Basic Research Foundation (2019A1515011189, 2020A1515010986, and 2020A1515010985), Science and Technology Planning Project of Guangdong Province (A2018315), Technology Project of Guangzhou (2018-1202-SF-0019), and Key project of Guangzhou Health Commission (2019-ZD-09).

SUPPLEMENTARY MATERIAL

The Supplementary Material for this article can be found online at: https://www.frontiersin.org/articles/10.3389/fnagi.2021.634213/full#supplementary-material.

REFERENCES

Ali, A. A., Abo, E. D., El-Emam, S. Z., Shahat, A. S., and El-Sayed, R. M. (2019). Physical & mental activities enhance the neuroprotective effect of vinpocetine & coenzyme Q10 combination against Alzheimer & bone remodeling in rats. *Life Sci.* 229, 21–35. doi: 10.1016/j.lfs.2019.05.006

Alrafiah, A., Al-Ofi, E., Obaid, M. T., and Alsomali, N. (2019). Assessment of the levels of level of biomarkers of bone matrix glycoproteins and inflammatory cytokines from saudi Parkinson patients. *Biomed. Res. Int.* 2019:2690205. doi: 10.1155/2019/2690205

Bradburn, S., McPhee, J. S., Bagley, L., Sipila, S., Stenroth, L., Narici, M. V., et al. (2016). Association between osteocalcin and cognitive performance in healthy older adults. *Age Ageing* 45, 844–849. doi: 10.1093/ageing/afw137

Camacho-Soto, A., Gross, A., Searles, N. S., Miller, A. N., Warden, M. N., Salter, A., et al. (2020). Fractures in the prodromal period of Parkinson disease. *Neurology* 94, e2448–e2456. doi: 10.1212/WNL.0000000000009452

Carecchio, M., and Comi, C. (2011). The role of osteopontin in neurodegenerative diseases. *J. Alzheimers Dis.* 25, 179–185. doi: 10.3233/JAD-2011-102151

Choi, S. M., Kim, B. C., Jung, H. J., Yoon, G. J., Kang, K. W., Choi, K. H., et al. (2017). The association of musculoskeletal pain with bone mineral density in patients with Parkinson's disease. *Eur. Neurol.* 77, 123–129. doi: 10.1159/000455009

Garcia-Olivares, J., Baust, T., Harris, S., Hamilton, P., Galli, A., Amara, S. G., et al. (2017). Gbetagamma subunit activation promotes dopamine efflux through the dopamine transporter. *Mol. Psychiatry* 22, 1673–1679. doi: 10.1038/mp.2017.176

Goulding, S. R., Sullivan, A. M., O'Keeffe, G. W., and Collins, L. M. (2019). Gene co-expression analysis of the human substantia nigra identifies BMP2 as a neurotrophic factor that can promote neurite growth in cells overexpressing wild-type or A53T alpha-synuclein. *Parkinsonism Relat. Disord.* 64, 194–201. doi: 10.1016/j.parkreldis.2019.04.008

Grgurevic, L., Christensen, G. L., Schulz, T. J., and Vukicevic, S. (2016). Bone morphogenetic proteins in inflammation, glucose homeostasis and adipose tissue energy metabolism. *Cytokine Growth Factor Rev.* 27, 105–118. doi: 10.1016/j.cytogfr.2015.12.009

Guedes, J., Esteves, J. V., Morais, M. R., Zorn, T. M., and Furuya, D. T. (2018). Osteocalcin improves insulin resistance and inflammation in obese mice: participation of white adipose tissue and bone. *Bone* 115, 68–82. doi: 10.1016/j.bone.2017.11.020

Guo, X. Z., Shan, C., Hou, Y. F., Zhu, G., Tao, B., Sun, L. H., et al. (2018). Osteocalcin ameliorates motor dysfunction in a 6-Hydroxydopamine-induced Parkinson's disease rat model through AKT/GSK3β signaling. *Front. Mol. Neurosci.* 11:343. doi: 10.3389/fnmol.2018.00343

Hill, H. S., Grams, J., Walton, R. G., Liu, J., Moellering, D. R., and Garvey, W. T. (2014). Carboxylated and uncarboxylated forms of osteocalcin directly modulate the glucose transport system and inflammation in adipocytes. *Horm. Metab. Res.* 46, 341–347. doi: 10.1055/s-0034-1368709

Iczkiewicz, J., Broom, L., Cooper, J. D., Wong, A. M., Rose, S., and Jenner, P. (2010). The RGD-containing peptide fragment of osteopontin protects tyrosine hydroxylase positive cells against toxic insult in primary ventral mesencephalic cultures and in the rat substantia nigra. *J. Neurochem.* 114, 1792–1804. doi: 10.1111/j.1471-4159.2010.06896.x

Jordan, J., Bottner, M., Schluesener, H. J., Unsicker, K., and Krieglstein, K. (1997). Bone morphogenetic proteins: neurotrophic roles for midbrain dopaminergic neurons and implications of astroglial cells. *Eur. J. Neurosci.* 9, 1699–1709. doi: 10.1111/j.1460-9568.1997.tb01527.x

Khan, S. A., Lopez-Chua, C. A., Zhang, J., Fisher, L. W., Sorensen, E. S., and Denhardt, D. T. (2002). Soluble osteopontin inhibits apoptosis of adherent endothelial cells deprived of growth factors. *J. Cell. Biochem.* 85, 728–736. doi: 10.1002/jcb.10170

Khrimian, L., Obri, A., Ramos-Brossier, M., Rousseaud, A., Moriceau, S., Nicot, A. S., et al. (2017). Gpr158 mediates osteocalcin's regulation of cognition. *J. Exp. Med.* 214, 2859–2873. doi: 10.1084/jem.20171320

Li, Y., Terauchi, M., Vikulina, T., Roser-Page, S., and Weitzmann, M. N. (2014). B cell production of both OPG and RANKL is significantly increased in aged mice. *Open Bone J.* 6, 8–17. doi: 10.2174/1876525401406010008

Lund, S. A., Giachelli, C. M., and Scatena, M. (2009). The role of osteopontin in inflammatory processes. *J. Cell. Commun. Signal.* 3, 311–322. doi: 10.1007/s12079-009-0068-0

Maetzler, W., Berg, D., Schalamberidze, N., Melms, A., Schott, K., Mueller, J. C., et al. (2007). Osteopontin is elevated in Parkinson's disease and its absence leads

to reduced neurodegeneration in the MPTP model. *Neurobiol. Dis.* 25, 473–482. doi: 10.1016/j.nbd.2006.10.020

Metta, V., Sanchez, T. C., and Padmakumar, C. (2017). Osteoporosis: a hidden nonmotor face of Parkinson's disease. *Int. Rev. Neurobiol.* 134, 877–890. doi: 10.1016/bs.irn.2017.05.034

Mizokami, A., Kawakubo-Yasukochi, T., and Hirata, M. (2017). Osteocalcin and its endocrine functions. *Biochem. Pharmacol.* 132, 1–8. doi: 10.1016/j.bcp.2017.02.001

Moser, S. C., and van der Eerden, B. (2018). Osteocalcin-a versatile bone-derived hormone. *Front. Endocrinol.* 9:794. doi: 10.3389/fendo.2018.00794

Pang, X., Gong, K., Zhang, X., Wu, S., Cui, Y., and Qian, B. Z. (2019). Osteopontin as a multifaceted driver of bone metastasis and drug resistance. *Pharmacol. Res.* 144, 235–244. doi: 10.1016/j.phrs.2019.04.030

Puig, J., Blasco, G., Daunis-i-Estadella, J., Moreno, M., Molina, X., Alberich-Bayarri, A., et al. (2016). Lower serum osteocalcin concentrations are associated with brain microstructural changes and worse cognitive performance. *Clin. Endocrinol.* 84, 756–763. doi: 10.1111/cen.12954

Redmond, J., Fulford, A. J., Jarjou, L., Zhou, B., Prentice, A., and Schoenmakers, I. (2016). Diurnal rhythms of bone turnover markers in three ethnic groups. *J. Clin. Endocrinol. Metab.* 101, 3222–3230. doi: 10.1210/jc.2016-1183

Rentsendorj, A., Sheyn, J., Fuchs, D. T., Daley, D., Salumbides, B. C., Schubloom, H. E., et al. (2018). A novel role for osteopontin in macrophage-mediated amyloid-beta clearance in Alzheimer's models. *Brain Behav. Immun.* 67, 163–180. doi: 10.1016/j.bbi.2017.08.019

Rittling, S. R., and Singh, R. (2015). Osteopontin in immune-mediated diseases. *J. Dent. Res.* 94, 1638–1645. doi: 10.1177/0022034515605270

Schoppet, M., Henser, S., Ruppert, V., Stubig, T., Al-Fakhri, N., Maisch, B., et al. (2007). Osteoprotegerin expression in dendritic cells increases with maturation and is NF-κB-dependent. *J. Cell. Biochem.* 100, 1430–1439. doi: 10.1002/jcb.21129

Shan, C., Ghosh, A., Guo, X. Z., Wang, S. M., Hou, Y. F., Li, S. T., et al. (2019). Roles for osteocalcin in brain signalling: implications in cognition- and motor-related disorders. *Mol. Brain* 12:23. doi: 10.1186/s13041-019-0444-5

Walsh, M. C., and Choi, Y. (2014). Biology of the RANKL-RANK-OPG System in Immunity, Bone and Beyond. *Front. Immunol.* 5:511. doi: 10.3389/fimmu.2014.00511

Wei, J., and Karsenty, G. (2015). An overview of the metabolic functions of osteocalcin. *Rev. Endocr. Metab. Disord* 16, 93–98. doi: 10.1007/s11154-014-9307-7

Xu, Y., Ma, X., Pan, X., He, X., Xiao, Y., and Bao, Y. (2018). Correlations between serum concentration of three bone-derived factors and obesity and visceral fat accumulation in a cohort of middle aged men and women. *Cardiovasc. Diabetol.* 17:143. doi: 10.1186/s12933-018-0786-9

Conflict of Interest: The authors declare that the research was conducted in the absence of any commercial or financial relationships that could be construed as a potential conflict of interest.

Copyright © 2021 Lin, Zhou, Dai, Guo, Qiu, Zhang, Mo, Ding, Ye, Wu, Zhu, Wu, Xu and Chen. This is an open-access article distributed under the terms of the Creative Commons Attribution License (CC BY). The use, distribution or reproduction in other forums is permitted, provided the original author(s) and the copyright owner(s) are credited and that the original publication in this journal is cited, in accordance with accepted academic practice. No use, distribution or reproduction is permitted which does not comply with these terms.

frontiers in Aging Neuroscience

ORIGINAL RESEARCH
published: 03 March 2021
doi: 10.3389/fnagi.2021.638718

Preanalytical Stability of CSF Total and Oligomeric Alpha-Synuclein

*Ilham Y. Abdi[1†], Nour K. Majbour[1†], Eline A. J. Willemse[2], Wilma D. J. van de Berg[3], Brit Mollenhauer[4,5], Charlotte E. Teunissen[2] and Omar M. El-Agnaf[1]**

[1]Neurological Disorders Research Centre, Qatar Biomedical Research Institute (QBRI), Hamad Bin Khalifa University (HBKU), Doha, Qatar, [2]Neurochemistry Laboratory, Department of Clinical Chemistry, Amsterdam Neuroscience, Amsterdam University Medical Center, Amsterdam, Netherlands, [3]Section Clinical Neuroanatomy and Biobanking, Department of Anatomy and Neurosciences, Amsterdam Neuroscience, Amsterdam University Medical Center, Vrije University Amsterdam, Amsterdam, Netherlands, [4]Paracelsus-Elena-Klinik, Klinikstraße, Kassel, Germany, [5]Department of Neurology, University Medical Center Göttingen, Göttingen, Germany

Background: The role of cerebrospinal fluid (CSF) alpha-synuclein as a potential biomarker has been challenged mainly due to variable preanalytical measures between laboratories. To evaluate the impact of the preanalytical factors contributing to such variability, the different subforms of alpha-synuclein need to be studied individually.

Method: We investigated the effect of exposing CSF samples to several preanalytical sources of variability: (1) different polypropylene (PP) storage tubes; (2) use of non-ionic detergents; (3) multiple tube transfers; (4) multiple freeze-thaw cycles; and (5) delayed storage. CSF oligomeric- and total-alpha-synuclein levels were estimated using our in-house sandwich-based enzyme-linked immunosorbent assays.

Results: Siliconized tubes provided the optimal preservation of CSF alpha-synuclein proteins among other tested polypropylene tubes. The use of tween-20 detergent significantly improved the recovery of oligomeric-alpha-synuclein, while multiple freeze-thaw cycles significantly lowered oligomeric-alpha-synuclein in CSF. Interestingly, oligomeric-alpha-synuclein levels remained relatively stable over multiple tube transfers and upon delayed storage.

Conclusion: Our study showed for the first-time distinct impact of preanalytical factors on the different forms of CSF alpha-synuclein. These findings highlight the need for special considerations for the different forms of alpha-synuclein during CSF samples' collection and processing.

Keywords: preanalytical factors, alpha-synuclein, oligomers, cerebrospinal fluid, biomarkers

OPEN ACCESS

Edited by:
Pingyi Xu,
First Affiliated Hospital of Guangzhou Medical University, China

Reviewed by:
Davide Chiasserini,
University of Perugia, Italy
Andrii Domanskyi,
Orion Corporation (Finland), Finland
Hengxu Mao,
Southern Medical University, China

****Correspondence:***
Omar M. El-Agnaf
oelagnaf@hbku.edu.qa

†These authors share first authorship

Received: *07 December 2020*
Accepted: *08 February 2021*
Published: *03 March 2021*

Citation:
Abdi IY, Majbour NK, Willemse EAJ, van de Berg WDJ, Mollenhauer B, Teunissen CE and El-Agnaf OM (2021) Preanalytical Stability of CSF Total and Oligomeric Alpha-Synuclein. Front. Aging Neurosci. 13:638718. doi: 10.3389/fnagi.2021.638718

INTRODUCTION

A vast majority of studies done on neurological disorders use cerebrospinal fluid (CSF) as the biofluid of choice to explore and assess biomarkers as CSF protein levels most closely reflect the pathophysiology of the brain (Robey and Panegyres, 2019). A major subset of these neurodegenerative disorders, referred to as "synucleinopathies," is hallmarked by the deposition

of the cytoplasmic protein alpha-synuclein (α-syn) as aberrant inclusions in neurons and glial cells in the brain (Spillantini et al., 1998). Levels of different forms of α-syn in CSF have been widely investigated in several studies as potential biomarkers of synuclein aggregation disorders. Most studies that sought to explore α-syn as a biomarker focused on total α-syn (t-α-syn) levels either alone or in combination with other biomarkers with more recent studies looking at modified forms of α-syn such as oligomeric (o-α-syn) and phosphorylated α-syn at Ser 129 (pS129-α-syn) (Mollenhauer et al., 2008, 2013; Parnetti et al., 2011, 2014a,b, 2019; Majbour et al., 2016, 2020)

However, despite the growing number of studies investigating CSF α-syn biomarkers, it remains a challenge to use these biomarkers in routine diagnostic or prognostic procedures as they lack the required accuracy (sensitivity and specificity) (Wang et al., 2015; Eusebi et al., 2017). Impaired biomarker standardization has been attributed to several possible confounding factors such as inter-individual variations in CSF protein measures or clinical heterogeneity, medications, blood contamination, assays protocols, and preanalytical variations (Kang et al., 2016; Ming et al., 2016; Mollenhauer et al., 2017a,b, 2019; Willemse et al., 2019; Barkovits et al., 2020). Preanalytical factors are defined as the variables present before biomarker assessment influencing its precise evaluation (Guder, 2014). Little is yet known about the influence of these preanalytical factors on CSF α-syn measurements (Stewart et al., 2019). In the current study, we aim to understand the stability of CSF α-syn biomarkers, mainly t-α-syn and o-α-syn, against potential preanalytical factors that occur during CSF handling and processing. The novelty of this study lies in it being the first to specifically look at o-α-syn stability in CSF, which is important as growing evidence suggest that it plays an important role in the pathogenesis of synuclein aggregation disorders and may even be a better marker compared to t-α-syn (El-Agnaf et al., 2003; Park et al., 2011; Majbour et al., 2016; Williams et al., 2016; Volc et al., 2020).

MATERIALS AND METHODS

CSF Sample Collection

Anonymous CSF samples that had inadequate clinical information or were not fit for clinical validation were collected from Alzheimer Center Biobank at the VU University Medical Center (VUmc, Amsterdam, The Netherlands) and University Medical Center (Göttingen, Germany). The samples were pooled and aliquoted as 500 µl aliquots. Samples collected from the Biobank at VUmc were used in α-syn stability and adsorption experiments while those from University Medical Center Göttingen were used in investigations done on adsorption of α-syn. Aliquots were stored at −80°C in 1.5 ml polypropylene tubes with screw caps (Sarstedt, Nümbrecht, Germany). All samples were blinded, and donors gave written informed consent at study entry for the use of clinical information and CSF material for scientific research purposes. The study was conducted according to the revised Declaration of Helsinki and Good Clinical Practice guidelines and approved by the local ethics committee of the VU University Medical Center.

Samples Processing and Treatment

Adsorption to Surface Walls of Storage Tubes

To assess the extent of adsorption of α-syn to the surface walls of storage tubes, three experimental approaches were followed: (1) we tested the difference in α-syn levels when using six different polypropylene (PP) types from different vendors (see **Table 1** for tube information) compared to Nunc tubes (NUNC, Rochester, NY, USA) used as control. The main samples stocks were thawed on ice and aliquoted into the different tubes and frozen back overnight at −80°C before testing the next day; (2) we looked to observe the effect of using non-ionic detergents by measuring α-syn levels in the presence and absence of 0.05% of Tween-20, Triton X-100, or NP-40 detergents. The detergent treatments were added after thawing CSF samples and then incubated at 4°C for 30 min before testing; and (3) lastly, CSF samples were exposed to up to six tube transfers before quantification with thorough mixing between transfers to measure the difference in α-syn levels following the multiple tube transfers (reference sample-no tube transfer). For all experiments except those testing different polypropylene tubes, Sarstedt 0.5 ml polypropylene tubes were used.

Alpha-Synuclein Stability-Freeze-Thaw Cycles and Delayed Storage

CSF pools were aliquoted into 19 (Sarstedt-0.5 ml) tubes per set (n = 3). The first five tubes of each set were subjected to 1–7 freeze-thaw cycles (reference sample-1 freeze-thaw cycle). The remaining tubes were split into two sets which were then exposed to delayed storage times: 1, 2, 4, 24, 72, or 168 h at either 4°C or room temperature (RT) before finally storing them at −80°C (the reference sample, t = 0, was directly stored at −80°C).

Oligomeric- and Total- Alpha-Synuclein Quantification

CSF total and oligomeric α-syn levels were measured using our previously described ELISA assays (Majbour et al., 2016). Briefly, 384-well Maxisorb (Nunc) microplates were coated with 0.1 µg/ml Syn-140 (sheep anti-α-syn polyclonal antibody against t-α-syn), or 0.2 µg/ml Syn-O_2 (o-α-syn specific monoclonal antibody) at 50 µl/well in 200 mM $NaHCO_3$, pH 9.6 and incubated overnight at 4°C. Plates were washed thrice in phosphate-buffered saline with 0.05% Tween-20 (PBST) then blocked with 100 µl/well of blocking buffer (PBST with 2.5% gelatin) for 2 h at 37°C. After washing plates again, CSF samples and assay standards prepared as serial dilutions of recombinant human α-syn and o-α-syn in artificial CSF were added to the plates in duplicates at 50 µl/well and incubated at 37°C for 2.5 h. Detection antibodies, 11D12 (mouse anti-α-syn monoclonal antibody) against t-α-syn and FL-140 (rabbit polyclonal antibody, Santa Cruz Biotechnology, Santa Cruz, CA, USA) against o-α-syn were used at the diluted concentration of 1:5,000 and 1:1,000, respectively. Following a washing step, 50 µl/well of species-appropriate secondary antibodies: donkey anti-mouse IgG HRP or goat anti-rabbit IgG HRP (Jackson Immuno Research, West Grove, PA, USA), was added to the respective plates at the diluted concentration of 1:20,000 and incubate at 37°C for 2 h. After a final wash, the plates

TABLE 1 | Summary information of polypropylene tubes.

Vendor	Catalog no.	Volume (ml)	Specifications
Nunc (reference tubes)	368632	1.8	Sterile, screw cap, non-pyrogenic, cryovial
Denville scientific	C19063	0.6	Silicon-coated, sterile. Enzyme and DNA free
Corning	430791	15	Sterile, screw cap, RNase, DNase free and non-pyrogenic
Sarstedt	72.730.005	0.5	Sterile, screw cap
Eppendorf	0030.120.086	1.5	Safe-lock, sterile, free of pyrogen, RNase, DNA and ATP. Autoclavable.
Extragene	104571010	1.5	Non-sterile, flip cap, DNase and RNase and Pyrogen safe
Costar	3213	2	Snap Cap, Non-sterile

were incubated with an enhanced chemiluminescent substrate (SuperSignal ELISA Femto, Pierce Biotechnology, Rockford, IL, USA; 50 µl/well). The chemiluminescence (relative light units) was immediately measured using a PerkinElmer Envision multilabel plate reader (PerkinElmer, Finland).

Data Analysis

Standard calibrator curves for ELISA assays were fitted using the sigmoidal, 4PL, nonlinear regression model, where X = log(concentration), and CSF α-syn concentrations were calculated by interpolating from the curves. The generated figures and as well as the calculations used to establish the curves generated and determine α-syn concentrations were carried out using GraphPad Prism 7.0. The variations in the α-syn concentration due to the type of storage tube used, repeated freeze-thaw cycles and tube transfers, and delayed storage are expressed as mean percentage change compared to the values of the reference samples. Normality tests were not productive due to the small sample size hence the statistical significance of observed variations was assessed through non-parametric analysis of variance (ANOVA) in repeated measures (Friedman's test) followed by post-test Dunn's multiple comparison tests compared to one control reference value using GraphPad Prism. A *p-value* < 0.05 was regarded as statistically significant. However, given the small sample size statistical values may not reach significance therefore a change of >20% from reference values was also considered relevant.

RESULTS

To investigate the preanalytical variations due to non-specific binding of α-syn species to storage tubes, the effect of different types of polypropylene tubes, use of non-ionic detergents, and multiple tube transfers on measured t- and o- α-syn concentrations was tested. The stability of the α-syn species (t- and o-α-syn) against multiple freeze-thaw cycles and delayed storage was also tested.

Siliconized Tubes Showed the Least Adsorption for Both Total- and Oligomeric-α-syn Levels

Three CSF pools were distributed and incubated in six types of polypropylene tubes from different vendors (**Table 1**) then measured for the t- and o-α-syn concentrations. Results in **Figure 1** are expressed as the percentage reduction in t- and o-α-syn levels in the six tube types relative to the control storage tube Nunc tubes (NUNC, Rochester, NY, USA). Siliconized

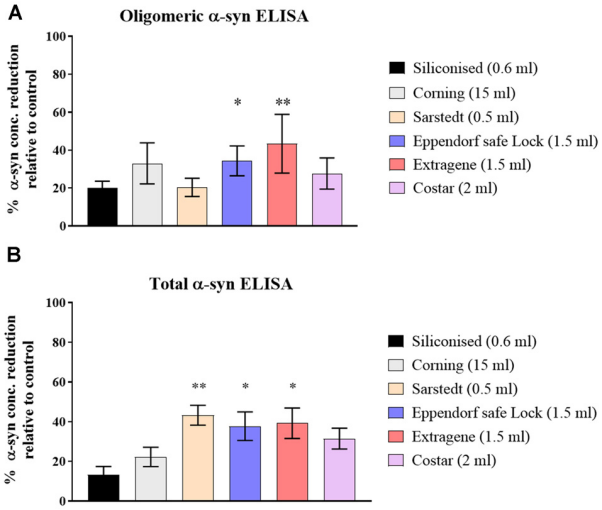


FIGURE 1 | Assessment of α-syn levels in different collection tube types. **(A)** O-α-syn, **(B)** t-α-syn levels in samples collected in different types of polypropylene (PP) tubes relative to control tube type (Nunc-1.8ml). Measurements were taken in duplicates from three cerebrospinal fluid (CSF) samples and results are expressed as the mean percentage reduction in CSF α-syn levels relative to control (Nunc tube). Error bars indicate standard error of the mean (± SEM). $^{**}p < 0.01$; $^{*}p < 0.05$.

polypropylene tubes showed the least reduction in both o-α-syn (19.5 ± 2.1% reduction) and t-α-syn (13.5 ± 7.8% reduction) concentrations. However, the results showed that the different types of storage tubes affect the levels of the two α-syn species differently. Samples incubated in Sarstedt tubes showed the second-lowest reduction in o-α-syn levels (22.5 ± 0.7%) nearly similar to levels recovered when siliconized polypropylene tubes were used whereas using the same Sarstedt tubes, a significant reduction in t-α-syn levels (44% reduction, $p = 0.003$) was observed. For measurements of both t- and o-α-syn levels, the use of Eppendorf Safe Lock, and Extragene tubes showed a significant reduction in the measured levels by 23 ± 4.2% ($p = 0.025$) and 35 ± 2.8% ($p = 0.042$) for t-α-syn and by 34 ± 13.4% ($p = 0.049$) and 51.5 ± 0.7% ($p = 0.004$) for o-α-syn levels, respectively.

The Use of Non-ionic Detergent Decreased Adsorption and Improved Sample Recovery

Treating CSF samples with non-ionic detergent showed a significant increase of 49.2 ± 3.2% in recovered o-α-syn for

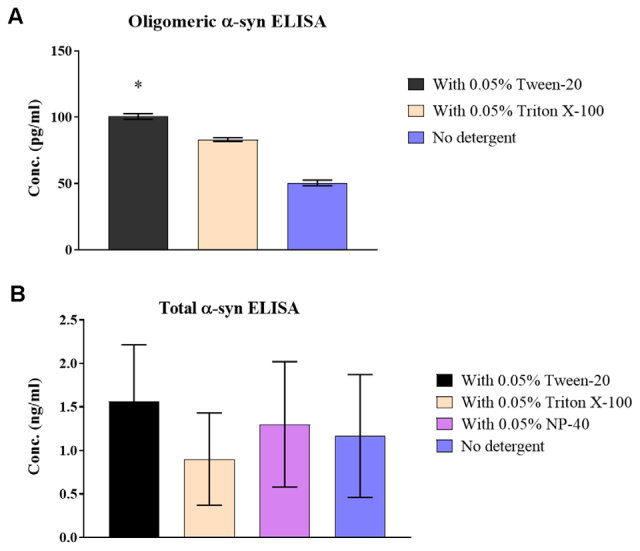


FIGURE 2 | Effect of non-ionic detergents on α-syn levels in samples. **(A)** O-α-syn, **(B)** t-α-syn concentration levels in CSF samples treated with non-ionic detergents Tween-20, Triton X-100, and NP-40 (total α-syn ELISA only) compared to no treatment. Results are expressed as the mean of duplicate measurements (n = 3) and error bars indicate the standard error of the mean (±SEM). *$p < 0.05$.

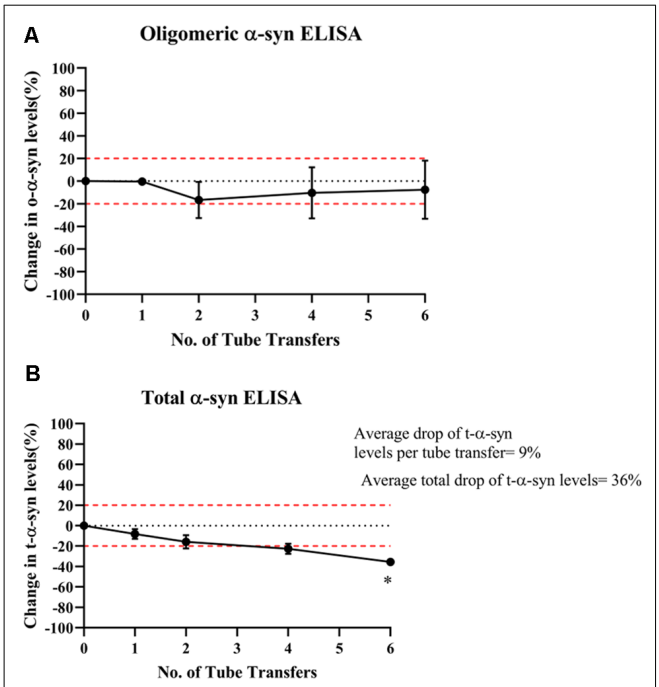


FIGURE 3 | Effect of multiple tube transfers on α-syn levels in samples. **(A)** O-α-syn, **(B)** t-α-syn levels in CSF samples subjected to multiple tube transfers. Measurements were taken in duplicates from three CSF samples and results are expressed as the mean percentage change in CSF α-syn levels. Error bars indicate the standard error of the mean. Red dotted lines represent reference lines at ±20% of the reference value. *$p < 0.05$.

Tween-20 treated samples (p = 0.046) while levels Triton X-100 treated samples increased by 39.2 ± 3.2% although statistical significance was not reached (**Figure 2A**). T-α-syn levels however showed variability in results with no clear effect of non-ionic detergents on protein recovery (**Figure 2B**).

Multiple Tube Transfers Decreased Total-α-syn Levels Measured Due to Adsorption to Tube Walls

In contrast, o-α-syn levels remained relatively stable following multiple tube transfers (**Figure 3A**) whereas t-α-syn steadily decreased by an average of 9% reduction per tube transfer with the statistically significant difference observed after at 6 tube transfers (p = 0.018; **Figure 3B**).

Multiple Freeze-Thaw Cycles Significantly Decreased Levels of Oligomeric-α-syn Measured in Samples

O-α-syn levels significantly decreased by 34% after the fourth thaw cycle and continued significantly decreasing with each cycle to a total drop of 42% after seven cycles (p=0.021; **Figure 4A**). However, levels of t-α-syn remained stable against freeze-thaw cycles (**Figure 4B**).

Delayed Storage Had Little or No Impact on α-syn Measured in Samples

Oligomeric-α-syn levels remained relatively stable despite a delay in sample storage (**Figure 5A**). While a gradual decrease in the measured t-α-syn concentration was observed with prolonged delay in storing samples at −80°C by keeping in RT with the decrease exceeding 20% reduction after 24 h however statistical significance was not reached (**Figure 5B**). α-syn measurements of samples kept at RT compared to those kept at 4°C prior storage at −80°C, showed no significant difference between both conditions, which could be attributed to the high variability in α-syn levels between samples.

DISCUSSION

The present study investigates preanalytical considerations for CSF t- and o-α-syn measurements, specifically the impact of potential confounding factors that can occur during sample handling, processing, and storage. To the best of our knowledge, similar studies were limited to analyzing the effect of preanalytical confounding factors on t-α-syn measurements but not o-α-syn CSF levels. This is important considering recent studies have shown improved diagnostic accuracy when combining multiple forms of α-syn, mainly the ratios of o- and pS129- α-syn to t-α-syn (Majbour et al., 2016).

First, we explored the non-specific binding or adsorption of α-syn to the storage tube surface. Studies have investigated this effect in Alzheimer's disease biomarkers, particularly in $A\beta_{1-42}$ peptide which has a hydrophobic C-terminal making it more prone to aggregate and bind non-specifically to the tube surface (Lewczuk et al., 2006; Pica-Mendez

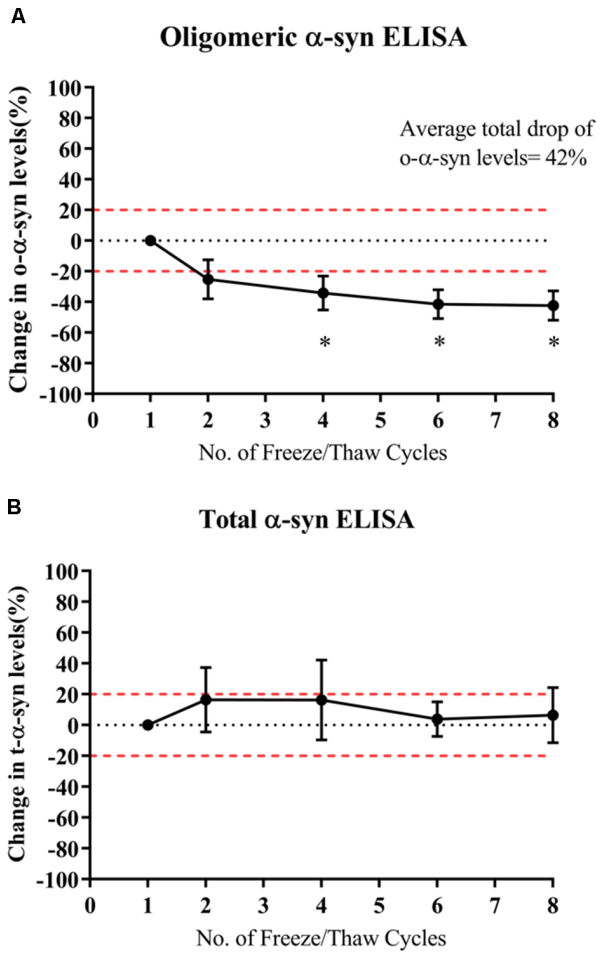


FIGURE 4 | Effect of multiple freeze-thaw cycles on α-syn levels in samples. **(A)** O-α-syn, **(B)** t-α-syn levels in CSF samples subjected to multiple freeze-thaw cycles. Measurements were taken in duplicates from three CSF samples expressed as a mean percentage change in CSF α-syn levels. Error bars indicate the standard error of the mean. Red dotted lines represent reference lines at ±20% of the reference value. *$p < 0.05$.

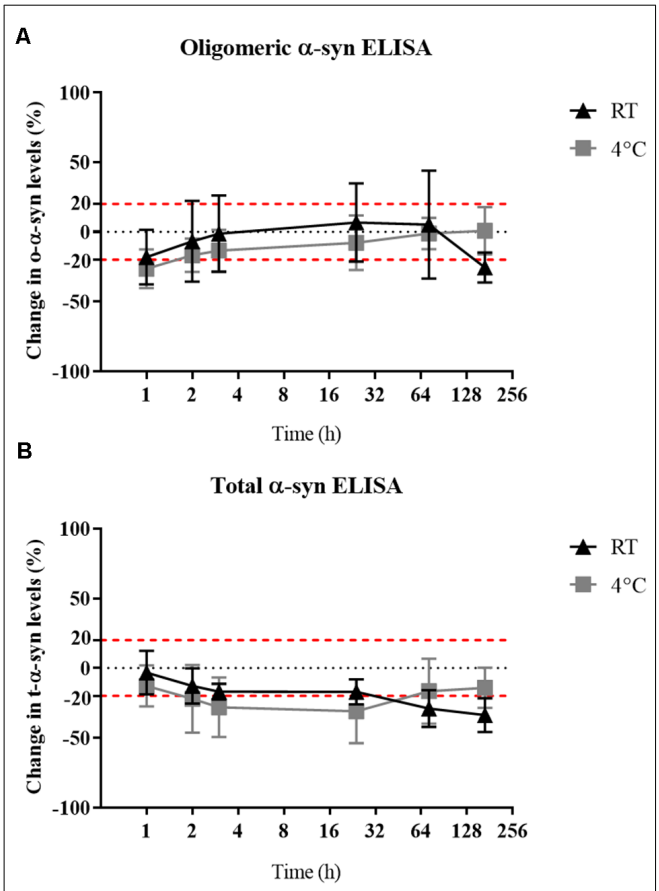


FIGURE 5 | Effect of delayed storage of samples on their α-syn levels. **(A)** O-α-syn, **(B)** t-α-syn levels in CSF samples delayed storage by: 0, 1, 2, 4, 24, 72, or 168 h at 4°C or room temperature (RT). Measurements were taken in duplicates from three CSF samples expressed as the mean percentage change in CSF α-syn levels. Error bars indicate the standard error of the mean. Red dotted lines represent reference lines at ±20% of the reference value.

et al., 2010; Perret-Liaudet et al., 2012). Similarly, α-syn protein in its aggregated form increases in hydrophobicity thereby increasing its propensity to be lipophilic and "sticky" (Breydo et al., 2012; Lee et al., 2018). As a result, α-syn could also be expected to adsorb to the storage tube surface.

According to recommended standards (Campo et al., 2012; Mollenhauer et al., 2017a) concerning storage tubes, we used Nunc PP tubes as reference tubes to test the effect of different PP tubes based on previously published work (Pica-Mendez et al., 2010). We demonstrated variable differences in CSF α-syn levels measured using PP tubes from different vendors. A similar observation was previously made in a study by Perret-Liaudet et al. (2012) for amyloid beta. They showed that PP tubes from different vendors resulted in different adsorption ratios despite the uniform use of polypropylene. A closer look revealed that the compositions of the tubes differed in that some were made from pure PP while others were co-polymers with other chemicals such as polyethylene (Perret-Liaudet et al., 2012). Our results showed that α-syn adsorption was largely attenuated by the use of siliconized polypropylene tubes, with a significant decrease in adsorption (∼20% and ∼25%) reduction of adsorption in siliconized tubes compared to other tubes for o- and t- α-syn levels, respectively. Silicone coating provides the tubes with a non-binding surface which significantly reduces adsorption of sticky proteins to the tube walls and low retention of protein in the tube (Chen et al., 2004). A trend of minimal retention of o-α-syn was noted when samples were stored in tubes with a smaller surface-volume ratio. This could be a factor influencing the adhesion of α-syn to storage tube walls as previous studies have reported that surface-volume ratio can potentially influence the measured concentrations of other CSF biomarkers (Vanderstichele et al., 2016; Delaby et al., 2019).

Previous studies showed the advantages of using non-ionic detergents such as Tween-20 in preventing loss of CSF amyloid proteins due to tube adsorption (Mollenhauer et al., 2008, 2017a; Pica-Mendez et al., 2010). In our study, the use of non-ionic detergents, Tween-20 and Triton X-100, was found to mitigate the magnitude of reduction in CSF o-α-syn levels, with Tween-20 detergent providing more effective results than Triton X-100 by at least 10%. Despite showing better stability against the different types of PP tubes, o-α-syn levels were remarkably affected by the absence of non-ionic detergents. It may be worth noting this observation as not solely a mechanism of reduced adsorption of o-α-syn but a possible result of effects of the detergents on the antibody-antigen complexes or formation of oligomers. Results of the non-ionic detergent effect on CSF t-α-syn levels were inconclusive due to the high variability noted among samples. Further experiments with a larger sample set are needed to better conclude the preventive impact provided by the use of detergents on CSF t-α-syn adsorption levels.

Examining the effect of multiple tube transfers, o-α-syn levels remained almost unaffected despite multiple tube transfers, while t-α-syn levels continuously declined with almost 36% of t-α-syn lost after the sixth transfer. Considering the capture and detection antibodies employed in our total ELISA (Syn-140, sheep anti-α-syn polyclonal antibody, and 11D12, mouse anti-α-syn monoclonal antibody) (Majbour et al., 2016), the assay measures monomers, aggregates, phosphorylated S129, and nitrated forms of α-syn. While our oligomeric ELISA, utilizing Syn-O2 (o-α-syn specific monoclonal antibody) for capture, measures aggregates of full-length α-syn. The differences between the impact of multiple tubes on the named analytes could be explained by the difference in the range of forms captured by each ELISA.

Investigating the stability of CSF α-syn over repeated freeze-thaw cycles is essential in dictating the conditions and methods used in storing CSF samples before testing. Results of our study show that t-α-syn levels are not affected by multiple freeze-thaw cycles whereas o-α-syn levels steadily decreased with each freeze-thaw cycle. However, another study demonstrated that t-α-syn levels declined with each cycle to up to 50% reduction after six cycles (Campo et al., 2012). Given the variability of reported results, it would be best to follow practices such as aliquoting CSF that have been recommended to avoid multiple freeze-thaw cycles and to not exceed two freeze-thaw cycles (Campo et al., 2012; Mollenhauer et al., 2017a).

In terms of α-syn stability against delayed sample storage, we found o-α-syn levels to be more stable than t-α-syn which showed a decrease in levels by 20% after 24 h of delayed storage, independent of the temperature the samples were kept during this delay. Previous reports showed a decrease in t-α-syn levels up to 40% when stored at 4°C for 4 days (Campo et al., 2012) while another study found no significant difference in α-syn levels in samples when exposed to prolonged delay in storage, 20 min–48 h, at either RT or 4°C after sample collection (Mollenhauer et al., 2017a). Samples frozen at −20°C for 1 month were stable and did not show a difference compared to reference samples directly frozen at −80°C (data not shown). The susceptibility of t-α-syn stability to delayed storage suggests the importance of sample handling guidelines stressing immediate processing and storage of samples.

To the best of our knowledge, this is the first study to assess the stability of o-α-syn along with t-α-syn against preanalytical confounding factors. The study also has some limitations: first, the lack of statistical power due to the small sample sets might have confounded our conclusions. Second, CSF sample pools from a biobank were used for our experiments. This meant that the samples used were already subjected to at least one freeze-thaw cycle and were stored long-term at −20 or −80°C before being exposed to our experimental conditions. Therefore, any alterations in α-syn chemistry that occurred due to this may have affected its stability and could not be assessed. Validation experiments to confirm the long-term stability of α-syn measurements after correct storage would be valuable to include in future studies.

CONCLUSION

Between lumbar puncture and laboratory analysis, collected CSF samples undergo variable sampling and storage methods, potentially different between individuals and sites processing the samples, which are often unknown to the scientists running the assays. We have investigated α-syn stability against these preanalytical variables and have shown that α-syn levels measured are affected, to different degrees, by the type of storage tube used, the addition of detergent, number of tube transfers, number of freeze-thaw cycles, and temperature and time to freeze. The impact of preanalytical factors was noticeably different between o- and t-α-syn forms, which means cautious awareness is required when analyzing the different forms. Our study revealed o-α-syn to be seemingly more stable, compared to t-α-syn, against most of the preanalytical variables tested, particularly adsorption to tube surface and delayed storage processing to −80°C. However, the opposite was noted when samples were exposed to multiple freeze-thaw cycles as t-α-syn levels remained stable while o-α-syn levels dropped considerably. In summary, the use of siliconized tubes, non-ionic detergents, immediate storage of samples, minimal freeze-thaw cycles, and tube-transfer provide the best preservation of t- and o-α-syn species. Our results emphasize the value of evaluating the impact of preanalytical factors on other subforms of α-syn emerging as potential biomarkers for synucleinopathies such as phosphorylated or truncated α-syn and employing different assessment methods such as protein misfolding cyclic amplification (PMCA) or Real-time quaking-induced conversion (RT-QuIC). Additionally, application studies assessing the correlation between the stability of α-syn forms and their impact on biomarkers studies would also be of great benefit to the research community.

DATA AVAILABILITY STATEMENT

The raw data supporting the conclusions of this article will be made available by the authors, without undue reservation.

AUTHOR CONTRIBUTIONS

NM and OE-A: study design and supervision. IA, NM and EW: conducting of the experiments. IA and NM: data analysis. IA: writing the first draft of the manuscript and incorporating revisions from other authors. IA, NM, WB, BM, CT and OE-A: data interpretation and critical revision of the manuscript for important intellectual content. OE-A: final review of the draft and approval to submit for publication. All authors contributed to the article and approved the submitted version.

FUNDING

This study was supported by Qatar Biomedical Research Institute.

ACKNOWLEDGMENTS

We would like to thank team members who provided technical support.

REFERENCES

Barkovits, K., Kruse, N., Linden, L., Tönges, L., Pfeiffer, K., Mollenhauer, B., et al. (2020). Blood contamination in CSF and its impact on quantitative analysis of α-synuclein. *Cells* 9:370. doi: 10.3390/cells9020370

Breydo, L., Wu, J. W., and Uversky, V. N. (2012). α-synuclein misfolding and Parkinson's disease. *Biochim. Biophys. Acta* 1822, 261–285. doi: 10.1016/j.bbadis.2011.10.002

Campo, M. D., Mollenhauer, B., Bertolotto, A., Engelborghs, S., Hampel, H., Simonsen, A. H., et al. (2012). Recommendations to standardize preanalytical confounding factors in Alzheimers and Parkinsons disease cerebrospinal fluid biomarkers: an update. *Biomark. Med.* 6, 419–430. doi: 10.2217/bmm.12.46

Chen, H., Brook, M. B., and Sheardown, H. (2004). Silicone elastomers for reduced protein adsorption. *Biomaterials* 25, 2273–2282. doi: 10.1016/j.biomaterials.2003.09.023

Delaby, C., Muñoz, L., Torres, S., Nadal, A., Bastard, N. L., Lehmann, S., et al. (2019). Impact of CSF storage volume on the analysis of Alzheimer's disease biomarkers on an automated platform. *Clin. Chim. Acta* 490, 98–101. doi: 10.1016/j.cca.2018.12.021

El-Agnaf, O. M. A., Walsh, D. M., and Allsop, D. (2003). Soluble oligomers for the diagnosis of neurodegenerative diseases. *Lancet Neurol.* 2, 461–462. doi: 10.1016/s1474-4422(03)00481-2

Eusebi, P., Giannandrea, D., Biscetti, L., Abraha, I., Chiasserini, D., Orso, M., et al. (2017). Diagnostic utility of cerebrospinal fluid α-synuclein in Parkinson's disease: a systematic review and meta-analysis. *Mov. Disord.* 32, 1389–1400. doi: 10.1002/mds.27110

Guder, W. G. (2014). History of the preanalytical phase: a personal view. *Biochemia Med.* 24, 25–30. doi: 10.11613/BM.2014.005

Kang, J. H., Mollenhauer, B., Coffey, C. S., Toledo, J. B., Weintraub, D., Galasko, D. R., et al. (2016). CSF biomarkers associated with disease heterogeneity in early Parkinson's disease: the Parkinson's progression markers initiative study. *Acta Neuropatholol.* 131, 935–949. doi: 10.1007/s00401-016-1552-2

Lee, J. E., Sang, J. C., Rodrigues, M., Carr, A. R., Horrocks, M. H., De, S., et al. (2018). Mapping surface hydrophobicity of α-synuclein oligomers at the nanoscale. *Nano. Lett.* 18, 7494–7501. doi: 10.1021/acs.nanolett.8b02916

Lewczuk, P., Beck, P., Esselmann, H., Bruckmoser, R., Zimmermann, R., Fiszer, M., et al. (2006). Effect of sample collection tubes on cerebrospinal fluid concentrations of tau proteins and amyloid β peptides. *Clin. Chem.* 52, 332–334. doi: 10.1373/clinchem.2005.058776

Majbour, N. K., Vaikath, N. N., Dijk, K. D. V., Ardah, M. T., Varghese, S., Vesterager, L. B., et al. (2016). Oligomeric and phosphorylated α-synuclein as potential CSF biomarkers for Parkinson's disease. *Mol. Neurodegeneration* 11:7. doi: 10.1186/s13024-016-0072-9

Majbour, N. K., Jan, O. A., Hustad, E., Thomas, M. A., Vaikath, N. N., Elkum, N., et al. (2020). CSF total and oligomeric α-synuclein along with TNF-α as risk biomarkers for Parkinson's disease: a study in LRRK2 mutation carriers. *Transl. Neurodegeneration* 9:15. doi: 10.1186/s40035-020-00192-4

Ming, X., Patel, R., Kang, V., Chokroverty, S., and Julu, P. O. (2016). Respiratory and autonomic dysfunction in children with autism spectrum disorders. *Brain Dev.* 38, 225–232. doi: 10.1016/j.braindev.2015.07.003

Mollenhauer, B., Cullen, V., Kahn, I., Krastins, B., Outeiro, T. F., Pepivani, I., et al. (2008). Direct quantification of CSF α-synuclein by ELISA and first cross-sectional study in patients with neurodegeneration. *Exp. Neurol.* 213, 315–325. doi: 10.1016/j.expneurol.2008.06.004

Mollenhauer, B., Trautmann, E., Taylor, P., Manninger, P., Sixel-Döring, F., Ebentheuer, J., et al. (2013). Total CSF α-synuclein is lower in *de novo* Parkinson patients than in healthy subjects. *Neurosci. Lett.* 532, 44–48. doi: 10.1016/j.neulet.2012.11.004

Mollenhauer, B., Batrla, R., El-Agnaf, O., Galasko, D. R., Lashuel, H. A., Merchant, K. M., et al. (2017a). A user's guide for α-synuclein biomarker studies in biological fluids: perianalytical considerations. *Mov. Disord.* 32, 1117–1130. doi: 10.1002/mds.27090

Mollenhauer, B., Caspell-Garcia, C. J., Coffey, C. S., Taylor, P., Shaw, L. M., Trojanowski, J. Q., et al. (2017b). Longitudinal CSF biomarkers in patients with early Parkinson disease and healthy controls. *Neurology* 89, 1959–1969. doi: 10.1212/WNL.0000000000004609

Mollenhauer, B., Bowman, F. D., Drake, D., Duong, J., Blennow, K., El-Agnaf, O., et al. (2019). Antibody-based methods for the measurement of α-synuclein concentration in human cerebrospinal fluid—method comparison and round robin study. *J. Neurochem.* 149, 126–138. doi: 10.1111/jnc.14569

Park, M. J., Cheon, S. M., Bae, H. R., Kim, S. H., and Kim, J. W. (2011). Elevated levels of α-synuclein oligomer in the cerebrospinal fluid of drug-naïve patients with Parkinson's disease. *J. Clin. Neurol.* 7, 215–222. doi: 10.3988/jcn.2011.7.4.215

Parnetti, L., Chiasserini, D., Bellomo, G., Giannandrea, D., Carlo, C. D., Qureshi, M. M., et al. (2011). Cerebrospinal fluid tau/α-synuclein ratio in Parkinson's disease and degenerative dementias. *Mov. Disord.* 26, 1428–1435. doi: 10.1002/mds.23670

Parnetti, L., Chiasserini, D., Persichetti, E., Eusebi, P., Varghese, S., Qureshi, M. M., et al. (2014a). Cerebrospinal fluid lysosomal enzymes and α-synuclein in Parkinson's disease. *Mov. Disord.* 29, 1019–1027. doi: 10.1002/mds.25772

Parnetti, L., Farotti, L., Eusebi, P., Chiasserini, D., Carlo, C. D., Giannandrea, D., et al. (2014b). Differential role of CSF α-synuclein species, tau and aβ42 in Parkinson's disease. *Front. Aging Neurosci.* 6:53. doi: 10.3389/fnagi.2014.00053

Parnetti, L., Gaetani, L., Eusebi, P., Paciotti, S., Hansson, O., El-Agnaf, O., et al. (2019). CSF and blood biomarkers for Parkinson's disease. *Lancet Neurol.* 18, 573–586. doi: 10.1016/S1474-4422(19)30024-9

Perret-Liaudet, A., Pelpel, M., Tholance, Y., Dumont, B., Vanderstichele, H., Zorzi, W., et al. (2012). Risk of Alzheimer's disease biological misdiagnosis linked to cerebrospinal collection tubes. *J. Alzheimer's Dis.* 31, 13–20. doi: 10.3233/JAD-2012-120361

Pica-Mendez, A. M., Tanen, M., Dallob, A., Tanaka, W., and Laterza, O. F. (2010). Nonspecific binding of Aβ42 to polypropylene tubes and the effect of tween-20. *Clin. Chim. Acta* 411:1833. doi: 10.1016/j.cca.2010.07.019

Robey, T. T., and Panegyres, P. K. (2019). Cerebrospinal fluid biomarkers in neurodegenerative disorders. *Future Neurol.* 14. doi: 10.2217/fnl-2018-0029

Spillantini, M. G., Crowther, R. A., Jakes, R., Cairns, N., Lantos, N. J., Goedert, M., et al. (1998). Filamentous α-synuclein inclusions link multiple system atrophy with Parkinson's disease and dementia with lewy bodies. *Neurosci. Lett.* 251, 205–208. doi: 10.1016/s0304-3940(98)00504-7

Stewart, T., Shi, M., Mehrotra, A., Aro, P., Soltys, D., Kerr, K. F., et al. (2019). Impact of pre-analytical differences on biomarkers in the ADNI and PPMI studies: implications in the era of classifying disease based on biomarkers. *J. Alzheimer's Dis.* 69, 263–276. doi: 10.3233/JAD-190069

Vanderstichele, H. M. J., Janelidze, S., Demeyer, L., Coart, E., Stoops, E., Herbst, V., et al. (2016). Optimized standard operating procedures for the analysis of cerebrospinal fluid Aβ42 and the ratios of Aβ isoforms using low protein binding tubes. *J. Alzheimer's Dis.* 53, 1121–1132. doi: 10.3233/JAD-160286

Volc, D., Poewe, W., Kutzelnigg, A., Lührs, P., Thun-Hohenstein, C., Schneeberger, A., et al. (2020). Safety and immunogenicity of the α-synuclein active immunotherapeutic PD01A in patients with Parkinson's disease: a randomised, single-blinded, phase 1 trial. *Lancet Neurol.* 19, 591–600. doi: 10.1016/S1474-4422(20)30136-8

Wang, L., Gao, L., Tang, H., Nie, K., Wang, L., Zhao, J., et al. (2015). Cerebrospinal fluid α-synuclein as a biomarker for Parkinson's disease diagnosis: a systematic review and meta-analysis. *Int. J. Neurosci.* 125, 645–654. doi: 10.1016/S1474-4422(20)30136-8

Willemse, E. A. J., Vermeiren, Y., Garcia-Ayllon, M. S., Bridel, C., Deyn, P. P. D., Engelborghs, S., et al. (2019). Pre-analytical stability of novel cerebrospinal fluid biomarkers. *Clin. Chim. Acta* 497, 204–211. doi: 10.1016/j.cca.2019.07.024

Williams, S. M., Schulz, P., and Sierks, M. R. (2016). Oligomeric α-synuclein and β-amyloid variants as potential biomarkers for Parkinson's and Alzheimer's diseases. *Eur. J. Neurosci.* 43, 3–16. doi: 10.1111/ejn.13056

Conflict of Interest: The authors declare that the research was conducted in the absence of any commercial or financial relationships that could be construed as a potential conflict of interest.

Copyright © 2021 Abdi, Majbour, Willemse, van de Berg, Mollenhauer, Teunissen and El-Agnaf. This is an open-access article distributed under the terms of the Creative Commons Attribution License (CC BY). The use, distribution or reproduction in other forums is permitted, provided the original author(s) and the copyright owner(s) are credited and that the original publication in this journal is cited, in accordance with accepted academic practice. No use, distribution or reproduction is permitted which does not comply with these terms.

frontiers in Aging Neuroscience

ORIGINAL RESEARCH
published: 17 March 2021
doi: 10.3389/fnagi.2021.653379

α-Synuclein Up-regulates Monoamine Oxidase A Expression and Activity *via* Trans-Acting Transcription Factor 1

Congcong Jia[1,2], *Cheng Cheng*[1,2], *Tianbai Li*[1,2], *Xi Chen*[1,2], *Yuting Yang*[1,2], *Xinyao Liu*[1,2], *Song Li*[1,2] *and Weidong Le*[1,2,3]*

[1]*Center for Clinical Research on Neurological Diseases, The First Affiliated Hospital, Dalian Medical University, Dalian, China,* [2]*Liaoning Provincial Key Laboratory for Research on the Pathogenic Mechanisms of Neurological Diseases, The First Affiliated Hospital, Dalian Medical University, Dalian, China,* [3]*Department and Institute of Neurology, Sichuan Academy of Medical Sciences, Sichuan Provincial Hospital, Chengdu, China*

Abnormal α-Synuclein (α-SYN) aggregates are the pathological hallmarks of Parkinson's disease (PD), which may affect dopamine (DA) neuron function and DA metabolism. Monoamine oxidase A (MAOA) is an enzyme located on the outer mitochondrial membrane that catalyzes the oxidative deamination of DA. Both α-SYN and MAOA are associated with PD pathogenesis, suggesting possible crosstalk between these two molecules. In the present study, we aimed to investigate the potential impacts of α-SYN on MAOA function and further explore the underlying mechanisms. Our study showed that overexpression of α-SYN [both wild-type (WT) and A53T] increased MAOA function *via* upregulating its expression without impacting MAOA stability. Overexpression of $\alpha\text{-SYN}^{WT}$ or $\alpha\text{-SYN}^{A53T}$ enhanced the transcription activity of the MAOA promoter region containing the binding sites of cell division cycle associated 7 like (R1, a transcriptional repressor of MAOA) and trans-acting transcription factor 1 (Sp1, a transcription factor of MAOA). Interestingly, α-SYN selectively increased Sp1 expression, thereby enhancing the binding capacity of Sp1 with MAOA promoter to increase MAOA expression. Taken together, our findings demonstrate that α-SYN can upregulate MAOA expression *via* modulation of Sp1 and may shed light on future studies of α-SYN associated PD pathogenesis.

Keywords: α-Synuclein, MAOA, Parkinson's disease, Sp1, dopamine

OPEN ACCESS

Edited by:
Shaogang Qu,
Southern Medical University, China

Reviewed by:
Jifeng Guo,
Central South University, China
Jian Wang,
Fudan University, China

***Correspondence:**
Weidong Le
wdle_sibs@163.com

Received: *14 January 2021*
Accepted: *25 February 2021*
Published: *17 March 2021*

Citation:
Jia C, Cheng C, Li T, Chen X, Yang Y, Liu X, Li S and Le W (2021) α-Synuclein Up-regulates Monoamine Oxidase A Expression and Activity via Trans-Acting Transcription Factor 1. Front. Aging Neurosci. 13:653379. doi: 10.3389/fnagi.2021.653379

INTRODUCTION

Parkinson's disease (PD) is a neurodegenerative disease pathologically characterized by progressive loss of dopamine (DA) neurons in the striatum and substantia nigra (Lees et al., 2009). Genetic alterations, such as the reduction or mutation of genes, can cause familial forms of PD (Kalia and Lang, 2015). Among them, α-Synuclein (α-SYN) gene (SNCA) was the first gene linked to PD. α-SYN is the principal constituent of Lewy bodies, and variation at its locus is the major genetic risk factor for sporadic disease. Polymeropoulos et al. (1997) identified the G209A mutation of SNCA, resulting in a substitution of Ala at position 53 to Thr (A53T), in familial forms of PD. Until now, there are six missense mutations of

α-SYN (A53T, A30P, A53E, E46K, G51D, and H50Q) associated with PD (Polymeropoulos et al., 1997; Kruger et al., 1998; Zarranz et al., 2004; Appel-Cresswell et al., 2013; Lesage et al., 2013; Proukakis et al., 2013). Mutations of α-SYN can form toxic protofibril or fibril (Giasson et al., 2002), affecting the functions of DA neurons and inducing neurodegeneration (Dev et al., 2003). Previous studies have shown that α-SYN affects the expressions of DA-related genes *via* Nurr1, a key factor involved in the development and functional maintenance of DA neurons (Saucedo-Cardenas et al., 1998; Jankovic et al., 2005; Jia et al., 2020a). Besides, α-SYN accumulation is also associated with tau spreading synaptic vesicles, autophagy, mitochondria, endoplasmic reticulum and Golgi complex, nucleus, cell-to-cell propagation, and neuroinflammation related functions (Wong and Krainc, 2017; Bassil et al., 2021). All these findings indicate the important functions of α-SYN in PD pathogenesis.

Monoamine oxidase (MAO), an enzyme for biogenic amines degradation, is located on the outer membrane of mitochondria (Green and Youdim, 1975). MAO has two isoforms (MAOA and MAOB), which locate on adjacent homologous genes of the X chromosome (Shih, 1991). While MAOA is a critical regulator of the metabolisms of serotonin (5-HT) and norepinephrine (NE), and MAOB prefers benzylamine and phenethylamine (Shih et al., 1999), both of them are involved in DA metabolism in most species (Westlund et al., 1988; Ugun-Klusek et al., 2019). Moreover, both MAOA and MAOB transcription levels and enzymatic activities are significantly increased in the induced pluripotent stem cells of dermal fibroblasts from PD patients with parkin mutations (Jiang et al., 2012). Besides, MAOA is also involved in apoptotic signaling and Shh-IL6-Rankl signaling pathways (Ou et al., 2006; Wu et al., 2017), indicating important roles of MAOA in DA neuron loss of PD. All these findings suggest the close association of MAO with PD pathogenesis.

Interestingly, the DA level was significantly reduced in the striatum tissue of mice with DA neurons specifically overexpressed human α-SYN-A53T (Chen et al., 2015), and the release of DA in the dorsal striatum of 1-month-old A53T mice is also reduced (Lin et al., 2012). Although α-SYN plays an important role in the DA-associated pathogenesis of PD, the molecular mechanism of α-SYN regulation on DA metabolism is still far from being clearly understood. One previous study reported that α-SYN can directly bind with MAOB and enhance MAOB enzyme activity (Kang et al., 2018). However, whether α-SYN modulates the expression and function of MAOA is still rarely investigated. In this study, we demonstrated that MAOA was up-regulated and activated in α-SYN overexpressed cells through increasing its transcription factor (Sp1) expression and the binding capacity of Sp1 with the MAOA promoter region. Our findings may shed light on future studies of α-SYN associated PD pathogenesis.

MATERIALS AND METHODS

Cell Lines and Culture

Mouse neuroblastoma N2a cells were maintained in Dulbecco's modified Eagle's medium (Gibco, Gaithersburg, MD, USA) containing 1% penicillin/streptomycin solution (Sigma–Aldrich, St. Louis, MO, USA) and 10% fetal bovine serum (Gibco). For the establishment of N2a cell lines stably expressing either wild-type (WT) α-SYN (N2a/α-SYN^{WT}) or A53T mutant α-SYN (N2a/α-SYN^{A53T}), N2a cells were transfected with p3XFLAG-CMV10, p3XFLAG-CMV10-human-SYNC, or p3XFLAG-CMV10-human-SYNC-A53T plasmids (kindly gift by Huaibin Cai professor) by lipofectamine 6000 (Beyotime, Shanghai, China) according to the manufacturer's instructions. Forty-eight hours after transfection, the cells were screened by cell culture medium containing 600 μg/ml of G418 (Sigma–Aldrich) until no more cell death. Real-time PCR and Western blot were used to verify the α-SYN level in cells.

Reagents

The antibodies used in the present study were shown as follows: anti-α-SYN antibody (Santa Cruz Biotechnology, Dallas, TX, USA), anti-MAOA antibody (Abcam, Cambridge, MA, USA), anti-Sp1 (Abcam, Cambridge, MA, USA), anti-R1 (ABclonal Technology, Wuhan, China), anti-Histone antibody (Cell Signaling Technology), anti-GAPDH antibody (Cell Signaling Technology, Danvers, MA, USA), anti-MAOB, anti-COMT, anti-ADH5, anti-FLAG, Goat anti-mouse IgG H&L and Goat anti-rabbit IgG H&L (Proteintech Group Inc., Rosemont, IL, USA), Goat anti-mouse Alexa 594 (Abcam) and Goat anti-rabbit Alexa 488 (Cell Signaling Technology).

Western Blot

N2a/α-SYN and N2a control cells were resuspended in RIPA lysis buffer (Beyotime) containing a protease inhibitor (cocktail, Sigma–Aldrich), lysed on ice for 30 min, and centrifuged at 12,000× *g* for 15 min. The supernatant protein concentration was detected by a BCA Protein Assay kit (Beyotime). Samples with equal amounts of total proteins (30–50 μg) were subjected to 10 or 12.5% SDS-polyacrylamide gel electrophoresis and then transferred to 0.45 μm polyvinylidene difluoride membranes (Millipore, Burlington, MA, USA). After blocking with 5% skimmed milk for 1 h at room temperature, the membrane was incubated with the primary antibody at 4°C overnight. Then, the membrane was incubated with a secondary antibody, and the protein bands were detected with the enhanced chemiluminescence detection kit (Wanlei Biotechnology, Shenyang, China) and quantified using the FluorChem Q system (Protein Simple, San Jose, CA, USA) and normalized against reference protein values.

Real-Time PCR

Total RNA was extracted and used to synthesize cDNA according to the manufacturer's instructions (TransGen Biotechnology, Beijing, China). The primers sequences and analysis methods used in the present study were described previously (Jia et al., 2020a,b).

Immunofluorescence

N2a/α-SYN and N2a control cells were fixed with 4% paraformaldehyde, punched by 0.2% Triton X-100 and blocked with 2% bovine serum albumin for 30 min, followed by incubation with the primary antibodies overnight at 4°C. After

washing with PBS, the cells were incubated with fluorescent secondary antibodies at room temperature for 1 h. Antifade Mounting Medium with DAPI (Beyotime) was used for nuclei staining. The cells were then washed with PBS three times. Fluorescence images were visualized using an A1R MP multiphoton confocal microscope (Nikon, Tokyo, Japan).

Immunoenzymatic Measurement

The samples were rinsed with ice-cold PBS and sonicated in PBS containing a protease inhibitor cocktail (Sigma–Aldrich). The homogenates were centrifugated for 10 min at 5,000× *g* to get the supernatant. Equal amounts of total supernatant protein were used to detect MAOA enzyme activity and DA content, using a mouse MAOA ELISA kit and a DA ELISA kit respectively, according to the manufacturer's instructions (Dalian Aimoke Biotechnology Company Limited, Dalian, China).

Luciferase Reporter Assay

N2a/α-SYN and N2a control cells were co-transfected with MAOA promoter fragment luciferase reporter plasmid (0.5 μg) and phRL-SV40 vector (0.05 μg) using lipofectamine 6000 (Beyotime) for 48 h according to our precious protocol (Jia et al., 2020b). Cells were sonicated in lysis buffer and then centrifuged for 10 min at 12,000× *g* to get the supernatant. The luciferase activities of the supernatant were detected with a dual-luciferase assay kit (Beyotime) in a microplate reader (BioTek Instruments, Inc., VT, USA) according to the manufacturer's instructions. The value of firefly luciferase was normalized to Renilla luciferase.

Chromatin Immunoprecipitation

A ChIP assay kit (Beyotime) was used to detect the binding amount of Sp1 or R1 with the MAOA promoter. Briefly, cells were crosslinked with 1% formaldehyde, sonicated with PBS containing 1 mM phenylmethylsulfonyl fluoride, and centrifuged at 12,000× *g* for 5 min. Equal amounts of total proteins were added anti-IgG, anti-R1, and anti-Sp1 antibodies, respectively. On the second day, protein A/G beads were added to bind the antibody-target protein-DNA complex. The precipitated complexes were washed and eluted to obtain the enriched target protein-DNA complex. The obtained complexes were purified with a DNA purification kit (Beyotime) and then detected with Real-time PCR. The methods of analyzed values were described previously (Jia et al., 2020a,b).

Immunoprecipitation

We seeded α-SYN overexpressed and control cells in 10 cm plates. The next day, the samples were washed with PBS, lysed in IP lysis buffer (Beyotime) containing cocktail, and centrifuged at 12,000× *g* for 15 min. Anti-FLAG magnetic beads (MedChemExpress LLC, Monmouth Junction, NJ, USA) were added into equal amounts of total proteins to make antibody-FLAG-protein complex. The complex was washed with PBS and then eluted in 1× SDS loading buffer for Western blot.

Statistical Analysis

All experiments were performed in triplicate and repeated a minimum of three times. Data were expressed as mean ± SEM. Statistical significance for multiple comparisons was performed by one-way analysis of variance (ANOVA) using GraphPad Prism (version 8.0.2, GraphPad Inc., San Diego, CA, USA). The significance was considered at $p < 0.05$.

RESULTS

Overexpression of α-SYN Decreases DA Level and Increases MAOA Activity

To explore the mechanism underlying the impacts of α-SYN on DA metabolism, we first constructed α-SYN^{WT} and α-SYN^{A53T} stably overexpressed N2a cell lines and detected the level of DA in these cells with a DA ELISA kit. The results showed that overexpression of α-SYN (both WT and A53T) induced 26% and 32% DA reduction for WT and A53T respectively, compared with control groups ($p < 0.01$, **Figure 1A**). We then detected the expression levels of several key proteins associated with DA metabolism, including MAOA, MAOB, alcohol dehydrogenase (ADH), and catechol O-methyltransferase (COMT). Western blot analysis showed that, among these proteins, MAOA was most sensitive to overexpression of α-SYN^{WT} and α-SYN^{A53T}, as evidenced by 1.67 and 1.69 folds upregulation, respectively ($p < 0.01$, **Figures 1B,C**). Other proteins (MAOB, ADH, and COMT) were not significantly changed by both α-SYN^{WT} and α-SYN^{A53T} overexpression (**Figures 1B,D–F**). Therefore, MAOA was selected for further analysis. We determined the total MAOA activity of cell lysates from α-SYN^{WT} and α-SYN^{A53T} overexpressed cells using a mouse MAOA ELISA kit. Consistent with protein expressions, the results showed that overexpression of α-SYN^{WT} and α-SYN^{A53T} markedly increased MAOA enzyme activity to 1.66 and 1.64 folds of controls ($p < 0.01$, **Figure 1G**). All these data indicated that overexpression of α-SYN^{WT} and α-SYN^{A53T} increased MAOA expression and activity, further confirming the association of α-SYN and PD pathology.

α-SYN Neither Binds With MAOA nor Alters the Degradation of MAOA

We previously found that α-SYN is located in both the nucleus and cytoplasm (Jia et al., 2020a). MAOA is mainly expressed on the outer membrane of mitochondria (Green and Youdim, 1975). To explore the mechanism of α-SYN on MAOA expression, we used the immunofluorescence staining to detect the colocalization of α-SYN and MAOA. As expected, our results showed that MAOA expression was increased in α-SYN^{WT} and α-SYN^{A53T} overexpressed cells (**Figure 2A**). Moreover, α-SYN showed clear colocalizations with MAOA in the cytoplasm. Due to the α-SYN^{WT} and α-SYN^{A53T} fragments of plasmids fused with a 3XFLAG label protein, we used an anti-FLAG antibody to pull down the transfected α-SYN to detect the direct binding between α-SYN and MAOA in the above cells. Interestingly, while α-SYN and MAOA colocalized in the cytoplasm (**Figure 2A**), no direct binding was observed between α-SYN and MAOA (**Figure 2B**).

One possibility for the increased level of MAOA in N2a/α-SYN cells might be due to the inhibited MAOA degradation. To further confirm this possibility, we cultured α-SYN^{WT} and

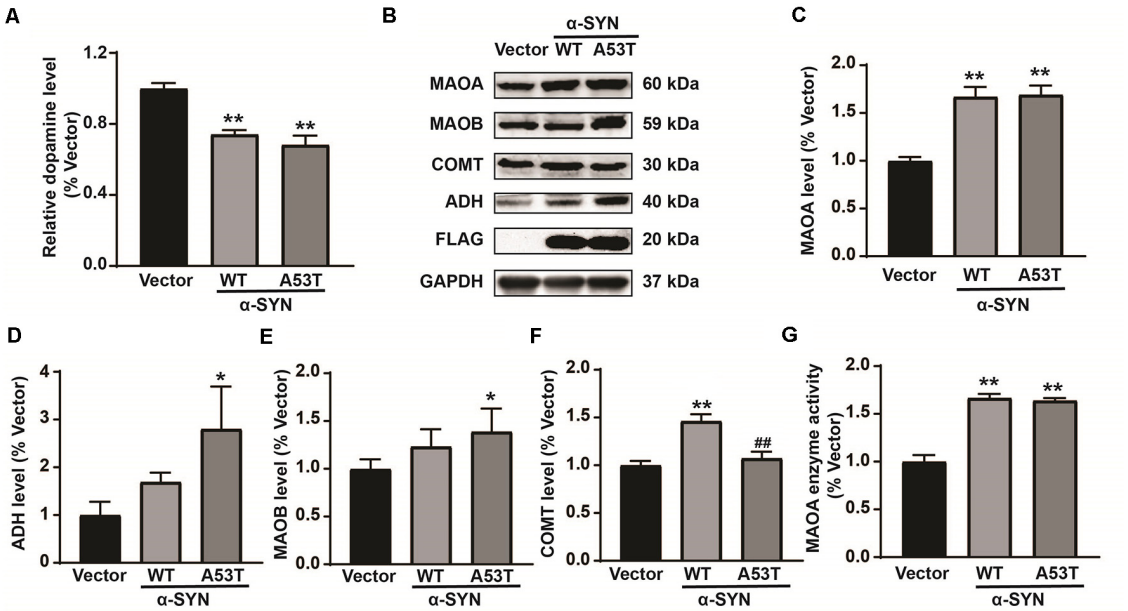


FIGURE 1 | Impacts of α-SYN^{WT} and α-SYN^{A53T} on dopamine (DA) content and DA metabolism-associated enzymes. The DA content was detected in α-Synuclein (α-SYN) [wild-type (WT), A53T] stably overexpressed and control (Vector) cells with a mouse DA Elisa kit **(A)**. Western blot detected the protein level of DA metabolism-associated enzymes [Monoamine oxidase A (MAOA), Monoamine oxidase B (MAOB), catechol O-methyltransferase (COMT), and alcohol dehydrogenase (ADH)] **(B–F)**. MAOA enzyme activity was detected in α-SYN overexpressed cells with a mouse MAOA Elisa kit **(G)**. Data were expressed as mean ± SEM. $^{**}p < 0.01$ vs. Vector transfected cells, $^{*}p < 0.05$ vs. Vector transfected cells, $^{\#\#}p < 0.01$ vs. α-SYN-WT transfected cells, $n = 3$.

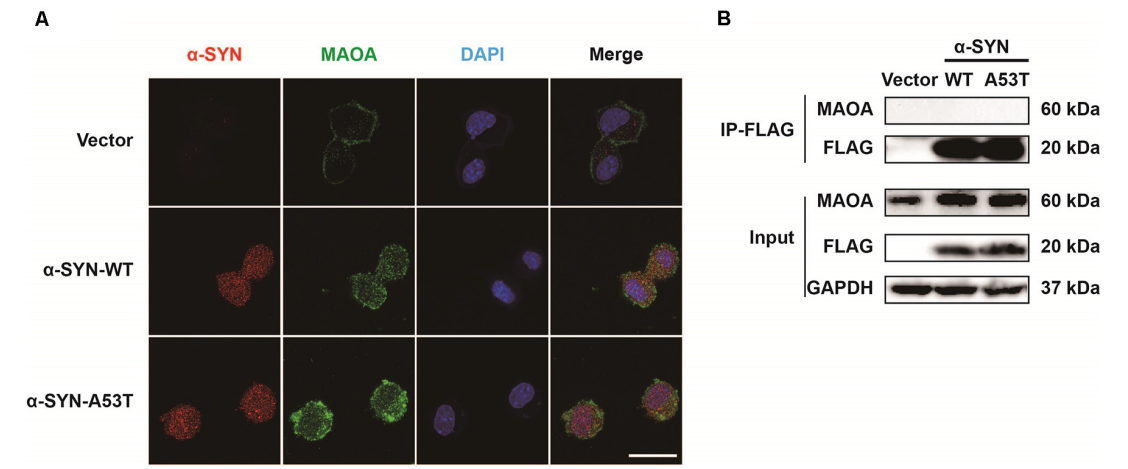


FIGURE 2 | Colocalization and interaction of α-SYN and MAOA. The intracellular protein level of MAOA was detected using immunofluorescent staining, α-SYN (red), MAOA (green), and nucleus (blue). Scale bare: 20 μm **(A)**. The transfected α-SYN was pulled down with an anti-FLAG antibody, and the direct binding between α-SYN and MAOA was detected in the control cells (Vector), α-SYN-WT and α-SYN-A53T stable expression cells **(B)**.

α-SYN^{A53T} overexpressed cells with a protein synthesis inhibitor puromycin (100 μM) for 0, 4, 8, 16, and 24 h. MAOA expression was determined by Western blot. The results showed that the half-life degradation of MAOA in N2a/α-SYN (WT and A53T) cells were not significantly different from that in the control cells (**Figures 3A–F**). These results indicated that α-SYN up-regulated MAOA expression not *via* inhibiting MAOA degradation.

α-SYN Affects the Protein Synthesis of MAOA *via* Sp1

After ruling out the possibility of direct effects of α-SYN on MAOA degradation, we detected the mRNA level of MAOA in α-SYN^{WT} and α-SYN^{A53T} overexpressed cells. Real-time PCR results showed that, together with significantly increased α-SYN mRNA level, MAOA level was up-regulated to 1.69 and

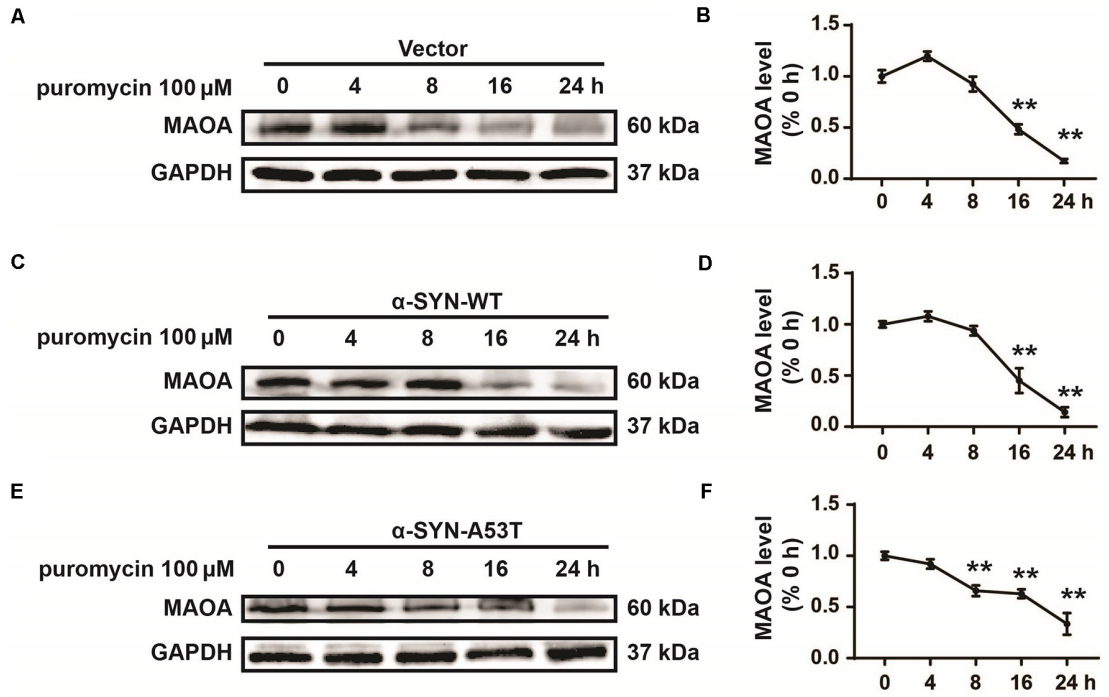


FIGURE 3 | Effects of overexpression of α-SYN^{WT} and α-SYN^{A53T} on MAOA degradation. The protein level of MAOA was detected using Western blot in α-SYN (WT and A53T) stably overexpressed and control (Vector) cells cultured with puromycin (100 μM) for 0, 4, 8, 16, and 24 h **(A–F)**. Data were expressed as mean ± SEM. $^{**}p < 0.01$ vs. the same cells at 0 h point, $n = 3$.

1.54-folds by α-SYN overexpression ($p < 0.01$, **Figure 4A**), indicating α-SYN altered the synthesis of MAOA from mRNA level. To further explore the mechanism, we subcloned the core fragment of the MAOA promoter into the pGL3-basic vector to obtain the MAOApromoter-luciferase plasmid, co-transfected with phRL-SV40 plasmids into α-SYN^{WT} and α-SYN^{A53T} overexpressed cells. The results of dual-luciferase reporter gene assay showed that both α-SYN^{WT} and α-SYN^{A53T} overexpression up-regulated the activity of MAOA-luciferase plasmid by 1.46 and 1.44 folds, respectively ($p < 0.01$, **Figure 4B**). We then used the JASPAR database to analyze the MAOA core promoter region of luciferase plasmid (Fornes et al., 2020). Bioinformatics analysis showed that the region contained the same binding sites of cell division cycle associated 7 like (R1, a transcriptional repressor of MAOA) and Sp1 (a transcription factor of MAOA; **Figure 4C**). α-SYN may affect the balance of R1 and Sp1 binding with MAOA promoter to impact MAOA expression. ChIP-Real-time PCR results showed that α-SYN did not significantly change the binding quantity of R1 with the MAOA promoter but increased that of Sp1 to 3.95 folds and 3.57 folds compared with controls, respectively ($p < 0.01$, **Figure 4D**).

Then, we determined the total protein levels of Sp1 in α-SYN^{WT} and α-SYN^{A53T} overexpressed cells, the results showed that α-SYN increased Sp1 expression to 2.06 folds and 2.10 folds compared with controls ($p < 0.05$, **Figures 5A,B**). Consistently, immunofluorescence staining obtained the same results as Western blot, confirming the significant increase in Sp1 expression in the nucleus of α-SYN overexpressed cells (**Figure 5C**). We separated cytoplasm-nucleus proteins and detected the expression levels of Sp1. Western blot results indicated that α-SYN did not significantly change the cytoplasm protein level of Sp1 (**Figures 5D,E**), it selectively increased the nucleus protein level of Sp1 to 1.92 folds and 2.10 folds compared with controls ($p < 0.05$, **Figures 5D,F**). Altogether, our results demonstrate that α-SYN can increase MAOA protein synthesis *via* up-regulating Sp1 expression (**Figure 6**).

DISCUSSION

α-SYN, as the important components of Lewy bodies, is closely associated with DA neuron loss and DA level reduction in the PD brain (Spillantini et al., 1997). One previous study showed that substantia nigra injection of AAV1/2-α-SYN^{A53T} reduced striatal DA and DOPAC levels and increased HVA levels (Ip et al., 2017). The dorsolateral striatum of α-SYN^{A53T} mice demonstrates a lower DA level than those of WT controls (Lin et al., 2012). In this study, we also found that overexpression of α-SYN (both WT and A53T) reduced DA contents *in vitro* (**Figure 1A**). These findings suggested a close correlation between α-SYN and DA metabolism. However, the exact mechanisms for this pathological impact of α-SYN on DA biosynthesis or degradation are still far from being fully investigated.

As for the biosynthesis of DA, L-tyrosine is hydroxylated by tyrosine hydroxylase (TH) to generate L-DOPA and then decarboxylated by aromatic acid decarboxylase (AADC) to form

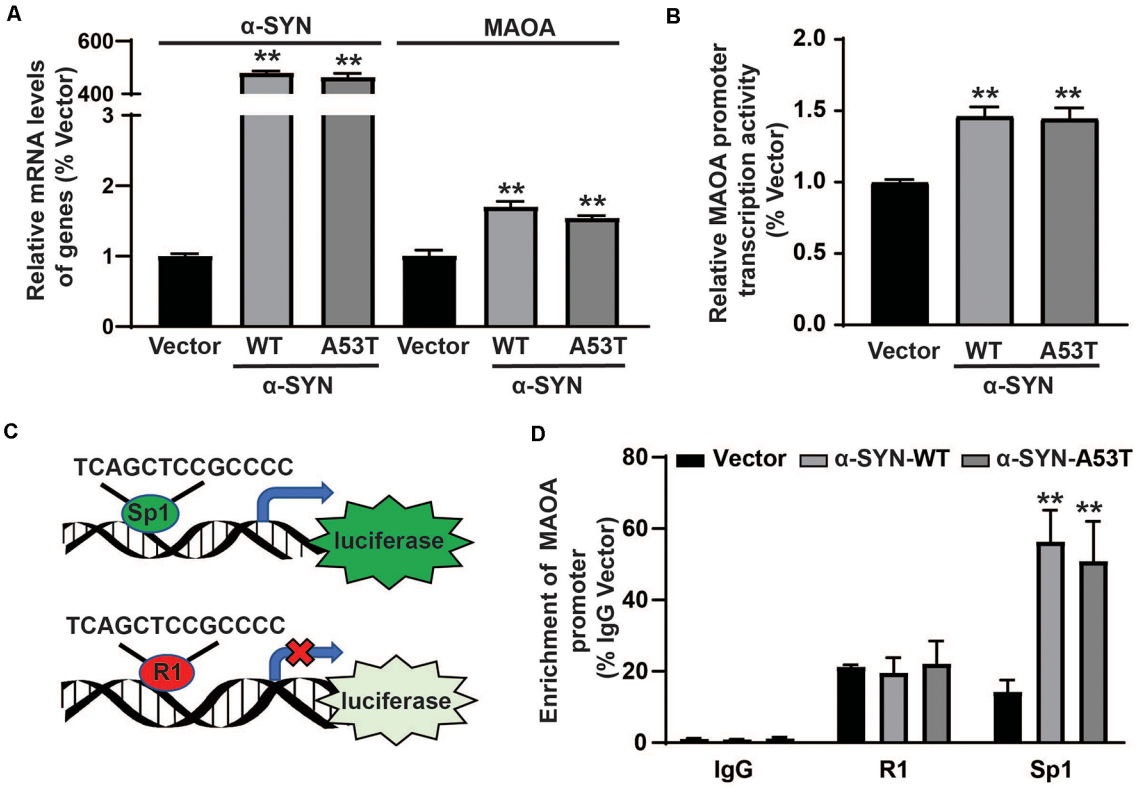


FIGURE 4 | α-SYN affected the protein synthesis of MAOA. The mRNA level of MAOA **(A)** and the activity of MAOA promoter luciferase **(B)** were analyzed in control cells (Vector), α-SYN^{WT} and α-SYN^{A53T} stably overexpressed cells. The transcription factor diagram of bioinformatics analysis MAOA promoter luciferase plasmid **(C)**. ChIP-Real-time PCR analyzed the binding quantity of R1 and Sp1 with the MAOA promoter region **(D)**. Data were expressed as mean ± SEM. $^{**}p < 0.01$ vs. Vector transfected cells, $n = 3$.

DA (Daubner et al., 2011; Monzani et al., 2019). Our previous study showed that α-SYN down-regulated the expression levels of TH and AADC *via* suppressing Nurr1 gene expression (Jia et al., 2020a), indicating an impact of α-SYN on DA biosynthesis through Nurr1-related mechanisms. In this study, we further explored the potential impacts and molecular mechanism of α-SYN on DA degradation. A previous study found that α-SYN can directly bind to MAOB and increase its activity and expression (Kang et al., 2018). Consistently, our present data also revealed that overexpression of α-SYN^{A53T} significantly up-regulated MAOB expression (**Figures 1B,E**). Except for MAOB, our results further suggested that α-SYN changed the expression levels of MAOA, COMT, and ADH (**Figures 1B–D,F**). Much more interestingly, among these proteins, MAOA was the only one that was significantly up-regulated by both α-SYN^{WT} and α-SYN^{A53T} overexpression, indicating an important role of MAOA in the α-SYN-regulated DA degradation.

To explore the mechanism of α-SYN on MAOA expression, we detected the co-localization of α-SYN and MAOA and the data revealed that there was no direct interaction between α-SYN and MAOA, which is consistent with previous findings (Kang et al., 2018). Our previous study and others showed that MAOA was degraded *in vitro* with the presence of a protein synthesis inhibitor (Jiang et al., 2006; Jia et al., 2020b). Kabayama et al. found that RING finger-type E3 ubiquitin ligase Rines/RNF180 increased the ubiquitination and degradation of MAOA (Kabayama et al., 2013). Moreover, the A30P mutation of α-SYN induced the activity of proteasome (Tanaka et al., 2001). α-SYN promotes the proteasome-dependent degradation of Nurr1 expression (Lin et al., 2012). These results raised the possibility that α-SYN up-regulated MAOA expression partially *via* changing the proteasome-dependent posttranscriptional levels. However, in our present study, both α-SYN^{WT} and α-SYN^{A53T} failed to induce a significant change in the half-life of MAOA protein (**Figure 3**). Our findings suggest possible transcription mechanisms underlying the impacts of α-SYN-increased MAOA level. In agreement with this hypothesis, our results showed that α-SYN increased MAOA mRNA level and the promoter activity (**Figures 4A,B**).

Previous studies reported that the human MAOA core promoter region has clusters of Sp1 binding sites, which can be competitively bound by R1 to repress MAOA expression (Zhu et al., 1994; Chen et al., 2005). The balance between Sp1 transcriptional activity and R1 repressor activity on the promoter regulates MAOA expression (Huang et al., 2012). Our bioinformatics analysis showed that the MAOA promoter-luciferase plasmid contained the binding site of

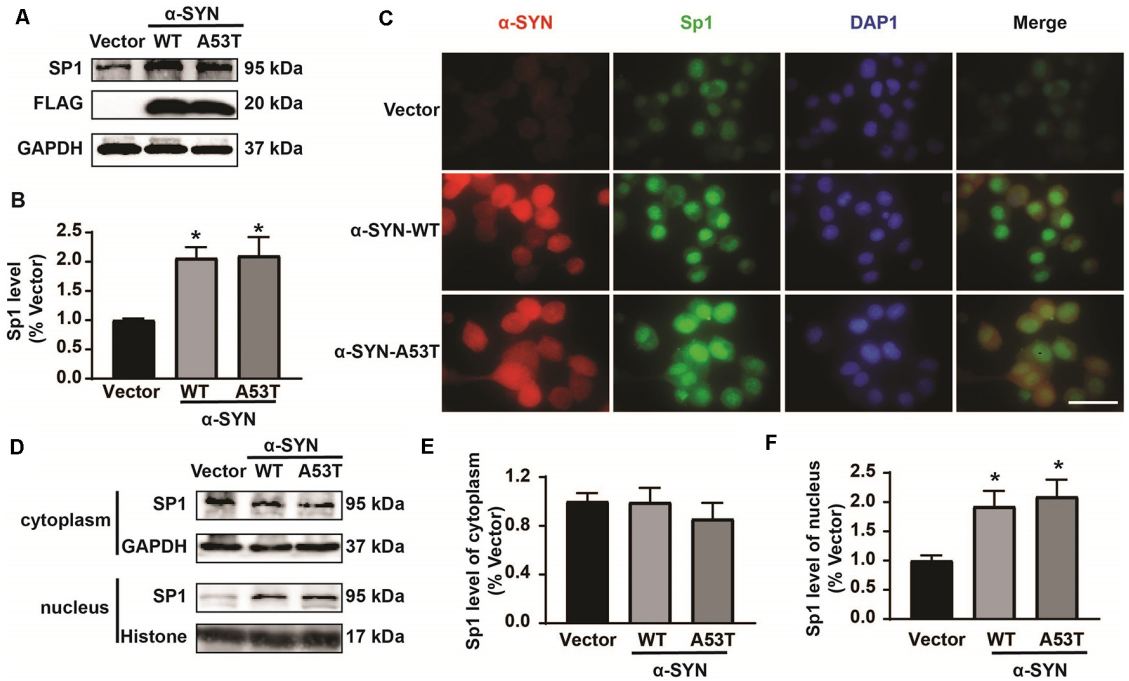


FIGURE 5 | α-SYN regulated the expression of Sp1. Western blot was used to detect the protein level of Sp1 in control cells (Vector), α-SYN^{WT} and α-SYN^{A53T} stably overexpressed cells **(A,B)**. The intracellular protein level of Sp1 was confirmed using immunofluorescent staining, α-SYN (red), Sp1 (green), and nucleus (blue). Scale bare: 50 μm **(C)**. Western blot detected the cytoplasm and nucleus protein level of Sp1 in control cells (Vector), α-SYN^{WT} and α-SYN^{A53T} stably overexpressed cells **(D–F)**. Data were expressed as mean ± SEM. *$p < 0.05$ vs. Vector transfected cells, $n = 3$.

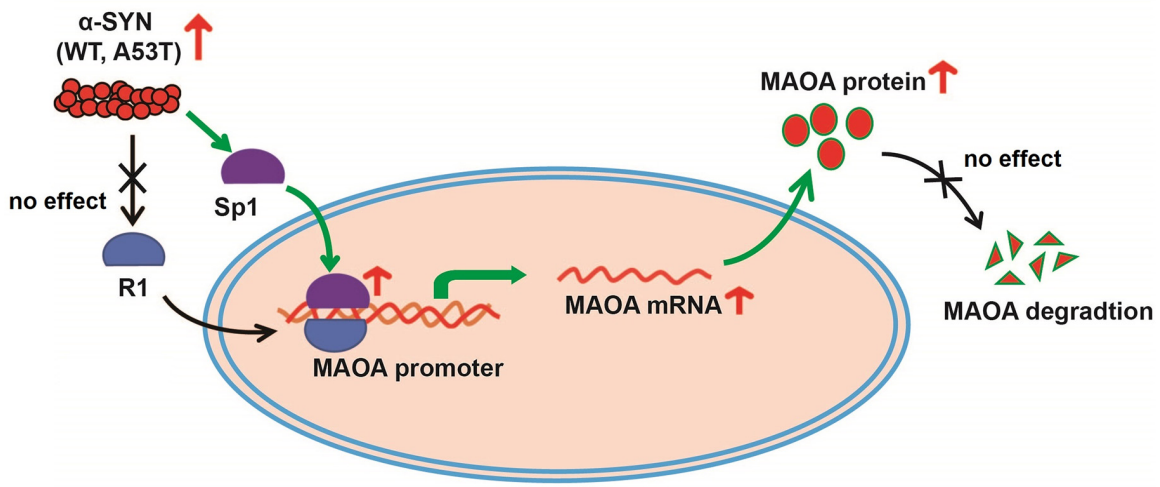


FIGURE 6 | The schematic illustration of mechanisms underlying α-SYN-induced MAOA increase. Overexpression of α-SYN^{WT} and α-SYN^{A53T} selectively up-regulated Sp1 expression and the binding quantity of Sp1 with MAOA promoter, thereby increasing MAOA expression and activity.

Sp1 and R1. ChIP-Real-time PCR results indicated that α-SYN selectively increased the binding quality of Sp1 with MAOA promoter, without change that of R1. Rather intriguingly, the protein level of Sp1, especially the nuclear Sp1, was increased by α-SYN overexpression. Our study showed that both α-SYN^{WT} and α-SYN^{A53T} can increase the activity and expression of MAOA *via* Sp1, suggesting that the increase of MAOA by α-SYN is one of the important molecular determinants for abnormal metabolism of DA in PD.

MAOA, as a flavoenzyme, can catabolize other neurotransmitters, including NE and 5-HT (Shih et al., 1999). The dysregulated functions of MAOA in neural signal

transmission may lead to depression, autism, or aggressive behavior phenotypes (Gu et al., 2017; Kolla and Bortolato, 2020), which may be involved as non-motor psychiatric manifestations of PD. Moreover, bypass of melatonin synthesis, MAOA converts 5-HT into 5-hydroxyindoleacetic acid (5-HIAA; Reiter, 1991), which may lead to a sleep disorder, another type of non-motor symptom of PD. These findings further predict the possible involvement of MAOA in non-motor symptoms of PD. Our results may provide a basis for studying the mechanism of α-SYN on the non-motor symptom of PD.

In summary, our present data reveal that α-SYN induces DA content *via* the effect on Sp1-mediated MAOA synthesis and activity, the finding of which is unknown for the α-SYN association with MAOA and its possible link to PD. Our study may shed new light on future studies to uncover the molecular mechanism of α-SYN on DA metabolism in PD pathogenesis and to facilitate the exploration of molecular targets for PD therapy.

DATA AVAILABILITY STATEMENT

The raw data supporting the conclusions of this article will be made available by the authors, without undue reservation.

AUTHOR CONTRIBUTIONS

CJ, CC, and TL conducted the experiments. CJ, XC, YY, and XL collected and analyzed the data. CJ and WL drafted the manuscript. WL and SL revised the manuscript. WL conceived and designed the experiments. The final manuscript was read and approved by all authors. All authors contributed to the article and approved the submitted version.

FUNDING

This work was supported by the National Natural Science Foundation of China (NSFC81771521), the National Key Research and Development Program of China (2016YFC1306600), Guangdong Provincial Key R & D Program (2018B030337001), Liaoning Provincial Department of Education Project (LZ2020067), and Dalian Medical Science Research Project (2012005).

ACKNOWLEDGMENTS

We appreciate all members of Weidong Le's Lab for their helpful technical support and constructive discussions.

REFERENCES

Appel-Cresswell, S., Vilarino-Guell, C., Encarnacion, M., Sherman, H., Yu, I., Shah, B., et al. (2013). α-synuclein p.H50Q, a novel pathogenic mutation for Parkinson's disease. *Mov. Disord.* 28, 811–813. doi: 10.1002/mds.25421

Bassil, F., Meymand, E. S., Brown, H. J., Xu, H., Cox, T. O., Pattabhiraman, S., et al. (2021). α-Synuclein modulates tau spreading in mouse brains. *J. Exp. Med.* 218:e20192193. doi: 10.1084/jem.20192193

Chen, K., Ou, X. M., Chen, G., Choi, S. H., and Shih, J. C. (2005). R1, a novel repressor of the human monoamine oxidase A. *J. Biol. Chem.* 280, 11552–11559. doi: 10.1074/jbc.M410033200

Chen, L., Xie, Z., Turkson, S., and Zhuang, X. (2015). A53T human α-synuclein overexpression in transgenic mice induces pervasive mitochondria macroautophagy defects preceding dopamine neuron degeneration. *J. Neurosci.* 35, 890–905. doi: 10.1523/JNEUROSCI.0089-14.2015

Daubner, S. C., Le, T., and Wang, S. (2011). Tyrosine hydroxylase and regulation of dopamine synthesis. *Arch. Biochem. Biophys.* 508, 1–12. doi: 10.1016/j.abb.2010.12.017

Dev, K. K., Hofele, K., Barbieri, S., Buchman, V. L., and van der Putten, H. (2003). Part II: α-synuclein and its molecular pathophysiological role in neurodegenerative disease. *Neuropharmacology* 45, 14–44. doi: 10.1016/s0028-3908(03)00140-0

Fornes, O., Castro-Mondragon, J. A., Khan, A., van der Lee, R., Zhang, X., Richmond, P. A., et al. (2020). JASPAR 2020: update of the open-access database of transcription factor binding profiles. *Nucleic. Acids Res.* 48, D87–D92. doi: 10.1093/nar/gkz1001

Giasson, B. I., Duda, J. E., Quinn, S. M., Zhang, B., Trojanowski, J. Q., and Lee, V. M. (2002). Neuronal α-synucleinopathy with severe movement disorder in mice expressing A53T human α-synuclein. *Neuron* 34, 521–533. doi: 10.1016/s0896-6273(02)00682-7

Green, A. R., and Youdim, M. B. (1975). Effects of monoamine oxidase inhibition by clorgyline, deprenil or tranylcypromine on 5-hydroxytryptamine concentrations in rat brain and hyperactivity following subsequent tryptophan administration. *Br J. Pharmacol.* 55, 415–422. doi: 10.1111/j.1476-5381.1975.tb06946.x

Gu, F., Chauhan, V., and Chauhan, A. (2017). Monoamine oxidase-A and B activities in the cerebellum and frontal cortex of children and young adults with autism. *J. Neurosci. Res.* 95, 1965–1972. doi: 10.1002/jnr.24027

Huang, L., Frampton, G., Rao, A., Zhang, K. S., Chen, W., Lai, J. M., et al. (2012). Monoamine oxidase A expression is suppressed in human cholangiocarcinoma *via* coordinated epigenetic and IL-6-driven events. *Lab Invest.* 92, 1451–1460. doi: 10.1038/labinvest.2012.110

Ip, C. W., Klaus, L. C., Karikari, A. A., Visanji, N. P., Brotchie, J. M., Lang, A. E., et al. (2017). AAV1/2-induced overexpression of A53T-α-synuclein in the substantia nigra results in degeneration of the nigrostriatal system with Lewy-like pathology and motor impairment: a new mouse model for Parkinson's disease. *Acta Neuropathol. Commun.* 5:11. doi: 10.1186/s40478-017-0416-x

Jankovic, J., Chen, S., and Le, W. D. (2005). The role of Nurr1 in the development of dopaminergic neurons and Parkinson's disease. *Prog. Neurobiol.* 77, 128–138. doi: 10.1016/j.pneurobio.2005.09.001

Jia, C., Qi, H., Cheng, C., Wu, X., Yang, Z., Cai, H., et al. (2020a). α-Synuclein negatively regulates Nurr1 expression through NF-κB-related mechanism. *Front. Mol. Neurosci.* 13:64. doi: 10.3389/fnmol.2020.00064

Jia, C. C., Li, G., Jiang, R., Liu, X., Yuan, Q., Le, W., et al. (2020b). B-cell receptor-associated protein 31 negatively regulates the expression of monoamine oxidase a *via* R1. *Front. Mol. Biosci.* 7:64. doi: 10.3389/fmolb.2020.00064

Jiang, H., Jiang, Q., Liu, W., and Feng, J. (2006). Parkin suppresses the expression of monoamine oxidases. *J. Biol. Chem.* 281, 8591–8599. doi: 10.1074/jbc.M510926200

Jiang, H., Ren, Y., Yuen, E. Y., Zhong, P., Ghaedi, M., Hu, Z., et al. (2012). Parkin controls dopamine utilization in human midbrain dopaminergic neurons derived from induced pluripotent stem cells. *Nat. Commun.* 3:668. doi: 10.1038/ncomms1669

Kabayama, M., Sakoori, K., Yamada, K., Ornthanalai, V. G., Ota, M., Morimura, N., et al. (2013). Rines E3 ubiquitin ligase regulates MAO-A levels and emotional responses. *J. Neurosci.* 33, 12940–12953. doi: 10.1523/JNEUROSCI.5717-12.2013

Kalia, L. V., and Lang, A. E. (2015). Parkinson's disease. *Lancet* 386, 896–912. doi: 10.1016/S0140-6736(14)61393-3

Kang, S. S., Ahn, E. H., Zhang, Z., Liu, X., Manfredsson, F. P., Sandoval, I. M., et al. (2018). Alpha-Synuclein stimulation of monoamine oxidase-B and legumain protease mediates the pathology of Parkinson's disease. *EMBO J.* 37:e98878. doi: 10.15252/embj.201798878

Kolla, N. J., and Bortolato, M. (2020). The role of monoamine oxidase A in the neurobiology of aggressive, antisocial and violent behavior: a tale of

mice and men. *Prog. Neurobiol.* 194:101875. doi: 10.1016/j.pneurobio.2020.101875

Kruger, R., Kuhn, W., Muller, T., Woitalla, D., Graeber, M., Kosel, S., et al. (1998). Ala30Pro mutation in the gene encoding α-synuclein in Parkinson's disease. *Nat. Genet.* 18, 106–108. doi: 10.1038/ng0298-106

Lees, A. J., Hardy, J., and Revesz, T. (2009). Parkinson's disease. *Lancet* 373, 2055–2066. doi: 10.1016/S0140-6736(09)60492-X

Lesage, S., Anheim, M., Letournel, F., Bousset, L., Honore, A., Rozas, N., et al. (2013). G51D α-synuclein mutation causes a novel parkinsonian-pyramidal syndrome. *Ann. Neurol.* 73, 459–471. doi: 10.1002/ana.23894

Lin, X., Parisiadou, L., Sgobio, C., Liu, G., Yu, J., Sun, L., et al. (2012). Conditional expression of Parkinson's disease-related mutant α-synuclein in the midbrain dopaminergic neurons causes progressive neurodegeneration and degradation of transcription factor nuclear receptor related 1. *J. Neurosci.* 32, 9248–9264. doi: 10.1523/JNEUROSCI.1731-12.2012

Monzani, E., Nicolis, S., Dell-Acqua, S., Capucciati, A., Bacchella, C., Zucca, F. A., et al. (2019). Dopamine, oxidative stress and protein-quinone modifications in Parkinson's and other Neurodegenerative diseases. *Angew. Chem. Int. Ed. Engl.* 58, 6512–6527. doi: 10.1002/anie.201811122

Ou, X. M., Chen, K., and Shih, J. C. (2006). Monoamine oxidase A and repressor R1 are involved in apoptotic signaling pathway. *Proc. Natl. Acad. Sci. U S A* 103, 10923–10928. doi: 10.1073/pnas.0601515103

Polymeropoulos, M. H., Lavedan, C., Leroy, E., Ide, S. E., Dehejia, A., Dutra, A., et al. (1997). Mutation in the α-synuclein gene identified in families with Parkinson's disease. *Science* 276, 2045–2047. doi: 10.1126/science.276.5321.2045

Proukakis, C., Dudzik, C. G., Brier, T., MacKay, D. S., Cooper, J. M., Millhauser, G. L., et al. (2013). A novel α-synuclein missense mutation in Parkinson disease. *Neurology* 80, 1062–1064. doi: 10.1212/WNL.0b013e31828727ba

Reiter, R. J. (1991). Pineal melatonin: cell biology of its synthesis and of its physiological interactions. *Endocr. Rev.* 12, 151–180. doi: 10.1210/edrv-12-2-151

Saucedo-Cardenas, O., Quintana-Hau, J. D., Le, W. D., Smidt, M. P., Cox, J. J., De Mayo, F., et al. (1998). Nurr1 is essential for the induction of the dopaminergic phenotype and the survival of ventral mesencephalic late dopaminergic precursor neurons. *Proc. Natl. Acad. Sci. U S A* 95, 4013–4018. doi: 10.1073/pnas.95.7.4013

Shih, J. C. (1991). Molecular basis of human MAOA and B. *Neuropsychopharmacology* 4, 1–7.

Shih, J. C., Chen, K., and Ridd, M. J. (1999). Monoamine oxidase: from genes to behavior. *Annu. Rev. Neurosci.* 22, 197–217. doi: 10.1146/annurev.neuro.22.1.197

Spillantini, M. G., Schmidt, M. L., Lee, V. M., Trojanowski, J. Q., Jakes, R., and Goedert, M. (1997). α-synuclein in Lewy bodies. *Nature* 388, 839–840. doi: 10.1038/42166

Tanaka, Y., Engelender, S., Igarashi, S., Rao, R. K., Wanner, T., Tanzi, R. E., et al. (2001). Inducible expression of mutant α-synuclein decreases proteasome activity and increases sensitivity to mitochondria-dependent apoptosis. *Hum. Mol. Genet.* 10, 919–926. doi: 10.1093/hmg/10.9.919

Ugun-Klusek, A., Theodosi, T. S., Fitzgerald, J. C., Burte, F., Ufer, C., Boocock, D. J., et al. (2019). Monoamine oxidase-A promotes protective autophagy in human SH-SY5Y neuroblastoma cells through Bcl-2 phosphorylation. *Redox Biol.* 20, 167–181. doi: 10.1016/j.redox.2018.10.003

Westlund, K. N., Denney, R. M., Rose, R. M., and Abell, C. W. (1988). Localization of distinct monoamine oxidase A and monoamine oxidase B cell populations in human brainstem. *Neuroscience* 25, 439–456. doi: 10.1016/0306-4522(88)90250-3

Wong, Y. C., and Krainc, D. (2017). α-synuclein toxicity in neurodegeneration: mechanism and therapeutic strategies. *Nat. Med.* 23, 1–13. doi: 10.1038/nm.4269

Wu, J. B., Yin, L., Shi, C., Li, Q., Duan, P., Huang, J. M., et al. (2017). MAOA-dependent activation of Shh-IL6-RANKL signaling network promotes prostate cancer metastasis by engaging tumor-stromal cell interactions. *Cancer Cell* 31, 368–382. doi: 10.1016/j.ccell.2017.02.003

Zarranz, J. J., Alegre, J., Gomez-Esteban, J. C., Lezcano, E., Ros, R., Ampuero, I., et al. (2004). The new mutation, E46K, of α-synuclein causes Parkinson and Lewy body dementia. *Ann. Neurol.* 55, 164–173. doi: 10.1002/ana.10795

Zhu, Q. S., Chen, K., and Shih, J. C. (1994). Bidirectional promoter of human monoamine oxidase A (MAO A) controlled by transcription factor Sp1. *J. Neurosci.* 14, 7393–7403. doi: 10.1523/JNEUROSCI.14-12-07393.1994

Conflict of Interest: The authors declare that the research was conducted in the absence of any commercial or financial relationships that could be construed as a potential conflict of interest.

Copyright © 2021 Jia, Cheng, Li, Chen, Yang, Liu, Li and Le. This is an open-access article distributed under the terms of the Creative Commons Attribution License (CC BY). The use, distribution or reproduction in other forums is permitted, provided the original author(s) and the copyright owner(s) are credited and that the original publication in this journal is cited, in accordance with accepted academic practice. No use, distribution or reproduction is permitted which does not comply with these terms.

frontiers in Aging Neuroscience

REVIEW
published: 23 March 2021
doi: 10.3389/fnagi.2021.645996

Biomarkers and the Role of α-Synuclein in Parkinson's Disease

*Tingting Du[1], Le Wang[2], Weijin Liu[3], Guanyu Zhu[4], Yingchuan Chen[4] and Jianguo Zhang[1,4,5]**

[1]Department of Functional Neurosurgery, Beijing Neurosurgical Institute, Capital Medical University, Beijing, China, [2]Molecular Biology Laboratory for Neuropsychiatric Diseases, Department of Neurobiology, Beijing Institute of Brain Disorders, Capital Medical University, Beijing, China, [3]Key Laboratory for Neurodegenerative Disease of the Ministry of Education, Key Laboratory of Neural Regeneration and Repair, Beijing Key Laboratory on Parkinson's Disease, Department of Neurobiology, School of Basic Medical Sciences, Capital Medical University, Beijing, China, [4]Department of Neurosurgery, Beijing Tiantan Hospital, Capital Medical University, Beijing, China, [5]Beijing Key Laboratory of Neurostimulation, Beijing Municipal Science and Technology Commission, Beijing, China

Parkinson's disease (PD) is a progressive neurodegenerative disorder characterized by the presence of α-synuclein (α-Syn)-rich Lewy bodies (LBs) and the preferential loss of dopaminergic (DA) neurons in the substantia nigra (SN) pars compacta (SNpc). However, the widespread involvement of other central nervous systems (CNS) structures and peripheral tissues is now widely documented. The onset of the molecular and cellular neuropathology of PD likely occurs decades before the onset of the motor symptoms characteristic of PD, so early diagnosis of PD and adequate tracking of disease progression could significantly improve outcomes for patients. Because the clinical diagnosis of PD is challenging, misdiagnosis is common, which highlights the need for disease-specific and early-stage biomarkers. This review article aims to summarize useful biomarkers for the diagnosis of PD, as well as the biomarkers used to monitor disease progression. This review article describes the role of α-Syn in PD and how it could potentially be used as a biomarker for PD. Also, preclinical and clinical investigations encompassing genetics, immunology, fluid and tissue, imaging, as well as neurophysiology biomarkers are discussed. Knowledge of the novel biomarkers for preclinical detection and clinical evaluation will contribute to a deeper understanding of the disease mechanism, which should more effectively guide clinical applications.

Keywords: Parkinson's disease, α-synuclein, biomarker, genetics, immune inflammation, imaging

OPEN ACCESS

Edited by:
Pingyi Xu,
First Affiliated Hospital of Guangzhou Medical University, China

Reviewed by:
Kurt A. Jellinger,
University of Vienna, Austria
Takahito Yoshizaki,
Keio University, Japan
Sravan Gs,
Hong Kong Baptist University, Hong Kong

****Correspondence:***
Jianguo Zhang
jg.zhang@ccmu.edu.cn

Received: *24 December 2020*
Accepted: *05 March 2021*
Published: *23 March 2021*

Citation:
Du T, Wang L, Liu W, Zhu G, Chen Y and Zhang J (2021) Biomarkers and the Role of α-Synuclein in Parkinson's Disease. Front. Aging Neurosci. 13:645996. doi: 10.3389/fnagi.2021.645996

INTRODUCTION

Parkinson's disease (PD) is a complex, chronic, and progressive neurodegenerative disease characterized by the presence of Lewy bodies (LBs) in vulnerable populations of neurons. The major component of LBs is insoluble α-synuclein (α-Syn) fibrils (Spillantini et al., 1997). The etiology of PD is likely multifactorial, and involves the interplay among aging, genetic susceptibility, and environmental factors (Pang et al., 2019); however, the α-Syn protein is a central component in the pathogenesis of the disease. Accumulating evidence suggests that α-Syn oligomers play a significant role in the PD neurodegenerative process by impairing many subcellular functions (Colla et al., 2012; Choi et al., 2013). Generally, degeneration of approximately 70% of dopaminergic (DA) neurons in the substantia nigra (SN) pars compacta (SNpc) of the midbrain region takes place before the clinical symptoms occur (Postuma et al., 2010; Heisters, 2011). According to clinical and imaging findings, the neurodegenerative process of PD may begin 7–10 years before the appearance

of the classic motor symptoms of bradykinesia, rigidity, and tremors (Hawkes, 2008; Schapira and Tolosa, 2010). PD is diagnosed from motor symptoms, but non-motor symptoms are often manifest during a prolonged prodromal phase as much as 20 years before the onset of the motor features (Kalia and Lang, 2015; Armstrong and Okun, 2020). Treatment can therefore only be initiated in the late phase of the disease. Although considerable progress has been made in understanding its pathogenesis, early and accurate diagnosis of PD is still a formidable challenge (Postuma et al., 2016). This is largely a result of the lack of well-established biomarkers for early diagnosis and monitoring of progression.

Biomarkers are required to detect the disease in the early stages when prevention is possible. Various biomarkers providing early diagnosis of the disease include clinical, imaging, pathological, physiological, biochemical, and genetic parameters. Moreover, biomarkers—alone or in combination—are used to diagnose and monitor the evolution of PD. This review article describes various biomarkers available for PD, discusses recent advances in their development, and focuses on the roles of α-Syn in the neurodegenerative process during PD.

GENETIC BIOMARKERS

SNCA

PD is typically a sporadic disease, but in a small proportion of patients, mutation of a dominantly or recessively inherited gene can cause PD. Although relatively rare, these genetic forms of PD have revealed much about the molecular pathogenesis of sporadic PD (Kalia and Lang, 2015). The first gene identified was *SNCA* (Polymeropoulos et al., 1997), which encodes α-Syn. *SNCA* mutations are associated with autosomal dominant PD. *SNCA* mutations as a genetic cause of PD led to the identification of α-Syn as a major component of LBs and neurites (Spillantini et al., 1997). In particular, α-Syn is implicated in the pathogenesis of PD, because it is a major component of LBs. The aggregation of α-Syn and its incorporation as a major component of LBs is the hallmark of PD. Approximately 90% of insoluble α-Syn in LBs is phosphorylated, and phosphorylation at Ser-129 (a major phosphorylation site) is characteristic of PD (Chen and Feany, 2005). Additionally, point mutations in the *SNCA* gene lead to familial PD (Polymeropoulos et al., 1997), as do relatively rare duplications or triplications of the *SNCA* locus, which result in elevated α-Syn in both the brain and blood (Miller et al., 2004). Point mutations, duplications, and triplications in the *SNCA* gene cause PD with high penetrance, and some SNPs of this gene have been identified as genetic risk factors for PD (Dekosky and Marek, 2003; Gasser, 2009). Highly penetrant familial mutations or multiplications in the *SNCA* have been shown to cause aggressive early-onset PD. Additionally, a common SNP in the *SNCA* gene that is enriched in PD patients has been shown to increase expression *in vitro* (Mizuta et al., 2013). Moreover, variants in the gene have been identified as a risk factor in Genome–Wide Association Studies (GWAS; Nalls et al., 2011). Thus, α-Syn in blood, plasma, or cerebrospinal fluid (CSF) is a promising candidate as a biomarker for diagnosing PD.

The first evidence showing that *SNCA* gene deregulation is directly associated with PD came from familial PD cases, where point mutations at the 53rd (alanine to threonine), 30th (alanine to proline), and the 46th (glutamine to lysine) amino acids were discovered, which led to an autosomal dominant form of disease inheritance along with early-onset (Polymeropoulos et al., 1997; Krüger et al., 1998; Zarranz et al., 2004). Both duplication and triplication of *SNCA* were strongly associated with severity and early onset in familial PD (Singleton et al., 2003; Chartier-Harlin et al., 2004). Several SNPs identified throughout *SNCA* were found to interfere with the normal transcriptional regulation of the gene and the binding of microRNA. The study revealed that the expression levels of microRNA miR-19b were downregulated in patients with idiopathic rapid eye movement sleep behavior disorder, and antedated the diagnosis of PD after 4.67 ± 2.61 years of follow-up (Fernández-Santiago et al., 2015). It, therefore, has the potential for early diagnosis of PD. Locascio et al. reported a consistent association of reduced *SNCA* transcripts in accessible peripheral blood and early-stage PD in 863 patients and suggested a clinical role as a potential predictor of cognitive decline (Locascio et al., 2015). At present, the most studied epigenetic-based biomarker for PD is DNA methylation in the *SNCA* gene. One report showed a 2-fold decrease in global DNA methylation in the cortex of human postmortem PD samples, with significant hypomethylation of the *SNCA* intron1 region (Desplats et al., 2011). Efforts have therefore considered using *SNCA* or some other PD-implicated gene methylation in peripheral tissues as a biomarker for PD (Jakubowski and Labrie, 2017). However, α-Syn, and subsequently LBs, are markers of other neurodegenerative diseases collectively termed α-synucleinopathies, a group that includes PD (with or without dementia), dementia with LBs, an LB variant of Alzheimer's disease, and multiple system atrophy (MSA). Therefore, a combination of imaging, biochemical analyses, and genetic biomarkers might be required.

Other Genes

In the past two decades, substantial progress has been made in the genetics of PD. Data from Mendelian genetics and GWAS have identified several chromosomal loci that cause or regulate the risk of PD (Hernandez et al., 2016; Deng et al., 2018). Genetic factors are associated with specific clinical pictures and may influence the response to therapy. Mutations of *SNCA*, Leucine-rich repeat kinase 2 (*LRRK2*), *Parkin*, PTEN-induced putative kinase 1 (*PINK1*), and *DJ-1* genes have been associated with monogenic forms of PD and linked to specific clinical characteristics slightly different from those observed in non-mutated patients (Koros et al., 2017).

Since the discovery of *SNCA* mutations as a cause of PD, five additional genes have been proposed to mediate autosomal dominant forms of PD: *LRRK2*, *VPS35*, *EIF4G1*, *DNAJC13*, and *CHCHD2* (Kalia and Lang, 2015). Mutations in *LRRK2* are the most common causes of dominantly inherited PD (Corti et al., 2011) because they are found in approximately 4% of familial PD patients and account for 1% of sporadic PD worldwide. The most common *LRRK2* mutation results in a Gly2019Ser amino acid substitution (Healy et al., 2008). *Parkin*, *PINK1*, and *DJ-1*

are associated with autosomal recessive forms of PD (Kalia and Lang, 2015). Mutations in *Parkin* are the most common cause of autosomal recessive PD. In patients with PD onset before the age of 45 years, *Parkin* mutations are seen in up to 50% of familial cases and about 15% of sporadic cases (Periquet et al., 2003). Patients with mutations in *Parkin* usually show juvenile PD (JPD, onset <21 years old) or early-onset PD (between 21 and 40 years old) with a slow clinical course, excellent response to low doses of levodopa, and frequent treatment-induced dyskinesias (Lohmann et al., 2009). Mutations in *PINK1* and *DJ-1* are less common causes (1–8% and 1–2% of early-onset sporadic PD, respectively; Singleton et al., 2013). *DJ-1*, also known as Parkinsonism-associated deglycase encoded by the *PARK7* gene, is a multifunctional protein that plays a neuroprotective role in oxidative stress during neurodegeneration (Saito, 2014). An increase of DJ-1 ultimately reflects oxidative stress in PD patients, making it a biomarker for PD. However, the DJ-1 level is very high in erythrocytes, and in the CSF and plasma, it is affected by hemolysis and contamination by erythrocytes (Saito, 2014). Therefore, when detecting DJ-1 level in the CSF and plasma, an evaluation of hemolysis and contamination by erythrocytes is very necessary. Generally, autosomal dominant PD tends to have an age of onset similar to sporadic PD, while recessively inherited Parkinsonism is more frequently associated with early onset (age <40 years; Schrag and Schott, 2006).

The greatest genetic risk factor for developing PD is a mutation in *GBA*, which encodes β-glucocerebrosidase (GCase), the lysosomal enzyme deficient in Gaucher disease (GD) (Sidransky and Lopez, 2012). The results of a large multicenter study of more than 5,000 patients with PD and an equal number of matched controls showed an odds ratio >5 for any *GBA* mutation in PD patients vs. control subjects (Sidransky et al., 2009). PD patients with some *GBA* mutations (GBA-PD) tend to have an earlier onset of symptoms, more aggressive disease, with more severe and earlier cognitive impairments and psychiatric manifestations (Balestrino and Schapira, 2018). One study reported that GCase activity was significantly lower in GBA-PD than in idiopathic PD patients, and even lower in GD-PD patients, suggesting that GCase activity could be a possible marker of mutated *GBA* (Ortega et al., 2016). Deficiency of GCase increases the risk of Parkinsonism, which appears to be driven by the direct effect of GCase deficiency and lysosomal dysfunction on α-Syn aggregation. The GCase activity in the CSF could therefore further serve as a PD biomarker (Magdalinou et al., 2014). Additional genes associated with Parkinsonism identified from relatives or patient cohorts include *ATP13A2*, *C9ORF72*, *FBXO7*, *PLA2G6*, *POLG1*, *SCA2*, *SCA3*, *SYNJ1*, and *RAB39B*. Parkinsonism due to mutations in these genes is quite rare and usually associated with features atypical for PD (e.g., prominent cognitive impairment, ophthalmological abnormalities, pyramidal signs, or ataxia; Kalia and Lang, 2015).

IMMUNE INFLAMMATORY BIOMARKERS

Immune Inflammation in PD

Under physiological conditions, the brain provides an immunosuppressive environment to maintain the function of the central nervous systems (CNS). When this environment is destroyed, such as in infectious diseases, autoimmune diseases, or neurodegenerative diseases, a series of immune responses are activated, sometimes even leading to chronic inflammation. Although it has been shown that various cells are involved, including peripheral immune cells, neurons, microglia, and astrocytes that infiltrate the brain tissue, the role of microglia is most conspicuous as resident macrophages of the CNS. Microglia are in the "resting or inactive" state under physiological conditions; however, almost any form of disturbance of the CNS microenvironment, such as infection, injury, and aging, can result in microglial activation.

Since the discovery of activated microglia in the SNpc of PD patients in 1988, increasing attention has been directed toward the study of neuro-immunoinflammatory pathogenesis of PD, characterized by microglial activation. Autopsies of PD patients have shown that the loss of DA neurons is accompanied by microglial activation, an inflammatory response, and the expressions of proinflammatory cytokines in microglia, such as TNF-α, IFN-γ, and IL-1β (Mirza et al., 2000). The early positron emission tomography (PET) results of PD patients have shown that the number of activated microglia was significantly increased, accompanied by the loss of DA neurons in the midbrain (Ouchi et al., 2005), which suggested that the neuroinflammatory response caused by excessive microglial activation had a significant impact on the progression of DA neuron degenerative in PD. These studies also suggest that assessing microglial activation in the substantia nigra (SN), as well as DA neuron injury by imaging techniques such as PET, can be an early diagnostic biomarker of PD.

A large number of activated microglia have also been found in the 1-methyl-4-phenyl 1,2,3,6-tetrahydropyridine (MPTP), rotenone, and 6-hydroxydopamine (6-OHDA) models and the activation of microglia can enhance their neurotoxicity to DA neurons, suggesting that microglial activation may be one of the main factors promoting the death of DA neurons (Zheng et al., 2008; Sui et al., 2009; Walsh et al., 2011). The systemic inflammation induced by IL-1β and LPS can exacerbate the death of DA neurons in PD animal models (Pott Godoy et al., 2008; Byler et al., 2009). However, some anti-inflammatory drugs, such as ibuprofen and minocycline, can reduce the inflammatory effects, lower microglia activation, and alleviate the degeneration of DA neurons in the SN in PD animal models (Wu et al., 2002; Zheng et al., 2008; Walsh et al., 2011), which suggests that suppressing microglial activation and proinflammatory cytokine release can inhibit neurodegeneration. Also, transgenic animal models have confirmed the association between microglia and PD (Lachenmayer and Yue, 2012; Deng and Yuan, 2014), in which microglia were activated and TNF-α secretion was increased in the SN of mice overexpressing α-Syn, with subsequent neuronal death (Su et al., 2008; Sanchez-Guajardo et al., 2010). Both transgenic and inflammatory PD models can explain some pathological changes of the disease, but they cannot fully explain the role of innate immunity and the slow onset of degenerative diseases; however, these studies fully demonstrate the involvement of immune inflammation in PD pathogenesis.

Activation of the immune system can affect the synthesis and secretion of many soluble immune factors, including cytokines, chemokines, and complement, which are significantly increased in the PD postmortem brain (Reale et al., 2009; Grozdanov et al., 2014). These increased cytokines are mainly present in the nigrostriatal system rather than in other brain regions, suggesting that they are produced only at the sites of DA neuron damage. Furthermore, the level of cytokines in CSF as a possible marker of early diagnosis or disease progression in PD is worthy of study and attention. In our opinion, the content of cytokines in CSF can be used as a marker for the progression of PD and can provide a target for PD treatment. However, a comprehensive assessment of PD should also be performed by including other biomarkers. Although microglial activation and neuroinflammation may provide directions and ideas for PD pathogenetic mechanisms and therapeutic strategies, it remains to be clarified whether microglial activation is the result or cause of DA neuron degeneration.

The Role of α-Syn in Immune Inflammation of PD

The α-Syn aggregates are thought to be the major component of PD LBs, and α-Syn is found both in the cytoplasm but also in intercellular space. Aberrant accumulation of α-Syn can promote both neuronal dysfunction and neuroinflammation. Microglia act as the resident immune cells of the brain, which closely monitor changes of the microenvironment and maintain microenvironment homeostasis. Experimental evidence has shown that α-Syn aggregates can be surrounded by microglia, and microglia can be activated by extracellular α-Syn aggregates, leading to increased extracellular superoxide, inflammatory cytokines, and the selective loss of DA neurons (Couch et al., 2011). Some studies have also shown that soluble α-Syn can also activate microglia (Klegeris et al., 2008).

Microglia can phagocytose extracellular α-Syn aggregates, which can be degraded by the autophagosome. Additionally, the Fc-γ receptor is required for uptake of extracellular, aggregated α-Syn and neuroinflammation induced by α-Syn (Cao et al., 2012). Fc-γ receptor knockout has been shown to attenuate the immune response, microglia activation, and DA neuron neurodegeneration, which is triggered by adeno-associated virus serotype 2 to selectively overexpress human α-Syn in the SN (Cao et al., 2010). The Fc-γ receptor$^{-/-}$ microglia do not exhibit an inflammatory response to aggregated α-Syn, suggesting that phagocytosis of α-Syn into microglia is required for inducing neuroinflammation and neurodegeneration in PD patients (Cao et al., 2012). Apart from Fc-γ receptor-mediated phagocytosis of α-Syn, toll-like receptors (TLRs) are also targeted by α-Syn treatment. The α-Syn can act as a damage-associated molecular pattern, which activates TLRs, and it may be an important mediator of neuroinflammation in PD patients. TLR2 and TLR4 expressions increase in postmortem brain tissue from PD patients (Drouin-Ouellet et al., 2014; Dzamko et al., 2017), and TLR2 is strongly localized to α-Syn positive LBs (Dzamko et al., 2017). Furthermore, both treatments with blocking antibody against TLR2 and depletion of TLR2 in microglia result in the elimination of cytokine release induced by conditioned medium from SH-SY5Y cells overexpressing α-Syn (Kim et al., 2013). Microglial phagocytic activity, proinflammatory cytokine release, and reactive oxygen species (ROS) production triggered by recombinant α-Syn treatment are downregulated in the TLR4 deficient murine (Fellner et al., 2013). The current findings suggest that TLR2 and TLR4 play a modulatory role in microglial activation and proinflammatory responses triggered by α-Syn in PD.

There is evidence that α-Syn can be secreted into the extracellular environment, and most of the extracellular α-Syn is aggregated, misfolded, and increased in amount. This extracellular α-Syn activates microglia and the immune system, to induce inflammatory responses during the pathogenesis of PD. Studies have assessed the effect of oligomeric or fibrillar α-Syn on microglia, and have shown that an increase in TNF-α (Daniele et al., 2015; Pradhan et al., 2017; Hughes et al., 2019), IL-1β (Daniele et al., 2015; Pradhan et al., 2017), IL-6 (Acuña et al., 2019), COX-2, and iNOS (Pradhan et al., 2017), as well as an increase in ROS or NO (Daniele et al., 2015; Pradhan et al., 2017; Panicker et al., 2019), are involved in neurotoxicity. Aggregated α-Syn also has been found to increase inflammasome activation and even pyroptosis. Fibrillary α-Syn in mouse microglia results in a delayed but robust activation of NLRP3 inflammasomes, leading to extracellular IL-1β and caspase recruitment domain release (Zhou et al., 2016; Gordon et al., 2018). Furthermore, phosphorylated and nitrated α-Syn also activates microglia, increases proinflammatory cytokines release, and induces inflammation (Reynolds et al., 2009; Christiansen et al., 2016; Duffy et al., 2018). Also, *in vitro* studies using different doses of monomeric recombinant α-Syn have stimulated both primary cultured microglia and microglia/macrophage cell lines, and have found that extracellular α-Syn can induce a pro-inflammatory response in microglia with an increase in proinflammatory cytokines (Boza-Serrano et al., 2014; Hu et al., 2016; Rabenstein et al., 2019; Shao et al., 2019; Wang L. et al., 2020), as well as an increase in reactive oxygen or COX-2 (Lee et al., 2010; Boza-Serrano et al., 2014; Hu et al., 2016), associated with inflammation. These results confirm that extracellular α-Syn has an important role in chronic inflammation during the pathogenesis of PD.

Microglia have stronger phagocytosis of extracellular α-Syn when compared to other cells in the CNS (Zhang et al., 2005), but different groups have found this phagocytic activity is different for different species of α-Syn. Microglia incubated with both wild-type and A53T α-Syn showed increased phagocytic activity, but an opposite effect was found in A30P and E46K α-Syn (Roodveldt et al., 2010). Also, monomeric α-Syn-stimulated microglia upregulated phagocytosis, while aggregated α-Syn inhibited both basal and LPS-induced phagocytosis (Park et al., 2008). Also, microglial phagocytic activity is increased after fibrillary α-Syn treatment dependent on TLR4 (Fellner et al., 2013). In contrast, microglia-overexpressed A30P or A53T α-Syn showed a pro-inflammatory response and impaired phagocytosis (Rojanathammanee et al., 2011). However, microglia from α-Syn knock-out mice showed increased basal levels of proinflammatory cytokines, increased expression of CD68, and impaired phagocytic ability, when compared with wild-type

microglia, suggesting that the levels of α-Syn may be related to phagocytosis.

During the progression of PD, extracellular α-Syn can undergo phagocytosis by microglia, leading to microglial activation, but the ability of activated microglia to degrade α-Syn is reduced, with increased α-Syn accumulation in the cytoplasm, which causes continuous activation of microglia, and eventually leads to chronic inflammation and long-term damage to DA neurons.

FLUID AND TISSUE BIOMARKERS

The α-Syn Species in CSF and Blood

As early as 2003, El-Agnaf and his colleagues first reported the identification of α-Syn in human CSF (El-Agnaf et al., 2003). Since then, different immunoassays for CSF α-Syn detection have been compared in different laboratories, and most studies suggested that CSF α-Syn is lower in PD patients (Eusebi et al., 2017; Parnetti et al., 2019). Reports on serum and plasma quantitative detection of α-Syn have provided ambiguous results, whether higher, lower, or not significantly different in PD patients when compared with controls (Ding et al., 2017; Lin et al., 2017; Chang et al., 2019; Fayyad et al., 2019). Several studies provide strong evidence that soluble α-Syn oligomers (o-α-Syn), which have been proven to be more toxic, have been commonly found at higher levels in the CSF and plasma of PD patients (Kayed et al., 2003; El-Agnaf et al., 2006). Furthermore, it has been reported that the ratio of CSF o-α-Syn/total α-Syn could improve the sensitivity and specificity of PD diagnosis (Parnetti et al., 2014). As for the detection of α-Syn aggregates, two highly specific and sensitive methods, protein-misfolding cyclic amplification (PMCA) and real-time quaking-induced conversion (RT-QuIC) have been recently developed, and higher levels of α-Syn aggregates have been detected in the CSF samples of PD patients (Shahnawaz et al., 2017; Rossi et al., 2020). Shahnawaz et al. (2020) also used PMCA and found distinctly aggregated α-Syn strains in the CSF from PD and MSA patients, with a sensitivity reaching 95.4%. Taken together, the results show that different forms of α-Syn, especially o-α-Syn and misfolded α-Syn aggregates, detected by ultrasensitive techniques, are promising markers for early diagnosis and differential diagnosis of PD.

The α-Syn phosphorylation at serine-129 (pSer129 α-Syn, p-α-Syn) has also been shown to be abnormally elevated in CSF and plasma of PD patients (Foulds et al., 2011; Landeck et al., 2016; Majbour et al., 2016). Furthermore, Lin et al. (2019) found that plasma p-α-Syn correlated with motor severity and progression in PD patients. Notably, p-α-Syn is relatively unstable due to environmental factors. Cariulo et al. recently used ultrasensitive immunoassays based on single-molecule counting technology and found that p-α-Syn in CSF was undetectable in PD patients, even though plasma p-α-Syn could be easily detected (Cariulo et al., 2019). These results showed that p-α-Syn detection still lacked further validation in independent laboratories, so it is recommended that phosphatase inhibitors be added to samples at the time of collection. In general, studies on α-Syn still lack confirmation, as immunoassays and standardized antigens for quantification have varied from different laboratories. Besides, red blood cell (RBC) contamination also limits the usefulness of CSF and blood α-Syn species measurements. A standardized process for sample collection and experimental analyses are therefore still needed for an accurate diagnosis of PD.

Other Biomarkers in CSF and Blood

In addition to α-Syn species, studies have also focused on searching for other PD biomarkers. Lamontagne-Proulx et al. (2019) found that extracellular vesicles (EV) in the plasma of PD patients contained a specific signature of proteins. These features could reliably differentiate control subjects from mild and moderate PD patients, which suggested that EV blood-based assays have the potential to be used as PD biomarker assays (Lamontagne-Proulx et al., 2019). In another study, Youn et al. (2018) found that the levels of LC3B, Beclin1, and LAMP-2 were higher in the CSF of PD patients, which means that CSF levels of some autophagy-related proteins might represent potential diagnostic and prognostic biomarkers of early-stage PD in patients (Youn et al., 2018). Also, Kim et al. (2019) evaluated the levels of β-amyloid 1–42 (Aβ1–42), α-Syn, tau, and phosphorylated tau181 in the CSF of PD patients, during a median follow-up of 4 years; only Aβ42 among these biomarkers were associated with the development of a freezing gait (Kim et al., 2019). Moreover, Posavi et al. (2019) used multicohort proteomics analyses to select blood-based biomarkers for PD patients. Their results showed that bone sialoprotein, osteomodulin, aminoacylase-1, and growth hormone receptor robustly associated with PD across multiple clinical sites (Posavi et al., 2019). Recently, a review showed that CSF and blood levels of amino acids might also become potential biomarkers for PD. They found decreased CSF levels of glutamate and taurine and increased CSF levels of tyrosine; decreased serum/plasma levels of aspartate, serine, tryptophan, and lysine, and increased serum/plasma proline and homocysteine levels (Jiménez-Jiménez et al., 2020). Taken together, these markers, and many other proteins such as circulating microRNAs and neurofilament light (He et al., 2018; Khalil et al., 2018; van den Berg et al., 2020; Wang H. et al., 2020), have all been reported to be associated with PD. However, Dos Santos et al. (2018) has also proposed that the potential biomarkers lacked robustness and reproducibility in supporting diagnosis in the early clinical stages of PD; therefore, we still need further validation to confirm these findings.

The α-Syn Species in RBCs

RBCs are the major source of α-Syn in peripheral blood cells (Barbour et al., 2008). In the last several years, expanded insights into PD had revealed some relationships between PD and RBC-α-Syn. Wang et al. found that the ratio of o-α-Syn/total RBC protein was higher in PD patients than in the control groups. However, there was no correlation between RBC o-α-Syn levels and the Unified Parkinson's disease Rating Scale (UPDRS) motor scale score or progression of motor degeneration (Wang et al., 2015). In another study, Abd-Elhadi

et al. (2015) found that the ratio of α-Syn/proteinase K-resistant α-Syn was significantly lower in PD patients when compared with healthy controls. Post-translational modifications (PTMs) of RBC-α-Syn have also been identified. Vicente Miranda et al. (2017) found that the levels of phosphorylated Y125, nitrated Y39, and glycated α-Syn were increased in RBCs from PD patients, while SUMOylated α-Syn was reduced. Moreover, these PTMs correlated with disease severity and duration. The combinatorial analyses of these PTMs in RBCs resulted in increased sensitivity in clinical trials (Vicente Miranda et al., 2017). Notably, there was a significant difference between the RBC-α-Syn from the membrane and cytosolic fractions. Zhang et al. (2005) found that, compared to healthy controls, the levels of total and aggregated α-Syn were significantly higher in the membrane fraction, but not in the cytosolic component of PD patients. Furthermore, the level of p-α-Syn was higher in PD patients in the cytosolic fraction, while to a lesser extent, it was also higher in the membrane fraction (Tian et al., 2019). Papagiannakis et al. (2018) also collected erythrocyte membranes and detected higher levels of α-Syn dimers and the dimer to monomer ratio in mutant carriers of the *GBA* gene (GBA-PD) and PD patients without known mutations (Papagiannakis et al., 2018). It is noteworthy that different forms of RBC-α-Syn also changed in GD and patients with MSA (Moraitou et al., 2016; Liu et al., 2019). It was also reported that there was no significant difference in the o-α-Syn/total protein ratio in RBCs between PD and MSA patients (Wang et al., 2015). Thus, further research is still needed to determine if RBC-α-Syn can be used for differential diagnosis of PD.

The α-Syn Species in Peripheral Tissues

Stokholm et al. (2016) found that gastrointestinal deposits of p-α-Syn were found in 56% of patients with prodromal PD when compared with 26% of control subjects, and they detected Lewy pathology in the gastrointestinal tract of patients up to 20 years before their diagnoses (Stokholm et al., 2016). Tolosa and co-workers also found aggregated α-Syn in submandibular gland tissues in patients with idiopathic rapid eye movement sleep behavior disorder (Vilas et al., 2016). Since then, studies have been conducted to detect abnormally aggregated α-Syn in multiple peripheral tissues and biofluids of PD patients (Tsukita et al., 2019; Chahine et al., 2020).

Peripheral biofluid samples such as saliva, tears, and urine are commonly used for clinical testing and diagnosis. Bougea et al. (2019) summarized the use of salivary α-Syn as a diagnostic biomarker for PD. They found that the potential use of salivary o-α-Syn but not total α-Syn was more promising (Bougea et al., 2019). In addition to o-α-Syn in salivary glands, Cao et al. (2019) reported that extracellular vesicles from PD saliva also obtained higher levels of o-α-Syn and higher o-α-Syn/α-Syn ratios (Cao et al., 2019). It was also suggested that salivary miR-153 and miR-223 levels may serve as non-invasive diagnostic biomarkers of idiopathic PD (Chahine et al., 2020). In addition to saliva, studies have also found higher levels of o-α-Syn in basal tears of PD patients (Hamm-Alvarez et al., 2019). Recently, Nam et al. found distinct forms of o-α-Syn in urine, which might be useful for PD diagnosis (Nam et al., 2020). In addition to these biological fluids, needle biopsies for labial minor salivary glands and submandibular glands, and detection of the deposition of α-Syn or p-α-Syn in PD patients are also possibilities for clinical applications (Adler et al., 2017; Iranzo et al., 2018; Shin et al., 2019). Furthermore, biopsy samples of submandibular glands were reported to have increased sensitivity and specificity, when compared to minor salivary glands (Campo et al., 2019). Manne et al. (2020) recently used the RT-QuIC technique to quantify pathological α-Syn level in paraffin-embedded submandibular glands of PD patients and healthy controls, where the sensitivity and specificity reached 100% and 94%, respectively (Manne et al., 2020).

Skin biopsy is also a promising diagnostic tool for PD. As early as 2014, Donadio et al. evaluated the skin biopsies from proximal and distal sites of small nerve fibers from idiopathic PD patients. They found that p-α-Syn was deposited in the proximal cervical skin, while nothing was detected in controls (Donadio et al., 2014). In subsequent studies, they also detected p-α-Syn both in proximal and distal sites of small nerve fibers from dementia with LB patients (Donadio et al., 2017). Similarly, it was reported that E46K-*SNCA* carriers had p-α-Syn aggregates in intraepidermal nerve fibers, and the severity of the latter skin abnormalities was correlated with sudomotor dysfunction in hands (Carmona-Abellan et al., 2019). Kuzkina et al. (2019) used conformation-specific antibodies and digestion with proteinase K to show that there was no obvious difference between α-Syn deposits in dermal cutaneous nerve fibers and midbrains of PD patients. In addition to early diagnosis of PD, abnormally aggregated α-Syn in skin nerve fibers might also be used for differential diagnosis with other diseases. Donadio et al. (2020) recently reported that the distribution difference of p-α-Syn in cutaneous nerves might help to distinguish MSA Parkinsonism type from PD with orthostatic hypotension. Wang et al. also used RT-QuIC/PMCA and found that skin α-Syn had aggregation seeding activity that was significantly higher in individuals with PD and other synucleinopathies, compared with those with tauopathies and non-neurodegenerative controls (Wang Z. et al., 2020).

In general, these results suggest that abnormally aggregated α-Syn in peripheral tissues and biofluids might be used for early diagnosis and differential diagnosis for PD. The development of new technologies, such as RT-QuIC and PMCA, has greatly assisted in these studies. However, it is also noteworthy that standardized methods for sample collection and detection are very important in the entire process, and related studies are still needed for further validations.

IMAGING BIOMARKERS

Imaging biomarkers have been increasingly used in the diagnosis of PD, to provide support for clinical observations. Neuroimaging using magnetic resonance imaging (MRI), positron emission tomography (PET), and transcranial sonography (TCS) can provide important information on brain structure and function in PD, and can also serve as an adjunct to clinical assessments. Imaging has been used to

differentiate PD from other movement disorders, and to facilitate diagnostic accuracy.

MRI

Traditional MRI is usually used to exclude secondary Parkinsonism, including neoplasms, vascular Parkinsonism, and multiple sclerosis. However, in recent years, new studies have reported that brain regions are widely involved in patients with PD. With the development of MRI, multiple sequences of MRI have been used to investigate change during PD.

T1-weighted (T1) and T2-weighted (T2) structural MRI has been used to estimate the cortical thickness and structural volume. Gerrits et al. (2016) performed voxel-based morphometry on PD patients to investigate the gray matter volume, and found that PD patients showed cortical thinning in the left pericalcarine gyrus, extending to the cuneus, precuneus, lingual areas, left inferior parietal cortex, bilateral rostral middle frontal cortex, and right cuneus, and increased cortical surface areas in the left pars triangularis (Gerrits et al., 2016). Lyoo et al. (2011) reported that the parieto-temporal associated cortex cortical thickness was negatively correlated with disease duration, total UPDRS motor score, and bradykinesia and axial motor deficit subscores. The SN plays an indispensable role in the pathology of PD (Lehéricy et al., 2014). Volumetric differences of SN have been investigated in some studies using MRI, with varying results. Minati et al. (2007) reported that loss of the SN was observed in PD patients, when compared with control subjects, nevertheless, some studies did not observe any volumetric differences of SN in PD patients (Oikawa et al., 2002; Péran et al., 2010). Also, a study performed 7T MRI of PD patients, and found higher volumes of the SN in PD patients, when compared with the unsmooth boundary between the SN and crus cerebri (Kwon et al., 2012). Cosottini et al. (2014) found that three-dimensional susceptibility-weighted 7T-MRI showed a three-layered organization of the SN, which allowed discrimination between PD patients and control subjects with a sensitivity and specificity of 100% and 96.2%, respectively (Cosottini et al., 2014).

Quantitative susceptibility mapping (QSM), which compensates for the nonlocality of magnetic field distribution, could provide a robust estimation of magnetic susceptibility that is correlated with the iron content of the brain. PD patients were divided into Hoehn–Yahr stage $\leq$2.5 and Hoehn–Yahr stage $\geq$3 into early-stage and late-stage PD groups. The QSM values of SNpc were significantly increased in the early-stage PD patients compared with the controls. In late-stage PD patients, QSM values were higher than those of the controls and early-stage PD patients (Guan et al., 2017). Magnetic resonance spectroscopy, relying on the resonance frequencies of protons, could be used to measure the number of biochemical molecules in the brain. The pre-supplementary motor area NAA/Cr was lower in PD patients and correlated negatively with age; however, it did not correlate with the UPDRS score, disease duration, or dopamine equivalents (Camicioli et al., 2007).

Diffusion tensor imaging, an *in vivo* tractography technique, allowed researchers to determine an indirect estimation of brain microstructural integrity in PD patients by analyzing water molecules (Saeed et al., 2017). Sampedro et al. (2019) investigated longitudinal changes in intracortical mean diffusivity (MD) in recently diagnosed and drug-naïve PD patients using a public database (the Parkinson's Progression Markers Initiative). They found that *de novo* PD patients showed a higher MD value in the frontal and occipital cortices after one year when compared with that of the control subjects, and these changes were correlated with changes in cognitive measures (Sampedro et al., 2019). Reduced fractional anisotropy (FA) of the SN was observed in PD patients when compared with that of control subjects, and the reduced FA of PD patients was greater in the caudal region compared with the rostral region of interest. The sensitivity and specificity of 100% for the diagnosis of PD were obtained when using caudal SN (Vaillancourt et al., 2009).

A functional MRI captures the patterns of coherent spontaneous fluctuations of blood oxygen levels, allowing investigation of functional connectivities and activates (Li et al., 2018). Zhang et al. (2019) observed an increased dynamic amplitude of low-frequency fluctuations in the left precuneus in PD patients, which was positively correlated with disease duration. Machine learning using these features indicated that 80.36% of the patients were correctly diagnosed (Zhang et al., 2019). Another study showed no difference between PD and control participants regarding dynamic functional connectivity of the default mode network or the frontoparietal network with the rest of the brain (Engels et al., 2018). In the late-stage of the disease, PD patients may suffer from the freezing of gait (FOG). The PD patients with FOG exhibited decreased voxel-mirrored homotopic connectivity in the inferior parietal lobe when compared with both PD patients without FOG and healthy controls, so these features could distinguish FOG^+ patients from FOG^- patients or healthy controls (Li et al., 2018).

PET

PET is an *in vivo* functional neuroimaging technique (Matthews et al., 2018). In fluorodeoxyglucose (FDG) PET meta-analyses, glucose hypometabolism was found in the bilateral inferior parietal cortex and left caudate nucleus (Albrecht et al., 2019). FDG-PET could also discriminate PD patients from control subjects and can predict the Hoehn and Yahr stage and UPDRS score, which indicates FDG-PET is an objective, sensitive biomarker of disease stage (Matthews et al., 2018). Another study found that PD patients with rapid eye movement sleep behavior disorder showed widespread reduced binding of ^{11}C-MeNER, which was correlated with electroencephalogram slowing, cognitive performance, and orthostatic hypotension (Sommerauer et al., 2018). The tau tangle ligand, ^{18}F-AV-1451, binds to neuromelanin in the midbrain. Hansen et al. investigated the value of ^{18}F-AV-1451 PET in measuring the concentration of nigral neuromelanin in PD patients and observed a decrease in the ^{18}F-AV-1451 signal in the midbrain, which indicated ^{18}F-AV-1451 might be the first radiotracer to reflect the loss of pigmented neurons in the SN (Hansen et al., 2016). ^{18}F-FP-CIT, a PET radiotracer, was used to reflect dopamine transporters. The dopaminergic depletion in all striatal subregions was negatively correlated with the UPDRS-III score (Park et al., 2019).

TCS

TCS, a noninvasive and widely available neuroimaging technique, uses ultrasound to estimate the echogenicity of brain tissues *via* the intact cranium. Increased echogenicity of the SN observed by TCS is considered a biomarker of idiopathic PD (Camicioli et al., 2007). Gaenslen et al. (2008) performed a prospective blinded study and found that the sensitivity of TCS at baseline was 90.7% and the specificity was 82.4%, according to endpoint diagnosis, and the positive predictive value and classification accuracy of TCS for idiopathic PD was 92.9% and 88.3%, respectively (Gaenslen et al., 2008). PD patients with an area of the SN echogenicity above a specific threshold value showed an early onset age, and the area of the SN echogenicity with a larger contralateral to the side was related to more severe symptoms (Berg et al., 2001).

PHYSIOLOGICAL BIOMARKERS

Deep brain stimulation (DBS) surgery provides an excellent opportunity to record local field potentials (LFPs) in PD patients, which has provided valuable insight into disease mechanisms and can be used as biomarkers to reflect the syndrome severity. Here we classified these biomarkers based on frequency bands, which will standardize the methodology and simplify the interpretation of these biomarkers.

Delta Band

PD is a neural degeneration disease, and the patients also have cognition problems. In PD dementia patients, there is strong delta activity in the nucleus basalis of Meynert (NBM) as measured using depth electrodes (Nazmuddin et al., 2018). The same frequency band activity is also elevated in LBs dementia (Gratwicke et al., 2020), which means that this frequency band is a potential biomarker to predict the cognitive decline in PD patients. This frequency band is especially important for NBM mapping (Nazmuddin et al., 2018). The phenomenon also shows that neurophysiology biomarker detection is related to the recording target. Although different targets can detect the same frequency band, a specific target is easy to detect a specific frequency band.

Theta and Alpha Bands

Several studies have referred to the theta and alpha bands as low-frequency bands (Wojtecki et al., 2017; Mazzoni et al., 2018), but we will discuss these frequency bands together. These frequency bands are related to cognitive processing and motor feedback. An augmentation of low-frequency activity in the subthalamic nucleus (STN) can be observed in conflicting tasks, including economic decision making and moral sentence evaluations (Fumagalli et al., 2011), which indicate that low frequency might be involved in conflict problem judgment. The low-frequency band activity is elevated in the STN after dopamine therapy, which sometimes is accompanied by impulse control disorder (Priori et al., 2004). This phenomenon indicates that a potential dopamine-dependent low-frequency band in the STN may be involved in conflictual and economic decision making. This frequency band is also related to motor feedback. After levodopa intake or DBS, the low-frequency activity is elevated in the STN and GPi, which often correlates with the improvement of some syndromes (Silberstein et al., 2003; Giannicola et al., 2013). Dyskinesia is a side effect of DBS or levodopa, and studies have found that the low-frequency band is elevated in this situation (Alonso-Frech et al., 2006). When combining this information, the low-frequency band is a good biomarker for a hyperkinetic state. A previous study indicated that the LF/beta power ratio was a good neural feedback biomarker to trigger stimulation in adaptive DBS (Giannicola et al., 2012). The low-frequency band is an important biomarker in supplementing the beta band because the beta band is spatially specific. Another important observation is that the alpha band activity is associated with gait. A previous study found the power of alpha oscillation was correlated with gait speed (Thevathasan et al., 2012). One study found that the alpha band power decrease was associated with the probability of freezing (Androulidakis et al., 2008), so this frequency band can be potentially used as a biomarker to regulate gait.

Beta Band

The beta band is the most popular frequency band used in PD studies. The beta power is elevated in PD patients and decreased after DBS and levodopa intake (Brown et al., 2001). This frequency band is closely related to movement, which decreases with movement initiation and rebounding after movement termination (Canessa et al., 2016). The beta band is a good biomarker to trigger stimulation in adaptive DBS because beta power is positively correlated with rigidity and bradykinesia in PD patients (Brittain and Brown, 2014). The beta power suppression is positively related to the improvement of motor impairment (Kühn et al., 2009). One previous study used the beta power as a biomarker in adaptive DBS, showing that the clinical effect was better than with conventional DBS (Beudel et al., 2018). The constancy of beta power has also contributed to adaptive DBS, and a study found that the long-term beta power could be recorded safely using Medtronic PC + S devices (Neumann et al., 2017).

The beta band is further divided into high beta and low beta bands. The low beta band is closely related to clinical syndromes like bradykinesia and rigidity (Tsiokos et al., 2017). Compared with the low beta band, the high beta band is more related to long-distance (interregional) coupling. The high-frequency oscillation of the cortical and high beta of the STN phase-amplitude coupling is prokinetic (Ozturk et al., 2020). This biomarker might be closely related to the hyper-direct pathway, because of shorter time delays in the high beta band and cortical signal-coupling delays, when compared with the low beta band (Alexander and Crutcher, 1990). This biomarker is more likely physiological rather than pathological during PD because it is related to force generation (Florin et al., 2013a).

As an important biomarker, the beta band has many other applications. The power of the low beta band increases when FOG appears (Chen et al., 2019). Notably, the increased 18 Hz activity is specifically observed in the STN during

freezing (Storzer et al., 2017). This biomarker also can be used to evaluate the bilateral hemisphere "crosstalk" network in the FOG syndrome; the low beta band coherence between two hemispheres is related to the possibility of FOG (Anidi et al., 2018). The low beta band can also be used to classify the PD phenotypes because this frequency band is increased in a kinetic rigid group rather than in tremor dominant patients (Trager et al., 2016). This biomarker is suitable for optimizing lead implantation and postoperative programming. Good beta-band activity and strong STN-cortex phase-amplitude coupling were found to be located in the dorsolateral STN. This feature can be used in intraoperative guidance (Zaidel et al., 2010). The beta band can also serve as a feedback biomarker to automatically screen possible optimal contacts. A previous study reported that the contact pair with maximal beta power in the STN was very likely to be the optimal contact, which will have a wide therapeutic window and which will lead to the best symptom control (Tinkhauser et al., 2018).

Gamma Band

The gamma-band is a prokinetic biomarker, which is elevated at the onset of movement (Florin et al., 2013b), and is completely different from the beta band. Another interesting phenomenon is that gamma activity shows an augmentation after administration of levodopa (Elben et al., 2018). One previous study combining the magnetoencephalogram and LFPs also supported the prokinetic features of gamma oscillation, which revealed a strong coherence in the gamma band between the STN and cortical areas during voluntary movement initiation (Litvak et al., 2012). The above features make the gamma band a suitable biomarker to add for adaptive DBS. During imagery gripping without actual action, we can still observe the enhancement of gamma oscillation (Fischer et al., 2017), which indicates that gamma power is suitable for the decoding movement force in PD patients.

The above frequency bands can be used as biomarkers to reflect the severity of the motor syndrome or the cognitive decline in PD patients. These biomarkers have close relationships with clinical parameters. In-depth analyses of these biomarkers will also aid in the development of future adaptive DBS for PD.

DISCUSSION

The mechanism of PD pathogenesis remains elusive, and conventional drug or surgery therapies have been unsatisfactory. Early diagnosis of PD is particularly important, but the classical clinical symptoms of PD occur in the middle or advanced stages of the disease and have many common clinical features with some other neurodegenerative diseases. Novel, reliable, sensitive, and early measured biomarkers are essential for early and accurate diagnosis, to predict and monitor disease occurrence and progression. The development of neuroimaging techniques can be used to detect early changes in PD patients and assess the progression of the disease, which should make it a reliable biomarker for PD, by evaluating the potential local structure, cell ultrastructural, perfusion pattern changes, and molecular alterations in PD patients. The emerging neurophysiological biomarkers sensitively reflect the specific syndromes in PD patients, which is well suited in developing the adaptive DBS and predicting the prognosis. Genetics has been associated with susceptibility to PD. To date, at least 20 risk genes have been confirmed to be involved in familial PD, so they may be born with or persist in patients for decades before the onset of clinical symptoms. Consequently, the positive genes or encoding related proteins in peripheral blood also can become potential biomarkers for the diagnosis of PD. Neuroinflammation is a feature of PD pathology and has received increasing attention. Microglial activation, and cytokines, complement or ROS in plasma, serum, or CSF also can provide diagnoses and reflect disease progression, and have the potential to be early diagnostic markers for PD. However, because PD is a complex and progressive neurodegenerative disease, the roles of various biomarkers are distinct at different stages of the disease process. Also, the profiles of biomarkers vary from person to person. A single biomarker may not be sufficient for early diagnostics and prediction of disease progression with adequate stability, sensitivity, or specificity, so a comprehensive biomarker dataset including clinical symptoms, neuroimaging, neurophysiology, and biochemical and genetic information should be used for early diagnostics to predict disease progression.

Also, α-Syn is the key protein associated with PD and is central to the pathogenesis of this disease. The α-Syn is both a promising candidate for a prognostic marker of PD and may act as a trigger during PD development. However, misfolded α-Syn forms oligomers and aggregates that are believed to be toxic for neurons, and α-Syn itself is the primary trigger of the immune response in PD, with its aggregates being sufficient to induce the inflammation. Neuroinflammation is a feature of PD pathology, which might also play a pivotal role in disease pathogenesis, due to chronic microglial activation, the release of cytokines and chemokines, component activation, and ROS. Other PD risk genes have also been implicated in α-Syn aggregation to varying degrees, such as *GBA*, *LRRK2*, *Parkin*, and *PINK1*. Misfolded and aggregated α-Syn is indeed a pathogenic event in PD. However, the actual factors that cause abnormal misfolding and aggregation of α-Syn leading to PD are not straightforward. Moreover, determining how α-Syn is released and taken up by neurons, and how it grows new aggregates in a healthy cell will facilitate a better understanding of the role of α-Syn in PD, and even its potential to act as a biomarker in support of improved clinical diagnoses. The development of biomarkers to help with early differential diagnosis and to predict disease progression from its earliest stage is of major importance, both for research and therapeutic development. Further understanding of the role of α-Syn in PD pathogenesis will provide novel insights for disease diagnosis and therapy, especially at the early stages of PD. The development of novel therapies against neurodegenerative disorders requires the ability to detect their early presymptomatic manifestations to enable treatment before irreversible cellular damage occurs.

AUTHOR CONTRIBUTIONS

TD and JZ conceived the manuscript. TD, LW, WL, GZ, and YC wrote the manuscript. All authors contributed to the article and approved the submitted version.

FUNDING

This study was supported by the National Natural Science Foundation of China (Nos. 61761166004 and 81830033), and the China Postdoctoral Science Foundation (No. 2018T110120).

REFERENCES

Abd-Elhadi, S., Honig, A., Simhi-Haham, D., Schechter, M., Linetsky, E., Ben-Hur, T., et al. (2015). Total and proteinase K-resistant α-synuclein levels in erythrocytes, determined by their ability to bind phospholipids, associate with Parkinson's disease. *Sci. Rep.* 5:11120. doi: 10.1038/srep11120

Acuña, L., Hamadat, S., Corbalán, N. S., González-Lizárraga, F., Dos-Santos-Pereira, M., Rocca, J., et al. (2019). Rifampicin and its derivative rifampicin quinone reduce microglial inflammatory responses and neurodegeneration induced *in vitro* by α-synuclein fibrillary aggregates. *Cells* 8:776. doi: 10.3390/cells8080776

Adler, C. H., Dugger, B. N., Hentz, J. G., Hinni, M. L., Lott, D. G., Driver-Dunckley, E., et al. (2017). Peripheral synucleinopathy in early Parkinson's disease: submandibular gland needle biopsy findings. *Mov. Disord.* 32, 722–723. doi: 10.1002/mds.27044

Albrecht, F., Ballarini, T., Neumann, J., and Schroeter, M. L. (2019). FDG-PET hypometabolism is more sensitive than MRI atrophy in Parkinson's disease: a whole-brain multimodal imaging meta-analysis. *Neuroimage Clin.* 21:101594. doi: 10.1016/j.nicl.2018.11.004

Alexander, G. E., and Crutcher, M. D. (1990). Functional architecture of basal ganglia circuits: neural substrates of parallel processing. *Trends Neurosci.* 13, 266–271. doi: 10.1016/0166-2236(90)90107-l

Alonso-Frech, F., Zamarbide, I., Alegre, M., Rodriguez-Oroz, M. C., Guridi, J., Manrique, M., et al. (2006). Slow oscillatory activity and levodopa-induced dyskinesias in Parkinson's disease. *Brain* 129, 1748–1757. doi: 10.1093/brain/awl103

Androulidakis, A. G., Khan, S., Litvak, V., Pleydell-Pearce, C. W., Brown, P., and Gill, S. S. (2008). Local field potential recordings from the pedunculopontine nucleus in a Parkinsonian patient. *Neuroreport* 19, 59–62. doi: 10.1097/WNR.0b013e3282f2e2d1

Anidi, C., O'Day, J. J., Anderson, R. W., Afzal, M. F., Syrkin-Nikolau, J., Velisar, A., et al. (2018). Neuromodulation targets pathological not physiological β bursts during gait in Parkinson's disease. *Neurobiol. Dis.* 120, 107–117. doi: 10.1016/j.nbd.2018.09.004

Armstrong, M. J., and Okun, M. S. (2020). Diagnosis and treatment of Parkinson disease: a review. *JAMA* 323, 548–560. doi: 10.1001/jama.2019.22360

Balestrino, R., and Schapira, A. H. V. (2018). Glucocerebrosidase and parkinson disease: molecular, clinical, and therapeutic implications. *Neuroscientist* 24, 540–559. doi: 10.1177/1073858417748875

Barbour, R., Kling, K., Anderson, J. P., Banducci, K., Cole, T., Diep, L., et al. (2008). Red blood cells are the major source of α-synuclein in blood. *Neurodegener. Dis.* 5, 55–59. doi: 10.1159/000112832

Berg, D., Siefker, C., and Becker, G. (2001). Echogenicity of the substantia nigra in Parkinson's disease and its relation to clinical findings. *J. Neurol.* 248, 684–689. doi: 10.1007/s004150170114

Beudel, M., Cagnan, H., and Little, S. (2018). Adaptive brain stimulation for movement disorders. *Prog. Neurol. Surg.* 33, 230–242. doi: 10.1159/000481107

Bougea, A., Koros, C., and Stefanis, L. (2019). Salivary α-synuclein as a biomarker for Parkinson's disease: a systematic review. *J. Neural Transm.* 126, 1373–1382. doi: 10.1007/s00702-019-02062-4

Boza-Serrano, A., Reyes, J. F., Rey, N. L., Leffler, H., Bousset, L., Nilsson, U., et al. (2014). The role of Galectin-3 in α-synuclein-induced microglial activation. *Acta Neuropathol. Commun.* 2:156. doi: 10.1186/s40478-014-0156-0

Brittain, J.-S., and Brown, P. (2014). Oscillations and the basal ganglia: motor control and beyond. *NeuroImage* 85, 637–647. doi: 10.1016/j.neuroimage.2013.05.084

Brown, P., Oliviero, A., Mazzone, P., Insola, A., Tonali, P., and Di Lazzaro, V. (2001). Dopamine dependency of oscillations between subthalamic nucleus and pallidum in Parkinson's disease. *J. Neurosci.* 21, 1033–1038. doi: 10.1523/JNEUROSCI.21-03-01033.2001

Byler, S. L., Boehm, G. W., Karp, J. D., Kohman, R. A., Tarr, A. J., Schallert, T., et al. (2009). Systemic lipopolysaccharide plus MPTP as a model of dopamine loss and gait instability in C57Bl/6J mice. *Behav. Brain Res.* 198, 434–439. doi: 10.1016/j.bbr.2008.11.027

Camicioli, R. M., Hanstock, C. C., Bouchard, T. P., Gee, M., Fisher, N. J., and Martin, W. R. W. (2007). Magnetic resonance spectroscopic evidence for presupplementary motor area neuronal dysfunction in Parkinson's disease. *Mov. Disord.* 22, 382–386. doi: 10.1002/mds.21288

Campo, F., Carletti, R., Fusconi, M., Pellicano, C., Pontieri, F. E., Di Gioia, C. R., et al. (2019). α-synuclein in salivary gland as biomarker for Parkinson's disease. *Rev. Neurosci.* 30, 455–462. doi: 10.1515/revneuro-2018-0064

Canessa, A., Pozzi, N. G., Arnulfo, G., Brumberg, J., Reich, M. M., Pezzoli, G., et al. (2016). Striatal dopaminergic innervation regulates subthalamic β-oscillations and cortical-subcortical coupling during movements: preliminary evidence in subjects with Parkinson's disease. *Front. Hum. Neurosci.* 10:611. doi: 10.3389/fnhum.2016.00611

Cao, S., Standaert, D. G., and Harms, A. S. (2012). The γ chain subunit of Fc receptors is required for α-synuclein-induced pro-inflammatory signaling in microglia. *J. Neuroinflammation* 9:259. doi: 10.1186/1742-2094-9-259

Cao, S., Theodore, S., and Standaert, D. G. (2010). Fcγ receptors are required for NF-κB signaling, microglial activation and dopaminergic neurodegeneration in an AAV-synuclein mouse model of Parkinson's disease. *Mol. Neurodegener.* 5:42. doi: 10.1186/1750-1326-5-42

Cao, Z., Wu, Y., Liu, G., Jiang, Y., Wang, X., Wang, Z., et al. (2019). α-Synuclein in salivary extracellular vesicles as a potential biomarker of Parkinson's disease. *Neurosci. Lett.* 696, 114–120. doi: 10.1016/j.neulet.2018.12.030

Cariulo, C., Martufi, P., Verani, M., Azzollini, L., Bruni, G., Weiss, A., et al. (2019). Phospho-S129 α-synuclein is present in human plasma but not in cerebrospinal fluid as determined by an ultrasensitive immunoassay. *Front. Neurosci.* 13:889. doi: 10.3389/fnins.2019.00889

Carmona-Abellan, M., Gabilondo, I., Murueta-Goyena, A., Khurana, V., Tijero, B., Luquin, M. R., et al. (2019). Small fiber neuropathy and phosphorylated α-synuclein in the skin of E46K-SNCA mutation carriers. *Parkinsonism Relat. Disord.* 65, 139–145. doi: 10.1016/j.parkreldis.2019.05.038

Chahine, L. M., Beach, T. G., Brumm, M. C., Adler, C. H., Coffey, C. S., Mosovsky, S., et al. (2020). *In vivo* distribution of α-synuclein in multiple tissues and biofluids in Parkinson disease. *Neurology* 95, e1267–e1284. doi: 10.1212/WNL.0000000000010404

Chang, C.-W., Yang, S.-Y., Yang, C.-C., Chang, C.-W., and Wu, Y.-R. (2019). Plasma and serum α-synuclein as a biomarker of diagnosis in patients with Parkinson's disease. *Front. Neurol.* 10:1388. doi: 10.3389/fneur.2019.01388

Chartier-Harlin, M. C., Kachergus, J., Roumier, C., Mouroux, V., Douay, X., Lincoln, S., et al. (2004). α-synuclein locus duplication as a cause of familial Parkinson's disease. *Lancet* 364, 1167–1169. doi: 10.1016/S0140-6736(04)17103-1

Chen, L., and Feany, M. B. (2005). α-synuclein phosphorylation controls neurotoxicity and inclusion formation in a *Drosophila* model of Parkinson disease. *Nat. Neurosci.* 8, 657–663. doi: 10.1038/nn1443

Chen, C.-C., Yeh, C.-H., Chan, H.-L., Chang, Y.-J., Tu, P.-H., Yeh, C.-H., et al. (2019). Subthalamic nucleus oscillations correlate with vulnerability to freezing of gait in patients with Parkinson's disease. *Neurobiol. Dis.* 132:104605. doi: 10.1016/j.nbd.2019.104605

Choi, B.-K., Choi, M.-G., Kim, J.-Y., Yang, Y., Lai, Y., Kweon, D.-H., et al. (2013). Large α-synuclein oligomers inhibit neuronal SNARE-mediated vesicle docking. *Proc. Natl. Acad. Sci. U S A* 110, 4087–4092. doi: 10.1073/pnas.1218424110

Christiansen, J. R., Olesen, M. N., Otzen, D. E., Romero-Ramos, M., and Sanchez-Guajardo, V. (2016). α-Synuclein vaccination modulates regulatory T cell activation and microglia in the absence of brain pathology. *J. Neuroinflammation* 13:74. doi: 10.1186/s12974-016-0532-8

Colla, E., Jensen, P. H., Pletnikova, O., Troncoso, J. C., Glabe, C., and Lee, M. K. (2012). Accumulation of toxic α-synuclein oligomer within endoplasmic reticulum occurs in α-synucleinopathy *in vivo*. *J. Neurosci.* 32, 3301–3305. doi: 10.1523/JNEUROSCI.5368-11.2012

Corti, O., Lesage, S., and Brice, A. (2011). What genetics tells us about the causes and mechanisms of Parkinson's disease. *Physiol. Rev.* 91, 1161–1218. doi: 10.1152/physrev.00022.2010

Cosottini, M., Frosini, D., Pesaresi, I., Costagli, M., Biagi, L., Ceravolo, R., et al. (2014). MR imaging of the substantia nigra at 7 T enables diagnosis of Parkinson disease. *Radiology* 271, 831–838. doi: 10.1148/radiol.14131448

Couch, Y., Alvarez-Erviti, L., Sibson, N. R., Wood, M. J., and Anthony, D. C. (2011). The acute inflammatory response to intranigral α-synuclein differs significantly from intranigral lipopolysaccharide and is exacerbated by peripheral inflammation. *J. Neuroinflammation* 8:166. doi: 10.1186/1742-2094-8-166

Daniele, S. G., Béraud, D., Davenport, C., Cheng, K., Yin, H., and Maguire-Zeiss, K. A. (2015). Activation of MyD88-dependent TLR1/2 signaling by misfolded α-synuclein, a protein linked to neurodegenerative disorders. *Sci. Signal.* 8:ra45. doi: 10.1126/scisignal.2005965

Dekosky, S. T., and Marek, K. (2003). Looking backward to move forward: early detection of neurodegenerative disorders. *Science* 302, 830–834. doi: 10.1126/science.1090349

Deng, H., Wang, P., and Jankovic, J. (2018). The genetics of Parkinson disease. *Ageing Res. Rev.* 42, 72–85. doi: 10.1016/j.arr.2017.12.007

Deng, H., and Yuan, L. (2014). Genetic variants and animal models in SNCA and Parkinson disease. *Ageing Res. Rev.* 15, 161–176. doi: 10.1016/j.arr.2014.04.002

Desplats, P., Spencer, B., Coffee, E., Patel, P., Michael, S., Patrick, C., et al. (2011). α-synuclein sequesters Dnmt1 from the nucleus: a novel mechanism for epigenetic alterations in Lewy body diseases. *J. Biol. Chem.* 286, 9031–9037. doi: 10.1074/jbc.C110.212589

Ding, J., Zhang, J., Wang, X., Zhang, L., Jiang, S., Yuan, Y., et al. (2017). Relationship between the plasma levels of neurodegenerative proteins and motor subtypes of Parkinson's disease. *J. Neural Transm.* 124, 353–360. doi: 10.1007/s00702-016-1650-2

Donadio, V., Incensi, A., Leta, V., Giannoccaro, M. P., Scaglione, C., Martinelli, P., et al. (2014). Skin nerve α-synuclein deposits: a biomarker for idiopathic Parkinson disease. *Neurology* 82, 1362–1369. doi: 10.1212/WNL.0000000000000316

Donadio, V., Incensi, A., Rizzo, G., Capellari, S., Pantieri, R., Stanzani Maserati, M., et al. (2017). A new potential biomarker for dementia with Lewy bodies: skin nerve α-synuclein deposits. *Neurology* 89, 318–326. doi: 10.1212/WNL.0000000000004146

Donadio, V., Incensi, A., Rizzo, G., De Micco, R., Tessitore, A., Devigili, G., et al. (2020). Skin biopsy may help to distinguish multiple system atrophy-parkinsonism from Parkinson's disease with orthostatic hypotension. *Mov. Disord.* 35, 1649–1657. doi: 10.1002/mds.28126

Dos Santos, M. C. T., Scheller, D., Schulte, C., Mesa, I. R., Colman, P., Bujac, S. R., et al. (2018). Evaluation of cerebrospinal fluid proteins as potential biomarkers for early stage Parkinson's disease diagnosis. *PLoS One* 13:e0206536. doi: 10.1371/journal.pone.0206536

Drouin-Ouellet, J., St-Amour, I., Saint-Pierre, M., Lamontagne-Proulx, J., Kriz, J., Barker, R. A., et al. (2014). Toll-like receptor expression in the blood and brain of patients and a mouse model of Parkinson's disease. *Int. J. Neuropsychopharmacol.* 18:pyu103. doi: 10.1093/ijnp/pyu103

Duffy, M. F., Collier, T. J., Patterson, J. R., Kemp, C. J., Luk, K. C., Tansey, M. G., et al. (2018). Lewy body-like α-synuclein inclusions trigger reactive microgliosis prior to nigral degeneration. *J. Neuroinflammation* 15:129. doi: 10.1186/s12974-018-1171-z

Dzamko, N., Gysbers, A., Perera, G., Bahar, A., Shankar, A., Gao, J., et al. (2017). Toll-like receptor 2 is increased in neurons in Parkinson's disease brain and may contribute to α-synuclein pathology. *Acta Neuropathol.* 133, 303–319. doi: 10.1007/s00401-016-1648-8

El-Agnaf, O. M., Salem, S. A., Paleologou, K. E., Cooper, L. J., Fullwood, N. J., Gibson, M. J., et al. (2003). α-synuclein implicated in Parkinson's disease is present in extracellular biological fluids, including human plasma. *FASEB J.* 17, 1945–1947. doi: 10.1096/fj.03-0098fje

El-Agnaf, O. M., Salem, S. A., Paleologou, K. E., Curran, M. D., Gibson, M. J., Court, J. A., et al. (2006). Detection of oligomeric forms of α-synuclein protein in human plasma as a potential biomarker for Parkinson's disease. *FASEB J.* 20, 419–425. doi: 10.1096/fj.03-1449com

Elben, S., Trenado, C., Vesper, J., Schnitzler, A., and Wojtecki, L. (2018). Human subthalamic oscillatory dynamics following somatosensory stimulation. *Clin. Neurophysiol.* 129, 79–88. doi: 10.1016/j.clinph.2017.10.015

Engels, G., Vlaar, A., Mccoy, B., Scherder, E., and Douw, L. (2018). Dynamic functional connectivity and symptoms of Parkinson's disease: a resting-state fMRI study. *Front. Aging Neurosci.* 10:388. doi: 10.3389/fnagi.2018.00388

Eusebi, P., Giannandrea, D., Biscetti, L., Abraha, I., Chiasserini, D., Orso, M., et al. (2017). Diagnostic utility of cerebrospinal fluid α-synuclein in Parkinson's disease: a systematic review and meta-analysis. *Mov. Disord.* 32, 1389–1400. doi: 10.1002/mds.27110

Fayyad, M., Salim, S., Majbour, N., Erskine, D., Stoops, E., Mollenhauer, B., et al. (2019). Parkinson's disease biomarkers based on α-synuclein. *J. Neurochem.* 150, 626–636. doi: 10.1111/jnc.14809

Fellner, L., Irschick, R., Schanda, K., Reindl, M., Klimaschewski, L., Poewe, W., et al. (2013). Toll-like receptor 4 is required for α-synuclein dependent activation of microglia and astroglia. *Glia* 61, 349–360. doi: 10.1002/glia.22437

Fernández-Santiago, R., Iranzo, A., Gaig, C., Serradell, M., Fernández, M., Tolosa, E., et al. (2015). MicroRNA association with synucleinopathy conversion in rapid eye movement behavior disorder. *Ann. Neurol.* 77, 895–901. doi: 10.1002/ana.24384

Fischer, P., Pogosyan, A., Cheeran, B., Green, A. L., Aziz, T. Z., Hyam, J., et al. (2017). Subthalamic nucleus β and γ activity is modulated depending on the level of imagined grip force. *Exp. Neurol.* 293, 53–61. doi: 10.1016/j.expneurol.2017.03.015

Florin, E., Dafsari, H. S., Reck, C., Barbe, M. T., Pauls, K. A., Maarouf, M., et al. (2013a). Modulation of local field potential power of the subthalamic nucleus during isometric force generation in patients with Parkinson's disease. *Neuroscience* 240, 106–116. doi: 10.1016/j.neuroscience.2013.02.043

Florin, E., Erasmi, R., Reck, C., Maarouf, M., Schnitzler, A., Fink, G. R., et al. (2013b). Does increased γ activity in patients suffering from Parkinson's disease counteract the movement inhibiting β activity? *Neuroscience* 237, 42–50. doi: 10.1016/j.neuroscience.2013.01.051

Foulds, P. G., Mitchell, J. D., Parker, A., Turner, R., Green, G., Diggle, P., et al. (2011). Phosphorylated α-synuclein can be detected in blood plasma and is potentially a useful biomarker for Parkinson's disease. *FASEB J.* 25, 4127–4137. doi: 10.1096/fj.10-179192

Fumagalli, M., Giannicola, G., Rosa, M., Marceglia, S., Lucchiari, C., Mrakic-Sposta, S., et al. (2011). Conflict-dependent dynamic of subthalamic nucleus oscillations during moral decisions. *Soc. Neurosci.* 6, 243–256. doi: 10.1080/17470919.2010.515148

Gaenslen, A., Unmuth, B., Godau, J., Liepelt, I., Di Santo, A., Schweitzer, K. J., et al. (2008). The specificity and sensitivity of transcranial ultrasound in the differential diagnosis of Parkinson's disease: a prospective blinded study. *Lancet Neurol.* 7, 417–424. doi: 10.1016/S1474-4422(08)70067-X

Gasser, T. (2009). Genomic and proteomic biomarkers for Parkinson disease. *Neurology* 72, S27–S31. doi: 10.1212/WNL.0b013e318198e054

Gerrits, N. J. H. M., Van Loenhoud, A. C., Van Den Berg, S. F., Berendse, H. W., Foncke, E. M. J., Klein, M., et al. (2016). Cortical thickness, surface area and subcortical volume differentially contribute to cognitive heterogeneity in Parkinson's disease. *PLoS One* 11:e0148852. doi: 10.1371/journal.pone.0148852

Giannicola, G., Rosa, M., Marceglia, S., Scelzo, E., Rossi, L., Servello, D., et al. (2013). The effects of levodopa and deep brain stimulation on subthalamic local field low-frequency oscillations in Parkinson's disease. *Neurosignals* 21, 89–98. doi: 10.1159/000336543

Giannicola, G., Rosa, M., Servello, D., Menghetti, C., Carrabba, G., Pacchetti, C., et al. (2012). Subthalamic local field potentials after seven-year deep brain stimulation in Parkinson's disease. *Exp. Neurol.* 237, 312–317. doi: 10.1016/j.expneurol.2012.06.012

Gordon, R., Albornoz, E. A., Christie, D. C., Langley, M. R., Kumar, V., Mantovani, S., et al. (2018). Inflammasome inhibition prevents α-synuclein pathology and dopaminergic neurodegeneration in mice. *Sci. Transl. Med.* 10:eaah4066. doi: 10.1126/scitranslmed.aah4066

Gratwicke, J., Oswal, A., Akram, H., Jahanshahi, M., Hariz, M., Zrinzo, L., et al. (2020). Resting state activity and connectivity of the nucleus basalis of Meynert and globus pallidus in Lewy body dementia and Parkinson's disease dementia. *NeuroImage* 221:117184. doi: 10.1016/j.neuroimage.2020.117184

Grozdanov, V., Bliederhaeuser, C., Ruf, W. P., Roth, V., Fundel-Clemens, K., Zondler, L., et al. (2014). Inflammatory dysregulation of blood monocytes in Parkinson's disease patients. *Acta Neuropathol.* 128, 651–663. doi: 10.1007/s00401-014-1345-4

Guan, X., Xuan, M., Gu, Q., Huang, P., Liu, C., Wang, N., et al. (2017). Regionally progressive accumulation of iron in Parkinson's disease as measured by quantitative susceptibility mapping. *NMR Biomed.* 30:e3489. doi: 10.1002/nbm.3489

Hamm-Alvarez, S. F., Okamoto, C. T., Janga, S. R., Feigenbaum, D., Edman, M. C., Freire, D., et al. (2019). Oligomeric α-synuclein is increased in basal tears of Parkinson's patients. *Biomark Med.* 13, 941–952. doi: 10.2217/bmm-2019-0167

Hansen, A. K., Knudsen, K., Lillethorup, T. P., Landau, A. M., Parbo, P., Fedorova, T., et al. (2016). *In vivo* imaging of neuromelanin in Parkinson's disease using 18 F-AV-1451 PET. *Brain* 139, 2039–2049. doi: 10.1093/brain/aww098

Hawkes, C. H. (2008). The prodromal phase of sporadic Parkinson's disease: does it exist and if so how long is it? *Mov. Disord.* 23, 1799–1807. doi: 10.1002/mds.22242

He, R., Yan, X., Guo, J., Xu, Q., Tang, B., and Sun, Q. (2018). Recent advances in biomarkers for Parkinson's disease. *Front. Aging Neurosci.* 10:305. doi: 10.3389/fnagi.2018.00305

Healy, D. G., Falchi, M., O'Sullivan, S. S., Bonifati, V., Durr, A., Bressman, S., et al. (2008). Phenotype, genotype and worldwide genetic penetrance of LRRK2-associated Parkinson's disease: a case-control study. *Lancet Neurol.* 7, 583–590. doi: 10.1016/S1474-4422(08)70117-0

Heisters, D. (2011). Parkinson's: symptoms, treatments and research. *Br. J. Nurs.* 20, 548–554. doi: 10.12968/bjon.2011.20.9.548

Hernandez, D. G., Reed, X., and Singleton, A. B. (2016). Genetics in Parkinson disease: mendelian versus non-Mendelian inheritance. *J. Neurochem.* 139, 59–74. doi: 10.1111/jnc.13593

Hu, Z., Wang, W., Ling, J., and Jiang, C. (2016). α-mangostin inhibits α-synuclein-induced microglial neuroinflammation and neurotoxicity. *Cell. Mol. Neurobiol.* 36, 811–820. doi: 10.1007/s10571-015-0264-9

Hughes, C. D., Choi, M. L., Ryten, M., Hopkins, L., Drews, A., Botia, J. A., et al. (2019). Picomolar concentrations of oligomeric α-synuclein sensitizes TLR4 to play an initiating role in Parkinson's disease pathogenesis. *Acta Neuropathol.* 137, 103–120. doi: 10.1007/s00401-018-1907-y

International Parkinson Disease Genomics Consortium, Nalls, M. A., Plagnol, V., Hernandez, D. G., Sharma, M., Sheerin, U.-M., et al. (2011). Imputation of sequence variants for identification of genetic risks for Parkinson's disease: a meta-analysis of genome-wide association studies. *Lancet* 377, 641–649. doi: 10.1016/S0140-6736(10)62345-8

Iranzo, A., Borrego, S., Vilaseca, I., Martí, C., Serradell, M., Sánchez-Valle, R., et al. (2018). α-Synuclein aggregates in labial salivary glands of idiopathic rapid eye movement sleep behavior disorder. *Sleep* 41:zsy101. doi: 10.1093/sleep/zsy101

Jakubowski, J. L., and Labrie, V. (2017). Epigenetic biomarkers for Parkinson's disease: from diagnostics to therapeutics. *J. Parkinsons Dis.* 7, 1–12. doi: 10.3233/JPD-160914

Jiménez-Jiménez, F. J., Alonso-Navarro, H., García-Martín, E., and Agúndez, J. A. G. (2020). Cerebrospinal and blood levels of amino acids as potential biomarkers for Parkinson's disease: review and meta-analysis. *Eur. J. Neurol.* 27, 2336–2347. doi: 10.1111/ene.14470

Kalia, L. V., and Lang, A. E. (2015). Parkinson's disease. *Lancet* 386, 896–912. doi: 10.1016/S0140-6736(14)61393-3

Kayed, R., Head, E., Thompson, J. L., Mcintire, T. M., Milton, S. C., Cotman, C. W., et al. (2003). Common structure of soluble amyloid oligomers implies common mechanism of pathogenesis. *Science* 300, 486–489. doi: 10.1126/science.1079469

Khalil, M., Teunissen, C. E., Otto, M., Piehl, F., Sormani, M. P., Gattringer, T., et al. (2018). Neurofilaments as biomarkers in neurological disorders. *Nat. Rev. Neurol.* 14, 577–589. doi: 10.1038/s41582-018-0058-z

Kim, C., Ho, D.-H., Suk, J.-E., You, S., Michael, S., Kang, J., et al. (2013). Neuron-released oligomeric α-synuclein is an endogenous agonist of TLR2 for paracrine activation of microglia. *Nat. Commun.* 4:1562. doi: 10.1038/ncomms2534

Kim, R., Lee, J., Kim, H.-J., Kim, A., Jang, M., Jeon, B., et al. (2019). CSF β-amyloid42 and risk of freezing of gait in early Parkinson disease. *Neurology* 92, e40–e47. doi: 10.1212/WNL.0000000000006692

Klegeris, A., Pelech, S., Giasson, B. I., Maguire, J., Zhang, H., McGeer, E. G., et al. (2008). α-synuclein activates stress signaling protein kinases in THP-1 cells and microglia. *Neurobiol. Aging* 29, 739–752. doi: 10.1016/j.neurobiolaging.2006.11.013

Koros, C., Simitsi, A., and Stefanis, L. (2017). Genetics of Parkinson's disease: genotype-phenotype correlations. *Int. Rev. Neurobiol.* 132, 197–231. doi: 10.1016/bs.irn.2017.01.009

Krüger, R., Kuhn, W., Müller, T., Woitalla, D., Graeber, M., Kösel, S., et al. (1998). Ala30Pro mutation in the gene encoding α-synuclein in Parkinson's disease. *Nat. Genet.* 18, 106–108. doi: 10.1038/ng0298-106

Kühn, A. A., Tsui, A., Aziz, T., Ray, N., Brücke, C., Kupsch, A., et al. (2009). Pathological synchronisztion in the subthalamic nucleus of patients with Parkinson's disease relates to both bradykinesia and rigidity. *Exp. Neurol.* 215, 380–387. doi: 10.1016/j.expneurol.2008.11.008

Kuzkina, A., Schulmeyer, L., Monoranu, C.-M., Volkmann, J., Sommer, C., and Doppler, K. (2019). The aggregation state of α-synuclein deposits in dermal nerve fibers of patients with Parkinson's disease resembles that in the brain. *Parkinsonism Relat. Disord.* 64, 66–72. doi: 10.1016/j.parkreldis.2019.03.003

Kwon, D.-H., Kim, J.-M., Oh, S.-H., Jeong, H.-J., Park, S.-Y., Oh, E.-S., et al. (2012). Seven-tesla magnetic resonance images of the substantia nigra in Parkinson disease. *Ann. Neurol.* 71, 267–277. doi: 10.1002/ana.22592

Lachenmayer, M. L., and Yue, Z. (2012). Genetic animal models for evaluating the role of autophagy in etiopathogenesis of Parkinson disease. *Autophagy* 8, 1837–1838. doi: 10.4161/auto.21859

Lamontagne-Proulx, J., St-Amour, I., Labib, R., Pilon, J., Denis, H. L., Cloutier, N., et al. (2019). Portrait of blood-derived extracellular vesicles in patients with Parkinson's disease. *Neurobiol. Dis.* 124, 163–175. doi: 10.1016/j.nbd.2018.11.002

Landeck, N., Hall, H., Ardah, M. T., Majbour, N. K., El-Agnaf, O. M., Halliday, G., et al. (2016). A novel multiplex assay for simultaneous quantification of total and S129 phosphorylated human α-synuclein. *Mol. Neurodegener.* 11:61. doi: 10.1186/s13024-016-0125-0

Lee, E.-J., Woo, M.-S., Moon, P. G., Baek, M. C., Choi, I. Y., Kim, W. K., et al. (2010). α-synuclein activates microglia by inducing the expressions of matrix metalloproteinases and the subsequent activation of protease-activated receptor-1. *J. Immunol.* 185, 615–623. doi: 10.4049/jimmunol.0903480

Lehéricy, S., Bardinet, E., Poupon, C., Vidailhet, M., and François, C. (2014). 7 Tesla magnetic resonance imaging: a closer look at substantia nigra anatomy in Parkinson's disease. *Mov. Disord.* 29, 1574–1581. doi: 10.1002/mds.26043

Li, J., Yuan, Y., Wang, M., Zhang, J., Zhang, L., Jiang, S., et al. (2018). Decreased interhemispheric homotopic connectivity in Parkinson's disease patients with freezing of gait: a resting state fMRI study. *Parkinsonism Relat. Disord.* 52, 30–36. doi: 10.1016/j.parkreldis.2018.03.015

Lin, C.-H., Liu, H.-C., Yang, S.-Y., Yang, K.-C., Wu, C.-C., and Chiu, M.-J. (2019). Plasma pS129-α-synuclein is a surrogate biofluid marker of motor severity and progression in Parkinson's disease. *J. Clin. Med.* 8:1601. doi: 10.3390/jcm8101601

Lin, C.-H., Yang, S.-Y., Horng, H.-E., Yang, C.-C., Chieh, J.-J., Chen, H.-H., et al. (2017). Plasma α-synuclein predicts cognitive decline in Parkinson's disease. *J. Neurol. Neurosurg. Psychiatry* 88, 818–824. doi: 10.1136/jnnp-2016-314857

Litvak, V., Eusebio, A., Jha, A., Oostenveld, R., Barnes, G., Foltynie, T., et al. (2012). Movement-related changes in local and long-range synchronization in Parkinson's disease revealed by simultaneous magnetoencephalography and intracranial recordings. *J. Neurosci.* 32, 10541–10553. doi: 10.1523/JNEUROSCI.0767-12.2012

Liu, G., Tian, C., Gao, L., Cao, Z., and Feng, T. (2019). α-synuclein in erythrocyte membrane of patients with multiple system atrophy: a pilot study. *Parkinsonism Relat. Disord.* 60, 105–110. doi: 10.1016/j.parkreldis.2018.09.012

Locascio, J. J., Eberly, S., Liao, Z., Liu, G., Hoesing, A. N., Duong, K., et al. (2015). Association between α-synuclein blood transcripts and early, neuroimaging-supported Parkinson's disease. *Brain* 138, 2659–2671. doi: 10.1093/brain/awv202

Lohmann, E., Thobois, S., Lesage, S., Broussolle, E., Du Montcel, S. T., Ribeiro, M. J., et al. (2009). A multidisciplinary study of patients with early-onset PD with and without parkin mutations. *Neurology* 72, 110–116. doi: 10.1212/01.wnl.0000327098.86861.d4

Lyoo, C. H., Ryu, Y. H., and Lee, M. S. (2011). Cerebral cortical areas in which thickness correlates with severity of motor deficits of

Parkinson's disease. *J. Neurol.* 258, 1871–1876. doi: 10.1007/s00415-011-6045-6

Magdalinou, N., Lees, A. J., and Zetterberg, H. (2014). Cerebrospinal fluid biomarkers in parkinsonian conditions: an update and future directions. *J. Neurol. Neurosurg. Psychiatry* 85, 1065–1075. doi: 10.1136/jnnp-2013-307539

Majbour, N. K., Vaikath, N. N., Van Dijk, K. D., Ardah, M. T., Varghese, S., Vesterager, L. B., et al. (2016). Oligomeric and phosphorylated α-synuclein as potential CSF biomarkers for Parkinson's disease. *Mol. Neurodegener.* 11:7. doi: 10.1186/s13024-016-0072-9

Manne, S., Kondru, N., Jin, H., Anantharam, V., Huang, X., Kanthasamy, A., et al. (2020). α-Synuclein real-time quaking-induced conversion in the submandibular glands of Parkinson's disease patients. *Mov. Disord.* 35, 268–278. doi: 10.1002/mds.27907

Matthews, D. C., Lerman, H., Lukic, A., Andrews, R. D., Mirelman, A., Wernick, M. N., et al. (2018). FDG PET Parkinson's disease-related pattern as a biomarker for clinical trials in early stage disease. *Neuroimage Clin.* 20, 572–579. doi: 10.1016/j.nicl.2018.08.006

Mazzoni, A., Rosa, M., Carpaneto, J., Romito, L. M., Priori, A., and Micera, S. (2018). Subthalamic neural activity patterns anticipate economic risk decisions in gambling. *eNeuro* 5:ENEURO.0366-17.2017. doi: 10.1523/ENEURO.0366-17.2017

Miller, D. W., Hague, S. M., Clarimon, J., Baptista, M., Gwinn-Hardy, K., Cookson, M. R., et al. (2004). α-synuclein in blood and brain from familial Parkinson disease with SNCA locus triplication. *Neurology* 62, 1835–1838. doi: 10.1212/01.wnl.0000127517.33208.f4

Minati, L., Grisoli, M., Carella, F., De Simone, T., Bruzzone, M. G., and Savoiardo, M. (2007). Imaging degeneration of the substantia nigra in Parkinson disease with inversion-recovery MR imaging. *Am. J. Neuroradiol.* 28, 309–313.

Mirza, B., Hadberg, H., Thomsen, P., and Moos, T. (2000). The absence of reactive astrocytosis is indicative of a unique inflammatory process in Parkinson's disease. *Neuroscience* 95, 425–432. doi: 10.1016/s0306-4522(99)00455-8

Mizuta, I., Takafuji, K., Ando, Y., Satake, W., Kanagawa, M., Kobayashi, K., et al. (2013). YY1 binds to α-synuclein 3'-flanking region SNP and stimulates antisense noncoding RNA expression. *J. Hum. Genet.* 58, 711–719. doi: 10.1038/jhg.2013.90

Moraitou, M., Dermentzaki, G., Dimitriou, E., Monopolis, I., Dekker, N., Aerts, H., et al. (2016). α-Synuclein dimerization in erythrocytes of Gaucher disease patients: correlation with lipid abnormalities and oxidative stress. *Neurosci. Lett.* 613, 1–5. doi: 10.1016/j.neulet.2015.12.013

Nam, D., Lee, J. Y., Lee, M., Kim, J., Seol, W., Son, I., et al. (2020). Detection and assessment of α-synuclein oligomers in the urine of Parkinson's disease patients. *J. Parkinsons Dis.* 10, 981–991. doi: 10.3233/JPD-201983

Nazmuddin, M., Oterdoom, D. L. M., Van Dijk, J. M. C., Van Zijl, J. C., Kampman, A. K., Drost, G., et al. (2018). Oscillatory activity and cortical coherence of the nucleus basalis of Meynert in Parkinson's disease dementia. *Parkinsonism Relat. Disord.* 52, 102–106. doi: 10.1016/j.parkreldis.2018.03.024

Neumann, W.-J., Staub-Bartelt, F., Horn, A., Schanda, J., Schneider, G. H., Brown, P., et al. (2017). Long term correlation of subthalamic β band activity with motor impairment in patients with Parkinson's disease. *Clin. Neurophysiol.* 128, 2286–2291. doi: 10.1016/j.clinph.2017.08.028

Oikawa, H., Sasaki, M., Tamakawa, Y., Ehara, S., and Tohyama, K. (2002). The substantia nigra in Parkinson disease: proton density-weighted spin-echo and fast short inversion time inversion-recovery MR findings. *Am. J. Neuroradiol.* 23, 1747–1756.

Ortega, R. A., Torres, P. A., Swan, M., Nichols, W., Boschung, S., Raymond, D., et al. (2016). Glucocerebrosidase enzyme activity in GBA mutation Parkinson's disease. *J. Clin. Neurosci.* 28, 185–186. doi: 10.1016/j.jocn.2015.12.004

Ouchi, Y., Yoshikawa, E., Sekine, Y., Futatsubashi, M., Kanno, T., Ogusu, T., et al. (2005). Microglial activation and dopamine terminal loss in early Parkinson's disease. *Ann. Neurol.* 57, 168–175. doi: 10.1002/ana.20338

Ozturk, M., Abosch, A., Francis, D., Wu, J., Jimenez-Shahed, J., and Ince, N. F. (2020). Distinct subthalamic coupling in the ON state describes motor performance in Parkinson's disease. *Mov. Disord.* 35, 91–100. doi: 10.1002/mds.27800

Pang, S. Y.-Y., Ho, P. W.-L., Liu, H.-F., Leung, C.-T., Li, L., Chang, E. E. S., et al. (2019). The interplay of aging, genetics and environmental factors in the pathogenesis of Parkinson's disease. *Transl. Neurodegener.* 8:23. doi: 10.1186/s40035-019-0165-9

Panicker, N., Sarkar, S., Harischandra, D. S., Neal, M., Kam, T. I., Jin, H., et al. (2019). Fyn kinase regulates misfolded α-synuclein uptake and NLRP3 inflammasome activation in microglia. *J. Exp. Med.* 216, 1411–1430. doi: 10.1084/jem.20182191

Papagiannakis, N., Koros, C., Stamelou, M., Simitsi, A. M., Maniati, M., Antonelou, R., et al. (2018). α-synuclein dimerization in erythrocytes of patients with genetic and non-genetic forms of Parkinson's disease. *Neurosci. Lett.* 672, 145–149. doi: 10.1016/j.neulet.2017.11.012

Park, S. B., Kwon, K.-Y., Lee, J.-Y., Im, K., Sunwoo, J.-S., Lee, K. B., et al. (2019). Lack of association between dopamine transporter loss and non-motor symptoms in patients with Parkinson's disease: a detailed PET analysis of 12 striatal subregions. *Neurol. Sci.* 40, 311–317. doi: 10.1007/s10072-018-3632-7

Park, J.-Y., Paik, S. R., Jou, I., and Park, S. M. (2008). Microglial phagocytosis is enhanced by monomeric α-synuclein, not aggregated α-synuclein: implications for Parkinson's disease. *Glia* 56, 1215–1223. doi: 10.1002/glia.20691

Parnetti, L., Farotti, L., Eusebi, P., Chiasserini, D., De Carlo, C., Giannandrea, D., et al. (2014). Differential role of CSF α-synuclein species, tau, and Aβ42 in Parkinson's disease. *Front. Aging Neurosci.* 6:53. doi: 10.3389/fnagi.2014.00053

Parnetti, L., Gaetani, L., Eusebi, P., Paciotti, S., Hansson, O., El-Agnaf, O., et al. (2019). CSF and blood biomarkers for Parkinson's disease. *Lancet Neurol.* 18, 573–586. doi: 10.1016/S1474-4422(19)30024-9

Péran, P., Cherubini, A., Assogna, F., Piras, F., Quattrocchi, C., Peppe, A., et al. (2010). Magnetic resonance imaging markers of Parkinson's disease nigrostriatal signature. *Brain* 133, 3423–3433. doi: 10.1093/brain/awq212

Periquet, M., Latouche, M., Lohmann, E., Rawal, N., De Michele, G., Ricard, S., et al. (2003). Parkin mutations are frequent in patients with isolated early-onset parkinsonism. *Brain* 126, 1271–1278. doi: 10.1093/brain/awg136

Polymeropoulos, M. H., Lavedan, C., Leroy, E., Ide, S. E., Dehejia, A., Dutra, A., et al. (1997). Mutation in the α-synuclein gene identified in families with Parkinson's disease. *Science* 276, 2045–2047. doi: 10.1126/science.276.5321.2045

Posavi, M., Diaz-Ortiz, M., Liu, B., Swanson, C. R., Skrinak, R. T., Hernandez-Con, P., et al. (2019). Characterization of Parkinson's disease using blood-based biomarkers: a multicohort proteomic analysis. *PLoS Med.* 16:e1002931. doi: 10.1371/journal.pmed.1002931

Postuma, R. B., Berg, D., Adler, C. H., Bloem, B. R., Chan, P., Deuschl, G., et al. (2016). The new definition and diagnostic criteria of Parkinson's disease. *Lancet Neurol.* 15, 546–548. doi: 10.1016/S1474-4422(16)00116-2

Postuma, R. B., Gagnon, J. F., and Montplaisir, J. (2010). Clinical prediction of Parkinson's disease: planning for the age of neuroprotection. *J. Neurol. Neurosurg. Psychiatry* 81, 1008–1013. doi: 10.1136/jnnp.2009.174748

Pott Godoy, M. C., Tarelli, R., Ferrari, C. C., Sarchi, M. I., and Pitossi, F. J. (2008). Central and systemic IL-1 exacerbates neurodegeneration and motor symptoms in a model of Parkinson's disease. *Brain* 131, 1880–1894. doi: 10.1093/brain/awn101

Pradhan, S. S., Salinas, K., Garduno, A. C., Johansson, J. U., Wang, Q., Manning-Bog, A., et al. (2017). Anti-inflammatory and neuroprotective effects of PGE2 EP4 signaling in models of Parkinson's disease. *J. Neuroimmune Pharmacol.* 12, 292–304. doi: 10.1007/s11481-016-9713-6

Priori, A., Foffani, G., Pesenti, A., Tamma, F., Bianchi, A. M., Pellegrini, M., et al. (2004). Rhythm-specific pharmacological modulation of subthalamic activity in Parkinson's disease. *Exp. Neurol.* 189, 369–379. doi: 10.1016/j.expneurol.2004.06.001

Rabenstein, M., Besong Agbo, D., Wolf, E., Dams, J., Nicolai, M., Roeder, A., et al. (2019). Effect of naturally occurring α-synuclein-antibodies on toxic α-synuclein-fragments. *Neurosci. Lett.* 704, 181–188. doi: 10.1016/j.neulet.2019.04.004

Reale, M., Iarlori, C., Thomas, A., Gambi, D., Perfetti, B., Di Nicola, M., et al. (2009). Peripheral cytokines profile in Parkinson's disease. *Brain Behav. Immun.* 23, 55–63. doi: 10.1016/j.bbi.2008.07.003

Reynolds, A. D., Stone, D. K., Mosley, R. L., and Gendelman, H. E. (2009). Nitrated α-synuclein-induced alterations in microglial immunity are regulated by CD4+ T cell subsets. *J. Immunol.* 182, 4137–4149. doi: 10.4049/jimmunol.0803982

Rojanathammanee, L., Murphy, E. J., and Combs, C. K. (2011). Expression of mutant α-synuclein modulates microglial phenotype *in vitro*. *J. Neuroinflammation* 8:44. doi: 10.1186/1742-2094-8-44

Roodveldt, C., Labrador-Garrido, A., Gonzalez-Rey, E., Fernandez-Montesinos, R., Caro, M., Lachaud, C. C., et al. (2010). Glial innate immunity generated by non-aggregated α-synuclein in mouse: differences between wild-type and Parkinson's disease-linked mutants. *PLoS One* 5:e13481. doi: 10.1371/journal.pone.0013481

Rossi, M., Candelise, N., Baiardi, S., Capellari, S., Giannini, G., Orru, C. D., et al. (2020). Ultrasensitive RT-QuIC assay with high sensitivity and specificity for Lewy body-associated synucleinopathies. *Acta Neuropathol.* 140, 49–62. doi: 10.1007/s00401-020-02160-8

Saeed, U., Compagnone, J., Aviv, R. I., Strafella, A. P., Black, S. E., Lang, A. E., et al. (2017). Imaging biomarkers in Parkinson's disease and Parkinsonian syndromes: current and emerging concepts. *Transl. Neurodegener.* 6:8. doi: 10.1186/s40035-017-0076-6

Saito, Y. (2014). Oxidized DJ-1 as a possible biomarker of Parkinson's disease. *J. Clin. Biochem. Nutr.* 54, 138–144. doi: 10.3164/jcbn.13-108

Sampedro, F., Martínez-Horta, S., Marín-Lahoz, J., Pagonabarraga, J., and Kulisevsky, J. (2019). Longitudinal intracortical diffusivity changes in *de-novo* Parkinson's disease: a promising imaging biomarker. *Parkinsonism Relat. Disord.* 68, 22–25. doi: 10.1016/j.parkreldis.2019.09.031

Sanchez-Guajardo, V., Febbraro, F., Kirik, D., and Romero-Ramos, M. (2010). Microglia acquire distinct activation profiles depending on the degree of α-synuclein neuropathology in a rAAV based model of Parkinson's disease. *PLoS One* 5:e8784. doi: 10.1371/journal.pone.0008784

Schapira, A. H., and Tolosa, E. (2010). Molecular and clinical prodrome of Parkinson disease: implications for treatment. *Nat. Rev. Neurol.* 6, 309–317. doi: 10.1038/nrneurol.2010.52

Schrag, A., and Schott, J. M. (2006). Epidemiological, clinical, and genetic characteristics of early-onset parkinsonism. *Lancet Neurol.* 5, 355–363. doi: 10.1016/S1474-4422(06)70411-2

Shahnawaz, M., Mukherjee, A., Pritzkow, S., Mendez, N., Rabadia, P., Liu, X., et al. (2020). Discriminating α-synuclein strains in Parkinson's disease and multiple system atrophy. *Nature* 578, 273–277. doi: 10.1038/s41586-020-1984-7

Shahnawaz, M., Tokuda, T., Waragai, M., Mendez, N., Ishii, R., Trenkwalder, C., et al. (2017). Development of a biochemical diagnosis of parkinson disease by detection of α-synuclein misfolded aggregates in cerebrospinal fluid. *JAMA Neurol.* 74, 163–172. doi: 10.1001/jamaneurol.2016.4547

Shao, Q.-H., Yan, W.-F., Zhang, Z., Ma, K.-L., Peng, S.-Y., Cao, Y.-L., et al. (2019). Nurr1: a vital participant in the TLR4-NF-κB signal pathway stimulated by α-synuclein in BV-2cells. *Neuropharmacology* 144, 388–399. doi: 10.1016/j.neuropharm.2018.04.008

Shin, J., Park, S.-H., Shin, C., Kim, J.-H., Yun, T. J., Kim, H.-J., et al. (2019). Submandibular gland is a suitable site for α synuclein pathology in Parkinson disease. *Parkinsonism Relat. Disord.* 58, 35–39. doi: 10.1016/j.parkreldis.2018.04.019

Sidransky, E., and Lopez, G. (2012). The link between the GBA gene and parkinsonism. *Lancet Neurol.* 11, 986–998. doi: 10.1016/S1474-4422(12)70190-4

Sidransky, E., Nalls, M. A., Aasly, J. O., Aharon-Peretz, J., Annesi, G., Barbosa, E. R., et al. (2009). Multicenter analysis of glucocerebrosidase mutations in Parkinson's disease. *N. Engl. J. Med.* 361, 1651–1661. doi: 10.1056/NEJMoa0901281

Silberstein, P., Kühn, A. A., Kupsch, A., Trottenberg, T., Krauss, J. K., Wöhrle, J. C., et al. (2003). Patterning of globus pallidus local field potentials differs between Parkinson's disease and dystonia. *Brain* 126, 2597–2608. doi: 10.1093/brain/awg267

Singleton, A. B., Farrer, M. J., and Bonifati, V. (2013). The genetics of Parkinson's disease: progress and therapeutic implications. *Mov. Disord.* 28, 14–23. doi: 10.1002/mds.25249

Singleton, A. B., Farrer, M., Johnson, J., Singleton, A., Hague, S., Kachergus, J., et al. (2003). α-Synuclein locus triplication causes Parkinson's disease. *Science* 302:841. doi: 10.1126/science.1090278

Sommerauer, M., Fedorova, T. D., Hansen, A. K., Knudsen, K., Otto, M., Jeppesen, J., et al. (2018). Evaluation of the noradrenergic system in Parkinson's disease: an 11C-MeNER PET and neuromelanin MRI study. *Brain* 141, 496–504. doi: 10.1093/brain/awx348

Spillantini, M. G., Schmidt, M. L., Lee, V. M., Trojanowski, J. Q., Jakes, R., and Goedert, M. (1997). α-synuclein in lewy bodies. *Nature* 388, 839–840. doi: 10.1038/42166

Stokholm, M. G., Danielsen, E. H., Hamilton-Dutoit, S. J., and Borghammer, P. (2016). Pathological α-synuclein in gastrointestinal tissues from prodromal Parkinson disease patients. *Ann. Neurol.* 79, 940–949. doi: 10.1002/ana.24648

Storzer, L., Butz, M., Hirschmann, J., Abbasi, O., Gratkowski, M., Saupe, D., et al. (2017). Bicycling suppresses abnormal β synchrony in the Parkinsonian basal ganglia. *Ann. Neurol.* 82, 592–601. doi: 10.1002/ana.25047

Su, X., Maguire-Zeiss, K. A., Giuliano, R., Prifti, L., Venkatesh, K., and Federoff, H. J. (2008). Synuclein activates microglia in a model of Parkinson's disease. *Neurobiol. Aging* 29, 1690–1701. doi: 10.1016/j.neurobiolaging.2007.04.006

Sui, Y., Stanić, D., Tomas, D., Jarrott, B., and Horne, M. K. (2009). Meloxicam reduces lipopolysaccharide-induced degeneration of dopaminergic neurons in the rat substantia nigra pars compacta. *Neurosci. Lett.* 460, 121–125. doi: 10.1016/j.neulet.2009.05.033

Thevathasan, W., Pogosyan, A., Hyam, J. A., Jenkinson, N., Foltynie, T., Limousin, P., et al. (2012). α oscillations in the pedunculopontine nucleus correlate with gait performance in parkinsonism. *Brain* 135, 148–160. doi: 10.1093/brain/awr315

Tian, C., Liu, G., Gao, L., Soltys, D., Pan, C., Stewart, T., et al. (2019). Erythrocytic α-Synuclein as a potential biomarker for Parkinson's disease. *Transl. Neurodegener.* 8:15. doi: 10.1186/s40035-019-0155-y

Tinkhauser, G., Pogosyan, A., Debove, I., Nowacki, A., Shah, S. A., Seidel, K., et al. (2018). Directional local field potentials: a tool to optimize deep brain stimulation. *Mov. Disord.* 33, 159–164. doi: 10.1002/mds.27215

Trager, M. H., Koop, M. M., Velisar, A., Blumenfeld, Z., Nikolau, J. S., Quinn, E. J., et al. (2016). Subthalamic β oscillations are attenuated after withdrawal of chronic high frequency neurostimulation in Parkinson's disease. *Neurobiol. Dis.* 96, 22–30. doi: 10.1016/j.nbd.2016.08.003

Tsiokos, C., Malekmohammadi, M., Auyong, N., and Pouratian, N. (2017). Pallidal low β-low γ phase-amplitude coupling inversely correlates with Parkinson disease symptoms. *Clin. Neurophysiol.* 128, 2165–2178. doi: 10.1016/j.clinph.2017.08.001

Tsukita, K., Sakamaki-Tsukita, H., Tanaka, K., Suenaga, T., and Takahashi, R. (2019). Value of *in vivo* α-synuclein deposits in Parkinson's disease: a systematic review and meta-analysis. *Mov. Disord.* 34, 1452–1463. doi: 10.1002/mds.27794

Vaillancourt, D. E., Spraker, M. B., Prodoehl, J., Abraham, I., Corcos, D. M., Zhou, X. J., et al. (2009). High-resolution diffusion tensor imaging in the substantia nigra of de novo Parkinson disease. *Neurology* 72, 1378–1384. doi: 10.1212/01.wnl.0000340982.01727.6e

van den Berg, M. M. J., Krauskopf, J., Ramaekers, J. G., Kleinjans, J. C. S., Prickaerts, J., and Briede, J. J. (2020). Circulating microRNAs as potential biomarkers for psychiatric and neurodegenerative disorders. *Prog. Neurobiol.* 185:101732. doi: 10.1016/j.pneurobio.2019.101732

Vicente Miranda, H., Cássio, R., Correia-Guedes, L., Gomes, M. A., Chegao, A., Miranda, E., et al. (2017). Posttranslational modifications of blood-derived α-synuclein as biochemical markers for Parkinson's disease. *Sci. Rep.* 7:13713. doi: 10.1038/s41598-017-14175-5

Vilas, D., Iranzo, A., Tolosa, E., Aldecoa, I., Berenguer, J., Vilaseca, I., et al. (2016). Assessment of α-synuclein in submandibular glands of patients with idiopathic rapid-eye-movement sleep behavior disorder: a case-control study. *Lancet Neurol.* 15, 708–718. doi: 10.1016/S1474-4422(16)00080-6

Walsh, S., Finn, D. P., and Dowd, E. (2011). Time-course of nigrostriatal neurodegeneration and neuroinflammation in the 6-hydroxydopamine-induced axonal and terminal lesion models of Parkinson's disease in the rat. *Neuroscience* 175, 251–261. doi: 10.1016/j.neuroscience.2010.12.005

Wang, Z., Becker, K., Donadio, V., Siedlak, S., Yuan, J., Rezaee, M., et al. (2020). Skin α-synuclein aggregation seeding activity as a novel biomarker for Parkinson disease. *JAMA Neurol.* 78, 1–11. doi: 10.1001/jamaneurol.2020.3311

Wang, L., Liu, Y., Yan, S., Du, T., Fu, X., Gong, X., et al. (2020). Disease progression-dependent expression of CD200R1 and CX3CR1 in mouse models of Parkinson's disease. *Aging Dis.* 11, 254–268. doi: 10.14336/AD.2019.0615

Wang, H., Wang, W., Shi, H., Han, L., and Pan, P. (2020). Cerebrospinal fluid and blood levels of neurofilament light chain in Parkinson disease: a protocol

for systematic review and meta-analysis. *Medicine* 99:e21458. doi: 10.1097/MD.0000000000021458

Wang, X., Yu, S., Li, F., and Feng, T. (2015). Detection of α-synuclein oligomers in red blood cells as a potential biomarker of Parkinson's disease. *Neurosci. Lett.* 599, 115–119. doi: 10.1016/j.neulet.2015.05.030

Wojtecki, L., Elben, S., Vesper, J., and Schnitzler, A. (2017). The rhythm of the executive gate of speech: subthalamic low-frequency oscillations increase during verbal generation. *Eur. J. Neurosci.* 45, 1200–1211. doi: 10.1111/ejn.13429

Wu, D. C., Jackson-Lewis, V., Vila, M., Tieu, K., Teismann, P., Vadseth, C., et al. (2002). Blockade of microglial activation is neuroprotective in the 1-methyl-4-phenyl-1,2,3,6-tetrahydropyridine mouse model of Parkinson disease. *J. Neurosci.* 22, 1763–1771. doi: 10.1523/JNEUROSCI.22-05-01763.2002

Youn, J., Lee, S.-B., Lee, H. S., Yang, H. O., Park, J., Kim, J. S., et al. (2018). Cerebrospinal fluid levels of autophagy-related proteins represent potentially novel biomarkers of early-stage Parkinson's disease. *Sci. Rep.* 8:16866. doi: 10.1038/s41598-018-35376-6

Zaidel, A., Spivak, A., Grieb, B., Bergman, H., and Israel, Z. (2010). Subthalamic span of β oscillations predicts deep brain stimulation efficacy for patients with Parkinson's disease. *Brain* 133, 2007–2021. doi: 10.1093/brain/awq144

Zarranz, J. J., Alegre, J., Gomez-Esteban, J. C., Lezcano, E., Ros, R., Ampuero, I., et al. (2004). The new mutation, E46K, of α-synuclein causes Parkinson and Lewy body dementia. *Ann. Neurol.* 55, 164–173. doi: 10.1002/ana.10795

Zhang, C., Dou, B., Wang, J., Xu, K., Zhang, H., Sami, M. U., et al. (2019). Dynamic alterations of spontaneous neural activity in Parkinson's disease: a resting-state fMRI study. *Front. Neurol.* 10:1052. doi: 10.3389/fneur.2019.01052

Zhang, W., Wang, T., Pei, Z., Miller, D. S., Wu, X., Block, M. L., et al. (2005). Aggregated α-synuclein activates microglia: a process leading to disease progression in Parkinson's disease. *FASEB J.* 19, 533–542. doi: 10.1096/fj.04-2751com

Zheng, L. T., Ock, J., Kwon, B.-M., and Suk, K. (2008). Suppressive effects of flavonoid fisetin on lipopolysaccharide-induced microglial activation and neurotoxicity. *Int. Immunopharmacol.* 8, 484–494. doi: 10.1016/j.intimp.2007.12.012

Zhou, Y., Lu, M., Du, R.-H., Qiao, C., Jiang, C.-Y., Zhang, K.-Z., et al. (2016). MicroRNA-7 targets Nod-like receptor protein 3 inflammasome to modulate neuroinflammation in the pathogenesis of Parkinson's disease. *Mol. Neurodegener.* 11:28. doi: 10.1186/s13024-016-0094-3

Conflict of Interest: The authors declare that the research was conducted in the absence of any commercial or financial relationships that could be construed as a potential conflict of interest.

Copyright © 2021 Du, Wang, Liu, Zhu, Chen and Zhang. This is an open-access article distributed under the terms of the Creative Commons Attribution License (CC BY). The use, distribution or reproduction in other forums is permitted, provided the original author(s) and the copyright owner(s) are credited and that the original publication in this journal is cited, in accordance with accepted academic practice. No use, distribution or reproduction is permitted which does not comply with these terms.

frontiers in Aging Neuroscience

ORIGINAL RESEARCH
published: 25 March 2021
doi: 10.3389/fnagi.2021.648982

Fatty Acid-Binding Protein 3 Expression in the Brain and Skin in Human Synucleinopathies

Hideki Oizumi[1], Kenshi Yamasaki[2], Hiroyoshi Suzuki[3], Takafumi Hasegawa[4], Yoko Sugimura[1], Toru Baba[1], Kohji Fukunaga[5] and Atsushi Takeda[1,6]*

[1] Department of Neurology, National Hospital Organization, Sendai Nishitaga Hospital, Sendai, Japan, [2] Department of Dermatology, Graduate School of Medicine, Tohoku University, Sendai, Japan, [3] Department of Clinical Pathology, National Hospital Organization, Sendai Medical Center, Sendai, Japan, [4] Department of Neurology, Graduate School of Medicine, Tohoku University, Sendai, Japan, [5] Department of Pharmacology, Graduate School of Pharmaceutical Sciences, Tohoku University, Sendai, Japan, [6] Department of Cognitive and Motor Aging, Graduate School of Medicine, Tohoku University, Sendai, Japan

Parkinson's disease (PD) and multiple system atrophy are types of adult-onset neurodegenerative disorders named synucleinopathies, which are characterized by prominent intracellular α-synuclein (αSyn) aggregates. We have previously found that αSyn aggregates and the vulnerability of dopaminergic neurons in the mouse brain are partly associated with the expression of fatty acid-binding protein 3 (FABP3, heart FABP). However, it remains to be elucidated whether FABP3 accumulation is associated with αSyn aggregates in human tissues. Here, we histologically studied FABP3 expression in human tissues obtained from patients with synucleinopathies, patients with Alzheimer disease (AD) and controls. We found that (1) a variety of neurons expressed the FABP3 protein in human brain tissues, (2) FABP3 was colocalized with αSyn aggregates in the brains of individuals with synucleinopathies but not with amyloid β or p-tau aggregates in the brains of individuals with AD, and (3) FABP3 was not present in p-αSyn deposits in biopsied skin tissues from individuals with PD. These findings suggest that FABP3 expression is associated with αSyn aggregation in synucleinopathies and provide new insights into the involvement of FABP3 in synucleinopathies.

Keywords: α-synuclein, multiple system atrophy, fatty acid-binding protein, human, Parkinson's disease

OPEN ACCESS

Edited by:
Liu Jun,
Shanghai Jiao Tong University, China

Reviewed by:
Makoto Hashimoto,
Tokyo Metropolitan Institute of Medical Science, Japan
Maria E. Jimenez-Capdeville,
Autonomous University of San Luis Potosí, Mexico

****Correspondence:***
Hideki Oizumi
ooizumi.hideki.ub@mail.hosp.go.jp

Received: *03 January 2021*
Accepted: *03 March 2021*
Published: *25 March 2021*

Citation:
Oizumi H, Yamasaki K, Suzuki H, Hasegawa T, Sugimura Y, Baba T, Fukunaga K and Takeda A (2021) Fatty Acid-Binding Protein 3 Expression in the Brain and Skin in Human Synucleinopathies. Front. Aging Neurosci. 13:648982. doi: 10.3389/fnagi.2021.648982

INTRODUCTION

Parkinson's disease (PD) is a secondary common neurodegenerative disorder affecting >1% of the population over 65 years of age worldwide (de Lau and Breteler, 2006). The histopathological features of PD include loss of dopaminergic (DA) neurons in the substantia nigra (SN) and the presence of cytoplasmic protein aggregates, known as Lewy bodies (LBs) (Gibb and Lees, 1988). α-Synuclein (αSyn), a 140-amino acid protein, is associated with synaptic vesicles in presynaptic nerve

Abbreviations: αSyn, α-synuclein; FABP, fatty acid-binding protein; DA, dopaminergic; PD, Parkinson's disease; CN, control; SN, substantia nigra; LBs, Lewy bodies; MSA, multiple system atrophy; GCIs, glial cytoplasmic inclusions; NCIs, neuronal cytoplasmic inclusions; DLB, dementia with Lewy bodies; MPTP, 1-methyl-1,2,3,6-tetrahydropyridine; FAs, fatty acids; p-αSyn, phosphorylated αSyn; ir, immunoreactive; p-tau, phosphorylated tau; NFT, neurofibrillary tangle; PUFAs, long-chain polyunsaturated fatty acids; AD, Alzheimer disease.

terminals, and β-sheet fibrillar αSyn aggregates are major components of LBs (Spillantini et al., 1998). αSyn aggregation is associated with progressive loss of DA neurons, implicating αSyn in PD pathogenesis. In addition, duplication/triplication and missense mutations (A53T, and A30P, etc.) in the αSyn gene *SNCA* are linked to familial early-onset PD (Polymeropoulos et al., 1997; Kruger et al., 1998; Singleton et al., 2003; Chartier-Harlin et al., 2004; Farrer et al., 2004; Zarranz et al., 2004). Therefore, PD and dementia with LBs (DLB) are designated as synucleinopathies, which are neurodegenerative disorders characterized by prominent intracellular αSyn aggregates (McCann et al., 2014). Multiple system atrophy (MSA) is an adult-onset neurodegenerative disorder that is clinically characterized by a combination of poorly levodopa (L-dopa)-responsive parkinsonism, cerebellar dysfunction and autonomic failure (Yabe et al., 2006). The histopathological features of MSA include the presence of glial and neuronal protein aggregates, known as glial cytoplasmic inclusions (GCIs) and neuronal cytoplasmic inclusions (NCIs), respectively (Wakabayashi et al., 1998; Wakabayashi and Takahashi, 2006; Homma et al., 2016). Similar to LBs, GCIs and NCIs are composed largely of αSyn aggregates. Thus, on the basis of histopathological observations, MSA is also classified as a synucleinopathy (McCann et al., 2014). However, the molecular mechanisms of αSyn aggregation remain to be elucidated.

There is increasing evidence that lipid metabolism plays crucial roles in the pathogenesis of synucleinopathies (Oueslati, 2016; Xicoy et al., 2019). In particular, fatty acid (FA) metabolism is noted to occur in αSyn aggregates (Mollenhauer et al., 2007a; Wada-Isoe et al., 2008a; Paisan-Ruiz et al., 2009; Yoshino et al., 2010; Tomiyama et al., 2011; Sumi-Akamaru et al., 2016). FA-binding proteins (FABPs) are lipid chaperones that mediate biological processes and systemic metabolic homeostasis through regulation of diverse lipid signals. Among FABPs, FABP3 is expressed mainly in the heart but is distributed in the kidneys, skeletal muscle, aorta, lungs, mammary glands, placenta, testes, ovaries, adrenal grands, stomach and brain (Furuhashi and Hotamisligil, 2008; Schulz-Schaeffer, 2010). Interestingly, in a previous study on model mice with PD induced by 1-methyl-1,2,3,6-tetrahydropyridine (MPTP), we found that αSyn binds to FABP3 and that αSyn aggregates with FABP3 accumulation are abundant in damaged DA neurons (Shioda et al., 2014). We also previously found that FABP3-knockout mice are resistant to MPTP-induced DA neurodegeneration in the SN and to MPTP-induced motor dysfunction (Shioda et al., 2014). Consistent with this finding, MPTP-induced αSyn aggregation in DA neurons is attenuated in FABP3-knockout mice (Shioda et al., 2014). Thus, FABP3 expression seems to be involved in the pathogeneses of αSyn aggregation and DA neuron degeneration in PD model mice. Serum FABP3 is a potential diagnostic marker for PD and DLB because the levels of this protein are higher in PD and DLB patients than in AD patients (Mollenhauer et al., 2007a; Wada-Isoe et al., 2008a). It has also been reported that elevated FABP3 levels in cerebrospinal fluid (CSF) are associated with future dementia in individuals with PD (Backstrom et al., 2015).

Although FABP3 has been suggested to promote αSyn aggregation in animal models and to potentially be a useful biomarker for synucleinopathies, it remains to be elucidated whether FABP3 accumulation is associated with αSyn aggregation in human tissues. Here, we pathologically studied FABP3 expression in human tissues obtained from patients with synucleinopathies, patients with Alzheimer disease (AD) and controls (CNs).

MATERIALS AND METHODS

Human Tissue Sources

Brain tissues from autopsies: We examined consecutive adult autopsy cases that had been registered at the National Hospital Organization (NHO) Sendai Medical Center. The ages of the subjects ranged from 58 to 89 years, with an average of 73.7 years. The 16 cases comprised eight female and eight male patients. The neuropathological diagnoses included four cases of PD, six cases of MSA, four CNs, and two cases of AD. None of the patients had kindred relationships with each other. The whole brains were fixed in 20% buffered formalin (Wako, Osaka, Japan) for 5–11 days. Serial coronal sections were dehydrated in a graded ethanol series, cleared in xylene, and embedded in paraffin using an automated tissue processor.

Biopsied skin tissues: Previous reports have shown that the presence of dermal αSyn deposits in proximal body sites is a sensitive biomarker for PD diagnosis, helping to differentiate PD from other parkinsonisms (Ikemura et al., 2008; Donadio et al., 2014; Zange et al., 2015). We recruited 10 PD patients fulfilling the diagnostic criteria of the UK PD brain bank (Gibb and Lees, 1988) for skin biopsy. All patients with PD showed late-onset disorder (at >45 years of age), were treated with L-dopa only or in combination with other medications and had well-controlled motor symptoms. None of the patients had kindred relationships with each other. In this study, 3-mm punch biopsies were taken from proximal body sites. Skin specimens were collected from the cervical C8 paravertebral area, i.e., close to the spinal ganglia (Donadio et al., 2014) and from an axilla. Skin biopsy was performed by using a 3-mm disposable punch with sterile technique after topical anesthesia with lidocaine. No suturing was required. We performed fixation in 4% paraformaldehyde for 24 h by using a previously described method (Ikemura et al., 2008), since this type of fixation increases immunohistochemical sensitivity for LB and Lewy neurite detection. Serial sections were dehydrated in a graded ethanol series, cleared in xylene, and embedded in paraffin using an automated tissue processor.

The procedures used were approved by the local human ethics committee and followed the Declaration of Helsinki regarding international clinical research involving humans. All subjects gave written informed consent to participate in the study.

Histological Immunofluorescence (IF) Staining

To enhance LB labeling, we pretreated all samples with formic acid (Sengoku et al., 2008). The sections were double-immunostained overnight with primary antibodies. The following antibodies were used in this study: rabbit polyclonal anti-FABP3 antibodies (1:100 dilution, Proteintech, Chicago, IL,

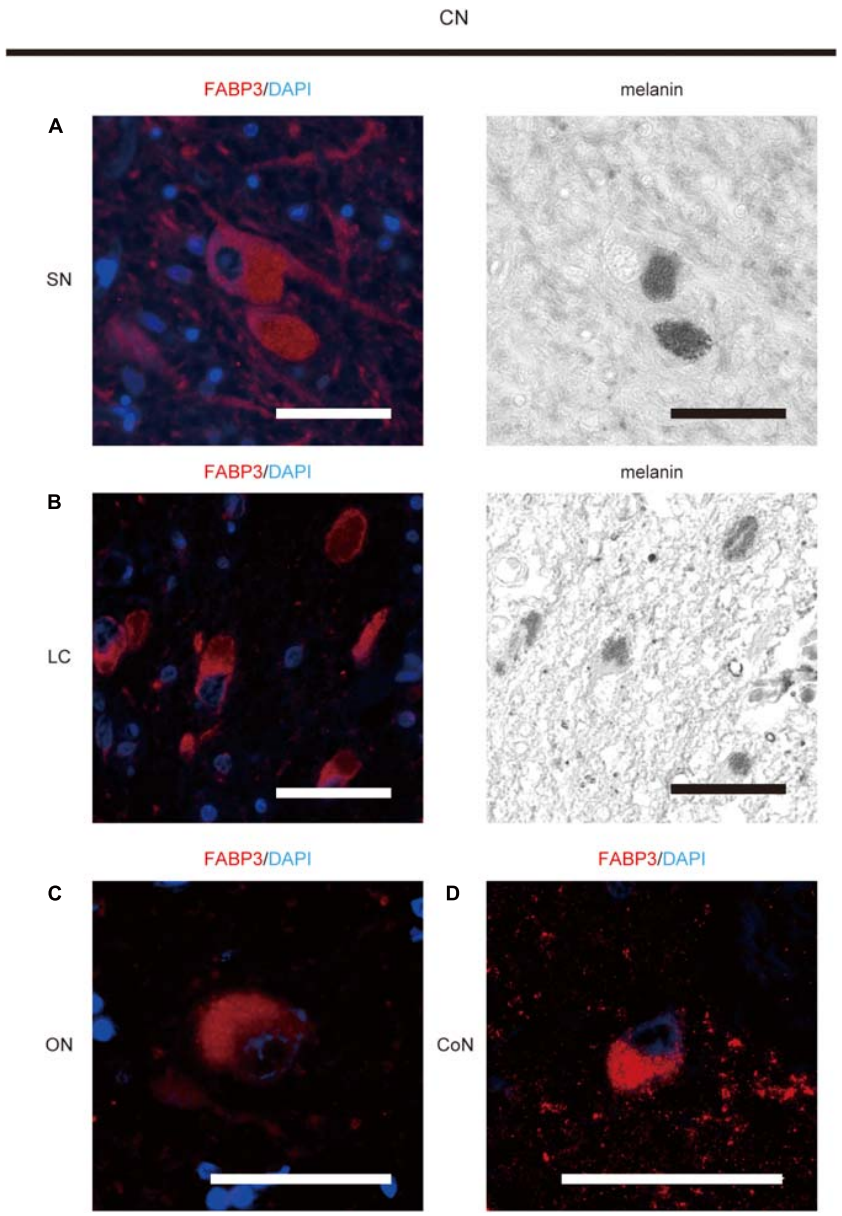


FIGURE 1 | Immunohistochemical analysis of FABP3 protein expression in autopsied brain tissues of CNs. We used fluorescence microscopy to show FABP3 expression and optical microscopy to identify melanin-positive DA neurons and locus coeruleus (LC) neurons. The nuclei of neurons were identified morphologically by DAPI (blue) staining. IF staining of FABP3 (red) and melanin (black) in DA neurons in the SN of CNs is shown in high-magnification images **(A)**. IF staining of FABP3 (red) and melanin (black) in LC neurons in the pons of CNs is shown in high-magnification images **(B)**. IF staining of FABP3 (red) in the oculomotor neurons (ON) of CNs is shown in high-magnification images **(C)**. IF staining of FABP3 (red) in the cortical neurons (CoN) in the EC of CNs is shown in high-magnification images **(D)**. FABP3-ir proteins in melanin-positive neurons were expressed mostly in the cytoplasm. FABP3-ir proteins were also expressed in oculomotor neurons and cortical neurons other than melanin-positive neurons. Scale bars = 50 μm.

United States), a mouse monoclonal p-αSyn (Ser 129) antibody (1:1,000 dilution, Wako, Richmond, VA, United States), a mouse monoclonal anti-αSyn aggregate antibody (BioLegend, San Diego, CA, United States), a mouse monoclonal anti-amyloid β antibody (1:100 dilution, Abcam, ab11132, Cambridge, MA, United States) and a mouse monoclonal anti-p-tau antibody (1:100 dilution, Innogenetics, Ghent, Belgium). The sections were then washed, and secondary antibodies were added for a 2-h incubation. The secondary antibodies, anti-mouse Alexa Fluor 488, anti-rabbit Alexa Fluor 594, anti-mouse Alexa Fluor 594, and anti-rabbit Alexa Fluor 488, were obtained from Jackson ImmunoResearch (West Grove, PA, United States) and were used at a 1:500 dilution. Then, a TrueBlack lipofuscin autofluorescence quencher (Biotium Inc. Fremont, CA, United States) was used to remove artifacts caused by lipofuscin in these tissues. The sections were viewed and analyzed under a microscope system

(BZ-X700, Keyence, Osaka, Japan). The oculomotor nucleus were identified by referring to the hematoxylin and eosin staining of the adjacent sections used for fluorescence staining.

Immunohistochemistry

We pretreated all samples with formic acid. The following primary antibodies were used: a mouse monoclonal anti-p-tau antibody (1:100 dilution, Innogenetics, Ghent, Belgium). The signals from monoclonal and polyclonal antibodies were detected by using the automatic system on a VENTANA NX20 with the I-View DAB Universal Kit (Roche, Basel, Switzerland) according to the manufacturer's instructions. Sections were counter-stained with hematoxylin.

Semiquantitative Analysis of IF Staining

For semiquantitative analysis of p-αSyn and αSyn fibril protein aggregation with FABP3 accumulation, double-positive cells were analyzed via immunohistochemical grading of double-positive aggregates in a 20× field according to the following scoring system; +++, more than 5 intracellular aggregates in a field; ++, 2–5 aggregates in a field; +, one aggregate in a field; and –, no aggregates. For semiquantitative analysis of p-αSyn deposits and FABP3 accumulations in biopsied skin tissues, positive areas were analyzed via immunohistochemical grading of double-positive deposits in a 20× field according to the following scoring system; ++, more than 30 deposits in a field; +, 1–29 deposits in a field; and –, no deposit. We also examined the ratio of FABP3-immunoreactive (ir) deposits to anti-p-αSyn or anti-αSyn fibril-ir aggregates. These ratios were measured by the software programs Hybrid Cell Count and Macro Cell Count (Keyence, Osaka, Japan) in 20×-magnified fields for brain tissues [the striatum for MSA and the entorhinal cortex (EC) for PD]. We quantify the luminance of the green-labeled aggregates and the luminance of the red-labeled target proteins expressed. The ratio was then calculated using the luminance of the green aggregates as the denominator and the red target protein as the numerator.

Statistical Evaluation

All values are expressed as the means ± SEs. Differences between groups were examined for statistical significance using independent *t*-tests. The data were analyzed with IBM Statistics software (version 25). A P value <0.01 was considered to indicate a statistically significant difference.

RESULTS

FABP3 Is Expressed in Neurons in Normal Brain Tissues

FABP3-ir proteins were expressed in melanin-positive DA neurons in the SN (**Figure 1A**), in melanin-positive locus coeruleus neurons in the pons (**Figure 1B**), in oculomotor neurons in the midbrain (**Figure 1C**) and cortical neurons in the EC (**Figure 1D**) in autopsied brain tissues from CNs. FABP3-ir proteins in melanin-positive neurons were expressed mostly in the cytoplasm. FABP3 proteins were also expressed in oculomotor neurons and cortical neurons other than melanin-positive neurons.

TABLE 1 | Demographic profiles of autopsy cases and the results of immunostaining for colocalization of p-αSyn and αSyn fibril aggregates with FABP3 accumulations.

Case	Disease	Age (years)	Sex	Disease duration (years)	Region	p-α Syn-ir+ and FABP3-ir+ aggregates	α Syn fibril-ir+ and FABP3-ir+ aggregates
1	PD	75	Male	NS	SN	++	++
					EC	++	++
2	PD	68	Female	10	SN	++	++
					EC	++	+
3	PD	87	Female	9	SN	++	+
					EC	+++	++
4	PD	75	Female	17	SN	++	++
					EC	++	+
5	CN	62	Male	NS	SN	–	–
6	CN	79	Male	NS	SN	–	–
7	CN	83	Female	NS	SN	–	–
8	CN	69	Male	NS	SN	–	–
9	MSA	77	Female	3	ST	+++	+++
10	MSA	62	Male	6	ST	+++	+++
11	MSA	68	Male	7	ST	+++	+++
12	MSA	64	Male	13	ST	+++	+++
13	MSA	76	Female	8	ST	+++	+++
14	MSA	87	Female	23	ST	+++	+++

PD, Parkinson's disease; MSA, multiple system atrophy; CN, control subject; SN, substantia nigra; ST, striatum; EC, entorhinal cortex; NS, not specified. Double-positive aggregates in a 20× field: +++, more than 5 intracellular aggregates in a field; ++, 2–5 aggregates; +, one aggregate; –, no aggregates.

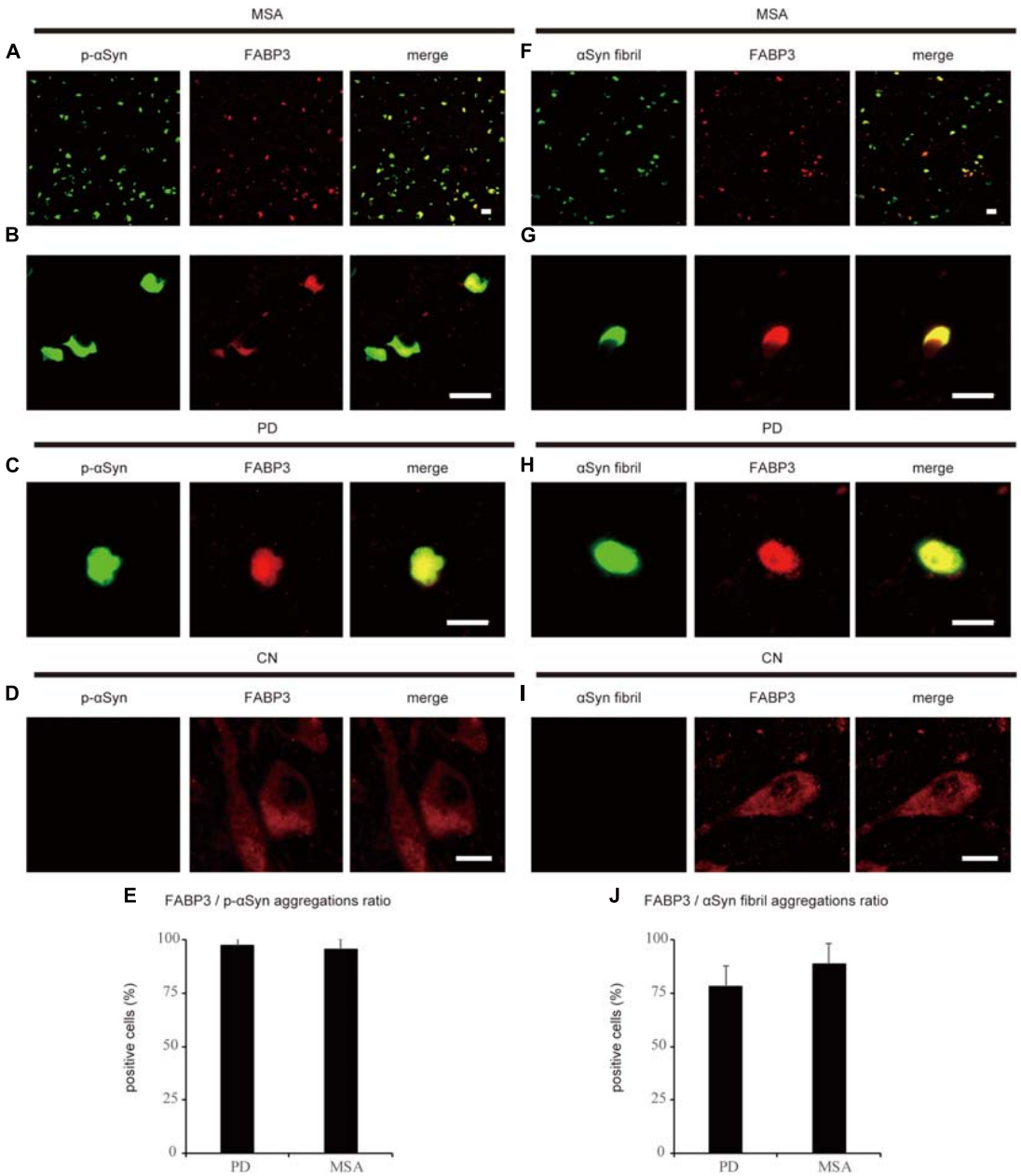


FIGURE 2 | Correlation between FABP3 protein accumulation and αSyn aggregation in synucleinopathies. IF staining of FABP3 (red) and p-αSyn (green) in the SN in MSA tissue is shown in low-magnification **(A)** and high-magnification **(B)** images; staining in the SN in PD tissue is shown in low-magnification images **(C)**; and staining in the SN in CN tissue is shown in high-magnification images **(D)**. **(A–C)** shows that FABP3 was colocalized with p-αSyn aggregates in synucleinopathies. In contrast, **(D)** shows that p-αSyn aggregates were not observed in the SN in CNs, although FABP3 protein was detected in DA neurons. The ratio of FABP3 protein accumulations to p-αSyn aggregates in the striatum in MSA tissue and in the EC in PD tissue was quantitatively analyzed **(E)** ($p = 0.666$). **(E)** shows that FABP3 accumulations were colocalized with most p-αSyn aggregates in both PD and MSA tissues. IF staining of FABP3 (red) and αSyn fibrils (green) in the SN in MSA tissue is shown in low-magnification **(F)** and high-magnification **(G)** images; staining in the SN in PD tissue is shown in low-magnification images **(H)**; and staining in the SN in CN tissue is shown in high-magnification images **(I)**. **(F–H)** shows that FABP3 accumulations were colocalized with αSyn fibrils in synucleinopathies. In contrast, **(I)** shows that αSyn fibrils were not observed in the SN in CNs, although FABP3 protein was detected in DA neurons. The ratio of FABP3 protein accumulations to αSyn fibrils in the striatum in MSA tissue and in the EC in PD tissue was quantitatively analyzed **(J)** ($p = 0.119$). **(J)** shows that FABP3 accumulations were colocalized with approximately 80% of αSyn fibrils in both PD and MSA tissues. Scale bars = 20 μm.

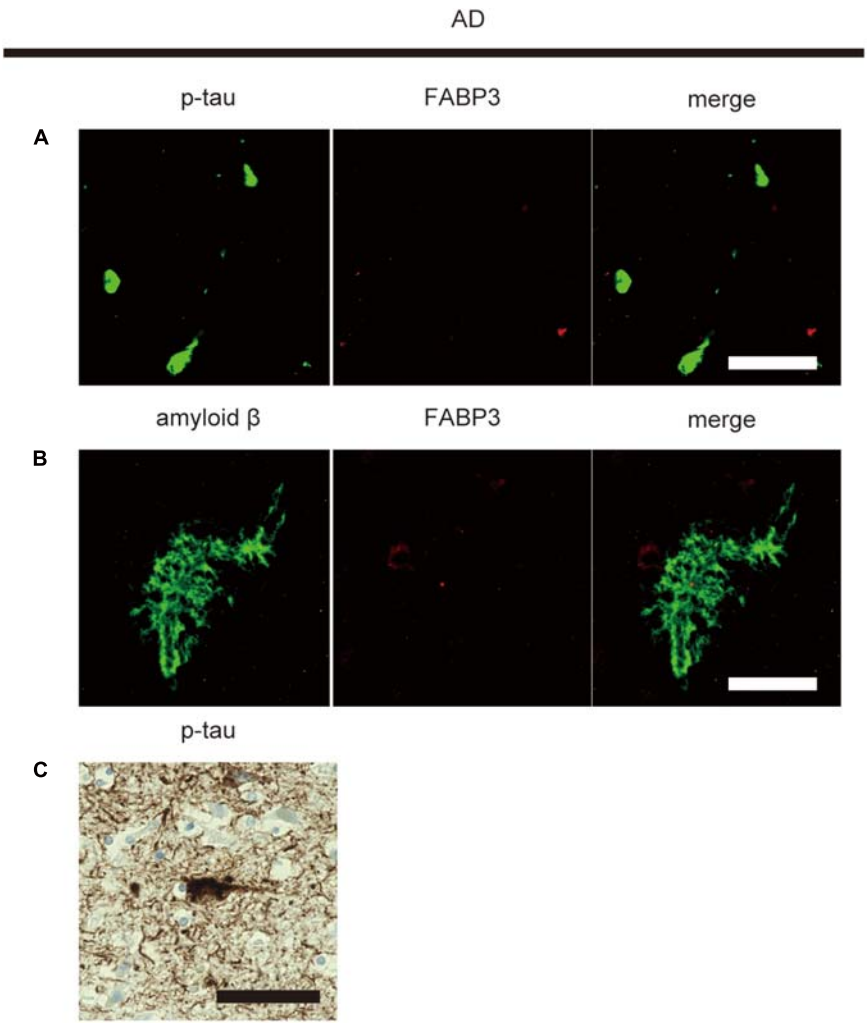


FIGURE 3 | No FABP3 protein expression in AD pathologyIF staining of FABP3 (red) and p-tau aggregates (green) in the frontal cortex in AD tissue **(A)**. IF staining of FABP3 (red) and amyloid β aggregates (green) in the frontal cortex in AD tissue **(B)**. FABP3 accumulation was not observed in amyloid β aggregates **(A)** or p-tau aggregates **(B)** in AD tissue. Nuclear staining with hematoxylin showed that p-tau-positive aggregates were NFTs **(C)**. Scale bars = 50 μm.

FABP3 Protein Expression Is Associated With α Syn Aggregates in Alpha Synucleinopathies

We next examined whether phosphorylated αSyn (p-αSyn) colocalized with FABP3 in synucleinopathies. As shown in **Table 1**, double-positive (p-αSyn-ir and FABP3-ir) aggregates were observed in the SN and EC in all four PD cases and in the striatum in all six MSA cases but not in the SN or EC in any of the four CNs. **Figures 2A–E** shows images of IF staining of FABP3 (red) and p-αSyn aggregates (green) in the striatum in MSA tissues (**Figure 2A**, low magnification; 2B, high magnification) and in the EC in PD tissues (**Figure 2C**, low magnification). There were no significant differences in the ratio of FABP3 accumulations to p-αSyn aggregates between PD and MSA tissues (**Figure 2E**) (t = 0.448, p = 0.666). FABP3 accumulations were colocalized with most p-αSyn aggregates in both PD and MSA tissues (**Figure 2E**). In contrast, p-αSyn aggregates were not observed in the SN in CNs, although FABP3 was detected in DA neurons (**Figure 2D**).

We next examined whether αSyn fibrils were colocalized with FABP3 in synucleinopathies. Similar to the correlation between p-αSyn and FABP3 protein expression in PD and MSA, a strong association between FABP3 protein expression and αSyn fibrils was observed in PD and MSA (**Table 1**). **Figures 2F–J** shows images of IF staining of FABP3 (red) and αSyn fibrils (green) in the striatum in MSA tissues (**Figure 2F**, low magnification; 2G, high magnification) and in the EC in PD tissues (**Figure 2H**, low magnification). There were no significant differences in the ratio of FABP3 accumulations to αSyn fibrils between PD and MSA tissues (**Figure 2J**) (t = 1.745, p = 0.119). FABP3 accumulations were colocalized with approximately 80% of the αSyn fibrils in both PD and MSA tissues (**Figure 2J**). In contrast, αSyn fibrils were not observed in the SN in CNs, although FABP3 was detected in DA neurons (**Figure 2I**).

TABLE 2 | Demographic profiles of PD patients with skin biopsy tissues and the results of immunostaining for FABP3 accumulations and p-α Syn deposits.

Case		Sex	Age	Duration	MMSE	FABP3 accumulaions	p-aSyn deposits
1	PD	Female	56	8	29	–	+
2	PD	Male	77	3	27	–	+
3	PD	Male	70	4	26	–	+
4	PD	Female	67	2	27	–	++
5	PD	Female	74	20	27	–	+
6	PD	Male	72	3	23	–	+
7	PD	Male	62	10	30	–	++
8	PD	Male	65	8	29	–	++
'9	PD	Female	74	8	28	–	+
10	PD	Male	61	2	29	–	++

PD, Parkinson's disease; MMSE, Mini-Mental State Examination. Double-positive deposits in a 20× field according to the following scoring system; ++, more than 30 deposits in a field; +, 1–29 deposits in a field; and –, no deposit.

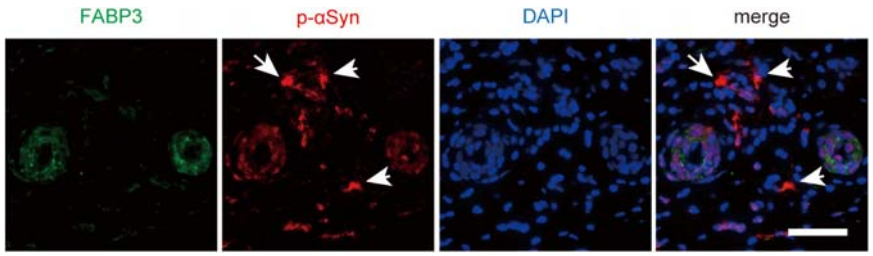


FIGURE 4 | No correlation between p-αSyn deposits and FABP3 accumulation in biopsied skin tissues of patients with PD. IF staining of p-αSyn (red) and FABP3 (green) in biopsied skin tissues of patients with PD. The nuclei were identified by DAPI (blue) staining. Weak FABP3 protein expression was observed in the cytoplasm of dermal sweat duct cells of patients with PD. On the other hand, p-αSyn deposits were observed in the dermal cells (arrows) of patients with PD. FABP3 accumulation was not observed in dermal p-αSyn deposits in PD tissues. Scale bars = 50 μm.

FABP3 Is Not Expressed in Senile Plaque-Related Amyloid β and Neurofibrillary Tangle (NFT)-Related Phosphorylated Tau (p-Tau) Aggregates in AD

Then, we examined whether senile plaque-related amyloid β or NFT-related p-tau aggregates are colocalized with FABP3 in AD. We did not observe FABP3 protein expression in amyloid β-positive senile plaques or p-tau-positive aggregates (**Figures 3A,B**). Nuclear staining with hematoxylin showed that p-tau-positive aggregates were NFTs (**Figure 3C**). FABP3 protein in neurons with p-tau-ir aggregates could not be detected in AD. In quantitative analysis, FABP3 accumulations were colocalized with 0% of the senile plaque-related amyloid β-ir aggregates and NFT-related p-tau-ir aggregates in the frontal cortex in AD. Thus, FABP3 accumulation is not associated with senile plaques or NFTs in AD.

FABP3-ir Accumulations Are Not Detectable in Biopsied Skin Tissues From Patients With PD

Finally, we examined whether αSyn deposits were colocalized with FABP3 in biopsied skin tissues from individuals with PD. We enrolled relatively early-stage PD patients with normal to mildly impaired cognition for skin biopsy (**Table 2**). However, dermal FABP3-ir accumulations were not observed in p-αSyn deposits in the samples of any of the patients with PD (**Figure 4** and **Table 2**).

DISCUSSION

Main Results of Our Study

The main results of the present study were that (1) a variety of neurons expressed the FABP3 protein in human brain tissues, (2) FABP3 was colocalized with αSyn aggregates in the brain tissues of patients with synucleinopathies but not with amyloid β or p-tau aggregates in the brain tissues of patients with AD, and (3) FABP3 was not present in p-αSyn deposits in biopsied skin tissues of patients with PD. These findings suggest that FABP3 is associated with αSyn aggregates in the brains of humans with synucleinopathies.

FABP3 Protein Expression in CNs and Patients With Synucleinopathies

We have previously reported that the FABP3 protein is specifically expressed in DA neurons in brain tissues of wild-type mice (Shioda et al., 2014). We have also previously reported neuron-specific expression of FABP3 mRNA in the rat brain (Owada et al., 1996). Immunohistochemical studies in monkey

brains have shown that cerebellar FABP3-positive cells are Purkinje cells and Bergmann glia (Boneva et al., 2010). Thus, FABP3 has been shown to be expressed in mouse, rat and monkey brain neurons. However, whether FABP3 is expressed in human brain tissues has remained unclear. Here, we histologically investigated FABP3 protein expression in autopsied human brain tissues and found that FABP3 was expressed in a variety of neurons, including DA neurons. These data suggest that FABP3 is commonly expressed in mammalian neurons.

We have previously suggested that the FABP3 protein plays crucial roles in αSyn aggregation in an MPTP-induced PD mouse model (Shioda et al., 2014). Long-term oral administration of the FABP3 ligand also significantly improves motor impairments, inhibits MPTP-induced αSyn aggregation, and prevents the loss of DA neurons in the SN (Matsuo et al., 2019). In the present study, we demonstrated, for the first time, that FABP3 colocalizes with αSyn aggregates in the contexts of PD and MSA. In this study, the number of co-localization of FABP3 with p-αSyn aggregates were more observed in MSA compared to PD. We speculated that this was because there was no significant difference in the ratio of FABP3 accumulations to p-αSyn aggregates between PD and MSA, but the number of p-αSyn aggregates were more observed in MSA compared to PD. On the other hand, FABP3 was not associated with amyloid β- and p-tau-positive aggregates in AD tissues. In summary, these results suggest that FABP3 is specifically associated with αSyn aggregates in individuals with synucleinopathies.

Blood FABP3 protein levels in PD were elevated but not in AD, and blood FABP3 protein levels is a potential diagnostic marker for PD (Mollenhauer et al., 2007b; Wada-Isoe et al., 2008b). On the other hand, cerebrospinal fluid FABP3 protein levels were elevated in AD (Guo et al., 2013; Chiasserini et al., 2017). It is reported that blood FABP3 levels were not elevated in AD, but FABP3 expression were observed in astrocyte structures in AD brain (Teunissen et al., 2011). Therefore, FABP3 expression in AD may be involved in the astroglia of the central nervous system. In this study, we analyzed the expression of FABP3 focusing on neurons. Pathological analysis relationship between FABP3 and astroglia should be performed in future studies, because we did not perform the analysis of FABP3 expression in astroglia.

αSyn aggregation is well recognized to contribute to the pathogenesis of synucleinopathies. Whereas only a small fraction of αSyn (<4%) is phosphorylated in healthy brains, distinct accumulation of αSyn phosphorylated at S129 (pS129) (>90%) is observed in LBs and GCIs (Oueslati, 2016). LBs and GCIs are composed of insoluble fibrillar protein aggregates and are responsible for cell death in synucleinopathies (Oueslati, 2016). Conversion of αSyn from a soluble monomer into oligomeric species and insoluble fibrils underlies the neurodegeneration associated with PD (Kalia et al., 2013). Previous reports have suggested that αSyn binds to FAs, particularly long-chain polyunsaturated fatty acids (Perrin et al., 2001; Sharon et al., 2001). Exposure to FAs enhances αSyn aggregation in cultured mesencephalic neuronal cells (Sharon et al., 2003; Liu et al., 2008). αSyn also binds to FABP3, and αSyn aggregates with FABP3 accumulation are detectable in damaged DA neurons in MPTP-induced PD model mice (Shioda et al., 2014). Therefore, αSyn aggregates and FABP3 may interact with each other and play a key role in the pathogeneses of synucleinopathies.

Recently, dermal αSyn deposits in biopsied skin tissue have been proposed to be useful biomarkers for the diagnosis of relatively early-stage PD (Ikemura et al., 2008; Donadio et al., 2014; Zange et al., 2015). Here, we histologically investigated FABP3 protein expression in biopsied skin tissues of patients with PD. However, FABP3 accumulation was not observed in p-αSyn deposits in these tissues. Generally, FABP3 is highly expressed in mature neurons in the central nervous system (Boneva et al., 2011). In the FABP family, myelin FABP (FABP8) is expressed in the peripheral nerves, and brain FABP (FABP7) and epidermal FABP (FABP5) are expressed mainly in glial cells and neurons of the immature brain (Boneva et al., 2011). Thus, p-αSyn deposits might colocalize with other FABPs (e.g., FABP5, FABP7 and FABP8) in PD skin. Further histological analyses of other FABPs (e.g., FABP5, FABP7 and FABP8) in PD skin should be performed in future studies.

CONCLUSION

In the present study, we demonstrated, for the first time, that FABP3 is associated with αSyn aggregates in autopsied brain tissues of patients with synucleinopathies but not with amyloid β or p-tau aggregates. These results provide new insights into the involvement of FABP3 in synucleinopathies.

DATA AVAILABILITY STATEMENT

The original contributions presented in the study are included in the article/supplementary material, further inquiries can be directed to the corresponding author/s.

ETHICS STATEMENT

The studies involving human participants were reviewed and approved by Sendai Nishitaga Hospital Local Human Ethical Committee. The patients/participants provided their written informed consent to participate in this study.

AUTHOR CONTRIBUTIONS

HO, KY, HS, TH, KF, and AT designed the study. HO, KY, HS, and YS performed the experiments. HO, KY, and HS analyzed the data. HO, KY, HS, TB, and AT wrote the manuscript. All authors contributed to the article and approved the submitted version.

FUNDING

The funding for this study was provided by Grants-in-Aid for Scientific Research from the Project of Translational and

Clinical Research Core Centers from the Japan Agency for Medical Research and Development (AMED) (grant numbers JP17dm0107071, and JP18dm0107071 to KF and AT) and the Ministry of Health, Labor and Welfare of Japan.

ACKNOWLEDGMENTS

We gratefully acknowledge Maki Takahashi, Shiryu Takemura, and Kikuko Hamanaka for technical support.

REFERENCES

Backstrom, D. C., Eriksson Domellof, M., Linder, J., Olsson, B., Ohrfelt, A., Trupp, M., et al. (2015). Cerebrospinal fluid patterns and the risk of future dementia in early, incident parkinson disease. *JAMA Neurol.* 72, 1175–1182. doi: 10.1001/jamaneurol.2015.1449

Boneva, N. B., Kaplamadzhiev, D. B., Sahara, S., Kikuchi, H., Pyko, I. V., Kikuchi, M., et al. (2011). Expression of fatty acid-binding proteins in adult hippocampal neurogenic niche of postischemic monkeys. *Hippocampus* 21, 162–171. doi: 10.1002/hipo.20732

Boneva, N. B., Mori, Y., Kaplamadzhiev, D. B., Kikuchi, H., Zhu, H., Kikuchi, M., et al. (2010). Differential expression of FABP 3, 5, 7 in infantile and adult monkey cerebellum. *Neurosci. Res.* 68, 94–102. doi: 10.1016/j.neures.2010.07.2028

Chartier-Harlin, M.-C., Kachergus, J., Roumier, C., Mouroux, V., Douay, X., Lincoln, S., et al. (2004). α-synuclein locus duplication as a cause of familial Parkinson's disease. *Lancet* 364, 1167–1169. doi: 10.1016/s0140-6736(04)17103-1

Chiasserini, D., Biscetti, L., Eusebi, P., Salvadori, N., Frattini, G., Simoni, S., et al. (2017). Differential role of CSF fatty acid binding protein 3, alpha-synuclein, and Alzheimer's disease core biomarkers in Lewy body disorders and Alzheimer's dementia. *Alzheimers Res. Ther.* 9:52. doi: 10.1186/s13195-017-0276-4

de Lau, L. M. L., and Breteler, M. M. B. (2006). Epidemiology of Parkinson's disease. *Lancet Neurol.* 5, 525–535. doi: 10.1016/s1474-4422(06)70471-9

Donadio, V., Incensi, A., Leta, V., Giannoccaro, M. P., Scaglione, C., Martinelli, P., et al. (2014). Skin nerve alpha-synuclein deposits: a biomarker for idiopathic Parkinson disease. *Neurology* 82, 1362–1369. doi: 10.1212/wnl.0000000000000316

Farrer, M., Kachergus, J., Forno, L., Lincoln, S., Wang, D. S., Hulihan, M., et al. (2004). Comparison of kindreds with parkinsonism and alpha-synuclein genomic multiplications. *Ann. Neurol.* 55, 174–179. doi: 10.1002/ana.10846

Furuhashi, M., and Hotamisligil, G. S. (2008). Fatty acid-binding proteins: role in metabolic diseases and potential as drug targets. *Nat. Rev. Drug Discov.* 7, 489–503. doi: 10.1038/nrd2589

Gibb, W. R., and Lees, A. J. (1988). The relevance of the Lewy body to the pathogenesis of idiopathic Parkinson's disease. *J. Neurol. Neurosurg. Psychiatry* 51, 745–752. doi: 10.1136/jnnp.51.6.745

Guo, L. H., Alexopoulos, P., and Perneczky, R. (2013). Heart-type fatty acid binding protein and vascular endothelial growth factor: cerebrospinal fluid biomarker candidates for Alzheimer's disease. *Eur. Arch. Psychiatr. Clin. Neurosci.* 263, 553–560. doi: 10.1007/s00406-013-0405-4

Homma, T., Mochizuki, Y., Komori, T., and Isozaki, E. (2016). Frequent globular neuronal cytoplasmic inclusions in the medial temporal region as a possible characteristic feature in multiple system atrophy with dementia. *Neuropathology* 36, 421–431. doi: 10.1111/neup.12289

Ikemura, M., Saito, Y., Sengoku, R., Sakiyama, Y., Hatsuta, H., Kanemaru, K., et al. (2008). Lewy body pathology involves cutaneous nerves. *J. Neuropathol. Exp. Neurol.* 67, 945–953. doi: 10.1097/NEN.0b013e318186de48

Kalia, L. V., Kalia, S. K., McLean, P. J., Lozano, A. M., and Lang, A. E. (2013). alpha-Synuclein oligomers and clinical implications for Parkinson disease. *Ann. Neurol.* 73, 155–169. doi: 10.1002/ana.23746

Kruger, R., Kuhn, W., Muller, T., Woitalla, D., Graeber, M., Kosel, S., et al. (1998). Ala30Pro mutation in the gene encoding alpha-synuclein in Parkinson's disease. *Nat. Genet.* 18, 106–108. doi: 10.1038/ng0298-106

Liu, X., Yamada, N., Maruyama, W., and Osawa, T. (2008). Formation of dopamine adducts derived from brain polyunsaturated fatty acids: mechanism for Parkinson disease. *J. Biol. Chem.* 283, 34887–34895. doi: 10.1074/jbc.M805682200

Matsuo, K., Cheng, A., Yabuki, Y., Takahata, I., Miyachi, H., and Fukunaga, K. (2019). Inhibition of MPTP-induced alpha-synuclein oligomerization by fatty acid-binding protein 3 ligand in MPTP-treated mice. *Neuropharmacology* 150, 164–174. doi: 10.1016/j.neuropharm.2019.03.029

McCann, H., Stevens, C. H., Cartwright, H., and Halliday, G. M. (2014). α-Synucleinopathy phenotypes. *Park. Relat. Disord.* 20, S62–S67. doi: 10.1016/s1353-8020(13)70017-8

Mollenhauer, B., Steinacker, P., Bahn, E., Bibl, M., Brechlin, P., Schlossmacher, M. G., et al. (2007a). Serum heart-type fatty acid-binding protein and cerebrospinal fluid tau: marker candidates for dementia with Lewy bodies. *Neurodegener. Dis.* 4, 366–375.

Mollenhauer, B., Steinacker, P., Bahn, E., Bibl, M., Brechlin, P., Schlossmacher, M. G., et al. (2007b). Serum heart-type fatty acid-binding protein and cerebrospinal fluid tau: marker candidates for dementia with Lewy bodies. *Neurodegener. Dis.* 4, 366–375. doi: 10.1159/000105157

Oueslati, A. (2016). Implication of alpha-synuclein phosphorylation at S129 in synucleinopathies: what have we learned in the last decade? *J. Parkinsons Dis.* 6, 39–51. doi: 10.3233/JPD-160779

Owada, Y., Yoshimoto, T., and Kondo, H. (1996). Spatio-temporally differential expression of genes for three members of fatty acid binding proteins in developing and mature rat brains. *J. Chem. Neuroanat.* 12, 113–122. doi: 10.1016/S0891-0618(96)00192-5

Paisan-Ruiz, C., Bhatia, K. P., Li, A., Hernandez, D., Davis, M., Wood, N. W., et al. (2009). Characterization of PLA2G6 as a locus for dystonia-parkinsonism. *Ann. Neurol.* 65, 19–23. doi: 10.1002/ana.21415

Perrin, R. J., Woods, W. S., Clayton, D. F., and George, J. M. (2001). Exposure to long chain polyunsaturated fatty acids triggers rapid multimerization of synucleins. *J. Biol. Chem.* 276, 41958–41962. doi: 10.1074/jbc.M105022200

Polymeropoulos, M. H., Lavedan, C., Leroy, E., Ide, S. E., Dehejia, A., Dutra, A., et al. (1997). Mutation in the alpha-synuclein gene identified in families with Parkinson's disease. *Science* 276, 2045–2047. doi: 10.1126/science.276.5321.2045

Schulz-Schaeffer, W. J. (2010). The synaptic pathology of alpha-synuclein aggregation in dementia with Lewy bodies. Parkinson's disease and Parkinson's disease dementia. *Acta Neuropathol.* 120, 131–143. doi: 10.1007/s00401-010-0711-0

Sengoku, R., Saito, Y., Ikemura, M., Hatsuta, H., Sakiyama, Y., Kanemaru, K., et al. (2008). Incidence and extent of Lewy body-related alpha-synucleinopathy in aging human olfactory bulb. *J. Neuropathol. Exp. Neurol.* 67, 1072–1083. doi: 10.1097/NEN.0b013e31818b4126

Sharon, R., Bar-Joseph, I., Mirick, G. E., Serhan, C. N., and Selkoe, D. J. (2003). Altered fatty acid composition of dopaminergic neurons expressing alpha-synuclein and human brains with alpha-synucleinopathies. *J. Biol. Chem.* 278, 49874–49881. doi: 10.1074/jbc.M309127200

Sharon, R., Goldberg, M. S., Bar-Josef, I., Betensky, R. A., Shen, J., and Selkoe, D. J. (2001). alpha-Synuclein occurs in lipid-rich high molecular weight complexes, binds fatty acids, and shows homology to the fatty acid-binding proteins. *Proc. Natl. Acad. Sci. U. S. A.* 98, 9110–9115. doi: 10.1073/pnas.171300598

Shioda, N., Yabuki, Y., Kobayashi, Y., Onozato, M., Owada, Y., and Fukunaga, K. (2014). FABP3 protein promotes alpha-synuclein oligomerization associated with 1-methyl-1,2,3,6-tetrahydropiridine-induced neurotoxicity. *J. Biol. Chem.* 289, 18957–18965. doi: 10.1074/jbc.M113.527341

Singleton, A. B., Farrer, M., Johnson, J., Singleton, A., Hague, S., Kachergus, J., et al. (2003). alpha-Synuclein locus triplication causes Parkinson's disease. *Science* 302:841. doi: 10.1126/science.1090278

Spillantini, M. G., Crowther, R. A., Jakes, R., Hasegawa, M., and Goedert, M. (1998). alpha-Synuclein in filamentous inclusions of Lewy bodies from Parkinson's disease and dementia with lewy bodies. *Proc. Natl. Acad. Sci. U. S. A.* 95, 6469–6473. doi: 10.1073/pnas.95.11.6469

Sumi-Akamaru, H., Beck, G., Shinzawa, K., Kato, S., Riku, Y., Yoshida, M., et al. (2016). High expression of alpha-synuclein in damaged mitochondria with

PLA2G6 dysfunction. *Acta Neuropathol. Commun.* 4:27. doi: 10.1186/s40478-016-0298-3

Teunissen, C. E., Veerhuis, R., De Vente, J., Verhey, F. R., Vreeling, F., van Boxtel, M. P., et al. (2011). Brain-specific fatty acid-binding protein is elevated in serum of patients with dementia-related diseases. *Eur. J. Neurol.* 18, 865–871. doi: 10.1111/j.1468-1331.2010.03273.x

Tomiyama, H., Yoshino, H., Ogaki, K., Li, L., Yamashita, C., Li, Y., et al. (2011). PLA2G6 variant in Parkinson's disease. *J. Hum. Genet.* 56, 401–403. doi: 10.1038/jhg.2011.22

Wada-Isoe, K., Imamura, K., Kitamaya, M., Kowa, H., and Nakashima, K. (2008a). Serum heart-fatty acid binding protein levels in patients with Lewy body disease. *J. Neurol. Sci.* 266, 20–24.

Wada-Isoe, K., Imamura, K., Kitamaya, M., Kowa, H., and Nakashima, K. (2008b). Serum heart-fatty acid binding protein levels in patients with Lewy body disease. *J. Neurol. Sci.* 266, 20–24. doi: 10.1016/j.jns.2007.08.018

Wakabayashi, K., and Takahashi, H. (2006). Cellular pathology in multiple system atrophy. *Neuropathology* 26, 338–345. doi: 10.1111/j.1440-1789.2006.00713.x

Wakabayashi, K., Yoshimoto, M., Tsuji, S., and Takahashi, H. (1998). Alpha-synuclein immunoreactivity in glial cytoplasmic inclusions in multiple system atrophy. *Neurosci. Lett.* 249, 180–182. doi: 10.1016/s0304-3940(98)00407-8

Xicoy, H., Wieringa, B., and Martens, G. J. M. (2019). The Role of Lipids in Parkinson's Disease. *Cells* 8:8010027. doi: 10.3390/cells8010027

Yabe, I., Soma, H., Takei, A., Fujiki, N., Yanagihara, T., and Sasaki, H. (2006). MSA-C is the predominant clinical phenotype of MSA in Japan: analysis of 142 patients with probable MSA. *J. Neurol. Sci.* 249, 115–121. doi: 10.1016/j.jns.2006.05.064

Yoshino, H., Tomiyama, H., Tachibana, N., Ogaki, K., Li, Y., Funayama, M., et al. (2010). Phenotypic spectrum of patients with PLA2G6 mutation and PARK14-linked parkinsonism. *Neurology* 75, 1356–1361. doi: 10.1212/WNL.0b013e3181f73649

Zange, L., Noack, C., Hahn, K., Stenzel, W., and Lipp, A. (2015). Phosphorylated alpha-synuclein in skin nerve fibres differentiates Parkinson's disease from multiple system atrophy. *Brain* 138, 2310–2321. doi: 10.1093/brain/awv138

Zarranz, J. J., Alegre, J., Gomez-Esteban, J. C., Lezcano, E., Ros, R., Ampuero, I., et al. (2004). The new mutation, E46K, of alpha-synuclein causes Parkinson and Lewy body dementia. *Ann. Neurol.* 55, 164–173. doi: 10.1002/ana.10795

Conflict of Interest: The authors declare that the research was conducted in the absence of any commercial or financial relationships that could be construed as a potential conflict of interest.

Copyright © 2021 Oizumi, Yamasaki, Suzuki, Hasegawa, Sugimura, Baba, Fukunaga and Takeda. This is an open-access article distributed under the terms of the Creative Commons Attribution License (CC BY). The use, distribution or reproduction in other forums is permitted, provided the original author(s) and the copyright owner(s) are credited and that the original publication in this journal is cited, in accordance with accepted academic practice. No use, distribution or reproduction is permitted which does not comply with these terms.

frontiers in Aging Neuroscience

ORIGINAL RESEARCH
published: 20 April 2021
doi: 10.3389/fnagi.2021.648531

Co-registration Analysis of Fluorodopa and Fluorodeoxyglucose Positron Emission Tomography for Differentiating Multiple System Atrophy Parkinsonism Type From Parkinson's Disease

Wen-biao Xian[1,2†], *Xin-chong Shi*[3†], *Gan-hua Luo*[3], *Chang Yi*[3], *Xiang-song Zhang*[3*] and *Zhong Pei*[1,2*]

[1] Department of Neurology, The First Affiliated Hospital, Sun Yat-sen University, Guangzhou, China, [2] Guangdong Provincial Key Laboratory of Diagnosis and Treatment of Major Neurological Diseases, National Key Clinical Department and Key Discipline of Neurology, Guangzhou, China, [3] Department of Nuclear Medicine, The First Affiliated Hospital, Sun Yat-sen University, Guangzhou, China

OPEN ACCESS

Edited by:
Pingyi Xu,
First Affiliated Hospital of Guangzhou Medical University, China

Reviewed by:
Shaogang Qu,
Southern Medical University, China
Yun-Cheng Wu,
Shanghai Jiao Tong University School of Medicine, China

***Correspondence:**
Zhong Pei
peizhong@mail.sysu.edu.cn
Xiang-song Zhang
zhxiangs@mail.sysu.edu.cn

[†]These authors have contributed equally to this work

Received: 31 December 2020
Accepted: 22 February 2021
Published: 20 April 2021

Citation:
Xian W-b, Shi X-c, Luo G-h, Yi C, Zhang X-s and Pei Z (2021) Co-registration Analysis of Fluorodopa and Fluorodeoxyglucose Positron Emission Tomography for Differentiating Multiple System Atrophy Parkinsonism Type From Parkinson's Disease. Front. Aging Neurosci. 13:648531. doi: 10.3389/fnagi.2021.648531

It is difficult to differentiate between Parkinson's disease and multiple system atrophy parkinsonian subtype (MSA-P) because of the overlap of their signs and symptoms. Enormous efforts have been made to develop positron emission tomography (PET) imaging to differentiate these diseases. This study aimed to investigate the co-registration analysis of ^{18}F-fluorodopa and ^{18}F-flurodeoxyglucose PET images to visualize the difference between Parkinson's disease and MSA-P. We enrolled 29 Parkinson's disease patients, 28 MSA-P patients, and 10 healthy controls, who underwent both ^{18}F-fluorodopa and ^{18}F-flurodeoxyglucose PET scans. Patients with Parkinson's disease and MSA-P exhibited reduced bilateral striatal ^{18}F-fluorodopa uptake ($p < 0.05$, vs. healthy controls). Both regional specific uptake ratio analysis and statistical parametric mapping analysis of ^{18}F-flurodeoxyglucose PET revealed hypometabolism in the bilateral putamen of MSA-P patients and hypermetabolism in the bilateral putamen of Parkinson's disease patients. There was a significant positive correlation between ^{18}F-flurodeoxyglucose uptake and ^{18}F-fluorodopa uptake in the contralateral posterior putamen of MSA-P patients ($rs = 0.558$, $p = 0.002$). Both ^{18}F-flurodeoxyglucose and ^{18}F-fluorodopa PET images showed that the striatum was rabbit-shaped in the healthy control group segmentation analysis. A defective rabbit-shaped striatum was observed in the ^{18}F-fluorodopa PET image of patients with Parkinson's disease and MSA-P. In the segmentation analysis of ^{18}F-flurodeoxyglucose PET image, an intact rabbit-shaped striatum was observed in Parkinson's disease patients, whereas a defective rabbit-shaped striatum was observed in MSA-P patients. These findings suggest that there were significant differences in the co-registration analysis of ^{18}F-flurodeoxyglucose and ^{18}F-fluorodopa PET images, which could be used in the individual analysis to differentiate Parkinson's disease from MSA-P.

Keywords: Parkinson's disease, mutiple system atrophy, PET, FDG, F-DOPA

INTRODUCTION

The diagnosis of Parkinson's disease (PD) is mainly based on the typical clinical presentation of cardinal signs and its being well-responsive to levodopa treatment (Armstrong and Okun, 2020); however, misdiagnosis of PD is not uncommon. The most common misdiagnoses are related to parkinsonism-plus syndromes, such as multiple system atrophy (MSA), which could be classified as the parkinsonian subtype (MSA-P) with predominant parkinsonism, and the cerebellar subtype (MSA-C) with predominant cerebellar features (Koga and Dickson, 2018). Asymmetry of the cardinal features of parkinsonism and good response to levodopa, which are characteristic manifestations associated with PD, could also be seen in some patients with MSA-P (Jost et al., 2019), which makes it difficult to make the differential diagnosis on the basis of clinical criteria alone. In clinical pathological studies, only 76% of postmortem-confirmed cases were diagnosed correctly as PD (Rajput et al., 1991), while 55% of postmortem-confirmed MSA cases were misdiagnosed (Litvan et al., 1997).

Many objective methods have been tested for the differential diagnosis between PD and MSA-P, such as serum neuronal exosomes (Jiang et al., 2020), proteins in cerebrospinal fluid (Singer et al., 2020), and neuroimaging (Saeed et al., 2020). Multiple imaging modalities such as magnetic resonance imaging (MRI) and positron emission tomography (PET) have been increasingly used to investigate the morphologic and functional characteristics of MSA, PD, and other atypical parkinsonisms (Zhao et al., 2020). The second consensus statement on the diagnosis of MSA (Gilman et al., 2008) and the recent Movement Disorders Society clinical diagnostic criteria for PD (Postuma et al., 2015) have included the results of a few of these neuroimaging techniques to serve as supportive criteria or exclusion criteria for the diagnosis of diseases. Thus, cerebral MRI and PET may aid in an early, accurate, and objective diagnostic classification by highlighting the underlying neurochemical and neuroanatomical changes that underlie the spectrum of disorders.

The differential diagnosis can be assisted by the characteristic features of MSA revealed by MRI, such as putaminal hyperintensive rim and "hot cross bun" sign of the pons (Hughes et al., 2002; Poewe and Wenning, 2002). However, putaminal hyperintensive rim occurs in only 31.8% of MSA-P patients and is also present in 6.7% of PD patients (Zhao et al., 2020). The "hot cross bun" sign exhibits the highest specificity in MSA-C patients but is not found in MSA-P patients (Zhao et al., 2020). In PET studies, ^{18}F-fluorodopa (^{18}F-Dopa) can only differentiate healthy subjects from parkinsonism patients, but it is inadequate for differentiating between MSA-P and PD because nigrostriatal dopaminergic neurons degenerate in these disorders (Burn et al., 1994). Imaging disease-specific patterns of regional glucose metabolism with ^{18}F-flurodeoxyglucose (^{18}F-FDG) PET allow for a highly accurate distinction between PD and MSA, such as PD-related pattern (Matthews et al., 2018) and MSA-related pattern (Akdemir et al., 2014). Due to the low spatial resolution of FDG PET images, visual analysis is difficult to detect significant anomalies; hence, these disease-specific patterns are calculated by voxel-based statistical analysis in comparison with healthy control subjects with statistical parametric mapping (SPM) software (Ko et al., 2017). SPM is useful in the group analysis of FDG PET images but is hampered in individual diagnosis. Single-patient SPM analysis could be also used, but this statistical method is controversial because only one patient is included in one group of the data. Single SPM analysis only derives a calculated image, which may differ from the actual brain structure of the patient; thus, the result could be affected by the selection of a normal control group. Variations in PET scanners and image reconstruction algorithms have been shown to systematically shift image quality in SPM analysis (Kogan et al., 2019).

We hypothesize that there are disease-specific patterns related to PD and MSA-P in both ^{18}F-Dopa and ^{18}F-FDG PET, and the two kinds of imaging modalities have their own advantages and disadvantages. In the present study, we used the co-registration analysis of ^{18}F-Dopa and ^{18}F-FDG PET to visualize the characteristics of the images without any calculation or image distortion, which could be easily used in the individual differential diagnosis between PD and MSA-P.

MATERIALS AND METHODS

Subjects and Clinical Assessments

Twenty-nine consecutive PD patients (mean age 57.0 ± 10.0 years), 28 MSA-P patients (mean age 60.6 ± 5.9 years), and 10 healthy controls (HCs, mean age 59.0 ± 8.2 years) were enrolled in this study. The PD patients were diagnosed according to Movement Disorders Society clinical diagnostic criteria for PD (Postuma et al., 2015), and MSA patients were diagnosed according to the second consensus statement on the diagnosis of MSA (Gilman et al., 2008). The patients were at a relatively early stage of disease: disease duration of MSA-P patients was within 5 years; Hoehn and Yahr stage (H&Y) of PD patients ranged from stage 1 to stage 3. Age-matched HCs without neurological disorders were also enrolled. The exclusion criteria for all participants were as follows: Patients with drug-induced parkinsonism, vascular parkinsonism, progressive supranuclear paralysis, corticobasal degeneration, and dementia with Lewy bodies; prior brain surgery, including deep brain stimulation; and other neurologic diseases, including head trauma, stroke, and brain tumor. Written informed consent was obtained from all participants in accordance with the Declaration of Helsinki, and the study was approved by the local Ethical Committee of the First Affiliated Hospital of Sun Yat-sen University.

Disease severity of the patients was measured with H&Y stage. Functional independence was measured using the Schwab and England Activities of Daily Living Scale (SEADL). Mini-Mental State Examination score and disease duration were also recorded. Patients in the PD group consisted of 16 males and 13 females, with a disease duration of 4.1 ± 1.7 years, H&Y stage 2.0 ± 0.6, Mini-Mental State Examination score of 28.6 ± 6.2, and SEADL score of 79.7 ± 6.7. Patients in the MSA-P group consisted of 16 males and 12 females, with a disease duration of 3.3 ± 1.0 years, H&Y stage 3.3 ± 0.7, Mini-Mental State Examination score of 26.6 ± 1.1, and SEADL score of 72.0 ± 3.8. There was no

significant difference between the PD and the MSA-P groups, except a more severe H&Y stage and a reduced SEADL score in the MSA-P group ($p < 0.05$).

PET Imaging

All participants underwent both cerebral ^{18}F-FDG and ^{18}F-Dopa PET examination using a Gemini GXL 16 PET/CT scanner (Philips, Amsterdam, the Netherlands) using the three-dimensional (3D) acquisition mode, with dopamine receptor agonists withdrawn for at least 72 h and levodopa withdrawn for at least 12 h. Participants were fasted for at least 8 h before ^{18}F-FDG PET imaging. Subjects lay comfortably in a supine position in a room with dimmed lighting and low background noise, to minimize any sympathetic response. A low-dose computerized tomography (CT, 120 KV, 250 mA) about 45 min after intravenous injection of ^{18}F-FDG (185 MBq) PET was performed immediately after CT for about 10 min. Transversal PET slices were reconstructed by means of CT-based attenuation correction using an iterative algorithm. ^{18}F-Dopa PET was performed on another day and the subjects fasted for at least 4 h. They were given oral entacapone (200 mg) 1 h prior to the injection of 370–444 MBq of ^{18}F-Dopa (Ruottinen et al., 1995). Each participant had a quiet rest lasting 90 min before a 10-min PET emission acquisition. PET images were reconstructed with low-dose CT images for attenuation correction.

Image Analysis

All the PET image data were processed and analyzed using the software MIPAV (version 7.0.1, US Department of Health and Human Services). The striatal regions of interest (ROIs) of PET images were defined using a technique developed at our institution (Shi et al., 2019). To accurately analyze the imaging profile characteristics of the subjects, we divided the striatum into anterior/posterior putamen (APu/PPu) and caudate nucleus in both ^{18}F-FDG and ^{18}F-Dopa PET image data. Specific uptake ratio (SUR) was calculated to evaluate the radioisotopic activity in the selected ROIs. The occipital cortex was regarded as the reference region in the ^{18}F-Dopa PET image and the average value of the whole brain was regarded as the reference region in ^{18}F-FDG PET image for calculating SUR by (target uptake—reference uptake)/reference uptake. In patients with PD and MSA-P, the contralateral ROIs were considered to be the opposite brain regions in relation to the predominantly affected limbs. The SUR was calculated by two expert radiologists (XS and XZ) who were blinded to participants' clinical data and co-registration analysis.

Image Co-registration Processing

The co-registration of three-dimensional PET and CT images was analyzed using software 3D Slicer (version 4.10.0, www.slicer.org). The 3D Slicer is a multiplatform developed to perform an interactive semiautomatic segmentation and image registration that allows the quantitation of features of interest from medical imaging including MRI, CT, and nuclear medicine. The first step was to make the co-registration of two CT images with a higher image resolution than PET, using a landmark registration algorithm of the software (**Figure 1A**). The second step was to use the "transforms" tool to make automatic registration of the ^{18}F-FDG and ^{18}F-Dopa PET images (**Figure 1B**). Segmentation of striatal ROIs was accomplished by

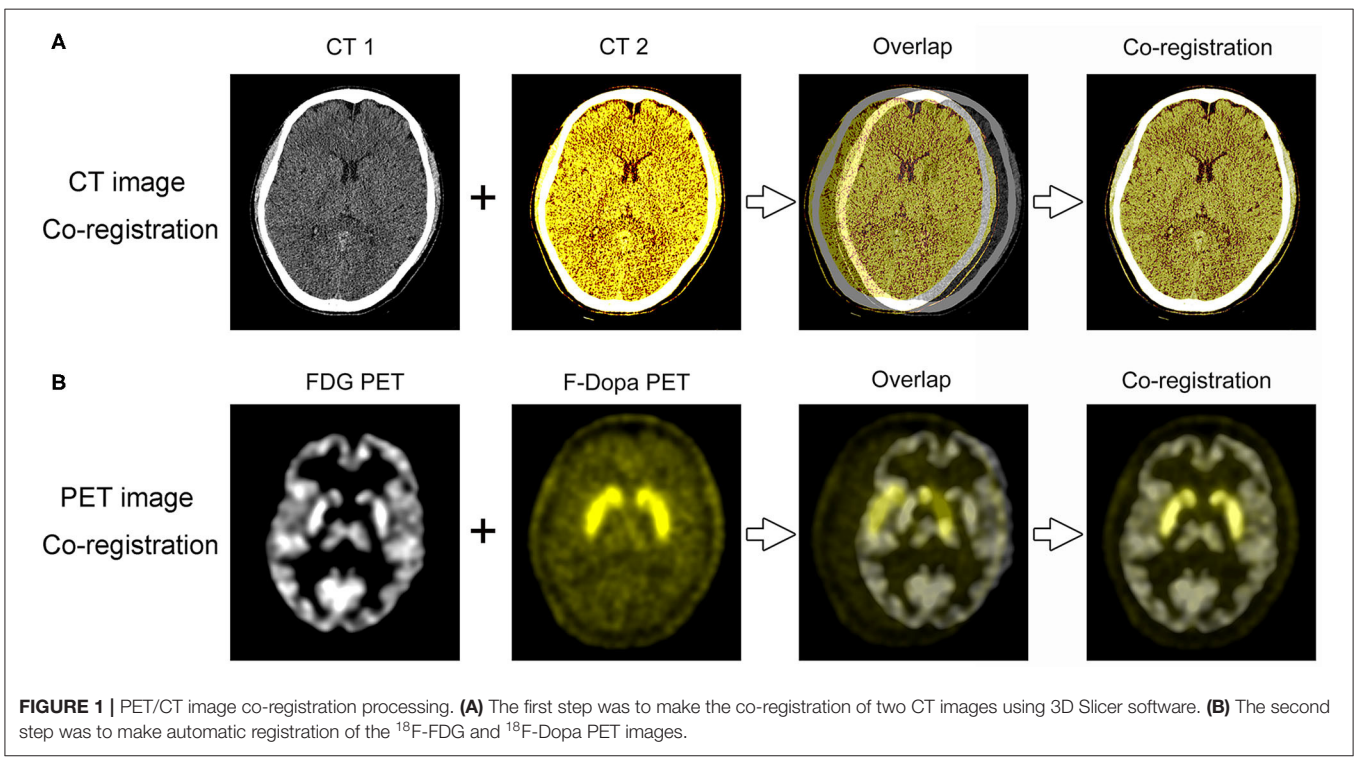


FIGURE 1 | PET/CT image co-registration processing. **(A)** The first step was to make the co-registration of two CT images using 3D Slicer software. **(B)** The second step was to make automatic registration of the ^{18}F-FDG and ^{18}F-Dopa PET images.

two methods: (1) Automatic brain structure segmentation. (2) Manual segmentation: an incorporated voxel made by automatic segmentation required a manual revision of the pixels, slice by slice, selected for a more precise segmentation. Segmentation of striatal ROIs in ^{18}F-FDG and ^{18}F-Dopa PET images was labeled with different colors to present the images more hierarchically. Finally, a 3D model was developed using the Model Maker to visualize the morphological structure of striatal ROIs. When the two models from ^{18}F-FDG and ^{18}F-Dopa PET overlapped in the co-registration analysis, the opacity of one model was reduced to 50% to visualize the 3D image more clearly. The co-registration processing was performed by two investigators (GL and CY) who were blinded to participants' clinical data and SUR analysis.

SPM Analysis

SPM analysis was performed using SPM5 (Wellcome Department of Cognitive Neurology, Institute of Neurology, University College London). To detect any regional metabolic pattern by SPM, all the images were analyzed using the appropriate voxel-by-voxel unvaried statistical tests of group comparisons (two-sample *t*-test, $p < 0.05$) within the two groups (PD vs. HC, MSA-P vs. HC). The results were displayed on the three orthogonal planes of an MRI.

Statistical Analysis

All analyses were conducted using SPSS 19.0 software (Version 19.0., IBM Corp., Armonk, NY, United States). Continuous data were given as mean ± standard deviation (SD); categorical data were given as frequencies or percentages. A Kruskal–Wallis test was applied to compare the mean differences between PD, MSA-P, and HC groups. The significant correlations between the SUR values in striatal ROIs of ^{18}F-FDG and ^{18}F-Dopa were evaluated using a Spearman's test. The statistical significance was set at $p < 0.05$.

RESULTS

Regional PET Analyses

In comparison with the HC group, significant reduction of ^{18}F-Dopa uptake was observed in the bilateral putamen and caudate nucleus in patients in both PD and MSA-P groups (**Table 1**). The reduction of ^{18}F-Dopa uptake in the putamen was more serious in the posterior than the anterior area, but there was no significant difference in the PPu/APu ratio of SUR values between PD and MSA-P groups. Significant differences in ^{18}F-FDG uptake were observed between PD, MSA-P, and HC groups. In comparison with the HC group, there was a significant increase in ^{18}F-Dopa uptake in the bilateral caudate nucleus and putamen of patients in the PD group. On the contrary, the ^{18}F-FDG uptake was significantly reduced in the bilateral putamen of patients in the MSA-P group when compared with the HC group. *Post-hoc* Bonferroni tests showed that the reduction of ^{18}F-FDG uptake in the putamen was more serious in the posterior than the anterior area in MSA-P patients compared to the PD and HC groups. The Spearman correlation analysis demonstrated a significant positive correlation of ^{18}F-FDG uptake with ^{18}F-Dopa uptake in the contralateral posterior putamen in MSA-P patients ($rs = 0.558$, $p = 0.002$). There was no significant correlation of tracer uptake between ^{18}F-FDG and ^{18}F-Dopa in other parts of the brain.

TABLE 1 | Specific uptake ratios of PET image of all participants.

Region	PD	MSA-P	HC	*p*
^{18}F-Dopa PET				
Contralateral Ca	2.25 ± 0.54^{c}	2.31 ± 0.36^{c}	3.00 ± 0.41^{ab}	<0.001
Ipsilateral Ca	2.34 ± 0.61^{c}	2.35 ± 0.40^{c}	3.00 ± 0.45^{ab}	0.003
Contralateral APu	2.27 ± 0.58^{c}	2.26 ± 0.36^{c}	3.83 ± 0.51^{ab}	<0.001
Ipsilateral APu	2.37 ± 0.58^{c}	2.37 ± 0.47^{c}	3.67 ± 0.58^{ab}	<0.001
Contralateral PPu	1.80 ± 0.32^{c}	1.74 ± 0.31^{c}	3.77 ± 0.62^{ab}	<0.001
Ipsilateral PPu	1.88 ± 0.36^{c}	1.92 ± 0.40^{c}	3.68 ± 0.61^{ab}	<0.001
Contralateral PPu/APu	0.81 ± 0.12^{c}	0.77 ± 0.10^{c}	0.96 ± 0.05^{ab}	<0.001
Ipsilateral PPu/APu	0.81 ± 0.09^{c}	0.79 ± 0.11^{c}	0.98 ± 0.10^{ab}	<0.001
^{18}F-FDG PET				
Contralateral Ca	2.12 ± 0.18^{c}	2.09 ± 0.22^{c}	1.89 ± 0.15^{ab}	0.007
Ipsilateral Ca	2.10 ± 0.20^{c}	2.15 ± 0.18^{c}	1.84 ± 0.18^{ab}	0.001
Contralateral APu	2.74 ± 0.30^{bc}	2.24 ± 0.22^{a}	2.36 ± 0.22^{a}	<0.001
Ipsilateral APu	2.72 ± 0.31^{bc}	2.42 ± 0.21^{a}	2.37 ± 0.15^{a}	<0.001
Contralateral PPu	2.86 ± 0.32^{bc}	1.71 ± 0.24^{ac}	2.28 ± 0.13^{ab}	<0.001
Ipsilateral PPu	2.91 ± 0.36^{bc}	2.00 ± 0.32^{ac}	2.37 ± 0.20^{ab}	<0.001
Contralateral PPu/APu	1.05 ± 0.06^{b}	0.76 ± 0.07^{ac}	0.97 ± 0.05^{b}	<0.001
Ipsilateral PPu/APu	1.07 ± 0.06^{b}	0.83 ± 0.12^{ac}	1.00 ± 0.05^{b}	<0.001

PD, Parkinson's disease; MSA-P, multiple system atrophy parkinsonian subtype; HC, healthy control; FDG, flurodeoxyglucose; Pu, putamen; Ca, caudate nucleus; Apu, anterior putamen; PPu, posterior putamen.
$p < 0.01$ compared to [a]PD, [b]MSA-P, and [c]HC.

PET Image Segmentation Analysis

The graphic comparison of the segmentations of striatal PET images between PD, MSA-P, and HC groups is shown in **Figures 2**, **3**. In the HC group, both ^{18}F-FDG and ^{18}F-Dopa PET images showed that the striatum had a full rabbit-shaped appearance in the segmentation analysis. In ^{18}F-Dopa PET image, the normal appearance of the striatum of patients in the PD and MSA-P groups was not completely displayed, and there were mainly graphic defects in the posterior part of the putamen. In ^{18}F-FDG PET image, the rabbit-shaped appearance of the striatum segment in PD patients was not impaired, whereas in MSA-P patients, there were significant defects of bilateral striatum segments in the posterior putamen. Co-registration image analysis showed that the segments of the striatum in ^{18}F-FDG and ^{18}F-Dopa PET of PD patients were mismatched, with intact striatal segments in ^{18}F-FDG PET but damaged striatal segments in ^{18}F-Dopa PET. The segments of the striatum in MSA-P and HC groups were matched in ^{18}F-FDG and ^{18}F-Dopa PET images. The striatal segments were defective in MSA-P patients but intact in the HC group. A significant difference was observed in the frequency of rabbit-shaped striatal segments in the segmentation analysis between PD, MSA-P, and HC groups (**Table 2**).

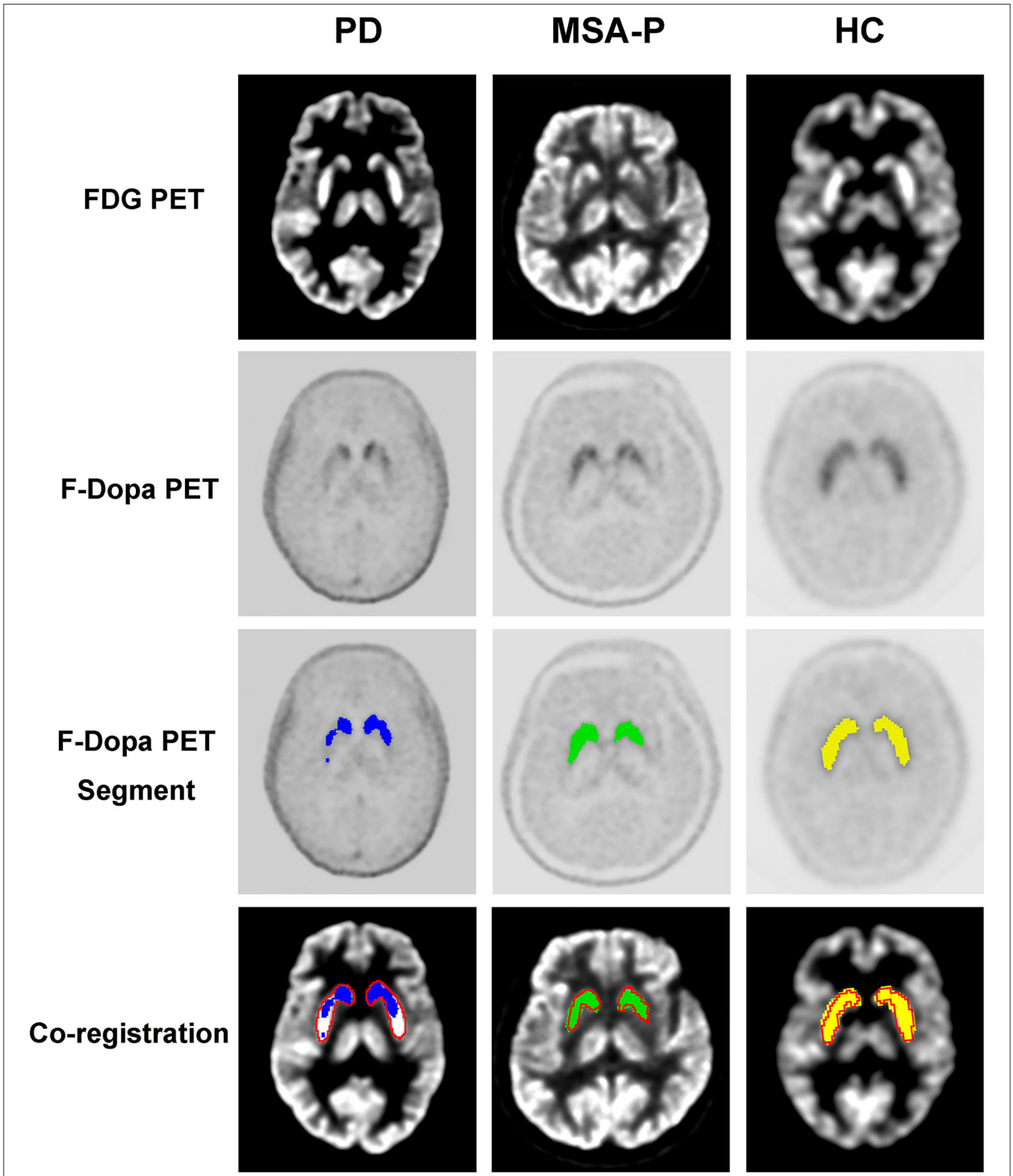


FIGURE 2 | Segmentation of striatal PET images of participants. The striatal segments of ^{18}F-Dopa PET (PD: blue color; MSA-P: green color; HC: yellow color) and ^{18}F-FDG PET (red color) images were labeled with different colors. Co-registration analysis showed that the segments of striatum in ^{18}F-FDG and ^{18}F-Dopa PET of PD patients were mismatched, with intact striatal segments in ^{18}F-FDG PET and damaged striatal segments in^{18}F-Dopa PET. The segments of striatum in MSA-P and HC groups were matched in ^{18}F-FDG and ^{18}F-Dopa PET images. The striatal segments were defective in MSA-P patients, whereas intact in the HC group.

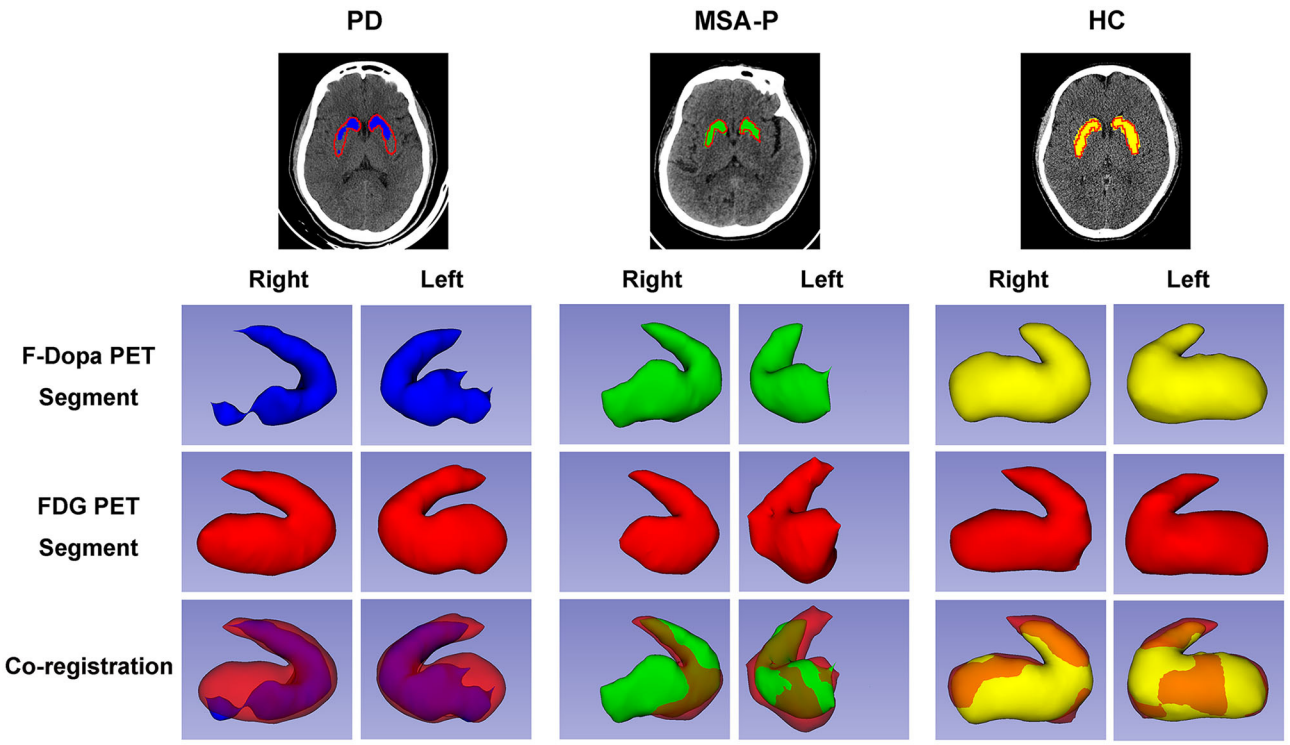


FIGURE 3 | Three-dimensional visualization of striatal PET images of participants. The striatal segments of ^{18}F-Dopa PET (PD: blue color; MSA-P: green color; HC: yellow color) and ^{18}F-FDG PET (red color) images were labeled with different colors. Both ^{18}F-FDG and ^{18}F-Dopa PET images showed that the striatum had a rabbit-shaped appearance in the HC group. A defective rabbit-shaped striatum was shown in the ^{18}F-Dopa PET image of patients with PD and MSA-P. In the ^{18}F-FDG PET image, an intact rabbit-shaped striatum was shown in PD patients, whereas a defective rabbit-shaped striatum was shown in MSA-P patients.

TABLE 2 | PET image segmentation analysis of all participants.

Striatal segment	PD (n = 29)		MSA-P (n = 28)		HC (n = 10)	
	^{18}F-FDG	^{18}F-Dopa	^{18}F-FDG	^{18}F-Dopa	^{18}F-FDG	^{18}F-Dopa
Intact rabbit-shaped	29	0	0	0	10	10
Defective rabbit-shaped	0	29	28	28	0	0

PD, Parkinson's disease; MSA-P, multiple system atrophy parkinsonian subtype; HC, healthy control; FDG, flurodeoxyglucose.

SPM Analysis of ^{18}F-FDG PET

In the MSA-P group, a significant glucose hypometabolism in the bilateral putamen was detected as compared with the HC group by statistical voxel-based analysis (**Figure 4A**). In comparison with the HC group, the PD patients were found to have a significant glucose hypermetabolism in the bilateral putamen, cerebellum, and occipital lobes, along with hypometabolism in the frontal, parietal, postcentral cortices, and cingulate areas (**Figure 4B**).

DISCUSSION

This study is the first to demonstrate the diagnostic value of co-registration analysis of ^{18}F-FDG and ^{18}F-Dopa PET for differentiating MSA-P from PD. Segmentation analysis of the rabbit-shaped appearance of the striatum segment of PET images not only could distinguish PD and MSA-P patients from healthy controls but also further differentiated PD from MSA-P. The segmentation analysis has also been verified by the traditional regional PET uptake value analysis and the latest SPM analysis used for identifying disease-specific metabolic patterns.

The segmentation analysis showed a full rabbit-shaped appearance of the striatal segment of PET images in both ^{18}F-Dopa and ^{18}F-FDG PET in the HC group, indicating intact integrity of the brain dopamine system and preserved function of the basal ganglia-related pathway. In patients with PD, a defective striatal segment was shown in ^{18}F-Dopa PET due to the degeneration of nigrostriatal dopaminergic neurons. However, the rabbit-shaped appearance of the striatal segment was intact in the ^{18}F-Dopa PET image, indicating that the postsynaptic function of the dopaminergic neurons and related pathways were

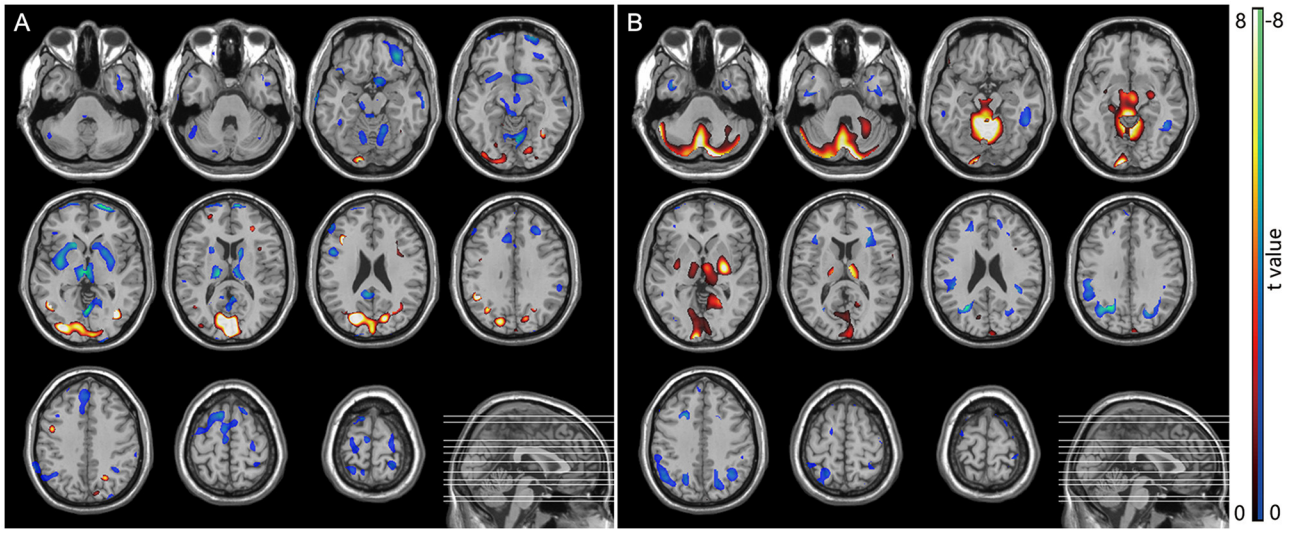


FIGURE 4 | SPM analysis of 18F-FDG PET. **(A)** MSA patients vs. normal controls showed hypometabolism in the bilateral putamen. **(B)** PD patients vs. normal controls showed hypermetabolism in the bilateral putamen, cerebellum, and occipital lobes, along with hypometabolism in the frontal, parietal, postcentral cortices, and cingulate areas.

not damaged (Ko et al., 2018; Shine et al., 2019). Defective striatal segments were shown in both ^{18}F-Dopa and ^{18}F-FDG PET images in patients with MSA-P, which is consistent with neuropathologic features of MSA (Yoshida, 2007; Jellinger, 2014). A neuropathologic study on MSA showed that the glial cytoplasmic inclusions, neuronal nuclear inclusions, and diffuse homogeneous alpha-synuclein staining in neuronal nuclei and cytoplasm were distributed widely in lesions in the pontine nuclei, putamen, substantia nigra, and other parts of the brain, indicating that both presynaptic function (detected by ^{18}F-Dopa PET) and postsynaptic pathway (detected by ^{18}F-FDG PET) of dopaminergic neurons were impaired.

The segmentation analysis could be verified by regional PET uptake value analysis. A significant reduction of ^{18}F-Dopa uptake was observed in the bilateral striatum of patients with PD and MSA-P. There was no significant difference in ^{18}F-Dopa uptake in the bilateral striatum between patients with PD and MSA-P, which is consistent with previous studies (Burn et al., 1994; Hu et al., 2002). The ^{18}F-Dopa and other presynaptic dopaminergic radiotracers of PET or single-photon emission computed tomography are useful to separate healthy subjects from Parkinsonism patients, but they are inadequate for differentiating between MSA-P and PD (Perju-Dumbrava et al., 2012; Kaasinen et al., 2019). The further ^{18}F-FDG PET showed a significant decrease in the bilateral putamen of patients with MSA-P and a significant increase in ^{18}F-FDG uptake in the bilateral striatum of patients with PD. The diametrically opposite results suggest that the pathogeneses of the two diseases are different. ^{18}F-FDG PET measures cerebral glucose metabolism, which reflects synaptic and neuronal activity. Loss of striatal dopamine in PD leads to changes of activity in both the direct and indirect striatal pathways, which could be detected by the ^{18}F-FDG PET. The primary pathological abnormality in PD is confined to the substantia nigra, and the degeneration of dopaminergic projection neurons from the substantia nigra to the striatum results in widespread alterations in the functional activity (Alexander et al., 1990; Parent and Hazrati, 1995) of the basal ganglia. The loss of inhibitory dopaminergic input to the striatum results in increased activity of the striatum, which is shown in striatal hypermetabolism in ^{18}F-FDG PET in patients with PD. The metabolic patterns in MSA-P represent regional postsynaptic neuronal loss directly related to abnormal protein deposition that characterizes the neurodegenerative disease (Tripathi et al., 2013). A susceptibility-weighted imaging study showed iron deposition in the putamen of patients with MSA-P caused by iron-mediated oxidative stress, which might appear as glucose hypometabolism in ^{18}F-FDG PET, which could differentiate MSA-P from PD (Yoon et al., 2015). We also observed a significant positive correlation of ^{18}F-FDG uptake with ^{18}F-Dopa uptake in the contralateral posterior putamen in MSA-P patients in our study, indicating that presynaptic function and postsynaptic pathway of dopaminergic neurons are synchronously damaged in MSA-P. In addition, regarding the similar disease duration, MSA-P patients in our study exhibited higher severity than PD patients with higher H&Y score, which is consistent with previous PET studies (Schönecker et al., 2019; Zhao et al., 2020), supporting the fact that MSA-P develops more rapidly than PD. PET studies showed that striatal uptake of ^{18}F-Dopa significantly correlated with the H&Y stage in both patients with PD (Eshuis et al., 2006) and MSA (Taniwaki et al., 2002). However, ^{18}F-FDG PET exhibited an opposite pattern of 18F-FDG uptake in the striatum between PD and MSA. For example, a longitudinal FDG-PET study showed that, as evidenced by PD-related pattern activity, a metabolic network characterized by hypermetabolism in the putamen increased linearly with disease progression of PD (Huang et al., 2007). In contrast, MSA-related

pattern, a metabolic network characterized by hypometabolism in the putamen, has been shown to have a positive correlation with disease duration in patients with MSA (Ko et al., 2017). Collectively, these studies suggest that with the progression of the disease, the striatal metabolism in PD patients increases, whereas the striatal metabolism in MSA patients decreases. Therefore, H&Y stage scores do not affect the differential diagnosis of the two diseases in our co-registration analysis of PET images.

Our SPM analysis also confirmed the results of the above segmentation analysis and ^{18}F-FDG uptake changes in patients with PD and MSA-P. PD patients were found to have a significant glucose hypermetabolism in the bilateral putamen, cerebellum, and occipital lobes, and a significant glucose hypometabolism in the bilateral putamen was detected in patients with MSA-P. SPM analysis can clearly differentiate between these two forms of parkinsonism: the glucose metabolism in the putamen is preserved or elevated in PD but significantly decreased in MSA-P, which is useful in the group analysis of FDG PET image. Our results are consistent with previous studies (Ma et al., 2007; Meles et al., 2020). However, the widespread implementation of such cerebral disease-related metabolic patterns in multicenter collaborations and clinical practice has been hindered by differences between PET scanners as well as reconstruction algorithms (Kogan et al., 2019). For example, hypermetabolism in the putamen was shown in the abnormal metabolic network in PD (Ma et al., 2007; Meles et al., 2020), but there was no significant change in metabolism of the putamen in the PD-related pattern analysis in several FDG PET studies (Holtbernd et al., 2015; Ko et al., 2017). The selection of a normal control group with differing ages, genders, and ethnicities could also cause potential bias in the SPM analysis (Kogan et al., 2019). It is interesting that significant glucose hypometabolism in the bilateral putamen can be found in MSA-P patients compared with healthy controls, but SPM analysis did not show reduced cerebellar metabolism. Our result is consistent with previous studies (Zhao et al., 2012, 2020), and the character of FDG PET image is consistent with the neuropathologic feature of MSA-P (predominated in basal ganglia) and MSA-C (predominated in cerebellum) (Ozawa et al., 2004).

There were several limitations in this study. First, our study sample was relatively small and longitudinal; hence, studies with a large sample size are needed in the future. Second, single-patient SPM analysis was not performed because there would have been the need to change the age-matched HC group from a large database if the patient's age changed. Finally, other types of parkinsonism-plus syndromes, such as progressive supranuclear paralysis and corticobasal degeneration, were not included in the study.

In conclusion, the co-registration analysis of ^{18}F-FDG and ^{18}F-Dopa PET demonstrated great diagnostic values for differentiating MSA-P from PD, which could be easily used in the individual analysis in clinics. Further studies are needed to evaluate the segmentation analysis in the differential diagnosis of other atypical Parkinsonisms, such as progressive supranuclear paralysis and corticobasal degeneration.

DATA AVAILABILITY STATEMENT

The raw data supporting the conclusions of this article will be made available by the authors, without undue reservation.

ETHICS STATEMENT

The studies involving human participants were reviewed and approved by local Ethical Committee of the First Affiliated Hospital of Sun Yat-sen University. The patients/participants provided their written informed consent to participate in this study.

AUTHOR CONTRIBUTIONS

W-bX: conceptualization, data curation and analysis, validation, and writing original draft. X-cS: data curation and analysis, validation, and writing original draft. G-hL and CY: data curation and analysis, and validation. X-sZ and ZP: project administration, resources, supervision, data analysis, review, and editing. All the authors read and approved the final manuscript.

FUNDING

This study was supported by grants from the National Key Research and Development Program of China, Stem Cell and Translational Research (No. 2017YFA0105104), the Southern China International Cooperation Base for Early Intervention and Functional Rehabilitation of Neurological Diseases (No. 2015B050501003), the Guangdong Provincial Engineering Center for Major Neurological Disease Treatment, the Guangdong Provincial Translational Medicine Innovation Platform for Diagnosis and Treatment of Major Neurological Disease, and the Guangdong Provincial Clinical Research Center for Neurological Diseases.

REFERENCES

Akdemir, Ü. Ö., Tokçaer, A. B., Karakuş, A., and Kapucu, L. Ö. (2014). Brain 18F-FDG PET imaging in the differential diagnosis of parkinsonism. *Clin. Nucl. Med*. 39, e220–226. doi: 10.1097/RLU.0000000000000315

Alexander, G. E., Crutcher, M., D', and DeLong, M. R. (1990). Basal ganglia-thalamocortical circuits: parallel substrates for motor, oculomotor, "prefrontal" and "limbic" functions. *Prog. Brain Res*. 85,119–146. doi: 10.1016/S0079-6123(08)62678-3

Armstrong, M. J., and Okun, M. S. (2020). Diagnosis and treatment of Parkinson Disease: a review. *JAMA*. 323, 548–560. doi: 10.1001/jama.2019.22360

Burn, D. J., Sawle, G. V., and Brooks, D. J. (1994). Differential diagnosis of Parkinson's disease, multiple system atrophy, and Steele-Richardson-Olszewski syndrome: discriminant analysis of striatal 18F-dopa PET data. *J. Neurol. Neurosurg. Psychiatry* 57, 278–284. doi: 10.1136/jnnp.57.3.278

Eshuis, S. A., Maguire, R. P., Leenders, K. L., Jonkman, S., and Jager, P. L. (2006). Comparison of FP-CIT SPECT with F-DOPA PET in patients with de novo

and advanced Parkinson's disease. *Eur. J. Nucl. Med. Mol. Imaging* 33,200–209. doi: 10.1007/s00259-005-1904-y

Gilman, S., Wenning, G. K., Low, P. A., Brooks, D. J., Mathias, C. J., Trojanowski, J. Q., et al. (2008). Second consensus statement on the diagnosis of multiple system atrophy. *Neurology* 71, 670–676. doi: 10.1212/01.wnl.0000324625.00404.15

Holtbernd, F., Ma, Y., Peng, S., Schwartz, F., Timmermann, L., Kracht, L., et al. (2015). Dopaminergic correlates of metabolic network activity in Parkinson's disease. *Hum. Brain Mapp*. 36, 3575–3585. doi: 10.1002/hbm.22863

Hu, M. T., Chaudhuri, K. R., Jarosz, J., Yaguez, L., and Brooks, D. J. (2002). An imaging study of parkinsonism among African-Caribbean and Indian London communities. *Mov. Disord*. 17,1321–1328. doi: 10.1002/mds.10261

Huang, C., Tang, C., Feigin, A., Lesser, M., Ma, Y., Pourfar, M., et al. (2007). Changes in network activity with the progression of Parkinson's disease. *Brain* 130,1834–1846. doi: 10.1093/brain/awm086

Hughes, A. J., Daniel, S. E., Ben-Shlomo, Y., and Lees, A. J. (2002). The accuracy of diagnosis of parkinsonian syndromes in a specialist movement disorder service. *Brain* 125, 861–870. doi: 10.1093/brain/awf080

Jellinger, K. A. (2014). Neuropathology of multiple system atrophy: new thoughts about pathogenesis. *Mov. Disord*. 29, 1720–1741. doi: 10.1002/mds.26052

Jiang, C., Hopfner, F., Katsikoudi, A., Hein, R., Catli, C., Evetts, S., et al. (2020). Serum neuronal exosomes predict and differentiate Parkinson's disease from atypical parkinsonism. *J. Neurol. Neurosurg. Psychiatry* 91,720–729. doi: 10.1136/jnnp-2019-322588

Jost, W. H., Lingor, P., Tönges, L., Schwarz, J., Buhmann, C., Kassubek, J., et al. (2019). Dyskinesia in multiple system atrophy and progressive supranuclear palsy. *J. Neural. Transm.* 126, 925–932. doi: 10.1007/s00702-019-02012-0

Kaasinen, V., Kankare, T., Joutsa, J., and Vahlberg, T. (2019). presynaptic striatal dopaminergic function in atypical Parkinsonism: a metaanalysis of imaging studies. *J. Nucl. Med*. 60,1757–1763. doi: 10.2967/jnumed.119.227140

Ko, J. H., Lee, C. S., and Eidelberg, D. (2017). Metabolic network expression in parkinsonism: clinical and dopaminergic correlations. *J. Cereb. Blood. Flow. Metab*. 37,683–693. doi: 10.1177/0271678X16637880

Ko, J. H., Spetsieris, P. G., and Eidelberg, D. (2018). Network structure and function in Parkinson's disease. *Cereb. Cortex* 28, 4121–4135. doi: 10.1093/cercor/bhx267

Koga, S., and Dickson, D. W. (2018). Recent advances in neuropathology, biomarkers and therapeutic approach of multiple system atrophy. *J. Neurol. Neurosurg. Psychiatry* 89, 175–184. doi: 10.1136/jnnp-2017-315813

Kogan, R. V., de Jong, B. A., Renken, R. J., Meles, S. K., van Snick, P. J. H., Golla, S., et al. (2019). Factors affecting the harmonization of disease-related metabolic brain pattern expression quantification in [18F]FDG-PET (PETMETPAT). *Alzheimers Dement (Amst)*. 11, 472–482. doi: 10.1016/j.dadm.2019.04.002

Litvan, I., Goetz, C. G., Jankovic, J., Wenning, G. K., Booth, V., Bartko, J. J., et al. (1997). What is the accuracy of the clinical diagnosis of multiple system atrophy? A clinicopathologic study. *Arch. Neurol*. 54, 937–944. doi: 10.1001/archneur.1997.00550200007003

Ma, Y., Tang, C., Spetsieris, P. G., Dhawan, V., and Eidelberg, D. (2007). Abnormal metabolic network activity in Parkinson's disease: test-retest reproducibility. *J. Cereb. Blood Flow Metab*. 27, 597–605. doi: 10.1038/sj.jcbfm.9600358

Matthews, D. C., Lerman, H., Lukic, A., Andrews, R. D., Mirelman, A., Wernick, M. N., et al. (2018). FDG PET Parkinson's disease-related pattern as a biomarker for clinical trials in early stage disease. *Neuroimage Clin*. 20,572–579. doi: 10.1016/j.nicl.2018.08.006

Meles, S. K., Renken, R. J., Pagani, M., Teune, L. K., Arnaldi, D., Morbelli, S., et al. (2020). Abnormal pattern of brain glucose metabolism in Parkinson's disease: replication in three European cohorts. *Eur. J. Nucl. Med. Mol. Imaging* 47, 437–450. doi: 10.1007/s00259-019-04570-7

Ozawa, T., Paviour, D., Quinn, N. P., Josephs, K. A., Sangha, H., Kilford, L., et al. (2004). The spectrum of pathological involvement of the striatonigral and olivopontocerebellar systems in multiple system atrophy: clinicopathological correlations. *Brain* 127,2657–2671. doi: 10.1093/brain/awh303

Parent, A., and Hazrati, L. N. (1995). Functional anatomy of the basal ganglia. I. The cortico-basal ganglia-thalamo-cortical loop. *Brain Res. Brain Res. Rev*. 20, 91–127. doi: 10.1016/0165-0173(94)00007-C

Perju-Dumbrava, L. D., Kovacs, G. G., Pirker, S., Jellinger, K., Hoffmann, M., Asenbaum, S., et al. (2012). Dopamine transporter imaging in autopsy-confirmed Parkinson's disease and multiple system atrophy. *Mov. Disord*. 27,65–71. doi: 10.1002/mds.24000

Poewe, W., and Wenning, G. (2002). The differential diagnosis of Parkinson's disease. *Eur. J. Neurol*. 9(Suppl 3), 23–30. doi: 10.1046/j.1468-1331.9.s3.3.x

Postuma, R. B., Berg, D., Stern, M., Poewe, W., Olanow, C. W., Oertel, W., et al. (2015). MDS clinical diagnostic criteria for Parkinson's disease. *Mov. Disord*. 30,1591–1601. doi: 10.1002/mds.26424

Rajput, A. H., Rozdilsky, B., and Rajput, A. (1991). Accuracy of clinical diagnosis in parkinsonism–a prospective study. *Can. J. Neurol. Sci*. 18, 275–278. doi: 10.1017/S0317167100031814

Ruottinen, H. M., Rinne, J. O., Ruotsalainen, U. H., Bergman, J. R., Oikonen, V. .J., Haaparanta, M. T., et al. (1995). Striatal [18F]fluorodopa utilization after COMT inhibition with entacapone studied with PET in advanced Parkinson's disease. *J. Neural. Transm. Park. Dis. Dement Sect*. 10, 91–106. doi: 10.1007/BF02251225

Saeed, U., Lang, A. E., and Masellis, M. (2020). Neuroimaging advances in Parkinson's disease and atypical Parkinsonian syndromes. *Front. Neurol*. 11:572976. doi: 10.3389/fneur.2020.572976

Schönecker, S., Brendel, M., Palleis, C., Beyer, L., Höglinger, G. U., Schuh, E., et al. (2019). PET imaging of astrogliosis and tau facilitates diagnosis of Parkinsonian syndromes. *Front. Aging Neurosci*. 11:249. doi: 10.3389/fnagi.2019.00249

Shi, X., Zhang, Y., Xu, S., Kung, H. F., Qiao, H., Jiang, L., et al. (2019). Decreased striatal vesicular monoamine transporter type 2 correlates with the nonmotor symptoms in Parkinson disease. *Clin. Nucl. Med*. 44, 707–713. doi: 10.1097/RLU.0000000000002664

Shine, J. M., Bell, P. T., Matar, E., Poldrack, R. A., Lewis, S. J. G., Halliday, G. M., et al. (2019). Dopamine depletion alters macroscopic network dynamics in Parkinson's disease. *Brain* 142, 1024–1034. doi: 10.1093/brain/awz034

Singer, W., Schmeichel, A. M., Shahnawaz, M., Schmelzer, J. D., Boeve, B. F., Sletten, D. M., et al. (2020). Alpha-synuclein oligomers and neurofilament light chain in spinal fluid differentiate multiple system atrophy from lewy body synucleinopathies. *Ann. Neurol*. 88,503–512. doi: 10.1002/ana.25824

Taniwaki, T., Nakagawa, M., Yamada, T., Yoshida, T., Ohyagi, Y., Sasaki, M., et al. (2002). Cerebral metabolic changes in early multiple system atrophy: a PET study. *J. Neurol. Sci*. 200,79–84. doi: 10.1016/S0022-510X(02)00151-X

Tripathi, M., Dhawan, V., Peng, S., Kushwaha, S., Batla, A., Jaimini, A., et al. (2013). Differential diagnosis of parkinsonian syndromes using F-18 fluorodeoxyglucose positron emission tomography. *Neuroradiology* 55, 483–492. doi: 10.1007/s00234-012-1132-7

Yoon, R. G., Kim, S. J., Kim, H. S., Choi, C. G., Kim, J. S., Oh, J., et al. (2015). The utility of susceptibility-weighted imaging for differentiating Parkinsonism-predominant multiple system atrophy from Parkinson's disease: correlation with 18F-flurodeoxyglucose positron-emission tomography. *Neurosci. Lett*. 584, 296–301. doi: 10.1016/j.neulet.2014.10.046

Yoshida, M. (2007). Multiple system atrophy: alpha-synuclein and neuronal degeneration. *Neuropathology* 27, 484–493. doi: 10.1111/j.1440-1789.2007.00841.x

Zhao, P., Zhang, B., and Gao, S. (2012). 18F-FDG PET study on the idiopathic Parkinson's disease from several parkinsonian-plus syndromes. *Park. Relat. Disord*. 18(Suppl 1), S60–62. doi: 10.1016/S1353-8020(11)70020-7

Zhao, P., Zhang, B., Gao, S., and Li, X. (2020). Clinical features, MRI, and 18F-FDG-PET in differential diagnosis of Parkinson disease from multiple system atrophy. *Brain Behav*. 10:e01827. doi: 10.1002/brb3.1827

Conflict of Interest: The authors declare that the research was conducted in the absence of any commercial or financial relationships that could be construed as a potential conflict of interest.

Copyright © 2021 Xian, Shi, Luo, Yi, Zhang and Pei. This is an open-access article distributed under the terms of the Creative Commons Attribution License (CC BY). The use, distribution or reproduction in other forums is permitted, provided the original author(s) and the copyright owner(s) are credited and that the original publication in this journal is cited, in accordance with accepted academic practice. No use, distribution or reproduction is permitted which does not comply with these terms.

frontiers in Aging Neuroscience

ORIGINAL RESEARCH
published: 28 May 2021
doi: 10.3389/fnagi.2021.665400

Decreased Exosomal Acetylcholinesterase Activity in the Plasma of Patients With Parkinson's Disease

Kyu Hwan Shim[1], Han Gyeol Go[1,2], Heewon Bae[1], Da-Eun Jeong[1], Danyeong Kim[2], Young Chul Youn[3], SangYun Kim[4], Seong Soo A. An[2] and Min Ju Kang[1]**

[1]Department of Neurology, Veterans Medical Research Institute, Veterans Health Service Medical Center, Seoul, South Korea, [2]Department of Bionano Technology, Gachon University, Seongnam-si, South Korea, [3]Department of Neurology, Chung-Ang University Hospital, Seoul, South Korea, [4]Department of Neurology, Seoul National University Bundang Hospital and Seoul National University College of Medicine, Seongnam-si, South Korea

Exosomes, which are small extracellular vesicles produced from various cell types, contain a variety of molecular constituents, such as proteins, lipids, and RNA. Recently, exosomal biomarkers have been investigated to probe the understanding and diagnosis of neurodegenerative disorders. Previous reports have demonstrated increased exosomal α-synuclein (α-syn) in patients with Parkinson's disease (PD) in comparison to healthy controls (HC). Interestingly, the cholinergic loss was revealed in the central and peripheral nervous systems in histopathology and molecular neuroimaging. Thereby, we simultaneously examined acetylcholinesterase (AChE) with α-syn as exosomal markers. Exosomes were isolated from the plasma of 34 FP-CIT PET proven patients with PD and 29 HC. Exosomal α-syn and AChE activity were quantified and the relationship with clinical parameters was analyzed. Remarkably, exosomal AChE activity was significantly decreased in PD compared to HC (P = 0.002). Moreover, exosomal AChE activity in PD revealed a strong negative correlation with disease severity, including H&Y (P = 0.007) and UPDRS part III (P = 0.047) scores. By contrast, no significant difference in exosomal α-syn concentration was observed between groups. These results support the occurrence of cholinergic dysfunction in PD, and they could be implicated with disease progression, especially motor deficits. Exosomal AChE activity with advanced exosome isolation techniques may be a reliable biomarker for the early diagnosis and prognosis of PD.

Keywords: Parkinson's disease, acetylcholinesterase, exosome, plasma, ultracentrifugation, alpha-synuclein

OPEN ACCESS

Edited by:
Shaomin Li,
Brigham and Women's Hospital and Harvard Medical School, United States

Reviewed by:
Roberta Marongiu,
Cornell University, United States
Laura Pasetto,
Istituto di Ricerche Farmacologiche Mario Negri (IRCCS), Italy

****Correspondence:***
Seong Soo A. An
seong.an@gmail.com
Min Ju Kang
minju0321@naver.com

Received: *08 February 2021*
Accepted: *26 April 2021*
Published: *28 May 2021*

Citation:
Shim KH, Go HG, Bae H, Jeong D-E, Kim D, Youn YC, Kim SY, An SSA and Kang MJ (2021) Decreased Exosomal Acetylcholinesterase Activity in the Plasma of Patients With Parkinson's Disease. Front. Aging Neurosci. 13:665400. doi: 10.3389/fnagi.2021.665400

INTRODUCTION

One of the pathophysiological characteristics of Parkinson's disease (PD) is the formation of Lewy bodies in the brain (Spillantini et al., 1997), which are mainly composed of insoluble aggregated α-synuclein (α-syn; Shults, 2006). Accordingly, α-syn has been studied extensively as a potential biomarker and indicator of disease progression in PD and its related synucleinopathies (El-Agnaf et al., 2003; Hong et al., 2010; Devic et al., 2011; Mollenhauer et al., 2011; Shi et al., 2011). However,

inconsistent plasma α-syn data in PD have been reported, and the diagnostic performance of α-syn in biofluids was still insufficient for application in PD diagnosis (Lee et al., 2006; Li et al., 2007; Foulds et al., 2011, 2013; Gorostidi et al., 2012; Ishii et al., 2015; Lin et al., 2017; Shim et al., 2020). The absence of reliable biofluidic biomarkers for PD has limited the monitoring of disease progression or treatment response.

Recent exosome studies have presented diverse possibilities for the etiology, diagnosis, and treatment of previously unexplained diseases (Lin et al., 2015). Exosomes, which are small extracellular vesicles with proteins and other components, are communication vehicles between cells or tissues. The mechanism of α-syn secretion via exosomes is not fully understood; however, several studies have demonstrated the secretion of α-syn on membrane vesicles of endocytic origin, sized 30–150 nm (Lee et al., 2005; Emmanouilidou et al., 2010; Alvarez-Erviti et al., 2011; Danzer et al., 2012; Tofaris, 2017). Recently, researchers have attempted to use exosomes in diagnosing PD by isolating them from their biofluids (Ho et al., 2014; Shi et al., 2014; Wu et al., 2017; Cerri et al., 2018; Zhao et al., 2019; Jiang et al., 2020; Niu et al., 2020). In particular, the levels of exosomal α-syn isolated from the blood were higher in the patients with PD than in the control group (Shi et al., 2014; Cerri et al., 2018; Zhao et al., 2019; Jiang et al., 2020). Accumulated results are required for explicit interpretations; therefore, detecting exosomal biomarkers from biofluids may contribute to the discovery of other potential PD biomarkers.

PD is a multifaceted and complex disorder, affecting multiple neurotransmissions rather than a single-system neurodegenerative disease (Braak et al., 2003; Langston, 2006). Growing evidence has suggested an association between degeneration of the nigrostriatal dopaminergic system and cholinergic denervation in PD (Müller and Bohnen, 2013). Interestingly, a study using positron emission tomography (PET), which measured acetylcholinesterase (AChE) activity, has reported severe cholinergic denervation in the brain of patients with PD when compared with Alzheimer's disease (AD; Bohnen et al., 2003). Moreover, 11C-donepezil uptake is significantly reduced in the peripheral organs in PD patients, indicating a decrease in AChE in the peripheral system (Gjerløff et al., 2014; Fedorova et al., 2017). Taken together, this suggests that AChE is extensively associated with the pathophysiological process of PD in the peripheral organs and the brain.

In the present study, exosomes were isolated from the plasma samples of patients with PD and healthy controls (HC) using ultracentrifugation. Exosomal AChE activity and α-syn levels were measured to investigate the correlation with clinical parameters and their biomarker potential.

MATERIALS AND METHODS

Participants

Patients with PD were recruited between May 2019 and June 2020 from the Veterans Health Service Medical Center. PD was diagnosed based on the UK Parkinson's Disease Society Brain Bank criteria. All patients underwent FP-CIT PET, were staged according to Hoehn and Yahr (H&Y) criteria, and evaluated by the Unified Parkinson's Disease Rating Scale (UPDRS). Age-matched HC who had no evidence of neurological or serious medical illnesses in their medical history or via neurological examination were recruited. All participants underwent brain magnetic resonance imaging and Mini-Mental State Examination (MMSE) to evaluate global cognitive impairments. All participants or their legal representatives provided written informed consent. The study protocol was approved by the Institutional Review Board of Veterans Healthcare Medical Center (2019-05-004).

Sampling

Blood samples were collected in tubes containing EDTA to prevent blood clotting. Plasma was separated within 4 h after blood collection. Samples were centrifuged for 10 min at 1,500 *g* to eliminate red blood cells, platelets, and cell debris. The separated plasma was transferred to the polypropylene tube and stored at −80°C until analysis.

Plasma Exosome Isolation

Plasma (1 ml) was centrifuged at 20,000 *g* for 1 h to remove large extracellular vesicles. The supernatant was transferred in an ultra-centrifugation tube filled with phosphate-buffered saline (PBS; 28348, Thermo Fisher) and ultra-centrifugated at 100,000 *g* (Optima XE-90 with 90Ti rotor, Beckman Coulter) for 1.5 h to pellet exosomes. The supernatant was discarded, and the pellets were resuspended in PBS with phosphate (4906845001, Roche) and protease (5892970001, Roche) inhibitors. Exosomes were lysed by incubating with M-PER (Cat. #78501; Thermo Fisher Scientific, Carlsbad, CA, USA), a mild detergent lysis buffer that yields highly efficient soluble proteins in a non-denatured state, for 30 min at 4°C (Guix et al., 2018). BCA assay (23227, Thermo Fisher Scientific, USA) was performed to quantify the exosomal protein concentration, according to the manufacturer's instructions. The plates were read using a plate reader (SpectraMax Plus 384; Molecular Devices, Sunnyvale, CA, USA) at 540 nm.

Transmission Electron Microscopy

The exosomes were fixed with 4% formaldehyde in PBS for 1 h at 4°C. Fixed samples were dropped onto formvar carbon film-coated 150 mesh copper grids for 1 min. The filter paper was used to remove any excess sample. The grids were negatively stained with 2% uranyl acetate. The excess liquid was washed using filter paper, and imaging was performed on a Hitachi H7600 transmission electron microscope, operated at 80 kV.

Nanoparticle Tracking Analysis

Nanoparticle tracking analysis was conducted with the isolated plasma exosomes to determine the concentration and the size distribution of particles using a ZetaView (Particle Metrix). The samples were diluted properly with particle-free PBS. Videos of the light-refracting particles were recorded with the following settings: 25°C fixed temperature, 11 positions, three cycles, sensitivity 80, shutter 100, 30 fps, 5 s videos/position, three measurements. The number and size distribution were analyzed by ZetaView Analyze 08.05.12. SP2.

Western Blot Analysis

The isolated exosomes (~20 μg proteins) were solubilized with Laemmli sample buffer and heated for 5 min at 98°C. The proteins were separated on an SDS-PAGE gel and transferred to a PVDF membrane. The membranes were blocked with 3% Nonfat-dried milk bovine (Sigma, M7409) in TBST (Thermo, #28360) for 1 h at room temperature (RT). Primary antibodies against Alix (Cell Signalling Technology, #2171) and GM130 (Cell signaling Technology, #12480) were diluted 1:1,000 in TBST with 3% Nonfat-dried milk bovine and incubated overnight at 4°C. The membranes were washed with TBST and incubated with HRP-conjugated secondary antibodies for 1 h at RT. The immunostained proteins were detected by applying chemiluminescent substrate (Thermo, #34577) and imaged by the DAVINCH-Chemi imager.

Exosomal Acetylcholinesterase Activity Measurement

AChE activity was determined using a fluorometric acetylcholinesterase assay kit (ab138872, Abcam). The following procedure was performed according to the manufacturer's instructions. Briefly, AChE standard and samples were diluted in assay buffer and applied to a 96-well plate in duplicate. The reaction mixture was added to each well and incubated for 1 h at RT. The fluorescence signal was monitored using a fluorescence microplate reader (FLUOstar Omega; BMG Labtech Inc., Cary, NC, USA; λex. = 490 nm, λem. = 520 nm).

Quantification of Exosomal α-Synuclein

Exosomal α-syn was measured by a commercial ELISA kit (AS-55550-H, Anaspec) according to the manufacturer's instructions. Briefly, exosomal lysates were diluted in sample buffer and added to each well in duplicate. After 4 h of incubation at RT, the microplate was washed six times, then TMB was applied to each well. Stop solution was added to terminate the reaction, and the optical signal was determined at 450 nm using a microplate reader.

Statistical Analysis

Statistical analyses were conducted using SPSS 24 (SPSS Inc., Chicago, IL). Fisher's exact test was used to assess the sex difference. Student's *t*- and Mann-Whitney *U* tests were performed to compare the biomarker between groups. $P < 0.05$ was regarded as statistically significant. Significant correlations were assessed using Spearman's correlation coefficient. The receiver operating characteristic (ROC) curve was analyzed to assess the accuracy of the diagnostic performance by calculating the area under the curve (AUC). The cutoff value was determined when the sum of the sensitivity and specificity maximized the Youden index.

RESULTS

Participant Demographics and Clinical Characteristics

Demographic characteristics and clinical features are summarized in **Table 1**. No significant differences in age or sex were found between groups; however, males were recruited more than females due to the specificity of recruitment from a veteran's hospital. There was no difference in MMSE score between groups. FP-CIT PET was performed in all patients with PD; all patients presented with reduced dopamine transport activity. In the HC group, seven individuals underwent FP-CIT PET; this revealed normal dopamine transport activity.

TABLE 1 | Demographics and clinical characteristics of the Parkinson's disease (PD) and healthy controls (HC) groups.

	PD	HC	*P*-value
N of individuals	34	29	-
Age	74.2 (4.7)	73.9 (4.6)	0.816[a]
Sex (M/F)	30/4	24/5	0.721[b]
MMSE	24.7 (3.8)	25.8 (2.5)	0.232[c]
H&Y score (1/1.5/2/2.5)	15/8/6/5	-	-
UPDRS part III	40.0 (13.1)	-	-
Disease duration (year)	5.1 (4.3)	-	-
FP-CIT PET (P/N)	34/0	0/7	0.000[b]

Data are presented as mean (standard deviation); [a]Student's t-test; [b]Fisher's Exact test; [c]Mann-Whitney test.

Analysis of Plasma Exosomal Biomarkers in Clinical Samples

Diagnostic performances were evaluated by measuring AChE activity and α-syn levels from the isolated plasma exosomes. Exosomes were isolated via ultracentrifugation, which was confirmed by visualization with transmission electron microscopy and nanoparticle tracking analysis (**Figure 1A** and **Supplementary Figure 1C**). The estimated size of exosomes was distributed around 140 nm by nanoparticle tracking analysis (**Figure 1B**). In Western blot, exosomes were enriched in Alix, but not in GM130 (**Figure 1C**). No differences in plasma exosome size and concentration were found between PD and HC (**Supplementary Figures 1A,B**). The total amount of proteins in the isolated exosomes may vary between individuals; therefore, total exosomal protein content was measured and used to normalize the two biomarkers. Total exosomal protein levels were highly correlated with the concentration of exosomes and the exosomal AChE activity, indicating the adequacy as a normalization factor (**Supplementary Figure 2**). The concentrations of exosomal α-syn showed no difference between groups (PD, 234.0 ± 183.2 pg/mg; HC, 219.7 ± 135.3 pg/mg; **Figure 2A**). Remarkably, exosomal AChE activity was significantly decreased in PD group (3.9 ± 1.0 mU/mg) when compared with HC group (4.7 ± 1.0 mU/mg; $P = 0.002$; **Figure 2B**). The ROC curve analysis revealed that exosomal AChE activity exhibited a moderate performance for PD diagnosis (AUC = 0.709; 95% confidence interval, 0.582–0.836; **Figure 2C**). When a cutoff value of 4.05 was applied, sensitivity and specificity were 61.8% and 79.3%, respectively.

Correlation Between Exosomal AChE Activity and PD Progression

Next, we analyzed the correlation between exosomal AChE activity and disease severity in patients with PD to investigate its clinical implication. Intriguingly, exosomal AChE activity was significantly correlated with H&Y ($p = 0.007$, $r^2 = 0.197$,

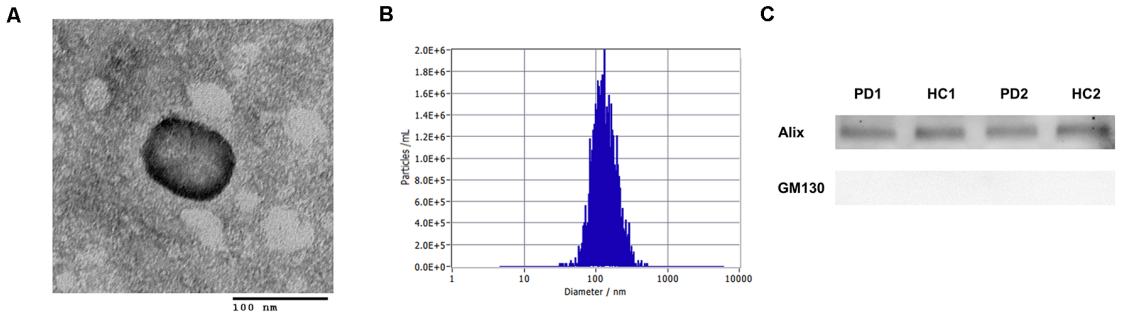


FIGURE 1 | Characteristics of the isolated exosomes by ultracentrifugation. **(A)** Representative transmission electron micrograph of isolated plasma exosomes (Scale bar = 100 nm). **(B)** A representative plot depicting the size and concentration of exosomes. **(C)** Western blot of the exosomes from Parkinson's disease (PD) and healthy controls (HC) individuals with specific antibodies against Alix and GM130 as positive and negative controls, respectively.

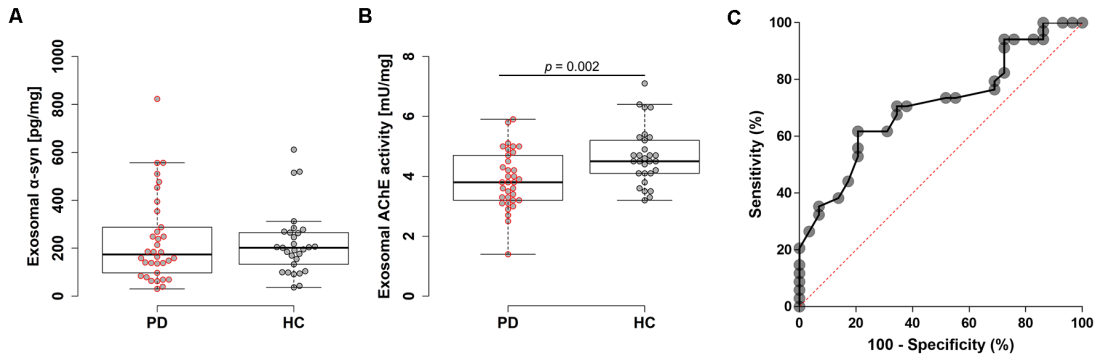


FIGURE 2 | Evaluation of plasma exosomal biomarkers. Box plots of exosomal α-syn levels **(A)** and acetylcholinesterase (AChE) activity **(B)**. Boxes represent the interquartile range; the horizontal lines mean medians and the whiskers. The Student's *t*-test was used for comparison of the two groups. **(C)** Receiver operating characteristic (ROC) analysis of exosomal AChE activity.

$\rho = -0.451$) and UPDRS part III scores ($p = 0.047$, $r^2 = 0.109$, $\rho = -0.342$; **Figures 3A,B**). Disease duration tended towards a moderate negative correlation with exosomal AChE activity ($\rho = 0.101$; **Figure 3C**). MMSE score and the administration of AChE inhibitors, including donepezil, galantamine, and rivastigmine, were not significantly correlated with exosomal AChE activity (**Figures 3D,E**).

DISCUSSION

In the current study, exosomal AChE activity was significantly reduced in the PD group compared to the HC group. Moreover, exosomal AChE activity was significantly negatively correlated with disease severity. Previous studies have examined the cholinergic deficits in PD via histopathology and molecular neuroimaging. A reduced number of cholinergic neurons was reported in the pedunculopontine nuclei of PD patients, which was correlated with H&Y scores (Rinne et al., 2008). A cholinergic PET study showed that patients of PD and PD with dementia had cholinergic denervation in the medial secondary occipital cortex (Müller and Bohnen, 2013). Additionally, the cholinergic loss was found using 11C-donepezil PET, which supported parasympathetic denervation in the peripheral nervous system of PD patients (Gjerløff et al., 2014; Fedorova et al., 2017). A significant decrease in colonic 11C-donepezil signal in the early stages of PD might explain the increased constipation as the first nonmotor symptom in the prodromal phase (Fedorova et al., 2017). Taken together, these studies demonstrate cholinergic dysfunction in the central and peripheral nervous systems of patients with PD, which supports the reduction in exosomal AChE activity found in this study. Furthermore, the strong association between the decreased exosomal AChE activity and disease severity highlights the importance of AChE in PD pathophysiology. Exosomal AChE activity was an insufficient single diagnostic biomarker for PD; however, it may have the potential to further elucidate PD pathophysiology. Despite the exosomal AChE levels had no difference between the two groups in the preliminary results (**Supplementary Figure 3**), we will keep considering the measurement of exosomal AChE levels to improve the diagnostic performance in the future.

The etiology of the decreased AChE activity in PD remains obscure. One hypothesis is that the decreased production and secretion of exosomal AChE are associated with α-syn-

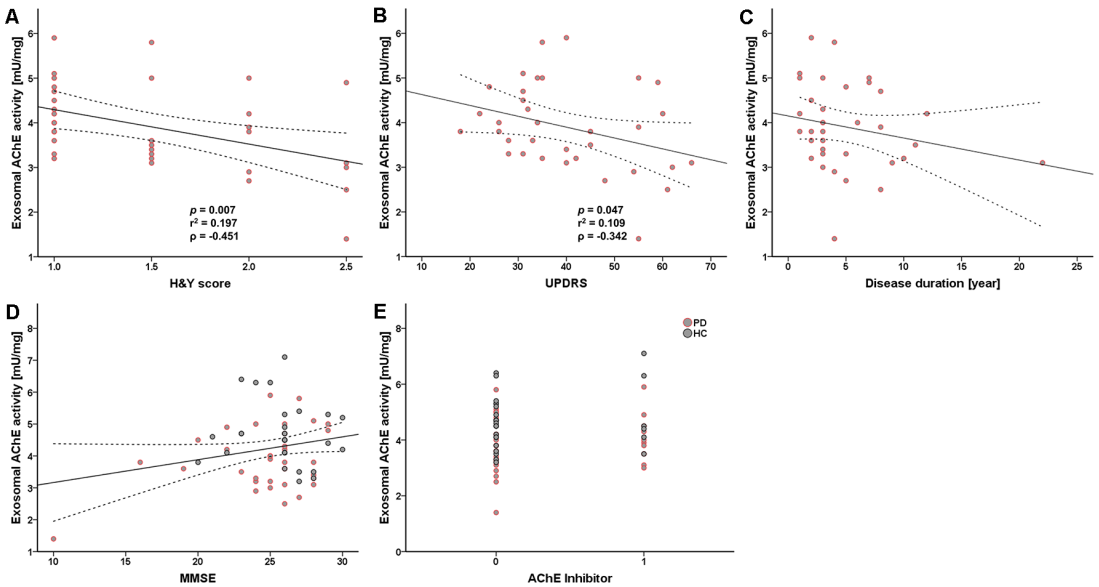


FIGURE 3 | Scatter plot of exosomal AChE activity and clinical data. Correlation between AChE activity and H&Y scores **(A)**, UPDRS part III score **(B)**, disease duration **(C)**, Mini-mental state examination (MMSE) score **(D)**, and AChE inhibitor use (donepezil, galantamine, and rivastigmine) **(E)**. 0 = without AChE inhibitors; 1 = with AChE inhibitors. The dashed line represents the 95% prediction interval of the regression line. ρ, Spearman's rho. Spearman's correlation analysis was used to determine any statistical significance.

induced neuronal death. Moreover, α-syn aggregates interfere with the axonal transport of protein (Chung et al., 2009; Chu et al., 2012); therefore, exosomal AChE activity might be decreased via related mechanisms. A different hypothesis relating to the balance between acetylcholine (ACh) and dopamine (DA) may explain this phenomenon (Spehlmann and Stahl, 1976; Aosaki et al., 2010). This balance is the main feature of motor activity control. DA deficiency in PD pathology can trigger a severe decline in basal ganglia circuit dynamics, leading to motor and cognitive impairment with cholinergic system imbalance (Aosaki et al., 2010). In a mouse PD model genetically modified for a decline in DA levels, an imbalance between ACh and DA exacerbated motor deficit (McKinley et al., 2019). Interestingly, administration of a high dose of donepezil highlighted that disturbing the balance of ACh and DA leads to medication-induced Parkinsonism (Rangseekajee et al., 2016). In the current study, it could be hypothesized that an imbalance between DA and ACh via DA depletion exacerbated the decrease in AChE activity.

In previous studies, exosomal α-syn was increased in PD when compared with HC (Shi et al., 2014; Cerri et al., 2018; Zhao et al., 2019; Jiang et al., 2020; Niu et al., 2020). By contrast, other studies have shown a decrease (Stuendl et al., 2016; Si et al., 2019) or no difference in exosomal α-syn between PD and HC groups (Tomlinson et al., 2015; Cao et al., 2019). These discrepancies may be due to biofluid type or technical differences in exosome isolation. For example, ultracentrifugation, as performed in this study, resulted in total exosome isolation from plasma; however, L1CAM antibody could specifically separate neuronal-derived exosomes in other studies. Subsequently, results may differ based on exosome origin, which suggests different pathways and significance. Therefore, comparing several exosome isolation techniques and subdividing them into specific cell-derived exosomes would best elucidate these mechanisms.

There are several limitations in the current study. First, the cohort was recruited from a limited number of individuals; therefore, the current study should be extended and reproduced with a larger cohort. Second, we recruited more male than female patients in a single center; therefore, the next study should recruit the samples from a multicenter cohort. Third, no organ-specific derived exosomes were extracted. Exosomes are released from various cells, including neurons, blood cells, and epithelial cells; therefore, priority should be given to isolating neuron-derived exosomes to investigate AChE activity in subsequent studies.

CONCLUSION

This study demonstrated the reduced AChE activity in plasma exosomes from patients with PD when compared with HC. Furthermore, a significant negative correlation between AChE activity and disease severity was observed in the PD group. These results suggested that plasma exosomal AChE could serve as a surrogate biomarker to monitor disease progression. Exosomal AChE activity showed a moderate diagnostic performance, which could be improved by applying an advanced exosome isolation technique. Exosomes may play pivotal roles in the occurrence and progression of PD; therefore, further studies will continue

to elucidate the pathophysiology of PD and develop diagnostic and therapeutic tools.

DATA AVAILABILITY STATEMENT

The raw data supporting the conclusions of this article will be made available by the authors, without undue reservation.

ETHICS STATEMENT

The studies involving human participants were reviewed and approved by Institutional Review Board of Veterans Healthcare Medical Center. The patients/participants provided their written informed consent to participate in this study.

AUTHOR CONTRIBUTIONS

KS, SA, and MK: conceptualization. HB: data curation. MK: funding acquisition. KS, HG, and DK: investigation. KS and MK: project administration. D-EJ and MK: resources. YY, SK, and SA: supervision. SA and MK: validation. KS and MK: writing—original draft. SA: writing—review and editing. All authors contributed to the article and approved the submitted version.

FUNDING

This research was supported by a National Research Foundation of Korea (NRF) grant awarded by the Korean government (NRF-2020R1F1A1075666; NRF-2020R1A2B5B01002463 to SA) and a VHS Medical Center research grant, South Korea (VHSMC 19041).

ACKNOWLEDGMENTS

We would like to express our gratitude to the participants for providing the samples and their agreement to participate in this research.

SUPPLEMENTARY MATERIAL

The Supplementary Material for this article can be found online at: https://www.frontiersin.org/articles/10.3389/fnagi.2021.665400/full#supplementary-material.

REFERENCES

Alvarez-Erviti, L., Seow, Y., Schapira, A. H., Gardiner, C., Sargent, I. L., Wood, M. J., et al. (2011). Lysosomal dysfunction increases exosome-mediated alpha-synuclein release and transmission. *Neurobiol. Dis.* 42, 360–367. doi: 10.1016/j.nbd.2011.01.029

Aosaki, T., Miura, M., Suzuki, T., Nishimura, K., and Masuda, M. (2010). Acetylcholine-dopamine balance hypothesis in the striatum: An update. *Geriatr. Gerontol. Int.* 10, S148–S157. doi: 10.1111/j.1447-0594.2010.00588.x

Bohnen, N. I., Kaufer, D. I., Ivanco, L. S., Lopresti, B., Koeppe, R. A., Davis, J. G., et al. (2003). Cortical cholinergic function is more severely affected in parkinsonian dementia than in Alzheimer disease: an *in vivo* positron emission tomographic study. *Arch. Neurol.* 60, 1745–1748. doi: 10.1001/archneur.60.12.1745

Braak, H., Del Tredici, K., Rüb, U., De Vos, R. A., Jansen Steur, E. N., Braak, E., et al. (2003). Staging of brain pathology related to sporadic Parkinson's disease. *Neurobiol. Aging* 24, 197–211. doi: 10.1016/s0197-4580(02)00065-9

Cao, Z., Wu, Y., Liu, G., Jiang, Y., Wang, X., Wang, Z., et al. (2019). α-Synuclein in salivary extracellular vesicles as a potential biomarker of Parkinson's disease. *Neurosci. Lett.* 696, 114–120. doi: 10.1016/j.neulet.2018.12.030

Cerri, S., Ghezzi, C., Sampieri, M., Siani, F., Avenali, M., Dornini, G., et al. (2018). The exosomal/total α-synuclein ratio in plasma is associated with glucocerebrosidase activity and correlates with measures of disease severity in PD patients. *Front. Cell. Neurosci.* 12:125. doi: 10.3389/fncel.2018.00125

Chu, Y., Morfini, G. A., Langhamer, L. B., He, Y., Brady, S. T., Kordower, J. H., et al. (2012). Alterations in axonal transport motor proteins in sporadic and experimental Parkinson's disease. *Brain* 135, 2058–2073. doi: 10.1093/brain/aws133

Chung, C. Y., Koprich, J. B., Siddiqi, H., and Isacson, O. (2009). Dynamic changes in presynaptic and axonal transport proteins combined with striatal neuroinflammation precede dopaminergic neuronal loss in a rat model of AAV alpha-synucleinopathy. *J. Neurosci.* 29, 3365–3373. doi: 10.1523/JNEUROSCI.5427-08.2009

Danzer, K. M., Kranich, L. R., Ruf, W. P., Cagsal-Getkin, O., Winslow, A. R., Zhu, L., et al. (2012). Exosomal cell-to-cell transmission of alpha synuclein oligomers. *Mol. Neurodegener.* 7:42. doi: 10.1186/1750-1326-7-42

Devic, I., Hwang, H., Edgar, J. S., Izutsu, K., Presland, R., Pan, C., et al. (2011). Salivary α-synuclein and DJ-1: potential biomarkers for Parkinson's disease. *Brain* 134:e178. doi: 10.1093/brain/awr015

El-Agnaf, O. M., Salem, S. A., Paleologou, K. E., Cooper, L. J., Fullwood, N. J., Gibson, M. J., et al. (2003). Alpha-synuclein implicated in Parkinson's disease is present in extracellular biological fluids, including human plasma. *FASEB j.* 17, 1945–1947. doi: 10.1096/fj.03-0098fje

Emmanouilidou, E., Melachroinou, K., Roumeliotis, T., Garbis, S. D., Ntzouni, M., Margaritis, L. H., et al. (2010). Cell-produced alpha-synuclein is secreted in a calcium-dependent manner by exosomes and impacts neuronal survival. *J. Neurosci.* 30, 6838–6851. doi: 10.1523/JNEUROSCI.5699-09.2010

Fedorova, T. D., Seidelin, L. B., Knudsen, K., Schacht, A. C., Geday, J., Pavese, N., et al. (2017). Decreased intestinal acetylcholinesterase in early Parkinson disease: An 11C-donepezil PET study. *Neurology* 88, 775–781. doi: 10.1212/WNL.0000000000003633

Foulds, P. G., Diggle, P., Mitchell, J. D., Parker, A., Hasegawa, M., Masuda-Suzukake, M., et al. (2013). A longitudinal study on α-synuclein in blood plasma as a biomarker for Parkinson's disease. *Sci. Rep.* 3:2540. doi: 10.1038/srep02540

Foulds, P. G., Mitchell, J. D., Parker, A., Turner, R., Green, G., Diggle, P., et al. (2011). Phosphorylated α-synuclein can be detected in blood plasma and is potentially a useful biomarker for Parkinson's disease. *FASEB J.* 25, 4127–4137. doi: 10.1096/fj.10-179192

Gjerløff, T., Fedorova, T., Knudsen, K., Munk, O. L., Nahimi, A., Jacobsen, S., et al. (2014). Imaging acetylcholinesterase density in peripheral organs in Parkinson's disease with ^{11}C-donepezil PET. *Brain* 138, 653–663. doi: 10.1093/brain/awu369

Gorostidi, A., Bergareche, A., Ruiz-Martínez, J., Martí-Massó, J. F., Cruz, M., Varghese, S., et al. (2012). α-synuclein levels in blood plasma from LRRK2 mutation carriers. *PLoS One* 7:e52312. doi: 10.1371/journal.pone.0052312

Guix, F. X., Corbett, G. T., Cha, D. J., Mustapic, M., Liu, W., Mengel, D., et al. (2018). Detection of aggregation-competent tau in neuron-derived extracellular vesicles. *Int. J. Mol. Sci.* 19:663.doi: 10.3390/ijms19030663

Ho, D. H., Yi, S., Seo, H., Son, I., and Seol, W. (2014). Increased DJ-1 in urine exosome of Korean males with Parkinson's disease. *Biomed. Res. Int.* 2014:704678. doi: 10.1155/2014/704678

Hong, Z., Shi, M., Chung, K. A., Quinn, J. F., Peskind, E. R., Galasko, D., et al. (2010). DJ-1 and alpha-synuclein in human cerebrospinal fluid as biomarkers of Parkinson's disease. *Brain* 133, 713–726. doi: 10.1093/brain/awq008

Ishii, R., Tokuda, T., Tatebe, H., Ohmichi, T., Kasai, T., Nakagawa, M., et al. (2015). Decrease in plasma levels of α-synuclein is evident in patients with

Parkinson's disease after elimination of heterophilic antibody interference. *PLoS One* 10:e0123162. doi: 10.1371/journal.pone.0123162

Jiang, C., Hopfner, F., Katsikoudi, A., Hein, R., Catli, C., Evetts, S., et al. (2020). Serum neuronal exosomes predict and differentiate Parkinson's disease from atypical parkinsonism. *J. Neurol. Neurosurg. Psychiatry* 91, 720–729. doi: 10.1136/jnnp-2019-322588

Langston, J. W. (2006). The Parkinson's complex: parkinsonism is just the tip of the iceberg. *Ann. Neurol.* 59, 591–596. doi: 10.1002/ana.20834

Lee, H. J., Patel, S., and Lee, S. J. (2005). Intravesicular localization and exocytosis of alpha-synuclein and its aggregates. *J. Neurosci.* 25, 6016–6024. doi: 10.1523/JNEUROSCI.0692-05.2005

Lee, P. H., Lee, G., Park, H. J., Bang, O. Y., Joo, I. S., Huh, K., et al. (2006). The plasma alpha-synuclein levels in patients with Parkinson's disease and multiple system atrophy. *J. Neural. Transm.* 113, 1435–1439. doi: 10.1007/s00702-005-0427-9

Li, Q. X., Mok, S. S., Laughton, K. M., Mclean, C. A., Cappai, R., Masters, C. L., et al. (2007). Plasma alpha-synuclein is decreased in subjects with Parkinson's disease. *Exp. Neurol.* 204, 583–588. doi: 10.1016/j.expneurol.2006.12.006

Lin, C.-H., Yang, S.-Y., Horng, H.-E., Yang, C.-C., Chieh, J.-J., Chen, H.-H., et al. (2017). Plasma α-synuclein predicts cognitive decline in Parkinson's disease. *J. Neurol. Neurosurg. Psychiatry* 88, 818–824. doi: 10.1136/jnnp-2016-314857

Lin, J., Li, J., Huang, B., Liu, J., Chen, X., Chen, X.-M., et al. (2015). Exosomes: novel biomarkers for clinical diagnosis. *Sci. World J.* 2015:657086. doi: 10.1155/2015/657086

McKinley, J. W., Shi, Z., Kawikova, I., Hur, M., Bamford, I. J., Sudarsana Devi, S. P., et al. (2019). Dopamine deficiency reduces striatal cholinergic interneuron function in models of Parkinson's disease. *Neuron* 103, 1056–1072.e1056. doi: 10.1016/j.neuron.2019.06.013

Mollenhauer, B., Locascio, J. J., Schulz-Schaeffer, W., Sixel-Döring, F., Trenkwalder, C., Schlossmacher, M. G., et al. (2011). α-Synuclein and tau concentrations in cerebrospinal fluid of patients presenting with parkinsonism: a cohort study. *Lancet Neurol.* 10, 230–240. doi: 10.1016/S1474-4422(11)70014-X

Müller, M. L. T. M., and Bohnen, N. I. (2013). Cholinergic dysfunction in Parkinson's disease. *Curr. Neurol. Neurosci.* 13, 377–377. doi: 10.1007/s11910-013-0377-9

Niu, M., Li, Y., Li, G., Zhou, L., Luo, N., Yao, M., et al. (2020). A longitudinal study on α-synuclein in plasma neuronal exosomes as a biomarker for Parkinson's disease development and progression. *Eur. J. Neurol.* 27, 967–974. doi: 10.1111/ene.14208

Rangseekajee, P., Paholpak, S., Aphisitphinyo, S., Pimpanit, V., and Paholpak, P. (2016). P.5.b.011—Severe medication-induced parkinsonism from a higher dose of donepezil (23 mg/day) in early-onset alzheimer's disease. *Eur. Neuropsychopharmacol.* 26:S646. doi: 10.26226/morressier.5785edcfd462b80296c99f8a

Rinne, J. O., Ma, S. Y., Lee, M. S., Collan, Y., and Röyttä, M. (2008). Loss of cholinergic neurons in the pedunculopontine nucleus in Parkinson's disease is related to disability of the patients. *Parkinsonism Relat. Dis.* 14, 553–557. doi: 10.1016/j.parkreldis.2008.01.006

Shi, M., Bradner, J., Hancock, A. M., Chung, K. A., Quinn, J. F., Peskind, E. R., et al. (2011). Cerebrospinal fluid biomarkers for Parkinson disease diagnosis and progression. *Ann. Neurol.* 69, 570–580. doi: 10.1002/ana.22311

Shi, M., Liu, C., Cook, T. J., Bullock, K. M., Zhao, Y., Ginghina, C., et al. (2014). Plasma exosomal α-synuclein is likely CNS-derived and increased in Parkinson's disease. *Acta Neuropathol.* 128, 639–650. doi: 10.1007/s00401-014-1314-y

Shim, K. H., Kim, S. C., Youn, Y. C., Sung, Y.-H., and An, S. S. A. (2020). Decreased plasma α-synuclein in idiopathic Parkinson's disease patients after adjusting hemolysis factor. *Mol. Cell Toxicol.* 16, 477–484. doi: 10.1007/s13273-020-00104-7

Shults, C. W. (2006). Lewy bodies. *Proc. Natl. Acad. Sci. U S A* 103, 1661–1668. doi: 10.1073/pnas.0509567103

Si, X., Tian, J., Chen, Y., Yan, Y., Pu, J., Zhang, B., et al. (2019). Central nervous system-derived exosomal alpha-synuclein in serum may be a biomarker in Parkinson's disease. *Neuroscience* 413, 308–316. doi: 10.1016/j.neuroscience.2019.05.015

Spehlmann, R., and Stahl, S. M. (1976). Dopamine acetylcholine imbalance in Parkinson's disease. Possible regenerative overgrowth of cholinergic axon terminals. *Lancet* 1, 724–726. doi: 10.1016/s0140-6736(76)93095-6

Spillantini, M. G., Schmidt, M. L., Lee, V. M., Trojanowski, J. Q., Jakes, R., Goedert, M., et al. (1997). Alpha-synuclein in Lewy bodies. *Nature* 388, 839–840. doi: 10.1038/42166

Stuendl, A., Kunadt, M., Kruse, N., Bartels, C., Moebius, W., Danzer, K. M., et al. (2016). Induction of α-synuclein aggregate formation by CSF exosomes from patients with Parkinson's disease and dementia with Lewy bodies. *Brain* 139, 481–494. doi: 10.1093/brain/awv346

Tofaris, G. K. (2017). A critical assessment of exosomes in the pathogenesis and stratification of Parkinson's disease. *J. Parkinsons Dis.* 7, 569–576. doi: 10.3233/JPD-171176

Tomlinson, P. R., Zheng, Y., Fischer, R., Heidasch, R., Gardiner, C., Evetts, S., et al. (2015). Identification of distinct circulating exosomes in Parkinson's disease. *Ann. Clin. Transl. Neurol.* 2, 353–361. doi: 10.1002/acn3.175

Wu, X., Zheng, T., and Zhang, B. (2017). Exosomes in Parkinson's disease. *Neurosci. Bull.* 33, 331–338. doi: 10.1007/s12264-016-0092-z

Zhao, Z.-H., Chen, Z.-T., Zhou, R.-L., Zhang, X., Ye, Q.-Y., Wang, Y.-Z., et al. (2019). Increased DJ-1 and α-synuclein in plasma neural-derived exosomes as potential markers for Parkinson's disease. *Front. Aging Neurosci.* 10:438. doi: 10.3389/fnagi.2018.00438

Conflict of Interest: The authors declare that the research was conducted in the absence of any commercial or financial relationships that could be construed as a potential conflict of interest.

Copyright © 2021 Shim, Go, Bae, Jeong, Kim, Youn, Kim, An and Kang. This is an open-access article distributed under the terms of the Creative Commons Attribution License (CC BY). The use, distribution or reproduction in other forums is permitted, provided the original author(s) and the copyright owner(s) are credited and that the original publication in this journal is cited, in accordance with accepted academic practice. No use, distribution or reproduction is permitted which does not comply with these terms.

frontiers in Aging Neuroscience

ORIGINAL RESEARCH
published: 31 May 2021
doi: 10.3389/fnagi.2021.650371

Cortical Structural Connectivity Alterations and Potential Pathogenesis in Mid-Stage Sporadic Parkinson's Disease

Xia Deng[1†], Zheng Liu[2†], Qin Kang[3†], Lin Lu[4†], Yu Zhu[3] and Renshi Xu[1,3]*

[1] Department of Neurology, The First Affiliated Hospital of Nanchang University, Nanchang, China, [2] Department of Neurology, The First Affiliated Hospital of Gannan Medical University, Ganzhou, China, [3] Department of Neurology, Jiangxi Provincial People's Hospital, The Affiliated People's Hospital of Nanchang University, Nanchang, China, [4] Department of Neurology, The First Affiliated Hospital of Guangzhou Medical University, Guangzhou, China

Many clinical symptoms of sporadic Parkinson's disease (sPD) cannot be completely explained by a lesion of the simple typical extrapyramidal circuit between the striatum and substantia nigra. Therefore, this study aimed to explore the new potential damaged pathogenesis of other brain regions associated with the multiple and complex clinical symptoms of sPD through magnetic resonance imaging (MRI). A total of 65 patients with mid-stage sPD and 35 healthy controls were recruited in this study. Cortical structural connectivity was assessed by seed-based analysis using the vertex-based morphology of MRI. Seven different clusters in the brain regions of cortical thickness thinning derived from the regression analysis using brain size as covariates between sPD and control were selected as seeds. Results showed that the significant alteration of cortical structural connectivity mainly occurred in the bilateral frontal orbital, opercular, triangular, precentral, rectus, supplementary-motor, temporal pole, angular, Heschl, parietal, supramarginal, postcentral, precuneus, occipital, lingual, cuneus, Rolandic-opercular, cingulum, parahippocampal, calcarine, olfactory, insula, paracentral-lobule, and fusiform regions at the mid-stage of sPD. These findings suggested that the extensive alteration of cortical structural connectivity is one of possible pathogenesis resulting in the multiple and complex clinical symptoms in sPD.

Keywords: Sporadic Parkinson's disease, magnetic resonance imaging, cortical structural connectivity, pathogenesis, brain

OPEN ACCESS

Edited by:
Shaomin Li,
Brigham and Women's Hospital and Harvard Medical School, United States

Reviewed by:
Jifeng Guo,
Central South University, China
Yi Guo,
Jinan University, China

****Correspondence:***
Renshi Xu
13767015770@163.com;
xurenshi@ncu.edu.cn

† These authors have contributed equally to this work

Received: *07 January 2021*
Accepted: *08 March 2021*
Published: *31 May 2021*

Citation:
Deng X, Liu Z, Kang Q, Lu L, Zhu Y and Xu R (2021) Cortical Structural Connectivity Alterations and Potential Pathogenesis in Mid-Stage Sporadic Parkinson's Disease. Front. Aging Neurosci. 13:650371. doi: 10.3389/fnagi.2021.650371

INTRODUCTION

Sporadic Parkinson's disease (sPD) is a neurodegenerative disorder, it is mainly caused by the progressive loss of dopaminergic neurons in the substantia nigra pars compacta projecting to the striatum. The damage of substantia nigra-striatum loops is believed to lead to the hallmarked motor dysfunctions of sPD including tremors, rigidity, bradykinesia, and postural instability (Jankovic, 2008; Göttlich et al., 2013). Apart from the substantia nigra-striatum loops, the deficit of other

Abbreviations: All abbreviations of names and coordinates of anatomical regions were cited from Anatomical Automatic Labeling of the Montreal Neurological Institute.

brain functions has been found in the different stages of sPD. These functional deficits in these brain regions result in multiple and complex clinical symptoms in sPD, which include behavioral disorders, cognitive dysfunction, and autonomic dysfunction such as orthostatic symptoms, incontinence, constipation, hyposmia, and/or dyssomnia (Göttlich et al., 2013; Khoo et al., 2013). However, the relational pathogenesis of brain area damage associated with these multiple and complex clinical symptoms of sPD still remains unclear.

Several neuroimage studies have assessed cortical morphometry using several different methods of magnetic resonance imaging (MRI) and revealed the existence of localized cortical atrophy in the early stages of sPD (Feldmann et al., 2008; Jubault et al., 2011; Gong et al., 2012; Göttlich et al., 2013; Xia et al., 2013; Chen et al., 2015). The motor functional connectivity of the posterior putamen, inferior parietal cortex, and striatum were examined and assessed in sPD patients, which revealed decreased and/or increased functional connectivity in several brain regions of sPD patients (Wu et al., 2009; Helmich et al., 2010; Hacker et al., 2012). A few studies have analyzed the patterns of cortical structural connectivity in sPD patients, and the partial results showed that several functional brain regions found abnormal alterations of cortical structural connectivity (Wu et al., 2009; Helmich et al., 2010; Hacker et al., 2012). However, the specific and typical alterations of cortical structural connectivity in sPD still needs further exploration. Up to now, these multiple and complex clinical symptoms of sPD cannot be completely explained by traditional pathogenesis such as a lesion of the simple typical extrapyramidal circuit between the striatum and substantia nigra, which need to be comprehensively investigated.

Cortical structural connectivity is currently extensively researched in multiple large-scale efforts worldwide, and leads to different definitions with respect to their connections as well as their elements. Perhaps the most promising avenue for defining the connection elements originates from the notion that the individual brain region maintains distinct connection profiles, such as long-range connectivity. These patterns of connectivity determine the functional properties of cortical regions and allow for their anatomical delineation and mapping (Tittgemeyer et al., 2018). The analysis of cortical structural connectivity can measure both global and local connectivity. Therefore, it can be used to assess global brain connectivity or local connectivity between the chosen brain regions (Castellanos et al., 2014; Irimia et al., 2014). Many neurological and psychiatric diseases can be considered as disconnection syndromes related to abnormal brain connectivity. Researchers expect to find and use altered brain connectivity metrics as disease biomarkers, pathological evidence, or treatment targets. For example, some studies have demonstrated specific changes in global and/or local brain connectivity in patients with Alzheimer's disease, schizophrenia, and focal brain lesions (Stam et al., 2007; Supekar et al., 2008; Gratton et al., 2012; Göttlich et al., 2013). In our previous MRI study, we also found that mid-stage sPD patients presented with reduced cortical thickness in several local clusters by applying the voxel-based morphometry (VBM) method (Deng et al., 2016). Therefore, we speculated that local reduced cortical thickness was possibly implicated in cortical atrophy and/or local cortical structural connectivity alteration in sPD patients (Apostolova and Thompson, 2007; Zarei et al., 2013; Irimia et al., 2014), which might be closely associated with the multiple and complex clinical symptoms and a potential pathogenesis basis of sPD. This study was to investigate the cortical structural connectivity alteration between the chosen cortex regions and potential pathogenesis of sPD through analyzing the alteration of cortical structural connectivity. It aimed to find new imaging alterations in functional magnetic resonance imaging (fMRI), which could explain the relationship between the alteration of cortical structural connectivity and potential pathogenesis of sPD.

In this study, we chose the brain regions of cortical thickness thinning derived from regression analysis using brain size as covariates. These brain regions were used as the seeds of the cortical connectivity assessment, because they were the most extensively altered brain regions and had the most representative cortical thickness thinning among the comparisons between sPD patients and controls (Deng et al., 2016). In total, the seeds consisted of 47 brain regions (**Supplementary Table 1**). A total of 67 mid-stage sPD patients and 35 healthy controls were recruited in this study. The alteration of their local cortical structural connectivity was assessed between the chosen brain regions according to 47 seed-based correlation analyses (SCA) regarding structural covariates using the VBM of MRI. Results revealed that a larger scale of local alteration of cortical structural connectivity occurred in mid-stage sPD. Our data suggested that the extensive lesion of local cortical structural connectivity was closely associated with the multiple and complex clinical symptoms of sPD, and was a potential pathogenesis of sPD.

MATERIALS AND METHODS

Participants

Participants were acquired from the First Affiliated Hospital of Nanchang University. A total number of 100 sPD patients were recruited for this study. In all of the sPD participants, sPD was diagnosed by three experienced neurologists, the severity of clinical symptoms was assessed according to the Unified Parkinson's Disease Rating Scale (UPDRS). Thirty-three patients were excluded due to the disqualification of clinical information or MRI data. Sixty-seven mid-stage sPD patients were included in this study based on a UPDRS Part III score of 34.11 ± 2.0 (part III; clinician-scored motor evaluation). All sPD patients were on medication (L-DOPA, agonists). Forty-five control participants were recruited. Ten control subjects were excluded due to disqualification of the clinical information or MRI data. The remaining 35 control subjects showed no sPD signs or any other neurological deficits according to the neurological examination. In order to precisely assess the classification of sPD course, we administered the assessment of modified Hoehn and Yahr and the UPDRS-III scale in sPD patients. The recruited mid-stage sPD patients had to present with all four major clinical signs including tremors, rigidity, bradykinesia, and postural instability, have a better dopaminergic reflection, and have modified Hoehn

and Yahr scale and UPDRS-III scale scores of 2.5–3 and 31–45, respectively. The brains of all subjects in this study had normal MRI images in both T1 and T2-weighted images. The relevant demographic and clinical information is summarized in **Supplementary Table 2**. All procedures have been approved by the ethical committee of the First Affiliated Hospital of Nanchang University and all subjects gave their written informed consent prior to participation. This study was performed in agreement with the Declaration of Helsinki.

MRI Data Acquisition

High-resolution structural MRI data were acquired from a 3.0 Tesla Siemens Tim Trio MRI scanner, participants were scanned at the Department of Radiology, the First Affiliated Hospital of Nanchang University using a three-dimensional T1-weighted MPRAGE sequence. The scanning parameters were as follows: TR/TE/TI: 1900/2.26/900 ms, flip angle: 9°, slice thickness: 1 mm, 176 slices, field of view 256 mm × 256 mm, acquisition matrix: 256 × 256, voxel size: 1 mm × 1 mm × 1 mm, 8-channels coil. Structural MRI sequences included T1-weighted 3D fast-spoiled gradient-recalled echo images. Other sequences including T2-weighted and FLAIR images were conducted in order to visualize and exclude focal lesions of the cortex or white matter (Deng et al., 2016).

Image Processing of Cortical Structural Connectivity Using Voxel-Based Morphometry (VBM)

All image processing was performed as per the previous protocol (Deng et al., 2016) and conducted in the State Key Laboratory of Cognitive Neuroscience and Learning and IDG/McGovern Institute for Brain Research, Beijing Normal University, China (Chen et al., 2015). Briefly, the CIVET pipeline was used to measure the cortical thickness and surface on VBM and corticometry. The native T1-weighted MRI images were first linearly aligned into the stereotaxic space and corrected for non-uniformity artifacts using the N3 algorithm (Tohka et al., 2004). The brain image results were then automatically segmented into the gray matter, the white matter, cerebrospinal fluid (CSF), and background by using a partial volume (PV) classification algorithm, in which a trimmed minimum covariance determinant method was applied for estimating the parameters of the PV effect model. The parameter β, controlling the relative strength of the Markov random field, was set to 0.1 (Kim et al., 2005). Next, the inner and outer gray matter surfaces were automatically extracted for each hemisphere using the constrained Laplacian-based automated segmentation with proximities (CLASP) algorithm (Lerch and Evans, 2005). The individual surfaces were further aligned with a surface template to allow comparisons across subjects at corresponding vertices. The cortical surfaces of both the internal and external cortex including 40,962 vertices were automatically extracted by CLASP algorithm.

The cortical surface was inversely transformed into the native space. Cortical thickness was measured between two surfaces on 40,962 vertices per hemisphere between the linked distance in the native space. Cortical thickness was detected by the link method which measured the Euclidean distance between the linked vertices of internal and external surfaces (Lyttelton et al., 2009). The middle cortical surfaces, defined by the geometric center between the internal and external cortical surfaces, were used to calculate the cortical surfaces in the native space. Both thickness and surface maps were further blurred using a 30 mm surface-based smooth diffusion kernel. Vertex-wise sphere-to-sphere warped non-linear surface registration was conducted into the unbiased iterative surface template. The thickness information on native surfaces was transformed into a template after diffusion smoothing by a 20 mm full-width half maximum to increase the signal to noise ratio and improve the detection ability of population changes using the surface registration (Chung et al., 2003). All cortical image processing was conducted by investigators blinded to the patient demographics, disease, and controls. Seven different clusters of cortical thickness thinning derived from the regression analysis using the brain size as covariates in sPD were selected as seeds. Cortical structural connectivity was investigated between the chosen brain regions according to information from 47 SCA regarding structural covariates using the VBM of MRI. The VBM, a technique based on the delineation of the cortex and normalization, can assess cortical atrophy including cortical volume, thickness, surface, and density (Ashburner and Friston, 2000; Deng et al., 2016). These methods have been validated using both manual measurements (Kabani et al., 2001) and a population simulation (Lyttelton et al., 2009), and have been widely applied. The protocol was similar with that of our previous study (Deng et al., 2016).

Statistical Analysis

We used one-way analysis of variance (ANOVA) with *post hoc* Bonferroni correction to examine the differences in age, education, sPD duration, mini mental state examination (MMSE), Hasegawa dementia scale revised (HDS-R), the forward digit span task (DF), the backward digit span task (DB), semantic verbal fluency test (SVFT), self-rating depression scale (SDS), Hamilton depression scale-17 (HAMD17), Hamilton depression scale-24 (HAMD 24), clock drawing task (CDT), clinical dementia rating (CDR), and the mean cortical thickness values of regions of interest (ROI) between sPD and control groups. A chi-squared test was used to assess the differences in the gender distribution between groups (Deng et al., 2016).

All cortical analyses were performed by the State Key Laboratory of Cognitive Neuroscience and Learning and IDG/McGovern Institute for Brain Research, Beijing Normal University, China. The cortical statistical analysis was performed at a vertex-wise level using an analysis of covariance (ANCOVA) with brain size and cortical surface as covariates and no covariates for comparisons among groups. For all cortical analyses, in order to correct for multiple vertex-wise comparisons, a random field theory (RFT)-based method was applied at the cluster level (Taylor and Adler, 2003), and the cortical clusters surviving a family-wise error (FWE)-corrected $p < 0.05$ were considered as significant. All statistical procedures were implemented

using SurfStat[1]. All names of anatomical regions were cited from Anatomical Automatic Labeling (AAL) of the Montreal Neurological Institute (MNI). The significance difference and correlation maps were created as applicable. The maps were corrected for multiple comparisons with permutation analysis at a threshold of $p < 0.05$. The values of cortical thickness and surface were expressed as mean ± SD. A 565comparison of uncorrected cortical thickness between sPD and control was also performed by Student's t-test with a significance of $p \leq 0.05$. The uncorrected $p \leq 0.05$ was the p value that was not corrected by the FWE, the corrected $p \leq 0.05$ was the p value that was corrected by the FWE. The cortical structural connectivity was expressed by mm, a comparison of cortical structural connectivity between sPD and control was also performed by Student's t-test with a significance of $p \leq 0.05$.

RESULTS

Clinical Characteristics of Mid-Stage sPD

A total of 67 patients with mid-stage sPD and 35 healthy controls were included in the final investigation and analysis. The details of demographics and disease-related characteristics in both sPD and healthy controls are shown in **Supplementary Table 2**. The average modified Hoehn and Yahr scale for mid-stage sPD patients was 2.7 ± 0.3, their total UPDRS score (sum of parts I–IV) was 83.17 ± 6.34 and their UPDRS part III score (motor examination) was 34.11 ± 2.0 (**Supplementary Table 2**).

Brain Regions of Abnormal Cortical Structural Connectivity Between sPD Patients and Control Group

The brain regions of thinning thickness in the regression analysis using brain size as a covariate were used as the chosen seeds, according to information from 47 SCA regarding structural covariates, cortical structural connectivity between the chosen brain regions was analyzed using the VBM of MRI (**Supplementary Table 1** and **Figures 1–7A**). Results revealed that an extensive alteration in cortical structural connectivity occurred in mid-stage sPD patients, the brain regions of abnormal cortical structural connectivity in the mid-stage sPD patients versus the controls are summarized in **Supplementary Tables 3–9**. Among them, the brain regions of significantly altered cortical structural connectivity compared with the cortical structural connectivity uncorrected by FWE between sPD and control in seeds 1–7 included the right temporal-pole-sup, the postcentral, the angular, the Rolandic-oper, the cuneus, the cingulum-ant, the occipital-sup, -mid, and –inf, the precuneus and the tectus regions, the left supramarginal, the sup-orb and the temporal-inf regions, the bilateral frontal-sup and -mid, the frontal-sup-medial, the inf-tri, the inf-oper, the inf- and mid-orb, the supp-motor-area, the precentral, the temporal-sup and -mid, the Heschl, the parahippocampal, the parietal-inf, the calcarine, the lingual, and the fusiform regions (**Figures 1–7B**). The brain regions of significantly altered cortical structural connectivity compared with the cortical structural connectivity corrected by FWE between sPD and control in seed 1 included the right frontal-sup, the mid-, inf-, and sup-orb, the frontal-sup-medial, supp-motor-area regions; the temporal-sup and Heschl regions; the left sup- and mid-tri regions, the paracentral-lobule and the insula regions; the bilateral inf-tri, the inf-oper, the Rolandic-oper, the precentral, the supramargina, the postcentral, the cingulum-post and -mid, and the precuneus regions (**Supplementary Table 3** and **Figure 1C**). Alterations in seed 2 included the right sup- and mid-medial, the precentral, the inf- and mid-cingulum regions; the left frontal-sup, the mid-orb, the rectus, the cingulum-ant, the temporal-pole-mid, the inf- and mid-parietal, and the supramarginal regions; the bilateral frontal-sup-medial, the parahippocampal, the calcarine, the lingual, the fusiform, the precuneus, the cuneus, the occipital-sup, and the postcentral regions (**Supplementary Table 4** and **Figure 2C**). Alternation in seed 3 included the right frontal mid-oper, inf- and mid-orb, inf-tri, the temporal-pole-sup, the parietal-inf, the angular, the supramarginal, the occipital-mid, the Rolandic-oper, the postcentral, the precentral, the paracentral-lobule and the cingulum-ant regions; the left insula and the cuneus regions; the bilateral inf-oper, the temporal-sup, the inf and mid, the Heschl, the cingulum-post and -mid, and the precuneus regions (**Supplementary Table 5** and **Figure 3C**). Alterations in seed 4 included the right parietal-sup, the occipital-sup, the cingulum-post, the parietal-mid and -ant, the precuneus, the cuneus, the rectus, and the olfactory regions; the left temporal-sup and -mid, the Rolandic-oper, the postcentral, and the occipital-inf regions; the bilateral frontal-sup and -mid, the frontal-sup-medial, the mid-, sup-, and inf-orb, the inf-tri, the inf-oper, the supp-motor-area, the precentral, the calcarine, the lingual, and the fusiform regions (**Supplementary Table 6** and **Figure 4C**). Alterations in seed 5 included the right temporal-sup, the cingulum-mid, the cingulum-post, and the precuneus regions; the left frontal-sup and -mid, the frontal-sup-medial, the temporal-pole-mid, -sup, and -inf, the temporal-mid, the supp-motor-area, and the parietal-inf regions; the bilateral frontal-inf-oper, the sup-, inf-, and mid-orb, the inf-tri, the Heschl, the supramarginal, the cingulum-ant, the rectus, the insula, the olfactory, the Rolandic-oper, the postcentral, and the precentral regions (**Supplementary Table 7** and **Figure 5C**). Alternations in seed 6 included the right postcentral and paracentral-lobule regions; the left frontal-mid, the temporal-pole-sup and -mid, the occipital-mid, and the calcarine regions; the bilateral frontal-sup, the parietal-sup, the occipital-sup, the precuneus, the cuneus, the precentral, the parahippocampal, the lingual, and the fusiform regions (**Supplementary Table 8** and **Figure 6C**). Alterations in seed 7 included the right frontal-sup and -mid, the frontal-sup-medial, the mid-orb, the cingulum-mid and -ant, and the rectus regions; the bilateral occipital-sup, -inf, and -mid, the calcarine, the lingual, the precuneus, and the cuneus regions (**Supplementary Table 9** and **Figure 7C**). In general, our result showed that the alteration of cortical structural connectivity comprehensively occurred in the frontal, limbic, temporal, parietal, and occipital lobes, especially in the frontal and limbic lobes, and to smaller

[1]http://www.math.mcgill.ca/keith/surfstat/

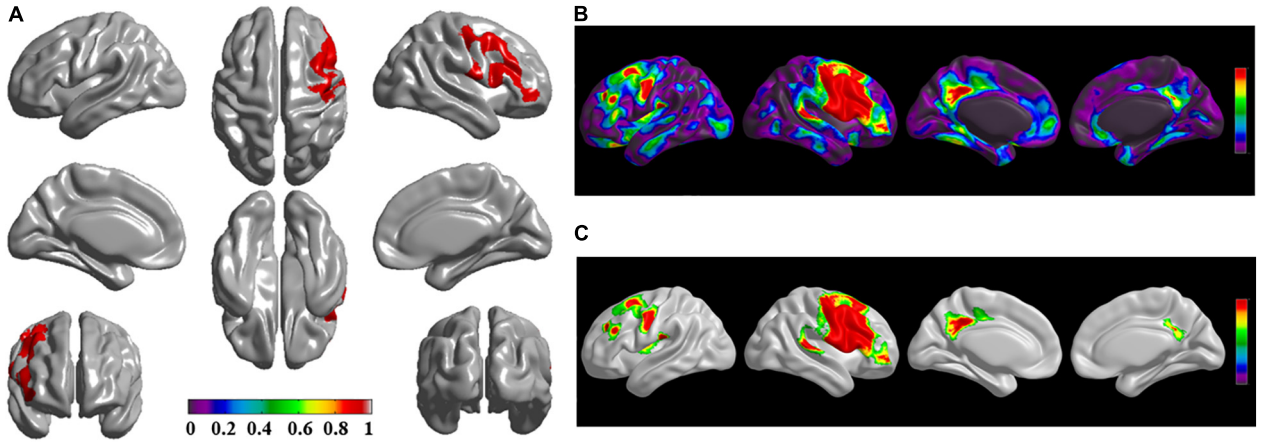


FIGURE 1 | The significantly altered brain regions of cortical structural connectivity in the sPD brain based on seed 1. **(A)** The brain regions of seed 1, the red brain regions represent the cortical thickness thinning regions. **(B)** The significantly altered brain regions in the F-map based on seed 1, the red, and green brain regions represent the brain regions of significant cortical structural connectivity alteration that were not corrected by the family-wise error (FWE). **(C)** The significantly altered brain regions after FWE correction based on seed 1, the red and green brain regions represent the brain regions of significant cortical structural connectivity alteration that were corrected by the FWE.

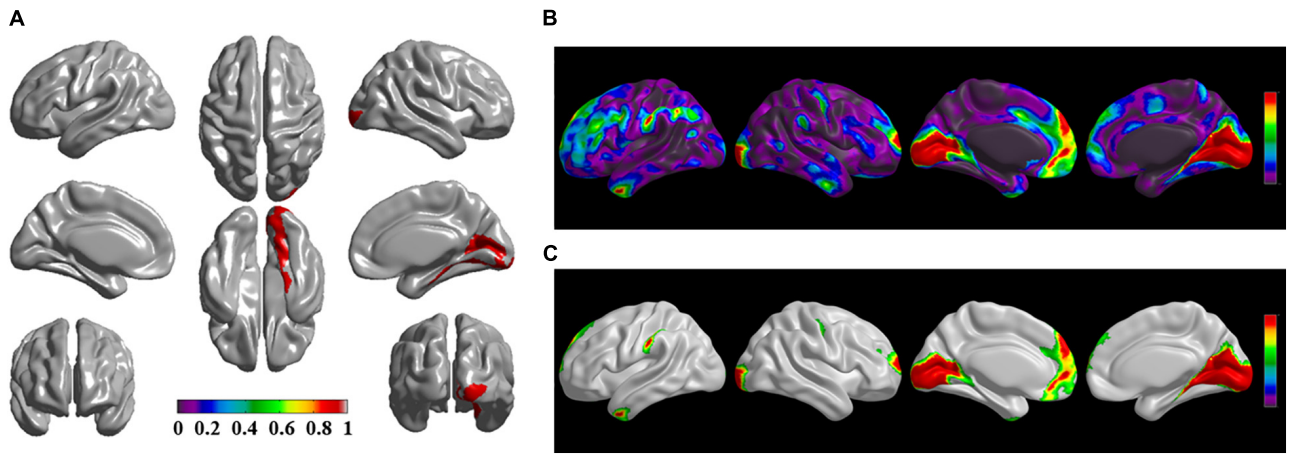


FIGURE 2 | The significantly altered brai n regions of cortical structural connectivity in the sPD brain based on seed 2. **(A)** The brain regions of seed 2, the red brain regions represent the cortical thickness thinning regions. **(B)** The significantly altered brain regions in the F-map based on seed 2, the red, and green brain regions represent the brain regions of significant cortical structural connectivity alteration that were not corrected by the FWE. **(C)** The significantly altered brain regions after FWE correction based on seed 2, the red and green brain regions represent the brain regions of significant cortical structural connectivity alteration that were corrected by the FWE.

extent in the temporal, parietal, and occipital lobes. The majority of alteration regions were symmetrical in both the right and left brain, while the minimum occurred only in the left brain.

DISCUSSION

The alteration of cortical structural connectivity might be one sign of cortex impairment. For this reason, we studied the alteration of cortical structural connectivity between the chosen brain regions of sPD and the control groups. Results showed that extensive alteration in cortical structural connectivity in many brain regions occurred in mid-stage sPD (**Figures 1–7B,C**). The brain regions of significantly altered cortical structural connectivity mainly focused on the following brain regions: the frontal cortex including the bilateral frontal-superior and -middle, the inferior-operculum, the inferior-pars triangularis, the inferior- and superior-orbitofrontal, the frontal-superior-medial, the precentral, the rectus, and the supplementary-motor-area cortex, and the right middle-orbitofrontal cortex regions. The temporal cortex alterations included the bilateral temporal-pole-superior, the temporal-superior, -middle, and -inferior, and the Heschl cortex and the left temporal-pole-middle cortex regions. The parietal cortex alterations included the bilateral parietal-inferior and -superior, the supramarginal, the postcentral and the precuneus cortex, the

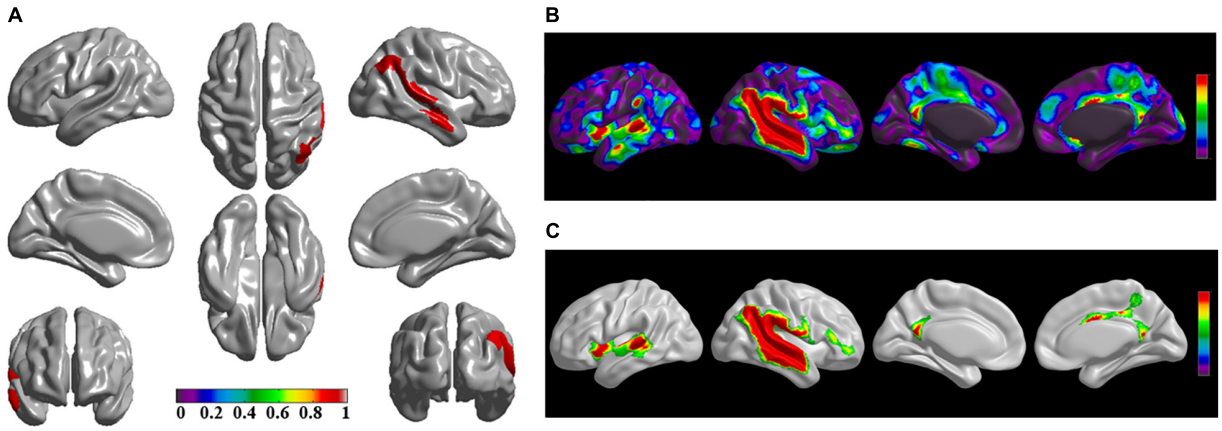


FIGURE 3 | The significantly altered brain regions of cortical structural connectivity in the sPD brain based on seed 3. **(A)** The brain regions of seed 3, the red brain regions represent the cortical thickness thinning regions. **(B)** The significantly altered brain regions in the F-map based on seed 3, the red, and green brain regions represent the brain regions of significant cortical structural connectivity alteration that were not corrected by the FWE. **(C)** The significantly altered brain regions after FWE correction based on seed 3, the red and green brain regions represent the brain regions of significant cortical structural connectivity alteration that were corrected by the FWE.

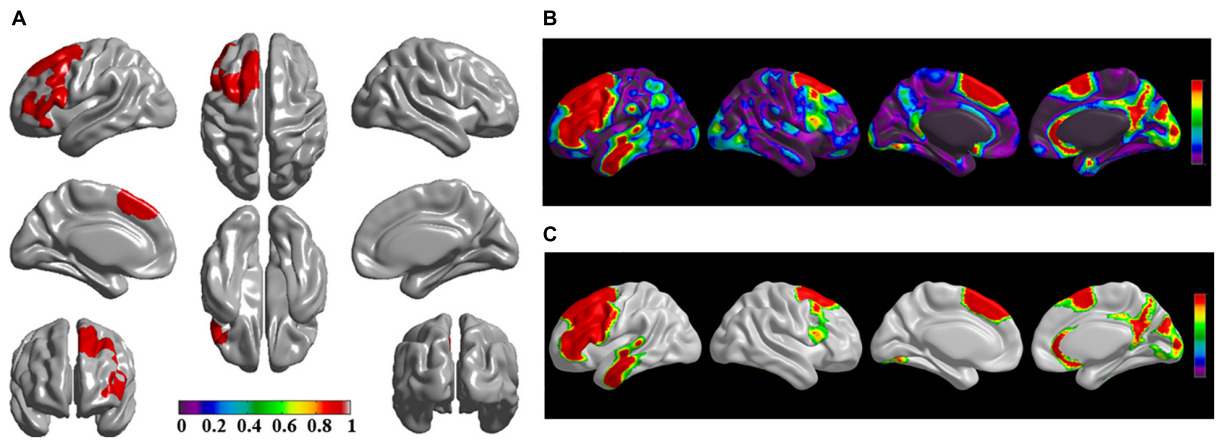


FIGURE 4 | The significantly altered brain regions of cortical structural connectivity in the sPD brain based on seed 4. **(A)** The brain regions of seed 4, the red brain regions represent the cortical thickness thinning regions. **(B)** The significantly altered brain regions in the F-map based on seed 4, the red, and green brain regions represent the brain regions of significant cortical structural connectivity alteration that were not corrected by the FWE. **(C)** The significantly altered brain regions after FWE correction based on seed 4, the red and green brain regions represent the brain regions of significant cortical structural connectivity alteration that were corrected by the FWE.

right postcentral-anterior, and the angular cortex regions. The occipital cortex alterations included the bilateral occipital-superior, -inferior, and -middle, the lingual, the cuneus, and the Rolandic-operculum cortex regions. The limbic cortex alterations included the bilateral cingulum-posterior, -middle, and -anterior, the parahippocampal and the calcarine cortex regions. Other cortex alterations included the bilateral olfactory, the insula, the paracentral-lobule, and the fusiform cortex regions (**Figures 1–7B,C**).

The frontal-sup (superior frontal gyrus) controls self-awareness and laughter (Fried et al., 1998; Goldberg et al., 2006), alteration of cortical structural connectivity in that area might be closely associated with coordination movement disorder and the mask face syndrome in sPD. The frontal-inf-oper (opercular part of the inferior frontal gyrus), also known as BA 44, comprises Broca's area together with the left-hemisphere BA 45, and is involved in semantic tasks. BA 44 controls phonological and syntactic processing. A recent neuroimage study showed that BA 44 was involved in selective response suppression in go/no-go tasks, therefore, it was believed to play an important role in the suppression of response tendencies. BA 44 was also demonstrated to be related to hand movements (Rizzolatti et al., 2002; Forstmann et al., 2008). Damage to the opercular part of the inferior frontal gyrus caused by the alteration of cortical structural connectivity might generate semantic, phonological, and syntactic processing dysphasia, and a coordination movement disorder in the hands such as tremors and bradykinesia in sPD.

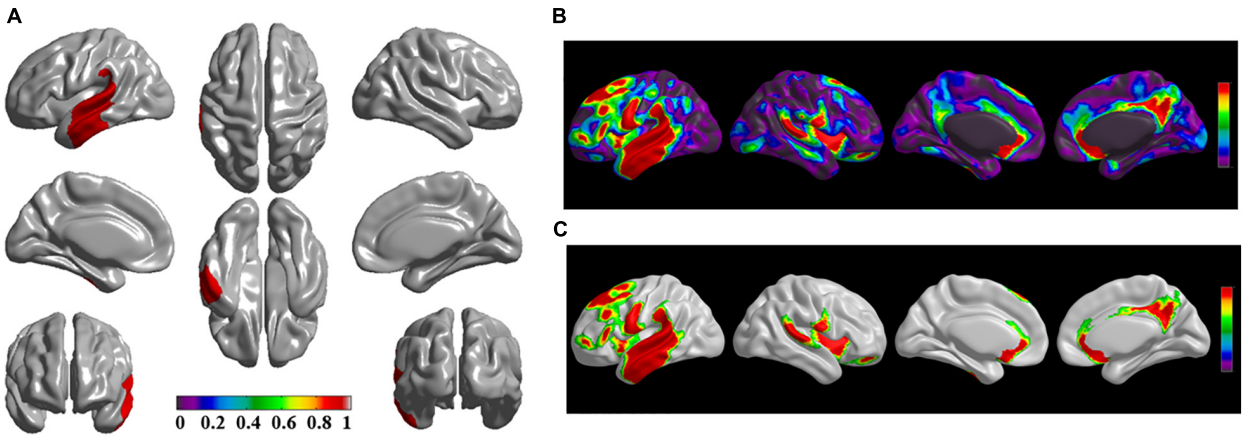


FIGURE 5 | The significantly altered brain regions of cortical structural connectivity in the sPD brain based on seed 5. **(A)** The brain regions of seed 5, the red brain regions represent the cortical thickness thinning regions. **(B)** The significantly altered brain regions in the F-map based on seed 5, the red, and green brain regions represent the brain regions of significant cortical structural connectivity alteration that were not corrected by the FWE. **(C)** The significantly altered brain regions after FWE correction based on seed 5, the red and green brain regions represent the brain regions of significant cortical structural connectivity alteration that were corrected by the FWE.

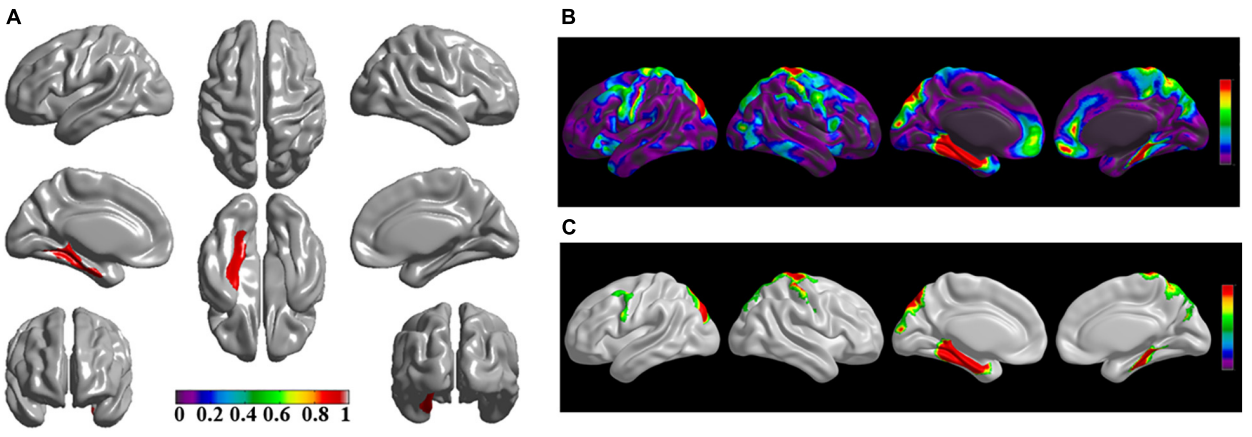


FIGURE 6 | The significantly altered brain regions of cortical structural connectivity in the sPD brain based on seed 6. **(A)** The brain regions of seed 6, the red brain regions represent the cortical thickness thinning regions. **(B)** The significantly altered brain regions in the F-map based on seed 6, the red, and green brain regions represent the brain regions of significant cortical structural connectivity alteration that were not corrected by the FWE. **(C)** The significantly altered brain regions after FWE correction based on seed 6, the red and green brain regions represent the brain regions of significant cortical structural connectivity alteration that were corrected by the FWE.

The frontal-mid (middle frontal gyrus) consists of Brodmann areas 9, 10, and 46. Brodmann area 9 is involved in short term memory (Babiloni et al., 2005), verbal fluency (Abrahams et al., 2003), error detection (Chevrier et al., 2007), auditory verbal attention (Nakai et al., 2005), inductive reasoning (Goel et al., 1997), attributing intention (Fink et al., 1999), sustained attention counting a series of auditory stimuli (Shallice et al., 2008), evaluates recency (Zorrilla et al., 1996), overrides automatic responses (Kübler et al., 2006), infers the intention of others (Goel et al., 1995), and comprehends spatial imagery (Knauff et al., 2002). The middle frontal gyrus on the left hemisphere is found to be at least partially responsible for empathy (Farrow et al., 2001), idioms (Maddock and Buonocore, 1997; Lauro et al., 2008), processing pleasant and unpleasant emotional scenes (Lane et al., 1997), self-criticism, and attention to negative emotions (Longe et al., 2010; Kerestes et al., 2012). The middle frontal gyrus on the right hemisphere is involved in attributing intention (Brunet et al., 2000), the theory of mind (Gallagher et al., 2002), suppressing sadness (Kaur et al., 2005), working memory (Zhang et al., 2003), spatial memory (Slotnick and Moo, 2006), recognition (Ranganath et al., 2003), recall (Düzel et al., 2001), the emotions of others (Bermpohl et al., 2006), planning (Fincham et al., 2002), calculation (Rickard et al., 2000), the semantic and perceptual processing of odors (Royet et al., 1999), and attention to positive emotions (Kerestes et al., 2012)[2]. The alteration of cortical structural connectivity in Brodmann area

[2]https://en.wikipedia.org/wiki/Brodmann_area_9

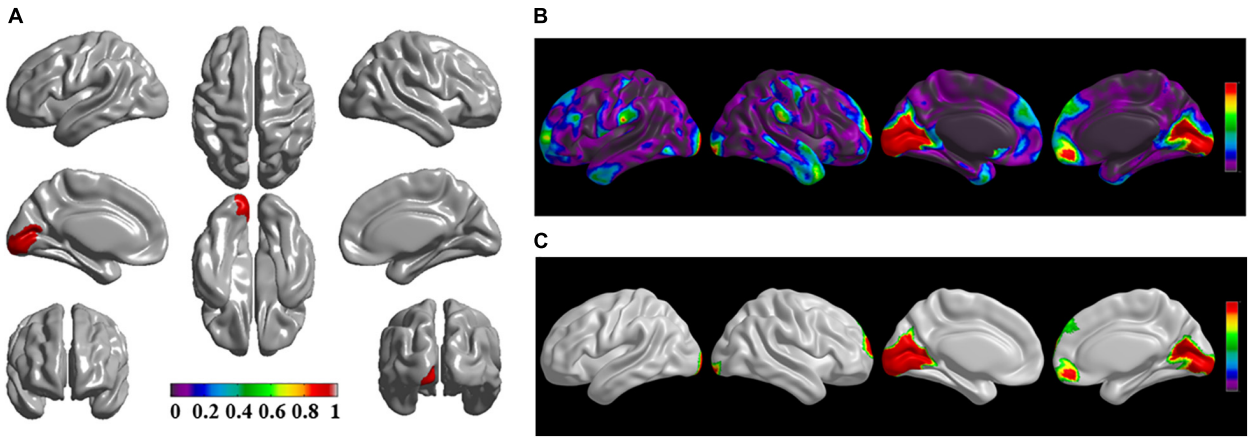


FIGURE 7 | The significantly altered brain regions of cortical structural connectivity in the sPD brain based on seed 7. **(A)** The brain regions of seed 7, the red brain regions represent the cortical thickness thinning regions. **(B)** The significantly altered brain regions in the F-map based on seed 7, the red, and green brain regions represent the brain regions of significant cortical structural connectivity alteration that were not corrected by the FWE. **(C)** The significantly altered brain regions after FWE correction based on seed 7, the red and green brain regions represent the brain regions of significant cortical structural connectivity alteration that were corrected by the FWE.

9 might result in lesions that affect memory, spatial imagery, auditory, intention, emotion, recognition, planning, calculation, and olfactory processes, leading to the corresponding multiple and complex clinical symptoms in sPD. Brodmann area 10's function is poorly understood. It may perform a domain general function in scheduling operations in working memory, episodic memory, and multiple-task coordination (Andrews et al., 2011). Brodmann area 46 plays a role in sustaining attention and in working memory (Buckner, 1996). The alteration of cortical structural connectivity in Brodmann areas 10 and 46 might damage memory, coordination, and attention, and generate the decline of working and episodic memory, multiple-task coordination, and sustaining attention in sPD.

The frontal-inf-tri (the pars triangularis of the inferior frontal gyrus), also known as Brodmann area 45, comprises Broca's area together with BA 44 and is active in semantic tasks, such as semantic decision tasks determining whether a word represents an abstract or a concrete entity and generation tasks generating a verb associated with a noun (Gabrieli et al., 1998; Kringelbach, 2005). Damaged cortical structural connectivity of this brain region might produce several types of dysphasia such as those described above in sPD.

The orb (orbitofrontal cortex, OFC) is among the least understood regions of the human brain, but it has been proposed that the OFC is involved in sensory integration, represents the affective value of reinforcers, decision-making and expectation, and adaptive learning (Talati and Hirsch, 2005). Sensing errors, abnormal emotions, and learning ability decline may result from cortical structural connectivity lesions in this area in sPD. The frontal-sup-medial (superior medial frontal gyrus) plays a role in executive mechanisms (Penfield and Welch, 1951). The precentral (precentral gyrus) is the primary motor cortex and controls the voluntary movement of the body. The rectus (or straight gyrus) may be associated with sexual desire. The supp-motor-area (supplementary motor area) controls postural stability during standing or walking, coordinates the temporal sequences of actions, bimanual coordination, and the initiation of internally generated as opposed to stimulus-driven movement (Roland et al., 1980; Halsband et al., 1994; Shima and Tanji, 1998; Serrien et al., 2002; Radua et al., 2010). The alteration of cortical structural connectivity in these brain regions might result in executive and control disorders of voluntary body movement, sexual dysfunction, abnormality of postural and walking stability, and coordination deficits, respectively, in sPD.

The temporal-sup (superior temporal gyrus) is involved in the perception of emotions from facial stimuli (Bigler et al., 2007), auditory processing, language function, and social cognition processes (Dupont, 2002), and is linked to the ability of processing information of the many changeable characteristics of the face. A lesion affecting cortical structural connectivity in this area might be related with the mask face syndrome, a decrease in auditory recognition, dysphasia, cognition impairment, and prosopagnosia in sPD.

The temporal-pole is important in autobiographical memory including taste and olfaction, face recognition, the visual discrimination of two-dimensional pictures, and the mnemonic functions of matching and learning (Acheson and Hagoort, 2013). Dysfunction caused by damaged cortical structural connectivity in these brain regions would generate disorders of taste and olfactory sense, visual recognition deficit, and learning dysfunction in sPD patients.

The exact function of the temporal-mid (middle temporal gyrus) is unknown, but it has been connected with the recognition of known faces and accessing the meaning of words while reading (Hickok et al., 2003). The temporal-inf (inferior temporal gyrus) is an essential region in recognizing patterns, faces, and objects. If cortical structural connectivity is damaged in these brain regions, it would result in the clinical significance of prosopagnosia, alexia, a deficit of semantic memory, and agnosia in sPD.

The temporal-sup (superior temporal gyrus) is involved in the perception of emotions from facial stimuli, auditory processing, and the function of vocabulary language, and potentially develops a sense of language. This region is an important structure in the pathway between the amygdala and prefrontal cortex and is involved in social cognition processes (Yagishita et al., 2008; Hartwigsen et al., 2010). A lesion in this area affecting cortical structural connectivity would produce the mask face syndrome, auditory decline, vocabulary-impaired dysphasia, and the obstacle of social cognition in sPD patients.

The Heschl gyrus (transverse temporal gyrus) is the first cortical structure to process incoming auditory information. The parietal-inf (inferior parietal lobule) is divided into the supramarginal gyrus and the angular gyrus, and is involved in the perception of emotions from facial stimuli, the interpretation of sensory information, and is concerned with language, mathematical operations, and body image (Bigler et al., 2007). The supramarginal gyrus interprets tactile sensory data and is involved in the perception of space and limb location. It also is involved in identifying the postures and gestures of other people (Lacey et al., 2012). The angular gyrus is the part of the brain associated with complex language functions (i.e., reading, writing, and the interpretation of what is written) (Koenigs et al., 2009). The parietal-sup (superior parietal lobule) contains Brodmann areas 5 and 7, is involved in spatial orientation, and receives a great deal of visual input as well as sensory input from the hands (Kjaer et al., 2002; Kamali et al., 2014a,b). The postcentral gyrus is the location of the primary somatosensory cortex. The precuneus gyrus is involved in self-consciousness (Fletcher et al., 1996; Lou et al., 2004), episodic memories, and visuospatial imagery (Cavanna and Trimble, 2006; Valyear et al., 2006). Lesions affecting cortical structural connectivity in these regions produce characteristic symptoms including an auditory lesion, the mask face syndrome, agraphesthesia, astereognosia, hemihypesthesia, alexia, agnosia, logagraphia, the loss of vibration, proprioception, and fine touch, disorder of episodic memories, visuospatial imagery, and hemineglect in sPD patients.

The occipital (occipital gyrus) is divided into several functional visual areas. Each visual area contains a full map of the visual world. The first functional area is the primary visual cortex. It contains a low-level description of local orientation, spatial-frequency, and color properties within small receptive fields. The primary visual cortex projects to the occipital areas of the ventral stream (visual area V2 and visual area V4), and the occipital areas of the dorsal stream (visual area V3, visual area V5, and the dorsomedial area). The ventral stream is known for processing the"wha" in vision, while the dorsal stream handles the "where/how" (Hadland et al., 2003; Bridge, 2011; Wandell and Winawer, 2011). The cuneus (Brodmann area 17) receives visual information from the contralateral superior retina, representing the inferior visual field. The lingula receives information from the contralateral inferior retina, representing the superior visual field (Wandell and Winawer, 2011). Occipital lesions resulting in the alteration of cortical structural connectivity could cause visual hallucinations, color agnosia, and movement agnosia in sPD patients. The Rolandic-oper (post-central operculum or occipital operculum) is responsible for light touch, pain and visceral sensation, and tactile attention (Wandell and Winawer, 2011). The cingulum (cingulate cortex) is an integral part of the limbic system and is involved in emotion formation and procession (Cingulate binds learning, 1997), learning (Stanislav et al., 2013), and memory (Takahashi et al., 2002; Kozlovskiy et al., 2012). It also plays a role in executive function and respiratory control. The parahippocampal (parahippocampal gyrus) plays an important role in the encoding and retrieval of memory (Spaniol et al., 2009; Simmons et al., 2013). The calcarine is the primary visual cortex. The olfactory (olfactory bulb) is involved in the sense of smell. The insula (insular cortex) is involved in consciousness and plays a role in diverse functions usually linked to emotion or the regulation of the body's homeostasis (Bramão et al., 2010; Gasquoine, 2014). The paracentral-lobule controls the motor and sensory innervations of the contralateral lower extremities. It is also responsible for the control of defecation and urination. The fusiform is linked to various neurological functions such as the processing of color information (Schwarzlose et al., 2005), face and body recognition (Carreiras et al., 2014), and word recognition (Sled and Pike, 1998). Lesions affecting the alteration of cortical structural connectivity in these brain regions were speculated to be associated with a series of neurological phenomena in sPD patients, such as abnormal synesthesia including abnormal light touch, pain, and visceral sensation, dyslexia, prosopagnosia, various visual disorders, autonomic nervous disorders like the disturbance of respiration, body homeostasis, defecation and urination, smell decline, and to a different extent the impairment of emotion, learning, and memory.

Through reviewing the functions of brain regions of significantly altered cortical structural connectivity in sPD, our results revealed that the functional defect of these regions might result in a series of clinical symptoms in mid-stage sPD. Such as the motor symptoms of bradykinesia, a movement coordination deficit, the mask face syndrome, and gait and postural instability. The non-motor symptoms included various disorders of speech, cognition, recognition, emotion, learning, and memory, and to a different extent impairments of smell, taste, auditory, visual, light touch, and pain sensations. Autonomic nervous dysfunctions include abnormal defecation and urination. There would also be a decline in learning, memory, and attention, dysphasia, alexia, agnosia, logagraphia, sexual dysfunction, and so on in sPD patients. The major functions in the regions of significantly altered cortical structural connectivity are strongly related to the generation of multiple and complex clinical symptoms in mid-stage sPD, especially complex non-motor symptoms. The alteration of extensive cortical structural connectivity may have resulted in multiple and complex clinical symptoms in our patients, which suggests that a series of motor and non-motor symptoms in the sPD patients may be derived from the impairment of different brain regions in mid-stage sPD, such as the alteration of cortical structural connectivity. Our results demonstrated that the above described brain regions of significantly altered cortical structural connectivity might result

in the impairment of their functions because of cortical damage which led to the clinical-related symptoms in sPD.

The resting-state functional connectivity alteration of the putamen and internal globus pallidus is associated with speech impairment in sPD patients (Manes et al., 2018). This clinically cognitive impairment was related to aberrant intrinsic activity and connectivity within the posterior cingulate, inferior parietal cortex, parahippocampus, entorhinal cortex, sensorimotor cortex (primary motor, pre/post-central gyrus), basal ganglia (putamen, caudate), and posterior cerebellar lobule VII in an sPD patient (Harrington et al., 2017). Up to date, a few investigations into levodopa-induced dyskinesia (LID) have focused on using fMRI. These studies identified the alterations in the brain network activity related to the onset and severity of LID. It was clear from these studies that the LID was associated with the bi-directional altered neuronal firing patterns between the basal ganglia and the neocortex, which led to the overactivation of frontal cortical areas, particularly in the motor, pre-motor, and prefrontal cortices (Cerasa et al., 2012; Cole et al., 2013; Esposito et al., 2013). The fMRI studies consistently demonstrated a linear relationship between the LID and the functional activity, shape, volume, or thickness of brain gray matter (Takeuchi et al., 2010; Zatorre et al., 2012; Fauvel et al., 2014). Although the pathogenesis of sPD symptoms has been looked into using fMRI in the past, the pathogenesis of the symptoms of sPD have not been completely understood yet and are awaiting further deep study.

In our study, we found that the brain regions of significantly altered cortical structural connectivity in mid-stage sPD extensively involved the frontal, temporal, parietal, occipital, and limbic lobe. The extensive alterations of cortical structural connectivity can explain a lot of the multiple and complex symptoms including a few motor and non-motor symptoms in mid-stage sPD. For example, the coordination movement disorder of the face, hands, and body, the abnormality of postural and walking stability (the frontal lobe), depression (the frontal, temporal, and limbic lobe), anxiety (the frontal, temporal, and limbic lobe), dyssomnia (the limbic lobe), cognitive impairment (the frontal and temporal lobe), memory decline (hippocampus), dysfunction of the autonomic nervous system (the parietal lobe), and visual spatial disorder (the occipital lobe). In general, our study provided fMRI evidence conferring that the pathological alteration of brain impairment contributed to some clinical symptoms of sPD. In addition, our study also provided a potential theory of pathogenesis for the multiple and complex clinical symptoms of sPD.

LIMITATIONS

Our study contained a few limitations, such as the small size of the sample, no direct analysis for disease symptom-related measures, and that only a single center was used. We did not perform direct correlation analyses for the potential relationship between brain alterations and clinical symptoms, and only indirectly speculated about their relationship through analyzing the brain function of cortical structural connectivity alteration.

CONCLUSION

In summary, our data suggested that the extensive alteration of cortical structural connectivity in mid-stage sPD patients resulted in the dysfunction of corresponding brain regions, generating a series of multiple and complex clinical symptoms. In addition, this study also provided neuroimage information for observing the distributed features of abnormal cortical alteration, understanding the relationship between the brain morphological abnormalities and the clinical symptoms, and reported some novel pathological lesions of the brain and the potential pathogenesis in mid-stage sPD patients. Furthermore, our study identified that the alteration of local cortical structural connectivity is one factor of cortex impairment in mid-stage sPD. Hence, the alteration of local cortical structural connectivity might be used as a diagnostic biomarker for sPD clinical symptoms.

DATA AVAILABILITY STATEMENT

The original contributions presented in the study are included in the article/**Supplementary Material**, further inquiries can be directed to the corresponding author.

ETHICS STATEMENT

The studies involving human participants were reviewed and approved by the ethical committee of the First Affiliated Hospital of Nanchang University and all participants gave their written informed consent prior to participate in the study. The study was performed in agreement with the Declaration of Helsinki.

AUTHOR CONTRIBUTIONS

RX and XD conceived and designed the experiments, contributed reagents, materials, analysis tools, wrote the manuscript, and processed the figures. XD, ZL, QK, LL, and YZ performed the experiments and analyzed the data. All authors were involved in the drafting, critical revision, final approval of the manuscript for publication, and agreed to be accountable for all aspects of the work in ensuring that questions related to the accuracy or integrity of any part of the work are appropriately investigated and resolved.

FUNDING

This work was supported by grants from the National Natural Science Foundation of China (30560042, 81160161, and 81360198), the Education Department of Jiangxi Province (GJJ13198 and GJJ170021), the Jiangxi Provincial Department of Science and Technology [(2014)-47, 20142BBG70062 and 20171BAB215022], the Health and Family Planning Commission of Jiangxi Province (20181019), and the Jiangxi Provincial

Department of Science and Technology Gan Po Elite 555 [Jiangxi Finance Elite Education refers to (2015) 108]. The funder had no role in study design, data collection and analysis, decision to publish, or preparation of the manuscript.

ACKNOWLEDGMENTS

We thank all volunteers and patients for their participation in our study. We also thank our colleagues for help with patient recruitment, the staff at the Functional Neuroimaging Unit at the First Affiliated Hospital of Nanchang University for technical assistance, and the State Key Laboratory of Cognitive Neuroscience and Learning and IDG/McGovern Institute for Brain Research, Beijing Normal University for data processing.

SUPPLEMENTARY MATERIAL

The Supplementary Material for this article can be found online at: https://www.frontiersin.org/articles/10.3389/fnagi.2021.650371/full#supplementary-material

REFERENCES

Abrahams, S., Goldstein, L. H., Simmons, A., Brammer, M. J., Williams, S. C., Giampietro, V. P., et al. (2003). Functional magnetic resonance imaging of verbal fluency and confrontation naming using compressed image acquisition to permit overt responses. *Hum. Brain Mapp.* 20, 29–40. doi: 10.1002/hbm.10126

Acheson, D. J., and Hagoort, P. (2013). Stimulating the brain's language network: syntactic ambiguity resolution after TMS to the inferior frontal gyrus and middle temporal gyrus. *J. Cogn. Neurosci.* 25, 1664–1677. doi: 10.1162/jocn_a_00430

Andrews, S. C., Hoy, K. E., Enticott, P. G., Daskalakis, Z. J., and Fitzgerald, P. B. (2011). Improving working memory: the effect of combining cognitive activity and anodal transcranial direct current stimulation to the left dorsolateral prefrontal cortex. *Brain Stimul.* 4, 84–89. doi: 10.1016/j.brs.2010.06.004

Apostolova, L. G., and Thompson, P. M. (2007). Brain mapping as a tool to study neurodegeneration. *Neurotherapeutics* 4, 387–400. doi: 10.1016/j.nurt.2007.05.009

Ashburner, J., and Friston, K. J. (2000). Voxel-based morphometry-the methods. *Neuroimage* 11, 805–821. doi: 10.1006/nimg.2000.0582

Babiloni, C., Ferretti, A., Del Gratta, C., Carducci, F., Vecchio, F., Romani, G. L., et al. (2005). Human cortical responses during one-bit delayed-response tasks: an fMRI study. *Brain Res. Bull.* 65, 383–390. doi: 10.1016/j.brainresbull.2005.01.013

Bermpohl, F., Pascual-Leone, A., Amedi, A., Merabet, L. B., Fregni, F., Gaab, N., et al. (2006). Attentional modulation of emotional stimulus processing: an fMRI study using emotional expectancy. *Hum. Brain Mapp.* 27, 662–677. doi: 10.1002/hbm.20209

Bigler, E. D., Mortensen, S., Neeley, E. S., Ozonoff, S., Krasny, L., Johnson, M., et al. (2007). Superior temporal gyrus, language function, and autism. *Dev. Neuropsychol.* 31, 217–238. doi: 10.1080/87565640701190841

Bramão, I., Faísca, L., Forkstam, C., Reis, A., and Petersson, K. M. (2010). Cortical brain regions associated with color processing: an FMRI study. *Open Neuroimag. J.* 4, 164–173. doi: 10.2174/1874440001004010164

Bridge, H. (2011). Mapping the visual brain: how and why. *Eye* 25, 291–296. doi: 10.1038/eye.2010.166

Brunet, E., Sarfati, Y., Hardy-Baylé, M. C., and Decety, J. (2000). A PET investigation of the attribution of intentions with a nonverbal task. *Neuroimage* 11, 157–166. doi: 10.1006/nimg.1999.0525

Buckner, R. L. (1996). Beyond HERA: contributions of specific prefrontal brain areas to long-term memory retrieval. *Psychon. Bull. Rev.* 3, 149–158. doi: 10.3758/BF03212413

Carreiras, M., Armstrong, B. C., Perea, M., and Frost, R. (2014). The what, when, where, and how of visual word recognition. *Trends Cogn. Sci.* 18, 90–98. doi: 10.1016/j.tics.2013.11.005

Castellanos, F. X., Cortese, S., and Proal, E. (2014). Connectivity. *Curr. Top Behav. Neurosci.* 16, 49–77. doi: 10.1007/7854_2013_244

Cavanna, A. E., and Trimble, M. R. (2006). The precuneus: a review of its functional anatomy and behavioural correlates. *Brain* 129, 564–583. doi: 10.1093/brain/awl004

Cerasa, A., Pugliese, P., Messina, D., Morelli, M., Gioia, M. C., Salsone, M., et al. (2012). Prefrontal alterations in Parkinson's disease with levodopa-induced dyskinesia during fMRI motor task. *Mov. Disord.* 27, 364–371. doi: 10.1002/mds.24017

Chen, Y., Li, P., Gu, B., Liu, Z., Li, X., Evans, A. C., et al. (2015). The effects of an APOE promoter polymorphism on human cortical morphology during non-demented aging. *J. Neurosci.* 35, 1423–1431. doi: 10.1523/JNEUROSCI.1946-14.2015

Chevrier, A. D., Noseworthy, M. D., and Schachar, R. (2007). Dissociation of response inhibition and performance monitoring in the stop signal task using event-related fMRI. *Hum. Brain Mapp.* 28, 1347–1358. doi: 10.1002/hbm.20355

Chung, M. K., Worsley, K. J., Robbins, S., Paus, T., Taylor, J., Giedd, J. N., et al. (2003). Deformation -based surface morphometry applied to gray matter deformation. *Neuroimage* 18, 198–213. doi: 10.1016/s1053-8119(02)00017-4

Cingulate binds learning (1997). Cingulate binds learning. *Trends Cogn. Sci.* 1:2. doi: 10.1016/S1364-6613(97)85002-4

Cole, D. M., Beckmann, C. F., Oei, N. Y., Both, S., Van Gerven, J. M., and Rombouts, S. A. (2013). Differential and distributed effects of dopamine neuromodulations on resting-state network connectivity. *Neuroimage* 78, 59–67. doi: 10.1016/j.neuroimage.2013.04.034

Deng, X., Zhou, M., Tang, C., Zhang, J., Zhu, L., Xie, Z., et al. (2016). The alterations of cortical volume, thickness, surface, and density in the intermediate sporadic Parkinson's Disease from the Han Population of Mainland China. *Front. Aging. Neurosci.* 8:185. doi: 10.3389/fnagi.2016.00185

Dupont, S. (2002). Investigating temporal pole function by functional imaging. *Epileptic. Disord.* 4, S17–S22.

Düzel, E., Picton, T. W., Cabeza, R., Yonelinas, A. P., Scheich, H., Heinze, H. J., et al. (2001). Comparative electrophysiological and hemodynamic measures of neural activation during memory-retrieval. *Hum. Brain Mapp.* 13, 104–123. doi: 10.1002/hbm.1028

Esposito, F., Tessitore, A., Giordano, A., De Micco, R., Paccone, A., Conforti, R., et al. (2013). Rhythm-specific modulation of the sensorimotor network in drug-naive patients with Parkinson's disease by levodopa. *Brain* 136, 710–725. doi: 10.1093/brain/awt007

Farrow, T. F., Zheng, Y., Wilkinson, I. D., Spence, S. A., Deakin, J. F., Tarrier, N., et al. (2001). Investigating the functional anatomy of empathy and forgiveness. *Neuroreport* 12, 2433–2438. doi: 10.1097/00001756-200108080-00029

Fauvel, B., Groussard, M., Chetelat, G., Fouquet, M., Landeau, B., Eustache, F., et al. (2014). Morphological brain plasticity induced by musical expertise is accompanied by modulation of functional connectivity at rest. *Neuroimage* 90, 179–188. doi: 10.1016/j.neuroimage.2013.12.065

Feldmann, A., Trauninger, A., Toth, L., Kotek, G., Kosztolanyi, P., Illes, E., et al. (2008). Atrophy and decreased activation of fronto-parietal attention areas contribute to higher visual dysfunction in posterior cortical atrophy. *Psychiat. Res.* 164, 178–184. doi: 10.1016/j.pscychresns.2008.01.006

Fincham, J. M., Carter, C. S., van Veen, V., Stenger, V. A., and Anderson, J. R. (2002). Neural mechanisms of planning: a computational analysis using event-related fMRI. *Proc. Natl. Acad. Sci. U.S.A.* 99, 3346–3351. doi: 10.1073/pnas.052703399

Fink, G. R., Marshall, J. C., Halligan, P. W., Frith, C. D., Driver, J., Frackowiak, R. S., et al. (1999). The neural consequences of conflict between intention and the senses. *Brain* 122, 497–512. doi: 10.1093/brain/122.3.497

Fletcher, P. C., Dolan, R. J., Shallice, T., Frith, C. D., Frackowiak, R. S., and Friston, K. J. (1996). Is multivariate analysis of PET data more revealing than the univariate approach? Evidence from a study of episodic memory retrieval. *Neuroimage* 3, 209–215. doi: 10.1006/nimg.1996.0023

Forstmann, B. U., van den Wildenberg, W. P., and Ridderinkhof, K. R. (2008). Neural mechanisms, temporal dynamics, and individual differences in

interference control. *J. Cogn. Neurosci.* 20, 1854–1865. doi: 10.1162/jocn.2008.20122

Fried, I., Wilson, C. L., MacDonald, K. A., and Behnke, E. J. (1998). Electric current stimulates laughter. *Nature* 391:650. doi: 10.1038/35536

Gabrieli, J. D., Poldrack, R. A., and Desmond, J. E. (1998). The role of left prefrontal cortex in language and memory. *Proc. Natl. Acad. Sci. U.S.A.* 95, 906–913. doi: 10.1073/pnas.95.3.906

Gallagher, H. L., Jack, A. I., Roepstorff, A., and Frith, C. D. (2002). Imaging the intentional stance in a competitive game. *Neuroimage* 16, 814–821. doi: 10.1006/nimg.2002.1117

Gasquoine, P. G. (2014). Contributions of the insula to cognition and emotion. *Neuropsychol. Rev.* 24, 77–87. doi: 10.1007/s11065-014-9246-9

Goel, V., Gold, B., Kapur, S., and Houle, S. (1997). The seats of reason? An imaging study of deductive and inductive reasoning. *Neuroreport* 8, 1305–1310. doi: 10.1097/00001756-199703240-00049

Goel, V., Grafman, J., Sadato, N., and Hallett, M. (1995). Modeling other minds. *Neuroreport* 6, 1741–1746. doi: 10.1097/00001756-199509000-00009

Goldberg, I. I., Harel, M., and Malach, R. (2006). When the brain loses its self: prefrontal inactivation during sensorimotor processing. *Neuron* 50, 329–339. doi: 10.1016/j.neuron.2006.03.015

Gong, G., He, Y., Chen, Z. J., and Evans, A. C. (2012). Convergence and divergence of thickness correlations with diffusion connections across the human cerebral cortex. *Neuroimage* 59, 1239–1248. doi: 10.1016/j.neuroimage.2011.08.017

Göttlich, M., Münte, T. F., Heldmann, M., Kasten, M., Hagenah, J., and Krämer, U. M. (2013). Altered resting state brain networks in Parkinson's disease. *PLoS One* 8:e77336. doi: 10.1371/journal.pone.0077336

Gratton, C., Nomura, E. M., Pérez, F., and D'Esposito, M. (2012). Focal brain lesions to critical locations cause widespread disruption of the modular organization of the brain. *J. Cogn. Neurosci.* 24, 1275–1285. doi: 10.1162/jocn_a_00222

Hacker, C. D., Perlmutter, J. S., Criswell, S. R., Ances, B. M., and Snyder, A. Z. (2012). Resting state functional connectivity of the striatum in Parkinson's disease. *Brain* 135, 3699–3711. doi: 10.1093/brain/aws281

Hadland, K. A., Rushworth, M. F., Gaffan, D., and Passingham, R. E. (2003). The effect of cingulate lesions on social behaviour and emotion. *Neuropsychologia* 41, 919–931. doi: 10.1016/s0028-3932(02)00325-1

Halsband, U., Matsuzaka, Y., and Tanji, J. (1994). Neuronal activity in the primate supplementary, pre-supplementary and premotor cortex during externally and internally instructed sequential movements. *Neurosci. Res.* 20, 149–155. doi: 10.1016/0168-0102(94)90032-9

Harrington, D. L., Shen, Q., Castillo, G. N., Filoteo, J. V., Litvan, I., Takahashi, C., et al. (2017). Aberrant intrinsic activity and connectivity in cognitively normal Parkinson's Disease. *Front. Aging Neurosci.* 9:197. doi: 10.3389/fnagi.2017.00197

Hartwigsen, G., Baumgaertner, A., Price, C. J., Koehnke, M., Ulmer, S., and Siebner, H. R. (2010). Phonological decisions require both the left and right supramarginal gyri. *Proc. Natl. Acad. Sci. U.S.A.* 107, 16494–16499. doi: 10.1073/pnas.1008121107

Helmich, R. C., Derikx, L. C., Bakker, M., Scheeringa, R., Bloem, B. R., and Toni, I. (2010). Spatial remapping of cortico-striatal connectivity in Parkinson's disease. *Cereb. Cortex* 20, 1175–1186. doi: 10.1093/cercor/bhp178

Hickok, G., Buchsbaum, B., Humphries, C., and Muftuler, T. (2003). Auditory-motor interaction revealed by fMRI: speech, music, and working memory in area Spt. *J. Cogn. Neurosci.* 15, 673–682. doi: 10.1162/089892903322307393

Irimia, A., Goh, S. Y., Torgerson, C. M., Vespa, P., and Van Hor, N. J. D. (2014). Structural and connectomic neuroimaging for the personalized study of longitudinal alterations in cortical shape, thickness and connectivity after traumatic brain injury. *J. Neurosurg. Sci.* 58, 129–144.

Jankovic, J. (2008). Parkinson's disease: clinical features and diagnosis. *J. Neurol. Neurosur. PS.* 79, 368–376. doi: 10.1136/jnnp.2007.131045

Jubault, T., Gagnon, J. F., Karama, S., Ptito, A., Lafontaine, A. L., Evans, A. C., et al. (2011). Patterns of cortical thickness and surface area in early Parkinson's disease. *Neuroimage* 55, 462–467. doi: 10.1016/j.neuroimage.2010.12.043

Kabani, N., Le Goualher, G., MacDonald, D., and Evans, A. C. (2001). Measurement of cortical thickness using an automated 3-D algorithm: a validation study. *Neuroimage* 13, 375–380. doi: 10.1006/nimg.2000.0652

Kamali, A., Flanders, A. E., Brody, J., Hunter, J. V., and Hasan, K. M. (2014a). Tracing superior longitudinal fasciculus connectivity in the human brain using high resolution diffusion tensor tractography. *Brain Struct. Funct.* 219, 269–281. doi: 10.1007/s00429-012-0498-y

Kamali, A., Sair, H. I., Radmanesh, A., and Hasan, K. M. (2014b). Decoding the superior parietal lobule connections of the superior longitudinal fasciculus/arcuate fasciculus in the human brain. *Neuroscience* 277, 577–583. doi: 10.1016/j.neuroscience.2014.07.035

Kaur, S., Sassi, R. B., Axelson, D., Nicoletti, M., Brambilla, P., Monkul, E. S., et al. (2005). Cingulate cortex anatomical abnormalities in children and adolescents with bipolar disorder. *Am. J. Psychiatry* 162, 1637–1643. doi: 10.1176/appi.ajp.162.9.1637

Kerestes, R., Ladouceur, C. D., Meda, S., Nathan, P. J., Blumberg, H. P., Maloney, K., et al. (2012). Abnormal prefrontal activity subserving attentional control of emotion in remitted depressed patients during a working memory task with emotional distracters. *Psychol. Med.* 42, 29–40. doi: 10.1017/S0033291711001097

Khoo, T. K., Yarnall, A. J., Duncan, G. W., Coleman, S., O'Brien, J. T., Brooks, D. J., et al. (2013). The spectrum of nonmotor symptoms in early Parkinson disease. *Neurology* 80, 276–281. doi: 10.1212/WNL.0b013e31827deb74

Kim, J. S., Singh, V., Lee, J. K., Lerch, J., Ad-Dab'bagh, Y., MacDonald, D., et al. (2005). Automated 3-D extraction and evaluation of the inner and outer cortical surfaces using a Laplacian map and partial volume effect classification. *Neuroimage* 27, 210–221. doi: 10.1016/j.neuroimage.2005.03.036

Kjaer, T. W., Nowak, M., and Lou, H. C. (2002). Reflective self-awareness and conscious states: PET evidence for a common midline parietofrontal core. *Neuroimage* 17, 1080–1086. doi: 10.1006/nimg.2002.1230

Knauff, M., Mulack, T., Kassubek, J., Salih, H. R., and Greenlee, M. W. (2002). Spatial imagery in deductive reasoning: a functional MRI study. *Brain Res. Cogn. Brain Res.* 13, 203–212. doi: 10.1016/s0926-6410(01)00116-1

Koenigs, M., Barbey, A. K., Postle, B. R., and Grafman, J. (2009). Superior parietal cortex is critical for the manipulation of information in working memory. *J. Neurosci.* 29, 14980–14986. doi: 10.1523/JNEUROSCI.3706-09.2009

Kozlovskiy, S. A., Vartanov, A. V., Nikonova, E. Y., Pyasik, M. M., and Velichkovsky, B. M. (2012). The cingulate cortex and human memory processes. *Psychol. Russia State Art* 5, 231–243. doi: 10.11621/pir.2012.0014

Kringelbach, M. L. (2005). The human orbitofrontal cortex: linking reward to hedonic experience. *Nat. Rev. Neurosci.* 6, 691–702. doi: 10.1038/nrn1747

Kübler, A., Dixon, V., and Garavan, H. (2006). Automaticity and reestablishment of executive control-an fMRI study. *J. Cogn. Neurosci.* 18, 1331–1342. doi: 10.1162/jocn.2006.18.8.1331

Lacey, S., Stilla, R., and Sathian, K. (2012). Metaphorically feeling: comprehending textural metaphors activates somatosensory cortex. *Brain Lang.* 120, 16–21.

Lane, R. D., Reiman, E. M., Bradley, M. M., Lang, P. J., Ahern, G. L., Davidson, R. J., et al. (1997). Neuroanatomical correlates of pleasant and unpleasant emotion. *Neuropsychologia* 35, 1437–1444. doi: 10.1016/s0028-3932(97)00070-5

Lauro, L. J., Tettamanti, M., Cappa, S. F., and Papagno, C. (2008). Idiom comprehension: a prefrontal task? *Cereb. Cortex* 18, 162–170. doi: 10.1093/cercor/bhm042

Lerch, J. P., and Evans, A. C. (2005). Cortical thickness analysis examined through power analysis and a population simulation. *Neuroimage* 24, 163–173. doi: 10.1016/j.neuroimage.2004.07.045

Longe, O., Maratos, F. A., Gilbert, P., Evans, G., Volker, F., Rockliff, H., et al. (2010). Having a word with yourself: neural correlates of self-criticism and self-reassurance. *Neuroimage* 49, 1849–1856. doi: 10.1016/j.neuroimage.2009.09.019

Lou, H. C., Luber, B., Crupain, M., Keenan, J. P., Nowak, M., Kjaer, T. W., et al. (2004). Parietal cortex and representation of the mental Self. *Proc. Natl. Acad. Sci. U.S.A.* 101, 6827–6832. doi: 10.1073/pnas.0400049101

Lyttelton, O. C., Karama, S., Ad-Dab'bagh, Y., Zatorre, R. J., Carbonell, F., Worsley, K., et al. (2009). Positional and surface area asymmetry of the human cerebral cortex. *Neuroimage* 46, 895–903. doi: 10.1016/j.neuroimage.2009.03.063

Maddock, R. J., and Buonocore, M. H. (1997). Activation of left posterior cingulate gyrus by the auditory presentation of threat-related words: an fMRI study. *Psychiatry Res.* 75, 1–14. doi: 10.1016/s0925-4927(97)00018-8

Manes, J. L., Tjaden, K., Parrish, T., Simuni, T., Roberts, A., Greenlee, J. D., et al. (2018). Altered resting-state functional connectivity of the putamen and internal globus pallidus is related to speech impairment in Parkinson's disease. *Brain Behav.* 8:e01073. doi: 10.1002/brb3.1073

Nakai, T., Kato, C., and Matsuo, K. (2005). An FMRI study to investigate auditory attention: a model of the cocktail party phenomenon. *Magn. Reson. Med. Sci.* 4, 75–82. doi: 10.2463/mrms.4.75

Penfield, W., and Welch, K. (1951). The supplementary motor area of the cerebral cortex; a clinical and experimental study. *AMA. Arch. Neurol. Psychiatry* 66, 289–317.

Radua, J., Phillips, M. L., Russell, T., Lawrence, N., Marshall, N., Kalidindi, S., et al. (2010). Neural response to specific components of fearful faces in healthy and schizophrenic adults. *Neuroimage* 49, 939–946. doi: 10.1016/j.neuroimage.2009.08.030

Ranganath, C., Johnson, M. K., and D'Esposito, M. (2003). Prefrontal activity associated with working memory and episodic long-term memory. *Neuropsychologia* 41, 378–389. doi: 10.1016/s0028-3932(02)00169-0

Rickard, T. C., Romero, S. G., Basso, G., Wharton, C., Flitman, S., and Grafman, J. (2000). The calculating brain: an fMRI study. *Neuropsychologia* 38, 325–335. doi: 10.1016/s0028-3932(99)00068-8

Rizzolatti, G., Fogassi, L., and Gallese, V. (2002). Motor and cognitive functions of the ventral premotor cortex. *Curr. Opin. Neurobiol.* 12, 149–154. doi: 10.1016/s0959-4388(02)00308-2

Roland, P. E., Larsen, B., Lassen, N. A., and Skinhøj, E. (1980). Supplementary motor area and other cortical areas in organization of voluntary movements in man. *J. Neurophysiol.* 43, 118–136. doi: 10.1152/jn.1980.43.1.118

Royet, J. P., Koenig, O., Gregoire, M. C., Cinotti, L., Lavenne, F., Le Bars, D., et al. (1999). Functional anatomy of perceptual and semantic processing for odors. *J. Cogn. Neurosci.* 11, 94–109. doi: 10.1162/089892999563166

Schwarzlose, R. F., Baker, C. I., and Kanwisher, N. (2005). Separate face and body selectivity on the fusiform gyrus. *J. Neurosci.* 25, 11055–11059. doi: 10.1523/JNEUROSCI.2621-05.2005

Serrien, D. J., Strens, L. H., Oliviero, A., and Brown, P. (2002). Repetitive transcranial magnetic stimulation of the supplementary motor area (SMA) degrades bimanual movement control in humans. *Neurosci. Lett.* 328, 89–92. doi: 10.1016/s0304-3940(02)00499-8

Shallice, T., Stuss, D. T., Alexander, M. P., Picton, T. W., and Derkzen, D. (2008). The multiple dimensions of sustained attention. *Cortex* 44, 794–805. doi: 10.1016/j.cortex.2007.04.002

Shima, K., and Tanji, J. (1998). Both supplementary and presupplementary motor areas are crucial for the temporal organization of multiple movements. *J. Neurophysiol.* 80, 3247–3260. doi: 10.1152/jn.1998.80.6.3247

Simmons, W. K., Rapuano, K. M., Kallman, S. J., Ingeholm, J. E., Miller, B., Gotts, S. J., et al. (2013). Category-specific integration of homeostatic signals in caudal but not rostral human insula. *Nat. Neurosci.* 16, 1551–1552. doi: 10.1038/nn.3535

Sled, J. G., and Pike, G. B. (1998). Standing-wave and RF penetration artifacts caused by elliptic geometry: an electrodynamic analysis of MRI. *IEEE Trans. Med. Imaging* 17, 653–662. doi: 10.1109/42.730409

Slotnick, S. D., and Moo, L. R. (2006). Prefrontal cortex hemispheric specialization for categorical and coordinate visual spatial memory. *Neuropsychologia* 44, 1560–1568. doi: 10.1016/j.neuropsychologia.2006.01.018

Spaniol, J., Davidson, P. S., Kim, A. S., Han, H., Moscovitch, M., and Grady, C. L. (2009). Event-related fMRI studies of episodic encoding and retrieval: meta-analyses using activation likelihood estimation. *Neuropsychologia* 47, 1765–1779. doi: 10.1016/j.neuropsychologia.2009.02.028

Stam, C. J., Jones, B. F., Nolte, G., Breakspear, M., and Scheltens, P. (2007). Small-world networks and functional connectivity in Alzheimer's disease. *Cereb. Cortex* 17, 92–99. doi: 10.1093/cercor/bhj127

Stanislav, K., Alexander, A., and Maria, P. (2013). Anatomical characteristics of cingulate cortex and neuropsychological memory tests performance. *Proc. Soc. Behav. Sci.* 86, 128–133. doi: 10.1016/j.sbspro.2013.08.537

Supekar, K., Menon, V., Rubin, D., Musen, M., and Greicius, M. D. (2008). Network analysis of intrinsic functional brain connectivity in Alzheimer's disease. *PLoS Comput. Biol.* 4:e1000100. doi: 10.1371/journal.pcbi.1000100

Takahashi, E., Ohki, K., and Miyashita, Y. (2002). The role of the parahippocampal gyrus in source memory for external and internal events. *Neuroreport* 13, 1951–1956. doi: 10.1097/00001756-200210280-00024

Takeuchi, H., Sekiguchi, A., Taki, Y., Yokoyama, S., Yomogida, Y., Komuro, N., et al. (2010). Training of working memory impacts structural connectivity. *J. Neurosci.* 30, 3297–3303. doi: 10.1523/JNEUROSCI.4611-09.2010

Talati, A., and Hirsch, J. (2005). Functional specialization within the medial frontal gyrus for perceptual go/no-go decisions based on "what,""when," and "where" related information: an fMRI study. *J. Cogn. Neurosci.* 17, 981–993. doi: 10.1162/0898929054475226

Taylor, J. E., and Adler, R. J. (2003). Euler characteristics for Gaussian fields on manifolds. *Ann. Probab.* 31, 533–563.

Tittgemeyer, M., Rigoux, L., and Knösche, T. R. (2018). Cortical parcellation based on structural connectivity: a case for generative models. *Neuroimage* 173, 592–603. doi: 10.1016/j.neuroimage.2018.01.077

Tohka, J., Zijdenbos, A., and Evans, A. (2004). Fast and robust parameter estimation for statistical partial volume models in brain MRI. *Neuroimage* 23, 84–97. doi: 10.1016/j.neuroimage.2004.05.007

Valyear, K. F., Culham, J. C., Sharif, N., Westwood, D., and Goodale, M. A. (2006). A double dissociation between sensitivity to changes in object identity and object orientation in the ventral and dorsal visual streams: a human fMRI study. *Neuropsychologia* 44, 218–228. doi: 10.1016/j.neuropsychologia.2005.05.004

Wandell, B. A., and Winawer, J. (2011). Imaging retinotopic maps in the human brain. *Vision Res.* 51, 718–737. doi: 10.1016/j.visres.2010.08.004

Wu, T., Wang, L., Chen, Y., Zhao, C., Li, K., and Chan, P. (2009). Changes of functional connectivity of the motor network in the resting state in Parkinson's disease. *Neuroci. Lett.* 460, 6–10. doi: 10.1016/j.neulet.2009.05.046

Xia, J., Wang, J., Tian, W., Ding, H., Wei, Q., Huang, H., et al. (2013). Magnetic resonance morphometry of the loss of gray matter volume in Parkinson's disease patients. *Neural. Regen. Res.* 8, 2557–2565. doi: 10.3969/j.issn.1673-5374.2013.27.007

Yagishita, S., Watanabe, T., Asari, T., Ito, H., Kato, M., Ikehira, H., et al. (2008). Role of left superior temporal gyrus during name recall process: an event-related fMRI study. *Neuroimage* 41, 1142–1153. doi: 10.1016/j.neuroimage.2008.03.008

Zarei, M., Ibarretxe-Bilbao, N., Compta, Y., Hough, M., Junque, C., Bargallo, N., et al. (2013). Cortical thinning is associated with disease stages and dementia in Parkinson's disease. *J. Neurol. Neurosurg. Psychiatry* 84, 875–881. doi: 10.1136/jnnp-2012-304126

Zatorre, R. J., Fields, R. D., and Johansen-Berg, H. (2012). Plasticity in gray and white: neuroimaging changes in brain structure during learning. *Nat. Neurosci.* 15, 528–536. doi: 10.1038/nn.3045

Zhang, J. X., Leung, H. C., and Johnson, M. K. (2003). Frontal activations associated with accessing and evaluating information in working memory: an fMRI study. *Neuroimage* 20, 1531–1539. doi: 10.1016/j.neuroimage.2003.07.016

Zorrilla, L. T., Aguirre, G. K., Zarahn, E., Cannon, T. D., and D'Esposito, M. (1996). Activation of the prefrontal cortex during judgments of recency: a functional MRI study. *Neuroreport* 7, 2803–2806. doi: 10.1097/00001756-199611040-00079

Conflict of Interest: The authors declare that the research was conducted in the absence of any commercial or financial relationships that could be construed as a potential conflict of interest.

Copyright © 2021 Deng, Liu, Kang, Lu, Zhu and Xu. This is an open-access article distributed under the terms of the Creative Commons Attribution License (CC BY). The use, distribution or reproduction in other forums is permitted, provided the original author(s) and the copyright owner(s) are credited and that the original publication in this journal is cited, in accordance with accepted academic practice. No use, distribution or reproduction is permitted which does not comply with these terms.

frontiers in Aging Neuroscience

REVIEW
published: 03 June 2021
doi: 10.3389/fnagi.2021.691881

The Cross-Links of Endoplasmic Reticulum Stress, Autophagy, and Neurodegeneration in Parkinson's Disease

Haigang Ren[1,2†], Wanqing Zhai[1†], Xiaojun Lu[1] and Guanghui Wang[1,2*]*

[1] *Department of Neurology, Center of Translational Medicine, Taicang Affiliated Hospital of Soochow University, The First People's Hospital of Taicang, Suzhou, China,* [2] *Jiangsu Key Laboratory of Translational Research and Therapy for Neuropsychiatric Disorders, Department of Pharmacology, College of Pharmaceutical Sciences, Soochow University, Suzhou, China*

Parkinson's disease (PD) is the most common neurodegenerative movement disorder, and it is characterized by the selective loss of dopaminergic (DA) neurons in the substantia nigra pars compacta (SNpc), as well as the presence of intracellular inclusions with α-synuclein as the main component in surviving DA neurons. Emerging evidence suggests that the imbalance of proteostasis is a key pathogenic factor for PD. Endoplasmic reticulum (ER) stress-induced unfolded protein response (UPR) and autophagy, two major pathways for maintaining proteostasis, play important roles in PD pathology and are considered as attractive therapeutic targets for PD treatment. However, although ER stress/UPR and autophagy appear to be independent cellular processes, they are closely related to each other. In this review, we focused on the roles and molecular cross-links between ER stress/UPR and autophagy in PD pathology. We systematically reviewed and summarized the most recent advances in regulation of ER stress/UPR and autophagy, and their cross-linking mechanisms. We also reviewed and discussed the mechanisms of the coexisting ER stress/UPR activation and dysregulated autophagy in the lesion regions of PD patients, and the underlying roles and molecular crosslinks between ER stress/UPR activation and the dysregulated autophagy in DA neurodegeneration induced by PD-associated genetic factors and PD-related neurotoxins. Finally, we indicate that the combined regulation of ER stress/UPR and autophagy would be a more effective treatment for PD rather than regulating one of these conditions alone.

Keywords: Parkinson's disease, ER stress, UPR, autophagy, α-synuclein, cross-link

OPEN ACCESS

Edited by:
Pingyi Xu,
First Affiliated Hospital of Guangzhou Medical University, China

Reviewed by:
Zhong Pei,
Sun Yat-sen University, China
David J. Koss,
Newcastle University, United Kingdom

****Correspondence:***
Xiaojun Lu
luxiaojun5215@163.com
Guanghui Wang
wanggh@suda.edu.cn

† These authors have contributed equally to this work

Received: *07 April 2021*
Accepted: *10 May 2021*
Published: *03 June 2021*

Citation:
Ren H, Zhai W, Lu X and Wang G (2021) The Cross-Links of Endoplasmic Reticulum Stress, Autophagy, and Neurodegeneration in Parkinson's Disease. Front. Aging Neurosci. 13:691881. doi: 10.3389/fnagi.2021.691881

INTRODUCTION

Parkinson's disease (PD), the most common neurodegenerative movement disorder, affects approximately 1% of the population over 60 years old, and its incidence dramatically increases to approximately 5% in the population greater than 85 years of age (Li and Le, 2020; Wang et al., 2020b). PD is a chronic, irreversible, and complex neurodegenerative disease with several typical motor impairments including resting tremor, bradykinesia, rigidity, and postural imbalance. These

are caused by the selective and progressive loss of dopaminergic (DA) neurons in the substantia nigra pars compacta (SNpc) and the deficiency of dopamine release in the striatum (Poewe et al., 2017). In addition to DA neuron loss, the presence of intracellular inclusions called Lewy bodies (LBs) with an accumulation of protein aggregates including α-synuclein (α-SYN), and abnormal dystrophic neurites termed Lewy neurites (LNs) in surviving DA neurons, are also the major hallmarks of PD pathology (Kalia and Lang, 2015). Recently, great achievements have been made in understanding PD pathogenesis, which may contribute to developing more optimal strategies for PD treatment.

The mechanisms of DA neuron damage in PD include a variety of cellular processes such as α-SYN aggregates, mitochondrial damage, oxidative stress, calcium homeostasis dysfunction, axonal transport disruption, and neuroinflammation injury, and also involve aging, and environmental and genetic factors (Shulman et al., 2011). Emerging evidence suggests that these disadvantages can perturb the balance of cellular homeostasis (proteostasis) in PD (Lehtonen et al., 2019). Endoplasmic reticulum (ER) stress-induced unfolded protein response (UPR) and autophagy, two major pathways that respond to an imbalance in cellular homeostasis, play particularly important roles in the pathology of neurodegenerative diseases including PD (Karabiyik et al., 2017; Costa et al., 2020).

Endoplasmic reticulum stress, UPR, and autophagy have become important targets for alleviating the damage of DA neurons, and they provide attractive clues for the treatment of PD (Moors et al., 2017; Martinez et al., 2019). However, UPR and autophagy are both related and independent cellular processes. Both the effects of their cross-talk and their unique mechanisms in PD must be considered in order to find an appropriate therapeutic target for PD treatment or to provide the basis for combination medication. In this review, we summarize the most recent advances in ER stress, UPR, autophagy, and their interactions in PD pathogenesis, and how to alleviate the toxic effects of cellular homeostasis imbalance in PD by targeting ER stress, UPR, and autophagy.

ER STRESS AND UPR

The ER is essential for cellular homeostasis. The ER organelles have a variety of important functions that are necessary for protein synthesis, protein quality control, Ca^{2+} homeostasis, and lipid and carbohydrate metabolism (Wang and Kaufman, 2016; Ghemrawi and Khair, 2020). Under physiological states, the ER uses the resident chaperone molecules to ensure the proper folding of newly synthesized proteins, and also can identify misfolded proteins through quality control mechanisms and employ proteasomes to implement ER-associated degradation (ERAD) (Walter and Ron, 2011). When the protein-folding capacity of the ER is saturated under various pathological conditions, such as aberrant aggregation of misfolded proteins or mutant proteins, accumulation of exogenous viral proteins, fluctuation of ER Ca^{2+} stores, perturbation of ATP levels, presence of environmental toxins, or occurrence of metabolic dysfunctions, the cells sense the ER stress and subsequently initiate an adaptive response referred to as UPR. This in turn attempts to alleviate ER stress by enhancing the protein-folding capacity and reducing the general synthetic load to restore ER homeostasis and maintain cell survival (Xu et al., 2012; Rashid et al., 2015).

The UPR is controlled by three ER-resident sensors: inositol-requiring kinase 1α (IRE1α), protein kinase RNA-activated (PKR)-like ER kinase (PERK), and activating transcription factor 6 (ATF6) (Manie et al., 2014). Both IRE1α and PERK are type I transmembrane Ser/Thr protein kinases, and possess similar structures with an NH_2-terminal ER luminal domain and a cytosolic kinase domain (Pandey et al., 2019). In addition, IRE1α has an extra RNase domain with endonuclease activity (Abdullah and Ravanan, 2018). ATF6 is a type II transmembrane protein with a COOH-terminal ER luminal domain and an NH_2-terminal cytosolic domain with bZIP transcription factor activity (Pandey et al., 2019).

In the absence of ER stress, all three UPR sensors remain inactive resulting from binding to the 78 kDa glucose-regulated protein 78 (GRP78), also known as binding-immunoglobulin protein (BIP), an abundant ER-resident chaperone encoded by gene *HSPA5*. When mutant, unfolded, or misfolded proteins accumulate in the ER, they release the inhibitory effect of GRP78 on PERK, IRE1α, and ATF6 activity through their high affinity for GRP78 (Oakes and Papa, 2015). In addition, the unfolded or misfolded proteins also act as active ligands for their activation (Credle et al., 2005; Gardner and Walter, 2011). All three UPR branches have outputs to attempt to alleviate ER stress for cell survival by distinct or partially overlapped mechanisms such as mitigating protein misfolding, reducing protein synthesis, or enhancing protein degradation (**Figure 1**). However, if the adaptive UPR fails to restore ER homeostasis, UPR signaling undergoes continuous activation to initiate pro-death signals through multiple pathways that eventually trigger intrinsic apoptosis (Hetz and Papa, 2018).

AUTOPHAGY

Autophagy is a highly conserved self-degradation process that delivers aggregated or misfolded proteins, lipid droplets, glycogens, and damaged organelles to lysosomes for degradation. It plays a fundamental role in the homeostasis of almost all types of cells, tissues, and organs (Levine and Kroemer, 2019). Autophagy has been divided into at least three subtypes: macroautophagy, chaperone-mediated autophagy (CMA), and microautophagy, with each involving different mechanisms of substrate delivery to the lysosome. Microautophagy degrades the cytosolic contents through small invaginations in the lysosomal membrane, while CMA mediates selective cytoplasmic proteins with a consensus KFERQ sequence motif into the lysosomal lumen for degradation upon recognition by heat shock cognate 71 kDa protein (HSC70) and targeting by lysosomal associated membrane protein 2A (LAMP2A) (Tekirdag and Cuervo, 2018). Macroautophagy (hereafter referred to autophagy) is the major and most thoroughly characterized autophagic pathway. It

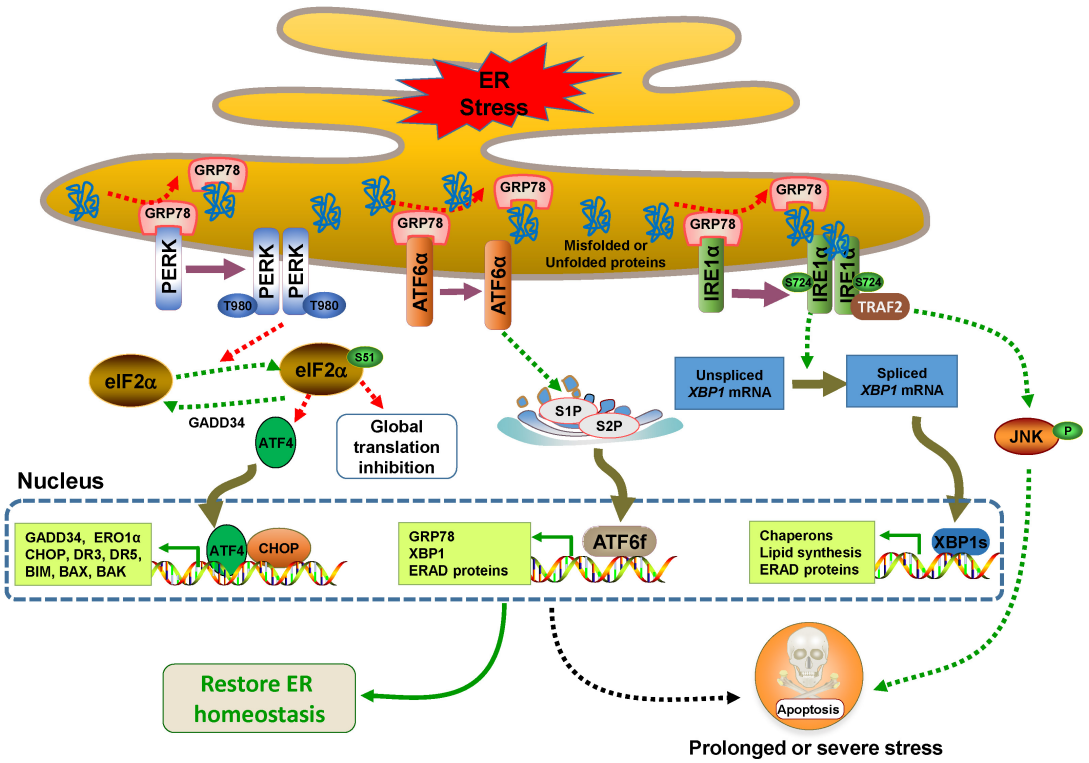


FIGURE 1 | Endoplasmic reticulum (ER) stress and UPR signaling pathways. The UPR is controlled by three major branches, IRE1α, PERK, and ATF6, which bind to GRP78 in the ER under normal conditions. In response to ER stress, the three sensors are activated by dissociating with GPR78. PERK undergoes dimerization, autophosphorylation, and then decreases protein synthesis by phosphorylating eIF2α at the Ser51, which selectively results in the translation of transcription factor 4 (ATF4), a factor that activates transcription of its downstream UPR genes such as CCAAT/enhancer binding protein (C/EBP) homologous protein (CHOP) (Harding et al., 2000). CHOP and ATF4 can upregulate the expression of genes involved in the UPR and apoptosis such as BIM, BAX, BAK, death receptor 3 (DR3), DR5, inositol 1,4,5-trisphosphate (IP3) receptor 1 (IP3R1) and ER oxidase 1α (ERO1α) (Iurlaro and Munoz-Pinedo, 2016). When the ER stress is relieved, CHOP and ATF4 induce the expression of growth arrest and DNA damage inducible protein 34 (GADD34), which directly dephosphorylates eIF2α and restarts global mRNA transcription (Novoa et al., 2001). IRE1α also undergoes dimerization, and even oligomerization and autophosphorylation, and then, its RNase activity is activated and *XBP1* mRNA is cleaved to generate XBP1s. The transcription factor XBP1s is responsible for the expression of a subset of downstream genes involved in ERAD, lipid synthesis, protein folding, translocation, and secretion (Korennykh and Walter, 2012; Hetz and Papa, 2018). Activated IRE1α also interacts with tumor necrosis factor receptor (TNFR)-associated factor-2 (TRAF2) and promotes a cascade of phosphorylation events that ultimately activates Jun amino-terminal kinase (JNK)-mediated cell death (Urano et al., 2000). The dissociation of GRP78 drives ATF6 to translocate to the Golgi, where it is cleaved by site-1 protease (S1P) and S2P to generate ATF6f, which transcriptionally activates the expression of a variety of genes involved in ERAD and ER chaperones including GRP78 and XBP1 (Haze et al., 1999; Shen et al., 2002; Yamamoto et al., 2007; Hillary and FitzGerald, 2018).

sequesters cytoplasmic contents within a double-membrane structure followed by fusion with lysosomes for degradation. According to the type of substrates it degrades, autophagy is also classified into non-selective autophagy and selective autophagy (Shimizu, 2018). Selective autophagy mediates specific substrates or organelles such as aggregate-prone proteins (aggrephagy), mitochondria (mitophagy), peroxisomes (pexophagy), pathogens (xenophagy), and ER (ERphagy) to the autophagic machinery for degradation via adaptor molecules (Stolz et al., 2014).

Under normal conditions, basal autophagy is ongoing at lower levels so that cells will optimally function after the removal of damaged organelles or unwanted substrates (Deegan et al., 2013). Autophagy is dramatically triggered by various stimuli such as nutrient deprivation, accumulation of protein aggregates, oxidative stress, hypoxia, and toxic molecule treatment (Corona Velazquez and Jackson, 2018). The complete processes of autophagy contain multiple sequential steps (autophagy induction, phagophore nucleation, elongation and closure, autophagosome maturation, and fusion with lysosomes to form autolysosomes) with complex mechanisms mediated by autophagy-related gene (ATG) proteins, their partners, and a variety of kinases (**Figure 2**).

INTERPLAY OF ER STRESS AND AUTOPHAGY

Although ER stress and autophagy can act as independent drivers, they share many common features such as protecting tissues by alleviating stress and inducing cell death when alleviating failure caused by extreme or chronic stress. Since it was first described in yeast in 2006, a large number of studies have revealed that ER stress and autophagy are mechanistically related (Bernales et al., 2006; Yorimitsu et al., 2006; Rashid et al., 2015). Changing

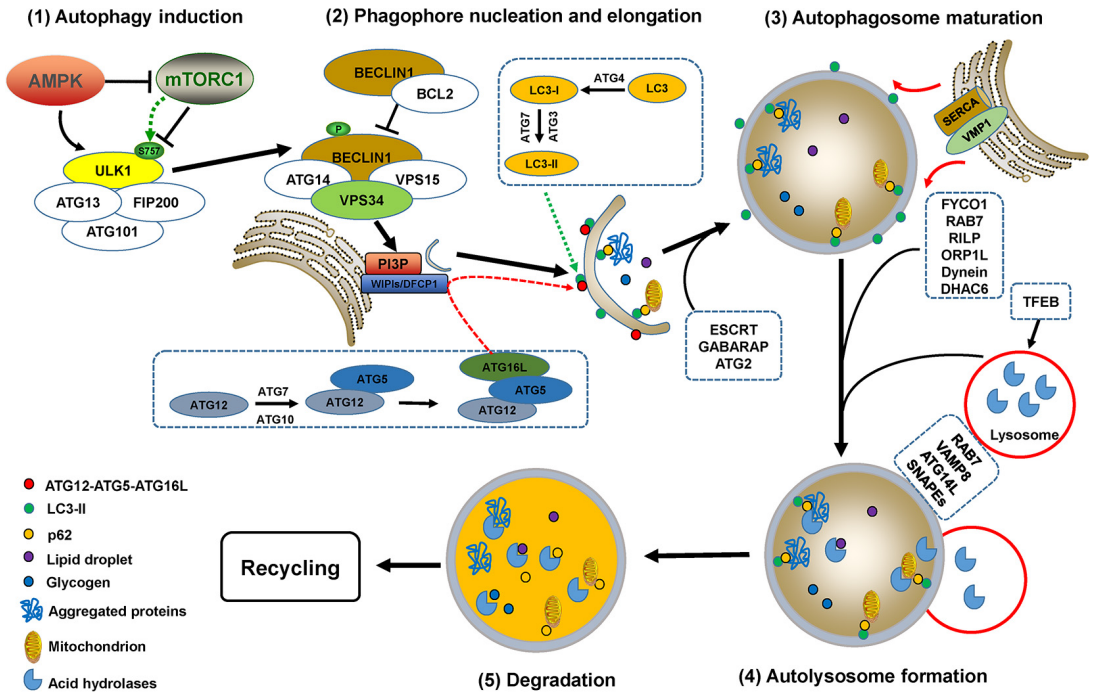


FIGURE 2 | The processes of autophagy. Autophagy processes include autophagy induction, phagophore nucleation, elongation and closure, autophagosome maturation, and fusion with lysosomes to form autolysosomes, which are mediated by multiple ATG proteins and a variety of kinases or partners with complex mechanisms. Autophagy initiation requires the activation of the uncoordinated-51-like kinase (ULK) complex, which is regulated by two kinases, AMP-activated protein kinase (AMPK) and mammalian target of rapamycin (mTOR) complex 1 (mTORC1). ULK1 activation causes phosphorylation of BECLIN1 and ATG14, thus promoting the formation of the PI3KC3 complex, which enhances the activity of VPS34 to generate phosphatidylinositol 3-phosphate (PI3P) (Russell et al., 2013; Nascimbeni et al., 2017). The enrichment of PI3P recruits double FYVE domain-containing protein 1 (DFCP1), downstream ATG proteins, and WD repeat proteins interacting with phosphoinositides 1 and 2 (WIPI1/2) for phagophore nucleation (Young and Wang, 2018). Phagophore elongation is mediated by two ubiquitin-like conjugation systems, ATG12-ATG5-ATG16L and the ATG8 (light chain 3, LC3) conjugation system (Noda and Inagaki, 2015). Phagophore closure is most likely accomplished by endosomal sorting complex required for transport (ESCRT) machinery-mediated membrane abscission (Tsuboyama et al., 2016; Takahashi et al., 2018, 2019). Additionally, the γ-aminobutyric acid receptor-associated protein (GABARAP) and ATG2 family are also critical for phagophore closure (Weidberg et al., 2010; Bozic et al., 2020). The ER-localized transmembrane protein vacuole membrane protein 1 (VMP1) mediates ER-phagophore dissociation via activating ER Ca^{2+} channel sarcoplasmic Ca^{2+}-ATPase (SERCA) and perturbing the local Ca^{2+} concentration (Zhao et al., 2017). Mature autophagosomes migrate to lysosomes involves the participation of proteins such as RAB7, FYVE coiled-coil domain-containing protein 1 (FYCO1), RAB-interacting lysosomal protein (RILP), Oxysterol-binding protein-related protein 1L (ORP1L), histone deacetylase 6 (HDAC6), kinesin or dynein (Nakamura and Yoshimori, 2017). RAB GTPases, soluble *N*-ethylmaleimide-sensitive factor attachment protein receptors (SNAREs), PI3K complex, and multiple tethering factors are involved in the fusion of autophagosomes with lysosomes to form autolysosomes, in which the autophagosomal contents are degraded by lysosomal acid hydrolases (Martini-Stoica et al., 2016; Zhao and Zhang, 2019). Transcription factor EB (TFEB) is a major regulator for autophagosome formation, lysosomal biogenesis, and lysosomal function (Martini-Stoica et al., 2016; Cortes and La Spada, 2019).

the functions of one system can affect the homeostasis of the other system, in which activation of autophagy triggered by ER stress-induced UPR is dominant. All three UPR branches can directly activate autophagy induction and autophagosome formation during ER stress through activating the expression of multiple ATG genes, inhibiting the expression of several autophagy inhibitors, or modulating several kinases including AMPK or mTORC1 (**Figure 3**). ER stress also regulates autophagy through mediating Ca^{2+} release. For example, ER stress stimulates Ca^{2+} release from the ER lumen into the cytosol through the IP3R channel, which activates the CaMKKβ/AMPK pathway and inhibits mTORC1 activity, thus triggering autophagy induction. In addition, the presence of Ca^{2+} in the cytosol leads to death-associated protein kinase 1 (DAPK1) activation, which phosphorylates BCL2 and BECLIN1 to induce autophagy (Verfaillie et al., 2010). However, whether ER stress affects autophagosome maturation, autolysosome formation, or lysosomal degradation is largely unknown.

PERK and Autophagy

Activation of the PERK pathway contributes to expression of multiple ATG genes (Cai et al., 2016). Under hypoxia, PERK-mediated ATF4 and CHOP activation transcriptionally activates LC3 and ATG5 expression (Rouschop et al., 2010; Rzymski et al., 2010). *ATG12* mRNA as well as its protein levels are increased by PERK-mediated eIF2α phosphorylation (Kouroku et al., 2007). ATF4 is sufficient for transcription of several ATG genes including *ATG3*, *BECLIN1*, *LC3*, *ATG12*, and *ATG16L1*, whereas CHOP expression transcriptionally upregulates ATG5, ATG10, and GABARAP expression (B'Chir et al., 2013). ATF4/CHOP heterodimer induces the transcriptional expression of *ATG7*, as well as *p62* and neighbor of BRCA1 gene 1 (*NBR1*), which act as

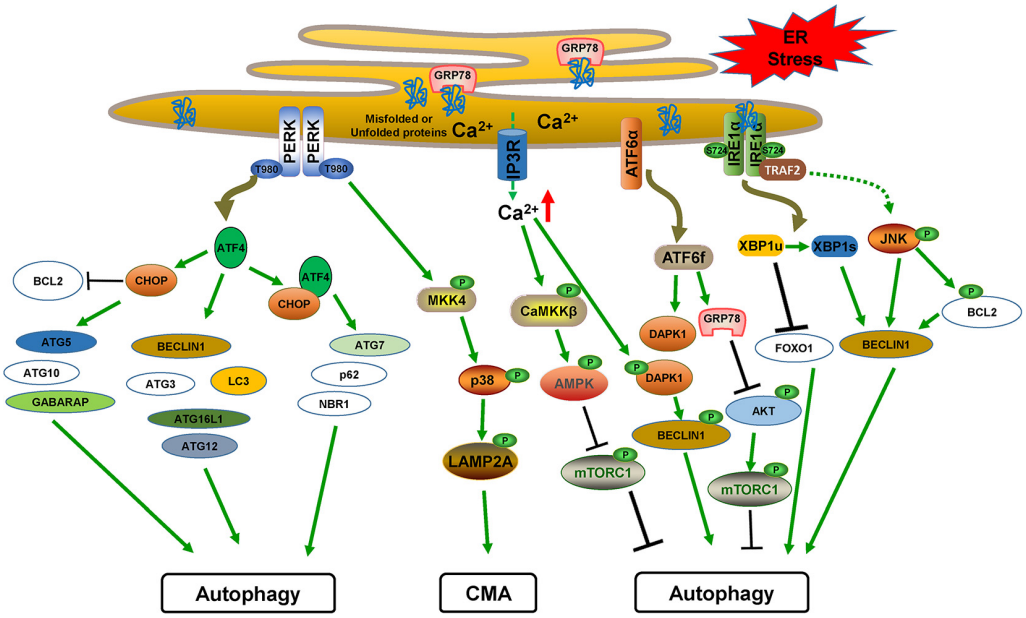


FIGURE 3 | The cross-links between ER stress/UPR and autophagy. PERK-mediated ATF4 translation induces CHOP. The transcriptional factors ATF4 and CHOP induce multiple ATG genes and autophagy regulatory factors alone or together. PERK also activates the MKK4/p38 pathway for CMA activation by phosphorylating LAMP2A. ATF6f activates the expression of GRP78, which inhibits AKT/mTORC1 activation, and DAPK1, which phosphorylates BECLIN1 to induce autophagy. IRE1α activation leads to JNK signaling, which induces BECLIN1 expression and also phosphorylates BCL2 to dissociate BECLIN1 for autophagy activation. XBP1s generation by IRE1α activation also transcriptionally activates BECLIN1 expression.

cargo receptors for selective autophagy of ubiquitinated targets (Lamark et al., 2009; B'Chir et al., 2013). CHOP can also promote autophagy through inhibiting the expression of BCL2, a protein that sequesters BECLIN1 in the ER and inhibits autophagosome formation (Pattingre et al., 2005; Rzymski et al., 2010).

The PERK pathway also initiates autophagy by activating AMPK and inhibiting mTORC1 activity (Avivar-Valderas et al., 2013). In addition, PERK-mediated ATF4/CHOP expression induces autophagy by inhibiting mTORC1 activity (Salazar et al., 2009; Bruning et al., 2013). Recently, The TFEB-mediated GADD34 expression may integrate mTORC1-mediated autophagy and ER stress (Gambardella et al., 2020). ER stress can also activate the CMA pathway by PERK activation, which recruits mitogen-activated protein kinase 4 (MKK4) and activates p38 to phosphorylate LAMP2A for CMA activation (Li et al., 2017).

IRE1α and Autophagy

IRE1α activation phosphorylates c-Jun N-terminal kinase (JNK) (Ogata et al., 2006), and this activation induces autophagy by directly phosphorylating BCL2 and disrupting its interaction with BECLIN1, which induces autophagosome formation (Wei et al., 2008). Moreover, JNK activation also upregulates BECLIN1 transcription (Li et al., 2009; Ren et al., 2010). The IRE1-dependent activation of AMPK is also involved in autophagy initiation (Meares et al., 2011). The generation of XBP1s, which is dependent on IRE1α RNase activity, also induces autophagy through direct transcriptional activation of BECLIN1 expression (Margariti et al., 2013). Interestingly, the unspliced form of XBP1 (XBP1u) negatively regulates autophagy through interacting with forkhead box O1 (FOXO1) and decreasing its levels (Zhou et al., 2011; Vidal et al., 2012; Zhao et al., 2013), suggesting that IRE1α-mediated XBP1 splicing during ER stress is critical for autophagy induction.

ATF6 and Autophagy

It has been suggested that the activation of the ATF6 branch triggers autophagy. ATF6-mediated GRP78 transcriptional expression induces autophagy initiation by inhibiting AKT activity (Yung et al., 2011). In addition, during ER stress, formed ATF6f induces the expression of DAPK1 (Kalvakolanu and Gade, 2012; Gade et al., 2014), which phosphorylates BECLIN1 so that it subsequently dissociates from its negative regulator BCL2, thus promoting autophagosome formation (Zalckvar et al., 2009).

ER STRESS, UPR, AND AUTOPHAGY CROSS TALK IN PD PATHOGENESIS

Dopaminergic neurons are particularly sensitive to unfolded, misfolded, and excessively aggregated proteins. ER stress and autophagy impairment are two essential events that lead to the imbalance of proteostasis, which contributes to DA neurodegeneration. In recent years, a large number of studies have focused on the relationship between ER stress and PD pathogenesis. For example, injection of an ER stress inducer, tunicamycin, into mouse brains causes high levels of oligomeric α-SYN, DA neuron death, locomotor deficiency, and

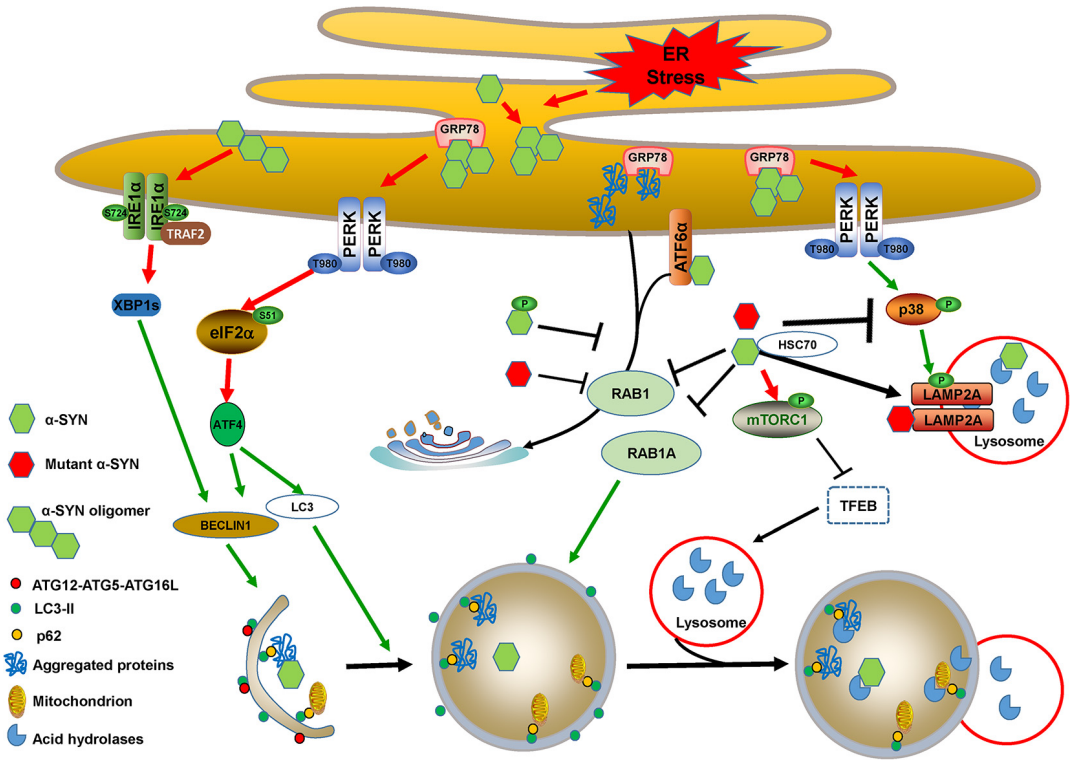


FIGURE 4 | Cross-links between ER stress and autophagy in α-SYN-mediated pathology. Accumulated α-SYN binds to GRP78 and activates ER stress. α-SYN also induces ER stress by binding to ATF6 and inhibiting its translocation to Golgi bodies. Additionally, wild-type, mutant, or phosphorylated α-SYN activates ER stress by inhibiting ER-Golgi trafficking, which leads to the accumulation of aggregated proteins. PERK/ATF4 activation that occurred due to ER stress induces BECLIN1 and LC3 expression. Oligomeric α-SYN directly activates the IRE1α/XBP1s branch and thus induces BECLIN1 expression. The expression of BECLIN1 and LC3 triggers autophagy induction. However, wild-type and mutant α-SYN inhibit autophagosome maturation by repressing RAB1A function. They also activate mTORC1 and sequester TFEB in the cytoplasm to block autophagic flux by impairing lysosomal biogenesis and function. PERK activation-mediated MKK4/p38/LAMP2A phosphorylation may promote CMA for wild-type α-SYN degradation, whereas wild-type and mutant α-SYN directly inhibit p38 activation to block CMA, and mutant α-SYN can also inhibit CMA uptake by interacting with LAMP2A.

glial activation (Coppola-Segovia et al., 2017), suggesting that administration of an ER stress inducer into the SNpc could be a novel animal model of PD. However, impaired autophagy, CMA, and mitophagy are frequently observed rather than autophagy activation in PD. Interestingly, conditional deletion of the *Atg7* gene in mice recapitulates many of the pathologic features of PD, including age-related loss of DA neurons, loss of striatal DA, accumulation of α-SYN, and ubiquitinated protein aggregates (Ahmed et al., 2012). Thus far, it is generally recognized that in PD patients as well as various PD cellular and animal models, ER stress activation, UPR markers, and autophagy dysfunction undoubtedly exist in the lesion regions, and are closely related to both genetic and neurotoxic factors that induce DA neurodegeneration.

ER Stress, UPR Activation, and Autophagy Dysfunction in Tissues of PD Patients

The UPR activation markers, including phosphorylation of PERK, eIF2α, and IRE1α, are observed in neuromelanin-containing DA neurons in the postmortem SNpc of PD patients rather than age-matched controls (Hoozemans et al., 2007; Hoozemans et al., 2012; Heman-Ackah et al., 2017). In addition, the immunoreactivity of phosphorylated PERK is co-localized with increased α-SYN immunoreactivity in DA neurons (Hoozemans et al., 2007). Importantly, UPR activation is an early event in neurodegeneration and is closely associated with the accumulation and aggregation of α-SYN (Hoozemans et al., 2012). GRP78 and CHOP, which are ER stress markers, are increased in the SNpc in PD patients (Selvaraj et al., 2012). Moreover, GRP78 is increased to a greater extent in dementia with LB (DLB) and PD with dementia (PDD) patients in the cingulate gyrus and parietal cortex (Baek et al., 2016). GRP78 is also dramatically upregulated in the brain tissues of autosomal recessive juvenile PD (AR-JP) patients caused by a loss of functional Parkin, a familial PD genetic factor (Imai et al., 2001). This is due to the defective function of Parkin's E3 ligase activity, which results in a lack of degradation and subsequent accumulation of its substrate, the PAEL receptor.

The protein disulfide isomerase (PDI) family participates in disulfide bond formation, reduction, isomerization, and accurate folding of nascent proteins, and they also are increased to constitute an adaptive response to ER stress

(Turano et al., 2002). It was found that a PDI member, pancreatic PDI (PDIp), accumulates in PD patient tissues (Conn et al., 2004). Homocysteine-induced ER protein (HERP) is a stress response protein that functions in ER folding and ERAD-mediated degradation, and ER load reduction is also increased in the SN of PD patients (Slodzinski et al., 2009). However, all PD patients do not experience an increase in the UPR in tissues. Baek et al. (2019) found that *GRP78* mRNA levels are upregulated, but they also showed that the protein levels of GRP78 are decreased in several brain regions, including the cingulate gyrus in PD patients. Recently, similar findings suggested that both GRP78 and ATF4 protein levels are decreased in the SNpc in PD patients (Esteves and Cardoso, 2020). These inconsistent results may be related to the different pathological degrees of PD patients. In the early stage of PD, UPR activation is an adaptive response to protect DA neurons from damage. However, in the late stage, excessive stress-induced neuron damage or severe DA neuron loss leads to inhibition of expression of these ER stress markers. Finally, ER stress and UPR activation are undoubted pathological processes in PD.

It was first discovered that autophagic degeneration of DA neurons occurred in the SN regions of PD patients in early studies (Anglade et al., 1997). Later, immunopositivity for LC3-II indicated that autophagosome formation occurred in the majority of LBs and LNs, and LC3-II colocalized with α-SYN in PD patients (Alvarez-Erviti et al., 2010; Dehay et al., 2010; Tanji et al., 2011), while the amount of lysosomes, and levels and activities of glucocerebrosidase (GCase) or protease cathepsin D (CTSD) were decreased within DA neurons in PD tissues (Dehay et al., 2010; Moors et al., 2019). Moreover, enlarged mitochondria have been observed within autophagosomes using confocal laser scanning microscopy in PD brains, suggesting PD-associated abnormal mitophagy (Zhu et al., 2003). Fiesel and Springer (2015); Fiesel et al. (2015) and Hou et al. (2018) confirmed that mitophagy indicated by ubiquitin Ser65 phosphorylation is specifically increased in PD patients and correlates with levels of LBs. Levels of HSC70 and LAMP2A were also dramatically decreased, which indicated that the CMA activity is significantly reduced in the SN tissues of PD patients (Alvarez-Erviti et al., 2010; Murphy et al., 2015).

The selective loss of LAMP2A protein and decreased levels of HSC70 were directly correlated with the increase in α-SYN levels and the accumulation of cytosolic CMA substrate proteins in PD samples (Murphy et al., 2015). Interestingly, crowded organelles and lipid membranes, including dystrophic lysosomes, mitochondria, and autophagosome-like structures, were observed in a recent PD postmortem study (Shahmoradian et al., 2019). Together, impairments in autophagy and CMA have been found in lesion regions in PD patients compared with matched controls using postmortem tissues. The increased autophagosomes and failed lysosomal clearance are common hallmarks in SN tissues of PD patients. The activated ER stress and UPR pathway may affect increases in autophagosome formation through the mechanisms described above. However, whether and how ER stress/UPR affects autophagosome fusion with lysosomes or lysosomal functions in PD are largely unclear.

Association of PD Genetic Factors With ER Stress, UPR, and Autophagy

Several PD-related genetic factors including gain of function of α-SYN and LRRK2, and loss of function of Parkin, PINK1, and DJ-1, affect ER stress/UPR and autophagy, and discussing the roles and mechanisms of these genetic factors in these two biological processes can greatly promote the understanding of PD pathology.

α-SYN in ER Stress, UPR, and Autophagy

α-SYN is encoded by the *SNCA* gene, the mutations of which such as A53T, or duplication or triplication, have been linked to autosomal-dominant forms of PD. Aggregated α-SYN, especially the accumulation in the brain of its soluble oligomers, is one of most important causative factors for both hereditary and sporadic PD. α-SYN is a major component deposited in LBs and LNs, in which it harbors extensive phosphorylation at Ser129, which mediates its aggregation and toxicity (Wang et al., 2020a). α-SYN can be degraded via multiple clearance machineries, including autophagy, CMA, and the ubiquitin proteasome system (Hou et al., 2020). Although wild-type, mutant, phosphorylated, and oligomeric α-SYN activate ER stress and promote autophagy induction, they block autophagic flux by impairing autophagosome maturation, fusion with lysosomes, and lysosomal biogenesis or functions (**Figure 4**).

α-SYN overexpression and its aggregated neurotoxic forms activate all three UPR branches and trigger chronic ER stress-induced apoptosis. It was discovered that overexpression of both wild-type and A53T mutant α-SYN affects RAB1, which is involved in trafficking substrates from the ER to the Golgi bodies, thus inducing UPR activation by blocking ER-Golgi trafficking. RAB1 overexpression reduces stress and protects against DA neurodegeneration in PD animal models (Cooper et al., 2006), and the Ser129 phosphorylation of α-SYN may mediate the ER-Golgi traffic disruption and trigger PERK/eIF2α branch activation in *in vitro* PD models (Sugeno et al., 2008; Jiang et al., 2010). A30P α-SYN disrupts the Golgi morphology and facilitates the susceptibility to ER stress. A53T α-SYN upregulates GRP78 levels and eIF2α phosphorylation, and results in mitochondrial cell death in neurons, as well as in astrocytes (Smith et al., 2005; Liu et al., 2018; Paiva et al., 2018).

Accumulation of α-SYN within the ER activates the PERK pathway by directly interacting with GRP78 *in vitro* and *in vivo* (Bellucci et al., 2011). α-SYN oligomers rather than monomers also activate the IRE1α-XBP1 pathway (Castillo-Carranza et al., 2012). In addition, α-SYN reduces ATF6 processing and leads to ERAD impairment by directly binding to ATF6 or indirectly restricting its incorporation into coat protein complex II (COPII) vesicles (Credle et al., 2015). ER stress also leads to the accumulation of α-SYN oligomers (Jiang et al., 2010), suggesting that ER stress plays an important role in α-SYN neurotoxicity. It is interesting to hypothesize whether α-SYN toxicity is a cause or a consequence of ER stress and UPR dysfunction. Additional evidence indicates that α-SYN accumulation within the ER is required for UPR activation, and toxic α-SYN oligomer formation precedes ER stress and UPR

activation (Colla et al., 2012a,b). Nevertheless, collaboration of α-SYN accumulation-induced ER stress and ER stress-enhanced α-SYN neurotoxicity is vital for PD pathogenesis.

Both wild-type and A53T mutant α-SYN can promote autophagy induction by upregulating BECLIN1 and LC3 expression (Yu et al., 2009; Decressac et al., 2013). The upregulation of BECLIN1 and LC3 expression may be involved in α-SYN-mediated ER stress and activation of the PERK/eIF2α/ATF4 pathway. However, wild-type α-SYN overexpression impairs autophagic flux via RAB1A inhibition, leads to ATG9 mislocalization, and inhibits the formation of autophagosomes (Winslow et al., 2010). RAB1 overexpression protects DA neurodegeneration in various PD animal models (Cooper et al., 2006; Gitler et al., 2008; Coune et al., 2012). Additionally, α-SYN binds to high mobility group box 1 (HMGB1) and strengthens BECLIN-BCL2 binding by blocking HMGB1-BECLIN1 interaction (Song et al., 2014). Both wild-type and A53T α-SYN can induce mTOR activity and impair autophagy (Jiang et al., 2013; Gao et al., 2015). In an AAV-mediated α-SYN overexpression mouse model, α-SYN impairs autophagic efflux by sequestering TFEB in the cytoplasm, accompanied by p62 and LC3-II accumulation (Decressac et al., 2013). Similarly, PC12 cells harboring A53T α-SYN display accumulated autophagic-vesicular structures and impaired lysosomal hydrolysis (Stefanis et al., 2001). Primary neurons seeded with α-SYN fibrils exist in phosphorylated α-SYN species with high neurotoxicity, named "pα-SYN*." These result from incomplete autophagic degradation of α-SYN, which colocalizes with GRP78 at mitochondria-associated ER membranes (Grassi et al., 2018), and this may play a role in the cross-linking between ER stress, mitochondrial fission, and mitophagy.

Interestingly, wild-type α-SYN contains a KFERQ sequence and is greatly degraded through the CMA pathway, while pathogenic α-SYN mutants act as CMA uptake inhibitors through interacting with LAMP2A on the lysosomal membrane (Cuervo et al., 2004). AAV-mediated overexpression of A53T α-SYN in neurons or A53T α-SYN in transgenic mice results in a reduction of CMA-mediated proteolysis of other substrates (Xilouri et al., 2009; Malkus and Ischiropoulos, 2012). Interestingly, modification of wild-type α-SYN by DA also impairs CMA proteolysis, similar to mutant α-SYN (Martinez-Vicente et al., 2008), which enables us to understand the selective vulnerability of the SNpc in PD. Although PERK activation has an active effect on LAMP2A through activating MKK4/p38 (Li et al., 2017), PERK activation induced by α-SYN is insufficient for activating LAMP2A activity, as both wild-type and pathogenic α-SYN have been reported that can directly inhibit p38 activation (Iwata et al., 2001). Whether wild-type and pathogenic α-SYN have an effect on phosphorylation and the activity of LAMP2A is not clear.

Parkin and PINK1 in ER Stress, UPR, and Autophagy

Mutations in Parkin (Kitada et al., 1998) and PTEN inducible kinase 1 (PINK1) (Valente et al., 2004a) have been identified as the most common causes of autosomal-recessive early-onset PD. *Parkin* mutations account for nearly 50% of young PD patients, and *PINK1* mutations account for 1–9% (Lucking et al., 2000; Puschmann, 2013). Parkin is an E3 ligase and functions in the ERAD of misfolded ER proteins (Shimura et al., 2000; Senft and Ronai, 2015). Parkin is upregulated by ATF4 under either ER stress or mitochondrial stress and inhibits stress-induced mitochondrial dysfunction and cell death via its E3 ligase activity (Imai et al., 2000; Bouman et al., 2011). Conversely, an accumulation of PAEL receptor, a substrate of Parkin, induces ER stress and cell death (Imai et al., 2001). Furthermore, the ER stress inhibitor salubrinal prevents rotenone-induced ER stress and cell death through the ATF4-Parkin pathway (Wu et al., 2014).

Parkin also regulates ER stress and UPR via transcription factor p53-dependent XBP1 transcription regulation (Duplan et al., 2013). It has been reported that Parkin participates in ER stress regulation in DA neurons and also in astrocytes (Ledesma et al., 2002; Singh et al., 2018). Moreover, an activation of the PERK branch of the UPR was observed that was induced by defective mitochondria, and PERK inhibition is neuroprotective in *parkin* mutant flies (Celardo et al., 2016), as well as in flies harboring mutants of *pink1*, a gene in which mutations in humans are associated with both genetic and sporadic PD (Valente et al., 2004a,b). It has been shown that PINK1 inhibits ER stress-induced damage to mouse primary cortical neurons (Li and Hu, 2015), and downregulation of ER stress response genes has been detected in aged *Pink1* knockout mice (Torres-Odio et al., 2017).

Parkin and PINK1 are two important regulators that control mitophagy and mitochondrial homeostasis (Swerdlow and Wilkins, 2020). Mitophagy, the process of removing damaged mitochondria, is compromised in PD pathogenesis, and its dysfunction is closely associated with DA neurodegeneration (Liu et al., 2019). The ATF4/CHOP heterodimer transcriptionally activates expression of p62 and NBR1 (B'Chir et al., 2013), which are two cargo adaptors involved in Parkin/PINK1-mediated mitophagy, and may be underlying the role of ER stress in mitophagy (Nguyen et al., 2016). It has been reported that the ER stress induced by tunicamycin (TM) and thapsigargin (TG) prevents Parkin loss and promotes its recruitment to the mitochondria, and also activates mitophagy during reperfusion after ischemia (Zhang et al., 2014). However, the crosslink and mechanisms between ER stress and mitophagy in PD pathogenesis are mainly unknown.

LRRK2 in ER Stress, UPR, and Autophagy

Mutations in the leucine-rich repeat kinase 2 (*LRKK2*) gene are the most common cause of autosomal-dominant forms of PD, as well as more than 3% of sporadic PD cases (Costa et al., 2020; Tolosa et al., 2020). LRRK2 possesses kinase function for catalyzing substrates and GTPase function for GTP-GDP hydrolysis. LRRK2 is co-localized with ER markers in DA neurons (Vitte et al., 2010), and LRKK2 depletion results in GRP78 downregulation in response to 6-hydroxydopamine (6-OHDA)-induced ER stress (Yuan et al., 2011). LRRK2 phosphorylates leucyl-tRNA synthetase (LRS), and this increases the number of misfolded proteins, causes ER stress, and induces autophagy initiation (Ho et al., 2018). LRRK2-G2019S mutation exacerbates these processes. It has recently been reported that LRRK2 regulates ER-mitochondria tethering through the

PERK-mediated activation of E3 ligases, and LRKK2 mutation enhances the sensitivity to ER stress and decreases mitochondrial biogenesis (Toyofuku et al., 2020). In addition, mutant LRKK2 binds to SERCA to repress its activity, leading to ER Ca^{2+} depletion and triggering ER stress, which ultimately results in mitochondrial Ca^{2+} overload and mitochondrial dysfunction in astrocytes (Lee et al., 2019).

It has been reported that LRRK2 functions in endosomal- and vesicle-trafficking pathways, plays roles in cytoskeleton dynamics and neurite outgrowth, and regulates multiple steps of the autophagy-lysosome pathway (Madureira et al., 2020). Although wild-type and mutant LRRK2 promote autophagy by ER stress induced by the phosphorylation of LRS, they impair the autophagic degradation in an LRS-independent manner (Ho et al., 2018). LRKK2-G2019S fibroblasts exhibit higher autophagic activity levels involved in activating ERK activity rather than the mTOR pathway (Bravo-San Pedro et al., 2013). An early and transient phosphorylation of ERK1/2 is involved in ER stress activation (Arai et al., 2004), indicating that LRKK2 may regulate autophagy initiation through the ERK pathway via LRS-meditated ER stress. LRRK2 and LRRK2-G2019S also regulate p62 phosphorylation, influence its affinity to ubiquitinated cargo (Park et al., 2016; Kalogeropulou et al., 2018), and decrease autophagic protein degradation. Additionally, LRKK2 and LRKK2-G2019S inhibit autophagosome formation and autophagosome-lysosome fusion in various LRRK2-related PD models may through regulating phosphorylation of a number of RAB proteins (Madureira et al., 2020). LRKK2 pathogenic mutants also impair lysosomal function, which is detected by abnormal lysosomal morphology, abnormal cellular lysosomal localization, increased lysosomal pH, or inhibition of lysosomal enzymes (Madureira et al., 2020).

Like α-SYN, LRKK2 can also be degraded by CMA, and unlike α-SYN mutants, which increase the binding affinity of HSC70 and LAMP2A, LRRK2 mutants block the formation of the CMA translocation complex by inducing LAMP2A and HSC70 accumulation at the lysosomal membrane (Orenstein et al., 2013; Ho et al., 2020). Although it has been reported that LRRK2-G2019S binds to MKK4/7 (Zhu et al., 2013), it is unclear whether LRRK2-G2019S participates in the PERK/MKK4/p38 pathway in CMA. Together, the promotion of autophagy initiation by LRRK2 and its pathogenic mutants is partly due to ER stress and UPR activation. However, they most likely inhibit autophagic flux, as well as CMA and lysosomal functions in an ER stress-independent manner.

DJ-1 in ER Stress, UPR, and Autophagy

DJ-1, a protein encoded by the *PARK7* gene, assumes multiple functions including antioxidative stress and chaperone properties (Mencke et al., 2021). Mutations or deletions of DJ-1 are associated with autosomal-recessive early-onset forms of PD (Bonifati et al., 2003). DJ-1 regulates ER stress and UPR by binding to and stabilizing ATF4 mRNA under both basal and stress conditions (Yang et al., 2019). DJ-1 can also protect against ER stress-induced cell death in Neuro2a cells (Yokota et al., 2003). Moreover, it has been shown that oxidized DJ-1 can interact with N-terminal arginylated GPR78, and thus facilitate the self-polymerization of p62 and the targeting of p62-cargo complexes to phagophores under oxidative stress (Lee et al., 2018). Interestingly, DJ-1 expression is regulated under ER stress such that XBP1 directly binds to its promoter and stimulates its expression (Duplan et al., 2013).

Overexpression of DJ-1 in DA neurons and in the SN of rat brains promotes ERK-dependent autophagy. Although there are no obvious effects of DJ-1 deficiency on autophagy in SH-SY5Y cells (Gonzalez-Polo et al., 2009; Ren et al., 2010), the loss of DJ-1 perturbs paraquat-induced autophagic initiation in SH-SY5Y cells by enhancing the mTOR activity (Gonzalez-Polo et al., 2009). In addition, DJ-1 deficiency in microglia impairs autophagy-mediated p62 degradation and reduces microglial-mediated α-SYN phagocytosis (Nash et al., 2017). DJ-1 protects against DA neurodegeneration through enhancing CMA in PD animal models, SH-SY5Y cells, and astrocytes (Xu et al., 2017; De Miranda et al., 2018). Together, the upregulation of DJ-1 expression in response to ER stress may enhance the CMA or autophagic degradation of aggregated proteins, which bridges the close link between ER stress and autophagy in PD pathogenesis.

Association of PD Neurotoxins With ER Stress and UPR

The well-known parkinsonian inducers including 1-methyl-4-phenyl-1,2,3,6-tetrahydropyridine (MPTP)/1-methyl-4-phenylpyridinium (MPP^+), 6-OHDA, and rotenone, all have profound effects on the regulation of ER stress/UPR and autophagy. Discussing the cross-link between ER stress/UPR and autophagy in these parkinsonian inducers may promote our understanding of PD pathology.

MPTP/MPP^+ in ER Stress, UPR, and Autophagy

MPTP is the best-known chemical for inducing a PD model *in vivo*. Intraperitoneally injecting mice with MPTP reproduces PD pathology, including the selective loss of DA neurons in the SN and accumulation of protein aggregates, and eventually leads to the onset of PD-like clinical symptoms (Bove et al., 2005). MPTP can efficiently cross the blood-brain barrier and is metabolized to the destructive MPP^+ by glial monoamine oxidase B (MAO-B). MPP^+ is transported into DA neurons via dopamine transporter (DAT) and induces DA neuron death by inhibiting mitochondrial functions and increasing mitochondrial superoxide.

MPP^+ triggers a significant increase in the expression of UPR genes including ATF4 and CHOP, which are involved in the activation of IRE1α and PERK in various cellular models (Ryu et al., 2002; Holtz and O'Malley, 2003). MPP^+ has been shown to activate cyclin-dependent-like kinase 5 (CDK5)-mediated XBP1s phosphorylation, which favors its nuclear translocation and promotes its transcriptional activity in rat primary cultured neurons (Jiao et al., 2017). The intracerebral injection of MPP^+ into the SNpc of rabbit brains induces ER stress involving the activation of the ATF6 and NF-κB signaling pathways (Ghribi et al., 2003). MPTP also promotes the phosphorylation of p38 and enhances the interaction between phosphorylated p38 and ATF6, leading to an increase in ATF6 transcriptional activity (Egawa et al., 2011). MPP^+ also activates the expression of UPR markers

such as PDIp, which accumulates in PD patient tissues (Conn et al., 2004). MPTP/MPP^+ activate ER stress and expression of the UPR markers GRP78 and CHOP by disturbing ER Ca^{2+} levels, which is accompanied by a decrease in AKT/mTOR activity (Selvaraj et al., 2012), and is closely associated with autophagy activation.

The regulatory effects of MPTP/MPP^+ on autophagy are not consistent among different studies. MPTP/MPP^+ treatment increases autophagosome formation, increases p62 levels, and decreases lysosomal activity (Dehay et al., 2010; Lim et al., 2011; Lim et al., 2014; Jovanovic-Tucovic et al., 2019), indicating that autophagy initiation is activated but autophagic flux is blocked by MPP^+ treatment. The activation of autophagy initiation by MPP^+ treatment probably occurs through activation of AMPK (Jovanovic-Tucovic et al., 2019). Further study indicates that mild MPP^+ exposure (10 or 200 μM for 48 h) predominantly inhibits autophagic degradation by reducing lysosomal hydrolase cathepsin D activity, whereas acute MPP^+ treatment (2.5 and 5 mM for 24 h) inhibits both autophagic degradation and basal autophagy by decreasing lysosomal density (Miyara et al., 2016). MPP^+ treatment increases autophagy activation and promotes mitochondrial degradation, which involves the activation of ERK signaling rather than the canonical pathway (Zhu et al., 2007, 2012; Dagda et al., 2008).

We speculate that MPP^+ treatment-induced mitochondrial degradation may not be due to the activation of autophagic flux, but it dramatically disrupts mitochondrial functions and impairs mitochondrial biogenesis (Zhu et al., 2012). MPP^+ treatment-induced ER stress and the UPR closely contribute to autophagy induction and autophagic flux blockage. All branches of the UPR are activated by MPTP/MPP^+ treatment, as well as subsequent events such as activation of AMPK (Jovanovic-Tucovic et al., 2019), decreased mTOR activity (Selvaraj et al., 2012), and increased NF-κB signaling (Ghribi et al., 2003),

TABLE 1 | The roles and mechanisms of PD-related factors in ER stress, autophagy and their cross-links.

PD-related factors	Roles and mechanisms in ER stress	Roles and mechanisms in autophagy	Cross-links
α-SYN	α-SYN directly binds to GRP78 to activate PERK and α-SYN reduces ATF6 processing; α-SYN oligomers activate the IRE1α-XBP1 pathway; Wild-type and mutant α-SYN affect RAB1 and disrupts traffic from the ER to the Golgi; ER stress leads to the accumulation of α-SYN oligomers.	α-SYN promotes autophagy induction by upregulating BECLIN1 and LC3 expression; α-SYN impairs autophagic flux via RAB1A inhibition, TFEB sequestration and lysosomal inhibition; α-SYN is degraded via autophagy and CMA; Oxidized α-SYN and A53T α-SYN reduce CMA-mediated proteolysis through binding to LAMP2A or inhibit p38 activation.	α-SYN-mediated BECLIN1 and LC3 expression via ER stress activation may be involved in its role in autophagy induction; The inhibition of RAB pathway by α-SYN is both involved in ER stress activation and autophagic flux impairment.
Parkin/PINK1	Parkin is upregulated by ER stress; Parkin inhibits PERK-mediated ER stress through its E3 ligase activity; Parkin also regulates ER stress via p53-XBP1 pathway; PINK1 inhibits ER stress via PERK branch.	Parkin and PINK1 control mitochondrial homeostasis by enhancing mitophagy.	PERK/ATF4/CHOP induced Parkin, p62 and NBR expression may be involved in Parkin/PINK1-mediated mitophagy.
LRRK2	LRRK2 is partly localized in ER; LRRK2 and its pathogenic mutant G2019S phosphorylate LRS, and cause ER stress; Mutant LRKK2 binds to SERCA and leads to ER Ca^{2+} depletion to trigger ER stress;	LRRK2 and LRKK2-G2019S induce autophagy initiation by phosphorylating LRS; LRRK2-G2019S promotes autophagy by activating ERK; LRRK2 and LRRK2-G2019S decrease autophagic degradation by regulating p62 phosphorylation, as well as inhibit autophagosome and autolysosome formation via phosphorylating a number of RAB proteins.	LRKK2 and it mutants trigger autophagy initiation by activating ERK via LRS-meditated accumulation of misfolded proteins and ER stress. LRKK2 and it mutants activate ER stress and impair autophagic flux may also through regulating RABs functions.
DJ-1	DJ-1 regulates ER stress/UPR by binding to and stabilizing ATF4 mRNA; Oxidized DJ-1 interact with arginylated GPR78; DJ-1 is upregulated under ER stress through XBP1 branch.	DJ-1 promotes ERK-dependent autophagy; Loss of DJ-1 perturbs paraquat-induced autophagic initiation by enhancing the mTOR activity; DJ-1 deficiency in microglia impairs autophagy-mediated p62 degradation and reduces microglial-mediated α-SYN phagocytosis. DJ-1 enhances CMA activity	Oxidized DJ-1 interact with arginylated GPR78 and facilitate p62-cargo complexes to phagophore; ER stress induced DJ-1 upregulation enhances the CMA or autophagic degradation.
MPTP/MPP^+	MPTP/MPP^+ activates IRE1α, PERK, and ATF6 branches through enhancing CDK5 and p38 activity, as well as disturbing ER Ca^{2+} levels.	MPTP/MPP^+ treatment increases autophagy initiation but blocks autophagic flux, probably through activating AMPK and ERK activity, and reducing mTOR activity and lysosomal hydrolase activity.	MPTP/MPP^+ treatment-induced ER stress and the UPR activation contribute to autophagy induction.
6-OHDA	6-OHDA activates ER stress/UPR by phosphorylating PERK and eIF2α.	6-OHDA treatment elicits autophagy activation by activating ERK and AMPK activity, as well as BECLIN1 expression; 6-OHDA promotes autophagic flux and CMA activity.	6-OHDA-activated ER stress/UPR contributes to excessive autophagy initiation and autophagic flux.
Rotenone	Rotenone triggers ER stress involving activation of all three branches of PERK, IRE1α, and ATF6.	Rotenone treatment increases autophagy induction but inhibits autophagic flux by impairing lysosomal functions; rotenone increases mitophagy.	Rotenone-mediated ER stress/UPR stimulates autophagy induction.

which contribute to autophagy initiation (Zhu et al., 2017). MPTP/MPP$^+$ treatment also disrupts lysosomal functions and leads to autophagic flux blockage (Dehay et al., 2010; Lim et al., 2011). The cross-link between autophagy initiation activation and autophagic flux blockage exaggerates the damage to DA neurons by MPTP/MPP$^+$ treatment.

6-OHDA in ER Stress, UPR, and Autophagy

6-OHDA, a selective catecholaminergic neurotoxin, is also widely used to induce DA neuron death as a PD model by eliciting the production of mitochondrial and cytosolic reactive oxygen species (ROS) (Simola et al., 2007). Increased levels of GRP78 and CHOP expression, as well as phosphorylated PERK and eIF2α, are detected in DA cellular models that are subjected to 6-OHDA treatment (Ryu et al., 2002; Holtz and O'Malley, 2003; Yamamuro et al., 2006; Deng et al., 2012; Xie et al., 2012; Ning et al., 2019b).

Like MPP$^+$, 6-OHDA treatment also elicits autophagy activation and promotes mitochondrial degradation involving the activation of ERK signaling (Dagda et al., 2008). Unlike MPP$^+$, 6-OHDA induces AMPK phosphorylation, followed by mTOR dephosphorylation, and increases LC3 conversion, p62 degradation, and cytoplasmatic acidification in SH-SY5Y cells (Arsikin et al., 2012). A recent study indicated that 6-OHDA treatment induces excessive autophagy with increased AMPK activity, decreased mTOR activity, reduced p62 levels, and also prevents alterations in lysosomal functions (Chung et al., 2018). In addition, 6-OHDA treatment stimulates CMA activity by increasing LAMP2A levels (Wang et al., 2018). 6-OHDA treatment induces BECLIN1 and decreases BCL2 expression and p62 levels, which are inhibited by PERK inhibition (Ning et al., 2019a,b), and this directly cross-links the ER stress and autophagy in 6-OHDA-induced PD pathogenesis. Together,

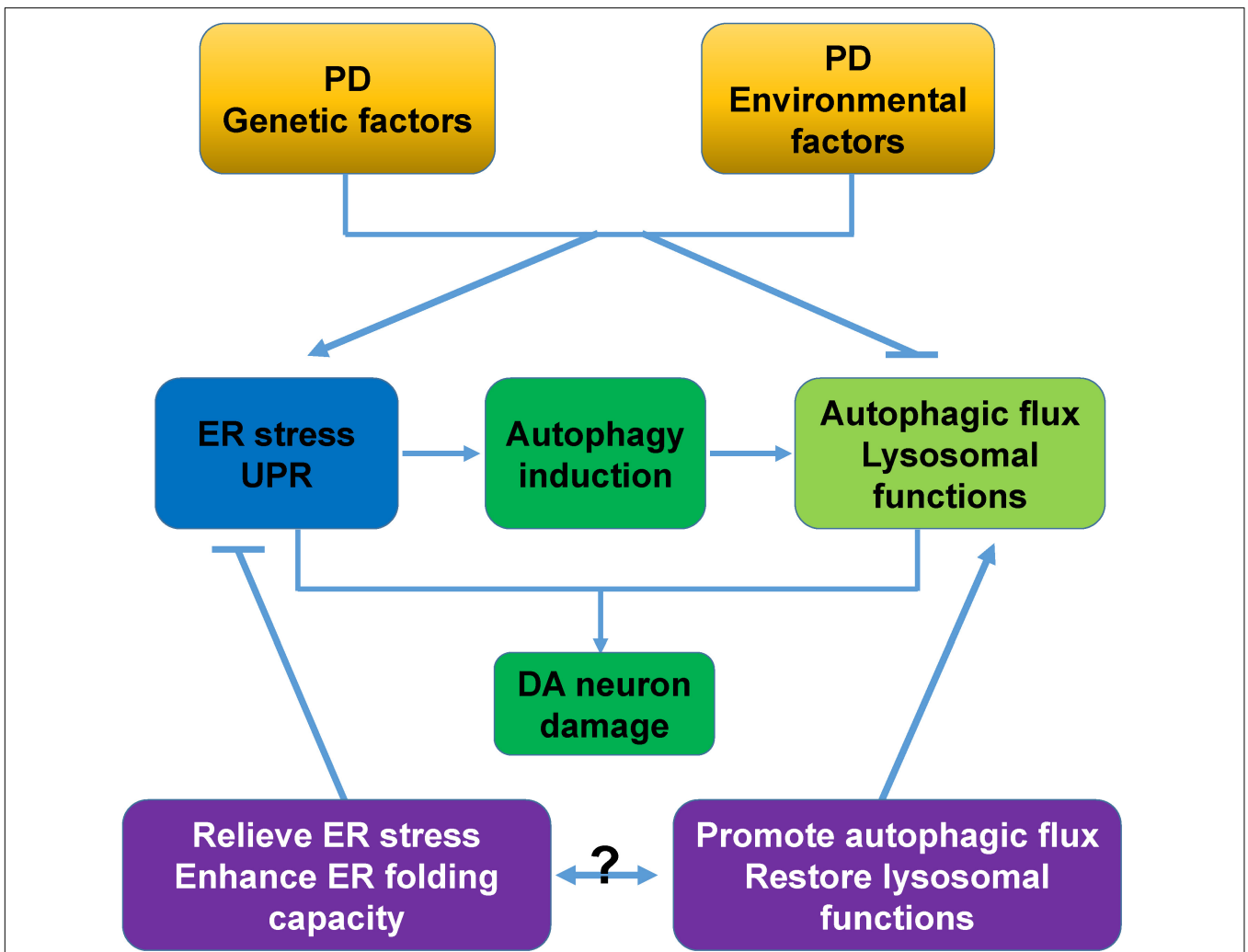


FIGURE 5 | Proposed model of cross-links between ER stress, autophagy, and DA neurodegeneration. PD-associated genetic and environmental factors trigger ER stress, and ER stress activates the UPR and induces autophagy to alleviate cellular stress. However, these PD-associated factors commonly block autophagic flux and impair lysosomal functions, and these changes synergistically cause severe damage and degeneration of DA neurons. Relieving ER stress/UPR, enhancing the ER folding capacity, promoting autophagic flux, and restoring lysosomal functions are neuroprotective for PD. The combined intervention of ER stress/UPR and autophagy would be a more attractive therapeutic approach for PD.

6-OHDA-induced excessive autophagy activation and autophagic flux contribute to PD pathogenesis.

Rotenone in ER Stress, UPR, and Autophagy

Rotenone treatment produces most of the movement disorder symptoms and the histopathological features of PD, including LBs (Betarbet et al., 2002). Rotenone also triggers ATF4 and CHOP expression involving activation of IRE1α and PERK in cellular models (Ryu et al., 2002; Ramalingam et al., 2019). An induction of the IRE1α and PERK branch of the UPR has also been shown in rotenone rat or mouse models of PD (Tong et al., 2016a,b; Ramalingam et al., 2019). Treatment of N2a cells with rotenone triggers ER stress and the UPR involving all three branches of PERK, IRE1α, and ATF6 (Gupta et al., 2019).

Rotenone induces an increase in autophagy related proteins LC3-II and BECLIN1, as well as in autophagy substrates such as α-SYN and p62 in cultured PC12 cells (Wu et al., 2015) and in SH-SY5Y cells (Xiong et al., 2013), suggesting that rotenone exerts bidirectional effects on autophagy initiation and autophagic flux. Rotenone increases oligomeric wild-type and A53T α-SYN in transfected cells through inhibiting their autophagic degradation (Yu et al., 2009). Similar to MPP^+, although rotenone treatment results in decreased autophagic flux, it increases mitophagy for mitochondrial degradation (Giordano et al., 2014), suggesting that the mitochondrial-specific degradation pathway used by MPP^+ and rotenone may be independent from that of autophagy. Therefore, rotenone-induced ER stress and the UPR initiate autophagy induction but block autophagic flux by impairing lysosomal functions, which aggravates the imbalance of cellular homeostasis and damage to DA neurons.

FUTURE PERSPECTIVES

The accumulation of unfolded, misfolded, and aggregated proteins, and the accumulation induced by cellular stress are essential mechanisms underlying the causes of PD. ER stress/UPR and autophagy, two major pathways that are used to respond to proteostasis imbalance, play especially important roles in PD pathology. In this review, we systematically examined the intrinsic molecular links between ER stress, the UPR, and autophagy, as well as the roles of these cross-links in PD pathology. ER stress, UPR activation, and dysregulated autophagy commonly coexist in patients and various cellular and animal models of PD, and are closely related to DA neurodegeneration caused by PD genetic and neurotoxic factors (**Table 1**). This is why targeting one of these processes would create a beneficial PD treatment (Moors et al., 2017; Martinez et al., 2019). More importantly, combining both ER stress/UPR and autophagy regulation, such as relieving ER stress/UPR or enhancing the ER folding capacity, and promoting autophagic flux or restoring lysosomal functions will be more neuroprotective for PD (**Figure 5**). In addition, the ER stress/UPR activation, upregulation of UPR genes, and accumulation of autophagosome markers and autophagic substrates are expected to be useful biomarkers or diagnostic parameters of PD.

For example, administration of GSK2606414, a PERK inhibitor, results in effective neuroprotection and prevents loss of SNpc DA neurons in mice that were treated with PD neurotoxin 6-OHDA (Mercado et al., 2018). Gene therapy that restores the folding capacity by administration of viral-mediated overexpression of GRP78 (Gorbatyuk et al., 2012) or UPR transcriptional factor XBP1s (Sado et al., 2009; Valdes et al., 2014) in the SNpc results in neuroprotection against neurotoxin- or genetic factors-induced damage to DA neurons. Rapamycin, an inhibitor of mTOR, initiates autophagy induction, enhances autophagic flux (Rubinsztein and Nixon, 2010), and confers significant protective effects on DA neurons in various PD models (Moors et al., 2017). Additionally, enhancing lysosomal biogenesis by TFEB overexpression or pharmacological stimulation of TFEB function by CCI-779 was shown to eliminate α-SYN oligomers and rescue midbrain DA neurons from α-SYN toxicity in rats (Decressac et al., 2013).

It is notable that PD-associated genetic or environmental factors lead to ER stress and UPR activation, which commonly initiate autophagy. However, these PD-associated factors also block autophagic flux and impair lysosomal functions. An intervention strategy for one of the two processes alone may not completely alleviate the imbalance in cellular homeostasis. However, a combined treatment strategy for both ER stress/UPR and the autophagy pathway has not yet been studied in PD. We recognize that combining ER stress/UPR and autophagy to explore the pathological mechanisms of PD and develop interventional strategies that combine ER stress/UPR and autophagy will be very meaningful in the future.

AUTHOR CONTRIBUTIONS

GW and XL designed the theme of the manuscript. HR and WZ wrote the manuscript. All authors approved the submitted version.

FUNDING

This research was funded by the National Natural Science Foundation of China (31970966, 32070970, and 31871023), Suzhou Clinical Research Center of Neurological Disease (Szzx201503), and the Priority Academic Program Development of Jiangsu Higher Education Institutions.

REFERENCES

Abdullah, A., and Ravanan, P. (2018). The unknown face of IRE1alpha - beyond ER stress. *Eur. J. Cell Biol.* 97, 359–368. doi: 10.1016/j.ejcb.2018.05.002

Ahmed, I., Liang, Y., Schools, S., Dawson, V. L., Dawson, T. M., and Savitt, J. M. (2012). Development and characterization of a new Parkinson's disease model resulting from impaired autophagy. *J. Neurosci.* 32, 16503–16509. doi: 10.1523/JNEUROSCI.0209-12.2012

Alvarez-Erviti, L., Rodriguez-Oroz, M. C., Cooper, J. M., Caballero, C., Ferrer, I., Obeso, J. A., et al. (2010). Chaperone-mediated autophagy markers in Parkinson disease brains. *Arch. Neurol.* 67, 1464–1472. doi: 10.1001/archneurol.2010.198

Anglade, P., Vyas, S., Javoy-Agid, F., Herrero, M. T., Michel, P. P., Marquez, J., et al. (1997). Apoptosis and autophagy in nigral neurons of patients with Parkinson's disease. *Histol. Histopathol.* 12, 25–31.

Arai, K., Lee, S. R., van Leyen, K., Kurose, H., and Lo, E. H. (2004). Involvement of ERK MAP kinase in endoplasmic reticulum stress in SH-SY5Y human neuroblastoma cells. *J. Neurochem.* 89, 232–239. doi: 10.1111/j.1471-4159.2004.02317.x

Arsikin, K., Kravic-Stevovic, T., Jovanovic, M., Ristic, B., Tovilovic, G., Zogovic, N., et al. (2012). Autophagy-dependent and -independent involvement of AMP-activated protein kinase in 6-hydroxydopamine toxicity to SH-SY5Y neuroblastoma cells. *Biochim. Biophys. Acta* 1822, 1826–1836. doi: 10.1016/j.bbadis.2012.08.006

Avivar-Valderas, A., Bobrovnikova-Marjon, E., Alan Diehl, J., Bardeesy, N., Debnath, J., and Aguirre-Ghiso, J. A. (2013). Regulation of autophagy during ECM detachment is linked to a selective inhibition of mTORC1 by PERK. *Oncogene* 32, 4932–4940. doi: 10.1038/onc.2012.512

Baek, J. H., Mamula, D., Tingstam, B., Pereira, M., He, Y., and Svenningsson, P. (2019). GRP78 level is altered in the brain, but not in plasma or cerebrospinal fluid in Parkinson's disease patients. *Front. Neurosci.* 13:697. doi: 10.3389/fnins.2019.00697

Baek, J. H., Whitfield, D., Howlett, D., Francis, P., Bereczki, E., Ballard, C., et al. (2016). Unfolded protein response is activated in Lewy body dementias. *Neuropathol. Appl. Neurobiol.* 42, 352–365. doi: 10.1111/nan.12260

B'Chir, W., Maurin, A. C., Carraro, V., Averous, J., Jousse, C., Muranishi, Y., et al. (2013). The eIF2alpha/ATF4 pathway is essential for stress-induced autophagy gene expression. *Nucleic Acids Res.* 41, 7683–7699. doi: 10.1093/nar/gkt563

Bellucci, A., Navarria, L., Zaltieri, M., Falarti, E., Bodei, S., Sigala, S., et al. (2011). Induction of the unfolded protein response by alpha-synuclein in experimental models of Parkinson's disease. *J. Neurochem.* 116, 588–605. doi: 10.1111/j.1471-4159.2010.07143.x

Bernales, S., McDonald, K. L., and Walter, P. (2006). Autophagy counterbalances endoplasmic reticulum expansion during the unfolded protein response. *PLoS Biol.* 4:e423. doi: 10.1371/journal.pbio.0040423

Betarbet, R., Sherer, T. B., and Greenamyre, J. T. (2002). Animal models of Parkinson's disease. *Bioessays* 24, 308–318. doi: 10.1002/bies.10067

Bonifati, V., Rizzu, P., van Baren, M. J., Schaap, O., Breedveld, G. J., Krieger, E., et al. (2003). Mutations in the DJ-1 gene associated with autosomal recessive early-onset parkinsonism. *Science* 299, 256–259. doi: 10.1126/science.1077209

Bouman, L., Schlierf, A., Lutz, A. K., Shan, J., Deinlein, A., Kast, J., et al. (2011). Parkin is transcriptionally regulated by ATF4: evidence for an interconnection between mitochondrial stress and ER stress. *Cell Death Differ.* 18, 769–782. doi: 10.1038/cdd.2010.142

Bove, J., Prou, D., Perier, C., and Przedborski, S. (2005). Toxin-induced models of Parkinson's disease. *NeuroRx* 2, 484–494. doi: 10.1602/neurorx.2.3.484

Bozic, M., van den Bekerom, L., Milne, B. A., Goodman, N., Roberston, L., Prescott, A. R., et al. (2020). A conserved ATG2-GABARAP family interaction is critical for phagophore formation. *EMBO Rep.* 21:e48412. doi: 10.15252/embr.201948412

Bravo-San Pedro, J. M., Niso-Santano, M., Gomez-Sanchez, R., Pizarro-Estrella, E., Aiastui-Pujana, A., Gorostidi, A., et al. (2013). The LRRK2 G2019S mutant exacerbates basal autophagy through activation of the MEK/ERK pathway. *Cell. Mol. Life Sci.* 70, 121–136. doi: 10.1007/s00018-012-1061-y

Bruning, A., Rahmeh, M., and Friese, K. (2013). Nelfinavir and bortezomib inhibit mTOR activity via ATF4-mediated sestrin-2 regulation. *Mol. Oncol.* 7, 1012–1018. doi: 10.1016/j.molonc.2013.07.010

Cai, Y., Arikkath, J., Yang, L., Guo, M. L., Periyasamy, P., and Buch, S. (2016). Interplay of endoplasmic reticulum stress and autophagy in neurodegenerative disorders. *Autophagy* 12, 225–244. doi: 10.1080/15548627.2015.1121360

Castillo-Carranza, D. L., Zhang, Y., Guerrero-Munoz, M. J., Kayed, R., Rincon-Limas, D. E., and Fernandez-Funez, P. (2012). Differential activation of the ER stress factor XBP1 by oligomeric assemblies. *Neurochem. Res.* 37, 1707–1717. doi: 10.1007/s11064-012-0780-7

Celardo, I., Costa, A. C., Lehmann, S., Jones, C., Wood, N., Mencacci, N. E., et al. (2016). Mitofusin-mediated ER stress triggers neurodegeneration in pink1/parkin models of Parkinson's disease. *Cell Death Dis.* 7:e2271. doi: 10.1038/cddis.2016.173

Chung, Y., Lee, J., Jung, S., Lee, Y., Cho, J. W., and Oh, Y. J. (2018). Dysregulated autophagy contributes to caspase-dependent neuronal apoptosis. *Cell Death Dis.* 9:1189. doi: 10.1038/s41419-018-1229-y

Colla, E., Coune, P., Liu, Y., Pletnikova, O., Troncoso, J. C., Iwatsubo, T., et al. (2012a). Endoplasmic reticulum stress is important for the manifestations of alpha-synucleinopathy in vivo. *J. Neurosci.* 32, 3306–3320. doi: 10.1523/JNEUROSCI.5367-11.2012

Colla, E., Jensen, P. H., Pletnikova, O., Troncoso, J. C., Glabe, C., and Lee, M. K. (2012b). Accumulation of toxic alpha-synuclein oligomer within endoplasmic reticulum occurs in alpha-synucleinopathy in vivo. *J. Neurosci.* 32, 3301–3305. doi: 10.1523/JNEUROSCI.5368-11.2012

Conn, K. J., Gao, W., McKee, A., Lan, M. S., Ullman, M. D., Eisenhauer, P. B., et al. (2004). Identification of the protein disulfide isomerase family member PDIp in experimental Parkinson's disease and Lewy body pathology. *Brain Res.* 1022, 164–172. doi: 10.1016/j.brainres.2004.07.026

Cooper, A. A., Gitler, A. D., Cashikar, A., Haynes, C. M., Hill, K. J., Bhullar, B., et al. (2006). Alpha-synuclein blocks ER-Golgi traffic and Rab1 rescues neuron loss in Parkinson's models. *Science* 313, 324–328. doi: 10.1126/science.1129462

Coppola-Segovia, V., Cavarsan, C., Maia, F. G., Ferraz, A. C., Nakao, L. S., Lima, M. M., et al. (2017). ER stress induced by tunicamycin triggers alpha-synuclein oligomerization, dopaminergic neurons death and locomotor impairment: a new model of Parkinson's disease. *Mol. Neurobiol.* 54, 5798–5806. doi: 10.1007/s12035-016-0114-x

Corona Velazquez, A. F., and Jackson, W. T. (2018). So many roads: the multifaceted regulation of autophagy induction. *Mol. Cell. Biol.* 38:e00303-18. doi: 10.1128/MCB.00303-18

Cortes, C. J., and La Spada, A. R. (2019). TFEB dysregulation as a driver of autophagy dysfunction in neurodegenerative disease: molecular mechanisms, cellular processes, and emerging therapeutic opportunities. *Neurobiol. Dis.* 122, 83–93. doi: 10.1016/j.nbd.2018.05.012

Costa, C. A. D., Manaa, W. E., Duplan, E., and Checler, F. (2020). The endoplasmic reticulum stress/unfolded protein response and their contributions to Parkinson's disease physiopathology. *Cells* 9:2495. doi: 10.3390/cells9112495

Coune, P. G., Schneider, B. L., and Aebischer, P. (2012). Parkinson's disease: gene therapies. *Cold Spring Harb. Perspect. Med.* 2:a009431. doi: 10.1101/cshperspect.a009431

Credle, J. J., Finer-Moore, J. S., Papa, F. R., Stroud, R. M., and Walter, P. (2005). On the mechanism of sensing unfolded protein in the endoplasmic reticulum. *Proc. Natl. Acad. Sci. U.S.A.* 102, 18773–18784. doi: 10.1073/pnas.0509487102

Credle, J. J., Forcelli, P. A., Delannoy, M., Oaks, A. W., Permaul, E., Berry, D. L., et al. (2015). alpha-Synuclein-mediated inhibition of ATF6 processing into COPII vesicles disrupts UPR signaling in Parkinson's disease. *Neurobiol. Dis.* 76, 112–125. doi: 10.1016/j.nbd.2015.02.005

Cuervo, A. M., Stefanis, L., Fredenburg, R., Lansbury, P. T., and Sulzer, D. (2004). Impaired degradation of mutant alpha-synuclein by chaperone-mediated autophagy. *Science* 305, 1292–1295. doi: 10.1126/science.1101738

Dagda, R. K., Zhu, J., Kulich, S. M., and Chu, C. T. (2008). Mitochondrially localized ERK2 regulates mitophagy and autophagic cell stress: implications for Parkinson's disease. *Autophagy* 4, 770–782. doi: 10.4161/auto.6458

De Miranda, B. R., Rocha, E. M., Bai, Q., El Ayadi, A., Hinkle, D., Burton, E. A., et al. (2018). Astrocyte-specific DJ-1 overexpression protects against rotenone-induced neurotoxicity in a rat model of Parkinson's disease. *Neurobiol. Dis.* 115, 101–114. doi: 10.1016/j.nbd.2018.04.008

Decressac, M., Mattsson, B., Weikop, P., Lundblad, M., Jakobsson, J., and Bjorklund, A. (2013). TFEB-mediated autophagy rescues midbrain dopamine neurons from alpha-synuclein toxicity. *Proc. Natl. Acad. Sci. U.S.A.* 110, E1817–E1826. doi: 10.1073/pnas.1305623110

Deegan, S., Saveljeva, S., Gorman, A. M., and Samali, A. (2013). Stress-induced self-cannibalism: on the regulation of autophagy by endoplasmic reticulum stress. *Cell. Mol. Life Sci.* 70, 2425–2441. doi: 10.1007/s00018-012-1173-4

Dehay, B., Bove, J., Rodriguez-Muela, N., Perier, C., Recasens, A., Boya, P., et al. (2010). Pathogenic lysosomal depletion in Parkinson's disease. *J. Neurosci.* 30, 12535–12544. doi: 10.1523/JNEUROSCI.1920-10.2010

Deng, C., Tao, R., Yu, S. Z., and Jin, H. (2012). Inhibition of 6-hydroxydopamine-induced endoplasmic reticulum stress by sulforaphane through the activation

of Nrf2 nuclear translocation. *Mol. Med. Rep.* 6, 215–219. doi: 10.3892/mmr.2012.894

Duplan, E., Giaime, E., Viotti, J., Sevalle, J., Corti, O., Brice, A., et al. (2013). ER-stress-associated functional link between Parkin and DJ-1 via a transcriptional cascade involving the tumor suppressor p53 and the spliced X-box binding protein XBP-1. *J. Cell Sci.* 126(Pt 9), 2124–2133. doi: 10.1242/jcs.127340

Egawa, N., Yamamoto, K., Inoue, H., Hikawa, R., Nishi, K., Mori, K., et al. (2011). The endoplasmic reticulum stress sensor, ATF6alpha, protects against neurotoxin-induced dopaminergic neuronal death. *J. Biol. Chem.* 286, 7947–7957. doi: 10.1074/jbc.M110.156430

Esteves, A. R., and Cardoso, S. M. (2020). Differential protein expression in diverse brain areas of Parkinson's and Alzheimer's disease patients. *Sci. Rep.* 10:13149. doi: 10.1038/s41598-020-70174-z

Fiesel, F. C., Ando, M., Hudec, R., Hill, A. R., Castanedes-Casey, M., Caulfield, T. R., et al. (2015). (Patho-)physiological relevance of PINK1-dependent ubiquitin phosphorylation. *EMBO Rep.* 16, 1114–1130. doi: 10.15252/embr.201540514

Fiesel, F. C., and Springer, W. (2015). Disease relevance of phosphorylated ubiquitin (p-S65-Ub). *Autophagy* 11, 2125–2126. doi: 10.1080/15548627.2015.1091912

Gade, P., Manjegowda, S. B., Nallar, S. C., Maachani, U. B., Cross, A. S., and Kalvakolanu, D. V. (2014). Regulation of the death-associated protein kinase 1 expression and autophagy via ATF6 requires apoptosis signal-regulating kinase 1. *Mol. Cell. Biol.* 34, 4033–4048. doi: 10.1128/MCB.00397-14

Gambardella, G., Staiano, L., Moretti, M. N., De Cegli, R., Fagnocchi, L., Di Tullio, G., et al. (2020). GADD34 is a modulator of autophagy during starvation. *Sci. Adv.* 6:eabb0205. doi: 10.1126/sciadv.abb0205

Gao, S., Duan, C., Gao, G., Wang, X., and Yang, H. (2015). Alpha-synuclein overexpression negatively regulates insulin receptor substrate 1 by activating mTORC1/S6K1 signaling. *Int. J. Biochem. Cell Biol.* 64, 25–33. doi: 10.1016/j.biocel.2015.03.006

Gardner, B. M., and Walter, P. (2011). Unfolded proteins are Ire1-activating ligands that directly induce the unfolded protein response. *Science* 333, 1891–1894. doi: 10.1126/science.1209126

Ghemrawi, R., and Khair, M. (2020). Endoplasmic reticulum stress and unfolded protein response in neurodegenerative diseases. *Int. J. Mol. Sci.* 21:6127. doi: 10.3390/ijms21176127

Ghribi, O., Herman, M. M., Pramoonjago, P., and Savory, J. (2003). MPP+ induces the endoplasmic reticulum stress response in rabbit brain involving activation of the ATF-6 and NF-kappaB signaling pathways. *J. Neuropathol. Exp. Neurol.* 62, 1144–1153. doi: 10.1093/jnen/62.11.1144

Giordano, S., Dodson, M., Ravi, S., Redmann, M., Ouyang, X., Darley Usmar, V. M., et al. (2014). Bioenergetic adaptation in response to autophagy regulators during rotenone exposure. *J. Neurochem.* 131, 625–633. doi: 10.1111/jnc.12844

Gitler, A. D., Bevis, B. J., Shorter, J., Strathearn, K. E., Hamamichi, S., Su, L. J., et al. (2008). The Parkinson's disease protein alpha-synuclein disrupts cellular Rab homeostasis. *Proc. Natl. Acad. Sci. U.S.A.* 105, 145–150. doi: 10.1073/pnas.0710685105

Gonzalez-Polo, R., Niso-Santano, M., Moran, J. M., Ortiz-Ortiz, M. A., Bravo-San Pedro, J. M., Soler, G., et al. (2009). Silencing DJ-1 reveals its contribution in paraquat-induced autophagy. *J. Neurochem.* 109, 889–898. doi: 10.1111/j.1471-4159.2009.06020.x

Gorbatyuk, M. S., Shabashvili, A., Chen, W., Meyers, C., Sullivan, L. F., Salganik, M., et al. (2012). Glucose regulated protein 78 diminishes alpha-synuclein neurotoxicity in a rat model of Parkinson disease. *Mol. Ther.* 20, 1327–1337. doi: 10.1038/mt.2012.28

Grassi, D., Howard, S., Zhou, M., Diaz-Perez, N., Urban, N. T., Guerrero-Given, D., et al. (2018). Identification of a highly neurotoxic alpha-synuclein species inducing mitochondrial damage and mitophagy in Parkinson's disease. *Proc. Natl. Acad. Sci. U.S.A.* 115, E2634–E2643. doi: 10.1073/pnas.1713849115

Gupta, S., Biswas, J., Gupta, P., Singh, A., Tiwari, S., Mishra, A., et al. (2019). Salubrinal attenuates nitric oxide mediated PERK:IRE1alpha: ATF-6 signaling and DNA damage in neuronal cells. *Neurochem. Int.* 131:104581. doi: 10.1016/j.neuint.2019.104581

Harding, H. P., Novoa, I., Zhang, Y., Zeng, H., Wek, R., Schapira, M., et al. (2000). Regulated translation initiation controls stress-induced gene expression in mammalian cells. *Mol. Cell* 6, 1099–1108. doi: 10.1016/s1097-2765(00)00108-8

Haze, K., Yoshida, H., Yanagi, H., Yura, T., and Mori, K. (1999). Mammalian transcription factor ATF6 is synthesized as a transmembrane protein and activated by proteolysis in response to endoplasmic reticulum stress. *Mol. Biol. Cell* 10, 3787–3799. doi: 10.1091/mbc.10.11.3787

Heman-Ackah, S. M., Manzano, R., Hoozemans, J. J. M., Scheper, W., Flynn, R., Haerty, W., et al. (2017). Alpha-synuclein induces the unfolded protein response in Parkinson's disease SNCA triplication iPSC-derived neurons. *Hum. Mol. Genet.* 26, 4441–4450. doi: 10.1093/hmg/ddx331

Hetz, C., and Papa, F. R. (2018). The unfolded protein response and cell fate control. *Mol. Cell* 69, 169–181. doi: 10.1016/j.molcel.2017.06.017

Hillary, R. F., and FitzGerald, U. (2018). A lifetime of stress: ATF6 in development and homeostasis. *J. Biomed. Sci.* 25:48. doi: 10.1186/s12929-018-0453-1

Ho, D. H., Kim, H., Nam, D., Sim, H., Kim, J., Kim, H. G., et al. (2018). LRRK2 impairs autophagy by mediating phosphorylation of leucyl-tRNA synthetase. *Cell Biochem. Funct.* 36, 431–442. doi: 10.1002/cbf.3364

Ho, P. W., Leung, C. T., Liu, H., Pang, S. Y., Lam, C. S., Xian, J., et al. (2020). Age-dependent accumulation of oligomeric SNCA/alpha-synuclein from impaired degradation in mutant LRRK2 knockin mouse model of Parkinson disease: role for therapeutic activation of chaperone-mediated autophagy (CMA). *Autophagy* 16, 347–370. doi: 10.1080/15548627.2019.1603545

Holtz, W. A., and O'Malley, K. L. (2003). Parkinsonian mimetics induce aspects of unfolded protein response in death of dopaminergic neurons. *J. Biol. Chem.* 278, 19367–19377. doi: 10.1074/jbc.M211821200

Hoozemans, J. J., van Haastert, E. S., Eikelenboom, P., de Vos, R. A., Rozemuller, J. M., and Scheper, W. (2007). Activation of the unfolded protein response in Parkinson's disease. *Biochem. Biophys. Res. Commun.* 354, 707–711. doi: 10.1016/j.bbrc.2007.01.043

Hoozemans, J. J., van Haastert, E. S., Nijholt, D. A., Rozemuller, A. J., and Scheper, W. (2012). Activation of the unfolded protein response is an early event in Alzheimer's and Parkinson's disease. *Neurodegener. Dis.* 10, 212–215. doi: 10.1159/000334536

Hou, X., Fiesel, F. C., Truban, D., Castanedes Casey, M., Lin, W. L., Soto, A. I., et al. (2018). Age- and disease-dependent increase of the mitophagy marker phospho-ubiquitin in normal aging and Lewy body disease. *Autophagy* 14, 1404–1418. doi: 10.1080/15548627.2018.1461294

Hou, X., Watzlawik, J. O., Fiesel, F. C., and Springer, W. (2020). Autophagy in Parkinson's disease. *J. Mol. Biol.* 432, 2651–2672. doi: 10.1016/j.jmb.2020.01.037

Imai, Y., Soda, M., Inoue, H., Hattori, N., Mizuno, Y., and Takahashi, R. (2001). An unfolded putative transmembrane polypeptide, which can lead to endoplasmic reticulum stress, is a substrate of Parkin. *Cell* 105, 891–902. doi: 10.1016/s0092-8674(01)00407-x

Imai, Y., Soda, M., and Takahashi, R. (2000). Parkin suppresses unfolded protein stress-induced cell death through its E3 ubiquitin-protein ligase activity. *J. Biol. Chem.* 275, 35661–35664. doi: 10.1074/jbc.C000447200

Iurlaro, R., and Munoz-Pinedo, C. (2016). Cell death induced by endoplasmic reticulum stress. *FEBS J.* 283, 2640–2652. doi: 10.1111/febs.13598

Iwata, A., Maruyama, M., Kanazawa, I., and Nukina, N. (2001). alpha-Synuclein affects the MAPK pathway and accelerates cell death. *J. Biol. Chem.* 276, 45320–45329. doi: 10.1074/jbc.M103736200

Jiang, P., Gan, M., Ebrahim, A. S., Lin, W. L., Melrose, H. L., and Yen, S. H. (2010). ER stress response plays an important role in aggregation of alpha-synuclein. *Mol. Neurodegener.* 5:56. doi: 10.1186/1750-1326-5-56

Jiang, T. F., Zhang, Y. J., Zhou, H. Y., Wang, H. M., Tian, L. P., Liu, J., et al. (2013). Curcumin ameliorates the neurodegenerative pathology in A53T alpha-synuclein cell model of Parkinson's disease through the downregulation of mTOR/p70S6K signaling and the recovery of macroautophagy. *J. Neuroimmune Pharmacol.* 8, 356–369. doi: 10.1007/s11481-012-9431-7

Jiao, F. J., Wang, Q. Z., Zhang, P., Yan, J. G., Zhang, Z., He, F., et al. (2017). CDK5-mediated phosphorylation of XBP1s contributes to its nuclear translocation and activation in MPP(+)-induced Parkinson's disease model. *Sci. Rep.* 7:5622. doi: 10.1038/s41598-017-06012-6

Jovanovic-Tucovic, M., Harhaji-Trajkovic, L., Dulovic, M., Tovilovic-Kovacevic, G., Zogovic, N., Jeremic, M., et al. (2019). AMP-activated protein kinase inhibits MPP+-induced oxidative stress and apoptotic death of SH-SY5Y cells through sequential stimulation of Akt and autophagy. *Eur. J. Pharmacol.* 863:172677. doi: 10.1016/j.ejphar.2019.172677

Kalia, L. V., and Lang, A. E. (2015). Parkinson's disease. *Lancet* 386, 896–912. doi: 10.1016/S0140-6736(14)61393-3

Kalogeropulou, A. F., Zhao, J., Bolliger, M. F., Memou, A., Narasimha, S., Molitor, T. P., et al. (2018). P62/SQSTM1 is a novel leucine-rich repeat kinase 2 (LRRK2) substrate that enhances neuronal toxicity. *Biochem. J.* 475, 1271–1293. doi: 10.1042/BCJ20170699

Kalvakolanu, D. V., and Gade, P. (2012). IFNG and autophagy: a critical role for the ER-stress mediator ATF6 in controlling bacterial infections. *Autophagy* 8, 1673–1674. doi: 10.4161/auto.21403

Karabiyik, C., Lee, M. J., and Rubinsztein, D. C. (2017). Autophagy impairment in Parkinson's disease. *Essays Biochem.* 61, 711–720. doi: 10.1042/EBC20170023

Kitada, T., Asakawa, S., Hattori, N., Matsumine, H., Yamamura, Y., Minoshima, S., et al. (1998). Mutations in the parkin gene cause autosomal recessive juvenile parkinsonism. *Nature* 392, 605–608. doi: 10.1038/33416

Korennykh, A., and Walter, P. (2012). Structural basis of the unfolded protein response. *Annu. Rev. Cell Dev. Biol.* 28, 251–277. doi: 10.1146/annurev-cellbio-101011-155826

Kouroku, Y., Fujita, E., Tanida, I., Ueno, T., Isoai, A., Kumagai, H., et al. (2007). ER stress (PERK/eIF2alpha phosphorylation) mediates the polyglutamine-induced LC3 conversion, an essential step for autophagy formation. *Cell Death Differ.* 14, 230–239. doi: 10.1038/sj.cdd.4401984

Lamark, T., Kirkin, V., Dikic, I., and Johansen, T. (2009). NBR1 and p62 as cargo receptors for selective autophagy of ubiquitinated targets. *Cell Cycle* 8, 1986–1990. doi: 10.4161/cc.8.13.8892

Ledesma, M. D., Galvan, C., Hellias, B., Dotti, C., and Jensen, P. H. (2002). Astrocytic but not neuronal increased expression and redistribution of parkin during unfolded protein stress. *J. Neurochem.* 83, 1431–1440. doi: 10.1046/j.1471-4159.2002.01253.x

Lee, D. H., Kim, D., Kim, S. T., Jeong, S., Kim, J. L., Shim, S. M., et al. (2018). PARK7 modulates autophagic proteolysis through binding to the N-terminally arginylated form of the molecular chaperone HSPA5. *Autophagy* 14, 1870–1885. doi: 10.1080/15548627.2018.1491212

Lee, J. H., Han, J. H., Kim, H., Park, S. M., Joe, E. H., and Jou, I. (2019). Parkinson's disease-associated LRRK2-G2019S mutant acts through regulation of SERCA activity to control ER stress in astrocytes. *Acta Neuropathol. Commun.* 7:68. doi: 10.1186/s40478-019-0716-4

Lehtonen, S., Sonninen, T. M., Wojciechowski, S., Goldsteins, G., and Koistinaho, J. (2019). Dysfunction of cellular proteostasis in Parkinson's disease. *Front. Neurosci.* 13:457. doi: 10.3389/fnins.2019.00457

Levine, B., and Kroemer, G. (2019). Biological functions of autophagy genes: a disease perspective. *Cell* 176, 11–42. doi: 10.1016/j.cell.2018.09.048

Li, D. D., Wang, L. L., Deng, R., Tang, J., Shen, Y., Guo, J. F., et al. (2009). The pivotal role of c-Jun NH2-terminal kinase-mediated Beclin 1 expression during anticancer agents-induced autophagy in cancer cells. *Oncogene* 28, 886–898. doi: 10.1038/onc.2008.441

Li, L., and Hu, G. K. (2015). Pink1 protects cortical neurons from thapsigargin-induced oxidative stress and neuronal apoptosis. *Biosci. Rep.* 35:e00174. doi: 10.1042/BSR20140104

Li, T., and Le, W. (2020). Biomarkers for Parkinson's disease: how good are they? *Neurosci. Bull.* 36, 183–194. doi: 10.1007/s12264-019-00433-1

Li, W., Zhu, J., Dou, J., She, H., Tao, K., Xu, H., et al. (2017). Phosphorylation of LAMP2A by p38 MAPK couples ER stress to chaperone-mediated autophagy. *Nat. Commun.* 8:1763. doi: 10.1038/s41467-017-01609-x

Lim, J., Kim, H. W., Youdim, M. B., Rhyu, I. J., Choe, K. M., and Oh, Y. J. (2011). Binding preference of p62 towards LC3-ll during dopaminergic neurotoxin-induced impairment of autophagic flux. *Autophagy* 7, 51–60. doi: 10.4161/auto.7.1.13909

Lim, J., Lee, Y., Jung, S., Youdim, M. B., and Oh, Y. J. (2014). Impaired autophagic flux is critically involved in drug-induced dopaminergic neuronal death. *Parkinsonism Relat. Disord.* 20(Suppl. 1), S162–S166. doi: 10.1016/S1353-8020(13)70039-7

Liu, J., Liu, W., Li, R., and Yang, H. (2019). Mitophagy in Parkinson's disease: from pathogenesis to treatment. *Cells* 8:712. doi: 10.3390/cells8070712

Liu, M., Qin, L., Wang, L., Tan, J., Zhang, H., Tang, J., et al. (2018). alphasynuclein induces apoptosis of astrocytes by causing dysfunction of the endoplasmic reticulumGolgi compartment. *Mol. Med. Rep.* 18, 322–332. doi: 10.3892/mmr.2018.9002

Lucking, C. B., Durr, A., Bonifati, V., Vaughan, J., De Michele, G., Gasser, T., et al. (2000). Association between early-onset Parkinson's disease and mutations in the parkin gene. *N. Engl. J. Med.* 342, 1560–1567. doi: 10.1056/NEJM200005253422103

Madureira, M., Connor-Robson, N., and Wade-Martins, R. (2020). LRRK2: Autophagy and Lysosomal activity. *Front. Neurosci.* 14:498. doi: 10.3389/fnins.2020.00498

Malkus, K. A., and Ischiropoulos, H. (2012). Regional deficiencies in chaperone-mediated autophagy underlie alpha-synuclein aggregation and neurodegeneration. *Neurobiol. Dis.* 46, 732–744. doi: 10.1016/j.nbd.2012.03.017

Manie, S. N., Lebeau, J., and Chevet, E. (2014). Cellular mechanisms of endoplasmic reticulum stress signaling in health and disease. 3. Orchestrating the unfolded protein response in oncogenesis: an update. *Am. J. Physiol. Cell Physiol.* 307, C901–C907. doi: 10.1152/ajpcell.00292.2014

Margariti, A., Li, H., Chen, T., Martin, D., Vizcay-Barrena, G., Alam, S., et al. (2013). XBP1 mRNA splicing triggers an autophagic response in endothelial cells through BECLIN-1 transcriptional activation. *J. Biol. Chem.* 288, 859–872. doi: 10.1074/jbc.M112.412783

Martinez, A., Lopez, N., Gonzalez, C., and Hetz, C. (2019). Targeting of the unfolded protein response (UPR) as therapy for Parkinson's disease. *Biol. Cell.* 111, 161–168. doi: 10.1111/boc.201800068

Martinez-Vicente, M., Talloczy, Z., Kaushik, S., Massey, A. C., Mazzulli, J., Mosharov, E. V., et al. (2008). Dopamine-modified alpha-synuclein blocks chaperone-mediated autophagy. *J. Clin. Invest.* 118, 777–788. doi: 10.1172/JCI32806

Martini-Stoica, H., Xu, Y., Ballabio, A., and Zheng, H. (2016). The Autophagy-Lysosomal pathway in neurodegeneration: a TFEB perspective. *Trends Neurosci.* 39, 221–234. doi: 10.1016/j.tins.2016.02.002

Meares, G. P., Hughes, K. J., Naatz, A., Papa, F. R., Urano, F., Hansen, P. A., et al. (2011). IRE1-dependent activation of AMPK in response to nitric oxide. *Mol. Cell. Biol.* 31, 4286–4297. doi: 10.1128/MCB.05668-11

Mencke, P., Boussaad, I., Romano, C. D., Kitami, T., Linster, C. L., and Kruger, R. (2021). The Role of DJ-1 in cellular metabolism and pathophysiological implications for Parkinson's disease. *Cells* 10:347. doi: 10.3390/cells10020347

Mercado, G., Castillo, V., Soto, P., Lopez, N., Axten, J. M., Sardi, S. P., et al. (2018). Targeting PERK signaling with the small molecule GSK2606414 prevents neurodegeneration in a model of Parkinson's disease. *Neurobiol. Dis.* 112, 136–148. doi: 10.1016/j.nbd.2018.01.004

Miyara, M., Kotake, Y., Tokunaga, W., Sanoh, S., and Ohta, S. (2016). Mild MPP(+) exposure impairs autophagic degradation through a novel lysosomal acidity-independent mechanism. *J. Neurochem.* 139, 294–308. doi: 10.1111/jnc.13700

Moors, T. E., Hoozemans, J. J., Ingrassia, A., Beccari, T., Parnetti, L., Chartier-Harlin, M. C., et al. (2017). Therapeutic potential of autophagy-enhancing agents in Parkinson's disease. *Mol. Neurodegener.* 12:11. doi: 10.1186/s13024-017-0154-3

Moors, T. E., Paciotti, S., Ingrassia, A., Quadri, M., Breedveld, G., Tasegian, A., et al. (2019). Characterization of brain Lysosomal activities in GBA-related and sporadic Parkinson's disease and dementia with Lewy bodies. *Mol. Neurobiol.* 56, 1344–1355. doi: 10.1007/s12035-018-1090-0

Murphy, K. E., Gysbers, A. M., Abbott, S. K., Spiro, A. S., Furuta, A., Cooper, A., et al. (2015). Lysosomal-associated membrane protein 2 isoforms are differentially affected in early Parkinson's disease. *Mov. Disord.* 30, 1639–1647. doi: 10.1002/mds.26141

Nakamura, S., and Yoshimori, T. (2017). New insights into autophagosome-lysosome fusion. *J. Cell Sci.* 130, 1209–1216. doi: 10.1242/jcs.196352

Nascimbeni, A. C., Codogno, P., and Morel, E. (2017). Phosphatidylinositol-3-phosphate in the regulation of autophagy membrane dynamics. *FEBS J.* 284, 1267–1278. doi: 10.1111/febs.13987

Nash, Y., Schmukler, E., Trudler, D., Pinkas-Kramarski, R., and Frenkel, D. (2017). DJ-1 deficiency impairs autophagy and reduces alpha-synuclein phagocytosis by microglia. *J. Neurochem.* 143, 584–594. doi: 10.1111/jnc.14222

Nguyen, T. N., Padman, B. S., and Lazarou, M. (2016). Deciphering the molecular signals of PINK1/Parkin mitophagy. *Trends Cell Biol.* 26, 733–744. doi: 10.1016/j.tcb.2016.05.008

Ning, B., Zhang, Q., Deng, M., Wang, N., and Fang, Y. (2019a). Endoplasmic reticulum stress induced autophagy in 6-OHDA-induced Parkinsonian

rats. *Brain Res. Bull.* 146, 224–227. doi: 10.1016/j.brainresbull.2019.01.001

Ning, B., Zhang, Q., Wang, N., Deng, M., and Fang, Y. (2019b). beta-Asarone regulates er stress and autophagy via inhibition of the PERK/CHOP/Bcl-2/Beclin-1 pathway in 6-OHDA-induced parkinsonian rats. *Neurochem. Res.* 44, 1159–1166. doi: 10.1007/s11064-019-02757-w

Noda, N. N., and Inagaki, F. (2015). Mechanisms of autophagy. *Annu. Rev. Biophys.* 44, 101–122. doi: 10.1146/annurev-biophys-060414-034248

Novoa, I., Zeng, H., Harding, H. P., and Ron, D. (2001). Feedback inhibition of the unfolded protein response by GADD34-mediated dephosphorylation of eIF2alpha. *J. Cell Biol.* 153, 1011–1022. doi: 10.1083/jcb.153.5.1011

Oakes, S. A., and Papa, F. R. (2015). The role of endoplasmic reticulum stress in human pathology. *Annu. Rev. Pathol.* 10, 173–194. doi: 10.1146/annurev-pathol-012513-104649

Ogata, M., Hino, S., Saito, A., Morikawa, K., Kondo, S., Kanemoto, S., et al. (2006). Autophagy is activated for cell survival after endoplasmic reticulum stress. *Mol. Cell. Biol.* 26, 9220–9231. doi: 10.1128/MCB.01453-06

Orenstein, S. J., Kuo, S. H., Tasset, I., Arias, E., Koga, H., Fernandez-Carasa, I., et al. (2013). Interplay of LRRK2 with chaperone-mediated autophagy. *Nat. Neurosci.* 16, 394–406. doi: 10.1038/nn.3350

Paiva, I., Jain, G., Lazaro, D. F., Jercic, K. G., Hentrich, T., Kerimoglu, C., et al. (2018). Alpha-synuclein deregulates the expression of COL4A2 and impairs ER-Golgi function. *Neurobiol. Dis.* 119, 121–135. doi: 10.1016/j.nbd.2018.08.001

Pandey, V. K., Mathur, A., and Kakkar, P. (2019). Emerging role of Unfolded Protein Response (UPR) mediated proteotoxic apoptosis in diabetes. *Life Sci.* 216, 246–258. doi: 10.1016/j.lfs.2018.11.041

Park, S., Han, S., Choi, I., Kim, B., Park, S. P., Joe, E. H., et al. (2016). Interplay between Leucine-rich repeat Kinase 2 (LRRK2) and p62/SQSTM-1 in selective Autophagy. *PLoS One* 11:e0163029. doi: 10.1371/journal.pone.0163029

Pattingre, S., Tassa, A., Qu, X., Garuti, R., Liang, X. H., Mizushima, N., et al. (2005). Bcl-2 antiapoptotic proteins inhibit Beclin 1-dependent autophagy. *Cell* 122, 927–939. doi: 10.1016/j.cell.2005.07.002

Poewe, W., Seppi, K., Tanner, C. M., Halliday, G. M., Brundin, P., Volkmann, J., et al. (2017). Parkinson disease. *Nat. Rev. Dis. Primers* 3:17013. doi: 10.1038/nrdp.2017.13

Puschmann, A. (2013). Monogenic Parkinson's disease and parkinsonism: clinical phenotypes and frequencies of known mutations. *Parkinsonism Relat. Disord.* 19, 407–415. doi: 10.1016/j.parkreldis.2013.01.020

Ramalingam, M., Huh, Y. J., and Lee, Y. I. (2019). The impairments of alpha-Synuclein and mechanistic target of rapamycin in rotenone-induced SH-SY5Y cells and mice model of Parkinson's disease. *Front. Neurosci.* 13:1028. doi: 10.3389/fnins.2019.01028

Rashid, H. O., Yadav, R. K., Kim, H. R., and Chae, H. J. (2015). ER stress: autophagy induction, inhibition and selection. *Autophagy* 11, 1956–1977. doi: 10.1080/15548627.2015.1091141

Ren, H., Fu, K., Mu, C., Li, B., Wang, D., and Wang, G. (2010). DJ-1, a cancer and Parkinson's disease associated protein, regulates autophagy through JNK pathway in cancer cells. *Cancer Lett.* 297, 101–108. doi: 10.1016/j.canlet.2010.05.001

Rouschop, K. M., van den Beucken, T., Dubois, L., Niessen, H., Bussink, J., Savelkouls, K., et al. (2010). The unfolded protein response protects human tumor cells during hypoxia through regulation of the autophagy genes MAP1LC3B and ATG5. *J. Clin. Invest.* 120, 127–141. doi: 10.1172/JCI40027

Rubinsztein, D. C., and Nixon, R. A. (2010). Rapamycin induces autophagic flux in neurons. *Proc. Natl. Acad. Sci. U.S.A.* 107:E181. doi: 10.1073/pnas.1014633107

Russell, R. C., Tian, Y., Yuan, H., Park, H. W., Chang, Y. Y., Kim, J., et al. (2013). ULK1 induces autophagy by phosphorylating Beclin-1 and activating VPS34 lipid kinase. *Nat. Cell Biol.* 15, 741–750. doi: 10.1038/ncb2757

Ryu, E. J., Harding, H. P., Angelastro, J. M., Vitolo, O. V., Ron, D., and Greene, L. A. (2002). Endoplasmic reticulum stress and the unfolded protein response in cellular models of Parkinson's disease. *J. Neurosci.* 22, 10690–10698.

Rzymski, T., Milani, M., Pike, L., Buffa, F., Mellor, H. R., Winchester, L., et al. (2010). Regulation of autophagy by ATF4 in response to severe hypoxia. *Oncogene* 29, 4424–4435. doi: 10.1038/onc.2010.191

Sado, M., Yamasaki, Y., Iwanaga, T., Onaka, Y., Ibuki, T., Nishihara, S., et al. (2009). Protective effect against Parkinson's disease-related insults through the activation of XBP1. *Brain Res.* 1257, 16–24. doi: 10.1016/j.brainres.2008.11.104

Salazar, M., Carracedo, A., Salanueva, I. J., Hernandez-Tiedra, S., Lorente, M., Egia, A., et al. (2009). Cannabinoid action induces autophagy-mediated cell death through stimulation of ER stress in human glioma cells. *J. Clin. Invest.* 119, 1359–1372. doi: 10.1172/jci37948

Selvaraj, S., Sun, Y., Watt, J. A., Wang, S., Lei, S., Birnbaumer, L., et al. (2012). Neurotoxin-induced ER stress in mouse dopaminergic neurons involves downregulation of TRPC1 and inhibition of AKT/mTOR signaling. *J. Clin. Invest.* 122, 1354–1367. doi: 10.1172/JCI61332

Senft, D., and Ronai, Z. A. (2015). UPR, autophagy, and mitochondria crosstalk underlies the ER stress response. *Trends Biochem. Sci.* 40, 141–148. doi: 10.1016/j.tibs.2015.01.002

Shahmoradian, S. H., Lewis, A. J., Genoud, C., Hench, J., Moors, T. E., Navarro, P. P., et al. (2019). Lewy pathology in Parkinson's disease consists of crowded organelles and lipid membranes. *Nat. Neurosci.* 22, 1099–1109. doi: 10.1038/s41593-019-0423-2

Shen, J., Chen, X., Hendershot, L., and Prywes, R. (2002). ER stress regulation of ATF6 localization by dissociation of BiP/GRP78 binding and unmasking of Golgi localization signals. *Dev. Cell* 3, 99–111. doi: 10.1016/s1534-5807(02)00203-4

Shimizu, S. (2018). Biological roles of alternative Autophagy. *Mol. Cells* 41, 50–54. doi: 10.14348/molcells.2018.2215

Shimura, H., Hattori, N., Kubo, S., Mizuno, Y., Asakawa, S., Minoshima, S., et al. (2000). Familial Parkinson disease gene product, parkin, is a ubiquitin-protein ligase. *Nat. Genet.* 25, 302–305. doi: 10.1038/77060

Shulman, J. M., De Jager, P. L., and Feany, M. B. (2011). Parkinson's disease: genetics and pathogenesis. *Annu. Rev. Pathol.* 6, 193–222. doi: 10.1146/annurev-pathol-011110-130242

Simola, N., Morelli, M., and Carta, A. R. (2007). The 6-hydroxydopamine model of Parkinson's disease. *Neurotox. Res.* 11, 151–167. doi: 10.1007/BF03033565

Singh, K., Han, K., Tilve, S., Wu, K., Geller, H. M., and Sack, M. N. (2018). Parkin targets NOD2 to regulate astrocyte endoplasmic reticulum stress and inflammation. *Glia* 66, 2427–2437. doi: 10.1002/glia.23482

Slodzinski, H., Moran, L. B., Michael, G. J., Wang, B., Novoselov, S., Cheetham, M. E., et al. (2009). Homocysteine-induced endoplasmic reticulum protein (herp) is up-regulated in parkinsonian substantia nigra and present in the core of Lewy bodies. *Clin. Neuropathol.* 28, 333–343.

Smith, W. W., Jiang, H., Pei, Z., Tanaka, Y., Morita, H., Sawa, A., et al. (2005). Endoplasmic reticulum stress and mitochondrial cell death pathways mediate A53T mutant alpha-synuclein-induced toxicity. *Hum. Mol. Genet.* 14, 3801–3811. doi: 10.1093/hmg/ddi396

Song, J. X., Lu, J. H., Liu, L. F., Chen, L. L., Durairajan, S. S., Yue, Z., et al. (2014). HMGB1 is involved in autophagy inhibition caused by SNCA/alpha-synuclein overexpression: a process modulated by the natural autophagy inducer corynoxine B. *Autophagy* 10, 144–154. doi: 10.4161/auto.26751

Stefanis, L., Larsen, K. E., Rideout, H. J., Sulzer, D., and Greene, L. A. (2001). Expression of A53T mutant but not wild-type alpha-synuclein in PC12 cells induces alterations of the ubiquitin-dependent degradation system, loss of dopamine release, and autophagic cell death. *J. Neurosci.* 21, 9549–9560.

Stolz, A., Ernst, A., and Dikic, I. (2014). Cargo recognition and trafficking in selective autophagy. *Nat. Cell Biol.* 16, 495–501. doi: 10.1038/ncb2979

Sugeno, N., Takeda, A., Hasegawa, T., Kobayashi, M., Kikuchi, A., Mori, F., et al. (2008). Serine 129 phosphorylation of alpha-synuclein induces unfolded protein response-mediated cell death. *J. Biol. Chem.* 283, 23179–23188. doi: 10.1074/jbc.M802223200

Swerdlow, N. S., and Wilkins, H. M. (2020). Mitophagy and the brain. *Int. J. Mol. Sci.* 21:9661. doi: 10.3390/ijms21249661

Takahashi, Y., He, H., Tang, Z., Hattori, T., Liu, Y., Young, M. M., et al. (2018). An autophagy assay reveals the ESCRT-III component CHMP2A as a regulator of phagophore closure. *Nat. Commun.* 9:2855. doi: 10.1038/s41467-018-05254-w

Takahashi, Y., Liang, X., Hattori, T., Tang, Z., He, H., Chen, H., et al. (2019). VPS37A directs ESCRT recruitment for phagophore closure. *J. Cell Biol.* 218, 3336–3354. doi: 10.1083/jcb.201902170

Tanji, K., Mori, F., Kakita, A., Takahashi, H., and Wakabayashi, K. (2011). Alteration of autophagosomal proteins (LC3, GABARAP and GATE-16) in Lewy body disease. *Neurobiol. Dis.* 43, 690–697. doi: 10.1016/j.nbd.2011.05.022

Tekirdag, K., and Cuervo, A. M. (2018). Chaperone-mediated autophagy and endosomal microautophagy: joint by a chaperone. *J. Biol. Chem.* 293, 5414–5424. doi: 10.1074/jbc.R117.818237

Tolosa, E., Vila, M., Klein, C., and Rascol, O. (2020). LRRK2 in Parkinson disease: challenges of clinical trials. *Nat. Rev. Neurol.* 16, 97–107. doi: 10.1038/s41582-019-0301-2

Tong, Q., Wu, L., Gao, Q., Ou, Z., Zhu, D., and Zhang, Y. (2016a). PPARbeta/delta agonist provides neuroprotection by suppression of IRE1alpha-caspase-12-mediated endoplasmic reticulum stress pathway in the rotenone rat model of Parkinson's disease. *Mol. Neurobiol.* 53, 3822–3831. doi: 10.1007/s12035-015-9309-9

Tong, Q., Wu, L., Jiang, T., Ou, Z., Zhang, Y., and Zhu, D. (2016b). Inhibition of endoplasmic reticulum stress-activated IRE1alpha-TRAF2-caspase-12 apoptotic pathway is involved in the neuroprotective effects of telmisartan in the rotenone rat model of Parkinson's disease. *Eur. J. Pharmacol.* 776, 106–115. doi: 10.1016/j.ejphar.2016.02.042

Torres-Odio, S., Key, J., Hoepken, H. H., Canet-Pons, J., Valek, L., Roller, B., et al. (2017). Progression of pathology in PINK1-deficient mouse brain from splicing via ubiquitination, ER stress, and mitophagy changes to neuroinflammation. *J. Neuroinflamm.* 14:154. doi: 10.1186/s12974-017-0928-0

Toyofuku, T., Okamoto, Y., Ishikawa, T., Sasawatari, S., and Kumanogoh, A. (2020). LRRK2 regulates endoplasmic reticulum-mitochondrial tethering through the PERK-mediated ubiquitination pathway. *EMBO J.* 39:e100875. doi: 10.15252/embj.2018100875

Tsuboyama, K., Koyama-Honda, I., Sakamaki, Y., Koike, M., Morishita, H., and Mizushima, N. (2016). The ATG conjugation systems are important for degradation of the inner autophagosomal membrane. *Science* 354, 1036–1041. doi: 10.1126/science.aaf6136

Turano, C., Coppari, S., Altieri, F., and Ferraro, A. (2002). Proteins of the PDI family: unpredicted non-ER locations and functions. *J. Cell. Physiol.* 193, 154–163. doi: 10.1002/jcp.10172

Urano, F., Wang, X., Bertolotti, A., Zhang, Y., Chung, P., Harding, H. P., et al. (2000). Coupling of stress in the ER to activation of JNK protein kinases by transmembrane protein kinase IRE1. *Science* 287, 664–666. doi: 10.1126/science.287.5453.664

Valdes, P., Mercado, G., Vidal, R. L., Molina, C., Parsons, G., Court, F. A., et al. (2014). Control of dopaminergic neuron survival by the unfolded protein response transcription factor XBP1. *Proc. Natl. Acad. Sci. U.S.A.* 111, 6804–6809. doi: 10.1073/pnas.1321845111

Valente, E. M., Abou-Sleiman, P. M., Caputo, V., Muqit, M. M., Harvey, K., Gispert, S., et al. (2004a). Hereditary early-onset Parkinson's disease caused by mutations in PINK1. *Science* 304, 1158–1160. doi: 10.1126/science.1096284

Valente, E. M., Salvi, S., Ialongo, T., Marongiu, R., Elia, A. E., Caputo, V., et al. (2004b). PINK1 mutations are associated with sporadic early-onset parkinsonism. *Ann. Neurol.* 56, 336–341. doi: 10.1002/ana.20256

Verfaillie, T., Salazar, M., Velasco, G., and Agostinis, P. (2010). Linking ER stress to autophagy: potential implications for cancer therapy. *Int. J. Cell Biol.* 2010:930509. doi: 10.1155/2010/930509

Vidal, R. L., Figueroa, A., Court, F. A., Thielen, P., Molina, C., Wirth, C., et al. (2012). Targeting the UPR transcription factor XBP1 protects against Huntington's disease through the regulation of FoxO1 and autophagy. *Hum. Mol. Genet.* 21, 2245–2262. doi: 10.1093/hmg/dds040

Vitte, J., Traver, S., Maues De Paula, A., Lesage, S., Rovelli, G., Corti, O., et al. (2010). Leucine-rich repeat kinase 2 is associated with the endoplasmic reticulum in dopaminergic neurons and accumulates in the core of Lewy bodies in Parkinson disease. *J. Neuropathol. Exp. Neurol.* 69, 959–972. doi: 10.1097/NEN.0b013e3181efc01c

Walter, P., and Ron, D. (2011). The unfolded protein response: from stress pathway to homeostatic regulation. *Science* 334, 1081–1086. doi: 10.1126/science.1209038

Wang, M., and Kaufman, R. J. (2016). Protein misfolding in the endoplasmic reticulum as a conduit to human disease. *Nature* 529, 326–335. doi: 10.1038/nature17041

Wang, R., Sun, H., Ren, H., and Wang, G. (2020a). alpha-Synuclein aggregation and transmission in Parkinson's disease: a link to mitochondria and lysosome. *Sci. China Life Sci.* 63, 1850–1859. doi: 10.1007/s11427-020-1756-9

Wang, R., Sun, H., Wang, G., and Ren, H. (2020b). Imbalance of Lysine Acetylation contributes to the pathogenesis of Parkinson's disease. *Int. J. Mol. Sci.* 21:7182. doi: 10.3390/ijms21197182

Wang, X., Zhai, H., and Wang, F. (2018). 6-OHDA induces oxidation of F-box protein Fbw7beta by chaperone-mediated Autophagy in Parkinson's model. *Mol. Neurobiol.* 55, 4825–4833. doi: 10.1007/s12035-017-0686-0

Wei, Y., Pattingre, S., Sinha, S., Bassik, M., and Levine, B. (2008). JNK1-mediated phosphorylation of Bcl-2 regulates starvation-induced autophagy. *Mol. Cell* 30, 678–688. doi: 10.1016/j.molcel.2008.06.001

Weidberg, H., Shvets, E., Shpilka, T., Shimron, F., Shinder, V., and Elazar, Z. (2010). LC3 and GATE-16/GABARAP subfamilies are both essential yet act differently in autophagosome biogenesis. *EMBO J.* 29, 1792–1802. doi: 10.1038/emboj.2010.74

Winslow, A. R., Chen, C. W., Corrochano, S., Acevedo-Arozena, A., Gordon, D. E., Peden, A. A., et al. (2010). alpha-Synuclein impairs macroautophagy: implications for Parkinson's disease. *J. Cell Biol.* 190, 1023–1037. doi: 10.1083/jcb.201003122

Wu, F., Xu, H. D., Guan, J. J., Hou, Y. S., Gu, J. H., Zhen, X. C., et al. (2015). Rotenone impairs autophagic flux and lysosomal functions in Parkinson's disease. *Neuroscience* 284, 900–911. doi: 10.1016/j.neuroscience.2014.11.004

Wu, L., Luo, N., Zhao, H. R., Gao, Q., Lu, J., Pan, Y., et al. (2014). Salubrinal protects against rotenone-induced SH-SY5Y cell death via ATF4-parkin pathway. *Brain Res.* 1549, 52–62. doi: 10.1016/j.brainres.2014.01.003

Xie, L., Tiong, C. X., and Bian, J. S. (2012). Hydrogen sulfide protects SH-SY5Y cells against 6-hydroxydopamine-induced endoplasmic reticulum stress. *Am. J. Physiol. Cell Physiol.* 303, C81–C91. doi: 10.1152/ajpcell.00281.2011

Xilouri, M., Vogiatzi, T., Vekrellis, K., Park, D., and Stefanis, L. (2009). Abberant alpha-synuclein confers toxicity to neurons in part through inhibition of chaperone-mediated autophagy. *PLoS One* 4:e5515. doi: 10.1371/journal.pone.0005515

Xiong, N., Xiong, J., Jia, M., Liu, L., Zhang, X., Chen, Z., et al. (2013). The role of autophagy in Parkinson's disease: rotenone-based modeling. *Behav. Brain Funct.* 9:13. doi: 10.1186/1744-9081-9-13

Xu, C. Y., Kang, W. Y., Chen, Y. M., Jiang, T. F., Zhang, J., Zhang, L. N., et al. (2017). DJ-1 inhibits alpha-synuclein aggregation by regulating chaperone-mediated Autophagy. *Front. Aging Neurosci.* 9:308. doi: 10.3389/fnagi.2017.00308

Xu, J., Zhou, Q., Xu, W., and Cai, L. (2012). Endoplasmic reticulum stress and diabetic cardiomyopathy. *Exp. Diabetes Res.* 2012:827971. doi: 10.1155/2012/827971

Yamamoto, K., Sato, T., Matsui, T., Sato, M., Okada, T., Yoshida, H., et al. (2007). Transcriptional induction of mammalian ER quality control proteins is mediated by single or combined action of ATF6alpha and XBP1. *Dev. Cell* 13, 365–376. doi: 10.1016/j.devcel.2007.07.018

Yamamuro, A., Yoshioka, Y., Ogita, K., and Maeda, S. (2006). Involvement of endoplasmic reticulum stress on the cell death induced by 6-hydroxydopamine in human neuroblastoma SH-SY5Y cells. *Neurochem. Res.* 31, 657–664. doi: 10.1007/s11064-006-9062-6

Yang, J., Kim, K. S., Iyirhiaro, G. O., Marcogliese, P. C., Callaghan, S. M., Qu, D., et al. (2019). DJ-1 modulates the unfolded protein response and cell death via upregulation of ATF4 following ER stress. *Cell Death Dis.* 10:135. doi: 10.1038/s41419-019-1354-2

Yokota, T., Sugawara, K., Ito, K., Takahashi, R., Ariga, H., and Mizusawa, H. (2003). Down regulation of DJ-1 enhances cell death by oxidative stress, ER stress, and proteasome inhibition. *Biochem. Biophys. Res. Commun.* 312, 1342–1348. doi: 10.1016/j.bbrc.2003.11.056

Yorimitsu, T., Nair, U., Yang, Z., and Klionsky, D. J. (2006). Endoplasmic reticulum stress triggers autophagy. *J. Biol. Chem.* 281, 30299–30304. doi: 10.1074/jbc.M607007200

Young, M. M., and Wang, H. G. (2018). Sphingolipids as regulators of Autophagy and Endocytic trafficking. *Adv. Cancer Res.* 140, 27–60. doi: 10.1016/bs.acr.2018.04.008

Yu, W. H., Dorado, B., Figueroa, H. Y., Wang, L., Planel, E., Cookson, M. R., et al. (2009). Metabolic activity determines efficacy of macroautophagic clearance of pathological oligomeric alpha-synuclein. *Am. J. Pathol.* 175, 736–747. doi: 10.2353/ajpath.2009.080928

Yuan, Y., Cao, P., Smith, M. A., Kramp, K., Huang, Y., Hisamoto, N., et al. (2011). Dysregulated LRRK2 signaling in response to endoplasmic reticulum stress leads to dopaminergic neuron degeneration in *C. elegans*. *PLoS One* 6:e22354. doi: 10.1371/journal.pone.0022354

Yung, H. W., Charnock-Jones, D. S., and Burton, G. J. (2011). Regulation of AKT phosphorylation at Ser473 and Thr308 by endoplasmic reticulum stress

modulates substrate specificity in a severity dependent manner. *PLoS One* 6:e17894. doi: 10.1371/journal.pone.0017894

Zalckvar, E., Berissi, H., Mizrachy, L., Idelchuk, Y., Koren, I., Eisenstein, M., et al. (2009). DAP-kinase-mediated phosphorylation on the BH3 domain of beclin 1 promotes dissociation of beclin 1 from Bcl-XL and induction of autophagy. *EMBO Rep.* 10, 285–292. doi: 10.1038/embor.2008.246

Zhang, X., Yuan, Y., Jiang, L., Zhang, J., Gao, J., Shen, Z., et al. (2014). Endoplasmic reticulum stress induced by tunicamycin and thapsigargin protects against transient ischemic brain injury: involvement of PARK2-dependent mitophagy. *Autophagy* 10, 1801–1813. doi: 10.4161/auto.32136

Zhao, Y., Li, X., Cai, M. Y., Ma, K., Yang, J., Zhou, J., et al. (2013). XBP-1u suppresses autophagy by promoting the degradation of FoxO1 in cancer cells. *Cell Res.* 23, 491–507. doi: 10.1038/cr.2013.2

Zhao, Y. G., Chen, Y., Miao, G., Zhao, H., Qu, W., Li, D., et al. (2017). The ER-Localized transmembrane protein EPG-3/VMP1 regulates SERCA activity to control ER-isolation membrane contacts for Autophagosome formation. *Mol. Cell* 67, 974–989.e976. doi: 10.1016/j.molcel.2017.08.005

Zhao, Y. G., and Zhang, H. (2019). Autophagosome maturation: an epic journey from the ER to lysosomes. *J. Cell Biol.* 218, 757–770. doi: 10.1083/jcb.201810099

Zhou, Y., Lee, J., Reno, C. M., Sun, C., Park, S. W., Chung, J., et al. (2011). Regulation of glucose homeostasis through a XBP-1-FoxO1 interaction. *Nat. Med.* 17, 356–365. doi: 10.1038/nm.2293

Zhu, J. H., Guo, F., Shelburne, J., Watkins, S., and Chu, C. T. (2003). Localization of phosphorylated ERK/MAP kinases to mitochondria and autophagosomes in Lewy body diseases. *Brain Pathol.* 13, 473–481. doi: 10.1111/j.1750-3639.2003.tb00478.x

Zhu, J. H., Gusdon, A. M., Cimen, H., Van Houten, B., Koc, E., and Chu, C. T. (2012). Impaired mitochondrial biogenesis contributes to depletion of functional mitochondria in chronic MPP+ toxicity: dual roles for ERK1/2. *Cell Death Dis.* 3:e312. doi: 10.1038/cddis.2012.46

Zhu, J. H., Horbinski, C., Guo, F., Watkins, S., Uchiyama, Y., and Chu, C. T. (2007). Regulation of autophagy by extracellular signal-regulated protein kinases during 1-methyl-4-phenylpyridinium-induced cell death. *Am. J. Pathol.* 170, 75–86. doi: 10.2353/ajpath.2007.060524

Zhu, X., Huang, L., Gong, J., Shi, C., Wang, Z., Ye, B., et al. (2017). NF-kappaB pathway link with ER stress-induced autophagy and apoptosis in cervical tumor cells. *Cell Death Discov.* 3:17059. doi: 10.1038/cddiscovery.2017.59

Zhu, Y., Wang, C., Yu, M., Cui, J., Liu, L., and Xu, Z. (2013). ULK1 and JNK are involved in mitophagy incurred by LRRK2 G2019S expression. *Protein Cell* 4, 711–721. doi: 10.1007/s13238-013-3910-3

Conflict of Interest: The authors declare that the research was conducted in the absence of any commercial or financial relationships that could be construed as a potential conflict of interest.

Copyright © 2021 Ren, Zhai, Lu and Wang. This is an open-access article distributed under the terms of the Creative Commons Attribution License (CC BY). The use, distribution or reproduction in other forums is permitted, provided the original author(s) and the copyright owner(s) are credited and that the original publication in this journal is cited, in accordance with accepted academic practice. No use, distribution or reproduction is permitted which does not comply with these terms.

frontiers in Aging Neuroscience

ORIGINAL RESEARCH
published: 01 July 2021
doi: 10.3389/fnagi.2021.701499

Identifying Mild Cognitive Impairment in Parkinson's Disease With Electroencephalogram Functional Connectivity

Min Cai[1,2†], Ge Dang[1,2†], Xiaolin Su[1,2], Lin Zhu[1,2], Xue Shi[1,2], Sixuan Che[3,4], Xiaoyong Lan[1,2], Xiaoguang Luo[1,2] and Yi Guo[1,2,5]*

[1] Department of Neurology, Shenzhen People's Hospital, The Second Clinical Medical College, Jinan University, Shenzhen, China, [2] The First Affiliated Hospital, Southern University of Science and Technology, Shenzhen, China, [3] Department of Medical, The Fourth People's Hospital of Chengdu, Chengdu, China, [4] MOE Key Lab for Neuroinformation, Chengdu Mental Health Center, The Clinical Hospital of Chengdu Brain Science Institute, University of Electronic Science and Technology of China, Chengdu, China, [5] Shenzhen Bay Laboratory, Gladstone Institute of Neurological Disease, Shenzhen, Guangdong, China

Objective: Cognitive impairment occurs frequently in Parkinson's disease (PD) and negatively impacts the patient's quality of life. However, its pathophysiological mechanism remains unclear, hindering the development of new therapies. Changes in brain connectivity are related to cognitive impairment in patients with PD, with the dorsolateral prefrontal cortex (DLPFC) being considered the essential region related to PD cognitive impairment. Nevertheless, few studies have focused on the global connectivity responsible for communication with the DLPFC node, the posterior division of the middle frontal gyrus (PMFG) in patients with PD; this was the focus of this study.

Methods: We applied resting-state electroencephalography (EEG) and calculated a reliable functional connectivity measurement, the debiased weighted phase lag index (dWPLI), to examine inter-regional functional connectivity in 68 patients with PD who were classified into two groups according to their cognitive condition.

Results: We observed that altered left and right PMFG-based functional connectivity associated with cognitive impairment in patients with PD in the theta frequency bands under the eyes closed condition ($r = -0.426$, $p < 0.001$ and $r = -0.437$, $p < 0.001$, respectively). Exploratory results based on the MoCA subdomains indicated that poorer visuospatial function was associated with higher right PMFG-based functional connectivity ($r = -0.335$, $p = 0.005$), and poorer attention function was associated with higher left and right PMFG-based functional connectivity ($r = -0.380$, $p = 0.001$ and $r = -0.256$, $p = 0.035$, respectively). Further analysis using logistic regression and receiver operating characteristic (ROC) curves found that this abnormal functional connectivity was an independent risk factor for cognitive impairment [odds ratio (OR): 2.949, 95% confidence interval (CI): 1.294–6.725, $p = 0.01$ for left PMFG; OR: 11.278, 95% CI: 2.578–49.335, $p = 0.001$ for right PMFG, per 0.1 U], and provided moderate classification power to discriminate between cognitive abilities in patients with PD [area under the ROC curve (AUC) = 0.770 for left PMFG; AUC = 0.809 for right PMFG].

OPEN ACCESS

Edited by:
Pingyi Xu,
First Affiliated Hospital of Guangzhou Medical University, China

Reviewed by:
Sandeep Malampati,
Nathan Kline Institute for Psychiatric Research, United States
Daojun Hong,
The First Affiliated Hospital of Nanchang University, China
Mahmoud Hassan,
University of Rennes 1, France

***Correspondence:**
Yi Guo
xuanyi_guo@163.com

[†] These authors have contributed equally to this work and share first authorship

***Received:** 28 April 2021*
***Accepted:** 10 June 2021*
***Published:** 01 July 2021*

Citation:
Cai M, Dang G, Su X, Zhu L, Shi X, Che S, Lan X, Luo X and Guo Y (2021) Identifying Mild Cognitive Impairment in Parkinson's Disease With Electroencephalogram Functional Connectivity. Front. Aging Neurosci. 13:701499. doi: 10.3389/fnagi.2021.701499

Conclusion: These preliminary findings indicate that abnormal PMFG-based functional connectivity patterns associated with cognitive impairment in the theta frequency bands under the eyes closed condition and altered functional connectivity patterns have the potential to act as reliable biomarkers for identifying cognitive impairment in patients with PD.

Keywords: Parkinson's disease, cognitive impairment, electroencephalography, functional connectivity, theta frequency band

INTRODUCTION

Parkinson's disease (PD) is clinically characterized by the presence of motor symptoms, including bradykinesia, tremor, rigidity, and postural instability (Sveinbjornsdottir, 2016). However, non-motor symptoms are currently receiving increased attention as they often precede the development of motor symptoms and can impose a significant burden on the patient, affecting independence in performing daily activities and negatively impacting the quality of life, independent of any motor symptoms (Tolosa et al., 2009). In particular, cognitive impairments frequently occur in patients with PD. Longitudinal studies have found that 10% of patients display cognitive deficits within three years of diagnosis; these numbers rise to 46% within 10 years and can reach as high as 83% within 20 years (Hanagasi et al., 2017). Therefore, it is essential to explore objective and non-invasive predictive biomarkers for this condition in its early stages.

The pathophysiological mechanisms responsible for cognitive impairment in patients with PD remain unclear. With the development of functional network science and neuroimaging approaches, it is now recognized that the pathophysiological disruptions associated with the development of neuropsychiatric disorders are rarely confined to a single region of the brain; rather, it is now known that there are alterations in functional connectivity within brain networks (Kehagia et al., 2013). Moreover, a dual syndrome hypothesis has been widely accepted, which distinguishes early frontal, dopaminergic-dependent dysexecutive syndrome, and later dopamine-independent posterior cortical syndrome (Fornito et al., 2015). Compared with other functional imaging methods, electroencephalography (EEG) has several advantages, predominantly its high temporal resolution, where specific frequency analysis enables precise investigation of connectivity changes (Donner and Siegel, 2011). Several EEG studies have found brain connectivity changes associated with cognitive impairment in patients with PD (Bertrand et al., 2016; Hassan et al., 2017; Chaturvedi et al., 2019; Sanchez-Dinorin et al., 2021), which might present potential markers for cognitive dysfunction, although various alterations in different frequency bands were observed in these studies. However, volume conduction issue resulting from the transient propagation of the electric fields engendered by the primary current source to most of the scalp sensors may influence connectivity estimates of EEG. Due to this linear mixing of signals from different brain regions detected by the same sensor, common methods used for functional connectivity evaluation (coherence or mutual information) may lead to the identification of transparent functional connections that do not accurately reflect the interactions between brain regions (Vinck et al., 2011). Several new functional connectivity assessment techniques have been developed to minimize the effects caused by volume conduction. In particular, the weighted phase lag index (wPLI), which weighs the contribution of the observed phase lead or lags by the magnitude of the imaginary component of the cross-spectrum, is less sensitive to additive volume-conducted noise sources (Lau et al., 2012). However, this measure has a positive bias. To solve this problem, Vinck et al. proposed a debiased estimator of the squared WPLI [i.e., dWPLI (Vinck et al., 2011)] that has been frequently applied to assess EEG data (Hardmeier et al., 2014; Wang et al., 2017).

Although there are many possible pathophysiological explanations for the correlation between EEG changes and the cognitive state of PD patients, the exact impaired circuitry responsible for these alterations is not clear. The dorsolateral prefrontal cortex (DLPFC), which transmits afferent projections to the caudate and putamen and is involved in higher-order cognitive functions, has been considered the essential region related to cognitive impairments in PD (Polito et al., 2012; Gratwicke et al., 2015; Rosero Pahi et al., 2020). Ko et al. demonstrated that stimulation of the right DLPFC, which is the most "sensitive" area related to PD-cognitive deficit-related metabolic pattern (PDCP), may normalize the altered PDCP network (Ko et al., 2014). In addition, non-invasive brain stimulation (NIBS) of the left DLPFC has been found to improve cognitive function in patients with PD (Beheshti and Ko, 2021). The posterior division of the middle frontal gyri (PMFG, left and right) are key nodes in the DLPFC that are widely used as accessible cortical stimulation sites for NIBS (Chen et al., 2013). In terms of the concept of brain networks, abnormal activity of a certain circuit component may modify its communication with other network components, which could be interpreted as modulation of functional connectivity throughout the brain (Gratwicke et al., 2015). Correspondingly, investigating the functional connectivity interacting with a focal targeted brain region may facilitate the development of a mechanism-specific intervention by identifying appropriate subgroups of clinical trials and providing objective measures of disease inhibition. Few studies have focused on global connectivity communicating with the particular region related to cognitive impairment in PD patients using resting-state EEG. Therefore, we hypothesized that the functional connectivity pattern of the PMFG might be a potential marker for identifying cognitive dysfunction in patients with PD.

To test this hypothesis, we applied resting-state EEG to measure potential PMFG-based functional connectivity (dWPLI) differences between PD patients with mild cognitive impairment (PD-MCI) and PD patients with normal cognition (PD-NC). In particular, we investigated whether abnormal functional connectivity was associated with cognitive function, and furthermore, whether this could discriminate between PD-MCI and PD-NC patients.

MATERIALS AND METHODS

Subjects

This study was approved by the Institutional Research Ethics Committee of Shenzhen People's Hospital and adheres to the recommendations of the Declaration of Helsinki. All PD patients were recruited from the inpatient or outpatient clinic at Shenzhen People's Hospital from March 2019 to November 2020, and written informed consent was obtained from each participant. The inclusion criteria were as follows: (1) age of 40–80 years; (2) idiopathic PD based on the UK Parkinson's Disease Society Brain Bank criteria (Hughes et al., 1992); (3) self-reported right-handedness. The exclusion criteria included the following: (1) documentation of serious organ dysfunction; (2) history of psychiatric disorders such as major depression, generalized anxiety disorder, or schizophrenia; (3) severe PD [Hoehn&Yahr (H&Y) scale stage $>$ 4]; (4) any kind of dementia; (5) changes in antiparkinsonian medication within one month prior to enrolment and use of drugs that may influence EEG.

Each patient underwent a series of clinical evaluations that assessed both motor and non-motor symptoms. Motor disability associated with PD was evaluated with the Unified Parkinson's Disease Rating Scale-III (UPDRS-III) (Movement Disorder Society Task Force on Rating Scales for Parkinson's Disease., 2003), and disease severity was assessed according to the H&Y stage (Hoehn and Yahr, 1967). The Hamilton Anxiety Rating Scale (HAMA) (Hamilton, 1959) and the Hamilton Depression Rating Scale (HAMD) (Hamilton, 1967) were used to assess anxiety and depression states, respectively. Sleep quality was estimated using the Pittsburgh Sleep Quality Index (PSQI) (Buysse et al., 1989).

Gobal cognitive abilities were evaluated using the Montreal Cognitive Assessment (MoCA) (Nasreddine et al., 2005). According to level I of the PD-MCI diagnostic criteria proposed by the Movement Disorder Society (Litvan et al., 2012), PD patients with a MoCA score of 24 or above (Lucza et al., 2015) and normal functionality were identified as PD-NC. Patients with a MoCA score below 24 and preserved functionality were identified as PD-MCI. All neurological functional assessments were conducted in the "on" status, and the individual drugs used were converted to the levodopa equivalent daily dose (LEDD) (Tomlinson et al., 2010).

EEG Acquisition and Preprocessing

Eight-minute resting-state EEGs of both the eyes closed (EC) and eyes open (EO) conditions were acquired using a BrainAmp DC amplifier (Brain Products, Munich, Germany) with a 64-channel EEG system. Participants were asked to sit in a comfortable chair and to remain relaxed during the EEG recording. A conductive gel was used to keep the electrode impedances below 5 kΩ. During the recording, participants were instructed to look at a fixation throughout the process. Using a sampling rate of 5,000 Hz, the EEG signals were referenced online to FCz. The EEG preprocessing was conducted offline with MATLAB (R2018a, The Mathworks Inc., Natick, MA, United States) using a home-made script that was structured based on that of EEGLAB (Delorme and Makeig, 2004) with the following steps: (1) down-sampling to 250 Hz; (2) removal of representative artifacts by visual inspection; (3) application of a zero-phase finite impulse response filter for band-pass filtering between 1 and 45 Hz and removal of 50 Hz line noise and harmonics by notch filtering; (4) rejection of corrupted channels and spherical interpolation of rejected channels; and (5) application of independent component analysis to remove remaining artifacts, including blinks, electrocardiogram signals, and high-frequency sustained muscle artifacts.

EEG Source Localization and Connectivity Analyses

EEG source localization and source spatial connectivity analyses were carried out using customized scripts and public toolboxes (including EEGLAB and Brainstorm) in MATLAB (Tadel et al., 2011). Specifically, the head model of the three-layer boundary element was calculated, and a rotating dipole with 3,003 vertices was then produced on the cortical surface. The lead field matrix of the dipole activities related to the EEG was acquired, and the minimum norm estimation (MNE) was used in the inverse model; the dipole direction is limited to the normal of the cerebral cortex (Lin et al., 2006). Functional connectivity based on the dWPLI correlation was computed among 31 regions of interest (ROIs) in the Montreal Neurological Institute space, stemmed from independent components analysis parcellation of functional magnetic resonance imaging connectivity of 38 healthy individuals used in a previous study (Toll et al., 2020). The dWPLI can be defined as:

$$\widehat{\Omega}^{w} = \frac{\sum_{j=1}^{N}\sum_{k=j+1} W_{j,k} d(X_j, X_k)}{N(N-1)\hat{W}} \quad (1)$$

where $\hat{W}$ represents the average weight, i.e., the weight normalization expressed as $\frac{1}{N(N-1)}\sum_{j=1}^{N}\sum_{k=j1} W_{j,k}$. The dWPLI ranges from 0 to 1. The higher the dWPLI value, the higher the coupling between neural oscillations (Vinck et al., 2011). Finally, excluding self-connectivity, 465 unique ROI pairs were calculated in each of the five frequency bands (delta: 1–4 Hz, theta: 5–7 Hz, alpha: 8–12 Hz, beta: 13–30 Hz, gamma: 31–45 Hz).

Statistical Analyses

Statistical analyses were conducted using the IBM Statistical Package for the Social Sciences (SPSS; IBM Corp., Armonk,

NY, United States) Version 25.0 and MATLAB. For analysis of variance, normality was tested by Shapiro–Wilk test; normally distributed data were represented as means and standard deviations, while non-normally distributed data were represented as medians and interquartile ranges. Group differences in age, education level, UPDRS-III score, and PSQI score were compared using independent-samples *t*-tests. Group differences in the disease course, H&Y stage, neuropsychological tests, and LEDD were compared using Mann–Whitney *U* tests, and sex differences between groups were compared using chi-squared tests. Network-based Statistics (NBS) (Zalesky et al., 2010), a nonparametric statistical test controlling for the family wise error rate resulting from multiple comparisons, was used to analyze differences in functional connectivity between the PD-MCI and PD-NC groups based on the following steps: (1) a two-sample *t*-test was conducted at each connection, and generating a test statistic value matrix demonstrating significant functional connectivity differences between the groups; (2) application of a component-forming threshold to obtain a set of supra-threshold matrices, and computing the size of the connected component in the matrices; (3) generating an empirical null distribution of largest component sizes by mean of randomly permuting the PD-MCI and PD-NC group membership, calculating the test statistic of interest, storing the largest component sizes, and repeating for 5,000 times; (4) estimating the *p*-value of the connected element (i.e., the proportion of the empirical null component sizes that was greater than the actual value), and $p < 0.05$ was defined as a significant difference between the groups. Partial correlation analysis was performed to evaluate the correlations between the seed-based functional connectivity and the MoCA score (as well as the MoCA subdomains, including executive, memory, visuospatial, language, and attention functions), adjusting for sex, age, and education level. To measure the power of the seed-based functional connectivity differences, receiver operating characteristic (ROC) curve analysis was performed. The statistical significance level was set at $p < 0.05$.

RESULTS

Demographic and Clinical Characteristics

Based on the above inclusion and exclusion criteria, 71 patients were initially included in this study; however, three participants were removed due to poor signal quality. Consequently, the final sample included 68 patients (37 males and 31 females), with 32 patients belonging to the PM-MCI group and the other 36 individuals to the PD-NC group. Relative to the PD-NC group, the PD-MCI group presented significantly lower MoCA scores (as well as the MoCA subdomains, including executive, memory, visuospatial, language, and attention functions; see **Supplementary Table 1**) and education levels, and a significantly higher mean age. No other significant differences were found between the two groups. The detailed demographic and clinical characteristics, as well as the statistical results, are shown in **Table 1**.

Seed-Based Functional Connectivity With Bilateral PMFG

NBS analysis revealed stronger brain-wide functional connectivity in the PD-MCI group than in the PD-NC group in the theta band under EC condition but not in any other bands or conditions. Specifically, components, including 216 edges connected to 31 nodes, showed enhanced connectivity strength between the groups, involving the visual, somatosensory, dorsal attention, default mode (DMN), frontoparietal control, and ventral attention networks (**Figures 1A,B**). When the left and right PMFG were selected as seed ROIs, the identified clusters involved multiple networks; for the left PMFG, the identified clusters involved the somatosensory, dorsal attention, default mode, frontoparietal control, and ventral attention networks; while the identified clusters for the right PMFG involved the visual, somatosensory, dorsal attention, default mode, frontoparietal control, and ventral attention networks

TABLE 1 | Main demographic and clinical characteristics in each group.

	All	PD-MCI	PD-NC	t/z/χ^2	*P* value
N	68	32	36		
Sex (M/F)	37/31	17/15	20/16	0.040	0.841
Age (year)	63.97 ± 9.09	66.67 ± 7.33	61.50 ± 9.92	−2.443	0.017*
Education (year)	8.59 ± 4.32	6.27 ± 4.06	10.72 ± 3.39	4.961	<0.001*
Duration (year)	2.5 (1.5, 5)	3 (1.5, 5.375)	2 (1, 5)	−0.321	0.748
UPDRS-III score	23.16 ± 11.30	24.79 ± 11.49	21.67 ± 11.08	−1.149	0.255
H&Y stage	2 (1.5, 2.5)	2 (1.5, 2.5)	1.75 (1, 2.375)	−1.053	0.292
PSQI score	9.36 ± 4.28	9.65 ± 4.33	9.05 ± 4.31	−0.431	0.669
LEDD (mg)	258.335 (118.75, 400)	233.335 (0,346.875)	275 (176.25, 446.875)	−1.044	0.297
HAMA	9 (6, 14.5)	9 (6, 17)	9 (5.25, 12.75)	−0.801	0.423
HAMD	11 (6.5, 15)	11 (4.5, 16)	11 (7, 14.75)	−0.096	0.923
MoCA	24 (19, 27)	19 (13.5, 22)	26.5 (25, 27.75)	−7.159	<0.001*

**p < 0.05 (comparison between PD-MCI and PD-NC group). HAMA, Hamilton Anxiety Rating Scale; HAMD, Hamilton Depression Rating Scale; H&Y, Hoehn and Yahr; LEDD, levodopa equivalent dose daily; MoCA, Montreal Cognitive Assessment; PD-MCI, Parkinson's Disease with mild cognitive impairment; PD-NC, Parkinson's Disease with normal cognition; PSQI, Pittsburgh Sleep Quality Index; UPDRS-III, Unified Parkinson's Disease Rating Scale-III.*

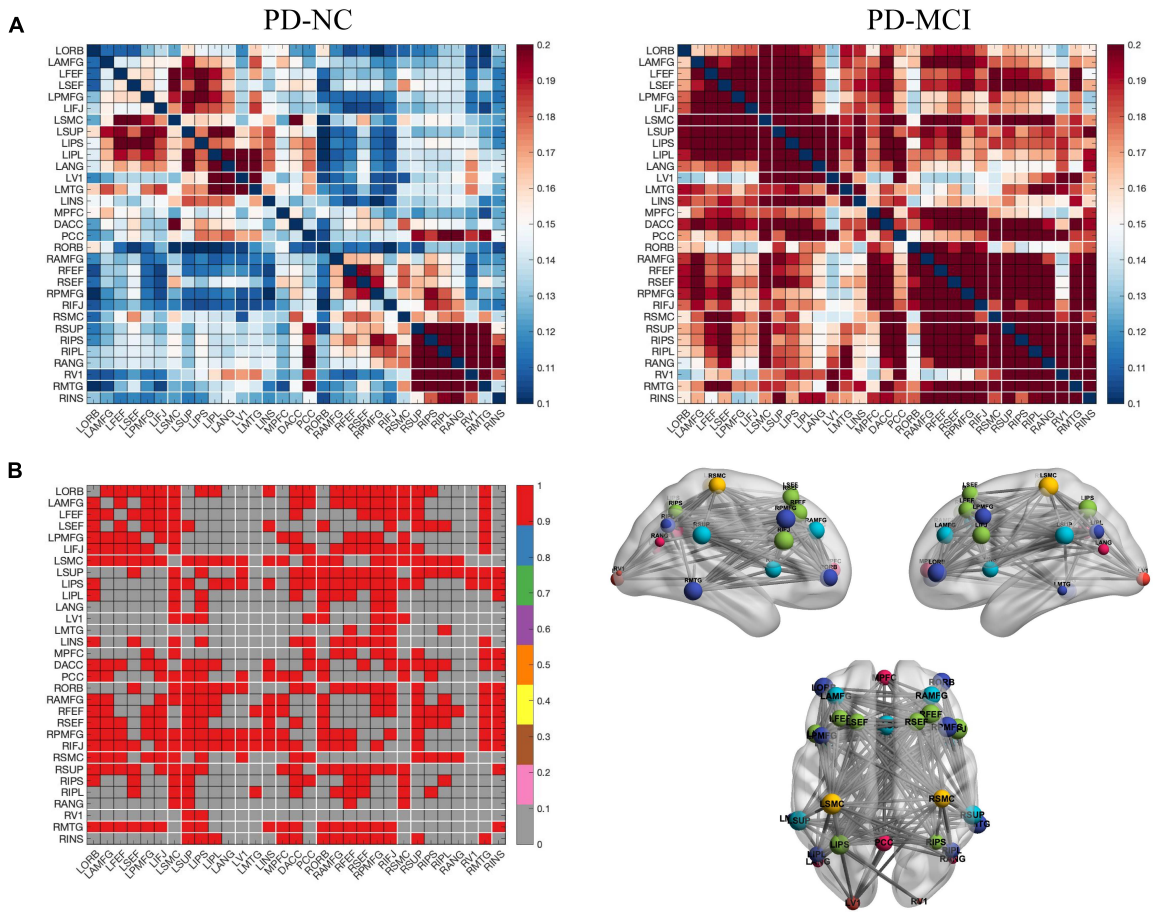


FIGURE 1 | Left and right PMFG-based functional connectivity changes in the theta frequency band under EC condition in PD-related mild cognitive impairment. **(A)** Functional connectivity matrices of the PD-MCI and PD-NC groups. **(B)** NBS analysis of group differences (PD-MCI group > PD-NC group, including the left PMFG and the right PMFG-based functional connectivity). Differential functional connectivity between the two groups (left), and 3D brain connectivity patterns showing the left side, right side, and the upper view, respectively (right). In **(B)**, the red matrix element represents the variant edges of the NBS analysis and the size of the node indicates the sum of the number of surviving edges for each node. EC, eyes closed; PD-MCI, Parkinson's disease with mild cognitive impairment; PD-NC, Parkinson's disease with normal cognition; NBS, network-based statistics; L, left; R, right; ORB, orbitofrontal cortex; AMFG, anterior division of the middle frontal gyrus; FEF, frontal eye field; SEF, supplementary eye field; PMFG, posterior division of the middle frontal gyrus; IFJ, inferior frontal junction; SMC, sensorimotor cortex; SUP, supramarginalgyrus; IPS, intraparietal sulcus; IPL, inferior parietal lobule; ANG, angular gyrus; MTG, middle temporal gyrus; V1, primary visual cortex; INS, insular cortex; MPFC, medial prefrontal cortex; DACC, dorsal anterior cingulate cortex; PCC, posterior cingulate cortex.

(**Figure 1B**). For all patients with PD, we next calculated the nodal functional connectivity for the selected ROIs as the average functional connectivity between the bilateral PMFG and all other identified clusters revealed by NBS. The seed-based functional connectivity significantly increased in the PD-MCI group, and the MoCA scores were negatively correlated with the left and right PMFG-based functional connectivity values ($r = -0.426$, $p < 0.001$ and $r = -0.437$, $p < 0.001$, respectively), after adjusting for sex, age, and education level (**Figure 2**). Concerning the subdomains of the MoCA, poorer visuospatial function was associated with higher right PMFG-based functional connectivity ($r = -0.335$, $p = 0.005$) and poorer attention function was associated with higher left and right PMFG-based functional connectivity ($r = -0.380$, $p = 0.001$ and $r = -0.256$, $p = 0.035$, respectively) after adjusting for sex, age, and education level (**Supplementary Figure 1**).

Prediction of Cognitive Outcome

Enter logistic regression analysis was performed for mild cognitive impairment based on the significant functional connectivity with the left and right PMFG, respectively, adjusting for sex, age, and education level. The logistic regression analysis results are shown in **Table 2**. The significant functional connectivity with the left and right PMFG were both independent risk factors for mild cognitive impairment in patients with PD [odds ratio (OR): 2.949, 95% confidence interval (C) 1.294–6.725, $p = 0.01$; OR: 11.278, 95% CI: 2.578–49.335, $p = 0.001$, respectively, per 0.1U]. In contrast to these findings, the logistic regression analysis based on the significant power spectral density from univariate analysis in the PMFG region failed to detect any significant results after adjusting for sex, age, and education level (data not shown). The ROC analysis results are shown in **Figure 3** and **Table 3**. The area under the ROC curve (AUC) of

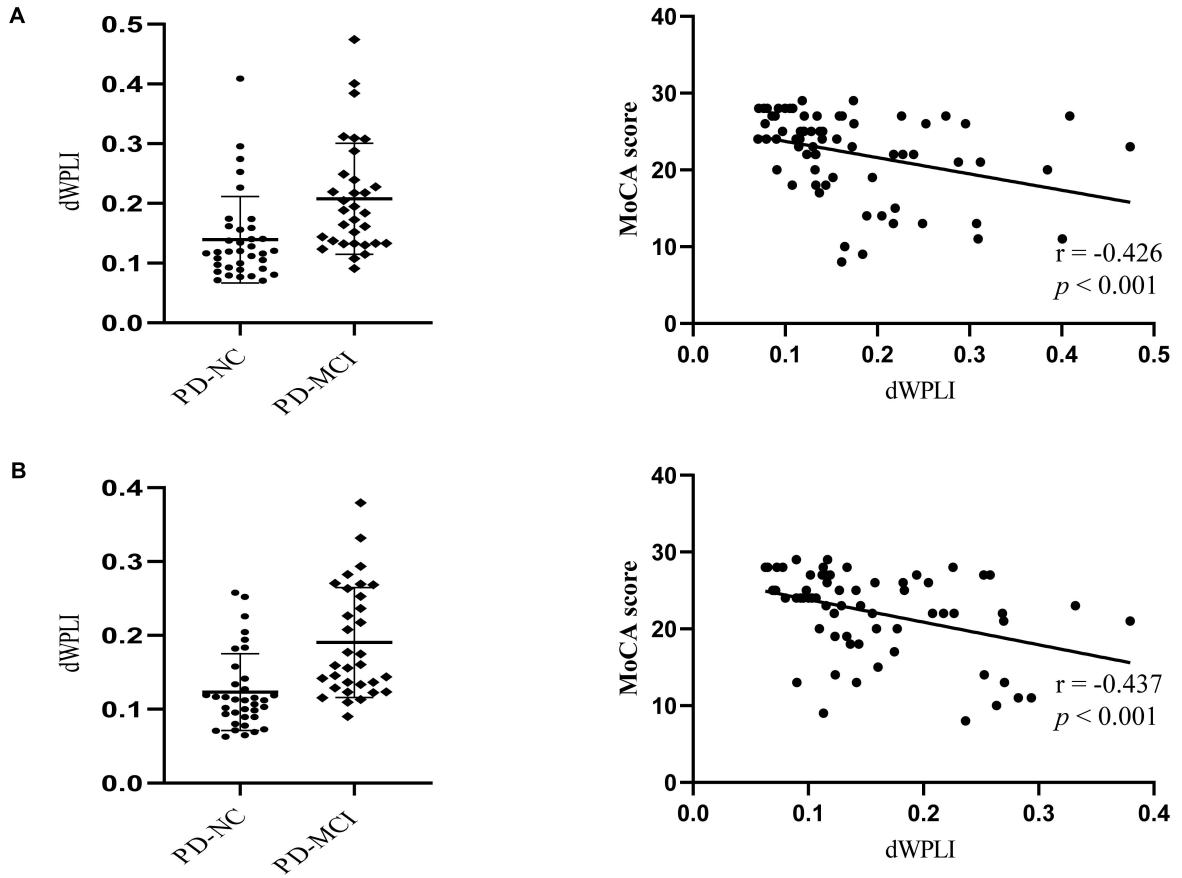


FIGURE 2 | The MoCA scores are negatively correlated with the left PMFG-based functional connectivity change **(A)** and the right PMFG-based functional connectivity change **(B)** after adjusting for sex, age, and education level. Scatterplot depicting seed-based functional connectivity significantly differed between the groups. dWPLI, debiased weighted phase lag index; MoCA, Montreal Cognitive Assessment; PD-MCI, Parkinson's disease with mild cognitive impairment; PD-NC, Parkinson's disease with normal cognition.

TABLE 2 | Logistic regression analysis for cognitive status in PD patients based on the significant functional connectivity with the left PMFG and right PMFG, respectively.

	B	S.E.	Wald	*p* value	OR	95% CI
Left PMFG, per 0.1 U	1.082	0.421	6.616	0.01	2.949	1.294–6.725
Right PMFGI, per 0.1 U	2.423	0.753	10.354	0.001	11.278	2.578–49.335

CI, confidence interval; OR, odds ratio; PMFG, posterior division of the middle frontal gyrus.

significant functional connectivity with the left PMFG was 0.770, with a sensitivity of 87.50% and a specificity of 61.10%. The AUC of significant functional connectivity with the right PMFG was 0.809, with a sensitivity of 87.50% and a specificity of 69.40%.

DISCUSSION

Using resting-state EEG dWPLI measurement, the present study revealed abnormal PMFG-based functional connectivity associated with cognitive impairment in patients with PD in the theta frequency bands under the EC condition. Logistic regression and ROC curves analyses found that such abnormal functional connectivity was an independent risk factor for cognitive impairment and could be used to discriminate the cognitive condition of patients with PD. Critically, based on PMFG regional power spectral density, a measure commonly used in previous EEG studies (Mostile et al., 2019), the logistic regression analysis did not identify any risk factors.

Cognitive Disruption in PD and Changes in Brain Connectivity

Cognitive dysfunction is pervasive in PD and negatively impacts patients' quality of life (Hanagasi et al., 2017). Therefore, investigations of the clinical features or predictive biomarkers for this condition in an early stage are essential. Electroencephalography functional connectivity could make a meaningful contribution to this procedure, given that altered signal rhythms in PD-MCI patients are related to underlying

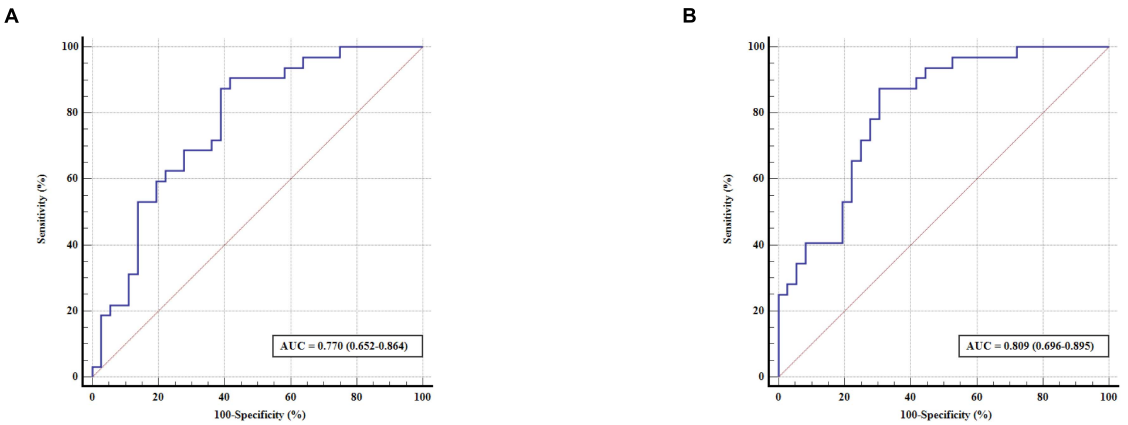


FIGURE 3 | ROC curve for predicting cognitive status in patients with PD based on the significant functional connectivity with the left PMFG **(A)** and right PMFG **(B)**.The x-axis indicates the percentage of (100 – specificity), and the y-axis indicates the percentage of sensitivity. AUC, area under the receiver operating characteristic curve; ROC, receiver operating characteristic; PMFG, posterior division of the middle frontal gyrus.

TABLE 3 | Receiver operating characteristic results predicting cognitive status in PD patients based on the significant functional connectivity with the left PMFG and right PMFG, respectively.

Variable	AUC	95% CI	Sensitivity (%)	Sensitivity (%)
Left PMFG	0.770	0.652–0.864	87.50	61.10
Right PMFG	0.809	0.696–0.895	87.50	69.40

AUC, area under the receiver operating characteristic curve; CI, confidence interval; PMFG, posterior division of the middle frontal gyrus.

neuropathological changes (Geraedts et al., 2018). Several studies have reported alterations in functional connectivity in patients with PD compared with healthy controls, and these abnormalities are exacerbated by cognitive impairments (Bertrand et al., 2016; Sanchez-Dinorin et al., 2021). The PD-MCI patients in the current study had stronger brain-wide functional connectivity in the theta frequency band compared with PD-NC patients. Different EEG bands have different normal functions and anatomical connections. Correspondingly, increased slow frequency (e.g., in the theta and delta bands) activity is characteristic of dysfunction in the diffuse gray matter in the cortical and subcortical regions along with local deafferentation in the cerebral cortex (Steriade et al., 1990). Thus, the hyper-synchronization in this frequency band is probably the result of a compensatory mechanism through which additional brain regions are enlisted to maintain cognitive performance (Gorges et al., 2015).

The DLPFC, thought to be a part of the limbic cortical-striatal-pallidal-thalamic network, has been proven to be one of the primary regions of interest for neuromodulation, and various imaging studies have demonstrated direct or indirect relationships between cognitive function and the DLPFC (Gratwicke et al., 2015; Rosero Pahi et al., 2020). In terms of the nodes located in the DLPFC, the bilateral PMFG are widely used as accessible cortical stimulation sites for NIBS (Chen et al., 2013). What happens to the brain connectivity patterns that interact with these sites? Our results demonstrate that the identified clusters involve multiple networks, implying that cognitive functions require coordinated communication among multiple brain regions. In support of these findings, a systematic review of neuroimaging studies investigating non-motor symptoms in PD suggested that several anatomically separated brain areas, including the sensorimotor and executive networks (particularly, the DLPFC and the anterior cingulate cortex), as well as the DMN, visual, auditory, salience (insular), frontal, parietal, and temporal networks, are all functionally connected during resting states, and the functional connectivity between these brain regions plays a pivotal role in coordinating complex cognitive processes (Prell, 2018). Furthermore, abnormal functional connectivity was associated with the MoCA score, which represents a global test scale for cognitive function, indicating that abnormal PMFG-based functional connectivity is involved in cognitive performance in patients with PD. Notably, Nissim et al. found that paired active-transcranial direct current stimulation (tDCS) over the left DLPFC together with cognitive training significantly increased working memory performance, as well as functional connectivity between the left DLPFC and right inferior parietal lobule in older adults (Nissim et al., 2019), which may also indicate that the DLPFC connectivity pattern plays a crucial role in cognitive function. On the other hand, our results also corroborate previous studies of changed functional connectivity in patients with PD that is related to their cognitive impairments (Bertrand et al., 2016; Hassan et al., 2017; Chaturvedi et al., 2019; Sanchez-Dinorin et al., 2021). Among them, Hassan et al. demonstrated that lower edge-wise connectivity in the alpha1 and alpha2 frequencies was associated with lower cognitive state, particularly in the frontotemporal areas (Hassan et al., 2017). While another study using the phase-locking value found enhanced functional connectivity within the frontal regions over all frequency bands, and changes in the delta and theta frequency bands were associated with poorer cognitive performance in PD patients (Sanchez-Dinorin et al., 2021). Indicators of

functional connectivity determined by different algorithms may disclose different underlying neural mechanisms. The results of functional connectivity measures depend on the type of functional connectivity measures and the cognitive behavioural measurement instrument used (Geraedts et al., 2018). Notably, the dWPLI correlation used in this study, could potentially exclude significant zero-lag connectivity caused by a mixture of true and spurious correlations; additionally, it is expected to detect real-time lagged functional couplings of brain source activities (Lau et al., 2012).

Furthermore, patterns of altered functional connectivity may be domain-specific, and relevant studies that consider functional connectivity in the context of cognitive domains are rare. While we only used the MoCA score as a measure of global cognitive function in the current study, we attempted to correlate the subitem scores of the MoCA with the significant functional connectivity in order to preliminarily explore the relationship between specific cognitive domain functions and the changes of PMFG-based functional connectivity. The performances of visuospatial and attention functions are associated with PMFG-based functional connectivity. These findings confirm the discoveries of a recent study: increased frontal synchronization of slow oscillations predicts global cognitive and visuospatial functions (Sanchez-Dinorin et al., 2021). In addition, another study found that attention and memory correlated significantly with the phase lag index in the beta and theta frequency bands, respectively (Chaturvedi et al., 2019). Nevertheless, as we did not have extensive reliable assessment measurements for specific cognitive domains, conclusions about specific cognitive domains need to be interpreted with caution and warrant further research.

EEG Measures Predict Cognitive Impairment in PD Patients

The reduction in EEG background frequency has been found to be associated with phosphorylated α-synuclein in autopsy tissue of the posterior cingulate cortex (Caviness et al., 2016), and several studies have also suggested that EEG features (frequency and power features of special regions) could be used to distinguish the severity of cognitive dysfunction or longitudinal cognitive decline in patients with PD using various approaches, including machine learning, which confirms the reliability and reproducibility of EEG in identifying cognitive impairment (Arnaldi et al., 2017; Betrouni et al., 2019; Zhang et al., 2021). Together, these findings provide strong evidence that EEG measures can be used as reliable biomarkers of cognitive decline in patients with PD. However, these studies only used the frequency and power features of EEG rather than functional connectivity that may better reflect the complexity of information processing in the cerebral cortex and may therefore be more closely related to behavior (Bullmore and Sporns, 2012). As described above, brain connectivity would be expected to disclose the properties of brain processing, and current studies have begun to address the issue of changes in brain connectivity, which broadens our understanding of the neural mechanisms of neurodegenerative diseases. Our results reveal that significant functional connectivity with the bilateral PMFG are independent risk factors for mild cognitive impairment in patients with PD, and, in addition, the ROC curve analysis demonstrated that the observed abnormalities of PMFG functional connectivity showed robust discriminative power when determining the cognitive condition in PD. Thus, the presence of such changes could be used as potential markers for identifying cognitive impairment in patients with PD. This corresponds to the higher theta band phase lag index in PD-MCI patients reported by Chaturvedi et al. (Chaturvedi et al., 2019). However, we paid more attention to the brain connectivity related to NIBS targets, which is essential for exploring the neural mechanisms and therapeutic mechanisms of diseases.

Clinical Significance

Generally, neuropsychological assessments are used to define the status and severity of cognitive impairment in patients with PD. However, it must be acknowledged that neuropsychological assessments require specialized neuropsychological experts, which is both time-consuming and requires good patient cooperation. Resting-state EEG is easily accessible with high test-retest reliability and objectively reflects the pathophysiological functioning of the brain (Salinsky et al., 1991). Furthermore, this procedure can be repeated multiple times without learning bias. Using this procedure, our study found that PMFG-based connectivity could predict the cognitive condition of patients with PD. Regarding clinical considerations, these findings hold promise as practical adjuncts to neuropsychological studies. Moreover, it may be possible to improve cognitive function in patients with PD by adjusting the EEG functional connectivity in specific regions.

This study has several limitations. First, it should be noted that we used the MoCA score as a global cognitive function measure to determine the level of cognition and cognitive impairment that meets the level I diagnostic criteria of PD-MCI; this measure does not assess specific cognitive domains and may, therefore, provide less diagnostic accuracy. To mitigate this issue, the diagnosis of idiopathic PD, as well as the determination of cognitive status in all included patients, were unanimously decided by movement disorder specialists and neuropsychological experts. Second, the alterations in connectivity observed in the present study are outwardly not specific to PD-MCI, as an increased slowing of activities is also common to other types of dementia. However, the pathophysiological mechanisms of dementias with different etiologies can be reflected through types of different brain connectivity; this aspect requires more extensive research in the future. Third, because of the heterogeneity of PD, it is difficult for a single marker to achieve an accurate diagnosis, and the combination of multimodal markers may improve the accuracy of diagnosis. Consequently, it would be of great significance to further explore multimodal markers for cognitive impairment associated with PD. Fourth, the current study is cross-sectional, and future longitudinal studies are warranted. It is expected that the methodology established in this study can be extended by integrating follow-up data to further predict the progression of cognitive impairment in patients with PD. In addition, the current study lacks an age-matched healthy control group, which

would be important to highlight unique features in the PD-NC group. Although our purpose was to identify patients with cognitive impairment from PD patients, future in-depth studies incorporating data from the control group are warranted.

CONCLUSION

We found abnormal PMFG-based functional connectivity patterns associated with cognitive impairment in patients with PD exclusively in the theta frequency bands under EC condition and demonstrated that this abnormal functional connectivity was an independent risk factor for cognitive impairment in PD. As such, abnormal PMFG-based functional connectivity patterns have the potential to act as reliable biomarkers for identifying cognitive impairment in patients with PD. These results provide a direction for elucidating the neuropathology of PD-MCI and the mechanism of NIBS.

DATA AVAILABILITY STATEMENT

The raw data supporting the conclusions of this article will be made available by the authors, without undue reservation.

ETHICS STATEMENT

The studies involving human participants were reviewed and approved by the Institutional Research Ethics Committee of Shenzhen People's Hospital. The patients/participants provided their written informed consent to participate in this study.

AUTHOR CONTRIBUTIONS

YG, MC, and GD: conception and study design. XlS, LZ, XS, SC, and XyL: data collection or acquisition. MC, GD, and XlS: data analysis and results interpretation. MC and GD: drafting the manuscript. LZ, XgL, and YG: revising the manuscript. All authors read and approved the final manuscript.

FUNDING

This work was supported by the National Natural Science Foundation of China (No. 81901208), the Shenzhen Basic Research Program (No. JCYJ20170818111012390), the Medical Science and Technology Research Foundation of Guangdong Province (No. A2019174), and the Shenzhen Health and Family Planning system Scientific Research discipline capacity Promotion Project (No. SZXJ2017034).

ACKNOWLEDGMENTS

We would like to acknowledge all the study staff for their contributions to the study. In the meantime, we would like to thank all the participants recruited in the current research.

SUPPLEMENTARY MATERIAL

The Supplementary Material for this article can be found online at: https://www.frontiersin.org/articles/10.3389/fnagi.2021.701499/full#supplementary-material

REFERENCES

Arnaldi, D., De Carli, F., Fama, F., Brugnolo, A., Girtler, N., Picco, A., et al. (2017). Prediction of cognitive worsening in de novo Parkinson's disease: Clinical use of biomarkers. *Mov. Disord.* 32, 1738–1747. doi: 10.1002/mds.27190

Beheshti, I., and Ko, J. H. (2021). Modulating brain networks associated with cognitive deficits in Parkinson's disease. *Mol. Med.* 27:24. doi: 10.1186/s10020-021-00284-5

Bertrand, J. A., McIntosh, A. R., Postuma, R. B., Kovacevic, N., Latreille, V., Panisset, M., et al. (2016). Brain connectivity alterations are associated with the development of dementia in Parkinson's disease. *Brain Connect.* 6, 216–224. doi: 10.1089/brain.2015.0390

Betrouni, N., Delval, A., Chaton, L., Defebvre, L., Duits, A., Moonen, A., et al. (2019). Electroencephalography-based machine learning for cognitive profiling in Parkinson's disease: preliminary results. *Mov. Disord.* 34, 210–217. doi: 10.1002/mds.27528

Bullmore, E., and Sporns, O. (2012). The economy of brain network organization. *Nat. Rev. Neurosci.* 13, 336–349. doi: 10.1038/nrn3214

Buysse, D. J., Reynolds, C. F. III, Monk, T. H., Berman, S. R., and Kupfer, D. J. (1989). The pittsburgh sleep quality index: a new instrument for psychiatric practice and research. *Psychiatry Res.* 28, 193–213. doi: 10.1016/0165-1781(89)90047-4

Caviness, J. N., Lue, L. F., Hentz, J. G., Schmitz, C. T., Adler, C. H., Shill, H. A., et al. (2016). Cortical phosphorylated alpha-Synuclein levels correlate with brain wave spectra in Parkinson's disease. *Mov. Disord.* 31, 1012–1019. doi: 10.1002/mds.26621

Chaturvedi, M., Bogaarts, J. G., Kozak Cozac, V. V., Hatz, F., Gschwandtner, U., Meyer, A., et al. (2019). Phase lag index and spectral power as QEEG features for identification of patients with mild cognitive impairment in Parkinson's disease. *Clin. Neurophysiol.* 130, 1937–1944. doi: 10.1016/j.clinph.2019.07.017

Chen, A. C., Oathes, D. J., Chang, C., Bradley, T., Zhou, Z. W., Williams, L. M., et al. (2013). Causal interactions between fronto-parietal central executive and default-mode networks in humans. *Proc. Natl. Acad. Sci. U.S.A.* 110, 19944–19949. doi: 10.1073/pnas.1311772110

Delorme, A., and Makeig, S. (2004). EEGLAB: an open source toolbox for analysis of single-trial EEG dynamics including independent component analysis. *J. Neurosci. Methods* 134, 9–21. doi: 10.1016/j.jneumeth.2003.10.009

Donner, T. H., and Siegel, M. (2011). A framework for local cortical oscillation patterns. *Trends Cogn. Sci.* 15, 191–199. doi: 10.1016/j.tics.2011.03.007

Fornito, A., Zalesky, A., and Breakspear, M. (2015). The connectomics of brain disorders. *Nat. Rev. Neurosci.* 16, 159–172. doi: 10.1038/nrn3901

Geraedts, V. J., Boon, L. I., Marinus, J., Gouw, A. A., van Hilten, J. J., Stam, C. J., et al. (2018). Clinical correlates of quantitative EEG in Parkinson disease: a systematic review. *Neurology* 91, 871–883. doi: 10.1212/WNL.0000000000006473

Gorges, M., Muller, H. P., Lule, D., Consortium, L., Pinkhardt, E. H., Ludolph, A. C., et al. (2015). To rise and to fall: functional connectivity in cognitively normal and cognitively impaired patients with Parkinson's disease. *Neurobiol. Aging* 36, 1727–1735. doi: 10.1016/j.neurobiolaging.2014.12.026

Gratwicke, J., Jahanshahi, M., and Foltynie, T. (2015). Parkinson's disease dementia: a neural networks perspective. *Brain* 138(Pt. 6), 1454–1476. doi: 10.1093/brain/awv104

Hamilton, M. (1959). The assessment of anxiety states by rating. *Br. J. Med. Psychol.* 32, 50–55. doi: 10.1111/j.2044-8341.1959.tb00467.x

Hamilton, M. (1967). Development of a rating scale for primary depressive illness. *Br. J. Soc. Clin. Psychol.* 6, 278–296. doi: 10.1111/j.2044-8260.1967.tb00530.x

Hanagasi, H. A., Tufekcioglu, Z., and Emre, M. (2017). Dementia in Parkinson's disease. *J. Neurol. Sci.* 374, 26–31. doi: 10.1016/j.jns.2017.01.012

Hardmeier, M., Hatz, F., Bousleiman, H., Schindler, C., Stam, C. J., and Fuhr, P. (2014). Reproducibility of functional connectivity and graph measures based on the phase lag index (PLI) and weighted phase lag index (wPLI) derived from high resolution EEG. *PLoS One* 9:e108648. doi: 10.1371/journal.pone.0108648

Hassan, M., Chaton, L., Benquet, P., Delval, A., Leroy, C., Plomhause, L., et al. (2017). Functional connectivity disruptions correlate with cognitive phenotypes in Parkinson's disease. *Neuroimage Clin.* 14, 591–601. doi: 10.1016/j.nicl.2017.03.002

Hoehn, M. M., and Yahr, M. D. (1967). Parkinsonism: onset, progression and mortality. *Neurology* 17, 427–442. doi: 10.1212/wnl.17.5.427

Hughes, A. J., Daniel, S. E., Kilford, L., and Lees, A. J. (1992). Accuracy of clinical diagnosis of idiopathic Parkinson's disease: a clinico-pathological study of 100 cases. *J. Neurol. Neurosurg Psychiatry* 55, 181–184. doi: 10.1136/jnnp.55.3.181

Kehagia, A. A., Barker, R. A., and Robbins, T. W. (2013). Cognitive impairment in Parkinson's disease: the dual syndrome hypothesis. *Neurodegener Dis.* 11, 79–92. doi: 10.1159/000341998

Ko, J. H., Choi, Y. Y., and Eidelberg, D. (2014). Graph theory-guided transcranial magnetic stimulation in neurodegenerative disorders. *Bioelectronic Med.* 1, 15–18. doi: 10.15424/bioelectronmed.2014.00004

Lau, T. M., Gwin, J. T., McDowell, K. G., and Ferris, D. P. (2012). Weighted phase lag index stability as an artifact resistant measure to detect cognitive EEG activity during locomotion. *J. Neuroeng Rehabil.* 9:47. doi: 10.1186/1743-0003-9-47

Lin, F. H., Belliveau, J. W., Dale, A. M., and Hamalainen, M. S. (2006). Distributed current estimates using cortical orientation constraints. *Hum. Brain Mapp.* 27, 1–13. doi: 10.1002/hbm.20155

Litvan, I., Goldman, J. G., Troster, A. I., Schmand, B. A., Weintraub, D., Petersen, R. C., et al. (2012). Diagnostic criteria for mild cognitive impairment in Parkinson's disease: movement disorder society task force guidelines. *Mov. Disord.* 27, 349–356. doi: 10.1002/mds.24893

Lucza, T., Karadi, K., Kallai, J., Weintraut, R., Janszky, J., Makkos, A., et al. (2015). Screening mild and major neurocognitive disorders in Parkinson's disease. *Behav. Neurol.* 2015:983606. doi: 10.1155/2015/983606

Mostile, G., Giuliano, L., Monastero, R., Luca, A., Cicero, C. E., Donzuso, G., et al. (2019). Electrocortical networks in Parkinson's disease patients with mild cognitive impairment. the PaCoS study. *Parkinsonism Relat. Disord* 64, 156–162. doi: 10.1016/j.parkreldis.2019.03.027

Movement Disorder Society Task Force on Rating Scales for Parkinson's Disease. (2003). The unified Parkinson's disease rating scale (UPDRS): status and recommendations. *Mov. Disord* 18, 738–750. doi: 10.1002/mds.10473

Nasreddine, Z. S., Phillips, N. A., Bedirian, V., Charbonneau, S., Whitehead, V., Collin, I., et al. (2005). The montreal cognitive assessment, MoCA: a brief screening tool for mild cognitive impairment. *J. Am. Geriatr. Soc.* 53, 695–699. doi: 10.1111/j.1532-5415.2005.53221.x

Nissim, N. R., O'Shea, A., Indahlastari, A., Kraft, J. N., von Mering, O., Aksu, S., et al. (2019). Effects of transcranial direct current stimulation paired with cognitive training on functional connectivity of the working memory network in older adults. *Front. Aging Neurosci.* 11:340. doi: 10.3389/fnagi.2019.00340

Polito, C., Berti, V., Ramat, S., Vanzi, E., De Cristofaro, M. T., Pellicano, G., et al. (2012). Interaction of caudate dopamine depletion and brain metabolic changes with cognitive dysfunction in early Parkinson's disease. *Neurobiol. Aging* 33:206 e229-e239. doi: 10.1016/j.neurobiolaging.2010.09.004

Prell, T. (2018). Structural and functional brain patterns of non-motor syndromes in Parkinson's disease. *Front. Neurol.* 9:138. doi: 10.3389/fneur.2018.00138

Rosero Pahi, M., Cavalli, J., Nees, F., Flor, H., and Andoh, J. (2020). Disruption of the prefrontal cortex improves implicit contextual memory-guided attention: combined behavioral and electrophysiological evidence. *Cereb. Cortex* 30, 20–30. doi: 10.1093/cercor/bhz067

Salinsky, M. C., Oken, B. S., and Morehead, L. (1991). Test-retest reliability in EEG frequency analysis. *Electroencephalogr. Clin. Neurophysiol.* 79, 382–392. doi: 10.1016/0013-4694(91)90203-g

Sanchez-Dinorin, G., Rodriguez-Violante, M., Cervantes-Arriaga, A., Navarro-Roa, C., Ricardo-Garcell, J., Rodriguez-Camacho, M., et al. (2021). Frontal functional connectivity and disease duration interactively predict cognitive decline in Parkinson's disease. *Clin. Neurophysiol.* 132, 510–519. doi: 10.1016/j.clinph.2020.11.035

Steriade, M., Gloor, P., Llinas, R. R., Lopes de Silva, F. H., and Mesulam, M. M. (1990). Report of IFCN committee on basic mechanisms. basic mechanisms of cerebral rhythmic activities. *Electroencephalogr. Clin. Neurophysiol.* 76, 481–508. doi: 10.1016/0013-4694(90)90001-z

Sveinbjornsdottir, S. (2016). The clinical symptoms of Parkinson's disease. *J. Neurochem.* 139(Suppl. 1), 318–324. doi: 10.1111/jnc.13691

Tadel, F., Baillet, S., Mosher, J. C., Pantazis, D., and Leahy, R. M. (2011). Brainstorm: a user-friendly application for MEG/EEG analysis. *Comput. Intell. Neurosci.* 2011:879716. doi: 10.1155/2011/879716

Toll, R. T., Wu, W., Naparstek, S., Zhang, Y., Narayan, M., Patenaude, B., et al. (2020). An electroencephalography connectomic profile of posttraumatic stress disorder. *Am. J. Psychiatry* 177, 233–243. doi: 10.1176/appi.ajp.2019.18080911

Tolosa, E., Gaig, C., Santamaria, J., and Compta, Y. (2009). Diagnosis and the premotor phase of Parkinson disease. *Neurology* 72(Suppl. 7), S12–S20. doi: 10.1212/WNL.0b013e318198db11

Tomlinson, C. L., Stowe, R., Patel, S., Rick, C., Gray, R., and Clarke, C. E. (2010). Systematic review of levodopa dose equivalency reporting in Parkinson's disease. *Mov. Disord* 25, 2649–2653. doi: 10.1002/mds.23429

Vinck, M., Oostenveld, R., van Wingerden, M., Battaglia, F., and Pennartz, C. M. (2011). An improved index of phase-synchronization for electrophysiological data in the presence of volume-conduction, noise and sample-size bias. *Neuroimage* 55, 1548–1565. doi: 10.1016/j.neuroimage.2011.01.055

Wang, C., Costanzo, M. E., Rapp, P. E., Darmon, D., Nathan, D. E., Bashirelahi, K., et al. (2017). Disrupted gamma synchrony after mild traumatic brain injury and its correlation with white matter abnormality. *Front. Neurol.* 8:571. doi: 10.3389/fneur.2017.00571

Zalesky, A., Fornito, A., and Bullmore, E. T. (2010). Network-based statistic: identifying differences in brain networks. *Neuroimage* 53, 1197–1207. doi: 10.1016/j.neuroimage.2010.06.041

Zhang, J., Gao, Y., He, X., Feng, S., Hu, J., Zhang, Q., et al. (2021). Identifying Parkinson's disease with mild cognitive impairment by using combined MR imaging and electroencephalogram. *Eur. Radiol.* doi: 10.1007/s00330-020-07575-1 [Epub ahead of print].

Conflict of Interest: The authors declare that the research was conducted in the absence of any commercial or financial relationships that could be construed as a potential conflict of interest.

Copyright © 2021 Cai, Dang, Su, Zhu, Shi, Che, Lan, Luo and Guo. This is an open-access article distributed under the terms of the Creative Commons Attribution License (CC BY). The use, distribution or reproduction in other forums is permitted, provided the original author(s) and the copyright owner(s) are credited and that the original publication in this journal is cited, in accordance with accepted academic practice. No use, distribution or reproduction is permitted which does not comply with these terms.

frontiers in Aging Neuroscience

ORIGINAL RESEARCH
published: 02 July 2021
doi: 10.3389/fnagi.2021.661505

PKC Delta Activation Promotes Endoplasmic Reticulum Stress (ERS) and NLR Family Pyrin Domain-Containing 3 (NLRP3) Inflammasome Activation Subsequent to Asynuclein-Induced Microglial Activation: Involvement of Thioredoxin-Interacting Protein (TXNIP)/Thioredoxin (Trx) Redoxisome Pathway

*Manikandan Samidurai, Bharathi N. Palanisamy, Alejandra Bargues-Carot, Monica Hepker, Naveen Kondru, Sireesha Manne, Gary Zenitsky, Huajun Jin, Vellareddy Anantharam, Anumantha G. Kanthasamy and Arthi Kanthasamy**

Department of Biomedical Sciences, Iowa Center for Advanced Neurotoxicology, Iowa State University, Ames, IA, United States

OPEN ACCESS

Edited by:
Pingyi Xu,
First Affiliated Hospital of Guangzhou Medical University, China

Reviewed by:
Rahul Srinivasan,
Texas A & M Health Science Center, United States
Senthilkumar Krishnamoorthi,
Hong Kong Baptist Hospital, Hong Kong, SAR China

***Correspondence:**
Arthi Kanthasamy
arthik@iastate.edu

Received: *30 January 2021*
Accepted: *08 June 2021*
Published: *02 July 2021*

Citation:
Samidurai M, Palanisamy BN, Bargues-Carot A, Hepker M, Kondru N, Manne S, Zenitsky G, Jin H, Anantharam V, Kanthasamy AG and Kanthasamy A (2021) PKC Delta Activation Promotes Endoplasmic Reticulum Stress (ERS) and NLR Family Pyrin Domain-Containing 3 (NLRP3) Inflammasome Activation Subsequent to Asynuclein-Induced Microglial Activation: Involvement of Thioredoxin-Interacting Protein (TXNIP)/Thioredoxin (Trx) Redoxisome Pathway. Front. Aging Neurosci. 13:661505. doi: 10.3389/fnagi.2021.661505

A classical hallmark of Parkinson's disease (PD) pathogenesis is the accumulation of misfolded alpha-synuclein (αSyn) within Lewy bodies and Lewy neurites, although its role in microglial dysfunction and resultant dopaminergic (DAergic) neurotoxicity is still elusive. Previously, we identified that protein kinase C delta (PKCδ) is activated in post mortem PD brains and experimental Parkinsonism and that it participates in reactive microgliosis; however, the relationship between PKCδ activation, endoplasmic reticulum stress (ERS) and the reactive microglial activation state in the context of α-synucleinopathy is largely unknown. Herein, we show that oxidative stress, mitochondrial dysfunction, NLR family pyrin domain containing 3 (NLRP3) inflammasome activation, and PKCδ activation increased concomitantly with ERS markers, including the activating transcription factor 4 (ATF-4), serine/threonine-protein kinase/endoribonuclease inositol-requiring enzyme 1α (p-IRE1α), p-eukaryotic initiation factor 2 (eIF2α) as well as increased generation of neurotoxic cytokines, including IL-1β in aggregated αSyn_{agg}-stimulated primary microglia. Importantly, in mouse primary microglia-treated with αSyn_{agg} we observed increased expression of Thioredoxin-interacting protein (TXNIP), an endogenous inhibitor of the thioredoxin (Trx) pathway, a major antioxidant protein system. Additionally, αSyn_{agg} promoted interaction between NLRP3 and TXNIP in these cells. *In vitro* knockdown of PKCδ using siRNA reduced ERS and led to reduced expression of TXNIP and the NLRP3 activation response in αSyn_{agg}-stimulated mouse microglial cells

(MMCs). Additionally, attenuation of mitochondrial reactive oxygen species (mitoROS) *via* mito-apocynin and amelioration of ERS *via* the eIF2α inhibitor salubrinal (SAL) reduced the induction of the ERS/TXNIP/NLRP3 signaling axis, suggesting that mitochondrial dysfunction and ERS may act in concert to promote the αSyn_{agg}-induced microglial activation response. Likewise, knockdown of TXNIP by siRNA attenuated the αSyn_{agg}-induced NLRP3 inflammasome activation response. Finally, unilateral injection of αSyn preformed fibrils (αSyn_{PFF}) into the striatum of wild-type mice induced a significant increase in the expression of nigral p-PKCδ, ERS markers, and upregulation of the TXNIP/NLRP3 inflammasome signaling axis prior to delayed loss of TH^+ neurons. Together, our results suggest that inhibition of ERS and its downstream signaling mediators TXNIP and NLRP3 might represent novel therapeutic avenues for ameliorating microglia-mediated neuroinflammation in PD and other synucleinopathies.

Keywords: ER stress, TXNIP, NLRP3, PKCδ, Parkinson's disease

INTRODUCTION

Parkinson's disease (PD) is the second most common age-related neurodegenerative disorder (Mhyre et al., 2012). The classical clinical manifestations include motor symptoms such as resting tremors and muscular rigidity, as well as non-motor symptoms including constipation, sleep disturbances, and depression (Demaagd and Philip, 2015). While the precise etiology of PD is not well understood, exposure to environmental toxicants and genetic factors are implicated in disease development (Davie, 2008). PD originates from the progressive loss of nigral dopaminergic (DAergic) neurons, which is accompanied by the accumulation of misfolded aggregated αSyn (αSyn_{agg}) within Lewy bodies and Lewy neurites which is a classical pathological hallmark of this disease (Dickson, 2012). Additionally, microglia-derived expression of pro-inflammatory cytokines such as IL-1β and TNF-α and the pro-oxidant NOS have been identified in the substantia nigra (SN), putamen, serum, and CSF of PD patients (Knott et al., 2000; Nagatsu et al., 2000; Frigerio et al., 2005; Teschke et al., 2014; Qin et al., 2016; Chen et al., 2018; Wijeyekoon et al., 2020). Numerous mechanisms have been implicated in PD pathogenesis, including mitochondrial dysfunction, endoplasmic reticulum stress (ERS), impaired proteostasis, and chronic neuroinflammation (Block et al., 2007) yet the exact mechanisms underlying increased vulnerability of nigral DAergic neurons to PD pathogenesis remains undefined. Interestingly, emerging evidence shows that the chronic microglia-driven inflammatory response plays a significant role in the progressive loss of nigral DAergic neurons and disease progression in animal models of PD (Gao et al., 2002; Qin et al., 2013; Duffy et al., 2018; Olanow et al., 2019). Therefore, it is imperative to better understand the contribution of chronic microglial activation to progressive nigral DAergic neurodegeneration in chronic neurodegenerative conditions including PD.

Microglia, the resident immune cells of the CNS, have been linked to the induction of the innate immune response in several neurodegenerative conditions including Alzheimer's disease (AD; Webers et al., 2020; Leng and Edison, 2021). Depending on the local microenvironment, and in a brain region-specific manner, microglia carry out a number of functions in the CNS (Bachiller et al., 2018) including immune surveillance, neuronal apoptosis, synaptic plasticity, and pruning, as well as phagocytosis and repair (Russo and McGavern, 2015; Salter and Stevens, 2017; Leng and Edison, 2021). Following exposure to chemical insult or infection, DAMP (Damage-associated molecular pattern) receptors present on the surface can recognize abnormal protein aggregates, cellular debris, and pathogens, thereby mounting a microglial activation response (Heneka et al., 2015). Secretion of cytokines from persistently activated microglia in aged brains may promote a low-grade inflammation, thereby culminating in dysfunctional neuron-microglia cross talk (Norden and Godbout, 2013; Spittau, 2017). Additionally, these detrimental responses may amplify neuronal damage, thereby leading to an exaggerated disease pathology in the context of proteinopathies (Webers et al., 2020). Given that the microglial density is particularly high in the SN pars compacta (SNpc), it is plausible that microglia-mediated neuroinflammation may contribute to PD-associated αSyn pathology (Calabrese et al., 2018; Olanow et al., 2019).

Protein kinase C delta (PKCδ) is a redox-sensitive kinase involved in various processes related to proliferation, cell cycle progression, differentiation, and apoptosis (Gordon et al., 2016a). Previously, our lab demonstrated that PKCδ is highly expressed in the nigral DAergic neurons of PD patients (Zhang et al., 2007; Gordon et al., 2012) and that caspase-3-mediated proteolytic activation of PKCδ promotes neuronal apoptosis in preclinical experimental models of PD (Gordon et al., 2012). Emerging evidence from our lab and others supports a role for microglial PKCδ in the induction of reactive microgliosis in response to diverse inflammogens including αSyn_{agg} (Wen et al., 2011; Gordon et al., 2012, 2016a). Although PKCδ activation has been linked to ERS and associated cellular damage (Qin and Mochly-Rosen, 2008; Larroque-Cardoso et al., 2013), the exact relationship between PKCδ-mediated ERS and reactive microgliosis in the context of α-synucleinopathy remains elusive.

ER dysfunction, following the accumulation of misfolded proteins, triggers the unfolded protein response (UPR) that restores ER proteostasis within the protein secretory machinery (Hetz et al., 2020). The UPR pathway is mediated *via* three ER-localized parallel signaling pathways, namely: (1) serine/threonine-protein kinase/endoribonuclease inositol-requiring enzyme 1α (IRE1α), (2) protein kinase R (PKR)-like endoplasmic reticulum kinase (PERK)-eukaryotic translation initiation factor (EIFα), and (3) activating transcription factor 6 (ATF6), which contributes to the restoration of protein-folding defects *via* modifying the cellular transcriptional and translational machinery (Grootjans et al., 2016). On the other hand, prolonged ERS *via* maladaptive UPR signaling can cause inflammatory damage *via* NLRP3 inflammasome activation eventually leading to cellular demise including cell death (Mercado et al., 2013; Lebeaupin et al., 2018; Reverendo et al., 2019). In fact, the central pathological hallmark of PD, namely the accumulation of misfolded αSyn within Lewy bodies, has been linked to ER-associated DAergic neuropathology (Gitler et al., 2008; Bellucci et al., 2011; Colla et al., 2012). In recent years, the pivotal role of ERS in promoting the activation of the NLRP3 inflammasome has been demonstrated in various inflammation-related disease models (Chen X. et al., 2019; Ji et al., 2019). Numerous studies have demonstrated the beneficial effects of UPR modulation in attenuating PD-associated DAergic neuronal injury (Boyce et al., 2005; Colla, 2019). To the best of our knowledge, the exact role of the ERS-dependent mechanism in microglia-mediated neuroinflammation in the context of α-synucleinopathy remains a conundrum. Hence, in this study, we investigated the roles of PKCδ, ERS-dependent pro-inflammatory signaling events, and mitochondria-dependent ERS mechanisms in the microglial activation response in α-synucleinopathy models of PD. Our studies for the first time unveil a novel microglial ERS-driven inflammatory signaling pathway involving TXNIP and NLRP3 activation in the expression of the neurotoxic microglial activation state in the context of α-synucleinopathy and that inhibition of microglial ERS and the TXNIP/NLRP3 signaling axis may represent a novel and effective therapeutic strategy for PD treatment.

MATERIALS AND METHODS

Chemicals and Biological Reagents

Modified Eagle's medium (MEM), fetal bovine serum (FBS), L-glutamine, MitoSOX for reactive oxygen species (ROS) assay, IRDye-tagged secondary antibodies, Hoechst nuclear stain, penicillin, streptomycin, and other cell culture reagents were purchased from Invitrogen (Carlsbad, CA, USA). ATF-4, p-IRE1α, p-eIF2α, PKCδ, and p-PKCδ Y311 antibodies were purchased from Cell Signaling Technology (Danvers, MA, USA). A comprehensive list of the antibodies used in this study has been provided in **Supplementary Table 1**. NLRP3, ASC, and caspase-1 antibodies were purchased from AdipoGen (San Diego, CA, USA). The TrX and TXNIP antibody purchased from the Abcam (Cambridge MA). The β-actin antibody was purchased from Sigma-Aldrich (St. Louis, MO, USA). Mito-apocynin (MitoApo) was obtained from Dr. Kalyanaraman (Medical College of Wisconsin, Milwaukee, WI, USA). Protein A/G magnetic beads were purchased from Thermo Fisher Scientific (Waltham, MA). The CD11b magnetic separation kit was purchased from Stem Cell Technologies (Vancouver, Canada). The Duo-link proximity ligation assay reagents were purchased from Sigma Aldrich (St. Louis, MO). The Bradford protein assay was purchased from Bio-Rad Laboratories (Hercules, CA). The quick western kit was purchased from the LICOR (Lincoln, NE, USA).

Human αSyn Purification and Aggregation

Ten milliliters of Luria broth medium with 100 μg/ml kanamycin was inoculated with BL21 (DE3) cells transformed with a pT7–7 plasmid encoding WT human αSyn from frozen stocks and incubated overnight at 37°C with shaking (pre-culture). The next day, the pre-culture was used to inoculate 1 liter of Luria broth/kanamycin medium. When the OD600 of the cultures reached 0.6, protein expression was induced with 1 mM isopropyl β-D-1-thiogalactopyranoside (Invitrogen), and the cells were further incubated at 37°C for 3 h before harvesting by centrifugation. Lysis was performed by resuspending the cell pellet in approximately 30 ml of 500 mM NaCl, 50 mM Tris HCl pH 7.6 using an Omni homogenizer at full speed for 5 min and ultra-sonicated with 30-s pulses followed by a 30-s pause, for a total ultra-sonication time of 3 min. Bacterial proteins were heat precipitated by incubating for 15 min in a 90°C water bath with gentle stirring. The solution was cooled by floating in ice water for 10 min then centrifuged at 10,000× *g* for 20 min. The supernatant was transferred to another tube and DNA was precipitated with streptomycin, 1 mg/ml of lysate, for 10 min at 4°C, and then ultracentrifuged at 24,500× *g*. The lysate was filtered through a 0.2-micron syringe filter into 3500 kD dialysis tubing and dialyzed against 20 mM Tris HCl pH 8.0 overnight. The lysate was collected from dialysis tubing and centrifuged at 15,000× *g* for 10 min, the supernatant was concentrated to a final volume of 10 ml, and the concentrate was filtered through a 0.2-μm syringe filter and applied to a GE Sephacryl S-200-HP column using the AKTA Pure FPLC unit. Fractions containing αSyn were identified by SDS-PAGE with Coomassie blue staining and pooled. Pooled fractions were then injected into a GE HiPrep Anion exchange column *via* AKTA Pure FPLC unit and eluted with a 20 mM Tris HCl and 2M NaCl solution. Fractions containing pure αSyn monomer were identified by SDS-PAGE and Coomassie blue staining was dialyzed against 20 mM Tris HCl pH 8.0 overnight. Protein concentration was determined *via* a NanoDrop 2,000 Spectrophotometer and aliquots of 1 mg were stored at −80°C until use.

Endotoxin-Free Mouse αSyn Purification and Aggregation

Recombinant mouse αSyn proteins were purified as previously reported (Mao et al., 2016). The ToxinEraser endotoxin removal kit (GenScript) was used to remove the bacterial endotoxin following the manufacturer's instructions. First, αSyn_{agg} was

prepared in PBS to 5 mg/ml by agitating the monomers at 1,000 rpm at 37°C for 5 days continuously and then stored at −80°C until use. To obtain the preformed fibrils, the αSyn_{agg} stock is diluted from 5 mg/ml to 2 mg/ml in sterile PBS in a 1.5 ml Eppendorf tube. This preparation is sonicated using the Bioruptor Plus at high power for 10 cycles (30 s on, 30 s off) at a constant temperature of 10°C. The endotoxin levels post Toxin Eraser treatment were 0.08 EU/μg protein. All batches of αSyn were found to have endotoxin levels of <0.5 EU/μg protein.

Transmission Electron Microscopy (TEM) Imaging

For TEM analysis αSyn_{agg} and αSyn_{PFF} were resuspended in 20 μl of sterile PBS and subsequently mixed with 2% uranyl acetate and incubated for 5 min at room temperature. Then, EM images were captured by adding 5 μl of the sample to carbon-coated copper grids and subsequently examined in a JEOL 2100 200-kV electron microscope operated at 80 kV. Additional analysis was performed using a Thermo Fisher Noran System 6 elemental analysis system.

Cell Cultures and Culture Media

Mouse Microglial Cell Cultures

A wild-type (WT) mouse microglial cell (MMC) line (kind gift from Dr. D. Golenbock, University of Massachusetts) was derived by viral transduction of primary microglia. The maintenance media for the MMCs was DMEM-F12 containing 10% FBS and 1% penicillin, streptomycin, glutamine, and sodium pyruvate, while the experiments were conducted in the same media with reduced FBS (2%). Cell cultures were maintained at 37°C with 5% CO_2 humidity.

MN9D DAergic Neuronal Cell Culture

The mouse DAergic MN9D cell line (RRID: CVCL_M067) was a kind gift from Dr. Syed Ali (National Center for Toxicological Research/Food and Drug Administration, Jefferson, AR) and cultured as described previously (Jin et al., 2011, 2014). Briefly, MN9D cells were grown in Dulbecco's modified Eagle's medium containing 10% fetal bovine serum (FBS), 2 mM L-glutamine, 1% penicillin, and 1% streptomycin and maintained at 37°C in a 5% CO_2 atmosphere. Microglia conditioned media (MCM) was initially collected following exposure of MMCs to αSyn_{agg} with or without the addition of salubrinal (SAL). MN9D cells were subjected to the following MCM with the following treatments: (1) CON MCM, (2) αSyn_{agg} MCM, (3) SAL pretreatment followed by the αSyn_{agg} treatment MCM, and (4) SAL alone MCM. At the end of the treatment period, cells were subjected to MTS cell viability assay.

Primary Microglial Culture

Primary microglial (mouse PMG) cells were cultured from WT postnatal day 1 mouse pups based on a technique described by Sarkar et al. (2017) but with slight modification. Brains were harvested from the pups devoid of their meninges in DMEM/F12 supplemented with 10% heat-inactivated FBS, 1% penicillin, streptomycin, L-glutamine, nonessential amino acids, and sodium pyruvate. Brain tissues were then incubated in 0.25% trypsin-EDTA for 15 min with gentle agitation. Trypsinization was stopped by adding twice the volume of DMEM/F12 complete medium followed by triple-washing the tissues in complete media. Tissues were then triturated gently to prepare a single-cell suspension. To remove cell debris, the cell suspension was strained through a 70 μm nylon mesh cell strainer. The single-cell suspension was then seeded into T-75 flasks and incubated at 37°C with 5% CO_2. As described by Sarkar et al. (2017), microglial cells were separated from mixed glial cultures using CD11b magnetic-bead separation to a 97% purity and were then allowed to recover for 48 h after plating. Upon isolation of microglia using the magnetic bead technique, the microglia-positive fraction was plated in T-75 flasks in growth media (DMEM/F12 complete medium). Following overnight incubation in growth media, the microglia were passaged again to begin various experiments.

αSyn Internalization Assay

Approximately 25,000 primary microglial cells were plated onto PDL-coated coverslips. Primary mouse microglial cells were incubated with 1 μM of αSyn aggregates (rPeptide) for 1 h. At the end of the incubation period, cells were washed 3 times in 1× PBS and subsequently fixed with 4% PFA, washed in PBS, and cells were made permeable by incubating with 0.25% Triton X-100, and 0.05% Tween-20, blocked with 2% BSA for 1 h at RT. Cells were then immunostained with the respective primary antibodies IBA1 (1:1,000, Rabbit polyclonal) and human αSyn (1:500, mouse monoclonal) diluted in PBS containing 1% BSA and incubated overnight at 4°C followed by staining with Alexa Fluor 488 and Alexa Fluor 555 dye-conjugated secondary antibodies respectively. Nuclei were counterstained using Hoechst stain (10 μg/ml), and coverslips were mounted with Fluoromount medium and examined using an inverted fluorescence microscope (Nikon, Tokyo, Japan), and images were analyzed using Keyence BZ-X810.

Animal Treatment

Six- to eight-week-old C57BL/6 mice were obtained from Charles River Labs (Wilmington, MA) and housed under standard conditions (22°C, 30% relative humidity, a 12-h light cycle, and *ad libitum* food and water). Given that males are at a higher risk of developing PD than women (Cerri et al., 2019), we utilized male mice in these studies. Mice were randomly divided into two groups (Control and αSyn_{PFF}). An intrastriatal αSyn_{PFF}-induced neuroinflammation model was used for this study as per Duffy et al. (2018). Briefly, the mouse was given continuous anesthesia throughout the procedure, and mouse-ear bars were placed firmly into each ear to secure the skull in place. The Angle 2 stereotaxic instrument was used with a 10-μl Hamilton syringe to inject the αSyn_{PFF} directly into the striatum (STR) at the following stereotaxic coordinates in relation to Bregma (mm): −2 ML, 0.5 AP, −4 DV. Prior to injection, αSyn_{PFF} is sonicated using a high-power bath sonicator system. The total volume of αSyn_{PFF} injected per site was 2 μl per mouse. The injection needle remained in place for an additional 2 min after completing the injection

before it was gently withdrawn over a period of at least 30 s to minimize leakage. Mice were euthanized either 2 months after the initial intrastriatal injection for molecular experiments or after 6 months for TH analysis. The STR and SN were collected and stored at −80°C until further experimentation. The use of animals and all animal-related procedures in this study were approved and supervised by the Institutional Animal Care and Use Committee (IACUC) at Iowa State University, Ames, IA, USA.

Immunohistochemistry: Diaminobenzidine Immunostaining

A mixture of 200 mg/kg ketamine and 20 mg/kg xylazine was used to deeply anesthetize mice for transcardial perfusion with freshly prepared 4% paraformaldehyde (PFA) solution. The perfused brains were immediately post-fixed in 4% PFA for 48 h as per our previous publication (Gordon et al., 2016b). Fixed brains were then cryoprotected in 10% sucrose before being sectioned into 30-μm coronal sections using a freezing microtome (Leica Microsystems, Wetzlar, Germany). DAB immunostaining in the coronal SN sections was performed as per Ghosh et al. (2013) with slight modification. Briefly, on the day of staining, 30-μm sections were washed with PBS, incubated with methanol containing 3% H_2O_2 for 30 min, washed with PBS 6x for 5 min each, and blocked with 10% normal goat serum, 0.5% Triton X-100 and 2% BSA in PBS for 1 h at room temperature (RT). Then, the sections were incubated with an anti-TH antibody (1:1,000, mouse monoclonal) overnight at 4°C and washed in PBS 6× for 10 min each. Biotinylated anti-rabbit secondary antibody was then used for 1 h at RT, washed in PBS 5× for 10 min each followed by incubation with avidin peroxidase and triple washed in PBS for 10 min each. Immunolabeling was observed using a DAB solution, which yielded a brown-colored stain. The stained sections were washed in PBS and carefully mounted on poly-L-lysine (PDL)-coated slides with organic solvent (DPX). Using the Stereo Investigator software (MBF Bioscience, Williston, VT, USA), the total numbers of TH^+ neurons were counted stereologically using every sixth section of the SN (Ghosh et al., 2010). Samples were visualized using an Eclipse TE2000-U (Nikon, Tokyo, Japan) inverted fluorescence microscope, and images were captured using Keyence BZ-0023 (Keyence, Osaka, Japan).

Immunohistochemistry and Immunofluorescence

Treated mice were sacrificed through transcardial perfusion performed using 4% PFA, and perfused brains were post-fixed in 4% PFA for 48 h. Next, 5-μm paraffin-embedded sections were cut on a microtome by the Department of Pathology, College of Veterinary Medicine, ISU. Sections underwent deparaffinization through a series of steps that includes xylene (x2), xylene:ethanol (1:1), 100% ethanol, 95% ethanol, 75% ethanol, ad 50% ethanol for 3 min each. Then, the sections underwent antigen retrieval using citrate buffer (10 mM sodium citrate, pH 8.5) for 30 min at 80°C. Next, the sections were blocked with 2% bovine serum albumin, 0.5% Triton X-100, and 0.05% Tween 20 in PBS for 1 h at RT. Sections were incubated with different primary antibodies such as anti-TXNIP (1:500; rabbit monoclonal), anti-eIF2α (1:500; rabbit monoclonal), and anti-Iba1 (1:500; goat polyclonal) overnight at 4°C. After washing with PBS, sections were incubated in appropriate secondary antibodies (Alexa Fluor 488 or 594 or 555) for 2 h followed by incubation with 10 μg/ml Hoechst 33342 for 5 min at RT to stain the nucleus. Then, the slides were mounted with Fluoromount medium (Sigma-Aldrich) on glass slides for visualization. Sections were viewed under a Keyence inverted fluorescence microscope.

Immunofluorescence studies in primary mouse microglia (PMG) cells were performed based on previously published protocols with few modifications (Ghosh et al., 2013). Approximately 25,000 cells were plated onto PDL-coated coverslips. After treatments, cells were fixed with 4% PFA, washed in PBS, and blocked with buffer (PBS containing 2% BSA, 0.5% Triton X-100, and 0.05% Tween-20) for 1 h at RT. Coverslips containing cells were probed with the respective primary antibodies IBA1 (1:1,000, goat polyclonal) and p-eIF2α (1:500, Rabbit polyclonal) diluted in PBS containing 1% BSA and incubated overnight at 4°C. Coverslipped cells were washed several times in PBS and incubated with Alexa Fluor 488 and Alexa Fluor 555 dye-conjugated secondary antibodies. Nuclei were counterstained using Hoechst stain (10 μg/ml), and coverslips were mounted with Fluoromount medium on glass slides for visualization. Samples were visualized using an inverted fluorescence microscope (Nikon, Tokyo, Japan), and images were captured using Keyence BZ-X810.

Intracellular MitoSOX Assay

As a measure of oxidative stress, mitochondrial superoxide levels were estimated using MitoSox. Primary microglial cells (∼20,000 cells per well) were seeded in a 96-well plate and treated with αSyn_{agg} at various time points after cell attachment. Following treatment, the cells were exposed to 5 μM MitoSOX dye and incubated for 20 min at 37°C, protected from light. The cells were then washed twice with Hank's Buffered Salt Solution (HBSS) before measuring the fluorescence intensity using a Spectramax^{TM} microplate reader at 510 and 580 nm of excitation and emission wavelengths, respectively.

Mitochondrial Membrane Potential (MMP) Measurement

Mitochondrial function, a key indicator of cell health, can be assessed by monitoring changes in MMP. Membrane potential changes in the mitochondria were monitored by 5,5′,6,6′-tetrachloro-1,1′,3,3′-tetraethyl-benzimidazolcarbocyanineiodide (JC-1) staining as previously described (Ghosh et al., 2010). Briefly, the cells were plated at 20,000 cells/well into a 96-well black-walled, clear-bottom plate. The assay plates were incubated overnight at 37°C for cell adhesion. After the respective incubation times, JC-1 dye solution was added to each well, and the cells were incubated at 37°C, 5% CO_2 for 30 min. The monomeric form of JC-1 dye in the cytosol was detected fluorometrically through the emission of green fluorescence at the excitation/emission wavelengths 485/535 nm and aggregates in healthy mitochondria were detected through the red fluorescence emitted at the excitation/emission wavelengths

of 550/600 nm using a Spectramax^{TM} microplate reader. The changes in MMP were calculated as the red/green ratio and expressed as a percentage of control.

Microglial Nitric Oxide Detection

Nitric oxide production by primary microglial cells was measured by Griess assay (Sigma-Aldrich) as described previously. The cells were plated at 20,000 cells/well into a 96-well plate. The assay plates were incubated overnight at 37°C for cell adhesion and exposed to αSyn_{agg} at various time points (6, 12, 18, 24 h). At the end of each treatment, 100 μl of supernatant was added to an equal volume of Griess reagent per well of a 96-well plate. The samples were then incubated at 37°C at RT for 15 min until their color stabilized. The absorbance was measured at 540 nm using a Synergy 2 multimode microplate reader (BioTek Instruments, Winooski, VT, USA). Sodium nitrate was used as the standard to determine the nitrite concentration in the samples.

MTS Assay

MTS assay using the Cell Titer 96® Aqueous One Solution Cell Proliferation (MTS) assay kit was conducted based on the method described in our previous publications (Charli et al., 2016; Singh et al., 2018). Briefly, 20,000 cells/well were seeded in a 96-well tissue culture plate and exposed to 100 μl of treatment media, and the respective conditioned media was collected from the microglia. Cells were then incubated with the MTS dye for 45 min in a humidified, 5% CO_2 atmosphere at 37°C. The supernatant was removed, the resulting formazan crystals were dissolved with 25 μl of dimethyl sulfoxide (Sigma-Aldrich), and the color change was measured spectrophotometrically at 490 nm. The values were expressed as % of control.

Real-Time Quantitative Reverse Transcription PCR (qRT-PCR)

SYBR Green qRT-PCR was performed on the harvested cells and tissues as described by Samidurai et al. (2020). RNA was extracted using the TRIZOL reagent (Invitrogen, Carlsbad, CA, USA) as per the manufacturer's protocol. The isolated RNA was converted into cDNA using a High-Capacity cDNA synthesis kit (Applied Biosystems, Waltham, MA, USA). The qRT-PCR was carried out on an Applied Biosystems QuantStudio 3 system with the SYBR master mix (Invitrogen, Carlsbad, CA, USA). QuantiTect Primer Assays (Qiagen, Germantown, MD, USA) for genes specific to the pro-inflammatory cytokines TNF-α, IL-1β (#330001), and IL-6 were used. Normalization was done with the housekeeping gene 18S rRNA. TNF-α and IL-6 were obtained from the Iowa State University DNA Facility ISU DNA Facility (sequences are provided in **Supplementary Table 2**), IL-1β (QT01048355), and 18S (#PPM57735E) purchased from the Qiagen. Dissociation curves were run to ensure a single amplicon peak in all the SYBR Green reactions. The results were graphed as fold change in the respective gene expression calculated using the ΔΔCt method.

Western Blotting (WB)

Cells and tissue were lysed and homogenized using modified RIPA buffer and subjected to fluorescent immunoblotting as previously described (Gordon et al., 2016b; Samidurai et al., 2020). Normalized protein (30 μg) from each sample was loaded into their respective wells and separated using a 12% SDS-PAGE gel. The proteins were then transferred to a nitrocellulose membrane, and the nonspecific-binding sites were blocked for 1 h at RT using an Odyssey blocking buffer (LI-COR, Lincoln, NE, USA). Membranes were then incubated overnight at 4°C in one of the following primary antibodies p-PKCδ, PKCδ, ATF-4, p-IRE1α, p-eIF2α (1:1,000, Rabbit monoclonal), NLRP3 (1:1,000, mouse monoclonal), ASC (1:1,000, rabbit polyclonal) caspase-1 (1:1,000, mouse polyclonal), TXNIP and TrX (1:1,000, Rabbit polyclonal). Next, the membranes were triple-washed with PBS, and then the membranes were visualized using IRDye-tagged secondary antibodies (incubated for 1 h at RT) on an LI-COR Odyssey infrared imaging system. To avoid variation in loading, the same blots were stripped *via* incubation in NewBlot Stripping Buffer for 30 min in RT and incubated with an anti-actin antibody; β-actin (1:10,000, mouse monoclonal) was used as a loading control to confirm the loading of equal protein concentration in each lane. Full blot images have been provided in the **Supplementary Figure 4**.

Co-immunoprecipitation (Co-IP) Studies

Immunoprecipitation studies were carried out as described previously but with minor modifications (Filhoulaud et al., 2019; Panicker et al., 2019). Approximately 6×10^6 MMCs were seeded and treated with αSyn_{agg} or vehicle for 18 h. Subsequently, for TXNIP immunoprecipitation experiments, cells were collected and spun down at 5,000× *g* and the cell pellets were resuspended and lysed with TNE buffer (10 mM Tris-HCl, pH 7.5, 1% Nonidet P-40, 0.15 M NaCl, 1 mM EDTA, and 1:1,00 protease inhibitor mixture), and kept on ice for 30 min. The lysates were then centrifuged at 17,400× *g* for 35 min at 4°C to remove the debris. The supernatant protein concentration was measured and normalized using the Bradford method. For the input fraction, approximately 50 μg protein was used. Approximately for immunoprecipitation analysis, 500 μg protein per sample in 500 μl TNE buffer was used. The extracted proteins were incubated with 5 μg of anti-TxNIP antibody and placed on an orbital shaker at 4°C overnight. The following day, bound proteins were recovered following the addition of protein A/G magnetic beads (Thermo-fisher) and subsequent placement on an orbital shaker for 1 h at RT. Protein A/G magnetic beads were centrifuged and subsequently subjected to four washes for 2–3 min each with TNE buffer. The bound proteins were eluted from the beads by boiling in Laemmli buffer for 10 min at 97°C. The eluted proteins were collected by centrifuging at 5,000 rpm for 5 min and separated on 12% SDS-PAGE gels and followed by immunoblotting using antibodies against TXNIP. Quick Western detection was used to avoid the visualization of denatured IgG. Membrane images were captured on an LI-COR Odyssey imaging system.

Duo-link Proximal Ligation Assay (PLA)

Proximity ligation assay (PLA) was carried out in PMG according to the manufacturer's protocol. Briefly, 10,000 primary microglial cells were seeded on PDL-coated coverslips in 96 well culture plates. After treatment of PMG with αSyn for 18 h, cells were

washed with PBS and fixed using 4% PFA, blocked with blocking buffer (PBS containing 1.5% BSA, 0.5% Triton X-100, and 0.05% Tween-20), and subsequently incubated with antibodies against NLRP3 and TXNIP at 4°C overnight. Secondary antibodies conjugated with positive and negative oligonucleotides (PLA probes) were then incubated with the cells. Next, ligase was added and these oligonucleotides hybridize to the PLA probes, and when close enough, form a closed circle. In the DNA circle, one of the antibody-conjugated DNA probes serves as a primer for rolling-circle amplification (RCA), and a repeated sequence (concatemeric) product was generated when DNA polymerase and nucleotides were added. Fluorescently labeled oligonucleotides proceed to bind to the RCA product, allowing visualization of the protein-protein interaction as single dots *via* fluorescence microscopy (Wang et al., 2015). The protein-protein interactions were visualized as green puncta and analyzed by fluorescence microscopy using a Keyence microscope (with 60X objective). The PLA signals were further quantified using the ImageJ software according to the previous publication (Gomes et al., 2016).

siRNA Transfection

The PKCδ siRNA was purchased from Santa Cruz Biotech (#SC-36246; Dallas, TX, USA), and TXNIP siRNA was purchased from life technologies (Ambion #4390771; Carlsbad, CA, USA). Lipofectamine 3,000 reagent was used for all the siRNA transfections according to the manufacturer's protocol. One-day-old MMCs seeded at the density of 1.5×10^6 in 6-well plates were used for transfection studies. Next, 700 pM of PKCδ siRNA, or 1.5 nM of TXNIP siRNA, or an equal amount of scrambled siRNA mixed with 5 μl of Lipofectamine 3,000 was added to the respective wells. The cells were then incubated with siRNA for 48 h, after which cells were treated with αSyn_{agg} for 24 h. Immunoblots were performed to check for the efficiency of target gene knockdown as well as for the determination of inflammation and ERS markers.

Data Analysis

Data were analyzed using a two-tailed *t*-test (two groups) or one-way or two-way ANOVA (multiple groups) followed by Bonferroni's *post hoc* analysis (PRISM 6.0 software, GraphPad, La Jolla, CA, USA), and are represented as mean ± SEM. Differences were considered statistically significant for p-values ≤ 0.05.

RESULTS

Aggregated αSyn (αSyn_{agg}) Enhanced Mitochondrial Impairment, PKCδ Activation, and ER Stress (ERS) *In vitro* in Mouse Primary Microglial Cells

Lewy bodies, which represent a classical pathological hallmark of PD and DLB exhibits microglial and neuronal inclusions enriched with αSyn_{agg} (Fellner et al., 2011; Hoffmann et al., 2019). Given that αSyn_{agg} positive inclusions appear prior to the development of clinical signs (Braak et al., 2006) and that they are taken up by the microglia and contribute to the templated conversion of endogenous monomeric αSyn (Earls et al., 2019; Pike et al., 2021). We initially characterized the αSyn fibrils. Therefore, in this study, we used the human αSyn_{agg} which was found to induce microglial activation response consistent with a previous finding from our lab (Panicker et al., 2019). In our previous studies, we examined αSyn fibrils using the thioflavin T assay to determine the extent of fibrillar content in the αSyn_{PFF} fractions. Consistent with a previous report our studies revealed that a majority of the αSyn_{agg} were composed of fibrillar species (Manne et al., 2019). We further validated the confirmation of fibrillar αSyn species using transmission electron microscopy (TEM; **Figure 1A**) prior to microglia treatment studies. Moreover, we found internalization and microglial activation capabilities by human αSyn_{agg} in mouse primary microglia as previously reported (Panicker et al., 2019). In fact, immunofluorescence staining verified that treatment of primary microglia with 1 μM αSyn_{agg} led to its internalization (**Figure 1B**) as determined using an antibody against human total αSyn, consistent with a previous finding from our lab (Panicker et al., 2019). Given that αSyn aggregation reportedly induces mitochondrial dysfunction, thereby contributing to disease pathology (Smith et al., 2005) next, we investigated the temporal pattern of mitoROS generation, mitochondrial membrane potential (MMP) collapse, and PKCδ activation in mouse primary microglia (mouse primary microglia) stimulated with 1 μM αSyn_{agg} based on previous reports (Boza-Serrano et al., 2014; Lee et al., 2018; Panicker et al., 2019) for increasing durations (6, 12, 18, 24 h; Hoffmann et al., 2016; Sarkar et al., 2020). Following treatment of primary microglial cells with 1 μM of αSyn_{agg} robust mitochondrial superoxide generation, mitochondrial membrane potential (MMP) generation and nitrite release were evidenced as determined by MitoSOX, JC-1, and Griess spectrophotometric plate reader assays, respectively. The cells treated with αSyn_{agg} exhibited a significant ($p < 0.001$) time-dependent increase in mitochondrial (mito)ROS generation with an accompanying dissipation of MMP (**Figures 1C,D**), as well as nitrite release in a time-dependent manner (**Supplementary Figure 1B**) as compared to vehicle-treated cells. These results indicate that αSyn_{agg} induced mitochondrial dysfunction in primary microglia *via* a mitochondrial oxidative stress mechanism and accompanying collapse of MMP.

Previous reports show that PKCδ is a critical regulator of the proinflammatory microglial activation state in response to diverse inflammogens including αSyn, TNF-α, and LPS (Wen et al., 2011; Gordon et al., 2016a). Next, we examined whether activated PKCδ, a redox-sensitive kinase, is associated with mitochondrial dysfunction. Our WB studies revealed that αSyn_{agg} stimulation of mouse primary microglia resulted in a pronounced time-dependent activation of PKCδ as evidenced by prominent PKCδ phosphorylation at site Tyr-311 at 12 h which remained elevated for the remainder of the treatment duration as compared to vehicle-treated cells (**Figure 1E**), suggesting that mitochondrial oxidative stress may serve as a trigger for PKCδ activation consistent with previous reports (Majumder et al., 2001; Steinberg, 2015). These data collectively suggest that PKCδ activation contributes to microglia activation presumably *via* mitochondrial oxidative stress mechanism. Several reports link

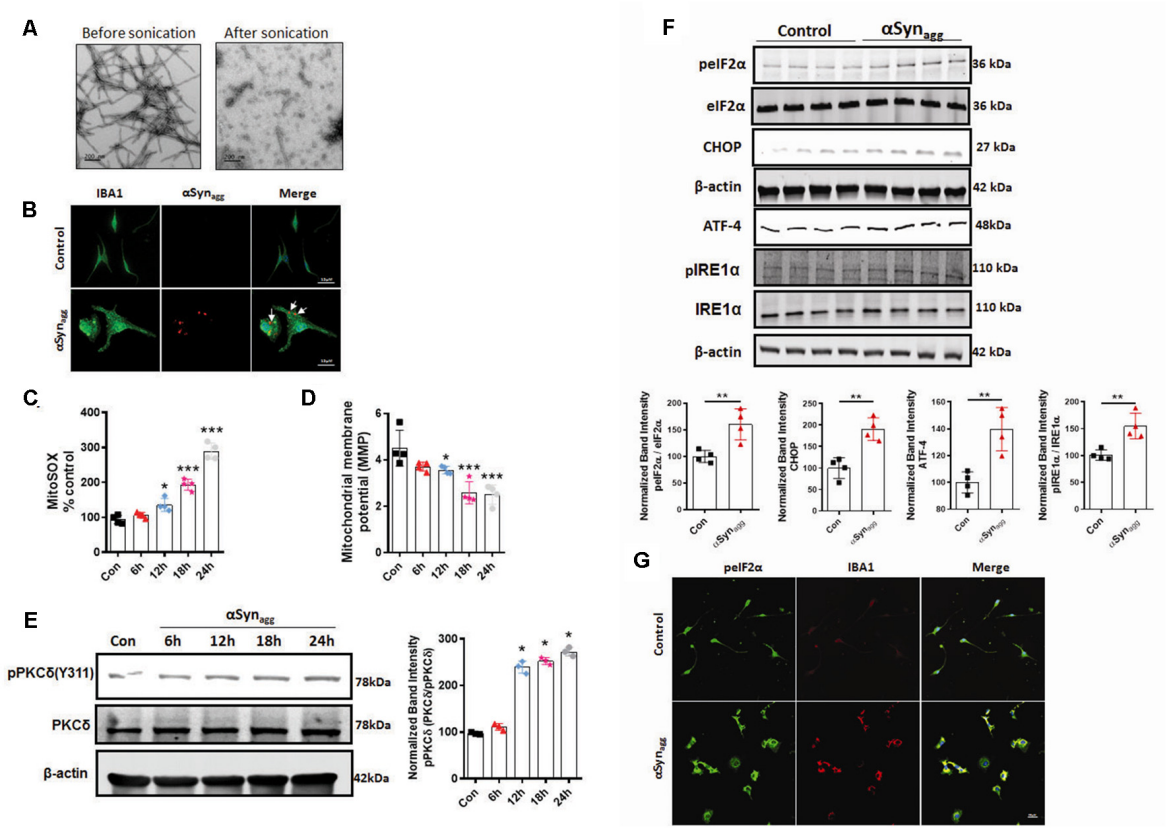


FIGURE 1 | Time-dependent mitochondrial dysfunction, PKCδ activation, and endoplasmic reticulum stress (ERS) markers in αSyn_{agg}-stimulated mouse primary microglia. Mouse primary microglial cells were exposed to 1 μM of αSyn_{agg} for increasing durations (6, 12, 18, and 24 h) and mitochondrial superoxide generation was measured using MitoSOX dye-based spectrofluorometric analysis. **(A)** Generation of human preformed fibrils (PFF) αSyn and validation of uptake of αSyn_{agg} by primary microglia. Representative scanning transmission electron microscopy (STEM) images of αSyn_{PFF} before scale bar = 200 (nm) and after scale bar = 200 (nm) sonication. Even after sonication the αSyn_{PFF} still retain their beta-sheet conformation. **(B)** Internalization of αSyn_{agg} in primary microglia. Representative immunohistochemical images of mouse primary microglia depicting uptake of hu-αSyn as determined using antibodies against human αSyn (red) and microglial marker-IBA-1 (green) in primary microglia treated with αSyn_{agg} for 1 h. Internalized human αSyn, visualized as red intracellular puncta), Scale bars, 15 μm. **(C)** MitoROS generation increased in a time-dependent manner in αSyn_{agg}-treated mouse primary microglia cells. Data shown are the mean ± SEM from at least three independent experiments. **(D)** Assessment of mitochondrial membrane potential [MMP ($\Delta\Psi$m)] using JC-1 spectrophotometric plate reader analysis. MMP decreased time-dependently post mouse PMG stimulation with αSyn_{agg}. Data shown are the mean ± SEM from at least three independent experiments. **(E)** Representative immunoblots and densitometric evaluation of p-PKCδ (Y311) in the whole-cell lysates indicating a time-dependent increase in PKCδ phosphorylation in αSyn_{agg}-treated mouse PMG. Data shown are the mean ± SEM from at least three independent experiments. **(F)** Representative immunoblots and densitometric analyses of mouse PMG cells treated with or without αSyn_{agg} for 24 h revealing significantly increased ATF-4, p-IRE1α, and and CHOP expression levels. The immunoblot is representative of at least three independent experiments. **(G)** Representative images from dual immunohistochemical staining for p-eIF2α (Red) IBA1 (green) in primary microglia treated with αSyn_{agg} for 24 h. Nuclei were counterstained with Hoechst stain (Blue). Results represent three independent experiments. Scale bar = 20 μm. Data were analyzed using one-way ANOVA followed by Bonferroni's *post hoc* analysis and two-tailed *t*-test. Asterisks (***$p < 0.001$, **$p < 0.01$ and *$p \leq 0.05$) indicate significant differences between control and treatment groups.

misfolded αSyn-induced PD pathology and ERS. For example, the overexpression of A53T αSyn promotes ER dysfunction, thereby eliciting pronounced ER stress (Smith et al., 2005; Karim et al., 2020), and blockage of ERS was found to protect against A53T αSyn-induced cell death (Boyce et al., 2005). Moreover, aberrant generation of mitoROS has been shown to contribute to ERS (Liu et al., 2019). Therefore, we further examined the magnitude of expression of ERS markers in αSyn_{agg} stimulated mouse primary microglia. As anticipated, the upregulation of ERS markers, including p-IRE1α, p-eIF2α, CHOP, and ATF-4, were observed in αSyn_{agg}-treated mouse primary microglia as compared with vehicle-treated cells (**Figure 1F**). Likewise, immunofluorescence analysis showed that αSyn_{agg} increased the p-eIF2α immunoreactivity in the primary microglia cells as compared to the vehicle treated cells further supporting the central role of ERS in microglial activation response in response to αSyn_{agg} (**Figure 1G**). To ensure that the observed effects were not due to cellular toxicity, we performed a cell viability assay using an MTS assay. MTS revealed little or no evidence of cell death at a concentration of 1 μM αSyn_{agg} (**Supplementary Figure 1A**). Given that αSyn concentrations ranging between 0.5–5 μM have been widely used in various cell culture studies and that the synaptic concentration of αSyn is believed to fall within the range of 2–4 μM

(Konno et al., 2012; Westphal and Chandra, 2013; Boza-Serrano et al., 2014; Domert et al., 2016; Lee et al., 2018; Hoffmann et al., 2019), we used 1 μM αSyn_{agg} in the remainder of the experiments unless otherwise stated. These results indicate that our αSyn_{agg} proteins are capable of inducing a reactive microglial activation state *via* mitochondrial oxidative stress and PKCδ activation mechanism as well as ERS in mouse primary microglia.

αSyn_{agg} Increased the Expression of TXNIP and NLRP3 Inflammasome Components With an Accompanying Elevation of Pro-inflammatory Cytokine Generation in Mouse Primary Microglia

Thioredoxin-interacting protein (TXNIP), also known as thioredoxin-binding protein-2 or vitamin D3-upregulated protein 1, has been shown to be an endogenous antagonist of the antioxidant protein thioredoxin (Trx) (Zhao et al., 2017b). In oxidatively stressed cells, in response to ERS, TXNIP has been linked to NLRP3 inflammasome activation (Wang C. Y. et al., 2019). To test whether TXNIP/Trx expression levels are altered by αSyn_{agg}, we treated primary microglia with αSyn_{agg}. As predicted, TXNIP expression was significantly increased while Trx expression levels were downregulated in mouse primary microglia stimulated with αSyn_{agg} (**Figure 2A**) as compared to controls. We next examined whether TXNIP upregulation is associated with increased expression of NLRP3 inflammasome activation markers as well as inflammatory cytokine generation. Our studies indicate that αSyn_{agg} treatment increased protein expression of NLRP3 inflammasome components alongside expression of the pro-inflammatory cytokines IL-1β, IL-6, and TNF-α in αSyn_{agg}-treated mouse primary microglia as compared to vehicle (con) treated cells (**Figure 2B**). Together these studies suggest that the microglial activation state induced by αSyn_{agg} may involve a functional interaction between NLRP3 and TXNIP in primary microglia.

αSyn_{agg} Stimulated the Interaction Between TXNIP and NLRP3 in Mouse Primary Microglia

Previous studies have identified mitoROS as a critical causative factor in promoting Trx disassociation from TXNIP, and its subsequent association with NLRP3, thereby leading to the generation of inflammasome activation markers (Zhou et al., 2010; Han et al., 2018). Therefore, we next assessed the interaction between NLRP3 and TXNIP using proximity ligation assay (PLA) in αSyn_{agg}-stimulated cells. Immunofluorescence analysis revealed a significant interaction between endogenous TXNIP and NLRP3 proteins in αSyn_{agg}-stimulated mouse primary microglia as compared to vehicle-treated cells (**Figure 3A**). We further validated our PLA findings using IP/IB analysis whereby a significant interaction between TXNIP and NLRP3 was evidenced in αSyn_{agg} stimulated mouse primary microglia as compared to controls (**Figure 3B**) suggesting that the TXNIP/NLRP3 association may at least in part trigger a reactive microglial activation state in the context of α-synucleinopathy.

Salubrinal (SAL), an eIF2α Inhibitor, Mitigates αSyn_{agg}-Induced Microglial Activation by Regulating TXNIP Expression, NLRP3 Inflammasome Activation, and Pro-inflammatory Cytokine Generation in Mouse Primary Microglia

Previous reports suggest that ERS is a critical regulator of the TXNIP/NLRP3 signaling axis and resultant inflammatory response in diverse experimental models of inflammation-related disorders (Chen X. et al., 2019; Feng and Zhang, 2019). Furthermore, pharmacological inhibition of ERS was found to afford neuroprotection in the A53T mouse model of PD (Boyce et al., 2005). However, the link between ERS and TXNIP/Trx, redoxisome dysfunction during an αSyn_{agg}-induced microglial pro-inflammatory signaling event remains poorly characterized. We hypothesized that the TXNIP-Trx system is a critical intermediate that links ERS to microglia-mediated NLRP3 inflammasome activation subsequent to αSyn_{agg} stimulation. Therefore, we examined the contribution of ERS in TXNIP-Trx dysfunction utilizing SAL, which is a selective inhibitor of eIF2α and has been shown to exhibit anti-inflammatory effects in a rodent model of traumatic brain injury (Logsdon et al., 2016). We first examined whether SAL inhibited αSyn_{agg}-induced dysregulation of the TXNIP/Trx system. Using mouse primary microglia, we first determined whether 50 μM of SAL (Huang et al., 2012) modulated the expression of ERS markers, including p-eIF2α, in αSyn_{agg}-treated cells. Pretreatment with SAL increased αSyn_{agg}-induced upregulation of p-eIF2α (data not shown). Next, we investigated the effect of SAL on αSyn_{agg}-induced dysregulation of the TXNIP/Trx pathway in mouse primary microglia treated with αSyn_{agg}. Our WB analysis revealed that SAL treatment attenuated αSyn_{agg}-induced TXNIP upregulation while upregulating Trx expression (**Figure 4A**). Together, these results indicate that ERS blockade *via* SAL reduced the αSyn_{agg}-induced dysregulation of the TXNIP/Trx signaling pathway which may, in turn, prevent the reactive microglial activation state. Emerging evidence suggests that ERS plays a critical role in TXNIP and resultant activation of the NLRP3 inflammasome (Lerner et al., 2012; Oslowski et al., 2012). However, to what extent ERS regulates NLRP3 inflammasome activation in response to αSyn_{agg} stimulation of mouse primary microglia remains poorly understood. Here we identified that NLRP3 inflammasome activation markers are activated in an ERS-dependent manner. Our immunoblot results showed that SAL attenuated the stimulatory effect of αSyn_{agg} on NLRP3 (**Figure 4**A), and its activation markers as evidenced by reduced pro-inflammatory cytokine mRNA expression of IL-1β and TNF-α (**Figure 4B**). These findings indicate that ERS blockade *via* SAL may in part ameliorate the αSyn_{agg}-induced neurotoxic microglial activation state *via* inhibition of TXNIP/NLRP3 inflammasome axis activation in αSyn_{agg}-stimulated primary microglia.

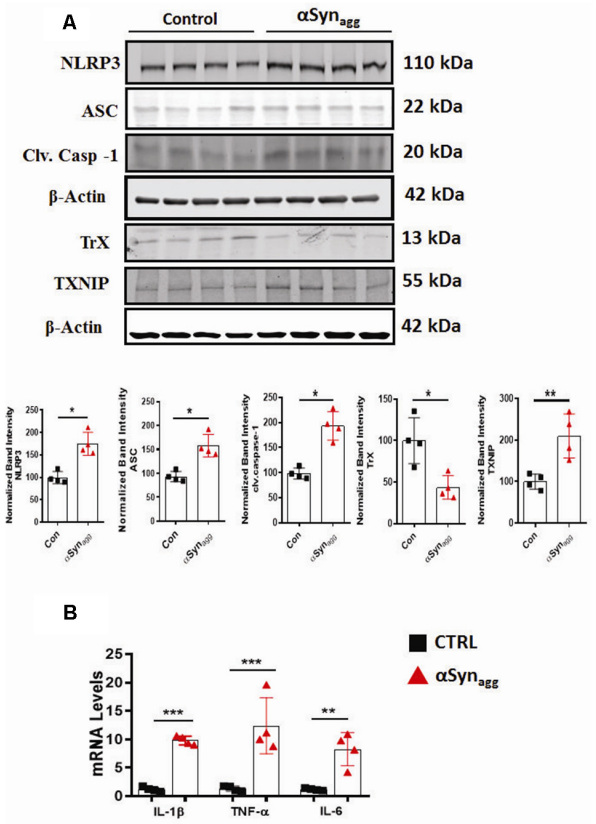


FIGURE 2 | Activation of TXNIP and TrX downregulation positively correlates with the induction of NLRP3 inflammasome activation markers and pro-inflammatory cytokine generation in αSyn$_{agg}$-stimulated mouse PMG. **(A)** Western blot analysis showing increased expression of NLRP3, ASC, caspase-1, TXNIP and downregulation of TrX expression following stimulation of mouse primary microglia with αSyn$_{agg}$ for 24 h and quantification of the expression levels of the aforementioned markers. β-actin was used as an internal loading control. Data presented as mean ± SEM from four independent experiments. **(B)** qRT-PCR analysis showing increased gene expression of pro-inflammatory cytokines including TNF-α, IL-1β, and IL-6 after αSyn$_{agg}$ stimulation for the indicated treatment period. Data are presented as the mean ± SEM and representative of three independent experiments. Data were analyzed using two-tailed *t*-test. Asterisks (***$p < 0.001$, **$p < 0.01$, and *$p \leq 0.05$) indicate significant differences between control and treatment groups.

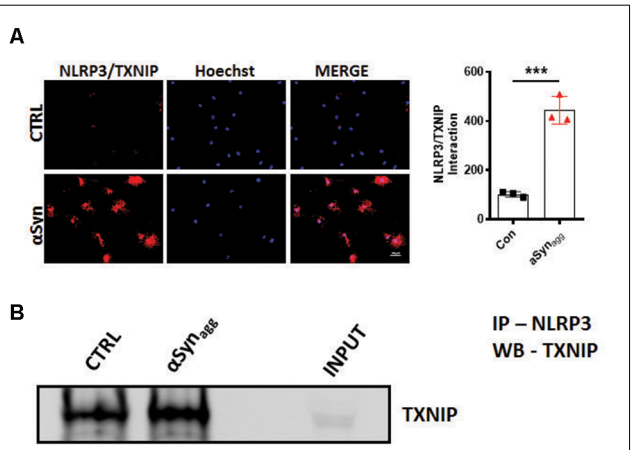


FIGURE 3 | αSyn$_{agg}$ promotes TXNIP interaction with NLRP3 in mouse primary microglia. **(A)** Representative immunofluorescence images of *in situ* proximity ligation assay (PLA) displaying interaction between TXNIP and NLRP3 in mouse primary microglia stimulated with αSyn$_{agg}$ for 24 h. Quantification of PLA puncta reveals the maximal amount of PLA puncta in αSyn$_{agg}$ stimulated mouse PMG. TXNIP-NLRP3 proximity ligation signal (red), and DAPI (blue). **(B)** Co-IP and WB analysis demonstrating the interactions between TXNIP and NLRP3 in αSyn$_{agg}$ stimulated primary microglia. Quantification of TXNIP-NLRP3 interactions using densitometric scanning analysis. Cell lysates were prepared from mouse primary microglia stimulated with or without αSyn$_{agg}$ for 24 h and subsequently immunoprecipitated (IP) with NLRP3 followed by immunoblotting with a TXNIP antibody. Data are shown as mean ± SEM. ***$p < 0.001$ vs. αSyn or controls using two-tailed *t*-test; $N = 3$).

Mito-Apocynin (MitoApo) Reduced NLRP3 Inflammasome Activation, ERS, and TXNIP/Trx Dysfunction in αSyn$_{agg}$-Stimulated MMC Microglial Cells

Since αSyn$_{agg}$ induces mitochondrial oxidative stress in primary microglia, next we explored the effects of (MitoApo), a mitochondrially targeted antioxidant on the αSyn$_{agg}$-induced ERS and TXNIP/NLRP3 signaling cascade. Owing to the fact that mouse microglial cell line, MMC closely mimic neonatal primary microglia (Sarkar et al., 2020), we utilized these cells to determine the activation of the aforementioned microglial pro-inflammatory mediators in MMCs treated with αSyn$_{agg}$ in the presence or absence of mitoapocynin. A previous report demonstrated that ER-mitochondria proximity promotes NLRP3 localization to mitochondria, triggering its activation (Shimada et al., 2012). Indeed, we previously demonstrated that the NLRP3 inflammasome translocated to the mitochondria in rotenone-stimulated microglial cells, which coincided with an elevated mitochondrial oxidative stress (Lawana et al., 2017). Based on these findings, we hypothesized that blocking mitochondrial oxidative stress *via* MitoApo would reduce ERS and the associated TXNIP/NLRP3 signaling pathway. To address this hypothesis, MMC microglial cells were treated with MitoApo (10 μM). We found that there was a significant upregulation of ERS markers including eIF2α, ATF-4, TXNIP, and NLRP3 protein expression, as well as pro-inflammatory cytokine mRNA expression (IL-1β and TNF-α) that was accompanied by an upregulation of Trx expression in MMC cells treated with αSyn$_{agg}$, which was markedly reduced by treatment of mitoapocynin (**Figures 5A–C**). Collectively, these results indicate that MitoApo ameliorates the αSyn$_{agg}$-induced ERS and TXNIP/NLRP3 signaling axis in a cell culture model of α-synucleinopathy.

PKCδ Knockdown in MMC Microglial Cells, Ameliorated αSyn-Induced ERS as Well as TXNIP and NLRP3 Inflammasome Activation

We next determined whether siRNA-mediated knockdown of PKCδ altered the αSyn$_{agg}$-induced microglial activation

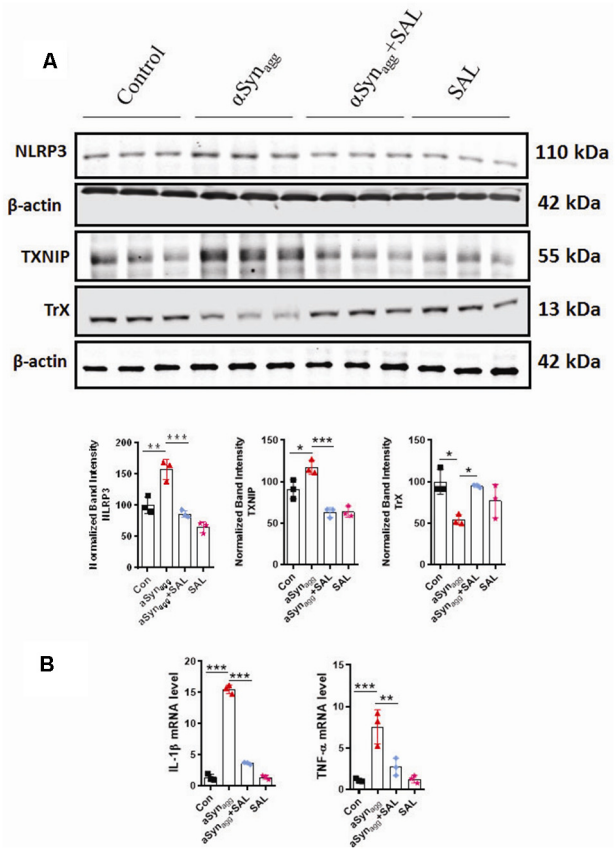


FIGURE 4 | Salubrinal (SAL) attenuates the αSyn_{agg}-induced activation of TXNIP, NLRP3 expression, and the release of pro-inflammatory cytokines in mouse primary microglia. Mouse primary microglia were pretreated with SAL (50 μM) for 3 h, followed by αSyn_{agg} for another 24 h. **(A)** Representative immunoblotting and densitometric quantification showing that SAL reduced the αSyn_{agg}-induced upregulation of NLRP3, TXNIP, and concurrent downregulation of TrX. **(B)** Quantitative gene expression analysis (qRT-PCR) showing that SAL abolished the αSyn_{agg}-induced mRNA expression of TNF-α, IL-1β in mouse primary microglia, 18S gene used for the normalizations. Data shown are the mean ± SEM from at least three independent experiments. Data were analyzed using one-way ANOVA followed by Bonferroni's *post hoc* analysis. Asterisks (***$p < 0.001$, **$p < 0.01$ and *$p \leq 0.05$) indicate significant differences between control and treatment groups.

response. We have demonstrated that the redox-sensitive kinase PKCδ is linked to microglial NLRP3 inflammasome activation and IL-1β generation under oxidative stress conditions (Lawana et al., 2017; Panicker et al., 2019), raising the possibility that PKCδ may be involved in NLRP3 inflammasome activation *via* the ERS response. To determine whether or how PKCδ expression influence the αSyn_{agg}-induced ERS-associated microglial activation response, MMC mouse microglial cells were transfected with either control siRNA or PKCδ siRNA and subsequently treated with αSyn_{agg}. MMC microglial cells that were transfected with a small interfering RNA (siRNA) against PKCδ for 48 h displayed markedly reduced endogenous PKCδ levels (60–70%) as compared with scrambled siRNA-transfected cells (**Supplementary Figure 2**). We next evaluated the effects of RNAi-mediated knockdown of PKCδ on the αSyn_{agg}-induced ER stress response in MMCs. Furthermore, as expected, downregulation of PKCδ remarkably repressed the αSyn_{agg}-induced ER stress response as exemplified by reduced expression of BIP (Binding immunoglobulin protein), p-eIF2α in MMCs (**Figure 6A**).

Next, we investigated the impact of PKCδ knockdown on the expression of TXNIP and its binding partner Trx in αSyn_{agg}-stimulated microglial cells using WB analysis. PKCδ downregulation dramatically decreased the expression of TXNIP while upregulating Trx expression in microglial cells treated with αSyn_{agg} (**Figure 6A**). Finally, we tested the causal relationship between PKCδ activation and NLRP3 inflammasome activation in microglial cells stimulated with αSyn_{agg}. PKCδ knockdown in MMC microglial cells treated with αSyn_{agg} significantly reduced the expression of NLRP3 (**Figure 6A**) and mRNA expression of proinflammatory cytokines including TNF-α and IL-1β (**Figure 6B**). Taken together, these results demonstrate that downregulation of PKCδ reduces the αSyn_{agg}-induced microglial activation response at least in part *via* amelioration of ERS and the TXNIP/NLRP3 signaling axis and the associated generation of proinflammatory cytokines in MMC microglial cells.

TXNIP Downregulation Mitigated NLRP3 Inflammasome Activation Markers in Mouse Primary Microglia Stimulated With αSyn_{agg}

Having demonstrated that TXNIP associates with NLRP3, we next determined whether TXNIP regulated NLRP3 inflammasome activation. Our approach was to assess NLRP3 activation markers since previous studies have demonstrated a positive association between TXNIP upregulation and activation and NLRP3 inflammasome activation markers (Tseng et al., 2016). Thus, in the initial set of experiments, we downregulated TXNIP expression using siRNA-mediated knockdown to determine its impact on NLRP3 inflammasome activation markers. Our WB analysis revealed a 65% knockdown efficiency (**Supplementary Figure 3**) of TXNIP that was accompanied by a marked reduction in the protein expression of NLRP3 inflammasome and cleaved caspase-1 expression (**Figure 7A**) in mouse primary microglia exposed to αSyn_{agg}. In parallel studies, qPCR analysis revealed that TXNIP siRNA ameliorated αSyn_{agg}-induced mRNA expression of IL-1β and TNF-α (**Figure 7B**). Our findings indicate a mechanistic link between TXNIP and the NLRP3 inflammasome activation in promoting a proinflammatory microglial phenotype and that downregulation of TXNIP ameliorates the proinflammatory microglial activation response in αSyn_{agg}-stimulated mouse primary microglia.

ERS Inhibition *via* SAL Decreased Indirect DAergic Neurotoxicity Mediated by αSyn_{agg} Stimulated Primary Microglia

To further test the influence of αSyn_{agg}-induced microglial ERS on DAergic neuronal survival we treated primary

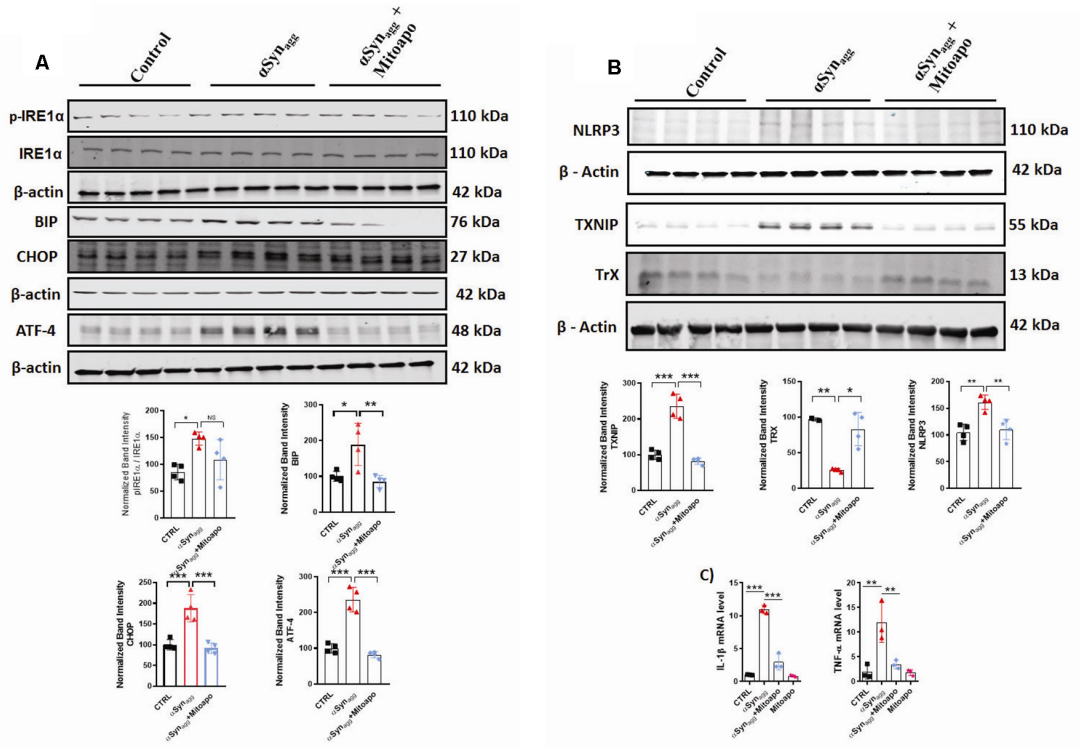


FIGURE 5 | Inhibition of mitoROS *via* mito-apocynin (Mitoapo) attenuates αSyn_{agg}-induced ERS, TXNIP/NLRP3 activation, and pro-inflammatory cytokine production in MMC microglial cells. MMCs were pretreated with Mito-Apo (10 μM) for 3 h, followed by a 24-h αSyn_{agg} treatment before being processed for WB and qRT-PCR analysis. **(A)** Representative immunoblot and densiometric quantification of protein expression showing that Mitoapo reduced the αSyn_{agg}-induced upregulation of p-IRE1α, BIP, CHOP, and ATF-4. **(B)** Representative immunoblot and densitometric quantification of protein expression showing that Mitoapo reduced the αSyn_{agg}-induced upregulation of TXNIP, NLRP3 while enhancing TrX expression levels. **(C)** qRT-PCR analyses showing mitoapo reduced the αSyn_{agg}-induced increased generation of proinflamamtory cytokines TNF-α and IL-1β. Data shown are the mean ± SEM from at least three independent experiments. Data were analyzed using one-way ANOVA followed by Bonferroni's *post hoc* analysis. Asterisks (***$p < 0.001$, **$p < 0.01$ and *$p \leq 0.05$) indicate significant differences between control and treatment groups. NS: not significant.

microglia with αSyn_{agg} in the presence or absence of the ERS inhibitor SAL followed by 3-(4, 5-dimethylthiazol-2-yl)-2, 5-diphenyltetrazolium bromide (MTT) cell viability assay in MN9D DAergic neuronal cells treated with microglia-conditioned media (MCM) collected from αSyn_{agg}-stimulated microglial cells treated with or without SAL. Mouse primary microglia were pretreated with SAL for 6 h and subsequently stimulated with αSyn_{agg} for 12 h, followed by washing and incubation with fresh cell culture media for another 24 h (**Figure 8A**). The resulting MCM was transferred to MN9D DAergic neuronal cells. After 18 h following MCM addition, cell viability was assessed using an MTT assay. The MCM collected from αSyn_{agg}-stimulated mouse primary microglia increased MN9D DAergic cell death whilst this effect was markedly reduced in MN9D cells that were treated with MCM from SAL-pretreated, αSyn_{agg}-stimulated microglial cells (SAL/αSyn_{agg}-MCM; **Figure 8B**). These results are in line with previous studies showing that a neurotoxic microglial activation state exerts detrimental effects on DAergic neuronal integrity subsequent to the αSyn-induced microglial inflammatory response (Yun et al., 2018).

Chronic Activation of ER Stress, TXNIP, and NLRP3 Inflammasome Activation Preceded Delayed Loss of TH+ Neurons in the Nigra of αSyn_{PFF}-Inoculated Mice

Our *in vitro* studies revealed that treatment of primary microglia induced PKCδ activation with an accompanying induction of the ERS-mediated TXNIP/NLRP3 signaling axis. Next, we sought to investigate the aforementioned signaling events in the αSyn_{PFF} mouse model of sporadic PD that reproduces several key PD pathological correlates including αSyn pathology, loss of DAergic neurons, and the microglial activation response *in vivo*. In this model, αSyn_{PFF} seeds are taken up by the striatum and transmitted to the nigra in a retrograde fashion *via* the nigrostriatal pathway where they function as a template and promote the seeding of endogenous murine αSyn to accumulate into misfolded phosphorylated pathological aggregates (Luk et al., 2012; Earls et al., 2019). Although microglia has been implicated in neuroinflammation and associated nigral TH neuronal loss (Duffy et al., 2018). To date, there is no published literature detailing TXNIP nor eIF2α-expression

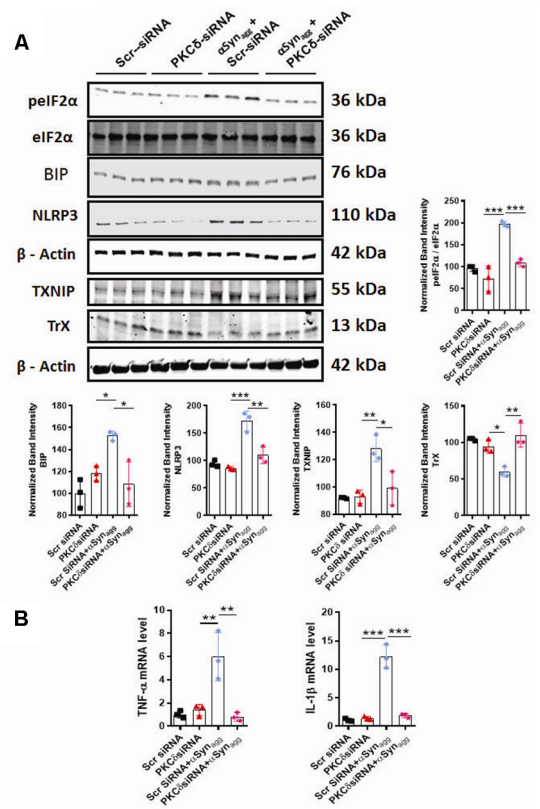


FIGURE 6 | siRNA-mediated PKCδ knockdown alle*viates* αSyn_{agg}-induced ERS, TXNIP, and NLRP3 inflammasome activation in mouse microglial cells (MMCs). MMCs were transfected with scrambled siRNA (Scr siRNA) or PKCδ siRNA for 48 h and were then treated with αSyn_{agg} for another 24 h before being processed for Western blot and qRT-PCR analyses. **(A)** Representative immunoblot and densitometric quantification revealing that PKCδ-silencing diminished the αSyn_{agg}-mediated activation of p-eIF2α, BIP, TXNIP, and NLRP3 and reversed the αSyn_{agg}-induced suppression of TrX. Data shown are the mean ± SEM from at least three independent experiments. **(B)** qRT-qPCR analysis depicting that PKCδ gene depletion significantly attenuated the αSyn_{agg}-induced mRNA expression of the pro-inflammatory markers IL-1β and TNF-α. Data shown are the mean ± SEM from at least three independent experiments. Data were analyzed using one-way ANOVA followed by Bonferroni's *post hoc* analysis. Asterisks (***$p < 0.001$, **$p < 0.01$, and *$p < 0.05$) indicate significant differences between control and treatment groups.

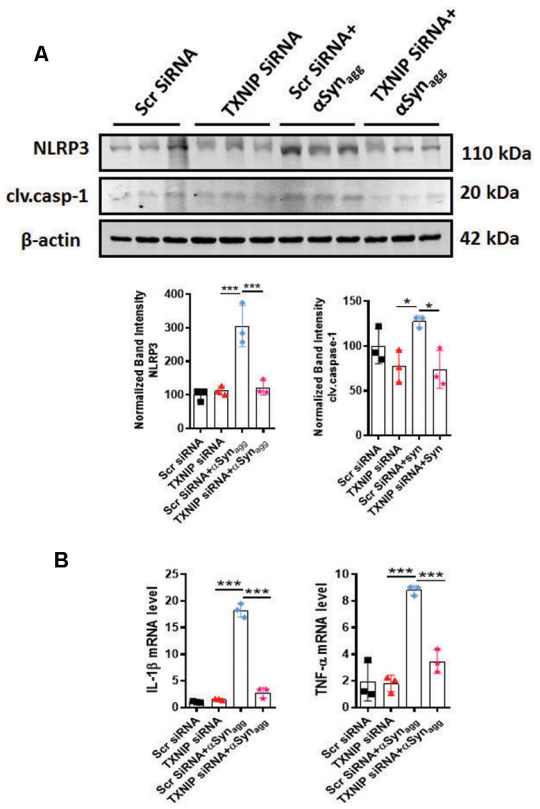


FIGURE 7 | siRNA-mediated TXNIP knockdown mitigates NLRP3 inflammasome activation markers in primary microglial cells stimulated with αSyn_{agg}. **(A)** Expression of caspase-1 and NLRP3 inflammasome activation marker in mouse PMG transfected with TXNIP siRNA for 48 followed by stimulation with αSyn_{agg} for another 24 h. Western blot analysis and quantification reveals inhibitory effects of TXNIP siRNA on αSyn_{agg}-induced upregulation of NLRP3 and cleaved caspase-1 in mouse PMG as compared with scramble siRNA transfected cells. β-actin used as an internal control. **(B)** qRT-PCR analysis of IL-1β and TNF-α in mouse PMG transfected with or without TXNIP siRNA with or without stimulation with αSyn_{agg} for 24 h. TXNIP siRNA attenuated αSyn_{agg}-induced upregulation of the aforementioned proinflammatory cytokine gene expression as compared to scramble transfected mouse PMG. Data shown are the mean ± SEM from at least three independent experiments. Significance is based on two-way ANOVA followed by a Bonferroni *post hoc* test. ***$p < 0.001$ and *$p < 0.05$ vs. controls.

within microglia in the context of synucleinopathy. Therefore, we used specific markers of ERS and inflammation to further support the role of microglial ERS in PD like pathology. To this end, we performed double immunolabeling for p-eIF2α or TXNIP a in nigral brain section from αSyn_{PFF} and PBS (control) infused mice. A previous study reported that TXNIP colocalizes with microglia after subarachnoid hemorrhage (SAH; Zhao et al., 2017a). As expected, control mice displayed scant expression of eIF2α or TXNIP. In contrast, αSyn_{PFF}-infused mice display considerable colocalization of eIF2α and TXNIP within IBA-1-positive microglia (**Figures 9A,B**). Thus, our results demonstrate that both p-eIF2α and TXNIP colocalized with microglia in the substantia nigra of αSyn_{PFF}-infused mice, suggesting that these inflammatory markers may aggravate nigral DAergic neurotoxicity by triggering pro-inflammatory signaling events. Moreover, we cannot exclude the possibility that activation of the aforementioned proinflammatory factors in other CNS cell types might contribute to the nigral DAergic neurotoxicity. Additionally, consistent with our *in vitro* results, our WB analysis further confirmed that αSyn_{PFF} intrastriatal infusion significantly upregulated the ERS markers p-eIF2α, CHOP (C/EBP Homologous Protein), BIP, and ATF-4 (**Figures 9C,D**) in the SNpc, which positively correlated with TXNIP upregulation and the associated downregulation of Trx levels as compared to PBS-infused mice (**Figure 9A**). Likewise, this effect was accompanied by PKCδ activation and upregulation of the NLRP3 inflammasome in the SNpc that was associated with enhanced generation of proinflammatory cytokine mRNA

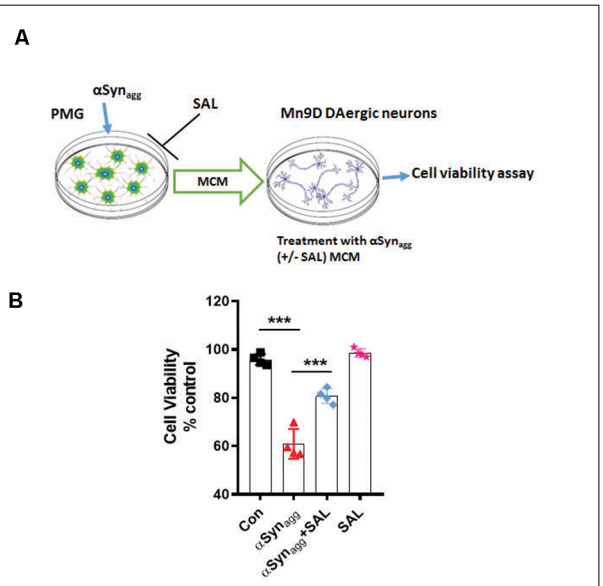


FIGURE 8 | Salubrinal attenuates αSyn_{agg}-stimulated microglia-conditioned media (MCM)-induced DAergic neurotoxicity. **(A)** Schematic diagram depicting the treatment of MN9D DAergic neuronal cells with MCM from αSyn_{agg}-stimulated primary microglia. **(B)** SAL reduced αSyn_{agg} MCM-induced DAergic cell death. Mouse PMG was incubated with αSyn_{agg} for 24 h, and subsequently, MCM from αSyn_{agg}-treated microglia with or without SAL was applied to MN9D DAergic neuronal cells for 12 h. At the end of the incubation period, an MTS assay was performed to determine the cell viability of MN9D DAergic neuronal cells. Data shown are the mean ± SEM from at least four independent experiments. Data were analyzed using one-way ANOVA followed by Bonferroni's *post hoc* analysis. Asterisks (***$p < 0.001$) indicate significant differences between control and treatment groups.

levels including Il-1β, TNF-α, and IL-6 in the striatum as compared to PBS-infused mice at 60 dpi (**Figure 9E**). Next, we determined whether TH neuronal loss occurs during the latter part of the disease (180 dpi) *in vivo* as demonstrated previously (Duffy et al., 2018). As expected, delayed TH^+ neuron loss in the SN of αSyn_{PFF}-infused mice was evidenced at 180 dpi as compared to PBS infused mice as determined by unbiased stereological analysis (**Figure 9F**). These results are consistent with our hypothesis that irremediable microglial ERS increases the susceptibility of nigral DAergic neurons to neurodegeneration in the context of α-synucleinopathy concomitant with the induction of TXNIP/NLRP3 mediated proinflammatory signaling events.

DISCUSSION

Microglia-mediated neuroinflammation has been linked to PD pathogenesis (Hirsch et al., 2012). Moreover, the identification of elevated inflammatory markers in postmortem PD brains (Ferrari et al., 2006; McCoy et al., 2006) and the discovery of PD risk genes that serve as risk factors of both sporadic and familial PD (Zimprich et al., 2004; Satake et al., 2009; Simón-Sánchez et al., 2009) further supports the link between neuroimmune dysfunction and PD pathogenesis. Intriguingly, Tokuda et al., have demonstrated elevated αSyn oligomer levels and an increased oligomer/total αSyn ratio in the CSF of PD patients, suggesting a pivotal role of this protein in the etiology of PD (Tokuda et al., 2010). Lewy bodies encompassing aggregated aSyn have been hypothesized to play a critical role in the pathogenesis of synucleinopathies (Larks, 1958).

Emerging evidence indicates that fibrillar αSyn can act as seeds to promote misfolding and aggregation of endogenous αSyn, in both cellular (Volpicelli-Daley et al., 2014) and animal models of PD (Luk and Lee, 2014) in the absence of αSyn overexpression. Intriguingly, a recent report suggested that the process of Lewy body formation involving interactions between membranous organelles and αSyn aggregates that contain αSyn competent seeding species, most likely in an rearranged fibrillar conformation is a major driver of neurodegeneration (Mahul-Mellier et al., 2020). This study suggested that the processes associated with LB formation and subsequent maturation are critical drivers of αSyn mediated neurotoxicity than αSyn fibril formation. Moreover, recent studies have shown that exogenously added aggregated αSyn can trigger misfolding and aggregation of endogenous αSyn, in cell culture (Panicker et al., 2019) while αSyn_{PFF} intrastriatal inoculation in rodents causes inclusion formation and associated nigral DAergic pathology within weeks post-injection (Paumier et al., 2015). Moreover, previous studies have shown that extracellular αSyn aggregates can induce the microglial activation response which, in turn, promotes the propagation of aggregated αSyn within interconnected brain regions (Boza-Serrano et al., 2014; Duffy et al., 2018; Yun et al., 2018) suggesting that microglia are major drivers of neuroinflammation and associated PD-like pathology. Given the positive association between αSyn pathology and microglial NLRP3 inflammasome activation in experimental Parkinsonism (Gordon et al., 2018; Panicker et al., 2019), we investigated the contribution of mitochondrial oxidative stress and ERS in the αSyn_{agg}-induced NLRP3-dependent microglial activation response. In this study, we provide compelling evidence that αSyn_{agg} elicits the microglial activation response in part *via* the induction of the PKCδ-dependent ERS-mediated TXNIP/NLRP3 signaling axis. In agreement with these results, prior work from our lab and others suggest that aggregated αSyn induced neurotoxic microglial activation state may exert deleterious effects on DAergic neuronal survival (Duffy et al., 2018; Gordon et al., 2018; Yun et al., 2018). Importantly, blockade of mitoROS *via* MitoApo attenuates ERS and the associated TXNIP/NLRP3 signaling axis in microglial cells. Likewise, the eIF2α inhibitor SAL not only attenuated αSyn_{agg}-induced microglial TXNIP/NLRP3 signaling but also indirect, microglia-mediated DAergic neurotoxicity. More interestingly, PKCδ activation correlated positively with the enhanced microglial ERS and TXNIP/NLRP3 signaling axis and was found to precede TH neuronal loss in the nigra of mice that received an intrastriatal injection of αSyn_{PFF}, implicating the interdependency between microglial PKCδ activation and induction of the TXNIP/NLRP3 signaling axis in α-synucleinopathy.

Given the central role of chronic neuroinflammation in promoting αSyn deposition in several synucleinopathy animal

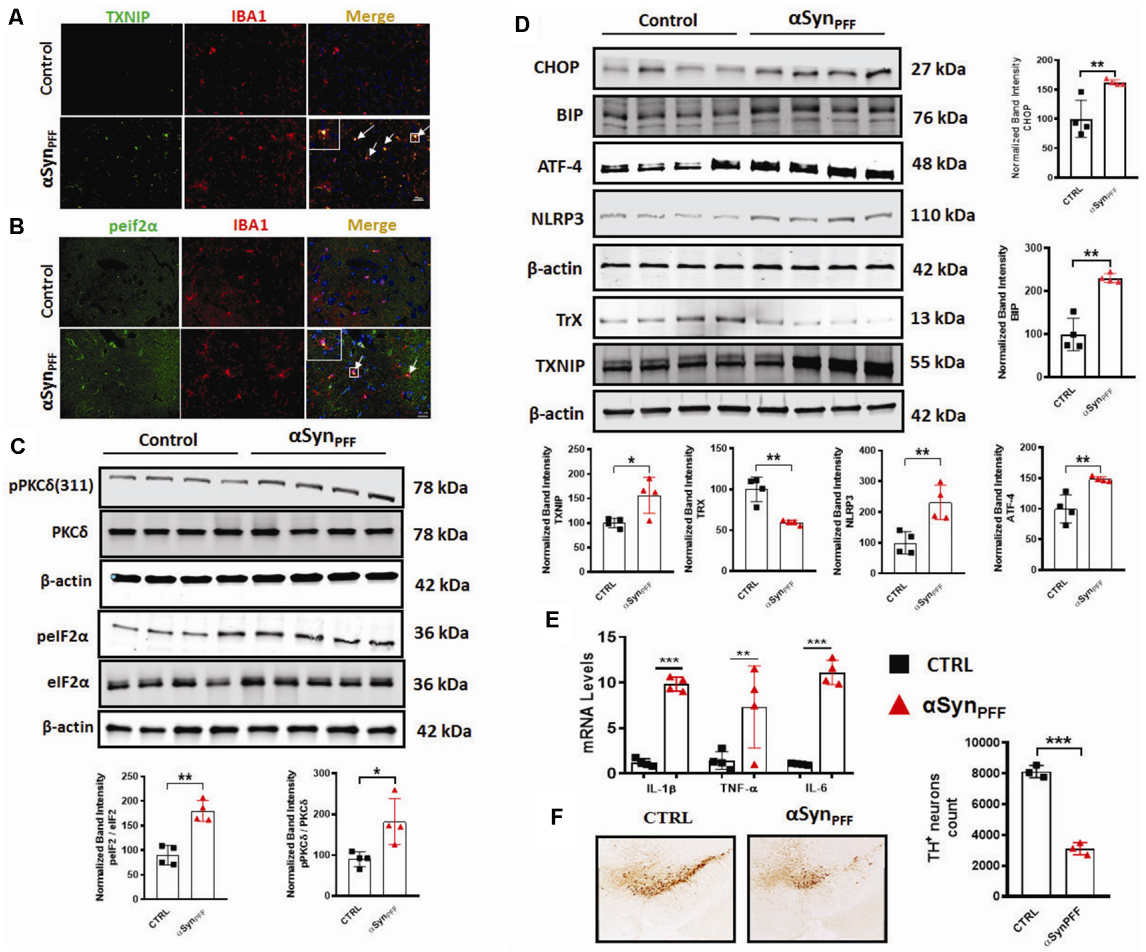


FIGURE 9 | Chronic early activation of PKCδ, endoplasmic reticulum stress (ERS), and the TXNIP/NLRP3 signaling axis precedes the delayed tyrosine hydroxylase (TH) neuronal loss in the αSyn_{PFF} mouse model of PD. C57BL/6 mice were intrastriatally infused with either 2 μl of αSyn_{PFF} or saline (PBS) *via* stereotaxic injection. **(A,B)** Increased colocalization of ERS or inflammation-related marker in the nigral microglia of αSyn_{PFF} infused mice. Representative immunohistochemical images showing colocalization of either TXNIP or p-eIF2α within IBA-1 positive microglia in the nigra of αSyn_{PFF} infused mice as compared to the PBS-injected mice. Nigral brain sections were double immunolabeled for p-eIF2α/IBA-1 or TXNIP/IBA-1, Nuclei were counterstained for hoechest. **(C)** Western blots showing increased expression of PKCδ and p-eIF2α in the nigra of αSyn_{PFF} inoculated mice. **(D)** Representative immunoblots showing that increased expression of CHOP, BIP, ATF-4, NLRP3, TXNIP, and downregulation of TrX in the SNpc of αSyn_{PFF} inoculated mice. Quantification of the relative expression of the aforementioned proteins at 60 dpi. **(E)** qRT-PCR analysis showing increased expression of IL-6, TNF-α, and IL-1β in the striata of αSyn_{PFF}-infused mice as compared to PBS-infused mice. **(F)** Representative photomicrographs of diaminobenzidine (DAB) immunostaining of TH in coronal midbrain sections of SN from perfused mouse brains at 180 dpi showing a dramatic reduction of TH-positive neurons in αSyn_{PFF}-treated mice vs. PBS-treated mice. Data are the mean ± SEM; $n = 4$ independent mice. Data shown are the mean ± SEM from at least three independent experiments. Asterisks (***$p < 0.001$, **$p < 0.01$ and *$p \leq 0.05$) indicate significant differences between control and treatment groups. NS: not significant.

models (Choi et al., 2009; Frank-Cannon et al., 2009; Gao et al., 2011), deciphering the molecular basis of the αSyn_{agg}-induced microglial activation response is critical. For this purpose, we analyzed the factors regulating NLRP3 inflammasome activation subsequent to the αSyn-induced microglial activation response. Exogenous αSyn_{agg} may interact with microglia *via* two different mechanisms. On the one hand, it may interact with CD36, class B scavenger receptor leading to the internalization of αSyn_{agg} by microglia leading to the microglial activation response *via* the Fyn-mediated NLRP3 inflammasome activation mechanism (Panicker et al., 2019). On the other hand, caspase-1-mediated truncation and aggregation of αSyn has been shown to promote uptake into microglial cells *via* TLR2 and TLR4 subsequently activating the NLRP3 inflammasome (Stefanova et al., 2011; Kim et al., 2013; Gustot et al., 2015; Chatterjee et al., 2020; Fan et al., 2020). Consistent with the former report, we observed that αSyn_{agg} was internalized within primary microglia suggesting that it may serve as a DAMP (Disease Associated Molecular Pattern) signal, thereby leading to NLRP3 inflammasome dependent, caspase-1-mediated IL-1β production (Codolo et al., 2013). Alternatively, recent studies from our group and others have demonstrated that many different types of cellular stress, including oxidative stressors/mitochondrial toxicants (Kim et al., 2014; Abais et al., 2015; Chen et al., 2015)

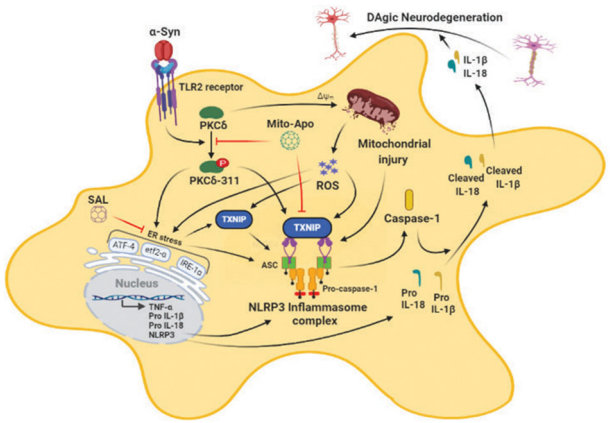


FIGURE 10 | Schematic representation of the role of mitoROS-PKCδ-mediated endoplasmic reticulum stress (ERS)-dependent induction of the TXNIP/NLRP3 signaling axis in response to the αSyn_{agg}-induced reactive microglial activation state. The treatment of microglial cells with αSyn_{agg} triggers mitoROS and PKCδ activation resulting in ERS-dependent activation of proinflamamtory signaling events including the TXNIP/NLRP3 activation response. Both mitochondria-driven oxidative stress and PKCδ activation contribute to the αSyn_{agg}-induced reactive microglial activation state *via* ERS through a feed-forward mechanism. An association between TXNIP and NLRP3 may partly explain the NLRP3 inflammasome-associated innate immune response. Moreover, αSyn_{agg}-induced microglial ERS causes indirect DAergic neurotoxicity. Importantly, Mitoapo and PKCδ-silencing suppress ERS and the associated TXNIP/NLRP3 signaling axis in response to αSyn_{agg}, thereby attenuating the reactive microglial activation state. Finally, salubrinal (SAL) attenuated the indirect DAergic neurotoxicity elicited by αSyn_{agg}, further highlighting the pivotal role of ERS in the expression of a neurodegenerative microglial phenotype and associated DAergic neurotoxicity.

or ERS inducers (Menu et al., 2012; Wali et al., 2014; Lebeaupin et al., 2015; Wang et al., 2017), may also promote NLRP3 inflammasome activation. Consistent with these findings, a positive association between robust mitoROS generation and NLRP3 inflammasome activation markers was evidenced in αSyn_{agg}-stimulated primary microglia. Importantly, Thioredoxin-interacting protein (TXNIP) a binding partner of thioredoxin (Trx) that inhibits the reducing activity of Trx through their disulfide exchange (Yoshihara et al., 2014), has been linked to NLRP3 inflammasome activation *via* increased oxidative stress (Chen et al., 2009; Oslowski et al., 2012). In line with these findings, we found that protein expression of TXNIP was upregulated while Trx expression was downregulated in αSyn_{agg}-stimulated primary microglia. Under divergent exogenous stress, TXNIP has been shown to bind to Trx thus disturbing the redox homeostasis, leading to ROS generation and resultant NLRP3 inflammasome activation, *via* a caspase-1-dependent IL-1β secretion mechanism which might be partially attributed to TXNIP interaction with Trx (Yoshihara et al., 2014; Zhao et al., 2017a). The significance of this interaction is further supported with data from αSyn_{agg} stimulated primary microglia demonstrating an interaction between TXNIP and the NLRP3 inflammasome that positively correlated with proinflammatory cytokine generation including IL-1β (Chen et al., 2009; Oslowski et al., 2012). Conversely, siRNA-mediated TXNIP knockdown attenuated NLRP3 inflammasome upregulation and proinflammatory cytokine generation including TNF-α, IL-1β. Additionally, we also demonstrated that inhibition of ERS *via* salubrinal also attenuated TXNIP through the upregulation of anti-oxidant protein Trx in αSyn_{agg}-stimulated microglial cells. Indeed, a previous study demonstrated that SAL treatment attenuated oxidative stress and neuroinflammation in a traumatic brain injury (TBI) rodent model further highlighting the pivotal role of ERS in neuroinflammation-related neurological disorders (Logsdon et al., 2016). Thus, the ability of TXNIP to interact with the NLRP3 inflammasome and its subsequent activation may serve as a critical regulator of microglial activation in response to αSyn_{agg}. While further studies are required, to demonstrate a direct contribution of NLRP3/TXNIP interaction to PD-like pathology, these studies raise the possibility that TXNIP and the NLRP3 inflammasome may be subject to regulation by both mitoROS and ERS and that the TXNIP/NLRP3 signaling axis may represent a feed-forward loop contributing to the enhancement of the αSyn_{agg}-induced neurotoxic microglial activation state. Despite this, the contribution of microglial activation to the secretion of neurotrophic factors, such as brain-derived neurotrophic factor (Trang et al., 2011), cannot be entirely ruled out.

ERS contributes to the initiation and progression of numerous immune disorders including type 2 diabetes, obesity, atherosclerosis, and neurodegenerative diseases (Oakes and Papa, 2015; Cao et al., 2016; Grootjans et al., 2016; Tao et al., 2018). The link between neuronal ERS and α-synucleinopathy has been intensely investigated in genetic models of PD following overexpression of αSyn (Colla, 2019). For example, toxicity associated with WT, A53T mutant, or C-terminal truncated αSyn was found to positively correlate with ERS and UPR activation (Cooper et al., 2006; Bellucci et al., 2011; Heman-Ackah et al., 2017; Karim et al., 2020). Moreover, treatment with ERS inhibitor salubrinal, afforded protection against A53T αSyn-induced cell death indicating that ERS is a central contributor to DAergic cell death (Smith et al., 2005). Despite this, the mechanisms by which aberrant ERS contribute to the αSyn_{agg}-induced microglial activation response remains poorly understood. Herein, we show that ERS markers, including p-eIF2α, ATF-4, p-IRE1α, BIP, are elevated in αSyn_{agg}-stimulated primary microglia concomitant with the TXNIP/NLRP3 signaling markers and that SAL not only attenuated ERS but also the TXNIP/NLRP3 signaling axis and proinflammatory cytokine generation in line with previous reports (Oslowski et al., 2012; Logsdon et al., 2016; Lebeaupin et al., 2018). Importantly, SAL inhibited microglia-mediated indirect DAergic neurotoxicity, suggesting that ERS can promote a deleterious microglial neurodegenerative phenotype eventually contributing to the nigral DAergic neurodegenerative process *in vivo*, suggesting that microglial NLRP3 and TXNIP may represent critical pathological correlates in PD pathogenesis and other synucleinopathies.

Both mitochondria-mediated oxidative stress and neuroinflammation have been identified as key pathological correlates in the pathophysiology of PD (Beal, 2003;

Rocha et al., 2018). Although mitochondrial dysfunction and ERS have been established as significant contributors to DAergic neuropathology (Chen C. et al., 2019), the impact of mitochondrial oxidative stress on ERS and associated microglia-mediated neuroinflammation remains poorly characterized. The generation of ROS *via* mitochondria has been linked to oxidative damage-induced pathologies including PD (Gao et al., 2008; Murphy, 2009; Dias et al., 2013). Our current study also revealed pronounced mitochondrial dysfunction characterized by robust mitoROS generation and an accompanying loss of MMP in αSyn-stimulated microglial cells. Moreover, we demonstrated that mitochondrial dysfunction preceded ERS in αSyn_{agg}-stimulated primary microglia, suggesting that mitochondrial oxidative stress acts as an upstream regulator of ERS and the TXNIP/NLRP3 inflammasome signaling axis. Indeed, treatment with the mitochondria-targeted antioxidant MitoApo attenuated ERS markers, including ATF-4 and p-IRE-1α, with an accompanying decreased expression of NLRP3 markers and TXNIP expression, as well as decreased proinflammatory cytokine generation in αSyn_{agg}-stimulated microglial cells. Our results suggest that the microglial inflammatory modulation triggered by mitochondrial oxidative stress is likely to promote the induction of ERS-dependent proinflammatory cell signaling events in synucleinopathies.

PKCδ-mediated cell signaling events occur in a cell type-specific and stimulus-specific manner. For example, recent findings from our lab and others have demonstrated that post-translational modification of PKCδ *via* a phosphorylation-dependent mechanism is associated with the Parkinsonian toxin-induced microglial activation response (Gordon et al., 2012; Panicker et al., 2015, 2019). Moreover, studies from our lab demonstrated that PKCδ is elevated in the microglia of postmortem PD brains and in animal models of PD (Gordon et al., 2016). Likewise, a similar increase in PKCδ was evidenced in human postmortem AD brains (Gordon et al., 2016b; Du et al., 2018). Despite this, the exact mechanism by which PKCδ contributes to the microglial activation response in the context of α-synucleinopathy remains undefined. Therefore, we hypothesized that PKCδ may have other effects, including the regulation of ERS-associated inflammatory signaling events in the microglia. Our results demonstrate that PKCδ is activated *via* a phosphorylation-dependent mechanism in αSyn_{agg}-treated microglial cells (as assessed *via* a time-dependent increase in phosphorylation of PKCδ at Tyr412 residue), which closely paralleled upregulation of ERS markers including ATF4, p-eIF2α, p-IRE1α and pro-inflammatory cytokine generation including IL-6, and TNF-α with concurrent upregulation of the NLRP3 inflammasome activation markers (cleaved caspase-1 and IL-1β) and TXNIP expression. Conversely, we found that siRNA-mediated knockdown of PKCδ attenuated the αSyn_{agg}-induced ERS response-mediated NLRP3/TXNIP signaling cascade, highlighting the regulatory effects of PKCδ on ERS and the associated proinflammatory response in microglial cells. Furthermore, using a mouse model of α-synucleinopathy known to recapitulate key pathological correlates of synucleinopathies, including the microglial activation response and DAergic neuropathology, we show that αSyn_{PFF} injection into the dorsal striatum resulted in pronounced PKCδ activation and ERS that was accompanied by upregulation of the NLRP3/TXNIP signaling axis in the nigra at 60 dpi, which represents an anatomically connected brain region. Therefore, aggregated αSyn may activate microglial PKCδ-dependent ERS-mediated activation of the TXNIP/NLRP3 signaling axis during the early stages of the pathology in the substantia nigra of αSyn_{PFF}-inoculated mice as compared to controls. Indeed, another study demonstrated the occurrence of pronounced microglial activation in the nigra several months prior to expression of nigral DAergic neurotoxicity (Duffy et al., 2018; Patterson et al., 2019). Moreover, perturbation of protein degradation machinery could lead to an increased protein load in the ER, thus making the cell more vulnerable to ERS. Indeed, αSyn aggregation was found to result in protein accumulation in the ER followed by induction of UPR and the resulting cell death in an *in vitro* cell culture model of PD (Cooper et al., 2006). In line with this finding, early induction of the nigral microglial ERS/TXNIP signaling cascade was found to precede significant TH neuronal loss at 180 dpi. Moreover, injection of αSyn_{PFF} into the striatum was also found to result in increased mRNA expression levels of TNF-α, IL-1b, IL-6 in this brain region. Importantly, we previously reported that proinflammatory cytokine such as TNF-α acting *via* TNFR1 induced PKCδ-mediated apoptotic death of DAergic neurons (Gordon et al., 2012). Thus, our observations raise the possibility that initial activation of the unfolded protein response (UPR) in α-synucleinopathy might have a neuroprotective role to compensate for the accumulation of misfolded proteins; however, persistent ERS may overwhelm the cellular antioxidant machinery *via* PKCδ and TXNIP upregulation eventually leading to the loss of nigral DAergic neurons. Thus, ERS and TXNIP are likely to play a causative role in nigral DAergic neuronal death in response to αSyn_{PFF}. Accordingly, increased TXNIP expression has been demonstrated in the hippocampus and cortex of the APP/PS1 transgenic mouse model of AD as an early disease phenotype (Wang Y. et al., 2019). Alternatively, ERS and TXNIP can also occur in other immune cell types such as astrocytes as well as other cells in the CNS further exaggerating nigral DAergic neurodegeneration, which requires further exploration. Given that males are at a higher risk of developing PD than women (Cerri et al., 2019) we utilized male mice in these studies. In light of the evidence demonstrating sex differences in inflammasome activation, we cannot rule out that different pathogenic mechanisms might be involved in the difference between men and women in expressing PD-related clinical correlates (Zhang et al., 2020).

Overall, our current findings coupled with other recent observations (Panicker et al., 2015; Gordon et al., 2016b), suggest that PKCδ and mitochondrial oxidative stress act as key regulators of ERs and TXNIP/NLRP3 inflammasome activation and support the hypothesis that PKCδ activation may drive the proinflammatory activation of microglia in response to αSyn_{agg} along with ERS and mitochondrial oxidative stress. The pathological significance of the aforementioned signaling pathways is further illustrated by the fact that *in vitro* PKCδ siRNA mediated knockdown, as well as pharmacological inhibition of mitochondrial oxidative stress and

ERS, ameliorates the microglial activation response subsequent to stimulation of microglial cells with αSyn_{agg}. Finally, our study highlights that intrastriatal αSyn_{PFF} injection, triggers microglial ERS and upregulation of the TXNIP/NLRP3 signaling axis are evidenced in the SN prior to late-stage nigral DAergic neurodegeneration providing further support for the significance of early induction of microglial ERS and TXNIP/NLRP3 signaling as an upstream instigating factor promoting PD-like pathology. Therefore, our studies unravel a previously unknown mechanism linking PKCδ, ERS, and the TXNIP/NLRP3 signaling axis to the microglial activation response in the context of α-synucleinopathy (**Figure 10**). Thus, therapeutic targeting of TXNIP and NLRP3 may represent a novel disease-modifying therapy for the treatment of PD.

DATA AVAILABILITY STATEMENT

The original contributions presented in the study are included in the article/**Supplementary Material**, further inquiries can be directed to the corresponding author.

ETHICS STATEMENT

The animal study was reviewed and approved by Institutional Animal Care and Use Committee (IACUC) at Iowa State University, Ames, IA, USA.

AUTHOR CONTRIBUTIONS

MS, AGK, and AK created the research design and conceptualized the study. MS, BP, GZ, HJ, and VA developed the methodologies detailed in the manuscript. MS, BP, AB-C, MH, NK, SM, VA, AGK, and AK conducted the experiments and analyzed the experimental results. MS, AGK, and AK wrote the original draft of the manuscript. MS, GZ, HJ, VA, AGK, and AK participated in manuscript discussions, and in the review and editing of the manuscript. AK and AGK secured funding and provided resources to successfully complete the proposed experiments. All authors have read and agreed to the published version of the manuscript. All authors contributed to the article and approved the submitted version.

FUNDING

This work was funded by the National Institutes of Health (NIH) grant NS088206 to AK and ES019267, NS100090, ES026892 to AGK. Other sources include the Lloyd Endowed Chair and Eminent Scholar and Armbrust Endowment to AGK and the Salsbury Endowed Chair to AK.

SUPPLEMENTARY MATERIAL

The Supplementary Material for this article can be found online at: https://www.frontiersin.org/articles/10.3389/fnagi.2021.661505/full#supplementary-material.

REFERENCES

Abais, J. M., Xia, M., Zhang, Y., Boini, K. M., and Li, P. L. (2015). Redox regulation of NLRP3 inflammasomes: ROS as trigger or effector? *Antioxid. Redox Signal.* 22, 1111–1129. doi: 10.1089/ars.2014.5994

Bachiller, S., Jiménez-Ferrer, I., Paulus, A., Yang, Y., Swanberg, M., Deierborg, T., et al. (2018). Microglia in neurological diseases: a road map to brain-disease dependent-inflammatory response. *Front. Cell. Neurosci.* 12:488. doi: 10.3389/fncel.2018.00488

Beal, M. F. (2003). Mitochondria, oxidative damage, and inflammation in Parkinson's disease. *Ann. N Y Acad. Sci.* 991, 120–131. doi: 10.1111/j.1749-6632.2003.tb07470.x

Bellucci, A., Navarria, L., Zaltieri, M., Falarti, E., Bodei, S., Sigala, S., et al. (2011). Induction of the unfolded protein response by α-synuclein in experimental models of Parkinson's disease. *J. Neurochem.* 116, 588–605. doi: 10.1111/j.1471-4159.2010.07143.x

Block, M. L., Zecca, L., and Hong, J.-S. (2007). Microglia-mediated neurotoxicity: uncovering the molecular mechanisms. *Nat. Rev. Neurosci.* 8, 57–69. doi: 10.1038/nrn2038

Boyce, M., Bryant, K. F., Jousse, C., Long, K., Harding, H. P., Scheuner, D., et al. (2005). A selective inhibitor of eIF2α dephosphorylation protects cells from ER stress. *Science* 307, 935–939. doi: 10.1126/science.1101902

Boza-Serrano, A., Reyes, J. F., Rey, N. L., Leffler, H., Bousset, L., Nilsson, U., et al. (2014). The role of Galectin-3 in α-synuclein-induced microglial activation. *Acta Neuropathol. Commun.* 2:156. doi: 10.1186/s40478-014-0156-0

Braak, H., Alafuzoff, I., Arzberger, T., Kretzschmar, H., and Del Tredici, K. (2006). Staging of Alzheimer disease-associated neurofibrillary pathology using paraffin sections and immunocytochemistry. *Acta Neuropathol.* 112, 389–404. doi: 10.1007/s00401-006-0127-z

Calabrese, V., Santoro, A., Monti, D., Crupi, R., Di Paola, R., Latteri, S., et al. (2018). Aging and Parkinson's disease: inflammaging, neuroinflammation and biological remodeling as key factors in pathogenesis. *Free Radic. Biol. Med.* 115, 80–91. doi: 10.1016/j.freeradbiomed.2017.10.379

Cao, S. S., Luo, K. L., and Shi, L. (2016). Endoplasmic reticulum stress interacts with inflammation in human diseases. *J. Cell. Physiol.* 231, 288–294. doi: 10.1002/jcp.25098

Cerri, S., Mus, L., and Blandini, F. (2019). Parkinson's disease in women and men: what's the difference? *J. Parkinsons Dis.* 9, 501–515. doi: 10.3233/JPD-191683

Charli, A., Jin, H., Anantharam, V., Kanthasamy, A., and Kanthasamy, A. G. (2016). Alterations in mitochondrial dynamics induced by tebufenpyrad and pyridaben in a dopaminergic neuronal cell culture model. *Neurotoxicology* 53, 302–313. doi: 10.1016/j.neuro.2015.06.007

Chatterjee, K., Roy, A., Banerjee, R., Choudhury, S., Mondal, B., Halder, S., et al. (2020). Inflammasome and α-synuclein in Parkinson's disease: a cross-sectional study. *J. Neuroimmunol.* 338:577089. doi: 10.1016/j.jneuroim.2019.577089

Chen, X., Guo, X., Ge, Q., Zhao, Y., Mu, H., and Zhang, J. (2019). ER stress activates the NLRP3 inflammasome: a novel mechanism of atherosclerosis. *Oxid. Med. Cell. Longev.* 2019:3462530. doi: 10.1155/2019/3462530

Chen, X., Hu, Y., Cao, Z., Liu, Q., and Cheng, Y. (2018). Cerebrospinal fluid inflammatory cytokine aberrations in Alzheimer's disease, Parkinson's disease and amyotrophic lateral sclerosis: a systematic review and meta-analysis. *Front. Immunol.* 9:2122. doi: 10.3389/fimmu.2018.02122

Chen, L., Na, R., Boldt, E., and Ran, Q. (2015). NLRP3 inflammasome activation by mitochondrial reactive oxygen species plays a key role in long-term cognitive impairment induced by paraquat exposure. *Neurobiol. Aging* 36, 2533–2543. doi: 10.1016/j.neurobiolaging.2015.05.018

Chen, G., Shaw, M. H., Kim, Y. G., and Nunez, G. (2009). NOD-like receptors: role in innate immunity and inflammatory disease. *Annu. Rev. Pathol.* 4, 365–398. doi: 10.1146/annurev.pathol.4.110807.092239

Chen, C., Turnbull, D. M., and Reeve, A. K. (2019). Mitochondrial dysfunction in Parkinson's disease-cause or consequence? *Biology* 8:38. doi: 10.3390/biology8020038

Choi, D.-Y., Liu, M., Hunter, R. L., Cass, W. A., Pandya, J. D., Sullivan, P. G., et al. (2009). Striatal neuroinflammation promotes Parkinsonism in rats. *PLoS One* 4:e5482. doi: 10.1371/journal.pone.0005482

Codolo, G., Plotegher, N., Pozzobon, T., Brucale, M., Tessari, I., Bubacco, L., et al. (2013). Triggering of inflammasome by aggregated α-synuclein, an inflammatory response in synucleinopathies. *PLoS One* 8:e55375. doi: 10.1371/journal.pone.0055375

Colla, E. (2019). Linking the endoplasmic reticulum to Parkinson's disease and α-synucleinopathy. *Front. Neurosci.* 13:560. doi: 10.3389/fnins.2019.00560

Colla, E., Coune, P., Liu, Y., Pletnikova, O., Troncoso, J. C., Iwatsubo, T., et al. (2012). Endoplasmic reticulum stress is important for the manifestations of α-synucleinopathy *in vivo*. *J. Neurosci.* 32, 3306–3320. doi: 10.1523/JNEUROSCI.5367-11.2012

Cooper, A. A., Gitler, A. D., Cashikar, A., Haynes, C. M., Hill, K. J., Bhullar, B., et al. (2006). α-synuclein blocks ER-Golgi traffic and Rab1 rescues neuron loss in Parkinson's models. *Science* 313, 324–328. doi: 10.1126/science.1129462

Davie, C. A. (2008). A review of Parkinson's disease. *Br. Med. Bull.* 86, 109–127. doi: 10.1093/bmb/ldn013

Demaagd, G., and Philip, A. (2015). Parkinson's disease and its management: part 1: disease entity, risk factors, pathophysiology, clinical presentation, and diagnosis. *P T* 40, 504–532.

Dias, V., Junn, E., and Mouradian, M. M. (2013). The role of oxidative stress in Parkinson's disease. *J. Parkinsons Dis.* 3, 461–491. doi: 10.3233/JPD-130230

Dickson, D. W. (2012). Parkinson's disease and parkinsonism: neuropathology. *Cold Spring Harb. Perspect. Med.* 2:a009258. doi: 10.1101/cshperspect.a009258

Domert, J., Sackmann, C., Severinsson, E., Agholme, L., Bergstrom, J., Ingelsson, M., et al. (2016). Aggregated α-synuclein transfer efficiently between cultured human neuron-like cells and localize to lysosomes. *PLoS One* 11:e0168700. doi: 10.1371/journal.pone.0168700

Du, Y., Zhao, Y., Li, C., Zheng, Q., Tian, J., Li, Z., et al. (2018). Inhibition of PKCδ reduces amyloid-β levels and reverses Alzheimer disease phenotypes. *J. Exp. Med.* 215, 1665–1677. doi: 10.1084/jem.20171193

Duffy, M. F., Collier, T. J., Patterson, J. R., Kemp, C. J., Luk, K. C., Tansey, M. G., et al. (2018). Lewy body-like α-synuclein inclusions trigger reactive microgliosis prior to nigral degeneration. *J. Neuroinflammation* 15:129. doi: 10.1186/s12974-018-1171-z

Earls, R. H., Menees, K. B., Chung, J., Barber, J., Gutekunst, C. A., Hazim, M. G., et al. (2019). Intrastriatal injection of preformed α-synuclein fibrils alters central and peripheral immune cell profiles in non-transgenic mice. *J. Neuroinflammation* 16:250. doi: 10.1186/s12974-019-1636-8

Fan, Z., Pan, Y.-T., Zhang, Z.-Y., Yang, H., Yu, S.-Y., Zheng, Y., et al. (2020). Systemic activation of NLRP3 inflammasome and plasma α-synuclein levels are correlated with motor severity and progression in Parkinson's disease. *J Neuroinflammation* 17:11. doi: 10.1186/s12974-019-1670-6

Fellner, L., Jellinger, K. A., Wenning, G. K., and Stefanova, N. (2011). Glial dysfunction in the pathogenesis of α-synucleinopathies: emerging concepts. *Acta Neuropathol.* 121, 675–693. doi: 10.1007/s00401-011-0833-z

Feng, L., and Zhang, L. (2019). Resveratrol suppresses Aβ-induced microglial activation through the TXNIP/TRX/NLRP3 signaling pathway. *DNA Cell Biol.* 38, 874–879. doi: 10.1089/dna.2018.4308

Ferrari, C. C., Pott Godoy, M. C., Tarelli, R., Chertoff, M., Depino, A. M., and Pitossi, F. J. (2006). Progressive neurodegeneration and motor disabilities induced by chronic expression of IL-1β in the substantia nigra. *Neurobiol. Dis.* 24, 183–193. doi: 10.1016/j.nbd.2006.06.013

Filhoulaud, G., Benhamed, F., Pagesy, P., Bonner, C., Fardini, Y., Ilias, A., et al. (2019). O-GlcNacylation links TxNIP to inflammasome activation in pancreatic β cells. *Front. Endocrinol.* 10:291. doi: 10.3389/fendo.2019.00291

Frank-Cannon, T. C., Alto, L. T., Mcalpine, F. E., and Tansey, M. G. (2009). Does neuroinflammation fan the flame in neurodegenerative diseases? *Mol. Neurodegener.* 4:47. doi: 10.1186/1750-1326-4-47

Frigerio, R., Elbaz, A., Sanft, K. R., Peterson, B. J., Bower, J. H., Ahlskog, J. E., et al. (2005). Education and occupations preceding Parkinson disease: a population-based case-control study. *Neurology* 65, 1575–1583. doi: 10.1212/01.wnl.0000184520.21744.a2

Gao, H.-M., Jiang, J., Wilson, B., Zhang, W., Hong, J. S., and Liu, B. (2002). Microglial activation-mediated delayed and progressive degeneration of rat nigral dopaminergic neurons: relevance to Parkinson's disease. *J. Neurochem.* 81, 1285–1297. doi: 10.1046/j.1471-4159.2002.00928.x

Gao, H.-M., Kotzbauer, P. T., Uryu, K., Leight, S., Trojanowski, J. Q., and Lee, V. M.-Y. (2008). Neuroinflammation and oxidation/nitration of α-synuclein linked to dopaminergic neurodegeneration. *J. Neurosci.* 28, 7687–7698. doi: 10.1523/JNEUROSCI.0143-07.2008

Gao, H.-M., Zhang, F., Zhou, H., Kam, W., Wilson, B., and Hong, J.-S. (2011). Neuroinflammation and α-synuclein dysfunction potentiate each other, driving chronic progression of neurodegeneration in a mouse model of Parkinson's disease. *Environ. Health Perspect.* 119, 807–814. doi: 10.1289/ehp.1003013

Ghosh, A., Chandran, K., Kalivendi, S. V., Joseph, J., Antholine, W. E., Hillard, C. J., et al. (2010). Neuroprotection by a mitochondria-targeted drug in a Parkinson's disease model. *Free Radic. Biol. Med.* 49, 1674–1684. doi: 10.1016/j.freeradbiomed.2010.08.028

Ghosh, A., Saminathan, H., Kanthasamy, A., Anantharam, V., Jin, H., Sondarva, G., et al. (2013). The peptidyl-prolyl isomerase Pin1 up-regulation and proapoptotic function in dopaminergic neurons: relevance to the pathogenesis of Parkinson disease. *J. Biol. Chem.* 288, 21955–21971. doi: 10.1074/jbc.M112.444224

Gitler, A. D., Bevis, B. J., Shorter, J., Strathearn, K. E., Hamamichi, S., Su, L. J., et al. (2008). The Parkinson's disease protein α-synuclein disrupts cellular Rab homeostasis. *Proc. Natl. Acad. Sci. U S A* 105, 145–150. doi: 10.1073/pnas.0710685105

Gomes, I., Sierra, S., and Devi, L. A. (2016). Detection of receptor heteromerization using in situ proximity ligation assay. *Curr. Protoc. Pharmacol.* 75, 2.16.11–12.16.31. doi: 10.1002/cpph.15

Gordon, R., Albornoz, E. A., Christie, D. C., Langley, M. R., Kumar, V., Mantovani, S., et al. (2018). Inflammasome inhibition prevents α-synuclein pathology and dopaminergic neurodegeneration in mice. *Sci. Transl. Med.* 10:eaah4066. doi: 10.1126/scitranslmed.aah4066

Gordon, R., Anantharam, V., Kanthasamy, A. G., and Kanthasamy, A. (2012). Proteolytic activation of proapoptotic kinase protein kinase Cδ by tumor necrosis factor α death receptor signaling in dopaminergic neurons during neuroinflammation. *J. Neuroinflammation* 9:82. doi: 10.1186/1742-2094-9-82

Gordon, R., Neal, M. L., Luo, J., Langley, M. R., Harischandra, D. S., Panicker, N., et al. (2016a). Prokineticin-2 upregulation during neuronal injury mediates a compensatory protective response against dopaminergic neuronal degeneration. *Nat. Commun.* 7:12932. doi: 10.1038/ncomms12932

Gordon, R., Singh, N., Lawana, V., Ghosh, A., Harischandra, D. S., Jin, H., et al. (2016b). Protein kinase Cδ upregulation in microglia drives neuroinflammatory responses and dopaminergic neurodegeneration in experimental models of Parkinson's disease. *Neurobiol. Dis.* 93, 96–114. doi: 10.1016/j.nbd.2016.04.008

Grootjans, J., Kaser, A., Kaufman, R. J., and Blumberg, R. S. (2016). The unfolded protein response in immunity and inflammation. *Nat. Rev. Immunol.* 16, 469–484. doi: 10.1038/nri.2016.62

Gustot, A., Gallea, J. I., Sarroukh, R., Celej, M. S., Ruysschaert, J. M., and Raussens, V. (2015). Amyloid fibrils are the molecular trigger of inflammation in Parkinson's disease. *Biochem. J.* 471, 323–333. doi: 10.1042/BJ20150617

Han, Y., Xu, X., Tang, C., Gao, P., Chen, X., Xiong, X., et al. (2018). Reactive oxygen species promote tubular injury in diabetic nephropathy: the role of the mitochondrial ros-txnip-nlrp3 biological axis. *Redox Biol.* 16, 32–46. doi: 10.1016/j.redox.2018.02.013

Heman-Ackah, S. M., Manzano, R., Hoozemans, J. J. M., Scheper, W., Flynn, R., Haerty, W., et al. (2017). α-synuclein induces the unfolded protein response in Parkinson's disease SNCA triplication iPSC-derived neurons. *Hum. Mol. Genet.* 26, 4441–4450. doi: 10.1093/hmg/ddx331

Heneka, M. T., Carson, M. J., El Khoury, J., Landreth, G. E., Brosseron, F., Feinstein, D. L., et al. (2015). Neuroinflammation in Alzheimer's disease. *Lancet Neurol.* 14, 388–405. doi: 10.1016/S1474-4422(15)70016-5

Hetz, C., Zhang, K., and Kaufman, R. J. (2020). Mechanisms, regulation and functions of the unfolded protein response. *Nat. Rev. Mol. Cell Biol.* 21, 421–438. doi: 10.1038/s41580-020-0250-z

Hirsch, E. C., Vyas, S., and Hunot, S. (2012). Neuroinflammation in Parkinson's disease. *Parkinsonism Relat. Disord.* 18, S210–212. doi: 10.1016/S1353-8020(11)70065-7

Hoffmann, A., Ettle, B., Bruno, A., Kulinich, A., Hoffmann, A. C., Von Wittgenstein, J., et al. (2016). α-synuclein activates BV2 microglia dependent

on its aggregation state. *Biochem. Biophys. Res. Commun.* 479, 881–886. doi: 10.1016/j.bbrc.2016.09.109

Hoffmann, A. C., Minakaki, G., Menges, S., Salvi, R., Savitskiy, S., Kazman, A., et al. (2019). Extracellular aggregated α synuclein primarily triggers lysosomal dysfunction in neural cells prevented by trehalose. *Sci. Rep.* 9:544. doi: 10.1038/s41598-018-35811-8

Huang, X., Chen, Y., Zhang, H., Ma, Q., Zhang, Y. W., and Xu, H. (2012). Salubrinal attenuates β-amyloid-induced neuronal death and microglial activation by inhibition of the NF-κB pathway. *Neurobiol. Aging* 33, 1007.e9–1017.e9. doi: 10.1016/j.neurobiolaging.2011.10.007

Ji, T., Han, Y., Yang, W., Xu, B., Sun, M., Jiang, S., et al. (2019). Endoplasmic reticulum stress and NLRP3 inflammasome: crosstalk in cardiovascular and metabolic disorders. *J. Cell. Physiol.* 234, 14773–14782. doi: 10.1002/jcp.28275

Jin, H., Kanthasamy, A., Anantharam, V., Rana, A., and Kanthasamy, A. G. (2011). Transcriptional regulation of pro-apoptotic protein kinase Cδ: implications for oxidative stress-induced neuronal cell death. *J. Biol. Chem.* 286, 19840–19859. doi: 10.1074/jbc.M110.203687

Jin, H., Kanthasamy, A., Harischandra, D. S., Kondru, N., Ghosh, A., Panicker, N., et al. (2014). Histone hyperacetylation up-regulates protein kinase Cδ in dopaminergic neurons to induce cell death: relevance to epigenetic mechanisms of neurodegeneration in Parkinson disease. *J. Biol. Chem.* 289, 34743–34767. doi: 10.1074/jbc.M114.576702

Karim, M. R., Liao, E. E., Kim, J., Meints, J., Martinez, H. M., Pletnikova, O., et al. (2020). α-Synucleinopathy associated c-Abl activation causes p53-dependent autophagy impairment. *Mol. Neurodegener.* 15:27. doi: 10.1186/s13024-020-00364-w

Kim, C., Ho, D. H., Suk, J. E., You, S., Michael, S., Kang, J., et al. (2013). Neuron-released oligomeric α-synuclein is an endogenous agonist of TLR2 for paracrine activation of microglia. *Nat. Commun.* 4:1562. doi: 10.1038/ncomms2534

Kim, S. R., Kim, D. I., Kim, S. H., Lee, H., Lee, K. S., Cho, S. H., et al. (2014). NLRP3 inflammasome activation by mitochondrial ROS in bronchial epithelial cells is required for allergic inflammation. *Cell Death Dis.* 5:e1498. doi: 10.1038/cddis.2014.460

Knott, C., Stern, G., and Wilkin, G. P. (2000). Inflammatory regulators in Parkinson's disease: iNOS, lipocortin-1 and cyclooxygenases-1 and -2. *Mol. Cell Neurosci.* 16, 724–739. doi: 10.1006/mcne.2000.0914

Konno, M., Hasegawa, T., Baba, T., Miura, E., Sugeno, N., Kikuchi, A., et al. (2012). Suppression of dynamin GTPase decreases α-synuclein uptake by neuronal and oligodendroglial cells: a potent therapeutic target for synucleinopathy. *Mol. Neurodegener.* 7:38. doi: 10.1186/1750-1326-7-38

Larks, S. D. (1958). The human electrohysterogram: wave forms and implications. *Proc. Natl. Acad. Sci. U S A* 44, 820–824. doi: 10.1073/pnas.44.8.820

Larroque-Cardoso, P., Swiader, A., Ingueneau, C., Negre-Salvayre, A., Elbaz, M., Reyland, M. E., et al. (2013). Role of protein kinase C δ in ER stress and apoptosis induced by oxidized LDL in human vascular smooth muscle cells. *Cell Death Dis.* 4:e520. doi: 10.1038/cddis.2013.47

Lawana, V., Singh, N., Sarkar, S., Charli, A., Jin, H., Anantharam, V., et al. (2017). Involvement of c-Abl kinase in microglial activation of NLRP3 inflammasome and impairment in autolysosomal system. *J. Neuroimmune Pharmacol.* 12, 624–660. doi: 10.1007/s11481-017-9746-5

Lebeaupin, C., Proics, E., De Bieville, C. H., Rousseau, D., Bonnafous, S., Patouraux, S., et al. (2015). ER stress induces NLRP3 inflammasome activation and hepatocyte death. *Cell Death Dis.* 6:e1879. doi: 10.1038/cddis.2015.248

Lebeaupin, C., Vallée, D., Hazari, Y., Hetz, C., Chevet, E., and Bailly-Maitre, B. (2018). Endoplasmic reticulum stress signalling and the pathogenesis of non-alcoholic fatty liver disease. *J. Hepatol.* 69, 927–947. doi: 10.1016/j.jhep.2018.06.008

Lee, S., Kim, S., Park, Y. J., Yun, S. P., Kwon, S. H., Kim, D., et al. (2018). The c-Abl inhibitor, Radotinib HCl, is neuroprotective in a preclinical Parkinson's disease mouse model. *Hum. Mol. Genet.* 27, 2344–2356. doi: 10.1093/hmg/ddy143

Leng, F., and Edison, P. (2021). Neuroinflammation and microglial activation in Alzheimer disease: where do we go from here? *Nat. Rev. Neurol.* 17, 157–172. doi: 10.1038/s41582-020-00435-y

Lerner, A. G., Upton, J.-P., Praveen, P. V. K., Ghosh, R., Nakagawa, Y., Igbaria, A., et al. (2012). IRE1α induces thioredoxin-interacting protein to activate the NLRP3 inflammasome and promote programmed cell death under irremediable ER stress. *Cell Metab.* 16, 250–264. doi: 10.1016/j.cmet.2012.07.007

Liu, X., Zhang, R., Huang, L., Zheng, Z., Vlassara, H., Striker, G., et al. (2019). Excessive oxidative stress contributes to increased acute ER stress kidney injury in aged mice. *Oxid. Med. Cell. Longev.* 2019:2746521. doi: 10.1155/2019/2746521

Logsdon, A. F., Lucke-Wold, B. P., Nguyen, L., Matsumoto, R. R., Turner, R. C., Rosen, C. L., et al. (2016). Salubrinal reduces oxidative stress, neuroinflammation and impulsive-like behavior in a rodent model of traumatic brain injury. *Brain Res.* 1643, 140–151. doi: 10.1016/j.brainres.2016.04.063

Luk, K. C., and Lee, V. M.-Y. (2014). Modeling Lewy pathology propagation in Parkinson's disease. *Parkinsonism Relat. Disord.* 20, S85–S87. doi: 10.1016/S1353-8020(13)70022-1

Luk, K. C., Kehm, V., Carroll, J., Zhang, B., O'Brien, P., Trojanowski, J. Q., et al. (2012). Pathological α-synuclein transmission initiates Parkinson-like neurodegeneration in nontransgenic mice. *Science* 338, 949–953. doi: 10.1126/science.1227157

Mahul-Mellier, A. L., Burtscher, J., Maharjan, N., Weerens, L., Croisier, M., Kuttler, F., et al. (2020). The process of Lewy body formation, rather than simply α-synuclein fibrillization, is one of the major drivers of neurodegeneration. *Proc. Natl. Acad. Sci. U S A* 117, 4971–4982. doi: 10.1073/pnas.1913904117

Majumder, P. K., Mishra, N. C., Sun, X., Bharti, A., Kharbanda, S., Saxena, S., et al. (2001). Targeting of protein kinase C delta to mitochondria in the oxidative stress response. *Cell Growth Differ.* 12, 465–470.

Manne, S., Kondru, N., Hepker, M., Jin, H., Anantharam, V., Lewis, M., et al. (2019). Ultrasensitive detection of aggregated α-synuclein in glial cells, human cerebrospinal fluid and brain tissue using the RT-QuIC assay: new high-throughput neuroimmune biomarker assay for parkinsonian disorders. *J. Neuroimmune Pharmacol.* 14, 423–435. doi: 10.1007/s11481-019-09835-4

Mao, X., Ou, M. T., Karuppagounder, S. S., Kam, T. I., Yin, X., Xiong, Y., et al. (2016). Pathological α-synuclein transmission initiated by binding lymphocyte-activation gene 3. *Science* 353:aah3374. doi: 10.1126/science.aah3374

McCoy, M. K., Martinez, T. N., Ruhn, K. A., Szymkowski, D. E., Smith, C. G., Botterman, B. R., et al. (2006). Blocking soluble tumor necrosis factor signaling with dominant-negative tumor necrosis factor inhibitor attenuates loss of dopaminergic neurons in models of Parkinson's disease. *J. Neurosci.* 26, 9365–9375. doi: 10.1523/JNEUROSCI.1504-06.2006

Menu, P., Mayor, A., Zhou, R., Tardivel, A., Ichijo, H., Mori, K., et al. (2012). ER stress activates the NLRP3 inflammasome *via* an UPR-independent pathway. *Cell Death Dis.* 3:e261. doi: 10.1038/cddis.2011.132

Mercado, G., Valdés, P., and Hetz, C. (2013). An ERcentric view of Parkinson's disease. *Trends Mol. Med.* 19, 165–175. doi: 10.1016/j.molmed.2012.12.005

Mhyre, T. R., Boyd, J. T., Hamill, R. W., and Maguire-Zeiss, K. A. (2012). Parkinson's disease. *Subcell. Biochem.* 65, 389–455. doi: 10.1007/978-94-007-5416-4_16

Murphy, M. P. (2009). How mitochondria produce reactive oxygen species. *Biochem. J.* 417, 1–13. doi: 10.1042/BJ20081386

Nagatsu, T., Mogi, M., Ichinose, H., and Togari, A. (2000). Cytokines in Parkinson's disease. *J. Neural Transm. Suppl.* 58, 143–151.

Norden, D. M., and Godbout, J. P. (2013). Review: microglia of the aged brain: primed to be activated and resistant to regulation. *Neuropathol. Appl. Neurobiol.* 39, 19–34. doi: 10.1111/j.1365-2990.2012.01306.x

Oakes, S. A., and Papa, F. R. (2015). The role of endoplasmic reticulum stress in human pathology. *Annu. Rev. Pathol.* 10, 173–194. doi: 10.1146/annurev-pathol-012513-104649

Olanow, C. W., Savolainen, M., Chu, Y., Halliday, G. M., and Kordower, J. H. (2019). Temporal evolution of microglia and α-synuclein accumulation following foetal grafting in Parkinson's disease. *Brain* 142, 1690–1700. doi: 10.1093/brain/awz104

Oslowski, C. M., Hara, T., O'Sullivan-Murphy, B., Kanekura, K., Lu, S., Hara, M., et al. (2012). Thioredoxin-interacting protein mediates ER stress-induced β

cell death through initiation of the inflammasome. *Cell Metab.* 16, 265–273. doi: 10.1016/j.cmet.2012.07.005

Panicker, N., Saminathan, H., Jin, H., Neal, M., Harischandra, D. S., Gordon, R., et al. (2015). Fyn kinase regulates microglial neuroinflammatory responses in cell culture and animal models of Parkinson's disease. *J. Neurosci.* 35, 10058–10077. doi: 10.1523/JNEUROSCI.0302-15.2015

Panicker, N., Sarkar, S., Harischandra, D. S., Neal, M., Kam, T. I., Jin, H., et al. (2019). Fyn kinase regulates misfolded α-synuclein uptake and NLRP3 inflammasome activation in microglia. *J. Exp. Med.* 216, 1411–1430. doi: 10.1084/jem.20182191

Patterson, J. R., Duffy, M. F., Kemp, C. J., Howe, J. W., Collier, T. J., Stoll, A. C., et al. (2019). Time course and magnitude of α-synuclein inclusion formation and nigrostriatal degeneration in the rat model of synucleinopathy triggered by intrastriatal α-synuclein preformed fibrils. *Neurobiol. Dis.* 130:104525. doi: 10.1016/j.nbd.2019.104525

Paumier, K. L., Luk, K. C., Manfredsson, F. P., Kanaan, N. M., Lipton, J. W., Collier, T. J., et al. (2015). Intrastriatal injection of pre-formed mouse α-synuclein fibrils into rats triggers α-synuclein pathology and bilateral nigrostriatal degeneration. *Neurobiol. Dis.* 82, 185–199. doi: 10.1016/j.nbd.2015.06.003

Pike, A. F., Varanita, T., Herrebout, M. A. C., Plug, B. C., Kole, J., Musters, R. J. P., et al. (2021). α-synuclein evokes NLRP3 inflammasome-mediated IL-1β secretion from primary human microglia. *Glia* 69, 1413–1428. doi: 10.1002/glia.23970

Qin, X., and Mochly-Rosen, D. (2008). The PKCdelta -Abl complex communicates ER stress to the mitochondria—an essential step in subsequent apoptosis. *J. Cell Sci.* 121, 804–813. doi: 10.1242/jcs.024653

Qin, L., Liu, Y., Hong, J.-S., and Crews, F. T. (2013). NADPH oxidase and aging drive microglial activation, oxidative stress and dopaminergic neurodegeneration following systemic LPS administration. *Glia* 61, 855–868. doi: 10.1002/glia.22479

Qin, X.-Y., Zhang, S.-P., Cao, C., Loh, Y. P., and Cheng, Y. (2016). Aberrations in peripheral inflammatory cytokine levels in Parkinson disease: a systematic review and meta-analysis. *JAMA Neurol.* 73, 1316–1324. doi: 10.1001/jamaneurol.2016.2742

Reverendo, M., Mendes, A., Argüello, R. J., Gatti, E., and Pierre, P. (2019). At the crossway of ER-stress and proinflammatory responses. *FEBS J.* 286, 297–310. doi: 10.1111/febs.14391

Rocha, E. M., De Miranda, B., and Sanders, L. H. (2018). α-synuclein: pathology, mitochondrial dysfunction and neuroinflammation in Parkinson's disease. *Neurobiol. Dis.* 109, 249–257. doi: 10.1016/j.nbd.2017.04.004

Russo, M. V., and McGavern, D. B. (2015). Immune surveillance of the CNS following infection and injury. *Trends Immunol.* 36, 637–650. doi: 10.1016/j.it.2015.08.002

Salter, M. W., and Stevens, B. (2017). Microglia emerge as central players in brain disease. *Nat. Med.* 23, 1018–1027. doi: 10.1038/nm.4397

Samidurai, M., Tarale, P., Janarthanam, C., Estrada, C. G., Gordon, R., Zenitsky, G., et al. (2020). Tumor necrosis factor-like weak inducer of apoptosis (TWEAK) enhances activation of STAT3/NLRC4 inflammasome signaling axis through PKCδ in astrocytes: implications for Parkinson's disease. *Cells* 9:1831. doi: 10.3390/cells9081831

Sarkar, S., Dammer, E. B., Malovic, E., Olsen, A. L., Raza, S. A., Gao, T., et al. (2020). Molecular signatures of neuroinflammation induced by αsynuclein aggregates in microglial cells. *Front. Immunol.* 11:33. doi: 10.3389/fimmu.2020.00033

Sarkar, S., Malovic, E., Plante, B., Zenitsky, G., Jin, H., Anantharam, V., et al. (2017). Rapid and refined CD11b magnetic isolation of primary microglia with enhanced purity and versatility. *J. Vis. Exp.* 122:55364. doi: 10.3791/55364

Satake, W., Nakabayashi, Y., Mizuta, I., Hirota, Y., Ito, C., Kubo, M., et al. (2009). Genome-wide association study identifies common variants at four loci as genetic risk factors for Parkinson's disease. *Nat. Genet.* 41, 1303–1307. doi: 10.1038/ng.485

Shimada, K., Crother, T. R., Karlin, J., Dagvadorj, J., Chiba, N., Chen, S., et al. (2012). Oxidized mitochondrial DNA activates the NLRP3 inflammasome during apoptosis. *Immunity* 36, 401–414. doi: 10.1016/j.immuni.2012.01.009

Simón-Sánchez, J., Schulte, C., Bras, J. M., Sharma, M., Gibbs, J. R., Berg, D., et al. (2009). Genome-wide association study reveals genetic risk underlying Parkinson's disease. *Nat. Genet.* 41, 1308–1312. doi: 10.1038/ng.487

Singh, N., Lawana, V., Luo, J., Phong, P., Abdalla, A., Palanisamy, B., et al. (2018). Organophosphate pesticide chlorpyrifos impairs STAT1 signaling to induce dopaminergic neurotoxicity: implications for mitochondria mediated oxidative stress signaling events. *Neurobiol. Dis.* 117, 82–113. doi: 10.1016/j.nbd.2018.05.019

Smith, W. W., Jiang, H., Pei, Z., Tanaka, Y., Morita, H., Sawa, A., et al. (2005). Endoplasmic reticulum stress and mitochondrial cell death pathways mediate A53T mutant α-synuclein-induced toxicity. *Hum. Mol. Genet.* 14, 3801–3811. doi: 10.1093/hmg/ddi396

Spittau, B. (2017). Aging microglia-phenotypes, functions and implications for age-related neurodegenerative diseases. *Front. Aging Neurosci.* 9:194. doi: 10.3389/fnagi.2017.00194

Stefanova, N., Fellner, L., Reindl, M., Masliah, E., Poewe, W., and Wenning, G. K. (2011). Toll-like receptor 4 promotes α-synuclein clearance and survival of nigral dopaminergic neurons. *Am. J. Pathol.* 179, 954–963. doi: 10.1016/j.ajpath.2011.04.013

Steinberg, S. F. (2015). Mechanisms for redox-regulation of protein kinase C. *Front. Pharmacol.* 6:128. doi: 10.3389/fphar.2015.00128

Tao, L., Lin, H., Wen, J., Sun, Q., Gao, Y., Xu, X., et al. (2018). The kinase receptor-interacting protein 1 is required for inflammasome activation induced by endoplasmic reticulum stress. *Cell Death Dis.* 9:641. doi: 10.1038/s41419-018-0694-7

Teschke, K., Marion, S. A., Tsui, J. K., Shen, H., Rugbjerg, K., and Harris, M. A. (2014). Parkinson's disease and occupation: differences in associations by case identification method suggest referral bias. *Am. J. Ind. Med.* 57, 163–171. doi: 10.1002/ajim.22272

Tokuda, T., Qureshi, M. M., Ardah, M. T., Varghese, S., Shehab, S. A., Kasai, T., et al. (2010). Detection of elevated levels of α-synuclein oligomers in CSF from patients with Parkinson disease. *Neurology* 75, 1766–1772. doi: 10.1212/WNL.0b013e3181fd613b

Trang, T., Beggs, S., and Salter, M. W. (2011). Brain-derived neurotrophic factor from microglia: a molecular substrate for neuropathic pain. *Neuron Glia Biol.* 7, 99–108. doi: 10.1017/S1740925X12000087

Tseng, H. H. L., Vong, C. T., Kwan, Y. W., Lee, S. M.-Y., and Hoi, M. P. M. (2016). TRPM2 regulates TXNIP-mediated NLRP3 inflammasome activation *via* interaction with p47 phox under high glucose in human monocytic cells. *Sci. Rep.* 6:35016. doi: 10.1038/srep35016

Volpicelli-Daley, L. A., Luk, K. C., and Lee, V. M.-Y. (2014). Addition of exogenous α-synuclein preformed fibrils to primary neuronal cultures to seed recruitment of endogenous α-synuclein to Lewy body and Lewy neurite-like aggregates. *Nat. Protoc.* 9, 2135–2146. doi: 10.1038/nprot.2014.143

Wali, J. A., Gurzov, E. N., Fynch, S., Elkerbout, L., Kay, T. W., Masters, S. L., et al. (2014). Activation of the NLRP3 inflammasome complex is not required for stress-induced death of pancreatic islets. *PLoS One* 9:e113128. doi: 10.1371/journal.pone.0113128

Wang, Y., Wang, Y., Bharti, V., Zhou, H., Hoi, V., Tan, H., et al. (2019). Upregulation of thioredoxin-interacting protein in brain of amyloid-β protein precursor/presenilin 1 transgenic mice and amyloid-β treated neuronal cells. *J. Alzheimers Dis.* 72, 139–150. doi: 10.3233/JAD-190223

Wang, C.-Y., Xu, Y., Wang, X., Guo, C., Wang, T., and Wang, Z.-Y. (2019). Dl-3-n-butylphthalide inhibits NLRP3 inflammasome and mitigates Alzheimer's-like pathology *via* Nrf2-TXNIP-TrX axis. *Antioxid. Redox Signal.* 30, 1411–1431. doi: 10.1089/ars.2017.7440

Wang, S., Yoo, S., Kim, H.-Y., Wang, M., Zheng, C., Parkhouse, W., et al. (2015). Detection of in situ protein-protein complexes at the Drosophila larval neuromuscular junction using proximity ligation assay. *J. Vis. Exp.* 95:52139. doi: 10.3791/52139

Wang, K., Zhu, X., Zhang, K., Yao, Y., Zhuang, M., Tan, C., et al. (2017). Puerarin inhibits amyloid β-induced NLRP3 inflammasome activation in retinal pigment epithelial cells *via* suppressing ROS-dependent oxidative and endoplasmic reticulum stresses. *Exp. Cell Res.* 357, 335–340. doi: 10.1016/j.yexcr.2017.05.030

Webers, A., Heneka, M. T., and Gleeson, P. A. (2020). The role of innate immune responses and neuroinflammation in amyloid accumulation and progression

of Alzheimer's disease. *Immunol. Cell Biol.* 98, 28–41. doi: 10.1111/imcb.12301

Wen, J., Ribeiro, R., and Zhang, Y. (2011). Specific PKC isoforms regulate LPS-stimulated iNOS induction in murine microglial cells. *J. Neuroinflammation* 8:38. doi: 10.1186/1742-2094-8-38

Westphal, C. H., and Chandra, S. S. (2013). Monomeric synucleins generate membrane curvature. *J. Biol. Chem.* 288, 1829–1840. doi: 10.1074/jbc.M112.418871

Wijeyekoon, R. S., Moore, S. F., Farrell, K., Breen, D. P., Barker, R. A., and Williams-Gray, C. H. (2020). Cerebrospinal fluid cytokines and neurodegeneration-associated proteins in Parkinson's disease. *Mov. Disord.* 35, 1062–1066. doi: 10.1002/mds.28015

Yoshihara, E., Masaki, S., Matsuo, Y., Chen, Z., Tian, H., and Yodoi, J. (2014). Thioredoxin/Txnip: redoxisome, as a redox switch for the pathogenesis of diseases. *Front. Immunol.* 4:514. doi: 10.3389/fimmu.2013.00514

Yun, S. P., Kam, T.-I., Panicker, N., Kim, S., Oh, Y., Park, J. S., et al. (2018). Block of A1 astrocyte conversion by microglia is neuroprotective in models of Parkinson's disease. *Nat. Med.* 24, 931–938. doi: 10.1038/s41591-018-0051-5

Zhang, D., Anantharam, V., Kanthasamy, A., and Kanthasamy, A. G. (2007). Neuroprotective effect of protein kinase C delta inhibitor rottlerin in cell culture and animal models of Parkinson's disease. *J. Pharmacol. Exp. Ther.* 322, 913–922. doi: 10.1124/jpet.107.124669

Zhang, J., Pei, L., Zang, D., Xue, Y., Wang, X., Chen, Y., et al. (2020). Gender differences of NLRP1 inflammasome in mouse model of Alzheimer's disease. *Front. Aging Neurosci.* 12:512097. doi: 10.3389/fnagi.2020.512097

Zhao, Q., Che, X., Zhang, H., Fan, P., Tan, G., Liu, L., et al. (2017a). Thioredoxin-interacting protein links endoplasmic reticulum stress to inflammatory brain injury and apoptosis after subarachnoid haemorrhage. *J. Neuroinflammation* 14:104. doi: 10.1186/s12974-017-0878-6

Zhao, Q., Che, X., Zhang, H., Tan, G., Liu, L., Jiang, D., et al. (2017b). Thioredoxin-interacting protein mediates apoptosis in early brain injury after subarachnoid haemorrhage. *Int. J. Mol. Sci.* 18:854. doi: 10.3390/ijms18040854

Zhou, R., Tardivel, A., Thorens, B., Choi, I., and Tschopp, J. (2010). Thioredoxin-interacting protein links oxidative stress to inflammasome activation. *Nat. Immunol.* 11, 136–140. doi: 10.1038/ni.1831

Zimprich, A., Biskup, S., Leitner, P., Lichtner, P., Farrer, M., Lincoln, S., et al. (2004). Mutations in LRRK2 cause autosomal-dominant parkinsonism with pleomorphic pathology. *Neuron* 44, 601–607. doi: 10.1016/j.neuron.2004.11.005

Conflict of Interest: AGK and VA have an equity interest in PK Biosciences Corporation located in Ames, IA. AGK also has an equity interest in Probiome Therapeutics located in Ames, IA. The terms of this arrangement have been reviewed and approved by Iowa State University in accordance with its conflict-of-interest policies.

The remaining authors declare that the research was conducted in the absence of any commercial or financial relationships that could be construed as a potential conflict of interest.

Copyright © 2021 Samidurai, Palanisamy, Bargues-Carot, Hepker, Kondru, Manne, Zenitsky, Jin, Anantharam, Kanthasamy and Kanthasamy. This is an open-access article distributed under the terms of the Creative Commons Attribution License (CC BY). The use, distribution or reproduction in other forums is permitted, provided the original author(s) and the copyright owner(s) are credited and that the original publication in this journal is cited, in accordance with accepted academic practice. No use, distribution or reproduction is permitted which does not comply with these terms.

frontiers in Aging Neuroscience

REVIEW
published: 08 July 2021
doi: 10.3389/fnagi.2021.702639

Alpha-Synuclein as a Biomarker of Parkinson's Disease: Good, but Not Good Enough

*Upasana Ganguly[1], Sukhpal Singh[1], Soumya Pal[1], Suvarna Prasad[1], Bimal K. Agrawal[2], Reena V. Saini[3] and Sasanka Chakrabarti[1]**

[1] Department of Biochemistry and Central Research Laboratory, Maharishi Markandeshwar Institute of Medical Sciences and Research, Maharishi Markandeshwar Deemed University, Ambala, India, [2] Department of General Medicine, Maharishi Markandeshwar Institute of Medical Sciences and Research, Maharishi Markandeshwar Deemed University, Ambala, India, [3] Department of Biotechnology, Maharishi Markandeshwar Engineering College, Maharishi Markandeshwar Deemed University, Ambala, India

Parkinson's disease (PD) is the second most common neurodegenerative disorder of the elderly, presenting primarily with symptoms of motor impairment. The disease is diagnosed most commonly by clinical examination with a great degree of accuracy in specialized centers. However, in some cases, non-classical presentations occur when it may be difficult to distinguish the disease from other types of degenerative or non-degenerative movement disorders with overlapping symptoms. The diagnostic difficulty may also arise in patients at the early stage of PD. Thus, a biomarker could help clinicians circumvent such problems and help them monitor the improvement in disease pathology during anti-parkinsonian drug trials. This review first provides a brief overview of PD, emphasizing, in the process, the important role of α-synuclein in the pathogenesis of the disease. Various attempts made by the researchers to develop imaging, genetic, and various biochemical biomarkers for PD are then briefly reviewed to point out the absence of a definitive biomarker for this disorder. In view of the overwhelming importance of α-synuclein in the pathogenesis, a detailed analysis is then made of various studies to establish the biomarker potential of this protein in PD; these studies measured total α-synuclein, oligomeric, and post-translationally modified forms of α-synuclein in cerebrospinal fluid, blood (plasma, serum, erythrocytes, and circulating neuron-specific extracellular vesicles) and saliva in combination with certain other proteins. Multiple studies also examined the accumulation of α-synuclein in various forms in PD in the neural elements in the gut, submandibular glands, skin, and the retina. The measurements of the levels of certain forms of α-synuclein in some of these body fluids or their components or peripheral tissues hold a significant promise in establishing α-synuclein as a definitive biomarker for PD. However, many methodological issues related to detection and quantification of α-synuclein have to be resolved, and larger cross-sectional and follow-up studies with controls and patients of PD, parkinsonian disorders, and non-parkinsonian movement disorders are to be undertaken.

Keywords: imaging biomarkers, cerebrospinal fluid, α-synuclein oligomers, phosphorylated α-synuclein, extracellular vesicles, metabolomics, brain-derived neurotrophic factor, uric acid

OPEN ACCESS

Edited by:
Yun-Cheng Wu,
Shanghai Jiao Tong University School of Medicine, China

Reviewed by:
Pooja Jadiya,
Temple University, United States
Lili-Naz Hazrati,
University of Toronto, Canada

****Correspondence:***
Sasanka Chakrabarti
profschakrabarti95@gmail.com

Received: *29 April 2021*
Accepted: *07 June 2021*
Published: *08 July 2021*

Citation:
Ganguly U, Singh S, Pal S, Prasad S, Agrawal BK, Saini RV and Chakrabarti S (2021) Alpha-Synuclein as a Biomarker of Parkinson's Disease: Good, but Not Good Enough. Front. Aging Neurosci. 13:702639. doi: 10.3389/fnagi.2021.702639

INTRODUCTION

Parkinson's disease (PD) is a complex and progressive neurodegenerative disorder that mainly affects the elderly population and appears sporadically and in familial forms. Familial type accounts for only 5–10% of PD patients, while the vast majority of PD subjects suffer from the sporadic form, which has a multi-factorial origin (Kalia and Lang, 2015). The cardinal signs of PD are motor impairments such as resting tremor, bradykinesia, muscular rigidity, postural instability (Jankovic, 2008; Greenland and Barker, 2018; Kouli et al., 2018). Flexed posture and 'freezing' are also characteristic of PD, and many secondary motor symptoms occur during the disease (Jankovic, 2008). Non-motor symptoms like autonomic dysfunction, anosmia, sleep disorders, hallucinations, depression, and dementia also appear; some non-motor symptoms appear even before the advent of the motor symptoms (Jankovic, 2008; Greenland and Barker, 2018). However, the term 'parkinsonian disorders' encompasses other diseases like multiple system atrophy (MSA), progressive supranuclear palsy, corticobasal degeneration, drug-induced parkinsonism, and post-encephalitic parkinsonism, with similar or overlapping clinical features as in PD (Dickson, 2012). The diagnosis of PD is essentially clinical, but when the presentation is not classical, PD may be confused with other parkinsonian disorders or several other movement disorders. Thus, a PD- specific biomarker would be useful for differential diagnosis in cases of non-classical presentation. Further, the motor symptoms of PD develop due to the dopaminergic neuronal loss of substantia nigra of the mid-brain, and there is already massive dopaminergic neurodegeneration by the time the patient presents clinically to the physician. A neuroprotective therapy initiated early would be an ideal treatment option for PD, but a clinically useful neuroprotective drug for PD is not available so far. Identifying and validating a putative neuroprotective drug through randomized controlled trials would be difficult unless PD can be identified unequivocally at a very early stage. Therefore, a conveniently detectable biomarker for early-stage diagnosis of PD will serve a very important purpose for clinical trials of neuroprotective compounds and early initiation of neuroprotective therapy.

Although the term 'biomarker' is often used in a vast sense, we will restrict the term in this review as a tool to aid in the diagnosis of the disease or its prognostic evaluation. The biomarker for PD is often categorized as genetic, imaging-based, or biochemical biomarkers (Emamzadeh and Surguchov, 2018; He et al., 2018). However, the genetic biomarker is especially useful for the familial form of PD, which accounts for a small subset of PD subjects usually presenting as early-onset cases with a positive family history. For most other cases of late-onset sporadic PD, an imaging-based or a biochemical biomarker would be the ideal choice. In this review, we would present an overview of epidemiology, diagnosis, pathogenesis, and pathology of the disease and briefly discuss the genetic and other biomarkers before going into a detailed analysis of α-synuclein as a candidate biomarker for PD. Ideally, a biomarker should be related to the pathogenesis of the disease, and α-synuclein meets this criterion very aptly in the context of PD. However, for a disease like PD affecting the basal ganglia and other discrete regions of the brain primarily, the changes in the level of α-synuclein may be manifested consistently only in cerebrospinal fluid (CSF), and this may impede its use as a promising biomarker for PD. Thus, it will be interesting to review the available studies measuring the levels of α-synuclein in peripheral circulation or other accessible body fluids in PD. Further, it will be essential to scrutinize the existing literature for various limitations of different studies on the biomarker potential of α -synuclein.

PD: AN OVERVIEW

Epidemiology

Parkinson's disease is the second most common neurodegenerative disease of the elderly population, whose prevalence is 0.5 to 1% in the age group of 65–69 years, and it gradually rises with the increasing age (Kouli et al., 2018). The global burden of PD increased from 2.5 million in 1990 to 5.1 in 2016, which is variably distributed in different countries, and the rise in PD population over time cannot be solely attributed to the increase in the aged population in different countries during this period (GBD 2016 Neurology Collaborators, 2018). Many studies have reported variable prevalence of PD according to gender and in different countries and age groups. A meta-analysis of PD prevalence reported in 2014 that the prevalence increases with age and is significantly higher in males in the age group of 50 to 59 years (Pringsheim et al., 2014). This meta-analysis further showed that in the age group of 70 to 79 years, a higher prevalence of PD is noted in Europe, North America, and Australia than in Asia. A detailed and recent meta-estimate of PD prevalence collected from different sources in several regions of North America found the prevalence of 572 per 1,00,000 above the age of 45 years (Marras et al., 2018). This study analyzed in detail the reasons for the variable prevalence of PD reported in earlier studies. As observed in this study, the prevalence was more in the males, increased with age, and showed some regional variations. In a study based in Korea, age and gender standardized prevalence of PD in 2015 was estimated to be 139.8 per 1,00,000 with females having a higher prevalence, and both the incidence and prevalence of PD increased continuously from 2010 to 2015 in this country (Park et al., 2019). In a comparative analysis of different descriptive studies and meta-analyses on the prevalence of PD in eastern and western nations, Abbas et al. (2018) showed an increased prevalence with age, male predominance, and interestingly a lower prevalence of this disorder in the eastern nations. The differences in the prevalence of PD in different countries could be related to inappropriate sample selections, limitations of various data collection methods and analyses, and different life expectancies in different populations. Alternatively, this difference may arise from the variances in genetic or environmental risk factors for PD present in different populations.

Diagnosis of PD

When PD presents with typical motor symptoms as described above, the diagnosis of the disease can be made with a great degree of certainty. The presence of autonomic dysfunction, some sensory loss like anosmia, ageusia, sleep disorders, unilateral onset and persistent asymmetry of symptoms, positive response to dopaminergic therapy, and levodopa-induced dyskinesia can strengthen the diagnosis (Jankovic, 2008; Greenland and Barker, 2018; Marsili et al., 2018). In many cases, the disease may be confused with other 'parkinsonian disorders,' where a careful recording of history, e.g., exposure to pesticides, encephalitis, certain antipsychotic drugs, or the presence of certain exclusion criteria or brain imaging studies may help to clinch the diagnosis. Since the confirmation of PD can be established only by post-mortem histopathology, many diagnostic criteria have been proposed by expert groups (Jankovic, 2008; Marsili et al., 2018). The severity of symptoms, associated disability, and the progress of the disease can be assessed by using several rating scales. Hoehn and Yahr (H-Y) scale was the oldest one which divides PD into several stages based on the presence or absence of a battery of clinical symptoms indicative of motor impairment and disability. Many other rating scales have since been utilized to obtain a global estimate of disease severity or specific aspects of the disease. The unified Parkinson's disease rating scale (UPDRS), later upgraded by the expert group of Movement Disorder Society (MDS-UPDRS) in 2008, takes into consideration of motor disability, motor complications, activities of daily living, non-motor symptoms, including changes in mood, behavior, and intellectual functions (Martínez-Martín et al., 2015). Other global assessment methods like the clinical impression of severity index for Parkinson's disease (CISI-PD), Parkinson's disease composite scale (PDCS), and several other forms of assessment of specific PD-related symptoms are also in use (Martínez-Martín et al., 2015, 2016; Pintér et al., 2019). The importance of these rating scales and their correlation with each other are important areas of clinical PD research (Martínez-Martín et al., 2016; Ayala et al., 2017; Skorvanek et al., 2017).

The familial forms of PD often have an earlier onset and sometimes an aggressive progression than sporadic forms. Still, clinical features are very similar to that of sporadic type in most cases. The differential diagnosis of PD includes not only 'parkinsonian disorders,' but also several other disorders like essential tremor, dystonic tremor, neurodegeneration with brain iron accumulation (NBIA), Huntington's disease, Wilson's disease, spinocerebellar ataxia, and idiopathic basal ganglia calcification (Greenland and Barker, 2018).

Pathology and Pathogenesis

The post-mortem macroscopic examination of a PD brain shows characteristically a loss of pigmented region in the substantia nigra of the mid-brain, which microscopically corresponds to a loss of neuromelanin-containing dopaminergic neurons of pars compacta of substantia nigra (Hartmann, 2004; Dickson, 2012). The neuronal loss in the PD brain is not restricted to substantia nigra only, but catecholaminergic as well as non-catecholaminergic neurons in the dorsal motor nucleus of the vagus, olfactory bulb, ventral tegmental region, locus coeruleus, raphe nucleus, and nucleus basalis of Meynert, and the neuronal loss is associated with reactive gliosis (Alexander, 2004; Hartmann, 2004; Dickson, 2012; Giguère et al., 2018). Another characteristic feature of PD pathology is the presence of eosinophilic inclusions (5–30 μ in diameter) in the soma of the surviving neurons (Lewy bodies or LBs) which are visible in routine histopathological staining (Hartmann, 2004; Dickson, 2012; Kouli et al., 2018). The LBs can be immunostained by using antibodies against α-synuclein, and such immuno-staining for α-synuclein also reveals the thread-like inclusion structures in the neuronal processes called Lewy neurites (LNs) (Hartmann, 2004; Dickson, 2012; Kouli et al., 2018). Although α-synuclein is the predominant protein in LBs and LNs, other proteins like ubiquitin, neurofilament protein, ubiquitin-binding protein p62, tubulin, and synphilin-1 also occur in such structures. Somewhat pale staining structures with an ill-defined outline, immuno-reactive to α-synuclein, which are presumably the early stages of LBs, are also seen within neurons in substantia nigra as well as other parts of the PD brain including cortex and amygdala (Braak et al., 2004; Hartmann, 2004; Dickson, 2012; Kouli et al., 2018). From extensive studies with post-mortem PD brains, Braak et al. (2004) have proposed a Lewy-pathology-based staging (1 to 6) of PD. According to their study, the disease begins (Stage 1and 2) in the anterior olfactory nucleus and dorsal vagal nuclei and spreads predictably to reach the locus coeruleus in the pons, substantia nigra, and other nuclei in the mid-brain and fore-brain (Stage 3 and 4) and finally in the different neocortical areas. However, other studies have contradicted this staging and propagation of PD pathology (Dickson, 2012; Jellinger, 2019). One characteristic feature of PD pathology has been the selective vulnerability of specific neurons to develop LBs and LNs and subsequent death while sparing others in close anatomical contact with degenerating neurons. Recent experimental studies further suggest that α-synuclein pathology might begin in the periphery, and the pathological form of the protein may be transferred via the vagal nerve by retrograde transport from the gut wall to the dorsal nucleus of the vagus in the brain, which was originally hypothesized by Braak et al. (2004; Holmqvist et al., 2014). The pathogenic mechanisms of PD have been explored in post-mortem PD brains and experimental models, including PD models in transgenic organisms, toxin-induced neurodegeneration in cultured catecholaminergic cell lines, and various toxin-based animal models of PD. Identifying genes responsible for familial PD and examining the mechanisms of actions of their protein products like α-synuclein, PARKIN, PINK1, LRRK2, and DJ-1 in model systems have provided important clues in understanding the PD pathogenesis both in the familial and sporadic forms. Similarly, exposure to pesticides like paraquat or other types of toxin like MPTP has been implicated in the genesis of PD, resulting in the development of several toxin-based animal models. In general, such studies indicate that oxidative stress, mitochondrial dysfunction, metal accumulation, proteinopathy, and inflammatory reactions are some of the interdependent mechanisms that contribute to neurodegeneration in PD (Jenner, 2003; Eriksen et al., 2005;

Schapira, 2007; Dawson et al., 2010; Jackson-Lewis et al., 2012; Gubellini and Kachidian, 2015; Wrangel et al., 2015; Ganguly et al., 2017). The details of PD pathogenesis are not within the purview of this review, and no coherent picture has so far emerged to define the neurodegenerative processes in PD clearly. However, it will not be out of place if we present a brief update of important elements of PD pathogenesis before analyzing the role of α-synucleinopathy in this process.

Mitochondrial Dysfunction in PD

Mitochondrial complex I inhibition in substantia nigra in post-mortem PD brain was an early finding which was later reported in platelets and skeletal muscles of PD patients (Schapira, 2007). Toulorge et al. (2016) elegantly compiled a detailed catalog of many mitochondrial bioenergetic deficits in post-mortem PD brain reported in the literature. Other studies have indicated altered mitochondrial biogenesis, mitochondrial fusion-fission homeostasis, defective mitophagy in post-mortem PD brain, PD transgenic animals, or toxin (rotenone, 6-hydroxydopamine, and MPTP) induced models of PD in animals or cultured cells of neural origin (Park et al., 2018; Jiang X. et al., 2019). Peroxisome proliferator-activated receptor-gamma coactivator-1 α (PGC-1α) coordinates the expression levels of many genes needed for mitochondrial biogenesis and electron transport chain activity. The expression of PGC-1α was reported to be decreased in substantia nigra of PD patients, which could be partially attributed to increased cytosine methylation at the promoter region of the PGC-1α gene (Eschbach et al., 2015; Su et al., 2015). PGC-1α regulated nuclear-genes encoding mitochondrial proteins were also downregulated in substantia nigra of the PD brain (Zheng et al., 2010). Familial PD-related genes like *PARKIN, PINK1, DJ1* encode proteins that regulate mitophagy and multiple other mitochondrial functions. The mutations of these genes in experimental genetic models of PD show many mitochondrial anomalies (Gandhi et al., 2009; Irrcher et al., 2010; Heeman et al., 2011; Thomas et al., 2011; Shaltouki et al., 2015; Chung et al., 2016). In a recent study, Zilocchi et al. (2018) reported altered mitochondrial morphology and decreased levels of optic atrophy 1 or OPA1, a mitochondrial fusion protein, and mitochondrial voltage-dependent anion channel (VDAC1 and VDAC2) proteins in substantia nigra of PD brains as well as in dopamine-induced neurodegeneration model in SH-SY5Y cells. Recent investigations also identified various deletion mutations and rearrangements of mtDNA with altered copy numbers in nigral neurons of sporadic PD patients and experimental models of PD, but their significance in PD pathogenesis could not be established as yet (Martín-Jiménez et al., 2020). Altogether an enormous body of data has been generated on mitochondrial anomalies in clinical and experimental PD models, and these have been linked to oxidative stress, neuroinflammation, calcium dysregulation, and finally, neurodegeneration.

Oxidative Stress in PD

The accumulation of transition metals like iron and copper, oxidative damage markers of phospholipids, proteins, and DNA, depletion of reduced glutathione (GSH) and increased activity of glutathione degradative enzyme, and elevated levels of peroxiredoxins were reported in substantia nigra of post-mortem PD brains (Jenner, 2003; Ayton and Lei, 2014; Toulorge et al., 2016; Guo et al., 2018). The accumulation of iron in the substantia nigra of PD patients was confirmed both in post-mortem brain samples or by antemortem imaging techniques (Ayton and Lei, 2014; Wang J. Y. et al., 2016). In post-mortem PD brain and toxin-based and genetic models, the key role of reactive oxygen species (ROS) and oxidative stress is apparent in PD pathology (Wu et al., 2003; Varcin et al., 2012; Sanders and Greenamyre, 2013). The accumulation of iron in substantia nigra can lead to ROS generation, especially when the iron is bound to proteins like α-synuclein. Apart from that, the mitochondrial complex I inhibition and other bioenergetic impairment, autoxidation or enzymatic oxidation of dopamine, and activation of microglial NADPH oxidase are also responsible for increased ROS formation in the PD brain (Jana et al., 2011; Bisaglia et al., 2014; Ganguly et al., 2017; Puspita et al., 2017; Guo et al., 2018). In turn, ROS can damage the mitochondrial DNA or electron transport chain components, causing a further increase in ROS production or interact with mitochondrial permeability transition pore to release apoptogenic factors or with the endoplasmic reticulum (ER) to cause Ca^{2+} dysregulation and ER stress (Puspita et al., 2017; Guo et al., 2018). ROS have a complex action on the proteasomal pathway of protein degradation, but with a high level of oxidative stress inactivation of ubiquitinating enzymes, 20S proteasomal catalytic and 19S regulatory units occur (Pajares et al., 2015). Thus increase in ROS may lead to intra-neuronal accumulation of proteins like α-synuclein, which is cleared from the cell in a significant way by the proteasomal pathway (Ebrahimi-Fakhari et al., 2011). In the context of oxidative damage in PD, it is to be mentioned that dopamine oxidation produces ROS as well as highly reactive quinones, which can avidly form conjugates with proteins through thiol residues inactivating their functions, and this process may have important implication in PD pathogenesis (Bisaglia et al., 2014).

Inflammation in PD Pathogenesis

The inflammatory response is an essential feature of PD pathogenesis, which has been validated by many published reports over the last several decades. In the striata of post-mortem PD brain, activated microglia, and elevated levels of pro-inflammatory cytokines were demonstrated in multiple studies (Stojkovska et al., 2015; Caggiu et al., 2019). Microglia are primarily responsible for the inflammatory response in the brain. In post-mortem PD brains, the increased number of microglial cells exhibiting activation markers like HLA-DR, ICAM-1, CD 68, and CD23 were reported in multiple studies (Toulorge et al., 2016; Caggiu et al., 2019). The activated microglia liberate a variety of pro-inflammatory cytokines and chemokines. Several studies reported elevated levels of TNF-α, IL1β, IL6, IFN-γ, TGF-β, and others in the striatum, substantia nigra, and CSF from post-mortem PD brains (Mogi et al., 1996; Nagatsu et al., 2000; Toulorge et al., 2016; Caggiu et al., 2019; Pajares et al., 2020). In conformity with these post-mortem findings, an upregulation of pro-inflammatory cytokines was observed in the brain of 6-hydroxydopamine or MPTP-based models of PD (Pajares et al., 2020). Microglial ROS production through activation of NADPH

oxidase is characteristic of the inflammatory response, which is also enhanced in the substantia nigra of post-mortem PD brain as well as in the brain of MPTP induced mice model of PD (Belarbi et al., 2017). The activation of microglia in the brain occurs through many triggers like aggregated α-synuclein, pesticides, MPTP, bacterial lipopolysaccharide (LPS), and cytokines, which have implications in dopaminergic neuronal death in PD as observed in different experimental systems (Sanchez-Guajardo et al., 2015; Caggiu et al., 2019; Lee et al., 2019; Zhao et al., 2019). It is already established that elevated peripheral cytokines can lead to the activation of brain microglia through neural and humoral pathways (Dilger and Johnson, 2008). Thus, it is interesting that a meta-analysis confirmed elevated levels of circulating pro-inflammatory cytokines in sporadic PD, and this may link systemic inflammatory and immune response to PD pathogenesis (Qin et al., 2016). Apart from the central role of microglia in brain inflammatory response, astrocytes have been implicated recently in the latter process, but their importance in PD pathogenesis is not clearly established (Toulorge et al., 2016; Pajares et al., 2020). On the other hand, activated microglia can affect the blood-brain barrier allowing the invasion of the brain by peripheral monocytes and lymphocytes, which might also contribute to the inflammatory response in the brain (Pajares et al., 2020).

α-Synucleinopathy and PD Pathogenesis

The importance of α-synuclein in the pathogenesis of PD is indicated by the fact that it is the most abundant protein component of LBs and LNs. Moreover, point mutations (A53T, A30P, E46K, G51D, and several others) and multiplications (duplications or triplications) of the *SNCA* gene (coding for α-synuclein) have been reported in individuals with familial PD with autosomal dominance (Polymeropoulos et al., 1997; Krüger et al., 1998; Zarranz et al., 2004; Klein and Westenberger, 2012; Kiely et al., 2013). This small acidic protein of 140 amino acids is expressed abundantly in the brain and located at the presynaptic terminals where it is presumably involved in the vesicular transport of neurotransmitters (Stefanis, 2012; Lashuel et al., 2013). This intrinsically unfolded protein takes up partially helical structures in contact with biomembranes (Stefanis, 2012). Under certain conditions, α-synuclein attains β-conformation and undergoes aggregation to form soluble oligomers of various types and finally insoluble fibrils (Breydo et al., 2012; Stefanis, 2012). α-Synuclein undergoes different post-translational modifications such as phosphorylation, nitration, acetylation, *o*-GlcNAcylation (*N*-acetylglucosamine attached through serine hydroxyl groups), truncation, and ubiquitination, and some of these may modify the aggregation, membrane-binding, metal-binding, and other properties of this protein (Oueslati, 2016; Zhang et al., 2019; He et al., 2021). Though α-synuclein can undergo both serine and tyrosine phosphorylation at multiple sites through different kinases, the phosphorylated α-synuclein at serine 129 has been linked to toxicity in different studies (Oueslati, 2016; Arawaka et al., 2017; Zhang et al., 2019).

Transgenic organisms (flies, worms, and mice) overexpressing human wild-type or mutant human α-synuclein exhibit dopaminergic neurodegeneration, LB pathology, and motor deficits to varying extents (Breydo et al., 2012; Stefanis, 2012). Accumulated evidence from a large number of experimental studies clearly demonstrates that the administration of human α-synuclein protein or lentivirus or recombinant adeno-associated virus-carrying wild or mutant human α-synuclein gene in the substantia nigra of rodents and monkeys can lead to progressive neurodegeneration and motor deficits, and these studies have been well-summarized in several reviews (Dehay and Fernagut, 2016; Ganguly et al., 2018). Likewise, catecholaminergic cell lines manipulated genetically or pharmacologically in culture to express high levels of wild or mutant α-synuclein undergo degeneration under basal conditions or cellular stress (Zhu et al., 2012; Ramalingam et al., 2019; Ganguly et al., 2020). The varied mechanisms of α-synuclein toxicity altering mitochondrial functions and endoplasmic reticulum (ER)-Golgi transport or causing ER -stress and autophagic impairment in different model systems are available in several reviews (Stefanis, 2012; Lashuel et al., 2013; Ganguly et al., 2018; Fields et al., 2019). Some of the recent studies have provided further insights into α-synuclein toxicity in different model systems, which could be important in the context of PD pathogenesis. For example, mitochondria and ER remain tethered to each other at certain zones through interactions of a mitochondrial outer membrane protein and an integral protein of ER. Paillusson et al. (2017) showed that over-expression of α-synuclein (wild or mutated) disrupted the interactions of mitochondria and ER, leading to defective Ca^{2+} exchange between these two compartments and decreased mitochondrial ATP production. Similarly, Ganguly et al. (2020) suggested that accumulated α-synuclein in SH-SY5Y cells exposed to iron interacted with mitochondrial permeability transition pore components to cause mitochondrial depolarization and loss of ATP production. This study also showed how iron-dependent oxidative inactivation of Parkin, an E3 ubiquitin ligase, could lead to intracellular accumulation of α-synuclein presumably by preventing its degradation in the proteasomal pathway. Consistent with this idea, Chung et al. (2020) showed that a cell-permeable form of Parkin could prevent the accumulation of α-synuclein aggregates and fibrils when SH-SY5Y cells overexpressing α-synuclein were exposed to a mitochondrial toxin like rotenone. This study also demonstrated that cell-permeable Parkin could remove damaged mitochondria by mitophagy and promote mitochondrial biogenesis. The authors further confirmed the findings in toxin-based animal models of PD (Chung et al., 2020). In another study using Drosophila and mice models of α-synucleinopathy, it was demonstrated that α-synuclein interacted with cytoskeletal proteins spectrin and actin to cause mitochondrial morphological and functional alterations through mislocalization of a mitochondrial fission protein (Ordonez et al., 2018). Ludtmann et al. (2018) using inducible pluripotent stem cells (iPSC)-derived neurons with triplication of *SNCA* gene showed that oligomeric α-synuclein through inhibition of mitochondrial complex I activity caused oxidation of a subunit of ATP synthase leading to the opening of mitochondrial permeability transition pore with consequent mitochondrial swelling and cell death. In a similar model of iPSC-derived cortical neurons carrying triplicate *SNCA* gene, increased

expressions (mRNA and protein) of ER stress and unfolded protein response (UPR) markers could be observed (Heman-Ackah et al., 2017). In a Drosophila model of α-synucleinopathy and neurodegeneration, the expression of human α-synuclein caused impairment of autophagolysosomal system leading to an accumulation of autophagosomes and mitophagosomes, and the process involved abnormal stabilization of actin filaments (Sarkar et al., 2021). Likewise, in PC12 cells, the overexpression of human wild-type or mutant α-synuclein prevented starvation-induced autophagic vesicle formation with downregulation of autophagic markers (Wang K. et al., 2016). This plethora of studies identifying different potential mechanisms of α-synuclein toxicity have significant implications in PD pathogenesis, but so far, no consensus mechanism of α-synuclein mediated neurodegeneration has emerged.

BIOMARKERS OF PD

Multiple studies have reported the usefulness of several biochemical or imaging biomarkers in the differential diagnosis of PD. However, no single biomarker is specific enough for routine use in the diagnostic or prognostic evaluation in clinical cases of PD. On the other hand, the genetic biomarkers are mutations in defined genes or susceptibility loci that have been useful only in establishing the familial nature of PD.

Imaging Biomarkers

Several imaging techniques such as magnetic resonance imaging (MRI), transcranial sonography (TCS), single-photon emission computed tomography (SPECT), and positron emission tomography (PET) have been used to identify structural changes in the substantia nigra. These techniques can estimate the levels of dopamine transporter (DAT), vesicular monoamine transporter (VMAT), post-synaptic dopamine receptors, aromatic amino acid decarboxylase activity, abnormal accumulation of proteins (α-synuclein, and tau) or iron in the mid-brain or other areas. Such measurements have assisted in understanding the pathogenesis of the disease or its progression or effects of drugs on it (Niethammer et al., 2012; Wang L. et al., 2012). However, the results from such studies are not unequivocal to recommend any particular imaging biomarker for PD diagnosis. High-resolution MRI can identify a unique cluster of dopaminergic neurons in substantia nigra, called nigrosome-1, and the 'swallow-tail' appearance of healthy nigrosome-1 is lost in PD (Schwarz et al., 2014). It appears that though routine structural MRI may not be of much use in the diagnosis of PD, advanced MRI techniques such as diffusion imaging and susceptibility-weighted imaging for iron-load could be useful for supportive diagnosis of PD (Pyatigorskaya et al., 2014). The efficacy of TCS in the diagnosis of PD has also been examined, but in 196 consecutive cases of clinically unclear parkinsonism, the diagnostic accuracy of TCS of substantia nigra in identifying early cases of PD could not be established (Bouwmans et al., 2013). The imaging of DAT with PET or SPECT scan has again been suggested as only a piece of supportive evidence in favor of PD diagnosis (Brooks, 2016). Nevertheless, ^{18}F-labeled L-6-fluoro-3,4-dihydroxyphenylalanine (^{18}F-DOPA) PET-scan could eventually become an important diagnostic tool for the differential diagnosis of PD (Calabria et al., 2016). Further, an ^{18}F-labeled 2-deoxy-2-fluoro-D-glucose (^{18}F-FDG) PET scan is being accepted as a good method for differential diagnosis of PD from other parkinsonian disorders or risk assessment of cognitive impairment in PD (Meyer et al., 2017).

Genetic Biomarkers

The familial nature of PD was first identified in some Italian and Greek families where an autosomal dominant inheritance of the disease was attributed to mutations in the *SNCA* gene (coding for α-synuclein) present in the long arm of chromosome 4 (Nussbaum and Polymeropoulos, 1997; Polymeropoulos et al., 1997). From that time onward, based on linkage analysis, exome sequencing, and genome-wide association studies (GWAS), nearly 28 chromosomal loci have been implicated in genetic forms of PD, and 18 of them have been included in the PARK family and named as PARK 1/4, PARK 2, PARK 3, PARK 5, PARK 6 and so on (Klein and Westenberger, 2012). Within these loci several genes have been identified in which mutations can lead to monogenic forms of familial PD with either autosomal dominant or recessive inheritance or some complex disorders with parkinsonism as an associated component; in such cases, the mutations by themselves are sufficient for causing the disease (Lesage and Brice, 2009; Klein and Westenberger, 2012). The other chromosomal loci without identified genes may also cause familial PD, while some other loci probably represent susceptibility or genetic risk for developing PD (Pankratz and Foroud, 2007; Lesage and Brice, 2009; Klein and Westenberger, 2012). Among the monogenic forms of PD, mutations in *LRRK2* (PARK8) coding for leucine-rich repeat kinase 2 protein and *SNCA* (PARK1/4) coding for α-synuclein cause autosomal dominant PD; LRRK2 mutations are responsible for a significant percentage of familial PD, but SNCA mutations are rare (Pankratz and Foroud, 2007; Lesage and Brice, 2009; Klein and Westenberger, 2012). However, duplication or triplication of SNCA locus is also reported to cause familial PD with an earlier onset of the disease seen in those with triplication (Singleton et al., 2003; Book et al., 2018). Mutations in *PARKIN* (PARK2) coding for an E3 ubiquitin ligase enzyme called Parkin, and *PINK1* (PARK6) coding for a protein kinase called phosphatase and tensin homolog (PTEN)-induced protein kinase 1 cause autosomal recessive disease accounting for the majority of familial PD cases, while mutations in *DJ-1* (PARK7) are seen in rare forms of familial PD with autosomal recessive inheritance (Pankratz and Foroud, 2007; Klein and Westenberger, 2012). As in PARK 1/4, PARK2, PARK7, some of the gene mutations cause early-onset PD (sometimes even juvenile-onset) with aggressive progress, while typical late-onset PD with slow progress as in sporadic disease is caused by other mutations in PARK8 (LRRK2), PARK13, and PARK17. Mutations in PARK9 (*ATP13A2*) cause a complex phenotype with associated parkinsonism (Klein and Westenberger, 2012). The inheritance patterns of monogenic familial PD get complicated because many mutations have incomplete or variable penetrance and

expressivity, making it difficult to identify some family members with the disease. In addition, a phenocopy may appear in the family, which means a person with similar clinical features of the disease caused by some unknown environmental factors or by a different genetic mechanism (Klein and Westenberger, 2012).

It is also important to analyze how genes related to monogenic familial PD can also be important in sporadic PD. Besides specific mutations causing familial PD, in a given population, there are other genetic variations (polymorphisms) within such genes, their promoters, or in other sites in the gene loci, which may pose as susceptibility or genetic risk factors in the genesis of sporadic PD. The heterozygous carriers of autosomal recessive PD could also be at a higher risk of developing sporadic PD (Lesage and Brice, 2009; Klein and Westenberger, 2012; Mullin and Schapira, 2015). Such genetic variants or heterozygous mutations of SNCA, LRRK2, PARKIN, PINK1, and GBP (coding for lysosomal β-glucocerebrosidase) genes have been implicated in sporadic PD, emphasizing the importance of gene-environment interactions in this disease (West et al., 2002; Abou-Sleiman et al., 2006; Winkler et al., 2007; Lesage and Brice, 2009; Ross et al., 2011; Mullin and Schapira, 2015; Do et al., 2019). Further, the familial PD-related genes and their protein products have helped us understand the molecular mechanisms underlying PD pathogenesis, and much experimental work is available to explain PD pathogenesis through the involvement of α-synuclein, Parkin, PINK1, and DJ-1. However, the identification of mutations related to monogenic PD is beneficial clinically only in a small set of patients with positive family history and early onset of the disease or presenting with some complex phenotype in addition to parkinsonism. The incomplete penetrance and expressivity of these mutations and the fact that some PARK loci are just indicative of PD susceptibility, genetic counseling, or routine genetic testing of all persons having a positive family history of PD is not recommended. As far as the vast majority of sporadic PD cases are concerned, the identification of susceptibility variants or heterozygous mutations of familial PD genes holds some promise for the future development of a genetic biomarker for PD, but for this, many large-scale statistically powered GWAS or other kinds of analyses would be necessary.

Biochemical Biomarkers

The biochemical biomarkers for PD include a broad range of molecules that have been analyzed in CSF, blood, or other biological fluids. These include dopamine and its catabolites, several other types of amine or amino acid neurotransmitters, neuropeptides, oxidative damage markers, purine catabolite like uric acid, inflammatory markers, neurotrophic factors like brain-derived neurotrophic factor (BDNF), microRNAs, and several proteins known to be associated with the pathogenesis of PD and other neurodegenerative disorders, and all these have been discussed elaborately in multiple reviews and meta-analyses (Jiménez-Jiménez et al., 2014; Emamzadeh and Surguchov, 2018; He et al., 2018; Wei et al., 2018; Jiang L. et al., 2019; Katayama et al., 2020). To avoid repetition and because no clinically useful blood or CSF biochemical biomarker specific for PD is still available, we will only briefly discuss a few of these biomarkers. Oxidative stress and inflammatory markers, are not specific for PD and are usually altered in multiple other neurological diseases where oxidative damage and inflammation are involved in the disease pathogenesis. BDNF, a member of the neurotrophin family, is an important regulator of neuronal differentiation, proliferation, and survival, and in several experimental models of PD, the neuroprotective role of BDNF was earlier demonstrated (Palasz et al., 2020). However, the alterations in BDNF levels in CSF and blood in PD patients as reported in multiple studies are complex and inconsistent, and its biomarker potential in this disorder is not established (Nagatsu et al., 2000; Salehi and Mashayekhi, 2009; Ventriglia et al., 2013; Jiang L. et al., 2019). The purine derivative and the potent antioxidant uric acid (measured both in the serum and CSF) have been explored as a candidate risk factor and a diagnostic and prognostic biomarker for PD (Cipriani et al., 2010; Paganoni and Schwarzschild, 2017). A meta-analysis of eligible studies on serum uric acid level as a diagnostic biomarker has shown that PD is associated with a low uric acid level in serum (Wen et al., 2017). Dopamine and its catabolites like dihydroxy phenylacetic acid (DOPAC) and homovanillic acid (HVA) in CSF have been analyzed for a long time to assess the loss of central dopaminergic functions and to correlate it with the motor impairment in PD. The CSF levels of HVA and DOPAC were reported to be elevated in PD patients at early stages, and the values increased further with the degree of motor impairment (Stefani et al., 2017). In contrast, a recent follow-up study showed that subjects with several PD-related risk factors had a higher chance of being afflicted with the disease if their baseline CSF levels of dopamine and DOPAC were low (Goldstein et al., 2018). In another study, the CSF level of HVA could not differentiate PD patients from the controls, but the ratio of xanthine/HVA clearly separated the two groups (LeWitt et al., 2011). However, many earlier studies reported a decline in CSF HVA levels in PD, and these studies as well as the changes in serotonin catabolites in PD have been well-reviewed elsewhere (Jiménez-Jiménez et al., 2014).

Metabolomics has opened up new avenues of research in biomarker identification for pathological conditions. In this approach, instead of a hypothesis-driven targeted search for a biochemical biomarker for disease, complete profiles of the metabolites are compared between the control and diseased subjects employing primarily a liquid chromatography-mass spectrometry (LC-MS) based separation-detection system. Multiple studies have adopted this approach using blood or CSF to identify sets of molecules to distinguish PD from control subjects. These metabolites are sugars, fatty acids, amino acids, peptides or molecules related to phosphoglyceride and sphingolipid metabolism, amino acid metabolism, mitochondrial functions, energy metabolism, and glutathione metabolism (Trupp et al., 2014; Wuolikainen et al., 2016; Stoessel et al., 2018; Willkommen et al., 2018; Zhao et al., 2018). Although a promising approach, a metabolomics-based search for a set of definitive and clinically useful biomarkers for the diagnosis of PD is yet to be achieved.

Identifying protein biomarkers of PD from familial PD gene products, which could help in the diagnosis or prognostic evaluation of the disease, forms an important area of PD research, and in this context, we will focus our attention on α-synuclein.

TABLE 1 | Biomarkers in Parkinson's disease (PD).

Biomarker	Techniques used	Targets analysed	Advantages	Limitations
Imaging biomarkers	Magnetic resonance imaging (MRI), transcranial sonography (TCS), single-photon emission computed tomography (SPECT), positron emission tomography (PET)	Dopamine transporter (DAT), vesicular monoamine transporter (VMAT), post-synaptic dopamine receptors, aromatic amino acid decarboxylase activity, accumulation of proteins (α-synuclein, tau), iron, etc.	Non-invasive. Good supportive evidence for diagnosis. ^{18}F-DOPA PET scan and ^{18}F-FDG PET scan showing great promise as diagnostic tools.	No unique biomarker found yet. Expensive and may not be easily available.
Genetic biomarkers	Linkage analysis Exome sequencing Genome-wide association studies (GWAS)	Mutations in genes and susceptibility loci in chromosomes (PARK family)	Confirmation of genetic nature of PD in patients with positive family history or with an early onset of the disease or having a complex phenotype in addition to PD.	Useful only for a small subset of PD patients. Due to incomplete penetrance and expressivity of the mutations, the genetic testing/counseling not recommended routinely.
Biochemical markers	HPLC, immuno-assays, biochemical assays, immuno-blotting, immuno-histochemistry, LC-MS	Dopamine metabolites (DOPAC, HVA), oxidative damage markers, inflammatory markers, miscellaneous markers (amino acid derivatives, uric acid, BDNF, peptides, miRNAs) Metabolomic profile, Protein markers (α-synuclein, LRRK2, DJ-1, tau, etc.)	Some markers can be assessed in easily accessible biofluids or tissues. Automated assays for a large number of samples possible in many cases. Some markers are related to disease pathogenesis directly. α-Synuclein is a promising protein biomarker. Metabolomic profiling could become an emerging technique.	Some biomarkers like oxidative damage or inflammatory markers are non-specific. Others like uric acid not directly related to pathology. No single unique biomarker is still available.

BDNF, brain-derived neurotrophic factor; DA, dopamine; DOPAC, dihydroxy phenyl acetic acid; HPLC, high performance liquid chromatography; HVA, homovanillic acid; LC-MS, liquid chromatography-mass spectrometry; LRRK2, leucine rich repeat kinase-2; ^{18}F-DOPA, ^{18}F-labeled L-6-fluoro-3,4-dihydroxyphenylalanine; ^{18}F-FDG, ^{18}F-labeled 2-deoxy-2-fluoro-D-glucose.

Table 1 summarizes the different types of PD biomarkers with their advantages and limitations.

α-SYNUCLEIN AS A BIOMARKER

Because of the involvement of α-synuclein in PD pathogenesis and its presence in the CSF, blood, and other body fluids, the biomarker potential of this protein has been examined extensively in PD as well as other synucleinopathies. However, α-synuclein is expressed by many different tissues, and there is a bi-directional movement of this protein between blood and the brain (Sui et al., 2014). Thus, it may be difficult to interpret if the alterations in the levels of α-synuclein in body fluids reflect PD pathology in the brain. Additionally, the protein can exist in monomeric and multiple oligomeric forms as well as post-translationally modified forms which can add to the complexity of measurement of this protein.

α-Synuclein in Cerebrospinal Fluid (CSF)

The CSF is an ideal body fluid to look for PD biomarkers as it is expected to provide the metabolic-pathological profile of the CNS. Multiple studies have investigated the alterations in the levels of α-synuclein in the CSF, but the results are varied. While many studies have reported a lower mean total α-synuclein in CSF of PD patients with respect to age-matched controls or other neurological controls, a few studies failed to find any significant difference between the PD and control groups (Tokuda et al., 2006; Mollenhauer et al., 2008, 2011, 2013; Ohrfelt et al., 2009; Hong et al., 2010; Park et al., 2011; Parnetti et al., 2011; Shi et al., 2011; Hall et al., 2012; Toledo et al., 2013; van Dijk et al., 2013; Hansson et al., 2014; Wennström et al., 2013). Most studies, systematic reviews, and meta-analyses which examined the validity of α-synuclein in the CSF as a putative biomarker for PD emphasized that a decreased level of α-synuclein in CSF reliably separated PD from control subjects, but the specificity of this measurement was low (Mollenhauer et al., 2011, 2013; Aerts et al., 2012; Gao et al., 2015; Zhou et al., 2015; Chahine et al., 2020). Further, in the differential diagnosis of PD from other movement disorders like MSA, progressive supranuclear palsy, corticobasal degeneration, and vascular parkinsonism, the utility of α-synuclein in CSF as a single biomarker is not established (Aerts et al., 2012; Gao et al., 2015; Zhou et al., 2015). Other workers attempted to measure oligomeric α-synuclein in CSF to examine its suitability as a biomarker for PD. Thus, increased levels of α-synuclein oligomers (o-α-syn) in CSF have been reported in PD with dementia compared to age-matched controls. Similarly, others have reported decreased levels of α-synuclein, raised levels of o-α-syn and increased o-α-syn/total α-synuclein ratio in the CSF of PD patients compared to that in age-matched control subjects or various non-PD neurological controls (Tokuda et al., 2010; Hansson et al., 2014; Park et al., 2011; Parnetti et al., 2014a,b; van Steenoven et al., 2018). Combined measurements of the ratios of o-α-synuclein/total α-synuclein and β-glucocerebrosidase activity or Aβ42/total-tau improved the specificity of PD diagnosis (Parnetti et al., 2014a,b). Likewise, the ratio of tau to α-synuclein in CSF has been claimed to be of high specificity in distinguishing PD from other parkinsonian syndromes or neurological controls (Parnetti et al., 2011; Heegaard et al., 2014). The measurement of CSF

α-synuclein in combination with FMS-like tyrosine kinase 3 ligand (FLT3L) or the percentage phosphorylated tau (p-tau) clearly distinguished PD from MSA in a study (Shi et al., 2011). A recent study employed single-molecule array (Simoa), an ultra-sensitive technology, to quantitate very low concentrations (picomolar to femtomolar) of α-synuclein protofibrils (PFs) in CSF of PD patients and observed an increased concentration of α-synuclein PFs in PD patients (von Euler Chelpin et al., 2020). The increased baseline level of misfolded α-synuclein aggregate in CSF (measured by protein misfolding cyclic amplification technique) has been reported in a follow-up study as a risk factor for the development of dementia in PD (Ning et al., 2019). These varied α-synuclein levels and forms in PD patients reported by various study groups might be the result of changes in the secretion, solubility, and aggregation of the protein, thereby affecting its overall turnover.

Post-translational modifications of α-synuclein affect its solubility and make it prone to aggregation. The most common pathological post-translational modification of α-synuclein is phosphorylation, particularly at Ser129. Phosphorylated α-synuclein (pS129) has been identified in CSF by mass spectrometry. A cross-sectional study reported higher pS129 in PD patients compared to healthy controls or MSA or PSP; the ratio of pS129/total α-synuclein is significantly higher in PD than in healthy controls or PSP (Wang Y. et al., 2012). Unlike the CSF levels of total α-synuclein, the levels of pS129 have a weak correlation with PD severity (Wang Y. et al., 2012). A study by the same group in the longitudinal DATATOP cohort (deprenyl and tocopherol antioxidative therapy of Parkinsonism) which included individuals with early PD in a placebo-controlled clinical trial reported increased CSF pS129 and pS129/total α-synuclein ratio over 2 years of disease progression (Stewart et al., 2015). Another important study corroborated the earlier findings of decreased α-synuclein and elevated levels of o-α-syn and pS129 in CSF in PD than that in controls, and further demonstrated that the combined measurements of o-α-syn/total α-synuclein and pS129/total α-synuclein could clearly improve the discrimination of PD from controls (Majbour et al., 2016). However, this study did not find any correlation of the CSF level of pS129 with the severity of PD and instead showed a modest inverse correlation with o-α-syn levels with the latter.

Although CSF appears to be an ideal body fluid to look for PD biomarkers, as it is in direct contact with the brain and the spinal cord, it may be mentioned that the process of obtaining CSF involves an invasive, painful procedure requiring skilled staff, and there may be additional technical and ethical issues related to CSF collection for a particular disease.

α-Synuclein as a Blood Biomarker of PD

The easy accessibility of blood makes it an important body fluid to monitor biomarker levels of disease for diagnostic or prognostic evaluation. α-Synuclein levels have been examined in plasma, serum, erythrocytes, and even in peripheral blood mononuclear cells in PD. The level of α-synuclein in plasma exceeds many times that of CSF, and the major source of plasma or serum α-synuclein is the erythrocytes (Barbour et al., 2008). In familial PD patients with SNCA multiplications, high levels of α-synuclein in blood were reported (Miller et al., 2004). One recent case-control study reported increased levels of α-synuclein in the peripheral circulation (plasma and serum) in PD with respect to age-matched healthy controls, and further, the serum levels correlated with the clinical severity of the disease (Chang et al., 2020). Other studies also observed increased levels of α-synuclein in the plasma of PD patients than that in controls, but the correlation of this parameter with the degree of motor disability was variably reported (Lee et al., 2006; Ding et al., 2017; Lin et al., 2017; Wang et al., 2019). A small study with 34 PD patients and 27 controls earlier reported an increased plasma level of soluble oligomeric α-synuclein in the patients' group (El-Agnaf et al., 2006). However, several other studies either showed decreased levels of α-synuclein in plasma in PD subjects than that in controls or failed to observe any significant difference in this parameter between the two groups (Li et al., 2007; Shi et al., 2010). In a longitudinal study, PD patients were followed for up to 20 years after initial presentations and plasma total α-synuclein and phosphorylated α-synuclein or pS129 were measured repeatedly (Foulds et al., 2013). Plasma levels of pS129 but not total α-synuclein were higher in PD subjects compared to healthy controls on the first presentation, but during the follow-up period of the PD patients, the levels of total α-synuclein in the plasma increased and that of pS129 remained unaltered (Foulds et al., 2013). These somewhat inconsistent results could be due to technical reasons such as contamination from erythrocyte α-synuclein as a result of hemolysis, different assay techniques employed, and the differential ability of the antibodies to bind to different forms of α-synuclein. In contrast to such studies, attempts have been made to validate the biomarker potential of erythrocyte α-synuclein in PD. In a recent extensive study, total and aggregated α-synuclein and also pS129 were separately measured in the membrane, and cytosolic fractions of erythrocytes; significantly increased levels of total and aggregated α-synuclein in the membrane fraction and remarkably high levels of pS129 in cytosolic fraction were observed in PD cases in comparison to that in healthy controls (Tian et al., 2019). Likewise, another large study of 334 healthy controls, 333 PD and 114 MSA patients, erythrocyte α-synuclein oligomers or o-α-syn were found to be much elevated in PD patients compared to that in other two groups, and apparently, this measurement could differentiate PD patients from control or MSA subjects with good sensitivity and specificity (Li et al., 2019). This study further showed in rat models that an increase in erythrocyte o-α-syn reflected an increased brain level of α-synuclein. An increased level of erythrocyte α-synuclein with respect to healthy controls was also reported in PD patients in another study which, however, showed that higher plasma levels of α-synuclein in PD than controls had better positive predictive value and stronger correlation with disease severity than erythrocyte α-synuclein levels (Wang et al., 2019). The erythrocyte levels of α-synuclein dimers were higher in idiopathic PD and those with GBA mutations than in age and sex-matched controls (Papagiannakis et al., 2018). Likewise, a decreased ratio of total to proteinase K resistant α-synuclein (phospholipid-bound α-synuclein) in red blood cells was shown to discriminate PD patients from healthy controls (Abd-Elhadi et al., 2015). The same group in a later study measured

multiple forms of α-synuclein consisting of total α-synuclein, proteinase-K resistant α-synuclein, oxidized α-synuclein, and pS129 and demonstrated that the higher levels of total and proteinase K resistant α-synuclein and pS129 differentiated PD patients with motor symptoms (without dementia) from healthy controls with a high degree of accuracy (Abd-Elhadi et al., 2019). On the other hand, a recent study estimated the levels of total α-synuclein, o-α-syn, total-tau, phosphorylated tau, α-synuclein-amyloid β42 complex, and α-synuclein-tau complex in red blood cells of PD patients; decreased total α-synuclein and increased levels of o-α-syn, phosphorylated-tau, and α-synuclein-amyloid β42 complex were observed in PD subjects with respect to controls (Daniele et al., 2018). This study also suggested that the level of α-synuclein-amyloid β42 complex in red blood cells correlated well with the degree of disease severity. Another extensive study detected different post-translationally modified α-synuclein in the lysate of red blood cells such as different types of phosphorylated α-synuclein apart from pS129, nitrated or glycated or small ubiquitin-like modifier or SUMO-ylated α-synuclein, and showed that phosphorylated, nitrated, and glycated α-synucleins were elevated and SUMO-ylated α-synuclein was decreased in PD patients with respect to that in controls (Miranda et al., 2017).

α-Synuclein in oligomerized or aggregated form is known to be released outside from the neurons packed in extracellular vesicles (EVs), and such EVs may be responsible for the neuron-to-neuron transfer of α-synuclein and the spread of PD pathogenesis in the brain (Lööv et al., 2016; Yu et al., 2020). The EVs from the brain likewise may carry toxic oligomeric α-synuclein to the peripheral circulation, and some studies examined the biomarker potential of EV-α-synuclein in blood (Vandendriessche et al., 2020; Yu et al., 2020). For the latter purpose, α-synuclein present in neuron-derived EVs, positive for neuronal cell adhesion molecule LCAM1, were analyzed (Lööv et al., 2016; Vandendriessche et al., 2020). Thus, a large study measured α-synuclein content in plasma as well as in LCAM1 positive EVs isolated from the blood of 267 PD and 215 controls; the plasma levels of α-synuclein did not differ in the groups, but LCAM1 positive EV-α-synuclein was significantly higher in the PD cases compared to that in the controls (Shi et al., 2014). Similarly, increased α-synuclein content of neuron-derived EVs in serum of PD patients could differentiate them from the controls not only in the presence of motor deficits but even during the prodromal phase (Jiang et al., 2020). The authors further showed that simultaneous measurements of α-synuclein and clusterin in neuron-derived EVs could distinguish PD from several other parkinsonian disorders.

α-Synuclein in Saliva

α-Synuclein has been detected in the saliva of PD patients. A decrease in the level of total α-synuclein in the saliva of PD patients in comparison to controls has been reported from several studies (Devic et al., 2011; Al-Nimer et al., 2014). Vivacqua et al. (2016) reported a significant increase in o-α-syn and o-α-syn/total α-synuclein ratio, but a decreased level of total α-synuclein in the saliva of PD patients. The authors suggested that the decrease in total α-synuclein in saliva in PD subjects could partly be accounted for by the oligomerization of monomeric α-synuclein. Similar findings were reported by Shaheen et al. (2020), which also showed a positive correlation between the level of o-α-syn and disease duration; further, in PD patients, higher levels of o-α-syn were seen in bradykinesia and rigidity-dominant than in tremor-dominant phenotypes. Another study measured the salivary total α-synuclein and o-α-syn between controls and PD cases and analyzed single nucleotide polymorphisms or SNP variants of *SNCA* in the PD group (Kang et al., 2016). The study failed to observe any significant difference in salivary total α-synuclein level between the PD and healthy control groups, but the o-α-syn level was significantly higher in the PD group. This study further showed that salivary level of total α-synuclein decreased with age with no correlation with disease duration or severity but depended upon the SNP variant of *SNCA* (Kang et al., 2016). A meta-analysis of existing studies on salivary α-synuclein as a biomarker for PD concluded that the association of increased o-α-syn in saliva with PD looks significant, but no such association with PD could be established for salivary total α-synuclein (Bougea et al., 2019). In various other tissues like the enteric nervous system, retina, and skin, α-synucleinopathy is being investigated vigorously to understand various non-motors features of PD and overall pathology of the disease, but the biomarker implications of these studies are not clear at this moment

α-Synuclein in Skin

Wang et al. (2013) compared the deposition of α-synuclein in the cutaneous nerves between PD patients and healthy controls. The study reported increased deposits of α-synuclein, detected by immunohistochemistry followed by confocal imaging, in the cutaneous sympathetic nerves (both cholinergic and adrenergic) in PD subjects with higher deposition observed in the advanced cases of the disease and with more autonomic dysfunction. In a similar study, Gibbons et al. (2016) reported a higher deposit of α-synuclein in the skin biopsy samples of PD patients than control subjects with a greater deposition in patients of more severity or longer duration or with autonomic dysfunction. The authors further observed that α-synuclein deposition was more in sympathetic adrenergic fibers than in cholinergic ones. In a recent study, the oligomeric form of α-synuclein or o-α-syn was detected for the first time in autonomic nerve terminals in skin biopsy samples using a proximity ligation assay; a significantly higher deposition of o-α-syn was seen in 38 consecutive PD patients in comparison to 29 consecutive healthy controls (Mazzetti et al., 2020). Interestingly, the authors of this study further analyzed o-α-syn deposition in skin biopsy samples of 19 pairs of monozygotic twins discordant for PD. Within this cohort of twins, a higher deposition of o-α-syn was noticed in PD patients.

Several studies demonstrated the deposition of pS129 in the cutaneous nerves in PD subjects in comparison to that in control subjects (Donadio et al., 2014, 2016). Zange et al. (2015) demonstrated that deposition of pS129 in skin sympathetic nerve fibers could distinguish PD from patients of MSA and essential tremor. Doppler et al. (2014) in their study observed the deposition of phosphorylated α-synuclein in skin nerve fibers in PD patients predominantly in autonomic nerves supplying

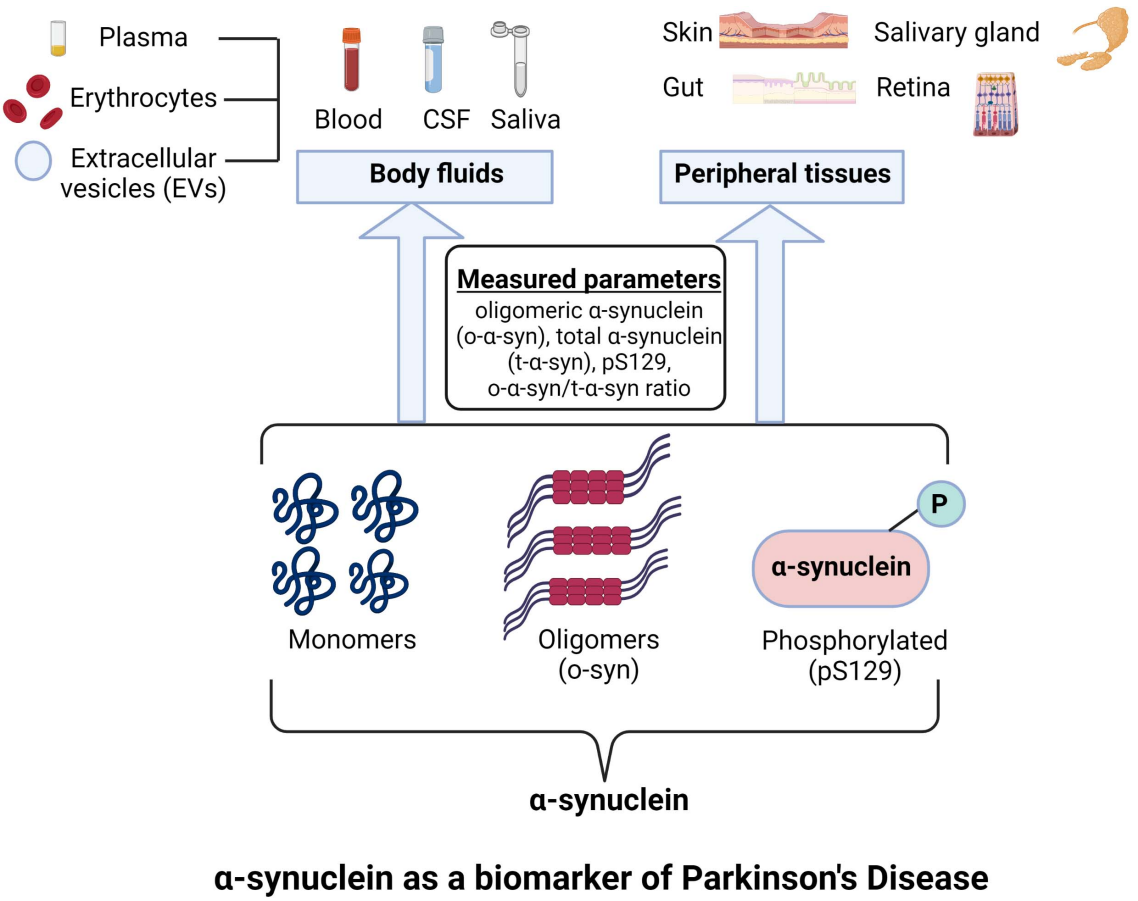


FIGURE 1 | Different forms of α-Synuclein as a prospective biomarkers in Parkinson's disease (PD). Image was created using BioRender.com.

blood vessels, erector pili muscles and sweat glands, but some deposition also occurred in somatosensory and other types of nerve fibers in the epidermis and dermis. This study suggested that the accumulation of phosphorylated α-synuclein caused peripheral neurodegeneration in PD. Another group utilized two new techniques, real-time quaking-induced conversion and protein misfolding cyclic amplification assays, to measure the aggregation-seeding activity of phosphorylatexd α-synuclein or pS129 in tissue samples (Wang et al., 2021). The authors then analyzed the aggregation-seeding activity of pS129 in autopsied skin samples from PD and non-PD control cadavers as well as skin biopsy samples from living PD patients and non-PD control subjects (Wang et al., 2021). A higher aggregation-seeding activity of pS129 was seen in skin samples from PD than that in non-PD controls in this study.

α-Synuclein in the Enteric Nervous System (ENS)

Most PD patients exhibit non-motor symptoms, including autonomic dysfunction of the gastrointestinal tract. The detection of LBs in the ENS of PD patients was made very early (Qualman et al., 1984). They identified these inclusions in the esophagus and colon of two PD patients with dysphagia (Qualman et al., 1984). Wakabayashi et al. (1988, 1990) reported in several publications the presence of LBs in Auerbach's and Meissner's plexuses and paravertebral and coeliac sympathetic ganglia in the human ENS. Other studies further confirmed the accumulation and aggregation of α-synuclein in the gut mucosa of PD patients (Braak et al., 2006; Lebouvier et al., 2010; Gold et al., 2013; Sánchez-Ferro et al., 2014). The aggregates of α-synuclein in the gastro-intestinal mucosa also contained a significant amount of the phosphorylated protein (Lebouvier et al., 2010; Barrenschee et al., 2017; Beck et al., 2020). A large-scale study demonstrated the accumulation of α-synuclein in mucosal biopsy samples from the gastrointestinal tract in the pre-motor phase of PD (Hilton et al., 2013). The aggregation of α-synuclein in ENS could be responsible for the enteric abnormality observed in clinical PD cases. It also strengthens the hypothesis that PD may begin peripherally in the gut wall and then proceed toward the central nervous system. As a diagnostic biomarker of PD, the identification of α-synuclein pathology in mucosal biopsy samples from the gastrointestinal tract could be important as well. α-Synuclein aggregates are frequent and of a higher degree in PD patients as compared to age-matched healthy controls (Lebouvier et al.,

2010; Forsyth et al., 2011; Shannon et al., 2012; Gold et al., 2013; Sánchez-Ferro et al., 2014; Yan et al., 2018). However, other studies with enteric tissue biopsy samples identified α-synuclein immunoreactivity in normal aged persons or could not find any difference in α-synuclein accumulation between PD patients and controls or observed increased immunoreactivity of phosphorylated but not total α-synuclein in PD subjects (Böttner et al., 2012; Chung et al., 2015; Lee et al., 2018; Beck et al., 2020). Another retrospective study with post-mortem gastro-intestinal mucosal samples of PD patients and controls even claimed decreased deposition of α-synuclein and pS129 in PD subjects (Harapan et al., 2020). In fact, there are multiple problems of using α-synuclein pathology in mucosal biopsies from the gastrointestinal tract in the diagnosis of PD (Visanji et al., 2013; Chung et al., 2015). Further, the content of mucosal α-synuclein in the gastrointestinal tract in sporadic PD patients was claimed to vary with *SNCA* variants present in those subjects (Chung et al., 2019). Nevertheless, a recent systematic review and meta-analysis confirmed a strong association between gut α-synuclein and PD (Bu et al., 2019).

The accumulation of α-synuclein in neural structures within the submandibular gland in PD was demonstrated in multiple studies showing a good degree of consistency. Del Tredici et al. (2010) analyzed the deposition of α-synuclein immunohistochemically in the submandibular gland and anatomically related sympathetic nerves and ganglion as well as the vagal nerve in autopsy study. The study included pathologically confirmed 9 PD patients, 19 controls, and some patients of MSA and incidental Lewy body disease. α-Synuclein immunoreactivity was observed in tissue samples in nearly all cases of PD, but none in the control or MSA subjects (Del Tredici et al., 2010). However, in a recent study of 59 cases of PD (early, moderate and advanced) and 21 healthy controls, biopsies from the submandibular gland showed immuno-reactivity to α-synuclein with a specific monoclonal antibody only in 56.1% cases but with 100% specificity (Chahine et al., 2020). Another study demonstrated that in the submandibular gland total α-synuclein (measured by a sensitive laser-based immuno-assay) in PD cases was similar to that in controls. However, the oligomeric form of α-synuclein (o-α-syn) content (measured by gel filtration followed by immuno-blotting) was higher in PD cases than in controls (Kang et al., 2016). This study further showed that total α-synuclein content in submandibular salivary gland tissue in PD cases varied with specific *SNCA* variants present in the patients. In a couple of studies, Beach and his group showed that immunoreactive pS129 was present conspicuously in submandibular salivary gland tissue collected from autopsied persons in a high percentage of PD cases that were absent in controls (Beach et al., 2013, 2016). The studies considered only the immunoreactive α-synuclein in nerve fibers within the salivary gland, and apart from PD cases, pS129 immunoreactivity was also present in a significant percentage of Lewy body dementia cases. Real-time quaking-induced conversion assay with the post-mortem submandibular salivary gland tissue (kept frozen or as paraffin-embedded tissue sections) reported a higher aggregation-seeding activity of pS129 in all cases of PD compared to control (Manne et al., 2020).

α-Synuclein in Retina

Endogenous α-synuclein is present in all three different layers but predominantly in the inner plexiform layer in the retina (Surguchov et al., 2001; Beach et al., 2014). Visual problems and structural alterations in the retina in PD are being investigated intensively especially with techniques like optical coherence tomography (OCT), electroretinography (ERG), and visual evoked potentials (VEP) (Indrieri et al., 2020). The visual alterations in PD could be linked to α-synucleinopathy in the retina, which may also reflect the PD pathology in the brain (Veys et al., 2019; Indrieri et al., 2020). Many animal models of PD develop α-synucleinopathy in the retina (Price et al., 2016; Mammadova et al., 2019). From the point of view of the biomarker potential of retinal α-synuclein in PD, only limited information is available. Bodis-Wollner et al. (2014) reported the existence of α-synuclein aggregates in the retina of patients with PD and implicated their role in impaired vision and retinal morphology in the latter condition. Beach et al. (2014) also reported the presence of pS129 in the nerve fibers at the inner retinal surface in PD in contrast to controls. Likewise, in another study, pS129 immunoreactivity was reported in the retina in PD patients but not in controls; the deposits of pS129 appearing like LBs and LNs were observed in ganglion cells in perikarya as well as axonal and dendritic processes (Ortuño-Lizarán et al., 2018). This study mentioned that α-synuclein immunoreactivity in the retina was similar in control and PD subjects. On the other hand, another group used enucleated eyes at autopsy and observed α-synuclein immunoreactivity in the retina both in PD patients (67%) and controls (50%) without any indication of LBs and LNs in the patients (Ho et al., 2014). **Figure 1** schematically summarizes the different forms of α-synuclein in biofluids and peripheral tissues studied to date as prospective biomarkers in PD.

CONCLUSION AND FUTURE DIRECTION

It is evident from the present discussion that though α-synuclein is a promising biomarker candidate, its specificity as a single diagnostic or prognostic biomarker of PD is far from established in any of the biological fluids or peripheral tissues. Some obvious reasons for this failure lie in the significant degree of inconsistencies among different studies, small sample sizes in predominantly cross-sectional studies, recruitment of patients with different degrees of disease severity and duration in different studies, and lack of participation of early PD patients in most studies. In addition, most studies compared PD with healthy controls or neurological controls but did not compare PD with other parkinsonian disorders or other kinds of movement disorders that may be confused with PD.

The technical issues of α-synuclein measurements in biological fluids are also very serious in the context of the variability of results in different studies. The chances of contamination of CSF with blood or that of plasma and serum with lysed red blood cells cannot be ignored. More serious could be the variations in immuno-assays, immuno-blotting methods, and various other purification procedures adopted

by the different groups. α-Synuclein exists in monomeric and different types of oligomeric forms as well as in different post-translationally modified forms, and it is not known with what efficacy the antibody to one form of α-synuclein (supplied by the commercial manufacturers or produced in the lab by different groups) cross-reacts with other forms of α-synuclein in a particular assay. This could add serious errors to the measurement, making comparisons difficult among different studies. As already indicated, SNCA variants can result in different amounts of α-synuclein in different PD subjects, which might have also contributed to differences between the two studies. Further, most studies did not mention the storage of biological samples (time period and temperature of storage) before immunoassays were performed. Further, the effect of storage on the conversion of monomeric to different oligomeric forms or the stability of post-translationally modified forms of α-synuclein were also not analyzed. In other words, properly validated immunoassay methods are paramount in establishing the biomarker role of α-synuclein in PD. Likewise, for the peripheral tissue α-synuclein, the variations in immunohistochemical techniques and the lack of knowledge on different forms of α-synuclein present in the tissue in normal and pathological conditions and the limited number of commercially available antibodies are the major concerns. In most publications with tissue α-synuclein, the presence of immuno-reactivity to α-synuclein or pS129 was thought to indicate LB pathology without ascertaining the oligomeric state of α-synuclein present in the tissue.

Having discussed these limitations, we can say that measurements of o-α-syn, total α-synuclein, pS129 with or without total tau in CSF or red blood cell lysate or the saliva could be important in finally developing a good biomarker for PD. Future studies should focus more on red blood cell lysate and saliva in this regard. Likewise, the measurement of total α-synuclein in neuron-derived EVs may be equally promising in this context. For tissue α-synuclein and its oligomers, the skin biopsy studies, though limited in number, so far have provided consistent results. Further, a skin biopsy is a minimally invasive procedure that would be acceptable to PD patients. So the assessment of α-synuclein deposition in cutaneous nerve fibers in skin biopsy specimens in PD patients may emerge as a future diagnostic method. The same may be said for submandibular salivary gland α-synuclein in PD cases where the published results are very consistent, and thus larger studies should be conducted in the future with needle biopsy specimens from this gland. It may be equally important to use dyes like Thioflavin-S, which can bind to α-synuclein oligomers to give rise to fluorescent products that could be detectable under a fluorescence microscope. This can provide better information on the oligomeric state of α-synuclein in peripheral tissue. Intra-vitreal administration of Thioflavin S or a similar compound for visualization of fluorescent dye-bound α-synuclein aggregates in the retina, taking into consideration the toxicity angle, should be a future endeavor. Overall, it appears that establishing α-synuclein as a good biomarker for PD will require well-validated detection methods and larger clinical studies (cross-sectional and follow-up) with PD patients, patients of parkinsonian disorders, and non-parkinsonian movement disorders. The use of a combination of imaging biomarkers or other biochemical biomarkers along with α-synuclein for the diagnostic and prognostic evaluation of PD should also be explored more vigorously.

AUTHOR CONTRIBUTIONS

UG contributed to the conceptualization, writing, editing, and project management. SS and SoP contributed to the writing. SuP and BA contributed to the editing and supervision. RS contributed to the conceptualization, editing, and supervision. SC contributed to the conceptualization, writing, editing, supervision, and project management. All authors contributed to the article and approved the submitted version.

ACKNOWLEDGMENTS

The authors thank the management at Maharishi Markandeshwar University (Deemed to be) for their support in writing this review article.

REFERENCES

Abbas, M. M., Xu, Z., and Tan, L. C. S. (2018). Epidemiology of Parkinson's disease-east versus west. *Mov. Disord. Clin. Pract.* 4, 14–28. doi: 10.1002/mdc3.12568

Abd-Elhadi, S., Grigoletto, J., Poli, M., Arosio, P., Arkadir, D., and Sharon, R. (2019). α-Synuclein in blood cells differentiates Parkinson's disease from healthy controls. *Ann. Clin. Transl. Neurol.* 6, 2426–2436. doi: 10.1002/acn3.50944

Abd-Elhadi, S., Honig, A., Simhi-Haham, D., Schechter, M., Linetsky, E., Ben-Hur, T., et al. (2015). Total and proteinase K-Resistant α-Synuclein Levels in erythrocytes, determined by their ability to Bind Phospholipids, Associate with Parkinson's disease. *Sci. Rep.* 5:11120. doi: 10.1038/srep11120

Abou-Sleiman, P. M., Muqit, M. M. K., McDonald, M. Q., Yang, Y. X., Gandhi, S., Healy, D. G., et al. (2006). A heterozygous effect for PINK1 mutations in Parkinson's disease? *Ann. Neurol.* 60, 414–419. doi: 10.1002/ana.20960

Aerts, M. B., Esselink, R. A. J., Abdo, W. F., Bloem, B. R., and Verbeek, M. M. (2012). CSF α-synuclein does not differentiate between parkinsonian disorders. *Neurobiol. Aging* 33, 430.e1–430.e3. doi: 10.1016/j.neurobiolaging.2010.12.001

Alexander, G. E. (2004). Biology of Parkinson's disease: pathogenesis and pathophysiology of a multisystem neurodegenerative disorder. *Dialogues Clin. Neurosci.* 6, 259–280. doi: 10.31887/DCNS.2004.6.3/galexander

Al-Nimer, M. S. M., Mshatat, S., and Abdulla, H. I. (2014). Saliva α-synuclein and a high extinction coefficient protein: a novel approach in assessment biomarkers of Parkinson's disease. *N. Am. J. Med. Sci.* 6, 633–637. doi: 10.4103/1947-2714.147980

Arawaka, S., Sato, H., Sasaki, A., Koyama, S., and Kato, T. (2017). Mechanisms underlying extensive Ser129-phosphorylation in α-synuclein aggregates. *Acta Neuropathol. Commun.* 5:48. doi: 10.1186/s40478-017-0452-6

Ayala, A., Triviño-Juárez, J. M., Forjaz, M. J., Rodríguez-Blázquez, C., Rojo-Abuin, J. M., and Martínez-Martín, P. (2017). Parkinson's disease severity at 3 years can be predicted from non-motor symptoms at baseline. *Front. Neurol.* 8:551. doi: 10.3389/fneur.2017.00551

Ayton, S., and Lei, P. (2014). Nigral iron elevation is an invariable feature of Parkinson's disease and is a sufficient cause of neurodegeneration. *Biomed Res. Int.* 2014:581256. doi: 10.1155/2014/581256

Barbour, R., Kling, K., Anderson, J. P., Banducci, K., Cole, T., Linnea, D., et al. (2008). Red blood cells are the major source of alpha-synuclein in blood. *Neurodegener. Dis.* 5, 55–59. doi: 10.1159/000112832

Barrenschee, M., Zorenkov, D., Böttner, M., Lange, C., Cossais, F., Scharf, A. B., et al. (2017). Distinct pattern of enteric phospho-alpha-synuclein aggregates and gene expression profiles in patients with Parkinson's disease. *Acta Neuropathol. Commun.* 5:1. doi: 10.1186/s40478-016-0408-2

Beach, T. G., Adler, C. H., Dugger, B. N., Serrano, G., Hidalgo, J., Henry-Watson, J., et al. (2013). Submandibular gland biopsy for the diagnosis of Parkinson disease. *J. Neuropathol. Exp. Neurol.* 72, 130–136. doi: 10.1097/NEN.0b013e3182805c72

Beach, T. G., Adler, C. H., Serrano, G., Sue, L. I., Walker, D. G., Dugger, B. N., et al. (2016). Prevalence of submandibular gland synucleinopathy in Parkinson's disease, dementia with Lewy Bodies and other Lewy Body disorders. *J. Parkinsons Dis.* 6, 153–163. doi: 10.3233/JPD-150680

Beach, T. G., Carew, J., Serrano, G., Adler, C. H., Shill, H. A., Sue, L. I., et al. (2014). Phosphorylated α-synuclein-immunoreactive retinal neuronal elements in Parkinson's disease subjects. *Neurosci. Lett.* 571, 34–38. doi: 10.1016/j.neulet.2014.04.027

Beck, G., Hori, Y., Hayashi, Y., Morii, E., Takehara, T., and Mochizuki, H. (2020). Detection of phosphorylated Alpha-synuclein in the Muscularis propria of the gastrointestinal tract is a sensitive predictor for Parkinson's disease. *Parkinsons Dis.* 2020:4687530. doi: 10.1155/2020/4687530

Belarbi, K., Cuvelier, E., Destée, A., Gressier, B., and Chartier-Harlin, M. C. (2017). NADPH oxidases in Parkinson's disease: a systematic review. *Mol. Neurodegener.* 12:84. doi: 10.1186/s13024-017-0225-5

Bisaglia, M., Filograna, R., Beltramini, M., and Bubacco, L. (2014). Are dopamine derivatives implicated in the pathogenesis of Parkinson's disease? *Ageing Res. Rev.* 13, 107–114. doi: 10.1016/j.arr.2013.12.009

Bodis-Wollner, I., Kozlowski, P. B., Glazman, S., and Miri, S. (2014). α-synuclein in the inner retina in parkinson disease. *Ann. Neurol.* 75, 964–966. doi: 10.1002/ana.24182

Book, A., Guella, I., Candido, T., Brice, A., Hattori, N., Jeon, B., et al. (2018). A meta-analysis of α-synuclein multiplication in familial Parkinsonism. *Front. Neurol.* 9:1021. doi: 10.3389/fneur.2018.01021

Böttner, M., Zorenkov, D., Hellwig, I., Barrenschee, M., Harde, J., Fricke, T., et al. (2012). Expression pattern and localization of alpha-synuclein in the human enteric nervous system. *Neurobiol. Dis.* 48, 474–480. doi: 10.1016/j.nbd.2012.07.018

Bougea, A., Koros, C., and Stefanis, L. (2019). Salivary alpha-synuclein as a biomarker for Parkinson's disease: a systematic review. *J. Neural Transm.* 126, 1373–1382. doi: 10.1007/s00702-019-02062-4

Bouwmans, A. E. P., Vlaar, A. M. M., Mess, W. H., Kessels, A., and Weber, W. E. J. (2013). Specificity and sensitivity of transcranial sonography of the substantia nigra in the diagnosis of Parkinson's disease: prospective cohort study in 196 patients. *BMJ Open* 3:e002613. doi: 10.1136/bmjopen-2013-002613

Braak, H., de Vos, R. A. I., Bohl, J., and Del Tredici, K. (2006). Gastric alpha-synuclein immunoreactive inclusions in Meissner's and Auerbach's plexuses in cases staged for Parkinson's disease-related brain pathology. *Neurosci. Lett.* 396, 67–72. doi: 10.1016/j.neulet.2005.11.012

Braak, H., Ghebremedhin, E., Rub, U., Bratzke, H., and Del Tridici, K. (2004). Stages in the development of Parkinson's disease-related pathology. *Cell Tissue Res.* 318, 121–134. doi: 10.1007/s00441-004-0956-9

Breydo, L., Wu, J. W., and Uversky, V. N. (2012). A-synuclein misfolding and Parkinson's disease. *Biochim. Biophys. Acta* 1822, 261–285. doi: 10.1016/j.bbadis.2011.10.002

Brooks, D. J. (2016). Molecular imaging of dopamine transporters. *Ageing Res. Rev.* 30, 114–121. doi: 10.1016/j.arr.2015.12.009

Bu, J., Liu, J., Liu, K., and Wang, Z. (2019). Diagnostic utility of gut α-synuclein in Parkinson's disease: a systematic review and meta-analysis. *Brain Behav. Res.* 364, 340–347. doi: 10.1016/j.bbr.2019.02.039

Caggiu, E., Arru, G., Hosseini, S., Niegowska, M., Sechi, G. P., Zarbo, I. R., et al. (2019). Inflammation, infectious triggers, and Parkinson's disease. *Front. Neurol.* 10:122. doi: 10.3389/fneur.2019.00122

Calabria, F. F., Calabria, E., Gangemi, V., and Cascini, G. L. (2016). Current status and future challenges of brain imaging with (18)F-DOPA PET for movement disorders. *Hell. J. Nucl. Med.* 19, 33–41. doi: 10.1967/s002449910335

Chahine, L. M., Beach, T. G., Brumm, M. C., Adler, C. H., Coffey, C. H., Mosovsky, S., et al. (2020). In vivo distribution of α-synuclein in multiple tissues and biofluids in Parkinson disease. *Neurology* 95, e1267–e1284. doi: 10.1212/WNL.0000000000010404

Chang, C. W., Yang, S. Y., Yang, C. C., Chang, C. W., and Wu, Y. R. (2019). Plasma and serum Alpha-synuclein as a biomarker of diagnosis in patients with Parkinson's disease. *Front. Neurol.* 10:1388. doi: 10.3389/fneur.2019.01388

Chung, E., Choi, Y., Park, J., Nah, W., Park, J., Jung, Y., et al. (2020). Intracellular delivery of Parkin rescues neurons from accumulation of damaged mitochondria and pathological α-synuclein. *Sci. Adv.* 6:eaba1193. doi: 10.1126/sciadv.aba1193

Chung, S. J., Kim, J., Lee, H. J., Ryu, H. S., Kim, K., Lee, J. H., et al. (2015). Alpha-synuclein in gastric and colonic mucosa in Parkinson's disease: limited role as a biomarker. *Mov. Disord.* 31, 241–249. doi: 10.1002/mds.26473

Chung, S. J., Konig, I. R., Lohmann, K., Hinrichs, F., Kim, J., Ryu, H. S., et al. (2019). Association of SNCA variants with α-synuclein of gastric and colonic mucosa in Parkinson's disease. *Parkinsonism Relat. Disord.* 61, 151–155. doi: 10.1016/j.parkreldis.2018.10.028

Chung, S. Y., Kishinevsky, S., Mazzulli, J. R., Graziotto, J., Mrejeru, A., Mosharov, E. V., et al. (2016). Parkin and PINK1 Patient iPSC-Derived midbrain dopamine neurons exhibit mitochondrial dysfunction and α-Synuclein accumulation. *Stem Cell Rep.* 7, 664–677. doi: 10.1016/j.stemcr.2016.08.012

Cipriani, S., Chen, X., and Schwarzschild, M. A. (2010). Urate: a novel biomarker of Parkinson's disease risk, diagnosis and prognosis. *Biomark. Med.* 4, 701–712. doi: 10.2217/bmm.10.94

Daniele, S., Frosini, D., Pietrobono, D., Petrozzi, L., Lo Gerfo, A., Baldacci, F., et al. (2018). α-Synuclein Heterocomplexes with β-Amyloid are increased in red blood cells of Parkinson's disease patients and correlate with disease severity. *Front. Mol. Neurosci.* 11:53. doi: 10.3389/fnmol.2018.00053

Dawson, T. M., Seok Ko, H., and Dawson, V. L. (2010). Genetic animal models of Parkinson's disease. *Neuron* 66, 646–661. doi: 10.1016/j.neuron.2010.04.034

Dehay, B., and Fernagut, P. O. (2016). Alpha-synuclein-based models of Parkinson's disease. *Rev. Neurol.* 172, 371–378. doi: 10.1016/j.neurol.2016.04.003

Del Tredici, K., Hawkes, C. H., Ghebremedhin, E., and Braak, H. (2010). Lewy pathology in the submandibular gland of individuals with incidental Lewy body disease and sporadic Parkinson's disease. *Acta Neuropathol.* 119, 703–713. doi: 10.1007/s00401-010-0665-2

Devic, I., Hwang, H., Edgar, J. S., Izutsu, K., Presland, R., Pan, C., et al. (2011). Salivary α-synuclein and DJ-1: potential biomarkers for Parkinson's disease. *Brain* 134:e178. doi: 10.1093/brain/awr015

Dickson, D. W. (2012). Parkinson's disease and parkinsonism: neuropathology. *Cold Spring Harb. Perpect. Med.* 2:a009258. doi: 10.1101/cshperspect.a009258

Dilger, R. N., and Johnson, R. W. (2008). Aging, microglial cell priming, and the discordant central inflammatory response to signals from the peripheral immune system. *J. Leukoc. Biol.* 84, 932–939. doi: 10.1189/jlb.0208108

Ding, J., Zhang, J., Wang, X., Zhang, L., Jiang, S., Yuan, Y., et al. (2017). Relationship between the plasma levels of neurodegenerative proteins and motor subtypes of Parkinson's disease. *J. Neural Transm.* 124, 353–360. doi: 10.1007/s00702-016-1650-2

Do, J., McKinney, C., Sharma, P., and Sidransky, E. (2019). Glucocerebrosidase and its relevance to Parkinson disease. *Mol. Neurodegener.* 14:36. doi: 10.1186/s13024-019-0336-2

Donadio, V., Incensi, A., Leta, V., Giannoccaro, M. P., Scaglione, C., Martinelli, P., et al. (2014). Skin nerve α-synuclein deposits: a biomarker for idiopathic Parkinson disease. *Neurology* 82, 1362–1369. doi: 10.1212/WNL.0000000000000316

Donadio, V., Incensi, A., Piccinini, C., Cortelli, P., Giannocarro, M. P., Baruzzi, A., et al. (2016). Skin nerve misfolded α-synuclein in pure autonomic failure and Parkinson disease. *Ann. Neurol.* 79, 306–316. doi: 10.1002/ana.24567

Doppler, K., Ebert, S., Uceyler, N., Trenkwalder, C., Ebentheuer, J., Volkmann, J., et al. (2014). Cutaneous neuropathy in Parkinson's disease: a window into brain pathology. *Acta Neuropathol.* 128, 99–109. doi: 10.1007/s00401-014-1284-0

Ebrahimi-Fakhari, D., Cantuti-Castelvetri, I., Fan, Z., Rockenstein, E., Masliah, E., Hyman, B. T., et al. (2011). Distinct roles in vivo for the ubiquitin-proteasome system and the autophagy-lysosomal pathway in the degradation of α-synuclein. *J. Neurosci.* 31, 14508–14520. doi: 10.1523/JNEUROSCI.1560-11.2011

El-Agnaf, O. M. A., Salem, S. A., Paleologou, K. E., Curran, M. D., Gibson, M. J., Court, J. A., et al. (2006). Detection of oligomeric forms of alpha-synuclein protein in human plasma as a potential biomarker for Parkinson's disease. *FASEB J.* 20, 419–425. doi: 10.1096/fj.03-1449com

Emamzadeh, F. N., and Surguchov, A. (2018). Parkinson's disease: biomarkers, treatment, and risk factors. *Front. Neurosci.* 12:612. doi: 10.3389/fnins.2018.00612

Eriksen, J. L., Wszolek, Z., and Petrucelli, L. (2005). Molecular pathogenesis of Parkinson disease. *Arch. Neurol.* 62, 353–357. doi: 10.1001/archneur.62.3.353

Eschbach, J., Einem, B. V., Müller, K., Bayer, H., Scheffold, A., Morrison, B. E., et al. (2015). Mutual exacerbation of peroxisome proliferator-activated receptor γ coactivator 1α deregulation and α-synuclein oligomerization. *Ann. Neurol.* 77, 15–32. doi: 10.1002/ana.24294

Fields, C. R., Bengoa-Vergniory, N., and Wade-Martins, R. (2019). Targeting Alpha-synuclein as a therapy for Parkinson's disease. *Front. Mol. Neurosci.* 12:299. doi: 10.3389/fnmol.2019.00299

Forsyth, C. B., Shannon, K. M., Kordower, J. H., Voigt, R. M., Shaikh, M., Jaglin, J. A., et al. (2011). Increased intestinal permeability correlates with sigmoid mucosa alpha-synuclein staining and endotoxin exposure markers in early Parkinson's disease. *PLoS One* 6:e28032. doi: 10.1371/journal.pone.0028032

Foulds, P. G., Diggle, P., Mitchell, J. D., Parker, A., Hasegawa, M., Masuda-Suzukake, M., et al. (2013). A longitudinal study on α-synuclein in blood plasma as a biomarker for Parkinson's disease. *Sci. Rep.* 3:2540. doi: 10.1038/srep02540

Gandhi, S., Wood-Kaczmar, A., Yao, Z., Plun-Favreau, H., Deas, E., Klupsch, K., et al. (2009). PINK1-associated Parkinson's disease is caused by neuronal vulnerability to calcium-induced cell death. *Mol. Cell* 33, 627–638. doi: 10.1016/j.molcel.2009.02.013

Ganguly, G., Chakrabarti, S., Chatterjee, U., and Saso, L. (2017). Proteinopathy, oxidative stress and mitochondrial dysfunction: cross talk in Alzheimer's disease and Parkinson's disease. *Drug Des. Devel. Ther.* 11, 797–810. doi: 10.2147/DDDT.S130514

Ganguly, U., Banerjee, A., Chakrabarti, S. S., Kaur, U., Sen, O., Cappai, R., et al. (2020). Interaction of α-synuclein and Parkin in iron toxicity on SH-SY5Y cells: implications in the pathogenesis of Parkinson's disease. *Biochem. J.* 477, 1109–1122. doi: 10.1042/BCJ20190676

Ganguly, U., Chakrabarti, S. S., Kaur, U., Mukherjee, A., and Chakrabarti, S. (2018). Alpha-synuclein, proteotoxicity and Parkinson's disease: search for neuroprotective therapy. *Curr. Neuropharmacol.* 16, 1086–1097. doi: 10.2174/1570159X15666171129100944

Gao, L., Tang, H., Nie, K., Wang, L., Zhao, J., Gan, R., et al. (2015). Cerebrospinal fluid alpha-synuclein as a biomarker for Parkinson's disease diagnosis: a systematic review and meta-analysis. *Int. J. Neurosci.* 125, 645–654. doi: 10.3109/00207454.2014.961454

GBD 2016 Neurology Collaborators (2018). Global, regional, and national burden of Parkinson's disease, 1990–2016: a systematic analysis for the Global Burden of Disease Study 2016. *Lancet Neurol.* 17, 939–953. doi: 10.1016/S1474-4422(18)30295-3

Gibbons, C. H., Garcia, J., Wang, N., Shih, L. C., and Freeman, R. (2016). The diagnostic discrimination of cutaneous α-synuclein deposition in Parkinson disease. *Neurology* 87, 505–512. doi: 10.1212/WNL.0000000000002919

Giguère, N., Nanni, S. B., and Trudeau, L. E. (2018). On cell loss and selective vulnerability of neuronal populations in Parkinson's disease. *Front. Neurol.* 9:455. doi: 10.3389/fneur.2018.00455

Gold, A., Turkalp, Z. T., and Munoz, D. G. (2013). Enteric alpha-synuclein expression is increased in Parkinson's disease but not Alzheimer's disease. *Mov. Disord.* 28, 237–241. doi: 10.1002/mds.25298

Goldstein, D. S., Holmes, C., Lopez, G. J., Xu, T., and Sharabi, Y. (2018). Cerebrospinal fluid biomarkers of central dopamine deficiency predict Parkinson's disease. *Parkinsonism Relat. Disord.* 50, 108–112. doi: 10.1016/j.parkreldis.2018.02.023

Greenland, J. C., and Barker, R. A. (2018). *The Differential Diagnosis of Parkinson's Disease. Parkinson's Disease: Pathogenesis and Clinical Aspects [Internet]*. Brisbane: Codon Publications. doi: 10.15586/codonpublications.parkinsonsdisease.2018.ch6

Gubellini, P., and Kachidian, P. (2015). Animal models of Parkinson's disease: an updated overview. *Rev. Neurol.* 171, 750–761. doi: 10.1016/j.neurol.2015.07.011

Guo, J. D., Zhao, X., Li, Y., Li, G. R., and Liu, X. L. (2018). Damage to dopaminergic neurons by oxidative stress in Parkinson's disease (Review). *Int. J. Mol. Med.* 41, 1817–1825. doi: 10.3892/ijmm.2018.3406

Hall, S., Ohrfelt, A., Constantinescu, R., Andreasson, U., Surova, Y., Bostrom, F., et al. (2012). Accuracy of a panel of 5 cerebrospinal fluid biomarkers in the differential diagnosis of patients with dementia and/or parkinsonian disorders. *Arch. Neurol.* 69, 1445–1452. doi: 10.1001/archneurol.2012.1654

Hansson, O., Hall, S., Ohrfelt, A., Zetterberg, H., Blennow, K., Minthon, L., et al. (2014). Levels of cerebrospinal fluid α-synuclein oligomers are increased in Parkinson's disease with dementia and dementia with Lewy bodies compared to Alzheimer's disease. *Alzheimers Res. Ther.* 6:25. doi: 10.1186/alzrt255

Harapan, B. N., Frydrychowicz, C., Classen, J., Wittekind, C., Gradistanac, T., Rumpf, J. J., et al. (2020). No enhanced (p-) α-synuclein deposition in gastrointestinal tissue of Parkinson's disease patients. *Parkinsonism Relat. Disord.* 80, 82–88. doi: 10.1016/j.parkreldis.2020.08.020

Hartmann, A. (2004). Postmortem studies in Parkinson's disease. *Dialogues Clin. Neurosci.* 6, 281–293. doi: 10.31887/DCNS.2004.6.3/ahartmann

He, R., Yan, X., Guo, J., Xu, Q., Tang, B., and Sun, Q. (2018). Recent advances in biomarkers for Parkinson's disease. *Front. Aging Neurosci.* 10:305. doi: 10.3389/fnagi.2018.00305

He, S., Wang, F., Yung, K. K. L., Zhang, S., and Qu, S. (2021). Effects of α-Synuclein-associated post-translational modifications in Parkinson's disease. *ACS Chem. Neurosci.* 12, 1061–1071. doi: 10.1021/acschemneuro.1c00028

Heegaard, N. H. H., Tanassi, J. T., Bech, S., Salvesen, L., Lüttge, P., Montezinho, L. C. P., et al. (2014). Cerebrospinal fluid α-synuclein in the differential diagnosis of parkinsonian syndromes. *Future Neurol.* 9, 525–532. doi: 10.2217/fnl.14.51

Heeman, B., Haute, C. V. D., Aelvoet, S. A., Valsecchi, F., Rodenburg, R. J., Reumers, V., et al. (2011). Depletion of PINK1 affects mitochondrial metabolism, calcium homeostasis and energy maintenance. *J. Cell Sci.* 124, 1115–1125. doi: 10.1242/jcs.078303

Heman-Ackah, S. M., Manzano, R., Hoozemans, J. J. M., Scheper, W., Flynn, R., Haerty, W., et al. (2017). Alpha-synuclein induces the unfolded protein response in Parkinson's disease SNCA triplication iPSC-derived neurons. *Hum. Mol. Genet.* 26, 4441–4450. doi: 10.1093/hmg/ddx331

Hilton, D., Stephens, M., Kirk, L., Edwards, P., Potter, R., Zajicek, J., et al. (2013). Accumulation of α-synuclein in the bowel of patients in the pre-clinical phase of Parkinson's disease. *Acta Neuropathol.* 127, 234–241. doi: 10.1007/s00401-013-1214-6

Ho, C. Y., Troncosco, J. C., Knox, D., Stark, W., and Eberhart, C. G. (2014). Beta-amyloid, phospho-tau and alpha-synuclein deposits similar to those in the brain are not identified in the eyes of Alzheimer's and Parkinson's disease patients. *Brain Pathol.* 24, 25–32. doi: 10.1111/bpa.12070

Holmqvist, S., Chutna, O., Bousset, L., Aldrin-Kirk, P., Li, W., Björklund, T., et al. (2014). Direct evidence of Parkinson pathology spread from the gastrointestinal tract to the brain in rats. *Acta Neuropathol.* 128, 805–820. doi: 10.1007/s00401-014-1343-6

Hong, Z., Shi, M., Chung, K. A., Quinn, J. F., Peskind, E. R., Galasko, D., et al. (2010). DJ-1 and alpha-synuclein in human cerebrospinal fluid as biomarkers of Parkinson's disease. *Brain* 133, 713–726. doi: 10.1093/brain/awq008

Indrieri, A., Pizzarelli, R., Franco, B., and Leonibus, E. D. (2020). Dopamine, Alpha-synuclein, and mitochondrial dysfunctions in parkinsonian eyes. *Front. Neurosci.* 14:567129. doi: 10.3389/fnins.2020.567129

Irrcher, I., Aleyasin, H., Seifert, E. L., Hewitt, S. J., Chhabra, S., Phillips, M., et al. (2010). Loss of the Parkinson's disease-linked gene DJ-1 perturbs mitochondrial dynamics. *Hum. Mol. Genet.* 19, 3736–3746. doi: 10.1093/hmg/ddq288

Jackson-Lewis, V., Blesa, J., and Przedborski, S. (2012). Animal models of Parkinson's disease. *Parkinsonism Relat. Disord.* 18, 183–185. doi: 10.1016/S1353-8020(11)70057-8

Jana, S., Sinha, M., Chanda, D., Roy, T., Banerjee, K., Munshi, S., et al. (2011). Mitochondrial dysfunction mediated by quinone oxidation products of dopamine: implications in dopamine cytotoxicity and pathogenesis of Parkinson's disease. *Biochim. Biophys. Acta* 1812, 663–673. doi: 10.1016/j.bbadis.2011.02.013

Jankovic, J. (2008). Parkinson's disease: clinical features and diagnosis. *J. Neurol. Neurosurg. Psychiatry* 79, 368–376. doi: 10.1136/jnnp.2007.131045

Jellinger, K. A. (2019). Is Braak staging valid for all types of Parkinson's disease? *J. Neural Transm.* 126, 423–431. doi: 10.1007/s00702-018-1898-9

Jenner, P. (2003). Oxidative stress in Parkinson's disease. *Ann. Neurol.* 53, S26–S38. doi: 10.1002/ana.10483

Jiang, C., Hopfner, F., Katsikoudi, A., Hein, R., Catli, C., Evetts, S., et al. (2020). Serum neuronal exosomes predict and differentiate Parkinson's disease from atypical parkinsonism. *J. Neurol. Neurosurg. Psychiatry* 91, 720–729. doi: 10.1136/jnnp-2019-322588

Jiang, L., Zhang, H., Wang, C., Ming, F., Shi, X., and Yang, M. (2019). Serum level of brain-derived neurotrophic factor in Parkinson's disease: a meta-analysis. *Prog. Neuropsychopharmacol. Biol. Psychiatry.* 88, 168–174. doi: 10.1016/j.pnpbp.2018.07.010

Jiang, X., Jin, T., Zhang, H., Miao, J., Zhao, X., Su, Y., et al. (2019). Current progress of mitochondrial quality control pathways underlying the pathogenesis of Parkinson's disease. *Oxid. Med. Cell. Longev.* 2019:4578462. doi: 10.1155/2019/4578462

Jiménez-Jiménez, F. J., Alonso-Navarro, H., García-Martín, E., and Agúndez, J. A. G. (2014). Cerebrospinal fluid biochemical studies in patients with Parkinson's disease: toward a potential search for biomarkers for this disease. *Front. Cell. Neurosci.* 8:369. doi: 10.3389/fncel.2014.00369

Kalia, L. V., and Lang, A. E. (2015). Parkinson's disease. *Lancet* 386, 896–912. doi: 10.1016/S0140-6736(14)61393-3

Kang, W., Chen, W., Yang, Q., Zhang, L., Zhang, L., Wang, X., et al. (2016). Salivary total α-synuclein, oligomeric α-synuclein and SNCA variants in Parkinson's disease patients. *Sci. Rep.* 6:28143. doi: 10.1038/srep28143

Katayama, T., Sawada, J., Takahashi, K., and Yahara, O. (2020). Cerebrospinal fluid biomarkers in Parkinson's disease: a critical overview of the literature and meta-analyses. *Brain Sci.* 10:466. doi: 10.3390/brainsci10070466

Kiely, A. P., Asi, Y. T., Kara, E., Limousin, P., Ling, H., Lewis, P., et al. (2013). α-Synucleinopathy associated with G51D SNCA mutation: a link between Parkinson's disease and multiple system atrophy? *Acta Neuropathol.* 125, 763–769. doi: 10.1007/s00401-013-1096-7

Klein, C., and Westenberger, A. (2012). Genetics of Parkinson's disease. *Cold Spring Harb. Perspect. Med.* 2:a008888. doi: 10.1101/cshperspect.a008888

Kouli, A., Torsney, K. M., Kuan, W. L., Stoker, T. B., and Greenland, J. C. (2018). *Parkinson's Disease: Etiology, Neuropathology, and Pathogenesis. Parkinson's Disease: Pathogenesis and Clinical Aspects [Internet]*. Brisbane: Codon Publications. doi: 10.15586/codonpublications.parkinsonsdisease.2018.ch1

Krüger, R., Kuhn, W., Müller, T., Woitalla, D., Graeber, M., Kösel, S., et al. (1998). Ala30Pro mutation in the gene encoding alpha-synuclein in Parkinson's disease. *Nat. Genet.* 18, 106–108. doi: 10.1038/ng0298-106

Lashuel, H. A., Overk, C. R., Oueslati, A., and Masliah, E. (2013). The many faces of α-synuclein: from structure and toxicity to therapeutic target. *Nat. Rev. Neurosci.* 14, 38–48. doi: 10.1038/nrn3406

Lebouvier, T., Neunlist, M., des Varannes, S. B., Coron, E., Drouard, A., N'Guyen, J. M., et al. (2010). Colonic biopsies to assess the neuropathology of Parkinson's disease and its relationship with symptoms. *PLoS One* 5:e12728. doi: 10.1371/journal.pone.0012728

Lee, E., Hwang, I., Park, S., Hong, S., Hwang, B., Cho, Y., et al. (2019). MPTP-driven NLRP3 inflammasome activation in microglia plays a central role in dopaminergic neurodegeneration. *Cell Death Differ.* 26, 213–228. doi: 10.1038/s41418-018-0124-5

Lee, H. J., Jung, K. W., Chung, S. J., Hong, S. M., Kim, J., Lee, J. H., et al. (2018). Relation of enteric α-Synuclein to gastrointestinal dysfunction in patients with parkinson's disease and in neurologically intact subjects. *J. Neurogastroenterol. Motil.* 24, 469–478. doi: 10.5056/jnm17141

Lee, P. H., Lee, G., Park, H. J., Bang, O. Y., Joo, I. S., and Huh, K. (2006). The plasma alpha-synuclein levels in patients with Parkinson's disease and multiple system atrophy. *J. Neural Transm.* 113, 1435–1439. doi: 10.1007/s00702-005-0427-9

Lesage, S., and Brice, A. (2009). Parkinson's disease: from monogenic forms to genetic susceptibility factors. *Hum. Mol. Genet.* 18, R48–R59. doi: 10.1093/hmg/ddp012

LeWitt, P., Schultz, L., Auinger, P., Lu, M., and Parkinson Study Group Datatop Investigators. (2011). CSF xanthine, homovanillic acid, and their ratio as biomarkers of Parkinson's disease. *Brain Res.* 1408, 88–97. doi: 10.1016/j.brainres.2011.06.057

Li, Q. X., Mok, S. S., Laughton, K. M., McLean, C. A., Cappai, R., Masters, C. L., et al. (2007). Plasma alpha-synuclein is decreased in subjects with Parkinson's disease. *Exp. Neurol.* 204, 583–588. doi: 10.1016/j.expneurol.2006.12.006

Li, X., Yang, W., Li, X., Li, X., Chen, Z., Wang, C., et al. (2019). Levels of oligomeric alpha-synuclein in red blood cells are elevated in patients with Parkinson's disease and affected by brain alpha-synuclein expression. *Int. J. Clin. Exp. Med.* 12, 10470–10477.

Lin, C. H., Yang, S. Y., Horng, H. E., Yang, C. C., Chieh, J. J., Chen, H. H., et al. (2017). Plasma α-synuclein predicts cognitive decline in Parkinson's disease. *J. Neurol. Neurosurg. Psychiatry* 88, 818–824. doi: 10.1136/jnnp-2016-314857

Ludtmann, M. H. R., Angelova, P. R., Horrocks, M. H., Choi, M. L., Rodrigues, M., and Baev, A. Y. (2018). α-synuclein oligomers interact with ATP synthase and open the permeability transition pore in Parkinson's disease. *Nat. Commun.* 9:2293. doi: 10.1038/s41467-018-04422-2

Lööv, C., Scherzer, C. R., Hyman, B. T., Breakefield, X. O., and Ingelsson, M. (2016). α-Synuclein in extracellular vesicles: functional implications and diagnostic opportunities. *Cell. Mol. Neurobiol.* 36, 437–448. doi: 10.1007/s10571-015-0317-0

Majbour, N. K., Vaikath, N. N., van Dijk, K. D., Ardah, M. T., Varghese, S., Vesterager, L. B., et al. (2016). Oligomeric and phosphorylated alpha-synuclein as potential CSF biomarkers for Parkinson's disease. *Mol Neurodegener.* 11:7. doi: 10.1186/s13024-016-0072-9

Mammadova, N., Summers, C. M., Kokemuller, R. D., He, Q., Ding, S., Baron, T., et al. (2019). Accelerated accumulation of retinal α-synuclein (pSer129) and tau, neuroinflammation, and autophagic dysregulation in a seeded mouse model of Parkinson's disease. *Neurobiol. Dis.* 121, 1–16. doi: 10.1016/j.nbd.2018.09.013

Manne, S., Kondru, N., Jin, H., Anantharam, V., Huang, X., Kanthasamy, A., et al. (2020). α-Synuclein real-time quaking-induced conversion in the submandibular glands of Parkinson's disease patients. *Mov. Disord.* 35, 268–278. doi: 10.1002/mds.27907

Marras, C., Beck, J. C., Bower, J. H., Roberts, E., Ritz, B., Ross, G. W., et al. (2018). Prevalence of Parkinson's disease across North America. *NPJ Parkinsons Dis.* 4:21. doi: 10.1038/s41531-018-0058-0

Marsili, L., Rizzo, G., and Colosimo, C. (2018). Diagnostic Criteria for Parkinson's disease: from James Parkinson to the concept of Prodromal disease. *Front. Neurol.* 9:156. doi: 10.3389/fneur.2018.00156

Martínez-Martín, P., Chaudhuri, K. R., Rojo-Abuin, J. M., Rodriguez-Blázquez, C., Alvarez-Sanchez, M., Arakaki, T., et al. (2015). Assessing the non-motor symptoms of Parkinson's disease: MDS-UPDRS and NMS Scale. *Eur. J. Neurol.* 22, 37–43. doi: 10.1111/ene.12165

Martínez-Martín, P., Rojo-Abuin, J., Rodríguez-Violante, M., Serrano-Dueñas, M., Garretto, N., Martínez-Castrillo, J. C., et al. (2016). Analysis of four scales for global severity evaluation in Parkinson's disease. *NPJ Parkinsons Dis.* 2:16007. doi: 10.1038/npjparkd.2016.7

Martín-Jiménez, R., Lurette, O., and Hebert-Chatelain, E. (2020). Damage in mitochondrial DNA associated with Parkinson's disease. *DNA Cell Biol.* 39, 1421–1430. doi: 10.1089/dna.2020.5398

Mazzetti, S., Basellini, M. J., Ferri, V., Cassani, E., Cereda, E., Paolini, M., et al. (2020). α-Synuclein oligomers in skin biopsy of idiopathic and monozygotic twin patients with Parkinson's disease. *Brain* 143, 920–931. doi: 10.1093/brain/awaa008

Meyer, P. T., Frings, L., Rücker, G., and Hellwig, S. (2017). 18 F-FDG PET in Parkinsonism: differential diagnosis and evaluation of cognitive impairment. *J. Nucl. Med.* 58, 1888–1898. doi: 10.2967/jnumed.116.186403

Miller, D. W., Hague, S. M., Clarimon, J., Baptista, M., Gwinn-Hardy, K., Cookson, M. R., et al. (2004). Alpha-synuclein in blood and brain from familial Parkinson disease with SNCA locus triplication. *Neurology* 62, 1835–1838. doi: 10.1212/01.wnl.0000127517.33208.f4

Miranda, H. V., Cássio, R., Correia-Guedes, L., Antonio Gomes, M., Chegão, A., Miranda, E., et al. (2017). Posttranslational modifications of blood-derived alpha-synuclein as biochemical markers for Parkinson's disease. *Sci. Rep.* 7:13713. doi: 10.1038/s41598-017-14175-5

Mogi, M., Harada, M., Narabayashi, H., Inagaki, H., Minami, M., and Nagatsu, T. (1996). Interleukin (IL)-1β, IL-2, IL-4, IL-6 and transforming growth factor-α levels are elevated in ventricular cerebrospinal fluid in juvenile parkinsonism

and Parkinson's disease. *Neurosci. Lett.* 211, 13–16. doi: 10.1016/0304-3940(96)12706-3

Mollenhauer, B., Cullen, V., Kahn, I., Krastins, B., Outerio, T. F., Pepivani, I., et al. (2008). Direct quantification of CSF alpha-synuclein by ELISA and first cross-sectional study in patients with neurodegeneration. *Exp. Neurol.* 213, 315–325. doi: 10.1016/j.expneurol.2008.06.004

Mollenhauer, B., Locascio, J. J., Schulz-Schaeffer, W., Sixel-Doring, F., Trenkwalder, C., and Schlossmacher, M. G. (2011). alpha-Synuclein and tau concentrations in cerebrospinal fluid of patients presenting with parkinsonism: a cohort study. *Lancet Neurol.* 10, 230–240. doi: 10.1016/S1474-4422(11)70014-X

Mollenhauer, B., Trautmann, E., Taylor, P., Manninger, P., Sixel-Doring, F., Ebentheuer, J., et al. (2013). Total CSF α-synuclein is lower in de novo Parkinson patients than in healthy subjects. *Neurosci. Lett.* 532, 44–48. doi: 10.1016/j.neulet.2012.11.004

Mullin, S., and Schapira, A. (2015). The genetics of Parkinson's disease. *Br. Med. Bull.* 114, 39–52. doi: 10.1093/bmb/ldv022

Nagatsu, T., Mogi, M., Ichinose, H., and Togari, A. (2000). "Changes in cytokines and neurotrophins in Parkinson's disease," in *Advances in Research on Neurodegeneration*, eds P. Riederer, et al. (Vienna: Springer). doi: 10.1007/978-3-7091-6301-6_19

Niethammer, M., Feigin, A., and Eidelberg, D. (2012). Functional neuroimaging in Parkinson's disease. *Cold Spring Harb. Perspect. Med.* 2:a009274. doi: 10.1101/cshperspect.a009274

Ning, H., Wu, Q., Han, D., Yao, T., Wang, J., Lu, W., et al. (2019). Baseline concentration of misfolded α-synuclein aggregates in cerebrospinal fluid predicts risk of cognitive decline in Parkinson's disease. *Neuropathol. Appl. Neurobiol.* 45, 398–409. doi: 10.1111/nan.12524

Nussbaum, R. L., and Polymeropoulos, M. H. (1997). Genetics of Parkinson's disease. *Hum. Mol. Genet.* 6, 1687–1691. doi: 10.1093/hmg/6.10.1687

Ohrfelt, A., Grognet, P., Andreasen, N., Wallin, A., Vanmechelen, E., Blennow, K., et al. (2009). Cerebrospinal fluid α-synuclein in neurodegenerative disorders—A marker of synapse loss? *Neurosci. Lett.* 450, 332–335. doi: 10.1016/j.neulet.2008.11.015

Ordonez, D. G., Lee, M. K., and Feany, M. B. (2018). α-synuclein induces mitochondrial dysfunction through Spectrin and the Actin cytoskeleton. *Neuron* 97, 108–124. doi: 10.1016/j.neuron.2017.11.036

Ortuño-Lizarán, I., Beach, T. G., Serrano, G. E., Walker, D. G., Adler, C. H., and Cuenca, N. (2018). Phosphorylated α-synuclein in the retina is a biomarker of Parkinson's disease pathology severity. *Mov. Disord.* 33, 1315–1324. doi: 10.1002/mds.27392

Oueslati, A. (2016). Implication of Alpha-Synuclein phosphorylation at S129 in synucleinopathies: What have we learned in the last decade? *J. Parkinsons Dis.* 6, 39–51. doi: 10.3233/JPD-160779

Paganoni, S., and Schwarzschild, M. A. (2017). Urate as a marker of risk and progression of neurodegenerative disease. *Neurotherapeutics* 14, 148–153. doi: 10.1007/s13311-016-0497-4

Paillusson, S., Gomez-Suaga, P., Stoica, R., Little, D., Gissen, P., Devine, M. J., et al. (2017). α-Synuclein binds to the ER-mitochondria tethering protein VAPB to disrupt Ca 2+ homeostasis and mitochondrial ATP production. *Acta Neuropathol.* 134, 129–149. doi: 10.1007/s00401-017-1704-z

Pajares, M., Jiménez-Moreno, N., Dias, I. H. K., Debelec, B., Vucetic, M., Fladmark, K. E., et al. (2015). Redox control of protein degradation. *Redox Biol.* 6, 409–420. doi: 10.1016/j.redox.2015.07.003

Pajares, M., Rojo, A. I., Manda, G., Boscá, L., and Cuadrado, A. (2020). Inflammation in Parkinson's disease: mechanisms and therapeutic implications. *Cells* 9:1687. doi: 10.3390/cells9071687

Palasz, E., Wysocka, A., Gasiorowska, A., Chalimoniuk, M., Niewiadomski, W., and Niewiadomska, G. (2020). BDNF as a promising therapeutic agent in Parkinson's disease. *Int. J. Mol. Sci.* 21:1170. doi: 10.3390/ijms21031170

Pankratz, N., and Foroud, T. (2007). Genetics of Parkinson's disease. *Gen. Med.* 9, 801–811. doi: 10.1097/GIM.0b013e31815bf97c

Papagiannakis, N., Koros, C., Stamelou, M., Simitsi, A. M., Maniati, M., Antonelou, R., et al. (2018). Alpha-synuclein dimerization in erythrocytes of patients with genetic and non-genetic forms of Parkinson's Disease. *Neurosci. Lett.* 672, 145–149. doi: 10.1016/j.neulet.2017.11.012

Park, J. H., Kim, D. H., Kwon, D. Y., Choi, M., Kim, S., Jung, J. H., et al. (2019). Trends in the incidence and prevalence of Parkinson's disease in Korea: a nationwide, population-based study. *BMC Geriatr.* 19:320. doi: 10.1186/s12877-019-1332-7

Park, J. S., Davis, R. L., and Sue, C. M. (2018). Mitochondrial dysfunction in Parkinson's disease: new mechanistic insights and therapeutic perspectives. *Curr. Neurol. Neurosci. Rep.* 18, 21. doi: 10.1007/s11910-018-0829-3

Park, M. J., Cheon, S. M., Bae, H. R., Kim, S. H., and Kim, J. W. (2011). Elevated levels of alpha-synuclein oligomer in the cerebrospinal fluid of drug-naive patients with Parkinson's disease. *J. Clin. Neurol.* 7, 215–222. doi: 10.3988/jcn.2011.7.4.215

Parnetti, L., Chiasserini, D., Bellomo, G., Giannandrea, D., De Carlo, C., Qureshi, M. M., et al. (2011). Cerebrospinal fluid Tau/alpha-synuclein ratio in Parkinson's disease and degenerative dementias. *Mov. Disord.* 26, 1428–1435. doi: 10.1002/mds.23670

Parnetti, L., Chiasserini, D., Persichetti, E., Eusebi, P., Varghese, S., Qureshi, M. M., et al. (2014a). Cerebrospinal fluid lysosomal enzymes and alpha-synuclein in Parkinson's disease. *Mov. Disord.* 29, 1019–1027. doi: 10.1002/mds.25772

Parnetti, L., Farotti, L., Eusebi, P., Chiasserini, D., De Carlo, C., Giannandrea, D., et al. (2014b). Differential role of CSF alpha-synuclein species, tau, and Aβ42 in Parkinson's Disease. *Front. Aging Neurosci.* 6:53. doi: 10.3389/fnagi.2014.00053

Pintér, D., Martinez-Martin, P., Janszky, J., and Kovács, N. (2019). The Parkinson's disease composite scale is adequately responsive to acute levodopa challenge. *Parkinsons Dis.* 2019:1412984. doi: 10.1155/2019/1412984

Polymeropoulos, M. H., Lavedan, C., Leroy, E., Ide, S. E., Dehejia, A., Dutra, A., et al. (1997). Mutation in the alpha-synuclein gene identified in families with Parkinson's disease. *Science* 276, 2045–2047. doi: 10.1126/science.276.5321.2045

Price, D. L., Rockenstein, E., Mante, M., Adame, A., Overk, C., Spencer, B., et al. (2016). Longitudinal live imaging of retinal α-synuclein: GFP deposits in a transgenic mouse model of Parkinson's Disease/Dementia with Lewy Bodies. *Sci. Rep.* 6:29523. doi: 10.1038/srep29523

Pringsheim, T., Jette, N., Frolkis, A., and Steeves, T. D. L. (2014). The prevalence of Parkinson's disease: a systematic review and meta-analysis. *Mov. Disord.* 29, 1583–1590. doi: 10.1002/mds.25945

Puspita, L., Chung, S. Y., and Shim, J. W. (2017). Oxidative stress and cellular pathologies in Parkinson's disease. *Mol. Brain* 10:53. doi: 10.1186/s13041-017-0340-9

Pyatigorskaya, N., Gallea, C., Garcia-Lorenzo, D., Vidailhet, M., and Lehericy, S. (2014). A review of the use of magnetic resonance imaging in Parkinson's disease. *Ther. Adv. Neurol. Disord.* 7, 206–220. doi: 10.1177/1756285613511507

Qin, X. Y., Zhang, S. P., Cao, C., Loh, Y. P., and Cheng, Y. (2016). Aberrations in peripheral inflammatory cytokine levels in Parkinson disease: a systematic review and meta-analysis. *JAMA Neurol.* 73, 1316–1324. doi: 10.1001/jamaneurol.2016.2742

Qualman, S. J., Haupt, H. M., Yang, P., and Hamilton, S. R. (1984). Esophageal Lewy bodies associated with ganglion cell loss in achalasia. Similarity to Parkinson's disease. *Gastroenterology* 87, 848–856.

Ramalingam, M., Huh, Y. J., and Lee, Y. I. (2019). The Impairments of α-synuclein and mechanistic target of Rapamycin in Rotenone-Induced SH-SY5Y cells and mice model of Parkinson's disease. *Front. Neurosci.* 13:1028. doi: 10.3389/fnins.2019.01028

Ross, O. A., Soto-Ortolaza, A. I., Heckman, M. G., Aasly, J. O., Abahuni, N., Annesi, G., et al. (2011). Association of LRRK2 exonic variants with susceptibility to Parkinson's disease: a case-control study. *Lancet Neurol.* 10, 898–908. doi: 10.1016/S1474-4422(11)70175-2

Salehi, Z., and Mashayekhi, F. (2009). Brain-derived neurotrophic factor concentrations in the cerebrospinal fluid of patients with Parkinson's disease. *J. Clin. Neuosci.* 16, 90–93. doi: 10.1016/j.jocn.2008.03.010

Sánchez-Ferro, A., Rabano, A., Catalan, M. J., Rodriguez-Valcarcel, F. C., Diez, S. F., Herreros-Rodriguez, J., et al. (2014). In vivo gastric detection of α-synuclein inclusions in Parkinson's disease. *Mov. Disord.* 30, 517–524. doi: 10.1002/mds.25988

Sanchez-Guajardo, V., Tentillier, N., and Romero-Ramos, M. (2015). The relation between α-synuclein and microglia in Parkinson's disease: recent developments. *Neuroscience* 302, 47–58. doi: 10.1016/j.neuroscience.2015.02.008

Sanders, L. H., and Greenamyre, J. T. (2013). Oxidative damage to macromolecules in human Parkinson disease and the rotenone model. *Free Radic. Biol. Med.* 62, 111–120. doi: 10.1016/j.freeradbiomed.2013.01.003

Sarkar, S., Olsen, A. L., Sygnecka, K., Lohr, K. M., and Feany, M. B. (2021). α-synuclein impairs autophagosome maturation through abnormal actin stabilization. *PLoS Genet.* 17:e1009359. doi: 10.1371/journal.pgen.1009359

Schapira, A. H. V. (2007). Mitochondrial dysfunction in Parkinson's disease. *Cell Death Differ.* 14, 1261–1266. doi: 10.1038/sj.cdd.4402160

Schwarz, S. T., Afzal, M., Morgan, P. S., Bajaj, N., Gowland, P. A., and Auer, D. P. (2014). The 'Swallow Tail' appearance of the healthy Nigrosome – a new accurate test of Parkinson's disease: a case-control and retrospective cross-sectional MRI Study at 3T. *PLoS One* 9:e93814. doi: 10.1371/journal.pone.0093814

Shaheen, H., Sobhy, S., El Mously, S., Abuomira, M., and Mansour, M. (2020). Salivary alpha-synuclein (total and oligomeric form): potential biomarkers in Parkinson's disease. *Egypt. J. Neurol. Psychiatry Neurosurg.* 56:22. doi: 10.1186/s41983-020-0159-7

Shaltouki, A., Sivapatham, R., Pei, Y., Gerencser, A. A., Momèiloviæ, O., Rao, M. S., et al. (2015). Mitochondrial alterations by PARKIN in dopaminergic neurons using PARK2 patient-specific and PARK2 knockout isogenic iPSC lines. *Stem Cell Rep.* 4, 847–859. doi: 10.1016/j.stemcr.2015.02.019

Shannon, K. M., Keshavarzian, A., Mutlu, E., Dodiya, H. B., Daian, D., Jaglin, J. A., et al. (2012). Alpha-synuclein in colonic submucosa in early untreated Parkinson's disease. *Mov. Disord.* 27, 709–715. doi: 10.1002/mds.23838

Shi, M., Bradner, J., Hancock, A. M., Chung, K. A., Quinn, J. F., Peskind, E. R., et al. (2011). Cerebrospinal fluid biomarkers for Parkinson disease diagnosis and progression. *Ann. Neurol.* 69, 570–580. doi: 10.1002/ana.22311

Shi, M., Liu, C., Cook, T. J., Bullock, K. M., Zhao, Y., Ginghina, C., et al. (2014). Plasma exosomal α-synuclein is likely CNS-derived and increased in Parkinson's disease. *Acta Neuropathol.* 128, 639–650. doi: 10.1007/s00401-014-1314-y

Shi, M., Zabetian, C. P., Hancock, A. M., Ginghina, C., Hong, Z., Yearout, D., et al. (2010). Significance and confounders of peripheral DJ-1 and alpha-synuclein in Parkinson's disease. *Neurosci. Lett.* 480, 78–82. doi: 10.1016/j.neulet.2010.06.009

Singleton, A. B., Farrer, M., Johnson, J., Singleton, A., Hague, S., Kachergus, J., et al. (2003). alpha-Synuclein locus triplication causes Parkinson's disease. *Science* 302:841. doi: 10.1126/science.1090278

Skorvanek, M., Martinez-Martin, P., Kovacs, N., Rodriguez-Violante, M., Corvol, J. C., Taba, P., et al. (2017). Differences in MDS-UPDRS Scores Based on Hoehn and Yahr Stage and Disease Duration. *Mov. Disord. Clin. Pract.* 4, 536–544. doi: 10.1002/mdc3.12476

Stefani, A., Pierantozzi, M., Olivola, E., Galati, S., Cerroni, R., D'Angelo, V., et al. (2017). Homovanillic acid in CSF of mild stage Parkinson's disease patients correlates with motor impairment. *Neurochem. Int.* 105, 58–63. doi: 10.1016/j.neuint.2017.01.007

Stefanis, L. (2012). α-Synuclein in Parkinson's disease. *Cold Spring Harb. Perspect. Med.* 2:a009399. doi: 10.1101/cshperspect.a009399

Stewart, T., Sossi, V., Aasly, J. O., Wszolek, Z. W., Uitti, R. J., Hasegawa, K., et al. (2015). Phosphorylated α-synuclein in Parkinson's disease: correlation depends on disease severity. *Acta Neuropathol. Commun.* 3:7. doi: 10.1186/s40478-015-0185-3

Stoessel, D., Schulte, C., Teixeira Dos Santos, M. C., Scheller, D., Rebollo-Mesa, I., Deuschle, C., et al. (2018). Promising metabolite profiles in the plasma and CSF of early clinical Parkinson's disease. *Front. Aging Neurosci.* 10:51. doi: 10.3389/fnagi.2018.00051

Stojkovska, I., Wagner, B. M., and Morrison, B. E. (2015). Parkinson's disease and enhanced inflammatory response. *Exp. Biol. Med.* 240, 1387–1395. doi: 10.1177/1535370215576313

Su, X., Chu, Y., Kordower, J. H., Li, B., Cao, H., Huang, L., et al. (2015). PGC-1α promoter Methylation in Parkinson's disease. *PLoS One* 10:e0134087. doi: 10.1371/journal.pone.0134087

Sui, Y. T., Bullock, K. M., Erickson, M. A., Zhang, J., and Banks, W. A. (2014). Alpha synuclein is transported into and out of the brain by the blood-brain barrier. *Peptides* 52, 197–202. doi: 10.1016/j.peptides.2014.09.018

Surguchov, A., McMahan, B., Masliah, E., and Surgucheva, I. (2001). Synucleins in ocular tissues. *J. Neurosci. Res.* 65, 68–77. doi: 10.1002/jnr.1129

Thomas, K. J., McCoy, M. K., Blackinton, J., Beilina, A., van der Brug, M., Sandebring, A., et al. (2011). DJ-1 acts in parallel to the PINK1/parkin pathway to control mitochondrial function and autophagy. *Hum. Mol. Genet.* 20, 40–50. doi: 10.1093/hmg/ddq430

Tian, C., Liu, G., Gao, L., Soltys, D., Pan, C., Stewart, T., et al. (2019). Erythrocytic α-Synuclein as a potential biomarker for Parkinson's disease. *Transl. Neurodegener.* 8:15. doi: 10.1186/s40035-019-0155-y

Tokuda, T., Salem, S. A., Allsop, D., Mizuno, T., Nakagawa, M., Qureshi, M. M., et al. (2006). Decreased alpha-synuclein in cerebrospinal fluid of aged individuals and subjects with Parkinson's disease. *Biochem. Biophys. Res. Commun.* 349, 162–166. doi: 10.1016/j.bbrc.2006.08.024

Tokuda, T., Qureshi, M. M., Ardah, M. T., Varghese, S., Shehab, S. A. S., Kasai, T., et al. (2010). Detection of elevated levels of α-synuclein oligomers in CSF from patients with Parkinson disease. *Neurology* 75, 1766–1772. doi: 10.1212/WNL.0b013e3181fd613b

Toledo, J. B., Korff, A., Shaw, L. M., Trojanowski, J. Q., and Zhang, J. (2013). CSF alpha-synuclein improves diagnostic and prognostic performance of CSF tau and Abeta in Alzheimer's disease. *Acta Neuropathol.* 126, 683–697. doi: 10.1007/s00401-013-1148-z

Toulorge, D., Schapira, A. H. V., and Hajj, R. (2016). Molecular changes in the postmortem parkinsonian brain. *J. Neurochem.* 139(Suppl. 1), 27–58. doi: 10.1111/jnc.13696

Trupp, M., Jonsson, P., Ohrfelt, A., Zetterberg, H., Obudulu, O., Malm, L., et al. (2014). Metabolite and peptide levels in plasma and CSF differentiating healthy controls from patients with newly diagnosed Parkinson's disease. *J. Parkinsons Dis.* 4, 549–560. doi: 10.3233/JPD-140389

van Dijk, K. D., Persichetti, E., Chiasserini, D., Eusebi, P., Beccari, T., Calabresi, P., et al. (2013). Changes in endolysosomal enzyme activities in cerebrospinal fluid of patients with Parkinson's disease. *Mov. Disord.* 28, 747–754. doi: 10.1002/mds.25495

van Steenoven, I., Majbour, N. K., Vaikath, N. N., Berendse, H. W., van der Flier, W. M., van de Berg, W. D. J., et al. (2018). α-Synuclein species as potential cerebrospinal fluid biomarkers for dementia with lewy bodies. *Mov. Disord.* 33, 1724–1733. doi: 10.1002/mds.111

Vandendriessche, C., Bruggeman, A., Van Cauwenberghe, C., and Vandenbroucke, R. E. (2020). Extracellular vesicles in Alzheimer's and Parkinson's disease: small entities with large consequences. *Cells* 9:2485. doi: 10.3390/cells9112485

Varcin, M., Bentea, E., Michotte, Y., and Sarre, S. (2012). Oxidative stress in genetic mouse models of Parkinson's disease. *Oxid. Med. Cell. Longev.* 2012:624925. doi: 10.1155/2012/624925

Ventriglia, M., Zanardini, R., Bonomini, C., Zanetti, O., Volpe, D., Pasqualetti, P., et al. (2013). Serum brain-derived neurotrophic factor levels in different neurological diseases. *Biomed Res. Int.* 2013:901082. doi: 10.1155/2013/901082

Veys, L., Vandenabeele, M., Ortuño-Lizarán, I., Baekelandt, V., Cuenca, N., Moons, L., et al. (2019). Retinal α-synuclein deposits in Parkinson's disease patients and animal models. *Acta Neuropathol.* 137, 379–395. doi: 10.1007/s00401-018-01956-z

Visanji, N. P., Marras, C., Hazrati, L. N., Liu, L. W. C., and Lang, A. E. (2013). Alimentary, my dear Watson? The challenges of enteric α-synuclein as a Parkinson's disease biomarker. *Mov. Disord.* 29, 444–450. doi: 10.1002/mds.25789

Vivacqua, G., Latorre, A., Suppa, A., Nardi, M., Pietracupa, S., Mancinelli, R., et al. (2016). Abnormal salivary total and oligomeric Alpha-synuclein in Parkinson's disease. *PLoS One* 11:e0151156. doi: 10.1371/journal.pone.0151156

von Euler Chelpin, M., Söderberg, L., Fälting, J., Möller, C., Giorgetti, M., Constantinescu, R., et al. (2020). Alpha-Synuclein Protofibrils in cerebrospinal fluid: a potential biomarker for Parkinson's disease. *J. Parkinsons Dis.* 10, 1429–1442. doi: 10.3233/JPD-202141

Wakabayashi, K., Takahashi, H., Ohama, E., and Ikuta, F. (1990). Parkinson's disease: an immunohistochemical study of Lewy body-containing neurons in the enteric nervous system. *Acta Neuropathol.* 79, 581–583. doi: 10.1007/BF00294234

Wakabayashi, K., Takahashi, H., Takeda, S., Ohama, E., and Ikuta, F. (1988). Parkinson's disease: the presence of Lewy bodies in Auerbach's and Meissner's plexuses. *Acta Neuropathol.* 76, 217–221. doi: 10.1007/BF00687767

Wang, J. Y., Zhuang, G. G., Zhu, L. B., Zhu, H., Li, T., Li, R., et al. (2016). Meta-analysis of brain iron levels of Parkinson's disease patients determined by postmortem and MRI measurements. *Sci. Rep.* 6:36669. doi: 10.1038/srep36669

Wang, K., Huang, J., Xie, W., Huang, L., Zhong, C., and Chen, Z. (2016). Beclin1 and HMGB1 ameliorate the α-synuclein-mediated autophagy inhibition in PC12 cells. *Diagn. Pathol.* 11:15. doi: 10.1186/s13000-016-0459-5

Wang, L., Wang, G., Duan, Y., Wang, F., Lin, S., Zhang, F., et al. (2019). A comparative study of the diagnostic potential of plasma and Erythrocytic α-synuclein in Parkinson's disease. *Neurodegener. Dis.* 19, 204–210. doi: 10.1159/000506480

Wang, L., Zhang, Q., Li, H., and Zhang, H. (2012). SPECT molecular imaging in Parkinson's disease. *J. Biomed. Biotechnol.* 2012:412486. doi: 10.1155/2012/412486

Wang, N., Gibbons, C. H., Lafo, J., and Freeman, R. (2013). α-Synuclein in cutaneous autonomic nerves. *Neurology* 81, 1604–1610. doi: 10.1212/WNL.0b013e3182a9f449

Wang, Y., Shi, M., Chung, K. A., Zabetian, C. P., Leverenz, J. B., Berg, D., et al. (2012). Phosphorylated α-synuclein in Parkinson's disease. *Sci. Transl. Med.* 4:121ra20. doi: 10.1126/scitranslmed.3002566

Wang, Z., Becker, K., Donadio, V., Siedlak, S., Yuan, J., Rezaee, M., et al. (2021). Skin α-synuclein aggregation seeding activity as a novel biomarker for Parkinson disease. *JAMA Neurol.* 78, 1–11. doi: 10.1001/jamaneurol.2020.3311

Wei, Z., Li, X., Li, X., Liu, Q., and Cheng, Y. (2018). Oxidative stress in Parkinson's disease: a systematic review and meta-analysis. *Front. Mol. Neurosci.* 11:236. doi: 10.3389/fnmol.2018.00236

Wen, M., Zhou, B., Chen, Y. H., Ma, Z. L., Gou, Y., Zhang, C. L., et al. (2017). Serum uric acid levels in patients with Parkinson's disease: a meta-analysis. *PLoS One* 12:e0173731. doi: 10.1371/journal.pone.0173731

Wennström, M., Surova, Y., Hall, S., Nilsson, C., Minthon, L., Boström, F., et al. (2013). Low CSF levels of both α-synuclein and the α-synuclein cleaving enzyme neurosin in patients with synucleinopathy. *PLoS One* 8:e53250. doi: 10.1371/journal.pone.0053250

West, A. W., Maraganore, D., Crook, J., Lesnick, T., Lockhart, P. J., Wilkes, K. M., et al. (2002). Functional association of the parkin gene promoter with idiopathic Parkinson's disease. *Hum. Mol. Genet.* 11, 2787–2792. doi: 10.1093/hmg/11.22.2787

Willkommen, D., Lucio, M., Moritz, F., Forcisi, S., Kanawati, B., Smirnov, K. S., et al. (2018). Metabolomic investigations in cerebrospinal fluid of Parkinson's disease. *PLoS One* 13:e0208752. doi: 10.1371/journal.pone.0208752

Winkler, S., Hagenah, J., Lincoln, S., Heckman, M., Haugarvoll, K., Lohmann-Hedrich, K., et al. (2007). α-Synuclein and Parkinson disease susceptibility. *Neurology* 69, 1745–1750. doi: 10.1212/01.wnl.0000275524.15125.f4

Wrangel, C. V., Schwabe, K., John, N., Krauss, J. K., and Alam, M. (2015). The rotenone-induced rat model of Parkinson's disease: behavioral and electrophysiological findings. *Brain Behav. Res.* 279, 52–61. doi: 10.1016/j.bbr.2014.11.002

Wu, D. C., Teismann, P., Tieu, K., Vila, M., Jackson-Lewis, V., Ischiropoulos, H., et al. (2003). NADPH oxidase mediates oxidative stress in the 1-methyl-4-phenyl-1,2,3,6-tetrahydropyridine model of Parkinson's disease. *Proc. Natl. Acad. Sci. U.S.A.* 100, 6145–6150. doi: 10.1073/pnas.0937239100

Wuolikainen, A., Jonsson, P., Ahnlund, M., Antti, H., Marklund, S. L., Moritz, T., et al. (2016). Multi-platform mass spectrometry analysis of the CSF and plasma metabolomes of rigorously matched amyotrophic lateral sclerosis, Parkinson's disease and control subjects. *Mol. Biosyst.* 12, 1287–1298. doi: 10.1039/c5mb00711a

Yan, F., Chen, Y., Li, M., Wang, Y., Zhang, W., Chen, X., et al. (2018). Gastrointestinal nervous system α-synuclein as a potential biomarker of Parkinson disease. *Medicine* 97:e11337. doi: 10.1097/MD.0000000000011337

Yu, H., Sun, T., An, J., Wen, L., Liu, F., Bu, Z., et al. (2020). Potential roles of exosomes in Parkinson's disease: from pathogenesis, diagnosis, and treatment to prognosis. *Front. Cell Dev. Biol.* 8:86. doi: 10.3389/fcell.2020.00086

Zange, L., Noack, C., Hahn, K., Stenzel, W., and Lipp, A. (2015). Phosphorylated α-synuclein in skin nerve fibres differentiates Parkinson's disease from multiple system atrophy. *Brain* 138, 2310–2321. doi: 10.1093/brain/awv138

Zarranz, J. J., Alegre, J., Gómez-Esteban, J. C., Lezcano, E., Ros, R., Ampuero, I., et al. (2004). The new mutation, E46K, of alpha-synuclein causes Parkinson and Lewy body dementia. *Ann. Neurol.* 55, 164–173. doi: 10.1002/ana.10795

Zhang, J., Li, X., and Li, J. D. (2019). The roles of post-translational modifications on α-synuclein in the pathogenesis of Parkinson's diseases. *Front. Neurosci.* 13:381. doi: 10.3389/fnins.2019.00381

Zhao, H., Wang, C., Zhao, N., Li, W., Yang, Z., Liu, X., et al. (2018). Potential biomarkers of Parkinson's disease revealed by plasma metabolic profiling. *J. Chromatogr. B Analyt. Technol. Biomed. Life Sci.* 1081-1082, 101–108. doi: 10.1016/j.jchromb.2018.01.025

Zhao, J., Bi, W., Xiao, S., Lan, X., Cheng, X., Zhang, J., et al. (2019). Neuroinflammation induced by lipopolysaccharide causes cognitive impairment in mice. *Sci. Rep.* 9:5790. doi: 10.1038/s41598-019-42286-8

Zheng, B., Liao, Z., Locascio, J. J., Lesniak, K. L., Roderick, S. S., Watt, M. L., et al. (2010). PGC-1α, a potential therapeutic target for early intervention in Parkinson's disease. *Sci. Transl. Med.* 2:52ra73. doi: 10.1126/scitranslmed.3001059

Zhou, B., Wen, M., Yu, W. F., Zhang, C. L., and Jiao, L. (2015). The diagnostic and differential diagnosis utility of cerebrospinal Fluid α-Synuclein levels in Parkinson's disease: a meta-analysis. *Parkinsons Dis.* 2015:567386. doi: 10.1155/2015/567386

Zhu, M., Li, W., and Lu, C. (2012). Role of Alpha-synuclein protein levels in mitochondrial morphology and cell survival in cell lines. *PLoS One* 7:e36377. doi: 10.1371/journal.pone.0036377

Zilocchi, M., Finzi, G., Lualdi, M., Sessa, F., Fasano, M., and Alberio, T. (2018). Mitochondrial alterations in Parkinson's disease human samples and cellular models. *Neurochem. Int.* 118, 61–72. doi: 10.1016/j.neuint.2018.04.013

Conflict of Interest: The authors declare that the research was conducted in the absence of any commercial or financial relationships that could be construed as a potential conflict of interest.

Copyright © 2021 Ganguly, Singh, Pal, Prasad, Agrawal, Saini and Chakrabarti. This is an open-access article distributed under the terms of the Creative Commons Attribution License (CC BY). The use, distribution or reproduction in other forums is permitted, provided the original author(s) and the copyright owner(s) are credited and that the original publication in this journal is cited, in accordance with accepted academic practice. No use, distribution or reproduction is permitted which does not comply with these terms.

frontiers in Aging Neuroscience

ORIGINAL RESEARCH
published: 12 July 2021
doi: 10.3389/fnagi.2021.703158

Development and Validation of a Prognostic Model for Cognitive Impairment in Parkinson's Disease With REM Sleep Behavior Disorder

Fangzheng Chen[1†], Yuanyuan Li[1†], Guanyu Ye[1], Liche Zhou[1], Xiaolan Bian[2‡] and Jun Liu[1,3*‡]*

[1]*Department of Neurology and Institute of Neurology, Ruijin Hospital, Shanghai Jiao Tong University School of Medicine, Shanghai, China,* [2]*Department of Pharmacy, Ruijin Hospital, Shanghai Jiao Tong University School of Medicine, Shanghai, China,* [3]*CAS Center for Excellence in Brain Science and Intelligence Technology, Ruijin Hospital, Shanghai Jiao Tong University School of Medicine, Shanghai, China*

OPEN ACCESS

Edited by:
Alessandra Nicoletti, University of Catania, Italy

Reviewed by:
Steven Gunzler, University Hospitals Cleveland Medical Center, United States
Svetlana Tomic, Osijek Clinical Hospital Center, Croatia

***Correspondence:**
Xiaolan Bian
bxl70029@163.com
Jun Liu
jly0520@hotmail.com

†These authors have contributed equally to this work and share first authorship

‡These authors share last authorship

Received: *30 April 2021*
Accepted: *21 June 2021*
Published: *12 July 2021*

Citation:
Chen F, Li Y, Ye G, Zhou L, Bian X and Liu J (2021) Development and Validation of a Prognostic Model for Cognitive Impairment in Parkinson's Disease With REM Sleep Behavior Disorder. Front. Aging Neurosci. 13:703158. doi: 10.3389/fnagi.2021.703158

The presentation and progression of Parkinson's disease (PD) are not uniform, but the presence of rapid eye movement sleep behavior disorder (RBD) in PD patients may indicate a worse prognosis than isolated PD. Increasing evidence suggests that patients with comorbid PD and RBD (PD-RBD) are more likely to develop cognitive impairment (CI) than those with isolated PD; however, the predictors of CI in PD-RBD patients are not well understood. This study aimed to develop a prognostic model for predicting mild cognitive impairment (MCI) in PD-RBD patients. The data of PD-RBD patients were extracted from the Parkinson's Progression Markers Initiative study (PPMI), and the sample was randomly divided into a training set (n = 96) and a validation set (n = 24). PD-MCI as defined by the level II Movement Disorder Society (MDS) diagnostic criteria was the outcome of interest. The demographic features, clinical assessments, dopamine transporter (DAT) imaging data, cerebrospinal fluid (CSF) analyses and genetic data of PD patients were considered candidate predictors. We found that performance on the University of Pennsylvania Smell Identification Test (UPSIT), the mean signal and asymmetry index of the putamen on DAT imaging, p-tau/α-syn and p-tau in CSF, and rs55785911 genotype were predictors of PD-MCI in PD-RBD patients. A C-index of 0.81 was obtained with this model, and a C-index of 0.73 was obtained in the validation set. Favorable results of calibrations and decision curve analysis demonstrated the efficacy and feasibility of this model. In conclusion, we developed a prognostic model for predicting MCI in PD-RBD patients; the model displayed good discrimination and calibration and may be a convenient tool for clinical application. Larger samples and external validation sets are needed to validate this model.

Keywords: Parkinson's disease, REM sleep behavior disorder (RBD), cognition, nomogram, mild cognitive impairment

INTRODUCTION

Parkinson's disease (PD) is the second most common neurodegenerative disease affecting elderly people worldwide and is mainly characterized by motor symptoms, including bradykinesia, resting tremor, rigidity, and postural instability. Moreover, PD is considered to be a complex and multifaceted disorder with many nonmotor symptoms (NMSs), such as constipation, cognitive impairment (CI), anxiety, and rapid eye movement (REM) sleep behavior disorder (RBD; Kalia and Lang, 2015). CI is an important and common NMS of PD, and studies have shown that the prevalence rate of CI in PD patients rises as the disease progresses, reaching 80% at 20 years since diagnosis (Aarsland et al., 2003; Hely et al., 2008). PD-CI is classified into mild CI in PD (PD-MCI) and PD with dementia (PDD; Litvan et al., 2012); PD-MCI represents the earlier of the two stages and is a risk factor for PDD (Janvin et al., 2006). The presence of CI in PD patients severely aggravates the burden on the patients and their families; therefore, early detection of PD-MCI, even before the transition stage of PDD, is necessary and vital for potential disease prevention and treatment.

RBD is a parasomnia characterized by a loss of REM sleep-related normal skeletal muscle atonia with remarkable motor activities and dream enactment behaviors (Stefani et al., 2018), and the presence of RBD in individuals indicates an increased risk of developing α-synucleinopathy, including PD (Mahowald and Schenck, 2013). Moreover, RBD is a common symptom in PD patients, and it is estimated that the frequency of RBD is approximately 33–48% in PD patients (De Cock et al., 2007; Sixel-Döring et al., 2011; Jozwiak et al., 2017). Studies have shown that patients with comorbid PD and RBD (PD-RBD) have certain characteristics; they tend to be elderly males with non-tremor-dominant or akinetic-rigid motor subtypes and may represent a more severe disease course than isolated PD, correlated with increased autonomic dysfunction, psychiatric comorbidities and falls, along with accelerated cognitive decline and degraded sleep quality (Massicotte-Marquez et al., 2008; Postuma et al., 2008; Kim and Jeon, 2014; Chahine et al., 2016; Pagano et al., 2018; Trout et al., 2019). Therefore, researchers have suggested that PD-RBD may be a relatively diffuse and complex subtype of PD (Postuma et al., 2008, 2012; Lin and Chen, 2018).

Moreover, in terms of cognition, there is a considerable amount of evidence suggesting that PD-RBD is a distinct subtype with worse cognitive outcomes than PD/non-RBD (PD-nRBD; Sinforiani et al., 2006, 2008; Vendette et al., 2007; Gagnon et al., 2009; Postuma et al., 2012; Manni et al., 2013; Nomura et al., 2017), and the presence of RBD in PD is predictive of progression in CI (Sinforiani et al., 2008; Manni et al., 2013; Nomura et al., 2013). PD-RBD patients were reported to perform worse on executive functioning, attention, verbal learning and memory, and visuospatial processing tasks than PD-nRBD patients (Gagnon et al., 2009; Postuma et al., 2012; Jozwiak et al., 2017; Kamble et al., 2019; Yan et al., 2019); however, Postuma et al. (2012) reported that PD-RBD patients showed no difference from PD-nRBD patients in nonverbal learning and memory tasks, indicating a particular CI pattern in PD-RBD patients. In 2012, Postuma et al. (2012) reported that PD-RBD patients with MCI at baseline were more prone to develop dementia than PD-nRBD patients in a 4-year follow-up study. However, to our knowledge, a prospective study investigating whether PD-RBD patients were more likely to develop MCI than PD-nRBD patients over a sufficiently long period has not yet been conducted.

Currently, the factors contributing to the development of CI in PD-RBD patients are not well understood. To our knowledge, no study has investigated risk factors for CI in PD-RBD patients. This study aims to develop and validate a prognostic model with comprehensive assessments for predicting PD-MCI in PD-RBD patients. In addition, the predictors identified in this study could contribute to a better understanding of the PD-RBD phenotype and may guide the prevention of MCI in PD-RBD patients.

MATERIALS AND METHODS

Study Design and Participants

The Parkinson's Progression Markers Initiative (PPMI) is a multicenter (throughout the United States, Europe, and Australia) longitudinal study with the aim of identifying biomarkers of PD progression (Parkinson Progression Marker Initiative., 2011). Written informed consent was provided by the PPMI participants, and the PPMI study was approved by the institutional boards of the study sites (Weintraub et al., 2015). The detailed methodology and information of the study assessments are available on the PPMI website[1]. The data were updated on April 20th, 2020, and were downloaded from the PPMI website on September 29th, 2020. The participants were enrolled and screened at baseline, which was between June 2011 and April 2013, and were followed up annually.

The REM Sleep Behavior Disorder Questionnaire (RBDSQ) is a widely used and accepted tool to evaluate RBD symptoms and has been validated in multiple populations (Stiasny-Kolster et al., 2007; Nomura et al., 2011; Wang et al., 2015; Ye et al., 2020). In this study, RBDSQ scores $\geq$5 were defined as probable RBD by PPMI standards, as previously described (Pagano et al., 2018), and PD patients with this condition were defined as PD-RBD patients. For this study, we included PD-RBD patients meeting the following criteria: (1) RBDSQ score $\geq$5 at baseline and follow-up visits; (2) the status of cognition was recorded in the subsequent visits; and (3) clinical assessment, dopamine transporter (DAT) imaging, cerebrospinal fluid (CSF), and genetic data were available at baseline. Patients with MCI at baseline or without subsequent records of cognition status were excluded from this study. Moreover, to prove that PD-RBD patients had a higher risk of CI, PD-nRBD patients were included. They met the same inclusion and exclusion criteria for this study as the PD-RBD group except for RBDSQ scores <5.

A total of 120 PD-RBD patients and 218 PD-nRBD patients with available baseline clinical assessment, DAT scans, CSF analyses, and genetic data were included in this study. The

[1]http://ppmi-info.org

patients were followed up, and their cognitive status was evaluated at 1-year intervals after baseline enrollment.

Outcome

The outcome was defined as PD-MCI. In this study, PD-MCI was defined by the PPMI protocol and the Movement Disorder Society (MDS) MCI task force level II guidelines and was originally recorded in the PPMI dataset (Litvan et al., 2011). The cognitive domains in the MDS MCI task force level II guidelines were assessed as follows in PPMI data: the Hopkins Verbal Learning Test (HVLT) total recall and HVLT recognition discrimination were used for verbal memory, Benton Judgment of Line Orientation (JOLO) was used for visuospatial processing, Letter-Number Sequencing (LNS) was used for executive function and working memory, the Semantic fluency Test (SFT) was used for speeded lexical search, and the Symbol-Digit Modalities Test (SDMT) was used for processing speed and attention (Parkinson Progression Marker Initiative., 2011; Schrag et al., 2017; Hogue et al., 2018).

According to the PPMI reference manual, PD-MCI was defined as scores on two or more of HVLT immediate/total recall, HVLT recognition discrimination, JOLO, LNS, SFT, and SDMT that were more than 1.5 standard deviations below normal, with no functional impairment due to CI. These criteria have been applied and validated in several studies (Parkinson Progression Marker Initiative., 2011; Schrag et al., 2017; Hogue et al., 2018).

Candidate Predictors

The assessments of participants in the PPMI baseline data, including demographic features, clinical assessment, DAT-SCAN, CSF, and genetic data, were considered candidate predictors. The demographic variables were age, gender, and years of education (age and years of education were transformed to categorized variables in PPMI at given cutoff values).

The clinical assessment variables were disease duration, age at symptom onset, and initial symptoms at diagnosis. PD symptoms were assessed using Hoehn and Yahr staging, Total Rigidity Scores, the tremor dominant/postural instability and gait difficulty (TD/PIGD) classification, tremor scores, and Movement Disorder Society Unified Parkinson's Disease Rating Scale (MDS-UPDRS) scores. The modified Schwab and England Activities of Daily Living (ADL) score was used to evaluate performance in ADL. Olfactory function was assessed with the University of Pennsylvania Smell Identification Test (UPSIT). Depression was assessed with the 15-item Geriatric Depression Scale (GDS). Sleep disturbance was assessed with the Epworth Sleepiness Scale (ESS). Autonomic function was assessed with the Scale for Outcomes in PD for Autonomic Symptoms (SCOPA-AUT). The anxiety level was assessed with the State-Trait Anxiety Inventory (STAI).

For DAT scan imaging data, we included the mean caudate and putaminal uptake relative to uptake in the occipital area and asymmetry of caudate and putaminal uptake. For CSF data, Aβ, α-synuclein, tau, and phosphorylated tau (p-tau) and their relative ratios were included. For genetic data, APOE 4 status, MAPT genotype, and SNPs recorded in PPMI were included (Nalls et al., 2016).

Statistical Analysis

The original categorical or ranked variables in the PPMI data were retained, while other continuous numeric variables were transformed into ordinal categorical variables according to best cutoffs produced by X-tile software for a better calibration ability of the model (Camp et al., 2004). The endpoint was defined as the time from baseline normal cognition to the occurrence of PD-MCI. We compared MCI-free survival between the PD-RBD group and the PD-nRBD group by Kaplan–Meier and log-rank tests.

We used two methods for predictor selection. Univariate Cox proportional hazards regression analysis was repeated to identify variables associated with MCI-free survival, and variables with significant P values ($P < 0.01$) were considered for entry into the multivariate model. The least absolute shrinkage and selection operator (LASSO) regression model was also used to select optimal candidate variables from the high-dimensional data, and variables with nonzero coefficients in LASSO regression were selected for further analysis (Friedman et al., 2010). The final model was formulated on the basis of the results of multivariate Cox regression by using backward stepwise elimination with Akaike information criteria (AIC) as the stopping rule (Ji et al., 2019). The predictive ability of the two models was assessed with the receiver operating characteristic curve (ROC) at 3, 5, and 7 years (Chen et al., 2019).

The best prediction model was visualized with a nomogram for predicting 3-, 5- and, 7-year MCI-free survival probabilities (Iasonos et al., 2008; Balachandran et al., 2015). The concordance index (C-index) was used to evaluate the discrimination of the models (Pencina and D'Agostino, 2004), and calibration curves were plotted to evaluate the calibration of the model (Kramer and Zimmerman, 2007). Decision curves were plotted to assess the clinical usefulness of the model in different years (Vickers and Elkin, 2006).

Statistical analysis was performed using R software (Version 3.6.1). $P < 0.05$ was considered statistically significant.

RESULTS

Participants Characteristics

There were 423 PD patients at baseline in the PPMI database. Among the 158 PD-RBD patients, 31 PD-RBD patients were diagnosed with MCI at baseline, seven patients had no cognitive status records at the subsequent visits, and they were removed from further analysis. The sample finally included 120 PD-RBD patients and 218 PD-nRBD patients. For model development and internal validation, we randomly divided the sample into a training set ($n = 96$) and a validation set ($n = 24$) at a ratio of 8:2 (**Figure 2A**). Kaplan–Meier analysis indicated median MCI-free survival times of 6 years in the PD-RBD group and 7 years in the PD-nRBD group ($P = 0.029$, **Figure 1A**), suggesting a worse prognosis in the PD-RBD group than in the PD-nRBD group. Cox regression showed that RBD was a predictor of MCI after adjustment for age, sex, and education (HR = 1.43, 95% CI: $P = 0.029$).

The patients were mainly male (65%) and over 65 years old, and most of them had received over 13 years of education. Most

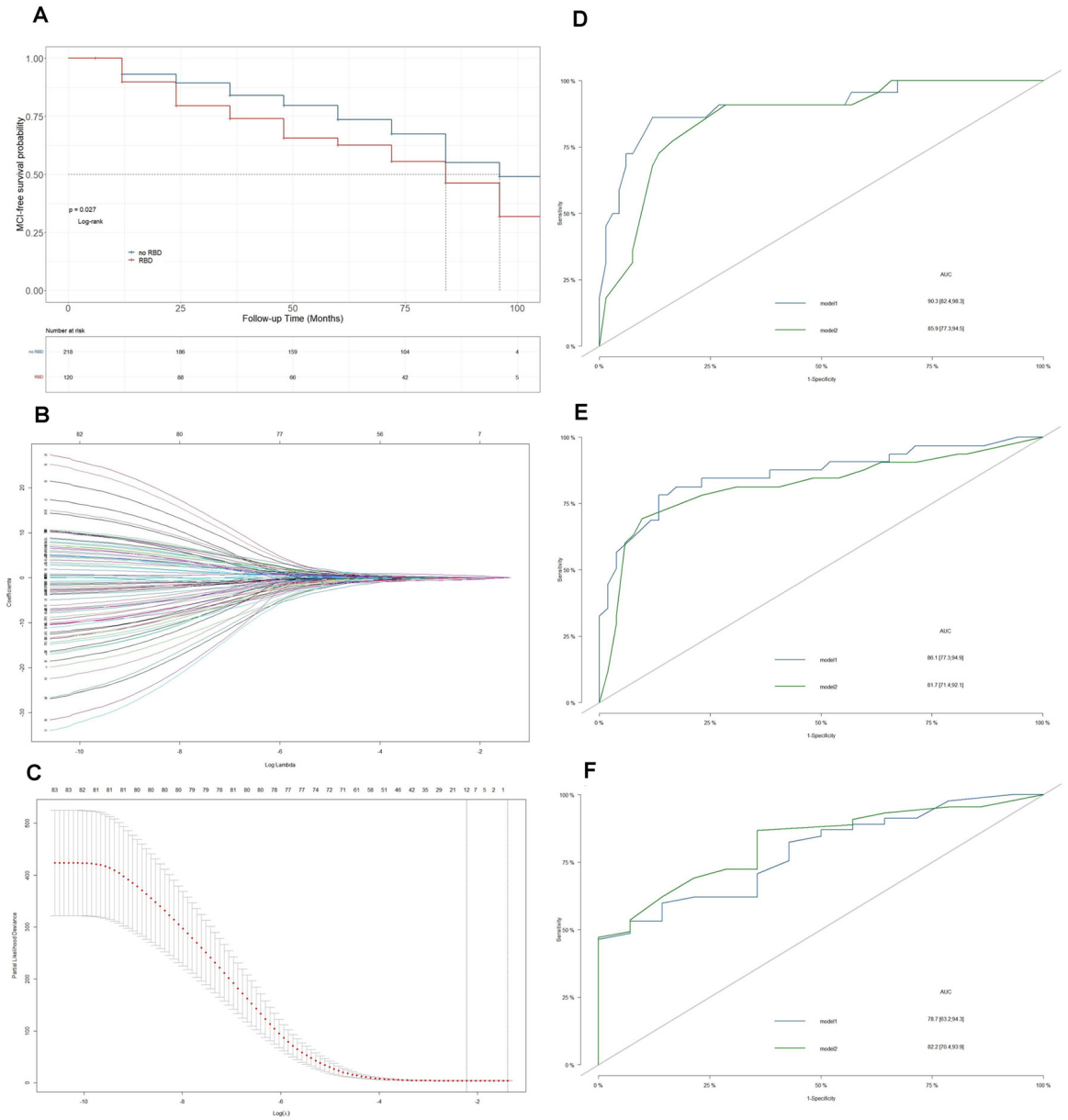


FIGURE 1 | Establishment of the prediction model. **(A)** Kaplan–Meier plots of mild cognitive impairment (MCI)-free survival between Parkinson's Disease (PD)-RBD patients and PD-nRBD patients. **(B)** Optimal parameter selection in the least absolute shrinkage and selection operator (LASSO) regression model. **(C)** The coefficient profiles of 83 variables in the LASSO model. The lambda we selected resulted in six variables with nonzero coefficients. **(D)** ROC curves of model 1 and model 2 for predicting MCI in PD-RBD patients at 3 years. **(E)** ROC curves of model 1 and model 2 for predicting MCI in PD-RBD patients at 5 years. **(F)** ROC curves of model 1 and model 2 for predicting MCI in PD-RBD patients at 7 years.

of their ages at symptom onset were over 55 years old, and their Hoehn and Yahr stages were all at or below level II (**Table 1**). Forty-nine patients in the training set and 13 patients in the validation set developed MCI.

Development of the Prediction Model

The predictors selected from univariate Cox regression and multivariate Cox regression models (model 1) are presented in **Table 2**. UPSIT score (HR = 0.36, P = 0.001), mean signal (HR = 0.44, P = 0.001), and asymmetry index of the putamen (HR = 0.35, $P < 0.001$) on DAT imaging, CSF p-tau/α-syn (HR = 4.27, P = 0.001), and p-tau (HR = 0.52, P = 0.05), and DDRGK1 rs55785911 genotype (HR_{AG} = 0.45, P = 0.016; HR_{AA} = 0.89, P = 0.66) were found to be final predictors of MCI in PD-RBD patients. A lambda value of 0.15 was applied to select candidate predictors (**Figures 1B,C**). The final predictors selected from the LASSO regression and multivariate Cox regression models (model 2) were hyposmia (HR = 0.55,

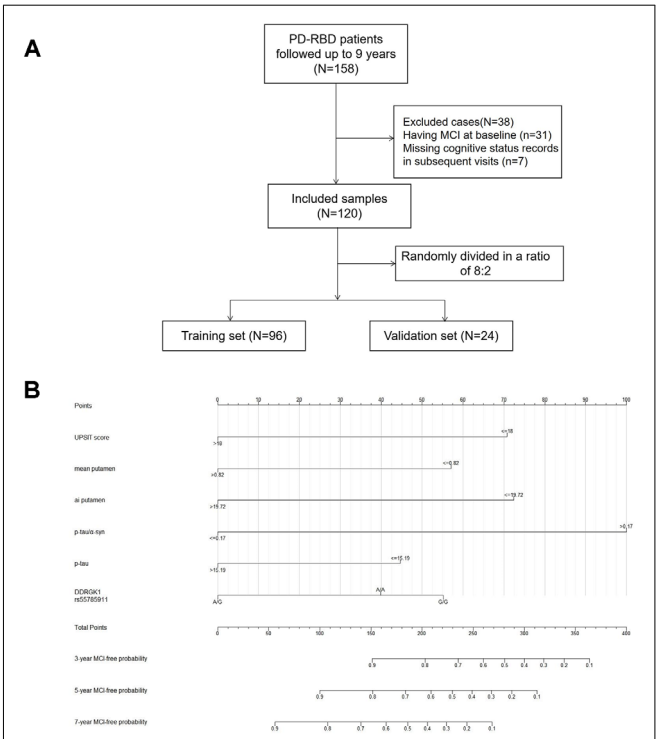


FIGURE 2 | Flow diagram of patient selection and allocation **(A)** and nomogram for predicting the MCI-free probabilities at 3, 5, and 7 years in PD-RBD patients **(B)**. Each level of every predictor corresponds to a score on the points scale, and the total points were acquired by adding the scores of each variable. The total points for each patient correspond to the estimation of the 3-, 5-, and 7-year probabilities of MCI-free survival in this nomogram. Abbreviations: PD, Parkinson's disease; RBD, Rapid eye movement sleep behavior disorder; MCI, mild cognitive impairment; ai, asymmetry index.

P = 0.45) and anosmia (HR = 1.28, P = 0.75) on the UPSIT, mean signal (HR = 0.4, P = 0.007) and asymmetry index of the putamen (HR = 0.37, P = 0.001) on DAT imaging, and CSF p-tau (HR = 3.74, P = 0.001).

ROC curves were plotted to compare the predictive abilities of the two models (**Figures 1D–F**). Model 1 exhibited a higher area under the curve (AUC) than model 2 at 3 years (90.3 vs. 85.9) and 5 years (86.1 vs. 81.7). Model 1 also had a lower AIC than model 2 (350 vs. 357).

Nomogram Construction

Model 1 was visualized with a nomogram (**Figure 2B**). Each level of every predictor corresponds to a score on the points scale, and the total points were acquired by adding the scores of each variable. The total points for each patient correspond to the estimation of the 3-year, 5-year, and 7-year MCI-free probabilities.

For example, suppose a PD-RBD patient scored 15 on the UPSIT, with a mean putamen DAT signal of 1, a putamen asymmetry index of 20 on DAT imaging, a p-tau/α-syn value of 0.5 and a p-tau level of 10 pg/ml in CSF, and had the G/G genotype of DDRGK1 rs55785911. This patient would receive a total score of 270 (UPSIT: 71; mean putamen DAT signal: 0; asymmetry index of putamen: 0; p-tau/α-syn: 100; p-tau: 44; DDRGK1 rs55785911: 55), and the corresponding MCI-free survival probabilities at 3 years and 5 years would be approximately 55% and 28%, respectively.

Discrimination, Calibration, Clinical Usefulness, and Validation

The C-index of model 1 was 0.811 (95% CI: 0.797–0.824, $P < 0.001$), and the C-index of model 2 was 0.782 (95% CI: 0.768–0.796, $P < 0.01$). The calibration plots of model 1 (**Figure 3A**) and model 2 (**Figure 3B**) at 3 years, 5 years, and 7 years suggested a better calibration of model 1. AUCs at different follow-up times were plotted for both models, and it was shown that model 1 always had AUCs higher than 0.75 (**Figure 4A**), and the AUC of model 1 was mostly higher than that of model 2. DCA at 3 years and 7 years showed that high proportions of patients would benefit from the two models. However, the net benefit is above zero only if the risk threshold

TABLE 1 | Basic characteristics of PD-RBD patients with different cognitive outcomes.

	Patients developed MCI (n = 62)	Patients did not develop MCI (n = 58)	P value
Age (years)			
<55	20 (34.5%)	15 (24.2%)	
55–65	18 (31%)	18 (29%)	0.327
>65	20 (34.5%)	29 (46.8%)	
Gender			
Male	32 (55.2%)	46 (74.2%)	0.046
Female	26 (44.8%)	16 (25.8%)	
Education level			
Primary or secondary (<13 years of schooling)	9 (15.5%)	6 (9.7%)	
Tertiary (13–23 years of schooling)	49 (85.5%)	56 (90.3%)	0.49
Age at symptom onset (years)			
<55	24 (41.4%)	17 (27.4%)	0.156
>55	34 (58.6%)	45 (72.6%)	
Hoehn and Yahr stage			
I	32 (55.2%)	26 (41.9%)	0.205
II	26 (44.8%)	36 (58.1%)	

Data are presented as n (%) and compared using the chi-square test.

TABLE 2 | Univariate and multivariate Cox regression analysis based on predictors of MCI in model 1.

Characteristic	Univariate analysis			Multivariate analysis		
	Coefficient	HR (95%CI)	*P* value	Coefficient	HR (95% CI)	*P* value
UPSIT score						0.001
≤18		Reference			Reference	
>18	−0.69	0.5 (0.3, 0.83)	0.007	−1.03	0.36 (0.19, 0.66)	
Mean putamen DAT signal						0.001
≤0.82		Reference			Reference	
>0.82	−1.05	0.35 (0.2, 0.64)	0.001	−0.82	0.44 (0.23, 0.85)	
Asymmetry index of putamen DAT signal						0.001
≤19.72		Reference			Reference	
>19.72	−0.82	0.44 (0.26, 0.73)	0.002	−1.05	0.35 (0.19, 0.66)	
p-tau/α-syn						0.001
≤0.17		Reference			Reference	
>0.17	1.08	2.94 (1.7, 5.06)	0.001	1.45	4.27 (2.2, 8.27)	
p-tau						0.05
≤15.19		Reference			Reference	
>15.19	−0.45	0.64 (0.39, 1.06)	0.081	−0.65	0.52 (0.27, 1.02)	
DDRGK1 rs55785911						
G/G		Reference			Reference	
A/G	−0.89	0.41 (0.24, 0.7)	0.001	−0.8	0.45 (0.23, 0.86)	0.016
A/A	−0.2	0.82 (0.38, 1.79)	0.623	−0.22	0.8 (0.29, 2.2)	0.665

of model 2 is <0.75 at 5 years. In general, the clinical usefulness of model 1 was better than that of model 2 (**Figure 4B**).

A C-index of 0.725 (95% CI: 0.65–0.80, $P = 0.017$) could still be obtained in the validation set. Moreover, the calibration plots of the validation set showed favorable calibration of model 1 at 3, 5, and 7 years (**Figure 5**).

DISCUSSION

MCI is common in PD patients, with a prevalence rate of 18.9–38.2%, and is known to be a risk factor for PDD (Litvan et al., 2011). Early diagnosis of MCI is important for clinicians to provide prompt intervention, and a means of estimating the probability of developing MCI helps both patients and clinicians. PD-RBD was reported to be a diffuse and malignant subtype of PD with more rapid progression in cognition and other NMSs (Postuma et al., 2009; Fereshtehnejad et al., 2015, 2017). PD-RBD patients had an increased risk of developing MCI, as confirmed in several studies (Massicotte-Marquez et al., 2008; Postuma et al., 2012; Manni et al., 2013; Jozwiak et al., 2017), and the coexistence of PD and RBD increased the risk of PDD (Anang et al., 2014). Chahine et al. (2016) first investigated the characteristics of PD-RBD patients from the PPMI database, and they found that PD-RBD patients had a greater rate of decline in global cognition than PD-nRBD patients from the 3-year follow-up data. Their conclusions were similar to those of this study, while we evaluated the patients *via* 9-year follow-up data. This study found that PD-RBD patients had a poorer prognosis of cognition in the 9-year cohort of PPMI. A prediction model conducted by Hogue O et al. showed that RBD was not significantly associated with early cognitive decline (Hogue et al., 2018). The sample they used was also from PPMI *de nova* PD patients, and their definition of early cognitive decline was the same as that in this study. However, the different evaluation times may lead to differences in our results. The prediction model developed by Schrag A showed that the RBDSQ score was associated with CI with an odds ratio of 1.13 at 2 years (Schrag et al., 2017), and a meta-analysis showed that the relative ratio of RBD for PD-CI was between 1.2–11.54, which supported our results (Manni et al., 2013; Guo et al., 2020).

In this study, we used two methods for candidate predictor selection, developed two models, and compared their performance. Model 1, which is based on univariate Cox regression, performed better than model 2 in terms of calibration, discrimination, and clinical usefulness. The C-index calculated from the training set and validation set suggested the favorable predictive ability of this model, and the calibration plots of both the training set and validation set were favorable. Although the AUC of model 1 decreased slightly with follow-up time, the overall AUC was >0.75. Moreover, the clinical usefulness suggested by DCA ensured that a large proportion of patients benefited from this model at subsequent visits.

UPSIT performance was found to be a predictor of PD-MCI in this study, and this result is corroborated by several other studies (Hu et al., 2014; Fullard et al., 2016; Hogue et al., 2018; Roos et al., 2019; Pekel et al., 2020). Moreover, olfactory deficits were found to be a risk and predictor of dementia and PD in iRBD patients (Postuma et al., 2019; Lyu et al., 2021). It has been reported that PD-MCI is more likely to be associated with severe olfactory impairment than PD patients with normal cognition (Park et al., 2018), and an imaging study found entorhinal cortex atrophy in early, drug-naive PD patients with MCI (Jia et al., 2019). Moreover, a study suggested that cortical thinning in the olfactory cortex is a marker for early dementia conversion in PD-MCI (Chung et al., 2019). The mechanisms behind this are still unclear, but deterioration in olfactory function has been suggested to reflect extrastriatal neurodegeneration in PD, and olfactory impairment suggests early involvement of the olfactory bulb in PD (Fullard et al., 2017).

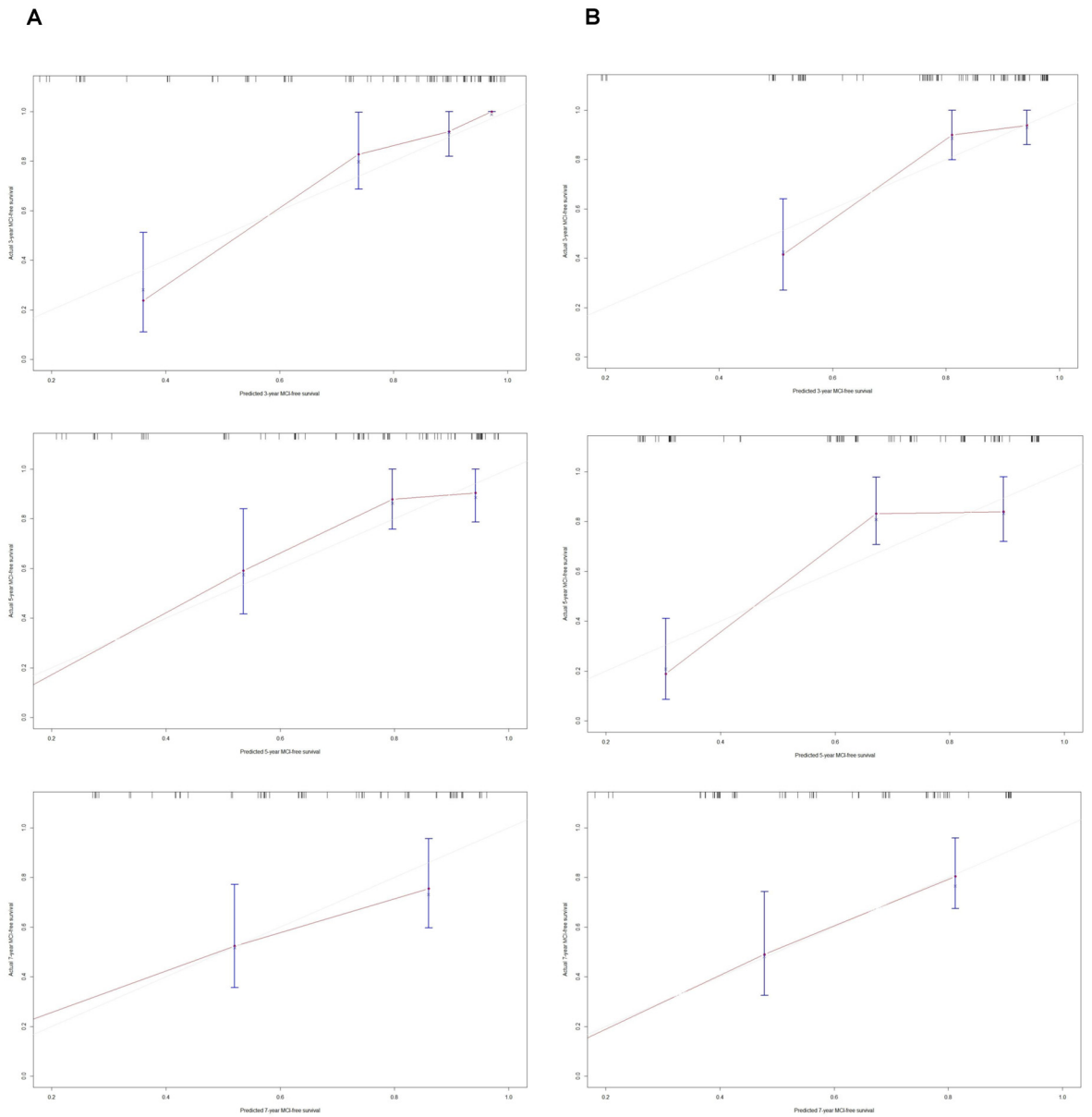


FIGURE 3 | Calibration plots of model-predicted MCI-free survival probabilities at 3 years, 5 years, and 7 years in PD-RBD patients. Model-predicted probabilities of overall survival are plotted on the x-axis; actual overall survival is plotted on the y-axis. **(A)** The calibration curve of model 1-predicted MCI-free survival probabilities at 3 years, 5 years, and 7 years in the training set, $n = 96$. **(B)** The calibration curve of the model 2-predicted probability of MCI-free survival probabilities at 3 years, 5 years, and 7 years in the training set, $n = 96$.

Patients in the early stages of PD often show decreased levels of DAT uptake, especially in the putamen (Benamer et al., 2000). A cohort study followed for 5.5 years found that lower striatal binding at baseline was associated with a higher risk for CI in de novo PD patients (Ravina et al., 2012). Similarly, this study found that a lower mean signal and asymmetry index of the putamen on DAT imaging were correlated with a higher risk of developing MCI. Moreover, it has been reported that PD-RBD patients exhibit a more rapid decrease in DAT binding, and the distinct pattern of striatal DAT binding may contribute to the more malignant subtype—PD-RBD (Cao et al., 2020).

P-tau was reported to induce defective autophagy and mitophagy in Alzheimer's disease (Reddy and Oliver, 2019) and was considered a potential biomarker for PD (Parnetti et al., 2019). A meta-analysis revealed that higher CSF p-tau could be observed in a PDD cohort than in PD patients with normal cognition, while CSF levels of p-tau between PD-CI patients and PD patients with normal cognition were not statistically significant (Hu et al., 2017). In this study, a higher ratio of p-

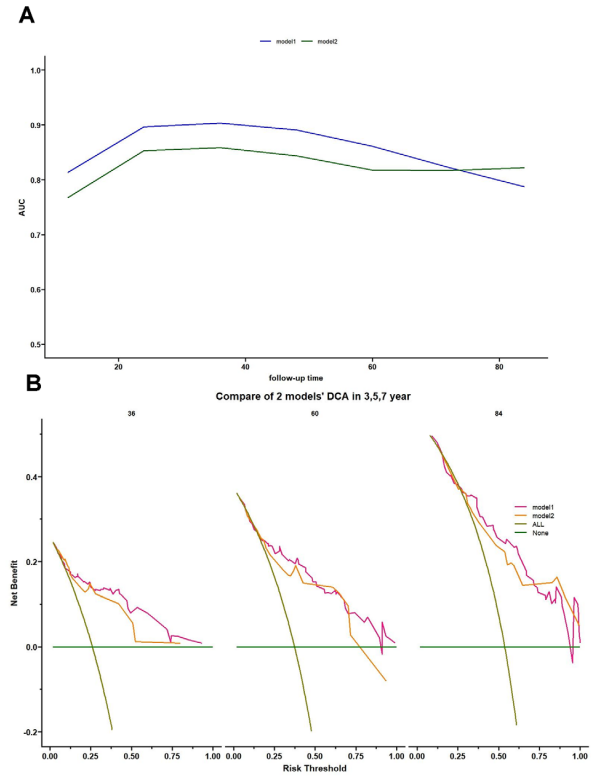


FIGURE 4 | Time-dependent AUC and decision curve analysis (DCA) for model 1 and model 2. **(A)** Time-dependent AUC plot showing how the AUCs of model 1 and model 2 changed with follow-up time. **(B)** DCA of model 1 and model 2 for 3-, 5-, and 7-year predictions. The brown line represents the assumption that all PD-RBD patients have MCI. DCA showed the following: (1) all patients would benefit from model 1 and model 2 for 3-year prediction; (2) for 5-year prediction, patients at risk threshold <0.75 would benefit from model 2, while patients at almost all risk thresholds would gain a positive net benefit in model 1; and (3) using model 1 and model 2 benefits patients more than the treat-all scheme or the treat-none scheme at almost all risk thresholds.

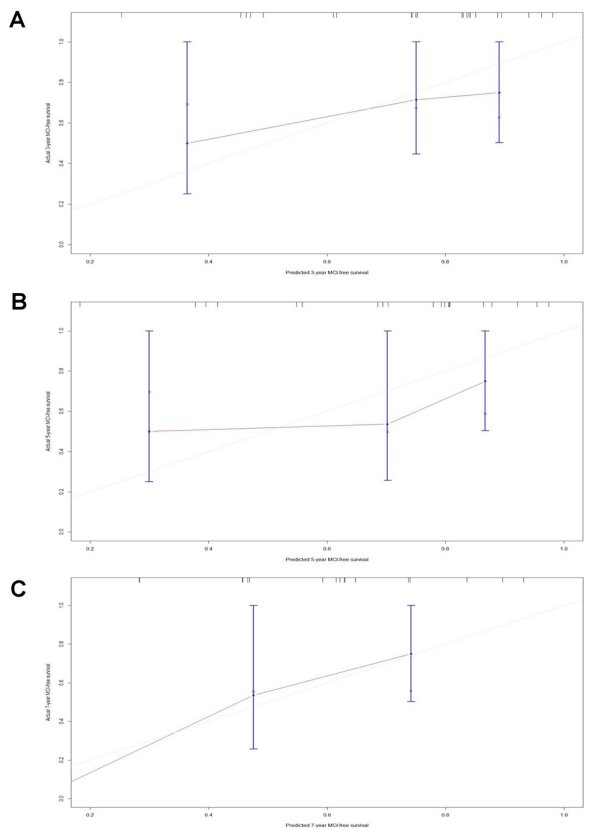


FIGURE 5 | Calibration plots of model 1-predicted probabilities of MCI-free survival at 3 years, 5 years, and 7 years in the validation set. Model-predicted probabilities of overall survival are plotted on the x-axis; actual overall survival is plotted on the y-axis. **(A)** The calibration curve of the model 1-predicted probability of MCI-free survival at 3 years in the validation set, $n = 24$. **(B)** The calibration curve of the model 1-predicted probability of MCI-free survival at 5 years in the validation set, $n = 24$. **(C)** The calibration curve of the model 1-predicted probability of MCI-free survival at 7 years in the validation set, $n = 24$.

tau/α-synuclein was found to be a risk factor for PD-MCI, and this may be specific to this PD-RBD subtype. The role of p-tau in this nomogram was merely to improve the performance of the model, as it was not statistically significant. Future studies with other cohorts are needed to validate the role of CSF p-tau/α-synuclein.

rs55785911/DDRGK1 was an SNP recorded in PPMI SNP data. A large-scale meta-analysis of genome-wide association data has identified DDRGK1 as a risk locus for PD (Nalls et al., 2014; Wang et al., 2016). DDRGK1 is an endoplasmic reticulum membrane protein and a critical component of the ubiquitin-fold modifier 1 (Ufm1) system and is critical for endoplasmic reticulum homeostasis (Liu et al., 2017). Ming Zou et al. investigated the association of variants of SIPA1 L2, MIR4697, GCH1, VPS13C, and DDRGK1 with PD in East Asians; however, they found that rs8118008/DDRGK1 was not correlated with PD (Wang et al., 2016). However, in this study, rs55785911/DDRGK1 was found to contribute to this model, and interestingly, patients with the A/G genotype had a better cognitive prognosis than patients with the G/G genotype. Although no studies have investigated the role of rs55785911/DDRGK1 in PD, the results need to be further confirmed because the results may be caused by sample size, and considering that overall 50 SNPs were tested, it is possible that some of the results were due to chance. Future studies with larger cohorts are needed.

There are several limitations to this study. First, seven patients were excluded from this study for missing cognitive status records in subsequent visits, which may cause bias to this study. Second, this model was only validated internally and should be validated in a different cohort. Third, the patients in this study were de novo and newly diagnosed patients without formal polysomnography (PSG) proven (which is absent from the PPMI database), but many studies using PPMI data were the same as this study, we all used RBDSQ score ≥5 as the cutoff value, and this criterion was validated in several populations. Therefore, this study pioneered further PSG-proven studies. Finally, the sample size of this study was limited.

The aim of this study was to develop a prognostic model for PD-RBD patients to predict the risk of MCI, and as a result, the model showed favorable discrimination, calibration, and clinical usefulness even at 7 years. In conclusion, this study is the first to develop and validate a prognostic model for de novo PD-RBD patients to practically assess MCI-free survival probabilities. This study demonstrated risk factors for MCI in the PD-RBD subgroup, thus contributing insights into the PD-RBD phenotype. As new disease-modifying treatments are being developed, strategies to identify PD-RBD patients at high risk of developing MCI could be useful to prevent or decelerate the progression of MCI in PD-RBD patients. Future studies are needed to validate the model and explore the role of predictors in this model.

DATA AVAILABILITY STATEMENT

Publicly available datasets were analyzed in this study. This data can be found here: http://ppmi-info.org.

ETHICS STATEMENT

The data included in this study are from the Parkinson's Progression Markers Initiative (PPMI) database. For the ethics statements, please see the detailed in http://www.ppmi-info.org.

AUTHOR CONTRIBUTIONS

FC: executed statistical analysis and wrote the first draft. YL: reviewed and critiqued the statistical analysis and the manuscript. GY and LZ: reviewed, critiqued, and revised the manuscript. JL and XB: produced the concept of this project, reviewed, and critiqued the manuscript. All authors contributed to the article and approved the submitted version.

FUNDING

Data used in the preparation of this article were obtained from the Parkinson's Progression Markers Initiative (PPMI) database (www.ppmi-info.org/data). For up-to-date information on the study, visit www.ppmi-info.org. PPMI—a public-private partnership—is funded by the Michael J. Fox Foundation for Parkinson's Research and funding partners, including AbbVie, Avid, Biogen, Bristol-Myers Squibb, Covance, GE Healthcare, Genentech, GlaxoSmithKline, Lundbeck, Eli Lilly, Merck, MesoScaleDiscovery, Pfizer, Piramal, Roche, Sanofi Genzyme, Servier, TEVA, and UCB. This study was supported by the National Natural Science Foundation of China (81873778) and the Science and Technology Commission of Shanghai Municipality (18JC1420303).

REFERENCES

Aarsland, D., Andersen, K., Larsen, J. P., Lolk, A., and Kragh-Sørensen, P. (2003). Prevalence and characteristics of dementia in Parkinson disease: an 8-year prospective study. *Arch. Neurol.* 60, 387–392. doi: 10.1001/archneur.60.3.387

Anang, J. B., Gagnon, J. F., Bertrand, J. A., Romenets, S. R., Latreille, V., Panisset, M., et al. (2014). Predictors of dementia in Parkinson disease: a prospective cohort study. *Neurology* 83, 1253–1260. doi: 10.1212/WNL.0000000000000842

Balachandran, V. P., Gonen, M., Smith, J. J., and DeMatteo, R. P. (2015). Nomograms in oncology: more than meets the eye. *Lancet Oncol.* 16, e173–e180. doi: 10.1016/S1470-2045(14)71116-7

Benamer, H. T., Patterson, J., Wyper, D. J., Hadley, D. M., Macphee, G. J., and Grosset, D. G. (2000). Correlation of Parkinson's disease severity and duration with 123I-FP-CIT SPECT striatal uptake. *Mov. Disord.* 15, 692–698. doi: 10.1002/1531-8257(200007)15:4<692::aid-mds1014>3.0.co;2-v

Camp, R. L., Dolled-Filhart, M., and Rimm, D. L. (2004). X-tile: a new bio-informatics tool for biomarker assessment and outcome-based cut-point optimization. *Clin. Cancer Res.* 10, 7252–7259. doi: 10.1158/1078-0432.CCR-04-0713

Cao, R., Chen, X., Xie, C., Hu, P., and Wang, K. (2020). Serial dopamine transporter imaging of nigrostriatal function in Parkinson's disease with probable REM sleep behavior disorder. *Front. Neurosci.* 14:349. doi: 10.3389/fnins.2020.00349

Chahine, L. M., Xie, S. X., Simuni, T., Tran, B., Postuma, R., Amara, A., et al. (2016). Longitudinal changes in cognition in early Parkinson's disease patients with REM sleep behavior disorder. *Parkinsonism Relat. Disord.* 27, 102–106. doi: 10.1016/j.parkreldis.2016.03.006

Chen, M., Cao, J., Bai, Y., Tong, C., Lin, J., Jindal, V., et al. (2019). Development and validation of a nomogram for early detection of malignant gallbladder lesions. *Clin. Transl. Gastroenterol.* 10:e00098. doi: 10.14309/ctg.0000000000000098

Chung, S. J., Yoo, H. S., Lee, Y. H., Lee, H. S., Ye, B. S., Sohn, Y. H., et al. (2019). Frontal atrophy as a marker for dementia conversion in Parkinson's disease with mild cognitive impairment. *Hum. Brain Mapp.* 40, 3784–3794. doi: 10.1002/hbm.24631

De Cock, V. C., Lannuzel, A., Verhaeghe, S., Roze, E., Ruberg, M., Derenne, J. P., et al. (2007). REM sleep behavior disorder in patients with guadeloupean parkinsonism, a tauopathy. *Sleep* 30, 1026–1032. doi: 10.1093/sleep/30.8.1026

Fereshtehnejad, S. M., Romenets, S. R., Anang, J. B., Latreille, V., Gagnon, J. F., and Postuma, R. B. (2015). New clinical subtypes of parkinson disease and their longitudinal progression: a prospective cohort comparison with other phenotypes. *JAMA Neurol.* 72, 863–873. doi: 10.1001/jamaneurol.2015.0703

Fereshtehnejad, S. M., Zeighami, Y., Dagher, A., and Postuma, R. B. (2017). Clinical criteria for subtyping Parkinson's disease: biomarkers and longitudinal progression. *Brain* 140, 1959–1976. doi: 10.1093/brain/awx118

Friedman, J., Hastie, T., and Tibshirani, R. (2010). Regularization paths for generalized linear models *via* coordinate descent. *J. Stat. Softw.* 33, 1–22. Available online at: https://pubmed.ncbi.nlm.nih.gov/20808728/.

Fullard, M. E., Morley, J. F., and Duda, J. E. (2017). Olfactory dysfunction as an early biomarker in Parkinson's disease. *Neurosci. Bull.* 33, 515–525. doi: 10.1007/s12264-017-0170-x

Fullard, M. E., Tran, B., Xie, S. X., Toledo, J. B., Scordia, C., Linder, C., et al. (2016). Olfactory impairment predicts cognitive decline in early Parkinson's disease. *Parkinsonism Relat. Disord.* 25, 45–51. doi: 10.1016/j.parkreldis.2016.02.013

Gagnon, J. F., Vendette, M., Postuma, R. B., Desjardins, C., Massicotte-Marquez, J., Panisset, M., et al. (2009). Mild cognitive impairment in rapid eye movement sleep behavior disorder and Parkinson's disease. *Ann. Neurol.* 66, 39–47. doi: 10.1002/ana.21680

Guo, Y., Liu, F. T., Hou, X. H., Li, J. Q., Cao, X. P., Tan, L., et al. (2020). Predictors of cognitive impairment in Parkinson's disease: a systematic review and meta-analysis of prospective cohort studies. *J. Neurol.* doi: 10.1007/s00415-020-09757-9 [Online ahead of print].

Hely, M. A., Reid, W. G., Adena, M. A., Halliday, G. M., and Morris, J. G. (2008). The Sydney multicenter study of Parkinson's disease: the inevitability of dementia at 20 years. *Mov. Disord.* 23, 837–844. doi: 10.1002/mds.21956

Hogue, O., Fernandez, H. H., and Floden, D. P. (2018). Predicting early cognitive decline in newly-diagnosed Parkinson's patients: a practical model. *Parkinsonism Relat. Disord.* 56, 70–75. doi: 10.1016/j.parkreldis.2018.06.031

Hu, M. T., Szewczyk-Królikowski, K., Tomlinson, P., Nithi, K., Rolinski, M., Murray, C., et al. (2014). Predictors of cognitive impairment in an early stage Parkinson's disease cohort. *Mov. Disord.* 29, 351–359. doi: 10.1002/mds.25748

Hu, X., Yang, Y., and Gong, D. (2017). Changes of cerebrospinal fluid Aβ42, t-tau and p-tau in Parkinson's disease patients with cognitive impairment relative to those with normal cognition: a meta-analysis. *Neurol. Sci.* 38, 1953–1961. doi: 10.1007/s10072-017-3088-1

Iasonos, A., Schrag, D., Raj, G. V., and Panageas, K. S. (2008). How to build and interpret a nomogram for cancer prognosis. *J. Clin. Oncol.* 26, 1364–1370. doi: 10.1200/JCO.2007.12.9791

Janvin, C. C., Larsen, J. P., Aarsland, D., and Hugdahl, K. (2006). Subtypes of mild cognitive impairment in Parkinson's disease: progression to dementia. *Mov. Disord.* 21, 1343–1349. doi: 10.1002/mds.20974

Ji, G. W., Zhu, F. P., Xu, Q., Wang, K., Wu, M. Y., Tang, W. W., et al. (2019). Machine-learning analysis of contrast-enhanced CT radiomics predicts recurrence of hepatocellular carcinoma after resection: a multi-institutional study. *EBioMedicine* 50, 156–165. doi: 10.1016/j.ebiom.2019.10.057

Jia, X., Wang, Z., Yang, T., Li, Y., Gao, S., Wu, G., et al. (2019). Entorhinal cortex atrophy in early, drug-naive Parkinson's disease with mild cognitive impairment. *Aging Dis.* 10, 1221–1232. doi: 10.14336/AD.2018.1116

Jozwiak, N., Postuma, R. B., Montplaisir, J., Latreille, V., Panisset, M., Chouinard, S., et al. (2017). REM sleep behavior disorder and cognitive impairment in Parkinson's disease. *Sleep* 40:zsx101. doi: 10.1093/sleep/zsx101

Kalia, L. V., and Lang, A. E. (2015). Parkinson's disease. *Lancet* 386, 896–912. doi: 10.1016/S0140-6736(14)61393-3

Kamble, N., Yadav, R., Lenka, A., Kumar, K., Nagaraju, B. C., and Pal, P. K. (2019). Impaired sleep quality and cognition in patients of Parkinson's disease with REM sleep behavior disorder: a comparative study. *Sleep Med.* 62, 1–5. doi: 10.1016/j.sleep.2019.04.001

Kim, Y. E., and Jeon, B. S. (2014). Clinical implication of REM sleep behavior disorder in Parkinson's disease. *J. Parkinsons Dis.* 4, 237–244. doi: 10.3233/JPD-130293

Kramer, A. A., and Zimmerman, J. E. (2007). Assessing the calibration of mortality benchmarks in critical care: the Hosmer-Lemeshow test revisited. *Crit. Care Med.* 35, 2052–2056. doi: 10.1097/01.CCM.0000275267.64078.B0

Lin, Y. Q., and Chen, S. D. (2018). RBD: a red flag for cognitive impairment in Parkinson's disease. *Sleep Med.* 4, 38–44. doi: 10.1016/j.sleep.2018.01.006

Litvan, I., Aarsland, D., Adler, C. H., Goldman, G., Kulisevsky, J., Mollenhauer, B., et al. (2011). MDS Task Force on mild cognitive impairment in Parkinson's disease: critical review of PD-MCI. *Mov. Disord.* 26, 1814–1824. doi: 10.1002/mds.23823

Litvan, I., Goldman, J. G., Tröster, A. I., Schmand, B. A., Weintraub, D., Petersen, R. C., et al. (2012). Diagnostic criteria for mild cognitive impairment in Parkinson's disease: movement disorder society task force guidelines. *Mov. Disord.* 27, 349–356. doi: 10.1002/mds.24893

Liu, J., Wang, Y., Song, L., Zeng, L., Yi, W., Liu, T., et al. (2017). A critical role of DDRGK1 in endoplasmic reticulum homoeostasis *via* regulation of IRE1α stability. *Nat. Commun.* 8:14186. doi: 10.1038/ncomms14186

Lyu, Z., Zheng, S., Zhang, X., Mai, Y., Pan, J., Hummel, T., et al. (2021). Olfactory impairment as an early marker of Parkinson's disease in REM sleep behaviour disorder: a systematic review and meta-analysis. *J. Neurol. Neurosurg. Psychiatry* 92, 271–281. doi: 10.1136/jnnp-2020-325361

Mahowald, M. W., and Schenck, C. H. (2013). REM sleep behaviour disorder: a marker of synucleinopathy. *Lancet Neurol.* 12, 417–419. doi: 10.1016/S1474-4422(13)70078-4

Manni, R., Sinforiani, E., Pacchetti, C., Zucchella, C., Cremascoli, R., and Terzaghi, M. (2013). Cognitive dysfunction and REM sleep behavior disorder: key findings in the literature and preliminary longitudinal findings. *Int. J. Psychophysiol.* 89, 213–217. doi: 10.1016/j.ijpsycho.2013.04.003

Massicotte-Marquez, J., Décary, A., Gagnon, J. F., Vendette, M., Mathieu, A., Postuma, R. B., et al. (2008). Executive dysfunction and memory impairment in idiopathic REM sleep behavior disorder. *Neurology* 70, 1250–1257. doi: 10.1212/01.wnl.0000286943.79593.a6

Nalls, M. A., Keller, M. F., Hernandez, D. G., Chen, L., Stone, D. J., Singleton, A. B., et al. (2016). Baseline genetic associations in the Parkinson's progression markers initiative (PPMI). *Mov. Disord.* 31, 79–85. doi: 10.1002/mds.26374

Nalls, M. A., Pankratz, N., Lill, C. M., Do, C. B., Hernandez, D. G., Saad, M., et al. (2014). Large-scale meta-analysis of genome-wide association data identifies six new risk loci for Parkinson's disease. *Nat. Genet.* 46, 989–993. doi: 10.1038/ng.3043

Nomura, T., Inoue, Y., Kagimura, T., and Nakashima, K. (2013). Clinical significance of REM sleep behavior disorder in Parkinson's disease. *Sleep Med.* 14, 131–135. doi: 10.1016/j.sleep.2012.10.011

Nomura, T., Inoue, Y., Kagimura, T., Uemura, Y., and Nakashima, K. (2011). Utility of the REM sleep behavior disorder screening questionnaire (RBDSQ) in Parkinson's disease patients. *Sleep Med.* 12, 711–713. doi: 10.1016/j.sleep.2011.01.015

Nomura, T., Kishi, M., and Nakashima, K. (2017). Differences in clinical characteristics when REM sleep behavior disorder precedes or comes after the onset of Parkinson's disease. *J. Neurol. Sci.* 382, 58–60. doi: 10.1016/j.jns.2017.08.3247

Pagano, G., De Micco, R., Yousaf, T., Wilson, H., Chandra, A., and Politis, M. (2018). REM behavior disorder predicts motor progression and cognitive decline in Parkinson disease. *Neurology* 91, e894–e905. doi: 10.1212/WNL.0000000000006134

Park, J. W., Kwon, D. Y., Choi, J. H., Park, M. H., and Yoon, H. K. (2018). Olfactory dysfunctions in drug-naïve Parkinson's disease with mild cognitive impairment. *Parkinsonism Relat. Disord.* 46, 69–73. doi: 10.1016/j.parkreldis.2017.11.334

Parkinson Progression Marker Initiative. (2011). The Parkinson progression marker initiative (PPMI). *Prog. Neurobiol.* 95, 629–635. doi: 10.1016/j.pneurobio.2011.09.005

Parnetti, L., Paciotti, S., Farotti, L., Bellomo, G., Sepe, F. N., and Eusebi, P. (2019). Parkinson's and Lewy body dementia CSF biomarkers. *Clin. Chim. Acta* 495, 318–325. doi: 10.1016/j.cca.2019.04.078

Pekel, N. B., Yildiz, D., Taymur, İ., Budak, E., Özmen, S., Çapkur, Ç., et al. (2020). Associations between olfactory impairment and cognitive functions in patients with Parkinson disease. *Noro Psikiyatr. Ars.* 57, 216–221. doi: 10.29399/npa.23070

Pencina, M. J., and D'Agostino, R. B. (2004). Overall C as a measure of discrimination in survival analysis: model specific population value and confidence interval estimation. *Stat. Med.* 23, 2109–2123. doi: 10.1002/sim.1802

Postuma, R. B., Bertrand, J. A., Montplaisir, J., Desjardins, C., Vendette, M., Rios Romenets, S., et al. (2012). Rapid eye movement sleep behavior disorder and risk of dementia in Parkinson's disease: a prospective study. *Mov. Disord.* 27, 720–726. doi: 10.1002/mds.24939

Postuma, R. B., Gagnon, J. F., Vendette, M., Charland, K., and Montplaisir, J. (2008). REM sleep behaviour disorder in Parkinson's disease is associated with specific motor features. *J. Neurol. Neurosurg. Psychiatry* 79, 1117–1121. doi: 10.1136/jnnp.2008.149195

Postuma, R. B., Gagnon, J. F., Vendette, M., and Montplaisir, J. Y. (2009). Markers of neurodegeneration in idiopathic rapid eye movement sleep behaviour disorder and Parkinson's disease. *Brain* 132, 3298–3307. doi: 10.1093/brain/awp244

Postuma, R. B., Iranzo, A., Hu, M., Högl, B., Boeve, B. F., Manni, R., et al. (2019). Risk and predictors of dementia and parkinsonism in idiopathic REM sleep behaviour disorder: a multicentre study. *Brain* 142, 744–759. doi: 10.1093/brain/awz030

Ravina, B., Marek, K., Eberly, S., Oakes, D., Kurlan, R., Ascherio, A., et al. (2012). Dopamine transporter imaging is associated with long-term outcomes in Parkinson's disease. *Mov. Disord.* 27, 1392–1397. doi: 10.1002/mds.25157

Reddy, P. H., and Oliver, D. M. (2019). Amyloid beta and phosphorylated tau-induced defective autophagy and mitophagy in Alzheimer's disease. *Cells* 8:488. doi: 10.3390/cells8050488

Roos, D. S., Twisk, J., Raijmakers, P., Doty, R. L., and Berendse, H. W. (2019). Hyposmia as a marker of (non-)motor disease severity in Parkinson's disease. *J. Neural Transm. (Vienna)* 126, 1471–1478. doi: 10.1007/s00702-019-02074-0

Schrag, A., Siddiqui, U. F., Anastasiou, Z., Weintraub, D., and Schott, J. M. (2017). Clinical variables and biomarkers in prediction of cognitive impairment in patients with newly diagnosed Parkinson's disease: a cohort study. *Lancet Neurol.* 16, 66–75. doi: 10.1016/S1474-4422(16)30328-3

Sinforiani, E., Pacchetti, C., Zangaglia, R., Pasotti, C., Manni, R., and Nappi, G. (2008). REM behavior disorder, hallucinations and cognitive impairment in Parkinson's disease: a two-year follow up. *Mov. Disord.* 23, 1441–1445. doi: 10.1002/mds.22126

Sinforiani, E., Zangaglia, R., Manni, R., Cristina, S., Marchioni, E., Nappi, G., et al. (2006). REM sleep behavior disorder, hallucinations and cognitive impairment in Parkinson's disease. *Mov. Disord.* 21, 462–466. doi: 10.1002/mds.20719

Sixel-Döring, F., Trautmann, E., Mollenhauer, B., and Trenkwalder, C. (2011). Associated factors for REM sleep behavior disorder in Parkinson disease. *Neurology* 77, 1048–1054. doi: 10.1212/WNL.0b013e31822e560e

Stefani, A., Heidbreder, A., Brandauer, E., Guaita, M., Neier, L.-M., Mitterling, T., et al. (2018). Screening for idiopathic REM sleep behavior disorder: usefulness of actigraphy. *Sleep* 41:zsy053. doi: 10.1093/sleep/zsy053

Stiasny-Kolster, K., Mayer, G., Schäfer, S., Möller, J. C., Heinzel-Gutenbrunner, M., and Oertel, W. H. (2007). The REM sleep behavior disorder screening questionnaire—a new diagnostic instrument. *Mov. Disord.* 22, 2386–2393. doi: 10.1002/mds.21740

Trout, J., Christiansen, T., Bulkley, M. B., Tanner, J. J., Sozda, C. N., Bowers, D., et al. (2019). Cognitive impairments and self-reported sleep in early-stage Parkinson's disease with versus without probable REM sleep behavior disorder. *Brain Sci.* 10:9. doi: 10.3390/brainsci10010009

Vendette, M., Gagnon, J. F., Décary, A., Massicotte-Marquez, J., Postuma, R. B., Doyon, J., et al. (2007). REM sleep behavior disorder predicts cognitive impairment in Parkinson disease without dementia. *Neurology* 69, 1843–1849. doi: 10.1212/01.wnl.0000278114.14096.74

Vickers, A. J., and Elkin, E. B. (2006). Decision curve analysis: a novel method for evaluating prediction models. *Med. Decis. Making* 26, 565–574. doi: 10.1177/0272989X06295361

Wang, L., Cheng, L., Li, N. N., Yu, W. J., Sun, X. Y., and Peng, R. (2016). Association of four new candidate genetic variants with Parkinson's disease in a Han Chinese population. *Am. J. Med. Genet. B Neuropsychiatr. Genet.* 171B, 342–347. doi: 10.1002/ajmg.b.32410

Wang, Y., Wang, Z. W., Yang, Y. C., Wu, H. J., Zhao, H. Y., and Zhao, Z. X. (2015). Validation of the rapid eye movement sleep behavior disorder screening questionnaire in China. *J. Clin. Neurosci.* 22, 1420–1424. doi: 10.1016/j.jocn.2015.03.008

Weintraub, D., Simuni, T., Caspell-Garcia, C., Coffey, C., Lasch, S., Siderowf, A., et al. (2015). Cognitive performance and neuropsychiatric symptoms in early, untreated Parkinson's disease. *Mov. Disord.* 30, 919–927. doi: 10.1002/mds.26170

Yan, Y. Y., Lei, K., Li, Y. Y., Liu, X. F., and Chang, Y. (2019). The correlation between possible RBD and cognitive function in Parkinson's disease patients in China. *Ann. Clin. Transl. Neurol.* 6, 848–853. doi: 10.1002/acn3.747

Ye, G., Li, Y., Zhou, L., Zhang, Y., Zhu, L., Zhao, A., et al. (2020). Predictors of conversion to α-synucleinopathy diseases in idiopathic rapid eye movement sleep behavior disorder. *J. Parkinsons Dis.* 10, 1443–1455. doi: 10.3233/JPD-202243

Conflict of Interest: The authors declare that the research was conducted in the absence of any commercial or financial relationships that could be construed as a potential conflict of interest.

Copyright © 2021 Chen, Li, Ye, Zhou, Bian and Liu. This is an open-access article distributed under the terms of the Creative Commons Attribution License (CC BY). The use, distribution or reproduction in other forums is permitted, provided the original author(s) and the copyright owner(s) are credited and that the original publication in this journal is cited, in accordance with accepted academic practice. No use, distribution or reproduction is permitted which does not comply with these terms.

frontiers in Aging Neuroscience

BRIEF RESEARCH REPORT
published: 12 August 2021
doi: 10.3389/fnagi.2021.648151

Genetic Analysis and Literature Review of *SNCA* Variants in Parkinson's Disease

Yi Guo[1], *Yan Sun*[2], *Zhi Song*[3], *Wen Zheng*[3], *Wei Xiong*[4], *Yan Yang*[3], *Lamei Yuan*[2,3,5]* *and Hao Deng*[2,3,5]*

[1] Department of Medical Information, School of Life Sciences, Central South University, Changsha, China, [2] Center for Experimental Medicine, The Third Xiangya Hospital, Central South University, Changsha, China, [3] Department of Neurology, The Third Xiangya Hospital, Central South University, Changsha, China, [4] Cancer Research Institute, Xiangya School of Medicine, Central South University, Changsha, China, [5] Disease Genome Research Center, Central South University, Changsha, China

Parkinson's disease (PD) is the fastest-growing neurodegenerative disorder. Aging, environmental factors, and genetics are considered as risk factors. The alpha-synuclein gene (*SNCA*), the first pathogenic gene identified in a familial form of PD, was indisputably involved as a heritable component for familial and sporadic PD. In this study, whole-exome sequencing and Sanger sequencing were performed to evaluate the association between the *SNCA* gene variants and PD. The genetic data of 438 clinically diagnosed patients with PD and 543 matched control populations of the Han Chinese were analyzed. The literature review of *SNCA* variants for 231 cases reported in 89 articles was extracted from the PubMed and the Movement Disorder Society Genetic mutation database. No potentially causative variant(s) in the *SNCA* gene, excepting two single-nucleotide nonsynonymous variants c.158C>T (p.A53V, rs542171324) and c.349C>T (p.P117S, rs145138372), were detected. There was no statistically significant difference in the genotypic or allelic frequencies for either variant between the PD group and the control group (all $P > 0.05$). No copy number variants of the *SNCA* gene were detected. The results of this study suggest that the variants in the exons of the *SNCA* gene may have less or no role in the development of PD in the Han Chinese populations. The literature review suggests that psychiatric signs and cognitive decline/dementia were more common among patients with *SNCA* duplication or triplication (psychiatric signs: $\chi^2 = 7.892$, $P = 0.005$; cognitive decline/dementia: $\chi^2 = 8.991$, $P = 0.003$).

Keywords: Parkinson's disease, *SNCA* gene, genetic analysis, whole-exome sequencing, Sanger sequencing, variant

OPEN ACCESS

Edited by:
Gianluigi Zanusso, University of Verona, Italy

Reviewed by:
Manabu Funayama, Juntendo University, Japan
Birgitt Schüle, Stanford University, United States

***Correspondence:**
Hao Deng
hdeng008@yahoo.com
Lamei Yuan
yuanlamei229@163.com

Received: *31 December 2020*
Accepted: *29 June 2021*
Published: *12 August 2021*

Citation:
Guo Y, Sun Y, Song Z, Zheng W, Xiong W, Yang Y, Yuan L and Deng H (2021) Genetic Analysis and Literature Review of SNCA Variants in Parkinson's Disease. Front. Aging Neurosci. 13:648151. doi: 10.3389/fnagi.2021.648151

INTRODUCTION

Parkinson's disease (PD), first reported by Dr. James Parkinson in his *An Essay on the Shaking Palsy* in 1817 and named by Jean-Martin Charcot, is the fastest-growing neurodegenerative disorder with an age-related prevalence of ∼3% among the population aged above 75 years and 4–5% of people older than 85 years (Hernandez et al., 2016; Emamzadeh, 2017; Billingsley et al., 2018; Hopfner et al., 2020). It is conservatively estimated that the PD cases will be 2-fold, i.e., from 6.2

million in 2015 to 12.9 million by 2040 (Dorsey and Bloem, 2018). Neuropathologically, PD is characterized by dopaminergic neuron loss in the substantia nigra pars compacta and insoluble alpha-synuclein-containing Lewy bodies formation in the remaining nigral neurons (Cook Shukla et al., 2004; Billingsley et al., 2018). Although the precise etiology has not been completely elucidated, advanced age, environmental influences, and genetics are thought to be the risk factors (Langston et al., 2015; Dorsey and Bloem, 2018). PD motor deficits include any or all of the following: bradykinesia/hypokinesia/akinesia, resting tremor, muscular rigidity, postural abnormality, gait disturbance, and freezing. The clinical pictures also include a range of nonmotor manifestations such as olfactory dysfunction, autonomic impairment, cognitive decline, and neuropsychiatric disturbance (Postuma et al., 2015; Liu and Le, 2020).

Although ∼5–10% of PD causation has been attributed to different monogenic causes, sporadic PD can be related to various additional genes and susceptibility loci (Balestrino and Schapira, 2020; Toffoli et al., 2020). Several technologies, including the high-throughput techniques such as whole-exome sequencing (WES) and whole-genome sequencing, as well as machine learning and single-cell RNA sequencing, have discovered a great number of genetic risk factors in PD (Deng et al., 2018; Blauwendraat et al., 2020). To date, at least 23 genes related to parkinsonism and a number of independent risk signals have been identified (Langston et al., 2015; Deng et al., 2018; Nalls et al., 2019; Blauwendraat et al., 2020).

The alpha-synuclein gene (*SNCA*) was indisputably considered as the first pathogenic gene responsible for autosomal dominant PD, supported by the fact that its protein aggregation is thought to be the primary pathological hallmark of the patients, though only a few mutations were identified (Polymeropoulos et al., 1997; Fields et al., 2019). In this study, WES and Sanger sequencing were performed to evaluate the association between *SNCA* gene variants and PD, and the literature review of *SNCA* variants was conducted.

MATERIALS AND METHODS

Study Subjects and Clinical Evaluation

The WES data of the *SNCA* gene were extracted from the internal PD-control database. A total of 981 Han Chinese participants from mainland China were recruited, including 438 clinically diagnosed patients with PD (male/female: 49.54%/50.46%, mean age: 59.19 ± 11.46 years, and mean age of onset: 55.67 ± 12.35 years) and 543 age- and sex-matched controls (male/female: 50.09%/49.91%, mean age: 58.11 ± 13.61 years) who had neither PD clinical symptoms nor a family history of PD. Among them, 438 patients with PD were consecutively recruited into this study, of which 308 were unrelated sporadic cases and 130 had a family history of PD. All PD individuals were evaluated by two experienced neurologists from the Third Xiangya Hospital, Central South University (Changsha, China) and were diagnosed with PD based on the official International Parkinson and Movement Disorder Society Clinical Diagnostic Criteria for PD (Postuma et al., 2015). The protocol was approved by the Institutional Review Board of the Third Xiangya Hospital, Central South University and was conducted in accordance with the tenets of the Declaration of Helsinki. Written informed consents were obtained from all participants. Moreover, a comprehensive literature review was performed to assess the associations between phenotypes and *SNCA* gene variants by PubMed (https://pubmed.ncbi.nlm.nih.gov/) and the Movement Disorder Society Genetic mutation database (MDSGene, https://www.mdsgene.org/). The following key search terms were used: "*SNCA*," "alpha-synuclein," "PD," "Parkinson's disease," "Parkinson disease," "point mutation," "mutation," "variant," "multiplication," "duplication," and "triplication."

WES and Sanger Sequencing

Genomic DNA (gDNA) was harvested from peripheral blood leukocytes according to the standard phenol–chloroform extraction as previously described (Yuan et al., 2015). WES was conducted on the gDNA to construct an internal PD-control database as previously described (Xiang et al., 2019). Frequencies of variants, such as single-nucleotide polymorphisms (SNPs) and insertions–deletions, were assessed using several public databases, such as the 1000 Genomes Project, the Single Nucleotide Polymorphism database (version 154), the Exome Aggregation Consortium, the Genome Aggregation Database, and the China Metabolic Analytics Project database (Xiang et al., 2019; Cao et al., 2020). The variant with an allele frequency over 1% was further filtered out, and the bioinformatics prediction software, such as Sorting Intolerant from Tolerant (SIFT), Protein Variation Effect Analyzer (PROVEAN), Polymorphism Phenotyping version 2 (PolyPhen-2), and MutationTaster, were utilized to evaluate the potential effects on the function and structure of the alpha-synuclein protein. The potential pathogenicity of identified variants was further assessed using the pathogenicity scoring algorithm and the category criteria of MDSGene (Klein et al., 2018). The conservation of amino acid sequences was analyzed by using the NCBI BLAST resources (https://blast.ncbi.nlm.nih.gov/Blast.cgi). The locus-specific PCR amplification and the bidirectional Sanger sequencing were performed to confirm variants using the primers 5′-CAATTTAAGGCTAGCTTGAGACTTATG-3′ and 5′-TCTTGAATACTGGGCCACAC-3′, as well as 5′-TCATCATGTTCTTTTTGTGCTTC-3′ and 5′-TGCAAGTTGTCCACGTAATGA-3′. In 100 PD cases, copy number variants (CNVs) were called using the CNVnator (version 0.3.2) read-depth algorithm (Abyzov et al., 2011).

Statistical Analysis

Fisher's exact test or Pearson's chi-squared test was applied to compare the categorical variables. The Hardy–Weinberg equilibrium for the genotype frequencies of PD subjects and controls was tested. The discrepancy of genotype and allele frequencies between the PD group and the control group was analyzed. Associations between different types of reported *SNCA* gene variants and recorded psychiatric signs as well as cognitive decline/dementia in the literature, which were reported to be common in PD (Book et al., 2018), were assessed. Two-sided $P < 0.05$ were considered statistically significant. The statistical

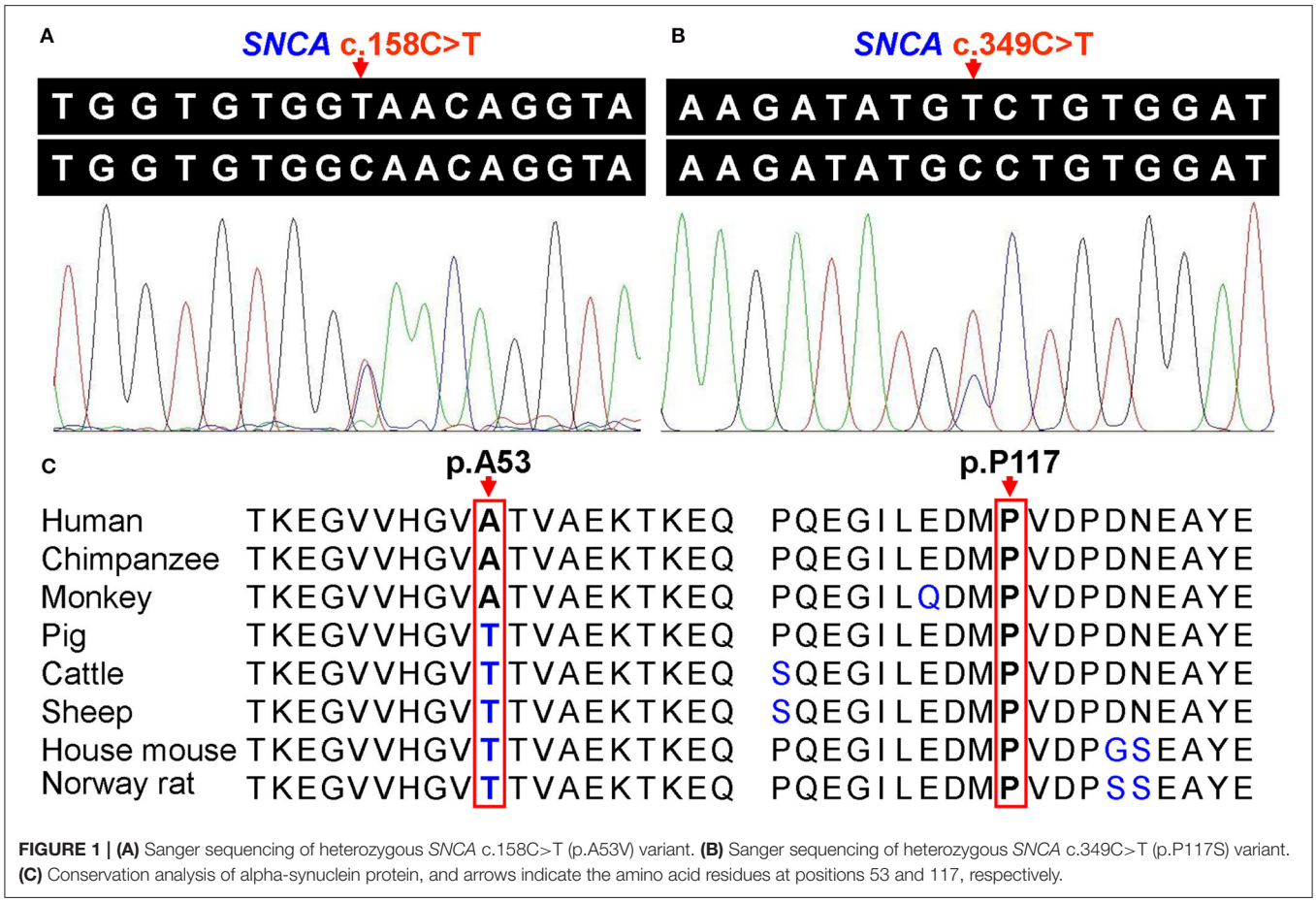


FIGURE 1 | (A) Sanger sequencing of heterozygous *SNCA* c.158C>T (p.A53V) variant. **(B)** Sanger sequencing of heterozygous *SNCA* c.349C>T (p.P117S) variant. **(C)** Conservation analysis of alpha-synuclein protein, and arrows indicate the amino acid residues at positions 53 and 117, respectively.

TABLE 1 | Allelic frequencies and bioinformatics predictions of the *SNCA* rs542171324 and rs145138372 variants.

dbSNP154	Variants	Bioinformatics predictions				MDSGene	Allelic frequencies			
		SIFT	PolyPhen-2	MutationTaster	PROVEAN		1000G	ExAC	gnomAD	ChinaMap
rs542171324	c.158C>T (p.A53V)	Damaging	Benign	Polymorphism	Neutral	Probably pathogenic	2×10^{-4}	8.24×10^{-6}	7.95×10^{-6}	1.89×10^{-4}
rs145138372	c.349C>T (p.P117S)	Tolerated	Benign	Disease causing	Neutral	Probably pathogenic	5.99×10^{-4}	7.43×10^{-5}	7.57×10^{-5}	8.03×10^{-4}

SNCA, the alpha-synuclein gene; dbSNP154, Single Nucleotide Polymorphism database version 154; SIFT, Sorting Intolerant from Tolerant; PolyPhen-2, Polymorphism Phenotyping version 2; PROVEAN, Protein Variation Effect Analyzer; MDSGene, Movement Disorder Society Genetic mutation database; 1000G, 1000 Genomes Project; ExAC, Exome Aggregation Consortium; gnomAD, Genome Aggregation Database; ChinaMap, China Metabolic Analytics Project.

analysis was performed by SPSS statistical software (version 25.0, SPSS Inc., Chicago, IL, USA).

RESULTS

The WES data of the coding regions of the *SNCA* gene and exon–intron boundaries revealed 17 variants, and other putative pathogenic variants for monogenic PD were not detected in these patients. Two known likely pathogenic single-nucleotide nonsynonymous variants (NM_000345.3), namely, c.158C>T (p.A53V, rs542171324) and c.349C>T (p.P117S, rs145138372), were separately detected in two and one patients with PD, respectively (**Supplementary Table 1**). Patient 1 with p.A53V variant was a 56-year-old female with an onset age of 53 years. The initial symptom was bradykinesia and "pill-rolling" rest tremor in her right upper limb, which subsequently progressed into the left lower limb. The rigidity was also presented on her right limbs. These motor symptoms slowly progressed. Over a period of 3 years, a sleep disorder was manifested. The skull MRI results were normal. Patient 2 with p.A53V variant was a 56-year-old female with an onset age of 52 years. She had similar phenotypic characteristics as those manifested in Patient 1. Patient 3 with p.P117S variant was a 76-year-old male. The initial symptoms were bradykinesia and rest tremor in both

upper limbs. He presented typical signs and symptoms of PD such as dystonia in both lower limbs, gait disturbance, and apathy, as well as a sleep disorder. No family history of PD or other related neurodegenerative disease was admitted in these three patients. Both identified variants were confirmed by Sanger sequencing (**Figures 1A,B**), and neither was observed in any of the 543 controls. SIFT predicted that rs542171324 would be "damaging," while no potential effects on protein structure or function were revealed by PROVEAN, PolyPhen-2, or MutationTaster. The rs145138372 was predicted to be "disease causing" by MutationTaster, while no potential effects on protein structure or function were revealed by SIFT, PROVEAN, or PolyPhen-2. According to the MDSGene criteria, *SNCA* c.158C>T (p.A53V) and c.349C>T (p.P117S) were interpreted as "probably pathogenic" with a score of 13 and 10, respectively (**Table 1**). Alanine at position 53 (p.A53) is not conserved between humans and rodents in which threonine is common in most species, while proline at position 117 (p.P117) is conserved in several species (**Figure 1C**). The Hardy–Weinberg equilibrium testing showed no deviation in either variant (all $P > 0.05$). For both variants (rs542171324 and rs145138372), the case–control study showed no statistically significant differences in genotype or allele frequencies between the PD group and the control group (all $P > 0.05$, **Table 2**). No CNVs of the *SNCA* gene were detected. Given that the *SNCA* gene mutations have been well confirmed to be responsible for PD worldwide, the *SNCA*-related phenotypes were assessed by extracting 231 cases with parkinsonism as reported in 89 articles (**Supplementary Table 2**). Psychiatric signs and cognitive decline/dementia were more common among patients with *SNCA* duplication or triplication (psychiatric signs: $\chi^2 = 7.892$, $P = 0.005$; cognitive decline/dementia: $\chi^2 = 8.991$, $P = 0.003$, **Supplementary Table 3**).

TABLE 2 | Genotypic and allelic distributions of rs542171324 and rs145138372 in the Han Chinese patients with PD and controls.

dbSNP154	Genotype/Allele	PD	Controls	*P*-value
rs542171324	Genotype			0.199
	CC	436	543	
	CT	2	0	
	TT	0	0	
	Allele			0.199
	C	874	1086	
	T	2	0	
rs145138372	Genotype			0.446
	CC	437	543	
	CT	1	0	
	TT	0	0	
	Allele			0.446
	C	875	1086	
	T	1	0	

PD, Parkinson's disease; dbSNP154, Single Nucleotide Polymorphism database version 154.

DISCUSSION

PD is the most frequent type of synucleinopathy which is pathologically characterized by proteinaceous cytoplasmic inclusions, primarily consisting of alpha-synuclein and ubiquitin (Tagliafierro and Chiba-Falek, 2016; Balestrino and Schapira, 2020; Toffoli et al., 2020). Genetic contributors exert a significant role in the complicated pathogenesis of PD, and considerable progress in establishing its genetic basis has been made since the first disease-causative gene was identified (Hernandez et al., 2016; Deng et al., 2018). Multiple susceptibility genes, disease-causing genes, and genetic risk loci attributed to PD have been identified (Hernandez et al., 2016; Liu and Le, 2020). Intriguingly, some pleomorphic risk loci overlap with the known causative genes of monogenic PD, such as *SNCA*, glucosylceramidase beta (*GBA*), leucine rich repeat kinase 2 (*LRRK2*), and vacuolar protein sorting 13 homolog C (*VPS13C*) (Singleton and Hardy, 2011; Nalls et al., 2019; Blauwendraat et al., 2020). Since the first point mutation of the *SNCA* gene was innovatively identified in 1997, at least 14 missense *SNCA* variants (p.M5T, p.L8I, p.A18T, p.A29S, p.A30P, p.A30G, p.E46K, p.H50Q, p.G51D, p.A53T, p.A53E, p.A53V, p.E57D, and p.P117S) have been discovered to date, which are classified as "pathogenic" or "likely pathogenic" (Polymeropoulos et al., 1997; Youn et al., 2019; Chen et al., 2020; Zhao et al., 2020; Brás et al., 2021; Liu et al., 2021). The CNVs of the *SNCA* locus were discovered in an Iowan kindred for the first time in 2003 (Singleton et al., 2003). Later, *SNCA* genomic multiplications (i.e., duplications and triplications) have been identified in at least 47 families and 18 sporadic cases worldwide (**Supplementary Table 2**, **Figure 2**). Apart from point variants and CNVs, some specific short structural variants located in the noncoding regions of the *SNCA* gene, such as promoter Rep1 allele, intron 2 poly-T allele, and intron 4 CT-rich allele, and SNPs, such as rs2736990 and rs356219, were reported to modulate susceptibility to PD (Mata et al., 2010; Miyake et al., 2012; Pan et al., 2013; Guo et al., 2014; Chiba-Falek, 2017; Piper et al., 2018).

The *SNCA* gene, which is mapped to chromosome 4q22.1, consists of six exons, and the latter five exons encode a presynaptic neuronal protein, i.e., alpha-synuclein, with 140 amino acids (Deng and Yuan, 2014; Xu et al., 2015). The protein, a member of the synuclein family, is comprised of an N-terminal with an amphipathic α-helix conformation associated with lipid membrane interactions, a central non-amyloid-component region, and a C-terminal involving fibrillization and aggregation inhibition (Ozansoy and Başak, 2013; Burré, 2015; Xu et al., 2015). Remarkably, almost all identified point variants are located in the N-terminal amphipathic region to date, underlining its significance to the pathogenic mechanism of the alpha-synuclein aggregation (Dehay et al., 2015; Brás et al., 2021). There is a dynamic equilibrium between a natively unfolded monomer and a membrane-bound form of alpha-synuclein protein (Burré, 2015; Dehay et al., 2015). The latter is crucial to mediate the physiological functions implicating synaptic activity and plasticity, neurotransmitter release, dopamine metabolism, synaptic vesicle reserve pool maintenance, and vesicle trafficking at the synapse (Deng and Yuan, 2014; Burré, 2015). The oligomerization or fibrillization of alpha-synuclein by causative

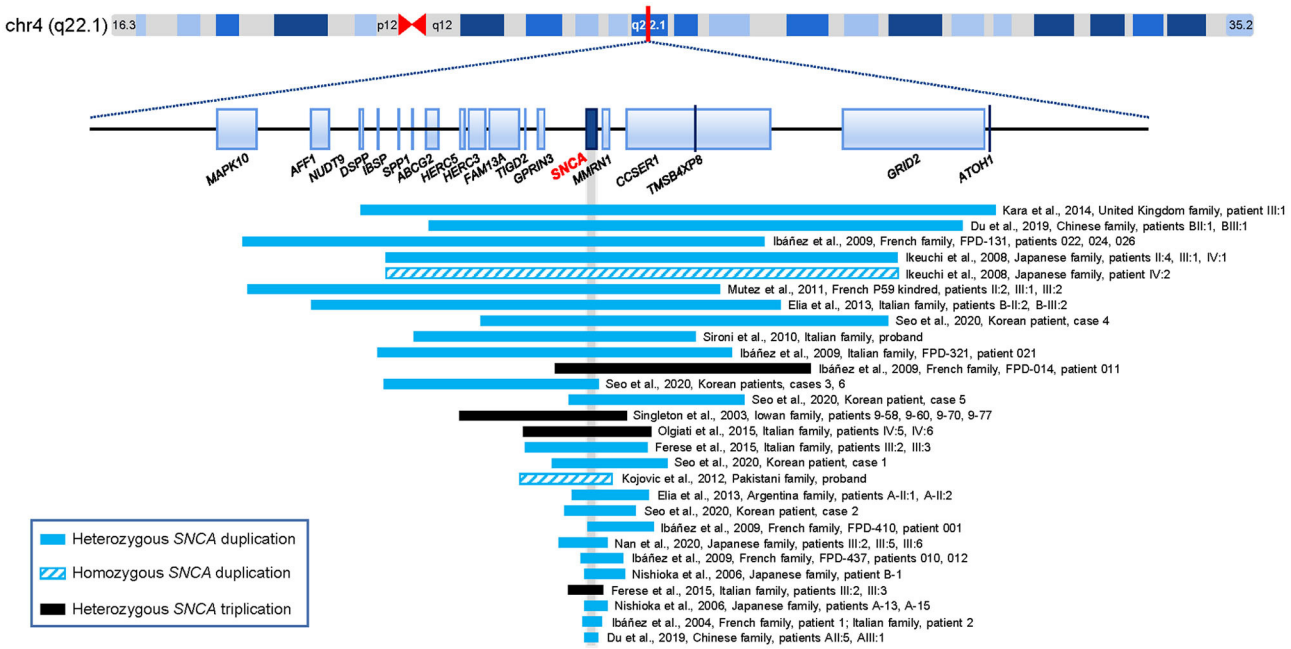


FIGURE 2 | The reported duplications and triplications including the *SNCA* locus for parkinsonism (i.e., bar sizes are not in proportion). The gray vertical bar indicates the position of the *SNCA* gene. The raw data and corresponding references are available in **Supplementary Table 2**. Genome size is based on human genome build 37.

point variants and the overexpression of alpha-synuclein by *SNCA* multiplications were proved to have a gain-in-toxic function and gene dosage-related effect, respectively (Tagliafierro and Chiba-Falek, 2016; Stojkovska et al., 2018; Balestrino and Schapira, 2020). The aggregated alpha-synuclein proteins accelerate dopaminergic neuron death and neurodegeneration, which are connected with neurological toxicity pathways, such as the impairment of mitochondrial and synaptic function, the autophagy lysosomal pathway, endoplasmic reticulum overload, and oxidative stress (Emamzadeh, 2017; Fields et al., 2019; Payne et al., 2019).

In this study, two single-nucleotide variants of the *SNCA* gene, namely, c.158C>T (p.A53V, rs542171324) and c.349C>T (p.P117S, rs145138372), were identified in three patients with PD. The rs542171324 has been previously reported in a Japanese autosomal dominant PD family in the homozygous state and three unrelated Chinese patients with early-onset PD (Yoshino et al., 2017; Chen et al., 2020). The rs145138372 has been found in a single patient of European ancestry with isolated/idiopathic rapid eye movement sleep behavior disorder and a Chinese patient with familial PD (Krohn et al., 2020; Zhao et al., 2020).

Considering p.A53V and p.P117S observed in sporadic PD cases and unaffected individuals of small families, as well as obtained weak bioinformatics evidence of pathogenicity and the relatively high frequency in Chinese patients, we inferred that these two variants may exert a high probability of susceptibility in PD rather than act as pathogenic variants in monogenic PD. To evaluate the relationship between *SNCA* gene variants and PD in the Han Chinese population, a well-characterized case–control comparison study was conducted to further investigate the relevance of two SNPs in the PD susceptibility in the Han Chinese individuals from mainland China. Despite the immense interest and considerable effort, no significant association between the two SNPs and the development of PD was detected (all $P > 0.05$). This study indicates that these SNPs in the coding regions of the *SNCA* gene have less or no effect on the development of PD in the Han Chinese population. No CNVs of the *SNCA* gene were detected.

Interestingly, an *in vitro* study showed that *SNCA* c.158C>T (p.A53V) variant increases the aggregation propensity and promotes oligomerization and fibrillation that are known to be related to the pathogenesis of PD (Mohite et al., 2018). It is also worth noting that the *SNCA* c.158C>T (p.A53V) variant, which is classified as "pathogenic," was detected in three unrelated Chinese patients sharing the same haplotype (Chen et al., 2020). The *SNCA* c.349C>T (p.P117S) variant identified in the Chinese patients was classified as "likely pathogenic," and its pathogenicity was supported by its effect on protein solubility (Zhao et al., 2020). However, the changes of *in vitro* functional experiments are not found to be enough to prove that those two variants may bring the carriers to reach the threshold of the development of PD. Recruitment of more families for detecting the variants and further functional analyses like *in vivo* experimental studies are warranted for their definite roles in PD.

Patients with PD, particularly those with *SNCA* gene multiplication, are usually complicated with neuropsychiatric symptoms, such as visual hallucination, delusion, and

cognitive decline/dementia (Book et al., 2018). We reviewed all reported cases with *SNCA* variants worldwide. Psychiatric signs and cognitive decline/dementia were more common in patients with *SNCA* multiplications. This study may be limited by the applied methods for not fully analyzing the variants in the noncoding region of the *SNCA* gene.

CONCLUSION

The two variants, namely, c.158C>T (p.A53V, rs542171324) and c.349C>T (p.P117S, rs145138372), of the *SNCA* gene were detected. The study shows that variants located in the coding regions of the *SNCA* gene may have less or no role in the development of PD in the Han Chinese population. Associations between different variant types of the *SNCA* gene and psychiatric signs as well as cognitive decline/dementia were assessed, which were found to be more common among patients with *SNCA* duplication or triplication.

DATA AVAILABILITY STATEMENT

The raw data presented in this article will be available by the authors, and reasonable requests to access the datasets by the qualified researchers should be directed to the corresponding author after legal permission.

ETHICS STATEMENT

The studies involving human participants were reviewed and approved by the Institutional Review Board of the Third Xiangya Hospital of Central South University. The patients/participants provided their written informed consent to participate in this study.

AUTHOR CONTRIBUTIONS

LY and HD contributed to the conception and design of the study. ZS, WZ, WX, and YY performed patient samples and clinical data acquisition. YG, YS, and YY performed the experiments. YG, YS, LY, and HD were involved in the data analysis and wrote the manuscript. All authors read and approved the final version of the manuscript.

FUNDING

This study was financially supported by the National Key Research and Development Program of China (2016YFC1306604), the National Natural Science Foundation of China (81670216, 81800219, and 81873686), the Scientific Research Project of Health and Family Planning Commission of Hunan Province, China (B20180729), and the Fundamental Research Funds for the Central Universities of Central South University, China (2020zzts299).

ACKNOWLEDGMENTS

The authors appreciate all the participants and investigators involved in this study for their contributions.

SUPPLEMENTARY MATERIAL

The Supplementary Material for this article can be found online at: https://www.frontiersin.org/articles/10.3389/fnagi.2021.648151/full#supplementary-material

REFERENCES

Abyzov, A., Urban, A. E., Snyder, M., and Gerstein, M. (2011). CNVnator: an approach to discover, genotype, and characterize typical and atypical CNVs from family and population genome sequencing. *Genome Res.* 21, 974–984. doi: 10.1101/gr.114876.110

Balestrino, R., and Schapira, A. H. V. (2020). Parkinson disease. *Eur. J. Neurol.* 27, 27–42. doi: 10.1111/ene.14108

Billingsley, K. J., Bandres-Ciga, S., Saez-Atienzar, S., and Singleton, A. B. (2018). Genetic risk factors in Parkinson's disease. *Cell Tissue Res.* 373, 9–20. doi: 10.1007/s00441-018-2817-y

Blauwendraat, C., Nalls, M. A., and Singleton, A. B. (2020). The genetic architecture of Parkinson's disease. *Lancet Neurol.* 19, 170–178. doi: 10.1016/S1474-4422(19)30287-X

Book, A., Guella, I., Candido, T., Brice, A., Hattori, N., Jeon, B., et al. (2018). A meta-analysis of α-synuclein multiplication in familial parkinsonism. *Front. Neurol.* 9:1021. doi: 10.3389/fneur.2018.01021

Brás, J., Gibbons, E., and Guerreiro, R. (2021). Genetics of synucleins in neurodegenerative diseases. *Acta Neuropathol.* 141, 471–490. doi: 10.1007/s00401-020-02202-1

Burré, J. (2015). The synaptic function of a-synuclein. *J. Parkinsons Dis.* 5, 699–713. doi: 10.3233/JPD-150642

Cao, Y., Li, L., Xu, M., Feng, Z., Sun, X., Lu, J., et al. (2020). The ChinaMAP analytics of deep whole genome sequences in 10,588 individuals. *Cell Res.* 30, 717–731. doi: 10.1038/s41422-020-0322-9

Chen, Y., Gu, X., Ou, R., Zhang, L., Hou, Y., Liu, K., et al. (2020). Evaluating the role of SNCA, LRRK2, and GBA in Chinese patients with early-onset Parkinson's disease. *Mov. Disord.* 35, 2046–2055. doi: 10.1002/mds.28191

Chiba-Falek, O. (2017). Structural variants in SNCA gene and the implication to synucleinopathies. *Curr. Opin. Genet. Dev.* 44, 110–116. doi: 10.1016/j.gde.2017.01.014

Cook Shukla, L., Schulze, J., Farlow, J., Pankratz, N. D., Wojcieszek, J., and Foroud, T. (2004). "Parkinson disease overview," in *GeneReviews®* [Internet], eds M. P. Adam, H. H. Ardinger, R. A. Pagon, S. E. Wallace, L. J. H. Bean, G. Mirzaa, and A. Amemiya (Seattle, WA: University of Washington), 1993–2021.

Dehay, B., Bourdenx, M., Gorry, P., Przedborski, S., Vila, M., Hunot, S., et al. (2015). Targeting α-synuclein for treatment of Parkinson's disease: mechanistic and therapeutic considerations. *Lancet Neurol.* 14, 855–866. doi: 10.1016/S1474-4422(15)00006-X

Deng, H., Wang, P., and Jankovic, J. (2018). The genetics of Parkinson disease. *Ageing Res. Rev.* 42, 72–85. doi: 10.1016/j.arr.2017.12.007

Deng, H., and Yuan, L. (2014). Genetic variants and animal models in SNCA and Parkinson disease. *Ageing Res. Rev.* 15, 161–176. doi: 10.1016/j.arr.2014.04.002

Dorsey, E. R., and Bloem, B. R. (2018). The Parkinson pandemic-a call to action. *JAMA Neurol.* 75, 9–10. doi: 10.1001/jamaneurol.2017.3299

Emamzadeh, F. N. (2017). Role of apolipoproteins and α-synuclein in Parkinson's disease. *J. Mol. Neurosci.* 62, 344–355. doi: 10.1007/s12031-017-0942-9

Fields, C. R., Bengoa-Vergniory, N., and Wade-Martins, R. (2019). Targeting alpha-synuclein as a therapy for Parkinson's disease. *Front. Mol. Neurosci.* 12:299. doi: 10.3389/fnmol.2019.00299

Guo, X. Y., Chen, Y. P., Song, W., Zhao, B., Cao, B., Wei, Q. Q., et al. (2014). SNCA variants rs2736990 and rs356220 as risk factors for Parkinson's disease but not for amyotrophic lateral sclerosis and multiple system atrophy in a Chinese population. *Neurobiol. Aging* 35, 2882.e1–2882.e6. doi: 10.1016/j.neurobiolaging.2014.07.014

Hernandez, D. G., Reed, X., and Singleton, A. B. (2016). Genetics in Parkinson disease: Mendelian versus non-Mendelian inheritance. *J. Neurochem.* 139 (Suppl 1), 59–74. doi: 10.1111/jnc.13593

Hopfner, F., Höglinger, G. U., Kuhlenbäumer, G., Pottegård, A., Wod, M., Christensen, K., et al. (2020). β-adrenoreceptors and the risk of Parkinson's disease. *Lancet Neurol.* 19, 247–254. doi: 10.1016/S1474-4422(19)30400-4

Klein, C., Hattori, N., and Marras, C. (2018). MDSGene: closing data gaps in genotype-phenotype correlations of monogenic Parkinson's disease. *J. Parkinsons Dis.* 8, S25–S30. doi: 10.3233/JPD-181505

Krohn, L., Wu, R. Y. J., Heilbron, K., Ruskey, J. A., Laurent, S. B., Blauwendraat, C., et al. (2020). Fine-mapping of SNCA in rapid eye movement sleep behavior disorder and overt synucleinopathies. *Ann. Neurol.* 87, 584–598. doi: 10.1002/ana.25687

Langston, J. W., Schüle, B., Rees, L., Nichols, R. J., and Barlow, C. (2015). Multisystem Lewy body disease and the other parkinsonian disorders. *Nat. Genet.* 47, 1378–1384. doi: 10.1038/ng.3454

Liu, H., Koros, C., Strohäker, T., Schulte, C., Bozi, M., Varvaresos, S., et al. (2021). A novel SNCA A30G mutation causes familial Parkinson's disease. *Mov. Disord.* doi: 10.1002/mds.28534

Liu, X., and Le, W. (2020). Profiling non-motor symptoms in monogenic Parkinson's disease. *Front. Aging Neurosci.* 12:591183. doi: 10.3389/fnagi.2020.591183

Mata, I. F., Shi, M., Agarwal, P., Chung, K. A., Edwards, K. L., Factor, S. A., et al. (2010). SNCA variant associated with Parkinson disease and plasma alpha-synuclein level. *Arch. Neurol.* 67, 1350–1356. doi: 10.1001/archneurol.2010.279

Miyake, Y., Tanaka, K., Fukushima, W., Kiyohara, C., Sasaki, S., Tsuboi, Y., et al. (2012). SNCA polymorphisms, smoking, and sporadic Parkinson's disease in Japanese. *Parkinsonism Relat. Disord.* 18, 557–561. doi: 10.1016/j.parkreldis.2012.02.016

Mohite, G. M., Kumar, R., Panigrahi, R., Navalkar, A., Singh, N., Datta, D., et al. (2018). Comparison of kinetics, toxicity, oligomer formation, and membrane binding capacity of α-synuclein familial mutations at the A53 site, including the newly discovered A53V mutation. *Biochemistry* 57, 5183–5187. doi: 10.1021/acs.biochem.8b00314

Nalls, M. A., Blauwendraat, C., Vallerga, C. L., Heilbron, K., Bandres-Ciga, S., Chang, D., et al. (2019). Identification of novel risk loci, causal insights, and heritable risk for Parkinson's disease: a meta-analysis of genome-wide association studies. *Lancet Neurol.* 18, 1091–1102. doi: 10.1016/S1474-4422(19)30320-5

Ozansoy, M., and Başak, A. N. (2013). The central theme of Parkinson's disease: α-synuclein. *Mol. Neurobiol.* 47, 460–465. doi: 10.1007/s12035-012-8369-3

Pan, F., Ding, H., Dong, H., Ye, M., Liu, W., Cui, G., et al. (2013). Association of polymorphism in rs2736990 of the α-synuclein gene with Parkinson's disease in a Chinese population. *Neurol. India* 61, 360–364. doi: 10.4103/0028-3886.117595

Payne, K., Walls, B., and Wojcieszek, J. (2019). Approach to assessment of Parkinson disease with emphasis on genetic testing. *Med. Clin. North Am.* 103, 1055–1075. doi: 10.1016/j.mcna.2019.08.003

Piper, D. A., Sastre, D., and Schüle, B. (2018). Advancing stem cell models of alpha-synuclein gene regulation in neurodegenerative disease. *Front. Neurosci.* 12:199. doi: 10.3389/fnins.2018.00199

Polymeropoulos, M. H., Lavedan, C., Leroy, E., Ide, S. E., Dehejia, A., Dutra, A., et al. (1997). Mutation in the alpha-synuclein gene identified in families with Parkinson's disease. *Science* 276, 2045–2047. doi: 10.1126/science.276.5321.2045

Postuma, R. B., Berg, D., Stern, M., Poewe, W., Olanow, C. W., Oertel, W., et al. (2015). MDS clinical diagnostic criteria for Parkinson's disease. *Mov. Disord.* 30, 1591–1601. doi: 10.1002/mds.26424

Singleton, A., and Hardy, J. (2011). A generalizable hypothesis for the genetic architecture of disease: pleomorphic risk loci. *Hum. Mol. Genet.* 20, R158–R162. doi: 10.1093/hmg/ddr358

Singleton, A. B., Farrer, M., Johnson, J., Singleton, A., Hague, S., Kachergus, J., et al. (2003). alpha-synuclein locus triplication causes Parkinson's disease. *Science* 302:841. doi: 10.1126/science.1090278

Stojkovska, I., Krainc, D., and Mazzulli, J. R. (2018). Molecular mechanisms of α-synuclein and GBA1 in Parkinson's disease. *Cell Tissue Res.* 373, 51–60. doi: 10.1007/s00441-017-2704-y

Tagliafierro, L., and Chiba-Falek, O. (2016). Up-regulation of SNCA gene expression: implications to synucleinopathies. *Neurogenetics* 17, 145–157. doi: 10.1007/s10048-016-0478-0

Toffoli, M., Vieira, S. R. L., and Schapira, A. H. V. (2020). Genetic causes of PD: a pathway to disease modification. *Neuropharmacology* 170:108022. doi: 10.1016/j.neuropharm.2020.108022

Xiang, Q., Yuan, L., Cao, Y., Xu, H., Li, Y., and Deng, H. (2019). Identification of a heterozygous mutation in the TGFBI gene in a Hui-Chinese family with corneal dystrophy. *J. Ophthalmol.* 2019:2824179. doi: 10.1155/2019/2824179

Xu, W., Tan, L., and Yu, J. T. (2015). Link between the SNCA gene and parkinsonism. *Neurobiol. Aging* 36, 1505–1518. doi: 10.1016/j.neurobiolaging.2014.10.042

Yoshino, H., Hirano, M., Stoessl, A. J., Imamichi, Y., Ikeda, A., Li, Y., et al. (2017). Homozygous alpha-synuclein p.A53V in familial Parkinson's disease. *Neurobiol. Aging* 57, 248.e7–248.e12. doi: 10.1016/j.neurobiolaging.2017.05.022

Youn, J., Lee, C., Oh, E., Park, J., Kim, J. S., Kim, H. T., et al. (2019). Genetic variants of PARK genes in Korean patients with early-onset Parkinson's disease. *Neurobiol. Aging* 75, 224.e9–224.e15. doi: 10.1016/j.neurobiolaging.2018.10.030

Yuan, L., Deng, X., Song, Z., Yang, Z., Ni, B., Chen, Y., et al. (2015). Genetic analysis of the RAB39B gene in Chinese Han patients with Parkinson's disease. *Neurobiol. Aging* 36, 2907.e11–2907.e12. doi: 10.1016/j.neurobiolaging.2015.06.019

Zhao, Y., Qin, L., Pan, H., Liu, Z., Jiang, L., He, Y., et al. (2020). The role of genetics in Parkinson's disease: a large cohort study in Chinese mainland population. *Brain* 143, 2220–2234. doi: 10.1093/brain/awaa167

Conflict of Interest: The authors declare that the research was conducted in the absence of any commercial or financial relationships that could be construed as a potential conflict of interest.

Publisher's Note: All claims expressed in this article are solely those of the authors and do not necessarily represent those of their affiliated organizations, or those of the publisher, the editors and the reviewers. Any product that may be evaluated in this article, or claim that may be made by its manufacturer, is not guaranteed or endorsed by the publisher.

Copyright © 2021 Guo, Sun, Song, Zheng, Xiong, Yang, Yuan and Deng. This is an open-access article distributed under the terms of the Creative Commons Attribution License (CC BY). The use, distribution or reproduction in other forums is permitted, provided the original author(s) and the copyright owner(s) are credited and that the original publication in this journal is cited, in accordance with accepted academic practice. No use, distribution or reproduction is permitted which does not comply with these terms.

frontiers in Aging Neuroscience

ORIGINAL RESEARCH
published: 17 August 2021
doi: 10.3389/fnagi.2021.686066

Significant Difference of Immune Cell Fractions and Their Correlations With Differential Expression Genes in Parkinson's Disease

Yilin Huang[1], Huisheng Liu[1], Jiaqi Hu[1], Chongyin Han[1], Zhenggang Zhong[1], Wei Luo[2], Yuhu Zhang[3]* and Fei Ling[1]**

[1] School of Biology and Biological Engineering, South China University of Technology, Guangzhou, China, [2] Clinical Research Institute, Foshan Hospital, Sun Yat-sen University, Foshan, China, [3] Department of Neurology, Guangdong Neuroscience Institute, Guangdong Provincial People's Hospital, Guangdong Academy of Medical Sciences, Guangzhou, China

OPEN ACCESS

Edited by:
Yun-Cheng Wu, Shanghai Jiao Tong University School of Medicine, China

Reviewed by:
Nirnath Sah, Johns Hopkins University, United States
Jae-Kyung Lee, University of Georgia, United States
Huijiao Liu, China Agricultural University, China

***Correspondence:**
Fei Ling
fling@scut.edu.cn
Yuhu Zhang
yhzhangsd@126.com
Wei Luo
luowei_421@163.com

Received: 26 March 2021
Accepted: 19 July 2021
Published: 17 August 2021

Citation:
Huang Y, Liu H, Hu J, Han C, Zhong Z, Luo W, Zhang Y and Ling F (2021) Significant Difference of Immune Cell Fractions and Their Correlations With Differential Expression Genes in Parkinson's Disease. Front. Aging Neurosci. 13:686066. doi: 10.3389/fnagi.2021.686066

Parkinson's disease (PD) is the second most neurodegenerative disease in the world. T cell infiltration in the central nervous system (CNS) has provided insights that the peripheral immune cells participate in the pathogenesis of PD. However, the association between the peripheral immune system and CNS remains to be elucidated. In this study, we analyzed incorporative substantia nigra (SN) expression data and blood expression data using the CIBERSORT to obtain the 22 immune cell fractions and then explored the molecular function to identify the potential key immune cell types and genes of PD. We observed that the proportions of naïve CD4 T cells, gamma delta T cells, resting natural killer (NK) cells, neutrophils in the blood, and regulatory T cells (Tregs) in the SN were significantly different between patients with PD and healthy controls (HCs). We identified p53-induced death domain protein 1 (*PIDD1*) as the hub gene of a PD-related module. The enrichment score of the neuron-specific gene set was significantly different between PD and HC, and genes in the neuron-related module were enriched in the biological process about mitochondria and synapses. These results suggested that the fractions of naïve CD4 T cells, gamma delta T cells, resting NK cells, and neutrophils may be used as a combined diagnostic marker in the blood, and Tregs in SN may be a potential therapeutic design target for PD.

Keywords: Parkinson's disease, immune cells, Tregs, *PIDD1*, blood, substantia nigra

INTRODUCTION

Parkinson's disease (PD) is the second most neurodegenerative disease. It is clinically defined as a progressive movement disorder, such as tremors, rigidity, and bradykinesia, and sometimes also with the presentation of non-motor symptoms like cognitive impairment (Blauwendraat et al., 2020). The pathological features of PD are the loss of dopaminergic neurons and the presence of Lewy bodies in the substantia nigra (SN). The pathogenic factors of PD are complex, and inflammation has been reported to be involved in the progress of neurodegeneration. Increasing evidence suggests that both the innate and adaptive immune systems contribute to neuron death

and PD pathogenesis (Earls et al., 2019). The synucleinopathy in the central nervous system (CNS) may alter the peripheral lymphocytic profile (Earls et al., 2019). Through analyzing the immune cells in the peripheral blood and cerebrospinal fluid (CSF), researchers observed that the periphery immune microenvironment changes, which may contribute to the progress of PD (Schroder et al., 2018). Increased monocyte precursors in the blood and enriched classical monocytes but decreased activated monocytes were observed in patients with PD (Grozdanov et al., 2014). CD8 T cell fraction increases in both CSF and peripheral blood (Schroder et al., 2018), and an increased proportion of circulating CD4 T cells was observed with decreased T helper (Th) 2, Th17, and regulatory T cell (Tregs) but increased Th1 in the peripheral blood (Baba et al., 2005; Kustrimovic et al., 2018). Tregs (CD4 + Foxp3+) frequency increases in patients with AD and PD by age, accompanied by the increased inhibitory activity of Tregs (Rosenkranz et al., 2007). Effector/memory T cell (Tem) activation and Tregs dysfunction seemed to be linked to PD pathobiology and disease severity rather than disease duration (Saunders et al., 2012). Research suggests that the percentages of natural killer (NK) cells, CD3 + T cells, and CD19 + B cells, and the Treg/Th17 ratio in peripheral blood may be used to predict the risk of PD in Chinese individuals (Cen et al., 2017). In women, the Tregs/Th17 ratio in patients with PD was higher than that in normal controls, implying the neuroprotective effects of estrogen (Cen et al., 2017). However, other immune cell compositions and activities present in PD and the relationship between the periphery and CNS still require further exploration. Furthermore, it is also important to screen more reliable diagnostic biomarkers, such as the proportional difference of lymphocyte subsets.

Due to the slow progression of neurodegenerative disease pathology, the infiltration dynamic of peripheral immune cells is more difficult to quantify (Greenhalgh et al., 2020). Recently, increasing evidence suggests that the adaptive immune system, including lymphocyte subpopulations and cytokines, is involved in the PD pathogenesis (Mosley et al., 2012; Galiano-Landeira et al., 2020). Microglia are the resident myeloid cells participating in maintaining homeostasis in CNS, and activated microglia in SN were signs of PD and were involved in a persistent proinflammatory event finally leading to neuron death (Tansey and Romero-Ramos, 2019). The relative proportions of CD4+ and CD8+ subsets of αβT cells are correlated with the variation in cellular proliferation in the hippocampus (Huang et al., 2010). Tregs, a subtype of CD4 T cell, has been regarded as a protective factor during neurodegeneration in the animal models with PD by suppressing immune activation and microglia responses to α-synuclein (α-syn) aggression (Reynolds et al., 2007). A previous study suggests that the cytotoxic attack of CD8 T cells may promote and initiate neuronal death and synucleinopathy in PD (Galiano-Landeira et al., 2020). In addition, the increased activated CD8 T cell fraction was found in the CSF from patients with PD (Schroder et al., 2018). Genetic analyses indicate that the inflammatory process can be risk factor for PD. The genome-wide association studies (GWAS) have revealed the HLA region variants as the susceptible locus of PD (Hamza et al., 2010). In addition, several polymorphisms in neuroinflammation-associated genes, such as *TNF*, *IL1B*, *CD14*, and *TREM2*, are the risk of PD (Hirsch and Hunot, 2009; Rayaprolu et al., 2013). Leucine-rich repeat kinase 2 (*LRRK2*) is expressed at higher levels in the immune cells, especially in patients with late-onset PD compared to age-matched controls, which may regulate the progression of PD (Cook et al., 2017). In addition, decreased mRNA levels in CD4 + T cells of signal transducer and activator of transcription 1 (*STAT1*), driving Th1 differentiation, and nuclear receptor subfamily 4 group A member 2 (*NR4A2*)/*STAT6* involved in the Treg development were detected in patients with PD having motor complications compared to those without motor complications, which gives a new opinion of the therapeutic management of PD (Kustrimovic et al., 2018; Contaldi et al., 2020). So, further studies to elucidate the relationship between gene expression and immune cell fraction/activity, as well as to explore the common/different points between peripheral and CNS immune systems, need to be performed.

CIBERSORT (Newman et al., 2015) is an analysis tool for evaluating the proportions of immune cells from gene expression data of each sample. It has been used to analyze the immune cell infiltration in a variety of diseases, including colorectal cancer (Ge et al., 2019), lupus nephritis (Cao et al., 2019), atopic dermatitis (Felix Garza et al., 2019), and osteoarthritis (Deng et al., 2020).

The goal of the study was to characterize the immune cell fractions in SN and blood and to investigate their links. First, we accessed the immune cell fractions in the peripheral blood and the SN via CIBERSORT based on the gene expression data. Then, we further probed into the association between gene expression values and the immune cell fractions. These results suggest that the naïve CD4 T cells, gamma delta T cells, and resting NK cells, as well as neutrophils in the blood, may be a potential combined diagnostic biomarker, and Tregs in the SN may be a potential therapeutic design.

MATERIALS AND METHODS

Data Downloaded, Processing, and Differential Gene Expression Analysis

We searched the blood microarray dataset with the keywords including "PD," "blood," and "Homo sapiens" from the GEO database[1] and finally selected GSE99039, including 205 patients with idiopathic PD and 233 healthy controls (HCs). The expression matrix and platform information of GSE99039 were downloaded, and then, the expression data were annotated by gene symbols in R software. Then, we screened the differential expression genes (DEGs) between PD and HC in GEO2R with $p < 0.05$ and $|\log2FC| > 0.3$.

We obtained the candidate microarrays that can get the unprocessed raw data (.cel file) with the keywords including "PD," "SN," and "Homo sapiens" from the GEO database (see text footnote 1). After preprocessing, we excluded datasets with large differences in expression values or numbers of probes.

[1] https://www.ncbi.nlm.nih.gov/geo/

We then retained only three datasets whose expression values were approximate for the subsequence analysis. The detailed information of the datasets is in **Supplementary Table 1**, and the detailed meta information of each sample is in **Supplementary Table 2**. We downloaded the raw data and platform information of GSE20164, GSE20292, and GSE7621 and then annotated the probe id after preprocessing the raw data. Their common genes merged three expression matrices, and the batch effect between them was removed. Raw data of GSE20164, GSE20292, and GSE7621 datasets were processed through the "affy" package to read the .cel file and RMA algorithm for background correction and data normalization. Then, we normalized three gene expression matrices, and the inter batch difference was removed using the "removebatcheffect" package of a limma. The boxplots and two-dimensional PCA plots before and after removing the batch effect are shown in **Supplementary Figures 3A–D**. After normalization, the median expression values of these samples from three datasets were on the same level, and the PCA plot showed that the difference between them was decreased, indicating that the merged expression matrix could be used for further analysis. Then, we used the "limma" package for differential expression analysis to identify DEGs between PD and HC, with $p < 0.05$ and $|\log2FC| > 1$.

Functional Enrichment Analysis of DEGs

We used the gene ontology (GO) enrichment function and Kyoto Encyclopedia of Genes and Genomes (KEGG) pathway enrichment analysis. We selected the significantly enriched functional GO terms and KEGG pathways with a p-value < 0.05 and false discovery rate (FDR) < 0.05.

Gene Set Enrichment Analysis and Gene Set Variation Analysis

We used the gene set enrichment analysis (GSEA) software to screen the significant KEGG pathway with a p-value < 0.05 and an FDR < 0.25.

The gene set variation analysis (GSVA) analysis was performed using the GSVA package with the method ssgsea. Neurons, microglia, astrocytes, and oligodendrocytes are the major cell types in CNS. Custom gene sets of the four cell types mentioned above were constructed using the top 15 high-fidelity genes from the published literature (Kelley et al., 2018). The differential analysis was performed using the limma package with the threshold adj. p-value < 0.05.

Weighted Gene Coexpression Network Analysis

We constructed the coexpression networks using the weighted gene coexpression network analysis (WGCNA) package in R, with the traits including disease, age, gender, platform, datasets, and the enrichment score (ES) of the gene sets of four major CNS cell types through GSVA. First, using the pickSoftThreshold function, we selected the soft thresholding powers β-value as long as the scale-free topology fitting indices R^2 reached 0.8. After obtaining the modules, we subsequently analyzed the association between modules and traits. We filtered the genes in each module with the criterion of gene significance (GS) > 0.2 and module membership (MM) > 0.8 and used a plug-in clueGO in Cytoscape software to explore the function of genes in green and cyan modules. The built-in function of the WGCNA, chooseTopHubInEachModule, is used to find the hub gene of each module. We exported the network file with the function exportNetworkToCytoscape and then visualized the network in Cytoscape with the plug-in cytoHubba.

Statistics

Statistical analysis and visualization were performed in GraphPad Prism 8 software (version 8.0.1, GraphPad Software, United States) and R (version 3.6.3). A two-tailed Student's t-test was performed to compare the difference between PD and HC groups. Correlations between two numerical variables were performed using Pearson's correlation test. The results were considered to be statistically significant for values of $p < 0.05$.

RESULTS

Result 1: Four Immune Cell Fractions in Blood From PD Compared With Those From HC Are Significantly Different and Their Correlation With DEGs in the Blood of Patients With PD

To understand the characteristics of peripheral immune cell fractions in patients with PD, we investigated the proportions of 22 immune cell types in peripheral blood using the CIBERSORT method. Compared with the immune cell proportions in blood samples of HC subjects, we found that both naïve CD4 T cells and gamma delta T cells were significantly decreased in groups with PD. In contrast, both resting NK cells and neutrophils were significantly increased (**Figure 1A**), which were reported separately in several previous studies by flow cytometry analysis (Niwa et al., 2012; Saunders et al., 2012; Cen et al., 2017; Zhou et al., 2020). In the blood of both PD and HC, we found that the naive CD4 + T cell fraction in a woman was significantly higher than that in a man, indicating that the naïve CD4 T cells vary between genders (**Supplementary Figures 1C,D**). Interestingly, GSEA of KEGG gene sets on blood expression profiles also revealed that NK cell-mediated cytotoxic pathways were enriched in PD (**Figure 1B**), implying that NK cells may be involved in clearing α-syn in the blood (Earls et al., 2020). To further investigate the relationship between immune cell fractions and gene expression, we screened 11 DEGs in the blood using GEO2R. We then performed the correlation analysis to confirm the correlation between DEG expression and immune cell fractions. These results showed that the mRNA level of prostaglandin D2 synthase (*PTGDS*) was positively correlated with the fraction of resting NK cells ($r = 0.47$, $p < 0.01$) (**Figure 1C**). In addition, the mRNA level of matrix metallopeptidase 9 (*MMP9*) was positively correlated with the fraction of neutrophils ($r = 0.41$, $p < 0.01$) and macrophages M0 ($r = 0.47$, $p < 0.01$) (**Figure 1D**). However, we found no correlation between any

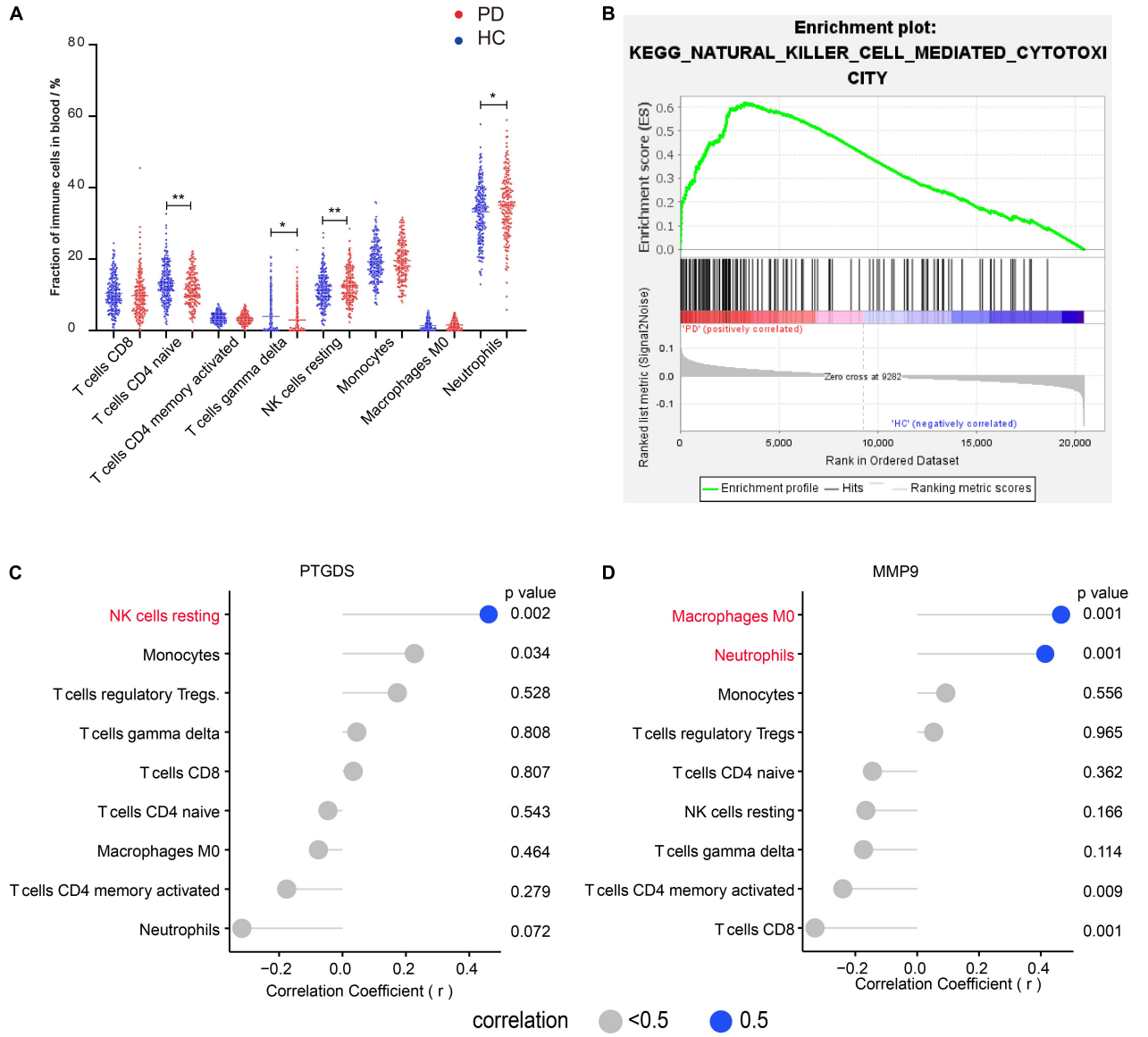


FIGURE 1 | Four immune cell fractions in the blood from PD compared with those from HC are significantly different and the correlation between immune cells and DEGs in the blood of patients with PD. **(A)** The main immune cell fractions in the blood from PD and HC. The ordinate represents the immune cell fractions, and the abscissa represents the immune cell types. The blue dots represent HC samples, and the red dots represent PD samples. **(B)** KEGG pathway–NK cell-mediated cytotoxicity enriched in PD using GSEA. **(C)** Correlation between *PTGDS* and immune cells. **(D)** Correlation between *MMP9* and immune cells. $^{*}p < 0.05$, $^{**}p < 0.01$.

DEGs and naïve CD4 T cells and gamma delta T cells (**Supplementary Figure 1B**).

Result 2: Tregs Fraction in SN Was Significantly Different Between PD and HC

We evaluated the peripheral immune cell fractions in SN using the CIBERSORT and found that only the fraction of Tregs was significantly different in PD compared with that in HC (**Figure 2A**). However, those significantly differential immune cells in the blood showed no significant difference and a low proportion in the SN (**Supplementary Figure 3E**). We also observed that the proportions of both macrophage M2 and CD8 T cells were higher than those of other immune cells but without statistical difference between PD and HC in the SN (**Supplementary Figure 3E**). Interestingly, a much more dispersion of CD8 T cell fraction values was found in the group with PD. We identified a total of 1,297 DEGs, including 702 downregulated genes and 595 upregulated genes, as shown in the volcano map (**Figure 2B**), among which 24 genes showed up to significant 2-fold differences in PD compared with those in HC. Aldehyde dehydrogenase family 1 (*ALDH1A1*), with reduced mRNA and protein levels in the SN of patients

with PD, is associated with the progressive neurodegenerative disease (Galter et al., 2003). The polymorphism of DOPA decarboxylase (*DDC*), which can catalyze the decarboxylation of L-3,4-dihydroxyphenylalanine (DOPA) to dopamine, affects the L-DOPA response in patients with PD (Devos et al., 2014). To confirm the correlation between the immune cells and the DEGs, we performed correlation analysis on the expression values of DEGs and the immune cell fractions. Although no significant difference in the activated DC and gamma delta T cell fractions was observed (**Figure 2A** and **Supplementary Figure 3E**), correlation analysis indicated that a solute carrier family 18 member A2 (*SLC18A2*) was negatively correlated with the activated dendritic cells (DC) ($r = -0.64$, $p < 0.01$) and stathmin 2 (*STMN2*) ($r = -0.60$, $p < 0.01$), as well as synaptic vesicle glycoprotein 2C (*SV2C*) ($r = -0.76$, $p < 0.01$) was negatively correlated with gamma delta T cells, separately (**Figures 2C–E**), while no DEGs were identified to be correlated with Tregs (**Supplementary Figure 3F**). The result from the KEGG enrichment analysis showed that DEGs were enriched in PD, oxidative phosphorylation, retrograde endocannabinoid signaling, proteasome, and synaptic vesicle cycle (**Supplementary Figure 4A**). Biological processes enriched by DEGs included the response to hypoxia, cellular respiration, and mitochondrial respiration, and ATP synthesis coupled to electron transport (**Supplementary Figure 4B**). Cell composition was about the neuronal cell body and structures of mitochondrion and proteasome (**Supplementary Figure 4B**). To investigate the difference in the signature of major CNS cells, we performed the GSVA analysis. The results showed that the ES of the neuron-specific gene set was significantly different; however, the other three cell-specific gene sets had no statistical difference between PD and HC (**Figure 2F**).

Result 3: p53-Induced Death Domain Protein 1 as a Hub Gene in the PD Module by the WGCNA Analysis in SN

Hierarchical clustering of gene expression data using WGCNA partitioned the data set into 28 merged modules (**Figure 3A**). We observed that the dark-orange module and bisque4 module were highly correlated with PD and age, separately (**Supplementary Figure 5A**). Both the green and cyan modules were highly correlated with the neuron-specific gene set downregulated in PD. Notably, the PD-related dark-orange module (cor = 0.59, $p < 0.01$) involved eight genes after filtering (**Figure 3D**), among which the p53-induced death domain protein 1 (*PIDD1*), an adaptor protein in cell death-related signaling processes, is identified as the hub gene (**Figure 3E**). The neuron-specific gene set is positively correlated with the green module (cor = 0.77, $p < 0.01$) and the cyan module (cor = 0.89, $p < 0.01$) (**Figures 3B,C**). The neuron-related green module was enriched for the biological process, mainly including the regulation of the cellular amino acid metabolic process, endosome organization, phosphatidylinositol monophosphate phosphatase activity, autophagy, and apoptotic changes of the mitochondrion, as well as melanosome transport (**Figure 3F**). In addition, the major biological function of the neuron-related cyan module was about the vesicle-mediated transport in synapse, ATPase-coupled cation transmembrane transporter activity, cellular respiration neurofilament cytoskeleton organization, and dopamine receptor signaling pathway, as well as neuron project regeneration (**Figure 3G**).

DISCUSSION

We characterized the immune cell fractions in the SN and blood and investigated the links between them through gaining 22 lymphocyte fractions of an individual sample in two independent cohorts of blood and SN tissues using CIBERSORT. In this study, the fractions of naïve CD4 T cells, gamma delta T cells, and resting NK cells, as well as neutrophils, were significantly different between the blood of PD and HC but not SN. However, only the Tregs fraction was different in PD SN compared with that in HC. Although we have not found a solid relationship between the peripheral and CNS immunities, we provided some views for further study.

The role of inflammation in PD is well appreciated now, obviously, and it is essential to observe for reliable and effective markers for PD. To identify the potential biomarkers of PD, we analyzed the mRNA expression array of the readily available biological samples, peripheral blood. Other studies also reported that the naïve CD4 T cells and gamma delta T cells were decreased in PD compared with those in HC (Saunders et al., 2012; Zhou et al., 2020), while NK cells and neutrophils were increased in PD (Niwa et al., 2012; Saunders et al., 2012; Cen et al., 2017), which were all observed in this study. Naïve CD4 cells can differentiate into different subtypes of Th cells, among which Th1 and Th17 are pro-inflammatory, while Th2 and Tregs are anti-inflammatory (O'Shea and Paul, 2010). Thus, the altered fraction of naïve CD4 T cells may help to understand the underlying mechanism of the neuroinflammation during PD.

The expression level of *MMP9* was positively correlated with neutrophils and macrophages M0 fraction. Matrix metalloproteinases (MMPs), mainly secreted by macrophages and neutrophils, are a family of proteolytic enzymes participating in the immune response and may facilitate the neutrophils invading the brain through the blood–brain barrier (Elkington et al., 2005; Turner and Sharp, 2016; Ritzel et al., 2018). The *PTGDS* mRNA level was positively correlated with the resting NK cells. Others found *PTGDS* to be positively correlated with the KEGG pathway NK cell-mediated cytotoxicity (Jiang et al., 2020), implying the potential relationship between *PTGDS* and NK cells during the immune response. So, these four differential distributed cells and their relationship with genes may provide new insights into investigating how the periphery immune system participates in the development of PD.

Although no remarkable difference of Tregs fractions was observed in the blood of patients with PD (Cen et al., 2017), others found CD49d + Tregs increased in PD compared to that in HC (Karaaslan et al., 2021). Tregs dysregulation and its impaired function of suppressing the activation of effector T cells were linked to the pathology of PD and disease severity

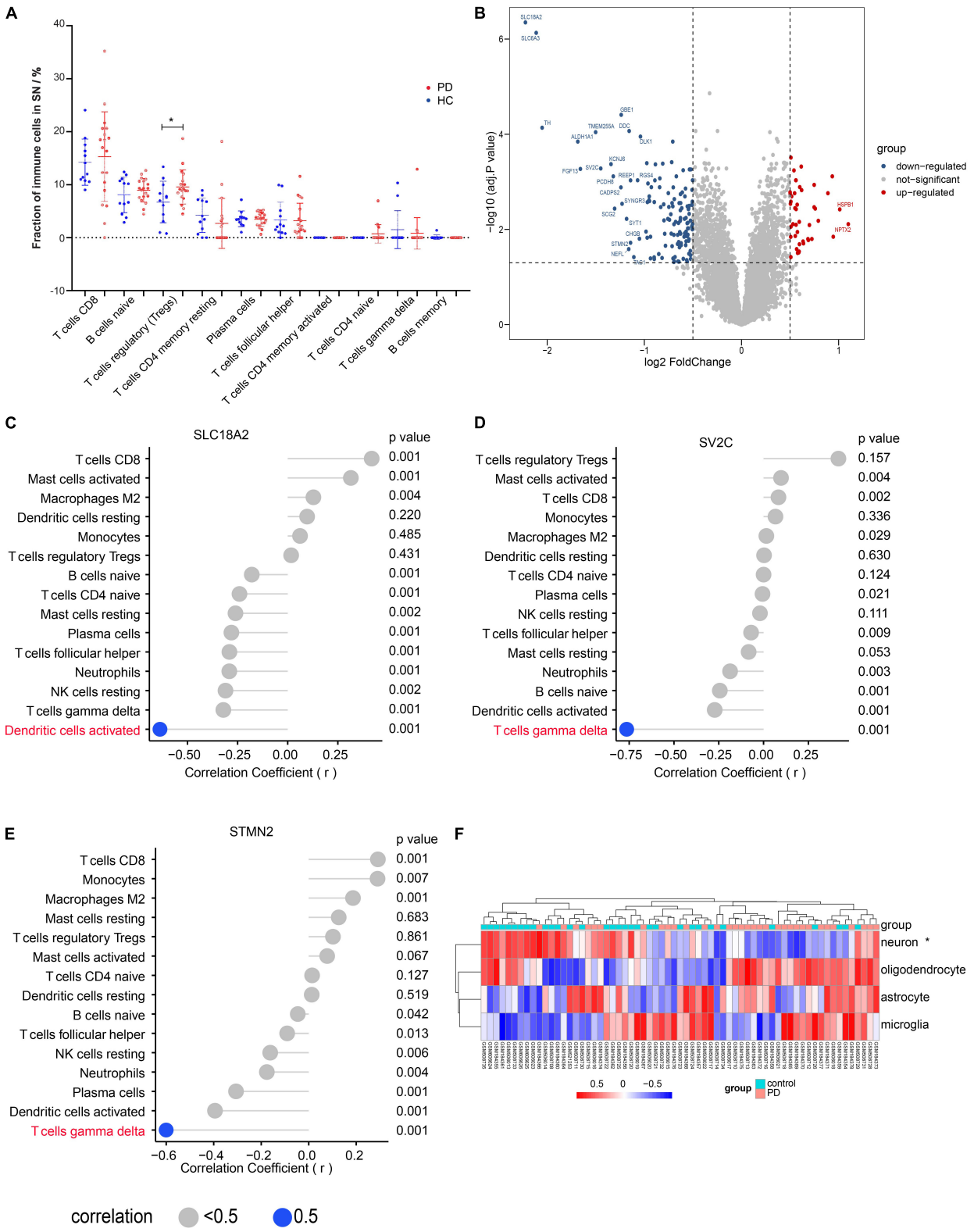


FIGURE 2 | Tregs fraction in substantia nigra (SN) was significantly different between PD and HC. **(A)** The main immune cell fractions in the SN from PD and HC. The ordinate represents the immune cell fractions, and the abscissa represents the immune cell types. The blue dots represent HC samples, and the red dots represent PD samples. **(B)** Volcano plot of the differential gene analysis of SN. **(C)** Correlation between *SLC18A2* and immune cells. **(D)** Correlation between *SV2C* and immune cells. **(E)** Correlation between *STMN2* and immune cells. **(F)** The heat map of the enrichment score through the GSVA analysis. *$p < 0.05$.

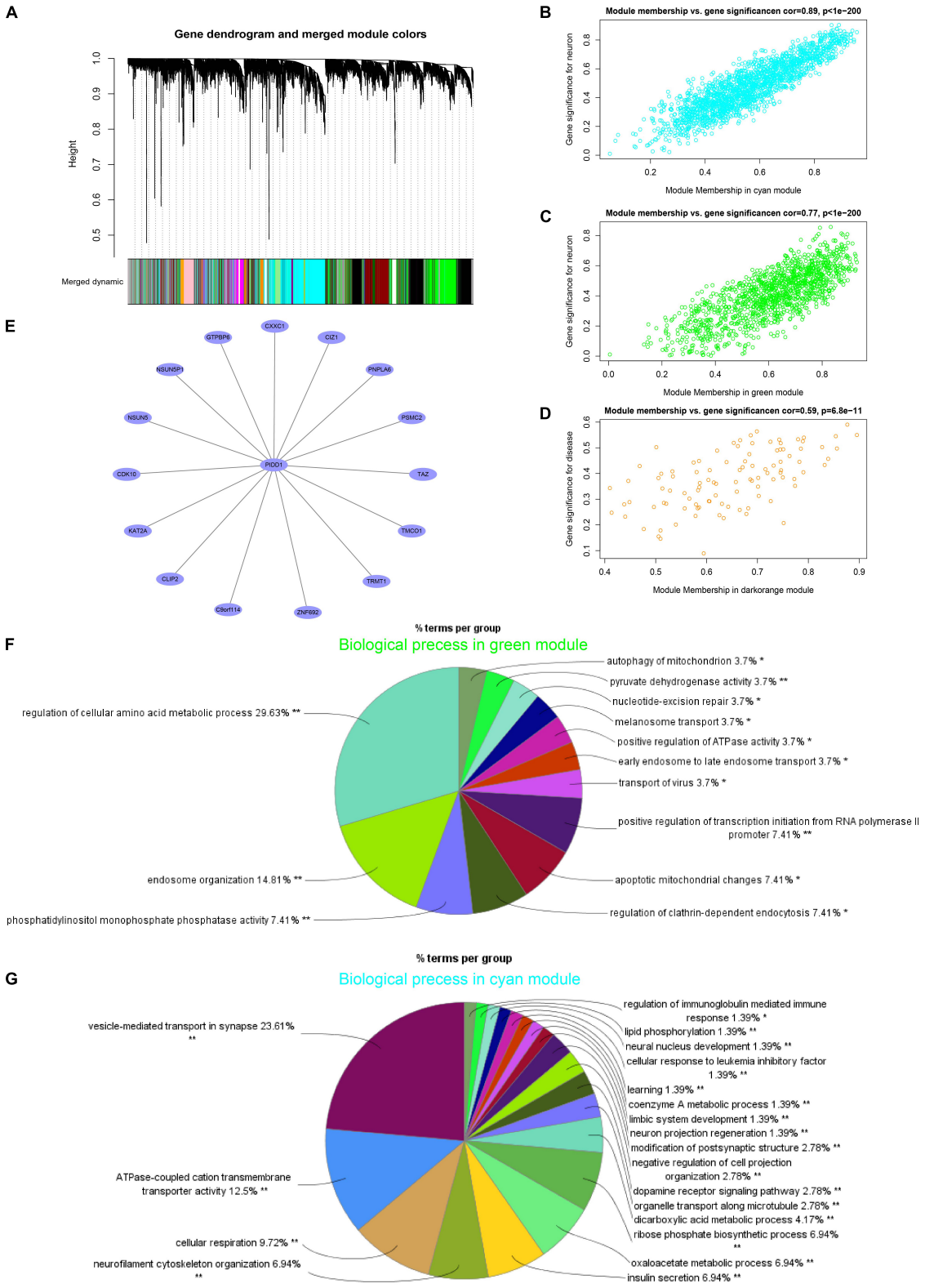


FIGURE 3 | p53-induced death domain protein 1 (*PIDD1*) as a hub gene in the module of PD by the WGCNA analysis in SN. **(A)** Dendrogram of all genes clustered based on a dissimilarity measure (1-TOM). **(B–D)** Correlation between the module membership and the gene significance in cyan, green, and dark-orange modules, separately. **(E)** The network graph of the hub gene *PIDD1* of the PD-related dark-orange module. **(F,G)** The biological process of the GO enrichment analysis of filtered genes in green and cyan modules, separately. $^{*}p < 0.05$, $^{**}p < 0.01$.

(Saunders et al., 2012). In this study, the Tregs was significantly increased in SN from PD compared with that in HC. The adoptive transfer of the activated Treg attenuated astrogliosis and microglia inflammation with concomitant neuroprotection, together with the upregulation of the brain-derived neurotrophic factor and the glial cell-derived neurotrophic factor expression and the downregulation of proinflammatory cytokines and oxidative stress (Liu et al., 2009). So, Tregs was thought to be neuroprotective. Thus, the Tregs fraction that is increased in PD may not be a trigger factor of the pathology of PD but a compensation mechanism to avoid the hyperactive inflammatory response under the pathological state. In these results, other T cell fractions had no statistical difference in SN between PD and HC, but we found that the frequency value of CD8 T cells was more dispersed in PD. CD4 and CD8 T cells had been found in the aged control SN, with only the density but not the percentage of CD8 T cells increasing in PD. They proposed that CD8 T cells contribute to the nigral dopaminergic neuron dysfunction and death in PD before apparent Lewy bodies appear (Galiano-Landeira et al., 2020). Although NK cells had been considered a highly relevant cell type in PD because of the involvement in clearing α-syn in the mouse model (Earls and Lee, 2020; Earls et al., 2020), few NK cells were observed in PD and HC SN. No significant differences in the activated DC and gamma delta T cell fractions were observed. However, we found that *SLC18A2* was negatively correlated with DC, and *STMN2* and SV2C were negatively correlated with gamma delta T cells. Decreased *SLC18A2*, *STMN2*, and *SV2C* expressions were found in the brain tissues from patients with PD. All three genes were considered a potential contributor to the pathogenesis of PD by regulating the synaptic vesicle function and then dopamine neuron function (Dunn et al., 2017; Lohr et al., 2017; Cho et al., 2019; Wang et al., 2019). The activated DC and gamma delta T cells may also have some potential links with the pathology of PD, which remains to be further explored.

Furthermore, we also analyzed the molecular function and coexpression network in SN from PD. These GSVA results showed that the set neuron-specific genes ES were decreased in PD compared with those in HC, indicating that mussy pathways altered may be caused by the neuron loss. *PIDD1*, as the hub gene of PD-related module, was slightly upregulated in PD and was a component of the DNA damage/stress response pathway that functions downstream of p53/*TP53* and could either promote cell survival or apoptosis (Tinel and Tschopp, 2004; Janssens et al., 2005; Tinel et al., 2006). Nuclear factor kappa-light-chain-enhancer of activated B cells (NF-κB) is a prototypical proinflammatory signaling molecule (Dolgacheva et al., 2019). *PIDD1* may promote the inflammatory process by activating the NF-κB signaling pathway (Zhong et al., 2017). Another two genes in the PD-related module, proteasome 26S subunit-ATPase 2 (*PSMC2*) and lysine acetyltransferase 2A (*KAT2A*), may also play roles in the neurodegenerative progression. *PSMC2*, involved in protein homeostasis, was downregulated in PD compared to that in HC in this study. Another study found that the *PSMC2* protein level decreased with age in neural stem cells (NSCs) derived from the subventricular zone on postnatal 7th day, 1 month, and 12-month-old mice suggested that *PSMC2* might accelerate aging or progression of PD (Wang et al., 2016). *KAT2A* was an essential regulator of the hippocampal memory consolidation by regulating a highly interconnected hippocampal gene expression network linked to neuroactive receptor signaling via the NF-κB pathway (Stilling et al., 2014) and played a role in regulating T cell activation (Gao et al., 2017). *PIDD1* as the hub gene may also take part in the progression of PD via regulating *PSMC2* or *KAT2A*. However, how these genes affect the progression of PD is undefined and remains to be further explored. The function of genes in the neuron-related modules suggested that these biological processes change, especially those regarding mitochondrion and synaptic functions, which contribute to neuron death and neurodegeneration in PD.

However, the study has some limitations. First, the results may be more reliable if we enlarged the sample size. Second, the blood and SN samples are not from the same individual, which affects our research in finding a similarity between blood and SN. Third, the reference signature matrix LM22 had only 22 lymphocyte subsets, and we may find links between blood and SN if we have more detailed lymphocyte subsets. Finally, further study to clarify the relationship between genes and immune cells and their underlying effect on the development of PD needs to be conducted in animal models and *in vitro* cell experiments.

CONCLUSION

In conclusion, we identified that the proportions of naïve CD4 T cells, gamma delta T cells, resting NK cells, and neutrophils were significantly different in the blood of PD compared with those of HC. Only Tregs fraction was observed to be significantly increased in PD SN compared to that in HC, and we identified *PIDD1* as a hub gene correlated with PD. Thus, the difference in the lymphocyte subsets in the blood between PD and HC may be used as combined diagnostic biomarkers, and Tregs in SN may be a potential therapeutic target of PD.

DATA AVAILABILITY STATEMENT

Publicly available datasets were analyzed in this study. This data can be found here: https://www.ncbi.nlm.nih.gov/geo/query/acc.cgi?acc=GSE99039; https://www.ncbi.nlm.nih.gov/geo/query/acc.cgi?acc=GSE20164; https://www.ncbi.nlm.nih.gov/geo/query/acc.cgi?acc=GSE20292; and https://www.ncbi.nlm.nih.gov/geo/query/acc.cgi?acc=GSE7621.

AUTHOR CONTRIBUTIONS

All authors listed have made a substantial, direct and intellectual contribution to the work, and approved it for publication.

FUNDING

This work was supported by National Natural Science Foundation of China (81972335) and the High-level Hospital Construction Project (No. DFJH201907).

ACKNOWLEDGMENTS

We thank Guangdong Province Key Laboratory of Fermentation and Enzyme Engineering for financial support.

SUPPLEMENTARY MATERIAL

The Supplementary Material for this article can be found online at: https://www.frontiersin.org/articles/10.3389/fnagi.2021.686066/full#supplementary-material

REFERENCES

Baba, Y., Kuroiwa, A., Uitti, R. J., Wszolek, Z. K., and Yamada, T. (2005). Alterations of T-lymphocyte populations in Parkinson disease. *Parkinsonism Relat. Disord.* 11, 493–498. doi: 10.1016/j.parkreldis.2005.07.005

Blauwendraat, C., Nalls, M. A., and Singleton, A. B. (2020). The genetic architecture of Parkinson's disease. *Lancet Neurol.* 19, 170–178. doi: 10.1016/S1474-4422(19)30287-X

Cao, Y., Tang, W., and Tang, W. (2019). Immune cell infiltration characteristics and related core genes in lupus nephritis: results from bioinformatic analysis. *BMC Immunol.* 20:37. doi: 10.1186/s12865-019-0316-x

Cen, L., Yang, C., Huang, S., Zhou, M., Tang, X., Li, K., et al. (2017). Peripheral lymphocyte subsets as a marker of Parkinson's disease in a Chinese population. *Neurosci. Bull.* 33, 493–500. doi: 10.1007/s12264-017-0163-9

Cho, S. S., Christopher, L., Koshimori, Y., Li, C., Lang, A. E., Houle, S., et al. (2019). Decreased pallidal vesicular monoamine transporter type 2 availability in Parkinson's disease: the contribution of the nigropallidal pathway. *Neurobiol. Dis.* 124, 176–182. doi: 10.1016/j.nbd.2018.11.022

Contaldi, E., Magistrelli, L., Milner, A. V., Cosentino, M., Marino, F., and Comi, C. (2020). Expression of transcription factors in CD4 + T cells as potential biomarkers of motor complications in Parkinson's disease. *J. Parkinsons Dis.* 11, 507–514. doi: 10.3233/JPD-202417

Cook, D. A., Kannarkat, G. T., Cintron, A. F., Butkovich, L. M., Fraser, K. B., Chang, J., et al. (2017). *LRRK2* levels in immune cells are increased in Parkinson's disease. *NPJ Parkinsons Dis.* 3:11. doi: 10.1038/s41531-017-0010-8

Deng, Y. J., Ren, E. H., Yuan, W. H., Zhang, G. Z., Wu, Z. L., and Xie, Q. Q. (2020). GRB10 and E2F3 as diagnostic markers of osteoarthritis and their correlation with immune infiltration. *Diagnostics (Basel)* 10:171. doi: 10.3390/diagnostics10030171

Devos, D., Lejeune, S., Cormier-Dequaire, F., Tahiri, K., Charbonnier-Beaupel, F., Rouaix, N., et al. (2014). Dopa-decarboxylase gene polymorphisms affect the motor response to L-dopa in Parkinson's disease. *Parkinsonism Relat. Disord.* 20, 170–175. doi: 10.1016/j.parkreldis.2013.10.017

Dolgacheva, L. P., Berezhnov, A. V., Fedotova, E. I., Zinchenko, V. P., and Abramov, A. Y. (2019). Role of DJ-1 in the mechanism of pathogenesis of Parkinson's disease. *J. Bioenerg. Biomembr.* 51, 175–188. doi: 10.1007/s10863-019-09798-4

Dunn, A. R., Stout, K. A., Ozawa, M., Lohr, K. M., Hoffman, C. A., Bernstein, A. I., et al. (2017). Synaptic vesicle glycoprotein 2C (*SV2C*) modulates dopamine release and is disrupted in Parkinson disease. *Proc. Natl. Acad. Sci. U. S. A.* 114, E2253–E2262. doi: 10.1073/pnas.1616892114

Earls, R. H., and Lee, J. K. (2020). The role of natural killer cells in Parkinson's disease. *Exp. Mol. Med.* 52, 1517–1525. doi: 10.1038/s12276-020-00505-7

Earls, R. H., Menees, K. B., Chung, J., Barber, J., Gutekunst, C. A., Hazim, M. G., et al. (2019). Intrastriatal injection of preformed alpha-synuclein fibrils alters central and peripheral immune cell profiles in non-transgenic mice. *J. Neuroinflammation* 16:250. doi: 10.1186/s12974-019-1636-8

Earls, R. H., Menees, K. B., Chung, J., Gutekunst, C. A., Lee, H. J., Hazim, M. G., et al. (2020). NK cells clear alpha-synuclein and the depletion of NK cells exacerbates synuclein pathology in a mouse model of alpha-synucleinopathy. *Proc. Natl. Acad. Sci. U. S. A.* 117, 1762–1771. doi: 10.1073/pnas.1909110117

Elkington, P. T. G., O'Kane, C. M., and Friedland, J. S. (2005). The paradox of matrix metalloproteinases in infectious disease. *Clin. Exp. Immunol.* 142, 12–20. doi: 10.1111/j.1365-2249.2005.02840.X

Felix Garza, Z. C., Lenz, M., Liebmann, J., Ertaylan, G., Born, M., Arts, I. C. W., et al. (2019). Characterization of disease-specific cellular abundance profiles of chronic inflammatory skin conditions from deconvolution of biopsy samples. *BMC Med. Genomics* 12:121. doi: 10.1186/s12920-019-0567-7

Galiano-Landeira, J., Torra, A., Vila, M., and Bove, J. (2020). CD8 T cell nigral infiltration precedes synucleinopathy in early stages of Parkinson's disease. *Brain* 143, 3717–3733. doi: 10.1093/brain/awaa269

Galter, D., Buervenich, S., Carmine, A., Anvret, M., and Olson, L. (2003). ALDH1 mRNA: presence in human dopamine neurons and decreases in substantia nigra in Parkinson's disease and in the ventral tegmental area in schizophrenia. *Neurobiol. Dis.* 14, 637–647. doi: 10.1016/j.nbd.2003.09.001

Gao, B., Kong, Q., Zhang, Y., Yun, C., Dent, S. Y. R., Song, J., et al. (2017). The histone acetyltransferase Gcn5 positively regulates T cell activation. *J. Immunol.* 198, 3927–3938. doi: 10.4049/jimmunol.1600312

Ge, P., Wang, W., Li, L., Zhang, G., Gao, Z., Tang, Z., et al. (2019). Profiles of immune cell infiltration and immune-related genes in the tumor microenvironment of colorectal cancer. *Biomed. Pharmacother.* 118:109228. doi: 10.1016/j.biopha.2019.109228

Greenhalgh, A. D., David, S., and Bennett, F. C. (2020). Immune cell regulation of glia during CNS injury and disease. *Nat. Rev. Neurosci.* 21, 139–152. doi: 10.1038/s41583-020-0263-9

Grozdanov, V., Bliederhaeuser, C., Ruf, W. P., Roth, V., Fundel-Clemens, K., Zondler, L., et al. (2014). Inflammatory dysregulation of blood monocytes in Parkinson's disease patients. *Acta Neuropathol.* 128, 651–663. doi: 10.1007/s00401-014-1345-4

Hamza, T. H., Zabetian, C. P., Tenesa, A., Laederach, A., Montimurro, J., Yearout, D., et al. (2010). Common genetic variation in the *HLA* region is associated with late-onset sporadic Parkinson's disease. *Nat. Genet.* 42, 781–785. doi: 10.1038/ng.642

Hirsch, E. C., and Hunot, S. (2009). Neuroinflammation in Parkinson's disease: a target for neuroprotection? *Lancet Neurol.* 8, 382–397. doi: 10.1016/S1474-4422(09)70062-6

Huang, G. J., Smith, A. L., Gray, D. H., Cosgrove, C., Singer, B. H., Edwards, A., et al. (2010). A genetic and functional relationship between T cells and cellular proliferation in the adult hippocampus. *PLoS Biol.* 8:e1000561. doi: 10.1371/journal.pbio.1000561

Janssens, S., Tinel, A., Lippens, S., and Tschopp, J. (2005). PIDD mediates NF-kappaB activation in response to DNA damage. *Cell* 123, 1079–1092. doi: 10.1016/j.cell.2005.09.036

Jiang, J., Pan, W., Xu, Y., Ni, C., Xue, D., Chen, Z., et al. (2020). Tumour-infiltrating immune cell-based subtyping and signature gene analysis in breast cancer based on gene expression profiles. *J. Cancer* 11, 1568–1583. doi: 10.7150/jca.37637

Karaaslan, Z., Kahraman, O. T., Sanli, E., Ergen, H. A., Ulusoy, C., Bilgic, B., et al. (2021). Inflammation and regulatory T cell genes are differentially expressed in peripheral blood mononuclear cells of Parkinson's disease patients. *Sci. Rep.* 11:2316. doi: 10.1038/s41598-021-81961-7

Kelley, K. W., Nakao-Inoue, H., Molofsky, A. V., and Oldham, M. C. (2018). Variation among intact tissue samples reveals the core transcriptional features of human CNS cell classes. *Nat. Neurosci.* 21, 1171–1184. doi: 10.1038/s41593-018-0216-z

Kustrimovic, N., Comi, C., Magistrelli, L., Rasini, E., Legnaro, M., Bombelli, R., et al. (2018). Parkinson's disease patients have a complex phenotypic and functional Th1 bias: cross-sectional studies of CD4+ Th1/Th2/T17 and Treg in drug-naive and drug-treated patients. *J. Neuroinflammation* 15:205. doi: 10.1186/s12974-018-1248-8

Liu, J., Gong, N., Huang, X., Reynolds, A. D., Mosley, R. L., and Gendelman, H. E. (2009). Neuromodulatory activities of CD4+CD25+ regulatory T cells in a murine model of HIV-1-associated neurodegeneration. *J. Immunol.* 182, 3855–3865. doi: 10.4049/jimmunol.0803330

Lohr, K. M., Masoud, S. T., Salahpour, A., and Miller, G. W. (2017). Membrane transporters as mediators of synaptic dopamine dynamics: implications for disease. *Eur. J. Neurosci.* 45, 20–33. doi: 10.1111/ejn.13357

Mosley, R. L., Hutter-Saunders, J. A., Stone, D. K., and Gendelman, H. E. (2012). Inflammation and adaptive immunity in Parkinson's disease.

Cold Spring Harb. Perspect. Med. 2:a009381. doi: 10.1101/cshperspect.a009381

Newman, A. M., Liu, C. L., Green, M. R., Gentles, A. J., Feng, W., Xu, Y., et al. (2015). Robust enumeration of cell subsets from tissue expression profiles. *Nat. Methods* 12, 453–457. doi: 10.1038/nmeth.3337

Niwa, F., Kuriyama, N., Nakagawa, M., and Imanishi, J. (2012). Effects of peripheral lymphocyte subpopulations and the clinical correlation with Parkinson's disease. *Geriatr. Gerontol. Int.* 12, 102–107. doi: 10.1111/j.1447-0594.2011.00740.x

O'Shea, J. J., and Paul, W. E. (2010). Mechanisms underlying lineage commitment and plasticity of helper CD4+ T cells. *Science* 327, 1098–1102. doi: 10.1126/science.1178334

Rayaprolu, S., Mullen, B., Baker, M., Lynch, T., Finger, E., Seeley, W. W., et al. (2013). TREM2 in neurodegeneration: evidence for association of the p.R47H variant with frontotemporal dementia and Parkinson's disease. *Mol. Neurodegener.* 8:19. doi: 10.1186/1750-1326-8-19

Reynolds, A. D., Banerjee, R., Liu, J., Gendelman, H. E., and Mosley, R. L. (2007). Neuroprotective activities of CD4+CD25+ regulatory T cells in an animal model of Parkinson's disease. *J. Leukoc. Biol.* 82, 1083–1094. doi: 10.1189/jlb.0507296

Ritzel, R. M., Lai, Y. J., Crapser, J. D., Patel, A. R., Schrecengost, A., Grenier, J. M., et al. (2018). Aging alters the immunological response to ischemic stroke. *Acta Neuropathol.* 136, 89–110. doi: 10.1007/s00401-018-1859-2

Rosenkranz, D., Weyer, S., Tolosa, E., Gaenslen, A., Berg, D., Leyhe, T., et al. (2007). Higher frequency of regulatory T cells in the elderly and increased suppressive activity in neurodegeneration. *J. Neuroimmunol.* 188, 117–127. doi: 10.1016/j.jneuroim.2007.05.011

Saunders, J. A., Estes, K. A., Kosloski, L. M., Allen, H. E., Dempsey, K. M., Torres-Russotto, D. R., et al. (2012). CD4+ regulatory and effector/memory T cell subsets profile motor dysfunction in Parkinson's disease. *J. Neuroimmune Pharmacol.* 7, 927–938. doi: 10.1007/s11481-012-9402-z

Schroder, J. B., Pawlowski, M., Meyer Zu Horste, G., Gross, C. C., Wiendl, H., Meuth, S. G., et al. (2018). Immune cell activation in the cerebrospinal fluid of patients with Parkinson's disease. *Front. Neurol.* 9:1081. doi: 10.3389/fneur.2018.01081

Stilling, R. M., Ronicke, R., Benito, E., Urbanke, H., Capece, V., Burkhardt, S., et al. (2014). K-Lysine acetyltransferase 2a regulates a hippocampal gene expression network linked to memory formation. *EMBO J.* 33, 1912–1927. doi: 10.15252/embj.201487870

Tansey, M. G., and Romero-Ramos, M. (2019). Immune system responses in Parkinson's disease: early and dynamic. *Eur. J. Neurosci.* 49, 364–383. doi: 10.1111/ejn.14290

Tinel, A., Janssens, S., Lippens, S., Cuenin, S., Logette, E., Jaccard, B., et al. (2006). Autoproteolysis of PIDD marks the bifurcation between pro-death caspase-2 and pro-survival NF-κB pathway. *EMBO J.* 26, 197–208. doi: 10.1038/sj.emboj.7601473

Tinel, A., and Tschopp, J. (2004). The PIDDosome, a protein complex implicated in activation of caspase-2 in response to genotoxic stress. *Science* 304, 843–846. doi: 10.1126/science.1095432

Turner, R. J., and Sharp, F. R. (2016). Implications of *MMP9* for blood brain barrier disruption and hemorrhagic transformation following ischemic stroke. *Front. Cell. Neurosci.* 10:56. doi: 10.3389/fncel.2016.00056

Wang, Q., Zhang, Y., Wang, M., Song, W. M., Shen, Q., McKenzie, A., et al. (2019). The landscape of multiscale transcriptomic networks and key regulators in Parkinson's disease. *Nat. Commun.* 10:5234. doi: 10.1038/s41467-019-13144-y

Wang, X., Dong, C., Sun, L., Zhu, L., Sun, C., Ma, R., et al. (2016). Quantitative proteomic analysis of age-related subventricular zone proteins associated with neurodegenerative disease. *Sci. Rep.* 6:37443. doi: 10.1038/srep37443

Zhong, J., Jiang, L., Huang, Z., Zhang, H., Cheng, C., Liu, H., et al. (2017). The long non-coding RNA Neat1 is an important mediator of the therapeutic effect of bexarotene on traumatic brain injury in mice. *Brain Behav. Immun.* 65, 183–194. doi: 10.1016/j.bbi.2017.05.001

Zhou, C., Zhou, X., He, D., Li, Z., Xie, X., and Ren, Y. (2020). Reduction of peripheral blood iNKT and γδT cells in patients with Parkinson's disease: an observational study. *Front. Immunol.* 11:1329. doi: 10.3389/fimmu.2020.01329

Conflict of Interest: The authors declare that the research was conducted in the absence of any commercial or financial relationships that could be construed as a potential conflict of interest.

Publisher's Note: All claims expressed in this article are solely those of the authors and do not necessarily represent those of their affiliated organizations, or those of the publisher, the editors and the reviewers. Any product that may be evaluated in this article, or claim that may be made by its manufacturer, is not guaranteed or endorsed by the publisher.

Copyright © 2021 Huang, Liu, Hu, Han, Zhong, Luo, Zhang and Ling. This is an open-access article distributed under the terms of the Creative Commons Attribution License (CC BY). The use, distribution or reproduction in other forums is permitted, provided the original author(s) and the copyright owner(s) are credited and that the original publication in this journal is cited, in accordance with accepted academic practice. No use, distribution or reproduction is permitted which does not comply with these terms.

frontiers in Aging Neuroscience

BRIEF RESEARCH REPORT
published: 22 September 2021
doi: 10.3389/fnagi.2021.717930

Detection of Cerebrospinal Fluid Neurofilament Light Chain as a Marker for Alpha-Synucleinopathies

Sezgi Canaslan[1†], Matthias Schmitz[1†], Anna Villar-Piqué[1,2,3], Fabian Maass[4], Karin Gmitterová[1,5,6], Daniela Varges[1], Paul Lingor[7], Franc Llorens[1,2,3], Peter Hermann[1] and Inga Zerr[1]*

[1] Department of Neurology, University Medical Center Göttingen and the German Center for Neurodegenerative Diseases (DZNE), Göttingen, Germany, [2] Network Center for Biomedical Research of Neurodegenerative Diseases (CIBERNED), Institute Carlos III, Madrid, Spain, [3] Neuroscience Area, Bellvitge Biomedical Research Institute (IDIBELL), L'Hospitalet de Llobregat, Spain, [4] Department of Neurology, University Medical Center, Göttingen, Germany, [5] Second Department of Neurology, Comenius University, Bratislava, Slovakia, [6] Department of Neurology, Slovak Medical University in Bratislava, Bratislava, Slovakia, [7] Department of Neurology, Technical University of Munich, Munich, Germany

Alpha-synucleinopathies, such as Parkinson's disease (PD), dementia with Lewy bodies (DLB), and multiple system atrophy (MSA), are a class of neurodegenerative diseases. A diagnosis may be challenging because clinical symptoms partially overlap, and there is currently no reliable diagnostic test available. Therefore, we aimed to identify a suitable marker protein in cerebrospinal fluid (CSF) to distinguish either between different types of alpha-synucleinopathies or between alpha-synucleinopathies and controls. In this study, the regulation of different marker protein candidates, such as alpha-synuclein (a-Syn), neurofilament light chain (NfL), glial fibrillary acidic protein (GFAP), and total tau (tau) in different types of alpha-synucleinopathies, had been analyzed by using an ultrasensitive test system called single-molecule array (SIMOA). Interestingly, we observed that CSF-NfL was significantly elevated in patients with DLB and MSA compared to patients with PD or control donors. To differentiate between groups, receiver operating characteristic (ROC) curve analysis resulted in a very good diagnostic accuracy as indicated by the area under the curve (AUC) values of 0.87–0.92 for CSF-NfL. Furthermore, we observed that GFAP and tau were slightly increased either in DLB or MSA, while a-Syn levels remained unregulated. Our study suggests NfL as a promising marker to discriminate between different types of alpha-synucleinopathies or between DLB/MSA and controls.

Keywords: alpha-synucleinopathies, biomarker, neurofilament light chain, SIMOA assay, cerebrospinal fluid

OPEN ACCESS

Edited by:
Shaogang Qu,
Southern Medical University, China

Reviewed by:
Zerui Wang,
Case Western Reserve University, United States
Fernando Goni,
New York University, United States

****Correspondence:***
Matthias Schmitz
matthias.schmitz@med.uni-goettingen.de

† These authors have contributed equally to this work

Received: *31 May 2021*
Accepted: *12 August 2021*
Published: *22 September 2021*

Citation:
Canaslan S, Schmitz M, Villar-Piqué A, Maass F, Gmitterová K, Varges D, Lingor P, Llorens F, Hermann P and Zerr I (2021) Detection of Cerebrospinal Fluid Neurofilament Light Chain as a Marker for Alpha-Synucleinopathies. Front. Aging Neurosci. 13:717930. doi: 10.3389/fnagi.2021.717930

INTRODUCTION

Alpha-synucleinopathies are a group of neurological disorders, including Parkinson's disease (PD), dementia with Lewy bodies (DLB), and multiple system atrophy (MSA). They share common overriding symptoms such as rigidity, rest tremor, akinesia, autonomic, behavioral, cognitive-motor dysfunctions like freezing, and speech problems (Kompoliti and Metman, 2010). PD is the common

Abbreviations: a-Syn, alpha-synuclein; AUC, area under the curve; CSF, cerebrospinal fluid, GFAP, glial fibrillary acidic protein; DLB, dementia with Lewy bodies; LB, Lewy bodies; MSA, multiple system atrophy; NfL, neurofilament light chain; PD, Parkinson's disease; ROC, receiver operating characteristic; SIMOA, single-molecule array; tau, total tau.

subgroup of synucleinopathies with a 1.6% of incidence rate among people over 65 years of age (De Rijk et al., 1997). The prevalence of synucleinopathies is around 21 per 100,000 person-years, and it increases excessively with age (Savica et al., 2013). The patients with PD show clinical symptoms when approximately 50% of substantia nigra cells and striatal dopamine are lost and patients with DLB experience visual hallucinations, cognitive impairments, and conscious problems (Kompoliti and Metman, 2010).

Alpha synucleinopathies are mainly characterized by alpha-synuclein (a-Syn) aggregates in the brain tissue. While PD and DLB possess the formation of Lewy bodies (LB) in neurons (Spillantini et al., 1997), MSA is characterized by glial cytoplasmic inclusions (GCIs) in non-neuronal cells, i.e., oligodendrocytes (Wakabayashi et al., 1998).

The misdiagnosis of alpha-synucleinopathies may occur due to a clinical overlap of symptoms and the lack of specific diagnostic tests or biomarkers. A confirmed diagnosis requires postmortem examination by autopsy, which confirms approximately 80% of premortal clinical diagnoses (Savica et al., 2013).

Until present, the colorimetric ELISA system and western blotting are commonly used for protein analysis in a diagnostic context. However, small changes in the protein concentration cannot be detected effectively by these standard methods for protein analyses. The high technological progress of protein analytics had been achieved by the development of the digital ELISA concept, such as the ultrasensitive single-molecule array (SIMOA) (Rissin et al., 2010). SIMOA measures proteins in femtomolar (fM) concentrations (Rissin et al., 2010) and can detect minuscule changes in protein concentrations related to the pathological processes in the brain, which were not measurable by the standard analog methods. These alterations may be important for diagnostic and understanding of neuropathological processes.

In this study, we analyzed the concentration of potential marker protein candidates, such as neurofilament light chain (NfL), glial fibrillary acidic protein (GFAP), a-Syn, and total tau (tau) in patients with different types of alpha-synucleinopathies. Diagnostic accuracies were estimated by the receiver operating characteristic (ROC) curve analysis.

METHODS

Patients

This study includes patients with alpha-synucleinopathies that were classified as PD (Postuma et al., 2015), DLB [criteria based on the McKeith criteria (McKeith et al., 2017)], and MSA (criteria based on the Gilman criteria) (Gilman et al., 1999, 2008); autopsies were not available (**Table 1**).

The control group was composed of cases diagnosed with non-primary neurodegenerative neurological and psychiatric conditions according to the acknowledged standard neurological, clinical, and para-clinical findings based on the ICD-10 definition cases, without cognitive impairment or dementia at the time of sampling. The number of patients in each group can be noted in the corresponding part in **Table 1**. Blood-contaminated cerebrospinal fluid (CSF) samples were excluded from the study.

Sample Pretreatment

All protein concentrations were measured with the SIMOA-SR-X machine (Quanterix, Billerica, MA, United States). We have used commercial assay kits from Quanterix. All assays have already been optimized for certain marker proteins. In this study, we followed the protocols provided by Quanterix and applied the recommended reaction conditions to obtain the most accurate outcome. In addition, each assay contains two internal controls with a defined protein concentration. Only when both internal assay controls were in the expected range (less than 10% variation), we subjected the data for further analysis.

Kits and samples were brought to room temperature before pipetting. CSF samples were vortexed for 10–20 s and centrifuged for 5 min at 10,000 rpm to remove impurities before use.

Initially, we analyzed each sample in duplicates and observed that the intra-assay variation was marginal and not statistically significant (**Supplementary Figures 1A,B**). Later, we proceeded with single measurements due to low sample volumes. All samples had an identification code and were analyzed blinded and randomly by the experimenter.

Determination of NfL

The CSF samples were diluted at 1:100 to a total volume of 100 μl. Capture antibody-coated beads (25 μl) and biotin-labeled detector antibodies (20 μl) were pipetted to the wells. Subsequently, the plate was incubated on an orbital shaker for 30 min at 30°C at 800 rpm using a black covering lid for protection from light. After washing, 100 μl of streptavidin β-galactosidase (SβG) was added to the wells, and the plates were incubated for 10 min at 30°C. After a couple of washing steps, the plate was placed in the SR-X machine for measurements.

Determination of Tau

For tau measurements, the reaction volume was 152 μl per well. We applied the same protocol mentioned before. The dilution of CSF was 1:10. Bead and detector antibody solutions were pipetted, and the plate was incubated at 35°C at 800 rpm for 20 min on an orbital shaker. The SβG solution was prepared by mixing diluent and reagent according to the described proportion. After incubation and washing, SβG solution was added to the samples and incubated for 10 min. After several steps of washing, the plate was placed on the machine for analysis using the tau protocol.

Determination of GFAP

We have followed the recommended dilutions according to the protocol of the manufacturer. CSF samples were diluted 1:40. Calibrators were prepared following the protocol on kit instructions. Bead solution was prepared from bead stock after washing and diluting in bead diluent. Detector reagent was also prepared according to the recommendation of the manufacturer. SβG stock solution (10 nM) was diluted to 0.150 nM. Bead (25 μl) and detector (20 μl) antibody solutions were pipetted

TABLE 1 | Summary of the demographic information about patients and biomarker concentration.

		DLB	MSA	PD	Controls
NfL	Number of Individuals (F/M)	23 (7:16)	26 (14:12)	29 (9:20)	35 (10:22)*
	Age ± S.D.	71.17 ± 10.13	65.15 ± 11.12	66.38 ± 11.44	60.75 ± 13.39
	Meant ± S.E.M (pg/mL)	2,190.76 ± 421.46	3,839.32 ± 615.85	960.55 ± 108.82	810.00 ± 104.81
GFAP	Number of Individuals (F/M)	27 (10:17)	26 (14:12)	32 (10:22)	28 (10:15)*
	Age ± S.D.	72.03 ± 9.55	65.15 ± 12.66	65.56 ± 10.36	62.32 ± 13.49
	Meant S.E.M (pg/mL)	9,451.86 ± 1,669.36	10,291.36 ± 1,736.94	4,938.28 ± 853.62	7,693.76 ± 839.87
a-Syn	Number of Individuals (F/M)	18 (5:13)	26 (14:12)	31 (9:22)	35 (11:20)*
	Age ± S.D.	72.61 ± 9.81	65.15 ± 12.66	65.97 ± 11.01	61.06 ± 13.76
	Meant S.E.M (pg/mL)	1,468.6 ± 350.69	1,532.30 ± 336.40	1,544.61 ± 249.51	1,299.91 ± 111.32
Total Tau	Number of Individuals (F/M)	20 (6:14)	27 (14:13)	25 (9:16)	21 (5:13)*
	Age ± S.D.	71.5 ± 10.64	65.07 ± 12.43	68.32 ± 9.11	62.28 ± 12.67
	Meant S.E.M (pg/mL)	140.36 ± 27.79	80.01 ± 7.16	62.53 ± 6.21	95.51 ± 10.40

**The rest is unknown.*

to the wells and incubated on an orbital shaker for 30 min at 30°C with shaking at 800 rpm. After washing, 100 µl of SβG solution were pipetted to wells and incubated again at the same condition for 10 min. After SβG treatment we followed the GFAP analysis protocol.

Determination of a-Syn

All CSF samples were diluted at 1:10 in sample dilution buffer. The preparation of bead and detector solutions was performed as described in the "Determination of GFAP" section. SβG solution was to a final concentration of 0.075 nM as the final concentration. All solutions were pipetted in the same order and the same amount as in GFAP measurement and incubated at 35°C for 35 min on an orbital shaker with shaking at 800 rpm. After washing and SβG addition, the plate was incubated for 10 min at the same condition, then the plate was transferred to the SR-X machine, and protocol for a-Syn analysis was performed.

Statistical Analysis

The normality of values was investigated by the Dallal–Wilkinson–Lille test. For multiple comparisons, we performed non-parametric testing by the Kruskal–Wallis one-way analysis with Dunn's test for *post hoc* comparisons. The ROC curves were calculated, and the area under the curve (AUC) values were extracted by using the software GraphPad Prism 6.0.1 (San Diego, CA, United States). All correlation studies were computed by using the non-parametric Spearman's correlation test (two-tailed) with a CI of 95%. The *p*-values below 0.05 are considered statistically significant.

Ethical Issues

The study was conducted according to the revised Declaration of Helsinki and Good Clinical Practice guidelines and has been approved by the Local Ethics Committee of the University Medicine Göttingen, No. 19/11/09 "Liquormarker als Prädiktoren für die Entwicklung einer Demenz bei Patienten mit Morbus Parkinson, Demenz mit Lewy Körperchen und Morbus Alzheimer" and by the Ethics Committee of the University Medicine Göttingen, No. 13/11/12 "LIX – Liquormarker zur Frühdiagnose und Krankheitsprogression bei Patienten mit Parkinson-syndromen und Motoneuronerkrankungen."

RESULTS

Determination of NfL-, GFAP-, Tau-, and a-Syn Levels in the CSF of Patients With Alpha-Synucleinopathy

The CSF samples from different subgroups of alpha-synucleinopathies (i.e., PD, DLB, and MSA) were subjected to the SIMOA analysis. The levels of four protein marker candidates, namely, NfL, GFAP, tau, and a-Syn, were measured by commercially available assay kits from Quanterix, following either a two- or a three-step protocol.

Our measurements indicated a significant increase in the NfL levels in patients with MSA compared to those with PD and controls ($p < 0.001$). In addition, patients with DLB exhibited higher NfL concentrations than patients with PD as well as control individuals ($p < 0.001$) (**Figure 1A** and **Table 1**).

A second neurodegenerative CSF-marker, tau, was moderately increased in patients with DLB compared to those with PD and the control group ($p < 0.05$) (**Figure 1B**).

When we compared CSF-GFAP levels in different types of alpha-synucleinopathies, our obtained data indicated elevated GFAP levels in patients with MSA compared with PD ($p < 0.05$) (**Figure 1C**). In the remaining groups, CSF-GFAP levels were not significantly regulated (**Figure 1C**).

The levels of a-Syn, the common causative player of all synucleinopathies, were not significantly changed between all groups and it did not correlate with age (**Figure 1D** and **Supplementary Figures 2A–C**).

Determination of Diagnostic Accuracy of NfL to Discriminate Patients With DLB and MSA From Patients With PD and Controls

To determine the diagnostic accuracy of CSF-NfL, we conducted the ROC curve analyses using the software GraphPad Prism 6.0.1.

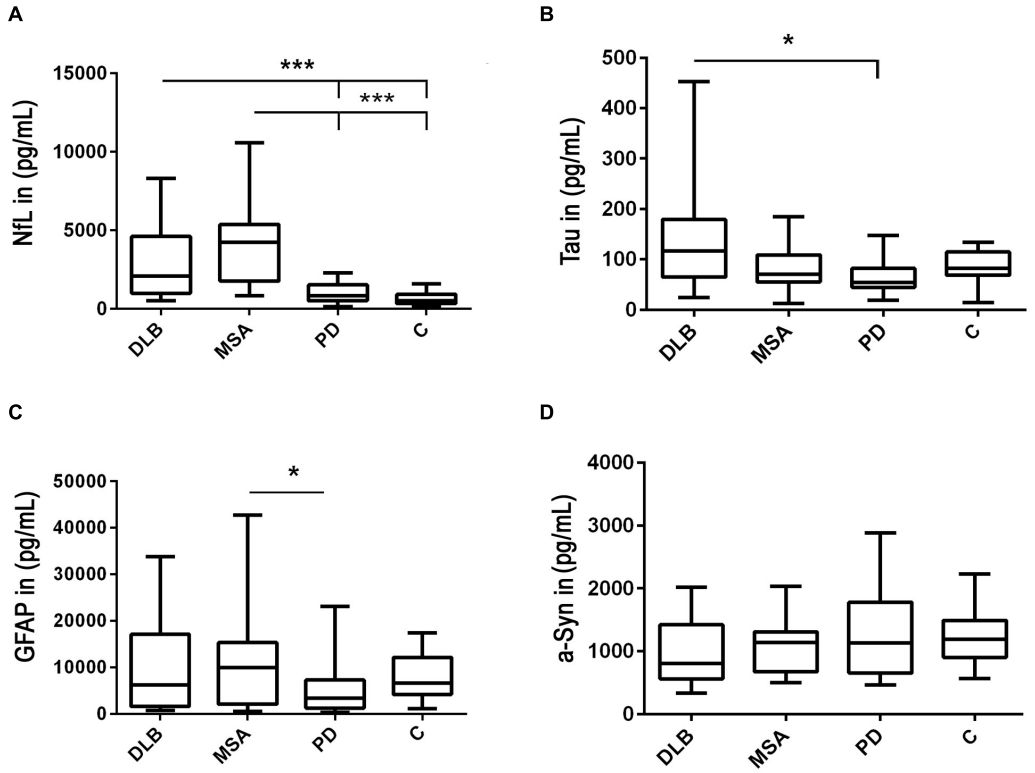
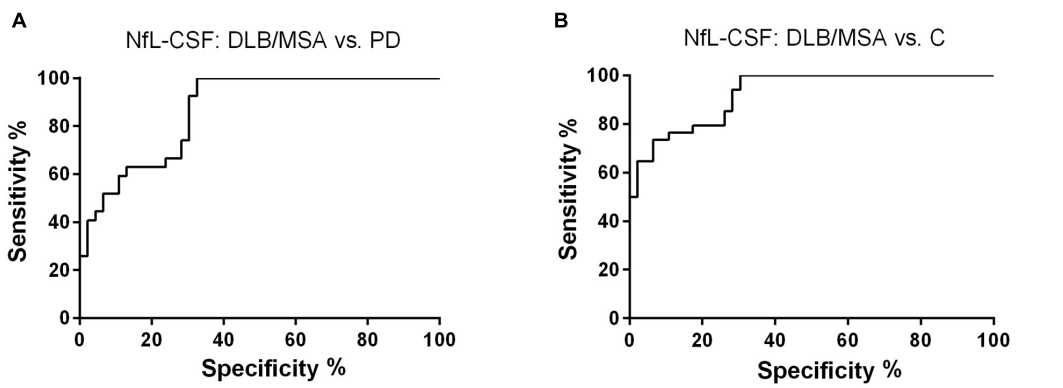


FIGURE 1 | Detection of neurofilament light chain (NfL), glial fibrillary acidic protein (GFAP), alpha-synuclein (a-Syn), and tau levels in cerebrospinal fluid (CSF). Potential marker candidate proteins were determined in CSF of synucleinopathy patients with Parkinson's disease (PD), dementia with Lewy bodies (DLB), multiple system atrophy (MSA), and controls (C). **(A)** The NfL levels were increased in patients with both MSA and DLB compared with PD and controls. **(B)** The tau levels were higher in patients with DLB than those with PD. **(C)** The GFAP levels were higher in patients with MSA than those with PD. **(D)** No significant changes in a-Syn concentrations were observed between groups. The values displayed are means and SDs. A ***p-value < 0.001 is considered as extremely significant, *$p < 0.05$ as significant, and $p \geq 0.05$ as not significant.



Area	0.8671
Std. Error	0.04044
95% confidence interval	0.7879 to 0.9464
P value	< 0.0001

Area	0.9246
Std. Error	0.02725
95% confidence interval	0.8711 to 0.9780
P value	< 0.0001

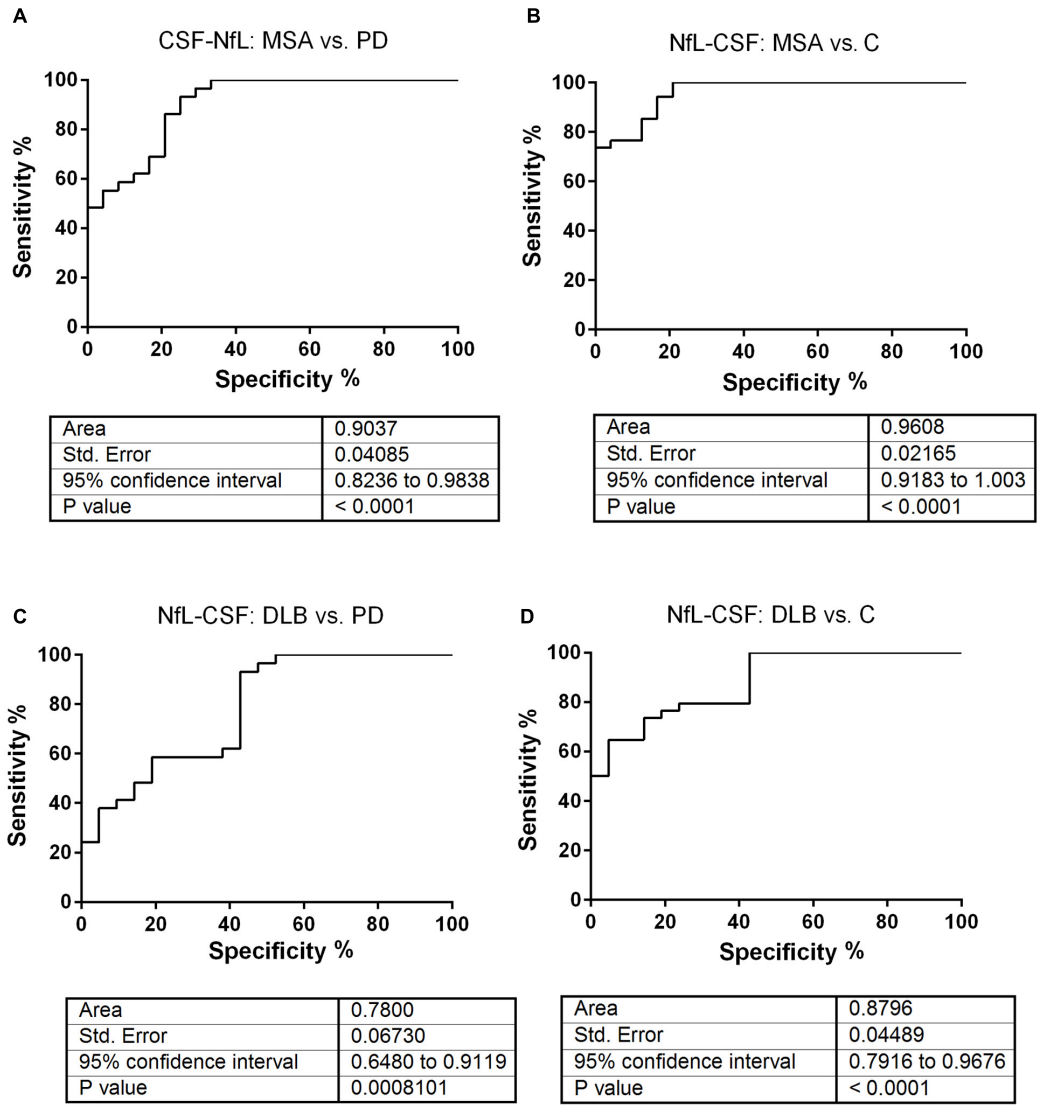
FIGURE 2 | Receiver operating characteristic (ROC) curve analysis of CSF-NfL levels. To increase the statistical power, we combined DLB and MSA in one group considered as other synucleinopathies. **(A)** The diagnostic accuracy of CSF-NfL was assessed with ROC-derived area under the curve (AUC) values (with 95% CI) for the discrimination of patients with other alpha-synucleinopathies from PD. The AUC values of 0.87 ± 0.04 SD, 95% CI of 0.79–0.95 indicated a very good diagnostic accuracy. **(B)** The diagnostic accuracy of CSF-NfL was assessed for the discrimination of patients with other alpha-synucleinopathies from controls (indicated as C). The AUC values of 0.92 ± 0.03 SD, 95% CI of 0.87–0.98 indicated a very good diagnostic accuracy.

We combined MSA and DLB to increase the statistical power. Interestingly, the ROC curve analysis indicated an AUC value of 0.87 to differentiate between DLB/MSA and PD ($p < 0.0001$) (**Figure 2A**). To distinguish between other synucleinopathy group and controls, our analysis revealed an AUC value of 0.92 ($p < 0.0001$) (**Figure 2B**). Both ROC curve analyses suggested CSF-NfL as a suitable marker to discriminate between other synucleinopathies and classical PD as well as between other synucleinopathies and controls.

Subsequently, we stratified the other synucleinopathy group in MSA and DLB. The ROC curve analysis indicated that CSF-NfL differentiated MSA from PD and control cases with a very good diagnostic accuracy. The AUC values were between 0.90 and 0.96, respectively (**Figures 3A,B**). In contrast, the ROC curve analysis produced a lower accuracy, when we assessed the diagnostic accuracy of CSF-NfL for differentiating DLB from PD and controls, indicated by the AUC values of 0.78 and 0.88 (**Figures 3C,D**).

DISCUSSION

With populations growing and aging worldwide, the development of novel and less-invasive diagnostic test systems has become an urgent need. Currently, the diagnostic application of certain biomarkers in body fluids of patients



Area	0.9037
Std. Error	0.04085
95% confidence interval	0.8236 to 0.9838
P value	< 0.0001

Area	0.9608
Std. Error	0.02165
95% confidence interval	0.9183 to 1.003
P value	< 0.0001

Area	0.7800
Std. Error	0.06730
95% confidence interval	0.6480 to 0.9119
P value	0.0008101

Area	0.8796
Std. Error	0.04489
95% confidence interval	0.7916 to 0.9676
P value	< 0.0001

FIGURE 3 | Receiver operating characteristic curve analysis of CSF-NfL levels from patients with MSA and DLB. ROC analyses were performed with the CSF-NfL concentrations obtained for the different diagnostic groups. **(A,B)** The diagnostic accuracy of CSF-NfL was assessed with ROC-derived AUC values (with 95% CI) for the discrimination of patients with MSA from PD and controls. The AUC values of 0.90 ± 0.04 SD, 95% CI of 0.82–0.98 and 0.96 ± 0.02 SD, 95% CI of 0.91–1.00 indicated a very good diagnostic accuracy. **(C,D)** The diagnostic accuracy of CSF-NfL was assessed for the discrimination of patients with DLB from PD and controls (indicated as C). The AUC values of 0.78 ± 0.07 SD, 95% CI of 0.65–0.91 and 0.88 ± 0.04 SD, 95% CI of 0.79–0.97 indicated a good diagnostic accuracy.

with alpha-synucleinopathies is still a matter of debate (Eller and Williams, 2011; Schade and Mollenhauer, 2014). Therefore, our aim is to analyze the expression of potential protein marker candidates in CSF to identify a suitable marker to differentiate either between different subgroups of alpha-synucleinopathies or between other synucleinopathies and controls without neurodegeneration. We have selected four promising marker protein candidates, namely, NfL, a-Syn, tau, and GFAP, to cover a certain spectrum of neurodegeneration to inflammation. Applying a novel technology, based on SIMOA, allows us an ultrasensitive detection of these four proteins to describe potential subtle differences between groups.

CSF-NfL as an Accurate Marker to Differentiate Between DLB/MSA and PD or Controls

In neurodegenerative diseases, CSF is a valuable source for biomarkers because it reflects neurodegenerative processes in the brain (Cramm et al., 2015, 2016; Schmitz et al., 2016a,b; Zerr et al., 2019; Llorens et al., 2020). When we determined CSF-NfL, a known marker for several neurodegenerative diseases, reflecting the neuroaxonal damage (Holmberg et al., 1998; Petzold, 2005), we obtained a highly significant increase of NfL levels in patients with DLB and MSA compared to those with PD and controls.

The ROC curve analyses suggested an accurate diagnostic accuracy of CSF-NfL to differentiate either between other synucleinopathies (i.e., DLB and MSA) from PD as indicated by an AUC value of 0.87 or between other synucleinopathies and controls as indicated by an AUC value of 0.92.

Previous studies on NfL detection in alpha-synucleinopathies already observed the elevated NfL levels in CSF of patients with MSA and DLB (Holmberg et al., 1998; Abdo et al., 2007). The diagnostic accuracy of CSF-NfL to differentiate MSA from PD was indicated by the AUC values of about 0.85–0.90 (Abdo et al., 2007; Hall et al., 2012; Magdalinou et al., 2015), which is in line with our observations. Potential differences between studies may depend on the composition of the patient cohort or the kind of methodology used for the measurement.

Regulation of Other CSF Biomarkers in Alpha-Synucleinopathies

In addition, we analyzed the regulation of other potential biomarker candidate proteins in CSF by using assays based on the SIMOA technology. We observed a moderate tau upregulated in CSF of DLB compared to PD cases. Since we have measured tau and not the phosphorylated forms of tau in PD and DLB, which might give further information about a potential implication of tau, the diagnostic relevance of tau in synucleinopathies is limited.

The upregulation of CSF-tau in DLB is in line with our previous study (Llorens et al., 2016) using a colorimetric detection system and others (Mollenhauer et al., 2011; Mondello et al., 2014).

In addition, we observed GFAP [a type III intermediate filament and the key component of the astrocyte cytoskeleton (Eng et al., 2000; Yang and Wang, 2015)] upregulated in patients with MSA. CSF-GFAP, mainly expressed in fibrillary astrocytes, was already described to be slightly upregulated in DLB, a distinct type of other synucleinopathies, compared with controls (Ishiki et al., 2016).

We observed no significant alterations of CSF-a-Syn levels between different diagnostic groups. Previous studies using a colorimetric a-Syn assay or an assay based on the Mesoscale technology revealed a moderated decrease of CSF-a-Syn in alpha-synucleinopathies compared with controls. No significant regulation was reported between different subgroups of synucleinopathies, such as PD, DLB, and MSA, which is in line with our current study (Llorens et al., 2017; Schmitz et al., 2019).

The strength of our study is that we applied the novel and ultrasensitive SIMOA to measure potential CSF protein marker candidates for alpha-synucleinopathies. The assays are commercially available and well-validated. In future studies, we also plan to develop a Homebrew assay for the detection of epigenetically modified a-Syn or tau species, such as different phosphorylated forms. A limitation of this analysis is the low number of available DLB cases that impeded a proper calculation of diagnostic accuracy. Therefore, a confirmation of our observations in larger cohorts or with alternative methodologies (e.g., analog or multiplexing detection systems) is suggested.

CONCLUSION

Our study applied an innovative digital methodology (i.e., SIMOA), which enabled us to detect even subtle regulations in CSF, suggesting NfL as a potential diagnostic marker for a reliable discrimination either between other synucleinopathies (i.e., DLB and MSA) and PD or between other synucleinopathies and controls. This is of particular interest because, in the daily clinical routine, it is more difficult to differentiate the PD-type of MSA (MSA-P) and PD than to differentiate MSA and DLB. Therefore, NfL may become important as a marker to identify those patients, allowing to include them in disease-modifying trials early in the disease course and to inform them about the quite different prognosis and characteristics of MSA disease.

DATA AVAILABILITY STATEMENT

The raw data supporting the conclusions of this article will be made available by the authors, on request.

ETHICS STATEMENT

The study was conducted according to the revised Declaration of Helsinki and Good Clinical Practice guidelines and has been approved by the Local Ethics Committee of the

University Medicine Göttingen, No. 19/11/09 "Liquormarker als Prädiktoren für die Entwicklung einer Demenz bei Patienten mit Morbus Parkinson, Demenz mit Lewy Körperchen und Morbus Alzheimer" and by the Ethics Committee of the University Medicine Göttingen, No. 13/11/12 "LIX – Liquormarker zur Frühdiagnose und Krankheitsprogression bei Patienten mit Parkinson-syndromen und Motoneuronerkrankungen." The patients/participants provided their written informed consent to participate in this study.

AUTHOR CONTRIBUTIONS

MS and IZ designed the study and wrote the manuscript. SC performed the experiments. SC, MS, AV-P, and PH analyzed and interpreted the data. AV-P, KG, PL, PH, FM, and FL critically revised the manuscript. KG, FM, and DV provided the samples and the clinical data. All authors contributed to the article and approved the submitted version.

FUNDING

This study was supported by the Alzheimer Forschung Initiative (AFI) project 20026.

SUPPLEMENTARY MATERIAL

The Supplementary Material for this article can be found online at: https://www.frontiersin.org/articles/10.3389/fnagi.2021.717930/full#supplementary-material

Supplementary Figure 1 | Analysis of intra-assay variations of NfL in CSF. We chose different concentrations (high and low) to compare pairwise the NfL levels measured in duplicates on the same plate **(A)**. Statistical analysis revealed no significant (ns) between both measurements **(B)**, $p > 0.05$.

Supplementary Figure 2 | Analysis of a potential correlation between a-Syn levels and age. **(A–C)** In synucleinopathy patients and controls, we correlated aSyn levels and age. No correlation was detected between all groups. All correlation studies were computed by using the non-parametric Spearman's correlation test (two-tailed) in a CI of 95%. A $*p$-value < 0.05 was considered as significant and $p \geq 0.05$ as not significant.

REFERENCES

Abdo, W. F., Bloem, B. R., Van Geel, W. J., Esselink, R. A. J., and Verbeek, M. M. (2007). CSF neurofilament light chain and tau differentiate multiple system atrophy from Parkinson's disease. *Neurobiol. Aging* 28, 742–747. doi: 10.1016/j.neurobiolaging.2006.03.010

Cramm, M., Schmitz, M., Karch, A., Mitrova, E., Kuhn, F., Schroeder, B., et al. (2016). Stability and reproducibility underscore utility of RT-QuIC for diagnosis of Creutzfeldt-Jakob disease. *Mol. Neurobiol.* 53, 1896–1904. doi: 10.1007/s12035-015-9133-2

Cramm, M., Schmitz, M., Karch, A., Zafar, S., Varges, D., Mitrova, E., et al. (2015). Characteristic CSF prion seeding efficiency in humans with prion diseases. *Mol. Neurobiol.* 51, 396–405. doi: 10.1007/s12035-014-8709-6

De Rijk, M. C., Tzourio, C., Breteler, M. M. B., Dartigues, J. F., Amaducci, L., Lopez-Pousa, S., et al. (1997). Prevalence of parkinsonism and Parkinson's disease in Europe: the EUROPARKINSON collaborative study. *J. Neurol. Neurosurg. Psychiatry.* 62, 10–15. doi: 10.1136/jnnp.62.1.10

Eller, M., and Williams, D. R. (2011). α-Synuclein in Parkinson disease and other neurodegenerative disorders. *Clin. Chem. Lab. Med.* 49, 403–408. doi: 10.1515/CCLM.2011.077

Eng, L. F., Ghirnikar, R. S., and Lee, Y. L. (2000). Glial fibrillary acidic protein: GFAP-thirty-one years (1969-2000). *Neurochem. Res.* 25, 1439–1451. doi: 10.1023/a:1007677003387

Gilman, S., Low, P. A., Quinn, N., Albanese, A., Ben-Shlomo, Y., Fowler, C. J., et al. (1999). Consensus statement on the diagnosis of multiple system atrophy. *J. Neurol. Sci.* 163, 94–98. doi: 10.1016/S0022-510X(98)00304-9

Gilman, S., Wenning, G. K., Low, P. A., Brooks, D. J., Mathias, C. J., Trojanowski, J. Q., et al. (2008). Second consensus statement on the diagnosis of multiple system atrophy. *Neurology* 71, 670–676. doi: 10.1212/01.wnl.0000324625.00404.15

Hall, S., Öhrfelt, A., Constantinescu, R., Andreasson, U., Surova, Y., Bostrom, F., et al. (2012). Accuracy of a panel of 5 cerebrospinal fluid biomarkers in the differential diagnosis of patients with dementia and/or Parkinsonian disorders. *Arch. Neurol.* 69, 1445–1452. doi: 10.1001/archneurol.2012.1654

Holmberg, B., Rosengren, L., Karlsson, J. E., and Johnels, B. (1998). Increased cerebrospinal fluid levels of neurofilament protein in progressive supranuclear palsy and multiple-system atrophy compared with Parkinson's disease. *Mov. Disord.* 13, 70–77. doi: 10.1002/mds.870130116

Ishiki, A., Kamada, M., Kawamura, Y., Terao, C., Shimoda, F., Tomita, N., et al. (2016). Glial fibrillar acidic protein in the cerebrospinal fluid of Alzheimer's disease, dementia with Lewy bodies, and frontotemporal lobar degeneration. *J. Neurochem.* 136, 258–261. doi: 10.1111/jnc.13399

Kompoliti, K., and Metman, L. V. (2010). *Encyclopedia of Movement Disorders*. Cambridge, MA: Academic Press. doi: 10.1016/c2009-1-03732-0

Llorens, F., Hermann, P., Villar-Piqué, A., Diaz-Lucena, D., Nägga, K., Hansson, O., et al. (2020). Cerebrospinal fluid lipocalin 2 as a novel biomarker for the differential diagnosis of vascular dementia. *Nat. Commun.* 11:619. doi: 10.1038/s41467-020-14373-2

Llorens, F., Kruse, N., Schmitz, M., Gotzmann, N., Golanska, E., Thüne, K., et al. (2017). Evaluation of α-synuclein as a novel cerebrospinal fluid biomarker in different forms of prion diseases. *Alzheimers Dement.* 13, 710–719. doi: 10.1016/j.jalz.2016.09.013

Llorens, F., Schmitz, M., Varges, D., Kruse, N., Gotzmann, N., Gmitterová, K., et al. (2016). Cerebrospinal α-synuclein in α-synuclein aggregation disorders: tau/α-synuclein ratio as potential biomarker for dementia with Lewy bodies. *J. Neurol.* 263, 2271–2277. doi: 10.1007/s00415-016-8259-0

Magdalinou, N. K., Paterson, R. W., Schott, J. M., Fox, N. C., Mummery, C., Blennow, K., et al. (2015). A panel of nine cerebrospinal fluid biomarkers may identify patients with atypical parkinsonian syndromes. *J. Neurol. Neurosurg. Psychiatry* 86, 1240–1247. doi: 10.1136/jnnp-2014-309562

McKeith, I. G., Boeve, B. F., DIckson, D. W., Halliday, G., Taylor, J. P., Weintraub, D., et al. (2017). Diagnosis and management of dementia with Lewy bodies. *Neurology*. 89, 88–100. doi: 10.1212/WNL.0000000000004058

Mollenhauer, B., Locascio, J. J., Schulz-Schaeffer, W., Sixel-Döring, F., Trenkwalder, C., and Schlossmacher, M. G. (2011). α-synuclein and tau concentrations in cerebrospinal fluid of patients presenting with parkinsonism: a cohort study. *Lancet Neurol.* 10, 230–240. doi: 10.1016/S1474-4422(11)70014-X

Mondello, S., Constantinescu, R., Zetterberg, H., Andreasson, U., Holmberg, B., and Jeromin, A. (2014). CSF α-synuclein and UCH-L1 levels in Parkinson's disease and atypical parkinsonian disorders. *Park. Relat. Disord.* 20, 382–387. doi: 10.1016/j.parkreldis.2014.01.011

Petzold, A. (2005). Neurofilament phosphoforms: surrogate markers for axonal injury, degeneration and loss. *J. Neurol. Sci.* 233, 183–198. doi: 10.1016/j.jns.2005.03.015

Postuma, R. B., Berg, D., Stern, M., Poewe, W., Olanow, C. W., Oertel, W., et al. (2015). MDS clinical diagnostic criteria for Parkinson's disease. *Mov. Disord.* 30, 1591–1601.

Rissin, D. M., Kan, C. W., Campbell, T. G., Howes, S. C., Fournier, D. R., Song, L., et al. (2010). Single-molecule enzyme-linked immunosorbent assay detects serum proteins at subfemtomolar concentrations. *Nat. Biotechnol.* 28, 595–599. doi: 10.1038/nbt.1641

Savica, R., Grossardt, B. R., Bower, J. H., Ahlskog, J. E., and Rocca, W. A. (2013). Incidence and pathology of synucleinopathies and tauopathies related to parkinsonism. *JAMA Neurol.* 70, 859–866. doi: 10.1001/jamaneurol.2013.114

Schade, S., and Mollenhauer, B. (2014). Biomarkers in biological fluids for dementia with Lewy bodies. *Alzheimers Res. Ther.* 6:72. doi: 10.1186/s13195-014-0072-3

Schmitz, M., Cramm, M., Llorens, F., Müller-Cramm, D., Collins, S., Atarashi, R., et al. (2016a). The real-Time quaking-induced conversion assay for detection of human prion disease and study of other protein misfolding diseases. *Nat. Protoc.* 11, 2233–2242. doi: 10.1038/nprot.2016.120

Schmitz, M., Ebert, E., Stoeck, K., Karch, A., Collins, S., Calero, M., et al. (2016b). Validation of 14-3-3 protein as a marker in sporadic Creutzfeldt-Jakob disease diagnostic. *Mol. Neurobiol.* 53, 2189–2199. doi: 10.1007/s12035-015-9167-5

Schmitz, M., Villar-Piqué, A., Llorens, F., Gmitterová, K., Hermann, P., Varges, D., et al. (2019). Cerebrospinal fluid total and phosphorylated α-synuclein in patients with Creutzfeldt–Jakob disease and synucleinopathy. *Mol. Neurobiol.* 56, 3476–3483. doi: 10.1007/s12035-018-1313-4

Spillantini, M. G., Schmidt, M. L., Lee, V. M. Y., Trojanowski, J. Q., Jakes, R., and Goedert, M. (1997). α-synuclein in Lewy bodies [8]. *Nature* 388, 839–840. doi: 10.1038/42166

Wakabayashi, K., Yoshimoto, M., Tsuji, S., and Takahashi, H. (1998). α-synuclein immunoreactivity in glial cytoplasmic inclusions in multiple system atrophy. *Neurosci. Lett.* 249, 180–182. doi: 10.1016/S0304-3940(98)00407-8

Yang, Z., and Wang, K. K. W. (2015). Glial fibrillary acidic protein: from intermediate filament assembly and gliosis to neurobiomarker. *Trends Neurosci.* 38, 364–374. doi: 10.1016/j.tins.2015.04.003

Zerr, I., Villar-Piqué, A., Schmitz, V. E., Poleggi, A., Pocchiari, M., Sánchez-Valle, R., et al. (2019). Evaluation of human cerebrospinal fluid malate dehydrogenase 1 as a marker in genetic prion disease patients. *Biomolecules* 9:800. doi: 10.3390/biom9120800

Conflict of Interest: The authors declare that the research was conducted in the absence of any commercial or financial relationships that could be construed as a potential conflict of interest.

Publisher's Note: All claims expressed in this article are solely those of the authors and do not necessarily represent those of their affiliated organizations, or those of the publisher, the editors and the reviewers. Any product that may be evaluated in this article, or claim that may be made by its manufacturer, is not guaranteed or endorsed by the publisher.

Copyright © 2021 Canaslan, Schmitz, Villar-Piqué, Maass, Gmitterová, Varges, Lingor, Llorens, Hermann and Zerr. This is an open-access article distributed under the terms of the Creative Commons Attribution License (CC BY). The use, distribution or reproduction in other forums is permitted, provided the original author(s) and the copyright owner(s) are credited and that the original publication in this journal is cited, in accordance with accepted academic practice. No use, distribution or reproduction is permitted which does not comply with these terms.

frontiers in Aging Neuroscience

ORIGINAL RESEARCH
published: 29 September 2021
doi: 10.3389/fnagi.2021.623977

Alterations of Erythrocytic Phosphorylated Alpha-Synuclein in Different Subtypes and Stages of Parkinson's Disease

Xu-Ying Li[1,2], Wei Li[1], Xin Li[1], Xu-Ran Li[1], Linjuan Sun[3], Weiwei Yang[1], Yanning Cai[1], Zhigang Chen[4], Jun Wu[5], Chaodong Wang[2,6] and Shun Yu[1]**

[1] Department of Neurobiology, Xuanwu Hospital of Capital Medical University, Beijing, China, [2] Department of Neurology, Xuanwu Hospital of Capital Medical University, Beijing, China, [3] Department of Neurology, Xiyuan Hospital, China Academy of Chinese Medical Sciences, Beijing, China, [4] Department of Neurology, Dongfang Hospital of Beijing University of Chinese Medicine, Beijing, China, [5] Department of Neurology, Peking University Shenzhen Hospital, Guangdong, China, [6] National Clinical Research Center for Geriatric Diseases, Beijing, China

Serine 129-phosphorylated alpha-synuclein (pS-α-syn) is a major form of α-syn relevant to the pathogenesis of Parkinson's disease (PD), which has been recently detected in red blood cells (RBCs). However, alterations of RBC-derived pS-α-syn (pS-α-syn-RBC) in different subtypes and stages of PD remains to be investigated. In the present study, by using enzyme-linked immunosorbent assay (ELISA) to measure pS-α-syn-RBC, we demonstrated significantly higher levels of pS-α-syn-RBC in PD patients than in healthy controls. pS-α-syn-RBC separated the patients well from the controls, with a sensitivity of 93.39% (95% CI: 90.17–95.81%), a specificity of 93.11% (95% CI: 89.85–95.58%), and an area under the curve (AUC) of 0.96. Considering motor subtypes, the levels of pS-α-syn-RBC were significantly higher in late-onset than young-onset PD ($p = 0.013$) and in those with postural instability and gait difficulty than with tremor-dominant (TD) phenotype ($p = 0.029$). In addition, the levels of pS-α-syn-RBC were also different in non-motor subtypes, which were significantly lower in patients with cognitive impairment ($p = 0.012$) and olfactory loss ($p = 0.004$) than in those without such symptoms. Moreover, the levels of pS-α-syn-RBC in PD patients were positively correlated with disease duration and Hoehn & Yahr stages (H&Y) (p for trend =0.02 and <0.001) as well as UPDRS III ($R^2 = 0.031$, $p = 0.0042$) and MoCA scores ($R^2 = 0.048$, $p = 0.0004$). The results obtained suggest that pS-α-syn-RBC can be used as a potential biomarker for not only separating PD patients from healthy controls but also predicting the subtypes and stages of PD.

Keywords: Parkinson's disease, phosphorylation, α-synuclein, red blood cells, biomarker

OPEN ACCESS

Edited by:
Shaogang Qu,
Southern Medical University, China

Reviewed by:
Jifeng Guo,
Central South University, China
Weili Yang,
Jinan University, China

****Correspondence:***
Shun Yu
yushun103@hotmail.com
Chaodong Wang
cdongwang01@126.com

Received: *30 October 2020*
Accepted: *03 February 2021*
Published: *29 September 2021*

Citation:
Li X-Y, Li W, Li X, Li X-R, Sun L, Yang W, Cai Y, Chen Z, Wu J, Wang C and Yu S (2021) Alterations of Erythrocytic Phosphorylated Alpha-Synuclein in Different Subtypes and Stages of Parkinson's Disease. Front. Aging Neurosci. 13:623977. doi: 10.3389/fnagi.2021.623977

INTRODUCTION

Parkinson's disease (PD) is an age-related neurodegenerative disorder, characterized by akinesia/bradykinesia, rigidity, tremor, and postural instability (Sveinbjornsdottir, 2016). According to motor symptoms, PD can be classified into two major subtypes: tremor-dominant (TD) and postural instability and gait difficulty (PIGD) phenotypes (Stebbins et al., 2013). In addition, PD patients also manifest various non-motor symptoms such as constipation, hyposmia,

depression, sleep disorders, and cognitive impairment (Sveinbjornsdottir, 2016). The complexity and variability of the PD symptoms reflects the heterogeneity of its neuropathology between individual patients.

The most characteristic neuropathologic change in PD is the formation of proteinaceous inclusions, known as Lewy bodies (LBs) and Lewy neurites (LNs), which are mainly composed of aggregated alpha-synuclein (α-syn) (Spillantini et al., 1998), a small soluble protein normally enriched in pre-synaptic terminals (Cheng et al., 2011). The presence of α-syn aggregates in Lewy pathology indicates an implication of this protein in the etiology and pathogenesis of PD. The implication of α-syn in PD is further evidenced by genetic studies showing that point mutations and copy number variants in the SNCA gene encoding α-syn are associated with early-onset familial PD (Polymeropoulos et al., 1997; Ahn et al., 2008; Olgiati et al., 2015). According to Braak staging, Lewy pathology processes in a stereotypic, topographic manner in the nervous system. It starts probably in the enteric nervous system and/or olfactory bulb, and then spreads via prion-like propagation to the substantia nigra (SN) and further areas in the central nervous system (CNS), inducing either dysfunction or degeneration of the affected neurons and various motor and non-motor symptoms (Braak and Tredici, 2017; Rietdijk et al., 2017). In addition to continuous progression, the load and distribution of Lewy pathology are varied in different clinical subtypes of PD (Selikhova et al., 2009; Van de Berg et al., 2012).

The close implication of α-syn in the etiology and pathogenesis of PD makes it an ideal biomarker for PD diagnosis. Multiple sources and species of α-syn, including those from the brain, cerebrospinal fluid (CSF), blood, saliva, and the peripheral tissues, have been tested for their utility in diagnosing PD and other synucleinopathies, among which serine 129-phosphorylated α-syn (pS-α-syn) in CSF and plasma is mostly investigated (Atik et al., 2016; Fogue Fayyad et al., 2019; Parnetti et al., 2019), due to its close association with the pathogenesis of PD (Anderson et al., 2006; Oueslati, 2016). All these studies demonstrate an elevation of pS-α-syn in the CSF and plasma of PD patients. However, the diagnostic performance of CSF- and plasma-derived pS-α-syn is low (Foulds et al., 2011, 2013; Wang et al., 2012, 2018; Majbour et al., 2016; Cariulo et al., 2019), possibly due to the presence of interacting factors such as lipid proteins, heterophilic antibodies, and contaminations by platelets and hemolysis (Anderson et al., 2006; Ishii et al., 2015; Atik et al., 2016; Emamzadeh and Allsop, 2017; Fogue Fayyad et al., 2019; Parnetti et al., 2019). Since red blood cells (RBCs) contain a high concentration of α-syn (Barbour et al., 2008), some researchers have turned to study the utility of the RBC-derived α-syn as a PD biomarker. This detection can not only avoid the interfering factors encountered in detecting plasma-derived α-syn, but also could be more stable due to its high concentration. Previous studies have demonstrated positive results for the association between the RBC-derived α-syn and PD. For example, studies by Abd-Elhadi et al. and ourselves provided evidence showing an increase in the levels of RBC-derived total and oligomeric-α-syn with PD (Abd-Elhadi et al., 2015; Wang et al., 2015); some studies also showed elevations of some post-translationally modified (PTM) α-syn (pY125, pS129, nY39, AGE, and SUMO-1) (Vicente Miranda et al., 2017; Tian et al., 2019) and proteinase K-resistant α-syn (Abd-Elhadi et al., 2015; Tian et al., 2019) in the RBCs of PD patients. However, if alterations of pS-α-syn in the RBCs (pS-α-syn-RBC) are associated with the subtypes and stages of PD remains to be elucidated.

In this study, an enzyme-linked immunosorbent assay (ELISA) was used to measure pS-α-syn-RBC, and the associations of pS-α-syn-RBC alterations with various clinical variables, including subtypes, age at onset (AAO), disease duration, Hoehn & Yahr (H&Y) stages, and UPDRS III (Unified Parkinson's disease Rating Scale III) scores were analyzed.

MATERIALS AND METHODS

Study Design and Participants

The PD patients in the study were recruited from Xuanwu Hospital of Capital Medical University, Dongfang Hospital of Beijing University of Chinese Medicine, and Peking University Shenzhen Hospital, from June 2018 to July 2020. During the same period, the healthy control subjects were enrolled from the Physical Examination Centers of Xuanwu Hospital and Xiyuan Hospital, China Academy of Chinese Medical Sciences. Clinical data of both PD patients and healthy controls were first reviewed by investigators from each hospital, and re-evaluated by two senior movement disorder specialists, specifically for the project. All patients were diagnosed based on the MDS clinical diagnostic criteria for PD released in 2015 (Postuma et al., 2015). *De novo* PD patients were identified using the following criteria: (i) disease duration <2 years; (ii) no history of present or past therapy with anti-parkinsonian agents (Mollenhauer et al., 2016). Patients with the following conditions were excluded: (i) Parkinsonian syndromes resulting from cerebrovascular, hypoxic, traumatic, infectious, metabolic, or systemic diseases affecting the CNS; (ii) Parkinson's plus syndromes, including multiple system atrophy (MSA), dementia with Lewy bodies (DLB), progressive supranuclear palsy (PSP), and corticobasal degeneration (CBD); (iii) ambiguous diagnosis due to uncertain clinical or imaging features; (iv) a first degree relative with PD. The control subjects were enrolled fulfilling the following criteria: (1) no motor symptoms (tremor, bradykinesia, restless legs); (2) no history and symptoms of functional constipation and rapid eye movement behavioral disorder (RBD), and less than two other non-motor symptoms, including cognitive decline, olfactory loss, depression, anxiety, according to the cut-off values of each scale for such symptoms; (3) no history and symptoms of stroke, dementia, hypoxia-related disorders (epilepsy, COPD, asthma, etc.); (4) no history and symptoms of blood diseases (anemia, erythremia, etc.). Case and control subjects were matched for age and gender. Participants with incomplete or missing demographic and clinical information were excluded from the study.

The study was approved by the Institutional Review Board and Ethics Committees of the participating hospitals. Written informed consent was obtained from each participant or their legal guardians before inclusion in the study.

Clinical Assessment and Subtype

All subjects were comprehensively assessed for demographic information and clinical characteristics by the site investigators. The quantitative severity of motor and non-motor symptoms (including cognitive impairment, olfactory loss, sleep, and neuro-psychiatric disturbances) was assessed using scales for each symptom (additional information was given in **Supplementary Methods**). Movement Disorder Society-sponsored revision of the Unified Parkinson's Disease Rating Scale (MDS-UPDRS) Part III score and H&Y stage were used to assess the severity of motor symptoms. The levodopa equivalent daily dose (LEDD) was calculated as previously described (Rabinak and Nirenberg, 2010). The PD patients were classified into distinct clinical subtypes using cut-offs on the (AAO), and the scores for motor and non-motor symptoms, as described before (Jankovic et al., 1990). Motor subtypes of PD were classified as the TD, PIGD, or mixed (MIX) phenotype, according to the ratio of mean tremor score/mean PIGD score in MDS-UPDRS. Non-motor subtypes were defined by the existence of cognitive impairment, neuropsychiatric symptoms, sleep disorders and olfactory decline, according to cut-off points on the scores quantifying these symptoms: Mini-mental State Examination (MMSE) and Montreal Cognitive Assessment (MoCA) for cognitive impairment, Hyposmia Rating Scale (AHRS) for olfactory loss, Rapid Eye Movement (REM) Sleep Behavior Disorder Questionnaire-Hong Kong (RBDQ-HK) for RBD, Hamilton Depression Scale (HAMD) for depression, and Hamilton Anxiety Scale (HAMA) for anxiety.

Preparation of RBC Samples

At the time of recruitment, whole blood samples (8 ml) were drawn into EDTA anti-coagulant tubes (1.8 mg per milliliter of blood) from the peripheral vein, let stand for 30 min in a vaccine carrier with ice packs (4–8°C), and then centrifuged at 4°C, 1,500 g for 15 min. The upper and middle layers, containing plasma, and white blood cells, were removed and stored for other uses, and the lower layer, containing RBCs, was washed with Hank's balanced salt solution [HBSS without Ca^{2+} and Mg^{2+}, 137.93 mM NaCl, 5.33 mM KCl, 0.34 mM Na_2HPO_4, 0.44 mM KH_2PO_4, 4.17 mM $NaHCO_3$, 5.56 mM D-Glucose (Dextrose), pH 7.2–7.4] for three times. Finally, the isolated RBC samples were collected, aliquoted, and preserved in a freezer (−80°C), and quality-checked every 3 months using fresh samples as the control. Protein concentrations were determined with a bicinchoninic acid (BCA) protein assay kit (Pierce Biotechnology, Rockford, IL, USA) before the assay.

Western Blot Analysis

Purified wild type α-syn and pS-α-syn proteins were separated by 12.5% sodium dodecyl sulfate-polyacrylamide gel electrophoresis (SDS-PAGE), transferred onto polyvinylidene fluoride (PVDF) membranes (Millipore Corp., Bedford, MA, USA), and blocked for 1 h with 5% non-fat milk in Tris-buffered saline containing 0.05% Tween-20 (TBST). The membranes were probed with either rabbit polyclonal anti-p-α-syn (Ser 129) (sc-135638, Santa Cruz Biotechnology, Santa Cruz, CA, USA) (1:5,000) or 3D5 mouse monoclonal anti-human α-syn antibody (RRID: AB_2315787) (1:10,000) (Yu et al., 2007; Vaccaro et al., 2015). After washing with TBST, the membranes were incubated with horseradish peroxidase-conjugated goat anti-rabbit or goat anti-mouse IgG (1:5,000; Vector Laboratories, Burlingame, CA, USA). Immunoreactive bands were visualized by enhanced chemiluminescence, and measured for densitometry with a Versadoc XL imaging apparatus (Bio-Rad). All experiments were conducted in triplicate. To rule out the possibility for the cross-reaction of the anti-pS-α-syn antibody with other proteins, the RBC lysates were first incubated at 4°C overnight with different concentrations of the 3D5 antibody and pS-α-syn antibody (Santa) conjugated to Protein A Sepharose 4B Fast Flow (P9424, Sigma-Aldrich, St. Louis, MO, USA) separately to pre-absorb the endogenous α-syn. Then, the protein A-antibody-α-syn/pS-α-syn complexes were precipitated, and the supernatants were subjected for Western blotting using a different anti-pS-α-syn antibody (Wako). All experiments were conducted in triplicates.

Enzyme-Linked Immunosorbent Assay

To establish the ELISA for measuring pS-α-syn concentrations, recombinant human wild type α-syn (WT-α-syn) and pS-α-syn were produced and purified (detailed in **Supplementary Methods**). The calibration curves were constructed using a series of concentrations of WT-α-syn and pS-α-syn. The assay used an anti-pS-α-syn as the capture and the biotinylated anti-WT-α-syn as the detection antibodies. Correlations between the standardized protein concentrations and the absorbances at 405 nm were analyzed. The lower limit of detection (LLOD) was calculated as the mean absorbance of 20 replicate readings of blank samples (buffer only) plus three standard deviations (SD) (Mathiesen et al., 2018). In addition, the lower limit of quantification (LLOQ) was calculated from the mean absorbance of 24 replicate readings of blank samples plus 10 SD. The accuracy of the assay and reproducibility in the sample matrix were assessed by spike-and-recovery and linearity-of-dilution assessments (detailed in **Supplementary Methods**). Quality control (QC) samples were used in each tested plate. Intra- and inter-test variations of tested and QC samples were expressed by the coefficient of variation (CVs) and calculated as follows: standard deviation/average concentration × 100% (Li et al., 2020).

For measuring pS-α-syn-RBC concentrations, a 96-well ELISA plate was coated with 100 μL/well of the non-biotinylated anti-pS-α-syn antibody (sc-135638, Santa Cruz Biotechnology, Santa Cruz, CA, USA) in coating buffer (0.1 μg/mL), and incubated overnight at 4°C (Liu et al., 2015). After washing with PBS containing 0.05% Tween-20 (PBST) and blocked with 10% BSA in PBST at 37°C for 2 h, 100 μl of RBC samples were added to each well and incubated at 37°C for 2 h. After washes with PBST, 100 μl/well of biotinylated 3D5 antibody (1 μg/mL) in blocking buffer was added. Plates were incubated for 2 h at 37°C. The wells were washed four times with PBST and incubated for 1 h with 100 μl of ExtrAvidin Alkaline Phosphatase (E-2636, Sigma-Aldrich, St. Louis, MO, USA) diluted 1:5,000

in blocking buffer. Following four washes with PBST, 100 μl of enzyme substrate p-nitrophenyl phosphate (pNPP, N1891, Sigma-Aldrich) was added per well, after which the absorbance was read at 405 nm using a Multiskan MK3 microplate reader (Thermo Scientific, UT, USA). All the samples were assayed blinded to the diagnosis and tested in triplicate within the same assay and on the same day.

Statistical Analysis

Demographic, clinical characteristics, and α-syn data were compared between groups according to the normality of their distributions. Analyses of variance (ANOVA), followed by *post-hoc* tests, was used for normally distributed data (age, AAO, etc.), and the Kruskal-Wallis test was used for skewed data (disease duration, LEDD, pS-α-syn-RBC levels, etc.) to compare differences among all the studied groups. The Chi-squared or Fisher's exact tests were performed to compare the distribution of categorical variables across groups.

Correlations of clinical variables (e.g., AAO, UPDRS III, MMSE, and MoCA scores) with pS-α-syn-RBC concentrations were examined by uni and multivariate linear regression models, with adjustment for confounding factors (e.g., age, sex, and AAO). Logistic regression models were used to analyze the correlation between the biomarker and PD. Receiver operating characteristic (ROC) curves were constructed and the area under the curve (AUC) was calculated to evaluate the performance of the models. A one-degree-freedom linear term was used for trend analysis of pS-α-syn-RBC alterations across intervals of disease duration and H&Y stages. All statistical analyses were performed using IBM SPSS Statistics® v22.0.0.0 (SPSS Inc., Chicago, IL, 2013), Medcalc (Microsoft), and GraphPad Prism® v6.0 (GraphPad Software Inc., La Jolla, CA, 2009), and P-values < 0.05 were regarded as statistically significant.

TABLE 1 | Demographic data of the study subjects.

Variable	Control	PD
Number	334	333
Sex (male/female)	174/160	192/141
Age	60.76 ± 10.99	60.37 ± 10.35
Age at onset	NA	55.28 ± 11.78
Education, years	–	9.95 ± 4.82
HandY stage	NA	2 (2, 3)
UPDRS III	NA	26.33 ± 12.70
Disease duration, years		
All	NA	5.03 ± 4.48
0–2	NA	1.44 ± 0.58
3–5	NA	3.68 ± 0.99
6–10	NA	7.77 ± 1.71
≥70	NA	13.78 ± 5.86
Medication		
Levodopa treatment, *n* (%)	NA	203 (60.96%)
LEDD, mg/day	NA	367.74 ± 382.04
Severity of non-motor signs		
MoCA scores	–	23.45 ± 4.28 ($n = 250$)
MMSE scores	–	26.26 ± 3.46 ($n = 201$)
RBDQ-HK scores	–	21.21 ± 18.02 ($n = 204$)
AHRS scores	–	20.41 ± 6.40 ($n = 195$)
HAMD scores	–	10.25 ± 6.58 ($n = 184$)
HAMA scores	–	9.85 ± 5.76 ($n = 226$)

All data are presented as Mean ± S.D. PD, Parkinson's disease; MSA, Multiple system atrophy; LEDD, Levodopa equivalent daily dose; UPDRS III, Unified Parkinson's Disease Rating Scale part III (motor) score; HandY stage, Hoehn and Yahr stage; MoCA, Montreal Cognitive Assessment; MMSE, Mini-Mental State Examination; RBDQ-HK, Rapid eye movement (REM) sleep behavior disorder questionnaire-Hong Kong; HAMD, Hamilton Depression Scale; HAMA, Hamilton Anxiety Scale; Definition of abnormal: for cognitive decline, MoCA score cut-offs of 17 (illiteracy), 20 (primary school education), 23 (secondary school education) of 30 points; for RBD, a cut-off of 19 on the RBDQ-HK score; for olfactory loss, a cut-off of 22 on the AHRS score; for depression, a cut-off of 8 on the HAMD score; for anxiety, a cut-off of 7 on the HAMA score. NA, not applicable; –, not available.

RESULTS

Between June 2018 and July 2020, 464 potentially eligible patients were recruited with consent. After clinical and neuroimaging re-evaluation and assurance of blood sample quality, our final analysis included 333 patients and 334 healthy controls. All PD patients were subjected to diagnosing, subtyping and staging analyses. Patients with missing scores for some non-motor symptoms were excluded from the latter analyses (**Supplementary Image 1**).

Demographic and clinical data for all participants are shown in **Table 1**. The AAO of the PD patients was 55.8 ± 11.78 years, and the disease duration was 5.03 ± 4.48 years. Most of the PD patients (90.99%) were in H&Y stages 1–3.

The specificity, accuracy, and reproducibility of the ELISA were evaluated using multiple assessments. As shown in our previous study (Li et al., 2020), after production and purification, Coomassie brilliant blue (CBB) staining confirmed a high purity of both the recombinant WT-α-syn and pS-α-syn proteins. In western blotting, the 3D5 anti-α-syn antibody specifically detected WT-α-syn (17 kDa). In contrast, the anti-pS-α-syn antibody did not bind WT-α-syn, but bound purified pS-α-syn (55 kDa) in a concentration-dependent manner. In the detection of RBC lysates using western blot, the anti-pS-α-syn antibody revealed several bands, including three major bands ranging from above 55 to 130 kDa and a very weak band at around 28 kDa. The three major bands were absorbed by pre-incubation of the lysates with overdose of the 3D5 anti-α-syn (Li et al., 2020) and pS-α-syn antibody (**Supplementary Image 2**) with the 28 kDa weak band remained unaffected, indicating that the pS-α-syn antibody mainly detects the pS-α-syn, which was in an aggregated form. Sine hemoglobin has peroxidase activity, the 28 kDa band may be the hemoglobin dimer, as revealed by the electrochemiluminescence (ECL) reaction (Abd-Elhadi et al., 2015). In the ELISA, the absorbances measured at 405 nm were positively correlated with the standardized pS-α-syn concentrations, with an R^2-value of 0.995 (Li et al., 2020). Further, using the blank samples, the LLOD and LLOQ of the assay were determined to be 0.18 and 0.60 μg/ml,

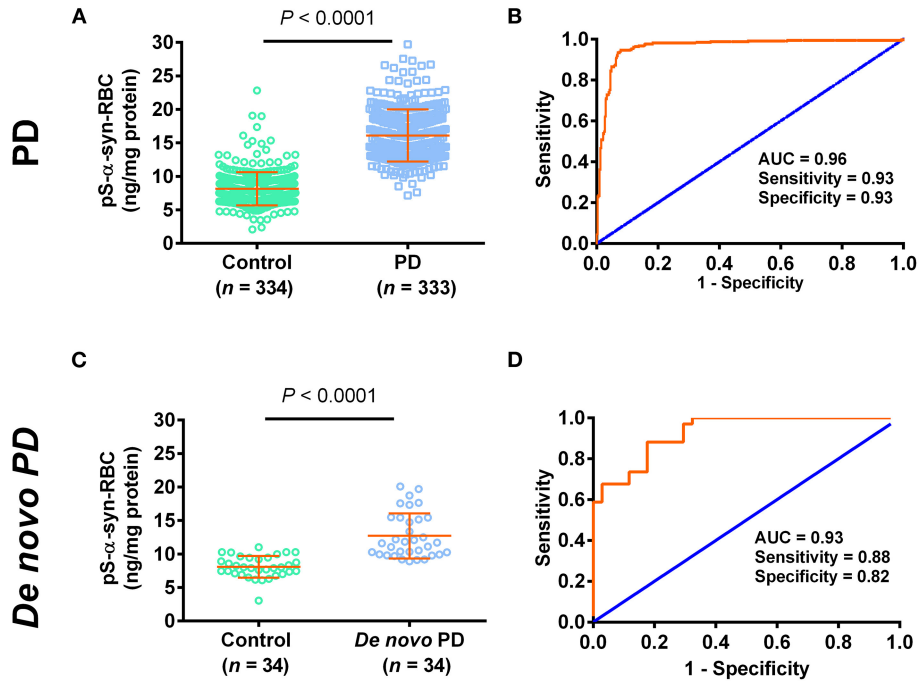


FIGURE 1 | Performance of pS-α-syn-RBC in diagnosing Parkinson's disease. **(A,C)** Concentrations of pS-α-syn-RBC in Parkinson's disease (PD) vs. controls in the PD (PD: 333, control: 334) and *de novo* (PD: 34, control: 34) study. **(B,D)** Receiver operating characteristic (ROC) curves for the diagnosis of PD in the PD and *de novo* PD study.

respectively. Spike-and-recovery assessment showed that the recovery rates of pS-α-syn in RBC lysates at low, median, and high spike levels were 87.7, 90.7, and 95.9%, respectively (**Supplementary Tables 1–4**).

We then used the ELISA to measure the levels of pS-α-syn-RBC. We showed that the levels of pS-α-syn-RBC were significantly higher in PD patients (14.17 ± 3.58 ng/mg) than in controls (7.22 ± 2.19 ng/mg; $p < 0.0001$). pS-α-syn-RBC separated the PD patients well from the controls, with a sensitivity of 93.39% (95% CI: 90.17–95.81%), a specificity of 93.11% (95% CI: 89.85–95.58%), and an AUC of 0.96 (**Figures 1A,B**). In a sub-analysis, pS-α-syn-RBC levels in the *de novo* PD patients ($n = 34$; 12.70 ± 3.36 ng/mg) were significantly higher than the age- and sex-matched controls ($n = 34$; 8.10 ± 1.62 ng/mg; $p < 0.0001$) (**Figures 1C,D**).

Multivariate linear regression analysis, adjusting for age, sex, and disease duration, showed that pS-α-syn-RBC levels in the PD patients were positively correlated with UPDRS III scores ($R^2 = 0.031$, $p = 0.0042$) and MoCA scores ($R^2 = 0.048$, $p = 0.0004$), but not with RBDQ-HK, AHRS, HAMD, or HAMA scores ($p > 0.05$, **Figure 2**). Considering the motor subtypes, the pS-α-syn-RBC levels were significantly higher in late-onset PD (LOPD) ($n = 288$; 14.57 ± 4.92 ng/mg) than in young-onset PD (YOPD) ($n = 45$; 14.06 ± 4.82 ng/mg; $p = 0.013$) as well as in patients with the PIGD ($n = 103$; 14.90 ± 5.79 ng/mg) than with the TD subtypes ($n = 50$; 13.05 ± 2.64 ng/mg; $p = 0.029$; **Table 2**). With respect to the non-motor subtypes, the pS-α-syn-RBC levels in patients with cognitive impairment and olfactory loss were significantly lower than those without such symptoms ($p = 0.012$ and 0.004, respectively; adjusting for age, sex, LEDD, and disease duration; **Table 3** and **Supplementary Table 5**). Moreover, the discrepancies in the level of pS-α-syn-RBC between motor and non-motor subtypes were associated with the AAO. Significant difference between the TD and PIGD subtypes was only observed in patients with the AAO <50 years ($p = 0.021$, adjusting for age, sex, disease duration, and LEDD), while between the cognitively normal and impaired PD patients was only found among those with the AAO between 60 and 69 years ($p = 0.004$; **Tables 2**, **3**; **Supplementary Image 3**).

Regarding the association of pS-α-syn-RBC with disease duration and H&Y stage of PD, pS-α-syn-RBC levels were progressively elevated with increasing disease duration (13.11 ± 4.21 ng/mg for 0–2 years; 13.10 ± 4.37 ng/mg for 3–5 years; 13.68 ± 5.03 ng/mg for 6–10 years, and 15.58 ± 4.97 ng/mg for >10 years; p for trend =0.020; **Figure 3A**) and advancing H&Y stages (11.44 ± 3.36 for stage 1, 13.16 ± 4.03 for stage 2, 14.09 ± 4.95 for stage 3, 16.40 ± 6.76 for stage 4–5; p for trend <0.001; **Figure 3E**). Concerning the motor subtypes, we found that higher pS-α-syn-RBC levels were associated with advancing H&Y stages in PIGD-PD ($p < 0.001$; **Figure 3G**) and increasing disease duration in MIX-PD patients ($p = 0.016$; **Figure 3D**), but not in TD-PD ($p > 0.05$; **Figures 3B,F**). With respect to the non-motor subtypes, pS-α-syn-RBC levels decreased with increasing disease duration in

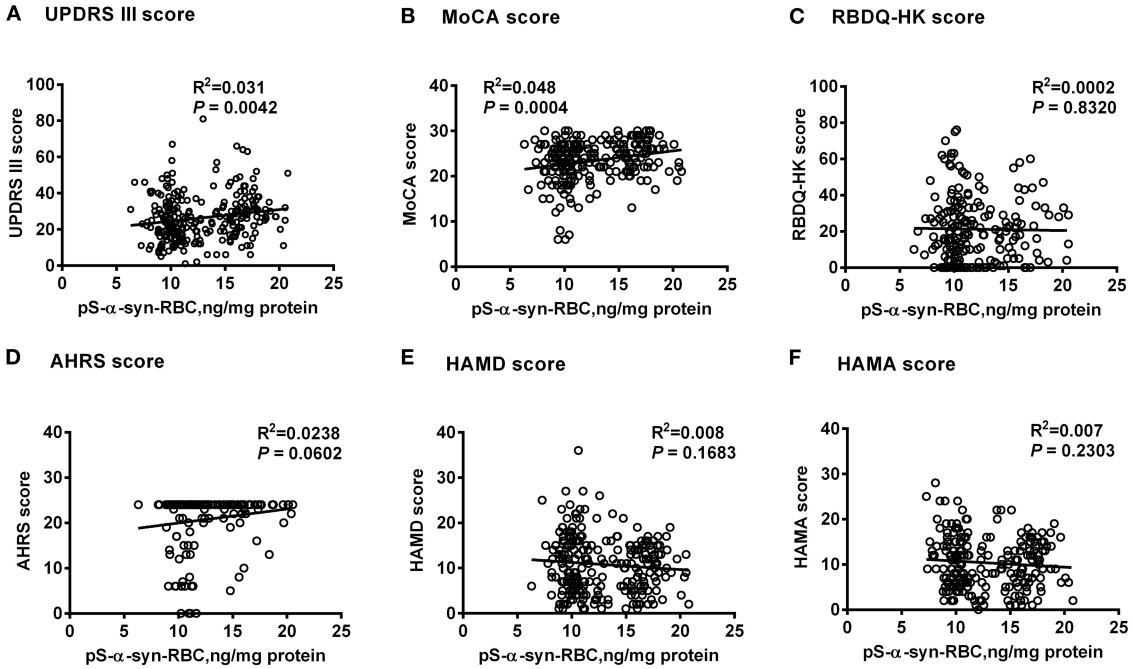


FIGURE 2 | Correlations between pS-α-syn-RBC and scores for motor and non-motor symptoms of Parkinson's disease. Correlations between pS-α-syn-RBC levels and scores for motor and non-motor symptoms were investigated using multivariate linear regression model adjusting age, sex, and disease duration. pS-α-syn-RBC, phosphorylated α-syn in red blood cells; **(A)** UPDRS III, Unified Parkinson's disease Rating Scale part III (motor); **(B)** MoCA, Montreal Cognitive Assessment; **(C)** RBDQ-HK, Rapid eye movement (REM) sleep behavior disorder questionnaire-Hong Kong; **(D)** AHRS, Hyposmia rating scale; **(E)** HAMD, Hamilton Depression Scale; **(F)** HAMA, Hamilton Anxiety Scale.

patients with cognitive impairment (p for trend =0.013), but not with other symptoms (RBD, olfactory dysfunction, depression, or anxiety; **Figure 4**).

DISCUSSION

The ELISA assay used for measuring pS-α-syn-RBC levels was established previously and has been applied to detect pS-α-syn in monkey brains (Liu et al., 2015) and pS-α-syn formed in PD plasma (Wang et al., 2016). The detection antibody was 3D5 mouse monoclonal anti-α-syn, which recognizes a sequence of 115–121 amino acids specific to human α-syn (Yu et al., 2007) and has been well-characterized previously for its specificity in detecting α-syn in human RBCs (Wang et al., 2015). The capture antibody was a rabbit polyclonal anti-pS-α-syn. The specificity of this anti-pS-α-syn in detecting pS-α-syn in human RBCs was confirmed by immunodepletion experiments, in which the immunoreactive signals revealed by this antibody in RBC lysates were disappeared by pre-incubating the lysates with the 3D5 anti-α-syn antibody and a different anti-pS-α-syn antibody. In order to further characterize our ELISA assay, we performed the spike-and-recovery and linearity-of-dilution assessments as well as LLOD and LLOQ analyses. The results, together with those from the immunodepletion experiments, suggested an enough sensitivity, specificity, accuracy, and reproducibility of this assay in detecting pS-α-syn in human RBCs.

As blood samples are more accessible and less invasive to obtain, detection of blood-derived α-syn as a biomarker is clinically preferable. Most previous studies have focused on detecting α-syn in blood plasma, which have yielded inconsistent results. Increased (Lee et al., 2006; Duran et al., 2010; Lin et al., 2018), decreased (Li et al., 2007; Ishii et al., 2015), and unchanged (Shi et al., 2010; Foulds et al., 2011; Goldman et al., 2018) levels of total plasma α-syn have been reported in PD patients. Although oligomeric α-syn and pS-α-syn levels in PD plasma tended to increase, their diagnostic values were low (Atik et al., 2016; Fogue Fayyad et al., 2019; Parnetti et al., 2019). The inconsistency and low diagnostic power in detecting plasma α-syn have been attributed to the presence of various interfering factors in the plasma such as lipoproteins, heterophilic antibodies, and contaminations by platelets and hemolysis (Anderson et al., 2006; Ishii et al., 2015; Atik et al., 2016; Emamzadeh and Allsop, 2017; Fogue Fayyad et al., 2019; Parnetti et al., 2019). Because RBCs contain abundant α-syn and the detection of RBC α-syn can avoid the interference encountered in the detection of plasma α-syn, it is believed that the RBC α-syn can be used as an alternative potential biomarker predicting the neuropathological changes of PD. Our present results showed that the levels of pS-α-syn-RBC were significantly higher in the PD patients than in the healthy controls. When this biomarker was used to diagnose PD, it produced a 93.39% sensitivity and a 93.11% specificity, with an AUC as high as 0.96. These values are much better than any reported values obtained in detecting plasma α-syn as

TABLE 2 | Overall and clinical variable-stratified comparisons of pS-a-syn-RBC levels between motor subtypes of Parkinson's disease.

Scale	All PD (n = 333)	TD (n = 50)	PIGD (n = 103)	MIX (n = 180)	p (TD vs. PIGD)	p (PIGD vs. MIX)	p (TD vs. MIX)
Sex (male/female)	192/141	20/30	64/39	108/72	**0.015**	0.800	**0.015**
Age	60.37 ± 10.35	62.54 ± 11.06	59.48 ± 10.63	60.13 ± 10.73	0.099	0.627	0.162
Age at onset	55.28 ± 11.78	58.13 ± 11.20	54.88 ± 11.34	53.69 ± 14.36	0.149	0.461	**0.034**
Disease duration, y	5.03 ± 4.48	4.42 ± 3.91	4.60 ± 3.24	5.06 ± 4.68	0.798	0.369	0.332
LEDD, mg/day	367.74 ± 382.04	318.03 ± 374.02	397.64 ± 373.56	371.85 ± 388.92	0.369	0.970	0.356
H and Y stage	2 (2, 3)	2 (2, 3)	2 (2, 3)	2 (1, 3)	0.833	0.628	0.339
pS-α-syn-RBC levels (raw data, μg/ml)	2.31 ± 0.70	2.19 ± 0.43	2.68 ± 1.11	2.21 ± 0.51	**0.001**	**<0.001**	0.855
pS-α-syn-RBC levels (normalized, μg/mg)	14.17 ± 3.58	13.05 ± 2.64	14.90 ± 5.79	14.56 ± 4.77	**0.029**	0.573	0.055
pS-α-syn-RBC levels in patients stratified by age at ONSET, ng/mg[a]							
<50	14.06 ± 4.82	11.47 ± 1.75	14.25 ± 5.75	14.40 ± 4.49	**0.021**	0.888	**0.017**
≥50	14.57 ± 4.92	12.18 ± 2.45	14.89 ± 5.79	14.56 ± 4.77	0.101	0.551	0.191
50–59	14.75 ± 5.44	12.33 ± 2.48	16.48 ± 7.07	14.14 ± 4.84	0.087	0.073	0.669
60–69	14.70 ± 4.53	12.21 ± 2.81	13.68 ± 3.75	15.60 ± 5.07	0.894	0.104	0.149
≥70	13.65 ± 4.21	11.76 ± 1.55	15.07 ± 5.56	12.99 ± 3.89	0.311	0.181	0.959
pS-α-syn-RBC levels in patients stratified by disease duration, ng/mg[b]							
0–2	13.11 ± 4.21	12.61 ± 2.72	13.74 ± 4.58	12.73 ± 4.44	0.588	0.557	0.929
3–5	13.10 ± 4.37	11.92 ± 2.38	13.91 ± 5.51	13.06 ± 3.95	0.176	0.380	0.431
5–10	13.68 ± 5.03	11.06 ± 0.96	13.48 ± 5.83	14.57 ± 4.88	0.411	0.259	0.092
>10	15.58 ± 4.97	12.30 ± 2.46	17.42 ± 6.68	15.68 ± 4.54	0.146	0.120	0.637
pS-α-syn-RBC levels in patients stratified by HandY STAGES, ng/mg[c]							
1	11.44 ± 3.36	10.90 ± 0.92	10.96 ± 3.27	11.84 ± 3.88	0.858	0.647	0.551
2	13.16 ± 4.03	12.01 ± 2.33	12.97 ± 4.39	13.81 ± 4.19	0.508	0.284	0.126
3	14.09 ± 4.95	12.56 ± 2.76	15.01 ± 5.73	14.01 ± 4.86	0.091	0.319	0.256
4–5	16.40 ± 6.76	12.21 ± 2.81	20.87 ± 7.84	15.39 ± 5.25	0.106	**0.050**	0.307

[a,b,c]Covariance analysis adjusting for sex, age, LEDD and disease duration; Bold: p < 0.05. YOPD, Young onset Parkinson's disease; LOPD, Late onset Parkinson's disease; TD, Tremor-dominant subtype; PIGD, postural instability and gait difficulty subtype.

well as other species of the RBC α-syn, including total α-syn, oligomeric α-syn, proteinase K-resistant α-syn, and some other PTMs (Glycation, SUMO-1, pY125, and nY39) (Abd-Elhadi et al., 2015; Vicente Miranda et al., 2017; Tian et al., 2019). The high performance of pS-α-syn-RBC in PD diagnosis can be explained not only by the high concentration of pS-α-syn in the RBCs and the lack of the interfering factors existent in the plasma, but also by the close relevance of pS-α-syn to the neuropathology of PD. Our results for the elevation of pS-α-syn-RBC in PD patients is supported by a recently published paper, which showed that erythrocytic pS-α-syn levels in PD patients were increased by more than nine times in comparison to the control values, although the AUC was only 0.71, possibly due to the higher degree of overlap of the measured pS-α-syn values between PD and controls (Tian et al., 2019).

Previous studies have shown that the neuropathological progression and total α-syn levels in plasma and CSF are different between PD subtypes (Selikhova et al., 2009; Van de Berg et al., 2012; Ding et al., 2017; Goldman et al., 2018). Since the levels of pS-α-syn-RBC were significantly increased in PD patients, we questioned if alterations of pS-α-syn-RBC are also different between PD subtypes. We showed that the levels of pS-α-syn-RBC were higher in the PIGD than in the TD subtypes. This discrepancy is in agreement with previous observations that patients with the PIGD subtype have more severe motor disorders, more rapid progression, and more frequent non-motor symptoms than patients with the TD subtype (Jankovic et al., 1990; Van der Heeden et al., 2016; Wu et al., 2016), suggesting a role of pS-α-syn in the motor phenotype and severity of PD. However, how pS-α-syn in the RBCs is correlated with that in the CNS is unclear. Evidence has accumulated that α-syn can be secreted from neuronal cells possibly by exocytosis and transported across the blood-brain barrier (BBB) bi-directionally, blood-to-brain and brain-to-blood. Therefore, it is possible that the brain-derived pS-α-syn can be released into the plasma, where it is further taken up by the RBCs in an unknown mechanism (Matsumoto et al., 2017).

Although PD patients with cognitive impairment have more severe neocortical Lewy body scores and higher plasma α-syn levels than those without cognitive impairment (Selikhova et al., 2009; Van de Berg et al., 2012; Ding et al., 2017; Goldman

TABLE 3 | Overall and clinical variable-stratified comparisons of pS-a-syn-RBC levels between non-motor subtypes of Parkinson's disease.

Scale	Cognitive decline			RBD			Olfactory loss		
	No (n = 184)	Yes (n = 66)	p-value	No (n = 104)	Yes (n = 100)	p-value	No (n = 139)	Yes (n = 56)	p-value
Sex (male/female)	108/76	30/36	–	99/45	45/55	–	74/65	25/31	–
Age	59.22 ± 10.68	64.12 ± 8.55	–	60.28 ± 11.03	63.41 ± 8.41	–	60.91 ± 10.43	63.36 ± 8.56	–
Age at onset	55.10 ± 11.99	58.75 ± 10.77	–	52.06 ± 18.20	58.41 ± 10.03	–	56.06 ± 12.63	57.78 ± 10.13	–
Disease duration, y	4.73 ± 4.12	4.85 ± 4.82	0.969	4.80 ± 4.52	5.08 ± 4.43	0.180	4.46 ± 4.23	5.66 ± 4.58	0.325
LEDD, mg/day	425.51 ± 424.51	377.12 ± 379.36	0.334	365.84 ± 415.33	394.71 ± 345.73	0.456	360.41 ± 399.05	393.31 ± 319.44	0.612
HandY stage	2 (2, 3)	2 (2, 3)	–	2 (2, 3)	2 (2, 3)	–	2 (2, 3)	2 (2, 3)	–
pS-α-syn-RBC	12.91 ± 3.43	11.64 ± 3.10	**0.012**	11.96 ± 3.23	11.42 ± 2.96	0.101	12.02 ± 3.18	10.74 ± 2.37	**0.004**
pS-α-syn-RBC levels in patients stratified by age AT ONSET, ng/mg[a]									
<50	12.58 ± 3.52	12.63 ± 3.07	0.844	11.09 ± 2.32	11.65 ± 3.26	0.866	11.01 ± 2.58	10.56 ± 2.31	0.660
50–59	12.81 ± 3.40	11.16 ± 2.80	0.095	11.59 ± 2.95	11.50 ± 2.96	0.980	12.06 ± 3.15	11.20 ± 2.31	0.288
60–69	13.18 ± 3.45	10.86 ± 2.52	**0.004**	12.04 ± 2.88	12.46 ± 3.31	0.907	12.73 ± 3.43	11.53 ± 2.16	0.477
≥70	11.55 ± 3.14	12.39 ± 4.01	0.137	12.42 ± 3.87	11.43 ± 2.92	0.347	11.66 ± 3.30	10.53 ± 4.11	0.249
pS-α-syn-RBC levels in patients stratified by disease duration, ng/mg[b]									
0–2	12.62 ± 3.56	12.72 ± 3.54	0.973	11.77 ± 3.18	12.36 ± 3.53	0.414	12.63 ± 3.46	11.43 ± 2.89	0.281
3–5	12.87 ± 3.56	11.74 ± 2.75	0.565	11.92 ± 3.06	11.54 ± 2.86	0.199	12.15 ± 3.20	11.05 ± 2.20	0.121
5–10	12.77 ± 3.13	10.38 ± 2.48	**0.038**	11.18 ± 2.36	11.27 ± 2.58	0.997	10.89 ± 2.64	10.30 ± 1.88	0.949
>10	14.40 ± 2.95	10.42 ± 2.79	**0.038**	11.16 ± 1.89	13.00 ± 3.66	0.130	11.10 ± 1.84	14.16 ± 2.29	0.137
pS-α-syn-RBC levels in patients stratified by HandY stages, ng/mg[c]									
1	12.61 ± 3.17	11.62 ± 3.13	0.244	11.62 ± 3.28	12.15 ± 3.76	0.935	12.26 ± 3.51	11.74 ± 2.91	0.690
2	13.34 ± 3.15	11.66 ± 3.15	**0.002**	11.97 ± 2.91	11.39 ± 2.50	0.153	11.76 ± 2.83	11.43 ± 2.50	0.067
3	13.14 ± 3.74	10.78 ± 2.33	**0.002**	11.19 ± 2.64	12.44 ± 3.66	0.374	12.38 ± 3.63	11.31 ± 2.14	0.463
4–5	15.50 ± 4.03	11.88 ± 2.99	0.504	11.44 ± 2.60	12.72 ± 3.05	0.807	10.14 ± 0.03	10.72 ± 3.05	0.765

[a,c]Covariance analysis adjusting for sex, disease duration, and LEDD; [b]Covariance analysis adjusting for sex, age and LEDD. Definition of abnormal: for cognitive decline, MoCA score cut-offs of 17 (illiteracy), 20 (primary school education), 23 (secondary school education) of 30 points; for RBD, a cut-off of 19 on the RBDQ-HK score; for olfactory loss, a cut-off of 22 on the AHRS score. Bold values: p< 0.05.

et al., 2018), we did not find an increase in the level of pS-α-syn-RBC in the cognitively impaired patients. Conversely, the cognitively impaired patients had lower levels of pS-α-syn-RBC in comparison to the cognitively normal patients. Because the PD patients with worse olfaction were more likely to have cognitive impairment (Fullard et al., 2016), it is reasonable that the patients with olfactory loss also had lower levels of pS-α-syn-RBC compared to those with normal olfactory function. The mechanism is not clear. It has been demonstrated that PD patients with cognitive impairment and olfactory dysfunction are associated with increased Aβ and tau pathology (Fujishiro et al., 2008; Irwin et al., 2013), and in the RBCs of PD patients, these proteins were found to interact with α-syn to form the α-syn-Aβ or the α-syn-Aβ heterocomplex (Daniele et al., 2018a,b). Therefore, the lower levels of pS-α-syn-RBC detected in the patients with cognitive impairment and olfactory loss may not be due to the actual reduction of pS-α-syn-RBC but rather to its interaction with Aβ and tau, which affects its accurate detection.

The present study also revealed that higher pS-α-syn-RBC levels were associated with worse motor symptoms, as indicated by UPDRS III scores. Moreover, the levels of pS-α-syn-RBC were positively correlated with disease duration and H&Y stages. These results are in agreement with previous studies showing that dopaminergic neuronal loss is positively correlated with total α-syn burden and disease duration (Dijkstra et al., 2014), suggesting that alterations of the pS-α-syn-RBC level may reflect the neuropathological conditions in PD.

Age at onset (AAO) is an important factor that affects the progression, severity, and phenotype of PD. We found that the levels of pS-α-syn-RBC in LOPD were significantly higher than those in YOPD. This is in line with a recent prospective study showing that an older AAO was associated with a more severe PD phenotype and a greater impairment of dopaminergic function (Pagano et al., 2016). In addition, we found that the differences in the level of pS-α-syn-RBC between the patients with the TD and PIGD subtypes and between the patients with and without cognitive and olfactory impairments were also affected by the AAO. However, with the increase in the AAO, the differences were disappeared, indicating that the neuropathological changes of PD tend to be homogenized with the increase in the AAO.

In conclusion, our study demonstrates that pS-α-syn-RBC levels are increased in PD patients, which separate PD patients from healthy controls, differ in different subtypes and stages of

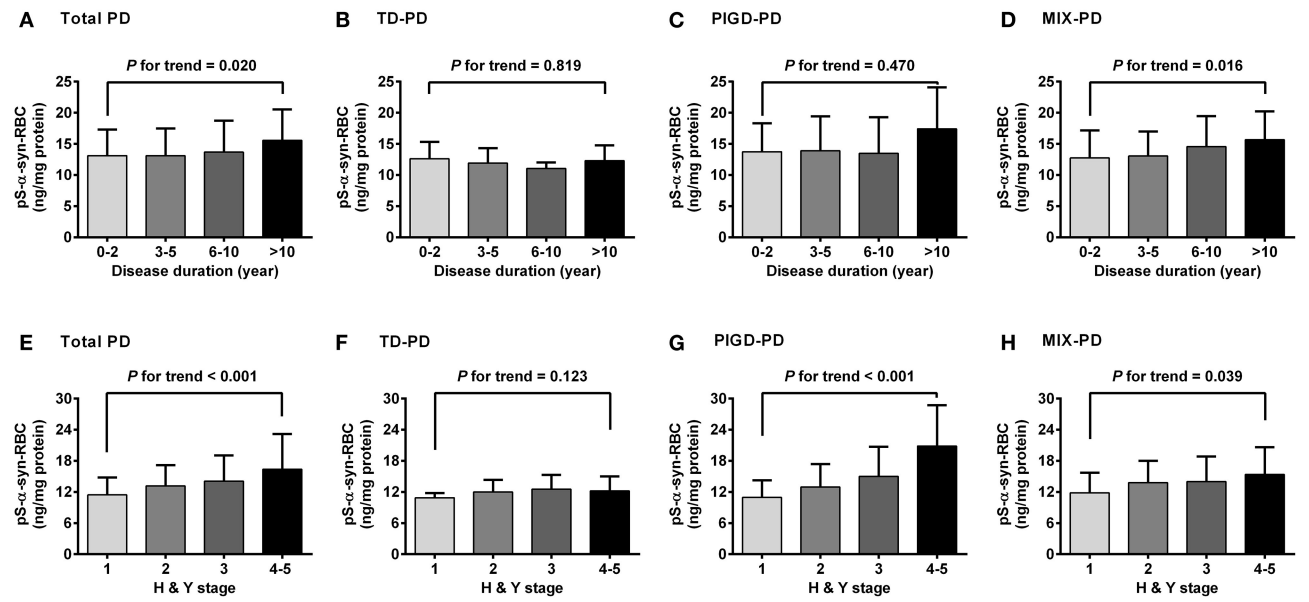


FIGURE 3 | Correlations of pS-α-syn-RBC with disease duration **(A–D)** and HandY stages **(E–H)** of Parkinson's disease and its motor subtypes. Trend was analyzed by using one-degree-freedom linear term. TD-PD, Parkinson's disease (PD) subtype with tremor dominant phenotype; PIGD-PD, PD subtype with postural instability and gait difficulty (PIGD)-dominant phenotype; MIX-PD, PD subtype with intermediate phenotype between TD and PIGD.

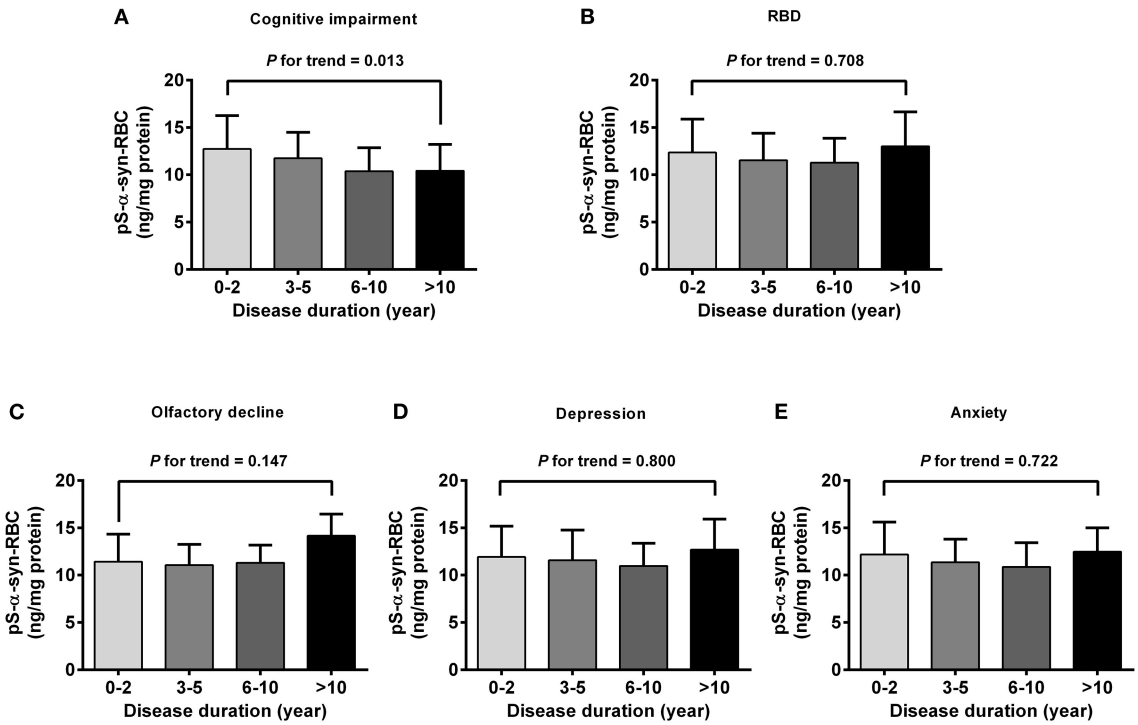


FIGURE 4 | Correlations of pS-α-syn-RBC with disease duration in PD patients with different non-motor subtypes. Correlations between pS-α-syn-RBC and intervals of disease duration in PD patients with non-motor subtypes was analyzed by using one-degree-freedom linear term for trend analysis. **(A)** Cognitive impairment; **(B)** RBD; **(C)** olfactory loss; **(D)** depression; **(E)** anxiety. *p*-values for the changing trend of pS-α-syn-RBC levels across increased disease durations were calculated.

PD, and may reflect the heterogeneity and progression of the neuropathological changes of PD.

DATA AVAILABILITY STATEMENT

The original contributions presented in the study are included in the article/**Supplementary Materials**, further inquiries can be directed to the corresponding authors.

ETHICS STATEMENT

The studies involving human participants were reviewed and approved by Xuanwu Hospital of Capital Medical University, Dongfang Hospital of Beijing University of Chinese Medicine, Peking University Shenzhen Hospital and Xiyuan Hospital, China Academy of Chinese Medical Sciences. The patients/participants provided their written informed consent to participate in this study.

AUTHOR CONTRIBUTIONS

SY and CW: had full access to all of the data in the study and takes responsibility for the integrity of the data, the accuracy of the data analysis, concept, design, obtained funding, and supervision. All authors: acquisition, analysis, or interpretation of data. CW, SY, and X-YL: drafting of the manuscript. LS, ZC, and JW: critical reversion of the manuscript for important intellectual content. CW and X-YL: experiments performance and statistical analysis. WL, XL, X-RL, WY, YC, LS, ZC, and JW: technical and material support.

FUNDING

This work was supported by grants from National Natural Science Foundation of China (NSFC) (82071428 and 81671244) to SY, grants from Ministry of Science and Technology of the People's Republic of China (MOST) (Key Project No. 2016YFC1306000), National Natural Science Foundation of China (NSFC) (No. 81771212), and Special Fund from the Key laboratory of Neurodegenerative Diseases, Ministry of Education of China (PXM2019_026283_000002) to CW.

ACKNOWLEDGMENTS

We gratefully thank the study participants and staff of the Department of Neurobiology and Neurology, Xuanwu Hospital, Capital Medical University, for their cooperation and assistance in participant recruitment, sample collection and data analyses.

SUPPLEMENTARY MATERIAL

The Supplementary Material for this article can be found online at: https://www.frontiersin.org/articles/10.3389/fnagi.2021.623977/full#supplementary-material

REFERENCES

Abd-Elhadi, S., Honig, A., Simhi-Haham, D., Schechter, M., Linetsky, E., Ben-Hur, T., et al. (2015). Total and proteinase K-resistant α-synuclein levels in erythrocytes, determined by their ability to bind phospholipids, associate with Parkinson's disease. *Sci. Rep.* 5:11120. doi: 10.1038/srep11120

Ahn, T. B., Kim, S. Y., Kim, J. Y., Park, S. S., Lee, D. S., Min, H. J., et al. (2008). alpha-Synuclein gene duplication is present in sporadic Parkinson disease. *Neurology* 70, 43–49. doi: 10.1212/01.wnl.0000271080.53272.c7

Anderson, J. P., Walker, D. E., Goldstein, J. M., de Laat, R., Banducci, K., Caccavello, R. J., et al. (2006). Phosphorylation of Ser-129 is the dominant pathological modification of alpha-synuclein in familial and sporadic Lewy body disease. *J. Biol. Chem.* 281, 29739–29752. doi: 10.1074/jbc.M600933200

Atik, A., Stewart, T., and Zhang, J. (2016). Alpha-synuclein as a biomarker for Parkinson's disease. *Brain Pathol.* 26, 410–418. doi: 10.1111/bpa.12370

Barbour, R., Kling, K., Anderson, J. P., Banducci, K., Cole, T., Diep, L., et al. (2008). Red blood cells are the major source of alpha-synuclein in blood. *Neurodegener. Dis.* 5, 55–59. doi: 10.1159/000112832

Braak, H., and Tredici, D. K. (2017). Neuropathological staging of brain pathology in sporadic Parkinson's disease: separating the wheat from the chaff. *J. Parkinsons Dis.* 7, S71–S85. doi: 10.3233/JPD-179001

Cariulo, C., Martufi, P., Verani, M., Azzollini, L., Bruni, G., Weiss, A., et al. (2019). Phospho-S129 alpha-synuclein is present in human plasma but not in cerebrospinal fluid as determined by an ultrasensitive immunoassay. *Front. Neurosci.* 13:889. doi: 10.3389/fnins.2019.00889

Cheng, F., Vivacqua, G., and Yu, S. (2011). The role of α-synuclein in neurotransmission and synaptic plasticity. *J. Chem. Neuroanat.* 42, 242–248. doi: 10.1016/j.jchemneu.2010.12.001

Daniele, S., Frosini, D., Pietrobono, D., Petrozzi, L., Lo Gerfo, A., Baldacci, F., et al. (2018a). α-Synuclein heterocomplexes with β-amyloid are increased in red blood cells of Parkinson's disease patients and correlate with disease severity. *Front. Mol. Neurosci.* 11:53. doi: 10.3389/fnmol.2018.00053

Daniele, S., Pietrobono, D., Fusi, J., Iofrida, C., Chico, L., Petrozzi, L., et al. (2018b). α-Synuclein aggregates with β-amyloid or tau in human red blood cells: correlation with antioxidant capability and physical exercise in human healthy subjects. *Mol. Neurobiol.* 55, 2653–2675. doi: 10.1007/s12035-014-9070-5

Dijkstra, A. A., Voorn, P., Berendse, H. W., Groenewegen, H. J., Netherlands Brain Bank, Rozemuller, A. J. et al. (2014). Stage-dependent nigral neuronal loss in incidental Lewy body and Parkinson's disease. *Mov. Disord.* 29, 1244–1251. doi: 10.1002/mds.25952

Ding, J., Zhang, J., Wang, X., Zhang, L., Jiang, S., Yuan, Y., et al. (2017). Relationship between the plasma levels of neurodegenerative proteins and motor subtypes of Parkinson's disease. *J. Neural. Transm.* 124, 353–360. doi: 10.1007/s00702-016-1650-2

Duran, R., Barrero, F. J., Morales, B., Luna, J. D., Ramirez, M., and Vives, F. (2010). Plasma alpha-synuclein in patients with Parkinson's disease with and without treatment. *Mov. Disord.* 25, 489–493. doi: 10.1002/mds.22928

Emamzadeh, F. N., and Allsop, D. (2017). α-Synuclein interacts with lipoproteins in plasma. *J. Mol. Neurosci.* 63, 165–172. doi: 10.1007/s12031-017-0967-0

Fogue Fayyad, M., Salim, S., Majbour, N., Erskine, D., Stoops, E., Mollenhauer, B., et al. (2019). Parkinson's disease biomarkers based on α-synuclein. *J. Neurochem.* 150, 626–636. doi: 10.1111/jnc.14809

Foulds, P. G., Diggle, P., Mitchell, J. D., Parker, A., Hasegawa, M., Masuda-Suzukake, M., et al. (2013). A longitudinal study on α-synuclein in blood plasma as a biomarker for Parkinson's disease. *Sci. Rep.* 3:2540. doi: 10.1111/ene.14208

Foulds, P. G., Mitchell, J. D., Parker, A., Turner, R., Green, G., Diggle, P., et al. (2011). Phosphorylated α-synuclein can be detected in blood plasma and is potentially a useful biomarker for Parkinson's disease. *FASEB J.* 25, 4127–4137. doi: 10.1096/fj.10-179192

Fujishiro, H., Tsuboi, Y., Lin, W. L., Uchikado, H., and Dickson, D. W. (2008). Co-localization of tau and α-synuclein in the olfactory bulb in Alzheimer's disease with amygdala Lewy bodies. *Acta Neuropathol.* 116, 17–24. doi: 10.1007/s00401-008-0383-1

Fullard, M. E., Tran, B., Xie, S. X., Toledo, J. B., Scordia, C., Linder, C., et al. (2016). Olfactory impairment predicts cognitive decline in early Parkinson's disease. *Parkinsonism Relat. Disord.* 25, 45–51. doi: 10.1016/j.parkreldis.2016.02.013

Goldman, J. G., Andrews, H., Amara, A., Naito, A., Alcalay, R. N., Shaw, L. M., et al. (2018). Cerebrospinal fluid, plasma, and saliva in the BioFIND study: relationships among biomarkers and Parkinson's disease features. *Mov. Disord.* 33, 282–288. doi: 10.1002/mds.27232

Irwin, D. J., Lee, V. M., and Trojanowski, J. Q. (2013). Parkinson's disease dementia: convergence of α-synuclein, tau and amyloid-β pathologies. *Nat. Rev. Neurosci.* 14, 626–636. doi: 10.1038/nrn3549

Ishii, R., Tokuda, T., Tatebe, H., Ohmichi, T., Kasai, T., Nakagawa, M., et al. (2015). Decrease in plasma levels of α-synuclein is evident in patients with Parkinson's disease after elimination of heterophilic antibody interference. *PLoS ONE* 10:e0123162. doi: 10.1371/journal.pone.0123162

Jankovic, J., McDermott, M., Carter, J., Gauthier, S., Goetz, C., Golbe, L., et al. (1990). Variable expression of Parkinson's disease: a base-line analysis of the DATATOP cohort. *Neurology* 40, 1529–1534. doi: 10.1212/wnl.40.10.1529

Lee, P. H., Lee, G., Park, H. J., Bang, O. Y., Joo, I. S., and Huh, K. (2006). The plasma alpha-synuclein levels in patients with Parkinson's disease and multiple system atrophy. *J. Neural. Transm.* 113, 1435–1439. doi: 10.1007/s00702-005-0427-9

Li, Q. X., Mok, S. S., Laughton, K. M., McLean, C. A., Cappai, R., Masters, C. L., et al. (2007). Plasma alpha-synuclein is decreased in subjects with Parkinson's disease. *Exp. Neurol.* 204, 583–588. doi: 10.1016/j.expneurol.2006.12.006

Li, X. Y., Yang, W. W., Li, X., Li, X. R., Li, W., Song, Q. H., et al. (2020). Phosphorylated alpha-synuclein in red blood cells as a potential diagnostic biomarker for multiple system atrophy: a pilot study. *Parkinsons Dis.* 2020:8740419. doi: 10.1155/2020/8740419

Lin, C. H., Yang, S. Y., Horng, H. E., Yang, C. C., Chieh, J. J., Chen, H. H., et al. (2018). Plasma biomarkers differentiate Parkinson's disease from atypical Parkinsonism syndromes. *Front. Aging Neurosci.* 10:123. doi: 10.3389/fnagi.2018.00123

Liu, G., Chen, M., Mi, N., Yang, W., Li, X., Wang, P., et al. (2015). Increased oligomerization and phosphorylation of α-synuclein are associated with decreased activity of glucocerebrosidase and protein phosphatase 2A in aging monkey brains. *Neurobiol. Aging* 36, 2649–2659. doi: 10.1016/j.neurobiolaging.2015.06.004

Majbour, N. K., Vaikath, N. N., van Dijk, K. D., Ardah, M. T., Varghese, S., Vesterager, L. B., et al. (2016). Oligomeric and phosphorylated alpha-synuclein as potential CSF biomarkers for Parkinson's disease. *Mol. Neurodegener.* 11:7. doi: 10.1186/s13024-016-0072-9

Mathiesen, R., Chriél, M., Struve, T., and Heegaard, P. M. H. (2018). Quantitative immunoassay for mink immunoglobulin in serum and milk. *Acta Vet. Scand.* 60:36. doi: 10.1186/s13028-018-0391-7

Matsumoto, J., Stewart, T., Sheng, L., Li, N., Bullock, K., Song, N., et al. (2017). Transmission of α-synuclein-containing erythrocyte-derived extracellular vesicles across the blood-brain barrier via adsorptive mediated transcytosis: another mechanism for initiation and progression of Parkinson's disease? *Acta Neuropathol Commun.* 5:71. doi: 10.1186/s40478-017-0470-4

Mollenhauer, B., Zimmermann, J., Sixel-Döring, F., Focke, N. K., Wicke, T., Ebentheuer, J., et al. (2016). Monitoring of 30 marker candidates in early Parkinson disease as progression markers. *Neurology* 87, 168–177. doi: 10.1212/WNL.0000000000002651

Olgiati, S., Thomas, A., Quadri, M., Breedveld, G. J., Graafland, J., Eussen, H., et al. (2015). Early-onset parkinsonism caused by alpha-synuclein gene triplication: clinical and genetic findings in a novel family. *Parkinsonism Relat. Disord.* 21, 981–986. doi: 10.1016/j.parkreldis.2015.06.005

Oueslati, A. (2016). Implication of alpha-synuclein phosphorylation at S129 in synucleinopathies: what have we learned in the last decade? *J. Parkinsons Dis.* 6, 39–51. doi: 10.3233/JPD-160779

Pagano, G., Ferrara, N., Brooks, D. J., and Pavese, N. (2016). Age at onset and Parkinson disease phenotype. *Neurology* 86, 1400–1407. doi: 10.1212/WNL.0000000000002461

Parnetti, L., Gaetani, L., Eusebi, P., Paciotti, S., Hansson, O., El-Agnaf, O., et al. (2019). CSF and blood biomarkers for Parkinson's disease. *Lancet Neurol.* 18, 573–586. doi: 10.1016/S1474-4422(19)30024-9

Polymeropoulos, M. H., Lavedan, C., Leroy, E., Ide, S. E., Dehejia, A., Dutra, A., et al. (1997). Mutation in the alpha-synuclein gene identified in families with Parkinson's disease. *Science* 276, 2045–2047. doi: 10.1126/science.276.5321.2045

Postuma, R. B., Berg, D., Stern, M., Poewe, W., Olanow, C. W., Oertel, W., et al. (2015). MDS clinical diagnostic criteria for Parkinson's disease. *Mov. Disord.* 30, 1591–1601. doi: 10.1002/mds.26424

Rabinak, C. A., and Nirenberg, M. J. (2010). Dopamine agonist withdrawal syndrome in Parkinson disease. *Arch. Neurol.* 67, 58–63. doi: 10.1001/archneurol.2009.294

Rietdijk, C. D., Perez-Pardo, P., Garssen, J., van Wezel, R. J., and Kraneveld, A. D. (2017). Exploring Braak's hypothesis of Parkinson's disease. *Front. Neurol.* 8:37. doi: 10.3389/fneur.2017.00037

Selikhova, M., Williams, D. R., Kempster, P. A., Holton, J. L., Revesz, T., and Lees, A. J. (2009). A clinico-pathological study of subtypes in Parkinson's disease. *Brain* 132, 2947–2957. doi: 10.1093/brain/awp234

Shi, M., Zabetian, C. P., Hancock, A. M., Ginghina, C., Hong, Z., Yearout, D., et al. (2010). Significance and confounders of peripheral DJ-1 and alpha-synuclein in Parkinson's disease. *Neurosci. Lett.* 480, 78–82. doi: 10.1016/j.neulet.2010.06.009

Spillantini, M. G., Crowther, R. A., Jakes, R., Hasegawa, M., and Goedert, M. (1998). α-Synuclein in filamentous inclusions of Lewy bodies from Parkinson's disease and dementia with Lewy bodies. *Proc. Natl. Acad. Sci. U.S.A.* 95, 6469–6473. doi: 10.1073/pnas.95.11.6469

Stebbins, G. T., Goetz, C. G., Burn, D. J., Jankovic, J., Khoo, T. K., and Tilley, B. C. (2013). How to identify tremor dominant and postural instability/gait difficulty groups with the movement disorder society unified Parkinson's disease rating scale: comparison with the unified Parkinson's disease rating scale. *Mov. Disord.* 28, 668–670. doi: 10.1002/mds.25383

Sveinbjornsdottir, S. (2016). The clinical symptoms of Parkinson's disease. *J. Neurochem. Suppl.* 1, 318–324. doi: 10.1111/jnc.13691

Tian, C., Liu, G., Gao, L., Soltys, D., Pan, C., Stewart, T., et al. (2019). Erythrocytic α-synuclein as a potential biomarker for Parkinson's disease. *Transl. Neurodegener.* 8:15. doi: 10.1186/s40035-019-0155-y

Vaccaro, R., Toni, M., Casini, A., Vivacqua, G., Yu, S., D'este, L., et al. (2015). Localization of α-synuclein in teleost central nervous system: immunohistochemical and Western blot evidence by 3D5 monoclonal antibody in the common carp, *Cyprinus carpio*. *J. Comp. Neurol.* 523, 1095–1124. doi: 10.1002/cne.23722

Van de Berg, W. D., Hepp, D. H., Dijkstra, A. A., Rozemuller, J. A., Berendse, H. W., and Foncke, E. (2012). Patterns of α-synuclein pathology in incidental cases and clinical subtypes of Parkinson's disease. *Parkinsonism Relat. Disord. Suppl.* 1, S28–S30. doi: 10.1016/S1353-8020(11)70011-6

Van der Heeden, J. F., Marinus, J., Martinez-Martin, P., Rodriguez-Blazquez, C., Geraedts, V. J., and van Hilten, J. J. (2016). Postural instability and gait are associated with severity and prognosis of Parkinson disease. *Neurology* 86, 2243–2250. doi: 10.1212/WNL.0000000000002768

Vicente Miranda, H., Cássio, R., Correia-Guedes, L., Gomes, M. A., Chegão, A., Miranda, E., et al. (2017). Posttranslational modifications of blood-derived alpha-synuclein as biochemical markers for Parkinson's disease. *Sci. Rep.* 7:13713. doi: 10.1038/s41598-017-14175-5

Wang, H., Stewart, T., Toledo, J. B., Ginghina, C., Tang, L., Atik, A., et al. (2018). Alzheimer's disease neuroimaging initiative. A longitudinal study of total and phosphorylated α-synuclein with other biomarkers in cerebrospinal fluid of Alzheimer's disease and mild cognitive impairment. *J. Alzheimers. Dis.* 61, 1541–1553. doi: 10.3233/JAD-171013

Wang, P., Li, X., Li, X., Yang, W., and Yu, S. (2016). Blood plasma of patients with Parkinson's disease increases alpha-synuclein aggregation and neurotoxicity. *Parkinsons Dis.* 2016:7596482. doi: 10.1155/2016/7596482

Wang, X. M., Yu, S., Li, F., and Feng, T. (2015). Detection of α-synuclein oligomers in red blood cells as a potential biomarker of Parkinson's disease. *Neuroscience Lett.* 599, 115–119. doi: 10.1016/j.neulet.2015.05.030

Wang, Y., Shi, M., Chung, K. A., Zabetian, C. P., Leverenz, J. B., Berg, D., et al. (2012). Phosphorylated α-synuclein in Parkinson's disease. *Sci. Transl. Med.* 4:121ra20. doi: 10.1126/scitranslmed.3002566

Wu, Y., Guo, X. Y., Wei, Q. Q., Ou, R. W., Song, W., Cao, B., et al. (2016). Non-motor symptoms and quality of life in tremor dominant vs postural instability gait disorder Parkinson's disease patients. *Acta Neurol. Scand.* 133, 330–337. doi: 10.1111/ane.12461

Yu, S., Li, X., Liu, G., Han, J., Zhang, C., Li, Y., et al. (2007). Extensive nuclear localization of alpha-synuclein in normal rat brain neurons revealed by a novel monoclonal antibody. *Neuroscience* 145, 539–555. doi: 10.1016/j.neuroscience.2006.12.028

Conflict of Interest: The authors declare that the research was conducted in the absence of any commercial or financial relationships that could be construed as a potential conflict of interest.

Publisher's Note: All claims expressed in this article are solely those of the authors and do not necessarily represent those of their affiliated organizations, or those of the publisher, the editors and the reviewers. Any product that may be evaluated in this article, or claim that may be made by its manufacturer, is not guaranteed or endorsed by the publisher.

Copyright © 2021 Li, Li, Li, Li, Sun, Yang, Cai, Chen, Wu, Wang and Yu. This is an open-access article distributed under the terms of the Creative Commons Attribution License (CC BY). The use, distribution or reproduction in other forums is permitted, provided the original author(s) and the copyright owner(s) are credited and that the original publication in this journal is cited, in accordance with accepted academic practice. No use, distribution or reproduction is permitted which does not comply with these terms.

Advantages of publishing in Frontiers

OPEN ACCESS
Articles are free to read for greatest visibility and readership

FAST PUBLICATION
Around 90 days from submission to decision

HIGH QUALITY PEER-REVIEW
Rigorous, collaborative, and constructive peer-review

TRANSPARENT PEER-REVIEW
Editors and reviewers acknowledged by name on published articles

Frontiers
Avenue du Tribunal-Fédéral 34
1005 Lausanne | Switzerland

Visit us: www.frontiersin.org
Contact us: frontiersin.org/about/contact

REPRODUCIBILITY OF RESEARCH
Support open data and methods to enhance research reproducibility

DIGITAL PUBLISHING
Articles designed for optimal readership across devices

FOLLOW US
@frontiersin

IMPACT METRICS
Advanced article metrics track visibility across digital media

EXTENSIVE PROMOTION
Marketing and promotion of impactful research

LOOP RESEARCH NETWORK
Our network increases your article's readership